PROCEEDINGS OF THE

32nd International Symposium on Analytical and Environmental Problems

Szeged, Hungary

October 12-13, 2026

University of Szeged

Edited by:
Tünde Alapi
Róbert Berkecz
István Ilisz

Publisher:
University of Szeged, H-6720 Szeged, Dugonics tér 13, Hungary

ISBN 978-963-688-175-7

2026.
Szeged, Hungary

The 32nd International Symposium on Analytical and Environmental Problems

Organized by:
SZAB Kémiai Szakbizottság Analitikai és Környezetvédelmi Munkabizottsága

Supporting Organizations
Hungarian Academy of Sciences
Hungarian Chemical Society Group of Csongrád County
Institute of Pharmaceutical Analysis, University of Szeged
Department of Molecular and Analytical Chemistry, University of Szeged

Symposium Chairman:
István Ilisz, DSc

Honorary Chairman:
Zoltán Galbács, PhD

Organizing Committee:
István Ilisz, DSc
professor of chemistry
University of Szeged, Institute of Pharmaceutical Analysis
Tünde Alapi, PhD
assistant professor
University of Szeged, Department of Molecular and Analytical Chemistry
Róbert Berkecz, PhD
associate professor
University of Szeged, Institute of Pharmaceutical Analysis

Scientific Committee:
István Ilisz, DSc
Tünde Alapi, PhD
Róbert Berkecz, PhD
Daniela Sojic Merkulov, PhD
full professor
University of Novi Sad, Faculty of Sciences, Department of Chemistry, Biochemistry and Environmental Protection

Lecture Proceedings

ECOTOXICOLOGICAL EVALUATION OF $CsPbI_3$ AND Cs_2SnI_6 PEROVSKITES ON *DAPHNIA MAGNA* MODEL ORGANISMS

Adrienn-Dorisz Dávid[1], László Szandra-Leila[1], Krisztina Albert[1], Lilla Szalma[2], Tamás Gyulavári[2], Karolina Solymos[2], Lujza Keresztes[1], Zoltán Kónya[2], Zsolt Pap[1,2,3]

[1]Babeş-Bolyai University, Faculty of Biology and Geology, Hungarian Department of Biology and Ecology
[2]University of Szeged, Faculty of Science and Informatics, Applied & Environmental Chemistry Department
[3] Babeş-Bolyai University, STAR-UBB Institute
e-mail: adrienn.david@ubbcluj.ro

Abstract

In this study, we investigated the environmental impacts of $CsPbI_3$ and Cs_2SnI_6 materials synthesized in the laboratory via a solvothermal method at 120/130°C, 150°C, and 180°C to enable the examination of various crystal sizes. For the materials science characterization of these compounds, three analytical methods were employed: crystal structure analysis via X-ray diffraction (XRD), crystal morphology characterization using scanning electron microscopy (SEM), and evaluation of optical properties by diffuse reflectance spectroscopy (DRS). The environmental impacts of both materials were tested in an aqueous medium using the model organism *Daphnia magna*, a microscopic yet macroscopically visible organism that is easy to culture and highly suitable for conducting acute (24-hour) immobilization tests. These assays were performed using the Daphtoxkit F test kit following OECD guidelines, which provides all necessary materials for testing, excluding the substance under evaluation. Our primary objective in the present study was the dose-response assessment of $CsPbI_3$ and Cs_2SnI_6, focusing on the determination of the median effective concentration (EC_{50}). To achieve this, statistical Hill and Weibull models—commonly employed in ecotoxicology—were utilized. Concentration shifts in $CsPbI_3$ a steep, rapid onset of effect, whereas the curve for Cs_2SnI_6 was considerably less steep; consequently, the Hill model was applied to the former and the Weibull model to the latter. The results confirmed that the toxicity of these perovskites is strongly dependent on the synthesis temperature: crystals synthesized at lower temperatures (120/130°C) were less toxic (with EC_{50} values around 1.8 mg/L), whereas those synthesized at higher temperatures (150°C and 180°C) exerted more potent effects at significantly lower concentrations (EC_{50} values ranging between 90 and 480 µg/L). Although Cs_2SnI_6 represents a lead-free alternative, its toxicity level was nearly identical to that of $CsPbI_3$ indicating that the environmental release of either compound could entail severe consequences.

REDUCTION INSTEAD OF OXIDATION – THE POTENTIAL FOR REMOVING PFAS "FOREVER CHEMICALS" USING THE UV/SULFITE ARP PROCESS

Kornél Erdős, Bence Veres, Tünde Alapi

Department of Molecular and Analytical Chemistry, University of Szeged, H-6720 Szeged, Dóm tér 7, Hungary
e-mail: erdoskornel05@gmail.com

Per- and polyfluoroalkyl substances (PFAS) are highly persistent and toxic synthetic chemicals, which are regularly detected in surface water, groundwater, and even in drinking water. Under the recast EU Drinking Water Directive, systematic PFAS monitoring became mandatory in 2026, with strict limits (0.5 µg/L for total PFAS and 0.1 µg/L for the sum of 20 individual PFAS) [1-2]. Advanced oxidation processes (AOPs) effectively remove many organic pollutants, but their efficiency is limited for compounds such as PFAS. Therefore, Advanced Reduction Processes (ARPs), such as UV/sulfite (UV/SO_3^{2-}) process, have attracted increasing attention. ARPs rely primarily on the generation of the hydrated electrons (e_{aq}^-), which can attack and break the carbon–fluorine bonds in PFAS molecule. Photochemical water treatment commonly uses low-pressure mercury lamps emitting UV radiation at 254 nm and vacuum ultraviolet (VUV) radiation at 185 nm. Wavelength influences the photolysis of oxidants (AOPs) or reducing agents (ARPs), thereby affecting treatment efficiency [3-4].

In this work, UV/sulfite and UV/VUV/sulfite processes were investigated for the transformation of perfluorooctanoic acid (PFOA) and other PFAS compounds, such as trifluoroacetic acid (TFA) and perfluoropropionic acid (PFPA), with particular attention to the effects of sulfite concentration, pH, and dissolved oxygen. Experiments were conducted in Milli-Q water and in biologically treated domestic wastewater, and the effects of matrix components, such as organic content, HCO_3^- and Cl^- were systematically investigated. PFAS degradation was monitored using a fluoride ion-selective electrode (F-ISE), since C-F bond breaking releases F^- into solution.

VUV photolysis can decompose PFAS directly; the fluoride ion formation rate and the treatment time required for mineralization depend on carbon-chain length. Transformation efficiency decreased at lower pH and higher O_2 content, indicating that, in addition to direct VUV photolysis of PFAS, the reaction with e_{aq}^- generated by VUV photolysis of water contributes to defluorination. Addition of SO_3^{2-} to the UV or UV/VUV irradiated solution enhanced the transformation, since its UV and VUV photolysis results in e_{aq}^-. Besides efficiency, these processes were extremely sensitive to pH, O_2, and HCO_3^- content. Moreover, dissolved organic content inhibited PFAS transformation.

The negative effect of HCO_3^- and organic content was eliminated in a two-step pretreatment procedure. First, pH was increased to 4.0, and intensive stirring was applied to drive HCO_3^- out as CO_2. Second, the UV/PDS AOP mineralized the solution's organic content. The practical applicability of the method was evaluated for determining PFAS concentration in a special wastewater. This PFAS-containing wastewater was generated during the cleaning of pipeline systems used to store or transport firefighting foam.

Acknowledgements
This study was financially supported by the Ministry of Innovation and Technology through the National Talent Programme, under grant no. [NTP-NFTÖ-26-0865].

References

[1] AZ EURÓPAI PARLAMENT ÉS A TANÁCS (EU) 2020/2184 IRÁNYELVE," 2020.
[2] https://www.eea.europa.eu/en/analysis/publications/pfas-pollution-in-european-waters
[3] J. Chen, P.-Y. Zhang és J. Liu, „Photodegradation of perfluorooctanoic acid by 185 nm vacuum ultraviolet light," *Journal of Environmental Sciences,* 1. vol19, pp. 387-390, 2007.
[4] X. Xin, J. Li and C.-H. Huang, "Far-UVC (222 nm) Enchances the Advanced Reduction Process for Per- and Polyfluoroalkyl Substance (PFAS) Destruction," *Environmental Science and Technology,* vol. 5, pp. 6048-6057., 2025.

A LITERATURE REVIEW OF MICROPLASTIC DETECTION QUANTIFICATION AND REMOVAL ENHANCED BY 3D PRINTED SPACERS

Salma Elrehaimah[1,2], Aws N. Al-Tayawi[1,2,3], Hadid Sukmana[1], Timea Miklós[1,2], Nóra Ábrahám[4], Zsuzsanna László[1], Szabolcs Kertész[1]*

[1]Department of Biosystems Engineering, Faculty of Engineering, University of Szeged, Moszkvai krt. 9, Szeged H-6725, Hungary
[2]Doctoral School of Environmental Sciences, University of Szeged, Tisza Lajos krt. 103, H-6725 Szeged, Hungary
[3]Department of Environmental Technology, Faculty of Environmental Sciences, University of Mosul, 41002 Mosul, Iraq
[4]"Unichem" Chemical, Manufacturing and Trading Ltd., Kőiskola út 3, Kistelek H-6760, Hungary
e-mail: kertesz@mk.u-szeged.hu

Abstract

This narrative literature review compares micro-Fourier transform infrared spectroscopy (*μFTIR*), micro-Raman spectroscopy (*μRaman*) and pyrolysis gas chromatography–mass spectrometry (*Py-GC/MS*) for assessing microplastics (*MPs*) and nanoplastics (*NPs*) removal by membrane filtration. Published studies show that particle counts, polymer mass and size range are different endpoints. In a paired drinking-water study, count-based removal was 78.1% by μFTIR and 43.2% by μRaman, but both gave approximately 80% when restricted to particles above 6.6 μm. Dairy wastewater studies report membrane treatment and reduced fouling with three-dimensional (3D) printed spacers, without measuring *MPs* and *NPs* removal. We conclude that size-matched, polymer-confirmed feed–permeate measurements with blanks and recovery controls are needed. Applying these methods to dairy wastewater and testing printed spacers for *MPs* retention remain proposed work; *NPs* below the validated detection range cannot be assessed.

Introduction

For this review, *MPs* are operationally defined as plastic particles from 1 μm to 5 mm and *NPs* as particles below 1 μm; definitions vary [1]. Retention cannot be inferred from nominal membrane pore size alone. This narrative review compares what each method measures (polymer identity, count, size or mass), its accessible size interval and its suitability for assessing filtration efficiency. It separates measured outcomes in water and dairy studies from a proposed dairy experiment. No new experimental data or systematic meta-analysis are reported.

Literature findings and discussion

Published detection evidence. An interlaboratory comparison found substantial variation in particle counts, polymer identity and mass across methods [2]. Yang and co-workers developed a *μFTIR* workflow for 10–500 μm particles in seawater, freshwater and wastewater, with attention to sample preparation [3]. The complementary outputs and limitations are summarized in Table 1 [2,3,5].

Table 1. Analytical outputs relevant to feed–permeate comparisons.

Method	Useful output	Limit for a removal claim
μFTIR	Polymer identity and size-resolved particle counts.	Misses particles below its validated size limit; matrix preparation affects recovery.
μRaman	Polymer identity and counts of smaller particles.	Different size limits and spectral interference affect comparison.
Py-GC/MS	Polymer-specific bulk mass.	Destructive; no particle count, size or morphology.

Published filtration evidence. Yang and co-workers applied *μFTIR* to assess *MPs* across drinking-water, wastewater and seawater treatment processes [4]. A separate paired-method study of a drinking-water works reported 78.1% count-based removal by *μFTIR* and 43.2% by *μRaman*; when both datasets were restricted to particles above 6.6 μm, each indicated approximately 80% removal [5]. These measurements demonstrate why removal estimates require a shared size interval. In dairy wastewater, microfiltration (*MF*) before ultrafiltration (*UF*) reduced fouling [6]. Published studies of 3D-printed spacers in dairy wastewater modules report improved filtration performance and reduced fouling [7,8]. Those dairy studies did not quantify plastic particles in feed, permeate and retentate, so they cannot establish *MPs* or *NPs* removal by the printed components.

Proposed dairy application. A future study could sample feed, permeate and retentate at each membrane stage in dairy wastewater, with procedural blanks, spike-recovery tests and a sample-cleanup procedure checked for plastic loss. Polymer-confirmed *μFTIR* and *μRaman* counts would be compared within a common validated size window; *Py-GC/MS* could add polymer-mass information. A conventional module and a module with a printed promoter should be tested under matched operating conditions while recording flux, fouling and particle breakthrough. Blanks should also check whether the printed component sheds plastic. This is a proposed protocol, not a result of the cited dairy studies; particles below the validated removal limit would remain unresolved.

Conclusion

Effective management of *MPs* and *NPs* requires an integrated approach that couples reliable identification and quantification with separation and membrane fouling control. The reviewed studies show that *μFTIR* and *μRaman* particle counts must be compared over the same size range, while *Py-GC/MS* adds a complementary measure of polymer mass. Membrane processes retain measurable MPs in studied waters, and dairy wastewater research supports pretreatment and 3D-printed spacers for improving filtration efficiency. The cited dairy studies do not establish plastic-particle removal by printed components. Validated measurements of feed, permeate, and retentate are needed before improved microplastic removal can be claimed for dairy wastewater; claims concerning nanoplastics will require methods with an appropriate validated detection range.

Acknowledgements

This work was supported by the NKFI-FK-142414 and 2022-1.2.6-TÉT-IPARI-TR-2022-00011 projects of the National Research, Development and Innovation Office, Hungary.

References

[1] N.B. Hartmann, T. Hüffer, R.C. Thompson, et al., Are we speaking the same language? Recommendations for a definition and categorization framework for plastic debris, Environmental Science & Technology 53(3) (2019) 1039–1047. doi:10.1021/acs.est.8b05297.

[2] Y.K. Müller, T. Wernicke, M. Pittroff, et al., Microplastic analysis—are we measuring the same? Results on the first global comparative study for microplastic analysis in a water sample, Analytical and Bioanalytical Chemistry 412(3) (2020) 555–560. doi:10.1007/s00216-019-02311-1.

[3] J. Yang, M. Monnot, Y. Sun, et al., Microplastics in different water samples (seawater, freshwater, and wastewater): Methodology approach for characterization using micro-FTIR spectroscopy, Water Research 232 (2023) article 119711. doi:10.1016/j.watres.2023.119711.

[4] J. Yang, M. Monnot, Y. Sun, et al., Microplastics in different water samples (seawater, freshwater, and wastewater): Removal efficiency of membrane treatment processes, Water Research 232 (2023) article 119673. doi:10.1016/j.watres.2023.119673.

[5] L. Maurizi, L. Iordachescu, I.V. Kirstein, et al., It matters how we measure—Quantification of microplastics in drinking water by µFTIR and µRaman, Heliyon 9(9) (2023) article e20119. doi:10.1016/j.heliyon.2023.e20119.

[6] M. Zielińska, M. Galik, Use of ceramic membranes in a membrane filtration supported by coagulation for the treatment of dairy wastewater, Water, Air, & Soil Pollution 228(5) (2017) article 173. doi:10.1007/s11270-017-3365-x.

[7] S. Kertész, A.N. Al-Tayawi, G. Gergely, et al., Investigation of different pre-treatment techniques and 3D printed turbulence promoter to mitigate membrane fouling in dairy wastewater module, Materials 16(8) (2023) article 3117. doi:10.3390/ma16083117.

[8] A.N. Al-Tayawi, N.S. Gulyás, G. Gergely, et al., Enhancing ultrafiltration performance for dairy wastewater treatment using a 3D printed turbulence promoter, Environmental Science and Pollution Research 30(50) (2023) 108907–108916. doi:10.1007/s11356-023-30027-4.

AN OVERVIEW ON THE STRATEGIES TO RECYCLE PEROVSKITE AND CIGS SOLAR CELLS TO REDUCE ENVIRONMENTAL IMPACTS

Saji Thomas Kochuveedu[1], Bodnárné Sándor Renáta[1], Pedro Anacleto[2], Francesco De Nicola[3]

[1]Department of System Design, Bay Zoltán Applied Research Nonprofit Ltd, Hungary
[2]International Iberian Nanotechnology Laboratory, Department of Quantum & Energy Materials, Laboratory of Nanostructured Solar Cells, Av. Mestre José Veiga s/n 4715-330 Braga, Portugal
[3]National Research Council (CNR), Institute of Structure of Matter (ISM), Via del Fosso del Cavaliere, Rome, Italy
e-mail: saji.thomas.kochuveedu@bayzoltan.hu

Abstract
Photovoltaic installations will be an important asset in achieving net zero target and developing a more sustainable world economy. This fast deployment will lead to generation of huge volume of waste after their service life. Perovskite solar cells (PSCs) achieved an impressive performance in the last decade. CIGS solar cells (CIGSSCs) are another fast-evolving commercial solar cell. The environmental impacts material used in these solar panels and the strategies to recover valuable materials from spent solar panels are discussed in detail. The environmental impacts of recycling are also analyzed.

Introduction
Achieving net-zero emissions by 2050 intensely relies on decarbonizing electricity sector, and this demands aggressive expansion of renewable energy sector. Projection studies by IRENA and IEA in 2023 indicate this target will require 18.2 TW1 and 18.8 TW2 of solar PV installed capacity by 2050. This demands aggressive deployment of solar panels. *TRANSMIT* project develops a semi-transparent photovoltaic technology with high average visual transparency and power conversion efficiency with an aim to contribute to the generation of on-site sustainable electricity in net-zero buildings. The techniques adopted are micro-structuring CIGS on glass using photolithography, sputtering, and lift-off techniques and printing print the perovskite material and use laser ablation to make clear micro-lines, thus creating transparency. This produced micro-striped semi-transparent photovoltaic devices validated in a relevant environment. CIGSSCs can be easily integrated into building design rather than sit on top of it. These modules can be embedded into facades, glass, and even semi-transparent surfaces without compromising on aesthetics and adaptability. which is something silicon solar panels struggles with. The project aims to reach TRL5.

Current solar panel industry is more linear economy oriented. Estimation studies say a global volume between 1.7 and 8 million tons of solar waste is expected arrive the waste recycling facilities by 2030. The depletion of natural resources and the emission of several pollutants to the environment during the whole life cycle of the device represent concerning environmental issues as well as GHG emissions. Therefore, an efficient end-of-life plan is the call of the time to establish circular economy and to reduce reliance on primary materials. Seeing the supply chain risks and concentrated productions of PV technology, a carefully designed EoL management could be an added benefit to the PV value chain since a large stock valuables materials are locked in the panels. Recovering locked raw materials and other valuable components and injecting them back to the supply chain can help the production of new panels with lower environmental impacts. Also, it can alleviate the security risks and

improve resilience of primary resources. Life Cycle Assessment (LCA) is one of the main methodologies helps an early-stage evaluation of all the environmental impacts. We overviewed the existing recycling strategies to device an efficient EoL management plan of the devices developed in this project and analysed the enviormental impacts of recycling using LCA.

Results and discussion

Despite high-efficiency and low production cost, material toxicity of lead-containing PSCs and low stability are the major challenges towards its widespread commercialization. The perovskite solar panels will contain up to ~6000 tons of lead, if only 20% of anticipated 8500-gigawatt PV market in 2050 is occupied by PSCs. Recycling 70 dm2 of perovskite film yields around 600 mg of PbI2, which is enough to prepare 1 mL of a 1.25 M PbI2 solution. This permits the production of recycled MAPbI3 films with an area of around 2 dm^2. The Au layer of PSCs can be peeled off using adhesive tape, and about 100 % recovery is reported. N,N-dimethylformamide (DMF) is a widely used solvent for dissolving the perovskite active layer during recycling. Hematite nanoparticles, diethyl ether or weakly acidic cation-exchange resin can be used to recover lead from DMF. The recycled DMF was reused to fabricate PSCs, achieving a PCE of 25.02%, which was comparable to the 25.12% efficiency of the control PSCs. Water is also used as a solvent, exploiting the temperature-dependent solubility of PbI2. Chlorobenzene is used to dissolve spiro-OMeTAD. The recovered substrates can be utilized to fabricate new PSC devices. The Au film of the SCs can be detached using scotch tape or via solvent extraction using acetone.

Despite many advantages of CIGSSCs in thin film PV technology, challenges remain in terms of material availability and production costs. Indium, being an energy-critical element, raises concerns over the sustainability of metal mining and reserves. Additionally, copper is toxic, and gallium is another critical metal that must be managed carefully. The valuable components of spent CIGS are concentrated in the light-absorption layer. The recycling starts with delamination of encapsulant, followed by recovery of metals. Hydrometallurgy is the commonly adapted methos to dissolute and precipitate metals. Oxidative roasting followed by acid leaching is another approach to recover metals. The leaching efficiency of Indium is above 90 % when sulfuric acid is used. A combination of hydrometallurgical leaching and electrochemical technology is another approach to recover the valuable components in CIGS waste. Electrodeposition can be used to recover Se and copper using Ti and Pt as working electrode, respectively.

Though recycling can reduce the environmental impacts significantly, and new panel can be produced with recycled materials, the solvents, DMF, ethyl acetate and DMSO, used for dissolving perovskite layers raise serious environmental concerns. DMF is included in the Candidate List of Substances of Very High Concern (SVHC), as part of Regulation by the European Chemical Agency. Thus, it is important to reduce the use of these solvents, and using green solvents instead. In CIGS recycling, using strong acids like sulfuric acid and nitric acid for leaching cause significant environmental burden. In this regard, the leaching process carried out by citric acid and H2O2 can reduce the environmental burden with the lowest impact of the CA production process.

Conclusion

We tried to develop an EoL plan for the project. Recycling cell materials at the end of life could contribute to reducing the environmental impact by keeping valuable materials in the cycle of use for longer. However, recycling is not free from environmental burdens. The environmental footprints of material and energy should be carefully analyzed using LCA. Solvents with lower environmental impacts and less energy intensive methods are suggested for recycling. Along

with recycling, suggestions for fabricating new devices with lower environmental concerns is also discussed.

Acknowledgements
This research, TRANSMIT, was funded by CET Partnership, the Clean Energy Transition Partnership under the 2022 Joint Call for research proposals, co-funded by the European Commission (GA nº101069750) and supported by the Hungarian Ministry of Culture and Innovation from the National Research Development and Innovation Fund, financed by the 2023-1.2.2HE_PARTNERSÉG application program.

References
[1] IRENA, World energy transitions outlook 2023 : 1.5°C pathway, International Renewable Energy Agency IRENA, 2023.
[2] Energy Agency, Net Zero Roadmap: A Global Pathway to Keep the 1.5 °C Goal in Reach - 2023 Update, 2023.
[3] N. Rodrigues, J. Fonseca, P. Santos, R. Gutzler, W. Witte, S. Shital, P. J. Dale, P. Anacleto, S. Sadewasser. RRL Solar (2026); 1-8
[4] B. Chen, C. Fei, S. Chen, H. Gu, X. Xiao, J. Huang. Nat. Commun. 12 (2021); 5859.
[5] F. Barayeva, A. Beisenbayev, B. Zhussipbay, Y. Olzhabay, D. Aidarkhanov, A. Ng. Eurasian Chem.-Technol. J. 27 (2025) 199─208.
[6] D. Hu, B. Ma, X. Li, Y. Lv, Y. Chen. J. Clean. Prod. 350 (2022)131426.
[7] Y. Taneja, R. Singh. EES Sol. 2 (2026); 706-714.

SOL-GEL IMMOBILIZED BIOCATALYSTS FOR THE ENZYMATIC PRODUCTION OF FLAVOR ESTERS IN SOLVENT-FREE SYSTEM

Anemona-Mariana Cornea [1], Ana Cristina Paul[2*]

[1]"Coriolan Drăgulescu" Institute of Chemistry, Romanian Academy, Mihai Viteazu 24 Blv., 300223, Timisoara, Romania
[2] Faculty of Chemical Engineering, Biotechnology and Environmental Protection, Politehnica University of Timisoara, Vasile Parvan 6 Blv., Timisoara, Romania*
[*]e-mail: cristina.paul@upt.ro

Abstract

The concept of biocatalysis has become an essential component of green and sustainable chemistry, offering an efficient alternative to conventional chemical procedures. This is attributed to the high degree of selectivity, rapid reaction rates, and mild operating conditions characteristic of enzymes. However, the industrial application of enzymes is often hindered by their inherent instability when exposed to extreme pH values, elevated temperatures, and organic solvents. In addition, the recovery and reuse of native enzymes from homogeneous solutions often pose significant challenges, frequently resulting in their classification as "single-use" components and consequently increasing the overall process costs. To address these challenges, enzyme immobilization is employed, defined as the association of a biocatalyst with a support material, in order to enhance stability, facilitate separation from reaction mixtures, and enable enzyme reuse [1-6].

The industrial use of lipases immobilized by the sol-gel method has been extensively documented across numerous domains, including the synthesis of flavor esters and biodiesel, as well as the production of high-value chiral pharmaceutical compounds. It is evident that the inherent limitations of free enzymes, such as reduced operational stability and difficulties in recovery, can be overcome through sol-gel immobilization, often enhanced by the use of hydrophobic precursors and the incorporation of various support materials. The sol-gel technique for enzyme immobilization enables the development of economically viable and sustainable biocatalytic processes [7-10].

The sol-gel process is a useful technique that can be employed for the immobilization of various enzymes, particularly lipases, with the aim of enhancing their stability and enabling their reuse. Numerous examples of enzymes stabilized using this technique have been reported in the literature. For example: *Candida antarctica* lipase B (CalB), *Candida Rugosa*, *Pseudomonas cepacia*, *Pseudomonas Stutzeri*, etc. [3,11-14].

The aim of this study was to develop new immobilized biocatalists using **(***Pseudomonas Stutzeri* and *Candida antarctica* lipase B**)** for the enzymatic production in solvent-free system of flavor esters, with a particular focus on pentyl hexanoate and pentyl octanoate. To evaluate the effectiveness of the biocatalyst, gas chromatography (GC) analyses were performed to assess the reaction yield, the biocatalytic efficiency, and the relative total activity.

The best results were obtained using the sol-gel biocatalyst based on *Candida antarctica* lipase B (CalB), achieving yields above 60% for both esters.

References

[1] R.A. Sheldon, S. Van Pelt, Enzyme immobilisation in biocatalysis: why, what and how. Chem Soc Rev. (2013);42(15):6223-35. doi:10.1039/C3CS60075K;
[2] M.S. Robescu, T. Bavaro, A Comprehensive Guide to Enzyme Immobilization: All You Needto Know. Molecules. (2025);30(4):939. doi:10.3390/molecules30040939;

[3] D. Weiser, F. Nagy, G. Bánóczi, M. Oláh, A. Farkas, A. Szilágyi, et al. Immobilization engineering – How to design advanced sol–gel systems for biocatalysis? Green Chem. (2017);19(16):3927-37. doi:10.1039/C7GC00896A;
[4] H.T. Imam, K. Hill, A. Reid, S. Mix, P.C. Marr, A.C. Marr, Supramolecular Ionic Liquid Gels for Enzyme Entrapment. ACS Sustainable Chem Eng. (2023);11(18):6829-37. doi:10.1021/acssuschemeng.3c00517
[5] H.T. Imam, P.C. Marr, A.C. Marr, Enzyme entrapment, biocatalyst immobilization without covalent attachment. Green Chem. (2021);23(14):4980-5005. doi:10.1039/D1GC01852C
[6] R. A. Rahman, &, S. M. Shaarani (Eds.), Enzyme immobilization for bioprocessing, 2022 Capitolul 1, Penerbit UTM.ISBN: 978-983-52-1889-7.
[7] S. Cebrián-García, A.M. Balu, A. García, R. Luque, Sol-Gel Immobilisation of Lipases: Towards Active and Stable Biocatalysts for the Esterification of Valeric Acid. Molecules. (2018);23(9):2283. doi:10.3390/molecules23092283
[8] M.E. Moisă, C.G. Spelmezan, C. Paul, J.H. Bartha-Vári, L.C. Bencze, F.D. Irimie, et al. Tailored sol–gel immobilized lipase preparates for the enzymatic kinetic resolution of heteroaromatic alcohols in batch and continuous flow systems. RSC Adv. (2017);7(83):52977-87. doi:10.1039/C7RA10157K
[9] T.C. Honaiser, A.M.M. Ficanha, R.M. Dallago, D. Oliveira, J.V. Oliveira, N. Paroul, et al. Immobilization of Lipase NS-40116 (Thermomyces lanuginosus) by Sol-Gel Technique Using Polyethyleneglycol as Additive. Industrial Biotechnology. (2019);15(1):35-40. doi:10.1089/ind.2018.0028
[10] J.P. Chen, W.S. Lin. Sol-gel powders and supported sol-gel polymers for immobilization of lipase in ester synthesis. Enzyme and Microbial Technology. (2003);32(7):801-11. doi:10.1016/S0141-0229(03)00052-8
[11] C. Vasilescu, C. Paul, S. Marc, I. Hulka, F. Péter. Development of a Tailored Sol-Gel Immobilized Biocatalyst for Sustainable Synthesis of the Food Aroma Ester n-Amyl Caproate in Continuous Solventless System. Foods. (2022);11(16):2485. doi:10.3390/foods11162485
[12] S.H. Lee, T.T.N. Doan, S.H. Ha, Y.M. Koo. Using ionic liquids to stabilize lipase within sol–gel derived silica. Journal of Molecular Catalysis B: Enzymatic. (2007);45(1-2):57-61. doi:10.1016/j.molcatb.2006.11.008
[13] S. Datta, L.R. Christena, Y.R.S. Rajaram. Enzyme immobilization: an overview on techniques and support materials. 3 Biotech. (2013);3(1):1-9. doi:10.1007/s13205-012-0071-7
[14] M. Dragomirescu, I. Radulov, A. Berbecea, I. Hotea, L. Crista, O. Iordanescu1, et al. Stabilization of enzymes for biotechnological applications. Journal of Pharmaceutical Negative Results. (2022);125-34. doi:10.47750/pnr.2022.13.S09.015

IN SILICO IDENTIFICATION OF NOVEL IKKβ INHIBITORS BASED ON BILIRUBIN-LIKE COMPOUNDS

Lucia Gradinaru, Alina Bora, Luminita Crisan*

"Coriolan Dragulescu" Institute of Chemistry, 24 Mihai Viteazu Ave., 300223 Timisoara, Romania;
e-mail: lumi_crisan@acad-icht.tm.edu.ro

IκB kinase β (IKKβ) plays a key role in the activation of the NF-κB signaling cascade and represents an important molecular target in inflammation-related diseases [1]. Bilirubin has attracted increasing interest beyond its established role as a biomarker of hepatic function, owing to its reported anti-inflammatory and cytoprotective properties [2]. However, its unfavorable aqueous solubility and limited bioavailability restrict its direct therapeutic application [3]. Here, we explored the possibility that bilirubin-like chemical structures could provide suitable starting points for the identification of potential IKKβ inhibitors through a computational drug-design workflow. Pharmacophore-based virtual screening was used to identify structurally compatible compounds, which were subsequently evaluated using predictive models to characterize their pharmacokinetic properties and potential toxicity. The selected structures were further investigated by quantum chemical calculations, providing insight into their electronic characteristics and chemical reactivity. Molecular docking was then employed to examine their interactions within the IKKβ binding site and to prioritize the most promising candidates. Among the investigated structures, one candidate showed a favorable predicted binding mode and a promising docking score, supporting its selection for further computational assessment. Molecular dynamics simulations will be performed in a subsequent step to further assess the stability of the predicted IKKβ-ligand complexes and the maintenance of key protein-ligand interactions during the simulation. These computational findings provide a basis for further investigation, while their biological activity and therapeutic potential remain to be established through subsequent *in vitro* and *in vivo* studies.

Acknowledgements
The authors would like to thank BIOVIA Software Inc. (BIOVIA Discovery Studio Visualizer, v. 19.1.0) for the free academic licenses. This work was partially supported by Program no 1, from the "Coriolan Dragulescu" Institute of Chemistry Timisoara, Romania, and by project "ICT-Interdisciplinary Center for Smart Specialization in Chemical Biology (RO-OPENSCREEN)", MySMIS code: 127952, Contract no. 371/20.07.2020, co-financed by the European Regional Development Fund under the Competitiveness Operational Program 2014–2020.

References
[1] Prescott, J.A.; Cook, S.J. Targeting IKKβ in Cancer: Challenges and Opportunities for the Therapeutic Utilisation of IKKβ Inhibitors. Cells 2018, 7, 115. https://doi.org/10.3390/cells7090115
[2] Kipp ZA, Pauss SN, Martinez GJ, et al (2025) Bilirubin Hepatic and Intestinal Transport and Catabolism: Physiology, Pathophysiology, and Benefits. Antioxidants 14:1326. https://doi.org/10.3390/antiox14111326
[3] Adin CA (2021) Bilirubin as a Therapeutic Molecule: Challenges and Opportunities. Antioxidants 10:1536. https://doi.org/10.3390/antiox10101536

BISMUTH-BASED MATERIALS FOR RECOVERY OF GOLD FROM AQUEOUS MEDIA AND ANTIMICROBIAL STUDIES

Cătălin Ianăși[1], Paula Svera[2], Orsina Verdes[1], Mariana Suba[1], Adina Negrea[3], Petru Negrea[3], Narcis Duteanu[3], Mihaela Ciopec[3], Nicoleta Nemes[4]

1"Coriolan Drăgulescu" Institute of Chemistry (ICT), B-dul. Mihai Viteazu 24, Timişoara, Romania
2 National Institute of Research and Development for Electrochemistry and Condensed Matter (INCEMC), Str. Dr. A. Păunescu Podeanu 144, Timişoara, Romania
3 Faculty of Industrial Chemistry and Environmental Engineering, Politehnica University Timişoara, 2 Victoriei Square, 300006 Timisoara, Romania
4 Research Institute for Renewable Energies-ICER, Politehnica University Timisoara, 138 Gavril Musicescu Street, 300501 Timisoara, Romania
e-mail: cianasic@yahoo.com

Abstract

Bismuth oxide–based materials have attracted considerable attention because of their tunable physicochemical properties, antimicrobial activity, and potential for the recovery of valuable metals from aqueous systems. In this study a prelimary approach for developing multifunctional bismuth-based materials by combining sol–gel-derived bismuth oxide and functionalized with carbonaceous supports. The synthesis conditions, including the type of acidic medium, incorporation of polyvinyl alcohol and graphite, and addition of gold or platinum species, strongly influence the resulting phase composition, crystallite size, surface morphology, thermal stability, and functional performance. Reported materials exhibit nanoscale crystallites, diverse morphologies, and enhanced antimicrobial activity. In parallel, carbon-supported bismuth materials provide increased surface area and favorable adsorption sites for the selective recovery of Au(III) from aqueous solutions. The carbon black/bismuth composite demonstrated an adsorption capacity of ~ 13 mg Au(III) g^{-1}, with optimum performance at low pH and approximately 90.5% recovery efficiency from real solutions. These results shows the versatility of bismuth oxide–carbon and metal-doped bismuth nanocomposites as multifunctional materials for antimicrobial applications and sustainable metal recovery. Further optimization of composition, surface chemistry, regeneration, and selectivity could support their practical use in environmental remediation and resource-recovery technologies.

NOVEL PALLADIUM(II) AND PLATINUM(II) COMPLEXES WITH SCHIFF BASES AND α-DIOXIMES: SYNTHESIS, PHYSICO-CHEMICAL CHARACTERIZATION, AND BIOLOGICAL STUDY

Csaba Várhelyi jr.[1], Roland Szalay[2], János Madarász[3], Melinda Simon-Várhelyi[1], Róbert Tőtős[1], Raluca-Anca Mereu[1], Judit Papp[4], Judith Mihály[5]

[1]Faculty of Chemistry and Chemical Engineering, "Babeş-Bolyai" University, RO-400 028 Cluj-Napoca, Arany János str. 11, Romania
[2]Institute of Chemistry, "Eötvös Loránd" University, H-1117 Budapest, Pázmány Péter str. 1/a, Hungary
[3]Faculty of Chemical Technology and Biotechnology, Budapest University of Technology and Economics, H-1111 Budapest, Műegyetem rkp. 3, Hungary
[4]Faculty of Biology and Geology, "Babeş-Bolyai" University, RO-400 084 Cluj-Napoca, Mihail Kogălniceanu str. 1, Romania
[5]Institute of Materials and Environmental Chemistry, HUN-REN Research Centre for Natural Sciences, H-1117 Budapest, Magyar tudósok körútja 2, Hungary
e-mail: ifj.varhelyi.cs@gmail.com

Abstract
New palladium(II) and platinum(II) complexes were synthesized with Schiff bases and α-dioximes, namely [Pd(butyrophenone)$_2$A(2-aminopyridine)$_2$] (A = hydrazine, phenyl-hydrazine, ethylenediamine, *o*-phenylenediamine, 1,2- and 1,3-propylenediamine) and [Pt(DioxH)$_2$L$_2$], (DioxH$_2$: diethyldioxime, i-butyl-methyl-dioxime; L = 2-aminopyrimidine, t-butylamine, 4-aminopyridine), by the reaction of Schiff bases or α-dioximes with $PdCl_2$ or $PtCl_2$ in suitable solvent. Following a brief literature survey on the classification, evolution, and applications of palladium and platinum complexes, the physicochemical properties of the new compounds were investigated by FTIR, NMR, UV-VIS spectroscopy, powder X-ray diffraction (XRD), mass spectrometry, thermal analysis (TG, DTG, DTA). The antibacterial activity of the complexes was also evaluated against several bacterial strains. Given their promising antibacterial and potential antitumor properties, these compounds represent an interesting class for further biochemical and pharmacological investigation.

Introduction

Transition metals hold significant potential as a core component for anticancer drugs. Palladium complexes are closely related to their platinum analogs, since the chemical and physical properties of palladium and platinum are highly comparable. Like platinum, palladium is incorporated into anticancer drugs in either metallic or ionic form (Pd^{2+} or Pd^{4+}) [1].

Beyond their cytotoxic potential, palladium and platinum complexes also exhibit antiamoebic activity, and in recent years their antimicrobial and antifertility properties have likewise been reported [2].

More recently, transition metal nanoparticles have attracted growing interest in both scientific research and industrial applications, owing to their distinctive optical, electronic, and catalytic properties. Noble metals such as palladium and platinum, in particular, have received considerable attention across diverse fields including sensors, energy conversion, biomedical treatment, and catalysis [3].

In this context, the present paper reports the synthesis and characterization of novel palladium(II) and platinum(II) complexes with Schiff bases and α-dioximes.

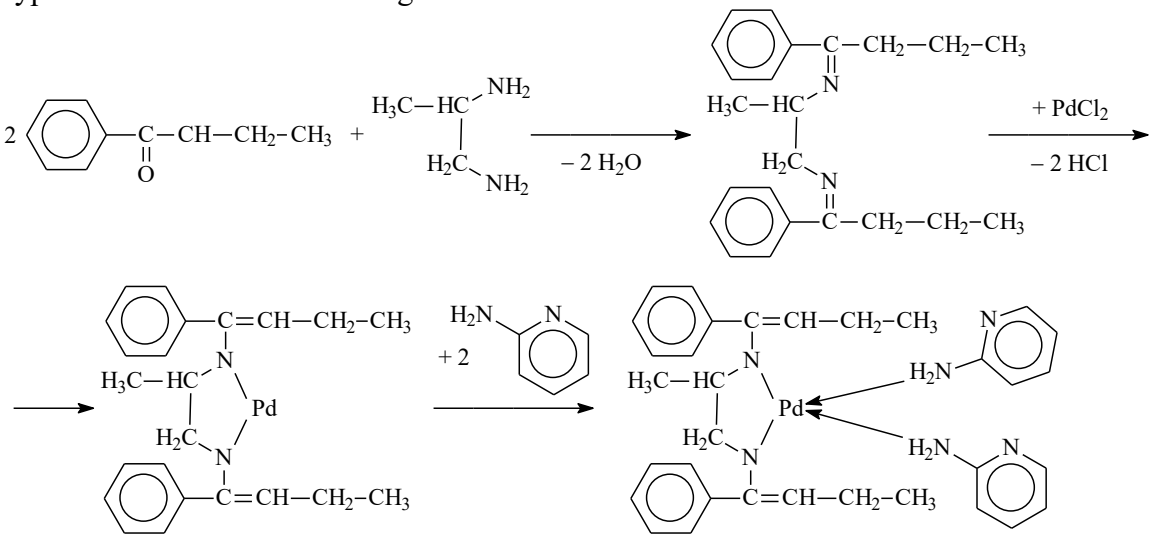
Experimental

Used materials: $PdCl_2$, $PtCl_4$, butyrophenone, i-Bu-Me-Dioxh$_2$, di-Et-Dioxh$_2$, hydrazine, phenylhydrazine, ethylene-diamine (en), 1,2-propylene-diamine (1,2-pn), 1,3-propylene-diamine (1,3-pn), *o*-phenylene-diamine (o-fen), 2-amino-pyridine, 2-amino-pyrimidine, t-butyl-amine, 4-amino-pyridine, MeOH, EtOH, HCOOH.

Methods:

- *Synthesis of [Pd(butyrophenone)$_2$A(L$_2$)] type complexes*

10 mmol *butyrophenone* and 5 mmol diamine (hydrazine, phenylhydrazine, en, 1,2-pn, 1,3-pn or *o*-phenylene-diamine) were dissolved in 10–25 ml EtOH and then refluxed for 1–2 hours. Aqueous solution of $PdCl_2$ (5 mmol, dissolved in HCl) was added to the resulting colored solution. In the last step, 10 mmol 2-amino-pyridine dissolved in 10 ml EtOH was added. The obtained mixture was refluxed in a water bath for 2–3 hours. After cooling the crystalline complexes were filtered off, washed with MeOH–water mixture (1:1), and finally dried on air. A typical reaction is the following:

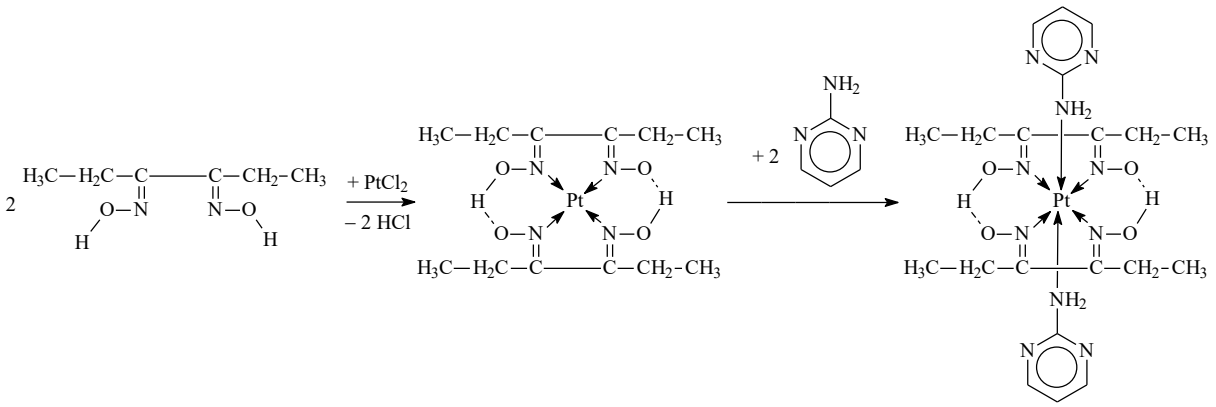


- *Synthesis of [Pt(DioxH)$_2$L$_2$] type complexes*

1 mmol $PtCl_4$ (0.34 g) was reduced with 1 ml formic acid (95 %) and dissolved in 5 ml distilled water prior to use in the complex synthesis:

$$PtCl_4 + HCOOH \rightarrow PtCl_2 + CO_2 + 2\ HCl$$

2 mmol α-dioxime (i-Bu-Me-Dioxh$_2$ or di-Et-Dioxh$_2$) was dissolved in 20 ml EtOH and then added to the aqueous solution of 1 mmol reduced platinum salt ($PtCl_2$). Afterwards 2 mmol amine (2-amino-pyrimidine, t-butyl-amine or 4-amino-pyridine) dissolved in 5 ml EtOH was added. The obtained solution was heated for 2–3 hours on a water bath. After cooling the crystalline complexes were filtered off, then washed with MeOH–water mixture (1:1). A typical reaction as an example is shown below:



Results and discussion

Microscopic characterization and yields of the prepared complexes are presented in Table 1.

Table 1. Microscopic characterization, calculated molar masses and yields of the prepared complexes.

Nr.	Compound	Calc. mol. mass	Yield (%)	Microscopic characterization
1.	[Pd(butyrophenone)$_2$(o-fen)]	472.92	10	Orange, small triangle-based prisms (microcrystals)
2.	[Pd(butyrophenone)$_2$(en)]	424.88	10	Grey, irregular microcrystals
3.	[Pd(butyrophenone)$_2$(1,3-pn)]	438.90	15	Yellow, flat prisms
4.	[Pd(butyrophenone)$_2$(hydrazone)]	396.82	10	Yellowish-brown triangle-based prisms (microcrystals)
5.	[Pd(butyrophenone)$_2$ (Ph-hydrazone)]	473.93	20	Brown, irregular microcrystals (plates)
6.	[Pd(butyrophenone)$_2$(hydrazone) (2-amino-pyridine)$_2$]	585.06	10	Black, small triangle-based prisms
7.	[Pd(butyrophenone)$_2$ (Ph-hydrazone)(2-am.-pyridine)$_2$]	662.16	10	Black, triangle-based prisms (microcrystals)
8.	[Pd(butyrophenone)$_2$(en) (2-amino-pyridine)$_2$]	613.11	25	Reddish-brown, long triangle-based prisms
9.	[Pd(butyrophenone)$_2$(1,2-pn)]	438.90	20	Khaki green, needle form crystals
10.	[Pd(butyrophenone)$_2$(1,2-pn) (2-amino-pyridine)$_2$]	627.14	15	Light brown, small triangle-based prisms (microcrystals)
11.	[Pd(butyrophenone)$_2$(1,3-pn) (2-amino-pyridine)$_2$]	627.14	20	Yellow, long triangle-based prisms
12.	[Pt(Me-i-Bu-DioxH)$_2$ (4-amino-pyridine)$_2$]	697.69	52	Light brown, long triangle-based prisms (needles)
13.	[Pt(di-Et-DioxH)$_2$(t-butyl-amine)$_2$]	627.68	47	Brown, long needle form crystals
14.	[Pt(di-Et-DioxH)$_2$(2-amino-pyrimidine)$_2$]	671.61	48	Reddish-brown, long triangle-based prisms

Infrared spectroscopic study

The mid-IR spectra were recorded with a Bruker Alpha FTIR spectrometer (Platinum single reflection diamond ATR), at room temperature, in the wavenumber range of 4000–400 cm^{-1}, and the far-IR range of 500–50 cm^{-1}, respectively, on a Bio Rad – FTS 60A, PIKE Gladi ATR

spectrometer, with a resolution of 4 cm^{-1}. The samples were measured in solid state (in powder form). The data of the most characteristic IR bands for some selected complexes are presented in Table 2.

The most important bands for the characterization of complexes are $\nu_{C=N}$ (1531–1567 cm^{-1}), ν_{N-O} (1206–1255 cm^{-1}) and ν_{Pt-N} (495–518 cm^{-1}) in case of *[Pt(DioxH)$_2$L$_2$]* type complexes. In the far IR region δ_{N-Pt-N} deformation vibrations appear (339–365 cm^{-1}). In case of Schiff bases, like *[Pd(butyrophenone)$_2$(o-fen)]* the $\nu_{C=N}$ valence band appear at 1497 cm^{-1} and ν_{Pd-N} at 439 cm^{-1}. The δ_{N-Pd-N} deformation vibrations appear at 293 cm^{-1}. The mentioned bands appear with very strong or strong intensities [4].

Table 2. IR data of selected complexes.

Comp. / cm^{-1}	[Pd(butyro-phenone)$_2$(o-fen)]	[Pt(Me-i-Bu-DioxH)$_2$ (4-amino-pyridine)$_2$]	[Pt(di-Et-DioxH)$_2$ (t-butyl-amine)$_2$]	[Pt(di-Et-DioxH)$_2$ (2-am.-pyrimidine)$_2$]
ν_{O-H}	3405 w	3648 w	-	3375 m
ν_{N-H}	3174 m	3186 m	3232 w	3286 m
ν_{C-H}	2915 m	2956 s	2938 m	2938 m
$\nu_{C=C}$	1616 s	1653 s	1738 m	1633 vs
$\nu_{C=N}$	1497 vs	1531 vs	1535 s	1567 vs
δ_{CH2}	1459 s	1463 s	1459 vs	1489 s
δ_{CH3}	1276 vs	1367 s	1377 m	1363 vs
ν_{N-O}	-	1255 vs	1241 vs	1206 vs
ν_{N-OH}	-	1113 s	1107 s	1110 m
τ_{O-H}	1034 m	1040 s	916 vs	1017 s
γ_{C-H}	737 vs	734 vs	713 s	786 vs
ν_{Pd-N}	439 s	-	-	-
ν_{Pt-N}	-	504 s	518 s	495 vs
δ_{N-Pd-N}	293 vs	-	-	-
δ_{N-Pt-N}	-	365 vs	357 vs	339 vs

(Abbreviations: vs = very strong, s = strong, m = medium, w = weak)

Mass spectrometry

Mass spectra of the samples were recorded on an Agilent 1200/6410B Triple Quad LC-MS/MS system using electrospray ionization (ESI). In the spectra we could detect the molecular ions and some fragments from in-source decomposition.

NMR spectroscopic study

The ^{1}H NMR spectra were recorded in DMSO-d_6 in 5 mm tubes at RT on a Bruker DRX 500 spectrometer at 500 MHz, using TMS as internal reference. In the spectra of dioxime complexes the aliphatic protons appear at 0.9–2.8 ppm, in nitrogen containing aromatic rings at 6.7–8.5 ppm, the NH protons appear between 3.2–4.2 ppm and the OH protons appear between 8.1–9.7 ppm.

Thermoanalytical measurements (TG-DTG-DTA)

Thermal measurements were performed with a 951 TG and 910 DSC calorimeter (TA Instruments), in Ar or N_2 at a heating rate of 10 $K \cdot min^{-1}$ (sample mass of 4–10 mg).

The thermal stability of *[Pt(DioxH)$_2$L$_2$]* type complexes is limited within the temperature range of 97–225 °C. The first step of the decomposition mechanism is the loss of the amino (L) groups between 100–320 °C, then the glyoxime units leave between 277 – 616

°C. The end of the process is between 515–626 °C. Subsequently, the decomposition of the glyoxime unit is accompanied by big exothermic peaks. This behavior can be explained with the presence of oxygen in the molecule. The general mechanism for decomposition is as follows:

$$[Pt(DioxH)_2L_2] \rightarrow [Pt(DioxH)_2L] \rightarrow [Pt(DioxH)_2] \rightarrow [Pt(DioxH)] \rightarrow PtO$$

UV–VIS spectroscopy

The electronic spectra for *[Pt(DioxH)$_2$L$_2$]* type complexes were recorded with a Jasco V-670 spectrophotometer in 10% EtOH/water solutions containing the substance in 10^{-4} mol/dm^3 concentration. Using Sörensen buffer solutions the electronic spectra were also recorded as a function of pH, and then the acidity constants were calculated, too. The obtained values were between $2.5 \cdot 10^{-12} – 2.2 \cdot 10^{-11}$, which indicate, that the studied complexes are weak acids.

Powder X-ray diffraction measurements

The crystal structure of the complexes was studied with powder XRD measurements, carried out on a PANalytical X'pert Pro MPD X-ray diffractometer. As being novel compounds their diffractograms cannot be found in the Cambridge database. The dioxime type complexes exhibit partially crystalline form.

Biological study

The antimicrobial effects of complexes were studied on *Staphylococcus aureus* Gram-positive bacterium. The investigations were carried out by Kirby-Bauer disk diffusion method. The complexes were dissolved in DMSO in 2 mmol/l concentration, and 20 µl was applied on sterile paper discs. The diameter of inhibition zones were: [Pt(Me-i-Bu-DioxH)$_2$(4-amino-pyridine)$_2$] – 14.66 mm, [Pt(di-Et-DioxH)$_2$(t-butyl-amine)$_2$] – 14.33 mm, [Pt(di-Et-DioxH)$_2$(2-amino-pyrimidine)$_2$] – 15.4 mm, which indicate a good antibacterial effect.

Conclusion

Fourteen novel palladium(II) and platinum(II) complexes with Schiff bases and α-dioximes were successfully synthesized and characterized by spectroscopic and physicochemical methods, confirming their proposed structures and providing insight into their thermal decomposition pathways and acid-base behavior. The antibacterial screening against *Staphylococcus aureus* revealed promising inhibitory activity for the [Pt(DioxH)$_2$L$_2$]-type complexes supporting their potential as candidates for further biological and pharmacological investigation.

Acknowledgement

The authors wish to express their thankfulness to the "Domus Hungarica Foundation" of Hungary for the several fellowships provided to Csaba Várhelyi jr.

References

[1] R. Czarnomysy, D. Radomska, O.K. Szewczyk, P. Roszczenko, K. Bielawski, International Journal of Molecular Sciences 22 (2021) 8271.
[2] K. Sharma, R. Singh, N. Fahmi, R.V. Singh, Spectrochimica Acta Part A: Molecular and Biomolecular Spectroscopy 75(1) (2010) 422
[3] M. Alaqarbeh, S.F. Adil, T. Ghrear, M. Khan, M. Bouachrine, A. Al-Warthan, Catalysts 13 (2023) 1343.
[4] K. Nakamoto, Infrared and Raman Spectra of Inorganic and Coordination Compounds. Part B: Applications in Coordination, Organometallic and Bioinorganic Chemistry, Wiley J., 38, NY 1997.

BIOPLASTICS. DEFINITION, EU REGULATION, INVESTIGATION METHODS

Mária Mörtl[1], Kingkham Paseutsakoun[2], Pap Klaudia[3], Tamás Varga[3], András Székács[1]

[1]Agro-Environmental Research Centre, Institute of Environmental Sciences, Hungarian University of Agriculture and Life Sciences (MATE), 2100 Gödöllő, Tessedik Sámuel u. 2, Hungary
[2]Doctoral School of Natural Sciences, Institute of Environmental Sciences, Hungarian University of Agriculture and Life Sciences (MATE), 2100 Gödöllő, Tessedik Sámuel u. 2, Hungary
[3]HUN-REN Institute for Nuclear Research (HUN-REN ATOMKI) 4026 Debrecen, Bem tér 18/c, Hungary
e-mail: mortl.maria@uni-mate.hu

Bioplastics are biobased and/or biodegradable materials. These two different properties are not strictly connected to each other, and biosources do not guarantee automatically less harmful effects to the environment. These are typically polyesters, and currently polybutylene adipate terephthalate (PBAT) is the most common biopolymer among the packaging materials. Problems related to the definition and examples of categories will be discussed in detail.
These polymers are usually more expensive compared to the conventional materials and their biocontent depends mainly on the legal regulatory requirements. Biobased plastics used to be required to contain at least 10% of material derived from renewable biosources, but it has lately been set to 20% of carbon derived from recent biomass. Thus, the corresponding regulation in the European Union (EU) [1] is changing. To enforce compliance with the regulations, the biocomponent ratio in bioplastic products, suitable analytical determination methods have to be applied. Regarding these protocols, radiocarbon methods using isotope ratio mass spectrometry analysis are applied, preferred in the EU as well.
According to the corresponding communication in the EU, biodegradation must be regarded as a system property, and the use of biodegradable plastics should be limited [2]. Some polymers can degrade under household circumstances characterized by uncontrolled temperature and generally aerobic conditions, whereas others decompose only under controlled industrial conditions. A severe limitation of the standard analytical method based on the emission of CO_2 monitoring at 58°C is that it does not consider the conversion of polymer carbon into soil organic matter [3]. Identification of the polymers is usually based on vibrational spectra (FT-IR), which may not be sufficient to identify all the components of the polymer, as we have observed for PBAT/PLA blends. As PLA is compostable under industrial conditions, its detection is of high importance. Based on pyrolysis GC-MS spectra, monomers can be identified, but recently solid phase NMR measurements have been also reported. Our recently developed GC-MS method for monitoring the decomposition of PBAT using silylation in sample preparation [4] provided further details about the actual composition of the polymer and its biodegradation. Using this alternative GC-MS method, monomers of PBAT polymer were detected over a year in maturated compost [4].

Acknowledgements
This research was supported by the Research Excellence Program and by the Flagship Research Groups Program of the Hungarian University of Agriculture and Life Sciences (MATE).

References

[1] European Commission (2026) https://environment.ec.europa.eu/topics/plastics/bio-based-biodegradable-and-compostable-plastics_en
[2] COM/2022/682 https://eur-lex.europa.eu/legal-content/EN/TXT/?uri=celex:52022DC0682
[3] M. Cucina, Environ. Sci. Technol. Lett. 13 (2026) 322.
[4] M. Mörtl, M. Damak, M. Gulyás, et al. Polymers 16(24) (2024) 3450.

THE EVOLUTION OF THE ISO 14001 ENVIRONMENTAL MANAGEMENT SYSTEMS

László Berényi

Faculty of Public Governance and International Studies, Ludovika University of Public Service, Budapest, H-1038 Budapest, Üllői út 82., Hungary
e-mail: berenyi.laszlo@uni-nke.hu

Abstract
A common understanding of sustainability concepts and terminology drives successful action. Management system standards have provided this understanding for organizations. In the field of environmental management, ISO 14001 has played a key role for decades in promoting environmental thinking in international trade. The latest edition of the standard was released in 2026. The study reviews and compares standard revisions and how sustainability has come to the fore. A clear shift is demonstrated from a procedural and compliance-oriented environmental management system towards a strategically integrated sustainability management tool. The findings may help managers, engineers, and researchers understand the role of contemporary environmental management systems and their contribution to their work.

Introduction
Growing awareness of global problems in the 1970s encouraged various institutions to take action. The United Nations organized the first environmental conference in 1972 (Stockholm), and later events clearly show how the approach shifted from environmental protection to interpretations of sustainability [1] [2]. The Club of Rome was founded in 1968 and published its first report in 1972. The European Economic Community gradually integrated environmental protection and social issues into the contracts and the regulations (see [3] [4]).
Beyond the grand global initiatives, business needed a more tangible way to implement the principles successfully. The British Standards Institution (BSI) published the first related standard, entitled: BS 7750 – Environmental Management Systems. It later served as the basis for the International Organization for Standardization to build the ISO 14001 standard. The use of standards aligned more with corporate thinking, and the growing role of supply chains in global trade from the 1970s called for a coordination tool [5].
Interestingly, environmental management standards did not offer a breakthrough in management approaches. The debate on the importance of environmental and social problems, as well as selecting the relevant interested parties, including the natural and built environment next to the customers and suppliers, made the practical application difficult. At the same time, a group of experts cut the Gordian knot: limiting the scope of the management system to one stakeholder – no other than the customer –, achieving its satisfaction was a tangible, easily measurable, understandable goal for the organizations. That is why the first quality management standards were published much earlier (BS 5750 in 1979 and ISO 9001 in 1987).
Since ISO standards are designed for use across a broad range – recently any type and size of organizations –, the requirements included must fit all of them. Of course, larger organizations with extensive experience and significant resources can be well ahead of others; meeting the requirements may be a serious challenge for others.
The revisions to the standard mirror changes in management approaches. The growing relevance of strategic management, supply chain management, and the development of environmental thinking must have been considered to maintain the applicability of the standards. Although the goal of the standard is to support organizational operations, in a

particular sense, it serves as an indicator of prevailing management expectations. The study aims to review and evaluate these changes.

Experimental

A comparative content analysis was conducted to review the changes and development of the ISO 14001 standard between 1996 and 2026. The four editions are as follows:

- ISO 14001:1996 – Environmental management systems — Specification with guidance for use
- ISO 14001:2004 – Requirements with guidance for use
- ISO 14001:2015 – Requirements with guidance for use
- ISO 14001:2026 – Requirements with guidance for use

The comparison criteria include the goal of the standard, the scope, focus points, new concepts, structural issues and fit with other management system standards.

The main limitation of the study is that, although ISO 14001 is the core environmental management system standard, environmental management is much broader. Several additional standards support the organizations towards sustainability. Similarly, EMAS regulations [4] [6] of the European Union are out of scope.

Results and discussion

The first publication of the first environmental management standard (Figure 1) was in 1992 (BS 7750). It marked the end of an active period of defining principles, action programs, and establishing international collaborations. Translating these ideas into requirements was pioneering, but changes in the 1980s made the situation chaotic. The disintegration of the Soviet Union, the rise of Eastern economies, and the cautious progress of European integration slowed ISO-level publication. Moreover, the ISO 9001 standard on quality issues proved sufficient for a long time.

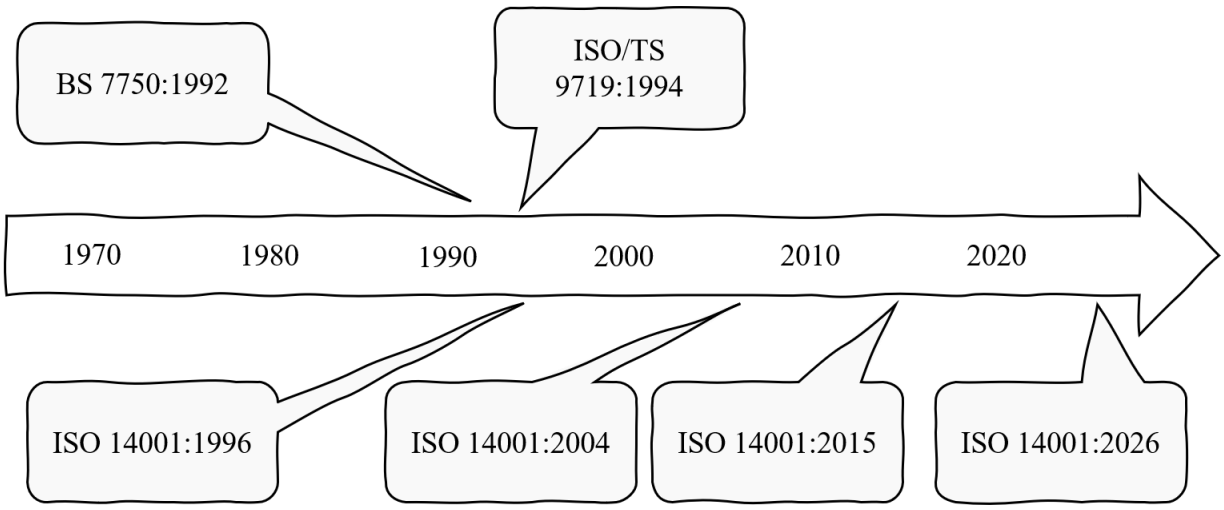


Figure 1. ISO 14001 editions

ISO 14001:1996 aimed to establish a framework for Environmental Management System (EMS). PDCA [7] was selected as background logic for continuous improvement, in part because it worked well in quality assurance. Similarly, the standard emphasized procedure orientation and documentation systems. Later versions have added several aspects; Table 1 summarizes the main changes and the continuous expansion of sustainability aspects in the regulations.

ISO 14001:2004 was the second edition of the EMS standard, following the third edition of its "brother," ISO 9001. The latter standard brought about a major change by highlighting process orientation and pointing out that, regardless of the size and activity of the organization, the key to success is identifying, planning, and performing the related processes. This concept was also presented in ISO 14001, enabling better integration of management systems. Common concepts and documentation systems supported this. Environmental planning and monitoring required separate processes in the standards, which confirmed that planning environmental actions had to be integrated into daily operations. Objectives, targets, and programs had to be highly compliant.

	ISO 14001:1996	**ISO 14001:2004**	**ISO 14001:2015**	**ISO 14001:2026**
Focus	Laying the basis for EMS	Refined requirements	Building strategic EMS, introducing risk-based approach	Refined and actualized requirements
Role of leadership	Limited to processes	Extended to organizational level coordination	Strong stakeholder orientation	Environmental and social responsibility
Risk management	Missing	Suggested by supplementary standards but not included in requirements	Risks and opportunities highlighted	New guidance on risks and opportunities
Stakeholder approach	Hidden	Limited	Included	Strengthened
Climate change issues	Missing	Missing	Not included in the requirements	Emphasized
Documentation	Procedure-based	Highlighted documentation system	Introduction of documented information	Refinements made
Integration with other standards	Difficult to feasible	Available	Focus point	Focus point

Table 1. Comparison of ISO 14001 standard editions (own edition)

ISO 14001:2015 was published together with ISO 9001:2015. These standards introduced the High Level Structure (HLS) as the backbone of future ISO management system standards (Figure 2).



Figure 2. Clauses in High Level Structure of ISO management system standards (own edition)

Beyond the main standard points and common basic terminology, the management approach was made more uniform than before. In terms of content, the new approach applied the main steps of strategic planning. Up to this edition, environmental management system processes were in parallel with organizational processes. The new concept required organizations to integrate them. Stakeholder orientation has become important; it highlights the organization's goals and context, allowing a customized system.

The responsibility of management is enhanced. Previously, a designated responsible person was key to coordination, but this shifted to defining responsibility across all organizational members.

Preventive actions were removed from the standard, and a risk-based approach was prioritized. Although the standard and its Annex point out that the approach focuses not only on risks (as effects of uncertainty) but also on opportunities (as potential beneficial effects) that are important and considerable, practice usually focuses on identifying, managing, or eliminating risks.

ISO 14001:2026 did not bring about as much progress as the previous one; the case is similar to the development between the first two editions. The 2015 revision made EMS a strategic tool of organizations, while the 2026 revision refined it. Moreover, climate change, biodiversity, and application opportunities across the entire supply chain have gained greater relevance.

Certification to the ISO 14001 standard supports uniform, global application of requirements and, through this, consistent interpretation of sustainability concepts.

Conclusion

The evolution of the ISO 14001 standard shows how the approach to environmental management has developed over the years. Management system standards are often disliked because they cause extra administration and stress from external audits, but they offer a common language for coordination among organizations. Changes in requirements aim to expand customization, but they seem to be softened. That is the cost of the opportunity; seeking

the best practices replaces the command-like requirements. Flexibility and integration opportunities with other management system standards can strengthen cooperation. The study highlighted quality management systems, but more importantly, energy management (ISO 50001) and occupational health and safety management systems (ISO 45001) are close to sustainability.

In accordance with the purpose of the conference, the implication of the study is indirect. Several product and process standards, along with good manufacturing and laboratory practices, help engineers focus on specific tasks. Meanwhile, the organization provides the framework and resources for the work; therefore, its controlled and transparent operation on sustainability issues, as emphasized in ISO 14001:2026, plays an essential role. The high integrability with other management system standards through the HLS structure can increase the acceptance among managers, engineers, and researchers.

References

[1] L. Elliott, The Global Politics of the Environment, Palgrave Macmillan, Basingstoke, 2004, pp. 296.
[2] P.S. Chasek, D.L. Downie, J.W. Brown, Global Environmental Politics (8th ed.), Routledge, New York, 2020, pp. 342.
[3] S. Kerekes, A környezetgazdaságtan alapjai, Aula Kiadó, Budapest, 2007, pp. 238
[4] L Berényi, A környezetmenedzsment feladatai és lehetőségei, Publio, Budapest, 2014, pp. 296.
[5] M. Christopher, Logistics & Supply Chain Management (4th ed.), Financial Times/Prentice Hall, 2011, pp. 276.
[6] European Parliament and Council. (2009). Regulation (EC) No 1221/2009 on the voluntary participation by organisations in a Community Eco-Management and Audit Scheme (EMAS). Official Journal of the European Union, L342, 1-45.
[7] W.E. Deming, Out of the Crisis, MIT Press, Cambridge, 2000, pp. 524.

SURFACTANT-ENGINEERED LIPOSOMES FOR LAMOTRIGINE DELIVERY: COMPARATIVE FORMULATION, PHYSICOCHEMICAL CHARACTERISATION, AND RELEASE KINETICS

Zita Farkaš Agatić, Vesna Tepavčević, Ana Pilipović, Mladena Lalić-Popović, Nemanja Todorović, Mihajlo Milošević, Ana Filipović, Mihalj Poša

University of Novi Sad, Medical Faculty, Department of Pharmacy, Novi Sad, Serbia
Corresponding author e-mail: zita.farkas@mf.uns.ac.rs

Abstract

Lamotrigine (LTG) is a poorly water-soluble antiseizure drug for which lipid-based carriers can improve formulation performance. This study comparatively evaluated LTG-loaded liposomes engineered with four surfactant systems: sodium cholate/Tween 80 (SCT), Poloxamer 188/Tween 80 (P188T), Poloxamer 407/Tween 80 (P407T), and Poloxamer 407/Brij 58 (P407B). Thirty-six egg-lecithin formulations were prepared by systematically varying the lecithin-to-cholesterol ratio and surfactant level; 24 selected compositions were additionally reproduced using soybean lecithin. Particle-size distribution, experimentally recovered entrapment efficiency (EE), Franz-cell release, and kinetic model fitting were assessed. The formulations differed markedly in size distribution, EE, and release behaviour. P407T02 and P407T03 produced the smallest particle populations, whereas P407T01 showed the highest EE in the complete dataset (85.99%). Release profiles were composition dependent and could not be described by a single universal kinetic model. The data show that LTG liposome performance is governed by the combined effects of surfactant system, cholesterol content, and lecithin source rather than by any isolated component.
Keywords: lamotrigine; liposomes; surfactants; entrapment efficiency; Franz diffusion cells; release kinetics

Introduction

Lamotrigine is a second-generation antiseizure drug used in epilepsy therapy, but its poor aqueous solubility and pH-dependent dissolution make it a formulation challenge [1,2]. Liposomes are attractive for LTG delivery because their phospholipid bilayer can accommodate poorly water-soluble molecules while allowing aqueous dispersion. However, the membrane of a liposome is a multicomponent physicochemical system: phospholipid source, cholesterol content, and incorporated surfactants can alter bilayer packing, fluidity, permeability, vesicle size, drug retention, and release [3, 4]. The present work was designed to compare chemically distinct surfactant-stabilized LTG liposomes and to identify composition-structure-performance relationships across a broad formulation space.

Materials and methods

All formulations contained LTG (50 mg), lecithin (250 mg), glycerol (1% v/v), cholesterol according to the selected lecithin-to-cholesterol ratio (6:1, 4:1, or 3:1), and isotonic phosphate buffer pH 5.8 to 10 mL. Four surfactant systems were tested: SCT, P188T, P407T, and P407B. In each egg-lecithin series, nine compositions were prepared by combining three surfactant levels with three lecithin-to-cholesterol ratios. Selected compositions were repeated with soybean lecithin, with the lecithin source as the only intended compositional change (Figure 1).

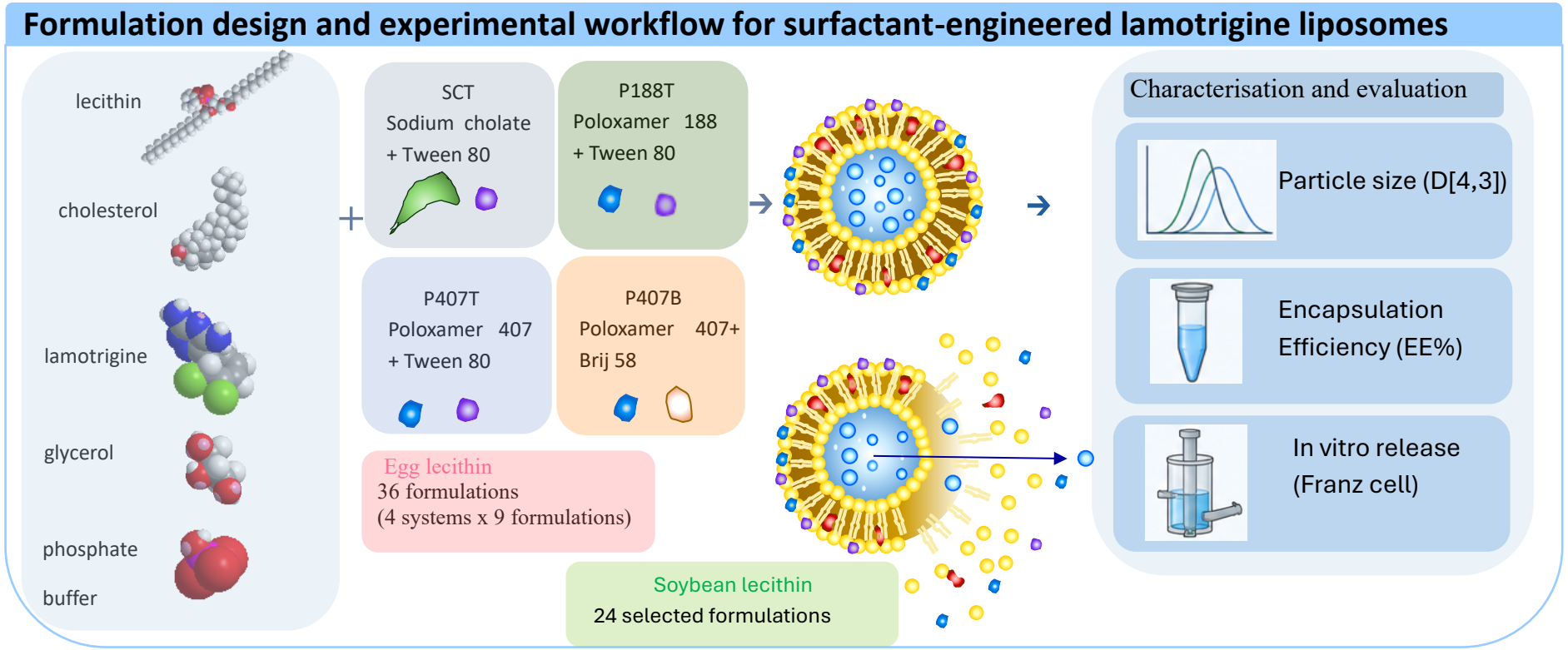


Figure 1. Formulation design and experimental workflow for surfactant-engineered lamotrigine liposomes

Liposomes were prepared by a modified thin-film dehydration-rehydration method [2]. The lipid phase was formed from LTG, lecithin, and cholesterol in ethanol, evaporated at approximately 40 °C, dried, and rehydrated with the surfactant-containing aqueous phase. Particle-size distributions were measured by laser diffraction. Entrapment efficiency was calculated from the experimentally recovered total LTG after methanol disruption and free LTG in the aqueous supernatant. In vitro release was investigated in 3D-printed Franz diffusion cells at 37 °C using a cellulose membrane and phosphate buffer as receptor medium. Corrected cumulative release was analysed by zero-order, first-order, Higuchi, Weibull, and Korsmeyer-Peppas models.

Results and discussion

Particle-size analysis showed that surfactant identity alone did not predict dispersion behaviour. The P407/Tween 80 series generated the smallest measured particle populations, especially P407T02 and P407T03, both with D[4,3] values close to 0.20 µm and narrow d(0.1)-d(0.9) intervals. In contrast, several P407/Brij 58 formulations showed broader distributions and greater contributions from larger particles. Sodium cholate/Tween 80 generally produced submicron-to-micrometer distributions, while selected P188/Tween 80 formulations showed intermediate submicron populations. These findings indicate that the accompanying surfactant and quantitative composition strongly influence particle-size behaviour. At the series level, the descriptive mean D[4,3] values further illustrate differences among the four surfactant systems and between lecithin sources (Figure 2A).

Table 1. Formulation-dependent performance indicators selected from the comparative dataset.

Endpoint	Leading formulation(s)	Key value(s)	Interpretation	Selection implication
Smallest particle populations	P407T02, P407T03	D[4,3] ≈ 0.20 µm	P407/Tween 80 created the most pronounced particle-size reduction.	Best candidates when particle size is prioritised.
Highest EE	P407T01	85.99%	Highest experimentally determined LTG association in the complete dataset.	Strong candidate for drug-loading capacity, but not sufficient alone.
High EE within P188T	P188T03	82.23%	P188T also enabled high LTG entrapment in selected compositions.	Useful comparator to P407T systems.
High EE within SCT	SCT08	79.22%	Bile-salt/Tween system can provide high entrapment in selected compositions.	Shows composition-specific benefit of sodium cholate.
High EE within P407B	P407B07	75.74%	P407/Brij 58 performance was variable but included high-EE formulations.	Requires balancing with broader particle distributions.

Entrapment efficiency ranged from 18.61 to 85.99% for egg-lecithin formulations and from 22.03 to 70.84% for soybean-lecithin formulations. The clearest lecithin-source effect was observed in the P407T series, where soybean substitution decreased EE for every directly comparable formulation. In contrast, SCT, P188T, and P407B showed mixed egg-to-soy responses. This confirms that lecithin source cannot be optimised independently of the remaining surfactant/cholesterol environment. The descriptive mean EE values at the series level further illustrate the formulation-dependent effect of lecithin source across the four surfactant systems (Figure 2B).

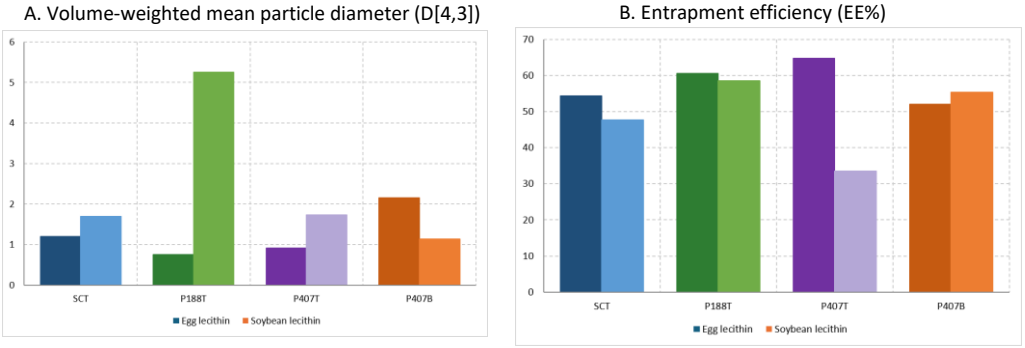


Figure 2. Physicochemical characteristics of lamotrigine liposomes

Release profiles were strongly formulation dependent. No single model adequately described all formulations. Representative egg-lecithin systems included Higuchi-described profiles such as SCT06 and P188T04, zero-order profiles such as SCT08, P407T06, and P407T09, and Korsmeyer-Peppas-described profiles such as P188T09 and P407B05. Several soybean-lecithin reformulations showed irregular profiles with no adequate fit to the tested models. Thus, kinetic model assignment should be treated as a comparative mathematical descriptor rather than definitive proof of a unique molecular mechanism (Figure 3) [5,6].

Table 2. Representative kinetic behaviour of selected formulations.

Formulation	Lecithin	Selected model	Representative parameter(s)	Relevance
SCT06	Egg	Higuchi	k_H = 39.66; R^2 = 0.989	Well-defined square-root-of-time release region.
SCT08	Egg	Zero-order	R^2 = 0.981	Approximately constant receptor-phase LTG appearance.
P188T04	Egg	Higuchi	k_H = 46.51; R^2 = 0.972	Good Higuchi fit across 15-180 min.
P188T09	Egg	Korsmeyer-Peppas	R^2 = 0.984	Strong early-stage release description.
P407T06	Egg	Zero-order	R^2 = 0.985	Sustained, nearly linear cumulative release profile.
P407B05	Egg	Korsmeyer-Peppas	R^2 = 0.999	Excellent empirical fit to initial release behaviour.

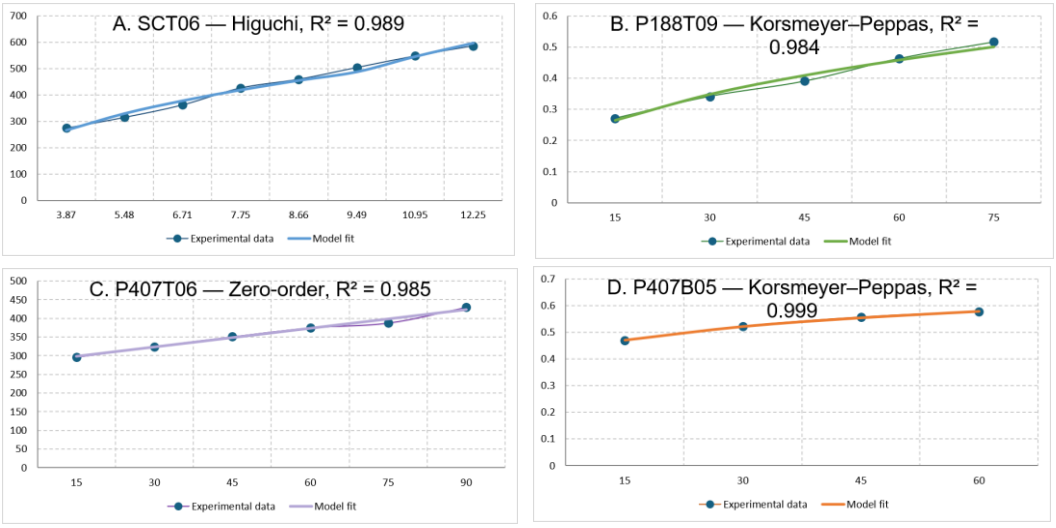


Figure 3. In vitro release profiles and kinetic modelling of representative lamotrigine liposomes (egg lecithin).

Conclusion

Surfactant-engineered LTG liposomes showed pronounced composition-dependent behaviour. P407T02 and P407T03 were most favourable from the particle-size perspective, while P407T01 gave the highest EE. However, high EE, small particle size, and controlled release did not coincide in a single universal formulation. The most defensible formulation selection therefore requires integrated assessment of particle-size distribution, distribution breadth, entrapment efficiency, release magnitude, and kinetic-model adequacy. The results support further optimisation of selected P407T and P188T formulations, while retaining SCT and P407B compositions as mechanistically informative comparators.

Acknowledgements

This research was carried out with support from the Provincial Secretariat for Higher Education and Scientific Research of the Autonomous Province of Vojvodina, Republic of Serbia, within the projects “Development of Innovative Pharmaceutical-Technological Preparations for the Pediatric Population in the Republic of Serbia” (“Razvoj inovativnih farmaceutsko-tehnoloških preparata za pedijatrijsku populaciju u Republici Srbiji”), Project No. 003817825 2025 09418 003 000 000 001, and “Integration of Digitalization and 3D Printing with Artificial Intelligence Support in the Development of Solid and Liquid Pharmaceutical Dosage Forms”, Project No. 003876072 2025 09418 003 000 000 001 04 004.

References

[1] Alam, T., Pandit, J., Vohora, D., Aqil, M., Ali, A., & Sultana, Y. Expert Opinion on Drug Delivery, 2015, 12, 181-194.
[2] Praveen, A., Aqil, M., Imam, S. S., Ahad, A., Moolakkadath, T., & Ahmad, F. J. Colloids and Surfaces B: Biointerfaces, 2019, 174, 553-562.
[3] Memoli, A., Annesini, M. C., & Petralito, S. International Journal of Pharmaceutics, 1999, 184, 227-235.
[4] Bollenbach, L., Buske, J., Mäder, K., & Garidel, P. International Journal of Pharmaceutics, 2022, 620, 121706.
[5] Costa, P., & Sousa Lobo, J. M. European Journal of Pharmaceutical Sciences, 2001, 13, 123-133.
[6] Higuchi, T. Journal of Pharmaceutical Sciences, 1963, 52, 1145-1149.

THE EFFECT OF DIFFERENT ALGAE SPECIES AND THEIR ETHANOL EXTRACTS ON TOMATO (*SOLANUM LYCOPERSICUM* L.) SEED GERMINATION

Đorđe Vojnović[1], Jelena Pavličević[2], Bojana Ikonić[2], Tamara Erceg[2], Halis Can Mörel[3], Davut Laçin[4], Emine Okudan[5], Ayşe Zehra Aroğuz[3], Vesna Teofilović[2]

[1]University of Novi Sad, Faculty of Agriculture, Trg Dositeja Obradovića 8, 21102 Novi Sad, Serbia
[2]University of Novi Sad, Faculty of Technology, Bul. Cara Lazara 1, 21000 Novi Sad, Serbia
[3] Faculty of Pharmacy, Biruni University, Merkezefendi, 75. Sokak No: 1-13 (M.G), 34015 Zeytinburnu/Istanbul, TÜRKİYE
[4] Department of Geology Engineering, Istanbul University-Cerrahpaşa, Avcılar Yerleşkesi, Mühendislik Fakültesi, J Blok, 34320 Avcılar/ Istanbul, TÜRKİYE
[5] Akdeniz University, Faculty of Fisheries, Department of Basic Aquatic Science, Section of Marine Biology, Dumlupınar Bulvarı, 07058 Konyaaltı/Antalya, TÜRKİYE
**Corresponding author's e-mail address:* vesnateofilovic@uns.ac.rs

Seaweed-based biostimulants are increasingly used as sustainable alternatives to synthetic fertilizers and conventional plant growth products. In this work, the influence of different macroalgae species (*Liagora viscida, Sargassum vulgare*, and *Ulva rigida*), as well as the effect of ethanol extracts from *Ulva rigida* and *Sargassum vulgare*, on the germination properties and hypocotyl length of tomato seeds (*Solanum lycopersicum* L.) were examined. The obtained results show that different macroalgae species possess biostimulatory potential during the early stages of tomato seed development, which depends strongly on the algae's chemical composition. Regarding germination energy, the highest values were achieved with the application of raw *Ulva rigida* (76.33%), which was slightly higher compared to the control treatment (74.67%). These results indicate that *Ulva rigida* can positively influence the initial metabolic processes preceding seed emergence. Based on total germination results, the highest germination percentage was achieved with the *Liagora viscida* treatment (78.00%), followed by *Ulva rigida* (77.67%), while the control stood at 76.33%. The most pronounced differences among the tested algae were observed in hypocotyl development, where the maximum hypocotyl length was recorded with the *Ulva rigida* treatment (6.27 mm). Conversely, ethanol extracts of *Ulva rigida* and *Sargassum vulgare* showed a pronounced inhibitory effect across all examined parameters. Germination energy was reduced to 56.00% with the *Ulva rigida* extract and to 54.33% with the *Sargassum vulgare* extract, representing a decrease of approximately 25–27% compared to the control. This negative effect was even more pronounced in hypocotyl development, yielding lengths of 3.53 mm (*Ulva rigida* extract) and 4.17 mm (*Sargassum vulgare* extract). The results indicate that ethanol extraction led to the isolation of compounds that, at the applied concentration, exert a phytotoxic effect, or that essential hydrophilic bioactive components were lost during the extraction process. Overall, raw biomass of *Ulva rigida* and *Liagora viscida* shows strong potential for use as sustainable biostimulants, whereas extraction methods and concentrations must be carefully optimized to avoid phytotoxicity.

Keywords: Marine algae fertilizers, bioactive substances, microbeads, biopolymers, germination energy, germination, hypocotyl length

Acknowledgement
This research was funded by the Bilateral Scientific cooperation between The Ministry of Science, Technological Development and Innovation of the Republic of Serbia (NITRA) (Nr. 026 02 11) and Scientific and Technological Research Council of Türkiye (TUBITAK) (Nr. 123N938), as well as by programs of Ministry of Science, Technological Development, and Innovation, Republic of Serbia No. 451-03-33/2026-03/200134, 451-03-34/2026-03/200134, and 451-03-34/2026-03/200117

CHIRAL HPLC SEPARATION OF PHARMACEUTICALLY RELEVANT COMPOUNDS: RETENTION, SELECTIVITY, AND STRUCTURAL ASPECTS

Gábor Németi*, Antal Péter, István Ilisz

Institute of Pharmaceutical Analysis, University of Szeged, H-6720 Szeged, Somogyi u. 4, Hungary
e-mail: nemeti.gabor@szte.hu

Numerous chiral compounds are present in living organisms, and their enantiomers may exhibit distinct biological and pharmacological effects. Consequently, the investigation of chiral active pharmaceutical ingredients, the preparation of enantiomerically pure compounds, and the enantioselective separation of racemic mixtures are of considerable importance. In high-performance liquid chromatography, chiral stationary phases are widely employed for this purpose, with macrocyclic antibiotics- and cinchona alkaloid-based chiral selectors being among the most extensively used. When utilizing reversed-phase, polar-organic, and polar-ionic chromatographic modes, employing "greener" solvents can provide effective alternatives. Given the biological and pharmaceutical relevance of the investigated fluorinated tryptophan derivative chiral compounds, the efficient separation and characterization of their enantiomers represent important steps in drug development. In this work, the enantioseparation of the investigated compounds was examined on macrocyclic antibiotics- and cinchona alkaloid-based chiral stationary phases. The effects of mobile-phase composition, the nature of the acid and base additives, and temperature on the chromatographic separation were evaluated. The elution order of the enantiomers was determined in all cases. Furthermore, the relationships between structural features, retention properties, and thermodynamic parameters were investigated.

Acknowledgments
This work was supported by Project No. TKP2021-EGA-32, implemented with funding from the National Research, Development and Innovation Fund of Hungary under the TKP2021-EGA funding scheme of the Ministry of Innovation and Technology.

XENOBIOTICS IN FOCUS

Linda Szilasi[1,2], István Ilisz[2], Roland Weiczner[2], Róbert Berkecz[1,2]

[1]Institute of Pharmaceutical Analysis, Faculty of Pharmacy, University of Szeged Somogyi utca 4, 6720, Szeged, Hungary
[2]Department of Forensic Medicine, Albert Szent-Györgyi Health Centre, Kossuth Lajos sgt. 40, 6724, Szeged, Hungary
peczelinda@gmail.com

Abstract

Wastewater-based epidemiology provides a valuable tool for assessing population-level exposure to pharmaceuticals and illicit drugs through the analysis of xenobiotics in wastewater. In this presentation, an analytical method was developed for the sensitive determination of more than 70 xenobiotic compounds using liquid chromatography–tandem mass spectrometry (LC–MS/MS).

The work focused on sample preparation, optimisation of one-dimensional reversed-phase separation, and the ongoing development of a two-dimensional hydrophilic interaction liquid chromatography–reversed-phase (HILIC–RP) approach. Wastewater samples underwent solid-phase extraction, followed by evaporation under a stream of nitrogen and reconstitution in 0.1% formic acid in a 70:30 (v/v) water–methanol mixture.

Compound identification was based on retention times, peak-area ratios, and MS/MS spectra. Reversed-phase separation was optimised using a C18 column, while several HILIC columns were evaluated for use in the first chromatographic dimension. The developed approach provides a basis for the subsequent online coupling of the two chromatographic dimensions and for the analysis of complex wastewater samples.

Introduction

Wastewater-based epidemiology has emerged as a complementary approach for monitoring population-level patterns of substance use. By analysing human excretion products and other xenobiotic residues in wastewater, it can provide near real-time and anonymous information on the occurrence of pharmaceuticals, illicit drugs, and their metabolites within a community.

The analysis of wastewater is analytically challenging because of the complexity of the matrix, the wide range of physicochemical properties of target compounds, and their typically low concentrations. Efficient sample preparation and highly selective chromatographic separation are therefore essential for reliable determination. The use of complementary separation mechanisms, such as hydrophilic interaction liquid chromatography and reversed-phase chromatography, may broaden analyte coverage and improve the separation of chemically diverse xenobiotics. These considerations provide the basis for the development of multidimensional chromatographic approaches for comprehensive wastewater analysis.

Experimental

Wastewater samples were centrifuged for 10 min. A 45 mL aliquot of the supernatant was processed by solid-phase extraction. After washing, extracts were evaporated under nitrogen and reconstituted in 200 µL of 0,1% formic acid in 70:30 (v/v) water–methanol. We performed analyses on a Shimadzu Nexera X2 UHPLC coupled to a Thermo Scientific TSQ Fortis triple-quadrupole mass spectrometer operated in positive ESI and MRM modes. For RP-LC, 1%

formic acid in water and acetonitrile were used as eluents; HILIC separations were evaluated using 5 mM ammonium acetate in water and acetonitrile.

Results and discussion

An MS/MS method suitable for the identification of more than 70 illicit drugs and benzodiazepines was successfully established. The optimised reversed-phase separation was performed at a flow rate of 0.4 mL min^{-1}, with a 7.5 µL injection volume and a column temperature of 50 °C, resulting in a total run time of 15 min.

Several HILIC columns were evaluated, showing clear differences in analyte retention and internal-standard behaviour. The ACQUITY UPLC BEH Amide columns provided only limited retention for several target compounds, whereas the other stationary phases exhibited distinct retention characteristics. These results indicate that further optimisation of the HILIC separation is necessary before online coupling with the reversed-phase dimension.

Conclusion

A sample-preparation procedure and an LC–MS/MS method were successfully established for the analysis of a broad range of xenobiotics in wastewater. The reversed-phase separation was optimised, while HILIC column selection and development of the first chromatographic dimension are still in progress. The next step will be the online coupling of the HILIC and reversed-phase dimensions to enable a more comprehensive analysis of complex wastewater samples.

Acknowledgement

This work was supported by the National Research, Development and Innovation Office (NKFIH) through the National Laboratory of Translational Neuroscience (NLTN) projects Neurodevelopmental Disorders and Adult Nervous System Disorders (RRF-2.3.1-21-2022-00011). Project No. TKP2021-EGA-32 was implemented with the support of the Ministry of Innovation and Technology of Hungary from the National Research, Development and Innovation Fund under the TKP2021-EGA funding scheme.

COMPARISON OF ADVANCED OXIDATION PROCESSES FOR THE TRANSFORMATION OF N-METIL-2-PYRROLIDON IN WATER

Bence Veres, Marcell Matetits, Bora Buchholcz, Judit Waldhauser, Tünde Alapi

Department of Molecular and Analytical Chemistry, University of Szeged, H-6720 Szeged, Dóm square 7, Hungary
e-mail: veres.bence@chem.u-szeged.hu

N-methyl-2-pyrrolidone (NMP) is an organic solvent widely used in industrial processes such as petrochemicals, pharmacology, surface treatment or cleaning, and lithium battery production; its annual production has been growing recently. However, NMP poses serious ecological and health risks; the EU classifies it as a teratogenic agent, and in Hungary the emission limit has been lowered to 2 mg/m^3 [1]. Meanwhile, environmental protection authorities recommend a limit as low as 300 µg/l for drinking water. Therefore, efficiently removing NMP from water is an urgent task. Advanced oxidation processes (AOPs) are viable water treatment methods that rely on radical generation to transform persistent or toxic pollutants into less harmful ones. Many of these methods can also be scaled up for industrial use.

UV/PDS, UV/H_2O_2, UV/Fenton, ozonation, UV/O_3, and peroxone (O_3/H_2O_2) processes were tested for the transformation of NMP and its toxic product [2], N-methyl succinimide (MSI). The effects of oxidant concentration and pH were investigated. Measurements were conducted in a synthetic matrix containing inorganic ions (NO_3^-, Cl^-, and HCO_3^-) to assess the matrix effect on efficiency.

In the UV/H_2O_2 and UV/PDS processes, using 100 ppm oxidant, NMP was transformed in 10 minutes, and the emerging MSI in ~60 minutes. With optimal UV/H_2O_2 parameters, around 60% of the initial TOC was removed, while the matrix reduced this to around 40%. Increasing pH (3 to 11) did not affect the NMP transformation rate but slowed MSI transformation. The Fenton process (1:5 Fe(II):H_2O_2 molar ratio) significantly increased NMP and MSI transformation, but the matrix considerably reduced efficiency. Ozonation and ozone-based processes were also tested, as they are among the most often used AOPs. Ozonation was less effective than UV-based AOPs. UV/O_3, on the other hand, proved to be superior, especially for MSI transformation and TOC decrease. Moreover, inorganic ions had a less pronounced impact on the efficiency in the case of ozone-based methods.

Operating UV light sources and generating ozone are both energy-intensive processes, however. We evaluated the methods based on energy efficiency and found UV/H_2O_2/Fe(II) to be the most energy-efficient process for NMP removal.

Acknowledgements

Bence Veres is grateful for the support by the EKÖP-26-4 – SZTE-536 University Research Scholarship Program of the Ministry for Culture and Innovation from the sources of the National Research, Development and Innovation Fund.

References

[1] https://eur-lex.europa.eu/legal-content/HU/ALL/?uri=celex:32008R1272 (last access: 2026.06.15.)

[2] Á. Tögyesi, C. Goncalves, E. Benes, A. Simon, V. K. Sharma, Journal of Chromatography A 1766 (2026) 466599

INVESTIGATION OF LUMINESCENT DNA-SILVER NANOCLUSTERS FOR SENSING AND BIOIMAGING APPLICATIONS

Bálint Hajdu[1,2], Annamária Tóth[2], Simon Holm Jacobsen Eiby[3], Pratik Shah[4], Hari Chandana Yadavalli[5], Seong Wook Yang[5], Morten Jannik Bjerrum[1], Lars Hemmingsen[1], Peter Waaben Thulstrup[1]*

[1]Department of Chemistry, University of Copenhagen, Copenhagen, Denmark
[2]Department of Molecular and Analytical Chemistry, University of Szeged, Szeged, Hungary
[3]Globe Institute, University of Copenhagen, Copenhagen, Denmark
[4]Department of Science and Environment, Roskilde University, Roskilde, Denmark
[5]Department of Systems Biology, Institute of Life Science and Biotechnology, Yonsei University, Seoul, Korea
e-mail: balinth11@chem.u-szeged.hu; baha@chem.ku.dk

Bionanotechnology is a prominent research area, with numerous possible applications (e.g. catalysis, molecular machines, nanofabrication, nanoelectronics, drug delivery, cancer treatment, nanophotonics, sensing and bioimaging)[1,2]. The use of DNA and RNA is especially advantageous as it allows the design of monodisperse and biocompatible biomaterials in the nano-size range. However, nanoconstructs consisting only from oligonucleotides with classical Watson-Crick base pairs often lack sufficient stability. A solution to this may be the design of metal-containing nanoconstructs, where metal ions/metal nanoclusters can increase structural stabilization and protection against nucleases *in vivo*. Our research group demonstrated earlier, that C-loop hairpin structured oligonucleotides can form luminescent clusters with Ag/Ag^+ [3].
In our current work, we investigated whether this luminescent interfacially dimerized DNA-silver nanoconstruct is stable enough to be applied as a sensor for detecting DNA or RNA fragments in serum or within cells.

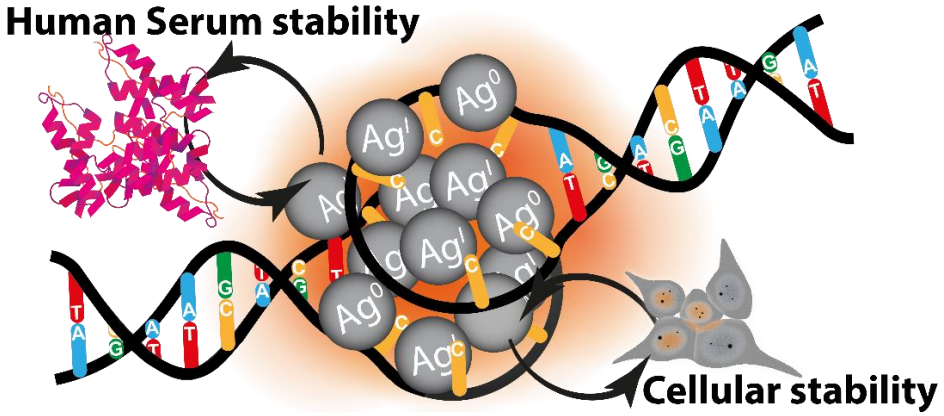


Figure 1. Schematic of the luminescent interfacially dimerized DNA-silver nanoconstruct

Acknowledgements
Funded by the European Union (MSCA, DNANOMETAL, 101151525).

References
[1] S S. Dey, et al. Nat. Rev. Methods. Primers. 1 (2021) 13.
[2] N. C. Seeman, J. Theor. Biol. 99 (1982) 237–247.
[3] R. Geczy, et al. Angew. Chem. 132 (2020) 16225-16231.

EVALUATING THE ENVIRONMENTAL IMPACT OF NEW COPPER(II) SCHIFF BASE COMPLEXES USING A CELLULAR BIOASSAY

Ildiko Buta[1], Mara Bogdan[1], Abedulkadir Abudalleh[2], Cseh Liliana[1], Radostina Alexandrova[2]

[1] "Coriolan Drăgulescu" Institute of Chemistry of the Romanian Academy
[2]Institute of Experimental Morphology, Pathology and Anthropology with Museum, Bulgarian Academy of Sciences, Sofia, Bulgaria
ildiko_buta@acad-icht.tm.edu.ro

Schiff base ligands incorporating thiophene and piperidine groups are promising scaffolds for developing ecocompatible, d-block metal complexes. [1] The inclusion of heterocyclic rings such as thiophene, contributes to electron-rich aromatic systems which can facilitate π-stacking and improve cellular uptake. [2] Though fewer studies combine both piperidine and thiophene scaffolds, recent work on piperidine-based heteroleptic Schiff base complexes has confirmed strong DNA and protein binding in vitro, which is a critical step toward anticancer activity. [3]

This study evaluates the environmental safety and ecotoxicological impact of a novel thiophene-derived Schiff base ligand (HL) and its binuclear copper(II) complex (LCu). The compounds were synthesized and structurally characterized using FT-IR, UV–Vis spectroscopy, elemental analysis, and single-crystal X-ray diffraction. To assess their interaction with biological systems exposed to environmental stressors, a cellular bioassay was performed using v-src-expressing rat cells (LSR-SF-SR) as a sensitive model of viral-induced biological stress. Cells were exposed to concentrations of 0.5–200 µg/mL for 24–72 h. Cellular response, viability, and morpho-functional alterations were evaluated using MTT, Neutral Red, Crystal Violet, AO/PI staining, scratch, and 3D colony formation assays. Both compounds exhibited concentration- and time-dependent biocompatibility profiles. The LCu complex modulated cell proliferation, migration, and colony formation more effectively than the free ligand, demonstrating that copper coordination influences cellular homeostasis under stress. These findings validate the LSR-SF-SR bioassay as a reliable tool for monitoring the environmental impact and biocompatibility of novel d-block coordination compounds, supporting their development as low-risk chemical systems.

Aknowledgements
This study was supported partially by the bilateral project between the Bulgarian Academy of Sciences and the Romanian Academy (Project No. IC-RO/04/2026–2028) and by Program No. 4, Project No. 4.1 from the "Coriolan Dragulescu".

References
[1] S. Nayab, A. Alam, N. Ahmad, S. W. Khan, W. Khan, D. Farhan, S. M. I. A. Shah, M. Ateeq, S. K. Shah, H. Lee, ACS Omega 8 (2023) 17620–17633.
[2] N. O. Boadi, M. Degbevi, S. A. Saah, M. Badu, L. S. Borquaye, N. K. Kortei, Sci. Afr. 12 (2021) e00846.
[3] B. Ari, M. Das, S. Mukherjee, D. Basak, A. Bera, A. Biswas, P. Kundu, P. Brandao, S. Mondal, B. C. Samanta, T. Maity, New J. Chem. 49 (2025) 13446-13462.

GREEN EXTRACTION OF DROUGHT-RESILIENT ROSEMARY: MODULATING EXTRACT COMPOSITION THROUGH SOLVENT SELECTIVITY FOR COSMETIC APPLICATIONS

Daniela Haidu[1], Manuela Crișan[1], Mariana Suba[1], Luminița Crișan[1], Ildiko Bută[1], Vlad Alexandru Enache[2], Camelia Oprean[3,4]

[1] "Coriolan Drăgulescu" Institute of Chemistry, Romanian Academy, 24 M. Viteazu Blvd., 300223 Timișoara, Romania
danielahaidu1@gmail.com
[2] Faculty of Food Engineering, University of Life Sciences „King Mihai I" from Timișoara – USVT, Calea Aradului Street, nr.119, 300645 Timișoara
[3]Faculty of Pharmacy, "Victor Babeș" University of Medicine and Pharmacy, E. Murgu Sq., No. 2, 300041 Timișoara, Romania
[4]OncoGen Centre, County Hospital Pius Brînzeu, 156 Liviu Rebreanu Blvd., 300736 Timișoara, România

Abstract

Climate change, increasing drought frequency, and the growing demand for naturally derived cosmetic ingredients encourage the valorization of resilient plant resources through more sustainable processing strategies. *Rosmarinus officinalis* L., a drought-tolerant aromatic plant rich in phenolic compounds and terpenoids, represents a promising renewable source of multifunctional cosmetic ingredients [1, 2].

Within a green chemistry framework, solvent selection can be used not only to improve extraction efficiency, but also to modulate extract composition while favoring cosmetic compatible media and reducing the need for extensive downstream processing. This study investigates rosemary extracts obtained using extraction media spanning a broad polarity range, from hydrophilic to lipophilic systems, to evaluate how solvent selectivity influences their chemical profile, antioxidant properties, and stability. Extracts were characterized by FT-IR, GC-MS, total phenolic content (TPC), DPPH antioxidant activity, color measurements, UV-Vis monitoring under controlled photoirradiation and varying pH conditions, and peroxide and *p*-anisidine values for oil extracts. Computational analyses complemented the characterization of the identified phytoconstituents.

TPC analysis showed comparable phenolic extraction from rosemary samples of different geographical origins (22.83 and 25.55 mg GAE/g), while combining solvents of different polarities increased TPC by up to 55.2%, reaching 35.43 mg GAE/g. Ethanolic extracts exhibited DPPH IC_{50} values of 169.58 and 182.02 µg/mL. FT-IR analysis highlighted solvent-dependent extraction selectivity, distinguishing lipophilic constituents from hydroxyl-containing and phenolic components preferentially extracted in more polar media. Photoirradiation induced changes in the characteristic UV-Vis bands at 280 and 320-340 nm, indicating the degradation of phenolic constituents and highlighting the importance of extract stability.

The results support solvent polarity as a practical tool for tailoring rosemary extracts according to their intended cosmetic application. Integrating drought-resilient plant resources with selective, cosmetic-compatible extraction media provides a promising approach for developing functional botanical ingredients in accordance with green chemistry and sustainable cosmetic production.

Acknowledgements
This work was supported by Program 2 of "Coriolan Dragulescu "Institute of Chemistry of Romanian Academy and by a grant of the Ministry of Education and Research, CCCDI-UEFISCDI, project number PN-IV-P6-6.1-CoEx-2024-0196, within PNCDI IV.

References
[1] Laftouhi A., Eloutassi N., Drioua S., Ech-Chihbi E., Rais Z., Abdellaoui A., Taleb A., Beniken M., Taleb A. (2023). Impact of Water Stress and Temperature on Metabolites and Essential Oil of Rosmarinus officinalis (Phytochemical Screening, Extraction, and Gas Chromatography). Journal of Ecological Engineering. 24. 237-248.
[2] Sahlabgi A., Lupuliasa D., Stanciu G., Lupșor S., Vlaia L.L., Rotariu R., Predescu N.C., Rădulescu C., Olteanu R.-L., Stănescu S.-G., Hîncu L., Mititelu M. The Development and Comparative Evaluation of Rosemary Hydroalcoholic Macerate-Based Dermatocosmetic Preparations: A Study on Antioxidant, Antimicrobial, and Anti-Inflammatory Properties. Gels. 2025 Feb 20;11(3):149.

GREENER APPROACHES TO THE SYNTHESIS OF PHOSPHORUS-BASED ANTIMICROBIAL COMPOUNDS

Aurelia VISA[1], Alexandru Buhai[1], Liliana Cseh[1]

[1] *"Coriolan Dragulescu" Institute of Chemistry, 24 Mihai Viteazu Blv., 300223 Timisoara, Romania*
e-mail: avisa@acad-icht.tm.edu.ro

Abstract
The increasing problem of antimicrobial resistance and the need for new bioactive compounds have encouraged the development of faster and more sustainable approaches to chemical synthesis. Phosphorus-containing compounds, such as phosphonates, bisphosphonates, phosphinic acids, quaternary phosphonium salts and α-aminophosphonates, are important classes of biologically active molecules, with several examples already used as therapeutic agents, including tenofovir and cidofovir [1,2]. However, their preparation can involve several synthetic steps, large amounts of solvents, and relatively long reaction times.
In this work, green chemistry approaches were investigated for the synthesis of phosphorus-based compounds, with particular attention to one-pot reactions and alternative energy sources such as ultrasound. The Kabachnik–Fields reaction was used to prepare α-aminophosphonate derivatives from aromatic aldehydes, aniline, and dialkyl phosphites. A conventional reflux method using oxalic acid as a catalyst was compared with a one-pot, solvent- and catalyst-free procedure under ultrasonic irradiation. The comparison focused on reaction efficiency, practical aspects, and the reduction of waste and solvent use in line with green chemistry principles [3]. These approaches show that simpler and more sustainable synthetic methods can be useful for preparing diverse phosphorus-containing compounds for further biological evaluation.

Acknowledgements
This work was partially supported by a grant of the Ministry of Education and Research, CCCDI-UEFISCI, project number PN-IV-P6-6.1-CoEx-2024-0106, within PNCDI IV and by supported by Program no 2, from the "Coriolan Drăgulescu" Institute of Chemistry Timisoara, Romania.

References
[1] K.D. Demadis, S.K. Adla, J. Timonen, P.A. Turhanen, Green Chem. 27 (2025) 863.
[2] J. Cui, K.-S. Ju, Curr. Opin. Microbiol. 87 (2025) 102630.
[3] P. Anastas, J. Warner, Green Chemistry: Theory and Practice, Oxford University Press, New York, 1998.

TAILORING MAGNESIUM-BASED COMPOUNDS THROUGH SYNTHESIS AND STABILITY

Marcela Iosivoni, Nicoleta Pleșu, Aurelia Vișa

"Coriolan Dragulescu" Institute of Chemistry, 24 Mihai Viteazu Blv., 300223 Timisoara, Romania
e-mail: miosivoni@gmail.com

Abstract
Bivalent metal-organic frameworks (MOFs) based on magnesium (Mg^{2+}) and 1-hydroxyethylidene-1,1-diphosphonic acid (HEDP) were synthesized following the 12 principles of green chemistry[1] via hydrothermal[2] and alternative synthesis methods (sonochemical and microwave-assisted synthesis), using water as solvent. The environmental and structural stability of the resulting materials was investigated in acidic media and under UV light irradiation using complementary techniques, namely X-ray Diffraction (XRD), Conductometric Analysis, Fourier Transformed Infrared Spectroscopy (FTIR), UV-Vis Spectroscopy and Thermogravimetric Analysis (TGA).

Introduction
The acceleration of global warming and environmental pollution demand the development of sustainable, eco-friendly materials, with a high stability in different conditions for outdoor applications. Metal–organic frameworks (MOFs) offer high surface area, tunable pore structures for environmental applications, thus far their structural stability and degradation behavior in chemically aggressive environments remains limited. To address this challenges, this study focuses on the greener synthesis and degradation behavior and stability of MOFs under UV light irradiation and acidic media.

Experimental
The MgHEDP compounds were synthesized using conventional methods (hydrothermal synthesis) and alternative greener routs (sonochemical and microwave-assisted synthesis), using water as the exclusive solvent (Figure 1).

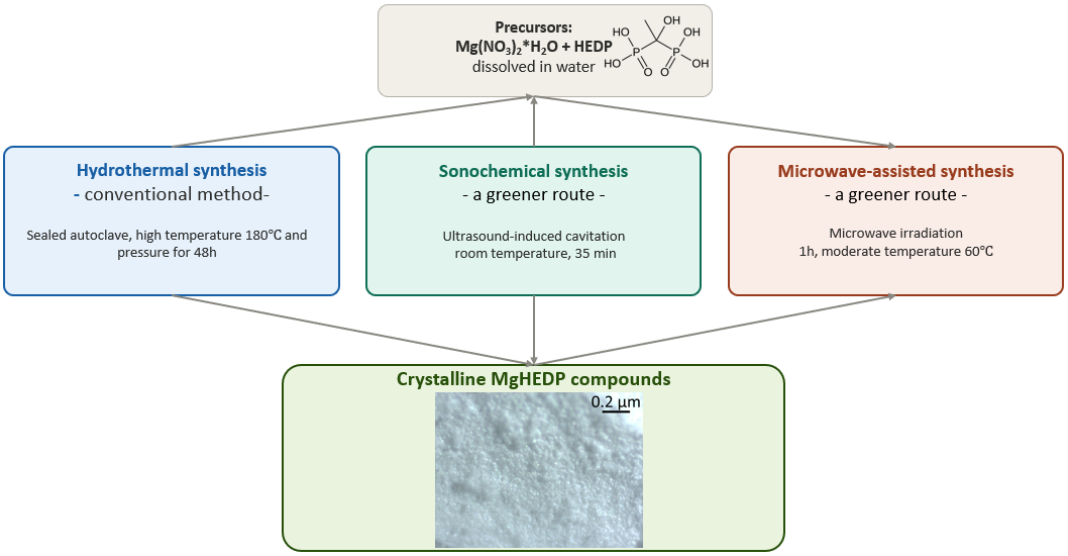


Figure 1. Synthesis routes for MgHEDP compounds, *conventional method versus greener routes*

Conductometric and UV-Vis measurements were used to monitor the periodic degradation behavior and chemical stability in acidic media. Additionally, photolytic degradation over 1–9 hours was analyzed using solid-state UV-Vis spectroscopy and X-ray diffraction.

Results and discussion

Under UV-Vis irradiation (1–9 h), the XRD spectra of MgHEDP showed a uniform decrease in diffraction peak intensities without abrupt peak disappearances, shifts, or sudden structural collapse. This uniform intensity decline confirms a non-selective degradation mechanism, without a major photolysis or aggressive oxidation.

Conductometric measurements at pH 2, 4 and 6, showed that the pH 2 induces surface protonation and ion release, the framework remains highly stable at pH 4 and 6 over 180 minutes (Table 1). Solid-state UV-Vis spectroscopy confirmed a linear surface release of phosphonate species without a major structural collapse.

Thermal analysis showed no major changes in the thermal profiles and weight loss, confirming the overall thermal and structural stability.

Fourier Transformed Infrared Spectroscopy spectra showed a progressive attenuation of intensity with increasing irradiation time in the range of 1200-900 cm^{-1}, without peak shifts, indicating gradual changes in the functional groups involved in surface interactions and/or in metal-phosphonate coordination.

Table 1. Synthetic scheme of processes occurring in solution at different pH

pH	**2**	**4**	**6**
H^+	↑	→	→
Protonation/Hydrolysis	↑	→	→
Ions in solutions	↑	→	→
Conductivity	↑	→	→

Conclusion

The MgHEDP compounds that were synthesized via greener, water-based routs display moderate to high chemical stability in acidic environments and mild photolytic degradation kinetics, demonstrating their potential for long-term environmental applications.

Acknowledgements

This work is supported by Program no 2, from the „Coriolan Dragulescu" Institute of Chemistry Timisoara, Romania.

References

[1] P. Anastas, J. Warner, Green Chemistry: Theory and Practice, Oxford University Press, New York, 1998.

[2] Y. Zhao, Z. Wang, Z. Bao, H. Xing, Z. Zhang, B. Su, Q. Yang, Sep. Purif. Technol. 2018, 195, 238-243.

MOLECULAR DETERMINANTS OF SOIL ORGANIC-CARBON PARTITIONING IN ENVIRONMENTAL CHEMICALS

Nicoleta Stoian[1], Liliana Halip[1]

[1]*Department of Computational Chemistry, „Coriolan Dragulescu" Institute of Chemistry,24 Mihai Viteazu Ave.,300223 Timisoara, Romania*
e-mail: nstoian@acad-icht.tm.edu.ro

Abstract

The mobility and persistence of organic compounds are strongly dependent on their interaction with soil and sediment organic matter, usually quantified by using the soil organic-carbon partition coefficient (Koc). This property is important for estimating how easily agrochemicals, and other potentially toxic compounds, could infiltrate into underground water sources. Precise Koc data accessibility is an issue within pollutant studies since experimental determinations that could provide such data involve time consuming and costly methods.[1] Therefore, QSAR methods are a valuable alternative used to estimate the environmental hazard for a new compound and creating safe disposal and management decisions.[2]
Using all pollutants in the NORMAN [3] database with measured Koc and known structures (~600 molecules) we built a 4-descriptor based model for LogKoc across different chemical classes. The compound mobility was defined using established vPvM (very Persistent, very mobile) thresholds. Molecular descriptors were calculated using RDKIT (KNIME), and multicolinearity screening was used to reduce the initial set of descriptors. Two independent validation strategies were applied: a conventional random split and a scaffold-based split, to assure no overlap between training and testing compounds.
The four-descriptor model showed an improved predictive power, (R^2=0.77 R^2_{adj} =0.7692, F statistic 432.7) compared to the single SlogP based model (R^2 = 0.7). An additional external pollutant dataset (~60 molecules) was used for external validation considering the applicability domain evaluated through Williams plot.

References

[1] Fu Liu, Fan Fan, Qingmiao Yu, Hongqiang Ren, Jinju Geng; Variable K_{OC} and Poor-Quality Data Sources Cause High Discrepancy in Current Mobility Assessment of Organic Substances. *ACS EST Water* 14 February 2025; 5 (2): 659–669
[2] Wang, Y.; Chen, J.; Yang, X.; Lyakurwa, F.; Li, X.; Qiao, X.In silico model for predicting soil organic carbon normalized sorption coefficient (K(OC)) of organic chemicals. Chemosphere 2015, 119, 438-444
[3]NORMAN Network. (2026). *NORMAN SusDat: Substance Database*. Accessed May 2026, from https://www.norman-network.com/nds/susdat/

METALATED PORPHYRIN DERIVATIVES AS SENSITIVE COMPOUNDS FOR DRUG QUANTIFICATION

Anca Lascu, Ionela Fringu, Nicoleta Plesu

Institute of Chemistry "Coriolan Drăgulescu", M. Viteazul Ave. 24, 300223-Timisoara, Romania
Email: ancalascu@yahoo.com

On the one hand, the simple, fast, environmentally friendly, and economic spectrophotometric detection and quantification [1] of a multitude of organic compounds is a highly relevant research topic; it offers real-time, instrumental readouts without the lengthy sample preparation required by chromatographic methods (like HPLC). On the other hand, electrochemical detection methods, including voltammetry and amperometry [2], are highly effective, cost-efficient, and easily miniaturized for point-of-care testing.

Due to their outstanding optical and electronic properties, porphyrins and their metallated derivatives play a central role in spectrophotometry as sensitive compounds [3]. Inserting metals like Zn(II), Pt(II), Co(II), or Mn(III) into the porphyrin core introduces axial coordination sites, allowing the sensor to bind strongly to drugs containing nitrogen or oxygen donor atoms [4]. A plethora of compounds in this family have been tested—varying either the central metal ion or the peripheral substituents of the porphyrin macrocycle—to detect and quantify minute quantities of drugs. The importance of quantifying drugs in the nanomolar concentration domain is critical due to their potential to induce toxicity [5].

References

1. Norvaiša K., Kielmann M., Senge M. O. Porphyrins as Colorimetric and Photometric Biosensors in Modern Bioanalytical Systems. Chembiochem. 2020;21(13):1793–1807. doi: 10.1002/cbic.202000067
2. Regueiro Pschepiurca M. E., Vadra N., Suarez S. A. Versatile Metalloporphyrin-Based Electrochemical Sensing Applications: From Small Gasotransmitters to Macromolecules. Eur. J. Inorg. Chem. 2023, 26(17), e202300005
3. DiNatale C., Monti D., Paolese Chemical sensitivity of porphyrin assemblies. Mat. Today 2010, 13(7-8), 46-52. 10.1016/S1369-7021(10)70127-9
4. Thakur, P.S., Gautam, L., Vyas, S.P., Sankar, M., Metalloporphyrin nanoparticles for diverse theranostic applications. In Inorganic nanosystems 2023. (pp. 489-507). Academic Press.
5. Thomas J., Kmar V., Sharma N., John N., Umesh M., Huligowda L.K.D., Kaur K., Utreja D. Recent approaches in nanotoxicity assessment for drug delivery applications: Challenges and prospects. Medicine in Drug Discovery 2025, 25, 100204, https://doi.org/10.1016/j.medidd.2025.100204

SELF-SUSTAINED COMBUSTION OF AMORPHOUS RIBBONS FOR THE SYNTHESIS OF Cu–Cu_2O/ZrO_2 MIXED OXIDE AS A SUPERCAPACITOR ELECTRODE MATERIAL

Mircea Nicolaescu[1], Carmen Lazau[1], Corina Orha[1], Cosmin Codrean[2], Cornelia Bandas[1]

[1]Condensed Matter Department, National Institute for Research and Development in Electrochemistry and Condensed Matter, A. P. Podeanu Street, No 144, 300569 Timisoara, Romania
[2]Politehnica University Timişoara, Materials and Manufacturing Engineering Department, Bd. Mihai Viteazul nr. 1, 300222, Timişoara, Romania
e-mail: mircea.nicolaescu@incemc.ro

Abstract

Recently, considerable attention has been devoted to the development of nanostructured electrode materials for high-performance supercapacitor applications. Among the various synthesis strategies, top-down approaches have gained increasing interest due to their relative simplicity, reduced processing complexity, and short synthesis times. In particular, combustion methods represent an attractive and rapid route for the preparation of oxide-based materials with complex compositions and structures. In this study, $Cu_{48}Zr_{47}Al_5$ amorphous ribbons were subjected to a self-sustained combustion process to obtain a Cu–Cu_2O/ZrO_2 mixed oxide, which was subsequently investigated as an electrode material for supercapacitor applications. The structural and morphological characteristics were analyzed by XRD and SEM, while the electrochemical performance was evaluated by cyclic voltammetry (CV) and galvanostatic charge–discharge (GCD) measurements. The CV curves exhibited a non-rectangular profile, indicating a predominantly pseudocapacitive charge-storage mechanism and confirming the potential of the Cu– Cu_2O/ZrO_2 material as a positive electrode. Overall, the results highlight the potential of Cu–Cu_2O/ZrO_2 mixed oxide obtained from amorphous ribbons as an electrode material for supercapacitor applications and demonstrate the suitability of the proposed synthesis approach [1].

References

[1] M. Nicolaescu, C. Lazau, C. Orha, C. Codrean, C. Bandas , Batteries. 12 (2026) 239.

Funding

This work was supported by the Project ‘‘Innovative Technological Approaches to Cir-cularity and Urban-Industrial Symbiosis within the Water-Energy-Materials-Fertilizers Nexus (ECO-NEXUS)’’, Smart Growth, Digitalization and Financial Instruments Program, 2021-2027, MySMIS under Grant 336912.

REMOVAL OF DYES FROM AQUEOUS SOLUTIONS USING ACTIVATED CARBON DERIVED FROM COFFEE WASTE: OPTIMIZATION OF THE ADSORPTION PROCESS

Maria-Andreea Nistor, Liliana Halip, Ana-Maria Lacrămă, Elisabeta-Ildyko Szerb, Simona-Gabriela Muntean

"Coriolan Drăgulescu" Institute of Chemistry, 24 Mihai Viteazu Bvd., 300223, Timisoara, Romania
e-mail: nistor_andreea1990@yahoo.com

Abstract

The increasingly widespread use of dyes in various industrial sectors, especially in the textile industry, has led to the continuous generation of wastewater contaminated with dyes, posing significant environmental concerns when inadequately treated [1]. In this context, the development of efficient, low-cost, and sustainable adsorbents derived from waste materials represents a promising approach for wastewater treatment [2]. In the present study, activated carbon prepared from coffee waste was investigated as an alternative adsorbent for the removal of dyes (Congo Red (CR) and Methylene Blue (MB)) from aqueous solutions. A pH_{PZC} value of 10.17 for the synthesized adsorbent was determined using the pH variation method (the pH drift method).

The effects of solution pH, initial dye concentration and adsorbent dosage on the adsorption efficiency were systematically investigated in single-component systems. The optimization of the adsorption process was performed using factorial design and Response Surface Methodology (RSM) based on a Central Composite Design, enabling the evaluation of both individual and interaction effects of the selected variables. The developed models demonstrated good predictive performance and identified the optimal operating conditions, under which the maximum predicted dye removal efficiencies were achieved: 97% for MB and 89% for CR, respectively. Model validation further confirmed the reliability of the predicted optimal conditions, and normal operating conditions, under which yields of 95% for MB and 85% for CR were achieved. To evaluate the applicability of the adsorbent (coffee-waste-derived activated carbon) under realistic conditions, the simultaneous adsorption of investigated dyes from a binary system was subsequently investigated yielding removal efficiencies of over 88% for MB and 59% for CR. Furthermore, kinetic analysis indicated that the adsorption process was more accurately described by the pseudo-second-order kinetic model.

Overall, the results demonstrate that activated carbon derived from coffee waste is an effective and sustainable adsorbent for the removal of both anionic and cationic dyes from aqueous media. The combination of high removal efficiencies, process optimization, and successful performance in binary systems highlights the potential of this waste-derived material for practical applications in the treatment of dye-containing wastewater.

Acknowledgements

This work was supported by a grant of the Ministry of Education and Research, CCCDI - UEFISCDI, through the project Center of Excellence in water management, materials, by-products and waste valorisation for circular bioeconomy implementation, proposal number PN-IV-P6-6.1-CoEx-2024-0056, contract 6 CoEx/02.06.2026, within PNCDI IV.

References

[1] J. Fito, M. Abewaa, A. Mengistu, K. Angassa, A.D. Ambaye, W. Moyo, T. Nkambule, Sci. Rep. 13 (2023) 5427.

[2] F. Aouay, A. Attia, L. Dammak, R. Ben Amar, A. Deratani, *Materials*. *17* (2024) 3078.

ACTIVATED CARBON AND COMPOZITES WITH IRON OXIDE, PREPARED FROM WASTE COFFEE: CHARACTERIZATION AND ADSORPTION PROPERTIES OF DYES

Ana-Maria Lacrămă, Maria-Andreea Nistor, Roxana Nicola, Simona-Gabriela Muntean, Elisabeta-Ildyko Szerb

"Coriolan Drăgulescu" Institute of Chemistry, Bv. Mihai Viteazul, No. 24, 300223 Timișoara, Romania
e-mail: *lacramaanamaria@yahoo.com*

Abstract
Following the principle of circular economy approach concerning the transformation of waste into useful materials, coffee waste was chosen as a precursor to obtain activated carbon materials [1]. The waste coffee was carbonized and next it was activated by using KOH and different procedures, like one, simple, or two, double time, activation treatments [2]. By incorporation of iron oxide into the obtained activated carbon, composites materials were obtained, as well. The obtained materials were characterised by nitrogen porosimetry and based on the obtained properties, some of them were selected to be further tested for dye adsorption. As a preliminary study the synthesized materials were tested as adsorbents for the removal of two anionic and three cationic dyes from aqueous solution. The results indicated that two materials, one with double time and one with simple activation treatment, had the highest adsorption capacities. Using the double treatment activated material as adsorbent, dye removal efficiencies between 85.51% and 99.76% were obtained under normal working conditions. In addition, using the simple activated material, yields between 59.06-79.96% were obtained for anionic dyes and 90.48-98.81% for cationic dyes, respectively. Preliminary results obtained working under normal conditions revealed that the obtained materials are promising adsorbents for the removal of dyes from aqueous solutions.

Acknowledgements
This work was supported by a grant of the Ministry of Education and Research, CCCDI - UEFISCDI, through the project Center of Excellence in water management, materials, by-products and waste valorisation for circular bioeconomy implementation, proposal number PN-IV-P6-6.1-CoEx-2024-0056, contract 6 CoEx/02.06.2026, within PNCDI IV.

References
[1] V. Lionetti, S. Bartucci, C. P. Bonaventura, G. Conte, G. Desiderio, A. Policicchio, R. G. Agostino, Int. J. Hydrog. Energy 136 (2025) 1029-1040.
[2] F. Aouay, A. Attia, L. Dammak, R. Ben Amar, A. Deratani, Materials 17(13) (2024) 3078.

MICROWAVE-ASSISTED SYNTHETIZED N-DOPED CARBON QUANTUM DOTS. FROM SYNTHESIS TO APPLICATIONS

Roxana Nicola*, Carmen Cretu, Alexandru Vişan, Silvana Borcănescu, Ana-Maria Lacrămă, Elisabeta Ildyko Szerb

"Coriolan Drăgulescu" Institute of Chemistry, Bv. Mihai Viteazu, No. 24, 300223 Timisoara, Romania
*e-mail:*cc.roxana@yahoo.com*

Abstract
Carbon dots are a relatively new class of carbon-based materials. They have attracted significant interest due to their distinctive structure and captivating properties. These properties include insignificant cytotoxicity with good biocompatibility, good solubility, tunable optical properties, numerous precursor sources, easy chemical surface functionalization, high chemical and photostability, as well as their small size [1,2]. In the present work, we present the synthesis of N-doped carbon quantum dots (N-CQDs) obtained using as precursors citric acid (CA) and diethylenetriamine (DETA) by microwave-assisted synthesis with controlled reaction parameters. Materials with different degree of carbogenic cores were obtained depending on the controlled reaction conditions. The temperature and time of reactions were varied, while pressure and microwave power were adapted for the synthesis conditions. The degree of carbogenic cores formation was evaluated and compared with a material obtained from banana peels as carbon source. The obtained materials were investigated in terms of their compositional, structural and optical properties using FT-IR and Raman spectroscopy, UV–Vis absorption and photoluminescence (PL) spectroscopy, X-ray diffraction (XRD), and elemental analysis. Representative samples were selected to investigate their sensitivity toward Fe^{3+} ions, while their antioxidant activity was assessed using the DPPH• radical scavenging assay.

1. Kostromin S., Borodina A., Pankin D., Povolotskiy A., Bronnikov S., *Chem. Phys. Lett.*, 841, 141175, **2024**
2. Nguyen K.G., Huš M., Baragau I.-A., Bowen J., Heil T., Nicolaev A., Abramiuc L.E., Sapelkin A., Sajjad M.T., Kellici S., *Small*, 20(24), **2024**

Acknowledgements
This work was supported by a grant of the Ministry of Education and Research, CCCDI - UEFISCDI, through the project Center of Excellence in water management, materials, by-products and waste valorisation for circular bioeconomy implementation, proposal number PN-IV-P6-6.1-CoEx-2024-0056, contract 6 CoEx/02.06.2026, within PNCDI IV.

EFFICIENT COUNTER ELECTRODE BASED ON PEDOT/GO AS SUSTAINABLE Pt-FREE COUNTER ELECTRODE FOR INDOOR DYE-SENSITIZED SOLAR CELLS

Daniel Ursu*, Melinda Vajda, Marinela Miclau, Cristian Casut, Radu Banica

National Institute for Research and Development in Electrochemistry and Condensed Matter, Dr. A. Păunescu-Podeanu Street no 144, 300569 Timişoara, Romania
e-mail: danielhoratiu@yahoo.com

Abstract

With the rise in living standards for people due to population modernization globally and rapid industrial transformations, lead to an explosion of Internet of things (IoT) devices, which according to IoT Analytics havealready reached 16.6 billion devices [1].

Dye-sensitized solar cells (DSSCs) have many advantages over other PV technologies such as lower manufacturing costs, longer lifespans, low light performance, mechanical strength, and diversity,they have emerged as a leading contender for producing electricity in interior light environments and can be successfully integrated into low power IoT systems, due to the incredibly high and stable power conversion efficiencies (PCE), up to 34% under 1000 lux [2]. Up to now, the platinum (Pt) has typically been used as CE material in DSSCs. However, the use of Pt as CE for the large-scale production and commercialization of DSSC is severely restricted due to its natural scarcity, high cost, and easy decomposition to PtI_4 by iodine redox electrolyte. From this perspective, low-cost conductive polymers, such as poly(3,4-ethylenedioxythiophene) (PEDOT), play an important role in replacing Pt as CE material in DSSCs, due to its high roomtemperature conductivity and remarkable stability [3]. Incorporation of graphene oxide (GO) into PEDOT improve the surface area and catalitic activity [4]

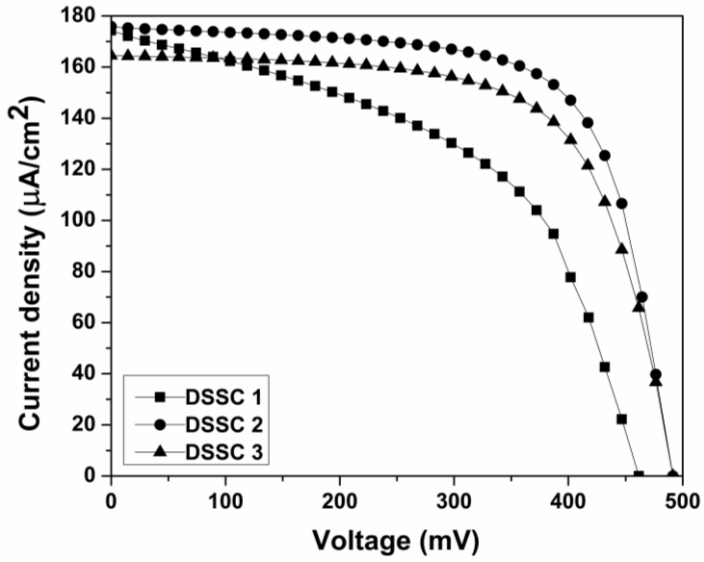


Figure 1 .J-V curves of DSSCs under 1000 lux illumination condition

In the present study, a simple and fast method was proposed to obtain efficient CE based on PEDOT/GO, using eco-friendly aqueous electrochemical deposition, and validated in indoor illumination conditions using commercial LED light sources and an electrolyte based on the I^-/I_3^- redox pair. The incorporation of GO enhances DSSC efficiency, increasing it from 13.35% for PEDOT-based CE to 19.75% for PEDOT/GO-based CE under 2700K LED illumination (Figure 1).

Acknowledgements
This work was supported by a grant of the Ministry of Education and Research, CCCDI - UEFISCDI, project number PN-IV-P6-6.1-CoEx-2024-0154, within PNCDI IV.

References
[1] H. Michaels, M. Rinderle, I. Benesperi, R. Freitag, A. Gagliardi, M. Freitag, Chemical Science, 14 (2023) pp. 5350-536
[2] M. Freitag, J. Teuscher, Y. Saygili, X. Zhang, F. Giordano, P. Liska, J. Hua, S.M. Zakeeruddin, J.-E. Moser, M. Grätzel, A. Hagfeldt, Nature Photonics, 11 (2017) pp. 372-378.
[3] L. Fagiolari, E. Varaia, N. Mariotti, M. Bonomo, C. Barolo, F. Bella, Advanced Sustainable Systems, 5 (2021) 2100025.
[4] D. Chen, H. Feng, J. Li, Graphene Oxide: Preparation, Functionalization, and Electrochemical Applications, Chemical Reviews, 112 (2012) 6027-6053.

CORROSION INHIBITION OF CARBON STEEL BY ORGANOPHOSPHORUS ACIDS: ELECTROCHEMICAL AND SURFACE-ADSORPTION STUDIES

Nicoleta Plesu[1], Kostas Demadis[2], Milica Țară-Lungă Mihali[1], Ionela Frîngu[1], Anca Lascu[1]

[1]"Coriolan Dragulescu" Institute of Chemistry, 24 Mihai Viteazul Blv, 300223 Timisoara, Romania
[2]Crystal Engineering, Growth and Design Laboratory, Department of Chemistry, University of Crete, Voutes Campus, Heraklion, Crete, GR-71003, Greece
e-mail: plesu_nicole@yahoo.com

Abstract
Electrochemical impedance spectroscopy (EIS) provides valuable insight into the relationship between the molecular structure of organophosphorus compounds and their corrosion-inhibition performance [1]. By monitoring parameters such as charge-transfer resistance, double-layer capacitance, and surface-film resistance, EIS can reveal how structural characteristics-including the number and arrangement of phosphonic acid groups, the presence of electron-donating or coordinating functionalities, and the overall molecular architecture-influence adsorption and protective-film formation at the metal/electrolyte interface [2]. The inhibitory action of six phosphonic acids was analyzed by electrochemical impedance spectroscopy (EIS), polarization curves (CP), gravimetric methos and optical microscopy. In this context, EIS and CP techniques offer a complementary perspective to gravimetric measurements: while gravimetry reflects the cumulative material loss resulting from corrosion over extended exposure periods, EIS and polarization measurements primarily describe the electrochemical state of the metal/electrolyte interface during a relatively short experimental period. Consequently, these electrochemical techniques can provide time-resolved information on changes in interfacial properties associated with inhibitor adsorption and film development, whereas gravimetric measurements provide an integrated assessment of corrosion damage. It was observed that in the case of phosphonic acids the length of the molecular chain can play an important role in determining the corrosion-inhibition efficiency. Longer chains can promote stronger intermolecular interactions and the formation of more compact and hydrophobic surface films, which may limit the access of corrosive species to the metal/electrolyte interface. However, the effect of chain length is not necessarily linear, since an increase in molecular size may also influence solubility, molecular mobility, orientation, and the accessibility of the phosphonic functional groups responsible for interaction with the metal surface.

Acknowledgements
This work was partially supported by Program no 3, from the "Coriolan Drăgulescu" Institute of Chemistry, Timișoara, Romania and by project "ICT—Interdisciplinary Center for Smart Specialization in Chemical Biology (RO-OPENSCREEN)", MySMIS code: 127952, Contract no. 371/20.07.2020, co-financed by the European Regional Development Fund under the Competitiveness Operational Program 2014–2020.

References
[1] K.L. Medard, H. Hamilton, S.C. van der Moore, J. Chem. Anal. 313 (2007) 163.
[2] Moschona A., Plesu N., Colodrero R.M.P., Cabeza A., Thomas A. G., Demadis K. D., Homologousalkyl side-chain diphosphonate inhibitors for the corrosion protection of carbon steels, Chem. Eng. J., 2021, 405, Article Number 126864.

FOOD-DERIVED ECDYSTEROIDS IN VERTEBRATE BLOOD: FROM INSECTIVOROUS BATS TO BROADER VERTEBRATE SCREENING

Mohamed Reda Essaih[1], Sándor Hornok[2,3], István Ilisz[1], Róbert Berkecz[1,4], Attila Hunyadi[5,6]

[1]Institute of Pharmaceutical Analysis, University of Szeged, Szeged, Hungary
[2]Department of Parasitology and Zoology, University of Veterinary Medicine, Budapest, Hungary
[3]HUN-REN UVMB Climate Change: New Blood-sucking Parasites and Vector-borne Pathogens Research Group, Budapest, Hungary
[4]Department of Forensic Medicine, Albert Szent-Györgyi Clinical Center, University of Szeged, Szeged, Hungary
[5]Institute of Pharmacognosy, University of Szeged, Szeged, Hungary
[6]HUN-REN-SZTE Biologically Active Natural Products Research Group, Szeged, Hungary.
Reda.essaih@um5r.ac.ma

Abstract

Ecdysteroids are steroid hormones that regulate essential developmental processes in arthropods and also occur in plants as phytoecdysteroids. In vertebrates, experimentally administered ecdysteroids have been associated with anabolic and metabolic effects. This contribution compares two targeted high-resolution mass spectrometric investigations of naturally acquired ecdysteroids in vertebrate blood: a study of insectivorous bats and a broader screening of birds, mammals, and reptiles. In the bat study, blood samples from 36 individuals representing eight insectivorous species were analyzed for ten natural ecdysteroids using ultra-high-performance liquid chromatography coupled to high-resolution quadrupole-Orbitrap mass spectrometry (UHPLC-HRMS). The fragmentation behaviour of the investigated ecdysteroids was also characterised by high-resolution tandem mass spectrometry to support structural identification. Nine ecdysteroids were detected, and 20-hydroxyecdysone (20E) was present in all evaluated bats. Mean 20E concentrations reached 232.82 ± 287.23 pmol/mL in Eptesicus serotinus and 38.49 ± 27.92 pmol/mL in Nyctalus noctula. In the subsequent vertebrate screening, 136 EDTA-anticoagulated blood samples were analyzed by targeted UHPLC-MS/HRMS. Only two samples were positive: a Common Kestrel (Falco tinnunculus) containing 58.9 nM 20E and a beech marten (Martes foina) containing 40.9 nM dacryhainansterone. The overall detection frequency was 1.47% (2/136; 95% CI 0.18–5.21%). Together, these findings support dietary acquisition as a source of circulating ecdysteroids in vertebrates and suggest that sustained insectivory is associated with more frequent detection than occasional or opportunistic insect consumption [1,2].

Introduction

Ecdysteroids are the principal steroid hormones of arthropods and regulate a wide range of physiological processes, including development, diapause, sexual maturation, reproduction, and behavior. Plants also biosynthesize phytoecdysteroids, which can influence herbivorous insects. Beyond these ecological roles, experimentally administered ecdysteroids have been reported to enhance energy utilization, protein synthesis, and tissue growth in vertebrates. Previous studies demonstrated that insectivorous passerine birds may contain low to high concentrations of circulating ecdysteroids, raising the question of whether similar dietary transfer occurs in other vertebrate groups. [1,2] The first study investigated whether insectivorous bats acquire circulating ecdysteroids from their prey. A subsequent screening study broadened this question to other amniote vertebrates, including zoo animals receiving

insect-containing diets, road-killed mammalian carnivores, and wild aquatic or predatory birds. This conference contribution presents the analytical workflow and compares the occurrence and quantitative levels of naturally acquired ecdysteroids observed in these two studies [1,2].

Experimental

In the bat study, 36 bats representing eight insectivorous species were evaluated. Whole blood was diluted with saline, spiked with poststerone (20E)-oxime as internal standard, precipitated and extracted with methanol, centrifuged, dried under nitrogen, and reconstituted in water/methanol (1:1, v/v). Ten ecdysteroids were targeted: 20-hydroxyecdysone, polypodine B, poststerone, 14-deoxy-20-hydroxyecdysone, 2-deoxy-20-hydroxyecdysone, ecdysone, ajugasterone C, calonysterone, dacryhainansterone and shidasterone. External calibration with an internal standard was used. Chromatographic separation was performed on an Accucore C30 column using water and acetonitrile, both with 0.1% formic acid. A Q Exactive Plus quadrupole-Orbitrap instrument was operated in positive mode, using SIM for quantification and PRM/HRMS-MS for identification. Mass tolerance was 5 ppm, and three replicate quantitative analyses were performed [1].

In the 2026 vertebrate screening, 136 blood samples collected between 2022 and 2025 were investigated. The samples included 30 regularly insect-fed zoo animals, 15 road-killed mammalian carnivores and 91 water-associated or predatory birds. For preparation, 50 µL whole blood was combined with internal standard and methanol, followed by protein precipitation/enrichment with ice-cold methanol, centrifugation, evaporation and reconstitution. Matrix-matched external calibration was applied. Targeted UHPLC-MS/HRMS was performed on an Orbitrap Exploris 240 in positive PRM mode. Identification relied on retention time, accurate precursor and fragment masses, and fragmentation patterns. The PRM mass tolerance was 5 ppm; five replicate quantitative analyses were performed for positive samples and the reported LOQ was 5 nM. The paper also reports an LOD of 0.5 nM for 20E and 1 nM for the other compounds [2].

Results and discussion

Nine ecdysteroids were detected in the blood of the eight investigated bat species. The most prevalent compound was 20E, detected in all evaluated bats. Among the larger bat species, E. serotinus showed a significantly higher mean 20E concentration (232.82 ± 287.23 pmol/mL, n = 8) than N. noctula (38.49 ± 27.92 pmol/mL, n = 11; P = 0.012). Bats predominantly feeding on beetles also showed a higher mean 20E concentration (204.96 ± 260.09 pmol/mL, n = 10) than bats predominantly feeding on flies (49.74 ± 59.58 pmol/mL, n = 15; P = 0.009). These observations support a relationship between dietary composition and circulating ecdysteroid profiles, although the study does not establish a causal physiological benefit [1]. In addition to quantitative determination, the fragmentation behaviour of the investigated ecdysteroids was characterised by high-resolution tandem mass spectrometry, providing further insight into their structural identification and supporting confident compound assignment. The broader vertebrate screening showed a markedly lower detection frequency. Ecdysteroids were absent at detectable levels from the regularly insect-fed zoo animals in that dataset. Among the 15 road-killed mammalian carnivores, one beech marten contained 40.9 nM dacryhainansterone (CV 1.4%). Among 91 water-associated and predatory birds, one Common Kestrel contained 58.9 nM 20E (CV 1.2%). Thus, 2 of 136 samples were positive, corresponding to 1.47% (95% CI 0.18–5.21%). Five replicate measurements for dacryhainansterone in the positive beech marten sample were 40.4, 40.2, 40.9, 41.6, and 41.4 nM, demonstrating good analytical repeatability [2]. The contrast between frequent detection in continuously insectivorous bats and rare detection in the broader vertebrate screening is consistent with the interpretation that repeated dietary exposure may help maintain measurable circulating concentrations. However,

negative samples do not exclude concentrations below the analytical detection limits, and neither study demonstrates sustained anabolic or health effects from the measured blood concentrations [1,2].

Conclusion

Targeted UHPLC-MS/HRMS enabled the selective identification and quantification of naturally acquired ecdysteroids in small-volume vertebrate blood samples. In addition, high-resolution tandem mass spectrometry allowed characterisation of the fragmentation pathways of the investigated ecdysteroids, supporting confident structural assignment. The two studies demonstrate that dietary ecdysteroids can enter vertebrate circulation, but their occurrence varies markedly with feeding ecology. Continuous insectivory in bats was associated with broad and frequent detection, whereas the broader vertebrate screening identified ecdysteroids in only two of 136 samples. These findings highlight the importance of dietary exposure, analytical sensitivity, and sampling context when interpreting circulating ecdysteroid concentrations. The available data demonstrate occurrence and enable quantitative assessment, but do not by themselves establish sustained physiological or anabolic effects in the sampled animals [1,2].

Acknowledgement

This work was supported by the National Research, Development and Innovation Office (NKFIH) through the National Laboratory of Translational Neuroscience (NLTN) projects Neurodevelopmental Disorders and Adult Nervous System Disorders (RRF-2.3.1-21-2022-00011). Project No. TKP2021-EGA-32 was implemented with the support of the Ministry of Innovation and Technology of Hungary from the National Research, Development and Innovation Fund under the TKP2021-EGA funding scheme.

References

[1] S. Hornok, R. Berkecz, E. Sós, A. D. Sándor, T. Körmöczi, N. Solymosi, J. Kontschán, A. Hunyadi, “Ecdysteroids as natural doping substances in the blood of insectivorous bats,” bioRxiv preprint, posted 14 May 2021. doi: 10.1101/2021.05.12.443761.

[2] S. Hornok, R. Berkecz, A. Pitó, P. Baro, K. M. Röper, J. Lanszki, A. Biácsi, K. Erdélyi, E. Sós, V. Molnár, E. Papp, S. Boldogh, S. Szabolcs, G. Keve, A. Hunyadi, “Do insect food-derived ecdysteroids appear in the blood of waterfowl, predatory birds, carnivorous mammals and primates?” PLOS ONE 21(9) (2026) e0357290. doi: 10.1371/journal.pone.0357290.

THE ROLE OF A HISTIDINE MUTATION IN THE PROPERTIES OF THE ARSENIC(III)-SENSING AFARSR PROTEIN

Réka S. Gyimesi, Annamária Tóth, Attila Jancsó, Béla Gyurcsik

Department of Molecular and Analytical Chemistry, University of Szeged, Hungary
e-mail: mesireka@gmail.com

Abstract

The occurrence of arsenic in the environment is a significant concern due to the toxicity of its compounds and the potential risks associated with exposure [1]. Reliable detection of arsenic species is therefore important for the assessment of contaminated environments. While conventional analytical techniques provide sensitive and accurate measurements, they generally depend on laboratory-based instrumentation and sample processing. Biological recognition of elements offer a complementary perspective, as they can respond to specific chemical species through molecular recognition mechanisms.

Members of the ArsR family represent such system for the recognition of arsenic(III). Their regulatory function is based on the interaction of the protein with the metalloid, which disrupts DNA binding of ArsR and consequently allows the expression of regulated genes. This molecular response can be exploited in assay systems to investigate arsenic recognition and to explore the characteristics required for selective metalloid sensing.

We examined how the H97D substitution affects the arsenic(III)-responsive properties of the AfArsR protein. The mutant protein was characterized both *in vivo* using the I-Block system based on intracellular gene regulation [2] and *in vitro* using spectrometric and electrophoretic approaches. Its interaction with As(III) was investigated alongside its response to selected divalent metal ions to assess the effect of the mutation on metalloid recognition and selectivity. Mass spectrometry demonstrated that the variant could bind metal(loid) ions, whereas circular dichroism spectroscopy indicated no substantial effect of these ions on the secondary structure of the protein.

The H97D substitution did not abolish the DNA-binding and regulatory activity of the AfArsR mutant. However, higher As(III) concentration was required for a response comparable to that of the wild-type protein. Consistently, electrophoretic mobility shift assays showed that disruption of the DNA-protein complex occurred at higher As(III) concentrations for the mutant. Comparison with other metal ions still indicated a preferential response toward As(III). Taken together, the results demonstrate that the H97D substitution alters the concentration range of AfArsR response to As(III), while preserving its regulatory function and As(III)-selective character. These findings provide insight into the molecular determinants governing metalloid-responsive regulation and support the investigation of ArsR-based systems as biological recognition elements for an environmentally relevant metal(loid).

Acknowledgements

We acknowledge the financial support of National Research, Development and Innovation Office, Hungary (No.: 150330), of the Hungarian Academy of Sciences and Japan Society for the Promotion of Science (JSPS NKM2024-15/2024)

References

[1] L.C. Platanias, J. Biol. Chem. 284, 18583-18587 (2009).
[2] S. Szentes, N. Zsibrita, M. Koncz, E. Zsigmond, P. Salamon, Z. Pletl, A. Kiss, Nucleic Acids Res., (2020) 48, e28.

Poster Proceedings

SUSTAINABLE BIOPROCESSING OF AGRO-FOOD RESIDUES FOR PREBIOTIC AND POSTBIOTIC PRODUCTION

Mirela Ahmadi[1], Ioan Peț[1], Maryam Ahmadi[1,2], Bogdan Peț[1,3], Aryan Ahmadi[1,4], Zeno Gârban[5]

[1]Faculty of Bioengineering of Animal Resources, University of Life Science "King Mihai I" from Timişoara, Timişoara-300645, Calea Aradului 119, Romania
[2] Faculty of Psychology and Educational Sciences, West University Timişoara, Bd. Vasile Parvan 4, Timisoara-300223, Romania
[3] Faculty of Dental Medicine, University of Medicine and Pharmacy „Victor Babes" Timisoara, B-dul Revoluției din 1989, Timisoara-300070, Romania
[4] Technical University of Munich, School of Engineering and Design, Boltzmannstraße 15, 85748-Garching bei München, Germany
[5]Working Group for Xenobiochemistry, Romanian Academy-Timişoara Branch, Bd. M. Viteazu 24, Timişoara-300223, Romania.
e-mail: ioan.pet@usvt.ro

Abstract
Agri-food residues contain carbohydrates, fibers, proteins, and bioactive compounds that can support the production of functional biotics. This review analyzes the transformation of residues from the processing of fruits, vegetables, cereals, legumes, and dairy-processing residues into prebiotic and postbiotic ingredients via enzymatic hydrolysis, extraction, and microbial fermentation. Analytical methods used to characterize the resulting products are also discussed. Although these processes can reduce organic waste and reliance on refined fermentation media, their environmental performance depends on pretreatment, resource consumption, process yield, and purification requirements. Therefore, sustainable implementation requires both technological optimization and environmental impact assessment.

Keywords: *agro-food residues, prebiotics, postbiotics, sustainable biotechnology.*

Introduction
Agro-food processing generates solid and liquid residues, including fruit pomace, peels, seeds, cereal bran, legume hulls, molasses and dairy side streams. These materials retain polysaccharides, soluble sugars, proteins, minerals and phenolic compounds that may be recovered or converted into functional ingredients. Their valorization can reduce the organic load directed towards disposal while providing substrates for microbial and enzymatic processes [1]. Plant-processing residues are particularly relevant to prebiotic production because they contain pectin, cellulose, hemicellulose and resistant starch. A prebiotic is defined as "a substrate that is selectively utilized by host microorganisms conferring a health benefit" [2]. Fiber content or fermentability alone does not establish prebiotic status, but agro-food residues may provide compounds with prebiotic potential or polymeric fractions that can be converted into oligosaccharides through extraction, enzymatic hydrolysis or microbial processing [3].
Residues containing fermentable carbohydrates may also support microorganisms used to obtain postbiotic preparations. A postbiotic is defined as "a preparation of inanimate microorganisms and/or their components that confers a health benefit on the host" [4]. Metabolites may be present, but purified metabolites or cell-free fermentation products without inanimate cells or cellular components do not satisfy this definition. Replacing refined culture media with suitable residues may decrease raw-material requirements and extend biomass utilization. However, pretreatment, sterilization, fermentation and product recovery also consume water and energy. Waste-derived processing should therefore be evaluated according to process yield, resource use and management of the remaining fractions [1,5]. This review examines the conversion of agro-food residues into prebiotic and postbiotic ingredients, with emphasis on bioprocessing methods, analytical characterization and environmental performance.

Agro-food residues as sources of functional substrates

The suitability of agro-food residue for prebiotic or postbiotic production depends on its chemical composition, availability, microbiological quality and response to processing. Plant residues are generally rich in structural polysaccharides, whereas liquid side streams contain soluble sugars and nitrogenous compounds that can be readily metabolized. Their composition varies with variety, maturity, processing method and storage conditions; each material must therefore be characterized before extraction, hydrolysis or fermentation [1,5].

Fruit and vegetable processing generates pomace, peels, seeds and fibrous pulp. Apple and citrus pomace contain pectin, cellulose and hemicellulose, while grape pomace also provides seed- and skin-associated polyphenols. Tomato processing produces a moist pomace composed mainly of skins and seeds. The skin fraction contains fiber and carotenoids, particularly lycopene, whereas the seeds supply proteins, lipids and fiber. Tomato seeds can be separated for oil and protein recovery, while the remaining seed material or complete pomace may be considered for further bioprocessing. However, its relatively high lipid content and limited availability of fermentable sugars may require defatting, hydrolysis or supplementation before microbial fermentation. Potato peels and sugar beet pulp provide starch, pectic substances and hemicellulose. These components can be recovered directly or converted into soluble fibers and oligosaccharides through mechanical, thermal or enzymatic treatment [1].

Cereal-processing residues, including wheat, rice and oat bran, contain cellulose, arabinoxylans, β-glucans and resistant starch. Enzymatic cleavage can release oligosaccharides, while hydrolyzed starch-rich fractions may support microbial growth. Legume hulls and seed coats also contain fiber, resistant starch and α-galactooligosaccharides. Phytates, tannins and protease inhibitors may nevertheless require controlled pretreatment [3,5].

Cheese whey contains lactose, soluble proteins, minerals and vitamins and can support lactic acid bacteria and yeasts. Fermentation can convert lactose into organic acids, microbial biomass and other products while reducing the organic load associated with untreated whey [6]. Molasses and fruit-processing liquids similarly provide fermentable sugars but may require dilution or supplementation.

Residue selection must also consider moisture, seasonality, transport, perishability and contamination with pesticides, mycotoxins, allergens or pathogenic microorganisms. A residue becomes a useful functional substrate only when its composition, safety and technological behavior are compatible with the intended bioprocess and final product.

Bioprocessing strategies for prebiotic production

Prebiotic ingredients can be obtained from agro-food residues by recovering naturally occurring compounds or converting complex carbohydrates into smaller fractions. Direct recovery applies to materials containing inulin-type fructans, resistant starch, pectin or other nondigestible carbohydrates and generally involves milling, extraction, separation, concentration and drying [7]. Purification should be adapted to the final application because extensive downstream processing increases resource consumption and may reduce yield [1,5].

Enzymatic hydrolysis provides controlled polymer degradation. Pectin-rich citrus peel, apple pomace and sugar beet pulp can be treated with pectinases to generate pectic oligosaccharides. Their composition depends on substrate structure, enzyme specificity, pH, temperature and reaction time. Excessive hydrolysis may produce monosaccharides, while membrane filtration or chromatography can provide fractions with defined molecular-weight distributions [8].

Cereal bran and lignocellulosic residues are sources of xylo- and arabinoxylo-oligosaccharides. Pretreatment increases hemicellulose accessibility, allowing endo-xylanases to release soluble oligomers. Hydrothermal and dilute-acid treatments are also effective, but severe conditions may generate monosaccharides, furfural derivatives and phenolic inhibitors [9].

Sucrose-rich molasses or fruit-processing streams can be converted into fructo-oligosaccharides by fructosyltransferases, whereas lactose-rich dairy streams can undergo β-galactosidase-catalyzed transgalactosylation to produce galacto-oligosaccharides. Substrate concentration, enzyme origin and reaction conditions influence the balance between synthesis and hydrolysis [6,10].

Microbial fermentation may release soluble carbohydrates by disrupting plant structures and removing simple sugars or antinutritional compounds. However, fermentability alone does not establish prebiotic status. Selective utilization by host microorganisms and an associated health benefit must be demonstrated [2]. Process selection should therefore balance functional evidence, product yield, purification requirements and resource consumption.

Fermentative production of postbiotics

Postbiotic production begins with selecting a characterized microorganism and a substrate that supports reproducible growth. Lactic acid bacteria, including species of *Lactiplantibacillus*, *Lacticaseibacillus*, *Lactobacillus* and *Leuconostoc*, are frequently investigated, although other bacteria and yeasts may also be suitable. Agro-food residues can replace conventional culture media when they provide accessible carbon, nitrogen, minerals and growth factors. Whey, molasses, fruit-processing liquids and hydrolysates from cereal or vegetable residues are among the substrates used for microbial conversion [6,11].

Solid residues usually require milling, hydration and enzymatic or thermal pretreatment to release fermentable compounds, whereas liquid substrates may need clarification, dilution or nutrient supplementation. Fermentation can be conducted under submerged or solid-state conditions. During cultivation, microorganisms produce biomass and metabolites such as organic acids, exopolysaccharides, peptides, enzymes and vitamins. Their formation depends on the strain, substrate composition, pH, temperature, oxygen availability and fermentation time [10,12]. Replacing a defined medium with residual biomass therefore requires process optimization.

Following fermentation, microorganisms must be inactivated while retaining components associated with the intended biological effect. Heat treatment is commonly used because it is accessible and readily controlled, but excessive temperature or treatment duration can alter membranes, surface proteins, enzymes and heat-sensitive metabolites. Alternative procedures include high-pressure processing, irradiation, pulsed electric fields and ultrasound. These techniques may preserve selected cellular structures but require specialized equipment and product-specific validation [13].

The final preparation may contain intact inanimate cells, cellular fragments and fermentation metabolites. It can be used as a liquid concentrate or stabilized by freeze-drying, spray-drying or encapsulation. The absence of viable microorganisms must be demonstrated through appropriate culture-based methods, complemented when necessary, by techniques assessing membrane integrity or metabolic activity [4,13].

The figure 1 shows how agro-food residues retain polysaccharides, proteins, polyphenols, lipids and minerals that can be recovered through sustainable bioprocessing. These components may be converted into prebiotics, postbiotics, enzymes and other bioactive ingredients, supporting resource recovery and waste reduction.

Not every fermented or inactivated agro-food residue qualifies as a postbiotic. The final product must contain inanimate microorganisms and/or their components and confer a demonstrated health benefit on the host [4]. Cell-free supernatants and isolated metabolites remain valuable fermentation products but should not be designated as postbiotics without microbial cellular material. Strain identity, substrate safety, inactivation efficiency, composition and biological effect must therefore be established for the final preparation.

Analytical characterization and quality assessment

Analytical characterization should confirm the composition, safety and functional properties of ingredients obtained from agro-food residues. For prebiotic fractions, total carbohydrates and dietary fiber provide initial information, but more selective methods are required to determine individual sugars, oligosaccharide profiles and degree of polymerization. High-performance liquid chromatography coupled with refractive-index, evaporative light-scattering or mass-spectrometric detection can separate mono-, di- and oligosaccharides. Size-exclusion chromatography and spectroscopic methods may provide additional information on molecular-weight distribution and structural features [8,9]. Residual monosaccharides, degradation products and phenolic compounds should also be measured because they can influence microbial utilization and product stability.

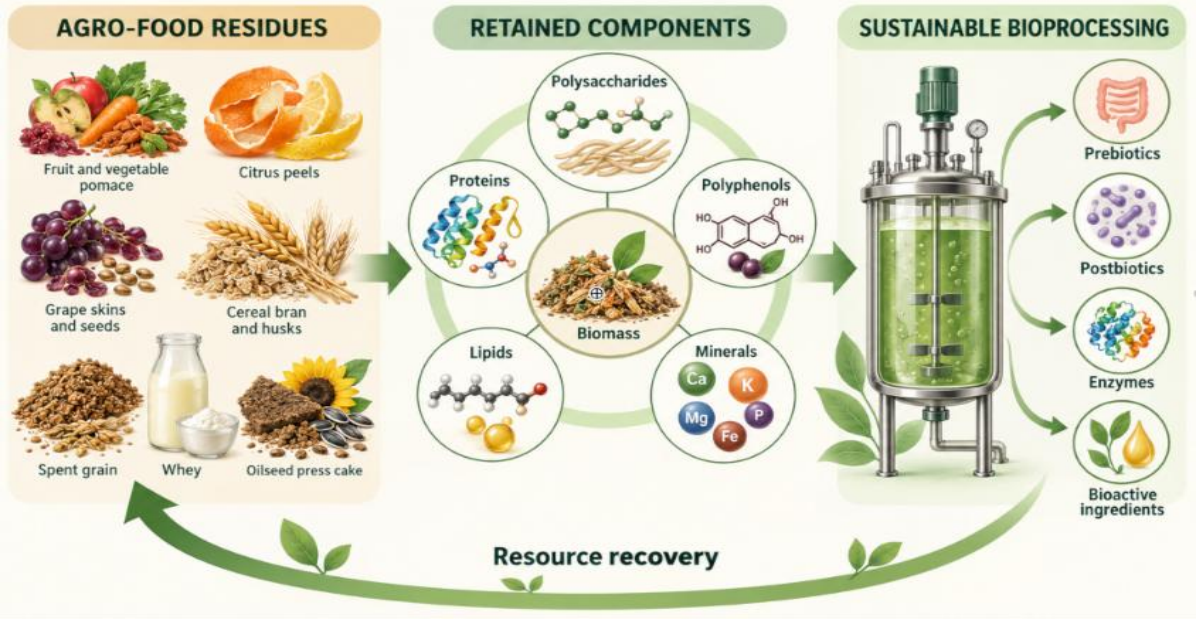


Figure 1. Valuable components in agro-food residues – sources for sustainable biotechnology

Functional assessment generally includes resistance to simulated gastrointestinal digestion, fermentation by selected microorganisms and monitoring of microbial growth, substrate consumption and short-chain fatty acid production. However, these assays indicate prebiotic potential rather than proving a health benefit, which requires evidence obtained in an appropriate host [2].

For postbiotic preparations, strain identity, fermentation conditions and inactivation parameters must be documented. The absence of cultivable cells should be confirmed by culture-based enumeration using suitable recovery conditions. Flow cytometry with viability dyes, microscopy or molecular methods may complement plate counting but should not replace the demonstration that viable microorganisms are absent [4,13]. Depending on the preparation, organic acids, peptides, exopolysaccharides, cell-wall components and other metabolites can be analyzed by chromatographic, electrophoretic, spectroscopic or immunochemical methods.

Quality assessment should also include microbial contaminants, mycotoxins, pesticide residues, heavy metals and allergens when relevant to the original substrate. Moisture content, water activity, pH and stability during storage are necessary for defining product specifications. Batch-to-batch consistency is particularly important because agro-food residues vary with origin, season and processing conditions.

Environmental benefits and technological limitations

Using agro-food residues as bioprocessing substrates can reduce the quantity of organic material directed towards landfill, uncontrolled decomposition or low-value disposal. It may also replace part of the refined carbohydrates and nutrients used in conventional fermentation

media and recover functional compounds before the remaining biomass is used for feed, energy or soil applications [1,5]. Local processing is preferable because many residues have high moisture content, deteriorate rapidly and are expensive to transport.
Drying, milling, sterilization, enzymatic hydrolysis, fermentation and purification require water, energy and auxiliary chemicals. Some pretreatments also generate inhibitory compounds or liquid effluents that require further treatment. Seasonal availability and compositional variability can affect process reproducibility, while contamination with microorganisms, pesticides, mycotoxins or allergens may restrict food applications [5,11].
Environmental performance should therefore be evaluated across the entire process rather than inferred from the use of residual biomass. Relevant indicators include material recovery, product yield, water and energy consumption, greenhouse-gas emissions and management of secondary residues. Life-cycle assessment and techno-economic analysis can identify whether a proposed process provides measurable advantages over conventional production and existing residue-management options.

Conclusions

Agro-food residues can provide carbohydrates, fibres and nutrients for producing prebiotic fractions and postbiotic preparations through extraction, enzymatic conversion and microbial fermentation. Their successful valorization depends on substrate composition, process control, product characterization and demonstrated biological function. However, using residual biomass does not by itself ensure environmental sustainability. Resource consumption, processing yield, safety, product stability and secondary waste generation must also be assessed. Integrating analytical control with technological and environmental evaluation is necessary to develop reproducible and genuinely sustainable bioprocesses

References

[1] E. Capanoglu, E. Nemli, F. Tomás-Barberán, J. Agric. Food Chem. 70 (2022) 6787–6804.
[2] G.R. Gibson, R. Hutkins, M.E. Sanders, S.L. Prescott, R.A. Reimer, S.J. Salminen, K. Scott, C. Stanton, K.S. Swanson, P.D. Cani, K. Verbeke, G. Reid, Nat. Rev. Gastroenterol. Hepatol. 14 (2017) 491–502.
[3] D. Davani-Davari, M. Negahdaripour, I. Karimzadeh, M. Seifan, M. Mohkam, S.J. Masoumi, A. Berenjian, Y. Ghasemi, Foods 8 (2019) 92.
[4] S. Salminen, M.C. Collado, A. Endo, C. Hill, S. Lebeer, E.M.M. Quigley, M.E. Sanders, R. Shamir, J.R. Swann, H. Szajewska, G. Vinderola, Nat. Rev. Gastroenterol. Hepatol. 18 (2021) 649–667.
[5] T.P.C. Ezeorba, A.N. Okeke, C.O. Okeke, C.N. Nweze, Bioresour. Technol. Rep. 25 (2024) 101728.
[6] T. Zotta, L. Solieri, L. Iacumin, C.Picozzi, M.Gullo, Appl.Microbiol. Biotechnol. 104 (2020) 2749–2764.
[7] Z. Gârban, Biochimie – Tratat comprehensiv, Vol. I, Bazele moleculare ale vieții, ed. a 6-a, Editura Academiei, București, 2024.
[8] B. Gullón, B. Gómez, M. Martínez-Sabajanes, R. Yáñez, J.C. Parajó, J.L. Alonso, Trends Food Sci. Technol. 22 (2011) 611–621.
[9] A.A. Aachary, S.G. Prapulla, Compr. Rev. Food Sci. Food Saf. 10 (2011) 2–16.
[10] S.I. Mussatto, I.M. Mancilha, Carbohydr. Polym. 68 (2007) 587–597.
[11] J.H. Saadoun, G. Bertani, A. Levante, F. Vezzosi, A. Ricci, V. Bernini, C. Lazzi, Foods 10 (2021) 707.
[12] N. Prajapati, A. Singh, R. Narsaiah, Front. Microbiol. 14 (2023) 1306192.
[13] T.C. Pimentel, A.G. Cruz, E. Pereira, W.K. Almeida da Costa, R. da Silva Rocha, G. Targino de Souza Pedrosa, C.S. Rocha, J.M. Alves, V.O. Alvarenga, A.S. Sant'Ana, M. Magnani, Trends Food Sci. Technol. 138 (2023) 199–214.

MINERAL COMPOSITION OF SWEET AND HOT PAPRIKA POWDER

Liana-Maria Alda[1], Simion Alda[2]*, Despina-Maria Bordean[1], Laura Rădulescu[1], Diana Moigrădean[1], Daniela Stoin[1], Ariana-Bianca Velciov[1], Corina Iuliana Megyesi[1], Daniela Scedei[2], Sofia Popescu[1], Alexandru Rinovetz[1]

[1]Faculty of Food Engineering, University of Life Sciences „King Mihai I" from Timisoara, Aradului Street No 119, 300645 Timișoara, Romania
[2]Faculty of Engineering and Applied Technology, University of Life Sciences „King Mihai I" from Timisoara, Aradului Street No 119, 300645 Timișoara, Romania
** corresponding author e-mail: simion_alda@usvt.ro*

Abstract
Capsicum annuum L. is one of the most widely cultivated vegetable crops worldwide and includes both sweet peppers (bell peppers) and hot peppers (chili peppers). These fruits are highly valued not only for their sensory properties, color and flavor, but also for their nutritional composition. In addition to vitamins, antioxidants, and dietary fiber, peppers represent an important source of essential minerals required for human health. Regular pepper consumption can contribute significantly to mineral intake because peppers contain a balanced spectrum of both macro- and microelements. The aim of this study was to evaluate the mineral composition and nutritional value of selected sweet and hot paprika powder samples using X-ray fluorescence (XRF) spectrometry. The obtained results demonstrated that paprika powder is characterized by high contents of potassium and calcium, as well as moderate levels of iron (Fe), manganese (Mn), copper (Cu), and zinc (Zn). These findings confirm the nutritional significance of paprika powder as a valuable source of essential minerals in the human diet.
Key words: *XRF, paprika powder, minerals, nutritional value, Capsicum annuum*

Introduction

Research indicates that the mineral composition of sweet and hot peppers is remarkably similar. Michel et al. (2022) found no statistically significant differences in the contents of phosphorus, potassium, calcium, magnesium, copper, iron, manganese, zinc, and sodium between the two varieties [5]. However, hot peppers generally contain slightly higher levels of dietary fiber, proteins, and polyphenolic compounds, whereas sweet peppers show higher moisture content and larger fruit size [5].

These fruits are highly valued not only for their sensory properties, color, and flavor but also for their nutritional composition. In addition to vitamins, antioxidants, and dietary fiber, peppers represent an important source of essential minerals required for human health [1]. Minerals such as potassium, calcium, magnesium, phosphorus, iron, zinc, copper, manganese, and sodium contribute to numerous physiological functions, including bone formation, enzymatic reactions, electrolyte balance, and immune function [2,5,7].

Regular consumption of peppers may contribute significantly to mineral intake because they contain a balanced spectrum of both macroelements and microelements [3,4,6,7,9,10].

Currently, European legislation on food contaminants (EU Regulation 2023/915) does not establish a maximum limit for copper in spices [11].

The aim of this study was to evaluate the mineral composition and nutritional value of selected sweet and hot paprika powder samples using X-ray fluorescence (XRF) spectrometry.

Experimental

Four samples of hot paprika powder (Ph1-Ph4) and four samples of sweet paprika powder (Ps1-Ps4) were purchased from leading supermarket chains in Romania.
According to the information provided on the packaging, all products were manufactured by Romanian producers.
The moisture content (%) of the investigated samples was measured using a Sartorius moisture analyzer.
Mineral composition was assessed by X-ray fluorescence spectroscopy (XRF) using a portable Hitachi X-MET8000 analyzer. Prior to analysis, the paprika samples were finely ground, dried to constant weight, and transferred into polyethylene sample bags. To ensure the reliability of the results, each sample was measured in triplicate.

Results and discussion

The moisture content of the samples ranged between 8% and 10%.
An evaluation of the nutritional characteristics declared on the product labels revealed that the eight paprika powder samples examined in this study exhibited an energy value ranging from 302 to 360 kcal/100 g.
The protein samples content varied between 11.8 % and 14.0%, while fat levels ranged from 9% to 14%.
Carbohydrates accounted for 52.7-56.0% of the total composition, whereas dietary fiber represented 33.4-37.7%.
The experimentally determined mineral concentrations in the paprika powder samples, expressed as mg/100 g DW or mg/kg DW, are illustrated in the following figures.

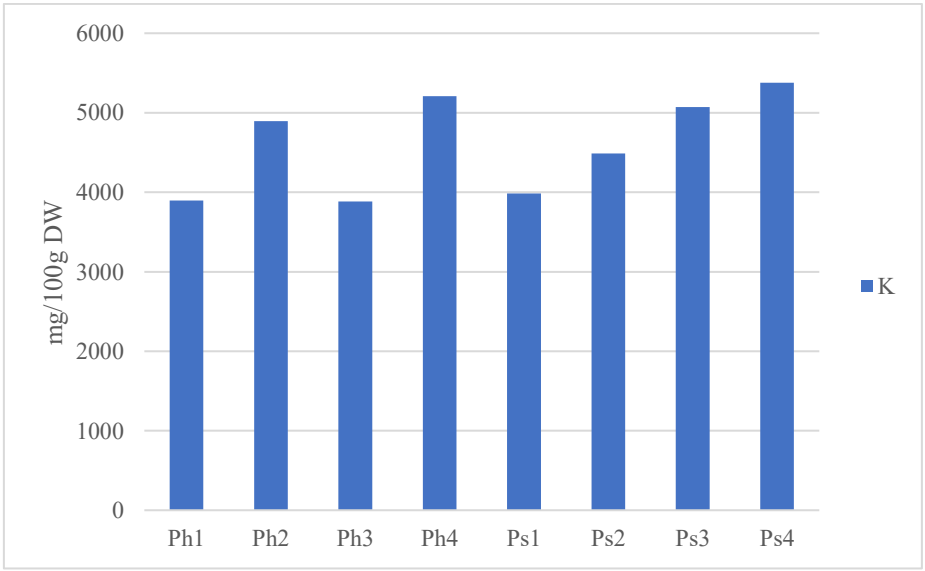


Figure 1. Potassium content (mg/100 g dry weight) in different paprika varieties
Legend: Ph1-Ph4= Hot paprika powder samples; Ps1-Ps4= Sweet paprika powder samples;

The potassium content ranged from approximately 3900 to 5400 mg/100 g DW, indicating moderate variability among the analyzed samples.
The highest potassium concentration was determined in sample Ps4, whereas the lowest values were observed in samples Ph1 and Ph3.

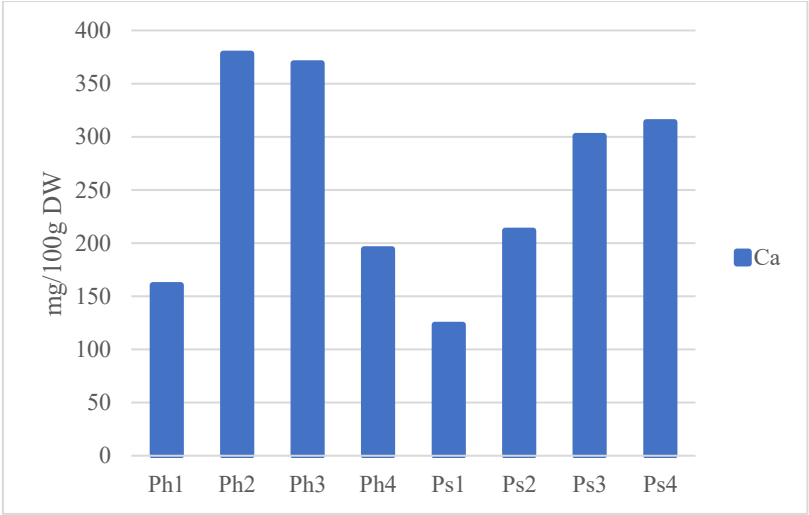


Figure 2. Calcium content (mg/100 g DW) of different paprika varieties
Legend: Ph1-Ph4= Hot paprika powder samples; Ps1-Ps4= Sweet paprika powder samples;

The calcium content ranged from approximately 125 to 380 mg/100 g DW. The highest calcium concentration was recorded in sample Ph2, whereas the lowest calcium contents were found in samples Ps1 and Ph1.

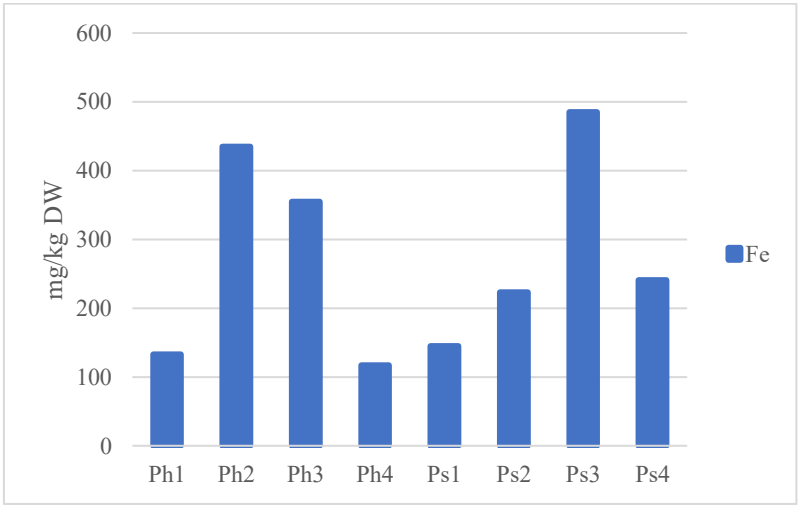


Figure 3. Iron content (mg/kg dry weight) in paprika samples
Legend: Ph1-Ph4= Hot paprika powder samples; Ps1-Ps4= Sweet paprika powder samples;

Iron exhibited the greatest variability among all the analyzed elements, with concentrations ranging from approximately 120 to 490 mg/kg DW.
Sample Ps3 showed the highest iron concentration, whereas the lowest levels were detected in samples Ph4 and Ph1.

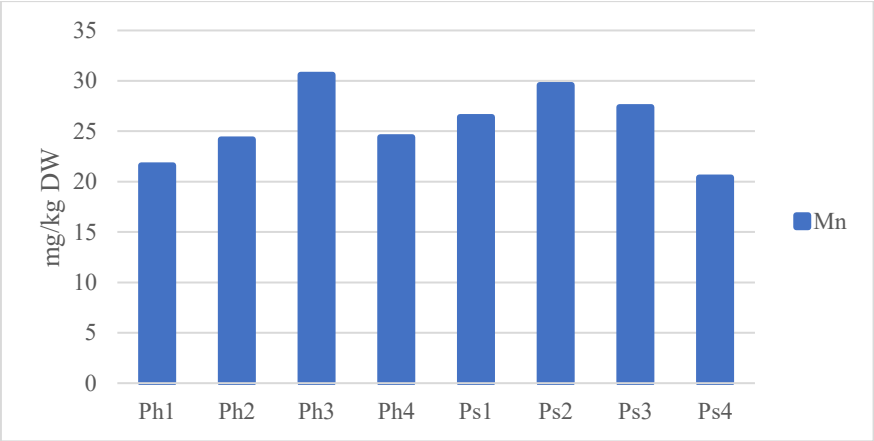


Figure 4. Manganese content (mg/kg dry weight) in paprika samples
Legend: Ph1-Ph4= Hot paprika powder samples; Ps1-Ps4= Sweet paprika powder samples;

Manganese content varied within a relatively narrow range, from 20.4 to 30.6 mg/kg DW. The highest manganese concentration was recorded in sample Ph3, whereas the lowest concentration was found in sample Ps4.

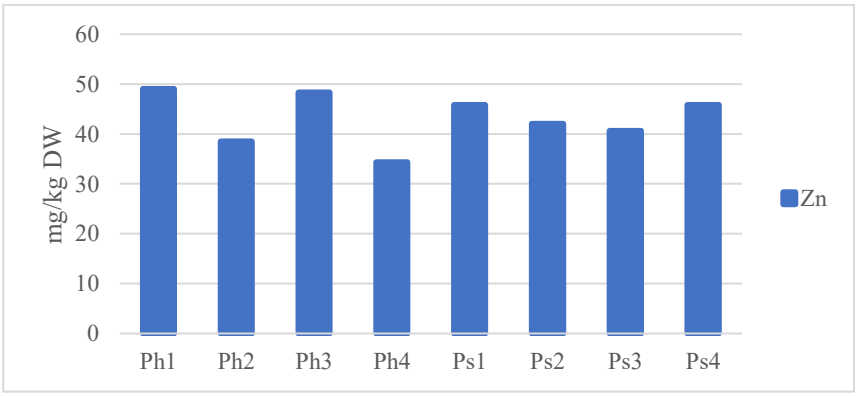


Figure 5. Zinc content (mg/kg dry weight) in paprika samples
Legend: Ph1-Ph4= Hot paprika powder samples; Ps1-Ps4= Sweet paprika powder samples;

Zinc concentrations ranged from approximately 35 to 50 mg/kg DW. The highest values were observed in Ph1 and Ph3, whereas the lowest concentration was recorded in Ph4.

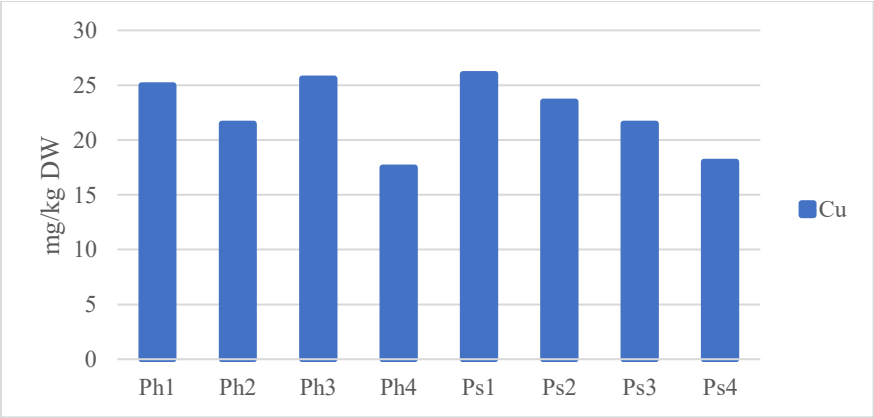


Figure 6. Copper content (mg/kg dry weight) in paprika powder samples
Legend: Ph1-Ph4= Hot paprika powder samples; Ps1-Ps4= Sweet paprika powder samples;

Copper content ranged from approximately 17.5 to 26 mg/kg DW. The highest concentrations were found in Ps1 and Ph3, while the lowest concentrations were detected in samples Ph4 and Ps4 (Figure 6).

Conclusion

The obtained results fall within the ranges reported in the literature for paprika (*Capsicum annuum*) [5,8,12].

The analysis of the mineral composition of the paprika powder samples revealed that potassium was the most abundant element, occurring at concentrations of several grams per 100 g dry weight, followed by calcium.

However, some values, particularly for Fe and Cu, are situated at the upper end of the frequently encountered ranges [5,8,12].

Among the trace elements, iron showed the highest variability, suggesting a strong influence of cultivar origin and cultivation conditions on its accumulation. In contrast, manganese, zinc, and copper were more uniformly distributed across the samples, indicating a relatively stable accumulation pattern in the pepper fruits used for paprika production.

Overall, the results confirm that both sweet and hot paprika powders represent valuable dietary sources of essential minerals and contribute significantly to their nutritional value.

References

[1] Hernández-Ortega, M., Ortiz-Moreno, A., Hernández-Navarro, M. D., Chamorro-Cevallos, G., Dorantes-Alvarez, L., Necoechea-Mondragón, H. Food Science and Human Wellness, 9(4), (2020), 329-339.

[2] Khan, N., Ahmed, M. J., Shah, S. Z. A. Pure and Applied Biology, 8(2), (2019), 1338-1347.

[3] Kim, J. S., Ahn, J., Lee, S. J., Moon, B. K. Foods, 11(22), (2022), 3684.

[4] Lakshmipriya, A., Shenbagavalli, S., Prabhu, T., Saravanapandiyan, P., Jayabalakrishnan, R. M., & Pavithra, S. I. Annals of Phytomedicine, 14(1), (2025), 377-387.

[5] Michel, N. A., Assanvo, B. J., Atchowo, E. J., Djaman, A. J. International Journal of Environment, Agriculture and Biotechnology, (2022),127-136.

[6] Michel, N. A., Mamadou, D., Adama, C., Joseph, D. A. European Journal of Applied Sciences–Vol, 9(4), (2021), 97-107.

[7] Nadeem, M., Anjum, F. M., Khan, M. I., Tehseen, S., El-Ghorab, A., & Sultan, J. I. International Journal of Food Properties, 24(1), (2021), 1516-1536.

[8] Ordog, A., Poór, P., Stajner, D., Popovic, B., Bátori, Z., & Tari, I. Journal of elementology, 23(2), (2018), 521-530.

[9] Pîrvulescu, L., Research Journal of Agricultural Science ,47(2), (2015), 259-262.

[10] Primožič, S., Terro, C., Strojnik, L., Šegatin, N., Poklar Ulrih, N., & Ogrinc, N. Foods, 14(13), (2025), 2323.

[11] https://eur-lex.europa.eu/eli/reg/2023/915/oj/eng

[12] https://www.5fructe.ro/valori-nutritionale/condimente-boia-de-ardei--i2028

ADSORPTION BEHAVIOR OF CATIONIC AND ANIONIC DYES ON A Ni(II)–CEPPA–PIPERAZINE COORDINATION MATERIAL

Diana Anghel, Vlad Chiriac, Dana Vlascici, Gheorghe Ilia

Department of Chemistry, West University of Timisoara, 16 Pestalozzi Street, 300115 Timisoara, Romania
e-mail: diana.anghel@e-uvt.ro

Abstract
A Ni(II) coordination material based on 2-carboxyethyl(phenyl)phosphinic acid (CEPPA) and piperazine was investigated for the removal of organic dyes from aqueous solutions. Preliminary adsorption screening was performed using Brilliant Green (BG), Congo Red (CR), Methyl Orange (MO), and Indigo Carmine (IC), and the changes were monitored by UV–Vis spectrophotometry. The highest apparent absorbance decrease was observed for Congo Red (33.1%), followed by Brilliant Green (21.9%) and Indigo Carmine (14.2%), whereas no measurable decrease was observed for Methyl Orange. Congo Red also exhibited a shift of the absorption maximum from approximately 498 to 488 nm after contact with the material. The different responses observed for the investigated dyes suggest that their behavior cannot be explained solely by ionic character and may also depend on molecular structure and adsorbent–adsorbate interactions.

Keywords: Ni(II); CEPPA; piperazine; dye adsorption; UV–Vis spectroscopy

Introduction
Synthetic dyes are widely used in textiles, pharmaceutical, food, and other industrial processes, and their release into aquatic environments represents an important environmental concern. Due to their intense coloration, structural diversity, and in some cases high chemical stability, even relatively low concentrations may affect water quality. Consequently, the development of efficient materials for dye removal from aqueous media remains an active area of research [1], [2].

Among the available treatment methods, adsorption is particularly attractive because of its operational simplicity and the possibility of employing a wide variety of solid materials as adsorbents. Metal–organic and coordination materials containing multifunctional ligands offer considerable structural and chemical versatility, allowing their properties to be tailored through the nature of the metal center and organic ligand [3]. In this context, phosphinate-based coordination materials are of interest because phosphinate groups can participate in different coordination modes, while the incorporation of additional organic components, such as piperazine, may further influence the physicochemical properties of the resulting material.

In the present study, a Ni(II) coordination material based on 2-carboxyethyl(phenyl)phosphinic acid (CEPPA) and piperazine was evaluated as an adsorbent for organic dyes in aqueous media. A preliminary comparative screening was performed using Brilliant Green (BG), Congo Red (CR), Methyl Orange (MO), and Indigo Carmine (IC), comprising both cationic and anionic dyes with different molecular structures. The aim was to investigate whether the material exhibits different affinities toward these dyes under identical experimental conditions and to assess its potential for further development as an adsorbent for organic contaminants.

Experimental

For the preliminary adsorption screening, 5 mg of the Ni(II)–CEPPA–piperazine material was added to 10 mL of each dye solution (20 mg L^{-1}). The suspensions were continuously stirred for 60 min at room temperature. After the adsorption experiment, the solid adsorbent was separated and the supernatants were analyzed by UV–Vis spectroscopy. Brilliant Green (BG), Congo Red (CR), Methyl Orange (MO), and Indigo Carmine (IC) were investigated under identical experimental conditions.

Results and discussion

The adsorption behavior of the Ni(II)–CEPPA–piperazine material was evaluated toward four dyes with different ionic and structural characteristics: Brilliant Green (BG), Congo Red (CR), Methyl Orange (MO), and Indigo Carmine (IC). The UV–Vis spectra recorded before and after 60 min of contact with the adsorbent revealed distinct responses depending on the investigated dye (Table 1).

Table 1.

Dye	Ionic character	λ max (nm)	A_0	A_{60}	Apparent absorbance decrease (%)
Congo Red	Anionic	498	1.361	0.910	33.1
Brilliant Green	Cationic	623	1.954	1.526	21.9
Indigo Carmine	Anionic	610	0.777	0.667	14.2
Methyl Orange	Anionic	470	1.628	1.678	No measurable decrease

For Congo Red, the absorbance measured at 498 nm decreased from 1.361 to 0.910, corresponding to an apparent absorbance reduction of approximately 33.1%, the highest value observed among the investigated dyes. In addition to the decrease in absorbance, the absorption maximum shifted from approximately 498 to 488 nm after contact with the material. This spectral shift may reflect changes in the molecular environment of CR after contact with the material. However, pH-controlled measurements and additional experiments are required to clarify the origin of this spectral change.

Brilliant Green, the cationic dye included in the study, also exhibited a substantial decrease in absorbance. At its experimental absorption maximum of 623 nm, the absorbance decreased from 1.954 to 1.526, representing an apparent reduction of approximately 21.9% after 60 min. Indigo Carmine showed a smaller but clearly observable change, with the absorbance at 610 nm decreasing from 0.777 to 0.667, corresponding to approximately 14.2%.

In contrast, Methyl Orange showed no decrease in absorbance under the investigated conditions. The absorbance at 470 nm changed from 1.628 to 1.678 after 60 min. Considering the relatively small magnitude of this variation, the result does not indicate measurable removal of MO during the preliminary screening experiment.

Conclusion

The Ni(II)–CEPPA–piperazine material exhibited different adsorption behavior toward the investigated dyes, following the order CR > BG > IC, while no measurable removal was observed for MO under the tested conditions. The strongest response was obtained for the anionic Congo Red, indicating that dye charge alone does not determine the interaction with

the material. These preliminary results suggest that factors beyond dye charge, including molecular structure and adsorbent–adsorbate interactions, may influence the observed behavior. Further studies are required to quantitatively evaluate the adsorption capacity and elucidate the underlying adsorption mechanisms.

Acknowledgements
The authors acknowledge the institutional support provided by the West University of Timisoara.

References
[1] M.J. Uddin, R.E. Ampiaw, W. Lee, Chemosphere 284 (2021) 131314.
[2] M.S. Khan, M. Khalid, M. Shahid, Mater. Adv. 1 (2020) 1575–1601.
[3] V.K.-M. Au, Front. Chem. 8 (2020) 708.

IRON SCRAPS DERIVED WASTES ANODE USED IN ELECTROCOAGULATION PROCESS FOR RECOVERY OF PHOSPHOROUS FROM WASTEWATER

Mihaela Gabriela Roșu[1], Anamaria Baciu [2], Corina Orha[3], Sorina Ilies[4], Costinel Flintă[1], Florica Manea [1*]

*[1] Department of Applied Chemistry and Engineering of Inorganic Compounds and Environment, Politehnica University of Timisoara, Blv. Vasile Parvan No. 6, 300223 Timisoara, Romania; mihaela-gabriela.staicu@student.tuiasi.ro, costinel.flinta@datcomp.ro, *florica.manea@upt.ro*

[2]Renewable Energy Research Institute, Politehnica University of Timisoara, Gavril Muzicescu Street, no. 138, 300501 Timisoara, Romania, anamaria.baciu@upt.ro*

[3]National Institute for Research and Development in Electrochemistry and Condensed Matter, Timisoara, Romania, orha.corina@gmail.com

[4]"Coriolan Drăgulescu" Institute of Chemistry, Romanian Academy, 24 Mihai Viteazu Bvd., 300223 Timisoara, Romania, sorinailies@acad-icht.tm.edu.ro

Abstract

In this study, iron wastes resulting from mechanical workshops were characterized and tested for recovery of phosphorous (P) from simulated wastewater. Iron wastes were characterized morpho-structurally through atomic force microscopy (AFM), energy dispersive X-ray (EDX) and X-ray diffraction (XRD). Electrochemical characterization by cyclic voltammetry (CV) provided valuable information for operating conditions of electrocoagulation (EC) in P recovery. Preliminary testing of EC using iron scraps anode allowed a P recovery degree higher than 90%.

Introduction

Electrocoagulation (EC) is one of the wastewater treatment technologies that is suitable to remove a large variety of both organic and inorganic contaminants. It also has been used in resource recovery, in which nutrient recovery, *e.g.*, phosphorous (P), completes the classical treatment objectives. Considering a broad-based treatment with a high pollutant removal efficiency [1]. EC does not require the storage of reagents because the coagulant is generated in situ. Also, it generates less sludge in comparison with conventional coagulation.

Considering recovery of P from municipal wastewater, the iron anodes can be taking into account through Fe^{2+} and Fe^{3+} species released and rapidly hydrolyzed to iron oxides, which binds phosphate through precipitation and adsorption [2-3]. The main operating cost of EC is given by the periodic replacement of the sacrificial anode. Thus, the use of metallic waste instead of the commercial electrode plates should reduce this cost and it is in accordance with the circular economy requirement [4]. The iron scraps resulting from the mechanical workshops are particularly suitable, being abundant, available at no cost and characterized by a high iron content. Their use as anodes has been reported for phosphate removal using magnetically attracted scraps [5], for the phosphate immobilization by the generated iron oxides [6] and, more recently, in packed-bed configurations for phosphonates removal, where the iron scrap anode proved to be less predisposed to passivation than a conventional iron anode [7]. However, the electrochemical behavior of this type of waste depends on its composition and surface state, which are variable and rarely characterized in detail. This study aims morpho-structural and electrochemical characterization of iron scrapes wastes for their testing as anode in EC process for recovery of P from simulated wastewaters.

Experimental

a. *Morpho-structural and electrochemical characterization*

The surface morphology of iron waste was examined by atomic force microscopy (AFM, Nanosurf EasyScan 2 Advanced Research), the images being processed with the Nanosurf EasyScan2 software. The elemental composition was determined semi-quantitatively by energy dispersive X-ray analysis (EDX), as a module of the scanning electron microscope (Inspect S, FEI Company, The Netherlands). The crystalline structure was characterized by X-ray diffraction (XRD, PANalytical X'Pert Pro MPD diffractometer) with Cu-Kα radiation and PixCEL detector, at 45 kV and 30 mA, the data processing for phase identification being performed with X'Pert HighScore Plus software. The diffuse reflectance spectra were recorded with a Lambda 950 UV-Vis-NIR spectrometer equipped with an integrating sphere.
The electrochemical characterization was performed by cyclic voltammetry (CV) using a classical three-electrode cell system and an Autolab potentiostat/galvanostat PGSTAT 302 (Eco Chemie, The Netherlands), consisting of the iron scraps working electrode, a platinum counter electrode and a saturated calomel electrode (SCE) as reference. The voltammograms were recorded in 0.1 M Na_2SO_4 and 0.1 M NaOH supporting electrolytes, within the potential range of -2 V to +1.5 V vs. SCE, at 0.05 $V \cdot s^{-1}$, and at scan rates ranged between 0.01 and 0.20 $V \cdot s^{-1}$.

b. *The electrochemical set-up and analytical methods for P recovery*

The electrochemical set-up presented in Figure 1, consisted of a soluble anode made of iron scraps resulting in waste from mechanical workshops, fixed within a perforated plexiglass casing, and a stainless-steel cathode, both placed vertically within a rectangular plexiglass cell and connected to a programmable DC power source. The active areas of the anode and of the cathode were 65 cm^2 and 70 cm^2, and all the experiments were carried out under galvanostatic regime. Before each experiment, the anode was activated by immersion in 10% NaOH solution for 2 min, followed by 10% H_2SO_4 solution for 2 min. For comparison, a conventional iron plate with an active area of 73 cm^2 was tested under the same operating conditions.

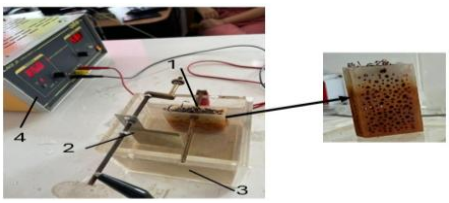


Figure 1. Image of the electrocoagulation (EC) set-up: 1 - anode electrode: Fe scrap, 2- cathode electrode: stainless steel, 3 - plexiglass rectangular cell, 4 - programmable DC power source.

The electrochemical dissolution tests were carried out in 700 cm^3 of solution, at the applied current of 0.25 A for 60 min. The theoretical amount of dissolved iron was calculated based on Faraday's law, in accordance with Equation (1), considering the two-electron oxidation of iron to Fe^{2+}:

$$m_{theorethic} = \frac{I \cdot t \cdot M}{n \cdot F}, (g) \quad (1)$$

where I is the applied current (A), t is the electrolysis time (s), M is the atomic mass of iron (55.845 $g \cdot mol^{-1}$), n is the number of electrons involved in the anodic dissolution and F is the Faraday constant (96,485 $C \cdot mol^{-1}$). The amount of iron actually dissolved from the anode (m_{exp}) was determined based on the mass loss of the electrode, and the soluble iron concentration by the 1,10-phenanthroline method, in accordance with the standard SR ISO 6332:1996, using a Varian Cary 100 Conc UV/VIS spectrophotometer (California, USA).

The energy consumption was assessed per volume of treated water (Wsp) using Equation (2):

$$W_{sp} = \frac{U \cdot I \cdot t}{V}, (W \cdot h \cdot dm^{-3}) \quad (2)$$

where U is the cell voltage (V), t is the electrolysis time (h) and Vs is the volume of the treated solution (dm^3).

The P recovery tests were carried out in 700 cm^3 of synthetic solution containing 140 $mg \cdot dm^{-3}$ PO_4^{3-}, at the applied current of 1.0 A for 60 min, and the recovery degree was calculated as $\eta = \frac{C_i - C_f}{C_f} \cdot 100, (\%)$, where C_i and C_f are the initial and the final phosphate concentrations.

The phosphate concentration was determined spectrophotometrically by the ammonium molybdate method, in accordance with the standard SR EN ISO 6878:2005, and the soluble iron concentration by the 1,10-phenanthroline method, in accordance with the standard SR ISO 6332:1996, using a Varian Cary 100 Conc UV/VIS spectrophotometer (California, USA).

Results and discussion

a. Morpho-structural and electrochemical characterization

The three-dimensional AFM map of the scanned area of 1.12 × 1.12 µm (Figure 2a) shows an irregular and rough surface, as it was expected for a material resulting from the mechanical machining. Figure 2b shows that the height distribution extends over a range of about 130 nm, with a maximum frequency at about 78 nm.

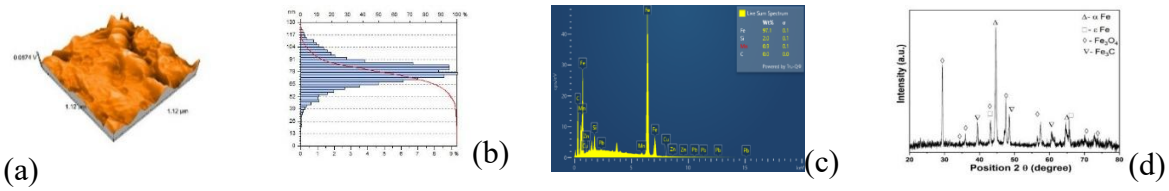


Figure 2. Characterization of the iron scraps electrode: (a) 3D AFM; (b) height distribution; (c) EDX spectrum; (d) XRD pattern;

The EDX analysis performed on three scanned areas (Figure 2c) shows a consistent composition, *i.e.*, 97.1–98.1% Fe, 1.1–2.0% Si and 0.8–0.9% Mn, which corresponds to a low-alloy carbon steel scrap. Figure 2d shows the diffraction peaks observed at 2θ = 43.5 °, 51.0° and 74.5 °, which were assigned to the (111), (200) and (220) planes of the face-centred cubic phase.

Cyclic voltammograms were recorded within the extended potential range in both supporting electrolytes in order to evaluate the anodic dissolution of the iron scraps electrode (Figure 3a).

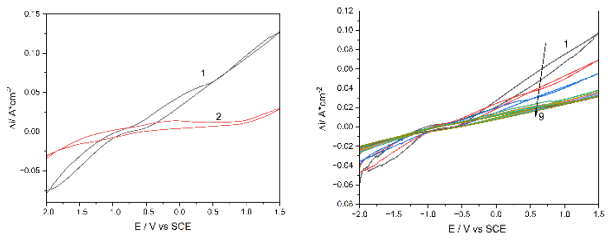


Figure 3. Cyclic voltammograms recorded in 0.1 M Na_2SO_4 (curve 1) and 0.1 M NaOH (curve 2) supporting electrolyte at the iron scraps electrode: (a) potential range: -2 V to +1.5 V vs. SCE at 0.05 $V \cdot s^{-1}$; (b) influence of the scan rate between 0.01 to 0.20 $V \cdot s^{-1}$ (curves 1-9), in 0.1 M Na_2SO_4 supporting electrolyte.

The electrochemical behaviour depends on pH, thus, in 0.1 M Na_2SO_4 supporting electrolyte, the anodic current increased continuously, which is characteristic of the active

dissolution of the metal. In 0.1 M NaOH supporting electrolyte, the anodic current remained low over the most part of the potential range. This behaviour is determined by the passivation of the iron surface through the oxide film formed in the alkaline medium.

The influence of the scan rate was studied in 0.1 M Na_2SO_4 supporting electrolyte (Figure 3c). No well-defined anodic peaks were noticed, but a continuous increase of the current with the potential, as it is characteristic of the active dissolution of a metal. The anodic current density decreased with the scan rate increasing, which shows a passivation effect of ireversible scan rate.

b. Electrochemical dissolution of the iron scraps anode and preliminary testing for phosphate removal

Before the electrocoagulation tests, the electrochemical dosing of Fe^{2+} was verified based on Faraday's law, for the iron scraps anode in comparison with the conventional iron plate anode, both tested under the same operating conditions. The results are gathered in Table 1.

Table 1. Operating conditions and the energy consumption parameters determined for the electrochemical dissolution of the iron scraps and of the iron plate anodes (0.25 A, 60 min, 700 cm^3 solution).

	Parameter	*Iron scraps*	*Iron plate*
Operating conditions	Anode geometric area, cm^2	65	73
	Current density, i, $mA \cdot cm^{-2}$	3.85	3.42
	Cell voltage, U, V	15.7	6.2
	Specific charge, Q', $A \cdot h \cdot dm^{-3}$	0.36	0.36
Results	Theoretical dissolved iron, $mg \cdot dm^{-3}$	372	372
	Dissolved iron, $mg \cdot dm^{-3}$	464	257
	W_{sp}, $kW \cdot h \cdot m^{-3}$	5.6	2.2

Considering the results of the dissolution tests, the iron scraps anode was tested in the electrocoagulation process applied for recovery of phosphate, in two replicates. The results are gathered in Table 2.

Table 2. Operating conditions and the results obtained for recovery of phosphate using the iron scraps anode (1.0 A, 60 min, 700 cm3 solution, initial concentration of PO_4^{3-} = 140 $mg \cdot dm^{-3}$), from simulated wastewater (0.1 M Na_2SO_4)

	Parameter	*Run 1*	*Run 2*
Operating conditions	Current density, i, $mA \cdot cm^{-2}$	15.4	15.4
	Cell voltage, U, V	16.5	16.5
	Specific charge, Q'A·h·dm^{-3}	1.43	1.43
Results	$PO_4^{3-}{}_{final}$, $mg \cdot dm^{-3}$	7	11
	Phosphate recovery degree, %	95.0	92
	Residual iron, $mg \cdot dm^{-3}$	0.6	0,2
	W_{sp}, $kW \cdot h \cdot m^{-3}$	23.6	23.6

Conclusion

The iron waste anode with de composition consisted of 97.1–98.1% Fe, 1.1–2.0% Si and 0.8–0.9% Mn, allowed good recovery degree of P (>90%) from simulated water containing 0.1 M Na_2SO_4. Electrochemical characterization by CV provided the useful information for selecting operation condition. To confront the passivation effect of the iron scraps anode, alkaline medium should be avoided.

Acknowledgements

This work was supported by the project "Innovative Technological Solutions to Circularity and Urban–Industrial Symbiosis within the Water–Energy–Materials–Fertilizers Nexus (ECO NEXUS)," Smart Growth, Digitization and Financial Instruments Program, 2021-2027, MySMIS no. 336912.

References

[1] S.Boinpally, A.Kolla, J.Kainthola, R. Kodali, J. Vemuri, Water Cycle, 4 (2023) 26, https://doi.org/10.1016/j.watcyc.2023.01.001.

[2] Z. Xu, Z. Chen, S. Peng, S. Bai, X. Li, G. Wang, R. Zheng, B.-J. Ni, J. Environn Chem. Eng. 13 (2025) 117695, https://doi.org/10.1016/j.jece.2025.117695.

[3] P.K. Holt, G. W. Barton, C. A. Mitchell, Chemosphere. 59 (2005) 355, https://doi.org/10.1016/j.chemosphere.2004.10.023. (EC)

[4] G. Li, B. Zheng, W. Zhang, Q. Liu, M. Li, Zhang, H. Sustainability 16 (2024) 3836, https://doi.org/10.3390/su16093836.

[5] D. Zhu, X. Hong, K. S. Hui, Water Sci Technol 84 (2021) 216, https://doi.org/10.2166/wst.2021.211.

[6] S. Xie, Z. Bai, W.Shao, C.Wang, J. Qin, Z. Liu, P. Liao, Environm. Sci. Adv. 2 (2023) 898, https://doi.org/10.1039/d3va00024a.

[7] H. Hu, J. Luo, Linyu He, Y. Lei, Water Res, 275 (2025) 123195, https://doi.org/10.1016/j.watres.2025.123195.

ELECTRODES BASED ON Ti/TiO_2-Au/rGO COMPOSITE MATERIAL FOR ELECTROCHEMICAL APPLICATION

Cornelia Bandas, Mina-Ionela Morariu, Corina Orha, Carmen Lazau, Mircea Nicolaescu

National Institute for Research and Development in Electrochemistry and Condensed Matter Timisoara, Condensed Matter Department, 300224 Timisoara,
e-mail: cornelia.bandas@incemc.ro

Abstract

The mechanical, chemical, and physical properties, composite materials represent a significant advancement in materials engineering. Since they are composed of at least two distinct constituents, synergistic interactions can arise within composite materials that surpass the individual properties of the components [1]. In this context, numerous nanostructured composites have been developed for electrochemical applications as a result of recent developments in materials science [2]. In recent years, electrochemical technologies have attracted a lot of interest due to their versatility, high sensitivity and rapid response, and because of their application in energy storage, clinical diagnosis and environmental monitoring fields [3].

This study presents a composite structure based on titanium foil/titanium dioxide/reduced graphene oxide functionalized with gold ions (Ti/TiO_2-Au/rGO) obtained by a simple and efficient spin-coating method, successfully applied in electrochemical doxorubicin (DOX) detection processes. The experimental protocol involves etching of the Ti foil to form a Ti/TiO_2 substrate, followed by the synthesis of the TiO_2-Au/rGO solution, which was deposited by a spin-coating technique on the surface of the Ti/TiO_2 support, to form electrodes based on a Ti/TiO_2-Au/rGO composite structure [4]. The structure and morphology of the as-synthesized composites were investigated in detail using X-ray analysis, Raman spectroscopy, and scanning electron microscopy coupled with an EDX. The electroactive surface area and apparent diffusion coefficient of the composite structures was evaluated by CV in a 1 M KNO_3 and in the presence of 4 mM $K_3Fe(CN)_6$. The potential application in electroanalysis of the electrodes was tested by CV for the detection of the DOX pollutant in 0.1 M NaOH and 1–5 mg L−1 DOX. The obtained results provide new insights into the development of electrochemical sensors for applications in water treatment processes.

Acknowledgements

The authors acknowledge the support of the project granted by the Ministry of Research, Innovation and Digitization, CNCS-UEFISCDI, project number PN-IV-P8-8.3-ROMD-2023-0227 within PNCDI IV and partially project number PN 23 27 01 02 INOMAT, 23-27 29N/2023.

References

[1] D.D.L. Chung, Chung, D.D.L., Ed.; Springer: London, UK, 2003; pp. 213–232.
[2] M.G. Musolino, Nanomaterials 2025, 15, 1638.
[3] G.A. Mello, S.R. Benjamin, F.de Lima, R.F. Dutra, Biosensors 2025, 15, 676.
[4] C. Bandas, M.-I. Morariu, C. Orha, C. Lazau, M. Nicolaescu, Crystals 2026, 16, 338

EXPERIMENTAL INVESTIGATION OF HEAT TRANSFER ENHANCEMENT IN A PCM-BASED THERMAL BATTERY

Radu Banica, Cristina Mosoarca, Florina Stefania Rus, Daniel Ursu, Nicolae Birsan, Alexandra Ioana Bucur, Dan Rosu, Bogdan Taranu

National Institute of Research and Development for Electrochemistry and Condensed Matter, Str. Dr. A. Paunescu Podeanu No.144, 300569 Timisoara, Romania

Phase-change material (PCM)-based thermal energy storage offers a promising approach for increasing the flexibility and efficiency of thermal energy systems by enabling heat storage at nearly constant temperature. In this study, a laboratory-scale thermal battery prototype was developed and experimentally investigated for domestic hot-water applications, using paraffin as the phase-change material. The prototype was designed at a 1:2 scale based on representative household hot-water consumption in Romania and provided an effective thermal storage capacity of approximately 1239 kJ. The system consisted of a 32 L plexiglass tank incorporating a bundle of aluminium tubes filled with paraffin with a melting range of 53–57 °C and immersed in a heat-transfer fluid. Plexiglass flow diffusers were integrated at the inlet and outlet of the tube bundle to improve fluid distribution and minimize flow channeling.

The thermal-hydraulic behaviour of the system was analysed using Reynolds, Nusselt, and Prandtl correlations, while thermal imaging and transient experiments were employed to characterize the charging and discharging processes. To address the intrinsically low thermal conductivity of paraffin, selected PCM-filled tubes were equipped with metallic conductive structures made of steel and copper. The experimental results revealed pronounced axial temperature gradients within the tube bundle, with higher temperatures observed in the lower region and lower temperatures in the upper region. A temperature inversion was also identified within the PCM-filled tubes, indicating the combined influence of heat conduction, natural convection, and internal air circulation during the phase-change process.

The incorporation of metallic conductive structures significantly affected the thermal response of the PCM. Copper-enhanced tubes reached higher temperatures and exhibited greater temperature variation along their height compared with steel-enhanced and unmodified paraffin tubes, indicating more effective heat propagation. The transient charging and discharging experiments further demonstrated that the low thermal conductivity of paraffin represents a major limitation for heat transfer and temperature homogenization within the storage medium. Overall, the results highlight the potential of metallic conductivity enhancement, particularly through copper structures, for improving the thermal response of compact PCM-based thermal batteries and provide experimental insights relevant to the design and optimization of domestic thermal energy storage systems.

Acknowledgment

This work was supported by a project financed by the Ministry of Research, Innovation and Digitization through PN 19 22 01 03 - Innovative technologies for the development of integrated devices for the generation and storage of electrical energy.

POST-HARVEST CHANGES IN THE PHYSICOCHEMICAL QUALITY INDICES OF APPLES DURING STORAGE

Beinșan Carmen[1], Șumălan Radu[1], Șumălan Renata[2*], Velicevici Giancarla[1], Borza Mariana[1], Panici Petre Alexandru[3]

[1]Department of Genetic Engineering, University of Life Sciences "King Michael I" from Timisoara, 300645, Timisoara, Romania; e-mail: carmenbeinsan@usvt.ro, radusumalan@usvt.ro, giancarlavelicevici@usvt.ro, mariana.borza@usvt.ro
[2]Department of Horticulture, University of Life Sciences "King Michael I" from Timisoara, 300645, Timisoara, Romania; e-mail: renatasumalan@usvt.ro
[3]Department of Forestry, University of Life Sciences "King Michael I" from Timisoara, 300645, Timisoara, Romania; e-mail: alexandrupanici@usvt.ro
**Corresponding author: renatasumalan@usvt.ro*

Abstract

This study describes the evolution of physical and physicochemical quality characteristics in three apple varieties – Ligol, Red Jonaprince, and Crimson Snow – over a period of 15 days of storage. The following indices were evaluated: fruit weight, diameter, soluble solids content, pH, titratable acidity, and firmness. Weight and diameter remained practically unchanged, while soluble solids content, pH, acidity, and firmness showed significant changes specific to each variety. In the case of the Ligol variety, the soluble solids content increased from 13.6 to 15.4 °Brix, and the titratable acidity decreased from 7.6 to 4.3 g malic acid/L. The Red Jonaprince variety exhibited a relatively stable soluble solids content and maintained a comparatively high final firmness. The Crimson Snow variety maintained the highest acidity on day 15, but recorded the lowest final firmness. The calculated ratio of soluble solids content to acidity increased in all varieties, with the most pronounced increase observed in the Ligol variety.

Introduction

Apple quality during storage reflects changes in both external physical attributes and internal physicochemical characteristics. Soluble solids, acidity, pH and firmness are widely used descriptors of apple quality and eating quality [2,3]. The supplied experimental report follows three cultivars with contrasting initial fruit size and physicochemical profiles over a 15-day storage period.

The objective of the research was to compare the apple cultivars Ligol, Red Jonaprince, and Crimson Snow regarding each parameter and, furthermore, to monitor the dynamics of the ripening process over the entire two-week period.

Experimental

The experimental material consisted of the Ligol, Red Jonaprince, and Crimson Snow varieties available in commercial centers in western Romania. The apples were stored for two weeks in an ultra-fresh chamber at a constant temperature between 4 and 6°C. Measurements were taken at three distinct time points: initially, after one week (day 8), and after two weeks (day 15).
To characterize the fruit as comprehensively as possible, six quality parameters - comprising the standard panel used in post-harvest studies - were determined: soluble solids (°Brix, measured refractometrically), weight (g), size or caliber (equatorial diameter, in mm), pH (determined using a pH meter on extracted juice), flesh firmness (measured with a penetrometer, in kgf/cm^2), and titratable acidity (expressed in g malic acid/L). These parameters

were selected because they capture both the physical characteristics of the fruit (mass, size, firmness) and the biochemical ones (sugar, pH, acidity), providing a balanced overview of the ripening stage.
The soluble-solids-to-acidity ratio was calculated as soluble solids divided by titratable acidity. Relative change was calculated as (Day 15 − Day 0) / Day 0 × 100.



The plant material used in the experiment

Results and Discussion

The results show a marked contrast between stable biometric traits and changing internal quality attributes. Red Jonaprince had the largest fruit throughout the experiment, Crimson Snow was intermediate, and Ligol was smallest. At Day 0, weight/diameter were 345 g/94 mm, 270 g/84 mm and 130 g/66 mm, respectively. By Day 15, the corresponding values were 340 g/93 mm, 265 g/84 mm and 130 g/66 mm (Figure 1,2). Fruit size and weight are important external quality attributes, but they do not fully describe eating quality [3].

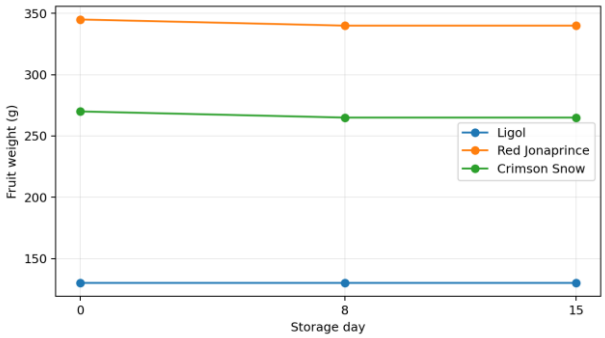


Figure 1. Fruit weight during storage

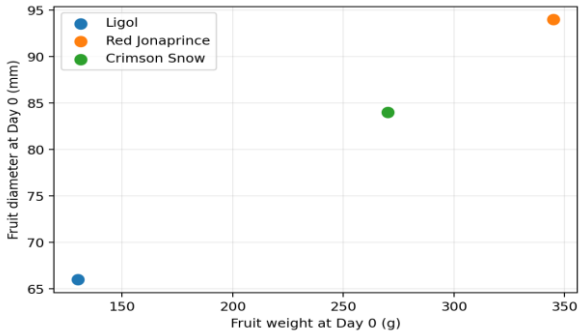


Figure 2. Descriptive relationship between fruit weight and diameter at the initial

Ligol showed a continuous increase in soluble solids from 13.6 to 15.4 °Brix (+13.2%). Crimson Snow increased from 12.2 to 13.4 °Brix (+9.8%), while Red Jonaprince increased at Day 8 and returned to 13.6 °Brix by day 15 (−0.7% net change) (Figure 3). Thus, the largest

net increase occurred in Ligol. The importance of soluble solids as an instrumental quality indicator is also supported by previous apple quality research [2,4].

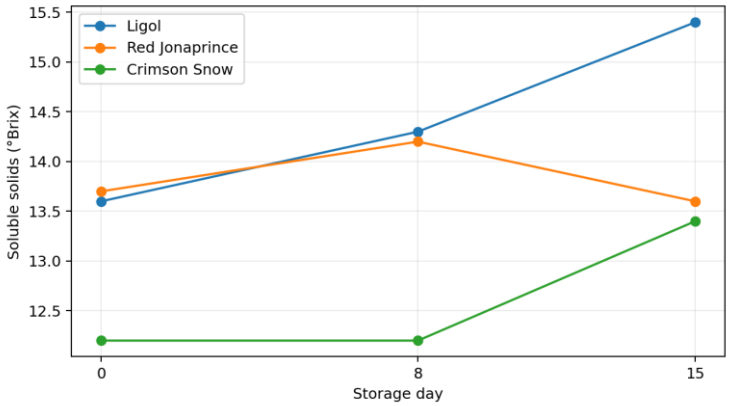


Figure 3. Soluble solids (°Brix) during storage

pH increased in all cultivars: Ligol 3.42→3.72, Red Jonaprince 3.49→3.76 and Crimson Snow 3.27→3.61. Titratable acidity decreased from 7.6→4.3, 6.2→5.3 and 7.7→6.0 g malic acid/L, respectively (Figure 4,5). The opposite trajectories are consistent with progressive maturation. Similar combinations of declining acidity and changing physicochemical quality indicators have been documented during apple storage [1].

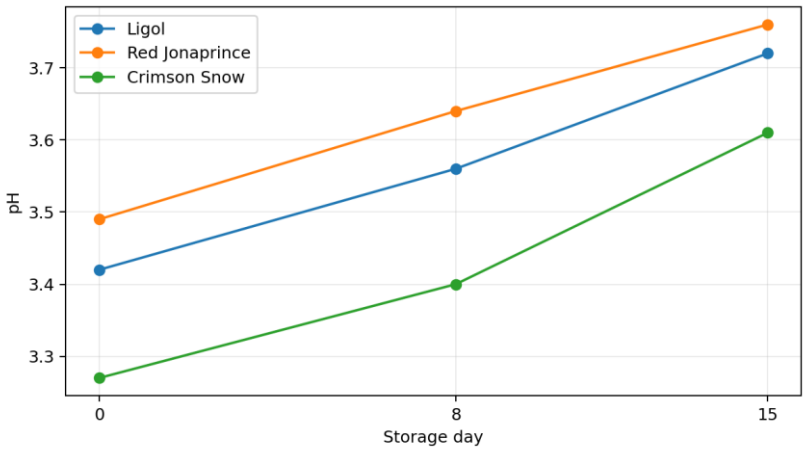


Figure 4. pH evolution during storage

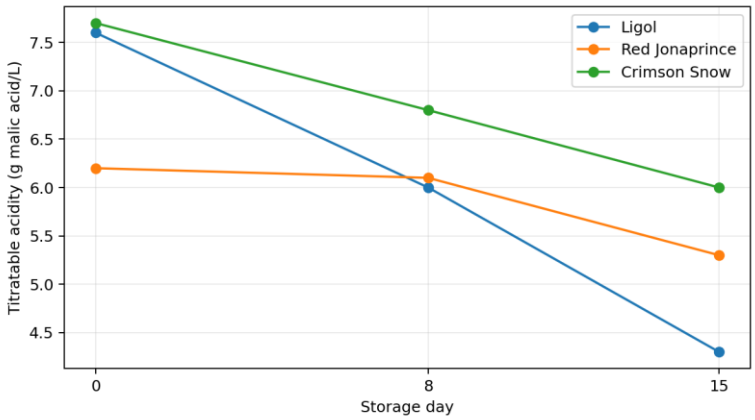


Figure 5. Titratable acidity during storage

Firmness declined in all cultivars. The Day 0→Day 15 changes were − 14.7% for Ligol, − 18.2% for Red Jonaprince and − 20.0% for Crimson Snow. Red Jonaprince retained 6.3 kgf/cm² at day 15, while Crimson Snow reached 5.6 kgf/cm² (Figure 6). Firmness is a commonly used postharvest quality and eating-quality indicator in apples [1,2,4].

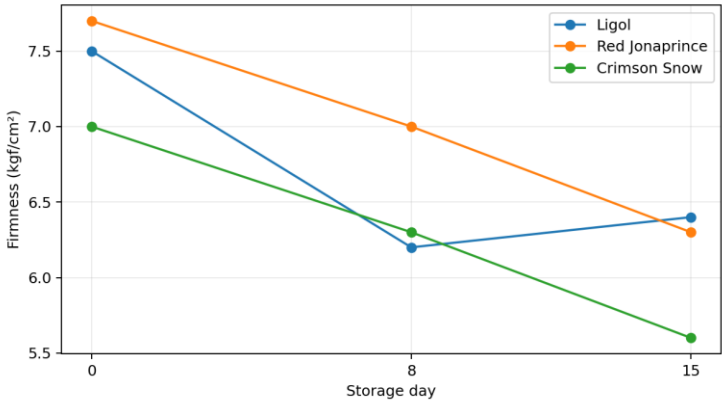


Figure 6. Firmness during storage

The soluble solids-to-acidity ratio increased from 1.79 to 3.58 in Ligol, 2.21 to 2.57 in Red Jonaprince, and 1.58 to 2.23 in Crimson Snow. This descriptive indicator reflects the combined increase in soluble solids and decrease in acidity (Figure 7).

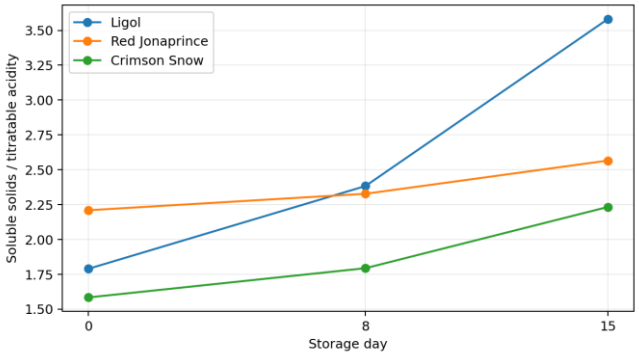


Figure 7. Soluble-solids-to-titratable-acidity ratio

Ligol had the largest relative increase in soluble solids and the largest decline in acidity. Red Jonaprince showed minimal net change in soluble solids. Crimson Snow showed an intermediate increase in soluble solids but the largest relative decline in firmness (Figure 8).

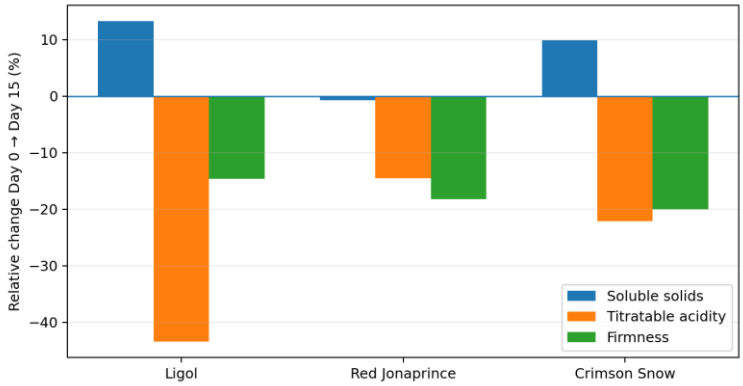


Figure 8. Relative change in selected quality attributes from initially to day 15

Conclusion

During 15 days of storage, fruit weight and diameter were practically stable, while soluble solids, pH, titratable acidity and firmness changed in cultivar-dependent ways. Ligol showed the strongest increase in soluble solids and reduction in acidity; Red Jonaprince retained relatively high firmness; and Crimson Snow retained the highest final acidity. These results are descriptive and support the conclusion that cultivar influences postharvest quality trajectories. Such cultivar - dependent trajectories are consistent with the recognized influence of cultivar and storage conditions on apple quality [3,5].

References

[1] Azzollini, D., et al. Postharvest quality assessment of apple during storage at ambient temperature. Heliyon, 7(8), e07714.(2021). https://doi.org/10.1016/j.heliyon.2021.e07714

[2] Hoehn, E., Gasser, F., Guggenbühl, B., & Künsch, U. Efficacy of instrumental measurements for determination of minimum requirements of firmness, soluble solids, and acidity of several apple varieties in comparison to consumer expectations. Postharvest Biology and Technology, 27(1), 27–37. (2003). https://doi.org/10.1016/S0925-5214(02)00190-4

[3] Musacchi, S., & Serra, S. Apple fruit quality: Overview on pre-harvest factors. Scientia Horticulturae, 234, 409 – 430(2018). https://doi.org/10.1016/j.scienta.2017.12.057

[4] Oraguzie, N., Alspach, P., Volz, R., Whitworth, C., Ranatunga, C., Weskett, R., & Harker, R. Postharvest assessment of fruit quality parameters in apples using both instruments and an expert panel. Postharvest Biology and Technology, 52(3), 279–287. (2009). https://doi.org/10.1016/j.postharvbio.2009.01.004

[5] Woodward, A., et al. Water Loss: A Postharvest Quality Marker in Apple Storage. Food and Bioprocess Technology. (2023). https://doi.org/10.1007/s11947-023-03305-9

ENVIRONMENTAL CONSCIOUSNESS AMONG HIGHER EDUCATION STUDENTS: DOES INCOME MATTER?

László Berényi

Faculty of Public Governance and International Studies, Ludovika University of Public Service, Budapest, H-1038 Budapest, Üllői út 82., Hungary
e-mail: berenyi.laszlo@uni-nke.hu

Abstract
Ultimately, solving global problems depends on individual intentions, decisions, and actions. Supporting pro-environmental behavior requires research because of the diversity of human existence. Even studies with a limited scope could serve as a foundation for further achievements. The study investigates whether opinions about environmental concerns differ among higher education students based on their income. The study examined five environmental attitude items using a sample of 581 Hungarian students. The results show that students with partial income displayed attitudes similar to those with regular income in most cases, while students without their own income showed lower values. However, the study can be considered a pilot experiment; it may contribute to developing targeted surveys to understand the factors influencing pro-environmental attitudes.

Introduction
The turning point in the environmental Kuznets curve hypothesis [1] represents the wealth of a nation, at which point protecting the environment becomes more important than economic growth. Although the hypothesis was not confirmed [2], its message aligns well with understanding individuals' approach to sustainability. Another frequently criticized but still influential theory is Maslow's hierarchy of needs [3]. Although the two theories operate at different levels and serve different purposes, they share a similar underlying logic. Finding evidence to support this idea requires much more effort. From a sustainability perspective, the hierarchy of needs suggests that a person does not address a higher-level need, so a lower-level need remains unsatisfied. If basic physiological and safety needs are sufficiently satisfied, individuals may place greater emphasis on social responsibility connected to belonging needs, self-esteem, and self-actualization.
Income is the source of buying goods and services as the means of satisfying needs. Assuming that better financial opportunities enable people to purchase products with better environmental performance, the question is whether this aligns with environmentally conscious thinking as well.
Several studies have empirically investigated environmental consciousness, including various influencing factors (see [4] [5]), and suggested a positive impact of income opportunities on pro-environmental behavior. However, the direct relationship with environmentally conscious behavior has not been confirmed; Mangleburg and Brown [6] found that the source of money is not a neutral factor, and that income earned from work and money received are associated with different patterns of consumer behavior.
Higher education students play an important transitional role in society. While they are currently learning professional and other skills and preparing themselves for their lives, they are already managing their affairs and making decisions. The increasing number of internship programs makes students more mature and responsible than before. Comparison of students with and without their own income therefore provides an opportunity to examine the relationship between economic autonomy and environmental consciousness. The research

question is whether students' opinions about environmental and sustainability issues differ based on whether they have their own income.

Experimental

The study presents a pilot experiment based on a survey on energy-consciousness [7], including a factor called environmentalism:

- I am concerned about climate change.
- I feel like I can do something to promote sustainability.
- I feel it is my moral duty to conserve energy.
- I turn off the lights and household appliances when I am not using them.
- I am interested in environmental and sustainability issues.

The statements were rated on a 7-point scale in a self-administered online survey. The grouping factor in the analysis was whether the respondent has their own income, with options yes, no, or partially (from scholarship, occasional work, or similar sources).

581 responses were available from students at various Hungarian higher education institutions in 2025 and 2026. 124 students have no own income, 177 have partial income, and 280 have regular own income. The non-parametric Kruskal-Wallis H test was used to test for significant differences among the groups, and the Mann-Whitney U test was used for testing pairwise comparisons.

The main limitations of the study come from its pilot nature. The paper presents only selected survey results. Although a large sample was available for statistical analysis, it is not representative. The questions were not designed for comprehensive evaluation of environmental consciousness, but the results can contribute to a better understanding of student opinions.

Results and discussion

The results show a generally positive attitude to environmental issues among the students. Considering the self-administered nature of data collection and the social expectations around sustainability, a positive-direction distortion can be expected. Sapiro-Wilk's test shows that the variables are not normally distributed ($p < 0.001$). Table 1 summarizes the descriptive statistics, and Figure 1 presents the mean values by grouping variable.

	Mean	Std. Deviation	Skewness (Std. Err. = 0.101)	Kurtosis (Std. Err. = 0.202)	Shapiro-Wilk (p<.001)
I am concerned about climate change.	5.361	1.551	-0.842	-0.019	0.876
I feel like I can do something to promote sustainability.	5.308	1.447	-0.885	0.472	0.889
I feel it is my moral duty to save energy.	5.115	1.455	-0.508	-0.352	0.918
I turn off the lights and household appliances when I am not using them.	6.420	0.964	-2.034	4.620	0.652
I am interested in environmental and sustainability issues.	5.150	1.515	-0.616	-0.281	0.909

Table 1. Descriptive statistics of the survey items

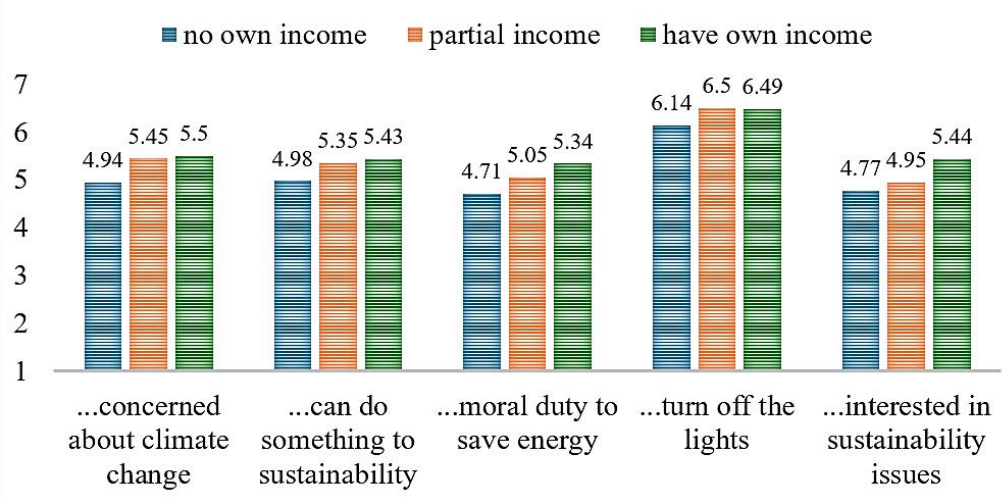


Figure 1. Mean values by grouping variable

The negative values of skewness and kurtosis indicators also confirm a skewed-to-the-left and flatter distribution than normal. An exception is the item about turning off the light and household appliances when not using them. The distribution (Table 2) is leptokurtic in all groups; responses that totally agree (7) are dominant. The Chi-square test for the contingency table ($\chi^2 = 22.47$, df = 12, p = 0.033) shows differences between the preferences in Table 2.

Options	No	Yes	Partially	Total	Total (%)
1	0	1	0	1	0.17%
2	1	1	0	2	0.34%
3	3	5	1	9	1.55%
4	9	4	7	20	3.44%
5	18	19	13	50	8.61%
6	27	61	37	125	21.51%
7	66	189	119	374	64.37%

Table 2. Distribution of the responses by grouping variable for the question 'I turn off the lights and household appliances when I am not using them'

Assuming the same distortion in the subsamples, the comparison offers valuable information. The Kruskal-Wallis H test results are summarized in Table 3. The analysis indicates differences in environmental attitudes among the groups, including the effect sizes (ε^2).

Question	Statistic	df	p	ε^2
...concerned about climate change	12.91	2	0.002	0.019
...can do something to sustainability	9.069	2	0.011	0.012
...moral duty to save energy	16.6	2	< .001	0.025
...turn off the lights	11.94	2	0.003	0.017
...interested in sustainability issues	23.48	2	< .001	0.037

Table 3. Kruskal-Wallis H test results

	...concerned about climate change	...can do something to sustainability	...moral duty to save energy	...turn off the lights	...interested in sustainability issues
Groups: no own income and partial income					
Mann-Whitney U	8940.0	9265.0	9457.5	9124.5	10163.5
Wilcoxon W	16690.0	17015.0	17207.5	16874.5	17913.5
Z	-2.800	-2.360	-2.080	-2.860	-1.112
Asymp. Sig. (2-tailed)	.005	.018	.038	.004	.266
Groups: no own income and have own income					
Mann-Whitney U	13687.0	14277.0	13059.5	14341.5	12770.5
Wilcoxon W	21437.0	22027.0	20809.5	22091.5	20520.5
Z	-3.480	-2.921	-4.061	-3.247	-4.340
Asymp. Sig. (2-tailed)	.001	.003	.000	.001	.000
Groups: patrial income and have own income					
Mann-Whitney U	23857.0	24060.0	22201.0	24647.0	20038.5
Wilcoxon W	39610.0	39813.0	37954.0	40400.0	35791.5
Z	-.692	-.539	-1.919	-.117	-3.529
Asymp. Sig. (2-tailed)	.489	.590	.055	.907	.000

Table 4. Mann-Whitney U test results

Because the Kruskal-Wallis H test results were significant, a pairwise analysis was conducted with the Mann-Whitney U test to explore the patterns (Table 4). Significant results ($p < 0.05$) were found for each question between students without and with their own income. Significant differences were also found between the no- and partial-income groups, except for interest in environmental and sustainability issues, which was the only question that differed significantly between the partial- and own-income groups. In summary, no income groups differ from the others, while students with partial or regular own incomes are close to each other.

Conclusion

The pilot study results among higher education students confirmed differences in environmental consciousness based on having their own income. The responses show generally positive environmental attitudes that may be subject to bias, and further justification was out of the scope of this study.

Students without their own income in the sample are less concerned about climate change; they do not feel a moral duty to save energy, and they are less interested in the topic. At the same time, this group does not feel they can contribute to sustainability. The findings are consistent with the assumption that the experience of having their own income may be associated with higher environmental consciousness. The relatively low effect sizes by the Kruskal-Wallis H test suggest that the problem is more complex than simplifying the influencing factors to having their own income. At the same time, the finding that students with partial income already resemble the group of students with a regular income in many respects emphasizes that the issue is worth addressing. The study implies that higher education students, particularly those without their own income, should be encouraged to develop environmental consciousness. Because no-income students are the least conscious, experiential learning methods, project-based activities, and sustainability-oriented campus initiatives may support these efforts.

References

[1] D.I. Stern, The Environmental Kuznets Curve, International Society for Ecological Economics, Internet Encyclopaedia of Ecological Economics. Rensselaer Polytechnic Institute, Troy, 2003

[2] D.I. Stern, The Rise and Fall of the Environmental Kuznets Curve. World Development 32(8) (2004), 1419-1439.

[3] A.H. Maslow, Motivation and Personality, Harper & Row, New York, 1954, p. 411.

[4] S. Du, G. Cao, Y. Huang, The effect of income satisfaction on the relationship between income class and pro-environment behavior. Applied Economic Letters 31(1) (2024), 61-64.

[5] X. Piao, S. Managi, Determinants of Pro-Environmental Behaviour: Effects of Socioeconomic, Subjective, and Psychological Well-Being Factors From 37 Countries, Humanities and Social Sciences Communications 11 (2024), 1293.

[6] T.F. Mangleburg, J.J. Brown, Teens' Sources of Income: Jobs and Allowances, Journal of Consumer Marketing, 12(1) (1995), 47-59.

[7] L. Berényi, Using Energy Saving Functions: Personal Opinions, Proceedings of the 31st International Symposium on Analytical and Environmental Problems, University of Szeged, Szeged, 2025, pp. 270-274.

SOME ASPECTS REGARDING THE IMPACT OF RENEWABLE ENERGY INFRASTRUCTURE ON SOIL AND AGRICULTURAL LAND USE

Blenesi Dima Attila[1], Popa Nelu Daniel[1], Casiana Mihuț[2], Anișoara Duma-Copcea[2], Okros Adalbert[2]

[1] Department of Agricultural Technologies, Faculty of Agriculture, "King Mihai I" University of Life Sciences of Timișoara, Calea Aradului nr. 119, 300645 Timișoara, Timiș county, Romania
[2] Department of Soil Sciences, Faculty of Agriculture, "King Mihai I" University of Life Sciences of Timișoara, Calea Aradului nr. 119, 300645 Timișoara, Timiș county, Romania
Email: anisoaradumacopcea@usvt.ro

Abstract

The transition towards an energy system based on renewable sources represents an important component of policies aimed at reducing greenhouse gas emissions and decreasing dependence on fossil fuels. However, the expansion of renewable energy infrastructure generates new interactions between energy systems, land resources, and terrestrial ecosystems. This paper critically analyses the scientific literature concerning the impact of renewable energy on soil and land use, with particular emphasis on agricultural land. The main effects associated with photovoltaic and wind energy infrastructure and energy biomass production are examined, together with the opportunities offered by agrivoltaic systems. The analysis shows that the impact on land depends on the technology, site characteristics, construction methods, and subsequent land management. In the case of photovoltaic systems, recent literature indicates changes in soil temperature and moisture, radiation regimes, and surface processes, while also identifying opportunities for water conservation and multifunctional land-use systems. Agrivoltaics may reduce direct competition between energy and agricultural production; however, its performance depends on crop type, panel configuration, and local pedoclimatic conditions. In the case of biomass, the main issue is the competition between land use for food, feed, and energy production. The paper advocates the integration of pedological, agricultural, hydrological, ecological, and energy criteria into land-use planning and identifies research priorities concerning long-term soil monitoring and the assessment of land multifunctionality.

Introduction

Renewable energy represents one of the fundamental components of the transition towards a low-emission energy system. Solar, wind, hydropower, geothermal energy, and bioenergy contribute to the diversification of energy sources and the reduction of dependence on fossil fuels. The integration of these sources into energy systems may provide important benefits in terms of reducing emissions and promoting sustainable development, including in agriculture, where renewable energy can be used for irrigation, transportation, processing, storage, and refrigeration [1].

At the same time, the energy transition generates a new dimension of competition for resources. Energy is not produced in an abstract space but requires infrastructure, land, and access to natural resources. Consequently, the expansion of renewable energy systems may influence land-use patterns, ecosystem functions, and soil properties.

This issue is particularly relevant to agriculture. Agricultural land simultaneously represents a basis for food production, a carbon reservoir, a habitat for organisms, a component of the hydrological cycle, and an economic resource. The Food and Agriculture Organization of the United Nations emphasizes the fundamental importance of land and soil for agri-food systems and terrestrial biodiversity [2].

Therefore, the development of energy infrastructure on agricultural land should be assessed not only in terms of the area occupied but also in terms of the functions performed by the land before, during, and after the operational period of the installation.
Recent literature demonstrates that the relationship between renewable energy and land is more complex than simply considering the area occupied. A recent global systematic review of photovoltaic systems identified many studies and reported significant changes in variables such as soil temperature, soil water content, surface temperature, and wind speed [3]. At the same time, a systematic review focusing on soil carbon identified only 18 studies worldwide concerning interactions between ground-mounted photovoltaic installations and soil carbon, indicating significant gaps in knowledge concerning long-term effects [4].
In this context, the aim of this paper is to analyze the interaction between renewable energy infrastructure, soil, and agricultural land use and to identify land-management approaches compatible with energy production, agricultural production, and the conservation of ecosystem functions.
The specific objectives of this paper are:

1. to identify the main forms of impact of renewable energy infrastructure on soil;
2. to analyze changes in land use and land functionality;
3. to compare the main renewable energy technologies from the perspective of their interaction with land;
4. to assess the role of agrivoltaics as a form of multifunctional land use;

Experimental

The paper represents an integrative review of the scientific literature, based on relevant studies concerning the relationship between renewable energy, soil, and land use. The analysis focused primarily on recent scientific literature, while also considering fundamental studies that contributed to the development of the concepts of land competition, land-use change, and energy biomass production.
The literature was thematically classified into the following categories: physical soil properties; thermal and hydrological regimes; soil organic carbon; land occupation and land-use change; agriculture and food production; agrivoltaics; wind energy; energy crops and bioenergy; biodiversity; land-use planning.
The literature search considered combinations of terms such as: renewable energy, solar energy, photovoltaic, wind energy, bioenergy, agricultural land, soil, soil properties, soil carbon, soil water, soil temperature, land use, land-use change, agrivoltaics, erosion, soil compaction.
For each technological category, the following aspects were considered: type of land affected; area and type of land occupation; changes in soil properties; changes in the hydrological regime; effects on vegetation; compatibility with agricultural activities; effects on biodiversity; potential for multifunctional use; impact mitigation measures. This approach makes it possible to move from a site-specific assessment of individual technologies towards an analysis of the land–energy–agriculture system.

Results and discussions

Renewable energy and pressure on land resources

The expansion of renewable energy does not eliminate pressure on natural resources but changes its nature. Fossil fuels require the extraction and processing of geological resources, whereas renewable energy sources use natural energy flows and require terrestrial infrastructure. This distinction is essential. Photovoltaic panels, wind turbines, hydropower infrastructure, and energy crops have different land-use footprints and generate different effects on soil and ecosystems. In the case of solar energy, the expansion of ground-mounted photovoltaic installations may generate a significant increase in land demand. Studies

concerning land requirements for solar energy development have shown that, under scenarios of high renewable energy penetration, the affected areas may become significant at regional level, while changes in land cover may also have implications for carbon balances [5]. This situation generates what may be described as land-use functional conflict, since the same area may simultaneously have: agricultural value; energy value; ecological value; hydrological value; landscape value; economic and social value. Consequently, the criterion of "land availability" is not sufficient when selecting energy infrastructure sites. It is necessary to assess the value and functions of the land.

Soil compaction and structural disturbance

The construction of renewable energy installations involves excavation, land levelling, access-road development, transportation of materials, and machinery traffic.

These activities may cause: increased bulk density; reduced porosity; changes in aggregate structure; reduced infiltration; increased surface runoff; degradation of the upper soil layer.

Soil compaction is important because it modifies the relationships between the solid, liquid, and gaseous phases of soil and may reduce its productive and hydrological functions.

In the case of energy infrastructure, the most significant effects are generally associated with the construction phase and auxiliary infrastructure, making site organization and construction management important elements of soil protection.

Thermal regime

The installation of photovoltaic panels changes the radiation balance of the surface and the distribution of solar radiation. An analysis published in 2026, synthesizing over a hundred studies, identified an average significant reduction in soil temperature of approximately 2.42 °C within photovoltaic systems compared with reference surfaces [3].

This value represents an aggregated result and should not be automatically extrapolated to every site. Soil response depends on climate, surface cover, panel configuration, orientation, height, and vegetation management.

Soil water regime, erosion and changes in surface runoff

The same meta-analysis reported an average significant increase in soil water content of approximately 38.6% within the analyzed photovoltaic systems [3].

This effect may be associated with reduced direct radiation and changes in the surface energy balance. However, the result must be interpreted carefully because rainfall reaching the panels is redistributed across the soil surface and may generate areas of increased accumulation or preferential runoff. Therefore, the effect on soil water may be simultaneously: beneficial through reduced evaporation and potentially adverse through rainfall redistribution.

Construction activities may increase land vulnerability to erosion through vegetation removal and disturbance of the upper soil layer. The risk is particularly relevant in: sloping areas; soils highly susceptible to erosion; areas exposed to intense rainfall; surfaces without vegetation cover; infrastructure with inadequate water drainage systems.

In photovoltaic systems, water runoff may become concentrated along panel edges. Consequently, installation design should consider panel geometry, row spacing, slope, and the hydrological properties of the soil. Erosion-control measures include: maintaining vegetation cover; limiting exposed soil surfaces; controlling machinery traffic; collecting and dispersing runoff in a controlled manner; rapidly restoring disturbed areas.

Photovoltaic energy and agricultural land

Ground-mounted photovoltaic parks located on agricultural land represent one of the most important contemporary issues concerning the relationship between energy and agriculture.

Their expansion may result in: reduction of available agricultural land; parcel fragmentation; changes in land accessibility; modification of the microclimatic regime; changes in land use.

However, a distinction must be made between land occupation and the permanent loss of agricultural function. Under certain configurations, the land between photovoltaic panels may

remain vegetated or may be used for grazing. In other situations, photovoltaic systems can be integrated into agricultural production systems. This approach leads to the concept of agrivoltaics. Agrivoltaics involves the simultaneous use of the same land area for agricultural production and electricity generation. The concept directly addresses one of the main issues identified in this paper: how can the conflict between food production and energy production be reduced without sacrificing the essential functions of agricultural land.

A previous systematic review published in 2024 shows that the effects of agrivoltaics on crop yield vary according to crop species and location, while also identifying potential benefits concerning water consumption and crop protection [6]. More recently, a 2026 meta-analysis based on more than sixty studies analyzed energy performance, soil parameters, and agricultural production simultaneously. The results indicated substantial heterogeneity among technological configurations and crops and highlighted the role of panel configuration and crop shade tolerance [7].

Wind energy and agricultural land use

Wind energy presents a distinctive situation regarding land use. The total area of a wind farm may be relatively large because of the distances required between turbines, while the area permanently occupied by foundations, platforms, access roads, and other infrastructure represents only a fraction of the total project area. Therefore, the land between turbines may, in many cases, continue to be used for agriculture or grazing. This situation demonstrates the need for a more precise indicator than simply "wind farm area". Impact assessment should distinguish between: project area → disturbed area → permanently occupied area → area retaining its agricultural function. At the same time, wind energy may generate landscape fragmentation and transformation.

Energy Biomass and Competition for Land

In the case of energy biomass, the relationship with land differs from that of solar and wind energy. Biomass may originate from: agricultural residues; forestry residues; energy crops; agro-industrial by-products; organic waste. When biomass is obtained from crops specifically cultivated for energy purposes, direct competition for land occurs. The scientific literature has long analyzed the "food versus fuel" issue, while more recent research proposes a broader food–feed–fuel perspective, in which the same resource may be required simultaneously for food, feed, and energy production [9].

A systematic review concerning biomass competition identified trade-offs between different land and resource uses and highlighted the importance of crop yields, land availability, and policy frameworks [10]. From the perspective of land-resource conservation, the use of agricultural and forestry residues and by-products may reduce direct competition with food production. The literature also supports directing energy biomass production towards residues and towards land that is not required for food or fibre production [11].

Biodiversity and ecosystem functions

Energy-related impacts should be assessed beyond the physical properties of soil.

A recent review of biodiversity and solar energy sitting indicates that the integration of biodiversity criteria into the site-selection process remains inconsistent [12]. Therefore, land assessment before renewable energy infrastructure development should consider not only soil fertility and economic value but also ecological value. From this perspective, degraded or highly artificialised land may offer advantages for energy infrastructure development, provided that technical and grid-connection conditions are favorable.

Conclusions

The expansion of renewable energy represents an important component of the transition towards a low-emission energy system; however, the development of associated infrastructure must be analyzed in direct relation to land resources.

The impact on soil and land is not uniform. It depends on technology, site characteristics, pedoclimatic conditions, intensity of intervention, and land-management practices.
For photovoltaic systems, recent literature indicates significant changes in soil temperature and moisture, although responses depend strongly on local conditions [3]. At the same time, knowledge concerning the effects on soil carbon remains limited [4].
Wind energy presents a different situation because the area permanently occupied by infrastructure may be considerably smaller than the total project area, allowing agricultural use to continue between turbines in many cases.
In the case of energy biomass, the main challenge is competition for resources between food, feed, and energy production. The utilisation of agricultural and forestry residues and by-products may help reduce this competition [10, 11].
Among the directions analysed, agrivoltaics is of particular interest for agricultural land, as it offers the possibility of simultaneously using the same area for energy and agricultural production. Nevertheless, its performance depends on crop type, climate, system configuration, and land properties [6, 7]. Consequently, renewable energy development should be accompanied by a change in land-use planning paradigms. The fundamental question should not be only "where can energy be produced?", but rather: "where can renewable energy be produced while maintaining or, where possible, improving the agricultural, hydrological, and ecological functions of the land?"
From this perspective, land should be regarded as a multifunctional resource – agricultural, ecological, hydrological, economic, and energetic. Maintaining its productive and ecological capacity should be a fundamental condition for the development of renewable energy infrastructure.

Bibliography

[1] FAO. *Renewable energy for agriculture*. Food and Agriculture Organization of the United Nations.
[2] FAO. *Land overview – Land, Soil and Water*. Food and Agriculture Organization of the United Nations.
[3] He, T., Zhang, L., Qiao, Z., Zheng, S., Li, X., Lu, K., Hao, Y. (2026). Land surface process alterations caused by solar photovoltaic systems: A systematic review and future framework from global evidence. *Geography and Sustainability*, 7(4), 100488.
[4] *Impacts of photovoltaic solar energy on soil carbon: A global systematic review and framework* (2025). *Renewable and Sustainable Energy Reviews*, 208, 115032.
[5] van de Ven, D.-J., Capellán-Pérez, I., Arto, I., Cazcarro, I., De Castro, C., Patel, P., González-Eguino, M. (2021). The potential land requirements and related land use change emissions of solar energy. *Scientific Reports*, 11, 2907.
[6] *Agrivoltaics, a promising new tool for electricity and food production: A systematic review* (2024). *Renewable and Sustainable Energy Reviews*, 192, 114277.
[7] Barros, J. S. G., Barros, T. A. S., Miele, M. J., Oleto, R. C. V., Teruel, B. (2026). Agrivoltaic Systems: Systematic Review and Meta-Analysis Relating Energy, Soil, and Crop Parameters. *Annual Review of Environment and Resources*, 51.
[8] Maximov, A. et al. (2026). Multi-dimensional ecological impacts of utility-scale solar and wind energy across terrestrial ecosystems: A systematic review. *Journal of Environmental Management*, 391, 129017.
[9] Rathmann, R., Szklo, A., Schaeffer, R. (2010). Land use competition for production of food and liquid biofuels: An analysis of the arguments in the current debate. *Renewable Energy*, 35(1), 14–22.
[10] *The battle for biomass: A systematic review of food-feed-fuel competition* (2020). *Global Food Security*, 25, 100330.

[11] Fritsche, U. R., Sims, R. E. H., Monti, A. (2010). Direct and indirect land-use competition issues for energy crops and their sustainable production – an overview. *Biofuels, Bioproducts and Biorefining*, 4, 692–704.
[12] Levin, M. O. et al. (2025). Bibliographic synthesis of biodiversity-relevant criteria for solar energy siting. *Renewable and Sustainable Energy Reviews*, 223, 116026.

SOME CONSIDERATIONS REGARDING THE ENERGY CROPS IMPACT ON AGRICULTURE AND AGRICULTURAL LAND

Blenesi Dima Attila[1], Popa Nelu Daniel[1], Casiana Mihuț[2], Anișoara Duma-Copcea[2], Okros Adalbert[2]

[1] Department of Agricultural Technologies, Faculty of Agriculture, "King Mihai I" University of Life Sciences of Timișoara, Calea Aradului nr. 119, 300645 Timișoara, Timiș county, Romania
[2] Department of Soil Sciences, Faculty of Agriculture, "King Mihai I" University of Life Sciences of Timișoara, Calea Aradului nr. 119, 300645 Timișoara, Timiș county, Romania
Email: adalbertokros@usvt.ro

Abstract

The increasing demand for renewable energy has intensified interest in biomass as an alternative energy resource and has stimulated the development of dedicated energy crops. The expansion of such crops creates new opportunities for agricultural diversification, rural development and the utilization of marginal or degraded land, but may also generate competition for agricultural land, water resources and other natural resources. The objective of this paper is to analyze the main effects of energy crops on agriculture and agricultural land, with particular emphasis on soil properties, soil organic carbon, water resources, erosion, biodiversity, greenhouse-gas emissions and the competition between food and energy production. Conversion of arable land to perennial energy crops may increase soil organic carbon and reduce the intensity of soil disturbance, whereas conversion of forests or other high-carbon ecosystems may result in carbon losses and negative environmental effects. Energy-crop systems may also influence biodiversity positively or negatively depending on landscape structure and management. The sustainable development of energy crops therefore requires an integrated land-management approach in which agricultural productivity, food security, soil conservation, water availability, biodiversity and greenhouse-gas emissions are considered simultaneously.

Introduction

The transition towards renewable and low-carbon energy systems has increased the importance of biomass as an energy resource. Agricultural biomass and dedicated energy crops may contribute to the production of heat, electricity, biogas and biofuels, while also creating opportunities for diversification within agricultural systems. Bioenergy is closely connected with agriculture, land use, food security, rural development and natural-resource management. The Food and Agriculture Organization of the United Nations (FAO) has consequently developed the Bioenergy and Food Security (BEFS) framework to support integrated assessment of the technical, environmental, economic and social implications of bioenergy development [1,2]. Energy crops comprise a heterogeneous group of plant species cultivated primarily for biomass production. Depending on their biological characteristics and production systems, they may include annual crops and perennial species. Among the latter, short-rotation coppice systems based on willow and poplar and perennial grasses have received considerable scientific attention because of their biomass productivity and their potential integration into agricultural landscapes. The development of perennial energy crops may reduce the frequency of soil disturbance after crop establishment and provide longer periods of soil cover. Land-use change is particularly important in this context. The conversion of arable land to perennial energy crops may produce different environmental consequences from the conversion of forests, grasslands or other ecosystems with substantial carbon stocks. Harris et al. [5]

demonstrated that the effects of land-use change to second-generation bioenergy crops on soil organic carbon vary according to the type of land converted. The expansion of energy crops can also generate competition between food and energy production. The FAO emphasizes that sustainable bioenergy development must be considered in relation to food security, land availability, water resources and agricultural development [1,3]. At European Union level, sustainability requirements also address the potential consequences of direct and indirect land-use change associated with bioenergy feedstocks [9–11]. The objective of this paper is therefore to provide an integrated assessment of the effects of energy crops on agriculture and agricultural land, emphasizing both potential benefits and environmental and socio-economic risks.

Experimental. Research approach

The present study was designed as a literature-based analytical review. Scientific publications and institutional documents dealing with energy crops, land-use change, soil quality, carbon stocks, biodiversity, water resources, food security and sustainable bioenergy were examined.
The methodological approach followed four main stages: identification of relevant scientific and institutional sources; classification of the sources according to the environmental and socio-economic aspects addressed; comparative analysis of the reported effects of energy crops; synthesis of the main opportunities, risks and management requirements. The analysis focused primarily on perennial energy crops and short-rotation woody crops because of their direct relationship with agricultural land management and their potential long-term effects on soil and landscape structure. The literature was analyzed according to the following criteria: changes in agricultural land use; effects on soil properties and soil organic carbon; water requirements and water-resource availability; erosion and land degradation; biodiversity and landscape structure; agricultural inputs and mechanization; greenhouse-gas emissions; food–energy competition; land tenure and rural development; sustainability criteria and land-use policies. The FAO BEFS framework was considered particularly relevant because it integrates natural-resource assessment with techno-economic, environmental and socio-economic considerations [1–4]. The FAO methodology explicitly identifies land, water, biodiversity, soil quality and greenhouse-gas emissions among the dimensions requiring assessment in sustainable bioenergy development [3,4].

Results and Discussion. Energy crops and agricultural land use

The introduction of energy crops into agricultural systems changes the functional use of land. The significance of this change depends not only on the surface area occupied by energy crops but also on the quality, productivity and previous use of the land.
From a sustainable land-management perspective, the use of marginal, degraded or low-productivity land may provide an opportunity to produce biomass without substantially reducing the productive potential of land required for food production. The FAO BEFS framework specifically considers land assessment as an essential component of evaluating sustainable bioenergy potential [1].
However, the conversion of highly productive agricultural land may generate direct competition between food and energy production. Furthermore, indirect land-use change may occur when the displacement of existing food or feed production from agricultural land contributes to agricultural expansion elsewhere. The European Union sustainability framework recognizes the potential significance of indirect land-use change (ILUC). Food and feed-crop-based biofuel production may contribute to agricultural expansion into areas with high carbon stocks, including forests, wetlands and peatlands, thereby potentially reducing the greenhouse-gas benefits associated with bioenergy [9–11]. The current EU framework therefore incorporates specific sustainability provisions concerning ILUC and the use of biomass for energy purposes

[9,10]. Consequently, the assessment of energy crops should incorporate not only the productivity of the crop itself but also the wider land-use consequences of its introduction.

Effects on soil properties and soil organic carbon

Soil represents one of the most important resources affected by the establishment of energy crops. The effects depend on crop type, management practices, duration of cultivation, previous land use and local soil conditions. Perennial energy crops may reduce the frequency of soil tillage following establishment and maintain vegetation cover for longer periods than annual crops. These characteristics can contribute to the stabilization of soil aggregates, reduced erosion and increased carbon inputs through root biomass and plant residues. One of the most relevant quantitative assessments was provided by Harris et al. [5], who conducted a analysis based on more than a hundred original studies. Their results indicated that conversion from arable land to short-rotation coppice systems based mainly on poplar or willow is associated with an average increase in soil organic carbon of approximately 5.0%, while conversion to perennial grasses, was associated with an increase of approximately 25.7%. However, the same study demonstrated that the direction and magnitude of the effect depend strongly on the previous land use. Conversion from forest to second-generation energy crops was associated with decreases in soil carbon [5]. These findings are particularly relevant for agricultural land management because they demonstrate that the environmental performance of an energy crop cannot be assessed independently of the land-use transition involved. Thus, conversion of arable land to a well-managed perennial energy crop may contribute to soil carbon accumulation, whereas conversion of ecosystems with high existing carbon stocks may result in an overall carbon loss.

Water resources and energy crops

Water availability is a critical factor in the productivity and sustainability of energy crops. Crop water requirements vary considerably according to species, climatic conditions, soil properties and production technology. Fast-growing woody species such as willow and poplar may achieve high biomass yields under favorable water conditions. However, their cultivation in regions characterized by persistent water deficits may increase competition for water resources, particularly where irrigation is required. The FAO BEFS framework identifies water-resource management as a major component of sustainable bioenergy assessment [1,3]. Water availability and water quality should therefore be evaluated before large-scale establishment of energy crops. From the perspective of agricultural engineering and land improvement, crop selection should be correlated with the hydrological characteristics of the land, including precipitation, irrigation potential, groundwater depth, soil water-holding capacity and drainage conditions. In regions affected by drought, the selection of drought-adapted energy crops may reduce pressure on irrigation resources. Conversely, crops with high water requirements should be carefully evaluated where water availability is limited.

Erosion and agricultural land degradation

Perennial energy crops may provide important soil-conservation functions because of their continuous or semi-continuous vegetation cover and developed root systems. Compared with annual cropping systems requiring repeated soil disturbance, perennial crops can reduce the period during which soil remains exposed to rainfall and wind. This may reduce surface runoff and soil detachment, particularly on erosion-prone agricultural land. Potential benefits include: reduction of water erosion; reduction of wind erosion; increased soil organic matter inputs; improved soil structural stability; increased infiltration capacity; reduction of soil disturbance. However, these benefits depend on crop establishment, harvesting technology, traffic intensity and soil-management practices. The FAO recommendations for sustainable bioenergy feedstock production emphasize conservation-oriented agricultural practices, including reduced or minimum tillage, integrated nutrient management and appropriate land and water

management [4]. Consequently, the use of energy crops should be integrated into broader soil-conservation strategies rather than regarded as an independent solution to land degradation.

Food–energy competition

The competition between food and energy production represents one of the most important challenges associated with the expansion of energy crops.

Agricultural land is a finite resource and performs multiple functions, including food production, feed production, carbon storage, biodiversity support, water regulation and rural development. When highly productive agricultural land is converted from food crops to dedicated energy crops, the resulting reduction in food production may increase pressure on other agricultural areas. FAO's BEFS approach emphasizes the importance of considering food security when evaluating bioenergy development [1–4]. The issue is not necessarily the existence of energy crops themselves, but rather where, how and at what scale they are introduced. The use of marginal or degraded land can provide one possible strategy for reducing direct competition with food production. Nevertheless, the suitability of marginal land must be assessed carefully because low productivity may result from limitations such as drought, salinity, poor soil structure, excessive wetness or nutrient deficiency. Consequently, land suitability assessment remains essential before the establishment of energy crops.

Land tenure and rural development

The development of energy crops can generate new economic opportunities for rural communities by creating markets for biomass and supporting local energy production.

At the same time, large-scale bioenergy development may influence land access and land tenure. FAO's analysis of bioenergy and land tenure emphasizes that expansion of biofuel production may affect access to land, particularly where competition for land resources is strong [8]. For agricultural holdings, energy crops may provide an alternative or complementary source of income. Their economic viability depends on biomass yield, production costs, market price, transport distance, storage requirements and the existence of a stable local demand for biomass. Therefore, energy crops should be integrated into rural development strategies rather than considered exclusively as an agricultural production activity.

Some principles for sustainable energy-crop development

The reviewed literature indicates that the sustainable development of energy crops should be based on several interconnected principles. First, the suitability of the land should be assessed before crop establishment. Soil properties, climate, water availability, topography and previous land use should be considered. Second, the conversion of habitats with high ecological value or high carbon stocks should be avoided. Third, the use of marginal and degraded land may be encouraged where appropriate crop productivity can be achieved without generating unacceptable environmental costs. Fourth, the cultivation system should minimize unnecessary soil disturbance and optimize the use of fertilizers, water and plant-protection products. Fifth, energy crops should be integrated into diversified agricultural landscapes rather than established exclusively as large-scale homogeneous monocultures. Finally, biomass production should be assessed from a life-cycle perspective, including cultivation, harvesting, transportation, storage and energy conversion.

Conclusions

Energy crops represent an important component of the transition towards renewable energy and can contribute to agricultural diversification, rural development and the productive use of certain categories of low-productivity or degraded land. The reviewed literature indicates that perennial energy crops may provide several environmental benefits, including reduced soil disturbance, improved soil protection and, under certain land-use transitions, increased soil organic carbon. The magnitude and direction of these effects, however, depend strongly on the type of crop, management system, environmental conditions and previous land use [5–7].

The conversion of arable land to perennial energy crops may generate favorable effects on soil carbon and landscape structure, whereas the conversion of forests or ecosystems with high carbon stocks may result in substantial environmental costs. Similarly, energy-crop plantations may contribute to biodiversity in homogeneous agricultural landscapes but may negatively affect biodiversity when they replace valuable natural or semi-natural habitats [6,7]. Water availability represents another critical constraint. Energy-crop development should be coordinated with regional water-resource management, especially in areas affected by drought. From the perspective of agricultural engineering, the selection of energy crops should therefore be correlated with soil characteristics, hydrological conditions, irrigation and drainage requirements, and available mechanization. The competition between food and energy production remains an important issue. Sustainable development requires careful spatial planning and the preferential consideration of land categories where biomass production can be achieved without significantly compromising food production, biodiversity or ecosystem services [1–4,9–11].

In conclusion, energy crops should not be regarded simply as an alternative to conventional agricultural crops. They should be considered as a component of an integrated agricultural land-management system, in which food production, energy generation, soil conservation, water management, biodiversity and rural development are evaluated simultaneously.

The sustainability of energy crops is therefore determined less by the crop itself than by the land on which it is cultivated, the production system applied, the resources consumed and the way in which the resulting biomass is integrated into the wider agricultural and energy system.

Bibliography

[1] FAO. *Bioenergy and Food Security: The BEFS Analytical Framework*. Environment and Natural Resources Management Working Paper No. 16. Rome: Food and Agriculture Organization of the United Nations; 2010. ISBN 978-92-5-106740-6.

[2] FAO. *The Bioenergy and Food Security (BEFS) Approach*. Food and Agriculture Organization of the United Nations. Available from: FAO Energy and Bioenergy and Food Security resources.

[3] FAO. *A Compilation of Tools and Methodologies to Assess the Sustainability of Modern Bioenergy*. Bioenergy and Food Security Criteria and Indicators (BEFSCI). Rome: Food and Agriculture Organization of the United Nations; 2012.

[4] Rossi, A. (ed.). *Good Environmental Practices in Bioenergy Feedstock Production: Making Bioenergy Work for Climate and Food Security*. Environment and Natural Resources Management Working Paper No. 49. Rome: Food and Agriculture Organization of the United Nations; 2012.

[5] Harris, Z.M., Spake, R., Taylor, G. Land use change to bioenergy: A meta-analysis of soil carbon and GHG emissions. *Biomass and Bioenergy*. 2015;82:27–39.

[6] Pedroli, B., Elbersen, B., Frederiksen, P., Grandin, U., Heikkilä, R., Krogh, P.H., Izakovičová, Z., Johansen, A., Meiresonne, L., Spijker, J. Is energy cropping in Europe compatible with biodiversity? Opportunities and threats to biodiversity from land-based production of biomass for bioenergy purposes. *Biomass and Bioenergy*. 2013;55:73–86.

[7] Vanbeveren, S.P.P., Ceulemans, R. Biodiversity in short-rotation coppice. *Renewable and Sustainable Energy Reviews*. 2019;111:34–43.

[8] Cotula, L., Dyer, N., Vermeulen, S. *Bioenergy and Land Tenure: The Implications of Biofuels for Land Tenure and Land Policy*. Land Tenure Technical Paper No. 1. Rome: Food and Agriculture Organization of the United Nations; 2008.

[9] European Commission. *Biofuels – Sustainability Criteria*. Directorate-General for Energy, European Commission.

[10] European Union. *Directive (EU) 2018/2001 of the European Parliament and of the Council of 11 December 2018 on the promotion of the use of energy from renewable sources*. Official Journal of the European Union; 2018, as amended.
[11] European Commission. *Report on the status of production expansion of relevant food and feed crops worldwide*. COM(2026) 36 final. Brussels; 20 January 2026.

DECOUPLED MICROBIAL AND PLANT RESPONSES TO EOM-ASSISTED RHIZOREMEDIATION IN *LOLIUM PERENNE* UNDER USED LUBRICANT OIL CONTAMINATION

Klaudia Hoffmann[1,2], Kitti Vastag[1], Enikő Mészáros[2], Kamilla Kovács[2], Zsófia Liska[2], Katalin Perei[1], Gábor Feigl[2], Attila Bodor[1]

[1]Department of Biotechnology and Microbiology, University of Szeged, H-6726 Szeged, Közép fasor 52, Hungary
[2]Department of Plant Biology, University of Szeged, H-6726 Szeged, Közép fasor 52, Hungary
e-mail: bodora@bio.u-szeged.hu

Abstract

Enhancing microbial activity in the rhizosphere is a promising strategy for improving the remediation of soils contaminated with used lubricant oil (ULO). However, stronger microbial stimulation does not necessarily lead to better plant performance, and the compatibility between the microbial treatment and the selected plant species may therefore be a critical determinant of remediation success. To explore this relationship in a monocot system, perennial ryegrass (*Lolium perenne* L.) was exposed to extracellular organic matter (EOM) derived from *Micrococcus luteus*, a preparation containing resuscitation-promoting factor (Rpf) and previously associated with increased microbial activity in contaminated soils. The effects of EOM were evaluated both under direct lubricant oil exposure and in ULO-contaminated soil. In semi-hydroponic assays, 10% EOM, 1% lubricant oil, and their combined treatment markedly reduced the germination index, demonstrating that direct exposure imposed substantial stress on early plant development. In soil, EOM produced a clear dose-dependent increase in rhizosphere microbial abundance. This microbial response was already significant at 5% EOM, yet it was not paralleled by a corresponding enhancement of plant growth. The divergence between microbial and plant responses was particularly evident when the results were considered alongside those obtained previously with dicotyledonous species. The *L. perenne* rhizosphere supported lower microbial abundance under comparable conditions, and, unlike *Lepidium sativum*, ryegrass showed only limited improvement in plant performance despite pronounced microbial stimulation. Root protein tyrosine nitration showed system-dependent responses: despite marked growth inhibition, only minor changes were observed under direct exposure, whereas in ULO-contaminated soil, 10% EOM shifted protein tyrosine nitration from the ULO-induced level toward that of the control. Together, these results reveal a clear decoupling between rhizosphere microbial stimulation and plant-level benefit in perennial ryegrass. They highlight the importance of considering plant species-specific responses when applying microbial stimulatory approaches under contaminant stress. Plant tolerance and stress responses should therefore be regarded as integral components in the development of EOM-assisted rhizoremediation strategies.

Acknowledgements

A.B. was supported by the János Bolyai Research Scholarship of the Hungarian Academy of Sciences (Grant no. BO/00108/25/8).

BEYOND BIODEGRADABILITY: ECOTOXICOLOGICAL EFFECTS OF BIODEGRADABLE MICROPLASTICS ACROSS MULTIPLE BIOLOGICAL SYSTEMS

Klaudia Hoffmann[1,2], Patrik Szabó[1], Bence Gálos[1], Etelka Kovács[1,2], Katalin Perei[1], Enikő Mészáros[2], Kamilla Kovács[2], Zsófia Liska[2], Gábor Feigl[2], Attila Bodor[1,2]

[1]Department of Biotechnology and Microbiology, University of Szeged, H-6726 Szeged, Közép fasor 52, Hungary
[2] MTA-SZTE Lendület "Momentum" Anthropogenic Stress and Plant Resilience Research Group, Department of Plant Biology, University of Szeged, H-6726 Szeged, Közép fasor 52, Hungary
e-mail: bodora@bio.u-szeged.hu

Abstract
The increasing use of biodegradable plastics in agriculture has been promoted as an alternative to conventional polymeric materials. Their environmental fate, however, is more complex than complete biodegradation: partial transformation may generate secondary microplastics (Bio-MPs) and release soluble organic constituents, potentially altering their interactions with exposed organisms. These changes may become particularly relevant after environmental ageing. This study therefore investigated the ecotoxicological effects of fresh and aged Bio-MPs across test systems representing different levels of biological organization. Microbial responses were assessed using the Gram-negative bacterium *Escherichia coli* and the Gram-positive *Bacillus licheniformis*. Exposure to Bio-MPs reduced culturable cell numbers in both species, although their sensitivity differed. In *E. coli*, a clear decrease was observed at 1% Bio-MP, whereas *B. licheniformis* responded already at 0.5%, with reduced cell numbers also detected at 1%. Plant-level effects were examined with *Brassica napus*. Under semi-hydroponic conditions, Bio-MPs altered the germination index in a concentration-dependent manner, while the response pattern changed when exposure occurred in soil. Effects were also detected at a higher level of biological complexity, as Bio-MP treatments reduced survival of the soil-dwelling collembolan test organism. Overall, the results show that biodegradable microplastics can elicit measurable biological effects across microbial, plant and soil invertebrate systems. Their environmental impact therefore cannot be inferred solely from their biodegradability or intended sustainability. Instead, the ecotoxicological behaviour of Bio-MPs appears to depend on both exposure conditions and the biological system considered, emphasizing the need to include transformed and environmentally aged materials in the safety assessment of biodegradable plastic alternatives.

Acknowledgements
The project was supported by the National Research, Development and Innovation Office, Hungary (NKFIH FK 142475) and by the 'Lendület' MOMENTUM programme of the Hungarian Academy of Sciences (LP2025-8/2025). A.B. was supported by the University Research Scholarship Programme (EKÖP), funded by the Ministry of Culture and Innovation from the National Research, Development and Innovation Fund (EKÖP-26-4-SZTE-494).

SYNTHESIS AND CHARACTERIZATION OF FUNCTIONALIZED GRAPHENE OXIDE NANOSHEETS DESIGNED FOR ENVIRONMENTAL APPLICATIONS

Tamás Bodor[1,2], Kolbert Zsuzsanna[2], Zoltán Kónya[3], Andrea Rónavári[3]

[1]Department of Plant Biology, University of Szeged, Szeged, Hungary
[2]Doctoral School of Biology, Faculty of Science and Informatics, University of Szeged, Szeged, Hungary
[3]Department of Applied and Environmental Chemistry, University of Szeged, Szeged, Hungary
e-mail: ronavari@chem.u-szeged.hu

Abstract

The primary objective of this study was to develop and characterize functionalized graphene oxide (GO) nanosheets designed for potential environmental applications. In particular, the GO nanosheets were functionalized to obtain a system designed as a potential nitric oxide donor. Nitric oxide (NO) is a vital signaling and regulating molecule that affects nearly every developmental stage of a plant's life cycle. Moreover, GO nanosheets demonstrate exceptional promising in enhancing plant growth and development, however careful optimization is required to mitigate potential concentration-dependent toxicity. These nanosheets were specifically engineered as a potential platform for NO delivery, facilitating a controlled and sustained release of nitric oxide. Comprehensive characterization of these functionalized nanosheets is imperative to evaluate their overall performance and prospective utility within environmental, agricultural and plant biotechnology.

Introduction

Upon exposure to diverse biotic (e.g., pathogens, herbivores) and abiotic (e.g., drought, salinity, heavy metal toxicity) stressors, plants enzymatically synthesize various redox-active molecules to orchestrate their defense mechanisms. This repertoire of highly reactive compounds, comprising both free radicals and non-radical derivatives, includes reactive nitrogen species (RNS), among which nitric oxide (NO) is of primary importance. It is a versatile signaling molecule that regulates nearly every developmental stage of a plant's life cycle, encompassing seed germination, root architecture, and senescence. Beyond development, it serves as a master regulator of plant resilience against both abiotic and biotic stresses by modulating stomatal closure during drought, mitigating oxidative damage, and driving immune responses against pathogens. Although the excessive accumulation of these molecules can lead to oxidative burst, they are essential for homeostasis, self-defense, development, and hormonal signaling [1].
Despite its biological importance, the targeted and sustained delivery of NO to plants remains challenging due to its highly reactive and transient nature.
GO nanosheets are a promising class of carbon-based materials that may be suitable for this purpose. GO is a key member of the graphene family, and represents an oxidized graphene structure with specific functional groups (carboxyl, hydroxyl, and epoxy groups), which contribute to its favorable physicochemical properties. Due to its unique physicochemical properties, specifically its high surface area, hydrophilicity, and abundant oxygen-containing functional groups GO acts as a highly potent, dose-dependent nano-regulator in plant biology. GO has been reported to promote seed germination rates, seedling establishment, and the formation of reproductive structures, drives overall biomass accumulation through increased plant height, shoot development, increased leaf area and highly branched root system architecture [2]. However, careful optimization is required to mitigate potential concentration-dependent toxicity associated with both NO and GO exposure.

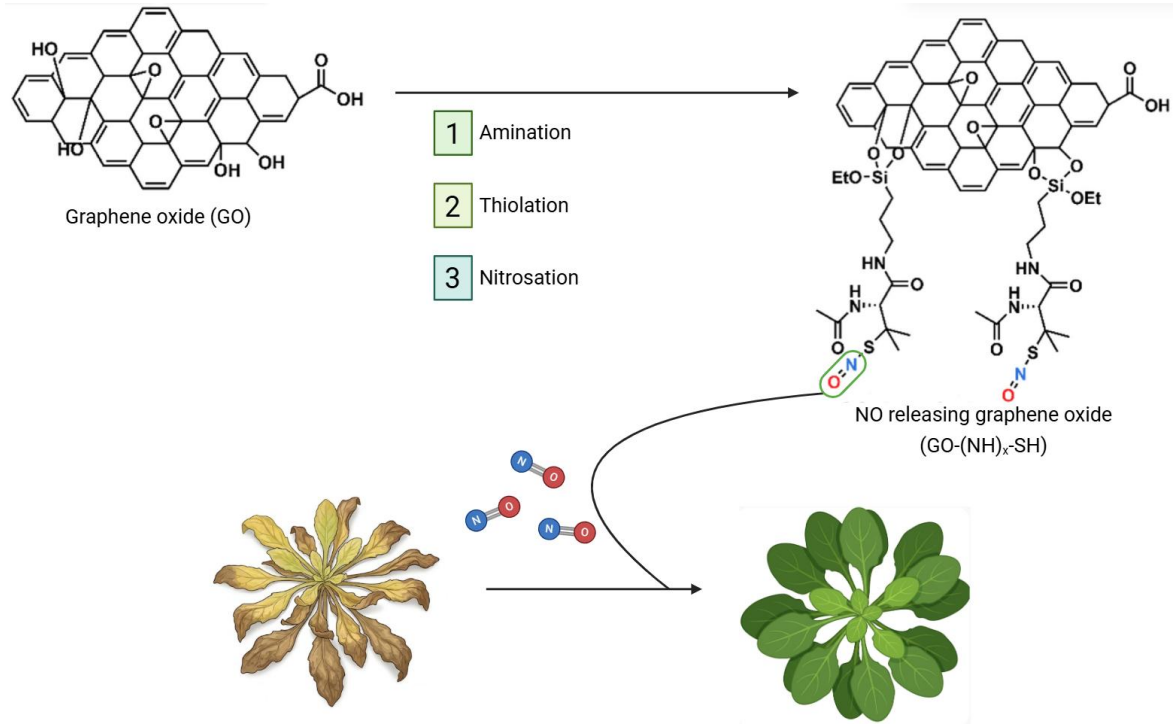


Fig 1.: Schematic figure of the synthesis of GO-$(NH)_x$-SNO and its proposed effect on plant development as potential nitric oxide reservoir

Experimental

A, Synthesis of NAPTH

For thiolation of aminated graphene oxide (GO-$(NH_2)_X$) 3-acetamido-4,4-dimethylthietan-2-one (NAPTH) (Fig 2.) needed to be synthesized following a reported protocol [3,4].

Firstly, 5 g of N-acetyl-D-penicillamine (NAP) was dissolved in 10 ml of acetic anhydride and 20 ml of pyridine, sealed and purged with argon gas. The reaction mixture was reacted for 15 h with protection from light. After the reaction, the solvent was removed via rotary evaporation and the crude precipitate was resuspended in 30 ml chloroform, washed three times with an equal volume of HCl (1 M), and the organic phase was dried over anhydrous magnesium sulfate.

The final mixture was condensed to a small volume and triturated in chilled hexanes at -20 °C overnight. The precipitated crystals were collected, washed with chilled hexanes, and further dried overnight. NAPTH was obtained as a pure white solid.

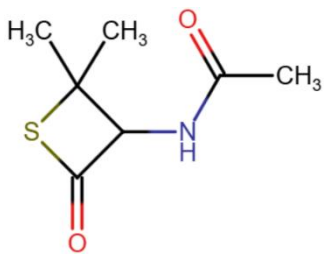


Fig 2.: 3-acetamido-4,4-dimethylthietan-2-one (NAPTH)

B, Synthesis of GO-(NH)x-SNO

Aminated graphene oxide (GO-$(NH_2)_x$) was synthesized following previous reported procedures [5,6]. Firstly 1 g of GO was suspended in anhydrous toluene (160 ml) and stirred under reflux in room temperature with N_2 atmosphere. Afterward, a molar amount of (3-aminopropyl) triethoxysilane (APTES) was dissolved in anhydrous 9 ml chloroform and injected into the reaction pot (0.020 mmol APTES/ mg GO). After 72 h, resulting crude product was vacuum filtered, washed with excess anhydrous chloroform, and dried under vacuum at 80 °C for 48 h.

Thiolated graphene oxide (GO-(NH)x -SH) was prepared by reacting GO-$[NH_2]_x$ with NAPTH following a modified protocol [7,8]. 500 mg GO-$(NH_2)_x$ was suspended in 50 ml MES Buffer (0.5 M, pH 6) with 10-fold stoichiometric excess of NAPTH provided relative to the quantitatively determined amine content measured by ninhydrin assay [9], which was used to quantify the amines of GO-$(NH2)_x$. Briefly, the GO-$(NH2)_x$ constructs were treated with excess ninhydrin in a 0.1% acetic acid solution and subjected to thermal incubation at 100 °C for 10 minutes. The functionalized nanomaterial was subsequently filtered out, allowing the optical absorbance of the resulting supernatant to be recorded at a wavelength of 570 nm. Final amine density was extrapolated using a standard curve generated from glycine. After adding the proper amount of NAPTH to the modified GO, the pot was purged under Ar gas and stirred for 48 h protected from light. Afterward the mixture was vacuum filtered, washed 3 times with 100 ml deionized water and dried under vacuum at room temperature for 12 h.

SNO-functionalized graphene oxide (GO-(NH)x-SNO) was prepared via dissolving 100 mg of GO-$(NH)_x$-SH in 25 ml HCl (2M), and chilled in ice bath, protected from light. DTPA was added to achieve a final concentration of 500 μM (act as a chelator). Finally, sodium nitrite was added in greater than a 10-fold stoichiometric excess relative to the quantitatively determined thiol content. The mixture was allowed to react for 2 h, after which it was centrifuged and washed with 10 ml chilled methanol three times. Finally, the functionalized GO was dried under vacuum at room temperature for 2 h.

Results and discussion

The synthesis of NAPTH was successful, in agreement with previously reported data. The zeta potential of GO nanosheets were -12.8 mV which increased to 4.04 mV after amination.

The hydrodynamic diameter of the GO nanosheets was about 2.6 -8.7 nm, according to DLS measurements. The XRD pattern showed a peak at 2θ = 14,044° and a broadened peak in the 20-35°range. The calculated layer distance is 7.32 Å which is lower than the expected distance of the GO-$(NH_2)_x$ after APTES functionalization. This contraction of GO layers can be caused by the loss of interstitial water and the possible partial reduction of the GO layers, that cause the loss of oxygen-containing functional groups. The second, broader peak further supports the hypothesis that the layers became unorganized partially, potentially due to the incomplete reaction with APTES and the formation of an unorganized siloxane network. This was further supported by the relatively low amine content determined by the ninhydrin assay.

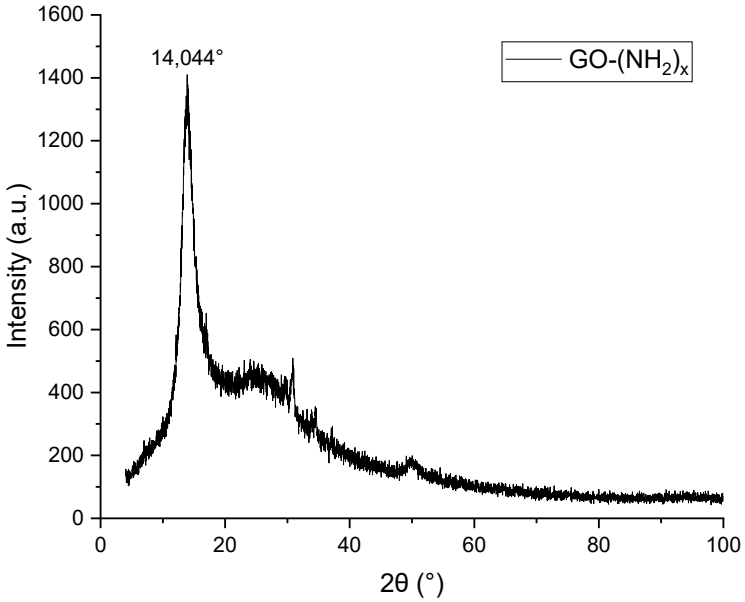


Fig 3.: XRD pattern of GO- $(NH_2)_x$

Conclusion

In conclusion, the synthesis of functionalized GO-(NH)x-SNO nanosheets contains several crucial steps that can substantially affect the final structure and physicochemical properties of the nanomaterial. The obtained results demonstrate the feasibility of the GO functionalization approach, while further optimization is required.

Future work will focus on confirming NO-release behavior, optimizing release characteristics, and evaluating the potential biological applicability of the resulting nanomaterials.

Acknowledgements

The research was supported by the Hungarian Research, Development and Innovation Office (grant no. PD 143320 and K146292).

References

[1] G. Fejes, T. Bodor, R. Szőllősi, S. Kondak, K. Kutasi, V. Fotopoulos, Zs. Kolbert, J. Exp. Bot. 76 (2025) 3669.
[2] Y. Yang, R. Zhang, X. Zhang, Z. Chen, H. Wang, P.C.H. Li, Plants 11 (2022) 2826.
[3] H.A. Moynihan, S.M. Roberts, J. Chem. Soc., Perkin Trans. 1 (1994) 797.
[4] M.C. Frost, M.E. Meyerhoff, J. Biomed. Mater. Res. A 72 (2005) 409.
[5] M. Garren, M. Ashcraft, D. Crowley, E.J. Brisbois, H. Handa, J. Biomed. Mater. Res. (2023)
[6] J. Huang, S. Ding, W. Xiao, Y. Peng, S. Deng, N. Zhang, Catal. Lett. 145 (2014) 1000.
[7] C. Ferris, M. Casas, M.J. Lucero, M.V. de Paz, M.R. Jimenez-Castellanos, Carbohydr. Polym. 111 (2014) 125.
[8] P. Espeel, F.E. Du Prez, Eur. Polym. J. 62 (2015) 247.
[9] S. Ghalei, S. Hopkins, M. Douglass, M. Garren, A. Mondal, H. Handa, J. Colloid Interface Sci. 590 (2021) 277.

PROTEIN-BASED BIODEGRADABLE FILMS FOR TOPICAL APPLICATION LOADED WITH NIACINAMIDE

Mina Bosnić, Jelena Milinković Budinčić, Sandra Bučko, Ljiljana Spasojević Pavlović, Jelena Ostojić, Željana Radonić, Jaroslav Katona, Lidija Petrović, Jadranka Fraj

Department of Pharmaceutical Engineering and Deparmtment of Applied and Engineering Chemistry, Faculty of Technology, University of Novi Sad, Bulevar Cara Lazara 1, 21000 Novi Sad, Serbia
e-mail: minabosnic@uns.rs

Abstract
As an approach to reducing the environmental problems that emerge from the excessive plastic consumption, new biodegradable materials are being developed. This study investigates the possibility of protein-based biodegradable films, specifically gelatin and sodium caseinate films, serving as niacinamide carriers for topical application.

Introduction
Niacinamide or nicotinamide (N), an amide derivative of vitamin B3, exhibits numerous dermal benefits including skin brightening, anti-ageing, skin barrier protection, and alleviation of dermatitis, psoriasis and acne vulgaris. Its potent activity on the skin may partly result from its role as a component of the coenzymes nicotineamide adenine dinucleotide (NAD^+), reduced nicotineamide adenine dinucleotide (NADH), and their phosphorylated forms ($NADP^+$and NADPH). [1,2]

Experimental
The gelatin/sodium caseinate films were prepared using the casting method, with the addition of 30% glycerol as a plasticizer and various concentrations (5, 7 and 9%) of N. Physico-chemical properties of the films (SEM, thickness, opacity, mechanical properties, water vapor permeability, swelling degree) were examined in order to assess the influence of N addition on the properties of the films.

Results and discussion
The SEM micrographs (Figure 1) show a uniform surface and cross-section of the 5% N gelatin/sodium caseinate films, which could indicate proper miscibility and incorporation of N within the protein matrix.

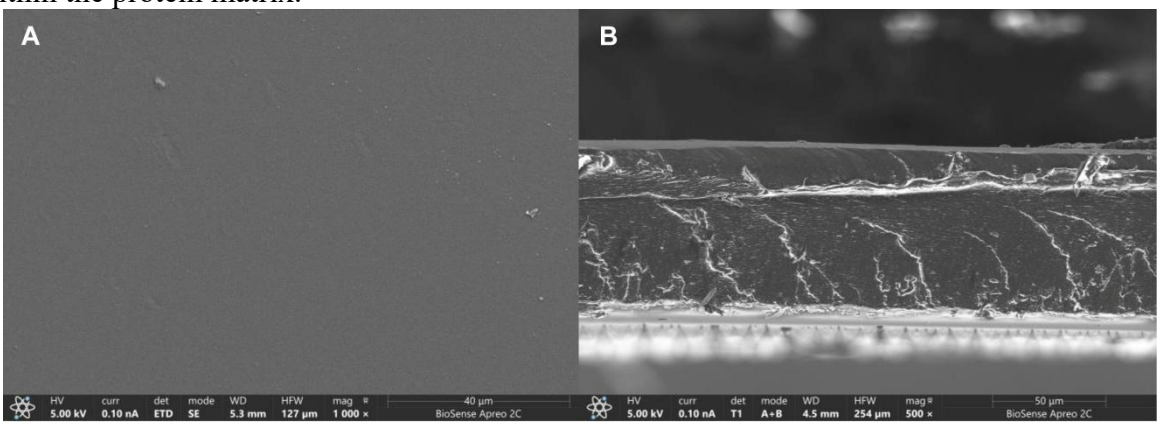


Figure 1. SEM micrographs of the surface (A) and cross-section (B) of gelatin/sodium caseinate films containing 5% niacinamide

The thickness of the films increased with the incorporation of N, while the opacity of the films was decreased, which is consistent with the typical effect of plasticizers. The influence of N addition on the mechanical properties of the films was also similar to the typical behavior of a plasticizer, with a decrease in tensile strength and an increase in elongation at break. This is likely due to the relatively low molecular weight and hydrophilicity of N. The increase in WVP of the films could also be related to the hydrophilicity of N. Interestingly, the differences in the film properties between the films containing different concentrations of N are not statistically significant. However, the swelling ratio of the films was concentration-dependent, decreasing with an increase in N concentration.

Conclusion

N was successfully incorporated into the gelatin/sodium caseinate films in concentrations of 5, 7 and 9%. Its influence on the film's physico-chemical properties was similar to that of a plasticizer, resulting in more flexible and pliable films suitable for topical application. The *in vitro* dissolution testing of the films could provide additional information on their potential for topical application.

Acknowledgements

This work was funded by the Ministry of Science, Technological Development and Innovation of the Republic of Serbia through two grant agreements with the University of Novi Sad – Faculty of Technology (Nos. 451-03-34/2026-03/200134 and 451-03-33/2026-03/200134).

References

[1] R.R. Ong, C.F. Goh, Drug Deliv. and Transl. Res. 14 (2024) 3512–3548.
[2] Y.C. Boo, Antioxidants 10 (2021) 1315.

NEW HETEROGENEOUS GREEN CATALYST ZnO/BANANA PEEL EXTRACT FOR WASTE WATER REMEDIATION UNDER SUBCRITICAL CONDITIONS

Tanja Brezo-Borjan[1], Jaroslava Švarc-Gajić[1], Szabolcs Bognár[2], Dušica Jovanović[2], Vesna Despotović[2], Nina Finčur[2], Sandra Jakšić[3] and Daniela Šojić Merkulov[2]

[1]Faculty of Technology, University of Novi Sad, Bulevar cara Lazara 1, 21000 Novi Sad, Serbia
[2]University of Novi Sad Faculty of Sciences, Department of Chemistry, Biochemistry and Environmental Protection, Trg Dositeja Obradovića 3, 21000 Novi Sad, Serbia
[3]Scientific Veterinary Institute "Novi Sad", Rumenački put 20, 21000 Novi Sad, Serbia
e-mail: tanja.brezo.borjan@uns.ac.rs

Abstract
The concentration of organic anthropogenic micropollutants (pesticides, pharmaceuticals, chemicals from personal care products) is rapidly increasing in wastewater, jeopardising aquatic ecosystems and the environment as a whole. The aim of this study was to investigate the treatment of contaminated waters under subcritical conditions in combination with a new heterogeneous green catalyst (ZnO/banana peel extract), as an environmentally friendly process for wastewater remediation without the use of oxidising agents. The catalyst was obtained by mixing aqueous banana peel extract with a $ZnSO_4$ solution, followed by the pH adjustment to 12. The process was tested on model systems containing different concentrations of the pesticides tembotrione and clomazone, the antibiotic ciprofloxacin, the synthetic estrogen hormone 17α-ethinylestradiol, and three mycotoxins (zearalenone, deoxynivalenol, and fumonisin B_1). The treatments were carried out at temperatures from 160 to 200 °C, during time from 30 to 120 min, in a nitrogen atmosphere (10 bar). The treated model systems were analysed by HPLC and compared to systems without catalysts to determine the degradation efficiency. The new catalyst ZnO/banana peel extract showed high efficiency (~83–100%) in the degradation processes and enabled a reduction in treatment time and temperature for almost all pollutants, except for clomazone. For clomazone, the addition of the new green catalyst led to a decrease in degradation efficiency from 71 to 35%.

Keywords: wastewater remediation; subcritical water treatment; heterogeneous green catalyst; micropollutants

Acknowledgements
This work was funded by the Science Fund of the Republic of Serbia (*In situ* pollutants removal from waters by sustainable green nanotechnologies–CleanNanoCatalyze, Grant No. 7747845). The authors are grateful to the Ministry of Science, Technological Development and Innovation of the Republic of Serbia (project numbers: 451-03-33/2026-03/ 200134, 451-03-34/2026-03/ 200134, 451-03-33/2026-03/20012, 451-03-34/2026-03/200125, and 451-03-33/2026-03/200031).

FUNCTIONAL MODIFICATION OF MARINE EXOSKELETONS BY THERMAL TREATMENT

Alexandra Ioana Bucur, Raul Alin Bucur, Andrei Racu, Cristina Mosoarca, George Dima, Paula Ianasi (Svera), Florina Stefania Rus, Bogdan-Ovidiu Taranu, Radu Banica

National Institute of R&D for Electrochemistry and Condensed Matter, 144 Dr. Aurel Păunescu-Podeanu, RO-300569 Timisoara, Romania
e-mail: iioitescu@yahoo.com

Abstract

Waste-derived materials have attracted increasing attention in the field of pollutant removal from surface water and groundwater. Ca-rich waste materials have demonstrated strong potential for phosphate removal [1] from water via adsorption. To increase their removal efficiency, these waste resources are frequently modified using thermal or chemical methods. Thermally treated marine shells, a promising Ca-based adsorbent, are currently studied for removing pollutants from wastewater; however, the optimal treatment type (pyrolysis or calcination), temperature, and duration of thermal modification remain to be clarified to maximize their performance.

The marine shells exoskeletons are mainly composed of calcium carbonate, whose thermal decomposition leads to the formation of calcium oxide, a highly reactive compound. This oxide further reacts with water to form calcium hydroxide, which promotes the precipitation of calcium phosphates. Thermal treatment of the shells eliminates the organic fraction that constitutes their structural backbone [4-5]; consequently, thermal modification leads to the formation of a highly porous material. The present study investigates the surface modification of marine exoskeleton fragments via thermal treatment, demonstrating the simultaneous generation of a useful calcium hydroxide solution and functionalized solid substrates for wastewater treatment.

Acknowledgements

This work was carried out through the Nucleu Program within the National Research Development and Innovation Plan 2022–2027, carried out with the support of MCID, project no PN 23 27 02 01, contract no. 29N/2023

The authors wish to thank Dr Eng Mihai Cosmin Pascariu for his valuable contribution to the concept of this work.

References

[1] X. Jian, A. Reza, F. Zeng, H. Li, A. Orlov, C. Gobler, X. Mao, Biomass Bioenergy 214 (2026) 109501

[2] Bucur A.I., Banica R., Pascariu M.C., Poienar M., Mosoarca C., Bucur R., Negrea A., Hulka I. Dig. J nanomat Biostruct. 17 (1) (2022), 153 - 160

[3] J. Zhang, B. Zheng, C. Zhang, L. Xie, C. Fang, J. Food Process. Eng. 46 (12) (2023) e14477

[4] J.-I. Lee, J.-K. Kang, J.-S. Oh, S.-C. Yoo, C.-G. Lee, E.H. Jho, S.-J. Park, J. Clean. Prod. 328 (2021).

[5] Bucur A.I., Poienar M., Bucur R.A., Mosoarca C., Banica R., Braz J Chem Eng, 40 (4) (2023), 1067 - 1076.

ENVIRONMENTALLY FRIENDLY CERAMICS FOR PIEZOELECTRIC BUZZERS WITH DUAL ELECTROMECHANICAL FUNCTIONALITY

Bucur Raul Alin, Badea Iuliana, Florina S. Rus, Radu Banica, Alexandra Ioana Bucur, Cristina Mosoarca, Dima George Daniel, Taranu Bogdan-Ovidiu, Andrei Racu

National Institute for Research and Development in Electrochemistry and Condensed Matter, Condensed Matter Department, No. 1 Plautius Andronescu, 300224 Timisoara, Romania.
e-mail: raul_alin_bucur@yahoo.com

Abstract

A major limitation of the widely used piezoelectric ceramic lead zirconate titanate, $Pb(Zr,Ti)O_3$ (PZT), is the high toxicity associated with lead compounds [1,2]. Consequently, increasing research attention has been directed toward environmentally friendly, lead-free piezoelectric materials, among which potassium sodium niobate, $(K,Na)NbO_3$ (KNN), is one of the most promising candidates [3,4]. KNN is a solid solution of orthorhombic ferroelectric $KNbO_3$ and $NaNbO_3$, and enhanced piezoelectric and ferroelectric properties have been reported near the morphotropic phase boundary (MPB), particularly around the equimolar composition $K_{0.5}Na_{0.5}NbO_3$ [3,4]. At room temperature, KNN exhibits a ferroelectric perovskite structure with orthorhombic symmetry.

The functional properties of KNN are strongly related to its crystal structure, phase transitions, composition, and microstructure. As previously reported [5,6,7], enhancement of the piezoelectric response can be achieved by shifting the orthorhombic–tetragonal polymorphic phase transition (PPT) toward room temperature or by modifying the composition through chemical additions and doping. In this context, incorporation of secondary perovskite phases represents an effective approach for tailoring the structural and electromechanical properties of KNN ceramics. In particular, the addition of $GdFeO_3$ has been reported to influence the physical and ferroelectric properties of $NaKNbO_3$-based ceramics [8], providing motivation for further investigation of the KNN–$GdFeO_3$ system.

In the present work, KNN ceramics doped with 0.25, 0.5, 0.75, 1, 2.5, and 5 mol% $GdFeO_3$ are investigated to establish relationships between composition, crystal structure, microstructure, dielectric response, and piezoelectric performance. X-ray diffraction (XRD) and Rietveld refinement are employed to examine phase evolution and determine the lattice parameters, while scanning electron microscopy is used to evaluate the influence of $GdFeO_3$ addition on grain morphology and grain size. The dielectric behavior is investigated at room temperature as a function of frequency, together with the piezoelectric coefficients and electromechanical coupling factors.

Beyond material characterization, the study demonstrates the practical application of the optimized KNN–$GdFeO_3$ ceramics in a piezoelectric buzzer. The device illustrates the inverse piezoelectric effect, in which an applied electrical signal produces mechanical deformation and acoustic vibrations. Conversely, the direct piezoelectric effect is demonstrated by mechanically striking the piezoelectric element, generating an electrical response sufficient to illuminate an LED. This dual electromechanical functionality highlights the potential of lead-free KNN–$GdFeO_3$ ceramics for environmentally friendly piezoelectric buzzers or other electromechanical energy-conversion applications.

References

[1] Jaffe, B., Cook, W. R., & Jaffe, H. (1971). Piezoelectric Ceramics. Academic Press.
[2] Rödel, J. et al. (2009). Perspective on the development of lead-free piezoceramics. Journal of the American Ceramic Society, 92, 1153–1177.

[3] Saito, Y. et al. (2004). Lead-free piezoceramics. Nature, 432, 84–87.
[4] Wang, K. & Li, J.-F. (2012). K,$NaNbO_3$-based lead-free piezoceramics: Phase transition, sintering and property enhancement. Journal of Advanced Ceramics, 1, 24–37.
[5] Wang, X. et al. (2021). "The mechanism for the enhanced piezoelectricity in multi-elements doped (K,Na)NbO_3 ceramics.", Nat Commun. 2021 Feb 9;12:881.
[6] Koruza, J. et al. (2018). "Sintering of Lead-Free Piezoelectric Sodium Potassium Niobate Ceramics." Materials, 11(1), 23.
[7] Rödel, J. et al. (2015). "Perspective on the Development of Lead-Free Piezoceramics." Journal of the American Ceramic Society, 98(7), 1905–1918.
[8] Rai, R. et al. (2011). Influence of $GdFeO_3$ addition on the physical properties of $NaKNbO_3$ lead-free ferroelectric ceramics. Materials Letters, 65, 2703–2706.

CARBON-BASED CONTAMINANTS FOUND IN GROUNDWATER FROM MARAMURES AND SATU MARE REGIONS

Anamaria Buda, Thomas Dippong

Technical University of Cluj-Napoca, Faculty of Science, 76 Victoriei Street, 430122, Baia Mare, Romania;
e-mail: thomas.dippong@cb.utcluj.ro

Abstract

Groundwater is one of the most important freshwater resources, supplying drinking water for a large proportion of the population, accounting for approximately 95% of the planet's accessible freshwater resources [1,2]. The presence and distribution of carbon-based compounds in groundwater are controlled by both natural hydrogeochemical processes and anthropogenic activities [1]. The determination of carbon fractions and carbon-containing contaminants provides valuable information on groundwater quality, geochemical evolution, and potential sources of pollution [1].

This study evaluates the occurrence of carbon-based components in groundwater collected from five natural groundwater sources located in the Maramureș and Satu Mare regions of northwestern Romania. The investigated parameters included total carbon (TC), total organic carbon (TOC), total inorganic carbon (TIC), organic acids, cyanide, anionic, nonionic, and cationic surfactants. These parameters were selected to characterize both the natural carbon cycle within the aquifers and the possible influence of human activities on groundwater quality. Total inorganic carbon is primarily associated with carbonate mineral dissolution and water–rock interactions, whereas total organic carbon reflects the presence of naturally derived organic matter as well as potential anthropogenic inputs [1,2]. Organic acids originate from microbial degradation of organic matter and influence groundwater acidity, complexation reactions, and metal mobility.

Cyanide is a highly toxic carbon-containing contaminant that may originate from industrial activities, mining operations, electroplating processes, and certain natural geochemical sources [3]. Surfactants represent an important group of emerging contaminants because they are widely used in domestic, industrial, and agricultural products. Their occurrence in groundwater may indicate infiltration of treated or untreated wastewater, leakage from septic systems, agricultural activities, or diffuse urban contamination [4,5].

Groundwater samples were collected from five sampling locations following standard sampling procedures to minimize contamination and preserve sample integrity. The analytical approach enabled the simultaneous assessment of natural carbon fractions and anthropogenic carbon-containing contaminants.

Total carbon (TC) ranged from 89.9 to 95.7 mg/L, with a mean of 94.2 mg/L. Total organic carbon (TOC) was recorded between 11.7 and 23 mg/L, with a mean of 17.8 mg/L. Together, these sources establish the natural organic carbon background in shallow groundwater, with concentrations generally decreasing and stabilizing with increasing depth [2]. High total organic carbon (TOC) concentrations in groundwater are directly influenced by surface-derived sources and the limited extent of subsurface processing, low TOC concentrations are characteristic of deep aquifers, where longer groundwater residence times allow the progressive mineralization of organic matter by microorganisms [1,2]. Total inorganic carbon (TIC) ranged from 73 to 81.1 mg/L, with a mean of 76.2 mg/L, reflecting the carbonate mineral dissolution and CO_2 dynamics characteristic of the local aquifer lithology [1,2].

The organic acid fraction ranged from 28.1 to 47.5 mg/L, with a mean of 38.2 mg/L across the five sampling points. Cyanide concentrations ranged from 0.016 to 0.024 mg/L across the five

sampling points, under the WHO drinking water guideline of 0.07 mg/L. Anionic surfactant concentrations, ranged from 0.423 to 0.649 mg/L, with a mean of 0.538 mg/L across the five sampling points. Nonionic surfactant concentrations ranged from 0.269 to 0.505 mg/L, with a mean of 0.385 mg/L Cationic surfactant concentrations, ranged from 0.504 to 1.105 mg/L, with a mean of 0.895 mg/L.

The obtained results provide information regarding the distribution of carbon species in groundwater from northwestern Romania. Variations in TC, TOC, and TIC concentrations reflected differences in local geology, groundwater residence time, and recharge conditions. The occurrence of organic acids, cyanide and surfactants allowed the identification of possible anthropogenic influences on individual groundwater sources [3-5].

The results demonstrate the importance of integrating classical carbon indicators with emerging organic contaminants when evaluating groundwater quality. Such an approach improves the identification of contamination sources, supports hydrogeochemical interpretation, and contributes to sustainable groundwater resource management. The significance of this study lies in its integrated investigation of traditional naturally occurring carbon contaminants alongside emerging contaminants that remain insufficiently studied in groundwater systems. The data obtained in this study also provide a valuable baseline for future monitoring programs in the Maramureș and Satu Mare regions, where natural mineral water resources represent an important environmental and socio-economic asset.

Acknowledgements: This work was supported by the Technical University of Cluj-Napoca through the doctoral research program within the IOSUD-UTCN. The authors gratefully acknowledge the financial support for participating in this conference.

References

[1] McDonough, L.K., Santos, I.R., Andersen, M.S., O'Carroll, D.M., Rutlidge, H., Meredith, K., Oudone, P., Bridgeman, J., Gooddy, D.C., Sorensen, J.P. and Lapworth, D.J., Changes in global groundwater organic carbon driven by climate change and urbanization. Nature Communication*s*, (2022), 11(1),.1279.

[2] Gooddy, D., Hinsby, K. Dissolved organic carbon in European groundwaters. In EGU General Assembly. European Geosciences Union (2007).

[3] Abdalla, O. A. E., Suliman, F. O., Al-Ajmi, H., Al-Hosni, T., Rollinson, H., Cyanide from gold mining and its effect on groundwater in arid areas, Yanqul mine of Oman. Environmental Earth Sciences, 60(4), (2010), 885–892.

[4] Gonçalves, R. A., Holmberg, K., Lindman, B., Cationic surfactants: A review. Journal of Molecular Liquids, 375, (2023), 121335.

[5] Kincses, N., Buda, A., Dippong, T., Mihali, C. Evaluation of the physico-chemical parameters of water in the lakes of Bocicoiu Mare. Scientific Bulletin of North University Center of Baia Mare Series D. Mining, Mineral Processing, Non-ferrous Metallurgy, Geology and Environmental Engineering, vol 40, nr 1, (2026), 77-87. DOI: https://doi.org/10.37193/SBSD.2026.1.08.

MECHANOCHEMICAL SYNTHESIS OF CHITOSAN-QUATERNARY PHOSPHONIUM SALT COMPOSITES FOR ANTIBACTERIAL APPLICATIONS

Alexandru Buhai[1*], Adriana Popa[1], Andrei Ivan[2], Ileana Nichita[2] Aurelia Vișa[1]
[1] "Coriolan Drăgulescu" Institute of Chemistry, 24 Mihai Viteazu Blv, 300223 Timişoara, Romania, email: buhaialex9@gmail.com
[2]Faculty of Veterinary Medicine, University of Life Science "King Michael I", 119 Calea Aradului, 300465, Timisoara, Romania

Abstract

With the seeking of more green approaches in synthesis and the growing interest in chitosan derivatives, specifically quaternary phosphonium salts (QPSs) chitosan derivatives due to their increased antibacterial effect, an often used method to obtain these derivatives is mechanochemistry. This study reports the green synthesis of chitosan-quaternary phosphonium salts composite materials.

Introduction

Chitosan is a renewable, biodegradable and biocompatible polysaccharide whose chemical functionalization provides an effective strategy for tailoring its physicochemical and biological properties. In particular, the incorporation of permanently charged quaternary phosphonium groups can improve the cationic character, water compatibility and antimicrobial performance of chitosan derivatives [1]. This type of derivatives are used in food preservation [2] and artifact preservation [3].

Green chemistry seeks to minimize adverse impacts on human health and the environment while enhancing the efficiency, sustainability, and resource efficiency of chemical processes through the implementation of its twelve fundamental principles [4]. Mechanochemistry promotes intimate contact between the solid reactants and can facilitate chemical transformations through mechanical energy, offering a potentially simpler and more sustainable alternative to conventional solution-based functionalization.

Experimental

In the present work, low molecular weight chitosan was combined with quaternary phosphonium salts (metyltriphenylphosphonium iodide, butyltriphenylphosphonium iodide, pentyltriphenylphosphonium iodide) through a mechanochemical approach, providing a solvent-free route for the preparation of chitosan derivatives. The obtained materials were characterized using solid state UV-Vis and FT-IR to confirm the interaction between the two components, respectively electronic microscope imaging to visualize the surface of the material.

Results and discussions

The composite was synthesized as follows: equimolar amounts (1:1) or (1:2) ratios of chitosan and QPSs were mixed by mechanochemical treatment for 30 min at a power of 30 Hz, resulting 6 samples.

The FTIR spectra exhibited the characteristic absorption bands of the phosphonium salts at 1434 cm^{-1}, while the characteristic bands of chitosan were observed as follows: a broad O–H and N–H stretching band at approximately 3200–3500 cm^{-1}, C–H stretching bands at 2870–2930 cm^{-1}, the amide I band at 1650 cm^{-1}, and the N–H bending band at in the region of 1580–1600 cm^{-1}.

The UV-Vis spectrum of the composite materials differ significantly from those of the individual starting components. In particular, changes in intensity and a shift to lower wavelengths (270-280 nm) compared with the spectrum of the QPs (340-360 nm).

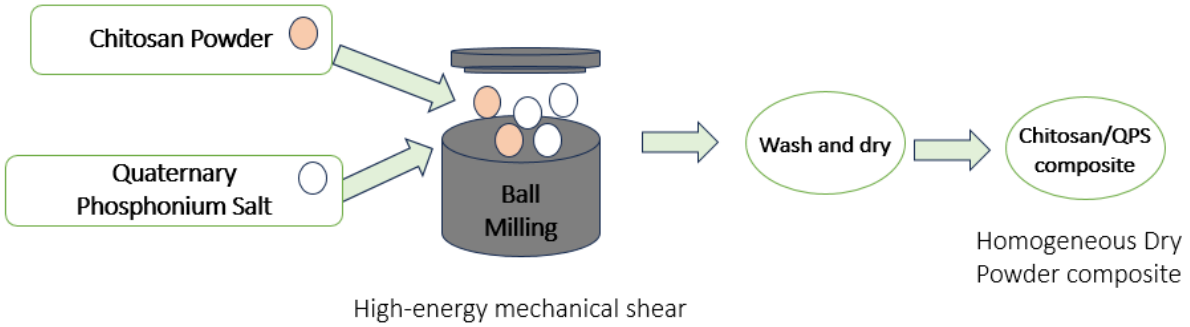


Fig. 1. Synthesis procedure of chitosan-quaternary phosphonium salts composites

Previous studies have demonstrated that QPs exhibit broad-spectrum antimicrobial activity against both Gram-positive and Gram-negative bacteria. Building on these findings, the incorporation of QPs into a chitosan-based matrix represents a promising strategy for the development of active food-packaging films [5].

By exploiting the non-covalent entrapment of the phosphonium salt within the renewable biopolymeric matrix, this composite demonstrates significant promise as an eco-friendly active food packaging material, successfully fulfilling the green design criterion for post-consumer degradation.

Conclusion

In conclusion this study presents the mechanosynthesis as a green approach to obtain chitosan-quaternary phosphonium salts composite materials. The unhindered mobility of the cationic phosphonium centers allows for a sustained, diffusion-controlled release that disrupts microbial cell membranes at the food interface, while the overarching chitosan framework maintains its intrinsic mechanical and gas-barrier integrity, thereby eliminating the reliance on persistent, petroleum-derived plastics, thus these materials that can further be used in antimicrobial applications.

Acknowledgements

This work is supported by Program no 2, from the „Coriolan Drăgulescu" Institute of Chemistry Timisoara, Romania.

References

[1] Freitas ED, Moura CF Jr, Kerwald J, Beppu MM. Polymers (Basel). 30 (2020) 12(12):2878
[2] Pan Q, Zhou C, Yang Z, He Z, Wang C, Liu Y, Song S, Gu H, Hong K, Yu L, Qu Y, Li P. Food Chem. 387 (2022) 132878.
[3] Bobu E, Nicu R, Obroce P, Ardelean E, Dunca S, Bălăeș T. Cellulose Chem. Technol. 50 (2016) 689-699
[4] Anastas P., Warner J., Green Chemistry: Theory and Practice, Oxford University Press, New York, 1998.
[5] Buhai A., Popa A., Visa A., Ivan A., Nichita I.; Proceedings of the 31st International Symposium on Analytical and Environmental Problems, University of Szeged, Szeged, 2025, 23-24

VALIDATION OF A MULTIRESIDUE METHOD FOR THE DETERMINATION OF INSECTICIDES IN SURFACE WATER: RELEVANCE TO DIRECTIVE (EU) 2026/805

Vojislava Bursić[1], Gorica Vuković[2], Antonije Žunić[1*], Bojan Konstantinović[1], Nataša Mandić[1], Tijana Stojanović[1], Nikola Puvača[3], Dušan Marinković[1]

[1]University of Novi Sad, Faculty of AgricultureTrg Dositeja Obradovića 8, 21000 Novi Sad, Serbia
[2]Field test, Vinogradarska 150 b, Belgrade, Serbia
[3]Faculty of Economics and Engineering Management in Novi Sad, Cvecarska 2, Novi Sad, Serbia
e-mail: antonije.zunic@polj.edu.rs

Abstract

The aim of this study was to validate a multiresidue method for the determination of fifteen insecticides in surface water using solid-phase extraction followed by liquid chromatography-tandem mass spectrometry (LC-MS/MS). Method performance was evaluated in terms of recovery, precision, linearity, limit of detection (LOD), limit of quantification (LOQ), and expanded measurement uncertainty. Validation was performed using spiked blank water samples at two concentration levels, 0.05 and 0.10 µg L^{-1}. Mean recoveries ranged from 84.7 to 102.7%, with RSD between 0.84 and 8.70%. The calibration curves showed good linearity for most analytes over the investigated concentration range, with coefficients of determination (R^2) ranging from 0.9620 to 0.9940, while chlorpyrifos showed a lower R^2 value of 0.9875. The LOQ established for all investigated analytes was 0.01 µg L^{-1}, and the expanded measurement uncertainty (k = 2) ranged from 38.19 to 49.04%, remaining below the 50% criterion specified in Commission Directive 2009/90/EC. The results demonstrate that the validated LC-MS/MS method provides suitable precision and measurement uncertainty under the validation conditions applied in this study. The results also highlight the importance of relating method performance characteristics, particularly LOQ and measurement uncertainty, to the applicable environmental quality standards when evaluating regulatory suitability under the evolving European water-quality framework, including Directive (EU) 2026/805.

Introduction

Directive (EU) 2026/805 of the European Parliament and of the Council of 30 March 2026 amending Directive 2000/60/EC, Directive 2006/118/EC and Directive 2008/105/EC represents an update of the existing EU legislative framework for water policy. Rather than establishing an entirely new regulatory framework, the Directive amends and strengthens the existing system for the protection and management of water resources. Its main objective is to further improve the protection of surface water and groundwater, particularly with regard to chemical pollution and to contribute to achieving good chemical and ecological status of European waters. Particular emphasis is placed on the risks associated with toxic and persistent pollutants, their potential for bioaccumulation. and their long-term presence in the aquatic environment.

The Directive was adopted by the European Parliament and the Council of the European Union on 30 March 2026 and published in the Official Journal of the European Union on 20 April 2026 as OJ L, 2026/805. It entered into force on 10 May 2026. Although the Directive is already in force at the EU level, Member States are required to adopt and publish the laws. regulations and administrative provisions necessary to comply with its provisions by 21 December 2027.

Directive (EU) 2026/805 strengthens and updates the EU framework for the monitoring and assessment of chemical pollutants in surface waters. Particular attention is given to priority substances and other pollutants posing a risk to the aquatic environment, as well as to the monitoring of substances that may accumulate in sediment or biota and emerging substances of concern. The Directive also promotes improvements in analytical and monitoring approaches and provides for the further development and standardisation of methods and technical specifications for assessing water quality.
Directive 2008/105/EC originally established EU-wide environmental quality standards (EQS) for 45 priority substances, together with eight other pollutants already regulated at EU level. Directive (EU) 2026/805 amends and extends this framework by introducing additional substances and revised requirements for the assessment and monitoring of chemical pollutants in surface waters. Among the substances and substance groups considered within the updated framework are pesticides, including groups of pesticides considered according to their mode of action. reflecting the increasing importance of comprehensive monitoring of pesticide contamination in the aquatic environment.
Within this regulatory context, reliable and sufficiently sensitive analytical methods are essential for the assessment of chemical status and the effective monitoring of pollutants in surface waters. Commission Directive 2009/90/EC establishes the technical specifications for chemical analysis and monitoring of water status and requires analytical methods used within the Water Framework Directive framework to be validated and documented in accordance with EN ISO/IEC 17025 or equivalent internationally accepted standards. Furthermore, Article 4 establishes minimum performance requirements, including a limit of quantification (LOQ) equal to or below 30% of the relevant EQS and a measurement uncertainty of 50% or below (k = 2). estimated at the level of the relevant EQS.
The aim of the present study was to validate a multiresidue analytical method for the determination of insecticides in surface waters, with particular emphasis on demonstrating adequate sensitivity, precision and reliability, as well as meeting the applicable requirements for LOQ and measurement uncertainty using liquid chromatography with tandem mass spectrometry (LC-MS/MS). The validated method is intended to support the reliable determination of insecticides in surface waters within the regulatory framework established by Directive (EU) 2026/805.

Experimental

Chemicals and reagents: The analytical standards of insekticides and Carbofuran-D3 (internal standard) were purchased from Dr. Ehrenstorfer (Augsburg, Germany), HCOOH (98–100%), MeCN (HPLC grade) and MeOH (HPLC grade) were purchased from Merck (Darmstadt, Germany).
Validation parameters: Recovery, repeatability, linearity, LOD, LOQ and measurement uncertainty (U(ex), %; k=2) were evaluated. The regulatory interpretation of method performance was considered according to 2009/90/EC, which establishes minimum performance criteria for method for pesticide residues monitoring in water. Blank samples (distilled water) were used to set the patameters of validation.
Sample extraction: After filtration through a 0.45 µm microfilter. 250 mL of spiking water The SPE columns (Bond Elut PLEXA) were mounted on a vacuum manifold and conditioned by passing 5 mL of methanol (2 × 2.5 mL) and then 5 mL of water. After conditioning, the entire volume of the spiked samples was passed through the SPE column. A vacuum pressure of 5 bar was applied to pass the samples through the column. The column was then washed twice with 3 mL of dichloromethane. The analytes were eluted with 6 mL of methanol (2 × 3 mL), with a 15 mL plastic tube placed beneath each column. The obtained extract was evaporated under a

stream of nitrogen and reconstituted in the mobile phase. After filtration through a 45 µm filter, the sample was analysed by LC-MS/MS.

LC-MS/MS conditions: An Agilent series 1200 HPLC system (Agilent Technologies) equipped with a G1312B binary pump, a G1367D auto sampler, a G1379B degasser, a G1316B column compartment thermostat, The HPLC system was coupled to an Agilent triple quadrupole mass spectrometer (6410B) coupled to an electrospray ionization source (ESI+). A Zorbax XDB C18 column (50x4.6 mm, 1.8 µm particle size) from Agilent (San Jose, CA, USA) was employed for the separation. The chromatographic determination of neonicotinoids was carried out employing a binary mobile phase with methanol (0.1% HCOOH, v/v - A) and an aqueous solution of formic acid (0.1%, v/v - B). A gradient elution started at 60% of B at the flow rate of 0.4 mL/min. This composition was reduced to 30% B in 10 min, and held for 5 min. The system was equilibrated during 5 min. The injection volume was 5 µL and column temperature was kept at 30 ºC. The ESI source values were as follows: drying gas (nitrogen) temperature 350 °C, drying gas flow rate 10 L/min, nebulizer pressure 40 psi and capillary voltage 4000 V. The detection was performed using the multiple reactions monitoring mode (MRM). The Agilent MassHunter software (version B.06.00 Agilent Technologies, 2012) was used for the optimization and quantification.

Results and discussion

The LC-MS/MS (ESI+) fragmentation of the protonated molecular ions of the investigated insecticides, yielding two product ions for each compound, is presented in Table 1. The average recoveries were calculated from the gained recovery values of spiking blank samples at concentrations of 0.05 and 0.1 µg L^{-1}, in three replicates and with the estimated measurement uncertainty (U(ex), %; k=2) are prsented in Table 1. The linearity of the method was evaluated for the analytes of interest over the concentration range of 0.01–0.20 µg L^{-1}. The coefficient of determination (R^2) was calculated for each pesticide and the corresponding values are presented in Table 1.

Table 1. MRM and validation parameters

Pesticide	Transition	R^2	Calibration Formula	R_T, min*	Recovery, % ± RSD, %	U(ex), %
Acetamiprid	223.1 - 126.0; 55.7	0.9861	y = 0.101147 * x + 0.009439	4.91	85.7 ± 2.52	45.21
Avermectin B1A	890.5 - 305.1; 145.2	0.9879	y = 0.002512 * x + 1.462292E-004	7.25	84.7 ± 6.28	42.11
Bendiocarb	224.1 - 167.1; 109.0	0.9925	y = 0.034545 * x + 0.002405	6.38	96.4 ± 2.31	49.04
Bifenazat-diazene	299.2 - 213.1; 197.1	0.9870	y = 0.087722 * x + 5.588268E-004	11.88	93.5 ± 3.87	47.26
Bifenazate	301.1 - 170.1; 198.0	0.9702	y = 53665.1112 * x - 205.160097	9.47	102.7 ± 2.77	38.19
Chlorantraniliprole	483.9 - 452.9; 286.1	0.9786	y = 0.006238 * x + 3.427578E-004	8.10	92.5 ± 3.58	40.84
Chlorpyriphos	349.9 - 97.0; 197.9	0.9875	y = 0.002282 * x + 1.340665E-004	12.64	101.2 ± 2.92	39.28
Cyantraniliprole	475.0 - 285.9; 444.0	0.9915	y = 0.006104 * x + 3.998538E-004	7.15	97.1 ± 2.30	44.36
Emamectin B1a	886.5 - 158.0; 126.1	0.9906	y = 0.099477 * x + 0.009023	9.56	96.4 ± 8.70	41.17
Indoxacarb	528.1 - 203.0; 150.0	0.9936	y = 0.004795 * x + 2.668410E-004	11.99	86.6 ± 6.34	43.95
Pirimifos-methyl	306.2 - 164.1; 108.0	0.9876	y = 0.425546 * x + 0.021476	10.77	92.0 ± 1.68	42.88
Prometryn	242.1 - 158.0; 200.1	0.9886	y = 0.880714 * x + 0.053103	6.23	91.4 ± 5.14	44.35
Spinosyn A	732.5 - 142.1; 98.2	0.9620	y = 0.193502 * x + 0.016463	8.48	96.7 ± 3.41	45.77
Spinosyn D	746.5 – 142; 98.2	0.9803	y = 0.045071 * x + 0.004115	8.71	94.9 ± 2.14	45.64
Thiamethoxam	292.0 - 211.1; 181.0	0.9940	y = 0.010851 * x + 7.811342E-004	4.16	93.1 ± 0.84	

Carbofuran – D3	225.1 – 165.0; 123.0			11.45		

*R_T- retention time, min

The expanded measurement uncertainty obtained for the fifteen insecticides for which validation was performed was below 50% (k = 2). However, this result alone should not be interpreted as evidence of full compliance with Article 4 of Commission Directive 2009/90/EC, as the Directive relates measurement uncertainty to the relevant environmental quality standard (EQS) and additionally requires the limit of quantification (LOQ) to be equal to or lower than 30% of the corresponding EQS. Therefore, the LOQ established for all analytes included in the study was 0.01 μg L^{-1}.

Conclusion

The validation of fifteen insecticides demonstrated acceptable precision and an expanded measurement uncertainty below 50% (k = 2) under the validation conditions used in this study. In the context of Commission Directive 2009/90/EC, a full regulatory assessment should additionally relate the method LOQ and measurement uncertainty to the applicable environmental quality standard (EQS), where such a standard is established. The evolving European water-quality framework, including Directive (EU) 2026/805, further emphasizes the need for analytical methods capable of reliable quantification at environmentally relevant concentrations.

Acknowledgements

The authors acknowledge the financial support of the Provincial Secretariat for Higher Education and Scientific Research (Project No.: 003864627 2025 09418 003 000 000 001 04 004) and the of the Ministry200117 of Agriculture, Forestry and Water Management, Project No. 451-03-34/2026-03/.

References

[1] Directive (EU) 2026/805 of the European Parliament and of the Council of 30 March 2026 amending Directive 2000/60/EC establishing a framework for Community action in the field of water policy, Directive 2006/118/EC on the protection of groundwater against pollution and deterioration and Directive 2008/105/EC on environmental quality standards in the field of water policy.

[2] Directive 2008/105/EC of the European Parliament and of the Council of 16 December 2008 on environmental quality standards in the field of water policy, amending and subsequently repealing Council Directives 82/176/EEC, 83/513/EEC, 84/156/EEC, 84/491/EEC, 86/280/EEC and amending Directive 2000/60/EC of the European Parliament and of the Council

[3] Commission Directive 2009/90/EC of 31 July 2009 laying down, pursuant to Directive 2000/60/EC of the European Parliament and of the Council, technical specifications for chemical analysis and monitoring of water status.

[4] SO/IEC 1725:2017. General requrements for the competence of testing and calibration laboratories

RADIATION-INDUCED VALENCE CONVERSION AND THERMAL OXIDATION OF TM-DOPED CAF_2 AND BAF_2 CRYSTALS

Gabriel Buse[1], Maria Poienar[2], Marius Stef[3], Carla Zeicu[4], Philippe Veber[1,2] Mathieu Duttine[3] and Daniel Vizman[2]

[1]ICAM, West University of Timisoara, Bvd. V.Parvan, No.4, Timisoara (Romania)
[2]Physics Faculty, West University of Timisoara, Bvd. V.Parvan, No.4, Timisoara (Romania)
[3]University of Bordeaux, CNRS, Bordeaux INP, ICMCB, UMR 5026, F-33600 Pessac (France)
Email: gabriel.buse@e-uvt.ro

Rare-earth-doped fluoride crystals are highly promising for luminescent, dosimetric, and photochromic applications due to their combination of low phonon energies, wide optical transparency across the UV–VIS–NIR range, and the chemical stability of the host lattice[1,2]. In this work, CaF_2 and BaF_2 single crystals doped with different concentrations of TmF_3 were grown by the vertical Bridgman–Stockbarger method [3]. Disks with a diameter of 10 mm and a thickness of 1 mm were prepared from the as-grown crystals and irradiated at room temperature with continuous flux of X-rays for 1, 2, 3, and 4 h. Room-temperature optical absorption spectra of the as-grown CaF_2 crystals revealed distinct absorption features associated with both Tm^{3+} and Tm^{2+} ions, whereas the BaF_2 crystals exhibited predominantly Tm^{3+}-related absorption bands. The absorption intensity was found to depend on both the TmF_3 concentration and the nature of the host matrix. X-ray irradiation produced pronounced changes in the UV–VIS absorption spectra, particularly an enhancement of the Tm^{2+}-related absorption bands. These results indicate that ionizing radiation promotes the conversion of Tm^{3+} to Tm^{2+} in both CaF_2 and BaF_2 hosts. To investigate the reversibility and thermal stability of this radiation-induced valence conversion, the irradiated crystals were subsequently annealed at temperatures up to 600 °C. The evolution of the absorption spectra during thermal treatment provides insight into the thermally activated oxidation of Tm^{2+} back to Tm^{3+} and the associated modification of the optical properties. Luminescence measurements were also performed to evaluate the effects of X-ray irradiation and subsequent thermal annealing on the emission characteristics of the Tm-doped fluoride crystals. The results demonstrate the strong influence of ionizing radiation and thermal treatment on the valence state and optical response of thulium ions in alkaline-earth fluoride hosts, highlighting the potential of these materials for radiation detection, dosimetry, and other radiation-responsive optical applications.

Acknowledgements
This work is supported by a grant PNRR/ 2022 /C 9 /MCID/I8, project title Enhanced Single Crystal Applications and Research in the Growth of new Optical rare earth based compounds for sustainable and efficient Technologies (ESCARGOT), contact number 136 15.11.2022.

References
[1] K.L. Medard, H. Hamilton, S.C. van der Moore, J. Chem. Anal. 313 (2007) 163.
[2] B.T. Metan, A. Milne, in: A.C. Thomson, P.T. Bell (Eds.), Introduction to General Chemistry, Chempublishing, Washington, 1994, pp. 547.

PREPARATION AND CHARACTERIZATION OF ANTHOCYANIN (RED PEONY)–B-CYCLODEXTRIN COMPLEXES

Adina Căta[1], Daniel H. Ursu[1], Anamaria Dabici[1], Paula Sfîrloagă[1], Nick S. Țolea[1], Dan Roșu[1], Oana-Raluca Pop[2], Ioana M.C. Ienașcu[1,3]

[1]National Institute of Research and Development for Electrochemistry and Condensed Matter, Dr. A. P. Podeanu 144, 300569, Timişoara, Romania
[2]University of Medicine and Pharmacy "Victor Babeş" Timişoara, Faculty of Pharmacy, 2 Eftimie Murgu Square, 300041 Timişoara,, Romania
[3]"Vasile Goldiş" Western University of Arad, Faculty of Pharmacy, Liviu Rebreanu 86, 310045, Arad, Romania
e-mail: adina.cata@yahoo.com

Abstract

Anthocyanins are natural pigments with attractive antioxidant properties and potential applications as natural colorants and functional ingredients. However, their physicochemical properties are strongly influenced by environmental conditions, which may limit their practical applications. Cyclodextrins can interact with suitable guest molecules through their hydrophobic cavities, providing an approach for modifying the molecular environment of natural compounds and obtaining inclusion complexes [1].

An anthocyanin-rich extract obtained from red peony petals (*Paeonia* spp.) was characterized in terms of anthocyanin content [2], total phenolic content [3], and antioxidant capacity using DPPH and FRAP assays [4,5]. The anthocyanin content was 2.010 ± 0.033 mg/g dry plant material. HPLC analysis revealed three anthocyanins, with two major compounds: pelargonidin-3,5-diglucoside and cyanidin-3,5-diglucoside.

Two inclusion complexes, containing different amounts of the anthocyanin-rich extract, were prepared by trituration with β-cyclodextrin. The resulting solid systems were characterized by UV-Vis-NIR spectroscopy, ATR-FTIR, X-ray diffraction and scanning electron microscopy. The UV-Vis spectra showed a shift of the characteristic anthocyanin absorption band from 524 nm in the extract to 541 nm in both complexes. FTIR analysis revealed shifts of characteristic β-cyclodextrin bands and a reduction or disappearance of selected anthocyanin-associated bands. XRD analysis indicated a decrease in β-cyclodextrin crystallinity, while SEM revealed a more pronounced amorphous morphology of the complexes. The complementary spectroscopic, structural and morphological results provide evidence for the formation of anthocyanin–β-cyclodextrin inclusion complexes. Further studies will focus on evaluating the physicochemical stability and functional properties of the obtained anthocyanin–β-cyclodextrin complexes.

References

[1] A. Cid-Samamed, J. Rakmai, J.C. Mejuto, J. Simal-Gandara, G. Astray, Food Chem. 384 (2022), 132467.
[2] M.M Giusti., R.E. Wrolstad, Unit F1.2. Anthocyanins. Characterization and Measurement of Anthocyanins by UV-Visible Spectroscopy, Current Protocols in Food Analytical Chemistry, John Wiley & Sons, Inc., 2001, pp. F1.2.1-F1.2.13.
[3] A.L. Waterhouse, Unit I1.1. Polyphenolics. Determination of Total Phenolics, Current Protocols in Food Analytical Chemistry, John Wiley & Sons, Inc., 2002, pp. I1.1.1-I1.1.8.
[4] W. Brand-Williams et al., LWT - Food Sci. & Technol. 28 (1995), 25-30.
[5] I.F.F. Benzie, J.J. Strain, Anal. Biochem. 239 (1996), 70.

INDOOR AIR QUALITY (IAQ)– RISKS TO HEALTH

Aleksandra Čavić[1], Marko Carić[1], Marko Koprivica[3], Miljan Šunjevic[2]

[1]University Business Academy in Novi Sad, Faculty of Economy and Engineering Management in Novi Sad, 21000 Novi Sad, Cvecarska 2, Serbia
[2]Department of Environmental Engineering and Occupational Safety and Health, Faculty of Technical Sciences, University of Novi Sad, Trg Dositeja Obradovića 6, 21000 Novi Sad, Serbia
[3]Faculty of Medicine, University of Novi Sad, Hajduk Veljkova 3, 21000 Novi Sad, Serbia
e-mail: Aleksandra.cavic22@gmail.com

Abstract
The modern urban population spends more than 90% of their time indoors, making indoor air quality a critical public health issue. Although environmental strategies traditionally focus on outdoor air pollution, indoor concentrations of specific toxicants can be significantly higher due to microclimatic conditions, building characteristics, and indoor emission sources. This paper analyzes the dynamics of the accumulation of chemical pollutants (such as formaldehyde and particulate matter) and the radioactive gas radon. The findings indicate that the hermetic sealing of buildings exponentially increases pollutant levels, particularly after prolonged periods of closure, leading to "sick building syndrome" and chronic health risks. Mitigation strategies must shift from passive ventilation to advanced engineering methods, including active soil depressurization, heat recovery ventilation (HRV), and real-time IOT monitoring, which demonstrate high cost-effectiveness in safeguarding public health.

Keywords: indoor air quality; radon; energy efficiency; ventilation; public health.

Introduction

Urban residents today spend more than 90% of their time indoors—primarily in apartments, schools, and workplaces. Consequently, indoor air quality has become one of the primary public health concerns [1]. Although public policies and environmental strategies traditionally focus on ambient air pollution, scientific research points to a completely different reality: the concentrations of certain toxicants in indoor environments can be several times higher than outdoors [2]. The dynamics and retention of pollutants inside buildings directly depend on fundamental microclimatic parameters, primarily temperature and relative humidity. Elevated humidity, for instance, creates an ideal breeding ground for biological contaminants such as mold spores and dust mites [2]. Generally speaking, indoor air quality is the result of a complex interaction between outdoor microclimatic factors, the architectural characteristics of the building itself, indoor emission sources, and the efficiency of ventilation systems [3].

Health Risks and Chemical Pollutants in Indoor Environments

Understanding building and environmental factors is a crucial prerequisite for preventing a wide range of chronic diseases [4]. Daily activities such as cooking, using household chemicals, or exposure to tobacco smoke generate high concentrations of particulate matter. These particles penetrate deep into the respiratory tract, triggering local and systemic inflammatory responses [4]. In scientific literature, prolonged exposure to this type of pollution is consistently linked to an increased incidence of chronic obstructive pulmonary disease (COPD), a decline in lung function, and an elevated risk of cardiovascular disorders in adults, as well as in vulnerable groups [4]. A specific health risk arises when returning to residential or commercial spaces that have been completely closed for an extended period, which is common after annual vacations

and school breaks, particularly in educational institutions. When a building is hermetically sealed, the lack of air exchange leads to the establishment of a so-called high-density equilibrium concentration of pollutants. In these situations, formaldehyde dominates—a gas continuously emitted by building components, polymeric materials, and lacquered furniture [4]. Staying in such a space without prior intensive ventilation exposes the body to a sudden inhalation of toxin-saturated air. This has been proven to initiate mucosal irritation, headaches, cognitive fatigue, and other manifestations classified under sick building syndrome [4]. Regarding the use of indoor plants for decontamination, contemporary studies have corrected earlier, overoptimistic expectations. Although certain plant species can absorb gases in highly controlled laboratory chambers, their actual performance in real residential and office conditions is negligibly small [5]. The natural air exchange rate in buildings eliminates pollutants orders of magnitude faster than plants ever could, which is why phytoremediation (air purification via plants) cannot be considered an adequate substitute for regular ventilation [5].

Specifics of Radon Accumulation and Ingress Mechanisms

In addition to standard chemical compounds, radon poses a specific risk. It is a naturally occurring radioactive gas without color, taste, or odor, produced by the decay of radium and uranium in soil and rocks [6]. The World Health Organization (WHO) classifies radon as the second most significant cause of lung cancer development in the general population, right behind tobacco smoking. It is estimated that radon causes between 3% and 14% of all cases of this cancer, depending on the national average of the environment being measured [6]. During inhalation, short-lived radioactive radon progeny attach to airborne particulate matter and enter the lungs, where they cause direct DNA damage to epithelial cells by emitting alpha particles [6]. Radon penetrates building interiors—primarily basements and ground-floor rooms—convectively and via diffusion through cracks in foundations, floor slabs, and utility cable conduits [7]. The gas also intensively migrates through unsealed joints, the building materials themselves, and openings around pipes [9]. Once inside the building, due to the so-called "stack effect", it tends to accumulate in lower zones but subsequently spreads progressively toward higher floors. This equally affects both old houses and energy-efficient new buildings [9]. This process of drawing gas from the ground is particularly pronounced during winter months. At that time, the large difference between indoor and outdoor temperatures amplifies the rising of warm air, creating a negative pressure in lower levels that literally sucks radon from the basement substrate [10]. The lack of ventilation in enclosed buildings leads to a rapid accumulation of radon, where concentrations can exceed recommended safety limits multiple times within just a few days [8]. On the other hand, the installation of mechanical systems can effectively reduce radon and carbon dioxide levels by over sixty percent [7].

Modern Architectural Trends and Engineering Mitigation Methods

The synergy between modern architectural trends and the dynamics of gas accumulation imposes an urgent need to redefine indoor space protection strategies. Contemporary energy efficiency trends, which involve the installation of highly airtight PVC or aluminum joinery and the application of thick thermal insulation layers on facades, inadvertently transform residential buildings into hermetically isolated units. While this approach successfully reduces thermal energy consumption, it simultaneously drastically reduces the infiltration of fresh outdoor air through the micro-cracks of window frames. Under such conditions, gases like radon lack a natural dispersion pathway to the outdoor environment, causing their accumulation rate to grow exponentially.Resolving this issue requires abandoning the old concept of passive ventilation and shifting toward advanced engineering mitigation techniques. This primarily entails installing active soil depressurization systems beneath the foundation slab, which extract

radon before it can even enter the building. Furthermore, the installation of sensor-controlled heat recovery ventilation (HRV) systems is crucial, along with the integration of one-way drainage valves in floor drains to prevent the backflow of gases from underground utility systems [11].In addition to structural modifications, an important step in comprehensive health protection is the implementation of smart systems for the continuous monitoring of indoor parameters. Traditional methods of periodic air sampling often fail to detect sudden spikes in gas concentrations, which fluctuate depending on atmospheric pressure, wind direction, and the occupants' own activities. The introduction of IoT (Internet of Things) sensor networks enables real-time monitoring of radon levels, total volatile organic compounds (TVOC), and carbon dioxide. These systems automatically trigger forced ventilation the moment pollutants exceed critical threshold values, thereby preventing the risk of acute exposure to toxins after prolonged periods of absence. The integration of such technologies with building management systems (BMS) is becoming a standard in modern green building, transforming passive structures into reactive systems that dynamically adapt to the health needs of their users [12].

Toxicological and Economic Aspects of Multi-Component Exposure

From a toxicological perspective, it is essential to consider the phenomenon of multi-component exposure, where the simultaneous presence of chemical toxicants and radon can induce synergistic or multiplicative health effects. It has been proven that the combined action of formaldehyde, inhaled particulate matter, and alpha radiation from radon progeny accelerates carcinogenic mechanisms by inducing oxidative stress and inhibiting cellular systems responsible for DNA repair [13]. This interaction poses a distinct risk in spaces where long-term work is conducted, wherein the absence of ventilation not only raises baseline toxin levels but also alters the size distribution of aerosol particles to which radioactive isotopes attach [14]. Consequently, health risk assessment methodologies are increasingly shifting from the analysis of individual pollutants toward integrated models of cumulative indoor toxicity [15]. Beyond immediate health outcomes, the economic dimension of compromised indoor air quality encompasses substantial direct and indirect costs for healthcare systems and the economy. Sick building syndrome and chronic radon exposure directly correlate with a decline in work productivity, increased absenteeism rates, and the development of occupational diseases among office employees [16]. Investments in advanced HVAC ventilation systems and low-emission volatile organic compound materials can therefore not be viewed exclusively as a construction expense, but rather as a cost-effective public health preventive measure. The introduction of stringent statutory regulations mandating radon level measurements prior to issuing building occupancy permits has demonstrated high economic justification through the long-term reduction of treatment costs for respiratory tract malignancies [17].

Conclusion

In conclusion, maintaining optimal indoor air quality (IAQ) has emerged as a critical public health priority for preventive medicine, population protection, and statutory regulation. While modern airtight, energy-efficient architectural designs and extended building vacancies inadvertently exacerbate the accumulation of hazardous chemical and radiological toxicants like radon, passive ventilation is no longer sufficient to mitigate these risks.

To achieve truly safe and health-sustainable living and working environments, a shift from passive measures to proactive engineering is required, built upon three foundational pillars:

- Source Control & Certification: Stringently monitoring indoor emission sources and verifying certified, low-emission building materials.
- Advanced Mitigation Engineering: Implementing combined systems such as active soil depressurization alongside sensor-controlled heat recovery ventilation.
- Continuous IOT Monitoring: Utilizing Internet of Things (IOT) frameworks to track air quality parameters in real time.

Ultimately, this study demonstrates that integrating smart, technology-driven ventilation solutions can reliably reduce indoor toxicant loads by over 60%. This approach proves that energy efficiency does not need to compromise public health, providing a scalable, cost-effective, and safe blueprint for the future of healthy urban infrastructure.

Acknowledgements
We would like to express our gratitude to the Provincial Secretariat for Higher Education and Scientific Research for financing this research project under grant number 003858394 2025 09418 003 000 000 001 04 002.

References
[1] K.L. Medard, H. Hamilton, S.C. van der Moore, J. Chem. Anal. 313 (2007) 163.
[2] B.T. Metan, A. Milne, in: A.C. Thomson, P.T. Bell (Eds.), Introduction to General Chemistry, Chempublishing, Washington, 1994, pp. 547.
[1] National Institute of Environmental Health Sciences (NIEHS). Indoor Air Quality and Human Health. NIH Report; 2022.
[2] U.S. Environmental Protection Agency (EPA). Indoor Air Quality in the Home Environment: Contaminants and Health Effects. US EPA Report; 2023.
[3] Vardoulakis S, Giagloglou K, Steinle S, et al. Indoor air quality guidelines and energy efficiency measures in building envelopes. Environ Int. 2015;77:118-137. doi:10.1016/j.envint.2014.12.013
[4] Duan P, Wang J, Ramalho O, et al. Indoor Exposure to Selected Air Pollutants in the Home Environment: A Systematic Review. Int J Environ Res Public Health. 2020;17(6):2105. doi:10.3390/ijerph17062105
[5] Cummings BE, Waring MS. Potted plants do not improve indoor air quality: a review and analysis of reported VOC removal efficiencies. J Expo Sci Environ Epidemiol. 2020;30(3):422-431. doi:10.1038/s41370-019-0175-9
[6] World Health Organization. Radon and health. World Health Organization fact sheet. Published January 25, 2023. Accessed September 21, 2026. who.int
[7] Gusev A, Tsapalov A, Kovler K, et al. Modeling and justification of indoor radon prevention and mitigation techniques in energy efficient buildings. J Environ Radioactiv. 2022;242:106790. doi:10.1016/j.jenvrad.2021.106790
[8] Yarmoshenko I, Malinovsky G, Vasilyev A, et al. Changes in radon concentration in multistory energy efficient residential buildings. Radiat Prot Dosimetry. 2024;198(4):210-218. doi:10.1093/rpd/ncad2024
[9] Radonshop. Radon in my house: How does Radon enter a house? Radonshop technical brief. Accessed September 21, 2026. radonshop.com
[10] Dranjer. What is the radon stack effect and how can you mitigate it? Dranjer white paper. Accessed September 21, 2026. dranjer.com
[11] Diallo T, Ménézo C, Wurtz E. Engineering solutions for radon mitigation and indoor air quality optimization in tightly sealed buildings: A review of active and passive methods. Build Environ. 2026;248:111204. doi:10.1016/j.buildenv.2025.111204
[12] Al-Khatib M, Martinez-Molina A, et al. Smart indoor air quality monitoring and responsive HVAC control systems in automated green buildings. Energy Build. 2026;310:114112. doi:10.1016/j.enbuild.2026.114112
[13] Møller P, Karottki DG, Jensen DM, et al. Oxidative stress, DNA damage, and inflammation induced by multi-component indoor air pollution exposure. Mutat Res Rev Mutat Res. 2024;793:108485. doi:10.1016/j.mrrev.2023.108485

[14] Ishikawa T, Tokonami S, Narazaki Y. Attachment of radon decay products to multi-component indoor aerosols and its deposition dynamics in the human respiratory tract. J Radiol Prot. 2023;43(2):021504. doi:10.1088/1361-6498/acd302
[15] Sarigiannis DA, Karakitsios SP, Gotti A, et al. Integrated methodology for cumulative risk assessment of multi-component exposures to indoor air pollutants. Toxicol Lett. 2025;340:87-98. doi:10.1016/j.toxlet.2024.11.009
[16] Wargocki P, Wyon DP. The effects of indoor air quality and temperature on the productivity and health of office workers. Indoor Air. 2024;34(1):e13201. doi:10.1111/ina.13201
[17] Lin L, Wang Q, Zheng X. Economic evaluation of policy interventions and ventilation techniques for indoor radon mitigation: A cost-benefit analysis. Health Policy. 2025;145:105123. doi:10.1016/j.healthpol.2025.01.008

HYBRID MATERIALS (LDH-CELLULOSE ACETATE AND LDH-SAWDUST) UTILIZED AS ADSORBENTS OF CONGO RED DYE FROM WATER

Larissa-Rusalina Floca[1], Adelina Cucu-Novăcuț[1], Adriana Popa[2], Lavinia Lupa[1], Laura Cocheci[1]

[1]Faculty of Chemical Engineering, Biotechnologies and Environmental Protection, Politehnica University Timisoara, 300223 Timisoara, 6 Parvan Blv., Romania
[2]"Coriolan Drăgulescu" Institute of Chemistry, 300223 Timisoara, 24 Mihai Viteazul Blv., Romania
e-mail: laura.cocheci@upt.ro

Abstract

The objectives of the study are the synthesis and characterization of two hybrid materials based on layered double hydroxides (LDH) and cellulosic polymers (cellulose acetate and wood sawdust), as well as the use of synthesized materials as adsorbents for the Congo Red dye. Thus, two materials named LDH-cellulose acetate and LDH-sawdust were synthesized from chemical reagents and polymers containing cellulose. Structural analysis through X-ray diffraction spectroscopy of the synthesized materials revealed that they have a layered double hydroxide structure, but their crystallinity and lattice parameters have undergone changes due to interaction between the LDH with the organic substrate. Their use as adsorbent materials in the adsorption process of Congo Red dye from aqueous solutions led to promising experimental results for the continuation of studies. The equilibrium adsorption capacities obtained under the studied experimental conditions were: 26.6 mg/g for LDH-sawdust and 13.8 mg/g for LDH-cellulose acetate.

Introduction

Layered double hydroxides, abbreviated as LDH, are also known as anionic clays or hydrotalcite-type compounds [1]. They represent a class of two-dimensional (2D) inorganic materials with a unique lamellar structure. They were first discovered in nature in 1842 in Sweden, in the form of a mineral called hydrotalcite [2].

Microscopically, layered double hydroxides typically exhibit a morphology of hexagonal stacks or 2D nanosheets. The width of the particles ranges from 50 to 300 nm, and their thickness ranges from 10 to 50 nm. As a result of various synthesis methods for these particles, it has been found that they can crystallize into more complex forms, such as "flower-like" structures—which are nanometric cones, microspheres, or nanotubes—providing a much larger surface area [3].

The chemical and crystalline structure of LDH is derived from that of brucite ($Mg(OH)_2$), a natural form of magnesium hydroxide, in which metal cations are surrounded by six hydroxyl groups, thus forming octahedral clusters that split at their ends to create infinite layers. The host layers are occupied by divalent (M^{2+}) and trivalent (M^{3+}) metal cations. Since some divalent cations are replaced by trivalent cations of similar size, the layers will carry a positive electric charge [2]. Anions and water molecules are inserted into the interlayer region to compensate for the positive electric charge of the layers. Since the anions are mobile, they can be easily exchanged, giving layered double hydroxides a high anion exchange capacity. The general formula for these compounds is as follows:

$$[M^{II}_{1-x}\, M^{III}_{x}\, (OH)_2]^{x+}\, [A^{n-}_{x/n}]^{x-} \cdot mH_2O,$$

where x represents the molar ratio of the metals (usually between 0.2 and 0.4) [2]

In terms of symmetry, LDH can most often be grouped into hexagonal configurations with two layers in the unit cell (2H) and rhombohedral configurations with three layers (3R).

A key application of these materials is environmental remediation through wastewater treatment. Layered double hydroxides act as highly effective adsorbents for removing toxic heavy metals such as lead, copper, or cadmium through surface complexation and ion exchange mechanisms. Their ability to capture persistent organic pollutants is demonstrated by the efficient retention of synthetic dyes and pharmaceutical residues such as antibiotics. Their porous structure and high specific surface area facilitate the electrostatic interactions and hydrogen bonds necessary for the immobilization of contaminants.
Hybrid materials formed by integrating layered double hydroxides into natural polymer matrices such as cellulose offer synergistic advantages over the individual components. In these systems, cellulose acts as a rigid support that prevents the agglomeration of inorganic particles and significantly improves structural stability and mechanical strength. LDH-cellulose hybrids exhibit enhanced hydrophilicity and accelerated adsorption kinetics and have been successfully applied in industrial processes for the separation of oil-water mixtures or in the selective recovery of phosphates from aqueous media. The use of bacterial cellulose allows for the production of extremely pure and flexible composites with a homogeneous dispersion of the inorganic phase [1,4].

Experimental

Two hybrid materials based on layered double hydroxides (LDH) and cellulosic polymers were synthesized in the laboratory using chemical reagents (to produce LDH) and cellulose acetate and wood sawdust, respectively. The synthesized materials are hereinafter referred to as LDH-cellulose acetate and LDH-sawdust.
A 200 cm³ solution of (Zn^{2+} + Al^{3+}) cations with a total concentration of 1 M and a Zn^{2+} : Al^{3+} ratio of 3 : 1 was prepared by measuring the required masses of $Zn(NO_3)_2 \cdot 6H_2O$ and $Al(NO_3)_3 \cdot 9H_2O$, both reagents of analytical grade. 5 g of cellulose acetate were placed in an 800 cm³ Berzelius beaker, to which 100 cm³ of distilled water and 10 cm³ of 2 M NaOH solution were added.
The cation solution was added slowly, drop by drop, to the reaction vessel over the cellulose acetate, maintaining the pH between 9 and 9.5 using the sodium hydroxide solution. The resulting precipitate is placed in an oven to mature for 18 hours at 80°C; then the precipitate is washed with distilled water, filtered through filter paper, and dried in an oven for 24 hours at 80°C.
The same procedure is followed for the LDH-sawdust sample.
The structural analysis of the synthesized materials was performed using X-ray diffraction analysis with a Rigaku Ultima IV diffractometer. This method made it possible to identify the crystalline phases in the synthesized material, as the instrument compared the diffractogram of the synthesized materials with diffractograms already in the database.
The adsorption capacity of the synthesized materials—LDH-cellulose acetate and LDH-sawdust, respectively—was experimentally tested using the batch adsorption method: both the hybrid materials and the simple organic substrate alone were brought into contact with different concentrations of Congo Red dye solutions. Dye solutions with initial concentrations of 10, 20, 40, 60, 80, and 150 mg/L were used. The contact time was 2 hours in a Julabo stirrer at room temperature. After 2 hours, the solutions were filtered, and their absorbance was measured at 498 nm, by using a Varian Carry 100 UV–VIS spectrophotometer. The equilibrium adsorption capacity was calculated using the formula:

$$q_e = \frac{c_i - c_f}{m} \cdot V \qquad (1)$$

where: q_e – equilibrium adsorption capacity (mg/g)
c_i – initial concentration of the Congo Red solution (mg/L)
c_f – final concentration of the Congo Red solution (mg/L)

m – mass of adsorbent (g)
V – volume of the Congo Red solution (L)

Results and discussion

The structural analysis of the synthesized materials was performed using X-ray diffraction analysis. This method made it possible to identify the crystalline phases in the synthesized materials, as the instrument compared the diffractograms of the synthesized materials with diffractograms already present in the database. For comparison, a layered double hydroxide of Zn_3Al-CO_3 type, referred to as Zn_3Al-reagents, synthesized from analytically pure reagents, was also analyzed.

The Zn_3Al–reagents sample was identified as a zaccagnaite-type layered double hydroxide belonging to the R–3m group, according to PDF card no. 9015034 [5].

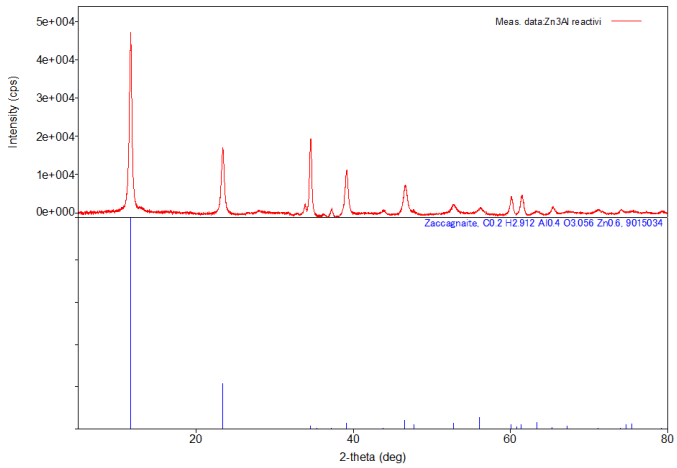
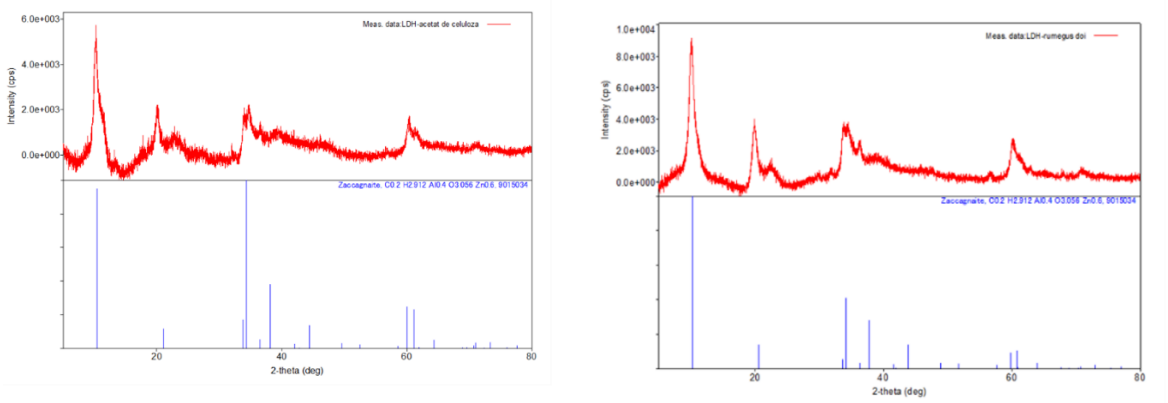


Figure 1. RXD pattern of Zn_3Al-reagents identified as zaccagnaite



a b

Figure 2. RXD patterns of ZnAl-cellulose acetate (a) and ZnAl-sawdust (b)

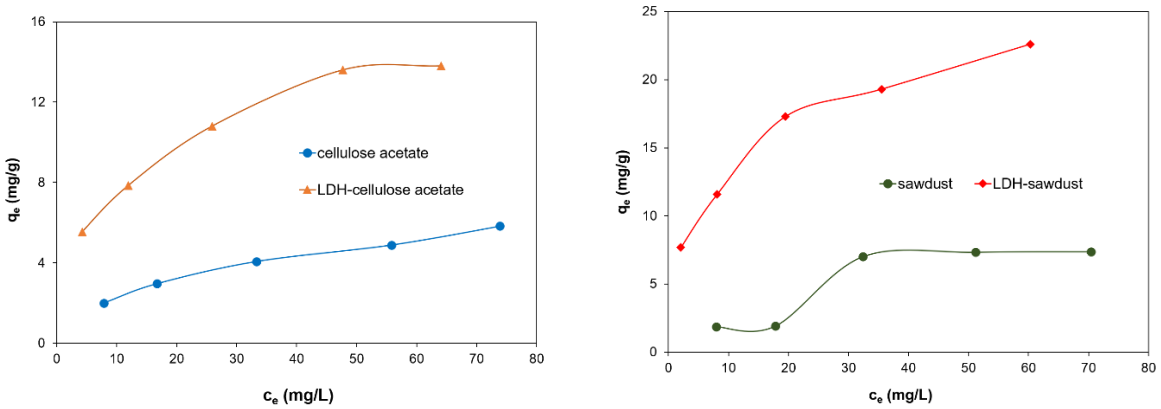
The instrument's software identified both the crystalline phase of LDH-cellulose acetate and that of LDH-sawdust as belonging to the same class of compounds, namely zaccagnaites. This leads to the conclusion that the synthesis of hybrids materials LDH–polymer with cellulose was successful, with the synthesized materials having a layered double hydroxide as their main crystalline phase.

Table 1 presents the lattice parameters *a* and *c* for the synthesized materials (LDH–cellulose acetate and LDH–sawdust), for Zn_3Al reagents, and for zaccagnaite.

Table 1. Lattice parameters *a* and *c* of the synthesized materials compared to those of zaccagnaite

Sample	*a* (Å)	*c* (Å)
LDH-cellulose acetate	3.092	24.768
LDH-sawdust	3.091	25.840
Zn_3Al-reagents	3.079	22.845
Zaccagnaite [5]	3.066	22.616

It can be observed that the values of the lattice parameter *a*, which represents the distance between two cations in the mixed hydroxide layer, are quite close to one another. In contrast, the values of the lattice parameter *c*, which represents the interlayer distance, are higher for the synthesized hybrid materials compared to the Zn_3Al-reagents and zaccagnaite. These higher values may be due to the presence of compounds containing cellulose (cellulose acetate, and sawdust, respectively) in the space between the layers of the layered double hydroxide.
The materials synthesized in the laboratory, LDH-cellulose acetate and LHD-sawdust, as well as cellulose acetate and sawdust, were used as adsorbents of the Congo Red dye in aqueous solutions, experimentally studying the equilibrium of the adsorption process.



a b

Figure 3. Adsorption equilibrium of Congo Red dye onto LDH-cellulose acetate and cellulose acetate (a), and onto LDH-sawdust and sawdust (b)

Figure 3a shows the equilibrium adsorption curve for the synthesized LDH-cellulose acetate material compared to that of cellulose acetate. When cellulose acetate was used as an adsorbent, it was observed that the adsorption process did not reach equilibrium for the concentrations of Congo Red solutions studied. The equilibrium adsorption capacity (q_e) increases continuously with increasing equilibrium dye concentration (c_e); this behavior may be due to the fact that cellulose acetate is not a good adsorbent. In contrast, when LDH-cellulose acetate was used as an adsorbent, the adsorption process reached equilibrium: the equilibrium adsorption capacity increases as the equilibrium concentration increases and then becomes constant. The equilibrium adsorption capacity experimentally determined when using LDH-cellulose acetate as an adsorbent is q_e = 13.8 mg/g. It can be seen from Figure 3a that, by using LDH-cellulose acetate, equilibrium adsorption capacities twice as high as those of cellulose acetate are obtained for the equilibrium concentrations studied.
Figure 3b shows the equilibrium curves for the adsorption of Congo Red dye on LDH-sawdust compared to adsorption on sawdust. The adsorption of Congo Red dye on sawdust has reached equilibrium; the equilibrium adsorption capacity of the sawdust, under the experimental

conditions studied, is q_e = 7.37 mg/g. In the case of dye adsorption on the synthesized LDH-sawdust material, the equilibrium adsorption capacity is q_e = 22.6 mg/g. It can be observed that the introduction of layered double hydroxide into the material's structure tripled the adsorption capacity.

Conclusion

The synthesized materials were structurally characterized by X-ray diffraction analysis, which revealed that the materials have a layered double hydroxide structure, but with some modifications in the crystal lattice parameters due to the presence of the organic substrate. Furthermore, the peaks characteristic of layered double hydroxides are less sharp and have shifted to smaller 2θ angles, leading to the conclusion that interactions exist between LDH and the organic substrate.

The experimental study of the Congo Red dye adsorption process was conducted using LDH-cellulose acetate and cellulose acetate, as well as LDH-sawdust and sawdust, as adsorbents.

The equilibrium adsorption capacities obtained under the experimental conditions studied were: 26.6 mg/g for LDH-sawdust and 13.8 mg/g for LDH-cellulose acetate. These values are three times and two times higher, respectively, than those of sawdust and cellulose acetate.

Acknowledgements

This work was supported by a grant of the Ministry of Research, Innovation and Digitization, CCCDI- UEFISCDI, proposal number PN-IV-P6-6.1-CoEx-2024-0056, within PNCDI IV.

References

[1] Bai S., Liu G., Shen T., Wu Z., Chen W., Song Y-F. (2025) Controllable synthesis of layered double hydroxides: From macroscopic morphology to microscopic coordination at the atomic level, *Coordination Chemistry Reviews*, 529, 216437

[2] Cavani F., Trifiro F., Vaccari A. (1991) Hydrotalcite-type anionic clays: preparation, properties and applications, *Catalysis Today*, 11, 173–301

[3] Agnaou H., EL Meziani S., Boumya W., Barka N., Chiban M., Elhalil A. (2026) Design and engineering of layered double hydroxides: From morphological-controlled synthesis to multifunctional applications, *Inorganic Chemistry Communications*, 183, 115832

[4] El Messaoudi N., Miyah Y., Georgin J., Franco D.S.P., Sewwandi B.V.N., Singh N., Knani S. (2025) A review of LDH–cellulose hybrid adsorbents for organic and inorganic pollutant removal from wastewater, *International Journal of Biological Macromolecules*, 330, 147986

[5] ***, PDF Card No. 9015034, Crystallography Open Database: Information card for entry 9015034

SUSTAINABLE VALORIZATION OF POULTRY EGGSHELL WASTE AS AN AGRICULTURAL SOIL AMENDMENT

Cozma Antoanela[1], Mihuț Casiana[1], Anișoara Duma Copcea[1], Okros Adalbert[1], Mircov D. Vlad[1], Popa Daniel[1], Lato Iaroslav[1], Chis Codruta[1], Petcu Mihaela[2], Daniela Scedei[2], Ilinca Imbrea[2*]

[1]Faculty of Agriculture, Department of Soil Sciences, University of Life Sciences "King Michael I" from Timisoara, 300645, Timisoara, Romania
[2]Faculty of Horticulture, Forestry and Plant Biotechnology, University of Life Sciences „King Michael I" from Timisoara, Aradului Street No 119, 300645 Timisoara, Romania
**author's email address: ilinca_imbrea@usvt.ro*

Abstract
This work aims to sustainably utilize eggshell waste from households, by transforming it into a product with potential for use in agricultural soil fertilization. The study aims to obtain eggshell powder and its physico-chemical characterization, mainly by determining the mineral profile, in order to evaluate its agronomic potential as a source of mineral elements for cultivated soils. The biological material used was represented by shells from chicken eggs obtained from laying hens raised in a household system and fed predominantly with cereals. The eggshells underwent processing stages to obtain a fine powder after which its mineral composition was analyzed. The data obtained in this study highlight the agronomic potential of poultry eggshell powder, which can constitute a natural source of macroelements, especially calcium and magnesium, as well as microelements, such as iron, manganese, zinc and copper. Under the conditions of the experiment, eggshell powder has a high calcium content, with values ranging between 35.08 and 39.24%, as well as magnesium, in concentrations of 0.37–0.56%. Regarding microelements, the analysis revealed the presence of iron at concentrations of 34.16–47.23 ppm, zinc in the range of 6.85–9.14 ppm, manganese with values between 3.72 and 5.38 ppm, and copper at concentrations of 4.61–6.47 ppm. Due to its mineral content, this by-product can be utilized as a soil amendment or mineral fertilizer to supplement nutrient levels in soils intended for plant cultivation, including in home gardens and container plantings.

Keywords: eggshell powder, microelement, agricultural fertilizer, eggshell waste

Introduction

The food industry generates annually significant amounts of eggshells as a by-product of egg processing and the manufacture of egg-based food products. In the absence of effective management and recovery strategies, these residues can represent an environmental problem, which highlights the need to identify sustainable solutions for their reuse and transformation into value-added products [1, 2, 3]. In the context of increasing concerns regarding sustainable waste management, the utilization of eggshells represents an important alternative for reducing environmental impact. By recycling, reusing and transforming them into value-added products, the quantities of waste disposed of, can be reduced and, at the same time, resources with economic and functional potential can be capitalized on. This waste can be recycled and transformed, through ecological methods, into calcium compounds with added value, thus representing a sustainable alternative for waste management in accordance with "zero waste" principles [4, 5].
Eggshell powder is a mineral-rich natural source, characterized by an ash content exceeding 94%. In terms of mineral composition, calcium is the predominant component, accompanied by magnesium and a series of mineral elements present in lower concentrations, such as iron,

zinc, copper, manganese, sulfur and silicon. This composition highlights the potential of eggshells as a raw material for obtaining value-added mineral products. The mineral composition of eggshells can vary within a relatively wide range, being influenced by a number of factors, such as the breed and age of the bird, the type and composition of the feed, as well as the conditions of its growth and exploitation, including the cage or free-range system [6,7,8]. Due to their high mineral content, especially calcium and magnesium, as well as the presence of microelements such as iron, zinc, manganese and copper, chicken eggshell waste has considerable potential for use in various agricultural activities. They can be used as mineral fertilizer, as an additive to improve soil physical properties, as well as to immobilize or reduce the bioavailability of heavy metals—particularly lead and cadmium—in contaminated soils. Eggshells can also be an alternative to naturally derived calcium carbonate and can be used as a nutritional supplement in animal feed [9, 10, 11]. An important advantage of using eggshells as a natural source of calcium is their accessibility and the possibility of utilizing this organic waste, thus contributing to a sustainable approach to resource management. At the same time, compared to some natural sources of calcium, eggshell powder stands out for its reduced content of potentially toxic compounds, an aspect that supports the opportunity of its use in household-scale fertilization practices.

Experimental

For the present study, chicken eggshells generated as a by-product from household food preparation were collected from two different locations and used as experimental samples.The eggs were obtained from free-range chickens raised under household conditions and fed primarily on wheat and corn. Eggshell powder was prepared using the methodology described in the literature by Radhika and Subhajit Ray et all. [12,13]. The powder thus obtained, stored in glass jars with ground corks, was subsequently analyzed to determine the total concentration of Ca, Mg, Fe, Mn, Cu and Zn.

The following **equipment and reagents** were used for sample preparation and analysis:

-Electric oven, used for drying eggshells
-Household grinder, used for grinding the dried eggshells
-Nabertherm temperature-controlled muffle furnace (model 6/11), used for the sample calcination
-Merck nitric acid, 65% (ρ = 1.39 g/cm3) essential to prepare the 0.5 N HNO_3
-Multi-element standard solution (1g/L) Merck - Germany, used to prepare working standards for Ca, Mg, Fe. Mn, Zn and Cu; distilled water
-Varian 280 FS flame atomic absorption spectrophotometer (air-acetylene), used to determine the absorbance of mineral elements in both standard solutions and sample solutions obtained following the mineralization process.

Mineral element concentrations of the eggshell samples were determined using atomic absorption spectrometry with an air–acetylene flame, after the calcination method, at 550 °C, followed by ash solubilization in 0.5 N nitric acid. The analytical procedure was adapted from the method reported by Ali, M. and W. Z. Badawy, with some modifications, and performed in accordance with the recommendations of Cozma et all [2,14]

Results and discussion

The content of essential mineral elements determined in the eggshell powder samples is presented in the Table below.

Table 1. The concentration of the essential mineral elements in chicken eggshell powder

Specification	Essential elements					
	Ca	Mg	Fe	Mn	Zn	Cu
	%	%	ppm	ppm	ppm	ppm
Limits	35.08 – 39.24	0.37 – 0.56	34.16 – 47.23	3.72– 5.38	6.85- 9.14	4.61 – 6.47
Mean values	**37.20 ± 2.08**	0.45± 0.09	40.54± 6.54	4.61± 0.83	7.95± 1.14	5.44± 0.94

The results presented in Table 1 indicate considerable variation in the mineral element content of the analyzed chicken eggshell powder, depending on the type of essential element and the origin of the eggshells. The determined concentrations ranged from 35.08 to 39.24% for calcium; 0.37 to 0.56% for magnesium; 34.16 to 47.23 ppm for iron; 3.72 to 5.38 ppm for manganese; 6.85 to 9.14 ppm for zinc, and 4.61 to 6.47 ppm for copper.

Calcium (Ca^{2+}) is an essential mineral macronutrient for plants, being required in relatively high quantities to support growth and development processes, playing a significant role in cellular structure and physiological processes. He plays a significant role influencing both the stability and normal functioning of the cell. The concentration limits (35.08 - 39.24%) and the average concentration (37.20±2.08) of calcium show that this is the predominant mineral macronutrient of the eggshell powder analyzed. The high Ca concentration determined in chicken eggshell powder indicates that it can serve as a natural source of calcium and has potential for use as a soil amendment or fertilizer to support plant growth and development. It also helps to reduce soil acidity, thus promoting nutrient availability and creating better conditions for crop growth and development.

Magnesium (Mg^{2+}) is an essential macronutrient for plants, playing a significant role in numerous physiological and biochemical processes. It constitutes the central component of the chlorophyll molecule and participates in the activation of a significant number of enzymes involved in plant metabolismIn the analyzed samples, magnesium was identified in concentrations ranging between 0.37 and 0.56 %, considerably lower values compared to those determined for calcium. Because the magnesium supply from soil minerals is generally insufficient to meet plant needs and maintain a high level of crop production and quality, supplementation of this element through fertilization may be necessary in many agroecosystems.

Iron (Fe^{2+}, Fe^{3+}) is an essential micronutrient for plant growth and development, playing an important role in numerous physiological and biochemical processes. Its role is associated with participation in the structure of cytochromes and in electron transport, the activation of certain enzymes, as well as processes involved in chlorophyll formation.In the analyzed eggshells, iron levels ranged from 34.16 to 47.23 ppm—concentrations lower than those determined for Ca and Mg, but higher than those recorded for Zn, Cu, and Mn. The average value of Fe content, of 40.54 ± 6.54 ppm, highlights the presence of this micronutrient in the composition of eggshells and suggests the possibility of using them as an additional source of iron for plants. However, the use of eggshells as a source of mineral nutrients should be done with caution, as the high carbonate input can alter the soil reaction and reduce the availability of iron to plants..

Manganese (Mn^{2+}) is an essential micronutrient involved in enzymatic activity, the synthesis of chlorophyll and amino acids, and in the process of photosynthesis. In the analyzed eggshells, Mn was determined at concentrations of 3.72–5.38 ppm, with a mean value of 4.61 ± 0.83 ppm. The Mn content was lower than that of Ca, Mg and Fe, but close to the values recorded for Zn and Cu, suggesting that the use of eggshells as a source of mineral nutrients could contribute to supplementing the Mn intake required by crop plants. The efficiency of manganese as a nutrient, however, is closely dependent on the chemical conditions of the soil, especially the pH value. The availability of Mn^{2+} in the soil solution decreases with increasing pH, the risk of manganese deficiency is higher in alkaline soils. At the opposite pole, in strongly acidic soils, with pH < 5, high concentrations of available Mn can cause toxicity phenomena in sensitive crops. Furthermore, interactions between mineral elements must be considered, as high levels of Cu, Fe, and Zn can limit manganese uptake by plants [15].

Zinc (Zn^{2+}) is an essential micronutrient for plants, involved in the activation of enzymes and in important processes such as chlorophyll synthesis, auxin formation, and chloroplast and starch development. In the analyzed eggshell samples, Zn was determined in concentrations ranging from 6.85 to 9.14 ppm, with an average value of 7.95 ± 1.14 ppm. This concentration is significantly lower than those of Ca and Mg (37.20 ± 2.08% and 0.45 ± 0.09%, respectively) and Fe (40.54 ± 6.54 ppm), but slightly higher than the values recorded for Cu and Mn (5.44 ± 0.94 ppm and 4.61 ± 0.83 ppm, respectively). The availability of zinc in soil is influenced by both soil properties and its source of origin. At high pH values, Zn can be immobilized by forming stable complexes, by precipitation or by interacting with phosphates, processes that reduce its availability to plants. Therefore, although eggshells can represent an additional source of Zn, their use as a fertilizer must be adapted to the characteristics of the soil, so that zinc immobilization processes are limited and its availability to plants is maintained [15,16]

Copper (Cu^{+}, Cu^{2+}) is an essential micronutrient involved in redox processes, photosynthesis, and carbohydrate and protein metabolism, while also contributing to plant resistance against pathogens and stress factors such as drought and low temperatures. In the analyzed eggshell samples, the copper concentration ranged from 4.61 to 6.47 ppm, highlighting the presence of this micronutrient in the analyzed material. Copper availability to plants is influenced by soil properties, particularly organic matter content and pH. Copper has a high affinity for organic matter, which can reduce the plant-available fraction as organic matter content increases. Furthermore, an increase in pH promotes Cu adsorption and precipitation, thereby reducing its availability, especially in neutral and alkaline soils [15,17].

Conclusion

In this context, eggshell powder can be considered a natural resource with dual agronomic functionality, serving both as a mineral supplement—by providing calcium and other nutrients essential for plant development—and as a potential soil amendment to improve certain soil properties. Therefore, the use of eggshells as a fertilizer must be considered in the context of soil characteristics and the balance of available mineral nutrients. The application of eggshells for fertilization purposes must be carried out taking into account the composition and properties of the soil. Due to their rich mineral content, chicken eggshells, transformed into powder, can represent a natural alternative for fertilizing and improving the properties of the soil used in growing trees, vegetables and flowers. At the same time, the large-scale recovery of eggshells can contribute to reducing environmental pollution caused by this waste and to reducing the costs associated with the purchase of mineral fertilizers and soil amendments.

References

[1] Liu Y., Wang K.W., Blanchard M., Li C., 2021, Eggshell powder compositions and methods of producing eggshell powder compositions, United States Patent No.: US 11,001,700 B2 (45), May 11;
[2] Ali, M. and W. Z. Badawy, 2017, Utilization of Eggshells By-Product as A Mineral Source for Fortification of Bread Strips, J. Food and Dairy Sci., Mansoura Univ., 8 (11), 455 - 459**;**
[3] Wijaya V. T and Teo S.S, 2019, Evaluation of eggshell as organic fertilizer on sweet basil International Journal of Sustainable Agricultural Research 6(2), 79-86, DOI: 10.18488/journal.70.2019.62.79.86;
[4] Burezq H. A, 2021, Utilization of Eggshell as Valuable Products for Sustainable Ecosystem and Agriculture (Review), *Poultry Science Journal*, 9(2), 147-165;
[5] Laohavisuti N., Boonchom B., Wimonmat B., Kittichai Chaiseeda & Seesanong S., 2021, Simple recycling of biowaste eggshells to various calcium phosphates for specifc industries, Sci Rep 11, 15143. https://doi.org/10.1038/s41598-021-94643-1**;**
[6] Arif S., I. Pasha, H. Iftikhar, F. Mehak, Sultana R., 2022, Effects of eggshell powder supplementation on nutritional and sensory attributes of biscuits, Czech Journal of Food Sciences, 40(1), 26–32.
[7] Islam M.K., Tusty T.A., Akhand A.A. and N. Ahsan, 2019, Human Uptake of eggshell powder as an alternate source of calcium, J. Pharm. Sci. **18**(2): 249-255.
[8] Schaafsma A., Pakan I., Hofstede G.J.H., Muskiet F.A.J., Van Der Veer E., De Vries P.J.F., 2000, Mineral, Amino Acid, and Hormonal Composition of Chicken Eggshell Powder and the Evaluation of Its Use in Human Nutrition. Poult. Sci., 79, 1833–1838.
[9] Hassan, N. M.M., 2015, Chicken Eggshell Powder as Dietary Calcium Source in Biscuits. World J. Dairy Food Sciences, 10, 199–206.
[10] Radhika Y, Sriram M & Aarti T., 2020, Egg shell powder as an unusual food ingredient for calcium fortification, Food and Agriculture Spectrum Journal. 1: 3.
[11] Dattatrav K. M., and Nair S.S., 2019, Study on eggshell and fruit peels as a fertilizer, Proceedings of International Conference on Sustainable Development in Association with Novateur Publications IJIERT-ISSN No: 2394-3696 ISBN. No. 978-93-87901-05-6 February
[12] Aditya, S., Stephen, J., & Radhakrishnan, M., 2021, Utilization of eggshell waste in calcium-fortified foods and other industrial applications: A review Trends in Food Science & Technology 115, pp. 422–432.
[13] Ray S., Barman A.K, Pradip Kumar Roy and Bipin Kumar Singh, 2017, Chicken eggshell powder as dietary calcium source in chocolate cakes, Pharma Innovation Journal; 6(9): 01-04;
[14] Cozma A., Mihut C., Mircov V. D., Okros A., Radu F., Cozma B., Niță L., Șmuleac L., 2020, Translocation of some heavy metals from the soil in root vegetables in the plain area of BANAT, Research Journal of Agricultural Science, 52 (2), 105-110.
[15] Soetan K.O., Olaiya C.O. and Oyewole O.E., 2010, The importance of mineral elements for humans, domestic animals and plants: A review, African Journal of Food Science Vol. 4(5) pp. 200-222.
[16] Santos W.O., Maria de Aquino P., Cuesta R.L., Saldanha I.M., Mattiello E.M., and Vergütz L., 2019, Zinc Diffusion and Availability Affected by Different Sources in Soils of Contrasting Textures, Journal of Agricultural Science; Vol. 11(5) ISSN 1916-9752
[17] Takáč P., Szabová T., Kozáková L., Benková M., 2009, Heavy metals and their bioavailability from soils in the long-term polluted Central Spiš region of SR, PLANT SOIL ENVIRON., 55 (4): 167–172.

MINERAL CHARACTERIZATION OF CHICKEN EGGSHELLS FROM EGGS SOLD ON THE LOCAL MARKET

Cozma Antoanela[1], Mihuț Casiana[1], Anișoara Duma Copcea[1], Okros Adalbert[1], Lia Rotariu[1], Corina Megyesi[2], Laura Radulescu[2], Radu Florina[2], Stoin Daniela[2], Mariana Poiana[2], Diana Utu[3], Maria Rada[3*]

[1]Department of Soil Sciences, University of Life Sciences "King Michael I" from Timisoara, 300645, Timisoara, Romania e-mail: cozma@usvt.ro
[2]Department of Food Science, University of Life Sciences "King Michael I" from Timisoara, 300645, Timisoara, Romania
*[3]University of Medicine and Pharmacy "Victor Babes" – Faculty of Medicine, 2 Eftimie Murgu Sq., 300041, Timisoara, Romania; *coresponding author e-mail:rada.maria@umft.ro*

Abstract
The aim of this study was to evaluate the mineral composition of chicken eggshells from eggs sold on the local market and assess their potential as a source of minerals for the fortification of food products. The concentrations of essential mineral elements, namely sodium (Na), potassium (K), calcium (Ca), magnesium (Mg), iron (Fe), manganese (Mn), zinc (Zn) and copper (Cu), were determined by flame atomic absorption-spectrometry in eggshell powders obtained from three different commercial sources. Concentrations were expressed in mg/100 g dry matter (DM). The results revealed variations between samples for all elements analyzed. Calcium presented by far the highest concentration, with values ranging between 34.472 and 38.531 mg/100 g DM and an average value of 36.763 ± 1.698 mg/100 g DM. For the other elements, the concentrations ranged between 36.3 and 48.7 mg/100 g DM for Na, 117–175 mg/100 g DM for K, 359–474 mg/100 g DM for Mg, 2.86–4.32 mg/100 g DM for Fe, 0.22–0.51 mg/100 g DM for Mn, 0.72–1.28 mg/100 g DM for Zn and 0.382–0.831 mg/100 g DM for Cu. The high calcium content highlights the potential of eggshells as a raw material for obtaining mineral ingredients and for fortifying food products. However, their use in food applications requires further evaluations regarding microbiological and chemical safety, mineral bioavailability, and optimal processing conditions.

Keywords: chicken eggshell; mineral composition, calcium, food fortification

Introduction

In the context of current concerns regarding the efficient use of resources and the reduction in the amount of by-products generated by the food industry, the recovery of agri-food waste represents a direction of interest for the development of value-added products. Transforming food by-product into a value-added ingredient can contribute to reducing waste and using resources more efficiently. The obtained eggshell powder has potential as a natural source of calcium, being utilized as an ingredient in the formulation of food products with improved mineral content. Its incorporation into the food matrix can represent a strategy for valorizing an agri-food by-product, while simultaneously obtaining products with increased nutritional value and an additional calcium intake [1, 2, 3]. Traditionally considered a low-value waste by-product, eggshell offers significant potential for valorization due to its mineral composition, characterized mainly by a high calcium carbonate content. Incorporating it into the food matrix can represent a strategy to valorize an agri-food by-product, while simultaneously yielding products with enhanced nutritional value and an additional calcium content. Processing eggshells into a powder can be an effective method of valorizing this by-product and reintroducing it into the food chain. To ensure the quality and safety of the product obtained, it is necessary to apply appropriate cleaning, treatment and grinding steps, as well as comply with

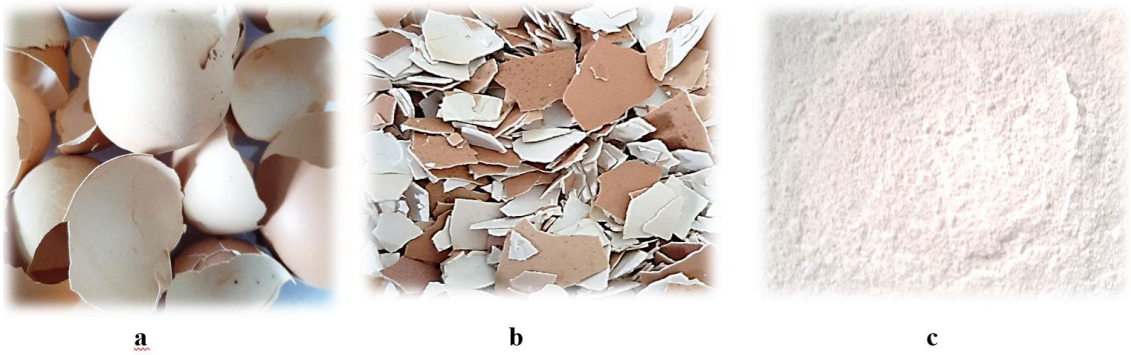
specific hygiene and food safety requirements. Numerous research studies have demonstrated the possibility of using eggshell powder to enrich various food products. Its application has been investigated in bakery products, dairy products, confectionery, and other food matrices [4, 5]. Eggshell powder is a mineral-rich natural source, characterized by an ash content exceeding 94%. In terms of mineral composition, calcium is the predominant component, accompanied by magnesium and a series of mineral elements present in lower concentrations, such as iron, zinc, copper, manganese, sulfur and silicon. Composition highlights the potential of eggshells as a raw material for obtaining value-added mineral products. The mineral composition of eggshells can vary within a relatively wide range, being influenced by several factors, such as the breed and age of the bird, the type and composition of the feed, as well as the conditions of its growth and exploitation, including the cage or free-range system. Schaafsma et al., in a comparative study of eggshell powders from different sources, reported approximately 39% elemental calcium and concluded that eggshell powder could represent a potential source of calcium for human nutrition [6, 7]. Park and Sohn, reported calcium concentrations of approximately 42.451–44.345 mg/100 g in eggshells from hens of different ages, along with significant differences in the concentrations of other mineral components. In another study, Xie et al., compared eggshells from free-range and conventionally raised hens and reported, calcium concentrations of approximately 36.631 and 34.256 mg/100 g, respectively, while magnesium concentrations were 604.2 and 536.3 mg/100 g. However, considerable variations in mineral concentrations have been reported depending on the source and characteristics of the analyzed eggshell samples. Tamanna et al., reported concentrations of 570.56 mg/g Ca, 24.17 mg/g Mg, 8.28 mg/g Fe, 27.44 mg/g Na, and 140.27 mg/g K in eggshell powder [8, 9, 10]. The aim of this study was to characterize the mineral composition of chicken eggshells sourced from eggs sold on the local market. The concentrations of sodium (Na), potassium (K), calcium (Ca), magnesium (Mg), iron (Fe), manganese (Mn), and copper (Cu) were determined using flame atomic absorption spectrometry. The resulting mineral profile was compared with values reported in the literature to characterize the material under investigation and to preliminarily assess its potential for utilization as a mineral raw material.

Experimental

Materials

Chicken eggshells were collected from eggs purchased from three local retail outlets. After removal of the egg contents, the eggshells were initially washed under running tap water. The inner membrane was subsequently removed, and the eggshells were rinsed with distilled water and boiled in water for 5 min. After cooling and removal of excess water, the eggshells were dried in a laboratory drying oven at 80 °C. The dried eggshells were subsequently ground using a kitchen grinder to obtain a fine powder.

Based on their origin, the samples were divided into three experimental groups, coded ES1 (eggshell 1), ES2 (eggshell 2), and ES3 (eggshell 3). Until analysis, the prepared samples were stored under refrigerated conditions in amber glass containers.



a b c

Figure 1. Appearance of chicken eggshell at different processing stages: raw eggshell (a), cleaned eggshell (b), and eggshell powder (c).

Methods

The concentrations of essential and potentially toxic mineral elements (Na, K, Ca, Mg, Fe, Mn, Zn, and Cu) in the eggshell samples were determined by flame atomic absorption spectrometry (FAAS) using an air–acetylene flame. The analytical procedure involved sample calcination followed by dissolution of the resulting ash in nitric acid. Elemental concentrations were subsequently measured using a Varian AA-240 atomic absorption spectrometer, according to the methodology described by Cozma et al. [11]. All samples were analyzed in triplicate, and the results were expressed as mg/100 g dry matter (DM).

Results and discussion

The concentrations of mineral elements determined in the chicken eggshell samples are presented in Table 1.

Table 1. Mineral composition of eggshell powder from eggs sold on the local market

Sample	Na	K	Ca	Mg	Fe	Mn	Zn	Cu
ES1	36,3	175	34.472	359	2,86	0,22	0,72	0,382
ES2	43,6	117	38.531	474	4,32	0,51	1,28	0,831
ES3	48,7	151	37.287	435	4,11	0,48	0,81	0,745
Mean value ± SD	42,87 ± 5,09	147,67 ± 23,80	36.763 ± 1.698	423 ± 47,45	3,76 ± 0,64	0,40 ± 0,13	0,94 ± 0,25	0,65 ± 0,19

For all the elements analyzed, differences were observed between samples from different commercial sources. The amplitude of the variations differed depending on the element analyzed, with the most obvious differences being observed in the case of potassium, calcium, magnesium and zinc. Calcium was the predominant element in the mineral composition of the analyzed shells, with individual concentrations ranging from 34.472 to 38.531 mg/100 g DM and a mean value of 36.763 ± 1.698 mg/100 g DM. The high calcium content aligns with the structural role of this mineral in eggshell formation and constitutes the primary characteristic of the analyzed mineral matrix. From the perspective of valorizing agri-food by-products, the high calcium concentration gives eggshells a potential interest as a raw material for obtaining mineral ingredients, provided that appropriate processing and safety control procedures are applied. Magnesium concentrations ranged from 359 to 474 mg/100 g DM, with a mean value of 423 ± 47.45 mg/100 g DM. Differences between samples may be associated with variability in the mineral composition of the raw material and, potentially, with factors related to bird

nutrition and rearing conditions. However, given the limited number of samples analyzed, these potential sources of variation should be regarded as hypotheses requiring verification through studies involving larger sample sizes and controlled data regarding the birds' origin and diet. For potassium, concentrations ranged from 117 to 175 mg/100 g DM, with a mean value of 147.67 ± 23.80 mg/100 g DM. Sodium showed lower values, ranging from 36.3 to 48.7 mg/100 g DM, with a mean of 42.87 ± 5.09 mg/100 g DM. Differences between samples were observed for both elements; however, the magnitude of these differences should be interpreted with caution, given the limited number of samples analyzed. Among the trace elements determined, iron showed concentrations ranging from 2.86 to 4.32 mg/100 g DM, with a mean value of 3.76 ± 0.64 mg/100 g DM. Manganese was determined within the range of 0.22–0.51 mg/100 g DM, with a mean value of 0.40 ± 0.13 mg/100 g DM. For zinc, concentrations of 0.72–1.28 mg/100 g DM were recorded, with a mean of 0.94 ± 0.25 mg/100 g DM, while copper ranged from 0.382 to 0.831 mg/100 g DM, with a mean value of 0.65 ± 0.19 mg/100 g DM. The variations observed in the analyzed elements may reflect differences in feed composition, the availability of minerals in feed and water, rearing conditions, the birds' age, breed or hybrid, and other physiological factors. Among the determined elements, calcium has one of the highest concentrations, the average value obtained experimentally being 36.763 mg/100 g DM. The value determined in the present study falls within the wide range of variation reported in the specialized literature [12-14]. For samples obtained from local commercial sources, the variability associated with their origin must also be taken into account. In the absence of detailed information regarding these factors, attributing the observed differences to a single cause is not justified. From the perspective of valorizing agri-food by-products, the results are particularly significant due to the high calcium concentration. Eggshell can thus serve as a promising raw material for producing mineral ingredients intended, under appropriate conditions for the fortification of food products. However, the total content of a mineral element is not sufficient, by itself, to assess the nutritional value of an ingredient. To confirm the food applicability, further investigations are needed regarding the bioavailability of minerals, their solubility, microbiological contamination and the presence of any chemical contaminants, including potentially toxic metals.

Conclusion

The analyzed eggshells showed a high mineral content, with calcium being the predominant element, with an average concentration of 36,763 ± 1,698 mg/100 g dry matter. This result confirms the importance of calcium in the mineral structure of the eggshell and highlights its potential as a calcium-rich raw material. In addition to calcium, measurable amounts of Mg, K, Na, Fe, Mn, Zn and Cu were identified, demonstrating that eggshell powder represents a complex mineral matrix, and not just a source of calcium. Differences were observed among the samples from the three commercial sources analyzed, with the most evident variations recorded for K, Ca, Mg, and Zn. These differences may be associated with the origin of the raw material and with biological, nutritional and technological factors, but attributing the variations to a single cause cannot be achieved based on the limited number of samples investigated. Comparison with data from the specialized literature revealed, overall, a concordance of the mineral profile, especially for Ca and Mg, while for some of the other elements more important differences were found. These differences can be explained, at least in part, by the natural variation of the raw material and by differences in the growing conditions, feeding and analytical methods used. The high calcium concentration indicates the potential to utilize eggshells for producing mineral ingredients, including for possible food fortification applications. However, the total concentration of minerals is not sufficient to establish nutritional value or suitability for consumption. Additional studies are underway, conducted on

a larger number of samples, to more accurately characterize the variability of mineral composition and to evaluate the safety and food applicability of eggshells.

References

[1] Aditya, S., Stephen, J., & Radhakrishnan, M., 2021, Utilization of eggshell waste in calcium-fortified foods and other industrial applications: A review Trends in Food Science & Technology 115, pp. 422–432.
[2] Liu Y., Wang K.W., Blanchard M., Li C., 2021, Eggshell powder compositions and methods of producing eggshell powder compositions, United States Patent No.: US 11,001,700 B2 (45), May 11;
[3] Ali, M. and W. Z. Badawy, 2017, Utilization of Eggshells By-Product as A Mineral Source for Fortification of Bread Strips, J. Food and Dairy Sci., Mansoura Univ., 8 (11), 455 - 459**;**
[4] Wijaya V. T and Teo S.S, 2019, Evaluation of eggshell as organic fertilizer on sweet basil International Journal of Sustainable Agricultural Research 6(2), 79-86, DOI: 10.18488/journal.70.2019.62.79.86;
[5] Arif S., I. Pasha, H. Iftikhar, F. Mehak, Sultana R., 2022, Effects of eggshell powder supplementation on nutritional and sensory attributes of biscuits, Czech Journal of Food Sciences, 40(1), 26–32.
[6] Islam M.K., Tusty T.A., Akhand A.A. and N. Ahsan, 2019, Human Uptake of eggshell powder as an alternate source of calcium, J. Pharm. Sci. 18(2): 249-255.
[7] Schaafsma A., Pakan I., Hofstede G.J.H., Muskiet F.A.J., Van Der Veer E., De Vries P.J.F., 2000, Mineral, Amino Acid, and Hormonal Composition of Chicken Eggshell Powder and the Evaluation of Its Use in Human Nutrition. Poult. Sci., 79, 1833–1838.
[8] Park Ji-Ae and Sohn Sea-Hwan, 2018, The influence of hen aging on eggshell ultrastructure and shell mineral components, Korean J. Food Sci. An. 38(5):1080~1091, pISSN: 1225-8563 eISSN: 2234-246X. DOI https://doi.org/10.5851/kosfa.2018.e41
[9] Xie, S., Hai, C., He, S., Lu, H., Xu, L., & Fu, H., 2023, Discrimination of Free-Range and Caged Eggs by Chemometrics Analysis of the Elemental Profiles of Eggshell. Journal of Analytical Methods in Chemistry, (1), 1271409.
[10] Tamanna, S. T., Amin, M. R., Rahman, M. T., Al Mamun, M. A., & Alauddin, M., 2025, Development of eggshell powder as an alternative source of Ca and Fe for human health: A compositional and comparative study. Food Chemistry Advances, 9, 101187.
[11] Cozma A., Popescu S., Rada M., Mihut C.,Velciov A., **2022**, Development and mineral characterization of milk chocolate fortified with chicken eggshell powder, SGEM Vienna, 22nd International Multidisciplinary Scientific GeoConference Surveying Geology and Mining Ecology Management, Advances in Biotechnology, ISSN: 1314- 2704, Vol.22 (6.2) 143 – 150.
[12] Ray S., Barman A.K, Pradip Kumar Roy and Bipin Kumar Singh, 2017, Chicken eggshell powder as dietary calcium source in chocolate cakes, Pharma Innovation Journal; 6(9): 01-04;
[13] Arnold, M., Rajagukguk, Y. V., & Gramza-Michałowska, A., 2021, Functional food for elderly high in antioxidant and chicken eggshell calcium to reduce the risk of osteoporosis—a narrative review. Foods, 10(3), 656.
[14] Hassan, N. M.M., 2015, Chicken Eggshell Powder as Dietary Calcium Source in Biscuits. World J. Dairy Food Sciences, 10, 199–206.

EVALUATION OF CHANGES IN CONSUMER BEHAVIOR REGARDING TEXTILE WASTE

Jovana Čugalj[1], Vuković Jelena[2], Una Marčeta[1],Bogdana Vujić[1], Batinić Bojan[3],

[1]University of Novi Sad, Technical faculty „Mihajlo Pupin" Zrenjanin, Serbia
[2] Faculty of Technology Zvornik - University of East Sarajevo
[3] University of Novi Sad, Faculty of Technical Sciences
e-mail: jovana.cugalj@uns.ac.rs

Abstract
The rapid expansion of fast fashion, driven by low-cost mass production and short consumption cycles, has made textile waste one of the fastest-growing environmental challenges globally. This study compares consumer behavior regarding textile consumption and waste management in Zrenjanin, Serbia, using surveys conducted in 2019 and 2026. It examines changes in purchasing habits, second-hand clothing use, disposal practices, and environmental awareness. Results indicate a positive shift toward reuse practices, with increased second-hand shopping and a strong willingness to participate in recycling campaigns. However, the frequency of purchasing new clothes also increased, revealing a persistent awareness-behavior gap where higher environmental knowledge does not consistently translate into sustainable consumption.

Introduction
Fashion trends encourage frequent wardrobe changes, increasing global fiber consumption and expansion of fast fashion which relies on the rapid production of affordable, trend-driven clothing with short collection cycles, designed to meet consumers' constantly changing preferences [1]. Overproduction driven by fast fashion and overconsumption drastically increases the fashion industry's environmental footprint, with 60% more clothing purchased today than in 2000 and around 30% never sold at full price [2].
Textile and clothing waste represents one of the fastest-growing waste streams globally, driven by fast fashion, low-cost mass production, and short consumption cycles, accounting for approximately 5.8% of the total global comunal waste disposed of in landfills (2018) [3]. Although textile waste constitutes a relatively small share of the total waste stream, its management remains a major environmental challenge. Globally, approximately 75% of total textile waste is disposed of in landfills, while only about 15-25% is reused or recycled, and less than 1% is recycled back into new clothing [4]. The total amount of textile waste generated in the EU was estimated at 6,95 million tonnes in 2020 (16 kg per capita), of which only 1,95 million tonnes (4,4 kg per capita) were separately collected [5]. Most of this waste ends up in landfills or is incinerated, causing negative environmental impacts [6].
In the Republic of Serbia, textile waste represented one of the categories of secondary raw materials subjected to recovery (R) operations, where R-codes designate waste recovery operations defined by waste legislation, including recycling, regeneration, and energy recovery. In 2024, textile waste accounted for 1,122 t of the total waste processed through R operations, while 1,593 t of textile waste were disposed of [7].
To gain a deeper understanding of the textile waste problem and identify potential solutions, it is essential to examine consumer behavior, particularly the factors influencing clothing purchase frequency, purchasing decisions, and disposal practices. In a previous study [8] mapped the fundamental patterns of consumer behavior regarding textile waste disposal at the local level. To assess how these patterns have evolved, a follow-up survey was conducted at the beginning of 2026. The aim was to determine whether the seven-year interval, marked by

rapid changes in the fashion industry and an increasing global emphasis on sustainability, has resulted in significant shifts in consumer purchasing and clothing disposal behavior.

Experimental

This research is based on a comparative analysis of two surveys conducted seven years apart (2019–2026) in the municipality of Zrenjanin, Serbia, building on a 2019 baseline study that identified the primary ways locals disposed of textile waste [8].

The survey in 2019. (S1) was conducted online over a 10-day period and distributed via social networks [8] with a total of 97 respondents participated. To understand whether and how these practices have changed, a follow-up survey was conducted in January 2026. (S2). The survey was carried out over a 15-day period and included a larger sample of 182. Both questionnaires were anonymous and online. Although S2 was more comprehensive, providing broader insights into respondents' consumption habits, some of the questions, and therefore the corresponding answers, could be used for comparison with S1, allowing the major conclusions to be drawn regarding changes in clothing consumption behavior over the previous seven-year period (Table 1).

Besides the general questions concerning respondents' age and sex, the specific questions selected for comparison from both surveys could be classified into four groups (QG):

- QG1: Frequency of purchasing new clothes
- QG2: Frequency of purchasing second hand clothes
- QG3: Fate of the old clothes
- QG4: Willingness to participate in recycling campaigns.

Table 1. Comparison of the question groups (QG) and corresponding survey questions used in the 2019 and 2026 questionnaires

QG	S1	S2
1	**Which of the following statements best describes you?**	**How often do you buy new clothes?**
	• I follow fashion trends and try to keep my wardrobe up to date.	• More than once a month
	• I buy new clothes as soon as a new collection arrives.	• Once a month
	• I buy clothes on sale from the previous season.	• Less than once a month
	• I do not usually follow fashion trends.	• Rarely
	• I do not buy clothes often; I wear them as long as they are usable	
	• None of the above	• Never
2	**Do you buy "second hand" clothing?**	**Have you ever purchased clothes from second-hand stores?**
	• Yes	• Yes, regularly
	• No	• Never
	• Sometimes	• Sometimes /Rarely
3	**The clothes I do not wear anymore**:	**What do you most often do with clothes that you no longer need or wear?** *(Multiple answers could be selected.)*
	• I gift to someone	• I donate them. • I give them away.
	• I sell	• I sell them.

	• I throw it in a container, • None of the above.	• I dispose of them together with household waste. • I leave them next to a waste container • None of the above.
4	**Do you know that there is a place in your city where you can put off your old wardrobe?**	**Would you support textile recycling or reuse programs in your community?** • Yes, I strongly support them. • Yes, I support them. • I am not sure. • No, I do not support them.`

Even though the questions in S1 and S2 were formulated differently, they addressed the same topics. Therefore, within QG1, the questions in both surveys assessed the frequency and habits of purchasing new clothes. In QG2, the questions provided insight into respondents' second-hand clothing purchasing patterns, with the 2026 survey offering more detailed response options. In QG3, the questions in both surveys were the most closely aligned, enabling a direct comparison of respondents' clothing disposal practices. Finally, although the questions in QG4 were not directly comparable, they provided valuable information on respondents' willingness to participate in textile recycling campaigns.

Results and discussion

The data were comprehensively analyzed, and the results are presented in the following sections. In terms of age distribution of respondents, this study included participants from all age groups, with a relatively balanced representation across categories. The largest share of respondents belonged to the 46-55 age group (29,7%), followed by participants aged 26-35 (19,8%), 36-45 (18,1%), 18-25 (16,5%), and those aged 56 and older (15,9%). In contrast to the study conducted in 2019, where the majority of respondents were from the younger population (mainly aged 18-24), with no participants older than 55 years. A limitation of this study is the gender imbalance in the sample, with 93.4% of respondents being female.

QG1: Frequency of purchasing new clothes.

In order to compare responses within QG1, the questions were matched according to the reported frequency of purchasing new clothes (Table 1). In both surveys, the largest proportion of respondents reported purchasing new clothing rarely (63.6% in S1 and 40% in S2). In contrast, purchasing new clothing less than once a month increased from 10.1% in S1 to 35% in S2, while monthly purchases increased from 1% to 15%. The proportion purchasing new clothing more than once a month was similar (12.1% in S1 and 10% in S2). Additionally, 13.1% of S1 respondents reported never purchasing new clothing, a response not recorded in S2. Overall, the findings indicate a higher frequency of new clothing purchases among respondents in S2 (Figure 1).

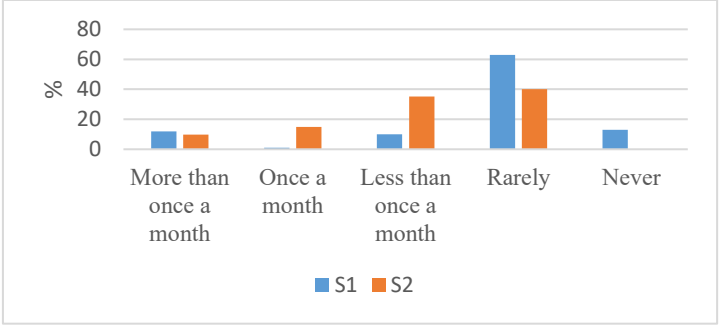


Figure 1. Frequency of purchasing new clothes

QG2: Frequency of purchasing second-hand clothes

The results related to second-hand clothing purchases showed that the largest proportion of respondents in both surveys selected "Sometimes" (52.6% in S1 and 40% in S2). The proportion purchasing second-hand clothing (Yes) almost doubled from 16.5% in S1 to 30% in S2, while those selecting "No" declined from 30.9% to 12%. The response "Rarely" was recorded only in S2 (18%). Overall, the findings indicate a greater tendency toward purchasing second-hand clothing among respondents in S2.

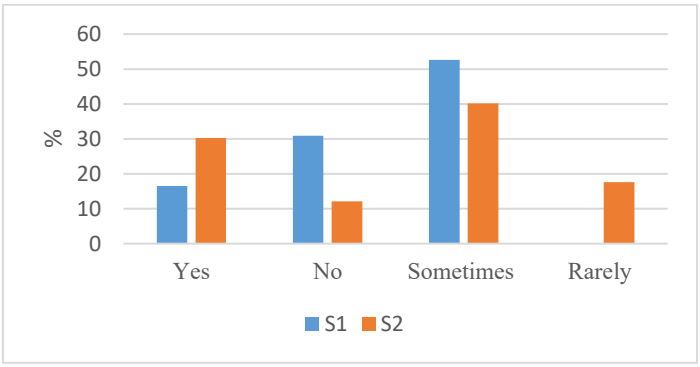


Figure 3. Purchasing of second-hand clothing

QG3: Fate of the old clothes

The response options within QG3 were consistent across both surveys, with donating/giving away combined into a single category in S2 (Table 1). However, in S1 respondents selected only one primary disposal method, whereas S2 allowed multiple strategies. As shown in Figure 4, donating or giving away clothes was the dominant method in both surveys, accounting for 83.5% in S1 and approximately 84% in S2. The "Dispose of" category increased from 4.1% in S1 to 28.6% in S2, while "Sell" increased from 0% to 6%. "None of the above" accounted for 8.2% in S1 and a minimal percentage in S2.

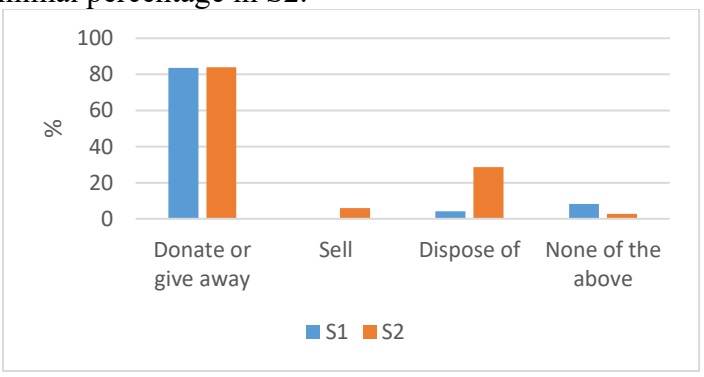


Figure 4. Fate of the old clothes

QG4: Willingness to participate in recycling campaigns.

In S1, awareness of local textile recycling infrastructure was limited, with 71.1% of respondents reporting that they did not know of any place in their city where old clothes could be deposited or recycled, while 28.9% were aware of such a location. In S2, 49.5% of respondents supported recycling campaigns and 42.3% expressed strong support, while only 6.6% were undecided and 1.6% disagreed. Overall, S1 reflects limited awareness of existing infrastructure, whereas S2 shows a strong willingness to participate in recycling initiatives.

Conclusion

This comparative study between 2019 (97 respondents) and 2026 (182 respondents) shows how textile consumption habits in Zrenjanin have evolved over seven years. The results indicate a shift toward more sustainable disposal and reuse practices. Purchasing second-hand clothing increased in 2026, and donating or giving away old clothes remained the primary disposal

method in both surveys (around 84%). Furthermore, environmental awareness improved significantly; while most S1 respondents were unaware of local collection points, over 91% of S2 participants expressed support for recycling campaigns. However, this growing awareness has not stopped the frequent consumption of new clothing. The overall frequency of buying new clothes is higher in 2026, with the "less than once a month" category being almost three times more common than in 2019. Additionally, 28,6% of respondents in S2 still dispose of textiles with regular household waste. Ultimately, the data confirms an awareness-behavior gap, where positive attitudes and a strong willingness to recycle do not fully translate into reduced fast fashion consumption.

References

[1] Y. Yu, H. Wang, and G. Li, "My Clothes, My Precious: Psychological Ownership and Compulsive Fashion Hoarding in Fast and Regular Fashion," Journal of Sustainable Marketing, 2025. doi: 10.51300/JSM-2025-147.

[2] N. Wüthrich, O. Talanova, B. Rosenthal, E. Wu, and C. Leong, From Waste to Worth. Munich, Germany: Roland Berger GmbH, 2024.

[3] U.S. EPA, Textiles: Material-Specific Data. United States Environmental Protection Agency, 2026. https://www.epa.gov/facts-and-figures-about-materials-waste-and recycling/textiles-material-specific-data

[4] J. P. Juanga-Labayen, I. L. Labayen, and Q. Yuan, "A Review on Textile Recycling Practices and Challenges," Textiles, vol. 2, no. 1, 2022. doi: 10.3390/textiles2010010.

[5] J. Deckers, T. Duhoux, and S. Due, Textile Waste Management in Europe's Circular Economy. European Environment Agency, European Topic Centre on Circular Economy and Resource Use, 2024.

[6] McKinsey & Company, Scaling Textile Recycling in Europe-Turning Waste into Value, 2022. https://vb.nweurope.eu/media/19019/2207-scaling-textile-recycling-in-europe-turning-waste-into-value.pdf

[7] SEPA, Report on the State of the Environment in the Republic of Serbia for 2024. Belgrade, Serbia: Republic of Serbia, Ministry of Environmental Protection, 2025. https://sepa.gov.rs/wp-content/uploads/2025/12/Izvestaj-2024.pdf

[8] J. Mićić, U. Marčeta, B. Vujić, and V. Mihajlović, "Identification of Final Disposal Ways of Waste Clothes in Zrenjanin Municipality," in Proc. XIII International Mineral Processing and Recycling Conference, Belgrade, Serbia, 2019.

COMBINING RANDOM-EFFECTS AND EXTREME VALUE THEORY FOR THE META-ANALYSIS OF RARE EVENT PROPORTIONS

Jovana Dedeić, Jelena Ivetić, Srđan Milićević, Katarina Vidojević, Marija Delić

Faculty of Technical Sciences, University of Novi Sad, Trg Dositeja Obradovića 6, 21000 Novi Sad, Serbia
e-mail: radenovicj@uns.ac.rs

Rare adverse events can be very important in a clinical context, but standard meta-analytic approaches are not built to give them special attention. Classical random-effects models (REM) provide reliable pooled estimates of overall event rates, but they do not distinguish studies with unusually high proportions, even though such studies may contain important information for risk assessment. This work introduces a two-component framework that combines the logit-normal REM with a Generalized Pareto Distribution (GPD) from extreme value theory (EVT). Studies are divided at a prespecified threshold. Those below the threshold are modeled using REM, while those above it are treated as tail observations and modeled separately using the GPD. This approach follows the peaks-over-threshold principle from EVT. The two components are separated deterministically rather than through a probabilistic mixture or a single composite density, which preserves identifiability of the maximum-likelihood estimator. Under standard regularity conditions, the estimator is also consistent as the number of studies increases.

A Monte Carlo simulation study considered several proportions of tail-heavy studies. The results showed that the combined model reduced bias and improved model fit relative to REM as the proportion of extreme studies increased. In more homogeneous scenarios, however, REM could perform better than XT-REM in terms of bias and error when little tail behavior was present, although XT-REM still provided a better overall fit. The method was also applied to real data from sixteen clinical trials reporting pneumonitis linked to immunotherapy, and the two-part model provided a substantially better fit than the classical REM. It yielded a pooled estimate of the central incidence and a separate characterization of the upper tail for trials with unusually high event rates.

Overall, the results show that separating central and extreme behavior at a prespecified threshold can provide a useful extension of random-effects meta-analysis for settings in which unusually high event rates are of particular interest.

A SUSTAINABLE BIOCATALYTIC ROUTE TO BIOACTIVE MYRICETIN GLYCOSIDES

Ildiko Bută[1], Alina Mogoşanu[1], Costin-Ioan Popescu[3], Liliana Cseh[1], Livia Deveseleanu-Corici[1*]

[1]"Coriolan Drăgulescu" Institute of Chemistry, Timisoara, Romania
[2]Victor Babeş University of Medicine and Pharmacy, Department of Biochemistry and Pharmacology, Timisoara, Romania
[3]Institute of Biochemistry of the Romanian Academy, Bucharest, Romania
e-mail: deveseleanulivia@gmail.com

Abstract

Flavonoid glycosides are increasingly recognized as high-value bioactive compounds due to their improved physicochemical and biological properties compared with their corresponding aglycones. Glycosylation can enhance aqueous solubility, chemical stability, and bioavailability, while preserving or, in some cases, improving the biological activities of flavonoids [1]. Among naturally occurring flavonols, myricetin is particularly attractive because of its broad spectrum of biological activities. However, its practical use in pharmaceutical and nutraceutical applications is limited by poor water solubility, chemical instability, and low bioavailability [2,3]. Enzymatic glycosylation using UDP-dependent glycosyltransferases (UGTs) provides a selective and environmentally friendly strategy for modifying myricetin. Compared with conventional chemical synthesis, UGT-catalyzed reactions can offer high regio- and stereoselectivity under mild reaction conditions, reducing the need for harsh reagents and energy-intensive processes [4,5].

In this study, recombinant UGTs were investigated for the enzymatic glycosylation of myricetin using UDP-glucose as the activated sugar donor. The influence of key reaction parameters, including pH, temperature, enzyme loading, and UDP-glucose concentration, was evaluated to determine their impact on glycoside formation and catalytic performance. Enzyme kinetic studies were also performed to characterize the interaction of the selected glycosyltransferase with myricetin and to provide further insight into its catalytic behavior.

The results demonstrate the potential of UGT-mediated glycosylation as a selective and sustainable approach for the production of bioactive myricetin glycosides. This study provides a basis for the further development of efficient biocatalytic processes for myricetin functionalization and the sustainable production of value-added flavonoid derivatives.

Acknowledgements

This work was supported by a grant of the Ministry of Research, Innovation and Digitization, CCCDI - UEFISCDI, project number PN-IV-P7-7.1-PED-2024-2513, within PNCDI IV.

References

[1]. Cunha M.-H., Ferrari I.B.S., Melo N.C., Carvalho L.M., Ortega M.M., Carvalho P.O., Antioxidants 15(5) (2026) 539.
[2]. Semwal D.K., Semwal R.B., Combrinck S., Viljoen A., Nutrients 16;8(2) (2016) 90.
[3]. Song X., Tan L., Wang M., Ren C., Guo C., Yang B., Ren Y., Cao Z., Li Y., Pei J., Biomed Pharmacother 134 (2021) 111017.
[4]. Li T., Nidetzky B., Enzyme Microb. Technol. 200 (2026) 110916.
[5]. Ding J., Li X., Jin Z., Svensson B., Bai Y., Biotechnol. Adv. 89 (2026) 108863.

PEELPRESSO – THE ECOFRIENDLY SNACK

Botond Dezső, Dorka Lukovszki, Benjámin Jancsó, Dóra Csercsics, Erzsébet Illés

Department of Food Engineering. University of Szeged. H-6724 Szeged. Mars tér 7. Hungary
e-mail: dezsobotond12@gmail.com

Abstract

One of the most pressing challenges facing the global food industry and modern hospitality is the management of organic by-products and waste streams generated during processing and consumption. Annually, vast amounts of easily biodegradable organic materials are sent to landfills or incinerated, with their current utilization rates remaining exceptionally low. The daily accumulation of spent coffee grounds in coffee shops, along with the fruit and vegetable fiber produced in juice bars and industrial processing plants, imposes significant environmental and financial burdens on both businesses and society. Landfilling these by-products leads to intense greenhouse gas emissions. Depositing 1 kg of wet spent coffee grounds results in a Global Warming Potential of approximately 2.1 kg CO_2 equivalent primarily due to the formation of methane (CH_4), which has a global warming potential 28 times higher than CO_2 over a 100-year horizon. Similarly, landfilling 1kg of fruit and vegetable fiber generates about 0.95 kg CO_2 equivalent in emissions. Upcycling of these organic residues not only minimizes direct emissions, but also indirectly reduces agricultural land use, intensive fertilizer application, and the consumption of embedded "virtual water" locked within primary raw materials.

The objective of our research was to unite these two streams of food industry by-products through the development of PeelPresso, a functional sandwich biscuit. The product consists of two crispy, fiber-rich biscuit shells surrounding a chocolate-like coffee filling. Based on our environmental impact assessments, producing a single 25 g sandwich biscuit repurposes 2.4 g of dried spent coffee grounds (equivalent to approximately 3.18 g of wet coffee grounds) and 2.8 g of dried fruit and vegetable fiber (22.4 g of fresh fiber). As a result, each unit directly prevents the release of 10.1 g of CO_2 equivalent into the atmosphere.

The technological novelty and creativity of this innovation lies in the unconventional pairing of raw materials and gentle processing methodologies. The fruit and vegetable pomace leftover from cold-pressed juice production is dried at low temperatures and finely milled to serve as a value-added flour substitute in the dough. Meanwhile, spent coffee grounds collected from local cafes are transformed into a smooth, homogeneous filling utilizing chocolate refining and conching technology.

The functionality of PeelPresso stems from the fact that fruit and vegetable fiber does not merely act as a bulking agent, but provides a physiologically valuable source of dietary fiber. The finished product contains 8.2 g / 100g of dietary fiber (approx. 2.0 g per 25 g biscuit), which actively supports healthy digestion. Furthermore, the natural organic compounds and the residual caffeine content within the spent coffee ground filling (approx. 28 mg / piece) exert a mild, natural stimulating effect, providing a Clean Label alternative free from synthetic additives compared to conventional confectionery.

Product consumer acceptance and market viability were evaluated through sensory testing and a questionnaire survey involving nearly 300 participants. The results demonstrated an overall concept attractiveness score of 4.39/5, with 86.7 % of respondents rating the product's flavor profile and harmonious texture exceptionally high. Furthermore, 65.2 % of participants expressed strong purchase intent. Consumer feedback confirmed that awareness of upcycling and environmental sustainability significantly enhanced the overall perceived quality and acceptance of the product.

RIVASTIGMINE (RVG) - CORROSION INHIBITOR FOR OLC52 CARBON STEEL IN ACETATE/ACETIC MEDIUM

George-Daniel Dima[1], Cristian George Vaszilcsin[2], Alexandra Ioana Bucur[2], Ștefania Rus[2]

[1]University Politehnica Timisoara, Faculty of Chemical Engineering, Biotechnology and Environmental Protection, Laboratory of Electrochemistry, Corrosion and Electrochemical Engineering, 6 Pârvan, 300223 Timisoara, Romania
[2]National Institute of Research and Development for Electrochemistry and Condensed Matter, Dr. A. P. Podeanu 144, 300569, Timişoara, Romania
e-mail: cristi_vasz@yahoo.com

Abstract
The corrosion process of carbon steel in low-acid environments is a crucial problem in many industrial applications, which may justify the trend in the literature towards the identification of organic compounds, used as active substances in medicines, which have the effect of reducing the rate of corrosion by limiting the anodic electrochemical oxidation processes, at the interface between the metal and the aggressive solution. The present study investigated the inhibitory effect of Rivastigmine, hereinafter abbreviated RVG, in acetic acid-potassium acetate buffer solution of concentration 0.5/0.25 mol L^{-1}, in a concentration range of 10^{-6} to 10^{-3} mol L^{-1} by using electrochemical techniques such as cyclic voltammetry, monitoring of the open-circuit potential value E_{OCP} in time, potentiodynamic polarization method and measurement of oxidation current over time at different fixed superpotentials.
The monitoring of the stabilization of the metallic surface subjected to corrosive attack was achieved by measuring the evolution of the open circuit potential, and in order to assess the modification of the electrode kinetics in the presence and absence of the inhibitor, in the studied agressive media, the potentiodynamic polarization method was used. The results provided from the last method mentioned, such as the corrosion current density i_{corr}, the corrosion potential E_{corr}, the anodic and cathodic slopes b_a and b_c slopes were obtained, values that represent the mean of the degree of corrosion inhibition by RVG.
The relationship between the RVG structure and its ability to adsorb to the metal surface and preventing further corrosive attacks can be studied by usng quantum molecular modeling calculations and obtaining molecular descriptors. From its structure, RVG contains several functional groups capable of donating non-participating electrons to the vacant molecular orbital of iron, namely, the tertiary amino group, the oxygen and nitrogen atoms in the carbamate group, and last but not least, the aromatic system of the organic molecule. The heteroatoms present in the aromatic system can contribute to the interaction of the inhibitor with active centers at the level of the carbon steel surface, and, the protonation of the amino group in the acetic acetate media, can contribute to the existence of potential electrostatic interactions during the initial adsorption stage.
From the preliminary electrochemical results, as well as from the molecular modeling results, it emerges that RVG modifies the interfacial processes and favors the formation of an adsorbed organic layer meant to reduce the metallic surface accessible to the species that corrodes, therefore RVG has potential for use as an organic corrosion inhibitor for OLC52 carbon steel in acetic acid - potassium acetate buffer medium, with potential for use in de-icing solution formulas.

Acknowledgements
This paper was supported by Politehnica University Timișoara in the frame of PhD studies.

References

[1] M. Arvand, P. Fallahi, Voltammetric determination of rivastigmine in pharmaceutical and biological samples using molecularly imprinted polymer modified carbon paste electrode, Sensors and Actuators B: Chemical, 188 (2013) 797-805.

[2] S.R. Poojary, D. Nayak, P.P. Kumari, *et al.*, Donepezil Drug as a Potential Inhibitor for the Corrosion Mitigation of EN24 Steel in Sulfamic Acid Medium: Electrochemical and Theoretical Investigation., J Bio Tribo Corros 12 (2026) 87.

[3] C. Verma, M.A. Quraishi, K. Y. Rhee, Present and emerging trends in using pharmaceutically active compounds as aqueous phase corrosion inhibitors, J. Mol. Liq., 328 (2021) 115395.

PRELIMINARY ELECTROCHEMICAL AND MOLECULAR STUDIES ON THE POTENTIAL OF PIPERINE AS A CORROSION INHIBITOR FOR OLC52 CARBON STEEL

George-Daniel Dima[1], Mircea Laurențiu Dan[1], Cristian George Vaszilcsin[2], Nataliia Rudenko[3], Voicu Librimir[1]

[1]University Politehnica Timisoara, Faculty of Chemical Engineering, Biotechnology and Environmental Protection, Laboratory of Electrochemistry, Corrosion and Electrochemical Engineering, 6 Pârvan, 300223 Timisoara, Romania
[2]National Institute of Research and Development for Electrochemistry and Condensed Matter, Dr. A. P. Podeanu 144, 300569, Timişoara, Romania
[3]University Politehnica Timisoara, Innovation and Technology Transfer Center, 2 V. Pârvan, 300223 Timisoara, Romania
e-mail: cristi_vasz@yahoo.com

Abstract

In the present study, the potential of use of Piperine (PIP) in the inhibition of corrosion of OLC52 carbon steel was preliminarily evaluated, in a corrosion medium of CH_3COOH 0.5 mol L^{-1}/ CH_3COOK 0.25 mol L^{-1}, by combining electrochemical methods with the molecular modeling method, in order to correlate the structural peculiarities in the PIP molecule, with the ability to decrease the rate of iron anodic oxidation process in the carbon steel alloy studied.

The PIP concentrations evaluated were in the range of 10^{-6} and 10^{-3} mol L^{-1}, and the electrochemical methods used to evaluate the behavior of the metal/aggressive solution system, to which the working PIP concentrations were added were: monitoring of open circuit potential E_{OCP}, cyclic voltammetry (CV), linear polarization method and chronoamperometry.

In order to complement the voltametric studies and to evaluate the ability of PIP to interact with the working metal surface, quantum molecular modeling calculations were performed, from which descriptors such as the energy of the higher occupied molecular orbital E_{HOMO}, the energy of the lower unoccupied molecular orbital E_{LUMO}, energy gap, molecular hardness and softness, values that assess the possibility, from a molecular point of view, of PIP to bind to the metal surface, preventing subsequent corrosive attacks of the aggressive environment. The molecular structure of PIP is rich in regions with high electron density, such as the amide group, through the carbonyl oxygen atom, the oxygen atoms from the methylenedioxy groups and the extended π systems of the aromatic ring, are the susceptible centers that favor the adsorption of the studied molecule at the level of the metal surface. However, the nitrogen atom of the amide group can contribute to the inhibitory effect, but the availability of its electron pair is reduced due to conjugation with the carbonyl group, which is why oxygen atoms and π systems are the centers of interaction of high importance.

From the correlation of the data obtained through voltammetric studies with quantum molecular modeling calculations, an inhibition mechanism based on the adsorption of the PIP molecule at the surface level of OLC52 is supported, the adsorption type and the adsorption mechanism being the subject of further research through the study of adsorption isotherms, electrochemical impedance spectroscopy, and surface morphology.

Acknowledgements

This paper was supported by Politehnica University Timișoara in the frame of PhD studies.

References

[1] K. Farhadi, R.E. Sabzi, A.S. Abdulnabi, Experimental and Theoretical Study of Piper Nigrum Seed: Isolation of Piperine, DFT/MD Adsorption Modeling and Nano-formulation as a Green Corrosion Inhibitor for Carbon Steel in 1.0 M HCl, Analytical and Bioanalytical Electrochemistry, 17 (2025) 696–720.

[2] V. Joshi, V. Bachhar, P. Singh, M. Duseja, R. Haldhar, K.P. Katin, E. Berdimurodov, R.K. Shukla, Rheological and anticorrosion study of Piper chaba extract and coating for mild steel in 2 M H_2SO_4, Colloids and Surfaces A: Physicochemical and Engineering Aspects, 708 (2025) 135989.

[3] A. Nawaz, K.M. Deen, S. Ishraq, W. Haider, An electrochemical analysis of green corrosion inhibitor for A335 pipe steel in produced water media, International Journal of Electrochemical Science, 19 (2024) 100680.

INFLUENCE OF MEMBRANE CUT-OFF AND DIAFILTRATION STAGES ON FLOW-PROMOTER PERFORMANCE IN SWEET WHEY FILTRATION

Réka Dobozi[1], Tímea Lilla Urr[1], Zoltán Péter Jákói[2], Balázs P. Szabó[1], Szabolcs Kertész[2]

[1]Department of Food Engineering, Faculty of Engineering, University of Szeged, H-6725 Moszkvai krt. 5-7., Hungary
[2]Department of Biosystems Engineering, Faculty of Engineering, University of Szeged, H6725 Moszkvai krt. 9., Hungary
e-mail: dobozireka@mk.u-szeged.hu

Abstract

The performance of hydrodynamically intensified membrane filtration may vary considerably with membrane characteristics and process stage. In this study, the effects of membrane molecular weight cut-off (*MWCO*), flow-promoter configuration and successive diafiltration *(DF)* stages were compared during the processing of industrial sweet whey. Polyethersulfone (*PES*) membranes with nominal *MWCO* values of 10, 30 and 50 kDa were evaluated in a stirred filtration cell. An initial ultrafiltration *(UF)* screening compared four 3D-printed flow-promoter configurations with an insert-free control. The most favorable backward-oriented spiral-vane configuration was subsequently tested against the control during *UF* followed by three consecutive *DF* stages. Statistical evaluation was performed using heteroscedastic fixed-effect models with Welch-type contrasts and Holm adjustment for multiple comparisons.

During the screening experiments, the selected promoter significantly reduced total filtration resistance relative to the control at all three *MWCO* values. Differences among promoter geometries were membrane-dependent: the selected configuration was clearly separated from the other designs at 10 and 30 kDa, whereas the two spiral-vane orientations could not be distinguished statistically at 50 kDa. Across the complete *UF-DF* sequence, total resistance was lower with the promoter in every membrane–stage combination, with nearly all comparisons remaining supported after correction for multiple testing. Reversible resistance showed the most consistent response, with lower values in all promoter–control comparisons, whereas irreversible resistance exhibited a less uniform pattern. Total resistance at the final DF stage was significantly lower than after *UF* for all membrane cut-offs and both hydrodynamic configurations, with reductions of 26.6-53.9% for the controls and 35.3-49.1% with the promoter. At the final endpoint, the 30 and 50 kDa membranes showed lower total resistance than the 10 kDa membrane, with no detectable difference between 30 and 50 kDa.

In contrast, no statistically detectable differences in final protein fraction were observed either between promoter and control treatments or among membrane cut-offs. The lactose fraction of the *DF3* retentates was significantly reduced by the promoter at 10 and 50 kDa, by 44.3% and 41.6%, respectively, while all 30 kDa promoter-treated retentates were below the analytical detection limit of 100 mg L^{-1}. Overall, hydrodynamic modification most consistently affected filtration resistance, whereas compositional responses were more condition-dependent.

Acknowledgements

The Authors are grateful for the support provided by the Ministry of Culture and Innovation's University Research Scholarship Program, financed by the National Research, Development and Innovation Fund (EKÖP-26-3-SZTE-244 and EKÖP-26-1-SZTE-238). Furthermore, this study was supported by the 142414 FK and 2022-1.2.6-TÉT-IPARI TR2022-00011 projects from the National Research, Development, and Innovation Office (NKFI), Hungary.

LADYBIRDS (COLEOPTERA: COCCINELLIDAE) AS PREDATORS OF *ALEUROCANTHUS SPINIFERUS* (QUAINTANCE) IN SATSUMA MANDARIN ORCHARDS ON THE COAST OF MONTENEGRO

Mitar Đukanović[1], Ivana Jovičić[2], Jovana Damjanović[3], Tatjana Perović[4], Dušan Marinković[1], Antonije Žunić[1*]

[1]Department for Plant and Environmental Protection, Faculty of Agriculture, University of Novi Sad
*mitardjukanovic2020@gmail.com; dusan.marinkovic@polj.edu.rs; antonije.zunic@polj.edu.rs**
[2]Institute of Pesticides and Environmental Protection, Belgrade
ivana.jovicic@pesting.org.rs
[3]Faculty of Sciences, University of Novi Sad
joca-jovana@hotmail.com
[4]Center for Subtropical Cultures, Biotechnical Faculty, University of Montenegro
tatjana.p@ucg.ac.me

Abstract

The whitefly *Aleurocanthus spiniferus* (Hemiptera: Aleyrodidae) continues to spread throughout Montenegro where it has caused significant damage to citrus orchards over the past decade. As of 2020, 69 species of ladybirds (Coleoptera: Coccinellidae) had been recorded in Montenegro. In order to identify potential predators of *A. spiniferus*, a two-year study (2024–2025) was conducted in two Satsuma mandarin orchards in southern Montenegro (Bar and Sutomore regions). The presence of ladybirds was monitored using yellow sticky traps (Bio Plantella, 24 x 17 cm) that were changed every 15 days from April to November. Collected material was preserved in vials containing 96% ethanol. The morphological determination of ladybird species was carried out at the Faculty of Sciences, University of Novi Sad, Department of Biology and Ecology, and at the Institute of Pesticides and Environmental Protection in Belgrade. Morphological examination was conducted using stereomicroscope Nikon S18 (30x) and Leica S9 E stereomicroscope (Leica Microsystems, Wetzlar, Germany, with a maximum zoom magnification of 55x). Species of the genus *Scymnus* Kugelann and the species *Clitostethus arcuatus* (Rossi) reached the highest abundance. In addition, *Oenopia conglobata* **(L.)** and *Chilocorus bipustulatus* **(L.)**, known predators of *A. spiniferus*, were observed at these sites.

Key words: predators, ladybirds, whitefly, citrus fruits

ON-SITE SPAD DIAGNOSTICS: EVALUATING THE IMPACT OF INSECTICIDES ON SATSUMA MANDARIN LEAF CHLOROPHYLL CONTENT

Mitar Đukanović[1], Antonije Žunić[1], Dušan Marinković[1], Tatjana Perović[2], Aleksandar Sedlar[1], Filip Vasić[1]

[1]Department for Plant and Environmental Protection, Faculty of Agriculture, University of Novi Sad
[2]Center for Subtropical Cultures, Biotechnical Faculty, University of Montenegro
Corresponding author: mitardjukanovic2020@gmail.com

Abstract
Based on the processed data, results were obtained regarding the analysis of chlorophyll content in Satsuma mandarin leaves in relation to the applied insecticides (acetamiprid, deltamethrin, spirotetramat, and pyriproxyfen). The chlorophyll content 3 days after treatment ranged from 53.2 to 57.8 SPAD units, and after seven days, it ranged from 48.3 to 58.4 SPAD units for all tested variants at both locations. The greatest negative impact was observed in the variants treated with deltamethrin (29.6%) and spirotetramat (16.8%), while the smallest effect was recorded with pyriproxyfen (7.2%). Overall, the tested Satsuma mandarin leaves showed varying degrees of fluctuation in chlorophyll concentration depending on the applied insecticides, suggesting that these minor changes will not significantly impact plant growth.

Keywords: insecticides, plant stress, mandarin, leaves, treatment

Introduction

Although the primary purpose of pesticide products is to increase yield and preserve the quality of agricultural products, their improper application can still directly or indirectly affect the physiological or biochemical processes of the plant [1]. Depending on the mechanism of action of certain pesticide substances, changes in photosynthesis and chlorophyll degradation can occur [1, 2]. Changes in the concentration of photosynthetic pigments in plants, as an indicator of photosynthetic efficiency is a reliable method for determining plant stress [3]. In leaves treated with pesticides, changes occur in the form of irregular chloroplast organization, expansion of the thylakoid membrane, and an increase in the number of plastoglobules [2]. The resulting oxidative stress leads to the degradation of chlorophyll and reduces the photosynthetic activity of plants. Oxidative stress occur when there is a critical imbalance between antioxidant defense and reactive oxygen species (ROS), which can damage various cellular macromolecules, such as lipids, proteins, and nucleic acids [4]. To mitigate and prevent further negative impacts of pesticides on cell organelles, the plant activates a defense system based on the detoxification or biotransformation of the damage-inducing compounds [2]. Detoxification implies that the plant activates an antioxidant defense system involving antioxidant enzymes and non-enzymatic antioxidants to maintain the level of ROS below the threshold that causes irreversible damage [5]. Through biotransformation, plants convert toxic compounds into less toxic ones via oxidation, reduction, and hydrolysis reactions; the compound is then conjugated by glutathione S-transferase and uridine diphosphate-glycosyltransferase to sugar, amino acid, or glutathione, and finally, these compounds are directed from the plant cytosol to the vacuoles and apoplast [6].

Field measurements using a SPAD device allow for rapid and simple assessment of the photosynthetic status of treated plants enabling the early detection of stress symptoms.

The aim of this study is to determine the effect of four insecticide active substances (deltamethrin, acetamiprid, spirotetramat, and pyriproxyfen) on the photosynthetic pigment content in mandarin leaves using a SPAD device (Konica Minolta). The data were statistically

analyzed using ANOVA and LSD tests at a 95% confidence level using the R statistical software.

Materials and Methods

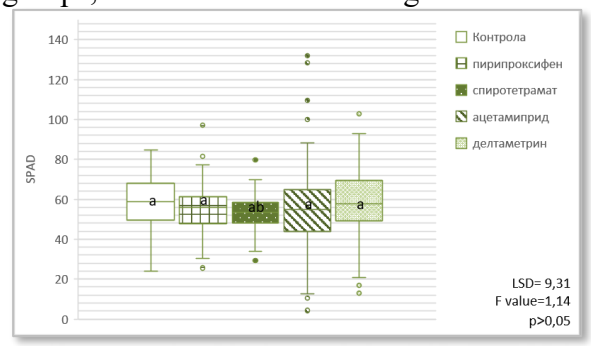
At two locations, Bar (42° 05' 15" N, 19° 06' 19" E) and Sutomore (42° 09' 27" N, 19° 01' 49" E) in Satsuma mandarin (*Citrus unshiu* Marc.) orchards, changes in chlorophyll content in mandarin leaves were measured using a portable SPAD device (Konica Minolta). The trial was conducted on August 25, 2025. Foliar application was carried out using a STIHL® SR 420 motorized atomizer. The following active substances were used: deltamethrin (Decis 2.5 EC, Bayer) at a dose of 5 mL/10 L, spirotetramat (Movento 100 SC, Bayer) at a dose of 15 mL/10 L, acetamiprid (Asset, Sharda Cropchem Espana AD) at a dose of 2.5 mL/10 L, and pyriproxyfen (Harpun EC, Galenika Fitofarmacija) at a dose of 7 mL/10 L. The experiment was set up according to the randomized block design with 4 replicates per treatment (4 trees per group, 25 randomly selected leaves per tree). The treatments were applied to trees that had served as control in a previous trial involving the efficacy assessment against the *A. spiniferus* [7]. SPAD assessments were taken 3 and 7 days after treatment.

Results and Discussion

Effect of Insecticides on Leaf Chlorophyll Content in the Bar Region

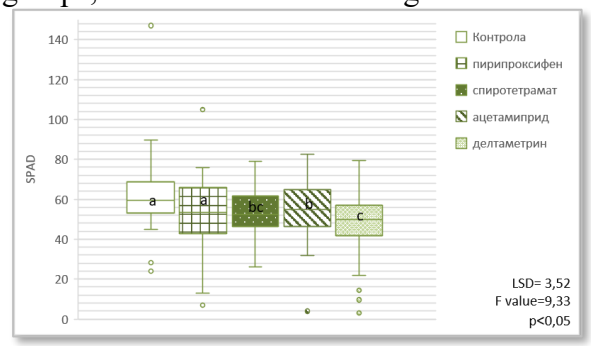
The results of the chlorophyll content assessment three and seven days after treatment in Bar are presented in Figures 1 and 2.

Figure 1. SPAD values 3 days after treatment (Bar, 2025); a, b - significant differences between groups; LSD - Fisher's Least Significant Difference test.



Three days after treatment, the chlorophyll values ranged from 53.2 to 57.8 SPAD units compared to the control. There is no statistically significant difference between the control and the treated groups ($F = 1.14$; $p > 0.05$).

Figure 2. SPAD values 7 days after treatment (Bar, 2025); a, b - significant differences between groups; LSD - Fisher's Least Significant Difference test

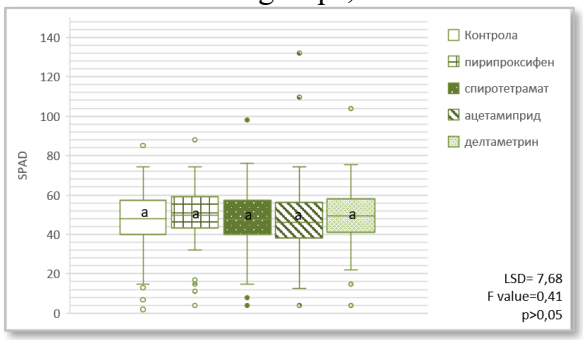


Seven days after treatment, values ranging from 49 to 58.9 SPAD units were recorded for all tested variants at both locations. The lowest chlorophyll content was recorded in the deltamethrin group, while the smallest difference compared to the control was recorded in the group treated with pyriproxyfen.

Effect of Insecticides on Leaf Chlorophyll Content in the Sutomore Region

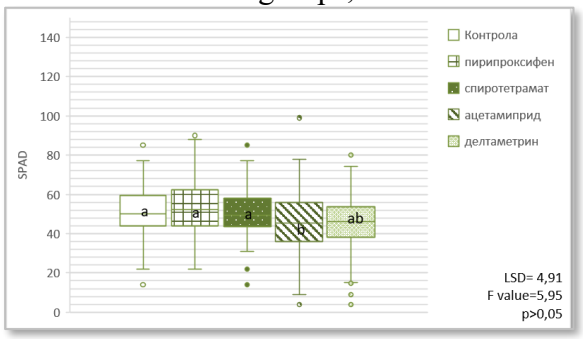
The chlorophyll content results obtained three and seven days after treatment at the Sutomore location are presented in Figures 3 and 4.

Figure 3. SPAD values in leaves 3 days after treatment (Sutomore, 2025); a, b - significant differences between groups; LSD - Fisher's Least Significant Difference test.



Three days after treatment the chlorophyll content ranged from 48.0 SPAD units in the group treated with acetamiprid to 55.2 SPAD units in the control group. There was no statistically significant difference between the groups ($F = 0.41$; $p > 0.05$).

Figure 4. SPAD values in leaves 3 days after treatment (Sutomore, 2025); a, b - significant differences between groups; LSD - Fisher's Least Significant Difference test.



Seven days after treatment at the Sutomore location, the greatest negative effect on chlorophyll content was observed in the acetamiprid treatment (around 50 SPAD units), while the control and the groups treated with pyriproxyfen and spirotetramat were at the same level of significance, with values ranging from 55 to 60 SPAD units.

During the assessments conducted three and seven days after treatment, no significant changes in chlorophyll content occurred. Therefore, it can be concluded that no stress was induced that would hinder the long-term growth and development of the treated plants at the applied doses.

References

[1] M. Lei, I. Raza, F. Deeba, M. Jamil, R. Naeem, A. Azizullah, B. Khattak, A. Shah, I. Ali, Z.S. Jin, M.D. Khan, Pol. J. Environ. Stud. 29 (2020) 2247.
[2] A. Žunić, I. Maksimović, M. Putnik-Delić, S. Vuković, D. Šunjka, S. Lazić, D. Bošković, Pol. J. Environ. Stud. 34 (2025) 5989.
[3] K. Sever, S. Bogdan, J. Franjić, Ž. Škvorc, Šumarski List 142 (2018) 247.
[4] A. Sharma, V. Kumar, A.K. Thukral, R. Bhardwaj, Planta Daninha 37 (2019) e019184291.
[5] A. Sereme, C. Dabire, M. Koala, M.K. Somda, A.S. Traore, J. Exp. Biol. Agric. Sci. 4 (2016) 414.
[6] L. Sun, H. Xua, W. Su, F. Xue, S. An, C. Lu, R. Wu, Plant Physiol. Biochem. 129 (2018) 101.
[7] M. Đukanović, T. Perović, V. Bursić, S. Tanasković, N. Magazin, B. Milić, M. Baloš, D. Marinković, A. Žunić, Chil. J. Agric. Res. 86 (2026) 628.

ASSESSMENT OF THE ENVIRONMENTAL IMPACT OF BRAKING SYSTEMS: A COMPARATIVE STUDY ON LIGHT AND COMMERCIAL VEHICLES

Anișoara Duma Copcea[1], Casiana Mihut[1], Okros Adalbert[1] Antoanela Cozma[1] Daniel Popa[2], Blenesi-Dima Attila[2], Daniela Scedei[3]

[1]Department of Soil Sciences, University of Life Sciences `King Mihai I from Timisoara, 119 Calea Aradului, Romania
[2]Department of Agricultural Tehnologies, University of Life Sciences `King Mihai I from Timisoara, 119 Calea Aradului, Romania
[3]Department of Horticulture, University of Life Sciences `King Mihai I from Timisoara, 119 Calea Aradului, Romania
e-mail: casiana_mihut@usvt.ro

Abstract

This study evaluates the correlation between the technical condition of braking systems and their environmental impact.
Utilizing digitized infrastructure and a Class 2 roller brake tester (4-tonne capacity, RO 328/06 certification) at a vehicle inspection station in Timișoara, a comparative study was conducted between a small passenger car (Renault Clio) and a light commercial vehicle (Ford Transit).
Braking has a direct and significant impact on the environment—a topic that has become central to new European regulations (such as the Euro 7 standard).
The results demonstrate that the early identification of braking imbalances and disc runout prevents uncontrolled fine particle emissions (PM2.5/PM10) resulting from asymmetric abrasion and optimizes the vehicle's energy efficiency.

Introduction

Public attention regarding automotive pollution has historically focused on exhaust emissions (CO_2, NOx). However, modern regulations (such as Euro 7) place increased emphasis on non-exhaust emissions, primarily consisting of particulate matter resulting from tire and brake pad wear [1, 2].
The braking system converts kinetic energy into thermal energy through friction [3, 4].
When a braking system operates in an unbalanced manner or exhibits deformation (ovality):
1. The wear rate of the friction material increases locally, releasing toxic heavy metal particles (copper, zinc, iron) and volatile organic compounds into the atmosphere.
2. Rolling resistance increases if the calipers do not fully retract, leading to additional fuel consumption and, consequently, a direct increase in CO_2 emissions. [5,6]
In recent decades, European Union environmental policies have focused primarily on reducing gaseous emissions resulting from the combustion of fossil fuels (CO_2, NOx, unburned hydrocarbons). [7,8].
Significant technological advancements in diesel particulate filters (DPF) and catalytic converters have considerably reduced tailpipe emissions [9,10]
Against this backdrop, the scientific community and regulatory bodies (through the upcoming Euro 7 legislative package) have shifted their focus heavily toward non-exhaust emissions. [11,12, 13]
Among these, particulate matter generated by the mechanical abrasion of braking systems represents one of the primary sources of fine particles in urban environments.
[14,15]. Converted through direct friction, the vehicle's kinetic energy becomes a continuous source of metallic micro-aerosols (copper, iron, zinc) and synthetic polymers that degrade air quality and penetrate directly into the human respiratory tract. [16, 17].

Experimental

The study was conducted in an industrial area of the municipality of Timișoara. The dynamic and environmental parameters of the braking system were determined using the SFR1 roller brake tester (Class 2).

Environmental and metrological specifications of the SFR1 tester

4-ton load capacity: provides a structural safety margin that eliminates slippage or measurement errors under heavy loads, preventing unnecessary tire wear during testing.

Corundum-coated rollers: the ultra-abrasive material ensures maximum grip and prevents tire slippage in winter or wet conditions.

Preventing roller slippage avoids the release of micro-emissions—such as burnt rubber and fine particles—into the enclosed space of the testing station.

Integrated weighing system (8 load cells): measures real-time mass at each wheel with 1 kg precision.

Relating braking force to actual mass prevents under-braking errors, which—in real-world driving—would lead to more severe and polluting emergency braking maneuvers.

8 kW (380V) motor providing constant speed (5.6 km/h): ensures stable rotation for the prompt detection of brake disc runout.

25% slip protection: automatic roller disengagement upon wheel locking protects the tire against excessive friction and reduces synthetic debris generation.

Paperless digital processing: the Eco Electro Platform software, integrated into a Linux-based system with a dual 21.5" LED monitor setup, ensures direct data acquisition from the electronic acquisition unit, eliminating the risk of human intervention or interpretation errors.

Results and discussion

The measurements performed on the SFR1 test stand for the two vehicles covered both regulatory parameters (RNTR) and energy sustainability parameters.

Table 1.

Renault Clio Test (Light passenger vehicle)

Renault Clio Test (Light passenger vehicle)	Recorded value (SFR1)	Minimum Legal Threshold	Ecological & Technical Assessment
Service brake efficiency	60.0% – 64.0%	≥ 50%	Approved. Optimal efficiency; short stopping distance, low heat generation per braking event. .
Parking brake efficiency	26.0% – 28.0%	≥ 16%	Passed. No hydraulic pressure loss or cable binding.
Axial imbalance	< 10%	< 20%	Passed. Even wear on left and right brake pads; fine particle emissions are uniform..
Disc runout	Within permissible limits	Minimized	No pedal vibration; uniform brake disc wea

Direct environmental impact (Renault Clio):

The vehicle's low mass, combined with a braking coefficient of ~62%, ensures low heat dissipation. The low level of imbalance indicates that braking does not affect the vehicle's steering, thereby eliminating asymmetric tire tread wear and minimizing brake pad dust emissions.

Table 2.

Ford Transit Testing (Light Commercial Vehicle)

Analyzed parameter	Recorded value (SFR1)	Minimum legal threshold	Ecological & Technical Assessment
Service brake efficiency	60.5% – 64.5%	≥ 50%	Approved. High load-bearing capacity under variable loads; prevents accelerated thermal wear.
Parking brake efficiency	21.2% – 28.6%	≥ 16%	Approved. Efficient ramp/slope locking mechanism under load..
Axial imbalance	Minimum (according to datasheet)	< 20%	Approved. Correct distribution of force on the rear axle (frequently subjected to dynamic loads).
Disc runout	Within permissible limits	Minimized	Prevents thermal micro-cracks in large drums/discs.

Direct environmental impact (Ford Transit):
The van's higher gross weight (often up to 3,500 kg) generates considerably higher kinetic energy ($E_k = \frac{1}{2}mv^2$).
The results obtained indicate that the van's braking system is correctly sized and maintained. A coefficient exceeding 60% prevents the overheating of brake discs—a process that would normally lead to the sublimation of friction materials and the massive release of toxic aerosols into the atmosphere.
Although both vehicles received a "RESULT: PASS" rating, the comparative analysis highlights differing environmental requirements:
Usage intensity and component lifecycle:
-Renault Clio (private use): Covers fewer kilometers; the biennial mandatory technical inspection (ITP) is sufficient to monitor wear resulting from the aging of friction linings.
-Ford Transit (commercial use): Subjected to intensive use. Although the mandatory inspection takes place annually (or every six months in special cases such as driving school vehicles or taxis), its annual environmental impact—in terms of brake particle emissions—is three to five times greater than that of a passenger car, due to daily routes and vehicle weight.
Weighing–Braking–Consumption Correlation:
-Automatic per-axle weighing performed by the SFR1 test stand allows for the identification of conditions where a brake caliper remains partially seized (residual braking).
A seized caliper on a Ford Transit, exerting a residual force of just 200 N, can increase diesel consumption by up to 0.5–0.8 l/100 km, generating tens of kilograms of additional CO_2 annually and causing premature brake disc wear.
Digitalization as an anti-pollution tool:
-Implementing the "Eco Electro Platform" software at the vehicle inspection center where the studies were conducted eliminates subjective interpretations.
A technical inspection report generated directly from sensor data guarantees that only vehicles with brakes operating within nominal parameters are driven on public roads, thereby limiting the risk of accidents and unnecessary pollution.

Conclusion
Technical and Environmental Compliance: both the Renault Clio passenger car and the Ford Transit van tested at the Timișoara vehicle inspection station meet national (RNTR/R.A.R.) and European standards, receiving a "PASS" result.
Reduction of Non-Exhaust Emissions: keeping axle imbalance below the critical threshold and preventing brake disc ovality—verified through Class 3 metrological testing—ensures a

significant reduction in fine particulate emissions (PM2.5 and PM10) resulting from brake system abrasion.

Energy efficiency: Rigorous testing on the SFR1 test stand—equipped with corundum-coated rollers and a real-time weighing system—directly contributes to identifying parasitic drag, thereby helping to keep fuel consumption within the manufacturer's design limits.

Importance of periodic inspection: For commercial vehicles, the rigor of brake testing has a significantly greater environmental impact than for passenger cars, due to the vehicle's mass and higher mileage.

References

[1] Amato, F., Cassee, F. R., Denier van der Gon, H. A. C., Gehrig, R., Gustafsson, M., Hafner, W., ... & Querol, X. (2014). Urban air quality: The challenge of non-exhaust road traffic emissions. Atmospheric Environment, 93, 340–350.

[2] Andreescu, C., & Stan, C. (2012). Dinamica autovehiculelor și impactul asupra mediului. Editura Matrix Rom, București.

[3] Burnete, N., Bogdan, A., & Moldovanu, D. (2016). Evaluarea emisiilor poluate generate de transportul rutier în mediul urban. Revista Transporturi, 23(2), 45–52.

[4] Căpățână, C., & Vancea, M. (2018). Cercetări privind uzura materialelor de fricțiune din componența frânelor auto și emisia de particule fine. Buletinul AGIR, (3), 112–118.

[5] Covaciu, D., & Florea, D. (2015). Analiza procesului de frânare la autovehicule și influența parametrilor de reglaj asupra performanțelor dinamice. Analele Universității „Transilvania” din Brașov, Seria I, 8(57), 89–96.

[6] Duma Copcea Anișoara, (2025), Termotehnică și motoare termice, Editura Agroprint, Timișoara

[7] Gaiginschi, R., & Filip, C. (2009). Poluarea generată de traficul rutier: Emisii de eșapament și non-eșapament. Editura Junimea, Iași.

[8] Iclodean, C., & Cordos, N. (2019). Impactul stării tehnice a autovehiculelor asupra siguranței rutiere și protecției mediului. Buletinul Științific al Universității Tehnice din Cluj-Napoca, Seria Autovehicule Rutiere, 29(1), 33–40.

[9] Macaria, C., & Oprean, I. (2014). Sisteme de frânare pentru autovehicule: Diagnosticare, metrologie și impact ecologic. Editura Universității Naționale de Știință și Tehnologie Politehnica București.

[10]Năstase, C., & Untaru, Ș. (2017). Cercetări privind generarea particulelor reziduale la frânarea autovehiculelor ușoare. Revista Română de Automobilism, (42), 21–28.

[11] Oprean, I., & Soloiu, V. (2008). Sisteme avansate de frânare și control al dinamicii autovehiculelor. Editura Politehnica Press, București.

[12] Popa, M., & Chiriac, R. (2013). Determinarea experimentală a coeficientului de frecare și a ratei de uzură pentru plăcuțele de frână fără azbest. Modtech International Journal, 1(2), 77–84.

[13] Soica, A., & Tarulescu, S. (2020). Monitorizarea calității aerului în zonele urbane aglomerate: Contribuția pulberilor provenite din uzura frânelor și anvelopelor. Journal of EcoAgriTourism, 16(1), 55–62.

[14] Ștefan, A., & Tofan, M. (2015). Metode metrologice de verificare a standurilor de frânare și evaluarea erorilor de măsurare. Revista de Metrologie, 62(4), 15–22.

[15] Thorpe, A., & Harrison, R. M. (2008). Sources and properties of non-exhaust particulate matter from road traffic: a review. Science of the Total Environment, 400(1-3), 270–282.

[16] Tudose, C., & Leahu, C. (2018). Optimizarea procesului de inspecție tehnică periodică (ITP) pentru reducerea amprentei de carbon a flotei rutiere. Analele Universității din Craiova, Seria Mecanică, 40(2), 101–108.

[17] Varga, B., & Todoruț, A. (2021). Analiza emisiilor non-eșapament în transportul rutier comercial ușor. Acta Technica Napocensis, Series: Applied Mathematics, Mechanics, and Engineering, 64(3), 412–420.

THE IMPACT OF THE MINIMUM TILLAGE SYSTEM ON CHERNOZEM IN THE WESTERN PLAIN

Anișoara Duma Copcea[1], Casiana Mihut[1], Veaceslav Mazăre[1] Okros Adalbert[1], Marius Stroia[1] Daniel Popa[2] Daniela Scedei[3] Attila Blenesi-Dima[2]

[1]Department of Soil Sciences, University of Life Sciences `King Mihai I from Timisoara, 119 Calea Aradului, Romania
[2]Department of Agricultural Technologies, University of Life Sciences `King Mihai I from Timisoara, 119 Calea Aradului, Romania
[3]Department of Horticulture, University of Life Sciences `King Mihai I from Timisoara, 119 Calea Aradului, Romania
e-mail: casiana_mihut@usvt.ro

Abstract

This study evaluates the impact of different tillage systems—specifically, the minimum tillage (Min-Till) system compared to the conventional moldboard plow system—on the physicochemical properties, water regime, organic matter dynamics, and phytopathological aspects of chernozem soil in Romania's Western Plain. The research was conducted at a farm in Timiș County.

The results demonstrate that shifting to the minimum tillage system promotes humus accumulation in the surface layer (4.0–4.5%), optimizes the water regime by reducing direct evaporation through a protective layer of crop residues (mulch), and maintains soil temperatures 3–8°C lower during critical summer periods.

A restructuring of the soil porosity network was also observed, characterized by the preservation of natural channels created by soil biota (earthworms) and roots. The main challenges identified with the minimum tillage system include the stratification of low-mobility nutrients (P and K) within the 0–10 cm horizon, the risk of temporary mineral nitrogen immobilization, and increased pressure from necrotrophic diseases transmitted via crop residues. The study concludes that effective chernozem management under a minimum tillage system requires localized fertilization (starter), rigorous crop rotation, and biostimulation of crop residue decomposition.

Introduction

The chernozems of Romania's Western Plain represent soil resources of exceptional agronomic value, characterized by high humus content, stable granular structure, and a high native cation exchange capacity[1, 2]. However, recent decades have been marked by intensifying aridification and soil structural degradation driven by aggressive mechanical tillage practices. [3, 4]

The conventional tillage system, based on furrow inversion via deep ploughing (25–30 cm), has historically ensured clean seedbeds and easy weed control. [5] Yet, the excessive aeration caused by ploughing stimulates the rapid mineralization of organic matter, destroys structural aggregates, and leads to the formation of a compacted layer known as "plough pan" (hardpan). [6, 7]

In the context of current climate change—characterized by prolonged droughts and extreme weather events—the adoption of conservation tillage systems (particularly Min-Till) has become imperative. [8] This study aims to provide a comparative analysis of the physicochemical and biological responses of chernozem soil to minimal mechanical

intervention, offering a tailored technological framework for maintaining the fertility and resilience of agro-ecosystems in the Western Plain. [9, 10]
Modern agro-ecosystems in Romania's Western Plain face major challenges driven by global climate change, manifested through prolonged periods of soil drought, an increased frequency of extreme soil-level temperatures, and an unbalanced redistribution of annual precipitation. Within this complex agrometeorological context, chernozems—historically recognized as soil resources of exceptional native fertility due to their well-developed clay-humus complex and stable granular structure—are subjected to intense degradation pressure resulting from intensive cultivation technologies. [11, 12]

Experimental

Field studies and measurements were conducted on a Chernozem soil at a farm located in Romania's Western Plain.
Soil and climatic conditions
The soil is a typical Chernozem with a loamy texture, high water-holding capacity, and an initial humus content in the arable layer ranging from 3.5% to 4.5%. The climate is temperate-continental with sub-Mediterranean influences, characterized by hot summers and a marked tendency toward soil drought during July and August.
Experimental variants
V1 – Conventional System (Control): annual moldboard plowing to a depth of 28–30 cm, followed by seedbed preparation using a field cultivator.
V2 – Minimum Tillage System (Min-Till): shallow loosening/non-inversion tillage (discs/chisel plow at 10–15 cm), maintaining at least 30% of crop residues on the soil surface as mulch.
Analysis methodologies
Physical properties: bulk density (g/cm^3) was determined using the known-volume cylinder method; total porosity and water infiltration rate were evaluated via penetrometry and the ring infiltrometer method.
Chemical properties: total humus was determined using the Walkley-Black method; total nitrogen (N) via the Kjeldahl method; available phosphorus (P_2O_5) and potassium (K_2O) via the Egner-Riehm-Domingo method; pH was measured potentiometrically in an aqueous suspension (1:2.5 ratio).
Phytopathological and thermal evaluations: the thermal microclimate was monitored using sensors buried at depths of 5 cm and 10 cm, while pathogen incidence was determined through periodic assessments of cereal and maize crops.

Results and discussion

Impact on soil physical properties
Aggressive ploughing mechanically disrupts soil aggregates and promotes surface crust formation caused by the direct impact of raindrops. In contrast, minimum tillage systems protect biomass and biological channels.
Repeated ploughing at the same depth (28–30 cm) leads to the formation of a "plough pan," obstructing root penetration and the vertical movement of water. Under conservation tillage systems, water retention is significantly superior due to the preservation of natural macropores.

Table 1

Physical properties of chernozem under the conventional system compared to the minimum tillage system

Property	Analytical parameter	Conventional system (Ploughing)	Minimum tillage system (Min-Till)
Physics	Soil structure	Unstable aggregates, risk of dusting	Granular/Glomerular; stable due to biota
Physics	Bulk density (g/cm³)	Stratified (reduction in the upper layer, compaction at 28–30 cm)	Medium and uniform; structural stability
Physics	Total porosity	Mechanically severed macropores	Dominated by permanent biological pores
Physics	Water infiltration	Low below the ploughing depth	High (earthworm burrows and root channels)
Physics	Ground temperature	High (massive heat absorption on dry soil)	3–5°C lower beneath the mulch layer

Humus dynamics and water regime

In the conventional system, massive soil aeration accelerates humus mineralization; a loss of just 0.1% humus per year equates to a reduction in water-holding capacity of approximately 10–15 t/ha.

The minimum tillage system shifts the balance toward humification. Plant residues retained on the surface form an insulating layer that reduces direct evaporation during critical periods. Consequently, the chernozem retains an optimal amount of water, with fine pores facilitating capillary rise from deeper soil layers (80–100 cm) during July and August.

Influence on chemical fertility (NPK)

The measurements taken reveal a clear change in the distribution of nutrients within the soil profile, depending on the tillage method:

Table 2

Nutrient (NPK) and humus dynamics in chernozem soil under a minimum tillage system

Chemical Element	Behavior in the Classical System	Minimal System Behavior	Technological Solution (Min-Till)
Nitrogen (N)	Soil structure	Unstable aggregates, risk of dusting	Granular/Glomerular; stable due to biota
Phosphorus (P)	Bulk density (g/cm³)	Stratified (reduction in the upper layer, compaction at 28–30 cm)	Medium and uniform; structural stability
Potassium (K)	Total porosity	Mechanically severed macropores	Dominated by permanent biological pores
Humus	Water infiltration	Low below the ploughing depth	High (earthworm burrows and root channels)

Phytopathological and agrotechnical aspects

Crop residues left on the soil surface create a moisture buffer zone but also generate microclimates favorable to the development of pathogens such as *Fusarium* spp., *Septoria* spp., or *Helminthosporium* spp. Additionally, an upward trend in slug and rodent populations has been observed.

To counteract these negative effects, experimental results indicate the need to implement the following measures:

1. Rational crop rotations avoiding cereal monoculture (introducing rapeseed, peas, or mustard).
2. Fine chopping and uniform spreading of straw or corn stalk residues.
3. Biological treatment of crop residues with bioremediation agents (e.g., *Trichoderma* spp.).

Conclusions

1. Restoration of physical structure: The minimum tillage (Min-Till) system halts the degradation of chernozem soil aggregates, eliminates the risk of plow pan formation, and reduces soil water evaporation by maintaining a mulch layer (resulting in soil temperatures 3–5°C lower).
2. Optimization of water reserves: Preserving biogenic channels (earthworm burrows) and the natural macropore network facilitates rapid precipitation infiltration and allows for the utilization of deep-seated water reserves (at 80–100 cm) during periods of severe drought.
3. Reorientation of fertility management: Due to the stratification of phosphorus and potassium in the 0–10 cm soil layer and the temporary immobilization of nitrogen, the minimum tillage system necessitates moving away from surface broadcasting in favor of localized fertilization (starter fertilizer) applied at the time of sowing.
4. Phytosanitary protection through biological management: Controlling pathogens favored by mulch no longer relies on soil inversion (plowing), but rather on strict crop rotation, fine chopping of crop residues, and the application of biological agents to accelerate decomposition.

References

[1] Canarache, A. (1990) – Fizica solurilor agricole, Editura Ceres, București.
[2] Duma-Copcea, A., Mateoc-Sîrb, N., Mihuț, C., Mateoc, T., Popa, N. D. (2025) – Soil Quality Assessment in Bihor County, Romania, IEP Conference Proceedings, pp. 589-596.
[3] Duma-Copcea, A., Mihuț, C., Popa, D. (2018) – Studies Regarding Minimum Soil Tillage, Scientific Papers Series Management, Economic Engineering in Agriculture and Rural Development, Vol. 18(4), pp. 105-112.
[4] Duma-Copcea, A., Mihuț, C., Sîrbu, C. C., Mazăre, R. (2020) – Sistemele de lucrare a solului și influența lor asupra calității cernoziomurilor, Research Journal of Agricultural Science, 52(2), pp. 45-52.
[5] Guș, P., Rusu, T. (2006) – Agrotehnică și tehnologii conservative, Editura Risoprint, Cluj-Napoca.
[6] Jităreanu, G., Ailincăi, C., Topa, D. (2012) – Managementul durabil al solului și influența sistemelor de lucrare asupra fertilității, Editura Ion Ionescu de la Brad, Iași.
[7] Mihuț, C., Duma-Copcea, A., Okros, A., Popa, D. (2022) – Influența tehnologiilor conservative asupra conservării apei în sol, Research Journal of Agricultural Science, Vol. 54(1), pp. 88-95.
[8] Mihuț, C., Niță, L., Duma-Copcea, A., Rinovetz, A. (2021) – Assessment of the Productive Capacity of Agricultural Lands for Their Sustainable Use, Scientific Papers Series Management, Economic Engineering in Agriculture and Rural Development, Vol. 21(3), pp. 515-522.
[9] Okros, A., Mihuț, C., Duma-Copcea, A., Mazăre, V., Stroia, M., Popa, D. (2025) – Analysis of the Agricultural System and Productive Resources in the Recaș Area, Timiș County, Romania, Annals of the University of Craiova - Agriculture Montanology Cadastre Series, Vol. 55(1), pp. 34-42.
[10] Popa, D., Duma-Copcea, A., Mihuț, C. (2019) – Cercetări privind eficientizarea energetică și fizică a sistemului Min-Till în Câmpia de Vest, Agrobuletin USAMVBT, Vol. 29, pp. 78-85.
[11] Rusu, T. (2014) – Tehnologii de lucrare minimă a solului (Min-Till și No-Till), Editura Academiei Române, București.
[12] Țărău, D., Mihuț, C. (2011) – Solurile Câmpiei de Vest a României – Geneză, evoluție și protecție, Editura Mirton, Timișoara.

GLUTEN-FREE SPONGE CAKE FORTIFIED WITH BAMBOO FLOUR: CHARACTERIZATION AND NUTRITIONAL PROPERTIES

Camelia Moldovan[1], Karolina Vrandečić[2], Delia Gabriela Dumbravă[1*], Viorica Mirela Popa[1], Diana Nicoleta Raba[3], Corina Dana Mișcă[1]

[1]Faculty of Food Engineering, University of Life Sciences "King Mihai I" from Timișoara, Calea Aradului 119A, 300645, Romania
[2] Faculty of Agrobiotechnical Sciences Osijek, Vladimira Preloga 1, 31000, Croatia
[3]Faculty of Management and Rural Tourism, University of Life Sciences "King Mihai I" from Timișoara, Calea Aradului 119A, 300645, Romania
e-mail: deliadumbrava@usvt.ro

Abstract
The evaluation of the quality characteristics of yogurt fortified with honey meets current consumer demand for natural functional foods with a clean label, offering a superior alternative to conventionally sweetened products. This research aimed to optimize the sensory profile and perform physicochemical characterization of yogurt by adding increasing proportions of honey (0%, 10%, 15%, 20%, and 25% relative to the yogurt mass). The evaluation of sensory and quality characteristics was carried out using hedonic testing on a 5-point scale and through physicochemical analyses of titratable acidity, soluble dry matter, salt content, antioxidant capacity, and proximate composition. Sensory analysis results indicated that the sample with 10% honey represents the optimal formulation, achieving the maximum score for taste (5.00) and consistency (5.00), while the added honey improved curd viscosity and substantially reduced the phenomenon of syneresis. From a physicochemical standpoint, the addition of honey led to a linear increase in soluble dry matter from 7.7°Bx to 23.5 °Bx and a reduction in acidity from 147 °T to 118 °T, mitigating excessive acidity. The antioxidant capacity increased significantly, directly correlating with the honey supplementation dose. Furthermore, energy density increased from 60 kcal/100g to 117 kcal/100g. Therefore, fortifying yogurt with honey enhances the rheological and functional properties of the product, with the 10% honey sample offering the ideal balance between organoleptic attributes and nutritional benefits.

ENHANCEMENT OF PHYSICOCHEMICAL PROPERTIES AND BIOACTIVE POTENTIAL OF DRINKABLE YOGURT FORTIFIED WITH NATURAL HONEY

Camelia Moldovan[1], Mehmet Kilinç[2], Delia Gabriela Dumbravă[1*], Viorica Mirela Popa[1], Diana Nicoleta Raba[3], Diana Veronica Dogaru[1], Mărioara Drugă[1]

[1]Faculty of Agrofood Processing Technology, University of Life Sciences "King Mihai I" from Timişoara, Calea Aradului 119A, 300645, Romania
[2] Afyon Kocatepe University, Faculty of Engineering and Architecture, Department of Food Engineering, Afyonkarahisar, Turkey
[3]Faculty of Management and Rural Tourism, University of Life Sciences "King Mihai I" from Timişoara, Calea Aradului 119A, 300645, Romania
e-mail: deliadumbrava@usvt.ro

Abstract
Given that whey separation (syneresis) remains a major technological drawback in drinkable yogurt formulations, this study evaluates the fortification of yogurt (3.5% fat) with natural honey (0–25% w/w) as a solution to stabilize the matrix and enhance its nutritional value. Analytical determinations tracked the evolution of titratable acidity, soluble solids content (°Brix), energy density, and centrifugation syneresis, alongside the quantification of total phenolic content (TPC) and antioxidant capacity (DPPH). The results revealed a dose-dependent improvement across all evaluated parameters. Honey incorporation moderated titratable acidity and increased soluble solids content from 7.7 °Brix up to a maximum of 23.5 °Brix, promoting aqueous phase retention and reducing syneresis by approximately 50% at the maximum fortification level. From a nutritional and bioactive perspective, honey addition nearly doubled the energy density (from 60 kcal/100g to 117 kcal/100g), increased phenolic content, and doubled DPPH radical scavenging activity (RSA), displaying a strong linear correlation between them ($R^2 > 0.9$). In conclusion, honey fortification represents an effective technological strategy to counter syneresis in drinkable yogurt, delivering a functional dairy product with optimized caloric density and enhanced antioxidant value.

BIODEGRADABLE SURFACTANT-STABILIZED NANOEMULSIONS FOR SUSTAINABLE MANAGEMENT OF INVASIVE STINK BUGS

Tamara Erceg[1], Vanja Travičić[1], Vesna Teofilović[1], Milica Aćimović[2], Irina Vulin[3], Dina Tenji[3]

[1]*University of Novi Sad, Faculty of Technology, Bul. Cara Lazara 1, 21000 Novi Sad, Serbia*
[2]*Institute of Field and Vegetable Crops, Novi Sad, Serbia*
[3]*University of Novi Sad, Faculty of Sciences, Serbia*
**Corresponding author's e-mail address: tamara.erceg@uns.ac.rs*

This research presents a fully bio-based, oil-in-water nanoemulsion platform designed as an eco-friendly replacement for synthetic, fossil-fuel-derived pesticides. Utilizing biodegradable surfactants—specifically saponins and alkyl polyglucosides—the delivery system encapsulates an active phase of neem oil combined with eucalyptus and lemongrass essential oils. The resulting formulations feature droplet sizes between 37 and 71 nm, low viscosity, excellent sprayability, and colloidal stability exceeding 60 days. Due to enhanced delivery efficiency and active synergies, the nanoemulsions achieved 100% mortality against two invasive stink bug species (*Halyomorpha halys* and *Nezara viridula*) within 48 hours. Beyond insecticidal efficacy, the water-based processing, fully biodegradable constituents, and confirmed biocompatibility in cytotoxicity assays significantly reduce ecotoxicological risks. These findings demonstrate that biosurfactant-stabilized nanoemulsions offer a scalable, low-impact crop protection alternative aligned with circular bioeconomy goals.

Keywords: Nanoemulsions, stink bugs control, biopesticides, biodegradable surfactants.

Acknowledgement: This research study was funded by the Provincial Secretariat for Higher Education and Scientific Research of Autonomous Province Vojvodina (Serbia) within the project "New generation nanoemulsion bioinsecticides: synergy of plant oils and extracts for environmentally friendly control of stink bugs—ECObiopest" (grant No. 003871936 2025 09418 003 000 000 001 04 003)

COMPARATIVE PHYSICOCHEMICAL EVALUATION OF GINGER-CONTAINING PEDIATRIC SYRUPS AND GRANULES

Zita Farkaš Agatić, Ana Pilipović, Vesna Tepavčević, Mladena Lalić-Popović, Nemanja Todorović, Kosta Popović, Mihalj Poša

Department of Pharmacy, Faculty of Medicine, University of Novi Sad, Hajduk Veljkova 3, 21000 Novi Sad, Serbia
e-mail: zita.farkas@mf.uns.ac.rs

Abstract

The development of age-appropriate oral formulations is particularly challenging when plant-derived active ingredients possess intense organoleptic properties. Ginger (Zingiber officinale Roscoe) contains bioactive phenolic constituents, while its characteristic pungent taste may limit acceptability in pediatric formulations. The aim of this study was to comparatively evaluate ginger-containing pediatric syrups and granules prepared using different taste-masking and formulation strategies. Three syrup formulations (SJ-1–SJ-3) and three granule formulations (G-1–G-3) were investigated. The approaches included β-cyclodextrin complexation, viscosity- or polymer-based taste masking, and pectin-based structuring or coating. Physicochemical and organoleptic properties were evaluated, while total phenolic content was determined using the Folin–Ciocalteu spectrophotometric method. In the syrup series, total phenolic content ranged from 263.03 to 392.22 mg GAE/L, with low matrix interference (13.49 mg GAE/L for the placebo). SJ-1, containing β-cyclodextrin, provided the most effective masking of the characteristic ginger taste and aroma. Among the granules, the β-cyclodextrin-containing G-1 formulation showed the most favorable overall technological and organoleptic characteristics. The results indicate that formulation strategy markedly influences the physicochemical and sensory properties of ginger-containing dosage forms and support β-cyclodextrin complexation as a promising taste-masking approach for further formulation development.

Introduction

Pediatric oral formulations require dose flexibility, physical and chemical stability, ease of administration and acceptable sensory properties. Ginger is widely investigated because of its bioactive constituents, particularly gingerols and shogaols, and its use in nausea and vomiting [1,2]. However, its characteristic pungent taste and aroma represent a relevant formulation challenge. Cyclodextrins are cyclic oligosaccharides capable of forming non-covalent inclusion complexes with suitable guest molecules and can be used to modify solubility, stability and organoleptic properties [3,4]. The present work compared two complementary oral dosage-form platforms, syrups and granules, and evaluated whether β-cyclodextrin-based complexation provides advantages over viscosity-, polymer- and coating-based approaches.

Results and discussion

Three syrup formulations and three granule formulations were prepared. SJ-1 employed β-cyclodextrin complexation; SJ-2 used a cyclodextrin-free viscosity/diffusion-masking strategy; and SJ-3 was a low-methoxyl pectin-structured system. G-1 combined β-cyclodextrin complexation with a pectin/polyethylene glycol coating; G-2 used a cyclodextrin-free polymer matrix with pectin/PEG coating; and G-3 represented a lower-complexity dilution-plus-coating approach. Syrups were characterized by pH, density, refractive index and organoleptic evaluation. Granules were evaluated by pH, refractive index, bulk and tapped density, Carr index, Hausner ratio and organoleptic properties. Total phenolic content was measured by the Folin–Ciocalteu method using gallic acid calibration (0–100 mg/L; $A = 0.0063c - 0.0024$; R^2

= 0.9998), with absorbance measured at 765 nm [5]. The main physicochemical, organoleptic and technological characteristics of the investigated formulations are summarized in Table 1.

Table 1. Comparative physicochemical, organoleptic, and technological characteristics of the investigated ginger-containing syrup and granule formulations.

Formulation	Key analytical/physical result	Organoleptic/technological observation	Overall interpretation
SJ-1	Total phenolics 263.03 mg GAE/L	Ginger taste and aroma almost completely masked; slight sedimentation, readily redispersible	Most effective syrup taste masking
SJ-2	pH 4.15; total phenolics 375.03 mg GAE/L	Moderate residual ginger character; viscosity and sweet–acid balance reduced pungency	Acceptable cyclodextrin-free alternative
SJ-3	Total phenolics 392.22 mg GAE/L	Most pronounced ginger character	Highest phenolic value, weaker sensory masking
G-1	pH 3.16; Carr index 14.75%; Hausner ratio 1.17	Homogeneous smaller particles; dry texture; mild ginger aroma	Best overall granule performance
G-2	pH 3.85; Carr index 17.24%; Hausner ratio 1.21	Larger aggregates and more intense ginger character	Further optimization required
G-3	pH 3.48; Carr index 12.90%; Hausner ratio 1.15	Homogeneous structure and favorable flow	Simple comparator with good processability

The syrup formulations showed clear formulation-dependent differences. Density values for SJ-1, SJ-2 and SJ-3 were 1.2844, 1.2680 and 1.2800 g/cm³, respectively, while the corresponding refractive indices were 1.4440, 1.4404 and 1.4249. Organoleptic evaluation most clearly differentiated the systems: SJ-1 almost completely masked the characteristic ginger taste and aroma, whereas SJ-2 produced moderate masking and SJ-3 retained the strongest ginger character. Total phenolic content ranged from 263.03 to 392.22 mg GAE/L; placebo contribution was only 13.49 mg GAE/L, indicating low matrix interference. Processing below 40 °C was used to limit degradation of sensitive constituents.

Granule formulations also differed in their technological behavior. The measured pH values were 3.16, 3.85 and 3.48 for G-1, G-2 and G-3, respectively; refractive indices of aqueous dispersions were 1.3736, 1.3718 and 1.3722. G-1 showed a favorable combination of particle uniformity, dry texture, mild ginger aroma and processability. The Carr index/Hausner ratio values were 14.75%/1.17 for G-1, 17.24%/1.21 for G-2 and 12.90%/1.15 for G-3. Although G-3 showed the most favorable numerical flow indices, the overall decision matrix used in the source study identified G-1 as the preferred formulation because it combined β-cyclodextrin-based taste masking with favorable technological and sensory properties. Taken together, the liquid and solid systems indicate that β-cyclodextrin complexation is particularly useful when taste masking is a critical formulation attribute. The total phenolic contents of the investigated syrup and granule formulations are compared in Figure 1. The overall formulation strategy, analytical characterization and selection of the most promising syrup and granule formulations are summarized schematically in Figure 2.

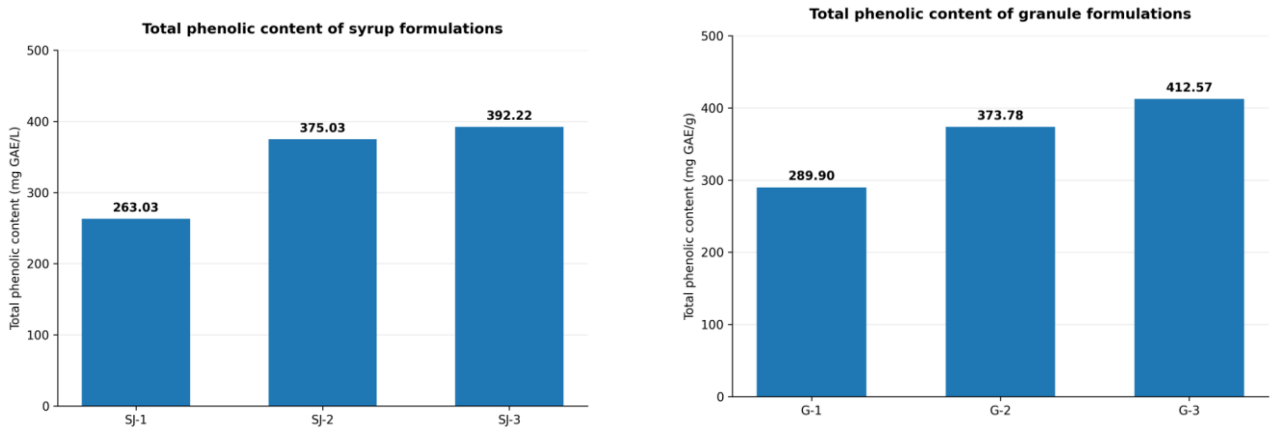


Figure 1. Total phenolic content of ginger-containing syrup and granule formulations determined by the Folin–Ciocalteu method.

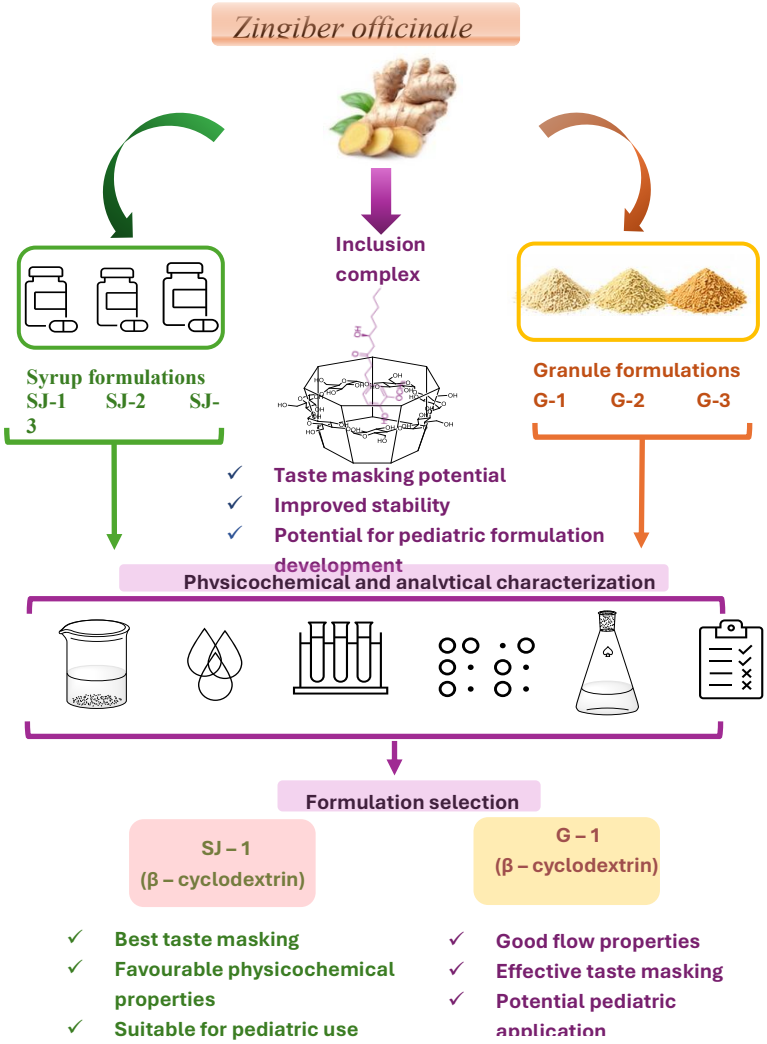


Figure 2. Schematic representation of the formulation and comparative evaluation of ginger-containing syrups and granules.

Conclusion

Six ginger-containing formulations representing two pediatric oral dosage-form platforms and several taste-masking strategies were comparatively evaluated. SJ-1 was the most promising syrup because β-cyclodextrin complexation provided the strongest masking of ginger pungency while preserving satisfactory physicochemical characteristics. G-1 was selected as the preferred granule formulation based on the combined technological and organoleptic assessment. The Folin–Ciocalteu measurements further indicated preservation of phenolic constituents under the applied processing conditions. Because total phenolic content is a non-specific analytical parameter, subsequent work should include marker-specific chromatographic quantification of gingerols and shogaols, together with stability and in vitro release studies.

Acknowledgements

This research was carried out within the project “Development of Innovative Pharmaceutical-Technological Preparations for the Pediatric Population in the Republic of Serbia” (“Razvoj inovativnih farmaceutsko-tehnoloških preparata za pedijatrijsku populaciju u Republici Srbiji”), funded by the Provincial Secretariat for Higher Education and Scientific Research of the Autonomous Province of Vojvodina, Republic of Serbia, under Project No. 003817825 2025 09418 003 000 000 001.

References

[1] E. Ernst, M.H. Pittler, Br. J. Anaesth. 84 (2000) 367–371.
[2] I. Lete, J. Allué, Integr. Med. Insights 11 (2016) 11–17.
[3] T. Loftsson, D. Duchêne, Int. J. Pharm. 329 (2007) 1–11.
[4] T. Loftsson, M.E. Brewster, J. Pharm. Pharmacol. 62 (2010) 1607–1621.
[5] V.L. Singleton, R. Orthofer, R.M. Lamuela-Raventós, Methods Enzymol. 299 (1999) 152–178.

REUSABILITY OF POLYDOPAMINE- AND TiO_2-MODIFIED PAN MEMBRANES DURING REPEATED OIL-EMULSION FILTRATION

Ákos Ferenc Fazekas, Brunet Wagner Rosildo Cassule, Gábor Veréb, Zsuzsanna László

Department of Biosystem Engineering, Faculty of Engineering, University of Szeged, Moszkvai Blvd. 9., H-6725 Szeged, Hungary
e-mail: fazekas.akos.ferenc@szte.hu

Abstract

Membrane filtration is a promising chemical-free and user-friendly method for the treatment of oil-contaminated water, as it can effectively remove both micro- and nanosized oil droplets. However, membrane fouling and the associated flux decline remain major obstacles to long-term application. Polydopamine modification forms a stable, homogeneous, and hydrophilic layer on the membrane surface, reducing the adhesion of contaminants such as oil droplets. Unlike chemical grafting, it proceeds spontaneously in a single step without UV irradiation, initiators, or cross-linking agents, making it a simple, cost-effective, and scalable method [1]. In this study, the repeated-use performance of polydopamine- and TiO_2-modified polyacrylonitrile ultrafiltration membranes (400 kDa) was investigated during oil-in-water emulsion filtration (c=100 ppm).

During the first filtration cycle, the PAN–PDA(40) membrane exhibited an oil-emulsion flux of 285 L m^{-2} h^{-1}, a flux recovery ratio of 71%, and a flux decline ratio of 29%. The incorporation of 20 mg TiO_2 markedly improved the filtration performance: the PAN–PDA(40)–TiO_2(20) membrane reached an oil-emulsion flux of 753 L m^{-2} h^{-1}, a flux recovery ratio of 97%, and a flux decline ratio of only 3%. Both membranes provided high purification efficiencies. COD removal was 98.5% for PAN–PDA(40) and 95.8% for PAN–PDA(40)–TiO_2(20), while turbidity removal reached 99.5% and 99.1%, respectively.

During repeated use, the flux of PAN–PDA(40) decreased considerably over four cycles. At VRR = 5, it declined from approximately 270 L m^{-2} h^{-1} in the first cycle to approximately 50 L m^{-2} h^{-1} in the fourth cycle. In contrast, the TiO_2-containing membrane maintained high flux values throughout eleven consecutive cycles, with final fluxes remaining approximately 550–740 L m^{-2} h^{-1}. These results demonstrate that TiO_2 immobilization substantially improves fouling resistance and the repeated-use performance of PDA-modified PAN membranes.

References

[1] Susan D., Mohammadreza O., Simin S. (2021) Role of polydopamine in the enhancement of binding stability of TiO_2 nanoparticles on polyethersulfone ultrafiltration membrane. Colloids and Surfaces A: Physicochemical and Engineering Aspects, 622, 126694

OPTICAL DETECTION OF TETRACYCLINE HYDROCHLORIDE USING AN A3B PORPHYRIN AND Zn-METALLODERIVATIVE

Ionela Fringu, Anca Lascu, Nicoleta Plesu

Institute of Chemistry "Coriolan Dragulescu", Mihai Viteazu Avenue 24, 300223 Timisoara, Romania
Email: ionelacreanga@yahoo.com

Tetracycline hydrochloride is one of the first antibiotics developed in medicine more than 70 years ago [1] and acts as a bacteriostatic antibiotic that does not directly kill bacteria, but instead blocks their multiplication and growth, preventing the infection from spreading. Despite its beneficial effects, long-term exposure to this antibiotic can lead to superinfections with *Candida albicans*, may affect the kidneys and liver [2], and may reduce the number of blood cells (platelets, eosinophils); therefore, precise dosing is necessary, both to avoid adverse effects and because of the growing concern regarding bacterial resistance to drugs.

In the present study, the ability of an A_3B-type porphyrin, namely 4-pyridyl-tris-(4-phenoxyphenyl) porphyrin (PyPPP), and its Zinc-metalated derivative (Zn-PyPPP) (Figure 1) [3] to detect tetracycline hydrochloride using a simple and easy-to-use optical method was investigated.

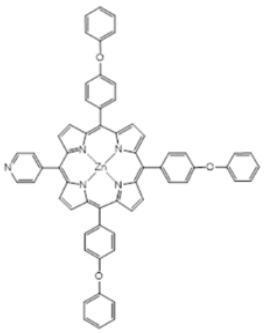


Figure 1. Structure of Zn (II)-4-pyridyl-tris-(4-phenoxyphenyl) porphyrin.

Due to the presence of several functional groups, as well as its acidic character, tetracycline hydrochloride represented an excellent candidate for testing the optical detection capability of the substituted porphyrin PyPPP and its zinc derivative (Zn-PyPPP).

The differences in the behavior of the two porphyrins in the presence of tetracycline are reflected in the morphological changes observed for both the porphyrin and its zinc-metalated derivative, indicating a more uniform arrangement of the triangular particles, which aggregate into H- and J-type structures. The tetracycline concentration range detectable by UV-Vis spectrometry is 10^{-5} M - 10^{-4} M.

References

1. Smilack, J.D. The tetracyclines. *Mayo Clin Proc.* 1999, 74, 7, 727-9.
2. Taneja, O.P.; Grover, N.K.; Thakur, L.C. Bhatia, V.N. *Chemo* 1974, 20, 4, 201–211.
3. Tărănu, B; Rus, S.F.; Fagadar-Cosma, E. *Coat.*, 2024, 14, 1048.

CORROSION PROCESSES IN AEROSOL PACKAGING INTENDED FOR THERMAL WATER - BASED COSMETIC PRODUCTS

Cristiana-Nicoleta Fuicu[1], Nataliia Rudenko[2], George Daniel Dima[1], Mircea-Laurențiu Dan[1], Nicolae Vaszilcsin[3,4]

[1]Faculty of Chemical Engineering, Biotechnologies and Environmental Protection, University Politehnica Timisoara, 300223 Timisoara, Romania
[2]Innovation and Technology Transfer Center, University Politehnica Timisoara, 300006 Timisoara, Romania
[3]Technical Sciences Academy of Romania, Bd. Dacia 26, 010414 Bucuresti, Romania
[4]Research Institute for Renewable Energies, University Politehnica Timisoara, Piata Victoriei 2, 300006 Timisoara, Romania
e-mail: mircea.dan@upt.ro

Aerosol packaging is a widely used technological solution for the conditioning and distribution of liquid cosmetic products, including thermal waters intended for skin application in the form of a fine spray. These packaging facilitate hygienic application, reduce direct contact between the user and the product, and partially protect the formulation from external contamination. At the same time, prolonged contact between the cosmetic product, the propellant gas, the valve components and the container material can lead to electrochemical degradation processes. Internal corrosion is relevant because it can affect the mechanical integrity of the container, the internal pressure, the operation of the spray system and the physicochemical stability of the product.

Thermal waters are natural systems with a variable chemical composition, determined by the geological context, water-rock interactions, source temperature and duration of underground circulation. Depending on the source, they may contain sodium, potassium, calcium, magnesium, bicarbonate, silicates, chlorides and sulphates, as well as dissolved gases, including carbon dioxide and, in some cases, sulphurous compounds. The corrosive character of a thermal water cannot be assessed exclusively by total mineralisation, being influenced by pH, conductivity, dissolved oxygen, alkalinity, ion and temperature ratios. Studies on geothermal and mineral waters have shown that the presence of chlorides and sulphates, together with acidic pH or dissolved gases, can favour corrosion processes and alter the stability of protective films formed on metal surfaces.

Aerosol containers for cosmetic products based on thermal waters are mainly made of aluminium, tinned sheet steel and, more rarely, stainless steel, their inner surface being usually protected by organic varnishes. The selection of the material must be correlated with the internal operating pressure, the mass and geometry of the packaging, the manufacturing technology, the possibility of recycling, the cost and, above all, the compatibility with the mineralised formula. Aluminium is frequently used in monoblock containers due to its low density, formability and spontaneous formation of a passive oxide film, which provides initial protection against corrosion. However, in contact with mineralised waters, especially in the presence of chloride ions, at pH values unfavourable to passivation or in the event of damage to the inner varnish, the protective film can be destabilised, favouring localised puncture corrosion. Tinplate, consisting of a low-carbon steel substrate coated with a thin layer of tin, offers mechanical rigidity and pressure resistance, but its protection depends on the continuity of the tin layer and the internal varnish. Pores, scratches, coating unevenness, or defects in the joint area can allow the electrolyte to enter the base steel and initiate local corrosion, including perforating corrosion. Stainless steel is distinguished by superior corrosion resistance due to its passive film rich in chromium oxides; austenitic molybdenum alloys, such as AISI 316, generally exhibit

better resistance to punctiform and crevice corrosion than AISI 304 in chloride-containing environments. However, the high cost and processing difficulties limit the use of stainless steel for the body of disposable aerosol containers, making it more suitable for functional components, filing equipment or reusable systems. Also, contact between the container body, valve cup, spring and other different metal components can lead to the formation of galvanic couples when the thermal water has sufficient conductivity to act as an electrolyte. Therefore, the use of high chemical compatibility inner varnishes and experimental testing of the product-packaging assembly are essential to reduce the migration of metal ions, prevent premature degradation and maintain the safety of the cosmetic product.

The morphology of internal corrosion can include uniform corrosion, point corrosion, crevice corrosion, galvanic corrosion, under-film corrosion, and thread corrosion. Point corrosion poses a particular risk to aluminum packaging because it produces localized cavities that can advance into the depth of the metal without a proportional and visible loss of mass. If there are defects in the organic coating, corrosion can propagate at the interface between the protective layer and the metal substrate. Evaluation of the susceptibility to filiform corrosion of organic coatings applied to metallic substrates can be performed using standardized guidelines, such as ASTM D2803. In addition, exposure to saline atmospheres or accelerated salt spray tests can be useful for comparing the relative strength of metal-coating systems, in accordance with the ASTM B117 methodology.

Figure 1 compares the three main categories of metallic materials used or relevant for aerosol packaging for cosmetic products based on thermal waters: aluminium, tinplate and stainless steel.



Figure 1. Schematic representation of metallic materials, protective coatings and possible corrosion mechanisms in aerosol packaging intended for cosmetic thermal waters. Created by the authors using an AI-assisted image-generation tool and scientifically reviewed by the authors.

The numbers in the figure correspond to the following elements:

1. Aluminum Container Wall - Represents the metal body of a one-piece aerosol container.
2. Indoor organic varnish applied to aluminum - The polymer layer physically isolates the thermal water and ionic species dissolved by the metallic substrate.

3. Passive aluminum oxide film; aluminum spontaneously develops a thin film of Al2O3, with a protective role, which limits the dissolution of the metal, but its stability depends on the pH of the solution, the ionic content and the presence of aggressive species.

4. Point corrosion of aluminum, localized attack initiated in an area with a lacquer defect or with discontinuities of the passive film.

5. Low-carbon steel substrate forms the mechanical basis of tinplate.

6. The tin layer deposited on the steel, which partially protects the steel substrate and contributes to the improvement of corrosion behaviour.

7. The inner varnish of the tinplate container is the main barrier against the interaction between the product and metal.

8. Passive film rich in chromium oxides of stainless steel (stainless steel forms an adherent passive film on the surface, rich in chromium oxides, which can recover in the presence of oxygen).

9. Protected stainless surface in contact with thermal water - The area depicted symbolizes the efficient operation of the passive film, which limits the transfer of electrons and reduces the speed of anodic dissolution processes.

At the bottom of Figure 1 the components of the spray system (the valve cup, spring, and actuator) show that an aerosol is not just made up of the body of the container. If different metal parts are electrically connected and are simultaneously in contact with the electrolyte, galvanic corrosion can occur.

At the same time, reddish-brown deposits are corrosion products, especially metal oxides and hydroxides. In the case of steel, they can be associated with the formation of iron oxides/hydroxides; in aluminum, the products may be less visible, but local degradation can progress in depth.

The figure highlights the fact that corrosion resistance is not determined only by the chosen metal, but by the entire thermal water – container – inner coating – valve – storage conditions system.

Corrosion processes in aerosol containers can have direct consequences on the quality of the cosmetic product. Metal ions resulting from dissolution, such as aluminum, iron or tin ions, can contribute to changes in the appearance of the product, turbidity, deposits or color changes. Corrosion products can also compromise the interior appearance of the container, damage the organic coating and affect the operation of the valve. In advanced situations, corrosion can lead to pressure losses, clogging of the spray ports or a decrease in the mechanical strength of the container. The electrochemical underpinnings of these phenomena, including anodic metal dissolution processes and cathode reactions associated with dissolved oxygen or hydrogen ions, are well described in the literature.

Corrosion prevention involves the evaluation of product-packaging compatibility from the development phase of the cosmetic formula. This evaluation must consider the ionic composition of the thermal water, the pH, the conductivity, the content of dissolved gases, the type of metallic material, the nature and thickness of the inner varnish, the materials of the valve system and the storage conditions. The use of organic coatings with high chemical resistance, the control of the continuity of the protective film, the compatible choice of metals in the aerosol assembly and the limitation of direct contact between the mineralized formula and the metallic substrate are essential measures. In situations where the product formula allows, the adjustment of the pH or the use of cosmetically compatible inhibitors can decrease the speed of electrochemical processes, but these solutions must be rigorously validated so as not to alter the dermato-cosmetic properties of the thermal water.

For the experimental investigation of corrosion phenomena, storage tests at room temperature and accelerated regime can be used, followed by gravimetric evaluations, visual inspections,

microscopic examinations and analysis of corrosion products. Electrochemical methods, such as open-circuit potential monitoring, linear polarization and electrochemical impedance spectroscopy, allow the assessment of corrosive activity and the efficiency of protective films. In addition, chemical analysis of thermal water and the calculation of stability indices can provide an initial estimate of the trend of corrosion or deposition formation.

In conclusion, corrosion of aerosol packaging for thermal water-based cosmetics is an interdisciplinary problem, located at the intersection of electrochemistry, materials engineering, mineral water chemistry and packaging technology. The natural variability of thermal water composition requires that each product-packaging system be tested individually, without direct extrapolation of the results obtained for other mineral sources. The integration of physicochemical water characterization, electrochemical tests, surface analyses and accelerated aging tests can support the design of more reliable aerosol packaging, reduce the risk of metal ion contamination, prevent container failure, and maintain the quality of cosmetics throughout their shelf life.

Acknowledgements
The authors used Perplexity AI image-generation tools to assist in preparing the conceptual illustration presented in Figure 1. The authors reviewed, edited, and verified the scientific accuracy, terminology, and relevance of the final figure and assume full responsibility for its content.

References

[1] Revie, R.W.; Uhlig, H.H. Corrosion and Corrosion Control: An Introduction to Corrosion Science and Engineering, 4th ed.; John Wiley & Sons: Hoboken, NJ, USA, 2008.
[2] Davis, J.R., Ed. Corrosion of Aluminum and Aluminum Alloys; ASM International: Materials Park, OH, USA, 1999.
[3] Revie, R.W., Ed. Uhlig's Corrosion Handbook, 3rd ed.; John Wiley & Sons: Hoboken, NJ, USA, 2011.
[4] Vasconcelos, H.C.; Fernández-Pérez, B.M.; González, S.; Souto, R.M.; Santana, J.J. Characterization of the Corrosive Action of Mineral Waters from Thermal Sources: A Case Study at Azores Archipelago, Portugal. Water 7, (2015), 3515–3530. https://doi.org/10.3390/w7073515
[5] Song, J.; Liu, M.; Sun, X. Model Analysis and Experimental Study on Scaling and Corrosion Tendencies of Aerated Geothermal Water. Geothermics 85, (2020), 101766. https://doi.org/10.1016/j.geothermics.2019.101766
[6] ASTM International. ASTM D2803-09(2020): Standard Guide for Testing Filiform Corrosion Resistance of Organic Coatings on Metal; ASTM International: West Conshohocken, PA, USA, 2020.
[7] ASTM International. ASTM B117-19: Standard Practice for Operating Salt Spray (Fog) Apparatus; ASTM International: West Conshohocken, PA, USA, 2019.

COMPARATIVE EVALUATION OF THREE TOTAL PROTEIN DETERMINATION METHODS

Borbála Gémes, Eszter Takács, Szandra Klátyik, András Székács

Agro-Environmental Research Center, Institute of Environmental Sciences, Hungarian University of Agricultural and Life Sciences, Tessedik S. u. 4, Gödöllő, Hungary, H-2100
e-mail: gemes.borbala.leticia@uni-mate.hu

Abstract

In ecotoxicological studies, determination of total protein content enables the standardized evaluation of biomarker responses, including changes in enzyme activities or heat shock protein levels [1,2]. Given the growing importance of biomarker analyses in ecotoxicological studies [3], the selection of the most reliable method for a given set of experimental conditions is crucial. The colorimetric Bradford assay and bicinchoninic acid (BCA) assay for total protein content determination, as well as the direct UV absorbance quantitation method were optimized for use in green alga species, and were evaluated comparing their sensitivity, dynamic range of determination, limit of detection, assay duration, and sample volume requirements. For measurement of optical density, the SpectraMax iD3 multimode reader (Molecular Devices, San José, CA, USA) was used, wavelengths for the Bradford assay and the BCA assay were determined at 595 nm and 562 nm, respectively. The UV absorbance method was performed on SpectraDrop™ micro-volume microplate (Molecular Devices, San José, CA, USA) according to the protocol provided by the manufacturer [4]. For systematic comparison of the methods, the same bovine serum albumin dilution series obtained in phosphate-buffered saline at the concentration range of 0–100 mg/mL were applied for all determination types.

Although strong positive correlations were detected among all three methods, sensitivity and limit of detection values differed among them. The UV absorbance quantitation process appeared to be the least sensitive procedure with a wide dynamic range. This protocol does not apply a dye or any other type of reagent, and is able to measure an order of magnitude higher concentrations than the colorimetric assays. Its advantage is, however, that it requires the lowest sample volume (4 µL). In contrast, the limit of detection values were more favorable (lower) for the two colorimetric assays. This latter feature may enable the assessment of treatment effects at the individual level in certain ecotoxicological tests, in contrast to the pooled-sample approach commonly employed in previous studies. Color development in the BCA assay required longer incubation periods (~ 30 minutes) than in the Bradford assay (~ 5 minutes). Incorporating kinetic measurement modes in determination protocols is strongly recommended to capture initial reaction rates, thereby expanding the linear dynamic range and ensuring accurate protein quantification.

Although all three methods are suitable for total protein determination, according to literature data and to the observed differences, the optimal choice may depend on the specific experimental conditions and analytical requirements.

Acknowledgements

This research was supported by the EKÖP-MATE/2026/27/K University Research Scholarship Programme of the Ministry of Science and Technology from the source of the National Research, Development and Innovation Fund and by the Flagship Research Groups Program of the Hungarian University of Agriculture and Life Sciences.

References

[1] A. Jemec, D. Drobne, T. Tišler, K. Sepčić, Environ. Sci. Pollut. Res.17(3) (2010) 571-581.
[2] C. Moreira-de-Sousa, R. B. de Souza, C. S. Fontanetti, Water Air Soil Pollut. 229(8) (2018) 264.
[3] S. E. Hook, E. P. Gallagher, G. E. Batley, Integr. Environ. Assess. Manag. 10(3) (2014) 327-341.
[4] Manufacturer's protocol: https://www.moleculardevices.com/sites/default/files/en/assets/app-note/br/direct-protein-quantitation-using-spectradrop-micro-volume-microplate.pdf (accessed 24.09.2026.)

CORROSION RESISTANCE OF SPIN-COATING Tb^{3+}-DOPED $Zn_3Nb_2O_8$ THIN FILMS IN NaCl AND HCl MEDIA

Mihaela Gherban, Bogdan Taranu, Mircea Nicolaescu, Carmen Lazau, Corina Orha, Cornelia Bandas, Mina Morariu*

National Institute for Research and Development in Electrochemistry and Condensed Matter Timisoara, Dr. A.P. Podeanu no.144, 300569, Timisoara Romania, email: mihaela.birdeanu@gmail.com, mina.popescu37@gmail.com
**Corresponding author: mina.popescu37@gmail.com*

Abstract

The study is based on the preparation of thin films using the spin-coating method, as well as on testing their corrosion resistance in aggressive media (NaCl and/or HCl). For the preparation of the thin films, $Zn_3Nb_2O_8$-type oxide materials doped with different concentrations of Tb^{3+} ions and synthesized using the hydrothermal method will be employed.

Introduction

The doping with Tb^{3+} ions is intended to improve the optical properties; however, it may slightly alter the density of crystal defects and the concentration of oxygen vacancies, thereby indirectly affecting the electrochemical stability. Tb^{3+} doping does not adversely affect its corrosion behavior and may even enhance its stability by optimizing the crystal structure and reducing surface defects [1-3].

In saline environments, the corrosion of Tb^{3+}-doped $Zn_3Nb_2O_8$ is mainly influenced by the presence of Cl^- ions, which are considered among the most aggressive species toward oxide materials. Although $Zn_3Nb_2O_8$ is a ceramic oxide with high chemical stability and good resistance to degradation, prolonged exposure to NaCl solutions may lead to changes in the surface layer and the development of localized corrosion processes.

In an acidic environment, the corrosion of the Tb^{3+}-doped $Zn_3Nb_2O_8$ ceramic material is governed by the interaction of H^+ and Cl^- ions with the oxide surface. Although $Zn_3Nb_2O_8$ exhibits high chemical stability due to the strong Nb–O bonds and the ceramic nature of its crystal lattice, prolonged exposure to HCl solutions leads to the progressive degradation of the surface through a complex mechanism involving selective dissolution and structural modification [4-8].

Experimental

Sample	Precusor 1	Precusor 2	Precusor 3	Molar ratio
1	Nb_2O_5	$Zn(NO_3)_2x4H_2O$	Tb_2O_3	1:3:0.05
2	Nb_2O_5	$Zn(CH_3COO)_2x2H_2O$	Tb_2O_3	1:3:0.05
3	Nb_2O_5	ZnO	Tb_2O_3	1:3:0.05
4	Nb_2O_5	$Zn(NO_3)_2x4H_2O$	$TbCl_3$	1:3:0.05
5	Nb_2O_5	$Zn(CH_3COO)_2x2H_2O$	$TbCl_3$	1:3:0.05
6	Nb_2O_5	ZnO	$TbCl_3$	1:3:0.05
7	Nb_2O_5	$Zn(NO_3)_2x4H_2O$	$Tb(NO_3)_3$	1:3:0.05
8	Nb_2O_5	$Zn(CH_3COO)_2x2H_2O$	$Tb(NO_3)_3$	1:3:0.05
9	Nb_2O_5	ZnO	$Tb(NO_3)_3$	1:3:0.05

Table 1. Precursors used in hydrothermal synthesis

The *spin coating technique* represents one of the most widely used methods for obtaining oxide thin films due to its process simplicity, low cost, reproducibility, and the possibility of precise control over the film thickness.

The deposition process involves the following steps: deposition of approximately 100–200 µL of precursor solution onto the substrate; rotation of the substrate at 2500–3500 rpm for 30–60 s;preheating of each deposited layer at 150–300 °C to remove the solvent and organic compounds;repetition of the deposition cycle until the desired film thickness (100–500 nm) is achieved. After deposition of the final layer, the films are thermally treated at 700–900 °C for 2–4 h in order to promote the crystallization of the $Zn_3Nb_2O_8$ phase and the activation of the Tb^{3+} luminescent centers.

Corrosion tests. Preparation and characterization of protective layers of undoped and 0.05 M Tb^{3+}-doped $Zn_3Nb_2O_8$ pseudo-binary oxide via the spin-coating technique.

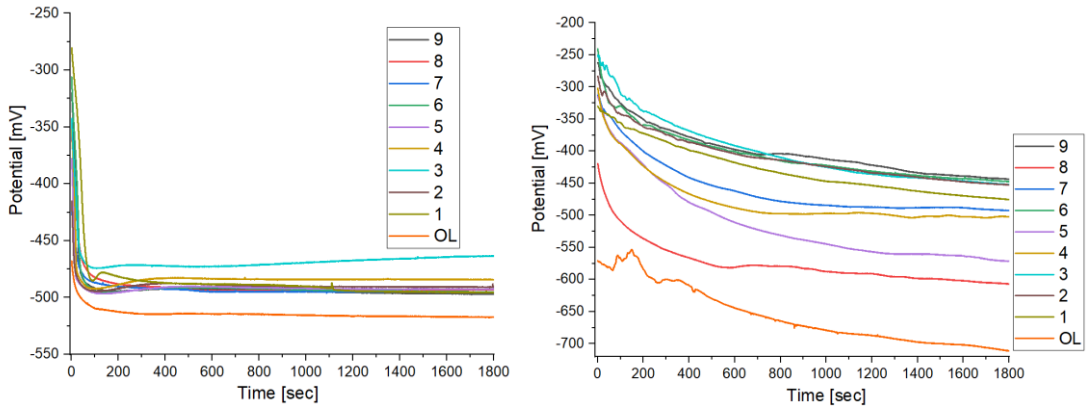
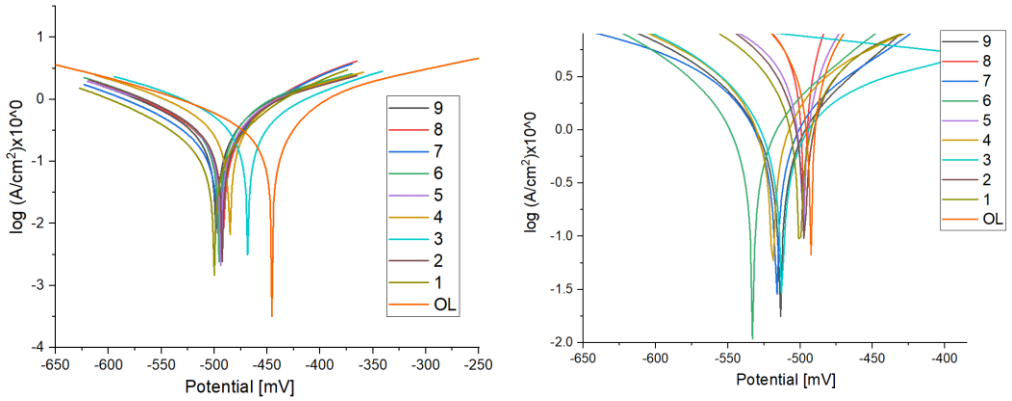


Figure 1. Open-circuit potential (OCP) measurements of electrodes modified by spin coating for 30 min: bare steel, $Zn_3Nb_2O_8$, and Tb^{3+}-doped $Zn_3Nb_2O_8$, obtained by the hydrothermal method in (a) 0.1 M HCl and (b) 0.3 M NaCl (notations as given in Table 1).

The OCP measurements presented in Figures 1a show that the coated electrodes stabilize after approximately 100–200 s, whereas in Figure 1b, the electrodes require a considerably longer time to stabilize, reaching a relatively stable state after approximately 1200 s and exhibiting a less uniform behavior. In contrast, the uncoated electrode stabilizes after approximately 1800 s. This result provides preliminary information about the nature of the processes occurring at the metal/thin-film/electrolyte interfaces.



a) b)

Figure 2. Tafel curves for electrodes modified by the spin-coating technique for 30 min: bare steel, $Zn_3Nb_2O_8$, and Tb^{3+}-doped $Zn_3Nb_2O_8$, obtained by the hydrothermal method in (a) 0.1 M HCl and (b) 0.3 M NaCl (notations as given in Table 1).

In all the analyzed cases, the steel electrodes modified by the deposition of thin films based on pseudo-binary oxides using the spin-coating technique exhibited an improvement in corrosion inhibition. Moreover, the highest corrosion inhibition efficiency (IE = 73.35%) among the electrodes modified by spin coating was obtained for the $Zn_3Nb_2O_8^{3+}$ structure synthesized by the hydrothermal method using Nb_2O_5, $Zn(NO_3)_2{\cdot}4H_2O$, and Tb_2O_3 as precursors in an acidic medium. This coating provided a smooth, non-porous, and uniformly covered surface, which contributed to its enhanced corrosion protection performance.

Results and discussion

Corrosion mechanism of Tb^{3+}-doped $Zn_3Nb_2O_8$ in a saline NaCl environment

In the initial stage, the material surface comes into contact with the electrolyte solution, and Cl^- ions and water molecules are adsorbed onto the oxide surface. Adsorption occurs preferentially in regions with high surface energy, such as crystal defects, grain boundaries, and oxygen vacancies. These regions become active sites for the initiation of degradation processes.

Subsequently, Cl^- ions penetrate the existing defects and locally destabilize the Zn–O bonds. Compared with Nb–O bonds, Zn–O bonds are more susceptible to electrochemical attack, leading to the selective dissolution of Zn^{2+} ions into the solution. The release of zinc generates oxygen vacancies and increases the density of structural defects in the surface layer. Micro-anodic regions develop in the vicinity of these defects, while intact surface areas act as cathodic regions, thereby promoting the occurrence of localized corrosion.

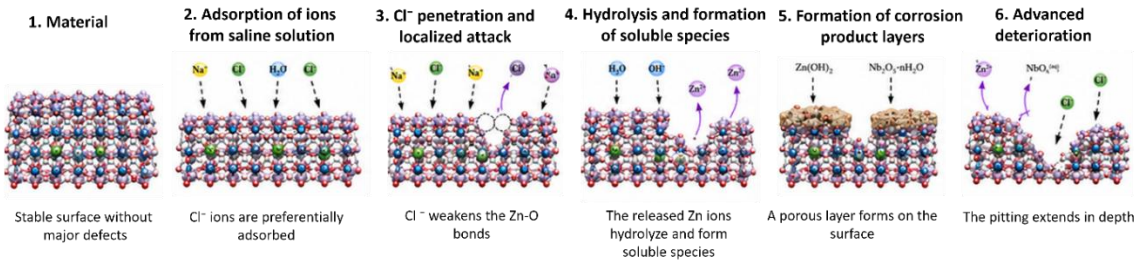


Figure 3. Corrosion mechanism of Tb^{3+}-doped $Zn_3Nb_2O_8$ in a saline NaCl environment

Experimental results obtained via potentiodynamic polarization and electrochemical impedance spectroscopy show that Tb^{3+}-doped samples exhibit lower corrosion current density (Icorr) values, higher polarization resistance (Rp) values, and larger Nyquist semicircle

diameters compared to the undoped material. These results confirm that Tb^{3+} doping improves corrosion resistance in a saline environment by reducing dissolution processes and enhancing the stability of the passive layer.

Corrosion mechanism of Tb^{3+}-doped $Zn_3Nb_2O_8$ in an acidic HCl medium

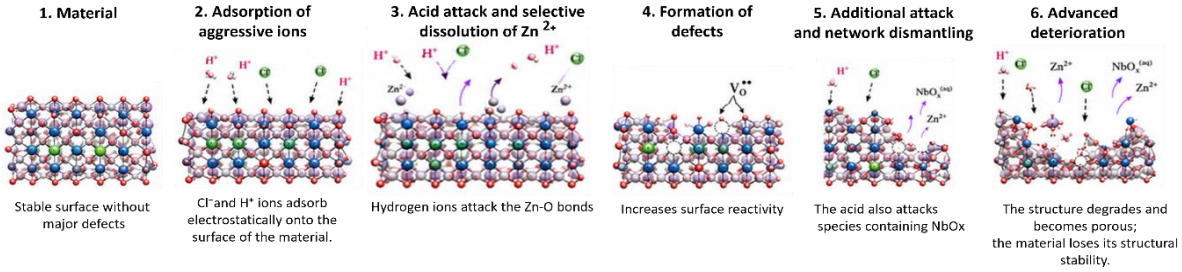


Figure 4. Corrosion mechanism of Tb^{3+}-doped $Zn_3Nb_2O_8$ in an acidic HCl medium

In the first stage, H^+ and Cl^- ions are adsorbed onto the material surface. Hydrogen ions protonate the oxygen atoms in the crystal lattice, which reduces the bond strength between Zn and O and promotes the breaking of Zn–O bonds. Cl^- ions do not react directly with the crystal lattice; however, they stabilize the dissolved metal ions and accelerate local dissolution processes.

The next stage is characterized by the preferential dissolution of zinc. The Zn–O bonds are more susceptible to acid attack than the Nb–O bonds; therefore, Zn^{2+} ions are released into the solution, generating oxygen vacancies and structural defects near the surface. The accumulation of these defects leads to increased porosity and facilitates the penetration of the electrolyte toward the inner layers of the material.

As dissolution progresses, the surface becomes enriched in niobium due to the higher stability of the Nb–O bonds. Through hydrolysis and structural rearrangement, a thin layer rich in hydrated niobium oxides may form, temporarily slowing ion transport and reducing the corrosion rate. However, in concentrated HCl solutions or after prolonged exposure, this protective layer may undergo partial dissolution, allowing the degradation process to continue.

Conclusion

Overall, the corrosion mechanism of $Zn_3Nb_2O_8^{3+}$ in an acidic HCl environment can be described as a sequence of the following stages: adsorption of H^+ and Cl^- ions onto the surface, protonation of lattice oxygen, breaking of Zn–O bonds, selective dissolution of Zn^{2+} ions, formation of defects and oxygen vacancies, development of a protective niobium oxide-rich layer, and, under aggressive conditions, degradation of this layer and propagation of corrosion into the bulk of the material. Due to the structural stabilization effect induced by Tb^{3+} ions, the doped material exhibits superior corrosion resistance compared with undoped $Zn_3Nb_2O_8$, making it a promising candidate for optoelectronic and luminescent applications in moderately acidic environments.

In conclusion, the corrosion mechanism of $Zn_3Nb_2O_8^{3+}$ in NaCl solution involves the adsorption of Cl^- ions, selective dissolution of zinc, formation of oxygen vacancies, development of a protective layer enriched in niobium compounds, and, under severe conditions, initiation of localized corrosion. Tb^{3+} doping reduces the susceptibility of the material to chloride-ion attack, enhances its structural stability, and improves its durability in saline environments, making it suitable for optoelectronic and functional applications under conditions of humidity or electrolyte exposure.

Acknowledgements
This research was funded by a grant from the Ministry of Research, Innovation and Digitization, project number PN 23 27 01 02 INOMAT, 23-27 29N/2023.

References
[1] R.W. Revie (Ed.), Uhlig's Corrosion Handbook, 3rd ed., Wiley, Hoboken, NJ, USA, (2011).
[2] P.R. Roberge, Handbook of Corrosion Engineering, 2nd ed., McGraw-Hill Education, New York, NY, USA, (2019).
[3] R.G. Kelly, J.R. Scully, D.W. Shoesmith, R.G. Buchheit, Electrochemical Techniques in Corrosion Science and Engineering, CRC Press, Boca Raton, FL, USA.
[4] D.A. Jones, Principles and Prevention of Corrosion, 2nd ed., Pearson Education.
[5]M.E. Orazem, "Electrochemical Impedance Spectroscopy," Current Opinion in Electrochemistry 13 (2019) 132–139.
[6]B. Ramírez-Barat, E. Cano, "In Situ Electrochemical Impedance Spectroscopy Measurements and Their Interpretation for the Diagnostic of Metallic Cultural Heritage: A Review," ChemElectroChem 5 (2018) 2968–2981.
[7] M.H. Nazir, Z.A. Khan, A. Saeed, "A Novel Non-Destructive Sensing Technology for On-Site Corrosion Failure Evaluation of Coatings," IEEE Access 6 (2018) 1042–1054.
[8] H. Hoshi, M. Itagaki, "Fundamental Electrochemical Methods for Corrosion Study—Electrochemical Impedance," Zairyo-to-Kankyo 67 (2018) 55–58.

IMPACT OF DIFFERENT DRYING METHODS ON THE PHENOLIC CONTENT AND ANTIOXIDANT ACTIVITY OF HOT TRUB EXTRACTS

Lenka Grubač[1], Alena Stupar[2], Anamarija Mandić[2], Aleksandra Mišan[2], Slađana Stajčić[1], Milana Pribić[1], Jelena Pejin[1]

[1]University of Novi Sad, Faculty of Technology Novi Sad, 21000 Novi Sad, Bulevar cara Lazara 1, Serbia
[2]University of Novi Sad, Institute of Food Technology Novi Sad, 21000 Novi Sad, Bulevar cara Lazara 1, Serbia
e-mail: lenka.grubac@uns.ac.rs

Global beer production yields substantial amounts of hot trub (HT), a protein-polyphenol-rich by-product generated during wort clarification. Although HT retains significant quantities of high-value hop-derived bioactive compounds, particularly prenylated chalcones such as xanthohumol, its industrial utilization is severely limited by an elevated moisture content (80 - 90%), which leads to rapid microbiological spoilage and chemical degradation. Due to this complex bioactive profile and the proven biological activities of its components, including antioxidant, anti-inflammatory, and antimicrobial properties, HT holds immense potential for high-value applications across the food, pharmaceutical, and cosmetic sectors. Matrix stabilization through drying is therefore a critical requirement for the long-term preservation and efficient recovery of these heat-sensitive polyphenols. However, traditional thermal drying often causes severe degradation of active constituents, emphasizing the need for optimized dehydration strategies.

This study evaluated the effect of various drying techniques applied to HT on the retention of total phenols and the resulting antioxidant activity of the extracts. The influence of conventional drying (50, 65, and 80 °C), vacuum drying (50, 65, and 80 °C at -0.95 bar), and freeze-drying (-40 °C at 0.128 mbar) on total phenols and DPPH radical scavenging capacity of the obtained HT extracts was systematically investigated. The results demonstrated that both the drying method and temperature significantly affected the stability and retention of total phenolic content. Under the tested conditions, vacuum drying consistently yielded extracts with superior total phenolic content and DPPH radical scavenging capacity compared to conventional drying at matching temperatures (0.42-0.45 vs. 0.31-0.38 g GAE/100 g DM hot trub for total phenolic content; and 9.69-11.69 vs. 4.28-6.65 μM TE/g DM hot trub for DPPH radical scavenging capacity). Among the vacuum-dried treatments, processing at 80 °C achieved a DPPH antioxidant capacity statistically equivalent to freeze-drying, while maintaining high polyphenol retention on par with the other vacuum conditions. Overall, vacuum drying emerges as a highly viable alternative to conventional thermal drying for HT stabilization. Although moderate temperatures (50-65 °C) provide a gentler thermal regime, 80 °C under vacuum maximizes the overall antioxidant response without compromising total polyphenol recovery.

Acknowledgements

This research was funded by the Ministry of Education, Science and Technological Development of the Republic of Serbia, University of Novi Sad – Faculty of Technology Novi Sad (Agreements No. 451-03-34/2026-03/200134 and 451-03-33/2026-03/200134) and Provincial Secretariat for Higher Education and Scientific Research of the Autonomous Province of Vojvodina (Agreements No. 002365668 2026 09418 002 000 000 001 04 002).

MESPILUS GERMANICA L. FRUIT DEVELOPMENT AND RIPENING IN RELATION TO CLIMATIC CONDITIONS AND ANTIOXIDANT PROPERTIES

Iasminca-Dușița Birta (Cugerean)[1], Nicoleta Gabriela Hadaruga[1,2]* , Cristina Mitroi[1], Alexandru-Erne Rinovetz[2], Mariana Atena Poiana[1,2], Despina - Maria Bordean[1,2]

[1]Doctoral School "Engineering of Vegetable and Animal Resources", University of Life Sciences "King Mihai I" from Timisoara, Calea Aradului 119, Timisoara, Romania;
[2]Faculty of Food Engineering, University of Life Sciences "King Mihai I" from Timisoara, 300645, Timisoara, Romania;
Corresponding author: nicoletahadaruga@usvt.ro

Abstract
The common medlar (*Mespilus germanica* L.) is a type of fruit tree that is not widely used; its fruits ripen later and contain substances that can help fight free radicals. The quality of these fruits varies depending on the diversity, cultivation methods, environment, and time of harvest. Fruits collected from the mountainous region of Banat, Romania, were analyzed to assess their appearance, edible portion, taste characteristics, and the antioxidant effect of the pulp. Nearly 5 kg of healthy fruit were hand-picked in the fall of 2023 in Caraș-Severin County, when the skin was brown, the pulp was white, and it had a firm texture. The antioxidant activity of the alcohol-extracted pulp extracts was measured using the DPPH method at a wavelength of 517 nm. The fruits had an average diameter of 31.13 ± 1.48 mm, an average length of 33.38 ± 2.98 mm, and an average weight of 15.68 ± 2.19 grams. The pulp accounted for 66.35 ± 2.32% of the total fruit weight, and the antioxidant activity was 62.9%, a figure higher than that obtained for pears and plums using the same measurement method [9]. These results indicate that this fruit has nutritional potential as a local fruit tree resource in the mountainous Banat region.
The aim of this study is to evaluate the shape characteristics, edible portion, sensory quality, and antioxidant activity of *M. germanica* L. fruits.

Keywords: *Mespilus germanica* L., climatic conditions, fruit development, ripening, antioxidant activity, bioactive compounds.

Introduction

The common medlar (*Mespilus germanica* L.) is a fruit-bearing perennial plant in the *Rosaceae* family. It has been cultivated and consumed for a long time, but is now less commonly used in many parts of Europe. There is growing interest in this plant due to the benefits of its fruit, which contains phenolic compounds, organic acids, minerals, and other biologically active substances [1,2]. The medlar can help diversify fruit tree crops, as it can grow in various soil types and environments [1]. Fruit quality depends on the plant's characteristics, environmental conditions, and the time of harvest. In the case of the serviceberry, the chemical composition and antioxidant properties of the fruit change as it ripens. Studies show that changes in the levels of phenolic acids, total phenols, and the ability to neutralize free radicals are observed at different stages of ripening. It has been found that most phenolic acids and antioxidant activity decrease as the fruit ripens [3,4]. Likewise, the levels of sugars, organic acids, and amino acids also change during these same stages [5]. These observations show us why it is important to choose the right time to harvest the fruit. Temperature and water have an impact on plant and fruit growth throughout the season. Differences in fruit composition can arise for several reasons, such as genotype, soil type, cultivation methods, and stage of ripening [1,2]. Recent research has also shown changes in polyphenols, organic acids, and antioxidant activity during the fall ripening process and thereafter [6]. The ripening of the medlar has a unique

characteristic: the fruits are often picked while still firm, then gradually soften through a process called postharvest ripening. During this process, their texture, color, flavor, and composition change. How we store the fruit after harvesting can influence both its taste and the number of antioxidants it contains. Some studies shows that storage under controlled conditions and packaging in a modified atmosphere can slow the softening process and reduce losses of phenolic compounds, flavonoids, and ascorbic acid [7,8]. This study aims to analyze *M. germanica* L. fruits from the mountainous region of Banat through measurements of their shape, determination of the edible portion, sensory evaluations, and assessment of antioxidant activity. The results are discussed in relation to what is known about the development and ripening of the wild cherry, as well as how the environment can affect these processes.

Materials and Methods

In the fall of 2023, approximately 5 kg of *M. germanica* L. fruit were hand-picked in Caraș-Severin County, in the mountainous region of Banat. Only fruit that looked healthy, with no signs of disease or insect damage, were selected. When harvested, the fruits had brown skin, white flesh with yellowish hues, and a firm texture. The fruits were immediately brought to the laboratory and those that could not be analyzed immediately were divided into packages of approximately 500 g and stored in a freezer at -30 °C until further analysis. Each fruit was weighed on a highly accurate scale capable of measuring down to 0.001 g. The width and length were measured and also the shape of the fruit was determined. To determine how much of the fruit was edible, the flesh was separated from the peel and seeds. The evaluation assessed the external appearance, internal appearance, taste, smell, and color using a five-point scale.

To investigate how the antioxidants mechanisms work, the peels, pulp, and seeds were separated. From the obtained pulp, three samples of 10 grams each were prepared and coded: MMg1, MMg2, and MMg3. The extraction process was carried out using 96% ethanol, under heat, for approximately 30 minutes. Afterward, the extracts were allowed to cool and then filtered. Antioxidant activity was measured using a spectrophotometer via the DPPH method: equal volumes of extract and DPPH solution were mixed, and the amount of light absorbed at 517 nm was monitored over a 5-minute period. The antioxidant activity (AO) was calculated using the following formula:

$$AO = 100 \cdot \left[1 - \frac{Absorbance_t}{Absorbance_{t=0}}\right] \qquad [\%]$$

Here, Abs_t is the amount of light absorbed by the mixture of extract and DPPH at a given time, and $Abs_{t=0}$ is the average amount of light absorbed by the DPPH control.

Results and Discussion

Figure 1 illustrate the average morphological and technological characteristics for the analyzed samples. The fruits were quite similar in size: diameter ranged from 29.14 to 33.81 mm, with an average of 31.13 ± 1.48 mm, length ranged from 29.43 to 38.98 mm, and the average was 33.38 ± 2.98 mm. Average shape index of 0.94 ± 0.06 suggests that the fruit has a predominantly round shape, similar to an apple. Weight ranged from 11.91 to 19.34 g, with an average of 15.68 ± 2.19 g.

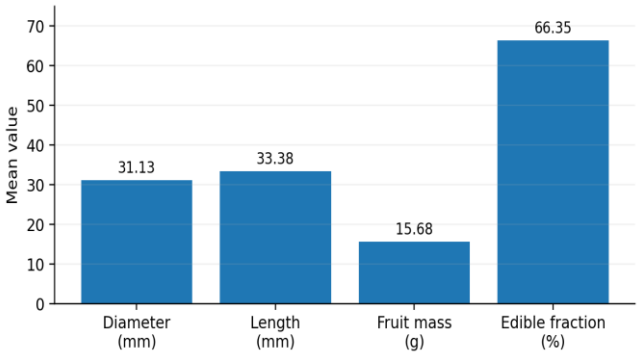


Figure 1. Mean morphological and technological characteristics of Mespilus germanica L. fruits.

Components of the fruits revealed an average weight of 1.56 ± 0.17 g for the peel, 3.73 ± 0.76 g for the seeds, and 10.40 ± 1.42 g for the pulp. The edible portion accounted for 66.35 ± 2.32% of the total fruit weight. This proportion is important for evaluating processing yield. In the sensory evaluation, taste and aroma were perceived more favorably than appearance. The external appearance received an average of 2.7 points, and the cross-section appearance was rated at 3.1 points, while color scored 2.4 points. Taste scored 4.6 points, and aroma scored 4.9 out of a maximum of 5 points. This variation may be related to the degree of ripeness of the medlar: its brownish hue and soft texture may seem less appealing to those unfamiliar with the fruit, even though its aroma is pleasant. Thus, the stage of ripeness influences both consumer acceptance and selection for technological uses. In the DPPH assay, shown in Figure 2, alcoholic extracts from medlar pulp demonstrated an average antioxidant activity of 62.9%. According to comparisons made in this experimental study, apple pulp scored 68.5%, pear pulp 51.6%, and plum pulp 46.4% [9]. Thus, *Mespilus germanica* proved to have a superior radical-scavenging capacity compared to pears and plums according to this protocol.

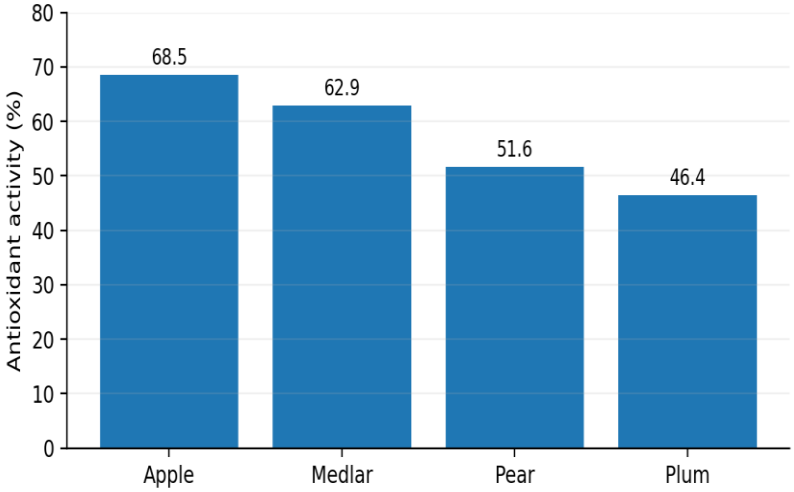


Figure 2. Antioxidant activity of medlar pulp compared with apple, pear and plum pulp under the applied DPPH assay conditions.[9]

Conclusions

The results should not be generalized to all fruit varieties or origins, nor to other extraction techniques. Samples used in this study were sourced from the mountainous region of Banat. However, temperature and precipitation were not monitored during the experiment. Previous studies suggest that the environment can influence variations in phytochemical composition, along with genotype, cultivation system, and the fruit's stage of ripeness. To investigate this correlation in the future, fruit analyses should be correlated with local records of temperature, precipitation, and soil moisture, as well as with the sum of temperature degrees.

Although appearance and color received lower sensory ratings, aroma and taste were rated positively. These variations reflect the specific characteristics of the moșmon ripening process

and are important for how the fruit might be used and appreciated by locals and even by future consumers of this fruit or products derived from it.
The peel and seeds could be investigated in future studies to determine whether they can be utilized, thereby helping to reduce waste generated during processing.

Acknowledgements
This study was funded by the University of Life Sciences "King Mihai I" from Timișoara. The research was initiated as part of the diploma thesis of Iasminca-Dușița Birta (Cugerean) and is currently being continued and further developed within her PhD research, under the supervision of Prof. Habil. Dr. Eng. Despina Maria Bordean.

References
[1] Voaides, C., Radu, N., Birza, E., & Babeanu, N. (2021). Medlar—A comprehensive and integrative review. *Plants*, *10* (11), 2344... https://doi.org/10.3390/plants10112344.
[2] Ercisli, S., Sengul, M., Yildiz, H., Sener, D., Duralija, B., Voca, S., & Purgar, D. D. (2012). Phytochemical and antioxidant characteristics of medlar fruits (*Mespilus germanica L.*). *Journal of Applied Botany and Food Quality*, *85*(1), 86.
[3] Gruz, J., Ayaz, FA, Torun, H., & Strnad, M. (2011). Phenolic acid content and radical scavenging activity of extracts from medlar (*Mespilus germanica* L.) fruit at different stages of ripening. *Food Chemistry*, *124* (1), 271-277. https://doi.org/10.1016/j.foodchem.2010.06.030
[4] Rop, O., Sochor, J., Jurikova, T., Zitka, O., Skutkova, H., Mlcek, J., ... & Kizek, R. (2010). Effect of five different stages of ripening on chemical compounds in medlar (*Mespilus germanica* L.). *Molecules*, *16*(1), 74-91.https://doi.org/10.3390/molecules16010074.
[5] Glew, R. H., Ayaz, F. A., Sanz, C., VanderJagt, D. J., Huang, H. S., Chuang, L. T., & Strnad, M. (2003). Changes in sugars, organic acids and amino acids in medlar (*Mespilus germanica* L.) during fruit development and maturation. *Food chemistry*, *83*(3), 363-369.
[6] Nistor, DI, Marc, RA, Vlassa, M., Filip, MR, Ungur, R., Crivei, I., & Mureşan, CC (2026). Comprehensive Analysis of Bioactive polyphenols, Organic acids and Antioxidant activity in Mespilus germanica L. fruits and leaves: Implications for Functional Food Applications. *Journal of the Indian Chemical Society* , 103083.https://doi.org/10.1016/j.jics.2026.103083.
[7] Selcuk, N., & Erkan, M. (2015). The effects of 1-MCP treatment on fruit quality of medlar fruit (Mespilus germanica L. cv. Istanbul) during long term storage in the palliflex storage system. *Postharvest biology and technology*, *100*, 81-90.https://doi.org/10.1016/j.postharvbio.2014.09.018.
[8] Selcuk, N., & Erkan, M. (2015). The effects of modified and palliflex controlled atmosphere storage on postharvest quality and composition of 'Istanbul' medlar fruit. *Postharvest biology and technology*, *99*, 9-19. https://doi.org/10.1016/j.postharvbio.2014.07.004.
[9] Birta, I., Cugerean, M. I., Mitroi, C. L., Rădulescu, L., Velciov, A. B., Megyesi, C. I., Cretu, A. M., Cureleac, C., Riviș, A., Hădărugă, N. G. (2022). Innovative vegan food products based on common medlar (*Mespilus germanica* L.) fruits and honey. *Book of Abstract, The 7th Student Conference "Life Sciences – Food Processing*", Timișoara, Romania, 4 July 2022, p. 20.

BALANCING PLANT STRESS AND RHIZOSPHERE STIMULATION DURING EOM-ASSISTED REMEDIATION OF USED LUBRICANT OIL-CONTAMINATED SOIL

Klaudia Hoffmann[1,2], Kitti Vastag[1], Enikő Mészáros[2], Kamilla Kovács[2], Zsófia Liska[2], Katalin Perei[1], Gábor Feigl[2], Attila Bodor[1]

[1]Department of Biotechnology and Microbiology, University of Szeged, H-6726 Szeged, Közép fasor 52, Hungary
[2]Department of Plant Biology, University of Szeged, H-6726 Szeged, Közép fasor 52, Hungary
e-mail: hoffmannklaudia99@gmail.com

Abstract

Used lubricant oil (ULO) contamination can impair both soil microbial activity and plant development. We investigated whether extracellular organic matter derived from *Micrococcus luteus* (EOM), containing resuscitation-promoting factor (Rpf), can modify early plant responses and rhizosphere activity in ULO-contaminated soil. The results reveal a dose-dependent balance between direct EOM-associated stress and beneficial, microbially mediated effects.

Rhizoremediation depends on coordinated plant-microbe interactions, yet contaminant stress may drive bacteria into a viable but non-culturable state and limit their contribution to biodegradation. Rpf-containing preparations can stimulate dormant microbial populations, but their effects on plants and the optimal application range remain insufficiently characterized.

The effects of *M. luteus*-derived EOM on garden cress (*Lepidium sativum* L.) were studied in an in vitro semi-hydroponic system and in ULO-contaminated soil. Germination index (GI%) was used to characterize early plant performance, rhizosphere microbial abundance was determined to assess microbial stimulation, and protein tyrosine nitration in roots was examined as a potential marker of nitrosative stress.

Direct exposure to 10% EOM in vitro reduced GI%, indicating an inhibitory effect. In contaminated soil, however, EOM produced a different, concentration-dependent response: 5% EOM significantly increased GI% to above 120% relative to the uncontaminated control, whereas 10% EOM resulted in values close to the control. Rhizosphere microbial abundance increased significantly with EOM concentration, suggesting that microbial stimulation may counteract oil-induced stress at an appropriate dose. Protein tyrosine nitration was detected in root tissues as a potential link between physiological stress responses and plant performance. The contrasting in vitro and soil responses indicate that EOM effects are determined by the interplay between direct plant exposure and indirect rhizosphere-mediated processes.

Appropriate EOM dosing can enhance rhizosphere activity and improve early plant performance in ULO-contaminated soil. Optimizing the balance between microbial stimulation and plant stress is therefore a key consideration for the application of Rpf-containing biostimulants in rhizoremediation.

Acknowledgements

A.B. was supported by the János Bolyai Research Scholarship of the Hungarian Academy of Sciences (Grant no. BO/00108/25/8).

CROSS-TROPHIC BIOLOGICAL RESPONSES TO FRESH AND NATURALLY AGED POLYETHYLENE MICROPLASTICS

Klaudia Hoffmann[1,2*], Patrik Szabó[1], Bence Gálos[1], Enikő Mészáros[2], Kamilla Kovács[2], Zsófia Liska[2], Etelka Kovács[1,2], Katalin Perei[1], Gábor Feigl[2], Attila Bodor[1,2]

[1]Department of Biotechnology and Microbiology, University of Szeged, Hungary
[2]MTA-SZTE Lendület "Momentum" Anthropogenic Stress and Plant Resilience Research Group, Department of Plant Biology, University of Szeged, Hungary
e-mail: hoffmannklaudia99@gmail.com

Abstract

Polyethylene (PE) is extensively used in agriculture, especially in mulch films, and its persistence promotes accumulation and fragmentation into microplastics (MPs) in soil. Because environmental aging may modify particle properties and biological interactions, the effects of fresh and naturally aged PE-MPs were evaluated across microbial, plant and soil-invertebrate test systems. The results demonstrate organism-specific responses that depend on exposure concentration, aging state and experimental matrix.

Agricultural soils represent an important sink for plastic residues originating from long-term use of PE-based materials. Assessing their ecological relevance requires approaches that integrate responses from different levels of biological organization rather than relying on a single test organism or endpoint.

Direct microbial effects were assessed using Gram-negative *Escherichia coli* and Gram-positive *Bacillus licheniformis*. Plant responses were examined with *Brassica napus* in in vitro semi-hydroponic and soil-based systems, while effects on soil fauna were evaluated using collembolans. Fresh and naturally aged PE-MPs were tested at different concentrations to identify concentration- and aging-dependent responses.

The bacterial species showed distinct sensitivity patterns. *E. coli* remained relatively tolerant at lower PE-MP concentrations, whereas culturable cell numbers significantly decreased at 1%. *B. licheniformis* responded at a lower exposure level, showing significant sensitivity already at 0.5%. In *B. napus*, PE-MPs altered the germination index in a concentration-dependent manner under semi-hydroponic conditions, but the response pattern differed in soil, indicating a strong influence of the exposure environment. Collembolan survival also decreased in the presence of PE-MPs. Together, these responses show that PE-MP effects vary considerably among biological models and are partly associated with physical interactions.

The biological impact of PE-MPs is shaped by concentration, aging state and the surrounding matrix. Combining microbial, plant and soil-fauna endpoints therefore provides a broader basis for evaluating the ecological consequences of conventional plastic residues in agricultural soils.

Acknowledgements

The project was supported by the National Research, Development and Innovation Office, Hungary (NKFIH FK 142475) and by the 'Lendület' MOMENTUM programme of the Hungarian Academy of Sciences (LP2025-8/2025). A.B. was supported by the University Research Scholarship Programme (EKÖP), funded by the Ministry of Culture and Innovation from the National Research, Development and Innovation Fund (EKÖP-26-4-SZTE-494).

ANTIOXIDANT ACTIVITY OF MERLOT GRAPE POMACE

Sara Hourani[1], Jelena Vukosavljević[1], Branimir Pavlić[1], Tatjana Jurić[2], Milica Petković[2], Ružica Ždero Pavlović[2], Boris M. Popović[2]

[1]University of Novi Sad, Faculty of Technology, Bulevar Cara Lazara 1, 21000 Novi Sad, Serbia
[2]University of Novi Sad, Chemistry Laboratory, Department of Field and Vegetable Crops, Faculty of Agriculture, Trg Dositeja Obradovića 8, 21102 Novi Sad, Serbia
e-mail: sarrahourani@gmail.com

Abstract

Grape pomace (*Vitis vinifera* L.) is a major by-product of the vinification process and a valuable source of bioactive compounds. This study aimed to evaluate Natural Deep Eutectic Solvents (NADES) as green alternatives for the extraction of phytochemicals from Merlot grape pomace and to assess the antioxidant potential of the obtained extracts. Phytochemicals were extracted using different NADES and reference solvents, namely 50% ethanol and acidified ethanol (50% ethanol with 1% HCl), under ultrasound-assisted conditions (40 °C, 30 min, 37 kHz). The antioxidant activity of the extracts was evaluated using DPPH, FRAP, and ORAC assays. The DPPH and FRAP assays are primarily based on electron transfer, whereas the ORAC assay predominantly involves hydrogen atom transfer [1]. DPPH IC_{50} values ranged from 1.88 mg/mL for the 50% ethanol extract to 10.91 mg/mL for ChCl:CitA:Ur (2:1:1). No significant differences were observed between the reference solvents and ChCl:Pro:Gly (1:1:2) or ChCl:LacA:Ur (1:1:1). The highest FRAP values were obtained for the ternary NADES ChCl:LacA:1,2PD, ChCl:LacA:Gly, and ChCl:LacA:Ur, showing activities comparable to the reference solvents. In the ORAC assay, Pro:LacA (1:2) showed slightly higher activity than 50% ethanol, while ChCl:LacA:1,2PD, ChCl:LacA:Gly, ChCl:LacA:Ur, and acidified ethanol exhibited comparable activities. In contrast, fructose-containing NADES generally showed the lowest antioxidant activity across the assays. Overall, ternary NADES based on choline chloride and lactic acid, particularly those containing 1,2-propanediol or urea, demonstrated favorable antioxidant performance and comparable activity to acidified ethanol. The results support the potential of NADES for the sustainable recovery of bioactive compounds from grape pomace and the valorization of winery by-products.

Acknowledgements

This research is financially supported by the Ministry of Science, Technological Devel opment, and Innovation of the Republic of Serbia, contracts No. 451 03-137/2025–03/200117, 451–03-136/2025–03/200117, and Grant No. 451–994/2024–03/3412, and Science Fund of Serbia (Program Ideas, APIDES project, Grant No. 7731993).

References

[1] Popović, B. M., Štajner, D., Slavko, K., & Sandra, B. (2012). Antioxidant capacity of cornelian cherry (Cornus mas L.) – Comparison between permanganate reducing antioxidant capacity and other antioxidant methods. Food Chemistry, 134(2), 734–741. https://doi.org/10.1016/J.FOODCHEM.2012.02.170

BIOCHAR ACCELERATES ANAEROBIC FUNGI–METHANOGEN INTERACTIONS AND RENEWABLE GAS PRODUCTION

Márta Huszár, Annabella Juhász-Erdélyi, Márk Szuhaj, Kornél L. Kovács, Zoltán Bagi, Etelka Kovács

Department of Biotechnology and Microbiology, Faculty of Science and Informatics, University of Szeged;

Abstract

Plant biomass represents a valuable renewable energy resource for biotechnological exploitation processes. One of the rate limiting steps in the bioconversion of lignocellulose-rich plant biomass is the microbial decomposition of lignocellulose, in which anaerobic fungi (AF) can play a key role [1, 2]. The performance of anaerobic fungi might be affected by their coexistence with other anaerobic microorganisms such as methanogens (M). Such syntrophic interaction is expected to augment substrate degradation and concomitant hydrogen and methane production [3, 4]. We assumed that the AF+M redox interaction is facilitated by biochar, depending on the microbial system composition and carbon substrate source [5]. In the present research we studied the effect of various biochar concentrations on anaerobic fungi (AF) and the mixture of anaerobic fungi and methanogens (AF+M) in the presence of different carbon sources.

Introduction

The complex structure of lignocellulose makes plant biomass resistant to microbial breakdown, which may lead to inefficiency of the bioconversion process [6]. Anaerobic fungi (AF) are the natural inhabitants of the digestive system of herbivores and are known for their efficiency of lignocellulose degradation. By developing an extensive rhizoidal network, anaerobic fungi physically break down plant cells, and the activity of their extracellular enzymes contributes to the degradation of structural polysaccharides from the cell wall of plants [7]. During the fermentation process, besides other products, anaerobic fungi produce hydrogen and carbon dioxide [8]. Hydrogenotrophic methanogens can utilize the resulting hydrogen and carbon dioxide for methane production, thereby reducing hydrogen accumulation in the system [9]. The removal of hydrogen may, in turn, influence the fermentation processes of anaerobic fungi, resulting in a syntrophic relationship between the two microbial groups [3] . Due to its physical and chemical properties, biochar may modify the environment and interactions of anaerobic microorganisms and may therefore affect the functioning of AF+M systems [5]. The aim of this study was to investigate how biochar concentration and a complex carbon source influence the activity of AF alone and in combination with methanogens (AF+M).

Materials and Methods

The experiments were conducted in 15 mL Hungate tubes containing 12 mL of Medium C [10], which was continuously flushed with carbon dioxide to maintain anaerobic conditions. Two different carbon sources were used. The glucose–maltose–cellobiose (GMC) mixture contained 10 g glucose, 10 g maltose, and 10 g cellobiose in 100 mL Milli-Q water, of which 0.5 mL was added to each tube. The complex carbon source mixture (CCM) contained 2.4 g xylose, 4.8 g water-soluble starch, 2.4 g rhamnose, 7.2 g Avicel, and 7.2 g α-cellulose in 100 mL Milli-Q water, of which 1 mL was added to each tube. To investigate the effects of biochar, either 0.5% w/v (0.06 g/tube) or 1% w/v (0.12 g/tube) biochar was added to each tube, while samples without biochar served as controls. Two different antibiotic treatments were used to investigate anaerobic fungi alone (AF) and anaerobic fungi in combination with methanogens (AF+M). The AF system was supplemented with 0.1 mg/mL chloramphenicol (Chl), whereas the AF+M system received a mixture of 0.25 mg/mL ampicillin (Amp) and streptomycin (Str). Following inoculation, the samples were incubated at 39°C. Changes in the gas-phase composition were monitored by gas chromatography for 14 days, starting on the second day after inoculation, to determine hydrogen and methane levels.

Results and Discussion

The effects of biochar varied depending on its concentration, the carbon source, and the composition of the microbial system. In the anaerobic fungi–methanogen (AF+M) system with GMC as the carbon source, the hydrogen concentrations were higher at both biochar concentrations than in the biochar-free control, whereas methane production was higher in the control. A distinct trend was observed with the complex carbon source: both hydrogen and methane levels were higher in the samples containing 1% biochar than in the control. In the anaerobic fungi-only (AF) system with GMC as the carbon source, higher hydrogen evolution was measured in the presence of 0.5% biochar, whereas lower hydrogen accumulation was measured with 1% biochar compared with the biochar-free control. Methane levels were very low in all treatments of the AF system. Comparison of the AF and AF+M systems revealed dissimilar gas production profiles. Elevated hydrogen accumulation was observed in the AF system, whereas in the presence of methanogens, hydrogen levels decreased and methane levels increased. This observation is consistent with the syntrophic relationship between anaerobic fungi and hydrogenotrophic methanogens, in which methanogens can utilize hydrogen and carbon dioxide produced during anaerobic fungal fermentation for methane production [2-4]. Overall, the effects of biochar were not consistent across the investigated systems, suggesting that both microbial system composition and the available carbon source may influence the response to biochar. Further studies are required to elucidate the microbial interactions underlying the observed differences.

Acknowledgements

This study was supported in part by the Hungarian National Research, Development, and Innovation Fund (NRDIF) project 2020-3.1.2-ZFR-KVG-2020-00009 and 2020-1.1.2-PIACI-KFI-2020-00117. Etelka Kovács, Kornél Kovács L. and Zoltán Bagi received support from the Hungarian NRDIF fund projects PD 128345, PD132145, K143198, FK123902, and 2019-2.1.13-TÉT_IN-2020-00016. This study was also supported by: EKÖP-26-3 - SZTE-407 awarded to Annabella Juhász-Erdélyi.

References

[1] C. A. Hooker, K. Z. Lee, and K. V Solomon, "Leveraging anaerobic fungi for biotechnology" *Curr. Opin. Biotechnol.*, 59, 103–110, 2019, doi: 10.1016/j.copbio.2019.03.013.

[2] —E. Kovács, C. Szűcs, A. Juhász-Erdélyi, Z. Bagi, and Kovács, K.L. "Anaerobic fungi: Effective warriors in lignocellulosic biomass degradation and fermentation" *FEMS Microbiol. Ecol.,* 101, fiaf108, 2025, doi: 10.1093/femsec/fiaf108.

[3] Y. F. Cheng, J. E. Edwards, G. G. Allison, W.-Y. Zhu, and M. K. Theodorou, "Diversity and activity of enriched ruminal cultures of anaerobic fungi and methanogens grown together on lignocellulose in consecutive batch culture" *Biores. Technol.*, 100(20), 4821–4828, 2009, doi: 10.1016/j.biortech.2009.04.031.

[4] D. O. Mountfort, R. A. Asher, and T. Bauchop, "Fermentation of Cellulose to Methane and Carbon Dioxide by a Rumen Anaerobic Fungus in a Triculture with *Methanobrevibacter* sp. Strain RA1 and *Methanosarcina barkeri*," *Appl. Environ. Microbiol.*, 44(1), 128–134, 1982, doi: 10.1128/aem.44.1.128-134.1982.

[5] H. M. Mazhar abbas, H. Sultan, A. Shah, A. Tahir, H. Iltaf, and L. Nie, "The role of biochar as a microbial carrier in enhancing biogas production efficiency in anaerobic digestion systems," *Renew. Sust. Energy Rev.*, 226, 116335, 2026, doi: 10.1016/j.rser.2025.116335.

[6] S. Malherbe and T. E. Cloete, "Lignocellulose biodegradation: Fundamentals and applications," *Rev. Environ. Sci. Biotechnol.*, 1(2), 105–114, 2002, doi: 10.1023/A:1020858910646.

[7] R. J. Gruninger *et al.*, "Anaerobic fungi (phylum Neocallimastigomycota): advances in understanding their taxonomy, life cycle, ecology, role and biotechnological potential," *FEMS Microbiol. Ecol.*, 90(1), 1–17, 2014, doi: 10.1111/1574-6941.12383.

[8] N. Yarlett, C. G. Orpin, E. A. Munn, N. C. Yarlett, and C. A. Greenwood, "Hydrogenosomes in the rumen fungus *Neocallimastix patriciarum*," *Biochem. J.*, 236(3), 729–739, 1986, doi: 10.1042/bj2360729.

[9] D. P. Morgavi, E. Forano, C. Martin, and C. J. Newbold, "Microbial ecosystem and methanogenesis in ruminants," *Animal*, 4(7), 1024–1036, 2010, doi: 10.1017/S1751731110000546.

[10] X. Peng, C. L. Swift, M. K. Theodorou, and M. A. O'Malley, "Methods for Genomic Characterization and Maintenance of Anaerobic Fungi," in *Meth. Molec. Biol.*, 2018, 53–67. doi: 10.1007/978-1-4939-7804-5_5.

AUTOMATED INTERPRETATION OF GANGLIOSIDE ION MOBILITY MASS SPECTROMETRY DATA USING A DEDICATED SOFTWARE TOOL

Raluca Ica[1,2], Mirela Sarbu[2], Sorin Nădăban[1], and Alina D. Zamfir[2,3]

[1]Faculty of Exact Sciences, Aurel Vlaicu University of Arad, Arad, Romania
[2]National Institute for Research and Development in Electrochemistry and Condensed Matter, Timişoara, Romania
[3]Department of Technical and Natural Sciences, Faculty of Food Engineering, Tourism and Environmental Protection, Aurel Vlaicu University of Arad, Arad, Romania
e-mail: raluca.ica@gmail.com

Abstract
Native gangliosides from human brain tissues, including normal samples and primary brain tumors, have been analyzed over the years using several high-resolution mass spectrometry (HR MS) approaches, including ion mobility mass spectrometry (IMS MS) in negative ion mode.Based on these data, we developed GIMSoft, a dedicated software tool for automated interpretation of IMS-resolved ganglioside spectra, combining accurate mass and charge state information with biosynthetically constrained compositional rules to assign plausible molecular classes. GIMSoft processed highly complex ganglioside profiles from both healthy and tumoral brain tissue, generating ranked candidate assignments that facilitate manual inspection, and its modular architecture defines a structured feature space suitable for future machine learning and artificial intelligence-based spectral interpretation.

Introduction
Gangliosides are sialylated glycosphingolipids abundantly expressed in the central nervous system and are regarded as tumor-associated antigens and candidate biomarkers in brain tumors [1]. However, comprehensive ganglioside profiling remains challenging due to pronounced molecular diversity and extensive isomerism.
In this context, IMS MS provides enhanced separation prior to mass analysis, but the resulting datasets are highly complex and require dedicated computational tools for efficient gangliosidomic interpretation [2].

Experimental
Native gangliosides from human brain tissues, including normal samples and primary brain tumors, were analyzed by IMS MS in negative ion mode. Based on these data, we developed GIMSoft, a software tool for automated interpretation of IMS-resolved ganglioside spectra. The current implementation enables feature detection, charge state recognition, neutral mass calculation, and molecular class assignment using accurate mass matching constrained by biosynthetic rules, with outputs prepared for integration into a comparative structural database.

Results and discussion
IMS MS enabled the separation of numerous components in highly complex ganglioside extracts from both healthy brain tissue and primary brain tumors, substantially reducing spectral overlap at the MS level. GIMSoft processes IMS-resolved spectral features by combining observed *m/z* values and charge state information to derive neutral molecular masses, which are matched against biosynthetically constrained theoretical ganglioside compositions to assign plausible molecular classes and compositional ranges.
For each detected feature, the software generates ranked candidate assignments that facilitate manual inspection and simplify the interpretation of complex ganglioside profiles. In addition,

the modular architecture of GIMSoft defines a structured feature space suitable for future integration of data-driven, machine learning, and artificial intelligence-based approaches for advanced spectral interpretation.

Conclusion

This study demonstrates the feasibility of automated molecular class assignment of gangliosides from IMS MS data using a dedicated software approach. GIMSoft integrates accurate mass and charge state information with biosynthetically constrained compositional rules, enabling efficient interpretation of complex datasets and supporting future integration of MS/MS and ML-assisted spectral analysis.

Acknowledgements

This work was supported by a grant of the Ministry of Research, Innovation and Digitization, CNCS-UEFISCDI, project number PN-IV-P2-2.1-TE-2023-0175, within PNCDI IV, and by Aurel Vlaicu University of Arad, Romania, grant number UAV-IRG-1-2025-8.

References

[1] M.R. Biricioiu, M. Sarbu, R. Ica, Ž. Vukelić, S. Kalanj-Bognar, A.D. Zamfir, Int. J. Mol. Sci. 25 (2024) 1335.
[2] M. Matsubara, M. Ishihara, M. Tiemeyer, K. Aoki, R. Ranzinger, BBA Adv. 7 (2025) 100161.

EVALUATION OF PHARMACOKINETIC AND TOXICOLOGICAL PROPERTIES OF SOME *N*-(2-BROMO-PHENYL)-2-HYDROXY-BENZAMIDE DERIVATIVES

Ioana M.C. Ienașcu[1,2], Adina Căta[1], Nick S. Țolea[1], Paula Sfîrloagă[1], Dan Roșu[1], Raluca Pop[3]

[1]*National Institute of Research and Development for Electrochemistry and Condensed Matter, 144 Dr. A. P. Podeanu, 300569, Timişoara, Romania*
[2]*"Vasile Goldiş" Western University of Arad, Faculty of Pharmacy, 86 Liviu Rebreanu, 310045, Arad, Romania*
[3]*"Victor Babeş" University of Medicine and Pharmacy, Faculty of Pharmacy, Timişoara, 2 Eftimie Murgu Square, 300041, Timişoara, Romania*

Abstract

The integrated evaluation of the pharmacokinetic and toxicological properties (ADMET) of the three structures of the N-(2-bromo-phenyl)-2-hydroxy-benzamide derivatives (ethyl ester EE, hydrazide HD, hydrazone HN) enabled a detailed characterization of their behavior in the body and the identification of the most suitable candidate for further development [1].

Intestinal absorption is a key determinant of oral bioavailability. EE shows very high absorption (94.42%), indicating excellent intestinal permeability. HD (72.76%) and HN (77.81%) exhibit good but lower absorption, potentially reflecting differences in lipophilicity, molecular size, and transporter interactions. EE (logS: −3.68) and HD (−3.70) show moderate ***aqueous solubility***, whereas HN has markedly lower solubility, limiting its in vivo absorption despite favorable theoretical permeability. ***Distribution*** was assessed using steady-state volume of distribution (VDss) and CNS permeability parameters (BBB and CNS permeability). EE shows moderate tissue distribution (VDss: 0.024 log L/kg), whereas HD (−0.245) and HN (−0.160) exhibit more limited distribution. EE shows the highest BBB permeability (0.072) and moderate CNS permeability (logPS: −2.984). HD (−0.788; −3.513) and HN (−1.103; −3.145) show low BBB/CNS penetration. Overall, EE has the greatest potential for CNS exposure, while HD and HN show predominantly peripheral distribution. ***Metabolism.*** Metabolic profiles were assessed based on interactions with major cytochrome P450 (CYP) isoforms. EE and HD showed no inhibition of major CYP enzymes, indicating favorable metabolic profiles and low drug–drug interaction potential. HN inhibited CYP3A4, suggesting a higher interaction risk. ***Elimination.*** EE shows high clearance (0.379 mL/min/kg), indicating rapid elimination, while HD (0.072) shows slow elimination and HN (0.152) an intermediate profile. No renal clearance was predicted, suggesting predominantly hepatic and/or biliary elimination. ***Toxicity.*** The AMES test predicts mutagenicity for HD, representing a major safety concern, while EE and HN show no mutagenic risk. Maximum Tolerated Dose (MTD) values indicate moderate tolerance for EE (0.214), the highest tolerance for HD (0.419), and lower tolerance for HN (−0.352). Despite its higher MTD, HD remains limited by its predicted mutagenicity.

Integrated ADMET analysis identifies EE as the most balanced candidate, combining excellent absorption, adequate solubility, favorable distribution and metabolism, and no predicted mutagenicity. Its main limitation is high clearance, which may shorten its duration of action but could be addressed through structural or formulation optimization.

References

[1] J. Lin, D.C. Sahakian, S.M.F. de Morais, J.J. Xu, R.J. Polzer, S.M. Winter. Curr. Top. Med. Chem. 3 (2003) 1125–1154.

CARCINOGENIC EFFECTS INDUCED BY LABORATORY SYNTHETIZED PLANT GROWTH REGULATORS ON MAMMALS

Georghe Ilia[1], Zeno Garban[2], Diana Anghel[1]

[1]Department of Chemistry, Faculty of Chemistry-Biology-Geography, West University of Timisoara, 16 Pestalozzi Str., Timisoara, Romania
e-mail:gheorghe.ilia@e-uvt.ro; gheorgheilia@gmail.com
[2]Working Group for Xenobiochemistry, Romanian Academy-Branch Timisoara, 24 M. Viteazu Bvd. , Timisoara-300223, Romania

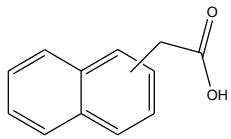
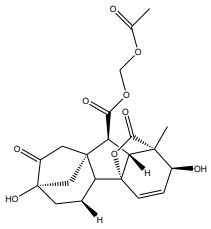
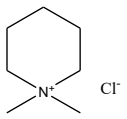
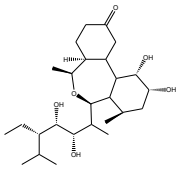
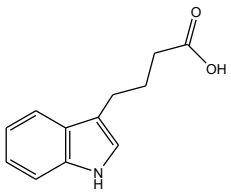
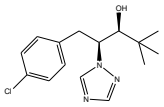
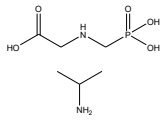
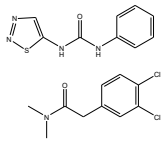
Abstract

Chemically synthesized plant growth regulators (PGRs) are chemicals of agrobiological importance for agriculture and contemporary farming methods. These chemicals have some physiological similarities to naturally occurring molecules produced by plant biosynthesis, often known as "plant growth bioregulators" (PGBRs), which control important metabolic processes. Mammal organisms may be impacted by a number of harmful consequences associated with exposure to PGRs.

Introduction

Synthetic plant growth regulators are active in plants even at extremely low doses and can be either bio-stimulators or bio-inhibitors. PGBRs and PGRs must be distinguished, as we mentioned in a prior article [1]. Under normal circumstances, PGBR is produced in plant organisms through biosynthesis in an amount suitable for normal physiological functions, whereas PGRs are obtained by synthesis. Human epidemiological findings and research on experimental animal models are frequently disregarded. Certain synthetic chemicals, which frequently have structures similar to those of natural molecules, raise certain concerns in these situations. The usage of terminological synonymy between synthetic (PGR) and natural plant growth bioregulators (PGBR) is another feature that draws the interest of experts in animal and plant physiology. Many physiologists believe that the term "plant hormones" is unsuitable in this context, where a comparison to "animal hormones" is drawn. The term "plant hormones" is often viewed as a marketing simplification that overlooks rigorous scientific details. It is essential to recognize, however, that Plant Growth Regulators (PGRs) encompass both natural plant compounds and synthetic substances not found in nature. Due to this inclusion, synthetic growth regulators are classified under pesticide regulations. To address the requirements of modern agriculture, numerous novel and naturally inspired plant growth regulators (PGRs) have been synthesized. A classification of these compounds, organized by their specific growth-regulating activity, is provided in the *Compendium of Pesticide Common Names*.[2] Scheme 1 illustrates a selection of representative compounds within the PGR category. Plant Growth Regulators (PGRs) and Plant Growth-Bioregulators (PGBRs), whether ingested through the consumption of raw plant material or processed dietary sources, exert significant effects on both human and mammalian systems.[3] Due to documented evidence linking PGRs to hepatotoxicity, nephrotoxicity, genotoxicity, neurotoxicity, carcinogenicity, and teratogenicity—as well as their suspected role in endocrine disruption—the presence of these residues in agricultural products represents a substantial public health concern. This paper reviews recent findings, primarily from the past decade, regarding the carcinogenicity of PGRs.

Scheme 1. PGR compounds with "similar structure" and "different structure" to natural PGBRs

 2-(1-naphthyl)acetic acid	 Gibberellins	 Mepiquat chloride	 Brassinolide
 4-indol-3-ylbutyric acid	 Paclobutrazol	 Glyphosate-isopropylamine	 Thidiazuron/ diuron

Toxic effects of plant growth regulators

The use of various synthetic plant growth regulators (PGRs) presents significant health risks, particularly in instances of improper application or when residues persist in agricultural products. Given their documented potential for hepatotoxicity, nephrotoxicity, genotoxicity, neurotoxicity, carcinogenicity, and teratogenicity, the presence of PGR residues constitutes a substantial threat to public health (Figure 1). [4]

Carcinogenicity

The cytotoxicity of ethephon and maleic hydrazide was evaluated in Vero, HepG2 (human hepatocellular carcinoma), and Hep2 (human epidermoid cancer) cell lines using (3-(4,5-dimethylthiazol-2-yl)-2,5-diphenyltetrazolium bromide) and LDH (lactate dehydrogenase) assays. For all cell lines tested, maleic hydrazide consistently exhibited lower IC50 values than ethephon. Following ethephon exposure, Vero cells demonstrated the lowest cytotoxicity, followed by HepG2 and Hep2 cells.[5] The genotoxic potential of flumetralin, a synthetic 2,6-dinitroaniline compound, was evaluated in human peripheral blood lymphocytes (PBLs). In vitro assessments, utilizing chromosome aberration (CA) and cytokinesis-block micronucleus assays, were conducted to determine the genotoxic and cytotoxic effects of the substance. During the 48-hour exposure period, binucleated cells were undetectable at the highest concentrations (500 and 1000 µg/mL), indicating severe cytostatic activity. Furthermore, flumetralin induced a statistically significant reduction in both the nuclear division index and the mitotic index across all tested doses and exposure durations when compared to the control groups.[6] The comet assay and γH2AX expression were utilized as genotoxicity endpoints to evaluate the potential genotoxic effects of ethephon on the murine embryonic fibroblast (MEF) cell line. At non-cytotoxic concentrations, ethephon induced a significant increase in both overall γH2AX expression and the number of γH2AX foci per cell. Elevated levels of lipid peroxidation (LPO) and reactive oxygen species (ROS) were observed only at concentrations exceeding 160 µg/ml. These results suggest that low, non-cytotoxic doses of ethephon increase mutagenic potential by facilitating DNA damage that subsequently influences cell proliferation.[7]

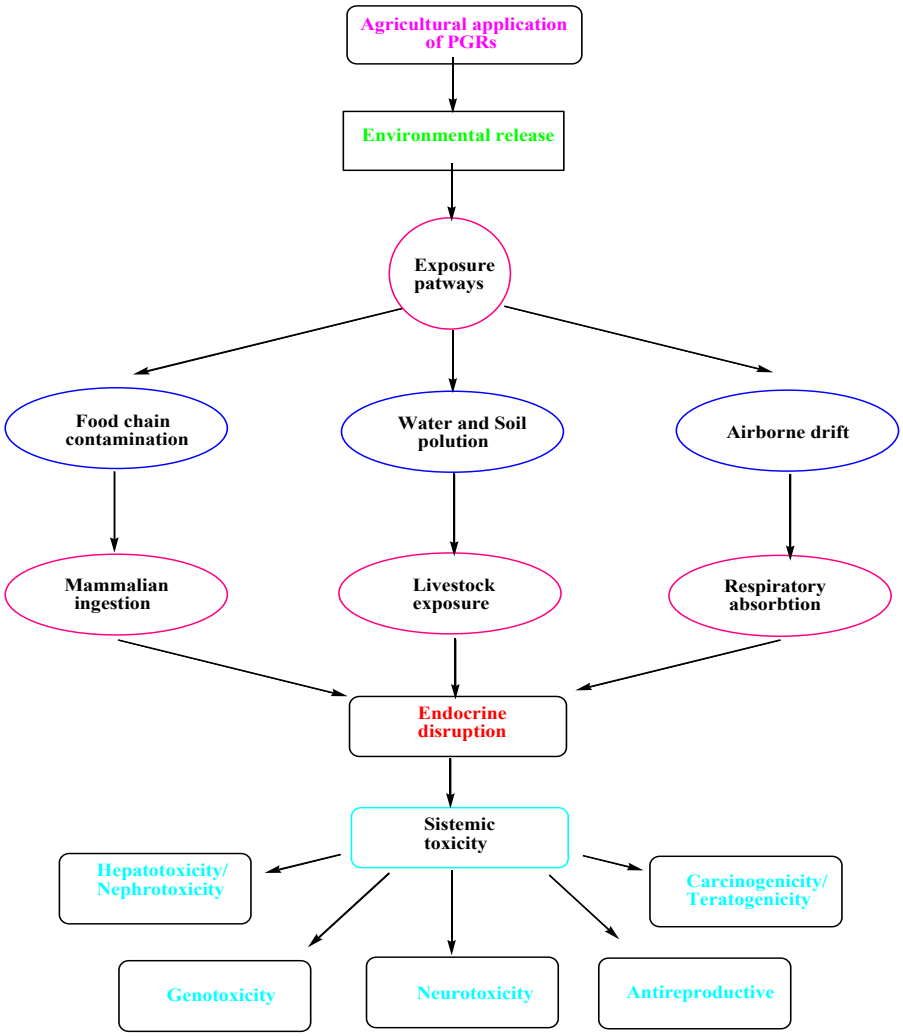


Figure 1. Exposure pathways to mammalian systems

The mutagenic potential of two plant growth regulators, kinetin and chlormequat chloride (CCC), was evaluated utilizing the Ames/Salmonella assay. The study employed *Salmonella typhimurium* strains TA 98 and TA 100, both in the presence (+S9) and absence (-S9) of metabolic activation enzymes. Each compound was tested across five non-cytotoxic concentrations, and results were determined by comparing observed mutation rates against those of spontaneous control plates. The analysis revealed that kinetin exhibited mutagenic activity at a dosage of 2500 µg/plate in strain TA 98 (both ±S9) and in strain TA 100 (-S9). Conversely, CCC demonstrated no mutagenic activity across the tested bacterial strains.[8] The potential cyto-genotoxicity of a commercial formulation of forchlorfenuron, a phenylurea cytokinin, was evaluated using chromosomal aberrations (CAs) and the mitotic index (MI) in human peripheral blood lymphocytes (PBLs). The results demonstrated that, relative to the negative control, forchlorfenuron significantly increased the frequency of structural CAs at concentrations of 1.00 and 2.00 µg/ml across both exposure durations. Furthermore, forchlorfenuron exhibited a cytotoxic effect on human PBLs at all tested concentrations, as evidenced by a statistically significant reduction in the MI compared to the negative control.[9]

Conclusion

Runoff from farm fields where synthetic PGRs have been applied, they can harm local ecosystems, potentially impacting wildlife and indirectly affecting mammalian health through the food chain. In general, although synthetic plant growth regulators fulfill valuable agricultural roles, their impacts on mammals deserve close attention, especially with respect to human health and environmental safety. To conclude, research into how synthetic plant growth regulators affect mammals uncovers a complex relationship between agricultural chemicals and mammalian biology.

References

[1] Garban, Z.; Ilia, G.; Structure-Activity of Plant Growth Bioregulators and their Effects on Mammals. *Molecules* 2024, 29, 5671, https://doi.org/10.3390/ molecules292356

[2] http://www.bcpcpesticidecompendium.org/class_plant_growth_regulators.html (accesed 19 March 20025)

[3] Mukherjee, A.; Gaurav, A.K.; Singh, S.; Yadav, S.; Bhowmick, S.; Abeysinghe, S.; Verma, J.P. The Bioactive Potential of Phytohormones: A Review. *Biotechnol. Rep.* 2022, 35, e00748, https://doi.org/10.1016/j.btre.2022.e00748.

[4] Xu, C-S.; Jiang, Z.; Shen, W.; Zou, S-H. Toxicological Characteristics of Plant Growth Regulators and their Impact on Male Reproductive Health. *Zhonghua. Nan. Ke. Xue.* 2018, 24,370-375.

[5] Yurdakok, B.; Baydan, E.; Okur, H.; Gurcan, I.S. Cytotoxic Effects of Etephon and Maleic Hydrazide in Vero, Hep2, HepG2 cells. *Drug. Chem. Toxicol.* 2014, 37, 459-465, DOI: 10.3109/01480545.2014.884112

[6] Kocaman, A.Y.; Bucak, S Genotoxic and Cytotoxic Effects of Flumetralin in Human Peripheral Blood Lymphocytes in Vitro. *Toxicol. Ind. Health* 2015, 32:1927-1934, doi:10.1177/0748233715595142.

[7] Hodjat, M.; Baeeri, M.; Rezvanfar, M.A.; Rahimifard, M.; Gholami, M.; Abdollahi, M. On the Mechanism of Genotoxicity of Ethephon on Embryonic Fibroblast cCells. *Toxicol. Mech. Meth*. 2017, 27, 173-180, DOI: 10.1080/15376516.2016.1273425.

[8] Yapici, S.; Uraz, G.; Beyzi, E.A Study on the Possible Mutagenicity of Different Types of Plant Growth Rregulators. *Int. J. Sec. Metabol.* 2021, 8, 425-435, DOI: 10.21448/ijsm.952423

[9] Kocaman, A.Y.; Yakar, B. Genotoxicity of a Synthetic Plant Growth Regulator, Forchlorfenuron (CPPU), on Human Lymphocytes Using Chromosome Aberration Assay. *Caryologia* 2023, 76,47-56. doi: 10.36253/ caryologia-2006.

VALIDATION OF THE METHOD FOR DETECTION OF *PSEUDOMONAS AERUGINOSA* IN IRRIGATION WATER SAMPLES

Renata Iličić, Vojislava Bursić, Bojan Konstantinović, Nataša Mandić, Antonije Žunić, Tijana Stojanović

University of Novi Sad, Faculty of Agriculture, Trg Dositeja Obradovića 8, Department for Environmental and Plant Protection, 21000 Novi Sad, Serbia
renatailicic@gmail.com

The quality of irrigation water is of particular importance for the production of safe agricultural products, especially in recent years, when droughts and high temperatures have become increasingly frequent. Therefore, regular monitoring of irrigation water quality is of particular importance and should be conducted routinely, especially during the summer months. Species of the genus *Pseudomonas* are ubiquitous microorganisms commonly found in soil and aquatic environments. Among the numerous described species, as an opportunistic pathogen bacteria *Pseudomonas aeruginosa* is of greatest importance due to its impact on human health. Its presence in water systems may compromise water quality and represents a potential public health risk. Irrigation water samples were collected during June (2026) from five locations in Vojvodina province, Republic of Serbia: Novi Sad, Zrenjanin, Žabalj, Vrbas and Vršac. Samples were collected using a telescopic sampling pole at a depth of approximately 50 cm, avoiding sediment disturbance, at sites located within agricultural production areas and outside the direct influence of wastewater discharges and tributaries. A total of ten water samples (250 mL each) were collected in sterile plastic bottles and transported to the laboratory in portable coolers under refrigerated conditions for further analysis. First the water samples (100 mL each) were filtered through 0.44 µm nitrocellulose membrane filters. The membrane filters were then placed onto King's B agar medium plates and incubated at 37 °C for three to five days. The plates were examined daily under ultraviolet light (360 nm). The presence of fluorescence at any time during the three-five-day incubation period was considered a positive result, the presence of *P. aeruginosa* in analyzed water samples. Following five days of incubation, *P. aeruginosa* was not detected in any of the analyzed irrigation water samples. This was confirmed by the absence of characteristic smooth, glistening, flat colonies on the medium, as well as the lack of fluorescence under UV illumination, indicating that none of the samples contained *P. aeruginosa.* In contrast, the medium inoculated with a *P. aeruginosa* isolate PA6 (positive control) exhibited the expected colony morphology and fluorescence, demonstrating the reliability of the detection method. Therefore, routine monitoring of water quality, regular microbiological testing, and the implementation of appropriate preventive and control measures are essential to ensure the safety of water intended for agricultural, environmental, and public use.

Key words: irrigation water; *P. aeruginosa*; Vojvodina.

Acknowledgments
This research was supported by the Provincial Secretariat for Higher Education and Scientific Research of the Autonomous Province of Vojvodina, Republic of Serbia, project: Assessment of irrigation water quality parameters in the context of food safety - AgriSAFE (003864627 2025 09418 003 000 000 001 04 004).

ELECTROCHEMICAL TECHNIQUES FOR DEVELOPMENT OF PERFLUOROOCTANOIC ACID CONTAINING WATER TREATMENT AND CONTROL

Adina Gavrilescu[1], Sorina Ilieș[2], Anamaria Baciu[3], Corina Orha[4], Florica Manea[1*]

[1]Department of Applied Chemistry and Engineering of Inorganic Compounds and Environment, Politehnica University of Timisoara, Blv. Vasile Parvan No. 6, 300223 Timisoara, Romania
[2]"Coriolan Dragulescu" Institute of Chemistry, Romanian Academy, 24 Mihai Viteazu Bvd.,300223 Timisoara, Romania; sorinailies@acad-icht.tm.edu.ro
[3]Renewable Energy Research Institute, Politehnica University of Timisoara, Gavril Muzicescu Street, no. 138, 300501 Timisoara, Romania, anamaria.baciu@upt.ro
[4]Condensed Matter Department, National Institute for Research and Development in Electrochemistry and Condensed Matter, 1 P. Andronescu Street, 300254 Timisoara, Romania; orha.corina@gmail.com
**e-mail: florica.manea@upt.ro*

Abstract

In this study, the double role of the electrochemical techniques using three-electrodes system was exploited to assess both perfluorooctanoic acid electrodegradation and process control through electrochemical detection. Two La-SnO_2/TiO_2 dimensionally-stable anodes (DSAs) synthesized by dip-coating and spin-coating were tested for PFOA degradation through electrooxidation. DSAs were characterized morpho-structurally through scanning electron microscopy coupled with energy dispersive Xray (SEM/EDX) and Xray diffraction (XRD). Cyclic voltammetry (CV) was tested in 0.1 M Na_2SO_4 supporting electrolyte for electrochemical characterization of DSAs and chronoamperometry was used to simulate the electrooxidation under potentiostatic conditions. Process control was assured by electrochemical detection using differential pulsed voltammetry (DPV) at molecular imprinted polymerized (MIP)-doped diamond electrode.

Introduction

Per- and polyfluoroalkyl substances (PFAS), including perfluorooctanoic acid (PFOA), are synthetic compounds widely used in industrial and domestic applications, owing to their chemical and thermal stability [1]. The strength of the carbon-fluorine bond makes them resistant to conventional treatment methods [2], and PFOA has become a priority contaminant due to its presence in contaminated water bodies and its demonstrated health impacts [1,2]. In natural waters, PFOA concentrations are typically in the range of pg/L to µg/L [3] while the maximum contaminant level established by the US EPA for PFOA and PFOS in drinking water is 4 ng/L [1-3]. Physical separation processes only transfer PFAS from one phase to another and leave a concentrated waste stream, which requires a following destruction step [4].
Electrochemical processes have shown promising potential for PFAS degradation, due to their treatment efficacy and cost-effectiveness, and they require electrode materials that ensure a sufficiently high overpotential for the oxygen evolution [1-4]. In addition, electrochemical methods have a dual character, in relation with both the detection and the destruction of pollutants [5], which allows the degradation process and its control to be carried out by the same type of technique.
Dimensionally stable anodes (DSA) consist of metal oxide films deposited onto titanium or other substrates, and they have been investigated in wastewater treatment due to their stable

size, long service life, electrocatalytic activity and low cost [6]. Their features depend on the synthesis method, and the preparation conditions, e.g., the structure-directing agent, the nature of the precursor and the sintering temperature, affect the physical properties and the stability of the electrodes [7].

Experimental

a) Synthesis and morphostructural characterization of the electrodes.

The Ti/SnO_2-La electrodes were prepared according to the previously reported procedure for Ti/SnO_2-Sb electrodes (Articol Ana Coatings,2023), in which $SbCl_3$ was replaced by La dopant. The Ti plates (1 × 1 cm) were imprinted in 10% oxalic acid, according to the protocol described in Articol Cori, Water, 2022. The SnO_2-La was deposited onto the imprinted Ti plates by two methods, dip coating (DSA 1), and spin-coating (DSA 2). The crystalline structure of the Ti/SnO_2-La electrodes was characterized by X-ray diffraction (XRD, PANalytical X'Pert PRO MPD Diffractometer, Almelo, The Netherlands) with Cu-Kα radiation (ʎ = 1.5418 Å) in the range 2θ = 10–80°. The surface morphology and the elemental composition were examined by scanning electron microscopy coupled with energy-dispersive X-ray spectroscopy (SEM/EDX, FEI Inspect S, Eindhoven, The Netherlands).

b) Electrochemical characterization and degradation

All electrochemical measurements were performed with an Autolab PGSTAT 302 potentiostat/galvanostat (Eco Chemie, Utrecht, The Netherlands) controlled by GPES 4.9 software, in a three-electrode cell consisting of the Ti/SnO_2-La working electrode, a platinum counter electrode and a saturated calomel electrode (SCE) as reference electrode. Before use, the electrodes were rinsed with distilled water and pretreated electrochemically by 10 successive cycles between -3.0 V and +3.0 V vs. SCE, at a scan rate of 0.05 $V*s^{-1}$, in 0.1 M Na_2SO_4 supporting electrolyte for electrode activation and characterization, and selection of operating conditions for further electrooxidation experiments. The electrooxidation of PFOA was carried out under potentiostatic conditions, using chronoamperometry applied at +2.5 V vs. SCE for 7200 s, in 0.1 M Na_2SO_4 supporting electrolyte and 3 nM PFOA.

c) Electrochemical detection of PFOA

The PFOA signal before and after electrolysis was determined electrochemically by differential pulsed voltammetry (DPV) at modified imprinted polymer (MIP)-boron dopped diamond electrode (BDD) [8], based on indirect electrochemical procedure for PFAS detection from water, using ferri/ferrocyanide redox couple, within the potential ranged from 0 to +0.5 V vs. SCE, with a modulation amplitude of 0.1 V, a step potential of 0.01 V and a modulation time of 0.05s. This method is based on the mitigating signal current assigned to ferri/ferrocyanide redox couple in the presence of different PFOA concentrations. The PFOA electrodegradation degree (η) was determined based on Equation (1):

$$\eta = \frac{(C_{PFOA,i} - C_{PFOA,f})}{C_{PFOA,i}} \times 100\ (\%) = \frac{(\Delta I_i - \Delta I_f)}{\Delta I_i} \times 100\ (\%) \qquad (1)$$

where, $C_{PFOA,i} - C_{PFOA,f}$ represents the change in the PFOA concentration, expressed in terms of current signal change (ΔI), determined by DPV voltammetry at MIP-BDD electrode using ferro/ferricyanide redox couple as reference.

Results and discussion

a) *Morphostructural characterization.* Since the two electrodes exhibited similar morphostructural characteristics, only the results obtained for DSA 1 are presented. Figure 1a presents the SEM image of the DSA1 electrode, which shows an irregulated morphology.

The presence of Sn, La, O and Ti is confirmed by EDX presented in the inset of Figure 1a. Also, XRD results identifies tin oxide and lanthanum oxide as components of DSA1, in accordance with EDX results.

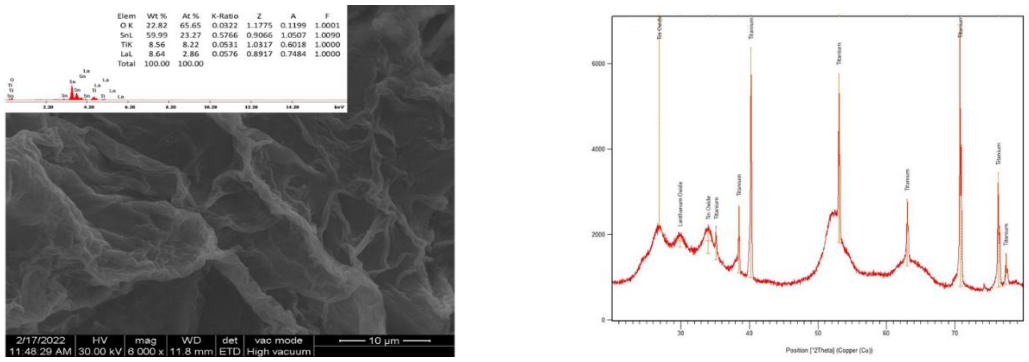
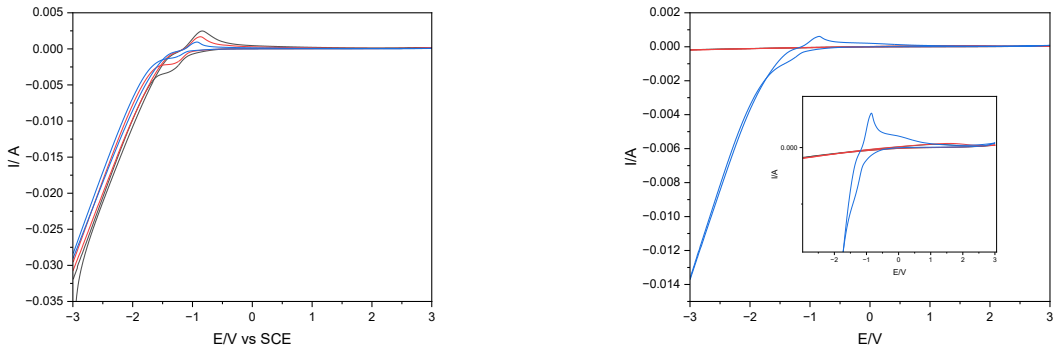


Figure 1. (a) SEM image (6000×) with the EDX spectrum and elemental composition (inset), and (b) XRD pattern of the DSA 1 electrode.

b) *Cyclic voltammetric measurements.* The electrochemical behaviour of the Ti/SnO_2-La electrodes was investigated by cyclic voltammetry in 0.1 M Na_2SO_4, between -3.0 and +3.0 V vs. SCE, at a scan rate of 0.05 $V \cdot s^{-1}$. Figure 2 compares the 1st, 3rd and 10th cycles of a continuous recording for DSA 26 and DSA 38. For DSA1 electrode, a reduction peak appeared at about -1.3 V vs. SCE during the cathodic scanning. This peak could be attributed to the reduction of Sn(IV) from SnO_2 at the electrode surface [9, 10]. During the reverse scanning, an oxidation peak appeared at about -0.85 V vs. SCE, corresponding to the reoxidation of the Sn layer formed during the cathodic scanning. It can be noticed that both peak currents of DSA1 decreased with the cycle number. A different behaviour was noticed for DSA2 electrode. During the 1st and 3rd cycles, very low currents were recorded over the whole potential range, without any oxidation or reduction peak, which informed about a highly resistive electrode surface. In the 10th cycle, the reduction peak at about -1.3 V vs SCE followed by the hydrogen evolution and the oxidation peak at about -0.84 V vs SCE appeared, similar to DSA1. A broad anodic shoulder was also noticed at about 0.5 V vs SCE. In the anodic region, no significant current was recorded up to +3.0 V vs. SCE at neither electrode, and the oxygen evolution did not occur within the potential range, SnO_2 anodes being characterized by a high overpotential for the oxygen evolution [11]. No significant influence related to the electrochemical behavoir of the La presence into electrode composition was found under these conditions.



a) b)

Figure 2. The cyclic voltammograms recorded at: DSA1 (a), and DSA2 (b), in 0.1 M Na_2SO_4 supporting electrolyte for 1st cycle (black line), 3rd cycle (red line), and 10th cycle (blue line), at a potential range between -3.0 V to +3.0 V vs SCE, at a scan rate of 0.05$V \cdot s^{-1}$. Inset: details of DSA2 electrode.

For testing PFOA electrooxidation, chronoamperometry was applied at +2.5 V vs. SCE, in 0.1 M Na_2SO_4 supporting electrolyte containing 3 nM PFOA, for 7200 s (Figure 3).

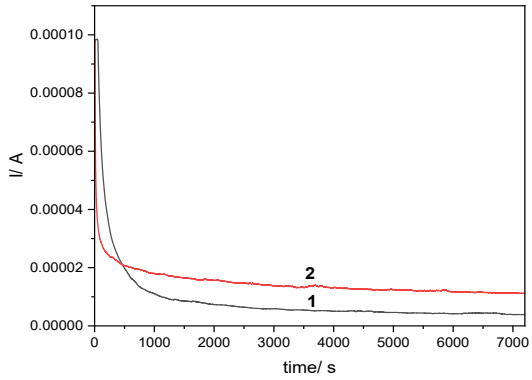


Figure 3. Chronoamperograms recorded at +2.5 V vs. SCE for 7200s in 0.1 M Na_2SO_4 supporting electrolyte containing 3 nM PFOA concentration at: (1) DSA1 and (2) DSA2 electrodes.

At both electrodes, the current decreased during the first minutes of polarization, as we expected, considering reaching the steady state, which was maintained during the whole electrooxidation time. It has to be underlined that for the similar voltage applying (+2.5 V/SCE), the current value is higher for DSA2, which remains relatively constant, showing a continous reactivation of the electrode surface vs DSA1, at which the current tendency is slightly decreasing.

PFOA concentration, before and after applying electrooxidation using chronoamperometry at both DSA electrodes, was assesed electrochemically using DPV at MIP-boron-doped diamond electrode (articol Sorinica) considering indirect detection based on reference signal assigned to ferri/ferrocyanide redox couple. Figure 4 shows DPVs recorded for PFOA before and after electrooxidation applying.

PFOA electrodegradation degree, determined by current signal change using DPV and MIP-boron-doped diamond electrode, at both DSAs are gathered in table 1.

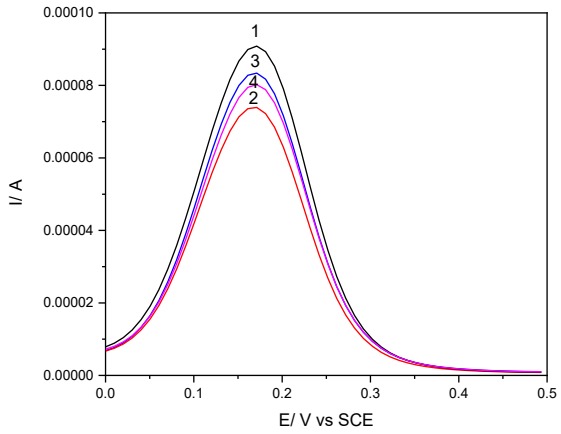


Figure 4. Differential pulse voltammograms (DPV) recorded at BDD electrode in: 1) 0.1 M KCl + 0.1 M Na_2SO_4 + 5 mM $K_3Fe(CN)_6$ supporting electrolyte; 2) 3 nM PFOA before electrolysis; 3) the solution electrolyzed with DSA2; 4) the solution electrolyzed with DSA1; 0.1 V modulation amplitude; 0.01V step potential; 0.05s modulation time; 0.02 $V*s^{-1}$scan rate.

Table 1. PFOA electrodegradation degree determined by DPV after 7200s of electrolysis at +2.5 V vs. SCE on both electrodes.

Electrode type	ΔI_i (A) (for 3 nM PFOA)	ΔI_f (A)	Ƞ (%)
DSA1	$1.67x10^{-5}$	$1.03x10^{-5}$	36.9
DSA2	$1.67x10^{-5}$ (de unit)	$0.71x10^{-5}$	56.8

Conclusion

Both DSAs electrodes synthesized by dip-coating and spin-coating exhibited good suitable features for PFOA degradation through electrooxidation. La integration within SnO_2/TiO_2 compositions did not affect significantly O_2 evolution, which informed that at potential value of +2.5 V/SCE, PFOA electrooxidation occurred on the electrode surface. Electrochemical techniques applied through three-electrodes system allowed to simulate conditions for both electrodegradation and process control through electrochemical detection. This advantage should be exploited as reference points for further scaling at pilot plant considering PFAS removal from water.

Acknowledgements

This work was supported by a grant of the Ministry of Research, Innovation and Digitization, CNCS/CCCDI - UEFISCDI, through the project Center of Excellence in water management, materials, by-products and waste valorisation for circular bioeconomy implementation, proposal number PN-IV-P6-6.1-CoEx-2024-0056, contract 6 CoEx/02.06.2026.

References

[1] S. Daghfous, E. Makhoul, E. Petit, G. Lesage, M. Bechelany, N. Bellakhal, M. Cretin, Materials 19 (2026) 1659.
[2] K.A. Akhilghosh, S. Farissi, V.P. Aiswriya, C.T. Aravindakumar, M. Muthuchamy, A. Muthukumar, Environ. Sci. Pollut. Res. (2025)
[3] X.Teng, Y. Qi, R.Guo, S. Zhang, J. Wei, J.S. Ajarem, S. Maodaa, A.A. Allam, Z. Wang, R. Qu, J. Hazard. Mater (2024).
[4] F.A. Zeidabadi, E.B. Esfahani, S.T. McBeath, K.L. Dubrawski, M. Mohseni, Chemosphere (2023).
[5] S. Motoc, A. Remes, A. Pop, F. Manea, J.Schoonman, J. Environ. Sci (2013).
[6] A. Baciu, C. Orha, R. Nicolae, M. Nicolaescu, S. Ilies, F. Manea, Coatings 13 (2023) 1127.
[7] C. Orha, C. Bandas, C. Lazau, M.I. Popescu, A.Baciu, F. Manea, Water 14 (2022) 821.
[8] S.-C.Negrea, L.A.Diaconu, D.Neidoni, A.Pacala, L.F. Pascu, S. Motoc, A. Baciu, E. Trif, F.Manea, Rom. J. Ecol. Environ. Chem. 6 (2024).
[9] S. Geiger, O. Kasian, A.M. Mingers, K.J.J Mayrhofer, S. Cherevko, Scientific Reports (2017).
[10] C.F. Sanz-Navarro, S.F. Lee, S.S. Yap, C.H. Nee, S.L. Yap, Thin solid films (2023).
[11] R. Kotz, S. Stucki, B. Carcer, J. Appl. Electrochem. 21 (1991).

SUSTAINABLE RECOVERY OF CELERY POMACE BIOACTIVE COMPOUNDS

Aleksandra Ivanovska[1], Ana Milivojević[2], Marija Ćorović[2]

[1]Innovation Center of the Faculty of Technology and Metallurgy in Belgrade Ltd., Karnegijeva 4, 11000 Belgrade, Serbia
[2]University of Belgrade, Faculty of Technology and Metallurgy, Karnegijeva 4, 11000 Belgrade, Serbia
e-mail: aivanovska@tmf.bg.ac.rs

Abstract

Celery pomace, the solid residue generated during celery juice processing, is an abundant agro-industrial by-product that is often underutilized or discarded despite retaining valuable bioactive compounds. It contains phenolic compounds, flavonoids, vitamins, chlorophylls, and other phytochemicals that may exhibit antioxidant, antimicrobial, and anti-inflammatory properties. The valorization of celery pomace through the recovery of these compounds represents a promising strategy for reducing agro-food waste while generating valuable bio-based resources for potential industrial applications. In particular, the efficient recovery of phenolic compounds may provide extracts suitable for incorporation into functional materials and products. In this investigation, extraction of phenolic compounds from celery pomace was optimized using a Box–Behnken design and response surface methodology. Extraction time (5–65 min), ethanol concentration (10–70%), and liquid-to-solid ratio (10–60 mL/g) were selected as independent variables, while total phenolic content was used as the main response. Response surface methodology showed that all three factors significantly affected total phenolic content, with the developed model showing a good fit to the experimental data ($R^2 = 0.9785$) and a non-significant lack of fit ($p = 0.0881$). The highest total phenolic content was predicted at a short extraction time (5 min), high ethanol concentration (70%), and a liquid-to-solid ratio of approximately 46 mL/g, reaching 1.71 mg GAE/g DW. Under these conditions, the corresponding predicted total chlorophyll content was 162.27 µg/g DW. Importantly, the response surface analysis indicated that similarly high phenolic content could be achieved over a broader range of liquid-to-solid ratios. This finding provides flexibility in selecting the final extraction conditions by considering not only extraction efficiency but also solvent consumption and overall process sustainability. The optimized extraction process demonstrates the potential of celery pomace as a valuable source of phenolic compounds that can be further utilized as functionalization agents in the textile industry and potentially in other value-added applications. The proposed approach contributes to the efficient utilization of agro-industrial residues, reduction of waste generation, and development of resource-efficient processes in accordance with circular economy and sustainable biorefinery principles.

Acknowledgements

This research was funded by the Ministry of Science, Technological Development and Innovation of the Republic of Serbia through the project EUREKA LinkUp 23921 (VALORGREEN). The authors thank Bubaja d.o.o., Serbia, for supplying the celery pomace.

ASSESSING THE BIODEGRADABILITY OF INDUSTRIAL SLUDGE WITH DIELECTRIC AND BIOKINETIC PARAMETERES

Zoltán Péter Jákói[1], Anar Imamverdiyev[2], Sándor Beszédes[1]

[1]Department of Biosystems Engineering, University of Szeged, H-6725 Szeged, Moszkvai krt. 9, Hungary
[2]Doctoral School of Environmental Sciences, University of Szeged, H-6720 Szeged, Rerrich Béla tér 1., Hungary
e-mail: jakoi.zoltan.peter@szte.hu

Abstract

This study investigated the effects of microwave (MW) pre-treatment and magnetic nanoparticles (MPs) on the anaerobic digestion (AD) of meat-processing sludge, integrating biokinetic modelling with dielectric measurements to assess methane production and explore opportunities for process monitoring. Five sludge variants were compared: an untreated control, an MP-only control, MW-pre-treated sludge, and two MW + MP treatments in which nanoparticles were either retained in or removed from the substrate before digestion. This design enabled evaluation of both pre-treatment effects and the influence of nanoparticle retention during the subsequent digestion stage. Methane production was normalized to volatile solids (VS), and cumulative production curves were fitted using the modified Gompertz, Logistic, and Weibull models to compare kinetic parameters across treatments. The highest biomethane potential and maximum methane production rate were obtained when MW pre-treatment was combined with MPs retained in the digestion medium. Biomethane potential reached 390 mL CH_4 g^{-1} VS, representing a 52% increase relative to the untreated control, while the maximum methane production rate increased by 85% to 37 mL CH_4 g^{-1} VS d^{-1}. These results indicate improvements in both methane recovery and production kinetics. Dielectric measurements revealed progressive changes in relative permittivity during digestion. The maximum rate of permittivity change exhibited a strong relationship with methane production rate ($R^2 > 0.98$), suggesting that dielectric responses may provide an indirect indicator of biochemical activity. Overall, the findings support the combined use of MW pre-treatment and magnetic nanoparticles as a promising approach for improving the anaerobic valorization of meat-processing sludge. They also highlight nanoparticle retention as a relevant treatment consideration and demonstrate the potential of integrating dielectric measurements with biokinetic modelling to support rapid assessment and monitoring of digestion performance.

Acknowledgements

The Authors are grateful for the financial support provided by the National Research, Development and Innovation Office (NKFIH) under the project number FK 146344 and EKÖP-26-4-SZTE-247.

TOWARDS A VALIDATED HPLC METHOD FOR ACRYLAMIDE DETERMINATION

Benjámin Jancsó, Lukács J. Németh, Balázs Jójárt

Department of Food Engineering, Faculty of Engineering, University of Szeged H-6724 Szeged, Mars tér 7, Hungary
e-mail: jancsob@mk.u-szeged.hu

Abstract

In a 2002 published report by the EU JRC it is stated that acrylamide ((2-propenamide), AA) does not pose a risk in the food chain, but it was discussed in detail its effects on human health resulting from industrial contamination [1]. In the same year, a Swedish research group identified the presence of AA in heated, carbohydrate-rich foodstuffs [2]. Mottram *et al.* [3,4] and Stadler *et al.* [5] discussed the presumably pivotal role of asparagine and reducing sugars (glucose) in the formation of AA while Zyzak *et al.* described the actual formation mechanism of AA *via* the Maillard reaction [6]. The International Agency for Research on Cancer classified AA as a probable human carcinogen (Group 2A) and set the maximum atmospheric concentration at 0.03 mg/m³ [7]. Six years later, on November 20, 2017, an EU regulation came into effect, setting different benchmark levels (for example: baby formulas 40, potato crips 750 and chicory 4000 µg/kg) for AA in foodstuffs [8].

Based on these considerations, it is evident that the determination of acrylamide levels is crucial for food safety. Therefore, this study aimed to develop a validated method using a HITACHI L2200 HPLC system (eluent: 95:5 UP water/methanol, flow rate: 0.4 ml/min, pressure: 30 bar, UV detector at 210 nm, injection volume 50 µl).

The calibration curve was established from three independent preparations (100 mg/250 cm³, dissolved in UP water) within a concentration range of 2–100 µg/100 cm³, and the resulting peak areas were determined using one or two Gaussian functions. The Gaussian curves were fitted using three different methods: via the Fityk software, the obtained curves were further refined, and both the analytical and numerical integrals of the curves were determined.

Since the data exhibited heteroscedasticity, a weighted approach was applied by scaling the data with both the $1/s^2$ and the VF3 methods [9] instead of standard OLS. The R^2 value reached 0.999 when using the VF3 method, and the intercept was not significantly different from zero ($p > 0.05$). When back-calculating intermediate concentrations, larger deviations were observed in the higher concentration range, indicating that the model, on average, overestimates the actual concentrations.

Based on these data, significant progress has been made toward developing a validated method; however, the determination of other important performance parameters (such as precision, reproducibility, and recovery, etc.) remains to be carried out.

References

[1] B. McSweeney, C. Day (Eds.), European Union Risk Assessment Report. Acrylamide. European Commission Joint Research Centre, EUR 19835 EN, Vol. 24 (2002) 1.
[2] E. Tareke, P. Rydberg, P. Karlsson, S. Eriksson, M. Törnqvist, J. Agric. Food Chem. 50 (2002) 4998.
[3] D.S. Mottram, B.L. Wedzicha, A.T. Dodson, Nature 419 (2002) 448.
[4] K. Mottram, J. Agric. Food Chem. 51 (2003) 802.
[5] R.H. Stadler, I. Blank, N. Varga, F. Robert, J. Hau, P.A. Guy, M.-C. Robert, S. Riediker, Nature 419 (2002) 449.

[6] D.V. Zyzak, R.A. Sanders, M. Stojanovic, D.H. Tallmadge, B.L. Eberhart, D.K. Ewalds, D.C. Gruber, T.R. Morsch, M.A. Strothers, G.P. Rizzi, M.D. Villagran, J. Agric. Food Chem. 51 (2003) 4782.
[7] J.W. Cherrie, M. Gorman Ng, A. Shafrir, M. van Tongeren, R. Mistry, O. Warwick, C. Corden, L. Rushton, S. Hutchings, IOM Research Project P937/9 (2011) 1.
[8] European Commitee, 2017/2158/EU Regulation, HL L 317 (2017) 21., Access: 2026.09.25.
[9] J. Tellinghuisen, Anal. Chem. 98 (2026) 11641.

IMPACT OF TEMPERATURE AND PRECIPITATION ON SOYABEAN YIELD IN THE REGION OF ŠUMADIJA AND WESTERN SERBIA

Darko Jaramaz[1], Marijana Jovanović Todorović[1], Aleksandra Stanojković-Sebić[2], Gordana Radović[1], Vladan Ugrenović[2], Darko Jakšić[1], Bojana Bekić Šarić[1]

[1]Institute of Agricultural Economics, Volgina 15, Belgrade, Serbia
[2]Institute of Soil Science, Teodora Drajzera 7, Belgrade, Serbia
e-mail: darko_ja@iep.bg.ac.rs

Abstract
Soyabean (Glycine max (L.) Merr.) plays a main role in global food security as a primary source of vegetable protein, in the same time recent studies on drought in Europe highlighted soyabean as one of the major crops affected by climate changes. The research area represents the statistical region of Šumadija and Western Serbia, which is one of the five statistical regions of Serbia and covers a total area of 26,493 km². The study employed monthly temperature and precipitation data recorded at seven meteorological stations across the region of Šumadija and Western Serbia during the growing seasons (April to September) from 2005 to 2024, as well as annual soyabean yield data for the same region and period. The Pearson correlation coefficient was applied to determine the strength and direction of the relationship between monthly meteorological indicators (temperature and precipitation) and soyabean yield. The study revealed a strong negative correlation between soyabean yield and mean temperature in July ($r = -0.71$), as well as a strong positive correlation between soyabean yield and total precipitation in July ($r = 0.66$).

Introduction
Soyabean (Glycine max (L.) Merr.) plays a main role in global food security as a primary source of vegetable protein and oil [1], and it is also used for biodiesel production and as an alternative energy source [2].
The increasing global population and the uncertainties of climate change have been considered one of the greatest future challenges for global food security [3]. Climate change significantly impacts agricultural production, with variations in precipitation patterns, temperature fluctuations, and rising atmospheric CO_2 concentrations [4].
Climate plays a crucial role in the growth and development of soyabean [5]. Recent studies on drought in Europe highlighted soyabean as one of the major crops severely affected by water scarcity and heat stress [6]. Especially temperature changes may cause decreases in yield and quality parameters (total biomass, pods per individual plant, grain weight), and shortening of the time from planting to maturity [7].
In Central and Eastern Europe the optimal sowing term falls in the range from mid-April to mid-May [8], when the soil temperature at sowing depth reaches 10–12 °C [9, 10]. In European countries, the soyabean growing season season typically lasts between 105 and 140 days [11].

Experimental
The research area represents the statistical region of Šumadija and Western Serbia, which is one of the five statistical regions of Serbia. It extends across the central and western parts of Serbia, covering a total area of 26,493 km². The topography of the statistical region of Šumadija and Western Serbia is extremely heterogeneous. The northern and northeastern parts include lowland and valley terrain, in the central parts prevails hilly and mountainous relief, while towards the west and southwest the elevation increases and the relief acquires a mountainous

character. The climate is predominantly temperate continental, but varies depending on the relief and elevation.

The study employed mean monthly temperatures and mean monthly precipitation totals during the soyabean growing season (from April to September), calculated using data from seven meteorological stations distributed throughout the region of Šumadija and Western Serbia [12], as well as annual soyabean yield data from the same region [13], for the period from 2005 to 2024. The spatial distribution of the meteorological stations is presented in Figure 1.

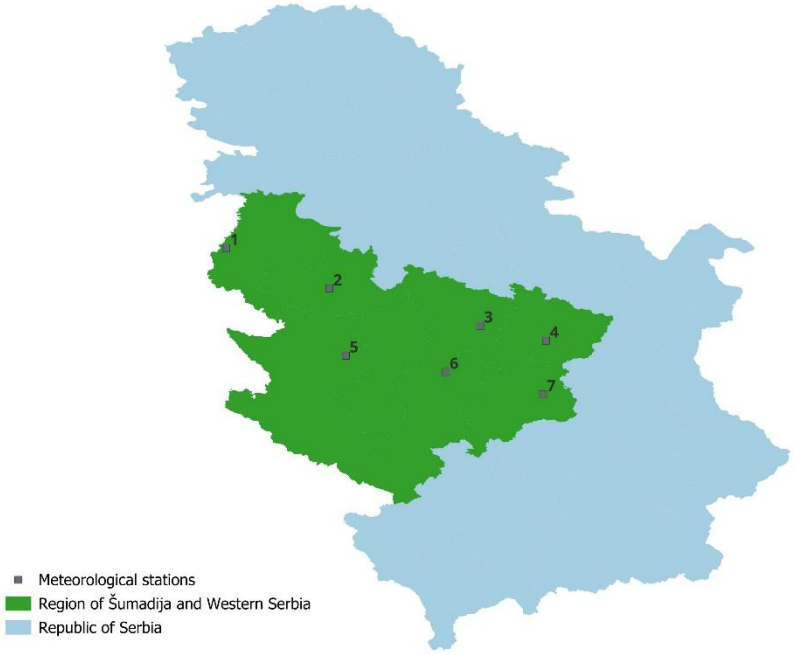


Figure 1. Research area and spatial distribution of the meteorological stations

The linear Pearson correlation coefficient was used to examine the relationship between the analyzed variables, assessing the strength and direction of the interrelationship between meteorological indicators at the monthly level (temperature and precipitation) and yield. Pearson's correlation coefficient was calculated using the following formula [14]:

$$r_{xy} = \frac{\sum_{i=1}^{n}(x_i - \bar{x})\,(y_i - \bar{y})}{\sqrt{\sum_{i=1}^{n}(x_i - \bar{x})^2 \sum_{i=1}^{n}(y_i - \bar{y})^2}}$$

where x_i and y_i represents the individual values of the variables, $\bar{x}$ and $\bar{y}$ are their arithmetic means, and n is the number of paired observations.

Results and discussion

The mean monthly temperatures (°C) for April, May, June, July, August, and September during the period 2005-2024, calculated using data from the seven meteorological stations within the region of Šumadija and Western Serbia, are presented in Figure 2. The highest mean temperatures were recorded in July 2024 (25.60 °C), August 2024 (25.54 °C), and July 2012 (25.15 °C).

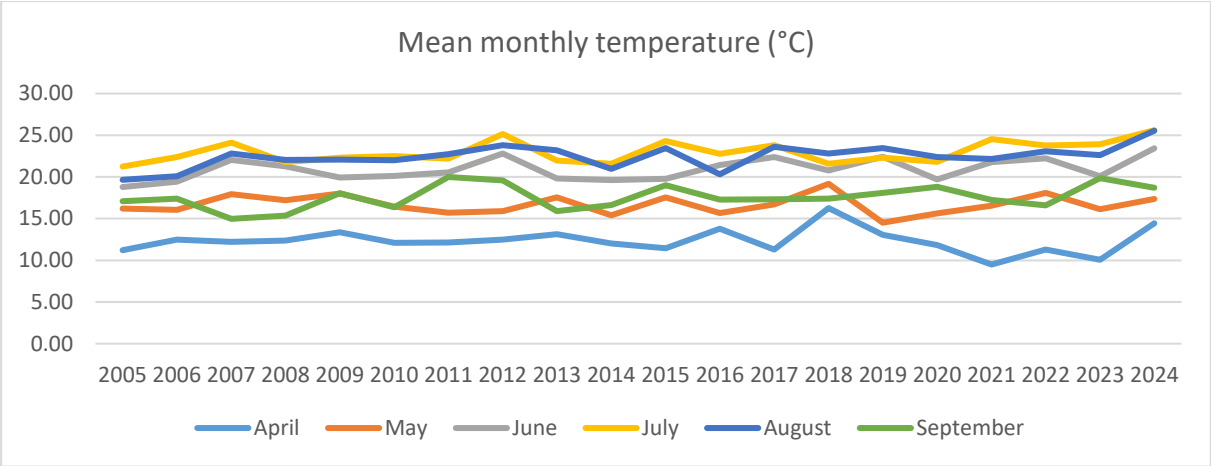


Figure 2. Mean monthly temperature (°C) for the region of Šumadija and Western Serbia (2005-2024)

The mean monthly precipitation totals (mm) for April, May, June, July, August, and September during the period 2005–2024, calculated using data from the seven meteorological stations within the region of Šumadija and Western Serbia, are presented in Figure 3.

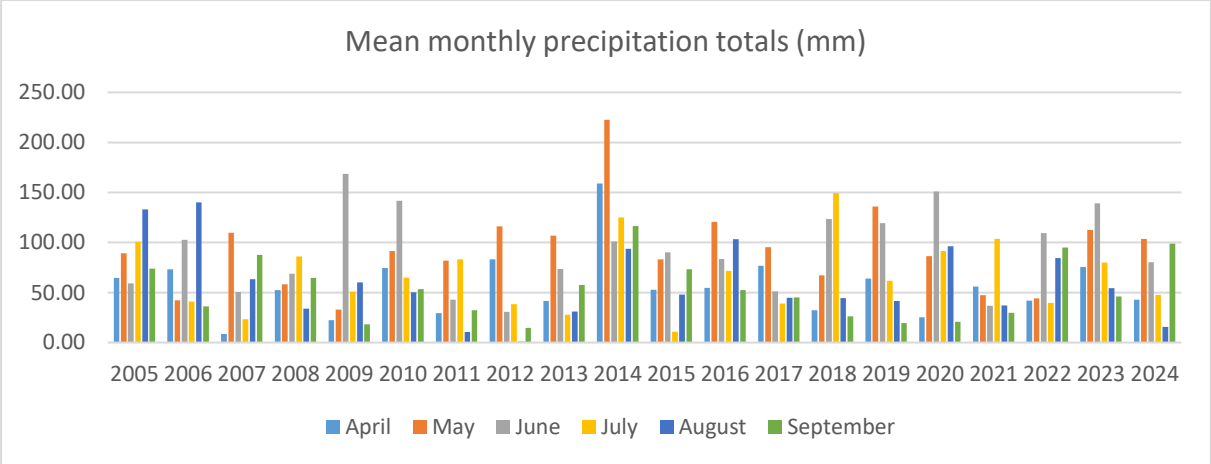


Figure 3. Mean monthly precipitation totals (mm) for the region of Šumadija and Western Serbia (2005-2024)

The annual soyabean yield (t/ha) for the region of Šumadija and Western Serbia during the period 2005–2024 are presented in Figure 4. The lowest soyabean yields were recorded in 2024 (1.3 t/ha), 2007 (1.4 t/ha), and 2012 (1.6 t/ha).

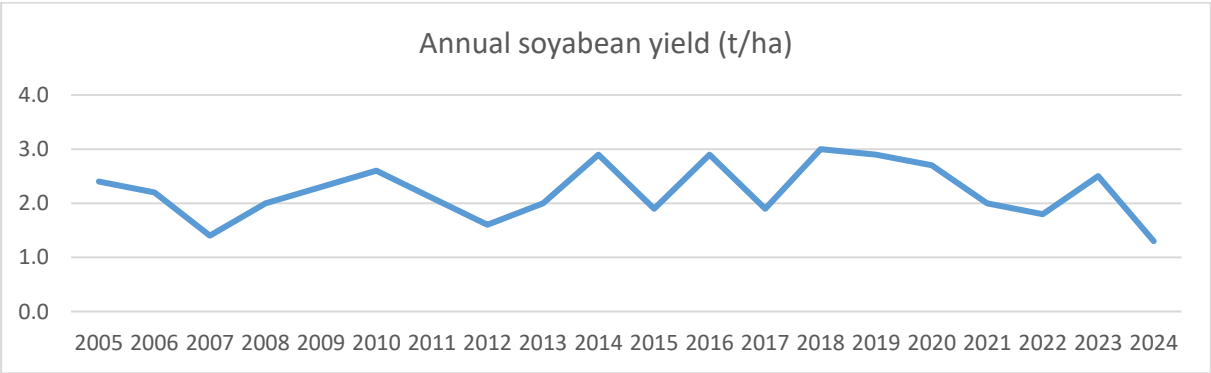


Figure 4. Annual soyabean yield (t/ha) for the region of Šumadija and Western Serbia (2005–2024)

The Pearson correlation coefficient (r) and its associated p-value between annual soyabean yield and mean monthly temperature (°C) in the region of Šumadija and Western Serbia during the period 2005–2024 are presented in Table 1. A strong negative correlation between soyabean yield and mean temperature was found for July (r = -0.71), while moderate negative correlations were found for August (r = -0.53) and June (r = -0.49). These correlations were statistically significant with $p < 0.05$.

Table 1. Pearson correlation between annual soyabean yield and mean monthly temperature (°C) in the region of Šumadija and Western Serbia (2005–2024)

		April (°C)	May (°C)	June (°C)	July (°C)	August (°C)	September (°C)
Yield (t/ha)	Pearson correlation coefficient (r)	0.195	-0.362	-0.487	-0.711	-0.528	0.042
	Statistical significance (p-value)	0.411	0.116	0.029	0.000	0.017	0.859

The Pearson correlation coefficient (r) and its associated p-value between annual soyabean yield and mean monthly precipitation totals (mm) in the region of Šumadija and Western Serbia during the period 2005–2024 are presented in Table 2. A strong positive correlation between soyabean yield and precipitation totals was found for July (r = 0.66), while moderate positive correlation was found for June (r = 0.56). Both correlations were statistically significant with $p < 0.05$.

Table 2. Pearson correlation between annual soyabean yield and mean monthly precipitation (mm) in the region of Šumadija and Western Serbia (2005–2024)

		April (mm)	May (mm)	June (mm)	July (mm)	August (mm)	September (mm)
Yield (t/ha)	Pearson correlation coefficient (r)	0.306	0.281	0.563	0.656	0.399	-0.282
	Statistical significance (p-value)	0.189	0.230	0.01	0.002	0.081	0.229

Conclusion

Soyabean production in the region of Šumadija and Western Serbia is mainly concentrated in the plains, basins, and valleys of the northern and central parts of the region. These areas are characterized by lower elevations and gentler terrain slopes, a longer growing season, and a larger share of arable agricultural land. Although the region of Vojvodina dominates Serbia's national soyabean production, the region of Šumadija and Western Serbia represents the main soyabean-producing area in Serbia south of the Sava and Danube rivers.

A strong negative correlation between soyabean yield and mean temperature was found for July (r= -0.71), while moderate negative correlations were found for August (r= -0.53) and June (r= -0.49). A strong positive correlation between soyabean yield and precipitation totals was found for July (r= 0.66), while a moderate positive correlation was found for June (r= 0.56).

A limitation of this study is the exclusion of factors that may also affect soyabean yield, such as soil properties, topographic characteristics, tillage practices, fertilizer application, and other meteorological parameters (minimum and maximum temperatures, solar radiation, relative humidity, wind speed, etc.). Future research should incorporate additional factors to provide a more comprehensive assessment of their relationships with soyabean yield.

Acknowledgements
Paper is a part of research financed by the Ministry of Science, Technological Development, and Innovation of the Republic of Serbia, agreed in decisions no. 451-03-33/2026-03/200009 from 5 February 2026, and no. 451-03-33/2026-03/ 200011.

References
[1] K.-H. Kim, S. H. Lim, S. D. Lim, J. Ha, B.-M. Lee, Agriculture 16/4 (2026) 445.
[2] S. Candemir, N. Kızılaslan, Turkish JAF Sci. Tech. 7/1 (2019) 43.
[3] A. Molotoks, P. Smith, T.P. Dawson, Food Energy Secur. 10/1 (2021) e261.
[4] J.L. Hatfield, K.J. Boote, B.A. Kimball, L.H. Ziska, R.C. Izaurralde, D. Ort, A.M. Thomson, D. Wolfe, Agron. J. 103 (2011) 351.
[5] B. Arslan, S.T.A. Aslan, B. Şen, Ecological Modelling 517 (2026) 111584.
[6] A. Toreti, D. Bavera, J. Acosta Navarro, C. Cammalleri, A. de Jager, C. Di Ciollo, A. Hrast Essenfelder, W. Maetens, D. Magni, D. Masante, M. Mazzeschi, S. Niemeyer, J. Spinoni, Publications Office of the European Union, Luxembourg (2022).
[7] C.H. Burroughs, C.M. Montes, C.A. Moller, N.G. Mitchell, A.M. Michael, B. Peng, H. Kimm, T.L. Pederson, A.E. Lipka, C.J. Bernacchi, K.J. Guan, Exp. Bot. 74/5 (2023) 1629.
[8] D.C. Dima, Agric. Sci. Procedia 2016 10 (2016) 10.
[9] M. Hrustic, S. Relic, D. Jockovic, Zbornik radova, 20 (1992) 483.
[10] J. Miladinovic, Magistarski rad, Univerzitet u Novom Sadu, Poljoprivredni fakultet, Novi Sad (1997).
[11] J. Księżak, J. Bojarszczuk, Agronomy 12/5 (2022) 1066.
[12] Republic of Serbia. Republic Hydrometeorological Service of Serbia (2005-2024), Meteorological Yearbook, Available online: https://www.hidmet.gov.rs/latin/meteorologija/klimatologija_godisnjaci.php (accessed on 6 July 2026).
[13] Statistical Office of the Republic of Serbia (2005-2024), Database: Plant Production, Available online: https://data.stat.gov.rs/Home/Result/130102?languageCode=sr-Cyrl (accessed on 10 July 2026).
[14] Pearson, K, Philosophical Transactions of the Royal Society of London, Series A, 187 (1896) 253.

IN VITRO GERMINATION OF SUNFLOWER (*Helianthus annuus* L.) SEEDS

Adriana Jicmon[1], Andreea Gabor[1], Narcis Baltag[1], Melisa Ciora[1], Emilian Onișan[1*], Irina Petrescu[1], Adalbert Okros[2]

[1]*University of Life Sciences "King Mihai I" from Timișoara, Calea Aradului 119, 300645 Timișoara, Romania*
[2]*Faculty of Agriculture, University of Life Sciences "King Mihai I" from Timișoara, Calea Aradului 119, 300645 Timișoara, Romania*
[*]*Corresponding author e-mail: Emilian.onisan@usvt.ro*

Abstract
This study evaluates the role of the pericarp in inhibiting the *in vitro* germination of sunflower (*Helianthus annuus* L.) seeds. Dehulled seeds and seeds with an intact pericarp (30 seeds per variant, two seeds per culture vessel) were surface-sterilised (5% NaClO, 2% PPM) and cultured on MS medium at 20 °C under continuous light, with evaluations at 7, 14 and 21 days. Dehulled seeds germinated faster and in a higher proportion (80%, 90% and 93.3% at 7, 14 and 21 days) than seeds with an intact pericarp (13.3%, 40% and 70%), the differences being significant at all three evaluation dates (Fisher's exact test). After 14 days, dehulled seeds formed complete seedlings with an elongated hypocotyl, expanded purple-green cotyledons and anthocyanin-pigmented roots. The results confirm that the pericarp acts as a physical and respiratory barrier that delays germination, and that its removal is an effective strategy for obtaining rapid and uniform *in vitro* cultures.

Introduction
Sunflower (*Helianthus annuus* L.) plays a crucial role in agriculture and the food industry, largely due to its high value as an oilseed crop. Its seeds are a rich source of oil, high-energy compounds and proteins. Expanding cultivation areas and a sustained interest in maximising crop value have secured sunflower a prominent place among the globally utilised oilseed crops [1]. At the same time, the growing demand for high-quality vegetable oils, together with the potential of sunflower oil for biodiesel production, has driven interest in improving the species. Consequently, breeding programmes focus on developing genotypes with higher yield potential, superior oil content, adaptation to current environmental conditions and enhanced resistance to biotic stress, particularly to diseases such as downy mildew [2–4].
In vitro tissue culture techniques allow researchers to study sunflower plant material under strictly controlled conditions, yielding reproducible and highly comparable results. These methods are widely applied in micropropagation, physiological research, plant breeding and biotechnology, and are the foundation of more advanced procedures, such as plant regeneration and genetic transformation [5], the rescue of immature embryos for the development of inbred lines [6] and the conservation of valuable genotypes through callus cultures [7]. However, plant response under such conditions is rarely uniform, as it is shaped by genotype, the origin and physiological state of the biological material and the composition of the nutrient medium [2].
Within these workflows, seed germination is a critical step, as the development of healthy, viable seedlings relies directly on its success. Carrying out germination *in vitro* ensures tight control over temperature, photoperiod, nutrient availability and culture medium composition, minimising external environmental noise [8]. As a result, *in vitro* germination is well suited both for producing uniform plant material and for monitoring seed response under standardised conditions, including the response to stress factors [9]. Mature seeds are easy to source and store, make experiments easy to schedule and repeat, and provide a reliable source of aseptic seedlings for the explants needed in downstream *in vitro* studies [1].

In vitro germination of sunflower seeds is primarily influenced by nutrient medium composition, temperature, light, carbon source, hormonal balance and sterilisation conditions [10], as well as by the hormonal and physiological state of the seeds, which affects the induction or release of dormancy [11]. Moderate temperatures are more favourable than extreme ones, which reduce both germination rate and speed [12]. Ethylene contributes to breaking dormancy [11], whereas abscisic acid (ABA) maintains it, and a reduction of its endogenous level can accelerate germination [8]. Auxins and cytokinins are primarily used in the subsequent rooting and regeneration stages and are not mandatory components of the germination medium [13], while seed sterilisation with agents such as ethanol, sodium hypochlorite or silver nitrate is necessary to limit contamination [14].

The aim of this study was to comparatively evaluate dehulled sunflower seeds and seeds with an intact pericarp cultured *in vitro* on MS medium at 20 °C under continuous illumination, by monitoring the germination rate and the morphological development of the seedlings over a 21-day period.

Experimental

Culture medium

Murashige and Skoog (MS) medium was prepared in a final volume of 1 L of distilled water, using 4.4 g MS powder, 30 g sucrose and 12 g agar. The components were dissolved and homogenised, the pH was adjusted to 5.7–5.8, and the medium was autoclaved, distributed into sterile glass culture vessels and allowed to solidify before inoculation.

Sterilisation and inoculation of plant material

The seeds were placed in a metal sieve and surface-sterilised successively with 5% sodium hypochlorite (NaClO) and 2% Plant Preservative Mixture (PPM), for 1 minute in each solution, then rinsed with sterile distilled water to remove residual sterilising agents. After approximately 2 minutes on a sterile Petri dish to remove excess water, the seeds were inoculated with sterile forceps onto the MS medium, with the apical end facing downward and completely inserted into the medium. All operations were carried out under aseptic conditions in a laminar flow hood, and the vessels were covered with sterile film, sealed and labelled.

Experimental design and culture conditions

Two experimental variants were compared: V1 – seeds with an intact pericarp and V2 – dehulled seeds. Each variant comprised 15 culture vessels (replicates, R1–R15) with two seeds per vessel, i.e. 30 seeds per variant. Cultures were maintained at 20 °C under continuous fluorescent illumination. Germination, morphological changes and possible contamination were recorded at 7, 14 and 21 days after inoculation.

Data analysis

The germination percentage was calculated for each variant and evaluation date as the ratio between the number of germinated seeds and the total number of inoculated seeds. Differences between variants at each date were tested with Fisher's exact test at a significance level of $\alpha = 0.05$.

Results and discussion

The germination results are summarised in Table 1 and the germination dynamics in Figure 1. Dehulled seeds (V2) germinated rapidly, reaching 80% after only 7 days, whereas seeds with an intact pericarp (V1) reached only 13.3%. The difference remained significant after 14 days (90% vs. 40%) and 21 days (93.3% vs. 70%), although it gradually narrowed from 66.7 to 50.0 and 23.3 percentage points. The pericarp therefore mainly delayed germination rather than preventing it completely: most of the V1 seeds germinated between days 7 and 21, while V2 reached a plateau after the first week.

Table 1. Number of germinated seeds per culture vessel (R1–R15, two seeds per vessel), total number of germinated seeds (n/30) and germination percentage (G) of intact (V1) and dehulled (V2) sunflower seeds

Day	Variant	R1	R2	R3	R4	R5	R6	R7	R8	R9	R10	R11	R12	R13	R14	R15	n/30	G (%)	p
7	V1	0	0	0	1	0	1	0	0	1	0	0	1	0	0	0	4	13.3	< 0.001
	V2	2	2	1	2	1	2	2	2	2	1	2	1	1	2	1	24	80.0	
14	V1	1	1	1	1	1	1	1	1	1	1	0	1	0	0	1	12	40.0	< 0.001
	V2	2	2	2	2	2	2	2	2	2	1	2	2	1	2	1	27	90.0	
21	V1	2	1	1	2	1	1	1	1	2	2	1	2	1	1	2	21	70.0	0.042
	V2	2	2	2	2	2	2	2	2	2	2	2	2	1	2	1	28	93.3	

p – Fisher's exact test between V1 and V2 at each evaluation date.

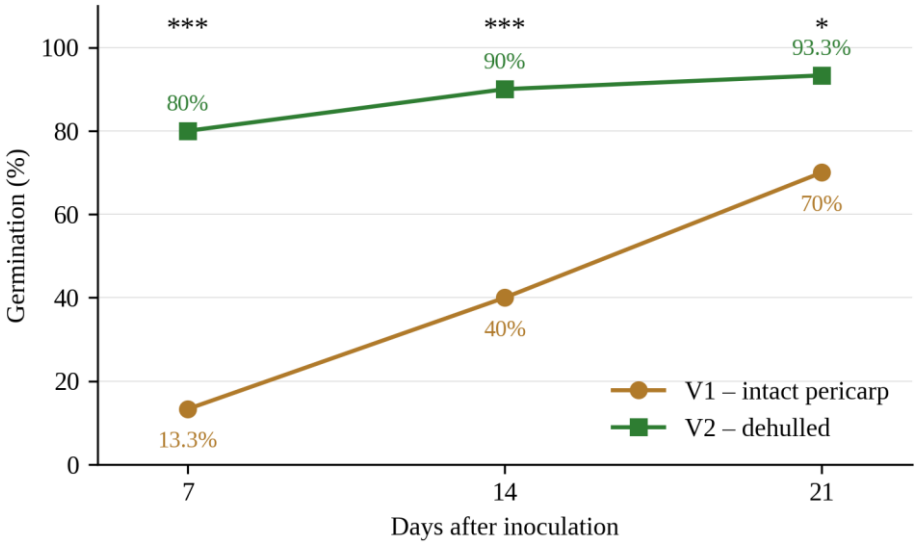


Figure 1. Germination dynamics of intact (V1) and dehulled (V2) sunflower seeds cultured *in vitro* on MS medium; *** $p < 0.001$, * $p < 0.05$ (Fisher's exact test)

The morphological differences were equally clear (Figures 2 and 3). After 14 days, the dehulled seeds formed well-developed seedlings with a prominent hypocotyl, expanded purple-green cotyledons and an elongated, strongly anthocyanin-pigmented root system penetrating deep into the agar medium. The increased condensation on the vessel walls suggests intense metabolic and respiratory activity. In contrast, most seeds with an intact pericarp remained at an early stage, showing only a short, creamy-white radicle barely piercing the pericarp, with minimal shoot growth and limited root penetration.

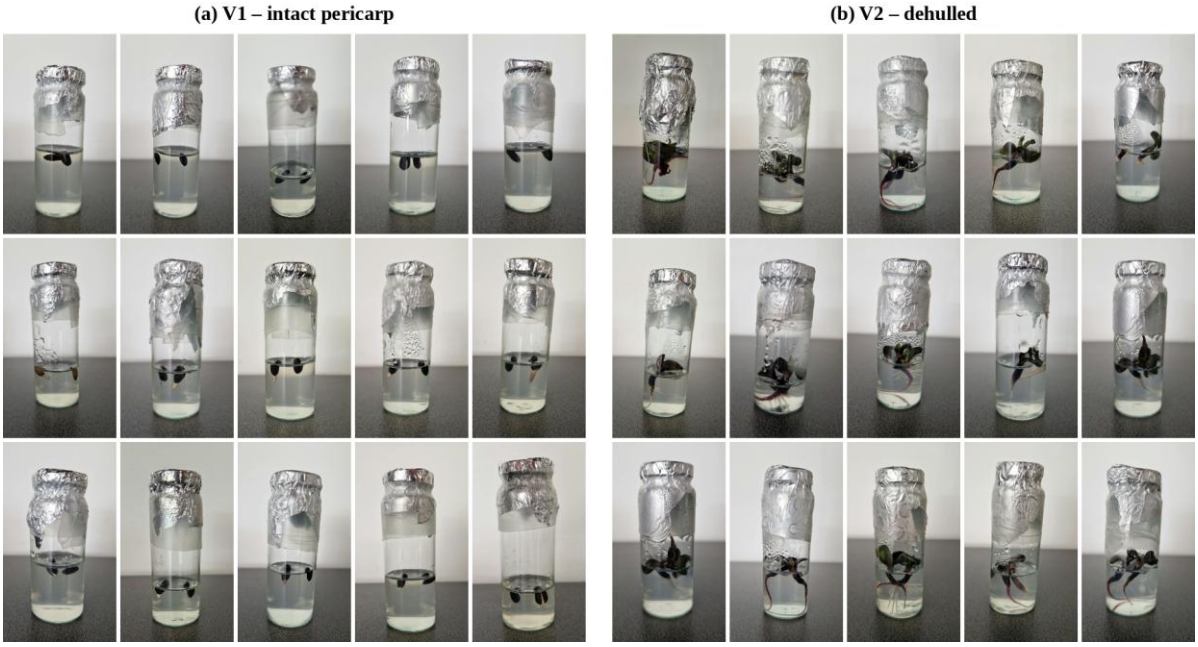


Figure 2. Seeds with an intact pericarp (a) and dehulled seeds (b) 14 days after inoculation

At 21 days, the dehulled seeds developed vigorous seedlings with long, branched root systems and well-differentiated aerial parts, whereas the seeds with an intact pericarp, although most of them had germinated, displayed short roots and reduced shoot growth, remaining clearly behind in development (Figure 3).

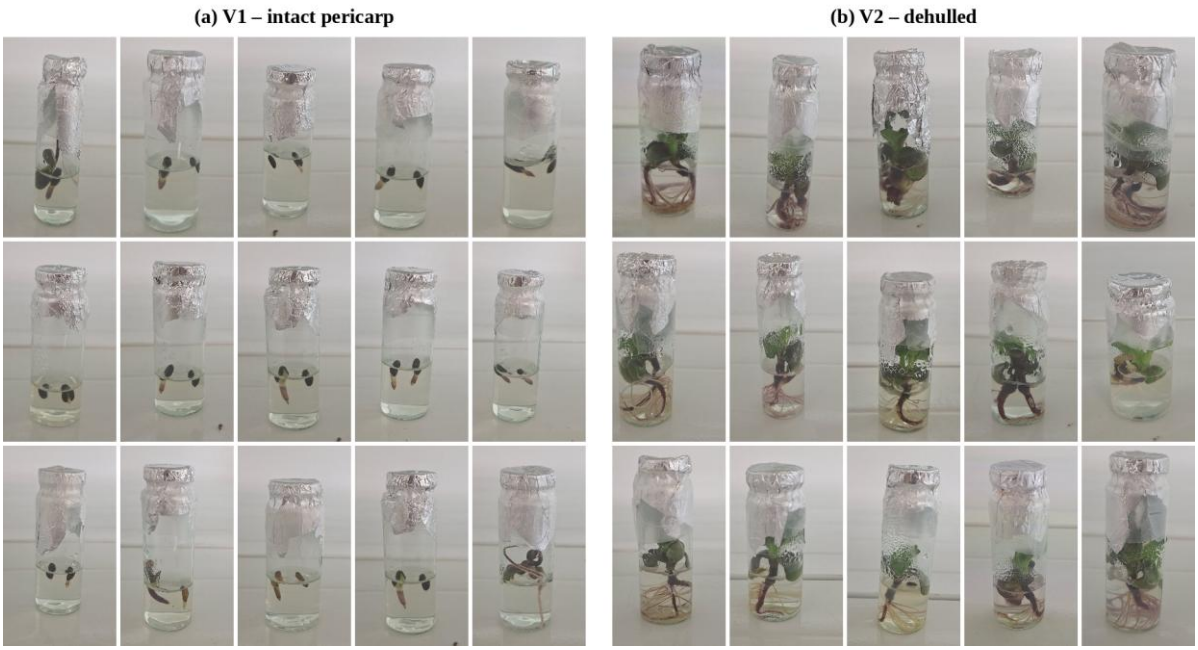


Figure 3. Seeds with an intact pericarp (a) and dehulled seeds (b) 21 days after inoculation

These differences stem primarily from the pericarp, which acts as a physical, mechanical and physiological barrier. The rigid, sclerenchymatous outer shell resists radicle expansion, delaying germination, while its removal significantly stimulates germination and yields higher germination percentages [15]. Partial damage or complete removal of the pericarp also facilitates water imbibition and helps alleviate seed dormancy [16]. In addition, sunflower seed dormancy is strongly regulated by hormonal balance, abscisic acid maintaining dormancy and

gibberellins promoting germination [17], and the pericarp and seed coats contribute to germination inhibition by restricting the availability of oxygen to the embryo [18]. The slow but continuous increase in the germination of intact seeds observed in this study is consistent with such a gradual, physically imposed delay rather than with a deep physiological dormancy.

Conclusion

Pericarp removal had a clear and significant effect on the germination and early seedling development of sunflower under *in vitro* conditions. Dehulled seeds reached 80% germination within 7 days and 93.3% after 21 days, forming well-differentiated seedlings with elongated, branched roots, whereas seeds with an intact pericarp germinated slowly (13.3% at 7 days, 70% at 21 days) and remained behind in development.

The pericarp acts as a physical, mechanical and physiological barrier that restricts water uptake, oxygen diffusion and radicle expansion, contributing, alongside hormonal mechanisms, to delayed germination. Dehulling is therefore recommended as a simple and effective step for obtaining rapid, synchronous and uniform *in vitro* sunflower cultures.

References

[1] I. Ozyigit, N. Gozukirmizi, B. Semiz, Russ. J. Plant Physiol. 53 (2006) 556.
[2] I.I. Ozyigit, N. Gozukirmizi, B.D. Semiz, Afr. J. Biotechnol. 6 (2007) 1498.
[3] E. Onișan, N.M. Horablaga, I. Samfira, C. Mate, I. Petrescu, Res. J. Agric. Sci. 58 (2026) 173.
[4] D. Pitariu, E. Onisan, M.N. Horablaga, P. Rain, Res. J. Agric. Sci. 57 (2025) 375.
[5] F. Chen, et al., PLoS ONE 19 (2024) e0298299.
[6] E. Onisan, C. Petolescu, A. Tenche-Constantinescu, I. Petrescu, et al., Appl. Sci. 15 (2025) 1576.
[7] M. Cristian, A. Simina, C. Petolescu, S. Popescu, A. Tenche-Constantinescu, et al., J. Hortic. For. Biotechnol. 29 (2025) 211.
[8] V. Mildažienė, et al., Sci. Rep. 9 (2019) 6437.
[9] E. Onisan, A. Simina, C. Petolescu, S. Popescu, A. Tenche-Constantinescu, et al., J. Hortic. For. Biotechnol. 29 (2025) 218.
[10] A.A. Khodabandeh, Optimizing *in vitro* culture conditions for sunflower (*Helianthus annuus* L.) seed germination and seedling growth, ResearchGate (accessed 13.09.2026).
[11] F. Corbineau, S. Bagniol, D. Côme, Isr. J. Plant Sci. 39 (1990) 313.
[12] A. Haj Sghaier, H. Khaeim, Á. Tarnawa, G.P. Kovács, C. Gyuricza, Z. Kende, Agriculture 13 (2023) 608.
[13] K. Inoka, N. Dahanayake, Int. J. Sci. Res. Publ. 5 (2015) 1.
[14] K. Ilyosiddinova, et al., Acta NUUz 3 (2025) 95.
[15] A.-S. Lachabrouilli, K. Rigal, F. Corbineau, C. Bailly, Eur. J. Agron. 124 (2021) 126209.
[16] A. Presotto, M. Poverene, M. Cantamutto, Ann. Appl. Biol. 164 (2014) 373.
[17] J. Bianco, G. Garello, M.T. Le Page-Degivry, Seed Sci. Res. 4 (1994) 57.
[18] C. Gay, F. Corbineau, D. Côme, Environ. Exp. Bot. 31 (1991) 193.

ENVIRONMENTAL AND DEVELOPMENT ASPECTS OF *Prunus persica* VARIETIES

Adriana Jicmon[1], Narcis Baltag[1], Melisa Ciora[1], Andreea Gabor[1], Emilian Onișan[1*], Irina Petrescu[1], Adalbert Okros[2]

[1]University of Life Sciences "King Mihai I" from Timișoara, Calea Aradului 119, 300645 Timișoara, Romania
[2]Faculty of Agriculture, University of Life Sciences "King Mihai I" from Timișoara, Calea Aradului 119, 300645 Timișoara, Romania
corresponding e-mail: Emilian.onisan@usvt.ro

Abstract

The peach (*Prunus persica*) is a fruit species whose growth, productivity and fruit quality are strongly shaped by pedoclimatic conditions, particularly low winter temperatures, late spring frosts and the water regime. This study assessed the morphological response of the fruits of two peach varieties frequently cultivated in western Romania, Champion and Redhaven, grown under the same local environmental conditions. Fruit weight, height, diameter and shape index (diameter/height ratio) were determined, characterised by descriptive statistics and compared between varieties using Welch's t-test. Champion produced significantly heavier (90.65 g vs. 40.28 g; $p = 0.010$) and wider fruits (53.03 mm vs. 42.06 mm; $p = 0.029$) than Redhaven, whereas fruit height (45.82 mm vs. 37.75 mm) and shape index (1.15 vs. 1.11) did not differ significantly. The results indicate a better use of water and nutrient resources by Champion, a more conservative ecological strategy in Redhaven and a higher stability of fruit shape compared to fruit size, information that is useful for orchard management under climate change.

Introduction

With an impressive annual fruit production worldwide, the peach (*Prunus persica*) is a species of particular importance, whose development and geographical distribution are strongly influenced by environmental factors. Among these, low temperatures are a major factor that delimits and restricts the growth and adaptability of the peach in various regions [1].Current climate change, characterized by extreme weather events such as late spring frosts and high temperatures that extend into the autumn months, seriously threatens peach production and the viability of fruit buds [2, 3]. Weather conditions during the growing season influence not only yield but also the physiological quality of the harvested product [4], and the development of genotypes adapted to the current environmental conditions of Romania has become a priority in plant breeding [5]. Thus, in addition to varietal diversity, the growing environment and climatic adaptability determine the quantity and quality of world production [6]. Depending on soil type, temperature and rainfall, peaches accumulate different amounts of nutrients, being a valuable source of vitamin C, vitamin A and antioxidants that protect cells from oxidative damage [7, 8]. Understanding how ecological conditions affect the phenotype is therefore key to ensuring a high-quality harvest [9].

The peach is a fruit tree species of the Rosaceae family. Its range has historically been shaped by extensive cultivation and by its adaptation to different pedoclimatic conditions, the species thriving in areas where its climatic requirements are met. The peach is a medium-sized tree whose vegetative characteristics are influenced by sunlight and water availability. In terms of climate, the peach prefers a temperate climate, with hot summers and cold winters. Quantitative exposure to low temperatures (the chilling requirement) is essential for the development of flower buds and for avoiding lethal spring frosts [3, 10, 11]. Stable temperatures from the spring months onwards are equally important, as a false spring can cause early budding

or bud freezing, exposing the tree to frost damage [6, 10, 12]. The peach prefers direct sun exposure (6–8 hours daily) and thrives in well-drained soils with a pH of 6.0–7.0 [13]. Soils with good porosity allow an efficient exploration by the root system, preventing water stress and root asphyxiation [14].

The aim of this paper was to assess the morphological parameters of the fruits of two peach varieties grown under identical conditions in western Romania and to evaluate their adaptability to the local growing environment.

Experimental

Experimental variants

The analysis focused on the impact of environmental factors on two varieties frequently cultivated in western Romania, a region whose climatic and edaphic conditions strongly shape the development of woody species [15] (Figure 1):

V1 – Champion. Adapted to areas with abundant insolation, it has good resistance to biotic (diseases and pests) and abiotic factors. The fruits can be affected by water stress, which makes water management essential.

V2 – Redhaven. A variety with high self-fertility and adaptability, optimally placed on southern or south-western exposures to make the most of the thermal and light regime. Its root system tolerates medium soils well and pH values between 5.7 and 7.5.



V1 – Champion V2 – Redhaven

Figure 1. The two peach varieties studied: V1 – Champion and V2 – Redhaven

Biological material and environmental conditions

The peach has high temperature requirements (optimum 14–35 °C) and is vulnerable to frosts below −24 °C. In Romania, the thermal amplitude and the precipitation regime (700–1,100 mm required annually) play a defining role in shaping the morphological development of the studied varieties. Both varieties were grown under the same local pedoclimatic conditions.

Measurements

Three fruits per variety (n = 3) were analysed. Fruit weight was determined with a digital balance, and fruit height (length) and diameter were measured with a digital calliper (Figure 2). The shape index was calculated as the ratio between fruit diameter and fruit height.

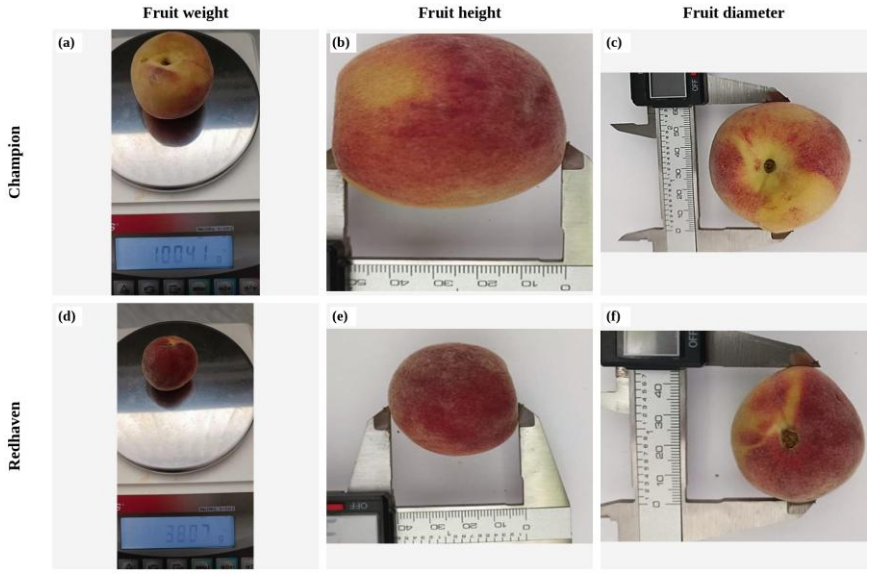


Figure 2. Measurement of fruit weight, height and diameter in Champion (a–c) and Redhaven (d–f).

Statistical analysis

For each trait, the mean, standard error of the mean (SE), standard deviation (SD), coefficient of variation (CV), minimum, maximum and the 95% confidence interval (CI) of the mean were calculated, an approach commonly used for the evaluation of morphological traits in crop plants [16]. Differences between the two varieties were tested with Welch's two-sample t-test (unequal variances) at a significance level of $\alpha = 0.05$.

Results and discussion

The descriptive statistics of the four morphological traits are presented in Table 1, the comparison between the two varieties in Table 2 and the graphical representation of the results, including the individual fruits, in Figure 3.

Table 1. Descriptive statistics of fruit morphological traits in the two peach varieties (n = 3)

Trait	Variety	Mean ± SE	SD	CV (%)	Min – Max	95% CI
Weight (g)	Champion	90.65 ± 5.85	10.14	11.2	80.15 – 100.40	65.45 – 115.86
	Redhaven	40.28 ± 1.30	2.25	5.6	38.07 – 42.56	34.70 – 45.86
Height (mm)	Champion	45.82 ± 0.74	1.28	2.8	44.90 – 47.29	42.64 – 49.01
	Redhaven	37.75 ± 2.47	4.28	11.3	33.80 – 42.29	27.13 – 48.37
Diameter (mm)	Champion	53.03 ± 2.17	3.77	7.1	48.72 – 55.71	43.66 – 62.40
	Redhaven	42.06 ± 2.46	4.26	10.1	38.34 – 46.72	31.45 – 52.66
Shape index	Champion	1.150 ± 0.036	0.062	5.4	1.080 – 1.200	0.995 – 1.305
	Redhaven	1.113 ± 0.008	0.014	1.3	1.100 – 1.130	1.077 – 1.149

SE – standard error; SD – standard deviation; CV – coefficient of variation; CI – confidence interval of the mean.

Table 2. Differences between Champion and Redhaven for the analysed traits (Welch's t-test)

Trait	Difference (Champion – Redhaven)	Relative difference (%)	t	p
Weight	50.37 g	+125.0	8.40	0.010 *
Height	8.07 mm	+21.4	3.13	0.072 n.s.
Diameter	10.97 mm	+26.1	3.34	0.029 *
Shape index	0.037	+3.3	1.01	0.411 n.s.

* significant difference ($p < 0.05$); n.s. – not significant.

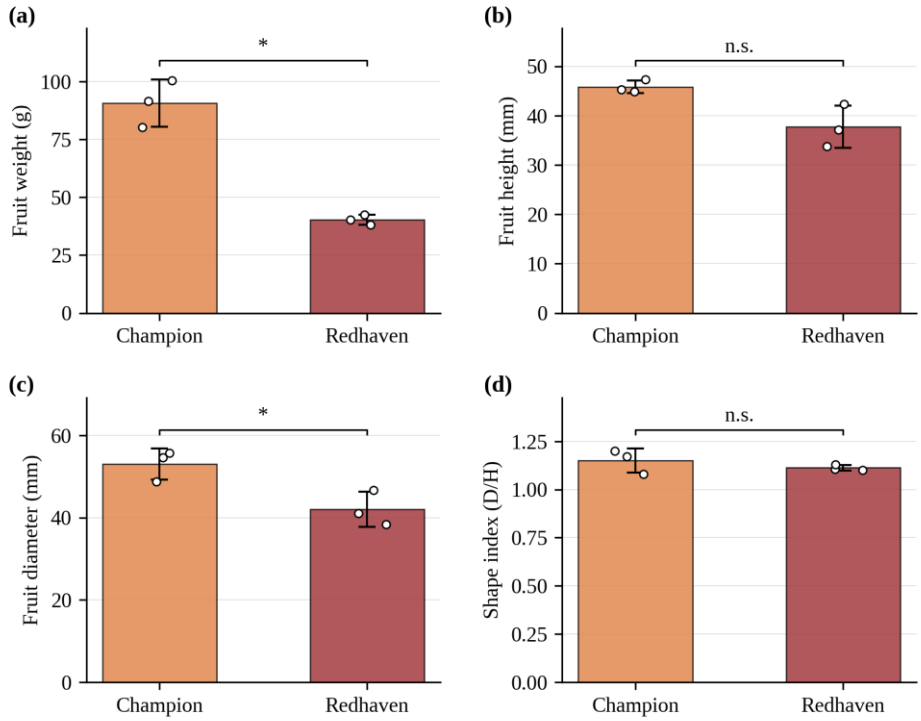


Figure 3. Fruit weight (a), height (b), diameter (c) and shape index (d) in the two peach varieties. Bars show the mean, error bars the standard deviation and dots the individual fruits; * $p < 0.05$, n.s. – not significant

Fruit weight

Under the influence of local climatic conditions, Champion produced fruits with a mean weight of 90.65 ± 5.85 g, more than twice the value recorded for Redhaven (40.28 ± 1.30 g). The difference of 50.37 g (+125%) was statistically significant ($p = 0.010$) and was the most pronounced varietal difference observed (Figure 3a). The fruits of Champion were also more variable (CV = 11.2%) than those of Redhaven (CV = 5.6%), which may reflect a stronger sensitivity of fruit growth to local water and nutrient availability [9, 13].

Fruit height

Factors such as solar radiation and precipitation resulted in a mean fruit height of 45.82 ± 0.74 mm for Champion and 37.75 ± 2.47 mm for Redhaven. Although the fruits of Champion were on average 21.4% taller, the difference was not statistically significant ($p = 0.072$), mainly because of the high variability of Redhaven (CV = 11.3%), whose fruits ranged from 33.80 to 42.29 mm (Figure 3b).

Fruit diameter

The availability of nutrients in the soil, a key factor for the expression of yield components [17], supported a mean fruit diameter of 53.03 ± 2.17 mm for Champion, significantly higher ($p = 0.029$) than that of Redhaven (42.06 ± 2.46 mm). Together with fruit weight, diameter was the trait that best differentiated the two varieties under the local growing conditions (Figure 3c).

Fruit shape index

The shape index was 1.15 for Champion and 1.11 for Redhaven, without significant differences between the varieties ($p = 0.411$). Values above 1 indicate slightly flattened fruits in both varieties, while the very low variability of Redhaven (CV = 1.3%) shows a highly uniform fruit shape (Figure 3d). Under the same growing conditions, fruit shape was thus more stable than fruit size, although chilling accumulation during endodormancy is known to influence fruit shape development in peach [11].

Overall, under identical growing conditions, Champion exceeded Redhaven by 125% in fruit weight and 26% in fruit diameter, whereas fruit height and shape index did not differ significantly. These results reflect the genotype-specific response of the two varieties to the same local environment and are consistent with the strong influence of the water regime on peach fruit size reported in other studies [9, 13]. Given the small number of fruits analysed, the results should be regarded as preliminary and confirmed on larger samples and over several growing seasons.

Conclusion

Adaptability to the environment directly influences the morphological characteristics of peach fruits. Under the pedoclimatic conditions of western Romania, the Champion variety produced significantly heavier (90.65 g vs. 40.28 g) and wider (53.03 mm vs. 42.06 mm) fruits than Redhaven, indicating an efficient use of water and nutrient resources. Fruit height and shape index did not differ significantly between the two varieties, and the low variability of the shape index suggests that fruit shape is a more stable trait than fruit size.

The smaller fruits of Redhaven suggest a different ecological plasticity, probably oriented towards resource conservation under water stress or temperature fluctuations. Assessing the interaction between the orchard and the growing environment remains essential for the sustainable management of peach orchards in the context of climate change.

References

[1] Y. Li, et al., Front. Plant Sci. 14 (2023) 1153902.
[2] C. Gottschalk, et al., Sci. Rep. 16 (2026) 18553.
[3] J. Liu, et al., Plants 10 (2021) 1266.
[4] V. Orkić, S. Kujundžić, S. Grubišić Šestanj, B. Ravnjak, S. Petrović, S. Vila, et al., Agronomy 15 (2025) 2115.
[5] E. Onișan, N.M. Horablaga, I. Samfira, C. Mate, I. Petrescu, Res. J. Agric. Sci. 58 (2026) 173.
[6] U. Caglar, J.M. Lawton, J.C. Melgar, K. Gasic, Agronomy 14 (2024) 302.
[7] M.I. Gil, F.A. Tomás-Barberán, B. Hess-Pierce, A.A. Kader, J. Agric. Food Chem. 50 (2002) 4976.
[8] C.M. Cantín, M.A. Moreno, Y. Gogorcena, J. Agric. Food Chem. 57 (2009) 4586.
[9] I. Toumi, O. Zarrouk, M. Ghrab, K. Nagaz, Plants 11 (2022) 1656.
[10] D.G. Bielenberg, K. Gasic, Front. Plant Sci. 13 (2022) 801606.
[11] Y. Li, et al., J. Integr. Agric. 15 (2016) 1267.
[12] E. Fadón, S. Herrera, B.I. Guerrero, M.E. Guerra, J. Rodrigo, Agronomy 10 (2020) 409.
[13] R. Alcobendas, J.M. Mirás-Avalos, J.J. Alarcón, E. Nicolás, Sci. Hortic. 164 (2013) 340.
[14] M.L. Amador, S. Sancho, B. Bielsa, J. Gomez-Aparisi, M.J. Rubio-Cabetas, Physiol. Plant. 144 (2012) 357.
[15] A.M. Țenche-Constantinescu, C. Berar, E. Onișan, I. Sărac, S. Popescu, et al., Plants 15 (2026) 603.
[16] E. Onișan, N.M. Horablaga, I. Samfira, C. Mate, G. Gorinoiu, Res. J. Agric. Sci. 58 (2026) 166.
[17] A.M. Baciu, K. Lorincz, G. Mike, I. Sărac, E. Onișan, et al., Appl. Sci. 16 (2026) 7103.

PRETREATMENT WITH SYNTHETIC CROSS-KINGDOM MICROBIAL CONSORTIA RADICALLY IMPROVES BIOGAS PRODUCTION FROM WHEAT STRAW

Annabella Juhász-Erdélyi [1], Kornél L. Kovács [1], Márta, Huszár[1], Roland Wirth [2], Márk Szuhaj [1], Attila Farkas [2], Gergely Maróti [2], Zoltán Bagi [1], Etelka Kovács [1]

[1] *Department of Biotechnology and Microbiology, Faculty of Science and Informatics, University of Szeged;*
[2] *Institute of Plant Biology, HUN-REN Biological Research Centre, Szeged*
email: erdelyi.annabella@stud.u-szeged.hu

Abstract
The primary objective of this research was to investigate biogas production from recalcitrant raw wheat straw by employing selectively assembled, rumen-derived microbial consortia (anaerobic fungi, methanogenic archaea, and bacteria) as pretreatment [1,2]. Results demonstrated that a 7-day pretreatment with the cross-kingdom consortia increased biomethane yields by 35–70% and augmented volatile fatty acid production.
This novel approach delineates a microbiological strategy to improve yields in advanced biogas technologies, strongly supporting the transition to a sustainable circular economy by efficiently converting agricultural residue into renewable energy [3-5].

Introduction
Lignocellulosic biomass represents a vast renewable resource for biogas production, but its complex structure makes degradation challenging [6]. Anaerobic fungi (AF) drive the efficient hydrolysis of plant fibers in herbivore rumen [7-9], but they are practically absent from conventional biogas reactors [10-14]. Previous in vitro studies have shown that co-cultivation of AF with methanogenic archaea (M) and fibrolytic acteria (B) significantly enhances methane yields [15]. Building on this knowledge, the present study aimed to identify optimal microbial partners for AF from the rumen microbiome and to apply these targeted, cross-kingdom synthetic consortia in pretreatment of wheat straw, thereby improving overall biogas production efficiency [5,16].
To track the active migration and syntrophic interactions of ruminal microorganisms, an innovative "microbial racecourse" reactor was employed [15]. A distinct colonization sequence of interacting partners on the wheat straw was observed: AF zoospores acted as the primary colonizers, followed closely by methanogenic archaea and specialized bacteria. Scanning electron microscopy (SEM) and volatile fatty acid (VFA) profiling validated this colonization, demonstrating extensive lignocellulose structural degradation within 72 hours.
Metagenomic characterization of active microbial participants uncovered the assembly of tailored synthetic consortia. These featured the anaerobic fungus *Neocallimastix lanati* associated with specific methanogens (*Methanobrevibacter gottschalkii* or *M. ruminantium*) and bacterial partners (*Butyrivibrio hungatei* or *Succiniclasticum ruminis*).

Results and Discussion
During subsequent biochemical methane potential (BMP) tests, the efficacy of the 7-day pretreatment became strikingly apparent. Wheat straw pretreated with the complete tripartite (AF + M + B) consortia yielded a 35–70% increase in biomethane compared to untreated samples. This enhancement was driven by profound mechanical and metabolic synergy: the AF zoospores develop invasive rhizoids to physically disrupt the tough lignocellulosic matrix, while surface-anchored bacteria and archaea efficiently metabolize the resulting hydrolysis

products. Distinct acetate and propionate profiles further indicated that the involvement of specific bacterial partners fundamentally optimized the underlying fermentation pathways.

Conclusion

This study successfully harnessed the potential of rumen-derived microbiota to overcome the recalcitrance of lignocellulosic biomass. By implementing the specialized cross-kingdom syntrophy found in the herbivore digestive tract, the targeted pretreatment with *N. lanati* and its optimal prokaryotic partners significantly boosted subsequent biomethane yields. Ultimately, these results highlight that maximizing methane production relies not merely on the individual fermentative capacities of microbes, but on the stability and redox balance of the entire metabolic network as well. Employing such tailored microbial communities can serve as a promising strategy for advancing renewable biogas technologies.

Acknowledgements

This study was supported in part by the Hungarian National Research, Development, and Innovation Fund (NRDIF) project 2020-3.1.2-ZFR-KVG-2020-00009 and 2020-1.1.2-PIACI-KFI-2020-00117. Etelka Kovács, Kornél Kovács L. and Zoltán Bagi received support from the Hungarian NRDIF fund projects PD 128345, PD132145, K143198, FK123902, and 2019-2.1.13-TÉT_IN-2020-00016. This study was also supported by: EKÖP-26-3 - SZTE-407.

References

1. Han, Y.; Chang, X.; Xiang, H.; Fang, Y.; Hao, L.; Gu, Y.; Han, X.; Zhao, B.; Zhao, Z.; Zhao, C.; et al. Exploring biomimetic potential of ruminant digestion strategies for lignocellulosic biomass utilization: A comprehensive review. Renew. Sustain. Energy Rev. 2023, 188, 113887.
2. Cheng, Y.F.; Edwards, J.E.; Allison, G.G.; Zhu, W.-Y.; Theodorou, M.K. Diversity and activity of enriched ruminal cultures of anaerobic fungi and methanogens grown together on lignocellulose in consecutive batch culture. Bioresour. Technol. 2009, 100, 4821–4828.
3. Sun, Y.; Cheng, J. Hydrolysis of lignocellulosic materials for ethanol production: A review. Bioresour. Technol. 2002, 83, 1–11.
4. Mosier, N.; Wyman, C.; Dale, B.; Elander, R.; Lee, Y.Y.; Holtzapple, M.; Ladisch, M. Features of promising technologies for pretreatment of lignocellulosic biomass. Bioresour. Technol. 2005, 96, 673–686.
5. Periyasamy, S.; Subrahmaniyan, V.; Mallick, S.; Santhalavan, S.; Kim, S.C.; Kim, S.W.; Sivakumar, S.; Varalakshmi, P. Recent advances in consolidated bioprocessing for conversion of lignocellulosic biomass into bioethanol—A review. Chem. Eng. J. 2023, 453, 139783.
6. Tong, X.; Smith, L.H.; McCarty, P.L. Methane fermentation of selected lignocellulosic materials. Biomass 1990, 21, 239–255.
7. Theodorou, M.K.; Mennim, G.; Davies, D.R.; Zhu, W.-Y.; Trinci, A.P.J.; Brookman, J.L. Anaerobic fungi in the digestive tract of mammalian herbivores and their potential for exploitation. Microbiology 1996, 142, 1573–1590.
8. Hartinger, T.; Zebeli, Q. The Present Role and New Potentials of Anaerobic Fungi in Ruminant Nutrition. Animals 2021, 11, 3127.
9. Kovács, E.; Szűcs, C.; Juhász-Erdélyi, A.; Bagi, Z.; Kovács, K.L. Anaerobic fungi: Effective warriors in lignocellulosic biomass degradation and fermentation. FEMS Microbiol. Ecol. 2025, 101, fiaf108.
10. Dollhofer, V.; Podmirseg, S.M.; Callaghan, T.M.; Griffith, G.W.; Fliegerová, K. Anaerobic fungi and their potential for biogas production. Adv. Biochem. Eng. Biotechnol. 2015, 151, 41–61.
11. Vinzelj, J.; Joshi, A.; Insam, H.; Podmirseg, S.M. Employing anaerobic fungi in biogas production: Challenges and opportunities. Bioresour. Technol. 2020, 300, 122687.

12. Bauchop, T.; Mountfort, D.O. Cellulose fermentation by a rumen anaerobic fungus in both the absence and the presence of rumen methanogens. Appl. Environ. Microbiol. 1981, 42, 1103–1110.
13. Jin, W.; Cheng, Y.F.; Mao, S.Y.; Zhu, W.Y. Isolation of natural cultures of anaerobic fungi and indigenously associated methanogens from herbivores and their bioconversion of lignocellulosic materials to methane. Bioresour. Technol. 2011, 102, 7925–7931.
14. Hobson, P.N.; Stewart, C.S. The Rumen Microbial Ecosystem; Springer: Berlin/Heidelberg, Germany, 1988.
15. Juhász-Erdélyi, A.; Huszár, M.; Farkas, A.; Maróti, G.; Wirth Szuhaj, M.; Bagi Z.; Kovács, K.L.; Kovács, E. Ruminal microbe consortia for biogas production from lignocellulosic substrate. Fermentation, 2026, 12, 247.
16. Lee, S.S.; Ha, J.K.; Cheng, K.-J. Relative contributions of bacteria, protozoa, and fungi to in vitro degradation of orchard grass cell walls and their interactions. Appl. Environ. Microbiol. 2000, 66, 3807–3813.

TARGETING FOOD SPOILAGE: EFFECT OF POTASSIUM SORBATE AND TYROSOL ON BACTERIAL GROWTH AND VIRULENCE TRAITS

Erika Beáta Kerekes[1], Urjinlkham Ryenchindorj[1], Viktória Gulyás[1], Csaba Vágvölgyi[1], Tamás Papp[1,2], Miklós Takó[1]

[1]Department of Biotechnology and Microbiology, Faculty of Science and Informatics, University of Szeged, H-6726 Szeged, Közép fasor 52, Hungary
[2]HUN-REN-SZTE Pathomechanisms of Fungal Infections Research Group, University of Szeged, H-6726 Szeged, Közép fasor 52, Hungary
e-mail: kerekeserika88@gmail.com

Food spoilage caused by bacterial contamination remains a critical challenge for food safety, economic stability and shelf-life extension. Food spoilage is often accelerated by biofilm formation regulated by the quorum sensing (QS) mechanism making these traits primary targets for modern food preservative strategies. While traditional chemical preservatives like potassium sorbate (POT) are widely used, there is a growing demand for combination with natural compounds to enhance efficiency and reduce chemical concentrations. Tyrosol is a natural bioactive phenolic compound exhibiting various health protective activities including antioxidant, antimicrobial, neuroprotective, anticancer and cardioprotective effects. In this study, the minimal inhibitory concentration (MIC), anti-biofilm and anti-QS potential of tyrosol and the synthetic preservative POT were assayed against *Bacillus cereus, Bacillus subtilis, Staphylococcus aureus, Escherichia coli* and *Pseudomonas putida* food-spoilage bacteria. The pigment producing biosensors *Chromobacterium violaceum* and *Serratia marcescens* were used for anti-QS experiments. Checkerboard experiments were prepared to assay the effect of the two compounds in combination. Results showed MIC values for tyrosol ranging between 2.5-5 mg/ml, while POT showed a wider range of 2-25 mg/ml. Tyrosol significantly inhibited biofilm formation in all bacteria except *S. aureus*. In contrast, POT inhibited only *E. coli* biofilm formation. Furthermore, POT inhibited the QS mechanism in both biosensor bacteria, whereas tyrosol affected only the pigment production of *S. marcescens*. In checkerboard experiments, an additive effect was recorded with the combination of POT and tyrosol against *P. putida* (FICI=1), *E. coli* (FICI=0.75), *B. subtilis* (FICI=0.75) and *C. violaceum* (FICI=0.62); in all other cases the combination was indifferent. Results indicate that these compounds can inhibit QS regulated traits, and the use of tyrosol alone or in combination can be a novel approach for food preservation. This research was funded by the National Research, Development and Innovation Office (NKFI grants PD 142122, 2024-1.1.1-KKV_FÓKUSZ-2024-00050 and 2025-1.2.4-TÉT-2025-00033).

PREPARATION OF TRICYCLIC 4-AMINOQUINAZOLINE DERIVATIVE BY ACID-CATALYZED ENVIRONMENTALLY BENIGN CASCADE REACTIONS

Shahd Seedahmed Siddig Khalfalla,[1,*] György Szőllősi[1,2,*]

[1]*SZTE, Institute of Pharmaceutical Chemistry, Eötvös utca 6, Szeged, 6720, Hungary.*
[2] *HUN-REN-SZTE, Stereochemistry Research Group, Institute of Pharmaceutical Chemistry, Eötvös utca 6, Szeged, 6720, Hungary.*
**Corresponding author: Shahd2481997@outlook.com ; szollosi@chem.u-szeged.hu*

Abstract

Nitrogen-containing heterocycles, particularly quinazolinone derivatives, are important scaffolds in medicinal chemistry because of their diverse biological activities. In this study, a sustainable, solvent-free approach for the synthesis of tricyclic quinazolinone derivatives was investigated through the reaction of anthranylhydrazide with ethyl levulinate, using acid catalysis. Initially, *p*-toluenesulfonic acid was employed to investigate the reaction pathway and the effects of temperature and reaction time on product formation. Subsequently, Amberlyst-15 was explored as a heterogeneous acid catalyst to improve the sustainability of the process and facilitate catalyst separation.

The reaction with *p*-toluenesulfonic acid afforded three tricyclic products: 4a-methyl-3,4,4a,5-tetrahydro-1*H*-pyridazino[6,1-*b*]quinazoline-2,10-dione; 4-amino-3a-methyl-2,3,3a,4-tetrahydropyrrolo[1,2-*a*]quinazoline-1,5-dione; 2-methyl-3H-pyridazino[6,1-*b*]quinazolin-10(4*H*)-one, with selectivity strongly dependent on temperature and reaction time. Importantly, the 4-amino-tetrahydropyrrolo[1,2-*a*]quinazolinone derivative, to the best of our knowledge, was not previously reported in the literature. Replacement of *p*-toluenesulfonic acid with the heterogeneous Amberlyst 15 followed by optimization of the reaction temperature, and catalyst amount in the presence of water significantly improved the selectivity toward the target product. Under the optimized conditions the 4-amino-tetrahydropyrrolo[1,2-*a*]quinazolinone derivative was obtained with approximately 93% selectivity. Overall, the study demonstrates that careful control of reaction conditions and the use of a heterogeneous acid catalyst enable selective formation of the previously unreported targeted quinolinone derivative under solvent-free conditions.

Introduction

N-containing heterocyclic compounds are among the most important structural scaffolds in medicinal chemistry [1]. Among these *N*-heterocycles, quinazolinone derivatives have attracted considerable attention because of their reported diverse pharmacological properties such as anticancer, antibacterial and anti-Alzheimer activities [2]. Quinazolinone derivatives have synthetic medicinal chemistry-friendly frameworks, which can be prepared via cyclocondensation reactions of anthranilamides with aldehydes or ketones. Moreover, carbonyl-containing compounds bearing an additional functional group can further increase the synthetic complexity of these reactions. When the second functionality is suitably positioned, as in γ-keto carboxylic acids and esters, a subsequent intramolecular cyclization can occur, allowing the formation of tricyclic quinazolinone scaffolds through one-pot cascade processes [3]. For further functionalization of these tricyclic quinazolinone derivatives, anthranylhydrazide can be used instead of the amide. An important precedent for the construction of tricyclic quinazolinone derivatives from anthranylhydrazide and a multifunctional carbonyl compound was reported by Schuler et al., as they prepared pyridazino[3,2-*b*]quinazoline derivatives by reacting anthranylhydrazides with levulinic acid,

and the reactions were performed in the presence of *para*-toluenesulfonic acid (*p*-TsOH) catalyst under reflux in benzene [4].

The development of more sustainable, environmentally benign synthetic methodologies has become increasingly important in modern organic chemistry, including the preparation of fine-chemicals and pharmaceutical intermediates. This aims to reduce solvent consumption, waste generation, and hazardous chemical use [5]. In this context, solvent-free reactions, one-pot processes, and catalytic methods have received significant attention. In particular, heterogeneous and recyclable acid catalysts offer advantages in catalyst recovery and product isolation [6]. Biomass-derived platform molecules are also attractive starting materials for sustainable synthesis. Levulinic acid, which can be obtained from lignocellulosic biomass [7], and its esters, such as ethyl levulinate [8], represent useful renewable building blocks for organic synthesis.

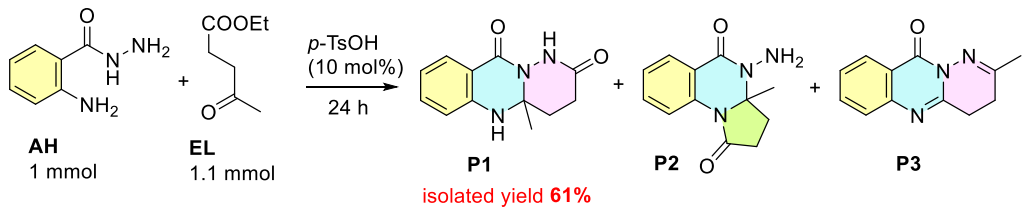
In our present study we aimed to develop environmentally benign, sustainable methods for the synthesis of a tricyclic quinazolinone derivatives by two subsequent cyclocondensations upon reacting anthranylhydrazide (**AH**) and ethyl levulinate (**EL**), as we attempted to use solvent-free reactions, one-pot processes, and heterogeneous recyclable acid catalysts.

Experimental

The anthranylhydrazide, ethyl levulinate, *para*-toluenesulfonic acid (*p*-TsOH) catalyst and the heterogeneous acid catalyst Amberlyst 15 (Amb-15) were obtained from commercial sources and used as received. The Amb-15 sold as beads was used after grinding with 30 Hz agitation frequency for 10 minutes in a 10 mL ZrO_2 grinding jar, applying 35 pieces of Ø 5 mm ZrO_2 grinding balls in a Retsch Mixing Mill MM 400 instrument. The reactions were carried out at one mmol scale in 4 mL closed glass vials under magnetic stirring and, when necessary, immersed in a preheated oil bath. After the given reaction time, the mixture was cooled to room temperature, then 3 mL methanol (MeOH) was added to dissolve the products. The heterogeneous Amb-15 catalyst was separated by centrifugation and washed twice with 2 mL MeOH, then the organic phases were combined. Thereafter, the resulting organic phases were analysed by GC-MSD. Products were purified by flash chromatography using a hexane/ethyl acetate eluent system or by crystallization from *i*Pr_2O-MeOH mixture and were analysed by NMR spectroscopy.

Results and discussion

We started our experiments with the reactions between the AH and EL using *p*-TsOH as a catalyst under solvent-free conditions, which were carried out in a conventional magnetically stirred system (Scheme 1).



Temperature	Selectivity (% by GC-MSD) P1	P2	P3
25°C	81	10	7
60°C	43	35	10

Scheme 1. Products obtained in the reaction of anthranylhydrazide with ethyl levulinate in the presence of *p*-TsOH catalyst, product **P1** was isolated from the reaction at 25°C in **61%** by flash chromatography or crystallization from *i*Pr_2O-MeOH mixture.

Firstly, the reactions were carried out at room temperature and stirred magnetically with 500 rpm for 24 h. 4a-Methyl-3,4,4a,5-tetrahydro-1*H*-pyridazino[6,1-*b*]quinazoline-2,10-dione (**P1**) was the major product isolated, as reported by Schuler et al. [4], beside two other products 4-amino-3a-methyl-2,3,3a,4-tetrahydropyrrolo[1,2-*a*]quinazoline-1,5-dione (**P2**) and 2-methyl-3*H*-pyridazino[6,1-*b*]quinazolin-10(4*H*)-one (**P3**). Then, while increasing the reaction temperature the selectivity of these three products changed dramatically (Scheme 1). The selectivity of **P2**, which is also a tricyclic quinazolinone derivative not described in the previous paper, increased [4]. Due to these observations, we started to examine the effect of temperature on product selectivity (Figure 1. a).

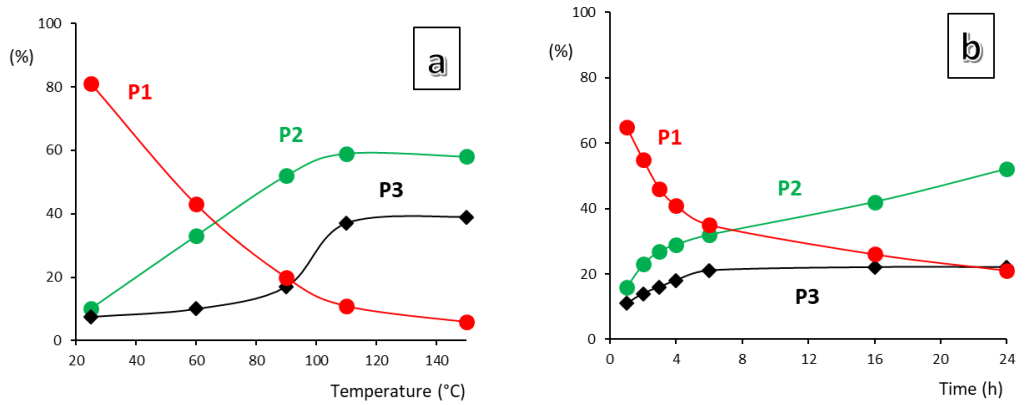


Figure 1. Effect of the temperature (**a**, 24 h) and evolution in time (**b**, 90°C) on the product composition (by GC-MSD) in the reaction of **AH** and **EL** using *p*-TsOH catalyst (10 mol%)

As Figure 1. **a** shows, at low temperature, **P1** had the highest selectivity, and as the temperature increased, **P2** selectivity increased and reached its maximum at 90°C. But at higher temperatures, we also had a significant amount of **P3**. These results demonstrate that increasing the temperature does not merely accelerate the reaction but changes the relative contribution of the competing reaction pathways. Low temperature favours **P1**, whereas elevated temperatures promote the formation of **P2** and, at still higher temperatures, **P3**. This behaviour suggests that **P1** is associated with a lower-energy, kinetically favoured pathway, while formation of **P2** and **P3** requires additional thermal activation.

Furthermore, to know how the reaction is proceeding the reaction was monitored as a function of time (Figure 1. **b**). The simultaneous decrease in **P1** and increase in **P2** and **P3** by time is particularly significant. This temporal relationship is consistent with the possibility that **P1** was formed initially as a kinetic product and subsequently undergoes further acid-catalyzed transformation (hydrolysis and cyclization) to give **P2**. Therefore, a sequential reaction process rather than three completely independent pathways occurred.

To improve the sustainability of the catalytic process, Amberlyst-15 (Amb-15), a heterogeneous acid catalyst, was used instead of homogeneous *p*-TsOH. The use of a heterogeneous catalyst may allow its easier separation and potentially enable its recovery and reuse. The effect of the reaction temperature on the product composition was also examined with this catalyst. The upper temperature limit was set at 110 °C to avoid the risk of compromising the stability of Amberlyst-15 [9].

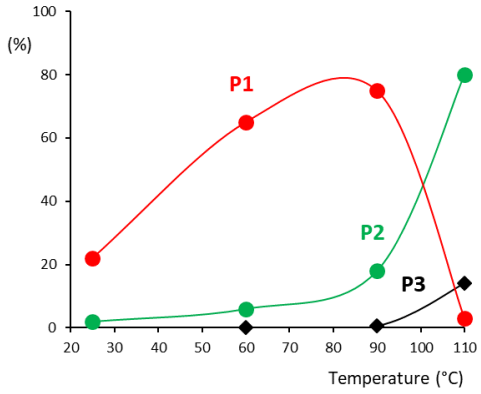
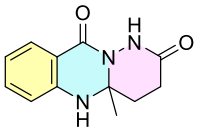


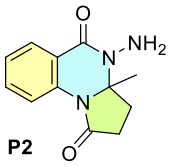
Figure 2. Effect of the temperature on the product composition (by GC-MSD) in the reaction of **AH** and **EL** using Amb-15 catalyst (100 mg, 47 mol%) in 24 h reactions

At lower temperatures, some intermediate compounds, mostly Schiff-bases based on their mass spectra, were detected, together with relatively low amounts of **P1**, **P2**, and **P3**. As the temperature was increased, **P1** selectivity also increased, whereas **P2** selectivity started to increase at 90 °C. Further increase of the temperature to 110 °C resulted in **P2** becoming the major product, while a significant amount of **P3** was also formed.

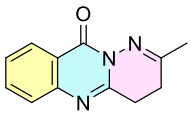
To further improve **P2** selectivity, a reaction temperature of 110 °C was initially selected based on the previous temperature-dependent experiment. We supposed that **P1** could undergo a subsequent acid-catalyzed transformation to **P2**, through hydrolytic cleavage of the tetrahydropyridazinone ring of **P1** followed by intramolecular cyclization to afford **P2**. To promote this possible transformation, a small amount of water was therefore added to the reaction mixture (Figure 3, entry 2). This resulted in decreased **P1** selectivity; however, it was accompanied by an increase in the formation of **P3** as well, and therefore slightly decreased **P2** selectivity (64%).



P1



P2



P3

Entry	Amb-15 (mg, mol%)	Temperature (°C)	Water additive (μL)	**Product** (% by GC-MSD) **P1**	**P2**	**P3**
1	100, 47 mol%	110	-	3	80	14
2	100, 47 mol%	110	100	1	64	28
3	75, 35 mol%	110	100	1	82	15
4	75, 35 mol%	90	100	-	93	2
5	§ 35 mol%	90	20 mmol scale		**77** (isolated yield, 3.56 g)	

Figure 3. Effect of the reaction conditions on the product selectivity (by GC-MSD) in the reaction of **AH** (1 mmol) and **EL** (1.1 mmol) using Amb-15 catalyst, 24 h; § reaction of 20 mmol **AH**, 22 mmol **EL** in presence of 1.5 g Amb-15 and 2 mL water, isolated yield following flash-chromatography

To decrease the formation of **P3**, the amount of Amberlyst-15 was subsequently reduced from 100 mg (47 mol%) to 75 mg (35 mol%) (Figure 3., entry 3). This modification resulted in a decrease in **P3** formation and a concomitant improvement in the selectivity toward **P2**, which increased to approximately 82%. As a further attempt to enhance the selectivity toward **P2**, the reaction temperature was lowered from 110 °C to 90 °C while maintaining the reduced catalyst

amount and the presence of water. Under these conditions, a remarkable increase in **P2** selectivity was observed, reaching approximately 93%, while the formation of **P3** was substantially suppressed. This optimized condition was subsequently applied on a much larger, 20 mmol scale, affording **P2** in an isolated yield of 77% following flash chromatography. The successful scale-up demonstrates that the optimized heterogeneous, recyclable Amb-15-catalyzed, solvent-free conditions provide an effective approach for the selective preparation of **P2**.

Conclusion

In summary, a solvent-free catalytic approach for the synthesis of tricyclic quinazolinone derivatives from anthranylhydrazide and ethyl levulinate was investigated. The reaction exhibited a strong dependence on both temperature and reaction time, resulting in the formation of three tricyclic products, a tetrahydro-1*H*-pyridazino[6,1-*b*]quinazolinedione (**P1**), a 4-amino-tetrahydropyrrolo[1,2-*a*]quinazolinedione (**P2**) and a pyridazino[6,1-*b*]quinazolinone (**P3**). Under homogeneous *p*-TsOH catalysis, **P1** was preferentially formed at lower temperatures, whereas increasing the reaction temperature favoured the formation of **P2** and, at higher temperatures, **P3**. The time-dependent study further showed a decrease in **P1** accompanied by an increase in **P2**, supporting the possibility of a sequential transformation in which **P1** undergoes further acid-catalyzed transformations.

To improve the sustainability of the process, Amberlyst-15 was investigated as a heterogeneous acid catalyst. Optimization of the catalyst amount, temperature, and addition of water enabled a significant improvement in the selectivity toward **P2**. Under the optimized conditions **P2** was obtained with approximately 93% yield by GC-MSD. Importantly, application of these conditions on a 20 mmol scale afforded **P2** in 77% isolated yield after purification. Overall, this study demonstrates that the use of a heterogeneous acid catalyst under solvent-free conditions provides an effective approach for the selective synthesis of the previously unreported tricyclic 4-amino-pyrrolo[1,2-*a*]quinazolinone derivative and highlights the potential of reaction-condition control for directing product selectivity in cascade cyclocondensation processes.

References

[1] É. Frank, G. Szőllősi, *Molecules* 26 (2021) 4617.
[2] S.K. Wahan, B. Sharma, P.A. Chawla, *J. Heterocycl. Chem.* 59 (2022) 239–257.
[3] V.J. Kolcsár, G. Szőllősi, *Molecules* 27 (2022) 5671.
[4] E. Schuler, N. Juanico, J. Teixidó, E.L. Michelotti, J.I. Borrell, *Heterocycles* 67 (2006) 161–173.
[5] P. Cintas, S. Tabasso, V.V. Veselov, G. Cravotto, *Curr. Opin. Green Sustain. Chem.* 21 (2020) 44–49.
[6] A. Kokel, C. Schäfer, B. Török, *Curr. Org. Synth.* 16 (2019) 615–649.
[7] E. Nzediegwu, M.-J. Dumont, *Waste Biomass Valor.* 12 (2021) 2825–2851.
[8] G.A.D. Castro, S.A. Fernandes, *Sustain. Energy Fuels* 5 (2021) 108–111.
[9] J. Guilera, E. Ramírez, C. Fité, M. Iborra, J. Tejero, *Appl. Catal. A: Gen.* 467 (2013) 301–309.

THE ROLE OF LACTIC ACID BACTERIA IN THE REDUCTION OF PESTICIDE RESIDUES IN FOOD AND FEED

Szandra Klátyik[1], Gergő Gyurcsó[1], Eszter Takács[1], Borbála Gémes[1], Mária Mörtl[1], Kewei Chen[2], Hui Shi[2], Muying Du[2], András Székács[1], Zsolt Zalán[3]

[1]Agro-Environmental Research Centre, Institute of Environmental Sciences, Hungarian University of Agriculture and Life Sciences, Tessedik S. u. 4, H-2100 Gödöllő, Hungary
[2]College of Food Science, Southwest University, No.2.Tiansheng Road, Beibei, Chongqing 400715, China
[3]Department of Bioengineering and Alcoholic Drink Technology, Institute of Food Science and Technology, Hungarian University of Agriculture and Life Sciences, Villányi út 29-43, H-1118 Budapest, Hungary
e-mail: klatyik.szandra@uni-mate.hu

Nowadays, intensive agricultural practices, the widespread use of pesticide formulations, as well as inappropriate harvesting technologies and timing can significantly contribute to the emergence of pesticide residues in agricultural commodities and food products. Due to the persistent characteristics of numerous pesticide active ingredients, their stability may be preserved both in the environment and during food processing. Consequently, various pesticide residues may be detectable in processed food products. The presence of such pesticide residues may pose risks to food safety and public health [1–2].

Lactic acid fermentation and lactic acid bacteria are known to provide beneficial effects from both nutritional and health perspectives. During lactic acid fermentation, the presence of lactic acid bacteria (primarily *Lactobacillus* and *Streptococcus* species) can contribute to the development and maintenance of a healthy gut microbiota, positively affect digestion, and support the immune system [3–5]. Furthermore, through various mechanisms (e.g., adsorption to the cell wall, enzymatic degradation, and biofilm formation), the levels of contaminants in food raw materials and products can be reduced by lactic acid bacteria [6–7].

In our initial model experiments, the inhibitory effects of the widely used and currently market-leading herbicidal active ingredient glyphosate (GLY) was tested in the form of pure active ingredient (GLY-isopropylammonium salt) and commercial herbicide formulation (Roundup Classic) containing a mixture of polyethoxylated tallow amines (POEA) as formulating agents. The inhibitory effect of POEA alone was also evaluated separately. The inhibitory effects of the tested compounds were studied on several lactic acid bacterial strains of probiotic, food technological, and nutritional significance (*Lactobacillus reuteri Protectis, Lactiplantibacillus plantarum 299v*, and *Lactobacillus acidophilus LA-5*). Although the applied GLY concentration of 400 mg/L GLY-isopropylammonium salt (equivalent to 296.4 mg/L GLY free acid) exceeds the residue levels typically detected in environmental samples and food products, the aim of the model experiments was to establish stress conditions that would allow a clearer evaluation of potential selection and adaptation processes. The selected concentration was also intended to improve the reproducibility and analytical reliability of the monitoring of possible biodegradation processes. The commercial formulation and the formulating agent were tested at concentrations corresponding to the selected GLY concentration, based on their respective proportions in the formulation.

Based on our results, the sensitivity of the investigated lactic acid bacteria varied considerably in response to the tested active ingredient, formulation agent, and commercial formulation, suggesting that strain-specific differences may play a decisive role in determining the efficiency of biodegradation and detoxification processes. In further studies, changes in pesticide residue

concentrations are planned to be monitored using environmental analytical methods, and the research will also be extended to include different food and feed matrices.

Acknowledgements
The authors gratefully acknowledge the support of the National Research, Development and Innovation Office through the Bilateral Scientific and Technological Cooperation project (2024-1.2.5-TÉT-2024-00043) and the project entitled “Support for Hungarian Participation in the Hungarian–Chinese Partner Institution Programme” (2025-1.2.7-HU-CN-PARTNER-2025-00022). This research was also supported by the Research Excellence Program of the Hungarian University of Agriculture and Life Sciences and by the Flagship Research Groups Program of the Hungarian University of Agriculture and Life Sciences.

References
[1] U. Bajwa, K.S. Sandhu, J. Food Sci. Technol. 51 (2014) 201–220.
[2] M.F. Ahmad, F.A. Ahmad, A.A. Alsayegh, M. Zeyaullah, A.M. AlShahrani, K. Muzammil, A.A. Saati, S. Wahab, E.Y. Elbendary, N. Kambal, M.H. Abdelrahman, S. Hussain, Heliyon 10 (2024) e29128.
[3] P. Petrova, A. Arsov, F. Tsvetanova, T. Parvanova-Mancheva, E. Vasileva, L. Tsigoriyna, K. Petrov, Nutrients 14 (2022) 2038.
[4] Y.L. Aguirre-Garcia, N.C. Cerda-Alvarez, R.M. Santiago Santiago, A.R. Chantre-López, S.D.C. Rangel-Ortega, R. Rodríguez Herrera, Fermentation 11 (2025) 378.
[5] M.M.A.N. Ranjha, B. Shafique, M. Batool, P.Ł. Kowalczewski, Q. Shehzad, M. Usman, M.F. Manzoor, S.M. Zahra, S. Yaqub, R.M. Aadil, Appl. Sci. 11 (2021) 11204.
[6] B. Maden, A.Y. Kumral, J. Agric. Food Chem. 68 (2020), 14988–14995.
[7] S. Yuan, C. Li, H. Yu, Y. Xie, Y. Guo, W. Yao, LWT 147 (2021) 111672.

COMPARATIVE ASSESSMENT OF THE ACUTE BEE TOXICITY OF NEONICOTINOID AND ANTHRANILIC DIAMIDE INSECTICIDES

Szandra Klátyik[1], Magda Hományiné Bohus[2], Eszter Takács[1], Borbála Gémes[1], Mária Mörtl[1], András Székács[1]

[1]Agro-Environmental Research Centre, Institute of Environmental Sciences, Hungarian University of Agriculture and Life Sciences, Tessedik S. u. 4, H-2100 Gödöllő, Hungary
[2]National Centre for Biodiversity and Gene Conservation, Department of Apiculture and Bee Biology, Isaszegi út 200, H-2100 Gödöllő, Hungary
e-mail: klatyik.szandra@uni-mate.hu

During the application of pesticide formulations, bees and other pollinators may be exposed to all components of these substances including their active ingredients through different exposure routes. The effects of neonicotinoid insecticides, inhibitors of the nicotinic acetylcholine receptors, on pollinators have been extensively studied, and bee-related risks associated with the use of imidacloprid, thiacloprid, thiamethoxam, and clothianidin, played a significant role in the restriction of their use within the European Union (EU) [1–4]. Anthranilic diamide insecticides, including chlorantraniliprole and cyantraniliprole, have a different mode of action based on the modulation of ryanodine receptors in target pests, and both active ingredients are currently on the market with valid approval in the EU [5]. The aim of the present comparative study was to compare the acute bee toxicity of five neonicotinoids (acetamiprid, clothianidin, imidacloprid, thiacloprid, and thiamethoxam) and two anthranilic diamides (chlorantraniliprole and cyantraniliprole).

Our comparative assessment was primarily based on the acute oral and contact LD_{50} values for the honey bee (*Apis mellifera*) reported in the Pesticide Manual and the Pesticide Properties DataBase (PPDB) [6–7]. The lowest acute oral LD_{50} values were reported for imidacloprid (0.004 µg/bee), clothianidin (0.004 µg/bee), and thiamethoxam (0.005 µg/bee). In contrast, values of 14.5 µg/bee for acetamiprid and 17.3 µg/bee for thiacloprid were reported, indicating differences of several orders of magnitude in acute toxicity among the neonicotinoids. Similar differences were observed for contact toxicity, with LD_{50} values of 0.024 µg/bee for thiamethoxam and 0.081 µg/bee for imidacloprid, compared with approximately 8.1 µg/bee for acetamiprid and 38.8 µg/bee for thiacloprid. Therefore, various neonicotinoids cannot be regarded as a homogeneous group in terms of acute bee toxicity.

Significant differences were also observed in the acute toxicity of the anthranilic diamides. For chlorantraniliprole, the oral LD_{50} was >104.0 µg/bee, while the contact LD_{50} was >4 µg/bee, indicating substantially lower acute toxicity, particularly via oral exposure, than that observed for imidacloprid, clothianidin, and thiamethoxam. For cyantraniliprole, the oral and contact LD_{50} values were >0.106 and >0.0934 µg/bee, respectively. Although the PPDB classifies these values as indicating high acute bee toxicity, the reported values represent lower limits. Consequently, the comparatively favourable acute toxicity profile of chlorantraniliprole cannot be generalized to anthranilic diamides as a whole.

In addition to acute toxicity, chronic and sublethal effects should also be considered. For thiacloprid, the PPDB reports a 10-day chronic LC_{50} of 3.1 µg/bee/day, whereas directly comparable chronic endpoints are not available in the same database for the other active ingredient assessed. However, the absence of such data should not be interpreted as evidence of an absence of chronic toxicity. Overall, the acute bee toxicity of the investigated active ingredients differed by several orders of magnitude. Chlorantraniliprole showed a more favourable acute toxicity profile than the highly acutely toxic neonicotinoids imidacloprid, clothianidin, and thiamethoxam. However, this conclusion cannot be directly extended to

cyantraniliprole or to anthranilic diamides as a whole. Additionally, the toxicity of pesticide formulations on bees may not be fully predicted from the individual toxicity of the active ingredient, since the presence of co-formulants may influence the overall toxicological profile of the formulation.

Acknowledgements
This research was supported by the EKÖP-MATE/2026/27/K University Research Scholarship Programme of the Ministry of Science and Technology from the source of the National Research, Development and Innovation Fund. The authors also gratefully acknowledge the support of the Flagship Research Groups Program of the Hungarian University of Agriculture and Life Sciences.

References
[1] EFSA, EFSA J. 11 (2013) 3066.
[2] EFSA, EFSA J. 11 (2013) 3068.
[3] EFSA, EFSA J. 11 (2013) 3067.
[4] EFSA, EFSA Support Publ. 15 (2018) 2397–8325.
[5] J.E. Casida, Chem. Res. Toxicol. 28 (2015) 560–566.
[6] J.A. Turner, The Pesticide Manual (2021)
[7] Pesticide Properties DataBase, https://sitem.herts.ac.uk/aeru/ppdb/en/atoz_insect.htm (accessed 25th September 2026)

ENHANCED BIOMETHANE PRODUCTION FROM BIODEGRADABLE PLASTICS FOLLOWING ANAEROBIC FUNGAL-METHANOGEN PRETREATMENT

Etelka Kovács[1], Roland Ancsa-Molnár[1], Annabella Juhász-Erdélyi[1], Márta Huszár[1], Márk Szuhaj[1], Gábor Feigl[2], Attila Bodor[1,2], Zoltán Bagi[1], Kornél Kovács[1]

[1]Department of Biotechnology and Microbiology, University of Szeged, Hungary
[2]MTA-SZTE Lendület "Momentum" Anthropogenic Stress and Plant Resilience Research Group, Department of Plant Biology, University of Szeged, Hungary

Abstract

The primary objective of this study was to investigate the potential of an anaerobic fungal–methanogen consortium to influence the anaerobic conversion of polymeric materials and to determine whether biological pretreatment can enhance subsequent biomethane production. Two biodegradable plastic materials, a corn starch-based poly(lactic acid) (Bio1) and a biodegradable agricultural mulch film (Bio2), were compared with conventional polyethylene (PE) and a polyurethane-based polymer dispersion (Impranil® DAH). The substrates were incubated with an anaerobic fungal–methanogen consortium isolated from chamois feces, followed by anaerobic digestion with industrial biogas digestate. Gas production, organic acid formation, esterase activity, and final methane production were monitored to characterize substrate-dependent responses.

The strongest response was observed for Bio1. During pretreatment, PLA generated substantially higher hydrogen and methane production than the other tested polymers, while subsequent anaerobic digestion resulted in 43.05 ± 1.29 mL methane following AF+M pretreatment compared with 24.65 ± 1.29 mL in the untreated control, corresponding to an approximately 74% increase. Bio1 also induced a pronounced increase in esterase activity, whereas PE and the other polymeric materials showed considerably weaker responses. These findings indicate that anaerobic fungal–methanogen pretreatment can substantially alter the subsequent anaerobic conversion of selected biodegradable plastics and may provide a promising biological approach for improving methane recovery from polymer-containing waste streams.

Introduction

Plastic accumulation represents a major environmental challenge because conventional synthetic polymers persist in terrestrial and aquatic environments and are resistant to biological degradation (1, 2). Although biodegradable plastics have been developed as alternatives to conventional polymers, their designation as "biodegradable" does not necessarily imply efficient degradation under all environmental conditions. In particular, the anaerobic conversion of biodegradable plastics under biogas fermentation conditions remains insufficiently understood (3).

Anaerobic digestion offers an attractive strategy for simultaneous waste treatment and renewable energy production. The process depends on a complex microbial network in which hydrolytic, fermentative, acetogenic and methanogenic microorganisms cooperate to convert organic substrates into methane and carbon dioxide (4). For polymeric substrates, however, hydrolysis and accessibility of the polymer structure can represent important limitations.

Anaerobic fungi (AF), members of the Neocallimastigomycota, possess highly efficient hydrolytic systems and invasive rhizoidal structures that enable extensive physical and enzymatic disruption of complex substrates. In natural anaerobic environments, they frequently interact syntrophically with methanogenic archaea, which utilize fungal fermentation products such as hydrogen and formate. Although the role of AF in lignocellulose degradation is well

established, their potential interaction with biodegradable polymers remains largely unexplored (5, 6).

Therefore, the present study investigated the response of conventional and biodegradable polymeric materials to anaerobic fungal–methanogen pretreatment. An AF+M consortium isolated from chamois feces was applied to two biodegradable plastics, conventional polyethylene and a polyurethane dispersion. Subsequent methane production was monitored to determine whether fungal–methanogen pretreatment could modify the biomethane potential of the tested materials. Esterase activity and fermentation-related parameters were additionally examined to provide functional evidence for substrate-dependent microbial responses.

Results and Discussion

Clear substrate-dependent differences were observed during the anaerobic pretreatment stage. Bio1 showed the strongest gas production response, generating 0.52 ± 0.21 mL hydrogen under AF+M conditions and 1.05 ± 0.10 mL under the cellulolytic control. In contrast, PE, Bio2 and Impranil® DAH showed only negligible hydrogen production. Methane production during pretreatment was similarly dominated by PLA, which produced 3.17 ± 0.27 mL methane under AF+M treatment, whereas methane formation remained below 0.2 mL for the other polymeric substrates.

The most pronounced effect of pretreatment became evident during the subsequent anaerobic digestion stage. Bio1 pretreated with the anaerobic fungal–methanogen consortium produced 43.05 ± 1.29 mL methane, compared with 24.65 ± 1.29 mL in the untreated control. Thus, AF+M pretreatment increased methane production by approximately 74%. Cellulolytic pretreatment also increased methane production, reaching 38.97 ± 1.31 mL, but remained below the yield obtained after AF+M treatment.

The response of the other polymers was considerably weaker. Conventional PE remained largely unaffected by AF+M pretreatment, producing 6.32 ± 2.05 mL methane compared with 6.18 ± 0.00 mL in the untreated control. Bio2 was similarly resistant, with methane production remaining within a narrow range of 5.33–5.92 mL across the treatments. Impranil® DAH showed no improvement following AF+M pretreatment. These differences indicate that the effect of anaerobic fungal pretreatment is strongly dependent on polymer composition and structure.

The enzymatic response further supported the substrate-dependent nature of the process. Bio1 treatments showed a pronounced increase in esterase activity during incubation, reaching approximately 0.067 under AF+M conditions and 0.061 under the cellulolytic treatment, compared with baseline values of approximately 0.004–0.006. In contrast, PE showed no measurable increase in esterase activity, while Bio1 displayed a moderate response and Bio2 only minor changes. Impranil® DAH remained close to baseline throughout the incubation period.

The strong response of Bio1 is consistent with the presence of hydrolysable ester bonds within its polymer backbone. Hydrolytic cleavage may generate soluble oligomeric and monomeric compounds that become accessible to anaerobic microbial metabolism. However, the observed esterase signal cannot by itself be interpreted as direct evidence of complete enzymatic Bio1 degradation, because abiotic hydrolysis and the release of soluble compounds from the polymer matrix may also contribute to the measured activity.

Taken together, the results suggest that the effect of AF+M pretreatment is not universal across polymer types. Rather, polymers with chemical structures susceptible to hydrolysis showed a substantially greater response than the chemically resistant PE control. The particularly strong response of Bio1 suggests that anaerobic fungal–methanogen consortia may modify the accessibility or availability of Bio1-associated carbon, resulting in more efficient subsequent conversion to methane. Importantly, the enhancement in methane production may reflect not

only direct polymer depolymerisation but also changes in soluble compounds and fermentation dynamics generated during pretreatment.

Conclusion

This study demonstrates a pronounced substrate-dependent effect of anaerobic fungal–methanogen pretreatment on the subsequent anaerobic conversion of polymeric materials. Among the tested substrates, PLA exhibited the strongest response, combining increased gas production during pretreatment, pronounced esterase activity and a 74% increase in subsequent methane production compared with the untreated control. In contrast, polyethylene and the second biodegradable polymer showed limited responsiveness, highlighting the importance of polymer chemistry in determining susceptibility to anaerobic biological treatment.

Overall, the results indicate that anaerobic fungal–methanogen consortia have potential as a biological pretreatment strategy for selected biodegradable plastics. Rather than representing a universal plastic-degradation system, the consortium appears to exert its strongest effects on polymers whose chemical structure permits hydrolytic transformation. Further investigation of the soluble products generated during pretreatment and their effects on methanogenic activity will be essential for distinguishing direct polymer conversion from changes in substrate accessibility and fermentation dynamics.

References

1.Sivan, A. (2011). New perspectives in plastic biodegradation. *Current Opinion in Biotechnology*, 22(3), 422–426.

2.Cózar, A., Echevarría, F., González-Gordillo, J. I., Irigoien, X., Ubeda, B., Hernández-León, S., et al. (2014). Plastic debris in the open ocean. *Proceedings of the National Academy of Sciences*, 111(28), 10239–10244.

3.Wei, R., & Zimmermann, W. (2017). Microbial enzymes for the recycling of recalcitrant petroleum-based plastics. *Microbial Biotechnology*, 10(6), 1308–1322.

4.Batstone, D. J., Keller, J., Angelidaki, I., et al. (2002). The IWA Anaerobic Digestion Model No.1 (ADM1). *Water Science and Technology*, 45(10), 65–73.

5.Youssef, N. H., Couger, M. B., Struchtemeyer, C. G., Liggenstoffer, A. S., Prade, R. A., Najar, F. Z., et al. (2013). The genome of the anaerobic fungus Orpinomyces sp. strain C1A reveals the unique evolutionary history of a remarkable plant biomass degrader. *Applied and Environmental Microbiology*, 79(15), 4620–4634.

6.Kovács, E., Szűcs, C., Juhász-Erdélyi, A., Bagi, Z., & Kovács, K. L. (2025). Anaerobic fungi: Effective warriors in lignocellulosic biomass degradation and fermentation. *FEMS Microbiology Ecology*, 101(11), fiaf108.

EARLY MORPHOLOGICAL CHANGES IN ROOT DEVELOPMENT INDUCED BY NANOPLASTICS AND PFAS CONJUGATES

Kamilla Kovács[1,2], Enikő Mészáros[1,2], Klaudia Hoffmann[1,2,3], Zsófia Liska[1,2] ,Bálint Bakk[4], István Szilágyi[4], Attila Bodor[2,3] Gábor Feigl[1,2]

[1]University of Szeged, Department of Plant Biology
[2]MTA-SZTE Lendület "Momentum" Anthropogenic Stress and Plant Resilience Research Group
[3]Department of Biotechnology and Microbiology, University of Szeged, Hungary
[4]MTA-SZTE Momentum Biocolloids Research Group, University of Szeged, Hungary
e-mail: kovacs.kamilla.03szte.hu

The increasingly frequent occurrence of micro- and nanoplastics in agricultural soils raises concerns regarding their effects on plant roots [1]. These effects may be particularly pronounced during the early stages of plant development, as changes in root growth can reflect disruptions in numerous fundamental physiological processes [2]. Therefore, changes in root morphology can serve as a useful tool for detecting plant responses to pollutants derived from plastics.

In this study, early root development was used as an indicator to evaluate the effects of model nanoplastics and their conjugates with per-and polyfluoroalkyl substances (PFAS). Sulfate-latex (SL; 120 nm, negatively charged) and amidine-latex (AL; 100 nm, positively charged) nanoparticles were tested individually as well as in combination with PFOA and PFOS.

Both latex nanoparticles stimulated root growth at a concentration of 10 ppm, whilst PFOA caused a significant reduction at the same concentration. Under the conditions studied, PFOS did not result in any detectable change in root growth. In the case of combined treatments, the SL conjugates continued to have a stimulating effect on root growth, whilst the effect characteristic of PFOA was absent. In contrast, in treatments combined with AL, the growth-promoting effect was reduced, and plant responses were primarily determined by the effect of PFAS concentration.

These results demonstrate the nanoplastic-PFAS interactions are non-additive, the biological outcome depends both on nanoplastic surface chemistry and on PFAS loading.

This work was supported by the PLAGROSYS - 2024-1.2.3-HU-RIZONT-2024-00010 project, funded by the National Research, Development and Innovation Office, Hungary, via the HU-RIZONT international research excellence cooperation program.

References

[1] Guo, Y., Zhang, D., Li, W., Zhao, Y., Su, W., Xing, Y., ... & Jiang, B. (2026). Interaction of Microplastics, Plants, and Rhizosphere: A Critical Review. *Molecules*, *31*(17), 3028.
[2] Yang, J., Chen, R., Zhang, H., Wang, R., & Zhang, Z. (2026). Molecular mechanism of silver nanoparticles inhibiting primary root growth of Oryza sativa L. *RSC advances*, *16*(17), 15187-15203.

EFFECTS OF COMBINED EXPOSURE TO POLYETHYLENE-BASED PLASTICS AND HEAVY METAL-CONTAMINATED WASTEWATER ON NITRO-OXIDATIVE HOMEOSTASIS IN OILSEED RAPE

Kamilla Kovács[1,2], Enikő Mészáros[1,2], Klaudia Hoffmann[1,2,3], Zsófia Liska[1,2], Attila Bodor[2,3], Gábor Feigl[1,2]

[1]University of Szeged, Department of Plant Biology
[2]MTA-SZTE Lendület "Momentum" Anthropogenic Stress and Plant Resilience Research Group
[3]Department of Biotechnology and Microbiology, University of Szeged, Hungary
e-mail: kovacs.kamilla.03szte.hu

Agricultural soils and their associated ecosystems are often exposed to complex mixtures of pollutants, the components of which may interact synergistically, antagonistically, or additively [1].
As a result, testing individual pollutants in isolation does not necessarily accurately reflect actual environmental conditions. This is particularly important in the case of plastics, which, as synthetic polymers, are widely used in many areas of modern life. Although plastics have numerous beneficial properties, after use, significant quantities end up in the environment, where they can persist for a long time and thus become a source of long-term contamination of ecosystems [2]. Irrigation with wastewater may further increase the accumulation of heavy metals in farmland, while the combined presence of plastic pollution and pollutants from wastewater may pose a complex abiotic stress to plants [3].

In this study, we investigated the effects of combined exposure to model wastewater containing multiple heavy metals, polyethylene (PE), and recycled polyethylene (rePE) on the dynamics of reactive oxygen and nitrogen species (ROS and RNS) in the root tips of oilseed rape (*Brassica napus* L.).

Based on the results, it can be concluded that the combined presence of plastics and wastewater in the investigated plant had a different effect on the balance of reactive oxygen and nitrogen species. This suggests a possible alteration in nitro-oxidative homeostasis. Morphological observations, meanwhile, suggest that incubation in wastewater modifies the effects of the plastic, and that the effect of the wastewater itself were also changes in the presence of plastic.

Our results suggested that interactions between polyethylene particles and pollutants present in wastewater do not simply elicit additive stress responses, but may result in complex physiological reactions involving a shift in the nitro-oxidative balance

The project was supported by the National Research, Development and Innovation Office, Hungary (NKFIH FK 142475) and by the Lendület "Momentum" Program of the Hungarian Academy of Sciences (LP2025-8/2025 to G.F).

[1] Vuong, A. M., Yolton, K., Braun, J. M., Lanphear, B. P., & Chen, A. (2020). Chemical mixtures and neurobehavior: a review of epidemiologic findings and future directions. *Reviews on environmental health*, *35*(3), 245-256.
[2] Geyer, R., Jambeck, J. R., & Law, K. L. (2017). Production, use, and fate of all plastics ever made. *Science advances*, *3*(7), e1700782.

[3] Jin, T., Tang, J., Lyu, H., Wang, L., Gillmore, A. B., & Schaeffer, S. M. (2022). Activities of microplastics (MPs) in agricultural soil: a review of MPs pollution from the perspective of agricultural ecosystems. *Journal of Agricultural and Food Chemistry*, *70*(14), 4182-4201.

SOLUTION EQUILIBRIA AND IRON BINDING PROPERTIES OF MDR-SELECTIVE 8-HYDROXYQUINOLINE DERIVATIVES

Hilda Kovács[1], Szilárd Tóth[2], István Szatmári[3], Gergely Szakács[2,4], Éva A. Enyedy[1]

[1]Department of Molecular and Analytical Chemistry, University of Szeged, Dóm tér 7-8, H-6720 Szeged, Hungary
[2]Drug Resistance Research Group, Research Centre for Natural Sciences, Hungarian Research Network (HUN-REN), Magyar tudósok körútja 2, H-1117 Budapest, Hungary
[3]Institute of Pharmaceutical Chemistry and Stereochemistry Research Group, Eötvös Loránd Research Network, University of Szeged, Eötvös u. 6, H-6720 Szeged, Hungary
[4]Center for Cancer Research, Medical University of Vienna, Borschkegasse 8a, A-1090 Vienna, Austria
e-mail: kovacs.hilda@chem.u-szeged.hu

Drug resistance is one of the biggest challenges in chemotherapy, and researchers are constantly searching for compounds that can overcome this problem. 8-Hydroxyquinoline (HQ) derivatives exhibit a broad spectrum of biological activities, including significant anticancer effects [1]. Among these compounds, HQ-based Mannich bases bearing a methyleneamine substituent at position 7 have been reported to have pronounced cytotoxicity, particularly against multidrug-resistant (MDR) cancer cell lines [2,3]. The biological activity of 8-hydroxyquinoline derivatives is frequently associated with their complexation with endogenous metal ions. Certain MDR-selective HQ derivatives have been reported to cause a significant reduction in intracellular iron levels, and some are capable of inducing the formation of redox-active copper(II) complexes [3].

Herein, we present a comparative study of the solution equilibrium properties of selected HQ derivatives, as well as their complexation with iron(II) and iron(III) ions. The investigated compounds include both MDR-selective derivatives and compounds exhibiting lower selectivity toward MDR cancer cells. The aim of this study is to elucidate the relationship between the physicochemical properties of the investigated HQ derivatives and their biological activity, with particular emphasis on their cytotoxic effects and selectivity toward MDR cancer cells. Such correlations may help to clarify the molecular features underlying their activity against MDR cancer cells and provide a more comprehensive understanding of the chemical determinants governing their biological effects.

Acknowledgements
This work was supported by the National Research, Development and Innovation Fund ANN 149481 project, and the EKÖP-26-4-SZTE-512 (H. K.) University Research Scholarship Program of the Ministry for Innovation and Technology, and Austrian Science Fund FWF 10.55776/PIN1280424.

References
[1] V. Oliveri, G. Vecchio, Eur. J. Med. Chem. 120 (2016) 252–274.
Y. Song, H. Xu, W. Chen, P. Zhan, X. Liu, Med. Chem.Commun. 6 (2015) 61–74.
[2] V. F.S. Pape, A. Gaál, I. Szatmári, N. Kucsma, N. Szoboszlai, C. Streli, F. Fülöp, É. A. Enyedy, G. Szakács, Cancers 13 (2021) 154.
[3] V. F. S. Pape, R. Palkó, S. Tóth, M. J. Szabó, J. Sessler, G. Dormán, É. A. Enyedy, T. Soós, I. Szatmári, G. Szakács, J. Med. Chem. 65 (2022) 7729–7745.

IRON CHELATION AND POTENTIAL MULTIDRUG RESISTANCE-SELECTIVE CYTOTOXICITY OF THE GRP78 INHIBITOR YUM70

Gerda T. Gátszegi[1], Szonja P. Pósa[2], Szilárd Tóth[3], Gergely Szakács[2], Éva A. Enyedy[1]

[1] *Department of Molecular and Analytical Chemistry, University of Szeged, Dóm tér 7-8, H-6720 Szeged, Hungary*
[2] *Center for Cancer Research, Medical University of Vienna, Borschkegasse 8a, A-1090 Vienna, Austria*
[3] *Drug Resistance Research Group, HUN-REN Research Centre for Natural Sciences, Magyar tudósok krt. 2, H-1117 Budapest, Hungary*

The GRP78 protein plays a key role in regulating the endoplasmic reticulum (ER) stress response, a process that tumour cells utilise to ensure their survival [1]. An 8-hydroxyquinoline derivative, YUM70 (*Figure 1*), is able to bind directly to GRP78, thereby inhibiting its function and inducing apoptosis in pancreatic cancer cells [1]. The compound has been shown to be effective in inhibiting tumour growth in both *in vitro* and *in vivo* studies. Notably, the structure of the YUM70 derivative contains a feature characteristic of multidrug resistance (MDR)-selective HQ derivatives (see the highlighted orange section) [2]. The mechanism of action of MDR-selective HQs is closely related to the stability of the complexes they form with Fe(II) and Fe(III) ions. However, the YUM70 derivative has not yet been tested on MDR cancer cell lines, and no solution equilibrium measurements have been reported.

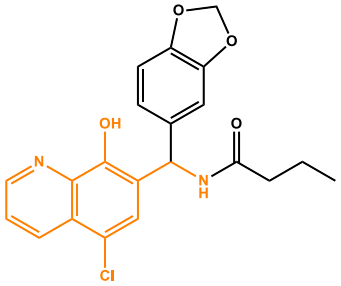


Figure 1. The chemical structure of YUM70.

In this study, we characterized the solution equilibrium properties and MDR-selectivity of YUM70. We investigated complex formation with iron(II) and iron(III) ions using UV-visible spectrophotometry, while the electrochemical properties of the resulting complexes were examined by cyclic voltammetry. We tested the compound's MDR-selective effect on parental and resistant cell lines. Furthermore, we synthesized derivatives incapable of chelation and examined their selectivity to confirm the role of chelation.

Acknowledgements
This work was supported by the National Research, Development and Innovation Fund ANN 149481 project, and the EKÖP-26-3-EKÖP-400 University Research Scholarship Program of the Ministry for Innovation and Technology (Hungary), and Austrian Science Fund FWF 10.55776/PIN1280424.

References
[1] S. Samanta, S. Yang, B. Debnath, D. Xue, Y. Kuang, K. Ramkumar, A.S. Lee, M. Ljungman, N. Neamati, Cancer Research 81 (2021) 1883–1895.
[2] V.F.S. Pape, R. Palkó, S. Tóth, M.J. Szabó, J. Sessler, G. Dormán, É.A. Enyedy, T. Soós, I. Szatmári, G. Szakács, J. Med. Chem. 65 (2022) 7729–7745.

CARBON QUANTUM DOTS FOR BENZYL ALCOHOL REMOVAL FROM AQUEOUS SOLUTION

Jelena Kozić[1], Jovana Prekodravac Filipović[1], Juan Carlos Colmenares Quintero[2], Biljana Todorović Marković[1]

[1]Vinca Institute of Nuclear Sciences-National Institute of the Republic of Serbia, University of Belgrade
[2]Institute of Physical Chemistry, Polish Academy of Sciences, Warsaw, Poland
e-mail: jelena.kozic@vin.bg.ac.rs

Abstract
Among organic contaminants in water, aromatic alcohols are an important group of compounds widely used as solvents, preservatives, and chemical intermediates in various industrial applications. [1,2] Benzyl alcohol (BnOH) is a neutral, non-chromophoric aromatic alcohol whose removal from aqueous systems can be challenging because of its chemical stability and low reactivity under mild conditions. [3]
Carbon Quantum Dots (CQDs) have attracted significant attention for their unique optical and surface properties. In presented work, pristine CQDs were synthesized from glucose as a carbon source. Compared with conventional synthesis approaches, this green, one-step, and low-cost method offers shorter reaction times, reduced energy consumption, and minimized formation of by-products. [4] The synthesized CQDs were subsequently investigated for their potential application in water treatment, focusing on the removal of BnOH through both adsorption and photocatalytic processes.
The obtained CQDs exhibited significant adsorption of BnOH in dark. Under 365 nm irradiation for 180 minutes, BnOH conversion remained stable at approximately 68-69%, corresponding closely to the adsorption equilibrium established during the dark period. Similarly, irradiation at 455 nm produced no evidence of photocatalytic degradation, with conversion remaining at approximately 56-59%. The lack of a progressive increase in BnOH conversion upon irradiation indicates that its removal by pristine CQDs is predominantly governed by adsorption rather than photocatalytic degradation. These results indicate the potential of pristine CQDs as sustainable adsorbents for the removal of neutral organic contaminants from aqueous systems.

Acknowledgements
This research was supported by the Ministry of Science, Technological Development and Innovations of the Republic of Serbia (grant number 451–03–33/2026–03/200017).

References
[1] H. Wu, R. Yan, A. Li, D. Huang, J. Pan, P. Zhao, Z. Xing, Efficient treatment of alcohol wastewater and its potential pollutant control strategies, Journal of Water Process Engineering 58 (2024) 104882. https://doi.org/10.1016/j.jwpe.2024.104882.
[2] G. Mu, D. Bian, M. Zou, X. Wang, F. Chen, Pollution and Risk Assessment of Polycyclic Aromatic Hydrocarbons in Urban Rivers in a Northeastern Chinese City: Implications for Continuous Rainfall Events, Sustainability 15 (2023) 5777. https://doi.org/10.3390/su15075777.
[3] Philip. Wexler, Encyclopedia of toxicology, Academic Press, 2014.
[4] J. Kozić, J.P. Filipović, D. Kleut, D. Mijin, Z. Marković, B. Ramadani, D. Giannakoudakis, B.T. Marković, Microwave–derived sustainable CQD as pH–robust nano–adsorbents for instant organic pollution adsorption, Materials Science and Engineering: B 332 (2026) 119647. https://doi.org/10.1016/j.mseb.2026.119647.

CLIMATE AND PEST-RELATED CHALLENGES IN HUNGARIAN WALNUT PRODUCTION

Pradeep Kumar and Mónika Máté

Department of Fruits and Vegetable Processing Technology, Institute of Food Science and Technology, Hungarian University of Agriculture and Life Sciences, Budapest, Hungary
e-mail: pradiip06@gmail.com

Abstract

Walnut (*Juglans regia* L.) is an important fruit crop in Hungary; however, national production has shown an unfavorable and increasingly variable trend in recent years despite the expansion of the cultivated area. According to data from the Hungarian Central Statistical Office, the total walnut orchard area increased from 6,396 ha in 2020 to 8,058 ha in 2024, while harvested production declined from 5,455 to 4,680 t (1). During the same period, the simple ratio of harvested production to total orchard area decreased from approximately 0.85 to 0.58 t ha^{-1}, indicating a substantial reduction in productivity. This short review summarizes the major environmental and phytosanitary factors that may contribute to declining and unstable walnut production in Hungary.

Among the environmental constraints, spring frost, prolonged drought and increasingly frequent periods of high temperature are of particular importance. Early vegetation development caused by mild late-winter and early-spring conditions may increase the vulnerability of walnut trees to subsequent frost events (2). At the same time, summer heat and water shortages can negatively affect fruit development, kernel filling and overall tree performance. Experimental studies have also demonstrated considerable differences in frost tolerance and environmental adaptation among walnut cultivars, emphasizing the importance of appropriate cultivar and site selection.

In addition to climatic stress, the invasive western walnut husk fly, *Rhagoletis completa*, represents a major phytosanitary challenge. The species was officially detected in Hungary in 2012 and has since become an important pest of walnut orchards. Larval feeding in the green husk can reduce nut quality, cause discoloration of the shell and kernel, and decrease the marketability of the harvested crop (3).

Future improvement of Hungarian walnut production will require an integrated approach combining climatic and phytosanitary monitoring with appropriate orchard management. A better understanding of these interacting factors is essential for developing effective adaptation and plant-protection strategies for sustainable walnut production in Hungary.

References

1. Hungarian Central Statistical Office (KSH). *Production and use of main fruits, 2020–2024*. STADAT Table 19.1.1.25. Hungarian Central Statistical Office, Budapest. Available at: https://www.ksh.hu/stadat_files/mez/en/mez0025.html
2. Szügyi-Bartha, K., Bujdosó, G., Froemel-Hajnal, V., Szügyi, S., Stefanovits-Bányai, É. & Szalay, L. (2022). Evaluation of the frost tolerance of Hungarian-bred walnut cultivars. *Acta Biologica Szegediensis*, **65**(2), 163–170. https://doi.org/10.14232/abs.2021.2.163-170
3. National Food Chain Safety Office (NÉBIH) (2012). *Megjelent diófáink újabb károsítója, a nyugati dióburok-fúrólégy (Rhagoletis completa)* [The western walnut husk fly, *Rhagoletis completa*, a new pest of walnut in Hungary]. National Food Chain Safety Office, Hungary.

CHARACTERIZATION, PHOTOCATALYTIC APPLICATIONS AND ENVIRONMENTAL EFFECTS OF $Ti_3C_2T_x$ MXENE

Laura Lakatos[1*], Aisa Tischner[1], Adrienn-Dorisz Dávid[2], Kincső Kozma[2], Tamás Gyulavári[1], Zsolt Pap[1,2,3], Kukovecz Ákos[1], Kónya Zoltán[1]

[1]Department of Applied and Environmental Chemistry, University of Szeged, H-6720 Szeged, Dóm tér 7, Hungary
[2]Babeş-Bolyai University, Institute for Interdisciplinary Research in Bio-Nano-Science, Treboniu Laurian 42, Cluj-Napoca, RO-400271 Romania
[3] Babeş-Bolyai University, 3B Centrum, Clinicilor 5–7, Cluj-Napoca, RO-400006 Romania
**e-mail: laura.lakatos@chem.u-szeged.hu*

Abstract

MXenes have attracted significant attention due to their unique physicochemical properties, including high electrical conductivity, large specific surface area and tuneable surface functionalities, making them promising for various applications [1]. However, the increasing use of these materials raises concerns regarding their potential environmental impact.

In the present work, the synthesis of $Ti_3C_2T_x$ MXene was carried out using a solvothermal method from a MAX-phase precursor in an HF-containing medium [2]. The synthesized MXene was characterized in terms of its structural, chemical and morphological properties using X-ray diffraction (XRD), infrared spectroscopy (IR) and scanning electron microscopy (SEM) (Figure 1). In addition, the stability of the prepared MXene was investigated in water and air, with further characterization of the (watered) samples (Figure 1).

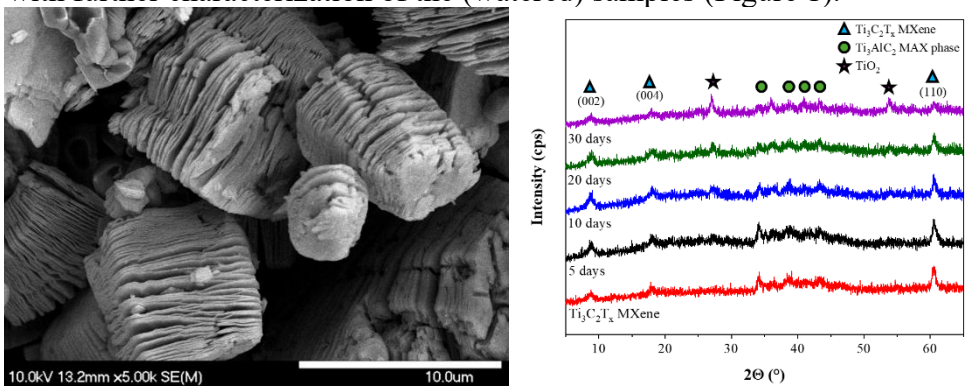


Figure 1. SEM micrograph of the synthesized MXene (left), and XRD diffractogram of the water stability test samples (right).

Based on these results, the photocatalytic activity of two different catalysts (P25 TiO_2, ZnO) was investigated in the presence of $Ti_3C_2T_x$ MXene to assess its effect on their photocatalytic performance. The influence of varying MXene content and synthesis parameters on the resulting catalytic activity was also examined, providing insight into the relationship between the preparation conditions, material composition and photocatalytic performance.

The potential effects of $Ti_3C_2T_x$ MXene on living organisms were also evaluated over a 4-week period at different concentrations (0.1%, 0.5% and 1.5% w/w relative to soil), alongside a control group. Each treatment and the control were tested in four replicates. Throughout the experiment, a fixed amount of fresh soil, appropriate humidity, shelter, and minimal protein and calcium sources were consistently provided. No additional food was supplied to promote increased soil consumption. The effects of MXene exposure on isopod morphology, including body mass, as well as mortality (Figure 2), were assessed, including the determination of the LD_{50} value.

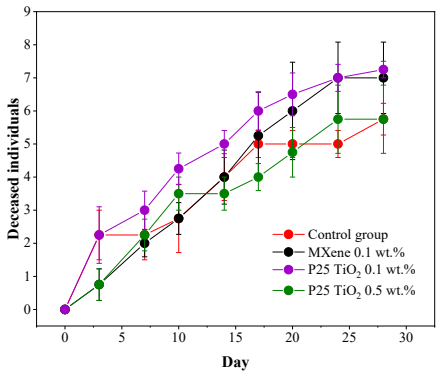


Figure 2. Mortality assay results from the toxicity assessment.

Acknowledgements

L. Lakatos was supported by the Pannonia Scholarship Program. Zs. Pap grateful for the Bolyai János research scholarship, the funding provided by the Hungarian Academy of Sciences. K. Kozma acknowledges the Hungarian Balassy Bálint Scholarschip Program and the Áron Márton Talent Development Scholarship. A.-D. Dávid was supported by Hungary's Talentum program.

References

[1] A.A. AL-Zahrani, H. Kochkar, Advancements in MXene synthesis: Novel methods and emerging applications, J. Alloys Compd. 1039 (2025) 183247.

[2] L. Chen, X. Ye, S. Chen, L. Ma, Z. Wang, Q. Wang, N. Hua, X. Xiao, S. Cai, X. Liu, Ti_3C_2 MXene nanosheet/TiO_2 composites for efficient visible light photocatalytic activity, Ceram. Int. 46 (2020) 25895–25904.

CALIBRATION OF A ULTRA-LOW-LEVEL LIQUID SCINTILLATION SPECTROMETER FOR THE DETERMINATION OF ^{90}Sr AND ^{210}Pb IN ENVIRONMENTAL WATER SAMPLES

Ana Lazić[1], Nataša Sarap[1], Dubravka Relić[2]

[1]University of Belgrade, Vinča Institute of Nuclear Sciences, National Institute of the Republic of Serbia, Radiation and Environmental Protection Department, Mike Petrovića Alasa 12-14, 11001 Belgrade
[2]University of Belgrade, Faculty of Physical Chemistry, Studentski trg 12-16, 11000 Belgrade, Serbia
e-mail: ana.lazic@vin.bg.ac.rs

Abstract

The determination of low activity concentrations of radionuclides in environmental waters requires sensitive analytical techniques capable of providing reliable results at low detection limits. Liquid Scintillation Counting (LSC) has been successfully applied for the determination of ^{90}Sr in water samples, including the assessment of detection limits, precision and accuracy [1], while recent studies have also demonstrated its applicability for the determination of ^{90}Sr and ^{210}Pb following appropriate radiochemical separation procedures [2]. In this study, a ultra-low-level liquid scintillation spectrometer Quantulus 1220 (PerkinElmer, Finland) was calibrated and its performance evaluated for the determination of ^{90}Sr and ^{210}Pb in different types of environmental waters, including drinking water, precipitation, surface water and groundwater. The calibration procedure included the evaluation of counting efficiency, as well as the minimum detectable activity (MDA) and investigation of quenching effects. For ^{90}Sr, a linear response between activity and count rate was obtained over the investigated activity range of 0.817–16.332 Bq, with an adjusted R^2 of 0.99923. The influence of counting time on the detection capability was also investigated, showing a decrease in MDA from 1.3986 Bq/L at 50 min to 0.2956 Bq/L at 1200 min. The determined detection efficiency was 34.1%. For ^{210}Pb, calibration was performed over the activity range of 10.912–436.478 Bq under low-level counting conditions, and the influence of quenching on the detector response was evaluated through changes in the spectral peak position and the corresponding quench factor. The minimum detectable activity for ^{210}Pb was determined to be 1.82 Bq/L at a counting time of 1200 min. The obtained results provide the basis for the reliable application of low-level liquid scintillation spectrometry for the determination of ^{90}Sr and ^{210}Pb in environmental water samples and its further use in routine environmental radioactivity monitoring.

Acknowledgements

The authors are grateful for the financial support of the Ministry of Science, Technological Development and Innovation of the Republic of Serbia (Contract No. 451-03-33/2026-03/200017).

References

[1] M.B. Nisti, C.H.R. Saueia, B. Castilho, B.P. Mazzilli, *Braz. J. Radiat. Sci.***7** (2019) 1–12.
[2] J. Martínez, M. de los Cobos, A. Peñalver, C. Aguilar, F. Borrull, *J. Radioanal. Nucl. Chem.*331 (2022) 629–637.

LOW-COST AUSTENITIC STAINLESS STEELS AS ANODE MATERIALS FOR ALKALINE FUEL CELLS FUELED BY C1–C3 ALCOHOLS

Voicu Librimir[1], Nataliia Rudenko[2], George Daniel Dima[1], Mircea Laurențiu Dan[1], Nicolae Vaszilcsin[1]

[1]University Politehnica Timisoara, Faculty of Chemical Engineering, Biotechnology and Environmental Protection, Laboratory of Electrochemistry, Corrosion and Electrochemical Engineering, 6 Pârvan, 300223 Timisoara, Romania
[2]University Politehnica Timisoara, Innovation and Technology Transfer Center, 2 V. Pârvan, 300223 Timisoara, Romania
e-mail: mircea.dan@upt.ro

Abstract

The growing global demand for energy, the need to reduce dependence on fossil fuels, and the requirement to implement energy-conversion technologies with a reduced environmental impact call for the development of efficient, durable, and economically affordable electrochemical systems. In this context, alkaline direct alcohol fuel cells represent a promising alternative for the direct conversion of the chemical energy of liquid fuels into electrical energy. Methanol, ethanol, and propanol, corresponding to C1–C3 lower alcohols, are of particular interest because they are easier to handle and store than gaseous hydrogen, possess favorable volumetric energy densities, and can be obtained from renewable resources, particularly in the case of ethanol. The performance of direct alcohol fuel cells is governed by the simultaneous occurrence of the anodic alcohol oxidation reaction and the cathodic oxygen reduction reaction. However, the slow kinetics of anodic oxidation, the formation of adsorbed intermediates, electrode degradation, and the use of noble-metal-based catalysts remain major factors limiting their large-scale implementation.

Compared with acidic systems, alkaline media may promote alcohol oxidation reactions through the involvement of hydroxide ions and the formation of oxygen-containing surface species that participate in the electrochemical transformation of organic molecules. Moreover, operation under alkaline conditions creates opportunities for the use of electrocatalysts based on earth-abundant and less expensive elements than platinum or palladium, such as nickel, iron, cobalt, copper, and their alloys. This approach is relevant both for reducing the overall cost of fuel-cell systems and for developing robust configurations adaptable to low-power stationary applications, portable devices, or demonstrative platforms for the electrochemical conversion of liquid fuels.

Introduction

This work proposes the evaluation of low-cost austenitic stainless steels as anode materials for alkaline fuel cells fueled by C1–C3 alcohols, with particular emphasis on AISI 304 stainless steel. This material, designated in the European system as X5CrNi18-10 or 1.4301, is among the most widely used austenitic stainless steels. AISI 304 is commonly referred to as “18/8” stainless steel because of its nominal composition of approximately 18% chromium and 8% nickel; the alloy also contains iron as the principal constituent, together with controlled amounts of carbon, manganese, silicon, phosphorus, and sulfur. Its Fe–Cr–Ni composition provides mechanical strength, good formability, broad commercial availability, and favorable corrosion resistance, which justify its investigation as a low-cost electrode material.Chromium contributes to the formation of a passive surface film responsible for the corrosion resistance of stainless steel. Under alkaline conditions and anodic polarization, this film may evolve through the formation of surface layers containing iron-, chromium-, and nickel-based oxides,

hydroxides, and oxyhydroxides. The properties of these layers depend on electrolyte composition, pH, applied potential range, activation time, and the presence of organic reactants. In particular, nickel- and iron-based surface species may participate in redox processes that facilitate the generation of oxygenated surface species and influence charge transfer at the electrode–electrolyte interface. Therefore, the electrochemical response of AISI 304 should be interpreted by correlating the bulk alloy composition with the chemical state, morphology, and actual composition of the surface film formed during operation.AISI 304 stainless steel is of interest not only as an available and mechanically robust metallic material but also as a platform that can be electrochemically activated or modified through mechanical, chemical, thermal, and electrochemical treatments. In its monolithic form, it can serve as a conductive electrode with a simple geometry, high mechanical strength, and low cost. Following activation, it may develop a rougher and more active surface with a larger electrochemically accessible area. In addition, the material can be used as a conductive support for oxides, hydroxides, porous layers, or noble-metal-free catalytic deposits.Oxidative activation of AISI 304 has been reported as a simple and scalable route for obtaining an active anodic electrode for the oxygen evolution reaction in alkaline and neutral media. Although these findings do not directly demonstrate activity toward alcohol oxidation, they support the potential of AISI 304 as an activatable and stable anode material under alkaline conditions.Methanol, ethanol, and propanol interact with the activated anodic surface of AISI 304 stainless steel, which may contain iron-, nickel-, and chromium-based oxide, hydroxide, and oxyhydroxide species. In the presence of OH^- ions from the alkaline electrolyte, the alcohols are oxidized at the anode, while the resulting electrons are transferred through the metallic material and the external circuit to the cathode, where the oxygen reduction reaction takes place. The anion-exchange membrane enables ionic transport and separates the anodic and cathodic compartments of the fuel cell.The electrochemical oxidation of C1–C3 alcohols on metallic surfaces depends on the molecular structure of the fuel, the adsorption of reactants and intermediate products, and the ability of the electrode to generate active oxygen-containing species. Methanol is a model fuel with a simple molecular structure and is widely employed for investigating anodic oxidation reactions. Ethanol is attractive because it can be produced from biomass, has lower toxicity, and benefits from existing production and transportation infrastructure; however, its complete oxidation is hindered by the need to cleave the C–C bond. Propanol has a higher volumetric energy density, but its oxidation mechanism may involve a broader range of intermediates and reaction products. Therefore, the comparative investigation of AISI 304 in alkaline electrolytes containing methanol, ethanol, or propanol may reveal the influence of alcohol structure on the oxidation onset potential, anodic current density, temporal stability, and passivation phenomena.

Experimental

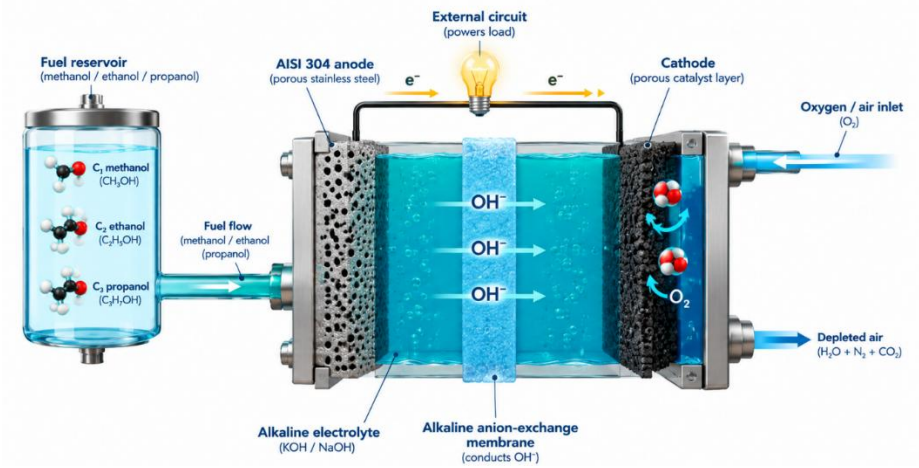


Figure 1. Schematic representation of an alkaline fuel cell fueled by C1–C3 alcohols, equipped with AISI 304 austenitic stainless-steel anode. Created by the authors using an AI-assisted image-generation tool and scientifically reviewed by the authors.)

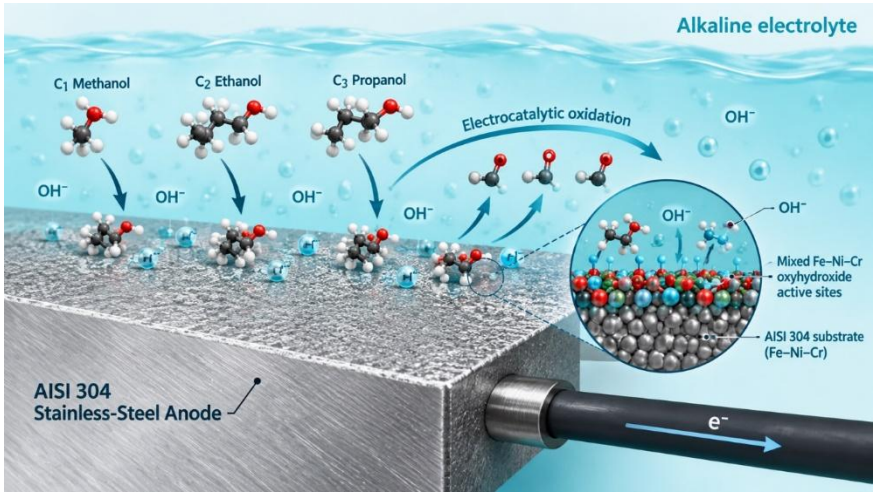


Figure 2. Conceptual representation of the electrocatalytic oxidation of C1–C3 alcohols on an AISI 304 austenitic stainless-steel anode, in an alkaline medium. Created by the authors using an AI-assisted image-generation tool and scientifically reviewed by the authors

Results and discussion

To evaluate AISI 304 as an anodic material, cyclic voltammetry, linear sweep voltammetry, Tafel analysis, chronoamperometry, and electrochemical impedance spectroscopy may be employed. Cyclic voltammetry enables the identification of surface redox regions and the observation of changes in anodic current in the presence of alcohols. Polarization curves can provide information on the oxidation onset potential and the current density associated with fuel oxidation, while Tafel analysis can assist in estimating apparent kinetic parameters. Chronoamperometry is useful for assessing time-dependent stability, the accumulation of adsorbed species, and the tendency toward passivation or deactivation. Electrochemical impedance spectroscopy can complement the analysis by determining charge-transfer resistance and changes at the electrode–electrolyte interface. Correlating these results with surface investigations, such as scanning electron microscopy, energy-dispersive X-ray spectroscopy, X-ray diffraction, and X-ray photoelectron spectroscopy, can clarify the electrode activation and degradation mechanisms.

Conclusion

In conclusion, AISI 304 austenitic stainless steel represents a relevant candidate for the development of low-cost anodic materials for alkaline fuel cells fueled by methanol, ethanol, and propanol. Its Fe–Cr–Ni composition, corrosion resistance, commercial availability, processability, and capacity for surface activation make this alloy suitable both as a monolithic electrode and as a substrate for noble-metal-free electrocatalytic coatings. The study aims to correlate surface structure and composition with electrocatalytic activity toward C1–C3 alcohol oxidation, stability in alkaline media, and the evolution of the passive film during anodic polarization. The results may contribute to the identification of more affordable and robust solutions for the direct electrochemical conversion of alcohols and to the development of alkaline fuel cells with practical application potential

Acknowledgements

The authors used Perplexity AI image-generation tools to assist in preparing the conceptual illustration presented in Figure 1. The authors reviewed, edited, and verified the scientific accuracy, terminology, and relevance of the final figure and assumed full responsibility for its content.

References

[1] E. Berretti, L. Osmieri, V. Baglio, H.A. Miller, J. Filippi, F. Vizza, M. Santamaria, S. Specchia, C. Santoro, A. Lavacchi, Electrochem. Energy Rev. 6 (2023) 30.
[2] Y. Li, H. Wang, J. Zhang, X. Liu, Y. Zhang, Adv. Sci. 12 (2025) e2408932.
[3] A. Mirzaei, S. Shahrokhian, S. Ghasemi, Front. Energy Res. 10 (2022) 843736.
[4] ASTM International, ASTM A240/A240M-24, Standard Specification for Chromium and Chromium-Nickel Stainless Steel Plate, Sheet, and Strip for Pressure Vessels and for General Applications, ASTM International, West Conshohocken, PA, 2024.
[5] H. Schäfer, S.M. Beladi-Mousavi, L. Walder, J. Wollschläger, O. Kuschel, S. Ichilmann, S. Sadaf, M. Steinhart, K. Küpper, L. Schneider, ACS Catal. 5 (2015) 2671–2680.
[6] E. Antolini, J. Power Sources 170 (2007) 1–12.
[7] S.P.S. Badwal, S. Giddey, A. Kulkarni, J. Goel, S. Basu, Appl. Energy 145 (2015) 80–103.
[8] L. An, T.S. Zhao, Y.S. Li, Renew. Sustain. Energy Rev. 50 (2015) 1462–1468.

EFFECTS OF POLYETHYLENE FIBERS ON GERMINATION AND EARLY ROOT DEVELOPMENT IN PLANTS

Zsófia Liska[1,2], Enikő Mészáros[1,2], Kamilla Kovács[1,2], Klaudia Hoffmann[1,2,3], Attila Bodor [2,3], Gábor Feigl[1,2]

[1]University of Szeged, Department of Plant Biology
[2]MTA-SZTE Lendület "Momentum" Anthropogenic Stress and Plant Resilience Research Group
[3]Department of Biotechnology and Microbiology, University of Szeged, Hungary

Abstract
Plastic pollution is an increasing environmental concern, with microplastics becoming widespread contaminants of terrestrial ecosystems. Polyethylene (PE), one of the most commonly used plastics, can enter agricultural environments and interact directly with plant roots. This study investigated the effects of PE fibers differing in size, concentration, and color on seed germination and early root development in five plant species: oilseed rape (*Brassica napus* L.), radish (*Raphanus sativus* L.), alfalfa (*Medicago sativa* L.), red clover (*Trifolium pratense* L.), and wheat (*Triticum aestivum* L.). Green and white PE fibers with sizes of 1 cm, 0.5 cm, and microsized fibers were applied at concentrations of 0.5% and 1%. Germination and primary root development were evaluated following exposure. The results demonstrated species-dependent responses to PE fiber size and color, with significant changes primarily observed in early root development. In contrast, germination responses were not statistically significant. These findings highlight the importance of particle characteristics and plant species when assessing the effects of polyethylene contamination on plants.

Introduction
Microplastics (MPs) are persistent environmental contaminants increasingly detected in terrestrial ecosystems, including agricultural soils. Polyethylene is one of the most widely used plastics and can enter the environment through the fragmentation of larger plastic materials [1,2]. Once present in soil, plastic particles can interact with plant roots and potentially influence water and nutrient availability, root development, and physiological processes [3].Previous studies have demonstrated that PE-based microplastics can affect plant growth, although responses vary considerably among plant species and experimental conditions [3,4]. Particle size may also influence plant responses, as smaller particles have a larger relative surface area and can interact differently with plant tissues [5].
The aim of this study was to investigate how PE fiber size, concentration, and color affect seed germination and early root development in five agriculturally relevant plant species: *B. napus*, *R. sativus*, *M. sativa*, *T. pratense*, and *T. aestivum*.

Experimental
Five plant species representing different plant families were used: oilseed rape (*Brassica napus*), radish (*Raphanus sativus*), alfalfa (*Medicago sativa*), red clover (*Trifolium pratense*), and wheat (*Triticum aestivum*).Green and white polyethylene fibers were tested in three size categories: 1 cm, 0.5 cm, and microsized fibers. Two concentrations, 0.5% and 1%, were applied together with untreated controls. Seeds were exposed to the different PE treatments under controlled experimental conditions. Germination was monitored throughout the experiment, while germination-related parameters and primary root length were recorded. Statistical differences were evaluated using Student's t-test, with $p < 0.05$ considered statistically significant.

Results and discussion

PE fiber exposure primarily affected early root development, whereas effects on germination were comparatively limited. Significant changes in primary root length were observed in several treatments, indicating that developing roots may be particularly sensitive to PE exposure.The magnitude and direction of the response differed among the five plant species and depended on fiber size. The responses to 1 cm, 0.5 cm, and microsized fibers were not uniform, indicating that particle size interacts with plant-specific characteristics. These findings are consistent with previous studies reporting species-dependent responses to polyethylene microplastics [3,4]. Fiber color also contributed to differences in root responses. Green and white PE fibers did not produce identical effects across all investigated species, suggesting that particle properties beyond concentration and size may influence plant–microplastic interactions.In contrast, germination was not significantly affected by the investigated treatments. This agrees with previous observations that microplastics may have relatively limited effects during germination while influencing subsequent seedling development [4]. Thus, primary root growth may represent a more sensitive endpoint for detecting early effects of PE exposure. Overall, the results indicate that the effects of PE fibers cannot be explained by concentration alone. Plant species, fiber size, and fiber color all contributed to the observed variation in root responses

Conclusion

This study demonstrated that polyethylene fibers can influence early plant development, particularly primary root growth, while germination remained largely unaffected. The five investigated species - *Brassica napus*, *Raphanus sativus*, *Medicago sativa*, *Trifolium pratense*, and *Triticum aestivum* - showed species-dependent responses to different PE fiber characteristics.

The observed differences in response to fiber size and color emphasize the importance of considering both particle properties and plant-specific sensitivity when assessing the ecological effects of plastic contamination. These findings contribute to a better understanding of plant–microplastic interactions and provide a basis for further research into the mechanisms underlying PE-induced changes in root development.

Acknowledgements

The project was supported by the National Research, Development and Innovation Office, Hungary (NKFIH FK 142475 and PLAGROSYS - 2024-1.2.3-HU-RIZONT-2024-00010) and by the Lendület "Momentum" Program of the Hungarian Academy of Sciences (LP2025-8/2025 to G.F)

References

[1] M. C. Rillig, L. Ziersch, and S. Hempel, "Microplastic transport in soil by earthworms," *Scientific Reports*, vol. 7, 1362, 2017. doi: 10.1038/s41598-017-01594-7.

[2] J. Boctor et al., "Microplastics and nanoplastics: fate, transport, and governance from agricultural soil to food webs and humans," *Environmental Sciences Europe*, vol. 37, 68, 2025. doi: 10.1186/s12302-025-01104-x.

[3] E. Mészáros et al., "Impacts of Plastics on Plant Development: Recent Advances and Future Research Directions," *Plants*, vol. 12, 3282, 2023.

[4] O. Bouaicha et al., "Plant species-specific impact of polyethylene microspheres on seedling growth and the metabolome," *Science of the Total Environment*, vol. 840, 156678, 2022. doi: 10.1016/j.scitotenv.2022.156678.

[5] X. Zhang et al., "Size/shape-dependent migration of microplastics in agricultural soil under simulative and natural rainfall," *Science of the Total Environment*, vol. 815, 152507, 2022. doi: 10.1016/j.scitotenv.2021.152507.

EFFECTS OF DIFFERENTLY SIZED AND CHARGED NANOPLASTICS ON EARLY ROOT DEVELOPMENT AND NITRO-OXIDATIVE STRESS IN *Brassica napus*

Zsófia Liska[1,2], Enikő Mészáros[1,2], Kamilla Kovács[1,2], Klaudia Hoffmann[1,2,3], Attila Bodor [2,3], Gábor Feigl[1,2]

[1]University of Szeged, Department of Plant Biology
[2]*MTA-SZTE Lendület "Momentum" Anthropogenic Stress and Plant Resilience Research Group*
[3]*Department of Biotechnology and Microbiology, University of Szeged, Hungary*

Abstract

Nanoplastics (NPLs) are increasingly recognized as emerging contaminants in terrestrial ecosystems, where their small size and high surface area facilitate interactions with plant roots. Their effects may depend on particle characteristics such as size, surface charge, and concentration. This research aimed to investigate the effects of differently sized and charged latex-based NPLs on early root development and nitro-oxidative stress in oilseed rape (*Brassica napus* L.). Two latex NPLs, amidine latex (AL; 50 nm) and sulfate latex (SL; 60 nm), were investigated using a controlled semi-hydroponic system. Root growth, architecture, and germination-related parameters were assessed, followed by fluorescence-based analysis of reactive oxygen and nitrogen species and protein tyrosine nitration. The study aimed to identify concentration-dependent responses and clarify potential links between NPL exposure, root development, and nitro-oxidative stress.

Introduction

Plastic pollution is an increasing environmental concern, and plastic particles are now widely detected in terrestrial ecosystems. Through physical and environmental degradation, larger plastic materials can form micro- and nanoplastics, which may enter agricultural soils and interact with plants [1–3]. Due to their small size, NPLs can interact closely with root surfaces and potentially enter plant tissues, raising concerns about their effects on crop development and food production [2,3].

Particle characteristics strongly influence plant–NPL interactions. In particular, surface charge can affect particle accumulation and localization in plant tissues [4]. Previous studies have demonstrated that NPL exposure can interfere with root meristem activity and root growth, although responses may differ between plant species and particle types [5,10]. NPL transport and distribution in soil are also influenced by environmental processes such as rainfall, soil structure, and biological activity [8,9].

Oure research therefore focused on the effects of latex-based NPLs differing in surface charge and particle size on early root development and nitro-oxidative stress in *B. napus*. Understanding these responses may contribute to a better assessment of the potential risks of NPL contamination in agricultural environments.

Experimental

Oilseed rape (*Brassica napus* L.) seedlings were exposed to two latex-based nanoplastics differing in particle size and surface charge under controlled semi-hydroponic conditions. A range of exposure concentrations were tested based on preliminary experiments.

Early root development was evaluated by measuring primary root length, lateral root number, and germination-related parameters. The obtained data were statistically analysed to identify

concentration- and particle-dependent responses and to select treatments for subsequent molecular analyses.
To investigate the potential mechanisms underlying the observed developmental responses, nitro-oxidative responses were assessed by fluorescence-based detection of selected reactive oxygen and nitrogen species.

Results and discussion
Latex-based nanoplastics induced particle-type- and concentration-specific responses in early oilseed rape development. Amidine latex stimulated primary root elongation at 10–25 ppm but inhibited it at 50 ppm, whereas sulfate latex strongly inhibited root elongation at 25–50 ppm. Amidine latex consistently increased DHE fluorescence, while sulfate latex produced a pronounced DHE fluorescence peak at 25 ppm. Other redox-related fluorescence markers showed more variable and non-monotonic responses. Overall, the results indicate distinct, non-linear developmental and redox responses to the two NPL types.

Conclusion
Our results revealed concentration-dependent alterations in early root development following exposure to both types of latex-based NPLs. The magnitude and direction of the responses differed depending on the NPL type and concentration, indicating that particle-specific characteristics may influence plant responses. Changes in oxidative parameters, particularly hydrogen peroxide and superoxide levels, were more pronounced than alterations in the investigated nitrosative parameters.

Acknowledgements
The project was supported by the National Research, Development and Innovation Office, Hungary (NKFIH FK 142475 and PLAGROSYS - 2024-1.2.3-HU-RIZONT-2024-00010) and by the Lendület "Momentum" Program of the Hungarian Academy of Sciences (LP2025-8/2025 to G.F).

References
[1] E. Mészáros et al., "The bioplastic paradox: Biodegradable microplastics trigger species-specific nitro-oxidative stress and root growth inhibition in Brassicaceae," *Journal of Hazardous Materials Advances*, vol. 20, 100936, 2025. doi: 10.1016/j.hazadv.2025.100936.
[2] J. Boctor et al., "Microplastics and nanoplastics: fate, transport, and governance from agricultural soil to food webs and humans," *Environmental Sciences Europe*, vol. 37, 68, 2025. doi: 10.1186/s12302-025-01104-x.
[3] F. Ren, J. Huang, and Y. Yang, "Unveiling the impact of microplastics and nanoplastics on vascular plants: A cellular metabolomic and transcriptomic review," *Ecotoxicology and Environmental Safety*, vol. 279, 116490, 2024. doi: 10.1016/j.ecoenv.2024.116490.
[4] X. D. Sun et al., "Differentially charged nanoplastics demonstrate distinct accumulation in Arabidopsis thaliana," *Nature Nanotechnology*, vol. 15, pp. 755–760, 2020. doi: 10.1038/s41565-020-0707-4.
[5] S. Ma et al., "Root Meristem Maintenance Mechanisms are Key to Plant Defense Against Nanoplastics," *Advanced Science*, vol. 12, e11837, 2025. doi: 10.1002/advs.202511837.
[6] Z. Lin et al., "Micro/Nanoplastics in plantation agricultural products: behavior process, phytotoxicity under biotic and abiotic stresses, and controlling strategies," *Journal of Nanobiotechnology*, 2025. doi: 10.1186/s12951-025-03314-0.
[7] J. Gigault et al., "Current opinion: What is a nanoplastic?," *Environmental Pollution*, vol. 235, pp. 1030–1034, 2018. doi: 10.1016/j.envpol.2018.01.024.

[8] M. C. Rillig, L. Ziersch, and S. Hempel, "Microplastic transport in soil by earthworms," *Scientific Reports*, vol. 7, 1362, 2017. doi: 10.1038/s41598-017-01594-7.
[9] X. Zhang et al., "Size/shape-dependent migration of microplastics in agricultural soil under simulative and natural rainfall," *Science of the Total Environment*, vol. 815, 152507, 2022. doi: 10.1016/j.scitotenv.2021.152507.
[10] C. Q. Zhou et al., "Response of rice (*Oryza sativa* L.) roots to nanoplastic treatment at seedling stage," *Journal of Hazardous Materials*, vol. 401, 123412, 2021. doi: 10.1016/j.jhazmat.2020.123412.
[11] A. R. Khan et al., "Micro/nanoplastics: Critical review of their impacts on plants, interactions with other contaminants (antibiotics, heavy metals, and polycyclic aromatic hydrocarbons), and management strategies," *Science of the Total Environment*, 2024. doi: 10.1016/j.scitotenv.2023.169420.

CO_2-ACTIVATED BIOCHARS FROM WASTE BIOMASS FOR WASTEWATER TREATMENT

Dragana Lukić, Sanja Panić, Jelena Prodanović, Teodora Subić, Vesna Vasić

University of Novi Sad, Faculty of Technology Novi Sad, Bul. cara Lazara 1, 21000 Novi Sad, Serbia
e-mail: dkukic@uns.ac.rs

Abstract

Heavy metals in aquatic environments, mainly from industrial activities and wastewater discharges, are a major environmental concern because they persist, are toxic, and can accumulate in living organisms. Unlike many organic pollutants, heavy metals cannot be degraded and may persist in the environment for long periods, posing risks to ecosystems and human health [1,2]. Although copper and chromium are essential trace elements involved in various biological processes, higher concentrations can cause various effects. Therefore, the development of efficient and economically feasible technologies for the removal of heavy metals from contaminated water is of considerable importance.

Adsorption is one of the most widely applied approaches for the removal of heavy metals from contaminated water, with activated carbon being a highly effective conventional adsorbent [3,4]. However, its relatively high production and regeneration costs have encouraged the development of alternative low-cost adsorbents. In this context, biological and waste-derived materials have attracted increasing attention due to their availability, low cost, and potential for valorization of agricultural and industrial residues [5,6]. Their conversion into adsorbents is also consistent with the principles of the circular economy, enabling waste biomass to be transformed into value-added materials while contributing to both waste reduction and resource recovery.

Biochar is a carbon-rich material obtained by the thermochemical conversion of biomass through pyrolysis under oxygen-limited conditions, with biochar, bio-oil, and synthesis gas formed as the main products [7]. Due to its porous structure and surface properties, biochar has considerable potential as a low-cost alternative to activated carbon for water treatment [6]. Its properties depend on the precursor biomass and pyrolysis conditions, while activation can further improve its porosity and adsorption performance. Physical activation using CO_2 is an effective approach for modifying biochar properties and enhancing its adsorption capacity [8]. Pyrolysis and activation can be performed either simultaneously in a one-step process or sequentially in a two-step process, in which the biochar is first produced and subsequently activated [9].

In this study, the adsorption performance of biochars derived from three waste lignocellulosic biomasses (walnut shells, spent sugar beet pulp, and raspberry stems) was investigated for the removal of Cu(II) and Cr(VI) ions from aqueous solutions. The biochars were produced by slow pyrolysis at 700 °C for 2 h under a nitrogen atmosphere. The resulting non-activated biochars were subsequently subjected to physical activation using CO_2, applying one- and two-step activation procedures. Both non-activated and activated biochars were evaluated in order to determine the effect of activation on their adsorption performance. Selected materials were characterized by scanning electron microscopy (SEM), energy-dispersive X-ray spectroscopy (EDS), and Fourier-transform infrared spectroscopy (FTIR) to obtain information on their elemental composition, surface morphology, and surface functional groups.

The EDS analysis demonstrated that the chemical composition of the obtained biochars varied depending on the precursor biomass, with carbon and oxygen representing the predominant elements and ranging from 49.8–85.3% and 7.6–24.1%, respectively. Phosphorus, sulfur, alkali

and alkaline-earth elements, as well as heavy metals, were also detected. SEM analysis revealed differences in surface morphology among the investigated materials. Biochars obtained from walnut shells and spent sugar beet pulp exhibited predominantly irregular and rough surfaces, whereas raspberry stem biochars were characterized by a more regularly oriented layered structure. Porosity was observed in the walnut shell biochars and was more obvious after CO_2 activation. FTIR analysis revealed a limited number or absence of detectable functional groups, which can be attributed to the degradation of surface functional groups during the high-temperature pyrolysis process.

The adsorption results demonstrated a clear improvement in performance after physical activation. Regardless of the precursor biomass, non-activated biochars exhibited the lowest adsorption capacities for both investigated metal ions, ranging from 3.5–8.0 mg/g for Cu(II) and 6–10 mg/g for Cr(VI). In contrast, activated biochars showed considerably higher adsorption capacities, ranging from 11–39 mg/g for Cu(II) and 24–49 mg/g for Cr(VI). The highest adsorption capacities for both metal ions were obtained using the raspberry stem biochar subjected to two-step CO_2 activation, with values of 39.4 mg/g for Cu(II) and 49.4 mg/g for Cr(VI). Overall, the investigated biochars exhibited higher adsorption capacities toward Cr(VI) than toward Cu(II).

The obtained results demonstrate that waste lignocellulosic biomasses can be converted into functional carbonaceous adsorbents through pyrolysis and subsequent physical activation. In particular, CO_2 activation significantly improved the adsorption performance of the investigated biochars, highlighting the importance of modification in tailoring their properties for environmental applications. The valorization of walnut shells, spent sugar beet pulp, and raspberry stems into adsorbents also represents a potentially valuable approach within the circular economy framework, as it combines waste biomass utilization with the treatment of contaminated water. The investigated materials therefore show promising potential for heavy-metal removal, particularly Cr(VI), although further research is required to evaluate their performance under realistic wastewater conditions, adsorption mechanisms, regeneration potential, and possible environmental risks associated with their practical application.

Acknowledgements

This work is a result of the programs 451-03-34/2026-03/200134 and 451-03-33/2026-03/200134 supported by the Ministry of Education, Science and Technological Development of the Republic of Serbia.

References

[1] X. Guo, A. Liu, J. Lu, X. Niu, M. Jiang, Y. Ma, X. Liu, M. Li, Adsorption mechanism of hexavalent chromium on biochar: Kinetic, thermodynamic, and characterization studies. ACS Omega 5 (2020) 26957–26966.

[2] X. Chen, G. Chen, L. Chen, Y. Chen, J. Lehmann, M.B. McBride, A.G. Hay, Adsorption of copper and zinc by biochars produced from pyrolysis of hardwood and corn straw in aqueous solution. Bioresour. Technol. 102 (2011) 8877–8884.

[3] A. Bhatnagar, M. Sillanpää, Utilization of agro-industrial and municipal waste materials as potential adsorbents for water treatment—A review. Chem. Eng. J. 157 (2010) 277–296.

[4] A. Abdolali, W.S. Guo, H.H. Ngo, S.S. Chen, N.C. Nguyen, K.L. Tung, Typical lignocellulosic wastes and by-products for biosorption process in water and wastewater treatment: A critical review. Bioresour. Technol. 160 (2014) 57–66.

[5] R.A. Canales-Flores, F. Prieto-García, Activation methods of carbonaceous materials obtained from agricultural waste. Chem. Biodivers. 13 (2016) 261–268.

[6] D. Kukić, M. Šćiban, J. Pejin, V. Vasić, J. Prodanović, Pivski trop kao potencijalni adsorbent za uklanjanje jona bakra iz vode. Zaštita Materijala 57 (2016) 397–403.

[7] P.R. Yaashikaa, P. Senthil Kumar, S. Varjani, A. Saravanan, A critical review on the biochar production techniques, characterization, stability and applications for circular bioeconomy. Biotechnol. Rep. 28 (2020) e00570.
[8] A. Colomba, F. Berruti, C. Briens, Model for the physical activation of biochar to activated carbon. J. Anal. Appl. Pyrolysis 1689 (2022) 10576.
[9] G. Greco, R.L.S. Canevesi, C. Di Stasi, A. Celzard, V. Fierro, J.J. Manyà, Biomass-derived carbons physically activated in one or two steps for CH_4/CO_2 separation. Renew. Energy 191 (2022) 122–133.

ALLELOPATHIC EFFECT OF *Ambrosia artemisiifolia* L. EXTRACTS ON GERMINATION OF MAIZE SEED

Nataša Mandić[1*], Bojan Konstantinović[1], Gordana Babić[4], Milena Popov[1], Tijana Stojanović[1], Jelena Gajić Umiljendić[2], Vojislava Bursić[1], Gorica Vuković[3]

[1] *University of Novi Sad, Faculty of Agriculture, Department of Environmental and Plant Protection, Trg Dositeja Obradovića 8,21000 Novi Sad, Serbia*
[2] *Institute of Pesticides and Environmental Protection, Laboratory of Weed Research, Banatska 31b, 11080 Belgrade, Serbia*
[3] *Field Test, Vinogradska 150b, 11000 Belgrade, Serbia*
[4]*Public Institution Agricultural Institute of the Republic of Srpska, Knjaza Miloša 17, 78000 Banja Luka, Bosnia and Herzegovina*
e-mail: natasa.mandic@polj.edu.rs

Abstract

Common ragweed (*Ambrosia artemisiifolia* L.) is one of the most invasive and economically important weed species in Europe, characterized by high reproductive capacity, rapid spread, and pronounced allelopathic potential. The aim of this study was to evaluate the allelopathic effects of aqueous extracts of *A. artemisiifolia* on seed germination and early seedling growth of maize (*Zea mays* L.) under controlled conditions. Whole ragweed plants were collected at the fruit development stage, dried at room temperature, ground into powder, and used to prepare aqueous extracts. Maize seeds were exposed to ragweed extracts at concentrations of 10, 20, 50, and 100%, while distilled water was used as the control. Germination percentage, hypocotyl and epicotyl length were assessed on the 10th day after the establishment of the experiment. The highest hypocotyl length (136 mm) was recorded at the 50% extract concentration, while the control value was 116.27 mm. Epicotyl length varied slightly among treatments, ranging from 29.80 mm at the 100% concentration to 38.15 mm in the control. Seed germination was higher in all extract treatments than in the control, where the lowest germination percentage (47%) was recorded. The highest germination percentages were observed at 20 and 50% extract concentrations. These findings indicate that *A. artemisiifolia* aqueous extracts may exert concentration-dependent allelopathic effects on maize, stimulating seed germination and hypocotyl growth while reducing epicotyl growth at higher concentrations. Further studies are required to identify the bioactive allelochemicals responsible for these effects and to evaluate their activity under field conditions.

Introduction

Modern agriculture faces complex agroecological challenges that directly threaten yield stability, the sustainability of cropping systems, and the economic viability of agricultural production, with weed species representing one of the major risk factors. Within the complex interactions occurring in agroecosystems, allelopathy emerges as a powerful mechanism, particularly among invasive plant species. This feature positions allelopathy as an important component in the development of environmentally sustainable weed management strategies.

Owing to pronounced morphological changes throughout their life cycle, their dominance within plant community structures, and their considerable influence on the surrounding environment, members of the family Asteraceae provide an excellent model for investigating allelochemical interactions [1]. As representatives of the most diverse family of angiosperms, species belonging to Asteraceae constitute important models for elucidating allelochemical interactions [2,3]. These compounds may exert both direct and indirect effects within

agroecosystems. Direct effects involve immediate impacts on neighboring plants and other organisms, manifested through altered germination, growth inhibition, or acute toxicity [4,5].
Common ragweed (*Ambrosia artemisiifolia* L.), a member of the Asteraceae family, is considered one of the most invasive and economically damaging weed species in Europe. Its rapid establishment and spread, high seed production, and pronounced allelopathic potential enable it to compete strongly with major arable crops, including maize (*Zea mays* L.), one of the most important cereal crops in the region. In addition to causing substantial yield reductions, the expansion of common ragweed can induce profound ecological changes within agroecosystems. At the same time, its highly allergenic pollen poses a considerable threat to human health, making this species a serious socio-ecological concern. Changes in agroecological conditions driven by climate change—particularly rising temperatures, prolonged growing seasons, and increasingly frequent soil disturbances—may further facilitate its establishment and spread.
Numerous studies have documented that common ragweed synthesizes a broad range of secondary metabolites, including phenolic acids, sesquiterpene lactones, and other bioactive compounds, which may exert strong inhibitory effects on seed germination and early crop growth [6-9].These allelopathic compounds are released into the surrounding environment through root exudates during active plant growth, as well as through the decomposition of plant residues in the soil.
The need for the proposed research arises from the substantial negative effects of common ragweed (*Ambrosia artemisiifolia* L.) on crop productivity and agroecosystem stability. The knowledge generated through this research may provide a scientific basis for improving agronomic practices and developing more effective integrated weed management strategies.

Experimental

Common ragweed (*Ambrosia artemisiifolia* L.) plants were sampled at the fruit development stage (phenological stages 71–79) [10], according to the distribution mapping reported by Babić and Trkulja [11], while species identification was performed using standard taxonomic keys [12,13]. The collected plant material (whole plants) was dried at room temperature at the JU PIRS, BL facilities, at the Ekonomija locality, after which the dried plant material was ground into a fine powder. Aqueous extracts of common ragweed were prepared according to Lehoczky *et al.* [14] and Bonea *et al.* [15], followed by incubation as described by Maksimović and Jotić [16], filtration using a modified method based on Chon *et al.* [17], and preparation of the required dilutions according to Maksimović and Jotić [16].
Prior to establishing the laboratory experiment, seeds of the selected maize genotype were surface-sterilized and subsequently rinsed with distilled water [18]. Filter paper placed in Petri dishes (150 mm × 25 mm), each containing 25 maize seeds, was moistened with aqueous common ragweed extracts at different concentrations (10, 20, 50, and 100%). The control treatment was prepared using distilled water. All Petri dishes containing the seeds were maintained in a growth chamber under a 12-h light/12-h dark photoperiod, at 24 °C during the light period and 20 °C during the dark period, with a relative humidity of 65%. Germination and shoot length will be assessed on the 10th day after the establishment of the experiment, according to Kazinczi *et al.* [19].

Results and discussion

The analysis of allelopathic effects represents a fundamental aspect of agronomy and plant ecology, as it directly contributes to the ability to predict weed succession, community stability, resilience to environmental stress factors, and, consequently, crop yield.
During the experiment that had the goal to prove alellopathic effects of *Ambrosia artemisiifolia* L. water extracts on maize seed germanination. The following results have been obtained:

In the experiments evaluating hypocotyl length, the results showed that the greatest hypocotyl length was recorded at the 50% extract concentration (136 mm). At extract concentrations of 10% and 20%, hypocotyl lengths were similar, reaching 106.25 and 107.99 mm, respectively, whereas the hypocotyl length recorded in the control treatment was 116.27 mm. The results are presented in Figure 1.

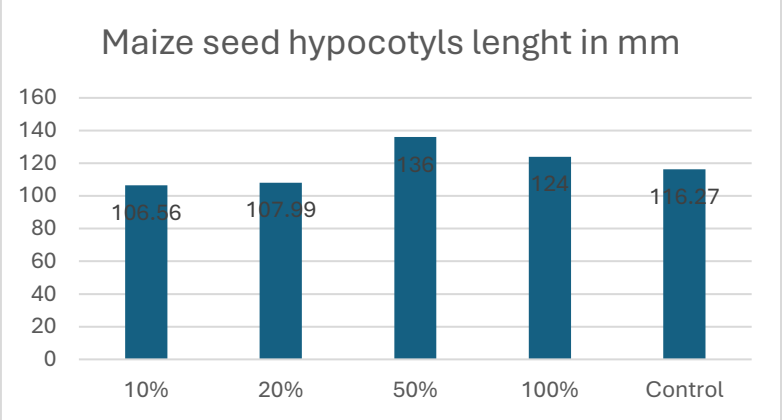


Figure 1 Measured values of maize seed hypocotyls after treatment with *Ambrosia artemisiifolia* L. extracts.

Measurements of epicotyl length showed relatively similar values across all treatments. Epicotyl length ranged from 29.80 mm at the 100% extract concentration to 38.15 mm in the control treatment with distilled water. At extract concentrations of 10%, 20%, and 50%, the recorded epicotyl lengths were 35.01, 33.99, and 35.70 mm, respectively. The epicotyl length values recorded after treatment with different concentrations of common ragweed aqueous extract are presented in Figure 2.

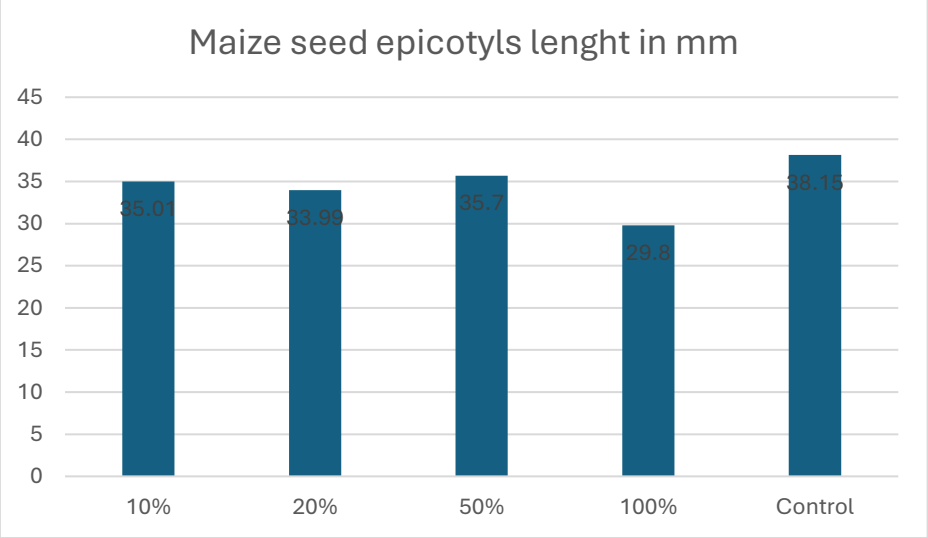


Figure 2 Measured values of maize seed epicotyls after treatment with *Ambrosia artemisiifolia* L. extracts.

The maize seed germination percentage showed a response pattern similar to that observed for epicotyl and hypocotyl length. The highest germination percentages were recorded at extract concentrations of 20% and 50%, whereas the lowest germination percentage (47%) was observed in the control treatment with distilled water. At extract concentrations of 10% and 100%, seed germination reached 69% and 68%, respectively. The results indicate that the

common ragweed aqueous extract exerted a stimulatory effect on maize seed germination at all tested concentrations compared with the control. The maize seed germination percentages recorded after treatment with different concentrations of common ragweed aqueous extract are presented in Figure 3.

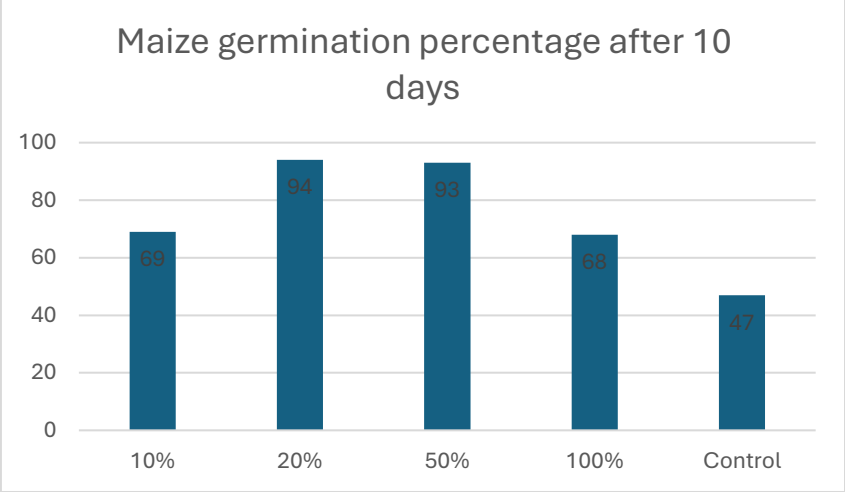


Figure 3 Seed germination of maize seeds after treatment with *Ambrosia artemisiifolia* L. extracts.

Conclusion

Based on the results of the conducted experiments, it can be concluded that *Ambrosia artemisiifolia* L. exhibited allelopathic effects on maize seed germination and early seedling growth. The aqueous extract of *A. artemisiifolia* had a more pronounced effect on hypocotyl length than on epicotyl length, with the magnitude and direction of the response depending on the extract concentration. The highest hypocotyl length was recorded at the 50% extract concentration, whereas epicotyl length showed relatively small variations among treatments and tended to decrease at higher extract concentrations.

The aqueous extracts of *A. artemisiifolia* stimulated maize seed germination at all tested concentrations compared with the control, with the highest germination percentages recorded at concentrations of 20% and 50%. These findings indicate a concentration-dependent response of maize to common ragweed aqueous extracts, suggesting that the allelopathic effect may be either stimulatory or inhibitory depending on the evaluated growth parameter and extract concentration.

The study was conducted under *in vitro* conditions, and the results indicate the allelopathic potential of *A. artemisiifolia* toward maize. However, further research under both controlled and field conditions is required to elucidate the mechanisms underlying these interactions and to determine their ecological and agronomic relevance.

Future studies should focus on the identification and characterization of the bioactive allelochemicals responsible for the observed effects, as well as on evaluating their effects on different crop and weed species. A better understanding of these compounds and their biological activity could contribute to assessing their potential application in the development of environmentally sustainable weed management strategies.

References

[1] A. Junaedi, A.M. Chozin, K. Kim, Current Research Status of Allelopathy. Scientific Journals of Bogor Agricultural University. Hayati, 13 (2) (2009), 79-84.

[2] R.M. McCoy, J.R. Widhalm, G.G. McNickle, Allelopathy as an evolutionary game. Plant Direct. 6(2) (2022) e382.

[3] X. Zhu, Y. Yi, L. Huang, C. Zhang, H. Shao, Metabolomics Reveals the Allelopathic Potential of the Invasive *Plant Eupatorium adenophorum*. Plants 10(7) (2021), 1473.
[4] C.H. Kong, T.D. Xuan, T.D. Khanh, H.D. Tran, N.T. Trung, Allelochemicals and Signaling Chemicals in Plants. Molecules. 24(15) (2019), 2737.
[5] L. Bakacsy, L.V. Kardos, A. Szepesi, K.N. Nagy, A. Vasas, G. Feig, Investigation of the Allelopathic Effect of Two Invasive Plant Species in Rhizotron System. Life (Basel), 14(4) (2024), 475.
[6] Q. Liu, X. Sun, L. Zhang, K. Li, X. Guo, Y. Guo, Z. Liu, Regulation mechanism of ρ-Hydroxybenzoic acid on grapevine root secretion characteristics. Scientia Horticulturae 256 (2019), 108541.
[7] G. Liang, Y. Niu, The allelopathic effect of para-hydroxybenzoic acid on the gene expression of photosynthesis and respiration in *Solanum lycopersicum*. Current Plant Biology 32(430) (2022), 100261.
[8] F. Zhang, J. Sun, C. Wang, C. Li, F. Chen, H. Xu, X. Chen, Bacillus benefits the competitive growth of *Ambrosia artemisiifolia* by increasing available nutrient levels. Front Plant Science 13 (2023), 1069016.
[9] C. Han, N. Kuchkarova, A. Ullah, Y. Arafat, Z. Toshmatov, H. Shao, Chemical profile and allelopathic potential of *Ambrosia artemisiifolia* root exudate. Chemistry&Biodiversity 23(2) (2026), e02986.
[10] M. Hess, G. Barralis, H. Bleiholder, H. Buhr, T. Eggers, H. Hack, R. Stauss, Use of the extended BBCH scale – general for the description of the growth, stages of mono and dicotyledonous species. Weed Research, 37 (1997), 433 – 441.
[11] G. Babić, V. Trkulja, Distribution mapping of selected invasive weed species in north western area of Republic of Srpska (Bosnia and Herzegovina). VIII. International Scientific Agricultural Symposium Agrosym, Jahorina. Book of Proceedings, (2017), 1524-1530.
[12] M. Josifović, (Ed.) Flora Republike Srbije, I-X, SANU, Beograd, (1970-1986).
[13] M. Sarić, N. Diklić, Eds Flora SR Srbije. Beograd: SANU, 10 (2) (1989).
[14] E. Lehoczky, R. Szabo, M.O. Nelima, P. Nagy, I. Beres, Allelopathic effects of ragweed (*Ambrosia artemisiifolia* L.) on cultivated plants. Communications in Agricultural and Applied Biological Sciences, 76 (3) (2011), 545– 549.
[15] D. Bonea, E. Bonciu, M. Niculescu, A.L. Olaru, The allelopathic, cytotoxic and genotoxic effect of Ambrosia artemisiifolia on the germination and root meristems of Zea mays, Caryologia, 71 (1) (2017), 24-28.
[16] T. Maksimović, K. Jotić, Allelopathic effects of ragweed on corn (*Zea mays* L.) and wheat (*Triticum aestivum* L.). Acta Scientifica Balcanica, 1(2) (2021), 13-21.
[17] S-U. Chon, Y-M. Kim, J-C. Lee, Herbicidal potential and quantification of causative allelochemicals from several Compositae weeds. Weed Research 43(6) (2003), 444-450
[18] J. Šućur, B. Konstantinović, M. Crnković, V. Bursić, N. Samardžić, Đ. Malenčić, D. Prvulović, M. Popov, G. Vuković, Chemical Composition of *Ambrosia trifida* L. and Its Allelopathic Influence on Crops. Plants, 10 (10) (2021), 2222.
[19] G. Kazinczi, I. Béres, A. Onofri, E. Nádasy, A. Takács, J. Horvát, M. Torma, Allelopathic effects of plant extracts on common ragweed (*Ambrosia artemisiifolia* L.). Journal of Plant Diseases and Protection, 21 (2008), 335–340.

WEEDS IN SUGAR BEET AND THEIR CONTROL

Nataša Mandić, Bojan Konstantinović, Milena Popov, Tijana Stojanović, Stefan Ugrinov, Sandra Cvjetković

University of Novi Sad, Faculty of Agriculture, Department of Environmental and Plant Protection, Trg Dositeja Obradovića 8, 21000 Novi Sad, Republic of Serbia
e-mail: natasa.mandic@polj.edu.rs

Abstract

During the 2023 growing season, the efficacy of a post-emergent herbicide in sugar beet was conducted at the Kula and Krivaja locations. The active ingredients used were foramsulfuron 50 g/L and thiencarbazone-methyl 30 g/L (OD formulation)(Conviso One). Treatments were conducted at the recommended application rate (1 L/ha) as well as at the minimum effective application rate (0.6 L/ha), while phytotoxicity on the crop was assessed using a double dose of the recommended application rate (2 L/ha). Efficacy was calculated relative to control plots. The tested product showed good efficacy against the following weed species: *Hibiscus trionum*, *Amaranthus retroflexus*, *Ambrosia artemisiifolia*, *Datura stramonium* and *Chenopodium album*. Satisfactory efficacy was observed against *Chenopodium hybridum* and *Xanthium strumarium*. Low efficacy was determined against the following weed species: *Cannabis sativa*, *Convolvulus arvensis* and *Sorghum halepense*. No phytotoxic effects of the tested product were recorded in the trials at any application rate.

Introduction

Agricultural production plays a vital role in providing sufficient food and industrial raw materials for the population and the food industry. The intensification of agriculture has increased the use of modern agronomic practices, high-yielding varieties and hybrids, and plant protection measures to achieve high and stable yields. According to Konstantinović *et al.* [1], a weed is any plant growing in a crop where it is unwanted by the producer. Weeds compete with crops for water, light, nutrients, and space, thereby reducing the yield and quality of agricultural products.

Sugar beet (*Beta vulgaris* subsp. *vulgaris*) is one of the most important industrial crops in temperate regions and a major source of sugar in Europe. Its importance extends beyond sugar production: sugar beet by-products are used in livestock production, the food industry, and energy production. Owing to favourable agroecological conditions, sugar beet has an important place in arable crop production in Serbia, particularly in Vojvodina.

Sugar beet is considered a demanding arable crop, primarily because it is vulnerable during the early stages of development. It emerges slowly and has limited competitive ability at these stages, allowing weeds to establish rapidly. Without timely and effective weed control, both root yield and sugar content may decline substantially.

Important weeds in sugar beet include *Amaranthus retroflexus*, *Chenopodium album*, *Ambrosia artemisiifolia*, *Datura stramonium*, *Abutilon theophrasti*, and *Xanthium strumarium*, as well as the perennial species *Convolvulus arvensis*, *Cirsium arvense*, and *Sorghum halepense*. Weed density and species composition depend on agroecological conditions, crop rotation, agronomic practices, and weather during the growing season.

This study examines the weed species present in sugar beet fields at Kula and Krivaja and evaluates the efficacy of different application rates of Conviso One (foramsulfuron and thiencarbazone-methyl) for their control. The findings are intended to improve knowledge of the weed flora in sugar beet and support more effective weed management under the production conditions at the study sites.

The critical period for weed control in sugar beet occurs during the first few weeks after crop emergence, when weeds can cause the greatest damage. Intense competition for water, light, and nutrients during this period may substantially reduce root yield and sugar content [2].
Sugar beet fields may contain a wide range of broadleaf and grass weeds with differing biological characteristics and competitive abilities. Common species include *Amaranthus retroflexus*, *Chenopodium album*, *Ambrosia artemisiifolia*, *Datura stramonium*, *Abutilon theophrasti*, and *Xanthium strumarium*, together with the perennial species *Convolvulus arvensis*, *Cirsium arvense*, and *Sorghum halepense* [3].
Because sugar beet is highly sensitive to weed competition, its production relies heavily on herbicides. In recent years, sugar beet varieties tolerant to acetolactate synthase (ALS) inhibitors have become more widely used, enabling new weed management systems and more effective weed control in the crop.

Experimental
During the growing season in 2023 (in May and June) the study conducted on the weed flora in sugar beet crops at two localities in the Republic of Serbia (Kula and Krivaja) was carried out. The assessment of the weed species in sugar beet fields involved counting the weeds in randomly chosen 1 m² quadrants within each 25 m² plot. This method allowed for a systematic evaluation of weed diversity in the crop. The identification of the weed species was done according to the literature sources [4,5]. The experiment was conducted using a randomized block design with four replicates, and a control group (untreated plots), following EPPO guidelines [6,7]. Weather conditions throughout the experiment were optimal for the effective performance of the herbicides under investigation. The results were compiled and analyzed at the University of Novi Sad, Faculty of Agriculture, Department of Environmental and Plant Protection, using MS Excel and Statistica 10. This analysis was based on the average values from four plots for each treatment, including the control. The efficacy of the studied herbicide was assessed using the following categories: poor efficacy (less than 75%), satisfactory efficacy (75-90%) and high efficacy (greater than 90%). foramsulfuron 50 g/L and thiencarbazone-methyl 30 g/L was applied at two application rates: 1.0 and 2.0 l/ha (phytotoxicity application), while the minimum effective application was applied at the rate 0.6 l/ha.

Results and discussion
At the Kula locality, the following weed species were recorded in the field trial: *Amaranthus retroflexus*, *Ambrosia artemisiifolia*, *Chenopodium album*, *Chenopodium hybridum*, *Cirsium arvense*, *Datura stramonium*, and *Xanthium strumarium*.

Efficacy of foramsulfuron 50 g/L and thiencarbazone-methyl 30 g/L at Kula locality are shown in Table 1.

Table 1. The efficacy of foramsulfuron 50 g/L and thiencarbazone-methyl 30 g/L at Kula locality.

Weed species	Control	Conviso One 0.6 l/ha		Conviso One 1.0 l/ha		Conviso One 2.0 l/ha	
	No./m^{2*}	No./m^2	Eff.*	No./m^2	Eff.	No./m^2	Eff.
First assessment							
Amaranthus retroflexus	5,75	1,75	69,57	0,00	100,00	0,00	100,00
Ambrosia artemisiifolia	5,25	1,50	71,43	0,25	95,24	0,00	100,00
Chenopodium album	4,25	1,00	76,47	0,00	100,00	0,00	100,00
Chenopodium hybridum	4,00	2,25	43,75	0,25	93,75	0,00	100,00
Cirsium arvense	4,25	1,50	64,71	0,25	94,12	0,00	100,00
Datura stramonium	4,00	1,50	62,50	0,00	100,00	0,00	100,00
Xanthium strumarium	5,50	1,50	72,73	0,25	95,45	0,00	100,00
Second assessment							
Amaranthus retroflexus	7,75	3,50	54,84	0,00	100,00	0,00	100,00
Ambrosia artemisiifolia	6,00	3,25	45,83	0,50	91,67	0,00	100,00
Chenopodium album	5,00	1,75	65,00	0,00	100,00	0,00	100,00
Chenopodium hybridum	4,75	3,00	36,84	0,25	94,74	0,00	100,00
Cirsium arvense	5,75	2,50	56,52	0,50	91,30	0,00	100,00
Datura stramonium	5,25	2,75	47,62	0,00	100,00	0,00	100,00
Xanthium strumarium	7,75	2,50	67,74	0,75	90,32	0,00	100,00

*No./m^2 – number per m^2; Eff. – efficacy

Chenopodium album and *Amaranthus retroflexus* were the most abundant species in the crop and were the main competitors of sugar beet during its early growth stages. *Ambrosia artemisiifolia* and *Datura stramonium* were also present in substantial numbers, whereas the perennial species *Cirsium arvense* was less abundant.

The efficacy of Conviso One at the Kula site is presented in Table 1. The highest levels of control were achieved for *Chenopodium album* and *Datura stramonium*, particularly at the higher application rates. Good control was also observed for *Amaranthus retroflexus*, which was highly sensitive to the treatments.

Chenopodium hybridum was less sensitive at the lower application rates, particularly following a single application of 0.6 L/ha. However, control improved considerably at higher rates. *Ambrosia artemisiifolia* was effectively controlled in most treatments, while higher application rates also provided effective control of *Xanthium strumarium*. The perennial species *Cirsium arvense* was less sensitive than the annual broadleaf weeds.

At the Krivaja locality, the following weed species were recorded in the field trial: *Abutilon theophrasti*, *Ambrosia artemisiifolia*, *Convolvulus arvensis*, *Cannabis sativa*, *Hibiscus trionum*, and *Sorghum halepense*.

Efficacy of foramsulfuron 50 g/L and thiencarbazone-methyl 30 g/L at Krivaja locality are shown in Table 2.

Table 2. The efficacy of Conviso One at Krivaja locality.

Weed species	Control	Conviso One 0.6 l/ha		Conviso One 1.0 l/ha		Conviso One 2.0 l/ha	
	No./m^{2*}	No./m^2	Eff.*	No./m^2	Eff.	No./m^2	Eff.
			First assessment				
Abutilon theophrasti	4,75	1,00	78,95	0,25	94,74	0,00	100,00
Ambrosia artemisiifolia	5,50	1,50	72,73	0,50	90,91	0,00	100,00
Convolvulus arvensis	4,25	2,00	52,94	1,50	64,71	0,00	100,00
Cannabis sativa	5,00	1,50	70,00	0,75	85,00	0,00	100,00
Hibiscus trionum	4,75	2,00	57,89	0,00	100,00	0,00	100,00
Sorghum halepense	5,50	1,75	68,18	0,75	86,36	0,00	100,00
			Second assessment				
Abutilon theophrasti	5,25	2,25	57,14	0,50	90,48	0,00	100,00
Ambrosia artemisiifolia	7,75	2,75	64,52	0,75	90,32	0,00	100,00
Convolvulus arvensis	5,50	3,00	45,45	2,00	63,64	0,00	100,00
Cannabis sativa	5,75	3,00	47,83	1,25	78,26	0,00	100,00
Hibiscus trionum	5,50	3,00	45,45	0,25	95,45	0,00	100,00
Sorghum halepense	6,25	3,50	44,00	1,00	84,00	0,00	100,00

*No./m^2 – number per m^2; Eff. – efficacy

Abutilon theophrasti and *Hibiscus trionum* were the most abundant species and represented substantial competition for sugar beet during the early stages of crop development.

The efficacy of Conviso One at the Krivaja site is presented in Table 2. High levels of control were achieved for *Abutilon theophrasti* and *Hibiscus trionum*, particularly at the higher application rates. *Ambrosia artemisiifolia* responded well to the treatments, while satisfactory control was also observed for *Cannabis sativa*.

The perennial species *Convolvulus arvensis* was the least sensitive to the treatments, especially at the lower application rates. *Sorghum halepense* was effectively controlled at the higher rates, whereas control was somewhat weaker at the lower rates.

At Krivaja, the highest overall efficacy was achieved with the 2.0 L/ha treatment, which provided a high level of control of most weed species present. These findings indicate that higher application rates provided more effective and consistent weed control in the sugar beet crop under the conditions of this trial.

Conclusion

The results showed substantial differences in the efficacy of Conviso One depending on the application rate, application method, and weed species present. At both study sites, the highest application rates produced the best results. The greatest adverse effects were observed in plots dominated by rapidly growing broadleaf weeds, including *Chenopodium album*, *Amaranthus retroflexus*, and *Ambrosia artemisiifolia*.

These findings indicate the potential value of ALS-inhibiting herbicides in sugar beet production, particularly when weather conditions prevent the timely application of conventional herbicides at the cotyledon stage. Conviso One provided control of a broad range of weed species at somewhat later growth stages, which may offer a practical advantage under the growing conditions at Kula and Krivaja. The results may therefore be relevant to weed management in sugar beet varieties tolerant to ALS inhibitors, especially as part of an integrated weed management approach.

.

References

[1] B. Konstatinović, M. Popov, N. Samardžić, N. *Osnovi herbologije praktikum*. Univerzitet u Novom Sadu, Poljoprivredni fakultet, Novi Sad (2021).
[2] B. Konstatinović, P. Štrbac, F. Balaž, M. Govedarica, M. Jarak. *Zaštita šećerne repe od štetočina, bolesti i korova*. „STYLOS " doo, Novi Sad (2021).
[3] R. Miličić. *Korovna flora šećerne repe i mogućnosti njena suzbijanja*. Sveučilište Josipa Juraja Štrosmajera, Osijek (2021).
[4] M. Josifović (Ed.), Flora SR Srbije I-X, SANU, Belgrade, Republic of Serbia, 1970-1986.
[5] T. Šarić, Atlas korova: 100 najvažnijih korovskih biljaka u Jugoslaviji, Svjetlost, Sarajevo, Bosnia and Herzegovina, 1991.
[6] OEPP. Guideline for the efficacy evaluation of herbicides (Weeds in sugar an fodder beet), OEPP/EPPO Standards for the efficacy evaluation of plant protection products, Herbicides and Plant Growth Regulators, PP 1/52 (3) (2014).
[7] OEPP. Guideline for the efficacy evaluation of plant protection products, Phytotoxicity assessment, Introduction, General and Miscellaneous Guidelines, New and Revised Guidelines (2014).

DEGRADATION OF SALICYLIC ACID IN AQUEOUS SOLUTION USING ELECTRON BEAM IRRADIATION AND OZONE: TOWARDS A COMBINED TREATMENT APPROACH

Krisztina Kovács[1], Anna Tegze[1], Monica Pavel[2], Anikó Bezsenyi[3,4], Erzsébet Takács[1], Mandula Petra[1], László Wojnárovits[1], Renáta Homlok[1]

[1]Radiation Chemistry Group, Surface Chemistry and Catalysis Department, Institute for Energy Security and Environmental Safety, HUN-REN Centre for Energy Research, Konkoly-Thege Miklós út 29–33, 1121 Budapest, Hungary
[2]"Ilie Murgulescu" Institute of Physical Chemistry of the Romanian Academy, 202 Spl. Independentei, 060021 Bucharest, Romania
[3]Institute of Environmental Engineering and Natural Sciences, Rejtő Sándor Faculty of Light Industry and Environmental Engineering, Óbuda University, Doberdó u. 6., 1034 Budapest, Hungary
[4]Budapest Sewage Works Pte Ltd., Asztalos Sándor út 4., 1087 Budapest, Hungary
e-mail: homlok.renata@ek.hun-ren.hu

Abstract

Salicylic acid may occur in aquatic environments as a pharmaceutical residue, making its removal from water of environmental interest. Advanced Oxidation Processes (AOPs) offer approaches for degrading organic contaminants through reactions involving highly reactive species. Previous studies have shown that ionizing radiation can degrade salicylic acid, with hydroxyl radicals playing an important role [1,2].

This study compared salicylic acid degradation by electron beam irradiation (e-beam) and ozonation as separate treatment processes. Aqueous solutions containing 20 mg L^{-1} salicylic acid were irradiated with a 4 MeV electron beam at absorbed doses of 0–50 kGy or treated with an ozone-containing gas stream for 0–30 min. The effects of both treatments were evaluated by monitoring salicylic acid degradation by measuring UV absorbance, pH, chemical oxygen demand (COD), and total organic carbon (TOC).

Both electron beam irradiation and ozonation induced the degradation of salicylic acid, accompanied by changes in COD and TOC consistent with oxidation and mineralization, respectively. In the irradiated solutions, reactive species formed by water radiolysis, particularly hydroxyl radicals, may have contributed to these processes. During ozonation, both molecular ozone and secondary hydroxyl radicals may have played a role. These results provide a basis for investigating a future combined electron beam–ozone treatment process.

Introduction

Salicylic acid is an aromatic hydroxycarboxylic acid widely used in pharmaceutical applications that may enter wastewater and other aquatic environments as a pharmaceutical residue. Its removal from water is therefore of environmental interest.

Advanced Oxidation Processes are promising methods for the degradation of organic pollutants because they generate highly reactive oxidizing species, particularly hydroxyl radicals (•OH). During electron beam irradiation, water radiolysis generates •OH, hydrated electrons, and hydrogen atoms.

Previous studies have shown that ionizing radiation degrades salicylic acid in aqueous solution, with •OH playing an important role [1]. Reported degradation products include 2,3-dihydroxybenzoic acid, 2,5-dihydroxybenzoic acid, and catechol [2].

Ozonation provides another approach to salicylic acid degradation. Its effectiveness depends on factors including pH and ozone dose, while both direct reactions with molecular ozone and

reactions involving secondary •OH may contribute [3]. Previous studies of O_3 and UV/O_3 treatment have examined salicylic acid removal, changes in total organic carbon, and the formation of oxidation products [4].
The aim of the present study was therefore to investigate the degradation of salicylic acid using electron beam irradiation and ozone treatment as individual processes, and to compare their degradation behaviour as a basis for the future development of a combined e-beam/O_3 treatment process.

Experimental

Aqueous salicylic acid solutions with an initial concentration of 20 mg L^{-1} were prepared for the irradiation and ozonation experiments.
For electron beam treatment, air-saturated solutions were irradiated using a 4 MeV electron beam at different absorbed doses in the range of 0–50 kGy.
Ozone treatment was performed using a newly established ozonation system. The ozone flow rate was maintained at 1.2 L min^{-1}, and treatment times between 0 and 30 min were used. The ozone-containing off-gas was passed through a 10% (w/V) Na_2SO_3 solution to absorb residual ozone. Following ozonation, 125 µL of 10% (w/v) Na_2SO_3 solution was added to each 200 mL sample to quench residual dissolved ozone. This corresponded to a nominal final Na_2SO_3 concentration of 62.5 mg L^{-1} (0.50 mmol L^{-1}).
The treatment effects were evaluated by monitoring salicylic acid degradation by measuring UV absorbance, pH, chemical oxygen demand (COD), and total organic carbon (TOC).

Results and discussion

Electron beam irradiation decreased the salicylic acid concentration, its removal increased with increasing absorbed doses. The observed degradation can be attributed mainly to reactions with reactive species generated during the radiolysis of water, particularly hydroxyl radicals. This behavior is consistent with previous studies on the radiation-induced degradation of salicylic acid in aqueous solution [1,2].
Ozonation also decreased the salicylic acid concentration over the investigated treatment period. The decrease in UV absorbance indicated changes in the aromatic structure of the molecule during oxidation. The observed changes in COD and TOC provided additional information on the oxidation and mineralization processes, respectively.
Previous ozonation studies have shown that salicylic acid degradation depends strongly on pH and ozone dosage, and that both direct ozone attack and hydroxyl-radical-mediated reactions may contribute to the degradation [3]. The O_3 and UV/O_3 processes have also been reported to influence both salicylic acid removal and the formation of oxidation products [4].
The comparison of the two individual treatments provides a basis for identifying their potentially complementary characteristics. While electron beam irradiation generates reactive species directly through water radiolysis, ozonation introduces molecular ozone and can additionally promote secondary radical reactions. The combination of these two processes is therefore of interest for further investigation.

Conclusion

The degradation of salicylic acid in aqueous solution was investigated using electron beam irradiation and ozone treatment as two individual Advanced Oxidation Processes.
Both treatment approaches demonstrated their applicability for the degradation of salicylic acid. Electron beam irradiation provided degradation through reactive species generated by water radiolysis, while ozonation promoted oxidation through reactions involving ozone and secondary reactive species.

The comparison of the two processes provides an experimental basis for the future combination of electron beam irradiation and ozonation. Further experiments will focus on the combined e-beam/O_3 treatment to investigate whether the two oxidation pathways can be effectively integrated for enhanced degradation and mineralization of organic contaminants in aqueous systems.

Acknowledgements
This work was supported by the Hungarian–Romanian bilateral inter-academic cooperation project NKM2025-90.

References
[1] L. Szabó, T. Tóth, R. Homlok, G. Rácz, E. Takács, L. Wojnárovits, Radiat. Phys. Chem. 97 (2014) 239.
[2] G. Albarrán, E. Mendoza, Radiat. Phys. Chem. 147 (2018) 27.
[3] R. Hu, L. Zhang, J. Hu, Chemosphere 153 (2016) 394.
[4] J. Chang, S. Wang, Y. Zhang, Y. Wang, W. Zhang, J. Lu, Z. Wang, Water Sci. Technol. 81 (2020) 753.

RADIOLYTIC DEGRADATION OF SULFADIAZINE IN DIFFERENT WATER MATRICES

Anna Pfeil[1], Anna Tegze[2], Anikó Bezsenyi[3,4], Petra Mandula[2], László Wojnárovits[2], Krisztina Kovács[2]

[1]Budapest University of Technology and Economics. Faculty of Chemical Technology and Biotechnology, Műegyetem rkp. 3., 1111 Budapest, Hungary
[2]HUN-REN Centre for Energy Research, Surface Chemistry and Catalysis Department, Radiation Chemistry Group, Konkoly-Thege Miklós út 29-33., 1121 Budapest, Hungary
[3]Institute of Environmental Engineering and Natural Sciences, Rejtő Sándor Faculty of Light Industry and Environmental Engineering, Óbuda University, Doberdó u. 6., 1034 Budapest, Hungary
[4]Budapest Sewage Works Pte Ltd., Asztalos Sándor út 4., 1087 Budapest, Hungary
e-mail: kovacs.krisztina@ek.hun-ren.hu

Abstract
The radiolytic degradation of sulfadiazine (SDZ) was investigated with particular focus on the reactivity of individual reactive species, the influence of the aqueous matrix, and the resulting changes in biodegradability and toxicity. Hydroxyl radicals were identified as the primary species responsible for SDZ decomposition. The degradation efficiency was found to be strongly matrix-dependent, being most limited in purified wastewater. Ionizing radiation treatment consistently enhanced biodegradability and reduced toxicity of the treated solutions, supporting its potential as a pre-treatment strategy for SDZ-contaminated waters.

Introduction
Sulfadiazine is a widely used sulfonamide antibiotic that is continuously released into aquatic environments due to its extensive application and incomplete metabolism [1]. Even at low concentrations, antibiotic residues may exert selective pressure on microbial communities, thereby promoting the development and spread of antibiotic resistance [2]. Their efficient removal from wastewater is therefore of considerable environmental and public health importance. Ionizing radiation generates highly reactive species, particularly hydroxyl radicals, that can efficiently degrade such persistent contaminants [3,4]. However, naturally occurring water constituents may compete for these reactive species and thereby significantly influence degradation efficiency. Therefore, this study investigates the radiolytic degradation of sulfadiazine in water matrices of varying complexity.

Experimental
Steady-state irradiation experiments were performed using a panoramic-type ^{60}Co γ-irradiation facility at a dose rate of 2.0 kGy h^{-1}. The absorbed dose and the dose rate were determined using an ethanol-chlorobenzene dosimetry system [5]. In most experiments the solutions were continuously bubbled with air to maintain oxygen saturation and prevent O_2 depletion during irradiation. To assess the contributions of the different reactive species generated during water radiolysis, the experiments were conducted under different conditions: air-saturated ($^{\bullet}OH$ + $O_2^{\bullet-}/HO_2^{\bullet}$), N_2O-saturated ($^{\bullet}OH$), N_2-saturated ($^{\bullet}OH$, e_{aq}^-, $H^{\bullet}$), and N_2-saturated solutions containing 5% (v/v) *tert*-butanol (e_{aq}^-). Following irradiation, changes in the UV-Vis absorption spectra of the samples were monitored using a UV-Vis spectrophotometer. The samples were further characterized by using conventional wastewater analytical methods to evaluate degradation efficiencies in different matrices: purified water, tap water, synthetic wastewater [6] and purified wastewater.

Chemical Oxygen Demand (COD), representing the amount of chemically oxidizable organic matter, was determined according to ISO 6060:1989. The Biochemical Oxygen Demand (BOD) measurements were carried out in an OxiTOP® Control BOD Respirator System in compliance with DIN EN 1899–1 (1999). For assessment of the toxic effects bioluminescence inhibition assay was applied with *Vibrio fischeri* bacteria according to DIN EN ISO 11348-2. Detailed descriptions of the analytical procedures are provided in our previous publications [7,8].

Results and discussion

In the first step, the reactivity of the individual radicals formed during water radiolysis (•OH, e_{aq}^-, H•) toward SDZ was studied under different reaction conditions using UV-Vis spectrophotometry to follow the dose-dependent decrease of the characteristic SDZ absorption band at 265 nm over the 0–5 kGy range (Fig. 1.). •OH proved to be the most reactive species toward SDZ, with essentially identical degradation efficiency observed in •OH-selective and •OH + $O_2^{\bullet-}$/$HO_2^\bullet$ systems. The hydrated electron also reacted appreciably with SDZ, though somewhat less efficiently. Notably, when all three primary water radiolysis products (•OH, e_{aq}^-, H•) were simultaneously present, the overall degradation efficiency was lower than that observed for either radical acting alone, suggesting a non-additive, competitive interplay among the radicals – likely due to radical–radical recombination reactions that reduce the fraction of reactive species available to attack the SDZ molecule.

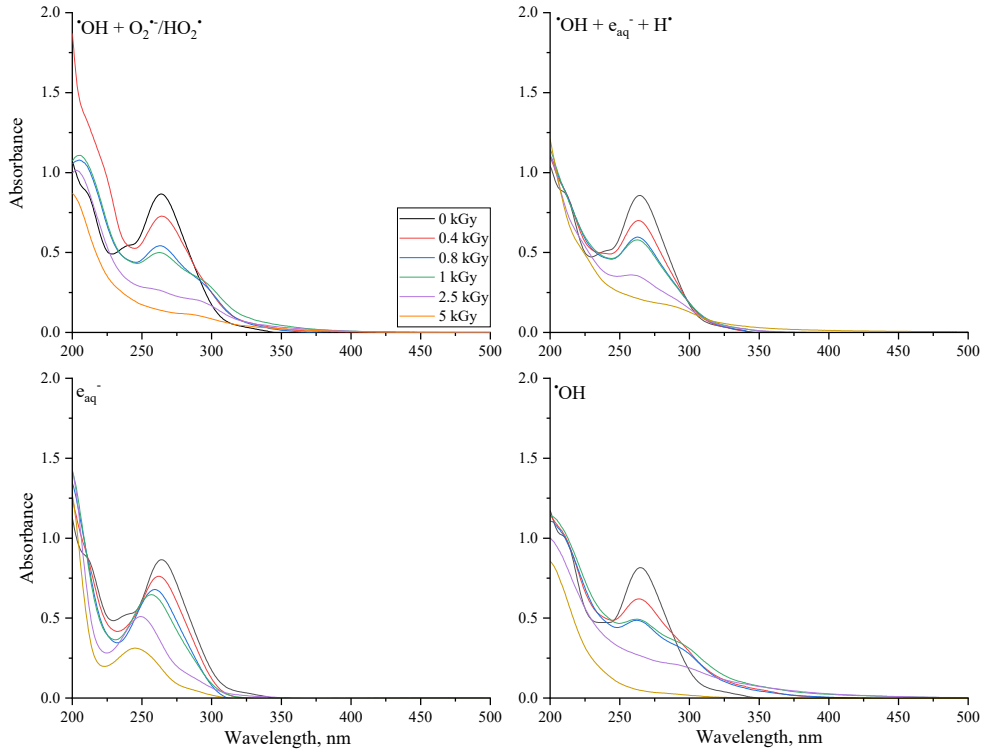


Figure 1. Dose-dependent UV-Vis spectral changes of SDZ (c_0 = 0.1 mmol dm^{-3}) in purified water under selective and combined water radiolysis radicals: •OH + $O_2^{\bullet-}$/$HO_2^\bullet$ (air-saturated), •OH + e_{aq}^- + H• (N_2-saturated), e_{aq}^- (N_2-saturated + *t*-BuOH), and •OH (N_2O-saturated).

In a further step, the effect of the aqueous matrix on SDZ degradation was examined by comparing pure water, tap water, synthetic wastewater, and purified wastewater (Fig. 2.). Degradation efficiency was found to be strongly matrix-dependent, following the order pure water ≈ synthetic wastewater > tap water > purified wastewater. The reduced degradation observed in tap water is attributed to the scavenging effect of carbonate/bicarbonate ions on •OH, while the markedly lower efficiency in purified wastewater indicates substantial

competition from residual dissolved organic matter and other matrix constituents for the reactive radicals. These results demonstrate that real water matrices considerably decrease the absorbed dose efficiency compared to model systems, which must be taken into account when designing radiation-based treatment strategies for SDZ removal.

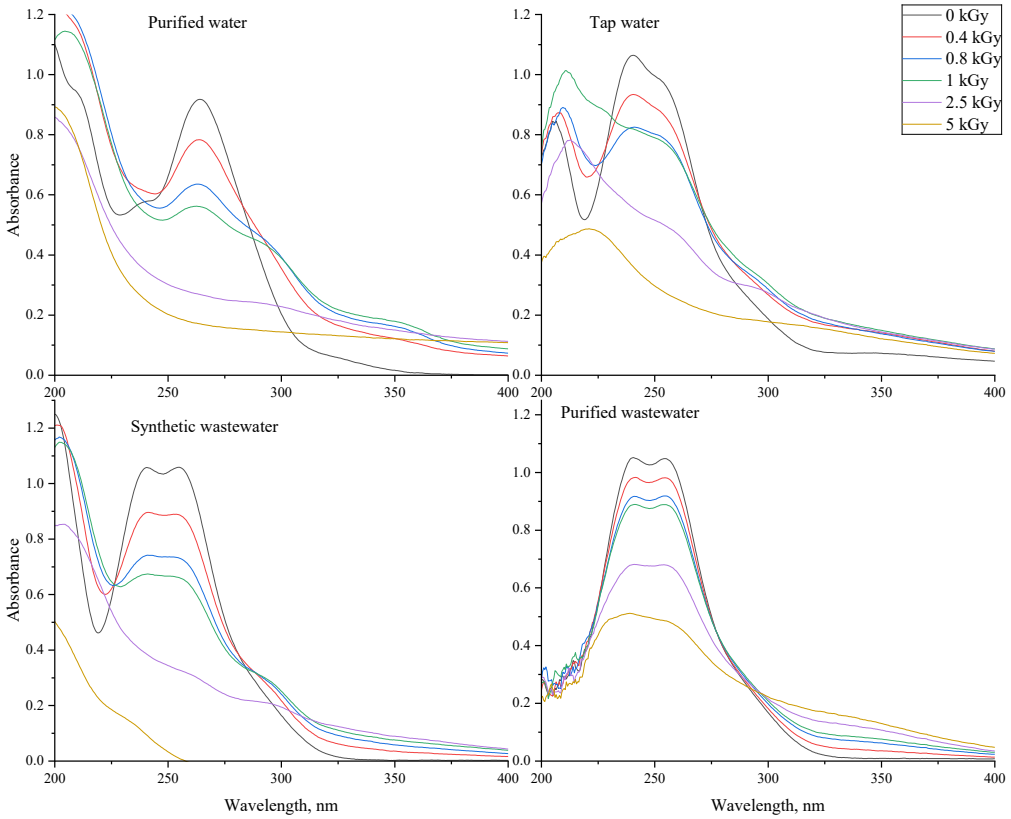


Figure 2. Dose-dependent UV-Vis spectral changes of SDZ in purified water, tap water, synthetic wastewater, and purified wastewater.

To further evaluate the environmental relevance of the radiolytic treatment, the biodegradability of the irradiated solutions was assessed by monitoring the chemical oxygen demand (COD) and the BOD_5/COD ratio, used as a biodegradability index, as a function of absorbed dose. In all matrices except purified wastewater, the COD decreased while the BOD_5/COD ratio increased markedly with increasing dose, indicating a progressive conversion of the initially non-biodegradable parent compound into more readily biodegradable transformation products. This effect was accompanied by a general decrease in luminescence inhibition, confirming a concurrent reduction in acute toxicity. Consistent with the matrix effects observed for SDZ removal, the enhancement in biodegradability was considerably less pronounced in purified wastewater, further supporting the role of the residual matrix components in limiting the efficiency of the radiolytic treatment.

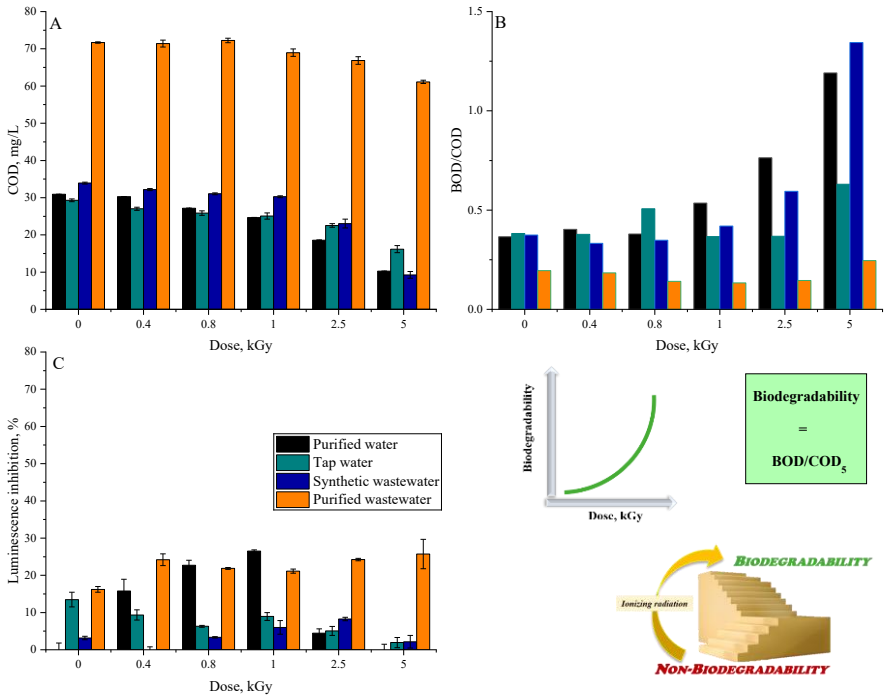


Figure 3. Effect of absorbed dose on (A) COD, (B) BOD_5/COD, and (C) luminescence inhibition (%) of SDZ solutions in different aqueous matrices together with a schematic summary illustrating the radiation-induced shift from non-biodegradable to biodegradable character.

Conclusion

The results demonstrate that ionizing radiation can effectively degrade SDZ in aqueous solutions. The non-additive behavior observed when all primary radiolytic species were simultaneously present suggests competitive radical–radical interactions that should be considered when optimizing treatment conditions. Importantly, the degradation efficiency and the extent of biodegradability improvement were strongly influenced by the composition of the aqueous matrix, being most pronounced in pure water and synthetic wastewater, moderately reduced in tap water, and considerably limited in purified wastewater due to competition from residual matrix constituents for the reactive radicals. Despite this matrix-dependent limitation, ionizing radiation treatment consistently improved the biodegradability (BOD_5/COD) and reduced the acute toxicity of the treated solutions, as reflected by decreased luminescence inhibition. These findings highlight the potential of ionizing radiation as a pre-treatment step to enhance the biological treatability of SDZ-contaminated waters, while underlining the need to account for matrix effects when applying this technology to real wastewater systems.

Acknowledgements

This research was supported by the János Bolyai Research Scholarship of the Hungarian Academy of Sciences and by the Ministry of Culture and Innovation of Hungary from the National Research, Development and Innovation Fund financed under the OTKA FK 23 funding scheme (Project No. 146883).

References

[1] W. Duan, H. Cui, X. Jia, X. Huang, Sci. Total. Environ. 820 (2022) 153178.
[2] V. Loureiro dos Louros, C. P. Silva, H. Nadais, M. Otero, V. I. Esteves, Environ. Res. 188 (2020) 109730.
[3] S. P. Mezyk, T. J. Neubauer, W. J. Cooper, J. R. Peller, J. Phys. Chem. A 111 (2007) 9019.

[4] B. T. Kengne, S. Wang, Y. Sun, J. Wang, S. Bulka, Water 17 (2025) 1077.
[5] ISO/ASTM 51538 Practical use of ethanol-chlorobenzene dosimetry system (2007).
[6] K. Kovács, A. Tegze, A. Bezsenyi, L. Wojnárovits, Environ. Technol. Inno. 43 (2026) 105039.
[7] K. Kovács, Á. Simon, Gy. T. Balogh, T. Tóth, L. Wojnárovits, Free Radic. Res. 54 (2020) 185.
[8] K. Kovács, Á. Simon, T. Tóth, L. Wojnárovits, Radiat. Phys. Chem. 196 (2022) 110141

ESTIMATED HEAVY METAL INPUTS TO SOIL FROM MANURE AND DIGESTATE APLICATION BASED ON NITRATE DIRECTIVE REQUIREMENTS

Maja Manojlović, **Dragan Kovačević**, **Klara Petković**, **Mirna Štrbac**

University of Novi Sad, Faculty of Agriculture, Trg Dositeja Obradovića 8, 21000 Novi Sad, Serbia
e-mail: maja.manojlovic@polj.uns.ac.rs

Abstract
The application of manure and biogas digestate to agricultural land has a positive effect on soil physical properties and plant nutrition, and enables the recycling of nutrients and organic matter, but simultaneously increases the risk of introducing heavy metals (HMs) into agricultural soil. The aim of this study was to quantify Pb, Cd, Cr, Ni, Cu and Zn inputs from selected manures and digestates based on input of 170 kg N ha^{-1} $year^{-1}$ through these materials, regulates by Nitrate directive (91/676/EEC). Concentrations of HMs expressed on a dry-matter basis were recalculated for 34 t ha^{-1} materials containing 70% water (10.2 t DM ha^{-1}). The highest inputs of HMs were for Zn (3559.8 g ha^{-1}) and Cu (958.8 g ha^{-1}) from digestate 5, while Cd input was 11.4 g ha^{-1} from manure 2. Relative to the Regulation on maximal input values per 2 years (Official Gazette of RS, No. 31/2018), the highest shares were 137% for Cu, 118.7% for Zn and 114.2% for Cd. The results demonstrate the importance of considering concentration, dry-matter content, application rate and application interval when evaluating HMs loading from organic fertilizers and soil improvers.

Introduction
Organic fertilizers and soil improvers are valuable sources of plant nutrients and organic matter, but they also contain HMs; and their composition can vary substantially with origin, feedstock, animal nutrition, processing and storage. Manure and digestate may therefore contribute to long-term HMs loading of agricultural soils [1–4], which can have long-term environmental and health risk [8]. Regarding HMs contents of manure, biogas digestate and other organic fertilizers, all policies set restrictions on the maximum allowable concentrations in those materials that can be spread on agricultural land. Expressing metal inputs on an area basis enhances concentration data because the actual soil load depends on both element concentration, fertilizer dry matter, and field application rate. The aim of this study is to evaluate HM concentrations in selected manures and digestates comparing them with prescribed maximum limits (Table 1), and calculating their soil loading based on the rate of 170 kg N/ha/year - a limit stipulated by the Nitrates Directive [5] for materials of manure origin.

Experimental
Heavy-metals concentrations for two manures and three biogas digestates were compiled from published data [1–4] and expressed as mg kg^{-1} DM. A field application scenario of 34 t ha^{-1} fresh organic material with 70% moisture was used, corresponding to 10.2 t DM ha^{-1} was based on N aplication rate of 170 kg/ha/year proposed by Nitrate directive [5]. Element input was calculated as concentration × 10.2 and expressed as g ha^{-1} per application. One application was assumed within a two-year cycle. For comparison, Serbian input values prescribed for a two-year period were taken from the cited regulation [6].

Table 1. Maximum permissible concentrations of heavy metals in fertilizers, supplementary for soil and supplementary for plants (mg kg^{-1}) and inputs regulation to soils[6]

Heavy metal	Maximum content in mg/kg by dry weight of plant nutrition products and soil improvers	
	Fertilizers*, soil improvers, other fertilizers and special products	g/ha in a period of two years
Lead (Pb)	100	600
Cadmium (Cd)	3	10
Chrome (Cr)	100	600
Nickel (Ni)	100	400
Mercury (Hg)	1	10
Copper** (Cu)	-	700
Zinc** (Zn)	-	3000

*Except for inorganic fertilizers with more than 5% P_2O_5; **Except for inorganic fertilizers with declared content of microelements

Results and discussion

Concentration of the HMs in digestate and manure (Table 2) was bellow maximum content proposed by Serbian Regulation for plant nutrition products and soil improvers [6] and bellow Regulation (EU) 2019/1009 [7].

Calculated inputs of HMs to agricultural land differed markedly among materials (Table 3). Digestate 5 produced the highest Cu and Zn loads, 958.8 and 3559.8 g ha^{-1}, respectively, while its Ni input was 143.8 g ha^{-1} but manure 2 supplied 11.4 g Cd ha^{-1}.

When compared with Serbian limit for HMs for two-year [6], some of the materials exceeded the limit values. The largest relative loads were for Cu in digestate 5 (137%), for Zn in digestate 5 (118.7%) and for Cd in manure 2 (114.2%).

Thus, extending the application interval reduces the frequency of loading but does not reduce the quantity of HMs entering the soil at the time of application. Both the single-application and the multi-year cumulative load should therefore be considered.

Table 2. The concentration of HMs in selected manure and digestate (mg kg^{-1} DM) and reference values, (mg kg^{-1} DM)[6]

Material	Pb	Cd	Cr	Ni	Cu	Zn
Manure 1[1]	9.04	n.r. *	19.2	n.r.	15.5	58.8
Manure 2[2]	6.9	1.12	17.6	13.3	n.r.	n.r.
Digestate 3[1]	n.r.	n.r.	16.4	n.r.	9.3	32.8
Digestate 4[3]	n.r.	n.r.	11.7	n.r.	36.0	39.0
Digestate 5[4]	7.7	0.56	22.3	14.1	94.0	349.0
Maximum content in mg/kg by dry weight of plant nutrition products and soil improvers [6]	100	3	100	100	-	-
Sets standards for products used as fertilizers, including digestate, ensuring safety for agricultural use, including heavy metals and pathogens[7]	120	1.5	100	50	300	800

**n.r. – not reported in the cited source*

Table 3. Estimated heavy-metal inputs from one application of 34 t ha^{-1} organic material (70% moisture) and reference values, g ha^{-1}

Material	Pb	Cd	Cr	Ni	Cu	Zn
Manure 1[1]	92.2	n.r.	195.8	n.r.	158.1	599.8
Manure 2[2]	70.4	11.4	179.5	135.7	n.r.	n.r.
Digestate 3[1]	n.r.	n.r.	167.3	n.r.	94.9	334.6
Digestate 4[3]	n.r.	n.r.	119.3	143.8	367.2	397.8
Digestate 5[4]	78.5	5.7	227.5	169.20	958.8	3559.8
Regulatory input value (2 yr) [6]	600	10	600	400	700	3000

n.r. – not reported in the cited source;
170 kg N ha^{-1} ÷ 5 kg N t^{-1} FM (0.5% N in FM) = 34 t FM ha^{-1}; at 70% moisture (30% DM), this equals 10.2 t DM ha^{-1}. Metal input (g ha^{-1}) = concentration (mg kg^{-1} DM) × 10.2.

Conclusion

Under the evaluated scenario of 34 t ha^{-1} application of the manure and biogas digestat every second years, for two of the selected organic materials (manure 2 and digestat 5) metal loads exceeded the derived two-year equivalent reference. Therefore, recommendation is to apply either less amount of manure and digestat than 34 t ha^{-1} or to increase a period between applications for two-year to three- or four-year.
Heavy metal analysis of organic materials as manure and digestat and calculation of area-based metal inputs are therefore important for planning repeated organic fertilizer use and limiting long-term HMs accumulation in soil.

Acknowledgment

The research funds were provided by the Ministry of Science, Technological Development and Innovation under Contract No. 451-03-33/2026-03/200117 dated 05 February 2026.

References

[1] D. Kovačević, M. Manojlović, R. Čabilovski, Z.S. Ilić, K. Petković, M. Štrbac, M. Vijuk, Agronomy 12 (2022) 871. https://doi.org/10.3390/agronomy12040871.

[2] T. Zeremski-Škorić, J. Ninkov, P. Sekulić, S. Milić, J. Vasin, D. Dozet, S. Jakšić, Ratar. Povrt. 47 (2010) 281–287.

[3] M. Manojlović, D. Kovačević, R. Čabilovski, K. Petković, M. Štrbac, Organic fertilizers as a source of microelements and potentially toxic elements, International Symposium on Soil Science and Plant Nutrition, Samsun, 2021.

[4] M. Sager, Soil Biol. Biochem. 39 (2007) 1383–1390.

[5] Nitrate directive (91/676/EEC).

[6] Official Gazette of the Republic of Serbia No. 31/2018, Rulebook on conditions for classification and determination of quality of plant nutrition products.

[7] European Union, 2019. Regulation (EU) 2019/1009 of the European Parliament and of the Council of 5 June 2019 laying down rules on the making available on the market of EU fertilising products and amending Regulations (EC) No 1069/2009 and (EC) No 1107/2009 and repealing Regulation (EC) No 2003/2003. Off. J. Eur. Union 170, 1–114. Available at: https://eur-lex.europa.eu/legal-content/EN/TXT/?uri=CELEX %3A32019R1009.

[8] Feng, L., Aryal, N., Li, Y., Horn, S.J., Ward, A.J., 2023. Developing a biogas centralised circular bioeconomy using agricultural residues - challenges and opportunities. Sci. Total Environ. 868, 161656.

FORMULATION AND FUNCTIONAL CHARACTERIZATION OF GLUTEN-FREE *GULAB JAMUN*-TYPE DESSERT: EFFECTS OF AGAVE SYRUP IMMERSION ON PHENOLIC CONTENT AND ANTIOXIDANT CAPACITY

Corina-Iuliana Megyesi[1], Ariana-Bianca Velciov[1], Mariana-Atena Poiană[1], Daniela Stoin[1], Moigrădean Diana[1], Popescu Sofia[1], Alda Liana[1], Rinovetz Alexandru[1], Andreea Ghițulescu[1], Cozma Antonela[2], Laura Rădulescu[1*]

[1] University of Life Sciences "King Mihai I" Timisoara, Faculty of Food Engineering, Calea Aradului, 300645, Timisoara, Romania
[2] University of Life Sciences "King Mihai I" Timisoara, Faculty of Agriculture, Calea Aradului, 300645, Timisoara, Romania
corresponding author, e-mail: laura.radulescu@usvt.ro

Abstract
This study aimed to develop and characterize a gluten-free *Gulab Jamun*-type dessert formulated with oat flour, rice semolina, psyllium, whole milk powder, and agave syrup, with particular emphasis on the effect of syrup immersion on its physicochemical, antioxidant, phenolic, and sensory characteristics. The product was evaluated before and after syrup immersion. Syrup immersion resulted in a decrease in moisture content from 17.65% to 13.21% and in ash content from 2.898% to 1.409%. In contrast, ferric reducing antioxidant power (FRAP) increased from 11.29 to 13.81 μM Fe^{2+}/g, while total phenolic content increased from 66.01 to 131.52 mg GAE/100 g. Sensory evaluation also indicated a positive effect of syrup immersion, with mean scores increasing from 4.48 before immersion to 4.76 after immersion. The most pronounced sensory improvement was observed for taste, which increased from 4.0 to 4.6, followed by aroma, which increased from 4.5 to 4.9. Overall, the findings indicate that syrup immersion substantially improved the sensory acceptability of the gluten-free *Gulab Jamun*-type dessert and was associated with increased FRAP values and total phenolic content. The developed product represents a promising gluten-free alternative to the conventional dessert.

Introduction
Traditional desserts represent an important part of the culinary heritage of many regions; however, their conventional formulations often rely on refined cereal ingredients and sugar-rich syrups. Growing consumer interest in gluten-free foods and alternative sweetening systems has encouraged the development of innovative formulations using non-traditional ingredients. *Gulab Jamun* is a popular South Asian dessert traditionally prepared from milk solids, shaped into small balls, fried, and immersed in warm, aromatic sugar syrup. Reformulation may affect dough structure, moisture retention, texture, flavour, and overall sensory quality, making the selection of alternative ingredients particularly important.
Gluten-free cereal ingredients offer opportunities to diversify traditional dessert formulations. Oats contain dietary fibre, proteins, lipids, vitamins, minerals, and bioactive compounds, contributing to their nutritional and functional potential in innovative food products [1,2]. Rice-derived ingredients are also widely used in gluten-free formulations due to their neutral flavour and technological versatility. However, the absence of gluten may reduce dough cohesiveness and structural stability. Consequently, hydrocolloid-rich ingredients such as psyllium are frequently incorporated because of their high water-binding capacity and ability to modify rheological and textural properties [3,4].
The sweetening system is another important consideration in dessert reformulation. Agave syrup has attracted interest as a natural alternative to conventional sweeteners and has been

investigated in bakery and confectionery applications [5,6]. It consists primarily of fructose and glucose and may also contain minor amounts of phenolic and other bioactive compounds, although its composition varies with botanical origin and processing conditions [5,7].
Despite increasing research on alternative ingredients for gluten-free products, the combined use of oat flour, rice semolina, and psyllium in a *Gulab Jamun*-type dessert remains insufficiently explored. Moreover, limited information is available on the effects of immersion in agave-based syrup on the physicochemical and functional characteristics of such products.
Therefore, this study aimed to formulate and characterize a gluten-free *Gulab Jamun*-type dessert containing oat flour, rice semolina, and psyllium, with particular emphasis on sensory acceptability and changes in selected physicochemical and functional parameters following immersion in agave syrup.

Experimental

2.1. Product formulation and preparation

A *Gulab Jamun*-type dessert was developed using a gluten-free formulation based on oat flour, rice semolina, psyllium, and milk powder. The selected ingredients were combined to obtain a homogeneous dough with adequate handling properties and subsequently shaped into small spherical units.
The recipe for obtaining the *Gulab Jamun*-type dessert is presented below:

Raw / auxiliary materials	Quantity	Raw / auxiliary materials	Quantity
Milk powder	130 g	Milk	80 ml
Oat flour	40 g	Oil	50 ml
Rice semolina	30 g	Agave syrup	200 ml
Clarified butter	30 g	Water	80 ml
Corn starch	10 g	Cardamom	2 g
Psyllium	5 g	Rose water	5 ml
Baking powder	4 g	Saffron	0,1 g

The formed products underwent heat treatment and were subsequently immersed in an agave-based syrup to obtain the finished product.

2.2. Sensory evaluation

Sensory evaluation was performed by a panel of 10 assessors. The product was evaluated according to five sensory attributes: appearance, taste, aroma, colour, and consistency, before and after syrup immersion.
A five-point hedonic scale was used, with higher values corresponding to greater sensory acceptability. Mean scores were calculated for each sensory attribute, and an overall mean score was determined to characterize the general acceptability of the product.

2.3. Physicochemical analyses

Physicochemical characteristics were evaluated before and after agave syrup immersion. Moisture and ash contents were determined gravimetrically after drying at 105°C and incineration at 550°C, respectively. Antioxidant capacity was assessed by the FRAP method at 593 nm, while total phenolic content was determined spectrophotometrically using the Folin–Ciocalteu assay. Results were expressed as mean values for the analyzed sensory and physicochemical parameters.

Results and discussion

3.1. Sensory characteristics

The sensory acceptability of the *Gulab Jamun*-type dessert was evaluated before and after syrup immersion based on five sensory attributes: appearance, taste, aroma, colour, and texture. The results are presented in Figure 1.

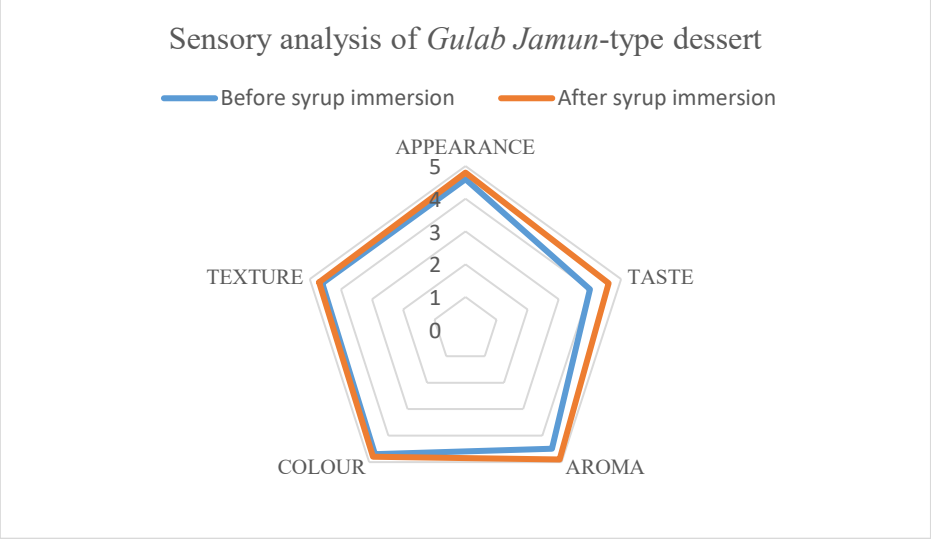


Figure 1. Graphic representation of sensory analysis for the developed *Gulab Jamun*-type dessert, before and after syrup immersion

Sensory acceptability was evaluated using a 5-point hedonic scale, where higher scores indicate greater acceptability. Syrup immersion was associated with increased scores for all evaluated attributes, from 4.0–4.7 before immersion to 4.6–4.9 after immersion. Taste showed the largest increase, from 4.0 to 4.6, which may be related to the contribution of the sweet syrup to the flavour profile of the *Gulab Jamun*-type dessert. Aroma increased from 4.5 to 4.9, becoming the highest-rated attribute after immersion. Appearance and colour increased slightly, from 4.6 to 4.8 and from 4.7 to 4.8, respectively, while texture increased from 4.6 to 4.7. Overall, the results indicate improved sensory acceptability following syrup immersion, particularly for taste and aroma, whereas the changes in colour, appearance, and texture were comparatively smaller.

3.2. Effect of syrup immersion on physicochemical and functional characteristics

The physicochemical and functional characteristics of the product before and after immersion in the agave-based syrup are presented in Table 2.

Table 2. Physicochemical and functional characteristics of the *Gulab Jamun*-type dessert before and after syrup immersion

Parameter	Before syrup immersion	After syrup immersion
Moisture, %	17.65	13.21
Ash, %	2.898	1.409
Antioxidant capacity, μM Fe^{2+}/g	11.29	13.81
Total phenolic content, mg GAE/100 g	66.01	131.52

The results demonstrate that immersion in the agave-based syrup was associated with measurable changes in both compositional and functional characteristics.

3.2.1. Moisture content

The moisture content decreased from 17.65% before syrup immersion to 13.21% in the final product. This result indicates that the syruping step altered the water-related characteristics of the product.

At first glance, a reduction in moisture following immersion in syrup may appear unexpected. However, the direction and magnitude of moisture changes in syrup-treated products can depend on the concentration and composition of the syrup, the osmotic gradient between the food matrix and the surrounding solution, and the duration and conditions of the treatment. The relatively high soluble-solids content of agave syrup may have contributed to water migration from the product matrix.

3.2.2. Ash content

Ash content decreased from 2.898% before syrup immersion to 1.409% after immersion. Ash content represents the inorganic mineral residue remaining after the combustion of organic matter and is commonly used as an indicator of the overall mineral fraction of a food product.

The reduction observed in the present study may reflect a dilution effect resulting from the incorporation of syrup into the final product. The relative contribution of the original product matrix to the total mass of the final syruped sample may have decreased following syrup uptake.

3.2.3. Antioxidant capacity

The antioxidant capacity, determined using the FRAP assay, increased from 11.29 μM Fe^{2+}/g before syrup immersion to 13.81 μM Fe^{2+}/g in the final product. This represents an increase of approximately 22%.

The FRAP assay evaluates the reducing capacity of compounds present in a sample and provides an indication of its antioxidant potential under the specific analytical conditions used. Therefore, the increase observed after syrup immersion suggests that the final product contained a greater concentration or availability of compounds capable of reducing ferric ions.

Agave syrup has been reported to contain phenolic compounds and other substances with potential antioxidant activity, although its composition can vary substantially according to agave species, geographical origin, and processing conditions [5–7]. Previous analyses of different agave syrups have demonstrated considerable variation in antioxidant activity and total phenolic content [7].

Consequently, the increase in FRAP values observed in the present study is consistent with the possibility that compounds present in the agave-based syrup contributed to the reducing capacity of the final product.

3.2.4. Total phenolic content

The most pronounced change associated with syrup immersion was observed for total phenolic content. The value increased from 66.01 mg GAE/100 g before syrup immersion to 131.52 mg GAE/100 g in the final product, representing an approximately two-fold increase.

This result indicates a substantial difference in the concentration of Folin–Ciocalteu-reactive compounds between the two analyzed product states. The increase occurred simultaneously with the increase in FRAP values, suggesting that syrup immersion modified the functional characteristics of the final product.

The findings are consistent with previous reports showing that agave syrups can contain variable concentrations of phenolic and other antioxidant-related compounds.

The substantially higher value obtained after syrup immersion suggests that the agave-based syrup contributed to the chemical characteristics measured by the assay.

Conclusion

A gluten-free *Gulab Jamun*-type dessert was successfully formulated using oat flour, rice semolina, psyllium, whole milk powder, and agave syrup. The comparison of the product before

and after syrup immersion demonstrated that this processing step influenced both its physicochemical and sensory characteristics.

Syrup immersion was associated with a decrease in moisture and ash contents, while FRAP values increased from 11.29 to 13.81 μM Fe^{2+}/g and total phenolic content increased from 66.01 to 131.52 mg GAE/100 g. The increase in total phenolic content was considerably greater than the change observed in FRAP, indicating that the two measurements did not change proportionally and should therefore be interpreted as complementary indicators of the product's functional characteristics.

The sensory evaluation showed an overall improvement in acceptability following syrup immersion, with the mean score increasing from 4.48 to 4.76. Taste exhibited the greatest improvement, increasing by 0.6 points, while aroma increased by 0.4 points. Appearance, colour, and texture showed smaller but consistent increases. These findings confirm the importance of syrup immersion in achieving a more favourable sensory profile of the developed dessert.

Overall, the results suggest that the proposed formulation and syrup immersion process have potential for the development of a gluten-free *Gulab Jamun*-type dessert with favourable sensory characteristics and measurable phenolic and reducing capacities.

References

[1] Rasane, P., Jha, A., Sabikhi, L., Kumar, A., Unnikrishnan, V.S., **2015**, Nutritional advantages of oats and opportunities for its processing as value-added foods—A review, *Journal of Food Science and Technology, 52*, 662–675, https://doi.org/10.1007/s13197-013-1072-1

[2] Alemayehu, G.F., Forsido, S.F., Tola, Y.B., Amare, E., **2023**, Nutritional and phytochemical composition and associated health benefits of oat (*Avena sativa* L.) grains and oat-based fermented food products, *The Scientific World Journal,* 2730175, https://doi.org/10.1155/2023/2730175

[3] Franco, E.A.N., Sanches-Silva, A., Ribeiro-Santos, R., Melo, N.R., **2020**, Psyllium (*Plantago ovata* Forsk): From evidence of health benefits to its food application, *Trends in Food Science & Technology, 96*, 166–175, https://doi.org/10.1016/j.tifs.2019.12.006

[4] Belorio, M., & Gómez, M. (2022). Psyllium: A useful functional ingredient in food systems, *Critical Reviews in Food Science and Nutrition, 62*(2), 527–538. https://doi.org/10.1080/10408398.2020.1829086

[5] Saraiva, A., Carrascosa, C., Ramos, F., Raheem, D., Raposo, A., **2022**, Agave syrup: Chemical analysis and nutritional profile, applications in the food industry and health impacts, *International Journal of Environmental Research and Public Health, 19*(12), 7022, https://doi.org/10.3390/ijerph19127022

[6] Ozuna, C., Franco-Robles, E., **2022**, Agave syrup: An alternative to conventional sweeteners? A review of its current technological applications and health effects, *LWT – Food Science and Technology, 162*, 113434, https://doi.org/10.1016/j.lwt.2022.113434

[7] Velázquez Ríos, I.O., González-García G., Mellado-Mojica E., Veloz Garcia, R.A., Dzul Cauich, J.G., López, M.G., Garcia-Vieyra, M., **2019**, Phytochemical profiles and classification of Agave syrups using ^{1}H-NMR and chemometrics, *Food Science & Nutrition, 7*, 3–13, https://doi.org/10.1002/fsn3.755

SPATIOTEMPORAL VARIABILITY OF WATER CHEMISTRY IN THE DTD CANAL IN THE VRBAS AREA

Maja Ajduković[1], Milica Vranešević[2], Jasna Grabić[2], Maja Meseldžija[1]

[1]Department of Plant and Environmental Protection, Faculty of Agriculture, University of Novi Sad, 21000 Novi Sad, Trg Dositeja Obradovića 8, Serbia
[2]Department of Water Management, Faculty of Agriculture, University of Novi Sad, 21000 Novi Sad, Trg Dositeja Obradovića 8, Serbia
e-mail: maja.meseldzija@polj.edu.rs

Abstract
The aim of this study was to determine spatial differences in the chemical composition of water within the Danube–Tisa–Danube Hydrosystem in the Vrbas area and to compare the results between two sampling campaigns. Water samples were collected at five sites on 25 April and 21 June 2026, and the concentrations of Na, K, Ca, Mg, NH_4^+, NO_3^-, NO_2^-, SO_4^{2-}, PO_4^{3-}, CO_3^{2-}, and HCO_3^- were determined. In April, the highest concentrations of Na, Mg, SO_4^{2-}, and HCO_3^- were recorded at site L1, whereas the highest concentrations of NH_4^+ and PO_4^{3-} were observed at the urban site L5. K concentrations were higher in June than in April at all five sites, while the mean concentrations of Mg, SO_4^{2-}, and HCO_3^- were lower. The results indicate spatial variability in water chemical composition and differences between the two sampling campaigns. Longer-term and more frequent water quality monitoring is required to identify seasonal patterns and potential sources of individual ions.

Introduction
The Danube-Tisa-Danube Hydrosystem (HS DTD) is one of the most important multipurpose water management systems in Serbia. In addition to a canal network approximately 960 km long, it includes various water management structures that ensure its functioning. The main purposes of the Hydrosystem include drainage, irrigation, and navigation. The Bačka section of HS DTD comprises 435.4 km of canals, including the 80.9 km long Vrbas-Bezdan section, where the study area is located [2]. Water quality in canals can be affected by various anthropogenic pressures, including those associated with urban areas and wastewater [1]. Many sections of the canal network are surrounded by agricultural land, and water quality may therefore also be influenced by diffuse agricultural pollution, as well as by municipal and industrial sources [3]. In addition, the physicochemical composition of surface waters varies spatially and temporally depending on natural conditions and human activities. Changes in hydrological and climatic conditions throughout the year can affect the concentrations of individual parameters, resulting in differences in water composition between sampling campaigns [4].
The aim of this study was to determine spatial differences in the chemical composition of water at five sites within HS DTD in the Vrbas area and to compare the values of the analyzed parameters in samples collected in April and June 2026.

Experimental
Water sampling was conducted at five sites within the Danube-Tisa-Danube Hydrosystem in the Vrbas area. The sites were selected to represent sections of the canal network differing in the surrounding land use. Samples were collected on 25 April and 21 June 2026 in two new 1 L PET bottles. With one sample from each site delivered to each of two laboratories at the Faculty of Agriculture, University of Novi Sad.

The concentrations of Na, K, Ca, and Mg were determined at the Laboratory for Soil, Fertilizer and Plant Material Testing. Following wet digestion with a mixture of HNO_3 and $HClO_4$ (4:1), the concentrations were determined by flame atomic absorption spectrophotometry [5, 6]. The concentrations of NH_4^+, NO_3^-, NO_2^-, SO_4^{2-}, PO_4^{3-}, CO_3^{2-}, and HCO_3^- were determined at the Water Laboratory of the Department of Water Management using a Lovibond MultiDirect multiparameter photometer, according to the manufacturer's procedures.

The locations of the sampling sites were mapped using QGIS, as shown in Figure 1, while the characteristics of the study sites are presented in Table 1. For each sampling campaign, minimum and maximum values, arithmetic means, and standard deviations were calculated for the analyzed parameters.

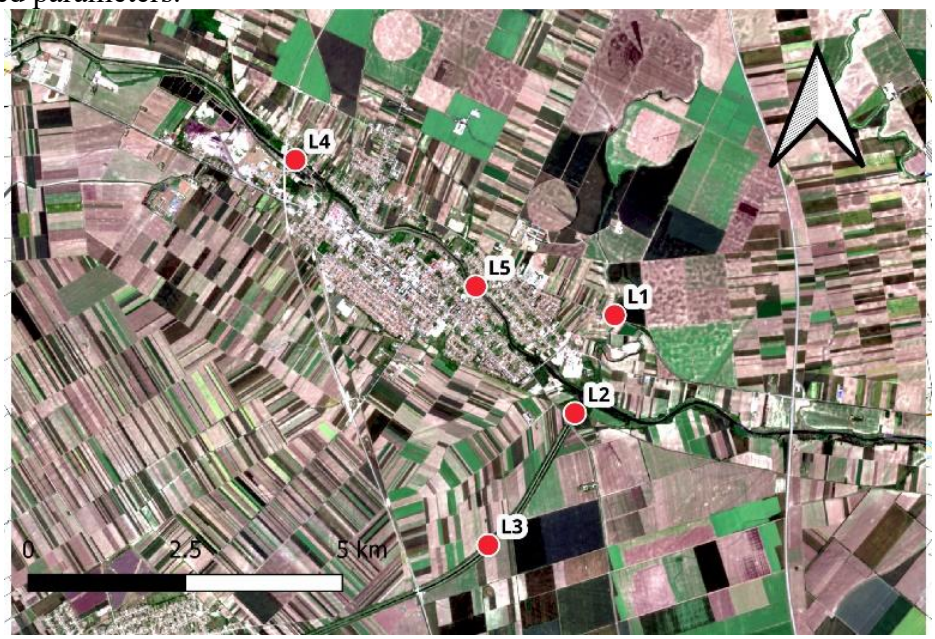


Figure 1. Location of the investigated sites

Table 1. Characteristics of the investigated sites with coordinates

Site	Surrounding area characteristics	Latitude (Y)	Longitude (X)
L1	Predominantly agricultural area, with cultivated land on both sides of the canal	45.56646	19.68349
L2	Orchard on one side of the canal and cultivated land on the other	45.55246	19.67537
L3	Predominantly agricultural area; located near an archaeological site and areas used by anglers	45.53359	19.65769
L4	Recreational area with a more intensively maintained canal bank; connected to a secondary canal	45.58864	19.61838
L5	Urban area of Vrbas; located within the immediate urban surroundings	45.57058	19.65516

Results and discussion

The results are presented separately for the April and June sampling campaigns, together with descriptive statistics for each campaign (Tables 2 and 3). This presentation enables comparison among sites and between sampling campaigns, similar to the approach applied by [7]. For NH_4^+, NO_3^-, and NO_2^-, some concentrations were below the detection limit of the method. These values are presented in their original form, and the arithmetic mean and standard deviation were not calculated for these parameters.

In April, site L1 had the highest concentrations of Na, Mg, SO_4^{2-}, CO_3^{2-}, and HCO_3^- among the investigated sites. Particularly notable were the concentrations of Na (256.61), SO_4^{2-} (181.5), and HCO_3^- (590), which were considerably higher at L1 than at the other sites. At site L5, located in the urban area of Vrbas, the highest April concentrations of K (57.79), NH_4^+ (7.36), and PO_4^{3-} (1.90) were recorded. These spatial differences indicate an uneven chemical composition of the water along the investigated canal section; however, the available data do not allow the sources of individual ions to be reliably determined.

The most consistent change between the April and June sampling campaigns was observed for K, whose concentration increased at all five sites. Its mean concentration increased from 24.45 in April to 116.85 in June, with the highest June value recorded at L2 (160.90). In contrast, the mean concentrations of Mg, SO_4^{2-}, and HCO_3^- were lower in June than in April, primarily due to the particularly high April values at L1. Mean concentrations of Ca and CO_3^{2-} differed considerably less between the two sampling campaigns. Therefore, changes in mean values should not be interpreted independently of the distribution of results among the individual sites.

In April, NO_3^- was measurable only at L3 (1.2), whereas in June a value of <1 was recorded at all sites. NO_2^- was measurable at L2 in April (0.04), and at L1 and L2 in June (0.02 at both sites). At L5, the concentrations of NH_4^+ and PO_4^{3-} were lower in June than in April. Since the study included five sites and only two sampling campaigns, the observed differences should be interpreted as findings specific to the investigated sampling dates rather than as a confirmed seasonal pattern. The same limitation in the amount of available data restricts the reliability of correlation analysis; therefore, such analysis was not performed.

Table 2. Concentrations of analyzed ions in water at five sampling sites in April 2026 (mg/L)

Site	K	Na	Ca	Mg	NH_4^+	NO_3^-	NO_2^-	SO_4^{2-}	PO_4^{3-}	CO_3^{2-}	HCO_3^-
L1	8,07	256,61	49,14	63,98	0,26	<1	<0,01	181,5	0,59	100	590
L2	21,95	51,31	55,8	17,38	2,46	<1	0,04	50,3	0,58	64	140
L3	15,69	45,69	51,38	16,76	<0,02	1,2	<0,01	46,4	0,19	72	156
L4	18,76	42,23	33,74	15,55	<0,02	<1	<0,01	58,5	0,11	94	58
L5	57,79	78,64	61,26	32,48	7,36	<1	<0,01	58,4	1,9	66	240
Minimum	8,07	42,23	33,74	15,55	—	—	—	46,4	0,11	64	58
Maximum	57,79	256,61	61,26	63,98	—	—	—	181,5	1,9	100	590
Mean	24,452	94,896	50,264	29,23	—	—	—	79,02	0,674	79,2	236,8
SD	19,33406	91,52917	10,33333	20,62275	—	—	—	57,52675	0,719604	16,64932	207,7431

Note: "<" indicates a concentration below the specified detection limit of the method; "—" indicates that the statistic was not calculated due to values below the detection limit. SD – standard deviation.

Table 3. Concentrations of analyzed ions in water at five sampling sites in June 2026 (mg/L)

Site	K	Na	Ca	Mg	NH_4^+	NO_3^-	NO_2^-	SO_4^{2-}	PO_4^{3-}	CO_3^{2-}	HCO_3^-
L1	80,42	59,18	52,4	17,6	0,05	<1	0,02	40,3	0,34	74	172
L2	160,9	70,56	62,22	16,07	1,76	<1	0,02	27,2	0,56	76	170
L3	142,14	87,77	53,87	17,58	0,04	<1	<0,01	26,7	0,39	98	182
L4	89,5	31,95	32,91	12,37	<0,02	<1	<0,01	40,3	0,1	92	38
L5	111,28	47,45	37,07	14,05	0,45	<1	<0,01	34,1	0,38	54	174
Minimum	80,42	31,95	32,91	12,37	—	—	—	26,7	0,1	54	38
Maximum	160,9	87,77	62,22	17,6	—	—	—	40,3	0,56	98	182
Mean	116,848	59,382	47,694	15,534	—	—	—	33,72	0,354	78,8	147,2
SD	34,22784	21,36442	12,27528	2,288827	—	—	—	6,680719	0,165167	17,23949	61,21438

Note: "<" indicates a concentration below the specified detection limit of the method; "—" indicates that the statistic was not calculated due to values below the detection limit. SD – standard deviation.

Conclusion

Analysis of water from five sites within the Danube–Tisa–Danube Hydrosystem in the Vrbas area revealed differences in chemical composition among the sites and between the two sampling campaigns. In April, the highest concentrations of Na, Mg, SO_4^{2-}, and HCO_3^- were recorded at site L1, while the highest concentrations of NH_4^+ and PO_4^{3-} were recorded at site L5, located in the urban area of Vrbas. In June, K concentrations were higher than in April at all five sites, while the mean concentrations of Mg, SO_4^{2-}, and HCO_3^- were lower.

The results indicate spatial variability in water chemical composition and changes between the investigated sampling dates. However, based on only two sampling campaigns, it is not possible to determine whether these changes represent a seasonal pattern or to reliably identify the sources of individual ions. A more comprehensive assessment of water quality would require continued monitoring at the same sites over a longer campaign, with more frequent sampling and the collection of data on hydrological conditions.

Acknowledgements

This research was funded by the Ministry of Science, Technological Development and Innovation, Republic of Serbia (Contract No. 451-03-34/2026-03/200117, dated 5 February 2026).

References

[1] Gaggia, F., De Feudis, M., Pagliarini, E., Trenti, W., Di Gioia, D., Vittori Antisari, L. (2026). Water quality of artificial canals used for agricultural purposes affected by urban and agricultural activities through a chemical and microbial perspective. *Agricultural Water Management, 324*, Article 110116. https://doi.org/10.1016/j.agwat.2025.110116

[2] Varga, L., Budinski, L. (2020). Matematičko modeliranje bačkog dela hidrosistema DTD primenom jednodimenzionalnog modela HEC-RAS. *Zbornik radova Fakulteta tehničkih nauka u Novom Sadu, 35*(12). https://doi.org/10.24867/10CG02Varga

[3] Savic, R., Stajic, M., Blagojević, B., Bezdan, A., Vranesevic, M., Nikolić Jokanović, V., Baumgertel, A., Bubalo Kovačić, M., Horvatinec, J., Ondrasek, G. (2022). Nitrogen and phosphorus concentrations and their ratios as indicators of water quality and eutrophication of the hydro-system Danube–Tisza–Danube. *Agriculture, 12*(7), Article 935. https://doi.org/10.3390/agriculture12070935

[4] Rahman, A., Jahanara, I., Jolly, Y. N. (2021). Assessment of physicochemical properties of water and their seasonal variation in an urban river in Bangladesh. *Water Science and Engineering, 14*(2), 139–148. https://doi.org/10.1016/j.wse.2021.06.006

[5] Adrian, W. J. (1973). A comparison of a wet pressure digestion method with other commonly used wet and dry-ashing methods. *Analyst, 98*, 213–216. https://doi.org/10.1039/AN9739800213

[6] Adrian, W. J., Stevens, M. L. (1977). Effect of different sample preparation methods on the atomic-absorption spectrophotometric determination of calcium in plant material. *Analyst, 102*, 446–452. https://doi.org/10.1039/AN9770200446

[7] El-Said Salem, Z., Attiah, A. M., Abu-Alam, T. (2024). Hydrochemical characterization and sustainability assessment of Ismailia canal water, Eastern Nile Delta, Egypt: Implications for human health and environmental safety. *Frontiers in Environmental Science, 12*, Article 1475082. https://doi.org/10.3389/fenvs.2024.1475082

INVASIVE PLANTS ACROSS THE AQUATIC–TERRESTRIAL GRADIENT OF IRRIGATION CANALS

Maja Ajduković[1], Maja Meseldžija[1], Branka Ljevnaić-Mašić[2], Dejana Džigurski[2], David Fic[2], Milica Vranešević[3]

[1]Department of Plant and Environmental Protection, Faculty of Agriculture, University of Novi Sad, 21000 Novi Sad, Trg Dositeja Obradovića 8, Serbia
[2]Department of Field and Vegetable Crops, Faculty of Agriculture, University of Novi Sad, 21000 Novi Sad, Trg Dositeja Obradovića 8, Serbia
[3]Department of Water Management, Faculty of Agriculture, University of Novi Sad, 21000 Novi Sad, Trg Dositeja Obradovića 8, Serbia
e-mail: maja.meseldzija@polj.edu.rs

Abstract
Invasive alien plant species occur in riparian ecosystems and may spread along watercourses into surrounding terrestrial habitats. This study investigated their distribution across different zones of the canal profile at survey sites within the Danube–Tisa–Danube canal network in the Municipality of Vrbas, South Bačka District, Autonomous Province of Vojvodina, Serbia. Field surveys were conducted on three occasions during the 2026 growing season. At each site, the canal profile was divided into four zones: aquatic, bank, canal slope, and adjacent terrestrial zone. A total of **18** invasive alien plant species were recorded. The highest number of taxa was recorded in the terrestrial zone (13), followed by the canal slope (7) and the aquatic zone (**3**). No invasive taxa were recorded in the bank zone. These findings indicate that invasive alien plants occurred more frequently in the terrestrial parts of the investigated canal profile than in the zones closer to the water.

Introduction
Invasive plant species are species that have been introduced into a new ecosystem, where they are able to adapt to local conditions and successfully spread. Their expansion may lead to the disruption of existing biodiversity and a decline in native species abundance, while the magnitude of their impact depends on climatic conditions, habitat characteristics, management practices, and anthropogenic influences [1].
Rivers and riparian areas represent important habitats for invasive alien plants, while also playing a significant role in their further spread into surrounding terrestrial areas. The Danube River Basin represents an important area for the distribution of invasive alien plant species in Europe, and studies conducted in the Middle Danube Basin in Serbia have revealed high levels of invasion in riparian areas, expressed through the richness and abundance of invasive alien plant species [2].
Changes in the composition and structure of riparian vegetation have been observed along gradients of increasing distance from surface water, with plant species composition changing with distance from the water [3]. The transition between aquatic and terrestrial ecosystems represents a spatial gradient characterized by changes in hydrological, geomorphological, and soil conditions, which are reflected in vegetation composition and structure [4. Such environmental heterogeneity allows the distinction of different zones across the transverse profile of a watercourse.
This study aimed to investigate the distribution of invasive alien plant species across four zones of the canal profile at six representative sites within the Danube–Tisa–Danube canal network in the Municipality of Vrbas, South Bačka District, Autonomous Province of Vojvodina, Serbia.

Experimental

The study was conducted during the 2026 growing season within the canal network in the area of Vrbas. Six representative sites (L1–L6) were selected along the investigated section of the canal network. At each site, an approximately 100 m long section of the canal was surveyed. Field surveys were conducted on three occasions, during spring, summer, and late summer, in order to record species occurring at different stages of the growing season.

At each site, vegetation flora/plant species was surveyed transversely across the canal profile, which was divided into four zones according to their position relative to the water surface: the aquatic zone (A), bank (B), canal slope (S), and adjacent terrestrial zone (T) (Figure 1.). The terrestrial zone included the inspection path and the area immediately adjacent to it. The presence of plant species was recorded separately for each zone during each field survey.

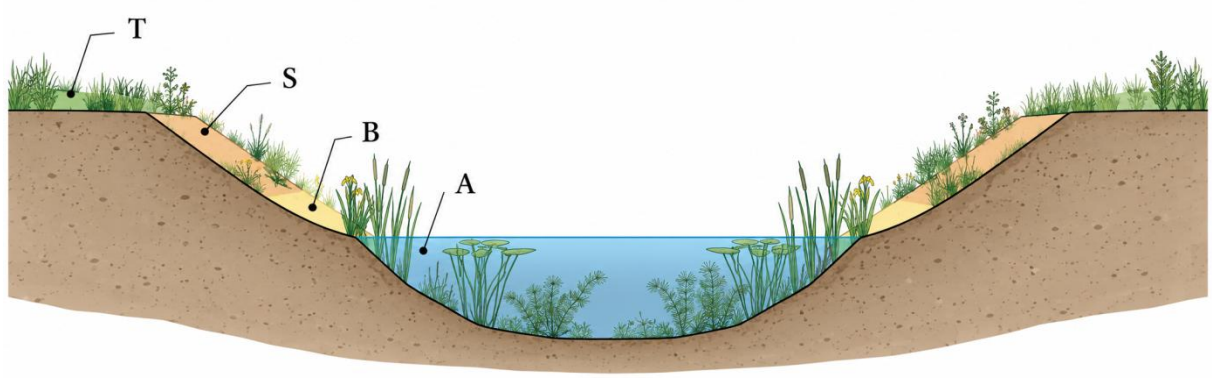


Figure 1. Drainage canal cross-section with survey zones (A, aquatic zone; B, bank; S, canal slope; T, adjacent terrestrial zone).

For the purposes of this study, invasive alien plant species were analyzed. A species was considered present in a zone if it was recorded there at least once during the three field surveys, and a dash (–) indicates that it was not recorded. Data on the presence of invasive alien plant species were organized into a binary presence/absence matrix (1/0). The total number of recorded invasive alien taxa was determined for each zone of the canal profile, and their distribution among zones and sites was described descriptively.

The identification and verification of the taxonomic identity of individual species were also carried out according to the Josifović [5], Felföldy [6], Jávorka and Csapody [7], while invasive status was determined according to [8]. Taxa classified in this source as invasive in Serbia and/or the Autonomous Province of Vojvodina were included in the analysis.

Results and discussion

A total of 18 invasive alien plant species were recorded during the survey of the canal network in the Vrbas area. Their occurrence varied among the investigated sites and across the different zones of the canal profile (Table 1). Riparian habitats vary in hydrological and environmental conditions across the transition from water to land, and these differences can shape plant community composition [3]. This makes the separate zones of the canal profile a useful basis for examining the occurrence of invasive alien plants. The total number of recorded invasive alien plant taxa differed among the zones of the canal profile. The highest number was recorded in the terrestrial zone (13), followed by the canal slope (7), while three invasive taxa were recorded in the aquatic zone.

Table 1. Distribution of invasive alien plant species across the investigated sites and zones of the canal profile

Taxon	L1	L2	L3	L4	L5	L6
Acer negundo L.	–	–	–	T	T	T
Ailanthus altissima (Mill.) Swingle	–	T	–	–	–	–
Amaranthus retroflexus L.	–	–	–	–	T	–
Ambrosia artemisiifolia L.	T	T	T	–	T	–
Artemisia annua L.	–	–	–	–	T	–
Asclepias syriaca L.	–	T	–	–	–	–
Azolla filiculoides Lam.	–	A	–	–	–	–
Cabomba caroliniana A.Gray	–	A	A	–	–	–
Consolida regalis Gray	–	S	T	–	–	–
Elodea nuttallii (Planch.) H.St.John	–	–	A	–	–	–
Erigeron annuus L. Pers.	–	–	S	–	–	–
Erigeron canadensis L.	–	S	S	–	–	–
Lepidium draba L.	S, T	–	–	–	–	–
Parthenocissus quinquefolia (L.) Planch.	–	–	–	T	S, T	–
Phytolacca americana L.	–	–	–	–	T	–
Robinia pseudoacacia L.	–	T	T	–	S, T	T
Sorghum halepense (L.) Pers.	–	–	–	–	T	–
Ulmus pumila L.	–	S, T	T	T	S, T	T

A = aquatic zone; B = bank; S = canal slope; T = adjacent terrestrial zone; – = not recorded.

No invasive plant species were recorded in the bank zone. These results indicate an uneven distribution of invasive alien plants along the aquatic–terrestrial gradient of the investigated canals (Figure 2).

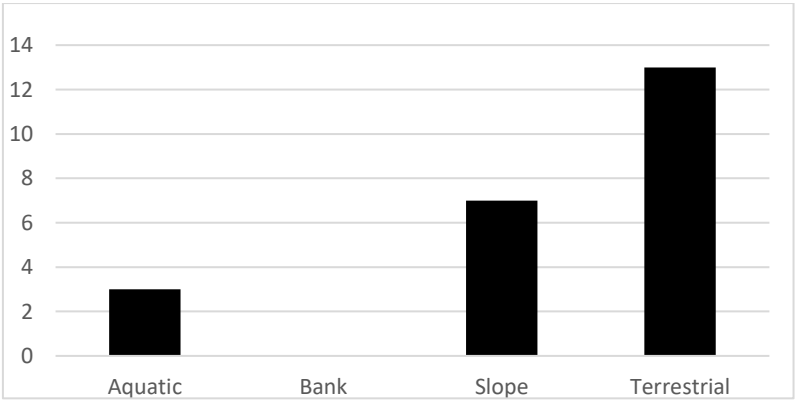


Figure 2. Distribution of invasive alien plant species (IAPs) along the aquatic–terrestrial gradient of the canal

The present study revealed differences in the distribution of invasive alien plant species among the different zones of the canal profile. These differences indicate that the occurrence of invasive plants varied along the aquatic–terrestrial gradient. Similar spatial variation in

vegetation composition along a gradient of increasing distance from surface water was reported in a study conducted in the Okavango Delta [4]. Differences in plant community composition among distance classes were associated with changes in moisture availability and other habitat conditions along the gradient. Although that study was not focused exclusively on invasive species, its findings demonstrate that position relative to the water can influence the spatial distribution of riparian vegetation.

In the present study, three invasive taxa, *Azolla filiculoides*, *Cabomba caroliniana*, and *Elodea nuttallii*, were recorded in the aquatic zone, while no invasive taxa were recorded in the bank zone. According to the authors Stojanović and Jovanović [8], *Cabomba caroliniana* was not recorded either in the investigated area, nor in Vojvodina or Serbia. At most sites, the bank zone was characterized by dense vegetation dominated by *Phragmites australis* and *Calystegia sepium*, while *Acorus calamus* was also recorded at site L4. The well-developed vegetation of the bank zone may have contributed to the absence of invasive taxa in this zone, although this relationship was not directly investigated.

A higher number of invasive taxa was recorded on the canal slope (7), while the highest number was found in the terrestrial zone (13), indicating a greater occurrence of invasive plants in the terrestrial parts of the investigated canal profile. The terrestrial zone included the inspection path and the area immediately adjacent to it, which at some sites were exposed to mowing, trampling, and other anthropogenic disturbances. The greater occurrence of invasive species in this zone may be associated with habitat disturbance; however, this relationship was not specifically investigated in the present study.

Conclusion

The results revealed an uneven distribution of invasive alien plant species among the different zones of the canal profile. The highest number of invasive taxa was recorded in the terrestrial zone, followed by the canal slope, while three taxa were recorded in the aquatic zone and none in the bank zone. These findings indicate a higher prevalence of invasive alien plants in the terrestrial sections of the surveyed canal profile compared to zones directly connected to areas with greater water availability.

Acknowledgements

This research was funded by the Ministry of Science, Technological Development and Innovation, Republic of Serbia (Contract No. 451-03-34/2026-03/200117, dated 5 February 2026), and by the Provincial Secretariat for Higher Education and Scientific Research (project entitled "Invazivne biljke kao indikatori ekološkog i hidrauličkog stanja drenažnih kanala"/“Invasive Plants as Indicators of the Ecological and Hydraulic Condition of Drainage Canals” – Contract No. 002368157 2026 09418 002 000 000 001 04 002).

References

[1] Zhu, Z., Fan, L., Fan, X., Yu, H., Cui, M., Wang, Y., Liu, S., Dai, Z., Wang, X., Ren, G., Du, D. (2026). Dynamic impact of alien plant invasion on plant diversity: A global meta-analysis. *Plant Diversity*. Advance online publication. https://doi.org/10.1016/j.pld.2026.07.002

[2] Anđelković, A. A., Pavlović, D. M., Marisavljević, D. P., Živković, M. M., Novković, M. Z., Popović, S. S., Cvijanović, D. L., Radulović, S. B. (2022). Plant invasions in riparian areas of the Middle Danube Basin in Serbia. *NeoBiota, 71*, 23–48. https://doi.org/10.3897/neobiota.71.69716

[3] Tsheboeng, G. (2018). Spatial variation of the influence of distance from surface water on riparian plant communities in the Okavango Delta, Botswana. *Ecological Processes, 7*, Article 32. https://doi.org/10.1186/s13717-018-0140-x

[4] Dodds, W. K., Barmuta, L. A., Bernal, S., Corman, J., Harms, T. K., Johnson, S. L., Li, L., Fernandes Cunha, D. G., Olden, J. D., Riis, T., Silva, L. C. R., Stella, J. C., Sullivan, P., Wohl, E. (2025). Defining stream riparian zones across multidimensional environmental gradients. *Journal of Environmental Quality, 54*(6), 1674–1697. https://doi.org/10.1002/jeq2.70080
[5] Josifović, M. (ed.). (1970-1977). Flora Sr Srbije (Tomovi I–IX). Srpska akademija nauka i umetnosti.
[6] Felföldy, L. (1990). Hínárhatározó: Edényes vízinövények. Környezetvédelmi és Vízgazdálkodási Minisztérium.
[7] Jávorka, S., Csapody, V. (1975). Iconographie der flora des südostlichen Mitteleuropa. Akadémiai Kiadó.
[8] Stojanović, V., Jovanović, I. (2018). Pregled invazivnih i potencijalno invazivnih vrsta biljaka u Republici Srbiji i okruženju u cilju utvrđivanja njihovog statusa na nacionalnom nivou. *Zaštita prirode, 68*(1–2), 41–59. https://doi.org/10.5937/ZasPri1802041S

COMPARATIVE EFFECTS OF BIODEGRADABLE AND POLYETHYLENE PLASTICS ON EARLY ROOT DEVELPOMENT IN RHIZOTRON SYSTEM

Enikő Mészáros[1], Kamilla Kovács[1], Klaudia Hoffmann[1,2], Zsófia Liska[1], Attila Bodor[1,2], Gábor Feigl[1]

[1]MTA-SZTE Lendület "Momentum" Anthropogenic Stress and Plant Resilience Research Group, Department of Plant Biology, University of Szeged, 6726 Szeged, Közép fasor 52, Hungary
[2]Department of Biotechnology and Microbiology, University of Szeged, 6726 Szeged, Közép fasor 52, Hungary
e-mail: meszaros.eniko@szte.hu

A robust and well-developed root system is vital for supporting healthy plant growth, facilitating efficient water and nutrient uptake, and enabling swift physiological adaptation to shifting environmental conditions. Today, terrestrial ecosystems are exposed to rising levels of microplastic contaminants, which accumulate in soils and alter physical soil properties [1]. However, despite the acknowledged risks of soil contamination, the immediate biological consequences of plastic particle exposure on early root dynamics, developmental and architectural orientation remain poorly understood [2,3].

This study evaluated the impact of diverse plastic contaminants on early root development using rapeseed (*Brassica napus* L.) and garden cress (*Lepidium sativum* L.) grown in a rhizotron system. Plants were exposed to two concentrations (0.5% and 1% w/w) of four plastic treatments: two biodegradable microplastics (<0.5 cm) and two polyethylene types (virgin and recycled, 0.5 cm).

Monitoring root growth over 14 days revealed that both biodegradable and conventional plastics significantly altered root architecture, specifically suppressing elongation and shifting spatial distribution in a type- and concentration-dependent manner. Notably, biodegradable options displayed distinct biological impacts, demonstrating that rapid degradation potential does not eliminate physiological risk.

These findings demonstrate that short-term exposure to microplastics - regardless of polymer type or origin - disrupts early root establishment, highlighting an urgent need to investigate long-term soil-plant feedback mechanisms.

This project was supported by the National Research, Development and Innovation Office, Hungary (NKFIH FK 142475).

[1] Saeed, T., Khan, T. A., Yusuf, M., & Bajguz, A. (2026). Microplastics in the rhizosphere: unraveling plant-microbe-soil interactions and consequences for crop resilience. *Plant Signaling & Behavior*, *21*(1), 2678701.

[2] Li, Y., Yang, G., Yu, C., Lei, X., Xing, X., Ma, X., & Sun, Y. (2024). The impact of microplastic concentration and particle size on the germination and seedling growth of Pisum sativum L. *Agronomy*, *14*(5), 923.

[3] Li, J., Yu, S., Yu, Y., & Xu, M. (2022). Effects of microplastics on higher plants: a review. Bulletin of Environmental Contamination and Toxicology, 109(2), 241-265.

CONTRASTING VIRGIN AND RECYCLED POLYETHYLENE IMPACTS ON ROOT ARCHITECURE AND NITRO-OXIDATIV BALANCE IN OILSEED RAPE

***Enikő Mészáros*[1,2], Bálint Kolossa[1], Kamilla Kovács[1,2], Klaudia Hoffmann[1,2,3], Zsófia Liska[1,2], Attila Bodor [2,3], Gábor Feigl[1,2]**

[1]*Department of Plant Biology, University of Szeged, 6726 Szeged, Közép fasor 52, Hungary*
[2]*MTA-SZTE Lendület "Momentum" Anthropogenic Stress and Plant Resilience Research Group, 6726 Szeged, Közép fasor 52, Hungary*
[3]*Department of Biotechnology and Microbiology, University of Szeged, 6726 Szeged, Közép fasor 52, Hungary*
e-mail: meszaros.eniko@szte.hu

Widespread plastic accumulation represents a major global environmental challenge, with polyethylene (PE) serving as one of the most persistent soil contaminants [1]. As plastic waste expands, terrestrial plants are increasingly exposed to both virgin and recycled PE fragments [2]. While such exposure can disrupt root system architecture and trigger cellular stress, the differential impacts of recycled versus virgin polymers remain insufficiently resolved [3].
In this study, we evaluated the effects of virgin PE and recycled PE (rePE) fragments (0.5 cm; applied at 0.5% and 1% w/w) on seed germination and early root development in oilseed rape (*Brassica napus* L.) under controlled *in vitro* conditions. To elucidate the underlying physiological mechanisms, we monitored reactive oxygen species (ROS) and reactive nitrogen species (RNS) dynamics to assess shifts in redox balance.
Surprisingly, virgin PE treatments stimulated root elongation relative to the control, whereas rePE treatments consistently suppressed root growth. This rePE-induced growth inhibition was strongly associated with disrupted nitro-oxidative homeostasis, with elevated nitrosative stress acting as the primary driver of root suppression.
These findings demonstrate that recycled and virgin plastics exert opposing physiological effects on early root development, underscoring that recycled polymers must be severely evaluated for their ecological risks rather than viewed solely through the lens of waste management.
The project was supported by the National Research, Development and Innovation Office, Hungary (NKFIH FK 142475) and by the Lendület "Momentum" Program of the Hungarian Academy of Sciences (LP2025-8/2025 to G.F).
[1] Jia, L., Liu, L., Zhang, Y., Fu, W., Liu, X., Wang, Q., ... & Huang, L. (2023). Microplastic stress in plants: effects on plant growth and their remediations. *Frontiers in plant science*, *14*, 1226484.
[2] Zhang, Y., Wang, X., Li, J., Yang, Y., Gao, Y., & Wang, P. (2025). Polyethylene microplastic: impacts on ryegrass seed germination and seedling development. *BMC Plant Biology*, *25*(1), 876.
[3] Wong, A. E., & Taylor, G. (2025). Plants and microplastics: Growing impacts in the terrestrial environment. *Frontiers in Plant Science*, *16*, 1666047.

GLOBAL BRAND, LOCAL BREW: A COMPARATIVE STUDY OF PRODUCTION AND QUALITY PARAMETERS ACROSS COUNTRIES

Márk Bakos[1], Balázs Lemmer[1], József Mihalkó[1]

[1]Department of Food Engineering, Faculty of Engineering, University of Szeged, H-6725 Szeged, Moszkvai krt. 5-7., Hungary
e-mail: mihalko@mk.u-szeged.hu

Abstract
The aim of our work was to compare batches of the same beer brand brewed in different countries based on various criteria and analyses. One of the methods frequently used by large beer companies is to brew their beers under a specific brand name in multiple countries using the same recipe, primarily for business and logistical reasons. The samples were collected in seven European countries during the summer of 2025. For each batch, we conducted the following tests: consumer price per liter, comparison of information on the label, alcohol content and color determination in accordance with Hungarian standards, and sensory evaluation. Overall, based on the results, we concluded that there are indeed differences between the batches brewed in different countries; these differences were particularly evident in the analytical tests and sensory evaluations.

Introduction
Prior work on beer industries shows that postwar consolidation in many markets coexists with waves of craft entrants, shaping a dynamic where large brewers pursue efficiency while remaining responsive to local styles and consumer tastes. Together, the seven country-case beers provide insights into how a leading brewer navigates concentration pressures, regional differentiation, sustainability imperatives, and evolving consumer demands in the contemporary beer landscape.

Experimental
This poster analyzes seven beers of a beer brand from seven countries to reveal how a single multinational brewer negotiates local terroirs, consumer preferences, and regulatory constraints within a global portfolio. The samples were collected in seven European countries during the summer of 2025: Hungary (HU), Belgium (BE), the Netherlands (NL), France (FR), the Czech Republic (CZ), Serbia (SE), Montenegro (MO). First, we compared the retail prices of the products and the information on their labels. The products were subjected to analytical tests also used in the beer industry – color measurement and alcohol content determination. Finally, the samples were also subjected to sensory evaluation.

Conclusion
Overall, based on the results, we concluded that there are indeed differences between the batches brewed in different countries; these differences were particularly evident in the analytical tests and sensory evaluations.

References
Cimini, A., & Moresi, M. (2021). Circular economy in the brewing chain. Italian Journal of Food Science, 33(3), 47–69. https://doi.org/10.15586/ijfs.v33i3.2123
Cuomo, G., & Vignali, C. (1996). The possibility of Boddingtons - “the cream of Manchester’s” - entry into the Dutch market. Management Decision, 34(8), 64–72. https://doi.org/10.1108/00251749610128149

Douma, S. (1988). Horizontale multinationalisatie als ondernemingsstrategie. Maandblad Voor Accountancy En Bedrijfseconomie, 62(12), 537–547. https://doi.org/10.5117/mab.62.13568
Garavaglia, C. (2021). Industry evolution: Evidence from the Italian brewing industry. Competition & Change, 26(1), 75–95. https://doi.org/10.1177/10245294211007408
González, J. M. G., & Ramírez, C. Z. (2013). Towards the consolidation of climate change strategies in organizations. International Journal of Climate Change Strategies and Management, 5(1), 6–20. https://doi.org/10.1108/17568691311299336
Sluyterman, K. (2017). B2B or B2C? BMGN - Low Countries Historical Review, 132(3), 11–36. https://doi.org/10.18352/bmgn-lchr.10397
Standard MSZ 8761-6:2002
Standard MSZ 8761-10:2002

SOIL CHARACTERIZATION AND ASSESSMENT OF THE MAIN LIMITING FACTORS OF PERMANENT GRASSLANDS IN THE LIPOVA AREA, ARAD COUNTY, ROMANIA

Casiana Mihuț[1], Anișoara Duma-Copcea[1], Antoanela Cozma[1], Daniela Scedei[3], Attila Blenesi[2], Carmen Durău[2], Adalbert Okros[1]*, Vlad-Dragoslav Mircov[2], Dan Nicolae Manea[1], Daniel Popa[2]

[1] Department of Agricultural Tehnologies, Faculty of Agriculture, University of Life Sciences "King Mihai I" from Timişoara, Calea Aradului nr.119, Timişoara, country Timiş, România
[2] Department of Soil Sciences, Faculty of Agriculture, University of Life Sciences "King Mihai I" from Timişoara, Calea Aradului nr.119, 300645 Timişoara, country Timiş, România
[3] Department of Horticulture, Faculty of Engineering and Applied Technologies, University of Life Sciences "King Mihai I" from Timişoara, Calea Aradului nr.119, 300645 Timişoara, country Timiş, România
e-mail: adalbertokros@usvt.ro

Abstract
Permanent grasslands are shaped by soil properties, relief, water regime, climate, and nutrient availability. This study characterized the main soils and pedological limitations of 1074.14 ha of permanent grasslands in Lipova, Arad County, western Romania, using pedological, agrochemical, topographic, and vegetation information from pastoral-management documentation and a 1:10,000 soil survey. The soil cover includes Preluvosols, Planosols, Eutric Cambisols, Gleysols, Stagnosols, Vertisols, Erodosols, Anthrosols, and soil associations. The principal constraints are acidity, humus reserves, slope, erosion, shallow soil conditions, and groundwater- or rainfall-induced excess moisture. Gleysols and Stagnosols are especially associated with wet-site vegetation such as *Juncus* and *Carex*. Nutrient supply is spatially uneven, with affected areas showing low nitrogen, moderate phosphorus, and high potassium. The findings support spatially differentiated grassland management according to soil, relief, hydrological, and fertility conditions.

Introduction
Permanent grasslands are important agricultural and ecological resources whose productivity and floristic composition depend on interactions among soil, relief, climate, water regime, and management. Soil characterization and land rating identify limiting factors and land suitability [1], while soil taxonomy provides a consistent interpretative framework [2]. In western and south-western Romania, variation in relief, parent material, and hydrology produces marked pedological diversity [3], including in Arad County, as reported by Dicu et al. (2025) [4]. Studies of Banat grasslands have linked vegetation structure with soil pH and N, P, and K supply (Sărățeanu and Moisuc, 2007) [5,6]; flooding and water stagnation can alter grassland vegetation [7], whereas management affects phytocoenotic biodiversity [8]. Sărățeanu et al. (2023) further documented climatic influences on grassland succession in western Romania [9]. Soil-resource assessment must integrate atmospheric conditions (Mihuț and Niță, 2018) [10], soil physical and chemical properties, fertility status [11], land-use-related constraints [12], and regional climatic variability [13]. In Lipova, the 1074.14 ha of permanent grasslands form a heterogeneous soil mosaic, with major limitations related to acidity, humus reserves, slope, erosion, and excess moisture [14]. The objective was therefore to characterize the main soil types and identify the dominant pedological limitations by integrating edaphic properties, relief, water regime, and vegetation as a basis for differentiated, sustainable management.

Experimental

1. Study area

The study covered 1074.14 ha of permanent grasslands belonging to Lipova, Arad County, distributed among 20 parcels in the Radna, Șoimoș, and Lipova grassland sectors [6,7]. Pedological, agrochemical, topographic, and floristic information was extracted from the pastoral management plan and its associated soil and agrochemical studies. Topography is variable, and altitude, slope, exposure, and landform affect local moisture and temperature conditions [12]; the source documentation reports a mean slope of 23° [7]. The climate is temperate continental with oceanic influences, modified locally by the Zarand Mountains and Lipova Hills [11]. Mean annual temperature is 9.2°C; the reported vegetation period averages about 245 days (230–260 days) [10,13].

2.2. Pedological and agrochemical characterization

The pedological and agrochemical documentation was prepared at 1:10,000 scale using the cadastral plan as the topographic base [3]. Main soil profiles were examined in management units 1B, 2B, 3B, 4C, 6, 9B, and 7A and analyzed by the Office for Pedological and Agrochemical Studies. Field observations addressed soil genesis and edaphic characteristics, water supply, parent material, and relief [1,4]. Agrochemical samples were collected according to ICPA methodology using diagonal sampling associated with the soil profiles [14]. Laboratory indicators reported in the source documentation included pH in water, humus content (Schollenberger method), base saturation (V%), nitrogen index (IN), mobile P (Egner–Riehm–Domingo), mobile K (flame photometry), and sum of exchangeable bases (modified Kappen method) [14].

2. Data analysis

Information was reorganized by soil type, morphological and physicochemical properties, moisture regime, relief position, and limiting factors. Taxonomic interpretation followed the Romanian System of Soil Taxonomy [2], while retaining soil names used in the original documentation. Vegetation information was integrated with edaphic conditions; the management plan distinguishes *Festuca valesiaca* grasslands (376 ha; 35%) and *Lolium perenne–Agrostis capillaris* grasslands (698 ha; 65%) [1]. The analysis was descriptive and comparative. Inferential statistics were not applied because the source data originated from pedological and agrochemical mapping rather than an experiment with independent replications.

Results and Discussion

1. Soil diversity and distribution

The Lipova grasslands show pronounced pedological heterogeneity. The principal soils are Preluvosols, Planosols, Eutric Cambisols, Gleysols, Stagnosols, Vertisols, Erodosols, and Anthrosols, together with associations of Eutric Cambisols, hydromorphic soils, and Gleysols [1]. Preluvosols occur in T1, T2, and T4; Planosols in T5; Eutric Cambisols in T4 and T6; Gleysols and Stagnosols in T1–T4; Vertisols in T1, T3, and T4; and Erodosols and Anthrosols in T1 and T2 [1]. Thus, the grasslands occupy a soil mosaic rather than a homogeneous pedological substrate.

The main constraints are soil acidity, humus reserves, slope, groundwater-related excess moisture, and rainfall-induced stagnant water. These chemical, physical, topographic, and hydrological limitations require management at land-unit scale. Regional pedological differentiation is also emphasized by Dicu et al. (2025) [4], while Țărău et al. (2010) [3] highlighted the role of soil and terrain properties in land-quality assessment in south-western Romania.

Table 1. Main soil groups and limiting factors in the Lipova permanent grasslands.

Soil / group	Distribution	Main limitation
Preluvosol	T1, T2, T4	Acidity; local relief constraints
Planosol	T5	Restricted internal drainage; temporary water stagnation
Eutric Cambisol	T4, T6	Locally shallow soil and erosion
Gleysol–Stagnosol	T1, T2, T3, T4	Groundwater and/or stagnant excess moisture
Vertisol	T1, T3, T4	Restrictive physical properties in some units
Erodosol–Anthrosol	T1, T2	Erosion and degraded/modified soil cover
Soil associations	T3	Pedological heterogeneity and variable water regime

2. Water regime, relief, and erosion

Excess moisture is one of the clearest constraints. Groundwater is generally close to the surface (0.5–1.5 m), while depressional landforms favor temporary stagnation after abundant rainfall. This is reflected by the distribution of Gleysols and Stagnosols and by wet-site vegetation. Parcel 9B, in the floodplain at about 143 m altitude, is characterized as Gleysol–Stagnosol; *Agrostis capillaris* and *Lolium perenne* occur together with *Juncus effusus*, which accounts for about 40% of the undesirable vegetation recorded there. Parcel 8, on level terrain at about 171 m, also has Gleysol–Stagnosol and includes *Juncus effusus* and *Carex–Juncus* tussocks. In parcel 7A, *Juncus* is an important undesirable component and pastoral value is rated poor. These observations indicate a spatial association between excess moisture and vegetation structure.

Relief adds further constraints through erosion and reduced effective soil volume. Parcel 2B (74.29 ha), located on hilly terrain and associated with Eutric Cambisol–Vertisol, has shallow soil, animal tracks and compacted paths, erosion exposure, and poor pastoral value. Consistent with Țărău et al. (2010) [3], these results support evaluating soil, relief, and water regime jointly rather than interpreting isolated indicators.

3. Soil fertility and management implications

Agrochemical information indicates uneven fertility: affected areas are poorly supplied with nitrogen, moderately supplied with phosphorus, and abundantly supplied with potassium. The source study reports very good K supply and recommends differentiating P requirements according to analytically determined mobile phosphates. Consequently, fertilization should be based on agrochemical evidence and spatial variability rather than uniform application. Recent work on soil chemical properties and fertility in western Romania [8] and the differentiated soil response to nutrient management reported by Șter et al. (2026) [9] support, in different agronomic contexts, the principle of adapting nutrient management to pedological conditions.

Climatic conditions also interact with soil functioning. Mircov et al. (2025) [13] highlighted the effects of extreme weather on crop production in western Romania, while Mihuț et al. (2026) [12] emphasized the integrated role of geological, climatic, and hydrological factors in soil and ecosystem differentiation. In Lipova, the relevant interaction is particularly between precipitation, relief position, and soil moisture regime. Overall, pastoral potential is controlled by soil type, water regime, relief, and fertility; therefore, ameliorative and management measures should be spatially differentiated across the 1074.14 ha.

Conclusions

The Lipova permanent grasslands are pedologically heterogeneous, with Preluvosols, Planosols, Eutric Cambisols, Gleysols, Stagnosols, Vertisols, Erodosols, Anthrosols, and soil associations. Water regime is a major limitation, especially on Gleysols and Stagnosols, where groundwater or stagnant excess moisture is associated with *Juncus* and *Carex* vegetation.

Acidity, humus reserves, slope, erosion, shallow soil conditions, and uneven nutrient supply further constrain pastoral use. Affected areas show low N, moderate P, and high K supply. The combined variability of soil, relief, hydrology, and fertility across 1074.14 ha justifies land-unit-specific management, particularly for drainage/water control, erosion-sensitive areas, and differentiated fertilization.

Acknowledgements
Contract de cercetare-dezvoltare nr. 4492/22.04.2026

References

[1] Paulette, L.; Buta, M. (2010). *Noțiuni teoretice și practice de cartare și bonitare a terenurilor agricole* [*Theoretical and practical notions of mapping and crediting of agricultural land*]. Risoprint, Cluj-Napoca.
[2] Florea, N.; Munteanu, I. (2012). *Sistemul Român de Taxonomie a Solurilor (SRTS) [Romanian Soil Taxonomy System]*. Editura Sitech, Craiova.
[3] Țărău, D.; Borza, I.; Dicu, D. (2010). Status of soil quality in south-west of Romania and its role in sustainable development of the rural space. *Acta Agraria Debreceniensis*, I, 273–278. https://doi.org/10.34101/ACTAAGRAR/I/8415.
[4] Dicu, D.; Vigh, A.; Șerb, R.; Țeț, D.; Bertici, R.; Herbei, M.; Horablaga, A.; Popescu, C. (2025). Characterization of soils in Arad County. *Research Journal of Agricultural Science*, 57(2), 268–276. https://doi.org/10.59463/RJAS.2025.2.29.
[5] Sărățeanu, V.; Moisuc, A. (2007). Influence of soil N, P, K supply on herbaceous invasive species from grasslands. *Scientific Papers, Faculty of Agriculture*, 39(1), 297–302.
[6] Sărățeanu, V.; Moisuc, A. (2007). Researches concerning soil pH on invasive species from grasslands. *Scientific Papers, Faculty of Agriculture*, 39(1), 303–308.
[7] Moisuc, A.; Samfira, I.; Cojocariu, L.; Horablaga, M.; Durău, C.C.; Sărățeanu, V. (2009). Vegetation evolution of grassland affected by flooding. *Research Journal of Agricultural Science*.
[8] Vântu, V.; Samuil, C.; Rotar, I.; Moisuc, A.; Razec, I. (2011). Influence of the management on the phytocoenotic biodiversity of some Romanian representative grassland types. *Notulae Botanicae Horti Agrobotanici Cluj-Napoca*, 39(1), 119–125. https://doi.org/10.15835/nbha3915867.
[9] Sărățeanu, V.; Cotuna, O.; Paraschivu, M.; Cojocariu, L.L.; Horablaga, N.M.; Rechițean, D.; Mircov, V.D.; Sălceanu, C.; Urlică, A.A.; Copăcean, L. (2023). Features of Natural Succession of Ex-Arable Forest Steppe Grassland (from Western Romania) under the Influence of Climate. *Plants*, 12(6), 1204. https://doi.org/10.3390/plants12061204.
[10] Mihuț, C.; Niță, L.D. 2018. Atmospheric factors used in the characterization of soil resources. *Research Journal of Agricultural Science*, 50, 114–120.
[11] Mircov, V.D.; Sărățeanu, V.; Mihuț, C.; Poșta, D.S.; Durău, C.C. (2025). Impact of extreme weather conditions on the production of the main field crops in Western Romania over the 2018–2023 period—case study. *Agriculture and Forestry*, 71(3), 103–112. https://doi.org/10.17707/AgricultForest.71.3.06.
[12] Stroia, M.S.; Stroia, C.; Mihuț, C.; Duma Copcea, A.; Mazăre, V.; Radu, D. (2026). Assessment of physical and mechanical soil constraints in Sânandrei, Western Romania. *Research Journal of Agricultural Science*, 58(2), 431 https://doi.org/10.59463/RJAS.2026.2.52.
[13] Stroia, M.S.; Mihuț, C.; Duma Copcea, A.; Stroia, C.; Okros, A. (2026). Comparative assessment of soil chemical properties and fertility in Sânandrei, Romania. *Research Journal of Agricultural Science*, 58(2), 442 https://doi.org/10.59463/RJAS.2026.2.53.

[14] Mihuț, C.; Duma Copcea, A.; Okros, A.; Popa, N.D.; Bungescu, S.T.; Mircov, V.D.; Blenești-Dima, A.; Mazăre, V.; Moatăr, M.M.; Stroia, M.S.; Mocanu, N. (2026). Soils, properties and limitations in relation to land use in Geoagiu. *Research Journal of Agricultural Science*, 58(2), 315 https://doi.org/10.59463/RJAS.2026.2.38.
[15] Amenajamentul pastoral al pajiștilor permanente aparținând orașului Lipova, județul Arad. Documentație pastorală, pedologică și agrochimică. [Pastoral arrangement of permanent grasslands belonging to the city of Lipova, Arad County. Pastoral, pedological and agrochemical documentation].

SUSTAINABLE SOIL MANAGEMENT UNDER HILLY LANDSCAPE CONDITIONS. CASE STUDY: DEJ AREA, ROMANIA

Casiana Mihuț[1], Anișoara Duma-Copcea[1], Antoanela Cozma[1], Daniela Scedei[3], Attila Blenesi[2], Daniel Popa[2], Adalbert Okros[1], Dan Nicolae Manea[1], Marius Stroia[1], Veaceslav Mazăre[1]

[1] Department of Soil Sciences, Faculty of Agriculture, University of Life Sciences "King Mihai I" from Timișoara, Calea Aradului nr.119, 300645 Timișoara, country Timiș, România
[2] Department of Agricultural Tehnologies, Faculty of Agriculture, University of Life Sciences "King Mihai I" from Timișoara, Calea Aradului nr.119, 300645 Timișoara, country Timiș, România
[3]Department of Horticulture, Faculty of Engineering and Applied Technologies, University of Life Sciences "King Mihai I" from Timișoara, Calea Aradului nr.119, 300645 Timișoara, country Timiș, România
e-mail: anisoaradumacopcea@usvt.ro

Abstract
Sustainable soil management is essential in hilly areas, where relief, climate, soil properties, and land use can intensify degradation. This study assessed the main soil vulnerabilities in the Dej area using available pedological, agrochemical, climatic, hydrological, and land-use information. The main limitations were erosion on slopes, acidic reaction in some soils, compaction associated with agricultural traffic, and temporary excess moisture in low-lying positions. Sustainable management should therefore be spatially differentiated and include soil-cover maintenance, reduced disturbance, crop rotation, organic-matter management, soil-test-based fertilization, erosion control, and appropriate excess-water management. The results support adapting agricultural practices to soil type, slope, drainage, and agrochemical status rather than applying uniform technologies across contrasting land units.

Introduction
Soil is a fundamental resource for agricultural production and ecosystem functioning. Sustainable management must maintain productivity while conserving soil functions over time [1,2]. Because soil quality is site-specific and multidimensional, its assessment should integrate indicators relevant to soil functions and major threats [3]. Organic matter supports aggregation, water retention, nutrient cycling, and carbon storage [4,5]. In hilly landscapes, slope increases runoff and soil redistribution, making erosion a major constraint to sustainable land use [6]. At European scale, erosion causes measurable productivity losses [7], and spatial assessments confirm the broad extent of water-erosion risk [8]. Conservation agriculture therefore emphasizes reduced soil disturbance, permanent soil cover, and crop diversification [9], although practices must be adapted to pedoclimatic and production conditions [10]. In Romania, soil diversity and diagnostic properties provide the basis for differentiated interpretation and land management [11]. Recent studies also show that fertility and land suitability vary among soil units [12], climatic variability affects agricultural production in western Romania [13], and degraded soils can recover under long-term revegetation and appropriate management [14,15]. The Dej area combines fragmented hilly relief with contrasting pedological and hydrological conditions. Slopes are vulnerable to fertile-soil loss, whereas low-lying positions may experience temporary excess moisture; uneven precipitation can intensify erosion and leaching, while dry periods increase the importance of soil-water conservation. Accordingly, this study aimed to identify the main soil vulnerabilities in the Dej area and to define differentiated

management priorities according to relief, soil properties, water regime, and agrochemical status.

Experimental

The study was conducted in the Dej area, northern Cluj County, within the Someș Plateau. The landscape is predominantly hilly and fragmented, with ridges, slopes, terraces, and floodplain areas (Figure 1).

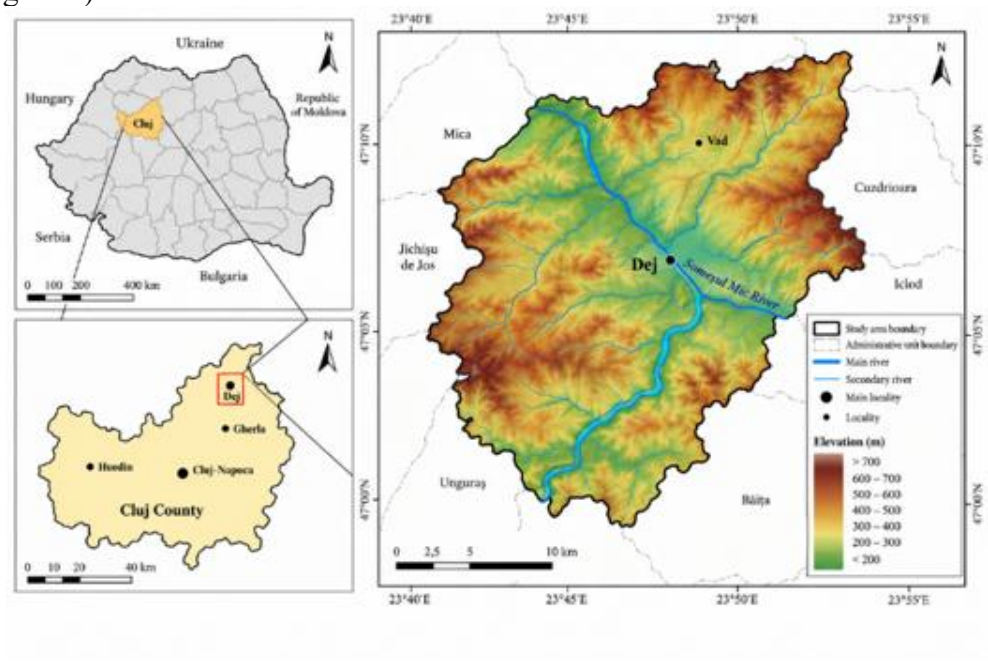


Figure 1. Location of the study area

The source documentation indicates elevations of approximately 300–600 m and a predominantly sedimentary substrate composed of marls, clays, sandstones, and colluvial or alluvial deposits.

The climate is moderately continental, with mean annual temperatures of about 7–9°C and annual precipitation of 600–700 mm. Uneven precipitation and torrential warm-season events are

The research is descriptive, comparative, and applied. Pedological and agrochemical information from the source documentation, including OSPA Cluj reports, was integrated with data on relief, climate, hydrology, land use, and anthropogenic pressures.

The analysis comprised three stages: (i) identification of the main vulnerabilities—erosion, acidity, compaction, and temporary excess moisture; (ii) qualitative association of these limitations with slopes, terraces, floodplains, and low-lying positions; and (iii) evaluation of compatible management options, including conservation tillage, soil cover, crop rotation, soil-test-based fertilization, liming where justified, erosion control, and excess-water management. Because the available database does not contain experimental replications of these management systems, no treatment effects, ANOVA, correlations, or regressions were calculated. The proposed practices are therefore management options supported by the identified vulnerabilities and the cited literature, not experimentally tested treatments in Dej.

Results and Discussion

Spatially Differentiated Land Vulnerability

Land vulnerability varied primarily with geomorphological position. On slopes, erosion was the dominant constraint because runoff and intense rainfall can accelerate topsoil loss,

consistent with the mechanism described by Montgomery (2007) [6] and European erosion assessments [8].
In low-lying positions and floodplains, temporary excess moisture becomes more important, reducing aeration and field accessibility. The source documentation therefore supports drainage where needed and avoidance of machinery traffic under wet conditions. These contrasts show that a single management system is not appropriate for the entire area.

Table 1. Relationship between land conditions, major vulnerabilities, and management priorities

Land condition	Main vulnerability	Priority management direction
Slopes	Erosion	Surface protection; contour farming
Acid soils	Acidity	pH monitoring; liming when justified
Compaction-prone soils	Structural degradation	Reduce traffic under wet conditions
Low-lying positions	Temporary excess water	Drainage management
Arable land	Organic matter loss	Rotations, crop residues, organic inputs
Vulnerable surfaces	Loss of fertile topsoil	Vegetative cover and erosion-control measures

Soil Conservation on Sloping Land

On sloping land, topsoil protection is the primary objective. Contour farming, grassed strips, maintenance of crop residues, cover crops, and reduced mechanical disturbance can limit erosion. These measures are consistent with conservation-agriculture principles [9], but their implementation must remain site-specific [10].
The available data do not demonstrate that no-till or any single practice is superior for all Dej soils. Where temporary excess moisture or compaction occurs, tillage and traffic must be adapted to the physical condition and water regime of the soil.
Accordingly, erosion-prone slopes require an integrated approach combining soil cover, reduced disturbance, contour-oriented operations, and permanently vegetated areas where risk is high.

Organic Matter and Fertility Management

Organic matter is central to soil structure, nutrient cycling, and resilience [4,5]. The source documentation indicates 2–4% humus and the presence of acidic soils in the Dej area, supporting organic-matter conservation and soil-test-based fertility management.
Crop rotation, legume integration, cover crops, and retention of organic inputs can help protect the soil surface and maintain organic matter. Fertilization and liming should be based on agrochemical analyses rather than applied uniformly across the area.
This differentiated approach agrees with Mihuț et al. (2025) [12], who reported differences in fertility and land suitability among Romanian soil units and emphasized management adapted to edaphic and hydrological limitations.
Water regime also requires differentiated management. Low-lying positions may experience temporary excess moisture, whereas warm-season dry periods increase the need to conserve soil water. Drainage and restricted traffic are appropriate where soils are wet; during water deficits, maintaining residues and improving infiltration can reduce evaporative losses.
Mircov et al. (2025) [13] likewise showed the importance of climatic variability for agricultural production in western Romania. Their results are not transferred quantitatively to Dej, but they support integrating temperature and precipitation variability into management decisions.

Conclusions

The Dej area has spatially differentiated soil vulnerabilities controlled mainly by relief, soil properties, and water regime.

Erosion is the principal limitation on slopes, while temporary excess moisture is important in low-lying positions; acidity and compaction are additional local constraints.

Management should therefore be differentiated by soil type, slope, drainage, and agrochemical status, with priority given to soil cover and erosion control on slopes and to drainage and traffic restriction on wet soils.

Crop rotation, cover crops, organic-matter conservation, and soil-test-based fertilization or liming can support long-term soil functionality. Overall, the results favor site-specific pedological management rather than uniform technologies.

References

[1] Doran, J.W.; Zeiss, M.R. (2000). Soil health and sustainability: Managing the biotic component of soil quality. Applied Soil Ecology, 15, 3–11. https://doi.org/10.1016/S0929-1393(00)00067-6.

[2] Pretty, J. 2008. Agricultural sustainability: concepts, principles and evidence. Philosophical Transactions of the Royal Society B, 363, 447–465. https://doi.org/10.1098/rstb.2007.2163.

[3] Bünemann, E.K.; Bongiorno, G.; Bai, Z.; et al. 2018. Soil quality—A critical review. Soil Biology and Biochemistry, 120, 105–125. https://doi.org/10.1016/j.soilbio.2018.01.030.

[4] Lehmann, J.; Kleber, M. 2015. The contentious nature of soil organic matter. Nature, 528, 60–68. https://doi.org/10.1038/nature16069.

[5] Lal, R. 2016. Soil health and carbon management. Food and Energy Security, 5, 212–222. https://doi.org/10.1002/fes3.96.

[6] Montgomery, D.R. 2007. Soil erosion and agricultural sustainability. Proceedings of the National Academy of Sciences, 104, 13268–13272. https://doi.org/10.1073/pnas.0611508104.

[7] Panagos, P.; Standardi, G.; Borrelli, P.; Lugato, E.; Montanarella, L.; Bosello, F. 2018. Cost of agricultural productivity loss due to soil erosion in the European Union. Land Degradation & Development, 29, 471–484. https://doi.org/10.1002/ldr.2879.

[8] Panagos, P.; Borrelli, P.; Poesen, J.; Ballabio, C.; Lugato, E.; Meusburger, K.; Montanarella, L.; Alewell, C. 2015. The new assessment of soil loss by water erosion in Europe. Environmental Science & Policy, 54, 438–447. https://doi.org/10.1016/j.envsci.2015.08.012.

[9] Hobbs, P.R.; Sayre, K.; Gupta, R. 2008. The role of conservation agriculture in sustainable agriculture. Philosophical Transactions of the Royal Society B: Biological Sciences, 363, 543–555. https://doi.org/10.1098/rstb.2007.2169.

[10] Kassam, A.; Friedrich, T.; Derpsch, R. 2019. Global spread of conservation agriculture. International Journal of Environmental Studies, 76, 29–51. https://doi.org/10.1080/00207233.2018.1494927.

[11] Florea, N.; Munteanu, I. 2012. Sistemul Român de Taxonomie a Solurilor (SRTS). Editura Sitech, Craiova.

[12] Mihuț, C.; Duma-Copcea, A.; Okros, A.; Cozma, A.; Mazăre, V.; Stroia, M.S. 2025. Integrated analysis of soil fertility, bonitation scores, and crop suitability in the Periam–Sânnicolau Mare area (Timiș County): Implications for sustainable land use. Annals of the University of Craiova – Agriculture, Montanology, Cadastre Series, 55(1), 321–328. https://doi.org/10.52846/aamc.v55i1.1699.

[13] Mircov, V.D.; Sărățeanu, V.; Mihuț, C.; Poșta, D.S.; Durău, C.C. 2025. Impact of extreme weather conditions on the production of the main field crops in Western Romania over the 2018–2023 period – case study. Agriculture and Forestry, 71(3), 103–112. https://doi.org/10.17707/AgricultForest.71.3.06.

[14] Buta, M.; Blaga, G.; Paulette, L.; Păcurar, I.; Roșca, S.; Borsai, O.; Grecu, F.; Pauliuc, E.S.; Negrușier, C. 2019. Soil Reclamation of Abandoned Mine Lands by Revegetation in Northwestern Part of Transylvania: A 40-Year Retrospective Study. Sustainability, 11, 3393. https://doi.org/10.3390/su11123393.
[15] Mihuț, C.; Niță, L. Atmospheric factors used in the characterization of soil resources. *Res. J. Agric. Sci.* **2018,** *50*, 114–120. https://www.rjas.ro/paper_detail/2612.

ECOLOGICAL RISKS OF TRACE METALS ALONG THE SERBIAN STRETCH OF THE DANUBE RIVER SEDIMENTS

Tatjana Mitrović[1], Marija Perović[2], Darija Obradović[1], Vladimir Vlatković[1]

[1]Institute of Physics Belgrade, University of Belgrade, Pregrevica 118, 11080 Belgrade, Serbia
[2]Jaroslav Černi Water Institute, Jaroslava Černog 80, 11225 Belgrade, Serbia
e-mail: tmitrovic@ipb.ac.rs

Abstract
Sediment quality along the Serbian stretch of the Danube River was assessed (2001-2023) using the mean Probable Effect Concentration Quotient (mPEC-Q) approach, an integrative index reflecting the potential toxicological risk of trace metal contamination to benthic biota (MacDonald et al., 2000) with the following equation:

$$mPEC - Q = \frac{\sum_{i=1}^{n} \frac{C_i}{PEC_i}}{n}$$

Ten monitoring stations were evaluated, spanning from Novi Sad to Kusjak downstream the Iron Gate I Reservoir (Figure 1). Based on the concentrations of As, Cu, Zn, Pb, Cr, Cd and Ni, mPEC-Q values were calculated and ranged from 0.29 (Novi Sad) to 0.76 (Veliko Gradište), with most stations falling within the 0.5–0.75 range (Table 1), indicating a low to moderate probability of adverse biological effects associated with sediment bound metals, according to established mPEC-Q toxicity thresholds.

Table 1. Mean mPEC-Q values of the Danube sediments with the highest contaminat contributor

Station	mPEC-Q values	Assosiated risk	Highest contributor
Novi Sad	0.29	Low	Ni (0.52)
Stari Banovci	0.32	Low	Ni (0.63)
Smederevo	0.66	High	Ni (1.64)
Ritopek	0.54	Moderate	Ni (1.40)
Ram	0.68	High	Ni (1.92)
Veliko Gradište	0.76	High	Ni (2.08)
Donji Milanovac	0.70	High	Ni (1.84)
Tekija	0.74	High	Ni (1.81)
Kladovo	0.67	High	Ni (1.56)
Kusjak	0.73	High	Ni (1.76)

Nickel (Ni) was identified as the dominant contributor to sediment contamination at eleven of the twelve stations, with individual PEC-Q values reaching as high as 2.08 at Veliko Gradište and 1.92 at Ram, both exceeding the threshold associated with probable toxicity (PEC-Q > 1).

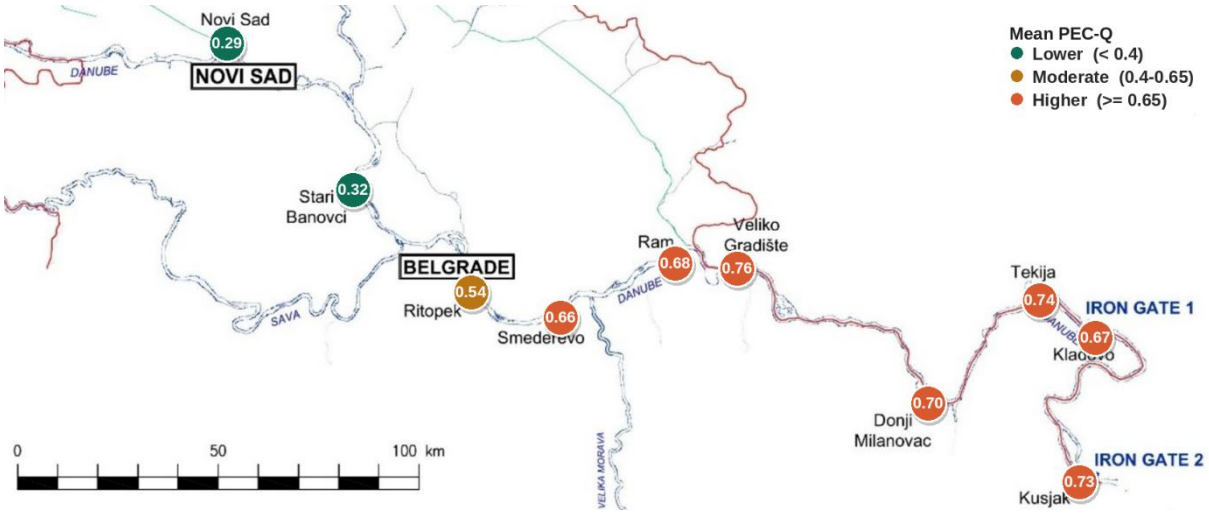


Figure 1. Average mPEC-Q values of Danube sediments

The spatial pattern shows generally higher mPEC-Q values at stations along the middle and lower Danube (e.g., Veliko Gradište, Donji Milanovac, Tekija, Kusjak,), while Novi Sad and Stari Banovci in the upper reach exhibited comparatively lower contamination levels. These findings suggest that Ni enrichment is the principal driver of sediment-associated ecological risk in this section of the Danube. But, since it was already found that it is likely linked to geogenic background levels (Mitrović et al., 2026) there is a reason to inspect bioavailability and site-specific ecological context rather than assume high risk from total concentration alone. A proper assessment should use bioavailability approaches and consider whether local biota is actually adapted, rather than relying solely on total concentration comparisons to generic thresholds.

References

[1] D. MacDonald, C.G. Ingersoll, T.A. Berger, Arch. Environ. Contam. Toxicol. 39 (2000) 20.
[2] T. Mitrović, M. Perović, D. Obradović, A. Petković, J. Čolić, T. Nenin, S. Lazović, Environ. Geochem. Health 48 (2026).

RESEARCH ON THE RESTORATION OF DEGRADED LAND IN THE OSTROVUL MOLDOVA VECHE IMPROVEMENT AREA

Moatăr Maria Mihaela[1], Panici Petre Alexandru[1], Dragomir Petru Ioan[1], Ștefan Carolina[1], Panici Cristina Gabriela[1], Scedei Daniela Nicoleta[2], Bora Marinela[3], Ceuca Vasile[4], Sîngeorzan Steluța-Maria[4]

[1]Department of Forestry, University of Life Sciences "King Michael I" from Timisoara, 300645, Timisoara, Romania; e-mail: mihaela.moatar@usvt.ro, alexandrupanici@usvt.ro, petruioandragomir@usvt.ro, carolinastefan@usvt.ro, panici.cristina-gabriela.fita@usvt.ro
[2]Department of Horticulture, University of Life Sciences "King Michael I" from Timisoara, 300645, Timisoara, Romania; e-mail: daniela.scedei@usvt.ro
[3]Department of Genetic Engineering, University of Life Sciences "King Michael I" from Timisoara, 300645, Timisoara, Romania; e-mail: bora.marinela.fita@usvt.ro
[4]Department of Forestry, University of Agricultural Sciences and Veterinary Medicine Cluj-Napoca, 300645, Timisoara, Romania; e-mail: vasy_ceuca@yahoo.com, *maria.sîngeorzan@usamvcluj.ro*
Corresponding author: alexandrupanici@usvt.ro, petruioandragomir@usvt.ro

Abstract
The study evaluates the ecological restoration of 29.00 ha of degraded land within the Ostrovul Moldova Veche improvement area, on the Danube River in Caraș-Severin County, Romania. The investigated land is affected mainly by wind erosion of sandy deposits (21.08 ha), bank undermining (3.97 ha), and waterlogging (2.95 ha). A site-based mapping approach was used to relate geomorphological, hydrological, geological and pedological constraints to restoration measures. The proposed technical complex combines riverbank stabilization, localized soil preparation, afforestation with species adapted to contrasting moisture conditions, and multiannual plantation maintenance. Black locust is emphasized on mobile and nutrient-poor sands, while black poplar, alder and ash are allocated to riverbank or wetter microsites. The investment assessment covers 29 ha, with a total estimated value of 240,116.22 RON, a specific investment reported in the source study as 8,824.7 RON ha^{-1}, and a seven-year implementation period. The restoration design is expected to reduce deflation and bank retreat, improve soil conditions and establish permanent protective forest vegetation [1–5].

Introduction
Land degradation on sandy alluvial islands results from the interaction of wind, water, soil properties and land use. Forestry-based reclamation seeks not only to establish tree cover, but also to reduce erosion, improve soil functioning and create a vegetation structure compatible with local hydrological constraints [1,5]. Recent restoration literature emphasizes the same site-based principle: soil texture, nutrient status, water availability and other edaphic limitations should guide afforestation design rather than applying a uniform planting prescription [7]. Long-term evidence from sandy soils also shows that tree establishment can alter organic layers and soil chemistry, but that responses depend strongly on soil type and species composition [8,10]. The present case study concerns the Ostrovul Moldova Veche improvement area, situated on a Danube island in Caraș-Severin County, within the Iron Gates Natural Park. The primary technical data and proposed works are taken from the bachelor thesis prepared for this perimeter [6].

Experimental

The research followed the degraded-land mapping method based on site units and site types. The perimeter was divided into homogeneous units, which were characterized using geomorphological, hydrological, geological and pedological criteria. Groundwater depth was particularly important because it differentiates dry mobile sands from moist interdunes and waterlogged low areas. Two main site groups and three site conditions were distinguished. The first group includes wind-degraded sandy land with typical psamosols, generally alkaline, very poor in humus and nutrients; groundwater is commonly below 2 m, but may rise to approximately 0.70 m near banks or interdunes. The second group includes low terrain periodically affected by water, with gleyed sandy soils for which excess moisture is the principal limiting factor.

Table 1. Degraded land categories in the Ostrovul Moldova Veche improvement area.

Degradation category	Area (ha)	Share (%)
Undermined riverbanks	3.97	11.69
Sandy land affected by deflation	21.08	78.69
Waterlogged land	2.95	9.62
Total	29.00	100.00

The improvement complex was matched to the identified degradation processes. On vulnerable eastern riverbanks, double wattle structures were proposed where bank height does not exceed 1.20 m, while gabions were proposed for higher sections. Willow stakes, fascines and fresh willow twigs are incorporated into the wattle structures so that living vegetation contributes progressively to stabilization. For planting, the soil is prepared manually in 0.60 × 0.80 m patches; 0.036 m³ of topsoil is allocated per planting pit. Based on 137,550 seedlings, the source study calculates 660.24 ares of prepared planting patches and 4,951.8 m³ of topsoil. Mounding is proposed for alder and ash on wet sites.

Species selection follows site requirements and protective function. Black locust (Robinia pseudoacacia) is the dominant species for dry, mobile and nutrient-poor sandy terrain because of its vigorous root system and capacity to stabilize sands. Black poplar (Populus nigra) is proposed in a protective belt along the Danube banks, whereas black alder (Alnus glutinosa) and ash (Fraxinus spp.) are assigned to wetter sites. For small planting stock, a 2 × 1 m rectangular spacing (5,000 seedlings ha^{-1}) is proposed; black poplar is planted at 4 × 2 m (625 seedlings ha^{-1}). Maintenance is planned for four to five years, with repeated soil mobilization and replacement of losses until canopy closure [1, 4, 5].

Results and Discussion

Wind erosion is the dominant degradation process, accounting for 21.08 ha (78.69%) of the 29 ha studied perimeter, whereas undermined banks and waterlogged terrain account for 3.97 ha and 2.95 ha, respectively (Table 1; Figure 1). This distribution explains why stabilization of sandy substrates and rapid establishment of protective vegetation form the core of the restoration design. The source study also notes that exposed sands may be mobilized at wind speeds of approximately 4.5 m s^{-1}, while strong winds are frequent in the perimeter, creating a persistent risk of renewed deflation where vegetation is sparse.

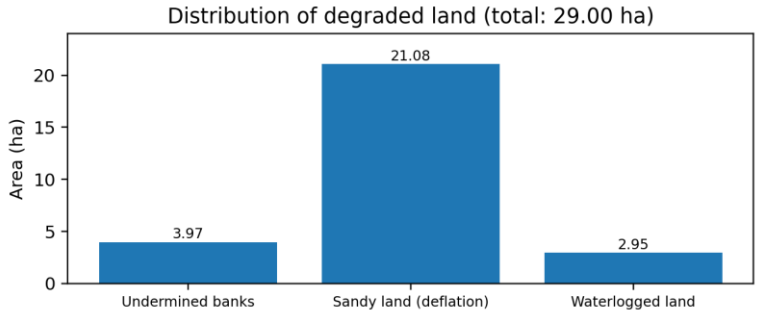


Figure 1. Area affected by the three principal degradation processes. Data derived from the bachelor thesis

The restoration measures are differentiated rather than uniform. On sandy sites, black locust is intended to accelerate soil protection and stand closure; the proposed 50% black locust–50% shrub/auxiliary composition is assigned to approximately 73% of the planted area. Along the riverbank, a 50% black poplar–50% associated woody-species composition is proposed on about 14% of the planted area to reinforce the bank through root development. On low, moist terrain (about 13%), a 50% alder–50% ash composition is proposed because these species are better suited to shallow groundwater and periodic excess moisture. This site-species matching is consistent with the silvicultural principle that reclamation success depends on adapting species and planting techniques to soil depth, moisture and degradation intensity [1, 4, 5].

Restoration design in relation to recent research

The site differentiation proposed for Ostrovul Moldova Veche is consistent with current restoration research. Prescott et al. [7] underline that successful forest restoration depends on matching species and treatments to soil constraints such as low organic matter, weak water-holding capacity, nutrient imbalance and erosion susceptibility. These constraints closely resemble the sandy, nutrient-poor and locally waterlogged conditions identified in the studied perimeter.

Romanian research also confirms the protective role of forest stands established on degraded land. Moldovan et al. [9] quantified substantial anti-erosion effects in afforested degraded areas and emphasized the influence of stand structure, rainfall and soil retention on runoff. Although their study concerns different site conditions, it is relevant methodologically because it demonstrates that restoration performance should be evaluated using measurable indicators rather than inferred only from plantation survival. In the Moldova Veche perimeter, suitable indicators would include vegetation survival, canopy closure, evidence of renewed wind erosion, bank stability, groundwater-related stress and the persistence of bare sandy patches.

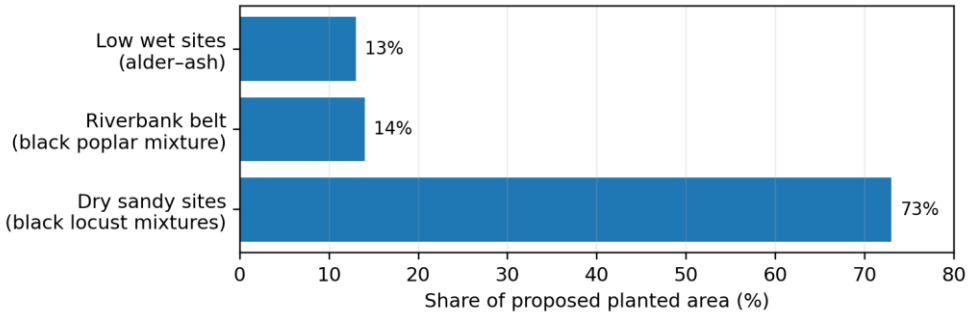


Figure 2. Distribution of the proposed planted area among the principal site-specific restoration solutions. Percentages are derived from the bachelor thesis [6].

Figure 2 highlights the predominance of the dry-sand restoration solution: approximately 73% of the proposed planted area is assigned to black-locust-based mixtures, compared with about 14% for the riverbank black-poplar mixture and 13% for alder–ash on wet lowlands [6]. This distribution mirrors the degradation pattern shown in Figure 1, where deflation-affected sandy land represents the largest affected category. The correspondence between degradation type and restoration allocation is a strength of the proposed design because resources are concentrated on the process occupying most of the perimeter while retaining distinct solutions for hydrologically contrasting microsites.

Table 2. Main restoration measures and technical parameters.

Component	Proposed measure / parameter
Bank stabilization	Double wattle structures on banks ≤1.20 m; gabions on higher vulnerable banks
Soil preparation	Manual 0.60 × 0.80 m patches; 0.036 m³ topsoil per pit; mounding for alder and ash
Dry sandy sites	Black locust-based mixtures; 2 × 1 m spacing for small planting stock (5,000 seedlings ha^{-1})
Riverbank belt	Black poplar-based mixture; 4 × 2 m spacing (625 seedlings ha^{-1})
Wet sites	Alder–ash mixture on low terrain with shallow groundwater
Maintenance	4–5 years, including repeated soil mobilization and replacement of losses

Implementation and monitoring considerations

The proposed intervention combines engineering works with biological stabilization, so implementation should follow a sequence that prevents one component from undermining another. Bank-protection works should be completed first in sectors exposed to wave action, followed by localized soil preparation and planting during the appropriate seasonal window. On mobile sands, unnecessary disturbance outside the planting patches should be avoided because freshly exposed material may be susceptible to renewed deflation. In wet depressions, planting operations should be timed according to groundwater conditions so that seedlings are neither installed into prolonged standing water nor subjected to avoidable drought stress immediately after planting. This sequencing is consistent with the general restoration principle that treatment intensity should respond to the dominant site limitation [7].

A simple field record can integrate these variables into an adaptive management cycle. Each year, the perimeter can be inspected by site unit, with observations on survival, erosion features, exposed soil, bank damage and hydrological stress. Results can then be compared with the previous year and used to prioritize replacement planting, supplementary stabilization or maintenance. Where repeated failure occurs in the same microsites, the cause should be diagnosed before replanting. This approach would make the project more consistent with contemporary restoration practice, in which success is evaluated through measurable ecological trajectories and management is adjusted when the observed response differs from the intended one [7,9,11].

Technical and economic assessment

The projected works cover the entire 29.00 ha degraded perimeter. The source study estimates a total investment of 240,116.22 RON, a specific investment reported as 8,824.7 RON ha^{-1} and implementation duration of seven years [6]. The source anticipates visible effects three to five years after plantation establishment; these values are project estimates and should not be interpreted as post-restoration measurements. The technical logic of the investment is that early expenditure on bank protection, soil preparation, planting and maintenance should reduce the

probability of renewed degradation and create the conditions for a self-sustaining protective stand.

A contemporary evaluation framework should complement these cost indicators with ecological monitoring. At minimum, annual records should include seedling survival by species and site type, replacement rate, height growth, percentage of bare soil, visible deflation features, bank retreat or stabilization, and waterlogging duration in low terrain. Soil pH and organic matter can be monitored at wider intervals to detect whether the substrate is developing in the intended direction [7,8,10]. This is particularly important because recent research on sandy disturbed sites shows that different tree species can produce contrasting effects on soil properties and those mixtures of planted stands and naturally developing vegetation may improve ecosystem diversity and resilience [11].

Conclusion

The Ostrovul Moldova Veche case demonstrates the need for a site-specific restoration strategy in which erosion control, hydrological constraints and afforestation are treated as a single technical system. Deflation is the dominant degradation process, but riverbank instability and waterlogging require separate engineering and silvicultural responses. The proposed combination of wattle and gabion protection, localized soil preparation, black-locust-based mixtures on dry sands, black poplar near the river and alder–ash on wet sites reflects this environmental heterogeneity [6]. The success of the project should therefore be judged not only by the initial establishment of 137,550 seedlings, but by sustained vegetation cover, reduced erosion, improved site stability and the capacity of the restored stands to persist under the local Danube hydrological regime.

References

[1] Ciortuz, I. Ameliorații Silvice. Editura Didactică și Pedagogică: Bucharest, 1981.
[2] Chiriță, C. Solurile României. Editura Academiei: Bucharest, 1977.
[3] Constandache, C.; Blujdea, V.; Nistor, S. (2010). Achievements and Perspectives on the Improvement by Afforestation of Degraded Lands in Romania. In The Management of Environmental Resources. Springer.
[4] Lăzăreanu, A. Tehnica lucrărilor de îngrijire în pepiniere și plantații forestiere. Editura Orizonturi Universitare: Timișoara, 2004.
[5] Traci, C. Împădurirea terenurilor degradate. Editura Ceres: Bucharest, 1985.
[6] Străin, D.-G. Cercetări privind lucrările de reconstrucție a terenurilor degradate din perimetrul de ameliorare Ostrovul Moldova Veche. Bachelor thesis, University of Life Sciences "King Michael I" from Timisoara, Timișoara, Romania.
[7] Prescott, C.E.; Katzensteiner, K.; Weston, C.J. Soils and restoration of forested landscapes. In Soils and Landscape Restoration; 2021; pp. 299–331. https://doi.org/10.1016/B978-0-12-813193-0.00011-4.
[8] Tew, E.R.; Vanguelova, E.I.; Sutherland, W.J. Alternative afforestation options on sandy heathland result in minimal long-term changes in mineral soil layers. Forest Ecology and Management 2021, 483, 118906. https://doi.org/10.1016/j.foreco.2020.118906.
[9] Moldovan, M.; Tăut, I.; Rebrean, F.A.; Szilard, B.; Arion, I.D.; Dîrja, M. Determining the Anti-Erosion Efficiency of Forest Stands Installed on Degraded Land. Sustainability 2022, 14, 15727. https://doi.org/10.3390/su142315727.
[10] Sławski, M.; Tarabuła, T.; Sławska, M. Does the enrichment of post-arable soil with organic matter stimulate forest ecosystem restoration—A view from the perspective of three decades after the afforestation of farmland. Forest Ecology and Management 2020, 478, 118525. https://doi.org/10.1016/j.foreco.2020.118525.

[11] Woś, B.; Likus-Cieślik, J.; Józefowska, A.; Pietrzykowski, M. Creation of a forest ecosystem mosaic of succession and afforestation on a site after sand mining—Stand characteristics and effects on soil properties. Ecological Engineering 2026, 227, 107977. https://doi.org/10.1016/j.ecoleng.2026.107977.

EVALUATION OF THE SENSORY PROPERTIES AND ANTIOXIDANT ACTIVITY OF FLAVORED VODKA OF SOME CHILI PEPPER VARIETIES

Diana Moigradean[1], Mariana-Atena Poiana[1*], Andreea Ghitulescu[1], Despina-Maria Bordean[1], Mihaela Lacatus[1], Ariana-Bianca Velciov[1], Daniela Stoin[1], Florina Radu[1], Corina-Iuliana Megyesi[1], Laura Radulescu[1], Simion Alda[2], Alexandru-Erne Rinovetz[1]

[1]Faculty of Food Engineering, University of Life Sciences "King Mihai I" from Timisoara, Romania, Aradului Street No 119, 300645 Timisoara, Romania
[2]Faculty of Engineering and Applied Technology, University of Life Sciences "King Mihai I" from Timisoara, Romania, Aradului Street No 119, 300645 Timisoara, Romania
[*] corresponding author e-mail: marianapoiana@usvt.ro

Abstract
This study aimed to produce and characterize flavored alcoholic beverages based on vodka and fresh chili peppers. For sample preparation, vodka with an alcohol concentration of 40% vol. was utilized, while three types of chili peppers were employed as plant materials: Cayenne (Green), Banana Chili (Yellow) and Hungarian Wax. The aromatization of the beverages was achieved through maceration, a method frequently employed in the production of flavored spirits due to the capacity of ethyl alcohol to extract aromatic compounds and bioactive substances from botanical sources. The results obtained confirm that the variety of pepper used influences both the sensory properties and the physicochemical characteristics of the flavored vodka, contributing to the obtaining of finished products with distinct aroma, taste and antioxidant activity profiles. The antioxidant activity and total phenolic content were investigated using standard analytical techniques, specifically the ferric-ion reducing antioxidant potential (FRAP assay) and the Folin-Ciocalteu method, respectively.

Introduction

The aromatization of spirit beverages relies on solid-liquid extraction to transfer volatile and bioactive components from botanical sources into an aqueous-alcoholic medium. This process depends on the nature of the solvent and the properties of the extracted compounds; ethanol is one of the most widely used solvents due to its ability to dissolve both hydrophilic and lipophilic compounds, thereby contributing to a complex aroma profile [8]. Standard extraction processes generally include maceration, digestion, decoction, infusion and percolation, alongside more advanced techniques such as Soxhlet extraction, supercritical fluid extraction, and ultrasound or microwave-assisted methods. Maceration is widely utilized as a conventional flavoring technique, involving the prolonged immersion of botanical biomass in a solvent at room temperature. Throughout this operation, the migration of bioactive constituents into the liquid phase is governed by a concentration gradient and the physicochemical attributes of the matrix solvent system. Although characteristically slow, this straightforward and economical method is highly preferred for isolating heat-sensitive compounds. Infusion is similar to maceration but employs higher temperatures to accelerate the extraction process. Raising the temperature intensifies diffusion and increases compound solubility, thereby reducing the time required to obtain the extract. However, high temperatures can lead to the degradation of certain volatile or thermolabile compounds, negatively affecting the sensory profile of the final product [1]. When processing chili peppers (*Capsicum spp*.), both maceration and infusion are effective for isolating capsaicinoids and key volatile aroma compounds. Capsaicin, the predominant pungent alkaloid, exhibits high solubility in ethanol, which streamlines its migration into hydro-alcoholic matrices. The final pungency of the spirit is heavily dictated by the extraction runtime and the ethanol titer. Ultimately, the selected extraction approach directly shapes the chemical

makeup and organoleptic properties of the beverage. Deciding between traditional maceration, hot infusion, or contemporary methodologies establishes the overall yield and the specific chemical profile obtained, resulting in distinct variations among flavored spirits [8].
Capsicum annuum (L.) is a widely consumed everyday spice renowned for its therapeutic and ethnobotanical features. Regular dietary intake of chili peppers has been shown to offer substantial health benefits. Rich in essential nutrients like vitamins and minerals, its fruits also deliver a high concentration of carotenoids and phenolic metabolites that act as powerful antioxidants [7]. Vodka is a neutral alcoholic alcoholic beverage produced primarily through the fermentation and distillation of grains. According to European Union regulations, it must maintain a minimum alcohol by volume (ABV) of 37.5% [4]. The lack of distinct flavor in the alcohol makes it an excellent base for maceration. This neutrality ensures that the aromatic compounds of the new ingredients are prominently highlighted, remaining unaffected by the underlying source material [1].
In this work, we analyzed the sensory properties, alcoholic strength and antioxidant activity of different chili pepper flavored vodkas.

Experimental

Three fresh chili pepper cultivars (*Capsicum* spp.) were purchased from a local market in Timisoara, Romania. Consequently, this study focuses on the following three cultivars: Green Cayenne, Banana Chili and Hungarian Wax. Each chili pepper variety was washed and sliced with a stainless-steel knife. For a flavorful drink with a medium spice level, some of the seeds and the inner white membranes were removed [2]. Maceration was used to flavor the drinks, which is a common practice when making infused alcohol. This technique is highly effective because ethyl alcohol easily extracts aromatic elements and beneficial compounds from plants [1]. Liquid extracts were prepared by macerating 10 g of hot peppers in 100 mL of Stalinskaya vodka (40% ABV), acting as the extraction solvent. The extraction of bioactive hot pepper compounds (flavor, colorants, and aromatics) into the solvent was achieved for maceration, maintained at room temperature and shielded from light. Following a maceration time of 48 h, the solid botanical mass was separated by filtration, and the clear liquid extracts were subjected to sensory and physicochemical analyses. Additionally, the antioxidant compounds in the fresh chili pepper samples were determined.

Physico-chemical analysis

Determination of alcohol by volume (ABV)
Quantifying the alcohol by volume (ABV) is an essential requirement for quality control management in commercial beverage production. Depending on the required precision, processing complexity and degree of automation, multiple protocols are available for daily laboratory operations; refractometric and densitometric techniques are widely favored for rapid ABV determination, particularly for real-time monitoring during the production process [1]. In this work, a refractometer method was used as a practical instrument to measure the alcohol concentration in the samples.
Determination of antioxidant activity and total phenolic content
The Ferric Reducing Antioxidant Potential (FRAP assay), as described by Benzie and Strain (1996) [5], was employed to evaluate the antioxidant activity. Additionally, the total phenolic content was quantified using the Folin-Ciocalteu method [6]. The TAC and TPC of the samples were quantified at 593 nm and 725 nm, respectively, using an Analytik Jena UV-VIS SPECORD 205 spectrophotometer. Gallic acid was utilized as the standard for TPC calibration. All measurements were performed in triplicate.
All solvents and reagents used in the experiments were of high analytical grade.

Results and discussion

Sensory analysis of the flavored alcoholic samples was performed to assess their organoleptic profiles, including appearance, odor, color and taste.

Pigment extraction efficiency depended strongly on the pepper variety. The vodka with Cayenne chili pepper demonstrated the most intense yellow-orange hue, whereas the Hungarian Wax pepper flavored vodka sample was very pale straw-yellow, nearly identical to the control. The Banana chili pepper sample fell between the two, presenting a light yellow tint. Notably, high transparency was preserved across all flavored vodka varieties. Evaluation of the chili extracts revealed distinct profiles in terms of scent strength, flavor endurance, and pungency. The Cayenne cultivar produced the strongest extract, characterized by a powerful, sharp aroma, a lingering spiciness, and the highest heat level. Conversely, the Hungarian Wax pepper was the least intense, offering a subtle fragrance and very low capsaicin impact. Positioned between these two, the Banana chili variety demonstrated balanced aromatic traits and a moderate level of heat. Also, called the yellow wax pepper, the Banana Chili is a milder cousin of the Hungarian Wax; it only slightly hotter than a bell pepper [12].

The varieties of vodka flavored with chili peppers presented appropriate organoleptic characteristics, being clear, without visible impurities or deposits. The differences between the samples were mainly observed in the aroma, color and intensity of the spicy taste; aspects determined by the variety of pepper used in the maceration process.

Stalinskaya vodka is colorless and has a clear appearance. Stalinskaya represents a prominent grain derived vodka manufactured in Romania based on traditional Russian formulations. Characterized by a standard ethanol concentration of 40%, the product is suitable for neat ingestion at lowered temperatures or as a primary spirit base designed to integrate efficiently with diverse beverage formulations [13].

The results presented in Table 1 highlight variations in the alcoholic strength of the flavored vodkas obtained by macerating different hot pepper varieties.

Table 1. Alcoholic strength of alcoholic extracts from different chili pepper varieties

Vodka variety	Alcohol by volume (ABV)
Vodka (control samples)	40.0
Vodka with Green Cayenne	36.9
Vodka with Banana Chilli	38.7
Vodka with Hungarian Wax	37.7

Regarding alcoholic strength, the Banana Chilli pepper formulation yielded the highest values, closely followed by the samples prepared with Hungarian Wax and green Cayenne varieties, respectively. Determination of alcoholic concentration revealed values ranging between 36.9 - 38.7% by volume (ABV), lower than the initial concentration of the vodka used for maceration. This decrease in alcoholic strength can be attributed to the migration of some botanical constituents from the plant material into the liquid phase and by the structural alterations occurring throughout the maceration time [1, 9].

Generally, *Capsicum annuum* species exhibit superior antioxidant capacity, which directly correlates with their elevated levels of capsaicinoids and phenolic compounds [3]. Characterization of these bioactive compound within the fresh chili pepper varieties (Table 2) and the fortified vodka samples (Table 3) relied on total phenolic levels (TPC) and ferric-ion reducing antioxidant potential (FRAP) measurements.

Table 2. Bioactive compound content of the analyzed fresh chili pepper varieties

Hot pepper variety	**TPC** (mg GAE/100 g FM)	FRAP (mM Fe^{2+}/100 g FM)
Green Cayenne pepper	148.22	71.89
Banana Chili pepper	248.56	58.50
Hungarian Wax pepper	196.08	26.10

Despite having the lowest initial phenolic content, the fresh Green Cayenne pepper demonstrated the highest antioxidant capacity (71.89 mM Fe^{2+}/100 g FM), outperforming the Hungarian Wax pepper by a factor of 2.75. Conversely, Banana Chili pepper possessed the highest TPC but only ranked second in FRAP values (58.50 mM Fe^{2+}/100 g FM). This structural discrepancy strongly suggests that the antioxidant power in these pepper varieties is not driven solely by total phenolics. Non-phenolic hydrophilic antioxidants, most notably ascorbic acid, along with highly potent specific capsaicinoids predominant in the green maturation stage of Cayenne peppers, likely exert a dominant synergistic effect in the FRAP assay mechanism [11].

Table 3. Bioactive compound content in flavored vodka formulations

Vodka variety	**TPC** (mg GAE/100 g FM)	FRAP (mM Fe^{2+}/100 g FM)
Vodka (control samples)	0	0
Vodka with Green Cayenne	348.46	N/A
Vodka with Banana Chili	359.12	N/A
Vodka with Hungarian Wax	307.21	N/A

N/A - Not Available

Furthermore, the migration of capsaicin, polyphenols and plant pigments into the ethyl alcohol fundamentally redefined the products final composition [10]. The highest total phenolic level was recorded for the Banana Chili flavored formulation (359.12 mg GAE/100 g FM), whereas the antioxidant potential of the samples remained below the detection limit of the FRAP method. The standard FRAP protocol measures absorbance after a brief incubation time (typically 10 minutes). However, certain polyphenols found in chili peppers exhibit slow reacting kinetics with the ferric-tripyridyltriazine (Fe^{3+}-TPTZ) complex, meaning the color development might not have progressed enough to be registered by the spectrophotometer within the designated timeframe [10]. Hydrophilic antioxidants like ascorbic acid are highly prone to degradation when exposed to light, oxygen, or prolonged storage during the infusion process, which could drastically diminish the samples overall reducing capacity [9].

The vodka maceration process demonstrated high efficiency in extracting bioactive compounds across all three chili pepper varieties, driving a significant increase in total phenolic content compared to the fresh raw material. The most pronounced effect was observed in the Green Cayenne variant, where the phenolic concentration escalated 2.35 fold (135.10%), followed by the vodka with Hungarian Wax pepper formulation with a 1.57 fold growth (56.68%) and with Banana Chili with a 1.44 fold enhancement (44.48%). These findings suggest that the hydroalcoholic medium acts as an ideal solvent: ethanol rapidly penetrates the plant cell membranes and dissolves lipids, successfully flushing out the polyphenols that would otherwise remain bound within the cell wall matrix. Furthermore, the alcohol concentration instantly denatures endogenous degradation enzymes (such as polyphenol oxidase) found in fresh chili, halting any enzymatic breakdown and maintaining the stability of the extracted antioxidants [11].

Conclusion

The varieties of vodka flavored with chili peppers presented appropriate organoleptic characteristics, being clear, without visible impurities or deposits. The differences between the samples were mainly observed in the aroma, color and intensity of the spicy taste; aspects determined by the variety of pepper used in the maceration process. This study highlights that utilizing a hydroalcoholic medium (vodka) represents an optimal and highly efficient approach for maximizing phenolic compound extraction from the cellular matrix of chili peppers, significantly outperforming the yields obtained from fresh raw material. Chili-flavored vodka can serve as an alternative for consumers interested in beverages with a distinct sensory profile, characterized by spicy notes and flavors specific to the plant-based ingredients used.

References

[1] A.R. Abubakar, M. Haque, J Pharm Bioallied Sci. (2020) 12(1) 1-10.

[2] R.S. Aleman, J.A. Marcia, I. Montero-Fernandez, J. King, S.K. Pournaki, R.T. Hoskin, M. Moncada, Foods 12 (2023) 369.

[3] E. Alvarez-Parrilla, L.A. De La Rosa, R. Amarowicz, F. Shahidi, J. Agric. Food Chem. 59 (2011), 163e173.

[4] AOAC (Association of Official Analytical Chemists). 1998. *Official Methods of Analysis* (16th edn, N°1-2). Association of Official Analytical Chemists: Washington D.C

[5] I.F. Benzie, J.J. Strain, Anal Biochem. 239(1) (1996) 70-76.

[6] O. Folin, V. Ciocalteu, J. Biol. Chem. 24 (1927) 627-650.

[7] I.M. Ivan, V. Popovici, C.L. Chitescu, L. Popescu, E.A. Luta, E.I. Ilie, L.I. Brasoveanu, C.M. Hotnog, O.T. Olaru, G.M. Nitulescu, R. Boscencu, C.E. Gird, Pharm.16(2) (2024) 245. doi: 10.3390/pharmaceutics16020245.

[8] J.E.Lee, J.T.M. Jayakody, J.J. Kim, J W. Jeong, K.M Choi, T.S. Kim, C. Seo, I. Azimi, J. Hyun, B. Ryu, *Foods 13*(19) (2024) 3151.

[9] M.R. Loizzo, A. Pugliese, M. Bonesi, F. Menichini, R. Tundis, LWT - Food Sci. Technol. 64 (2015) 623-631.

[10] I. Ogunlade, A.A. Alebiosu, A.I. Osasona, Int. J. Biol. Chem. Sci. 6(5) (2012) 2221-2227.

[11] M. Patra, E. Salonen, E. Terama, I. Vattulainen, R. Faller, B.W. Lee, J. Holopainen, M. Karttunen, Biophys J. 90(4) (2006) 1121-35.

[12] https://chilliworkshop.co.uk/chilli-varieties-from-a-to-z/banana-chilli/

[13] https://alcooldiscount.ro/vodca-stalinskaya-175l-40-alc-romania.html

DEVELOPMENT, FUNCTIONAL CHARACTERIZATION, AND SENSORY EVALUATION OF PHYTOCHEMICAL-ENRICHED RAW-VEGAN TRUFFLES

Delia-Gabriela Dumbrava[1], Camelia Moldovan[1*], Isabel Guiamba[2], Diana-Nicoleta Raba[3], Viorica-Mirela Popa[1], Diana-Veronica Radu[1], Corina-Dana Misca[1]

[1]Faculty of Agrofood Processing Technology, University of Life Sciences "King Mihai I" from Timişoara, Calea Aradului 119A, 300645, Romania
[2]Faculty of Engineering, Eduardo Mondlane University, Av. De Mozambique km 1,5 – C.P. 257, Maputo, Mozambique
[3]Faculty of Management and Rural Tourism, University of Life Sciences "King Mihai I" from Timişoara, Calea Aradului 119A, 300645, Romania
e-mail: cameliamoldovan@usvt.ro

Abstract
This study investigates the formulation, nutritional and functional profiling, and sensory evaluation of three raw-vegan truffle-type confectionery formulations, developed as minimally processed, refined sugar-free alternatives to conventional confectionery products. The investigated formulations comprise: RVT1 (dates, walnuts, fresh ginger), RVT2 (walnuts, dates, matcha powder), and RVT3 (coconut, dates, cocoa powder). Laboratory assays demonstrated that incorporating phytochemical-rich botanical ingredients significantly enhanced the functional attributes of the matrices. Among the raw ingredients, matcha and cocoa powders exhibited the highest total polyphenol concentrations and radical scavenging capacity, as assessed via the Folin-Ciocâlteu and DPPH assays. This profile directly translated to the finished products: RVT2 (matcha-enriched) displayed the highest total phenolic content and the highest antioxidant potential, followed by RVT1 and RVT3. Nutritional profiling revealed substantial protein levels (17 - 22 g/100g) across all formulations and a dietary fiber concentration exceeding 6\text g/100g - satisfying regulatory criteria for a "high fiber" claim—alongside low simple sugar content. Organoleptic testing conducted with a 20-member panel indicated high overall acceptability across all samples (>4.5 on a 5-point scale), with RVT3 attaining the highest scores for aroma and overall flavor profile. Ultimately, these findings demonstrate that phytochemically enriched raw-vegan confectionery, notably formulation RVT2, presents a nutritionally valuable, sustainable, and commercially viable functional food strategy.

DEVELOPMENT AND CHARACTERIZATION OF A PLANT-BASED MEATBALL ALTERNATIVE

Delia-Gabriela Dumbrava[1], Isabel Guiamba[2], Camelia Moldovan[1*], Diana-Nicoleta Raba[3], Viorica-Mirela Popa[1], Corina-Dana Misca[1], Diana-Veronica Radu[1]

[1]Faculty of Agrofood Processing Technology, University of Life Sciences "King Mihai I" from Timişoara, Calea Aradului 119A, 300645, Romania
[2]Faculty of Engineering, Eduardo Mondlane University, Av. De Mozambique km 1,5 – C.P. 257, Maputo, Mozambique
[3]Faculty of Management and Rural Tourism, University of Life Sciences "King Mihai I" from Timişoara, Calea Aradului 119A, 300645, Romania
e-mail: cameliamoldovan@usvt.ro

This study aimed to develop and comprehensively characterize a novel plant-based meatball formulation as a nutritious and sensory-appealing alternative to conventional meat products, using tofu and textured soy protein as primary matrix components. The vegan meatballs (VMB) were prepared by blending tofu, textured soy protein, grated carrot, onion, garlic, breadcrumbs, olive oil, and a selected blend of spices, followed by convection thermal processing in an air fryer at 190 °C for 20 minutes. Analytical evaluations included total polyphenol content (TPC) determination via the Folin–Ciocalteu assay, antioxidant capacity assessment using the DPPH radical scavenging assay, proximate profile and caloric value determination, and sensory evaluation using a 5-point hedonic scale with 20 assessors. The final product exhibited a TPC of 23.68 ± 0.25 mg GAE/100 g and a high radical scavenging activity (RSA) of 78.34 ± 0.21%, reflecting significant retention of bioactive compounds post-thermal treatment. Proximate analysis revealed a balanced nutritional profile containing 18.39 g/100 g protein, 13.84 g/100 g total carbohydrates, 10.44 g/100 g total lipids, and 3.84 g/100 g dietary fiber, corresponding to an energy yield of 223 kcal/100 g (caloric distribution: 42% lipids, 33% proteins, and 25% carbohydrates). Among the raw ingredients, mustard extract exhibited the highest phenolic concentration (55.46 ± 0.38 mg GAE/100 g), followed by carrot (33.22 ± 0.28 mg GAE/100 g) and tofu (25.36 ± 0.24 mg GAE/100 g). Sensory profiling demonstrated outstanding consumer acceptability, with scores exceeding 4.50 across all parameters, led by taste (4.65), followed by odor, aroma, and overall acceptability (4.60 each), as well as appearance and texture (4.50 each). Overall, these findings confirm that the formulated vegan meatballs represent a viable, high-protein, and antioxidant-rich plant-based alternative to traditional meat products with excellent sensory properties.

DEVELOPMENT OF Tb^{3+}-DOPED $Zn_3Nb_2O_8$ NANOMATERIALS WITH LUMINESCENT PROPERTIES

Mina Morariu, Mircea Nicolaescu, Carmen Lazau, Corina Orha, Cornelia Bandas, Mihaela Gherban*

National Institute for Research and Development in Electrochemistry and Condensed Matter Timisoara, Dr. A.P. Podeanu no.144, 300569, Timisoara Romania, email: mina.popescu37@gmail.com, mihaela.birdeanu@gmail.com
**Corresponding author: mihaelabirdeanu@gmail.com*

Abstract

The objective of this study is to conduct preliminary experiments, develop laboratory procedures, and obtain $Zn_3Nb_2O_8$ oxide nanomaterials doped with different concentrations of Tb^{3+} ions (0.01–1 mol%) using solid-state synthesis and hydrothermal synthesis methods. The obtained oxide nanomaterials will be subjected to comprehensive structural and optical characterization.

Introduction

In biomedicine, Tb^{3+} ions are used in imaging, biosensors, and immunoassays. Their distinctive properties include long luminescence lifetimes (ranging from microseconds to milliseconds), which enable time-resolved detection and reduce interference from autofluorescence. Organic terbium complexes are frequently employed in time-resolved fluorescence bioassays. Doped nanoparticles enable targeted delivery and selective detection [1-2]. Tb^{3+}-based optical sensors exploit the dependence of luminescence on temperature, pressure, or the composition of the surrounding environment. The intensity ratio between emission bands or variations in luminescence lifetime can be used for optical thermometry. This approach is relevant to both nanotechnology and biological applications [3-4].

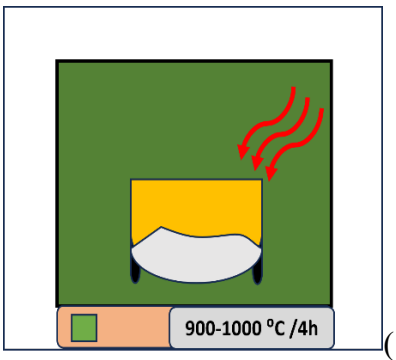
Experimental

Synthesis Methods - The synthesis method is a critical factor in obtaining high-performance luminescent materials, as it influences the crystal structure, particle size, dopant distribution, and structural defects. In the case of materials doped with rare-earth ions, controlling the morphology and ionic distribution is essential for optimizing luminescence efficiency and energy transfer. According to recent literature published in journals of the American Chemical Society and the Royal Society of Chemistry, modern synthesis methods are focused on obtaining nanostructures and materials with tunable optical properties.

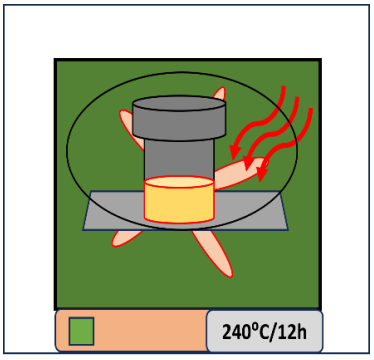
The solid-state reaction method (figure 1.) is one of the most widely used methods for the synthesis of inorganic phosphors. It involves mixing solid precursors (oxides, carbonates, or nitrates), followed by thermal treatment at high temperatures.
Advantages: high reproducibility; high crystalline purity; industrial scalability.
Disadvantages: high processing temperatures; limited control over particle size.
Solid-state synthesis was performed in a SNOL calcination furnace at a temperature of 900°C 1000°C or 1100°C for 4 hours, with heating and cooling rates of 5°C/min.

Hydrothermal method (figure 2.) involves solution-based reactions at high temperatures and pressures in an autoclave. The resulting materials are frequently used in bioimaging.
Advantages: morphological control, good crystallinity, moderate temperatures. Important parameters: pH, temperature, reaction time.

All samples were obtained by the hydrothermal method at a temperature of 240 °C for 12 h, with a filling degree of 80%. $Zn_3Nb_2O_8$ is a ternary oxide with a well-defined crystalline structure, which may be orthorhombic or monoclinic, depending on the synthesis conditions. Within the crystal lattice, Zn^{2+} and Nb^{5+} ions occupy distinct sites coordinated by oxygen atoms. The incorporation of Tb^{3+} ions into this matrix induces local structural modifications due to differences in ionic radius and charge.



(1)



(2)

Figure 1. The process of obtaining materials via the solid-state method and Figure 2. The hydrothermal synthesis process

The following precursors were used to obtain nanomaterials via hydrothermal and solid-state synthesis:

Sample	Precusor 1	Precusor 2	Precusor 3	Molar ratio
1a	Nb_2O_5	$Zn(NO_3)_2x4H_2O$	Tb_2O_3	1:3:0.02
1b	Nb_2O_5	$Zn(NO_3)_2x4H_2O$	Tb_2O_3	1:3:0.05
2a	Nb_2O_5	$Zn(CH_3COO)_2x2H_2O$	Tb_2O_3	1:3:0.02
2b	Nb_2O_5	$Zn(CH_3COO)_2x2H_2O$	Tb_2O_3	1:3:0.05
3a	Nb_2O_5	ZnO	Tb_2O_3	1:3:0.02
3b	Nb_2O_5	ZnO	Tb_2O_3	1:3:0.05
4a	Nb_2O_5	$Zn(NO_3)_2x4H_2O$	$TbCl_3$	1:3:0.02
4b	Nb_2O_5	$Zn(NO_3)_2x4H_2O$	$TbCl_3$	1:3:0.05
5a	Nb_2O_5	$Zn(CH_3COO)_2x2H_2O$	$TbCl_3$	1:3:0.02
5b	Nb_2O_5	$Zn(CH_3COO)_2x2H_2O$	$TbCl_3$	1:3:0.05
6a	Nb_2O_5	ZnO	$TbCl_3$	1:3:0.02
6b	Nb_2O_5	ZnO	$TbCl_3$	1:3:0.05
7a	Nb_2O_5	$Zn(NO_3)_2x4H_2O$	$Tb(NO_3)_3$	1:3:0.02
7b	Nb_2O_5	$Zn(NO_3)_2x4H_2O$	$Tb(NO_3)_3$	1:3:0.05
8a	Nb_2O_5	$Zn(CH_3COO)_2x2H_2O$	$Tb(NO_3)_3$	1:3:0.02
8b	Nb_2O_5	$Zn(CH_3COO)_2x2H_2O$	$Tb(NO_3)_3$	1:3:0.05
9a	Nb_2O_5	ZnO	$Tb(NO_3)_3$	1:3:0.02
9b	Nb_2O_5	ZnO	$Tb(NO_3)_3$	1:3:0.05

Table 1. Precursors used for solid-state and hydrothermal synthesis.

Results and discussion

The Tb^{3+} ion has an ionic radius larger than that of Zn^{2+} and different from that of Nb^{5+}, which results in: lattice strain, structural distortions, changes in lattice parameters.
$Zn_3Nb_2O_8$ is a complex ternary oxide in which: Zn^{2+} occupies tetrahedral or octahedral sites; Nb^{5+} is octahedrally coordinated by oxygen, there is a stable three-dimensional lattice, the structure is stabilized by networks of ZnO_4/ZnO_6 and NbO_6 polyhedra, mixed coordination exists. The Tb^{3+} ion can occupy: substitutional sites and interstitial sites.

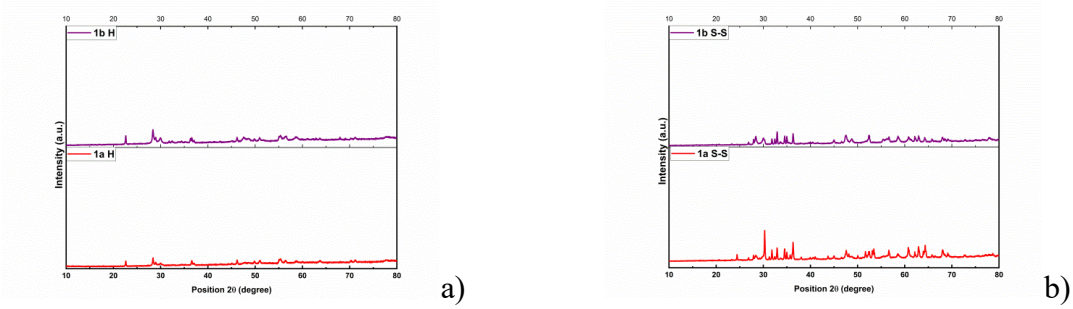


Figure 3. X-ray diffraction patterns of Tb^{3+}-doped $Zn_3Nb_2O_8$ materials (Zn:Nb:Tb molar ratios of 1:3:0.02 and 1:3:0.05) prepared by the hydrothermal method, corresponding to Figure 3 (a) and prepared by solid-state method corresponding to Figure 3 (b)

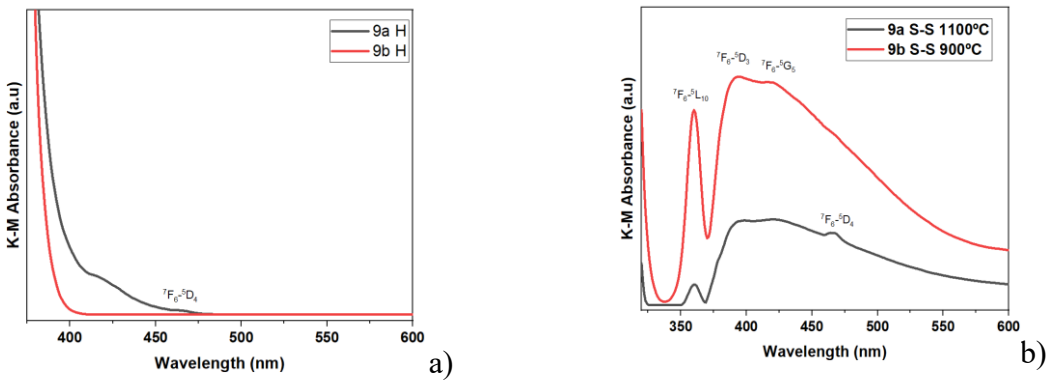


Figure 4. show the absorption spectra Tb^{3+}-doped $Zn_3Nb_2O_8$ compounds prepared via the hydrothermal method (a) and by solid-state method (b)

Absorbance spectra were derived from diffuse reflectance spectra using the Kubelka–Munk equations. The spectra were recorded in the 300–600 nm range at room temperature. In accordance with the Dieke energy level diagram and literature data [5–6], the observed absorption band is attributed to f–f electronic transitions of Tb^{3+} ions from the $^7F_6$ ground state term to various excited states.

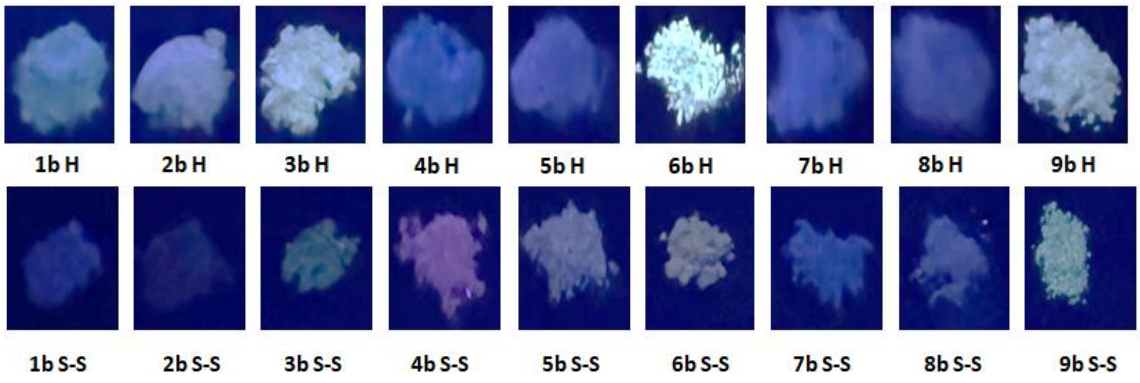


Figure 5. The images were recorded under UV irradiation at a wavelength of 366 nm for Tb^{3+}doped $Zn_3Nb_2O_8$.

The emission spectra of $Zn_3Nb_2O_8$ demonstrated that it is an intrinsic blue-light emitter. However, in the case of $Zn_3Nb_2O_8$:0.2 Tb^{3+}, an intense emission in the green region is produced

due to the $^5D_4 \rightarrow {}^7F_5$ transition, which is strongly influenced by the coordination environment of the Tb^{3+} ions.

As the concentration of Tb^{3+} dopant ions increases, the intensity of the transition from the excited level to the ground state also increases; consequently, the fluorescence intensity increases due to spontaneous radiative transitions.

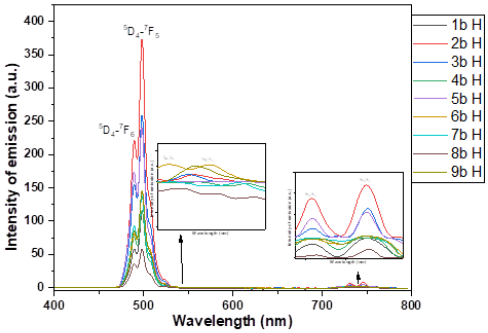


Figure 6. Room-temperature photoluminescence (PL) excitation spectra of Tb^{3+}-doped $Zn_3Nb_2O_8$ nanomaterials

Excitation occurs via UV absorption in the host matrix, followed by non-radiative transfer to the 4f levels of Tb^{3+}. The dominant emission corresponds to the $^5D_4 \rightarrow {}^7F_5$ transition (~542 nm). The absorption coefficient is correlated with the density of states and the interband transition probability.

Conclusion

The $^5D_4 \rightarrow {}^7F_5$ transition is the most intense and produces the characteristic green emission of Tb^{3+}-doped materials. Although the positions of the spectral lines remain relatively constant, the host matrix influences: the emission intensity, the lifetime of the excited state, the quantum efficiency, the broadening of the spectral bands, the energy-transfer processes. In the $Zn_3Nb_2O_8$ matrix, Tb^{3+} ions occupy crystallographic sites that favor emission originating from the $^5D_4$ level. The advantages of this host matrix include: a wide band gap, low phonon energy, high thermal stability, high luminescence efficiency, reduced non-radiative losses.

Acknowledgements

This research was funded by a grant from the Ministry of Research, Innovation and Digitization, project number PN 23 27 01 02 INOMAT, 23-27 29N/2023.

References

[1] S.G. Jamdade, P.S. Tambade, S.M. Rathod, Chem. Inorg. Mater. 1 (2023) 100020.
[2] A.M. Lakshmi, K. Kumari, P.V. Rao, N. Madaboosi, M. Özcan, P.S. Prasad, Ceram. Int. 51 (2025) 21501–21511.
[3] D.P. Aarti, R.B. Basavaraj, J.C. Abbar, M.B. Madhusudana Reddy, P.K. Jisha, J. Ind. Eng. Chem. 149 (2025) 645–656.
[4] L. Yi, R. Fu, F. Zhang, Z. Wei, M. Zhang, Ceram. Int. 50 (2024) 31976–31984.

[5] Z.X. Cheng, S. Zhang, F. Song, H.C. Guo, J.R. Han, H.C. Chen, J. Phys. Chem. Solids 63 (2002) 2011.
[6] W.T. Carnall, P.R. Fields, K. Rajnak, J. Chem. Phys. 49 (1968) 4424.

SILVER-BASED FUNCTIONALIZATION OF CELLULOSE-DERIVED CARBON AEROGELS FOR BIOFILM INHIBITION

Cristina Mosoarca, Radu Banica, Florina Stefania Rus, Mirela Iorga, Alexandra Bucur, George Dima, Bogdan-Ovidiu Taranu

National Institute of Research and Development for Electrochemistry and Condensed Matter, Str. Dr. A. Paunescu Podeanu No.144, 300569 Timisoara, Romania

The development of porous carbon-based materials with tailored antibacterial properties is of increasing interest for applications involving water purification and biofilm control. In this work, cellulose-derived carbon aerogels containing $CaCO_3$ were developed through a combined freeze-drying, thermal carbonization, and hydrothermal processing route, followed by silver-based functionalization. Cellulose fiber suspensions containing $CaCl_2$ and agarose were freeze-dried and thermally treated at 300 and 600 °C under an inert argon atmosphere. Subsequent hydrothermal treatment at 180 °C under pressurized CO_2/NH_3 conditions promoted the formation of a porous carbonaceous matrix containing partially or fully carbonized cellulose fibers and $CaCO_3$ (calcite), predominantly generated through gas–solid reactions.

The resulting materials were comprehensively characterized by X-ray diffraction, scanning electron microscopy coupled with energy-dispersive X-ray spectroscopy, thermogravimetric/differential thermal analysis, Fourier-transform infrared spectroscopy, and UV–VIS–NIR diffuse reflectance spectroscopy. To enhance their antibacterial functionality, selected aerogels were modified through ionic exchange with $AgNO_3$, resulting in the formation of Ag, AgCl, and Ag_2CO_3 surface phases. The estimated crystallite sizes were 9–11 nm for Ag and 46–230 nm for AgCl, as determined using the Debye–Scherrer equation.

The antibacterial performance of the pristine and silver-functionalized aerogels was assessed against Pseudomonas aeruginosa ATCC 27853 biofilms over five days. The Ag/AgCl-functionalized aerogels exhibited a strong antibacterial effect, resulting in a bacterial reduction exceeding 5 log, while the unmodified aerogels supported biofilm development and showed a log reduction of 2.477. These results demonstrate that silver-based surface functionalization can substantially enhance the antibacterial performance of cellulose-derived carbon aerogels. The combination of a highly porous carbonaceous architecture, $CaCO_3$ incorporation, and Ag-based functional phases provides a versatile platform for the development of multifunctional materials with potential applications in antibacterial water-treatment systems. The restricted optical accessibility of AgCl within the opaque porous structure may additionally influence its photoreduction and the subsequent availability of Ag^+ species, providing a possible mechanism for the observed antibacterial behavior and its evolution over time.

Acknowledgment

This work was supported by a project financed by the Ministry of Research, Innovation and Digitization through PN 19 22 01 03 - Innovative technologies for the development of integrated devices for the generation and storage of electrical energy.

ANTIBACTERIAN ACTIVITY OF A CHITOSAN-ALDEHYDE-ZINC SYSTEM IN LACTIC ACID SOLUTION

Ileana Nichita[1*], Aurelia Visa[2], Milica Tara-Lunga Mihali[2], Adriana Popa[2*], Andrei Ivan[1], Morariu Florica[3], Obistioiu Diana[4]

[1] *Faculty of Veterinary Medicine, University of Life Science "King Mihai I", 119 Calea Aradului, 300465 Timisoara, Romania*
[2] *"Coriolan Drăgulescu" Institute of Chemistry, 24 Mihai Viteazul Blvd., 300223, Timisoara, Romania*
[3] *Faculty of Bioengineering of Animal Resources, University of Life Science "King Mihai I", 119 Calea Aradului, 300465 Timisoara, Romania*
[4] *Faculty of Agriculture, University of Life Science "King Mihai I", 119 Calea Aradului, 300465 Timisoara, Romania*
[*] *coresponding e-mail:* nichita_ileana@yahoo.com; apopa_ro@yahoo.com

Abstract
Chit-BS-Zn system was prepared through a mechanochemical approach, obtaining a stable chitosan-based metal complex, which can be easily dissolved in lactic acid to form a homogeneous 1% (w/v) solution, the tested material showing promising antibacterial activity.

Introduction

Green chemistry is a modern approach aimed at developing sustainable chemical processes and products that reduce risks to the environment and human health by minimizing waste and eliminating hazardous substances [1,2]. In this context, mechanochemistry has become an efficient and environmentally friendly alternative for chemical synthesis, being particularly appreciated for its solvent-free processes, which significantly contribute to reducing environmental impact [3]. Chitosan (CS) is a non-toxic natural biopolymer, rich in free amino groups, which gives it high versatility and makes it useful in applications such as wastewater treatment, metal ion adsorption or the food and cosmetic industry [4-6]. Due to these functional groups, chitosan can form Schiff bases (Chit-BS) and stable metal complexes, being an important ligand in coordination chemistry [7].
We synthesized a Chit-BS-Zn system by a mechanochemical method, then we dissolved the product in lactic acid to obtain a 1% (m/v) homogeneous solution, the material showing promising antibacterial activity against *Escherichia coli*.

Experimental

We prepared Chit-BS-Zn system using a 1:1 molar ratio between $Zn(AcO)_2 \cdot 2H_2O$ and chitosan-aldehyde (Chit-BS), by grinding in a ball mill (25 Hz, 90 min), followed by washing with ethanol, filtration and drying in an oven at 50 °C for 24 h, and subsequently we dissolved 0.5 g of the product in 2% lactic acid, under continuous stirring at room temperature, to a final volume of 50 mL, obtaining a 1% (m/v) solution.
The antibacterial testing aimed to evaluate the effect of Chit-BS and Chit-BS-Zn solutions by measuring the inhibition zones (mm). The experiments were performed using catalog bacterial strains, including two Gram-negative species (*Pseudomonas aeruginosa* – ATCC 15692 and *Escherichia coli* – ATCC 25922) and two Gram-positive species (*Staphylococcus aureus* – ATCC 25923 and *Bacillus cereus* – ATCC 10878).

Results and discussion

Figure 1 shows the FTIR and TG analyses of the Chit BS-Zn sample.

Figure 2 illustrates the optical image corresponding to the same sample.

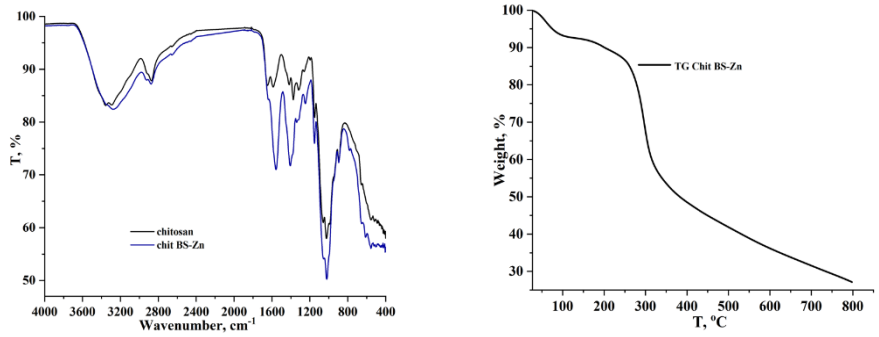


Figure 1. FTIR and TG for Chit BS-Zn sample.

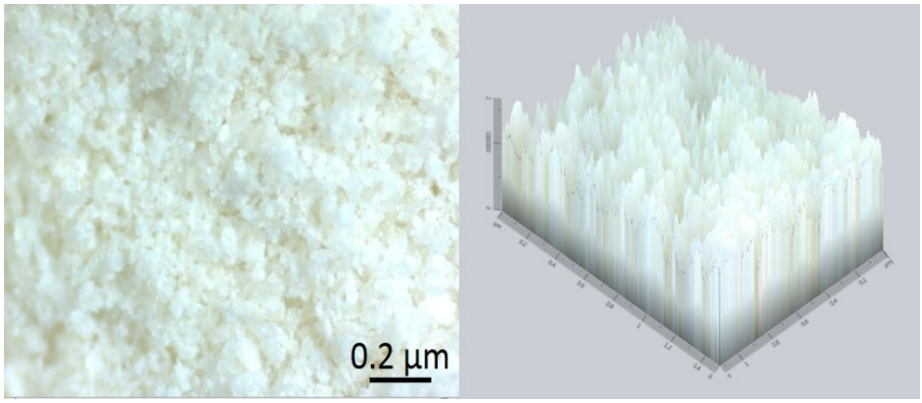


Figure 2. Optical Image for Chit BS-Zn sample.

Figure 1 highlights the structural characteristics and thermal stability of the Chit BS-Zn sample, while Figure 2 confirms its morphological appearance, together supporting the formation of the material.

The results of the antibacterial testing (see Table 1) revealed that both Chit-BS and the complexed system Chit-BS-Zn exhibit antimicrobial activity. However, it is observed that the inclusion of Zn^{2+} ions led to a slight increase in the inhibition zones. This effect can be attributed to the synergistic action between the chitosan-aldehyde matrix, known for its electrostatic interactions with bacterial membranes, and zinc ions, which can disrupt enzymatic processes and cellular integrity.

The percentage of inhibition is calculated with eq (1), such the interpretation becomes clearer and comparable between samples.

$$P_{\text{inhibition}}(\%) = \frac{Z_{\text{sample}}}{Z_{\text{antibiotic}}} \times 100$$

The percentage of inhibition ($P_{\text{inhibitie,}}$ %) can be determined by relating the diameter of the inhibition zone (Z_{samle} respective $Z_{\text{antibiotic}}$) of the sample (Chit-BS or Chit-BS-Zn) to a reference antibiotic (Gentamicin) (see Table 1).

Table 1. Inhibition zones (IZ, mm) and the percentage of bacterial inhibition ($P_{inhibitie}$, %) of the tested samples, compared to the antibiotic.

strains bacteria	antibiotic	Chit-BS		Chit-BS-Zn	
Bacillus cereus (ATCC 10878)	Gentamicin 22 mm	IZ	8 mm	IZ	10 mm
		$P_{inhibitie}$ (%)	36.36 %	$P_{inhibitie}$ (%)	45.45 %
Escherichia coli (ATCC 25922)	Gentamicin 18 mm	IZ	15 mm	IZ	17 mm
		$P_{inhibitie}$ (%)	83.33 %	$P_{inhibitie}$ (%)	94.44 %
Staphyloccocus aureus (ATCC 25923)	Gentamicin 22 mm	IZ	12 mm	IZ	13 mm
		$P_{inhibitie}$ (%)	26.40 %	$P_{inhibitie}$ (%)	59.09 %
Pseudomonas aeruginosa (ATCC 15692)	Gentamicin 26 mm	IZ	8 mm	IZ	8 mm
		$P_{inhibitie}$ (%)	30.76 %	$P_{inhibitie}$ (%)	30.76 %

Based on this calculation, the Chit-BS-Zn system will show slightly higher inhibition percentages than Chit-BS, confirming the increased efficiency due to Zn^{2+} ions. The material showing more pronounced antibacterial activity against *E. coli* compared to the other tested strains (Figure 3).

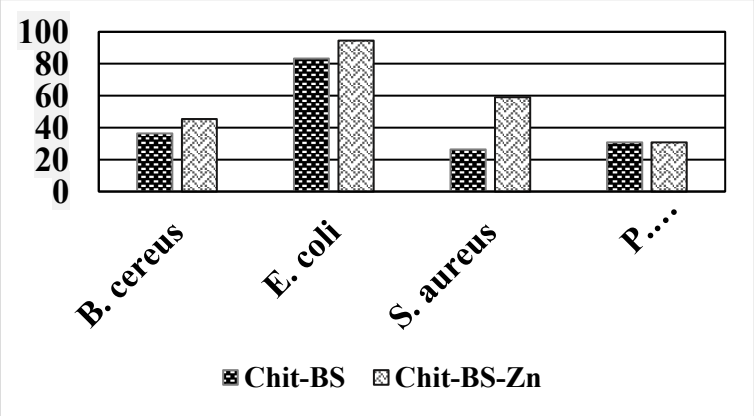


Figure 3. Percentage of microbial inhibition ($P_{inhibitie}$, %) of the tested samples vs strains bacteria, compared to the antibiotic.

Conclusion

The Chit-BS-Zn system obtained by mechanochemical method exhibits antibacterial activity, highlighting a more pronounced effect on *E. coli*, which suggests a potential for use in various applications.

References

[1] A.R. Sheldon, RSC 16 (2014) 950.
[2] M. Tobiszewski, M. Marc, A. Gałuszka, J. Namiesnik, Molecules 20 (2015) 10928.
[3] D. Hasa, W. Jones, Adv. Drug Deliv. Rev. 117 (2017) 147.
[4] P. Mukoma, B. R. Jooste, H.C.M. Vosloo, J. Power Sources 136 (2004) 16.
[5] M.F. Cervera, J. Heinamaki, M. Rasanen, S.L. Maunu, M. Karjalainen, O.M.N. Acosta, A.I. Colarte; Yliruusi, J. Carbohydr. Polym. 58 (2004) 401.
[6] P. Miretzky, F.A.Cirelli, J. Hazard. Mater. 167 (2009) 10.
[7] C. Verma, M.A. Quraishi, A. Alfantazi, K. Yop Rhee, Int. J. Biol. Macromol. 184 (2021) 135.

SOIL RESOURCE MANAGEMENT AND AGRICULTURAL LAND QUALITY IN DOMAȘNEA, CARAȘ-SEVERIN COUNTY

Okros Adalbert[1], Casiana Mihuț[1], Anișoara Duma-Copcea[1], Antoanela Cozma[1], Blenesi Attila[2], Stroia Marius[2], Popa Daniel[2], Daniela Scedei[3]

[1] Department of Soil Sciences, Faculty of Agriculture, "King Mihai I" University of Life Sciences of Timișoara, Calea Aradului nr. 119, 300645 Timișoara, Timiș county, Romania
[2] Department of Agricultural Technologies, Faculty of Agriculture, "King Mihai I" University of Life Sciences of Timișoara, Calea Aradului nr. 119, 300645 Timișoara, Timiș county, Romania
[3] Department of Horticulture, Faculty of Engineering and Applied Technologies, "King Mihai I" University of Life Sciences of Timișoara, Calea Aradului nr. 119, 300645 Timișoara, Timiș county, Romania
Email: casiana_mihut@usvt.ro

Abstract

Soil-resource management in hilly and submontane areas must account for the combined effects of soil properties, relief and water regime. This paper analyzes agricultural land use, soil cover, land-quality classes and the main limiting factors in Domașnea commune, Caraș-Severin County, south-western Romania, using data synthesized from the local pedological documentation. The investigated territory covers 4,317.45 ha, all included in agricultural use. Hayfields (1,569.38 ha; 36.35%) and pastures (1,499.85 ha; 34.74%) dominate the land-use structure, while orchards account for 825.67 ha (19.13%) and arable land for only 422.45 ha (9.78%). Luvisols are the dominant soil group, occupying 1,934.80 ha (44.81%), followed by soil associations (27.91%) and Eutricambosols (20.41%). Land evaluation confirms the suitability of permanent grasslands: pastures and hayfields are included on average in quality class II, whereas arable land is in class IV and orchards in class III. The most important restrictions are land unevenness, slope, erosion, low or moderate humus reserve, acidity, compaction and excess moisture on slopes. The results support a differentiated management strategy based on permanent vegetation on steep land, anti-erosion measures, maintenance of organic matter, localized liming, reduced traffic and drainage interventions adapted to local terrain conditions.

Introduction

Soil is a multifunctional natural resource whose agricultural value depends on the interaction between pedological properties, relief, climate, water regime and land use Pedological mapping and land evaluation therefore provide the basis for choosing appropriate land uses and for adapting cultivation technologies to site-specific constraints [1,6,8,11]. Romanian soil assessment combines national pedological methodologies and the Romanian System of Soil Taxonomy with internationally recognized approaches to soil description and classification. The FAO Guidelines for Soil Description, the World Reference Base for Soil Resources and the USDA Soil Survey Manual provide complementary concepts for interpreting morphology, texture, drainage and diagnostic horizons [3,12,13,15]. In south-western Romania, soil diversity is strongly controlled by parent material, relief and hydrological conditions, producing mosaics of cambic, luvisolic, alluvial and young eroded soils [2,5,7].Domașnea commune is located in Caraș-Severin County, within the Domașnea-Mehadia depression of the Timiș-Cerna intramontane corridor. The territory includes depression surfaces and dissected slopes with variable gradients. This geomorphological setting explains the limited extent of arable land and the predominance of hayfields, pastures and orchards. The local pedological study at 1:10,000

scale is the main documentary basis for evaluating soil distribution, quality classes and restrictive factors [10].The objective of this paper is to synthesize the main characteristics of the soil resources of Domașnea, quantify the principal limitations affecting agricultural suitability and formulate management directions compatible with the submontane character of the territory. Particular attention is given to the relation between land use, Luvisol dominance, slope-related degradation and the management of organic matter and water.

Experimental

The analysis is based on the numerical and descriptive information contained in the supporting chapter on soil-resource management in Domașnea and on the local pedological and agrochemical study cited in the bibliography [10]. No new field measurements were performed for this synthesis. The principal indicators were: area and share of agricultural land-use categories; distribution of soil types and soil associations; allocation of land uses to quality classes I-V; and the extent of limitations caused by acidity, humus reserve, texture, compaction, reduced effective soil volume, slope, erosion, landslides, land unevenness, excess moisture and climatic conditions. The interpretation was supported by Romanian and international works on pedology, land evaluation, soil physics and agrochemistry [3,4,6,8,11-15].The working method was descriptive and comparative.

Results and discussions

Reported percentages were retained from the source document, and each limitation was interpreted in terms of its agronomic significance and practical management implications. A representative stagnic Luvisol unit was also analyzed to illustrate how physical, chemical, hydrological and geomorphological restrictions interact at profile scale.

Land-use structure

Table 1. Distribution of agricultural land uses - Domașnea

Land use	Area (ha)	Share (%)
Arable land	422.45	9.78
Pastures	1,499.85	34.74
Hayfields	1,569.38	36.35
Vineyards	0.10	0.00
Orchards	825.67	19.13

Soil cover and land quality

Table 2. Principal soil types and soil associations identified in Domașnea

Soil type / complex	Symbol	Area (ha)	Share (%)
Regosols	RS	101.50	2.35
Aluviosols	AS	48.40	1.12
Eutricambosols	EC	881.00	20.41
Districambosols	DC	91.60	2.12
Preluvosols	EL	55.30	1.28
Luvisols	LV	1,934.80	44.81
Soil associations	-	1,204.85	27.91

Table 3. Agricultural land by quality class

Use	Area	Class I	Class II	Class III	Class IV	Class V	Mean score / class
Arable	422.45	0.00	0.00	204.15	179.05	39.25	36 / IV
Pastures	1,499.85	469.15	778.77	120.10	131.83	0.00	70 / II
Hayfields	1,569.38	8.85	1,168.61	300.10	86.57	5.25	64 / II
Vineyards	0.10	0.00	0.00	0.00	0.00	0.10	18 / V
Orchards	825.67	0.00	23.60	514.14	132.53	155.40	41 / III

Main limiting factors

Table 4. Limitations associated with soil acidity

Intensity	Area (ha)	Share of total (%)
Very severe	330.20	7.65
Moderate	357.10	8.27
Low	1,590.30	36.83

Table 5. Limitations associated with humus reserve

Intensity	Area (ha)	Share of total (%)
Severe	199.70	4.63
Moderate	2,959.75	68.55
Low	1,005.75	23.30

Table 6. Limitations associated with compaction and reduced effective soil volume

Factor / intensity	Area (ha)	Share (%)
Compaction - severe	54.20	1.25
Compaction - moderate	1,710.95	39.63
Reduced soil volume - very severe	235.20	5.45
Reduced soil volume - low	17.00	0.39

Table 7. Geomorphological limiting factors

Limiting factor	Affected area (ha)	Share (%)
Slope	3,270.75	75.76
Sheet erosion	1,058.70	24.52
Gully/deep erosion	490.65	11.36
Landslides	490.65	11.36
Rocks and boulders	383.60	8.88
Land unevenness	4,317.45	100.00

Table 8. Limitations associated with excess moisture

Type and intensity	Area (ha)	Share (%)
Groundwater excess - severe	8.00	0.19
Stagnant excess - low	200.90	4.65
Slope water excess - severe	717.45	16.62
Slope water excess - moderate	644.25	14.92
Slope water excess - low	795.35	18.42

Table 9. Climatic limitations

Climatic factor	Area (ha)	Share (%)
Temperature - moderate	199.70	4.63
Temperature - low	4,029.40	93.33
Moisture deficit - moderate	6.75	0.16
Moisture deficit - low	216.70	5.02

Representative soil unit

A representative unit was selected from the dominant Luvisols: soil unit US 32, a stagnic Luvisol, strongly stagnogleyed, developed on medium non-calcareous slope weathering materials and affected by slight water erosion. The unit covers 253.60 ha, representing 5.87% of the investigated territory. It occurs on uneven hills and slopes with gradients ranging from 5.1-10% to 35.1-50%, predominantly with north-western exposure; groundwater is deeper than 10 m. The representative profile has an Ap-Bt-Btw-B/C-C sequence. Texture is medium loam through the profile; total porosity is very high at 6-30 cm and medium between 30 and 82 cm. Soil reaction is moderately acid from 6 to 30 cm and slightly acid from 30 to 113 cm. The humus reserve in the upper 50 cm is moderate, whereas the nitrogen index is low between 6 and 55 cm. The reported limitation code O5 Z5 R5 F4 U4 W4 L4 A2 G2 P2 E2 indicates a combination of very severe and severe geomorphological, stoniness/trafficability, erosion and water-related restrictions. The unit illustrates why permanent land uses, anti-erosion measures, surface drainage and localized liming must be integrated with fertility management rather than applied independently.

Conclusions

The soil-resource assessment of Domașnea reveals an agricultural territory whose use is strongly controlled by relief and slope-related processes. The entire 4,317.45 ha investigated area is agricultural, but hayfields and pastures account for more than 71%, while arable land represents only 9.78%. This land-use structure is well adapted to submontane conditions and should be regarded as an important component of soil conservation rather than as a limitation of agricultural development.

Pedologically, Luvisols are dominant, occupying 44.81% of the territory, while soil associations account for 27.91% and Eutricambosols for 20.41%. The large share of soil associations demonstrates strong spatial heterogeneity. Land-quality assessment confirms that permanent grassland is the most suitable use: pastures and hayfields are in class II, orchards in class III, whereas arable land is in class IV. The main restrictions are geomorphological and physical. Land unevenness occurs across the entire analyzed territory, slope affects 75.76%, and important surfaces are exposed to erosion and landslides. Compaction affects more than 1,765 ha at moderate or severe intensity, while reduced effective soil volume imposes very severe restrictions on 235.20 ha. These factors directly influence mechanization, rooting depth, runoff and long-term soil stability. Chemical and biological fertility also require attention. Soil acidity affects more than half of the territory, and limitations associated with humus reserve occur on 96.48% of the investigated area. Management should therefore combine periodic agrochemical monitoring, localized liming where justified, organic fertilization, residue incorporation, green-manure crops and diversified rotations. These measures are especially important where physical degradation and low organic-matter status interact.Sustainable land management in Domașnea should preserve permanent grasslands and orchards on sloping and erosion-prone land, restrict the expansion of intensive arable cultivation on class IV and V surfaces, maintain surface-drainage systems and apply anti-erosion works according to slope position.

The representative stagnic Luvisol confirms that productive potential depends on the simultaneous management of acidity, organic matter, water excess, erosion and terrain stability.

References

[1]. Dicu, D., Bertici, R. (2018). Cartarea și bonitarea solurilor/terenurilor - caiet de lucrări practice. Eurobit, Timișoara.
[2]. Țărău, D., Rogobete, Gh., Dicu, D.D., Grozav, A., Niță, L.D., Iliuță, A.Ș., Tudor, C.M., Bertici, R. (2019). Pământuri și locuri dintre Dunăre-Vârful Gugu-Crișul Negru. Eurobit, Timișoara.
[3]. Florea, N., Munteanu, I. (2012). Sistemul Român de Taxonomie a Solurilor (SRTS-2012). Sitech, București.
[4]. Mihuț, C., Radulov, I. (2012). Științele Solului. Eurobit, Timișoara.
[5]. Țărău, D., Rogobete, Gh., Grozav, A., Dicu, D.D. (2018). Solurile din Sud-Vestul României. Eurobit, Timișoara.
[6]. Țărău, D. (2009). Bonitarea și evaluarea terenurilor cu elemente de fundamentare pedologică. Agroprint, Timișoara.
[7]. Țărău, D., Rogobete, Gh., Dicu, D. (2016). Solurile din vestul României. Caracterizare, evaluare și măsuri de îmbunătățire. Eurobit, Timișoara.
[8]. Florea, N., Bălăceanu, V., Canarache, A. et al. (1987). Metodologia elaborării studiilor pedologice, Vol. I-III. ICPA, București.
[9]. Niță, L., Țărău, D., Rogobete, Gh., Niță, S., Bertici, R., Tuța Sas, I., Sas, I., Dicu, D. (2018). The Role of Ecopedological Parameters in Management Sustainability of Banat Lands. Revista de Chimie, 69(3).
[10]. O.S.P.A. Caraș-Severin. Studiu pedologic și agrochimic elaborat în vederea realizării/reactualizării sistemului național și județean de monitorizare sol-teren pentru agricultură, teritoriul comunei Domașnea, scara 1:10,000.
[11]. Brady, N.C., Weil, R.R. (2016). The Nature and Properties of Soils. Pearson Education.
[12]. FAO (2006). Guidelines for Soil Description. Fourth edition. Food and Agriculture Organization of the United Nations, Rome.
[13]. IUSS Working Group WRB (2022). World Reference Base for Soil Resources. International soil classification system for naming soils and creating legends for soil maps. 4th edition. International Union of Soil Sciences, Vienna.
[14]. Lăcătușu, R. (2000). Agrochimie. Helicon, Iași.
[15]. USDA-NRCS (2017). Soil Survey Manual. USDA Handbook 18, Washington, D.C.

SOIL RESOURCE MANAGEMENT AND AGRICULTURAL LAND QUALITY IN REMETEA MARE, TIMIȘ COUNTY

Okros Adalbert[1], Casiana Mihuț[1], Anișoara Duma-Copcea[1], Blenesi Attila[2], Popa Daniel[2], Moldovan Camelia[3], Petrescu Irina[4], Rotariu Lia Sanda[5]

[1] Department of Soil Sciences, Faculty of Agriculture, "King Mihai I" University of Life Sciences of Timișoara, Calea Aradului nr. 119, 300645 Timișoara, Timiș county, Romania
[2] Department of Agricultural Technologies, Faculty of Agriculture, "King Mihai I" University of Life Sciences of Timișoara, Calea Aradului nr. 119, 300645 Timișoara, Timiș county, Romania
[3] Department of Food Control and Expertise, Faculty of Food Engineering, "King Mihai I" University of Life Sciences of Timișoara, Calea Aradului nr. 119, 300645 Timișoara, Timiș county, Romania
[4] Department of Horticulture, Faculty of Engineering and Applied Technologies, "King Mihai I" University of Life Sciences of Timișoara, Calea Aradului nr. 119, 300645 Timișoara, Timiș county, Romania
[5] Department of Management and Rural Development Faculty of Management and Rural Tourism "King Mihai I" University of Life Sciences of Timișoara, Calea Aradului nr. 119, 300645 Timișoara, Timiș county, Romania
Email: casiana_mihut@usvt.ro

Abstract

Soil resources determine the productive potential, environmental resilience and long-term sustainability of agricultural territories. This study analyzes the structure, quality and main limiting factors of agricultural soils in Remetea Mare commune, Timiș County, western Romania, using data synthesized from the local pedological and agrochemical study and from the territorial assessment presented in the supporting documentation. The investigated territory covers 10,124.74 ha, of which 8,691.08 ha (85.84%) are agricultural land. Arable land dominates the agricultural area with 7,256.90 ha (83.50%), while pastures, hayfields and orchards have considerably smaller shares. Nine principal soil types and 127 subtypes were identified, with Preluvosols (35.55%), Eutricambosols (27.69%) and Pelosols (14.32%) occupying the largest surfaces. Land-quality assessment indicates a predominantly medium productive potential: arable land, pastures and hayfields are mainly included in quality class III, whereas orchards fall in class IV. The most extensive restriction is soil compaction, with moderate limitations on 5,675.60 ha; stagnant excess moisture, acidity, fine texture, flooding and localized salinization-alkalization also affect land suitability. The results show that sustainable soil management in Remetea Mare requires differentiated measures, including traffic control, selective loosening, maintenance of drainage, organic-matter conservation, periodic agrochemical monitoring and localized liming where acidity becomes restrictive.

Introduction

Soil is a strategic natural resource because it simultaneously supports agricultural production, nutrient cycling, water regulation and terrestrial ecosystem functions. The productive value of agricultural land is determined not only by soil type, but also by texture, reaction, organic-matter status, hydrological regime and the intensity of physical degradation processes. Consequently, pedological mapping and land evaluation provide the scientific basis for matching crop technologies with local soil conditions and for preventing losses of fertility caused by inappropriate management [1,6,8,11]. In Romania, soil characterization and agricultural land-quality assessment are traditionally based on national pedological methodologies and the Romanian System of Soil Taxonomy, while international frameworks

such as FAO soil-description guidance, the World Reference Base for Soil Resources and the USDA Soil Survey Manual offer complementary principles for describing, classifying and interpreting soil profiles [3,12,13,15]. In the western and south-western part of the country, the soil cover is highly heterogeneous as a result of the interaction between relief, parent material, groundwater conditions, drainage and long-term land use [2,5,7]. This heterogeneity requires territorial analyses that move beyond general productivity averages and identify spatially differentiated constraints. Remetea Mare commune is a representative agricultural territory located east of Timișoara. The studied area includes sectors of high plain and low plain, as well as landscape elements associated with the Bega-Timiș interfluve. The agricultural function is dominant, but local soil resources are affected by several limiting factors, particularly fine texture, compaction, temporary water excess and, on smaller surfaces, acidity, flooding and salinization-alkalization. The local pedological and agrochemical study at 1:10,000 scale constitutes the principal documentary source for evaluating these constraints [10]. The objective of the present paper is to synthesize the main characteristics of the land fund and soil cover of Remetea Mare, to evaluate the distribution of agricultural land by quality classes, to quantify the principal limiting factors and to formulate soil-management directions adapted to local conditions. The analysis therefore combines descriptive pedology with an applied interpretation of land suitability, with emphasis on those properties that can be improved or managed through agricultural and hydrotechnical measures.

Experimentals

The study is based on the pedological and agrochemical information included in the territorial documentation for Remetea Mare and on the numerical data synthesized in the results chapter of the supporting material [10]. For the purposes of this paper, the information was organized into four analytical groups: land-use structure, distribution of soil types, land-quality classes and limiting factors affecting agricultural suitability. No new field measurements were generated for this synthesis; the work consisted of documentary extraction, verification of totals and descriptive-comparative interpretation of the available data. The following indicators were used: total surface and share of the main land-use categories; surface and percentage occupied by each principal soil type; allocation of arable land, pastures, hayfields and orchards to quality classes I-V; and the surface affected by acidity, humus reserve, coarse or fine texture, compaction/tillage pan, stagnant excess moisture, flooding and salinization-alkalization. Soil-profile interpretation was supported by national and international reference works on soil description, taxonomy, physical properties, agrochemistry and land evaluation [3,8,11-15].The approach is primarily descriptive and comparative. Percentages were retained as reported in the source material, and the discussion emphasizes the agronomic significance of each limitation. Particular attention was paid to the representative Eutricambosol unit described in the documentation because it integrates several characteristic restrictions of the territory: fine texture, compaction, differentiated soil reaction and temporary excess moisture.

Results and discussions

Land-use structure

Table 1. Distribution of agricultural land uses - Remetea Mare

Land use	Area (ha)	Share (%)
Arable land	7,256.90	83.50
Pastures	1,221.17	14.05
Hayfields	198.63	2.29
Orchards	14.38	0.17

Table 2. Main land-use categories in the investigated territory

Category	Area (ha)	Share of total (%)
Agricultural land	8,691.08	85.84
Forests	906.51	8.95
Water surfaces	203.45	2.01
Unproductive land	39.33	0.39
Roads	147.05	1.45
Buildings	137.32	1.36

Soil cover and land quality

Table 3. Principal soil types identified in Remetea Mare

Soil type	Symbol	Area (ha)	Share (%)
Aluviosols	AS	370.10	4.26
Eutricambosols	EC	2,406.79	27.69
Preluvosols	EL	3,089.90	35.55
Luvosols	LV	360.44	4.15
Pelosols	PE	1,244.89	14.32
Vertosols	VS	454.27	5.23
Gleiosols	GS	372.83	4.29
Stagnosols	SG	346.42	3.99
Erodosols	ER	47.43	0.55

Table 4. Agricultural land by quality class

Use	Area	Class I	Class II	Class III	Class IV	Class V	Mean score / class
Arable	7,256.90	138.02	2,653.13	3,165.18	945.55	355.02	53 / III
Pastures	1,221.17	194.76	406.29	385.15	173.02	61.95	59 / III
Hayfields	198.63	6.11	69.34	54.90	62.33	5.95	51 / III
Orchards	14.38	0.13	1.09	5.40	1.13	6.63	36 / IV

Limiting factors of agricultural production

Table 5. Limitations associated with soil acidity

Intensity	Area (ha)
Low	2,568.56
Moderate	886.19
Severe	16.32

Table 6. Limitations associated with humus reserve

Intensity	Area (ha)
Low	3,427.49

Intensity	Area (ha)
Moderate	706.49
Severe	33.52

Table 7. Limitations associated with soil texture

Limitation	Area (ha)
Coarse texture - low	68.77
Fine texture - low	4,170.41
Fine texture - moderate	408.36

Table 8. Limitations associated with compaction and soil packing

Intensity	Area (ha)
Low	1,450.13
Moderate	5,675.60

Table 9. Hydrological and localized chemical limitations

Factor / intensity	Area (ha)
Stagnant excess moisture - moderate	1,699.54
Stagnant excess moisture - severe	703.13
Stagnant excess moisture - very severe	34.21
Flooding - very severe	312.52
Salinization-alkalization - moderate	55.69

Representative soil unit

A representative unit selected from the Eutricambosols is described as a stagnic Eutricambosol, weakly gleyed and moderately stagnogleyed, developed on medium non-calcareous fluvial materials. The unit covers 44.20 ha (0.51% of the analyzed territory), occurs in the low plain on a depressional landform and has groundwater at approximately 2.1-3.0 m. The profile sequence is Ap-Atpw2-ABw3-Bvw4-BC-Cg1-Cg2. Texture is medium clay loam throughout the 0-150 cm profile. Total porosity is very low and bulk density very high between approximately 12 and 80 cm, confirming an important physical restriction. Soil reaction is moderately acid in the upper 0-22 cm, slightly acid between 22 and 80 cm and slightly alkaline below 80 cm. The humus reserve in the first 50 cm is high, but this favorable property is counterbalanced by compaction and excess moisture.

Conclusions

The analysis of soil resources in Remetea Mare shows a territory with a pronounced agricultural function and a heterogeneous pedological foundation. Agricultural land covers 8,691.08 ha, or 85.84% of the investigated area, and arable land represents 83.50% of the agricultural surface. Nine major soil types and 127 subtypes were identified, with Preluvosols, Eutricambosols and Pelosols forming the dominant soil groups. This diversity confirms that agricultural technologies cannot be applied uniformly across the commune.The land-quality assessment indicates mainly medium productive potential. Arable land, pastures and hayfields are classified on average in class III, while orchards are in class IV.

The main causes of this moderate suitability are not a single limiting factor but the combined effects of fine texture, compaction, soil reaction and hydrological restrictions. Compaction is the most extensive problem, with moderate limitations on 5,675.60 ha, while stagnant excess moisture affects more than 2,400 ha at moderate to very severe intensity.The sustainable

management of these soils should therefore prioritize the prevention and correction of physical degradation. Machinery traffic should be reduced or organized, tillage should be avoided at high soil moisture, and selective loosening should be applied only where compact layers are present. Chemical and biological fertility must be managed in parallel. Areas with moderate and severe acidity should be periodically mapped agrochemically and limed where analytical data justify intervention. These measures can improve aggregate stability and water relations and can reduce the sensitivity of fine-textured soils to compaction.

References

[1]. Dicu, D., Bertici, R. (2018). Cartarea și bonitarea solurilor/terenurilor - caiet de lucrări practice. Eurobit, Timișoara.
[2]. Țărău, D., Rogobete, Gh., Dicu, D.D., Grozav, A., Niță, L.D., Iliuță, A.Ș., Tudor, C.M., Bertici, R. (2019). Pământuri și locuri dintre Dunăre-Vârful Gugu-Crișul Negru. Eurobit, Timișoara.
[3]. Florea, N., Munteanu, I. (2012). Sistemul Român de Taxonomie a Solurilor (SRTS-2012). Sitech, București.
[4]. Mihuț, C., Radulov, I. (2012). Științele Solului. Eurobit, Timișoara.
[5]. Țărău, D., Rogobete, Gh., Grozav, A., Dicu, D.D. (2018). Solurile din Sud-Vestul României. Eurobit, Timișoara.
[6]. Țărău, D. (2009). Bonitarea și evaluarea terenurilor cu elemente de fundamentare pedologică. Agroprint, Timișoara.
[7]. Țărău, D., Rogobete, Gh., Dicu, D. (2016). Solurile din vestul României. Caracterizare, evaluare și măsuri de îmbunătățire. Eurobit, Timișoara.
[8]. Florea, N., Bălăceanu, V., Canarache, A. et al. (1987). Metodologia elaborării studiilor pedologice, Vol. I-III. ICPA, București.
[9]. Niță, L., Țărău, D., Rogobete, Gh., Niță, S., Bertici, R., Tuța Sas, I., Sas, I., Dicu, D. (2018). The Role of Ecopedological Parameters in Management Sustainability of Banat Lands. Revista de Chimie, 69(3).
[10]. O.S.P.A. Timiș. Studiu pedologic și agrochimic elaborat în vederea realizării/reactualizării sistemului național și județean de monitorizare sol-teren pentru agricultură, teritoriul comunei Remetea Mare, scara 1:10,000.
[11]. Brady, N.C., Weil, R.R. (2016). The Nature and Properties of Soils. Pearson Education.
[12]. FAO (2006). Guidelines for Soil Description. Fourth edition. Food and Agriculture Organization of the United Nations, Rome.
[13]. IUSS Working Group WRB (2022). World Reference Base for Soil Resources. International soil classification system for naming soils and creating legends for soil maps. International Union of Soil Sciences, Vienna.
[14]. Lăcătușu, R. (2000). Agrochimie. Helicon, Iași.
[15]. USDA-NRCS (2017). Soil Survey Manual. USDA Handbook 18, Washington, D.C.

SHORT-TERM RESPIROMETRIC AND SURVIVAL RESPONSE OF *EISENIA FETIDA* TO A COMMERCIAL COMPOSTABLE BIOPLASTIC BAG IN OECD ARTIFICIAL SOIL

Marianna Oláh[1], Mária Mörtl[1], Miklós Gulyás[2], András Székács[1]

[1]Agro-Environmental Research Centre, Institute of Environmental Sciences, Hungarian University of Agriculture and Life Sciences, Páter Károly str. 1, H-2100 Gödöllő, Hungary
[2]Department of Soil Science, Institute of Environmental Sciences, Hungarian University of Agriculture and Life Sciences, Páter Károly str. 1, H-2100 Gödöllő, Hungary
e-mail: olah.marianna@uni-mate.hu

Compostable bioplastics are increasingly used as alternatives to conventional plastics, but less is known about their short-term effects on soil organisms. Polybutylene adipate terephthalate (PBAT) one of the most widely used compostable polymer, and its degradation rate depends on environmental conditions and biological activity [1-3]

Earthworms such as *Eisenia fetida* are important soil organisms and bioindicators, while soil respiration provides an indirect measure of microbial activity. Under Regulation (EU) 2019/1009, Annex II, Part II, CMC 9 [4], as amended by Commission Delegated Regulation (EU) 2024/2787, certain polymers used in EU fertilising products are required to pass an earthworm acute toxicity test. This study investigated the effects of a commercial PBAT-based compostable bag on soil respiration and *E. fetida* under standardized conditions [5]. Earthworm survival, body mass and burrowing activity were assessed at the end of the incubation period.

Oxygen consumption increased in the presence of earthworms and/or bioplastic relative to the soil-only control, with the highest respiration observed in the combined earthworm–bioplastic treatment. Earthworms exposed to bioplastic exhibited reduced body mass and lower burrowing activity compared with earthworms in bioplastic-free soil, suggesting a measurable physiological response to bioplastic exposure.

Acknowledgements

This research was supported by the Research Excellence Program of the Hungarian University of Agriculture and Life Sciences and by the Flagship Research Groups Program of the Hungarian University of Agriculture and Life Sciences.

References

[1] A.S. Al Hosni, J.K., Pittman, G.D. Robson, (2019). Microbial degradation of four biodegradable polymers in soil and compost demonstrating polycaprolactone as an ideal compostable plastic. Waste Management, 97, 105–114.

[2] W. Ding, Z. Li, R. Qi, D.L. Jones, Q. Liu, Q. Liu, C. Yan, (2021). Effect thresholds for the earthworm Eisenia fetida: Toxicity comparison between conventional and biodegradable microplastics. Science of the Total Environment, 781, 146884.

[3] D. Gutiérrez-Rial, A. Lagoa, I. Villar, P. Feijoo, F. Mariño, J. Garrido, B. Soto, S. Mato (2025). Short- and medium-term effects of biodegradable microplastics (PLA and PHB) on earthworm development and reproduction. Ecotoxicology, 34(5), 701–711.

[4] Regulation (EU) 2019/1009 of the European Parliament and of the Council of 5 June 2019, Annex II, Part II, CMC 9 (Polymers other than nutrient polymers), point 3(b), as amended by Commission Delegated Regulation (EU) 2024/2787 of 23 July 2024.

[5] H. Platen, A. Wirtz (2010). Respiration activity of earthworms. Application Report Soils+solids.8, WTW/Xylem Analytics. Available online:

https://www.xylemanalytics.com/en/File%20Library/Resource%20Library/WTW/09%20Application%20Papers/AR_BOD_soils-solids.8--earthworms_lab_01_E.pdf

PEANUT SHELL-DERIVED ACTIVATED BIOCHAR FOR DICLOFENAC REMOVAL FROM WATER

Corina Orha[1*], Mina Ionela Morariu[1], Mircea Nicolaescu[1], Cornelia Bandas[1], Florina Stefania Rus[1], Carmen Lazau[1], Aniela Pop[2], Florica Manea[2]

[1]National Institute for Research and Development in Electrochemistry and Condensed Matter, Timisoara, Condensed Matter Department, 1 P. Andronescu Street, 300254, Timisoara, Romania
e-mails: orha.corina@gmail.com , mina.popescu37@gmail.com, nicolaescu.mircea13@yahoo.com , cornelia.bandas@gmail.com, rusflorinastefania@gmail.com , carmenlazau@yahoo.com ,
[2]Department of Applied Chemistry and Engineering of Inorganic Compounds and Environment, Politehnica University of Timisoara, Blv. Vasile Parvan No. 6, 300223, Timisoara, Romania
e-mails: aniela.pop@upt.ro , florica.manea@upt.ro;

Abstract
Vegetable waste has known as a new precursor for the obtaining of carbon-based materials due to its carbon richness, low cost, easily accessible and environmental-friendliness. In this study peanut shells were used to prepare biochar for diclofenac (DCF) removal from water. The biochar was activated chemically with KOH to enhance sorption charecteristics. The surface properties of the activated biochar obained through two different heat treatment at 550°C(BCA1) and 600°C (BCA2) were determined using X-ray Diffraction (XRD), Scanning Electron Microscopy (SEM) and RAMAN, which confirmed the successful activation of the biochar. Their preliminary testing for DCF removal showed a better performance of the sorption process using activated biochar treated at 600°C (BCA2).

Introduction
The conversion of agricultural waste into biochar has attracted considerable attention as a sustainable approach for water treatment. Biochar offer a porous structure, high surface area and abundant functional groups, making it a promising low-cost adsorbent for the removal of aqueous contaminants [1]. Moreover, this valorization pathway support the principles of the circular economy by transforming agricultural waste into added value materials. Among various agricultural residues, peanut husk represents an abundant and inexpensive precusors for biochar production. Its high cellulose content provides abundant functional groups that can facilitate the capture of various pollutants [2]. Various chemical agents, such as alkali metal salts, acids, or bases can be used for chemical activation, as they promote dehydration and the structural reorganization of the carbonaceous material's pores. Scientific literature indicates that KOH is the most effective activating agent, obtaining high specific surface areas and significant microporosity [3].

Consequently, peanut husk derived and functionalized carbon materials have been widely investigated for the removal of contaminates from aqueous solution such as dyes (~98,4%), [4] and pharmaceuticals (~1250 mg/g for Methylene Blue and ~303 mg/g for Tetracycline) [5,6].

The aim of this study was testing peanut husk as source for obtaining biochar by heat treatment in the absence of O_2 at 500°C and 600°C followed by its chemical and thermal activation to make it good sorbent for removal diclofenac-an emergent pollutant from water.

Experimental

The activated biochar (BCA) samples derived from peanut shells were prepared in three stages. First, the peanut shells were heat-treated at either 550°C (BCA1) or 600°C for 2 h (BCA2). Second, the resulting biochar was chemically activated with a 6M KOH solution at a biochar-KOH mass ratio of 1:2 for 60 min. Third, the samples were thermally activated under N_2 atmosphere at 700°C for 1h, using a N_2 flow rate of 100mL/min and a heating rate of 10°C/min. Following activation, the products were sequentially washed with 0,1M HCl solution and deionized water until de pH value of filtrate reached approximately 7. The residues were then dried at 60°C for 6h. The biochar (BC) was synthesized under similar conditions except the activation stage, being used for comparison in sorption test.

To study DCF sorption, an accurate weight of 0.025 g of activated biochar were shaken with 25 mL solution of 50 µg/L DCF for 120 min. The adsorption of DCF on biochar materials were studied using batch method and at certain running time, the suspension was sampled and filtered through a membrane filter. The concentration of DCF was measured in terms of absorbance at 275 nm (A_{275}) using a Varian Carry 100 spectrophotometer.

The DCF removal efficiency was calculated using the equation (1):

$$Removal\ efficiency = \frac{c_0 - c_t}{c_0} \times 100 \quad (\%) \qquad (1)$$

where: C_0 and C_t are the concentrations of DCF in aqueous solution in term of A_{275} at initial time and at each time t, respectively (mgL^{-1}).

Results and discussion

Figure 1 shows the XRD patterns of the activated biochar BCA_1 and BCA_2. From the analysis of the diffractograms of samples BCA1 and BCA2, it can be observed that they exhibit the charcteristic features of carbonaceous materials derived from biomass. Both samples show broad diffraction bands centered at approximatley 2θ=23° and 43–45°, which assigned to the (002) and (001) planes of disordered carbon structures and respective graphitic-type carbon structure. The broad and relatively low-intensity nature of these bands indicates a predominantly amorphous structure with a low degree of crystallinity and limited graphitic ordering. For BCA1, the broad diffraction bands observed around 23° and 45° indicated a predominantly amorphous carbon structure with a low degree of structural ordering. No intense and sharp diffraction bands characteristic of highly crystalline phase are observed in the analyzed range. Also, BCA2 exhibits a similar diffraction profile with broad bands around 23° and 45°, also indicating a predominantly amorphous structure and low crystallinity. The higher intensity of the (100) band observed for BCA1 compared with BCA2 indicates slight higher content graphytic type of carbon structure for BCA1, which may be related to the different heat-treated condition [7].

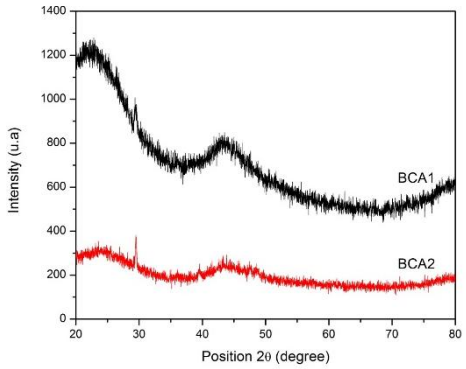


Figure 1. XRD patterns of biochar BCA1 and BCA2

The Raman spectrum of sample BCA1, presented in Figure 2, exhibits two characteristic bands of amorphous–graphitic carbon materials: the D band (~1350 cm^{-1}), associated with structural defects and amorphous regions, and the G band (~1580 cm^{-1}), attributed to C–C sp^2 vibrations in graphitic domains.

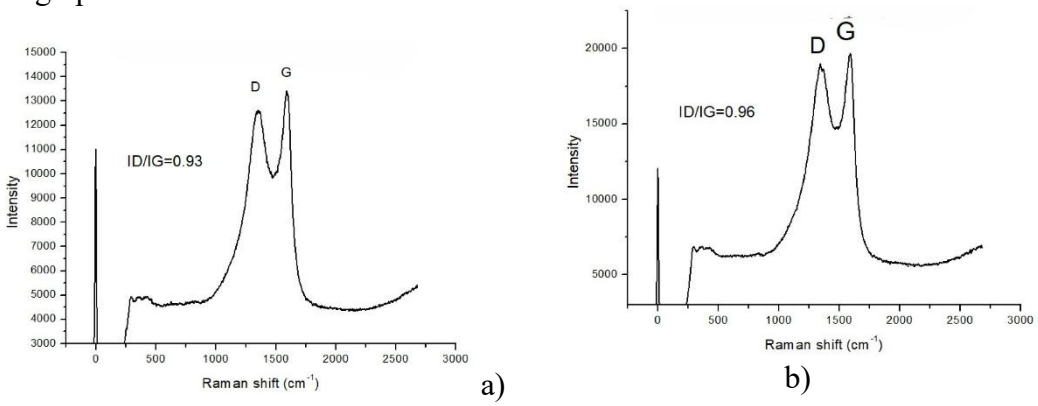


Figure 2. Raman patterns of biochar a) BCA1 and b) BCA2

The I_D/I_G ratio of 0.93 indicates a moderate degree of structural disorder, with the simultaneous presence of amorphous regions and sp^2 domains. The broadening of the Raman bands suggests the presence of relatively small but well-developed sp^2 domains. For sample BCA_2, the Raman spectrum also shows the characteristic D (~1350 cm^{-1}) and G (~1580 cm^{-1}) bands, which are well-defined. The I_D/I_G ratio of 0.96 likewise indicates a moderately disordered carbon structure, characterized by predominant amorphous regions and the presence of small sp^2 domains. Compared with BCA1, the slightly higher I_D/I_G ratio suggests a somewhat higher degree of structural disorder and more amorphous regions in BCA2.

The SEM images (Figure 3) of samples BCA1 and BCA2, obtained from peanut shell-derived biochar activated with KOH solution under different conditions, reveal a highly porous, three-dimensional morphology, characterized by an interconnected network of cavities and thin walls.

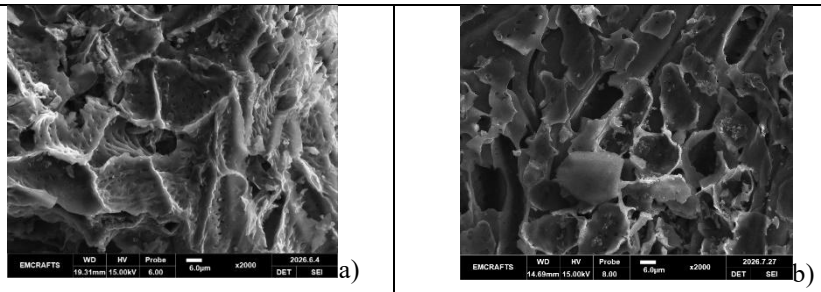


Figure 3. SEM images of the a)BCA1 and b)BCA2

Both samples exhibit pores of varying sizes, relatively uniformly distributed, forming a continuous sponge-like or reticulated structure. The irregular surfaces and numerous asperities observed on the pore walls indicate high microscopic roughness, associated with the chemical activation process using KOH. The morphological differences between BCA1 and BCA2 can be attributed to the different thermal treatment temperatures, which influence pore development and distribution.

Preliminary testing of BCA1 and BCA2 in sorption of DCF from water

The activated biochars (BCA1 and BCA2) were tested to check their sorption potential towards DCF from water. Also, the non-activated biochars (BC1 and BC2) obtained in similar conditions without activation were tested for comparison. The comparative results obtained until 120 minutes of sorption are shown in Figure 4.

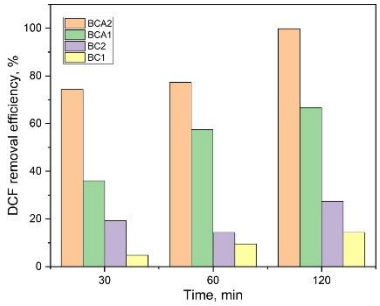


Figure 4. Evolution of DCF removal (50µg/L) efficiency versus time by sorption using BC1, BC2, BCA1 and BCA2

It is obviously that higher heating temperature and chemical activation enhanced sorption capacity of biochar towards DCF expressed in terms of DCF removal efficiency, *i.e.*, 14.36% BC1, 27.36% BC2, 66.75% BCA1 and 99.76% BCA2.

Conclusion

Activated biochar were successfully obtained using peanut shell biomass by heating at temperatures of 500°C and 600°C in the absence of O_2, followed by chemical activation using KOH. Higher heating temperature led to the degree of structural disorder and more amorphous regions that favored DCF sorption. Also, chemical activation with KOH enhanced significantly the biochar sorption capacity towards DCF-emergent pollutant from water.

Acknowledgements

This research is partially supported by the project "Innovative Technological Solutions to Circularity and Urban–Industrial Symbiosis within the Water–Energy–Materials–Fertilizers Nexus (ECO NEXUS)", Smart Growth, Digitization and Financial Instruments Program, 2021-2027, MySMIS no. 336912.

References

[1] K. I. Ogunwa, Ebenezer C. Nnadozie, N. Dube, P. O. Oladoye, K. S. Obayomi, Biomass and Bioenergy 208 (2026) 108844.
[2] A. A. Aryee, C. Gao, R. Han, L. Qu, Journal of Environmental Chemical Engineering 10 (2022) 108205.
[3] M. Mosbah, L. Mechi, R. Khiari, Y. Moussaoui, Processes (2020), 8, 1651.
[4] D. Garg, C.B. Majumder, S. Kumar, B. Sarkar, Journal of Environmental Chemical Engineering, 2019, 7, Issue 5.
[5] Md. T. Islam, AHM G. Hyder, R. Saenz-Arana, C. Hernandez, T. Guinto, Md A. Ahsan, B. Alvarado-Tenorio, J. C. Noveron, Journal of Environmental Chemical Engineering , (2019), 7, 102816.
[6] A. O. Egbedina, C. G. Ugwuja, · P. A. Dare, H. D. Sulaiman, · B. I. Olu-Owolabi, · K. O. Adebowale, Environmental Processes (2023) 10:20
[7] J. Zhou, S. Yuan, C. Lua, M. Yang, Y. Song, Journal of Electroanalytical Chemistry 878 (2020) 114704.

EFFICIENT REMOVAL OF ARSENIC FROM SIMULATED GROUNDWATER BY ZEOLITE FILTRATION

Adina Pacala

National Research and Development Institute for Industrial Ecology ECOIND, Timisoara Subsidiary, 300431 Timisoara, Bujorilor u. 115, Romania
e-mail: adina.pacala@ecoind.ro

Abstract

Arsenic contamination of groundwater represents a significant environmental and public health concern, particularly in areas where groundwater is used for drinking-water supply. Groundwater monitoring is nowadays mandatory in all member state level in European Union and our previous studies was focused to act in accordance with the legal provisions of the directive EU 2020/2184. Recent studies have reported high arsenic concentrations (over 200 µg/L) in groundwater sources in the Pannonian Basin (Hungary, Romania, Croatia, Serbia). Various technologies are available for the removal of arsenic from contaminated groundwater including chemical precipitation or coagulation, adsorption, lime softening, ion exchange and membrane separation. This study investigated the efficiency of a natural zeolite-based filtration process for arsenic removal from simulated groundwater. The simulated groundwater chemistry composition was given by 4 simulated pollutants added: arsenic (20 µg L^{-1}), iron (0,4 mg L^{-1}), manganese (0,2 mg L^{-1}), and ammonium (0,5 mg L^{-1}), into deionized water. The filtration medium consisted of natural zeolite clinoptilolite, a naturally occurring aluminosilicate mineral with ion-exchange and adsorption properties, with chemical formula $(Na,K)_6Si_{30}Al_6O_{72} \cdot 20 H_2O$ and high silicon content, Si/Al≥4. Romania has natural zeolite deposits with a high content of 90% clinoptilolite (e.g. Rupea deposit, Brașov), which makes it usable for various applications in technological processes for groundwater filtering for drinking purposes.

The fixed bed adsorption studies were conducted in glass columns designed by us, with an internal diameter of 4.9 cm and a length of 50 cm, equipped with quartz sand with a granulation of 2.5 mm and a fixed height of 5 cm at the base, over which natural Rupea zeolite with the granulation of 1.25 mm and a fixed height of the adsorbent layer of 10 cm was superimposed. A constant flow rate (100 mL·min^{-1}) was maintained using a peristaltic pump, the volume of simulated groundwater that was filtered remaining the same for all sets of experiments performed.

Following filtration through the clinoptilolite-rich zeolite medium, the residual arsenic concentration decreased to 3 µg/L, corresponding to an overall arsenic removal efficiency of 85%. The reduction in arsenic concentration demonstrates the potential of the natural zeolite to effectively remove arsenic from simulated groundwater under the investigated experimental conditions. The treated water contained an arsenic concentration below the commonly applied drinking-water limit of 10 µg/L.

The results indicate that clinoptilolite-rich natural zeolite may represent a simple, potentially low-cost filtration medium for arsenic removal and could be considered for the development of decentralized treatment systems for groundwater intended for drinking-water applications. Further investigations should evaluate the influence of arsenic speciation, pH, zeolite granulations, contact time, and filtration rate on treatment efficiency for a naturally arsenic-contaminated groundwater from a small rural community in Western Romania, with a similar water matrix chemistry content.

Acknowledgements
This work was carried out through the "Nucleu" Program within the National Research Development and Innovation Plan 2022-2027 with the support of Romanian Ministry of Research, Innovation and Digitalization, contract no. 3N/2022, Project code PN 23 22 03 03.

References
[1] Guidelines for drinking-water quality: fourth edition Incorporating the first and second addenda. Chemical fact sheets: Arsenic, World Health Organization (2022).
[2] EU, 2020, Directive (EU) 2020/2184 of the European Parliament and of the Council of 16 December 2020 on the quality of water intended for human consumption.
[3] A. Pacala, M. Stefanescu, G.G. Vasile, Proceedings of 29th ISAEP, Szeged, Hungary, (2023), 254-257.
[4] S. Aktar, S. Mia, T. Makino, M. M. Rahman, A. U. Rajapaksha, Sci. Total Environ. 862 (2023) 160821.
[5] H. Celebi, I. Bilican, T. Bahadir, J. Clin. Prod. 327 (2021) 129475.
[6] N.J. Raju, Environ. Res. 203 (2022) 111782.
[7] R. Patel, D. Shah, S. Shah, M. Shah, Mater. Today 62 (2022) 6890–6895.

SUSTAINABLE UTILIZATION OF RESIN IN THE MUNTELE MIC–POIANA MĂRULUI AREA, CARAȘ-SEVERIN COUNTY, ROMANIA

Panici Petre Alexandru[1], Dragomir Petru Ioan[1], Moatăr Maria Mihaela[1], Ștefan Carolina[1], Panici Cristina Gabriela[1], Scedei Daniela Nicoleta[2], Bora Marinela[3], Beinșan Carmen[3], Rădulescu Laura[4], Sîngeorzan Steluța-Maria[5]

[1]Department of Forestry, University of Life Sciences "King Michael I" from Timisoara, 300645, Timisoara, Romania; e-mail: alexandrupanici@usvt.ro, petruioandragomir@usvt.ro, mihaela.moatar@usvt.ro, carolinastefan@usvt.ro, panici.cristina-gabriela.fita@usvt.ro
[2]Department of Horticulture, University of Life Sciences "King Michael I" from Timisoara, 300645, Timisoara, Romania; e-mail: daniela.scedei@usvt.ro
[3]Department of Genetic Engineering, University of Life Sciences "King Michael I" from Timisoara, 300645, Timisoara, Romania; e-mail: bora.marinela.fita@usvt.ro, carmenbeinșan@usvt.ro
[4]Department of Science Food, University of Life Sciences "King Michael I" from Timisoara, 300645, Timisoara, Romania; e-mail: laura.radulescu@usvt.ro
[5]Department of Forestry, University of Agricultural Sciences and Veterinary Medicine Cluj-Napoca, 300645, Timisoara, Romania; e-mail: maria.sîngeorzan@usamvcluj.ro
**Corresponding author: petruioandragomir@usvt.ro, mihaela.moatar@usvt.ro*

Abstract

The purpose of this paper is to analyze resin as a non-timber forest product, with particular emphasis on its biological, economic, and silvicultural importance. The study aims to highlight how this resource can be responsibly utilized without causing significant damage to trees or contributing to the degradation of forest ecosystems.To achieve this purpose, the paper addresses several objectives. First, it aims to present the general characteristics of resin and its role in the life processes of trees. Second, the main products that can be obtained from resin and their applications in various fields are analyzed. Third, low-impact resin harvesting methods are presented; together with an assessment of the potential effects of resin extraction on tree health. The paper is structured into three chapters. The first chapter presents general aspects concerning forest resin, including its biological role, composition, characteristics, and the forest species that produce it. The second chapter focuses on the economic value of resin, the products obtained through its processing, and its applications in various fields. The third chapter comprises a case study on the utilization of resin in the Muntele Mic–Poiana Mărului area, Caraș-Severin County, with emphasis on the region's potential, harvesting methods, and their impact on trees.

Through this study, the aim is to emphasize that resin can represent a valuable resource for the forestry sector, provided that it is harvested and utilized rationally. The sustainable utilization of resin requires the appropriate selection of trees, the use of minimally invasive harvesting methods, continuous monitoring of stand conditions, and the maintenance of a balance between economic interests and forest conservation.For a better understanding of the analyzed area, the following figure presents a representation of the terrain in the Poiana Mărului Lake–Muntele Mic area. This region constitutes the geographical setting of the case study and is characterized by mountainous terrain, high elevations, and forested areas typical of the Carpathian region.

Introduction

Forests have always played an essential role in human life, providing resources for construction, heating, food, medicine, and various economic activities [1, 2]. Although timber is considered the most important forest product [2], forest ecosystems also provide numerous other resources,

collectively known as non-timber forest products (NTFPs) [5, 10]. Their importance has increased in recent years, particularly in the context of promoting the rational use of natural resources and reducing pressure on forest ecosystems [1, 6, 7].

Non-timber forest products include a wide range of resources, such as wild fruits, mushrooms, medicinal plants, sap, bark, apicultural products, and resin [5, 10]. These resources can be utilized without harvesting the trees themselves, thereby contributing to a more balanced use of forest ecosystems [1, 8]. Their integration into local economic activities highlights the forest not only as a source of timber, but also as a complex ecosystem capable of providing multiple benefits [1, 3, 10]. Forest resin represents one of the most significant non-timber forest resources [5, 9]. It is produced mainly by coniferous trees [4] and plays an important role in their natural defense mechanisms [2, 4]. When a tree is injured, resin is released onto the affected area, forming a protective barrier that helps prevent the penetration of insects, fungi, and other pathogens [2, 4].

Today, resin and its processed derivatives are widely used in the chemical, pharmaceutical, and cosmetic industries, as well as in the production of adhesives, varnishes, and paints [9, 11, 12]. The choice of this topic is motivated by the need for sustainable utilization of forest resources [1, 6, 7]. Resin harvesting can provide economic benefits, particularly in mountainous areas [5, 10]; however, it must be carried out carefully and responsibly [1, 8]. Since the process involves interventions on tree bark, improper harvesting can negatively affect tree health [2]. Deep, repeated, or incorrectly performed wounds may weaken trees, increase their susceptibility to diseases, and reduce the overall stability of forest stands [1, 2].

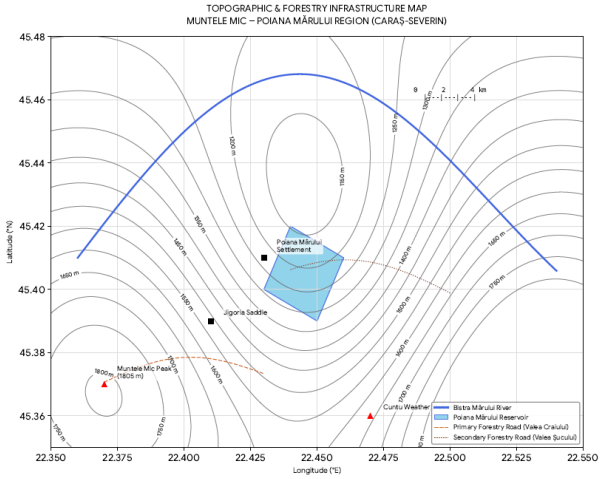


Figure 1. Topographic and Forestry Infrastructure Map of the Muntele Mic – Poiana Mărului Montane Corridor, Caraș-Severin County, Romania.

Experimental

The Muntele Mic–Poiana Mărului area, located in Caraș-Severin County, was selected as the study area [1, 3]. Situated in a mountainous region representative of western Romania, it is characterized by extensive forested areas comprising both coniferous and mixed stands [1, 4]. These natural conditions make the region suitable for assessing the potential utilization of resin as a non-timber forest product [5, 10]. The mountainous relief, high elevations, and cooler climate favor the development of coniferous species such as Norway spruce, silver fir, and pine [4]. These species are capable of producing resin, although resin yield and harvesting potential depend on species, age, health status, and local growing conditions [2, 4]. The area is of interest not only for its forest resources but also for the potential diversification of forest utilization [1, 7]. While forests are traditionally associated primarily with timber production, non-timber forest products can contribute to a more diversified and sustainable use of forest resources [5,

10]. Resin is particularly relevant in this context, as it can be harvested without felling trees, provided that extraction is properly controlled [9, 10].

The selection of this area is justified by the suitability of the mountain forests of Caraș-Severin for examining the balance between economic interests and forest ecosystem conservation [1, 6]. Resin harvesting should therefore be regarded not simply as an exploitation activity, but as an intervention integrated into a sustainable forest management system [1, 8]. The assessment of resin utilization potential was based on the presence and distribution of coniferous species, tree maturity and health status, forest stand characteristics, and the general suitability of the area for low-impact resin harvesting [2, 3]. Mature, vigorous, and healthy trees were considered more suitable for controlled harvesting, whereas trees affected by disease, decay, breakage, insect infestation, or other signs of deterioration should be excluded [2, 4]. Within the study area, resin harvesting should be restricted to mature and stable stands where such interventions do not compromise forest integrity [1, 3]. Protected areas, sites of high biodiversity, and stands showing signs of ecological or sanitary vulnerability should be excluded from harvesting [6, 7, 8]. The objective should not be to maximize short-term yield, but to ensure the moderate and sustainable utilization of a renewable resource [1, 10].

Species composition was also considered an important factor in assessing resin utilization potential [3, 4]. Areas dominated by healthy and well-developed conifers have greater potential, whereas harvesting is not recommended where conifers are scarce, young, or in poor phytosanitary condition [2, 4]. Consequently, the assessment should combine forest inventory information with direct field observations [3].

Resin harvesting generally involves stimulating resin secretion by making controlled injuries to the tree bark [2, 9]. Traditional methods relied on larger and deeper cuts, which could increase resin flow but also cause significant long-term damage to trees [2]. Currently, low-impact harvesting methods are preferable, particularly in areas such as Muntele Mic–Poiana Mărului, where forests also have important ecological and landscape functions [1, 7]. These methods aim to obtain moderate resin yields while maintaining tree health and forest stand stability [1, 2]. One suitable approach is controlled micro-tapping, which involves making small, shallow incisions that minimally affect the tree tissues [9]. The objective is to stimulate resin ducts without creating deep wounds, thereby allowing the tree to recover more effectively [2, 9].

Another option is passive resin collection, involving the collection of resin naturally released following minor injuries caused by broken branches, bark fissures, or other natural disturbances [5, 10]. Although yields are lower, this method has the advantage of avoiding additional direct intervention [10]. Limited extraction points may also be used by restricting harvesting to a small number of designated areas on the trunk [9]. After a harvesting period, these areas should be allowed to recover before extraction is resumed or transferred to other trees [1, 2]. Regardless of the method used, harvesting should be performed with appropriate, clean, and well-maintained tools. Deep, irregular, or extensive wounds may increase susceptibility to disease and reduce tree vitality. Harvesting should also be avoided under unfavorable conditions, such as drought, extreme temperatures, or pest outbreaks. For the study area, a combined low-impact approach is considered appropriate. Controlled micro-tapping may be applied selectively to suitable trees, while passive collection can supplement the harvested resin without placing additional pressure on the forest stand. Harvested resin can be used either as a raw material or processed into products with higher economic value [5, 9]. Processing allows this natural resource to be transformed into a diverse range of useful products [9, 10].

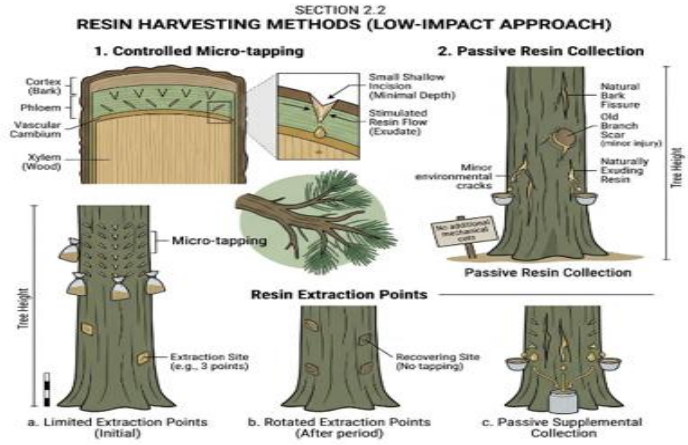


Figure 2. Resin Harvesting Methods

The two best-known resin derivatives are rosin and turpentine, obtained through the distillation of crude resin [9, 11, 12]. Rosin constitutes the solid fraction, while turpentine represents the volatile fraction [9, 11, 12]. Rosin has adhesive and hydrophobic properties and is used in the production of adhesives, varnishes, paints, paper, and various technical products [9, 11]. It is also used in the musical field, particularly for violin bows, contributing to its economic value [11]. Turpentine is primarily used as a solvent and as a raw material in the chemical industry, with applications in industrial, pharmaceutical, and cosmetic products [9, 12]. Due to its volatile nature, it requires controlled handling and appropriate safety conditions [12].

Results and Discussion

The assessment of the Muntele Mic–Poiana Mărului area indicates a favorable potential for the sustainable utilization of resin as a non-timber forest product. The presence of coniferous species, particularly Norway spruce, silver fir, and pine, provides suitable conditions for resin production. However, the potential for resin utilization is not uniform and depends on species composition, tree maturity, health status, and local environmental conditions. Among the coniferous species present in the area, pine may be considered particularly suitable for resin harvesting due to its generally higher resin-secretion capacity. Norway spruce and silver fir also produce resin, but harvesting interventions on these species should be approached more cautiously. Therefore, species composition represents an important factor in determining the suitability of a forest stand for resin utilization.

Passive resin collection provides an even less invasive alternative, although its lower yield limits its potential as a sole harvesting method.The findings further indicate that resin utilization should be considered as a complementary activity within sustainable forest management rather than as an intensive extraction practice. In the studied area, small-scale local processing could create additional opportunities for rural communities, particularly where resin-based products can be associated with local natural resources and tourism. Overall, the results support the potential of the Muntele Mic–Poiana Mărului area for sustainable resin utilization.

However, this potential depends on the application of selective harvesting practices, the careful selection of suitable trees and stands, and the adoption of low-impact extraction methods. The sustainable utilization of resin should therefore be based on moderate harvesting intensity and the long-term protection of forest ecosystem functions.

Conclusion

Based on the analysis conducted in this study, resin can be considered an important non-timber forest product, both from a biological and economic perspective. It is not only a resource of economic value, but also plays an essential natural role in the life of coniferous trees. Through

resin secretion, trees protect wounds, limit the penetration of pathogens, and defend themselves against harmful insects and microorganisms. Resin is characterized by a complex composition and distinctive physicochemical properties, including viscosity, a characteristic odor, insolubility in water, and the ability to harden upon exposure to air. These properties account for its wide range of applications in industry, medicine, cosmetics, handicrafts, and other fields. Processing resin can result in valuable products such as rosin, turpentine, resin oils, creams, ointments, and decorative products**.**

An important finding of this study is that resin can contribute to the diversification of the forest economy. Unlike timber harvesting, resin extraction does not require tree felling, providing an opportunity for more sustainable forest utilization. However, this advantage can only be maintained when harvesting is carried out properly, under controlled conditions, and in accordance with appropriate tree-protection measures. This case study indicates that mountainous regions with coniferous forests may have significant potential for resin utilization. Nevertheless, resin utilization should not be considered solely from an economic perspective. Harvesting involves creating wounds in the bark, and repeated or aggressive interventions may negatively affect tree health. Potential adverse effects include reduced tree vigor and growth, increased susceptibility to disease and insect attacks, and decreased stand stability. For this reason, traditional harvesting methods based on deep and repeated incisions should be applied with caution or replaced by less invasive techniques. Controlled micro-tapping, passive resin collection, and the use of limited extraction points represent more appropriate approaches for the responsible and sustainable utilization of resin.

References

[1] Giurgiu, V. Sustainable Management of Romania's Forests. Editura Academiei Române: Bucharest, (2004).
[2] Florescu, I.; Nicolescu, N.V. Silviculture. Editura Lux Libris: Brașov, (1996).
[3] Leahu, I. Forest Management Planning. Editura Didactică și Pedagogică: Bucharest, (2001).
[4] Clinovschi, F. Dendrology. Editura Universității „Ștefan cel Mare": Suceava, (2005).
[5] Rădulescu, A.V. Non-Timber Forest Products. Editura Universității Transilvania din Brașov: Brașov, (2006).
[6] National Forest Administration – Romsilva. Information on the Sustainable Management of the Publicly Owned State Forest Estate. (2024).
[7] Ministry of Environment, Water and Forests. National Forest Strategy 2030. Bucharest, (2023).
[8] Ministry of Environment, Water and Forests. Forest Code. Bucharest, (2024).
[9] Coppen, J.J.W.; Hone, G.A. Gum Naval Stores: Turpentine and Rosin from Pine Resin. Food and Agriculture Organization of the United Nations: Rome, (1995).
[10] FAO. Non-Wood Forest Products and Income Generation. Food and Agriculture Organization of the United Nations: Rome, (1999).
[11] Encyclopaedia Britannica. Rosin. (2024).
[12] Encyclopaedia Britannica. Turpentine. (2024).

BIRCH SAP –A NATURAL SOURCE OF BIOACTIVE COMPOUNDS AND VALORISATION PERSPECTIVES

Panici Petre Alexandru[1], Dragomir Petru Ioan[1], Moatăr Maria Mihaela[1], Ștefan Carolina[1], Panici Cristina Gabriela[1], Hățăgan-Toma Geanina Andrada[1], Scedei Daniela Nicoleta[2], Bora Marinela[3], Beinșan Carmen[3], Borza Mariana[3], Sîngeorzan Steluța-Maria[4]

[1]Department of Forestry, University of Life Sciences "King Michael I" from Timisoara, 300645, Timisoara, Romania; e-mail: alexandrupanici@usvt.ro, petruioandragomir@usvt.ro, mihaela.moatar@usvt.ro, carolinastefan@usvt.ro, panici.cristina-gabriela.fita@usvt.ro, geanina-andrada.hatagan-toma.fita@usvt.ro
[2]Department of Horticulture, University of Life Sciences "King Michael I" from Timisoara, 300645, Timisoara, Romania; e-mail: daniela.scedei@usvt.ro
[3]Department of Genetic Engineering, University of Life Sciences "King Michael I" from Timisoara, 300645, Timisoara, Romania; e-mail: bora.marinela.fita@usvt.ro, carmenbeinșan@usvt.ro, mariana.borza@usvt.ro
[4]Department of Forestry, University of Agricultural Sciences and Veterinary Medicine Cluj-Napoca, 300645, Timisoara, Romania; e-mail: maria.sîngeorzan@usamvcluj.ro
**Corresponding author: petruioandragomir@usvt.ro, mihaela.moatar@usvt.ro*

Abstract

At present, birch sap is increasingly being incorporated into modern food products, particularly beverages, syrups, and dietary supplements. It has gained recognition for its hydrating and detoxifying properties, as well as for providing a natural and healthier alternative to refined sugars and synthetic sweeteners used in processed foods. Moreover, the harvesting of birch sap is generally considered a sustainable practice, as it has no major adverse impact on forest ecosystems when properly managed. This makes birch sap an attractive ingredient in an era when consumers are becoming increasingly attentive to the origin of the foods they consume and to their environmental impact.

This paper aims to provide a comprehensive analysis of the chemical composition of birch sap, its harvesting and preservation processes, its diverse applications in the food industry, and the nutritional benefits it may provide to consumers. In addition, the challenges and opportunities facing the birch sap industry will be examined from the perspective of sustainability and the requirements of international markets. In this context, particular emphasis will be placed on the importance of this non-timber forest product not only as a food resource but also as a potential component of a more environmentally sustainable and responsible economic model capable of addressing current challenges associated with climate change and the use of natural resources. As interest in natural and functional products continues to grow, birch sap has considerable potential to become a key ingredient in the global market. At the same time, the integration of this resource into the food industry creates new economic opportunities, driven by increasing consumer demand for healthy, sustainable, and innovative food products.

Introduction

Birch sap harvesting represents one of the oldest forms of forest resource utilization that does not involve the removal of woody biomass and has been practiced for centuries in the temperate and boreal regions of Europe and Asia [1,6]. In regions such as Scandinavia, the Baltic States, Russia, and Central and Eastern Europe, including Romania, birch sap has traditionally served as a seasonal source of nutrients, being consumed either fresh or lightly fermented [6]. From a forest management perspective, this diversification has major implications. In a context of

increasing pressure on timber resources, combined with increasingly stringent societal requirements for biodiversity conservation and ecosystem protection, the utilization of non-timber forest products has become an essential component of multifunctional forest management [2], [10]. Birch sap harvesting provides an additional source of economic revenue, reducing exclusive dependence on timber exploitation and contributing to income stability in forested areas with limited opportunities for economic development [7]. The importance of this activity must, however, also be assessed from the perspective of ecological sustainability. Unlike timber harvesting, which involves structural changes to forest stands and directly affects carbon stocks, sap harvesting involves a localized and temporary intervention in the tree. When conducted within the biological capacity of the species, it does not result in the loss of the forest's fundamental ecosystem functions [11], [12]. The tree remains integrated within the ecosystem, continuing to contribute to soil protection, hydrological regulation, carbon sequestration, and the maintenance of associated biodiversity [10].

From a biological perspective, sap represents the principal medium for the transport of water and nutrients within the tree. During the dormant period, birch trees accumulate reserves of carbohydrates and other substances required for the resumption of growth [4], [5]. As spring temperatures increase, these reserves are mobilized, generating an intense upward flow of sap towards the buds and developing shoots. This physiological phase creates a unique opportunity for sap harvesting, as the volume of available sap is high and, provided that the intervention is limited in both duration and quantity, it does not significantly disrupt the tree's energy balance [3]. Aligning harvesting activities with the biological cycles of the species is essential from a management perspective. Synchronizing harvesting with the period immediately preceding leaf emergence reduces the risk of physiological stress and enables the resource to be harvested repeatedly over the long term [3], [6]. In the absence of such synchronization, harvesting may become a stress factor, affecting annual growth processes and the tree's ability to respond to abiotic and biotic stressors [4].

Experimental

The present study was conducted to assess the potential for utilizing birch sap as a non-timber forest product within a multifunctional forest management framework applicable to the Apuseni Mountains. The research has an applied character and focuses on the integration of ecological, technical, and economic aspects associated with birch sap harvesting under the specific conditions of the forest resources located in the vicinity of Gârda de Sus, Alba County, Romania [1].

The methodological approach was based on the analysis of information available in the scientific literature, correlated with the specific characteristics of the investigated area. The study did not involve direct field measurements; instead, a theoretical assessment was performed using productive and ecological parameters reported in European studies concerning birch sap production and harvesting [6]. The main objective was to estimate the available birch resource, determine the potential volume of sap that could be obtained under different harvesting scenarios, assess the economic potential of its utilization, and evaluate the sustainability of harvesting within the framework of sustainable forest management [11].

The study area is located in the central-western part of the Apuseni Mountains, in the vicinity of Gârda de Sus, Alba County, Romania. The investigated forest area is situated at elevations ranging from approximately 800 to 1,200 m. The main birch species considered were *Betula pendula* Roth. and *Betula pubescens* Ehrh., species widely described in European silvicultural literature [3]. The regional climate is temperate-continental, with mountain influences, characterized by a mean annual temperature of approximately 6–7 °C and mean annual precipitation exceeding 900 mm. These climatic conditions, together with the local hydrological regime, are considered favorable for birch sap flow during the spring harvesting period [4].

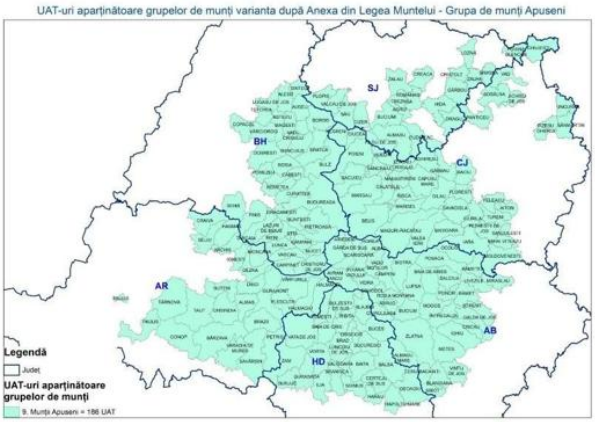


Figure 1. Location of the study area within the Apuseni Mountains

The research was designed as a descriptive-analytical and applied study based on several successive stages. First, the potential birch resource within the study area was estimated based on the proportion of forest occupied by birch, following general principles of non-timber forest product assessment [1]. Subsequently, the number of mature trees potentially suitable for sap harvesting was estimated using an average tree density derived from the scientific literature [3]. The assessment then considered the main technical criteria for selecting trees suitable for harvesting, including tree diameter and phytosanitary condition, criteria aligned with sustainable forest management guidelines [2]. Only mature and healthy trees were considered suitable for sap harvesting, in accordance with the principles of sustainable forest management [10].

Results and Discussion

The assessment of the birch resource in the investigated area indicates a significant potential for the utilization of birch sap as a non-timber forest product. Based on the estimated forest area of 500 ha and the assumed birch proportion of approximately 15%, the area potentially available for birch sap harvesting was estimated at 75 ha. Considering an average density of 120 mature birch trees/ha, the total birch resource was estimated at approximately 9,000 trees. Applying the eligibility criteria concerning tree diameter and phytosanitary condition, approximately 35% of the trees were considered suitable for sap harvesting, resulting in an estimated 3,150 trees.

Table 1. Main indicators used to estimate the birch sap harvesting potential

Indicator	Value	Explanation
Total analyzed area	500 ha	Area included in the case study
Birch participation	15%	Percentage of the area occupied by birch
Area occupied by birch	75 ha	500 ha × 15%
Average density	120 trees/ha	Estimated value based on specialized literature
Total number of trees	9.000 trees	75 ha × 120 trees/ha
Eligible trees (>25 cm, healthy)	3.150 trees	35% of the total number of trees

The estimated production potential varied considerably according to the assumed sap yield per tree. Under the pessimistic scenario, with an average yield of 5 L/tree, the estimated production reached 15,750 L per harvesting season. The moderate scenario, based on an average yield of 8 L/tree, resulted in an estimated production of 25,200 L, while the optimistic scenario, assuming 10 L/tree, resulted in approximately 31,500 L.

Table 2. Estimated birch sap production under different harvesting scenarios

Scenario	Average yield	Estimated production
Pessimistic	5 L/tree	15,750 L
Moderate	8 L/tree	25,200 L
Optimistic	10 L/tree	31,500 L

The moderate scenario was considered the most representative for the conditions of the Apuseni Mountains and was subsequently used for the economic assessment. Assuming a harvesting period of approximately 25 days, the estimated production of 25,200 L corresponds to an average daily volume of approximately 1,008 L. Such a production level suggests that birch sap harvesting could be organized as a seasonal activity requiring appropriate collection, temporary storage, transportation, and refrigeration infrastructure. From an economic perspective, the results indicate that the utilization of birch sap could generate an additional source of income within a multifunctional forest management system.

Table 3. Economic comparison of the two birch sap commercialization scenarios

Economic indicator	Fresh sap	Premium processed sap
Estimated production	25,200 L	25,200 L
Selling price	RON 8/L	RON 18/L
Gross revenue	RON 201,600	RON 453,600
Estimated costs	RON 75,000	RON 165,000
Estimated profit	RON 126,600	RON 288,600

The comparison demonstrates that processing and positioning birch sap as a higher-value product could substantially increase the economic benefits generated by the forest resource. Although the premium scenario involves higher production and marketing costs, the increase in selling price results in a significantly higher estimated profit. This finding suggests that local processing could represent an important strategy for increasing the added value of birch sap and reducing the dependence on the commercialization of raw sap. Beyond the direct economic benefits, birch sap harvesting could contribute to the diversification of forest-based activities in rural areas of the Apuseni Mountains. Overall, the findings support the integration of birch sap harvesting into a multifunctional approach to forest management, in which non-timber forest products contribute to economic diversification while maintaining the ecological functions and long-term stability of forest ecosystems. The development of local processing and commercialization capacities could further increase the value generated by birch resources and strengthen the role of sustainable non-timber forest product utilization in the socio-economic development of the Apuseni Mountains.

Conclusion

The present study assessed the potential for harvesting and utilizing birch sap as a non-timber forest product and evaluated its relevance within the framework of sustainable forest management. The results indicate that the forest resources in the Gârda de Sus area provide favorable conditions for the development of a controlled and economically viable birch sap harvesting activity. The estimated resource and production potential demonstrate that birch sap can represent a complementary source of income alongside conventional timber production. Under the moderate harvesting scenario, an estimated production of 25,200 L per harvesting

season was obtained, indicating the existence of a resource capable of supporting an organized seasonal activity.

The economic assessment showed that the degree of processing has a major influence on the profitability of birch sap utilization. While the commercialization of fresh sap can generate additional income, the processing and marketing of higher-value products can substantially increase the economic value of the resource. Therefore, the development of local processing facilities and short value chains represents an important opportunity for increasing the benefits generated at regional level. From an ecological perspective, birch sap harvesting can be integrated into sustainable forest management provided that appropriate harvesting practices are applied. The selection of mature and healthy trees, controlled tapping intensity, spatial rotation of harvesting areas, and regular phytosanitary monitoring are essential for maintaining tree vitality and ensuring the long-term availability of the resource. In conclusion, birch sap represents a promising renewable non-timber forest resource for Romania. Its integration into multifunctional forest management could contribute to the development of the forest bioeconomy and the diversification of forest-derived income, while maintaining the ecological functions and long-term stability of forest ecosystems.

References

[1] Cenușă, R.; Blujdea, V.; Teodosiu, M. Produse forestiere nelemnoase și rolul lor în dezvoltarea durabilă a pădurilor [Non-Timber Forest Products and Their Role in Sustainable Forest Development]. Editura Silvică: Bucharest, (2018).

[2] Filipescu, C.N. Silvicultură. Gestionarea durabilă a ecosistemelor forestiere [Silviculture. Sustainable Management of Forest Ecosystems]. Editura Universității „Ștefan cel Mare”: Suceava, (2014).

[3] Hynynen, J.; Niemistö, P.; Viherä-Aarnio, A. Silviculture of Birch Forests in Northern Europe. Finnish Forest Research Institute: Helsinki, (2010).

[4] Pallardy, S.G. Physiology of Woody Plants, 3rd Edition. Academic Press: New York, (2008).

[5] Kozlowski, T.T.; Kramer, P.J.; Pallardy, S.G. The Physiological Ecology of Woody Plants. Academic Press: San Diego, (1990).

[6] Svanberg, I.; Sõukand, R.; Łuczaj, Ł.; Kalle, R.; Zyryanova, O.; Dénes, A.; Papp, N. Uses of Tree Saps in Northern and Eastern Parts of Europe. Acta Societatis Botanicorum Poloniae, 81(4), 343–357, (2012).

[7] Enescu, C.M.; Dincă, L.; Crișan, V.E. Collection and Use of Birch Sap, a Less Known Non-Wood Forest Product in Romania. Notulae Botanicae Horti Agrobotanici Cluj-Napoca, (2017).

[8] Grabek-Lejko, D.; Kasprzyk, I.; Twardowski, T. The Bioactive and Mineral Compounds in Birch Sap. Baltic Forestry, 23(2), 394–401, (2017).

[9] Mănescu, C.; et al. Birch Sap Harvesting in Changing Spring Climate Conditions in Romania. Scientific Papers Series B, Horticulture, (2023).

[10] Stăncioiu, P.T. Silvicultură și Biodiversitate Forestieră [Silviculture and Forest Biodiversity]. Editura Universității Transilvania: Brașov, (2008).

[11] Forest Europe. State of Europe’s Forests 2020. Ministerial Conference on the Protection of Forests in Europe, (2020).

[12] Regia Națională a Pădurilor – Romsilva. Rapoarte privind gestionarea durabilă a fondului forestier din România [Reports on the Sustainable Management of Romania’s Forest Estate]. (2024).

STUDY ON BIOPLASTIC BAGS BY FT-IR AND RADIOCARBON METHODS

Kingkham Paseutsakoun[1], Mária Mörtl[2], Klaudia Papp[3], Tamás Varga[3], András Székács[2]

[1]Doctoral School of Natural Sciences, Institute of Environmental Sciences, Hungarian University of Agriculture and Life Sciences (MATE), Páter Károly u. 1, 2100 Gödöllő, Hungary
[2]Agro-Environmental Research Centre, Institute of Environmental Sciences, MATE, Tessedik Sámuel u. 4., 2100 Gödöllő, Hungary
[3]HUN-REN ATOMKI, Bem József út 18/C, 4026 Debrecen, Hungary
e-mail: Paseutsakoun.Kingkham@phd.uni-mate.hu

We have studied different packaging materials, including biopolymers as well as conventional polymers. Bioplastics are biobased and/or biodegradable materials. Over 40 types of plastic bags, collected mainly in Hungary also partly in countries were investigated. Among the samples studied, biopolymers were compostable either under household or industrial conditions, and there were recycled polymers as well. Bags were a) shopping bags, b) bags for vegetables and c) bags for organic waste collection.
Samples were identified by FT-IR spectroscopy measurements. Among the samples conventional polyethylene (PE), polypropylene (PP), polybutylene adipate terephthalate (PBAT) and polylactic acid (PLA) were found. PBAT is a biodegradable and fuel-based polymer, its biocomponent is usually a starch additive. In contrast, PLA is from renewable biosources, but an industrially compostable biopolymer. Vibrational spectra were evaluated and based on the intensities of some characteristic bands (e.g. carbonyl) further subcategories were determined. High variability of the FT-IR spectra has been observed for some PE samples. A different pattern was recorded for PBAT samples in the fingerprint region which is related to the composition of the material (e.g. starch content). PLA samples were blends with PBAT and starch. Vibrations of PBAT dominated the FT-IR spectra in the latter case, therefore detection of PLA was proven rather challenging.
The biocontent (percentage of modern carbon or pMC value) was measured by the radiocarbon method (acelerator mass spectrometry, AMS) using isotope ratio mass spectrometry analysis. This method is preferred for determination of the biocomponent ratio of regulated products in the European Union. Based on the results, a high variability has been observed in pMC values. The highest values were measured for bio-PE samples, which has the same persistence as its fuel-based counterpart. Its degradation requires hundreds of years. The other samples with significant biomaterial content were polyesters (PBAT or PLA/PBAT), and contained typically 10, 20 or over 50% of modern carbon. Compliance with the regulations in the European Union determines mainly the biocomponent ratio in bioplastic products.

Acknowledgements
This study was funded by the Tempus Public Foundation under the Stipendium Hungaricum scholarship. The research was supported by the Research Excellence Program of the Hungarian University of Agriculture and Life Sciences (MATE) and by the Flagship Research Groups Program of the Hungarian University of Agriculture and Life Sciences (MATE).

INFLUENCE OF ZnO ON BACTERIAL CELLULOSE

Paula Svera (m.Ianăși)[1], Cătălin Ianăși[2], Alexandra Ioana Bucur[1], Adina Căta[1], Nick Samuel Țolea[1], Paula Sfîrloagă[1]

1National Institute of Research and Development for Electrochemistry and Condensed Matter (INCEMC), Str. Dr. A. Păunescu Podeanu 144, Timișoara, Romania
2"Coriolan Drăgulescu" Institute of Chemistry (ICT), B-dul. Mihai Viteazu 24, Timișoara, Romania
e-mail: paulasvera@gmail.com

Abstract
Synthetic polymers are indispensable in our society, however, due to their lack of biodegradability resulting in waste accumulation and microplastic pollution, alternative materials with less impact on the environment are urgently needed. In this direction bacterial cellulose has a great potential [1-3]. However, there are many deficiencies that need improvement (maintaining sterile growth media, lack of antimicrobial activity, poor rehydration after drying, etc.). One solution to several of the aforementioned problems is the introduction of additional suitable materials. In this direction ZnO has antimicrobial and anti-mildew activity, inhibiting bacterial, fungal and mildew growth on surface and as well influences the mechanical properties as tensile strength and toughness when added to bioplastics [4-5]. In our study we investigate the surface of the bacterial cellulose after the introduction of 0.125g, 0.25g, 0.5g and 0.75g ZnO as well as the structural changes that take place. After the AFM (Atomic Force Microscopy) and WAXS/SAXS (Wide-Angle X-ray Scattering/ Small-Angle X-ray Scattering) analysis we demonstrated that the ZnO was incorporated in the material as well as the surface modifications that were obtained at different ZnO quantities.

References
[1] S.M. Choi, K.M. Rao, S.M. Zo, E.J. Shin, S.S. Han, Polymers 14 (2022) 1080.
[2] U.V. Kumar, S. Narayanasamy, S. Uthandi, Food. Bioprod. Process. 154 (2025) 153-174.
[3] L. Rosson, B. Tan, W. Best, N. Byrne, Cellulose 31 (2024) 10165-10190.
[4] M. Wasim, M.R. Khan, M. Mushtaq, A. Naeem, M. Han, Q. Wei, Coatings 10 (2020) 364.
[5] F. Wahid, Y-.X. Duan, X-.H. Hu, L-.Q. Chu, S-.R. Jia, J-.D. Cui, C. Zhong, Int.J.Biol.Macromol. 132 (2019) 692-700.

METEOROLOGICAL DRIVERS OF PM2.5 POLLUTION IN CENTRAL EUROPEAN CITIES: AN EXPLAINABLE MACHINE LEARNING APPROACH

Marija Paunović [1], Srđan Svrzić[2], Nebojša M. Ralević[3], Ljubo Nedović[3]

[1]*Department of Natural Science, University of Kragujevac, Faculty of Hotel Management and Tourism, Vrnjačka Banja, Serbia*
[2]*Department of Wood Science and Technology University of Belgrade, Faculty of Forestry, Belgrade, Serbia*
[3]*Department of Fundamental Science, University of Novi Sad, Faculty of Technical Sciences, Novi Sad, Serbia*
e-mail: majap@rcub.bg.ac.rs

Abstract
Fine particulate matter (PM2.5) is a major indicator of urban air pollution, while its daily concentrations are influenced by meteorological conditions as well as emission and atmospheric processes. This study investigates the meteorological drivers of daily PM2.5 variability in four Central European cities—Vienna, Budapest, Prague, and Warsaw—using an explainable machine learning approach. Daily PM2.5 observations for 2020–2024 were combined with ERA5-Land meteorological data on air temperature, relative humidity, wind speed, and precipitation, resulting in 6,947 city-day observations. A pooled XGBoost model was trained on data from 2020–2023 and evaluated on the temporally independent 2024 test set. The model achieved an R^2 of 0.417, with RMSE of 6.51 μg/m³ and MAE of 4.57 μg/m³. SHAP analysis identified temperature and wind speed as the most influential predictors, although differences in importance among the four meteorological variables were relatively small. Lower temperatures and weaker winds were generally associated with higher predicted PM2.5 concentrations, whereas precipitation tended to reduce predicted concentrations. The model substantially underestimated elevated PM2.5 concentrations, indicating that meteorology alone is insufficient to fully represent such episodes.

Introduction

Fine particulate matter (PM2.5) is one of the most important indicators of ambient air pollution due to its adverse effects on human health. Because of their small aerodynamic diameter (≤2.5 μm), these particles can penetrate deeply into the respiratory system and are associated with substantial health risks. The World Health Organization (WHO) recommends an annual mean PM2.5 concentration of 5 μg/m³ and a 24-hour mean of 15 μg/m³ [1]. Despite improvements in air quality across many European regions, daily PM2.5 concentrations continue to exhibit substantial temporal and spatial variability.

Ambient PM2.5 concentrations result from a complex interplay between emission sources, atmospheric processes, and meteorological conditions. Temperature, relative humidity, wind speed, and precipitation can affect particle formation, accumulation, dispersion, and removal. These relationships are often nonlinear and may vary across locations and atmospheric conditions, making machine-learning approaches particularly useful for their analysis [2,5,6].

Among such approaches, Extreme Gradient Boosting (XGBoost) can effectively capture nonlinear relationships and interactions among environmental predictors [3]. However, predictive performance alone does not reveal how individual variables contribute to model predictions. SHapley Additive exPlanations (SHAP) provide an interpretable framework for quantifying the relative contribution and direction of individual predictors. Recent studies have demonstrated the usefulness of combining machine learning with SHAP for investigating factors associated with PM2.5 concentrations [5,6]. However, less attention has been given to

the cross-city performance and limitations of parsimonious meteorology-only models when evaluated on a fully withheld future period. This study therefore examines meteorological contributions to daily PM2.5 variability and the limits of meteorology-only prediction across Vienna, Budapest, Prague, and Warsaw using a temporally validated XGBoost–SHAP framework. Daily PM2.5 observations for 2020–2024 are combined with ERA5-Land data on air temperature, relative humidity, wind speed, and precipitation. The model is trained on 2020–2023 data and evaluated on the temporally independent 2024 period, while SHAP analysis is used to assess the importance and direction of meteorological contributions to predicted PM2.5 concentrations.

Experimental

Daily PM2.5 concentrations for 2020–2024 were obtained from the European Environment Agency (EEA) Air Quality Download Service using validated measurement data (E1a) [7]. Vienna, Budapest, Prague, and Warsaw were selected to provide a comparative sample of major Central European urban environments, subject to the availability and continuity of PM2.5 observations during 2020–2024. Four monitoring sites representing urban conditions and providing sufficient temporal coverage were selected: Vienna (AKH), Budapest (HU0056A), Prague (Praha 5-Stodůlky, ASTOA), and Warsaw (Warszawa-Ursynów, PL0141A). Measurements flagged as valid were retained. For Prague, where hourly PM2.5 observations were used, daily concentrations were calculated only for days with at least 18 valid hourly measurements. No missing PM2.5 values were imputed. The resulting dataset contained 6,947 valid city-day observations.

Meteorological data were obtained from the ERA5-Land hourly time-series dataset [8] for the geographical coordinates of each air-quality monitoring station. The nearest available ERA5-Land grid point was automatically selected for each station location. Four meteorological variables were considered: 2-m air temperature, relative humidity, 10-m wind speed, and total precipitation. Relative humidity was derived from hourly 2-m air temperature and dew-point temperature, while wind speed was calculated from the hourly 10-m zonal and meridional wind components. Temperature, relative humidity, and wind speed were subsequently averaged to daily values, whereas hourly precipitation was summed to obtain daily totals. Daily aggregation was performed according to UTC calendar days. PM2.5 and meteorological data were then merged by city and date.

A pooled XGBoost [3] regression model was developed to estimate daily PM2.5 concentrations from temperature, relative humidity, wind speed, precipitation, and city. City was represented by one-hot encoded categorical variables. To provide a temporal rather than random validation, observations from 2020–2023 (n = 5,523) were used for model training, while the entire year 2024 (n = 1,424) was reserved as an independent test period. Model performance was evaluated using the coefficient of determination (R^2), root mean squared error (RMSE), and mean absolute error (MAE).

The XGBoost model used 500 boosting trees, a maximum tree depth of 3, a learning rate of 0.05, subsampling rate of 0.8, and column subsampling rate of 0.8. A fixed random seed of 42 was used to ensure reproducibility.

SHAP [4] were calculated for the independent 2024 test set to interpret model predictions. Global importance was assessed using mean absolute SHAP values, while the distribution and direction of SHAP values were used to examine whether different levels of each meteorological predictor were associated with increases or decreases in predicted PM2.5 concentrations.

Results and discussion

Daily PM2.5 concentrations showed noticeable differences among the four cities during 2020–2024 (Table 1). The highest mean concentrations were observed in Warsaw (13.74 µg/m³) and

Budapest (13.63 µg/m³), followed by Prague (12.50 µg/m³), while Vienna had the lowest mean concentration (10.25 µg/m³). Warsaw also exhibited the highest maximum daily concentration (97.93 µg/m³), indicating considerable variability and the occurrence of pronounced pollution episodes.

Table 1. Study sample and PM2.5 descriptive statistics by city

City	PM2.5 obs.	Mean (µg/m³)	SD	Min	Max
Budapest	1,718	13.63	9.54	1.31	65.38
Prague	1,640	12.50	7.42	2.68	52.96
Vienna	1,818	10.25	7.06	0.51	56.19
Warsaw	1,771	13.74	9.10	0.40	97.93
Total	6,947	-	-	-	-

The pooled XGBoost model demonstrated moderate predictive performance on the temporally independent 2024 test set (R^2 = 0.417, RMSE = 6.51 µg/m³, and MAE = 4.57 µg/m³; Table 2). Predictive performance varied across cities, with the highest R^2 obtained for Budapest (0.570), followed by Vienna (0.421), Prague (0.263), and Warsaw (0.246). Vienna showed the lowest MAE (3.83 µg/m³). These differences indicate that the extent to which daily PM2.5 variability can be represented by the selected meteorological predictors is not uniform across the four urban environments. The lower performance in Prague and Warsaw may reflect a greater influence of unmodelled factors, such as local emissions, boundary-layer conditions, and regional pollutant transport, although these were not directly evaluated. Previous European-scale research has similarly demonstrated spatial heterogeneity in machine-learning estimates of daily PM2.5 [2].

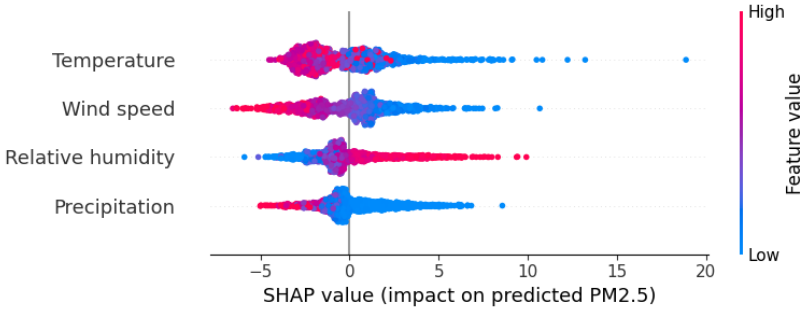
Table 2. XGBoost predictive performance on the independent 2024 test set

Sample	n	R^2	RMSE (µg/m³)	MAE (µg/m³)
Pooled	1,424	0.417	6.511	4.566
Budapest	356	0.570	6.754	5.018
Prague	341	0.263	6.750	4.468
Vienna	365	0.421	5.572	3.834
Warsaw	362	0.246	6.905	4.951

SHAP analysis provided further insight into the contribution of individual meteorological variables (Fig. 1). Temperature showed the highest global importance (mean |SHAP| = 1.941), closely followed by wind speed (1.879), relative humidity (1.666), and precipitation (1.465). The relatively small differences among these values suggest that daily PM2.5 variability was associated with a combination of meteorological conditions rather than being dominated by a single factor.

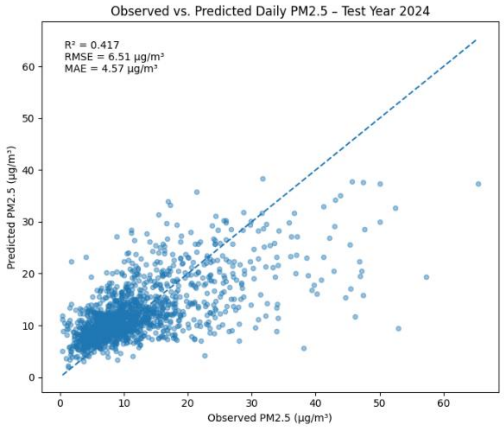
The direction of SHAP contributions revealed physically plausible patterns. Lower temperatures were generally associated with higher predicted PM2.5 concentrations, while higher temperatures tended to decrease model predictions. Stronger winds predominantly produced negative SHAP values, whereas weak winds contributed to increased predicted concentrations. This pattern is consistent with the role of wind in atmospheric dispersion and with recent explainable machine-learning studies identifying wind speed as an important meteorological driver of PM2.5 variability. Higher relative humidity was generally associated with increased predicted PM2.5, whereas higher precipitation tended to reduce predicted concentrations. These findings are broadly consistent with recent studies showing that temperature, humidity, wind and precipitation can exert important, nonlinear and location-dependent influences on PM2.5 concentrations [5,6].

Fig. 1. SHAP summary plot of meteorological predictors for the independent 2024 test set.



Despite capturing the general variation in daily PM2.5, the model showed a pronounced tendency to underestimate elevated PM2.5 concentrations (Fig. 2). Among the 65 test observations with measured PM2.5 concentrations ≥30 μg/m³, 96.9% were underestimated, with a mean prediction error (predicted − observed) of −16.21 μg/m³. This result indicates that the four basic meteorological variables and city information alone are insufficient to reproduce elevated PM2.5 concentrations. Such episodes may additionally depend on emission intensity, heating-related emissions, atmospheric stability, boundary-layer dynamics, secondary aerosol formation, and regional pollutant transport. Recent explainable machine-learning studies that jointly considered meteorological and emission-related variables have likewise shown that severe PM2.5 episodes cannot be attributed to meteorology alone [5,6].

Fig. 2. Observed versus XGBoost-predicted daily PM2.5 concentrations for the independent 2024 test set.



Overall, the results demonstrate that explainable machine learning can provide both predictive information and insight into the meteorological conditions associated with short-term PM2.5 variability. However, the findings should be interpreted as model-based associations rather than causal effects. The use of gridded ERA5-Land meteorology, representation of each city by a single monitoring site, differences in site classification, and the absence of direct emission and atmospheric-chemistry variables represent the main limitations.

Conclusion

This study applied an explainable machine-learning framework to investigate the meteorological factors associated with daily PM2.5 variability in four Central European cities. The XGBoost model demonstrated that basic meteorological conditions contain meaningful information for predicting day-to-day PM2.5 concentrations, although predictive performance varied across cities. SHAP analysis showed that temperature and wind speed were the most influential meteorological predictors, closely followed by relative humidity and precipitation. Colder conditions and weaker winds were generally associated with higher predicted PM2.5 concentrations, while precipitation tended to contribute to lower predictions. At the same time,

the pronounced underestimation of elevated PM2.5 concentrations indicates that meteorological variables alone cannot fully represent such episodes. Future models should therefore incorporate emission-related variables, atmospheric boundary-layer characteristics, and regional pollutant transport.

Acknowledgements
This research was partly supported by the Science Fund of the Republic of Serbia, GRANT No. 7632, Project "Mathematical Methods in Image Processing under Uncertainty"-MaMIPU. This research is supported by the Ministry of Science, Technological Development and Innovation of the Republic of Serbia by the Decision on the scientific research funding for teaching staff at the accredited higher education institutions in 2026 (No. 451-03-34/2026-03/200375, 451-03-34/2026-03/200156 and 451-03-65/2024-03/200169).

References
[1] World Health Organization, WHO global air quality guidelines: particulate matter (PM2.5 and PM10), ozone, nitrogen dioxide, sulfur dioxide and carbon monoxide, World Health Organization, Geneva, 2021.
[2] S. Shetty, P.D. Hamer, K. Stebel, A. Kylling, A. Hassani, T.K. Berntsen, P. Schneider, Daily high-resolution surface PM2.5 estimation over Europe by ML-based downscaling of the CAMS regional forecast, Environmental Research 264 (2025) 120363. https://doi.org/10.1016/j.envres.2024.120363
[3] T. Chen, C. Guestrin, XGBoost: A scalable tree boosting system, Proceedings of the 22nd ACM SIGKDD International Conference on Knowledge Discovery and Data Mining, 2016, pp. 785-794. https://doi.org/10.1145/2939672.2939785
[4] S.M. Lundberg, S.-I. Lee, A unified approach to interpreting model predictions, Advances in Neural Information Processing Systems 30 (2017) 4765-4774.
[5] C. Zhao, Z. Lin, L. Yang, M. Jiang, Z. Qiu, S. Wang, Y. Gu, W. Ye, Y. Pan, Y. Zhang, T. Wang, Y. Jia, Z. Chen, A study on the impact of meteorological and emission factors on PM2.5 concentrations based on machine learning, Journal of Environmental Management 376 (2025) 124347. https://doi.org/10.1016/j.jenvman.2025.124347
[6] Q. Yang, J. Gao, J. Chen, T. Ma, H. Xu, F. Wang, Y. Wei, J. Liu, Q. Sun, Y. Feng, G. Shi, Interpretable machine learning for exploring multiple influencing factors of PM2.5 and their interaction effects, Journal of Environmental Sciences (2026) 105560. https://doi.org/10.1016/j.jes.2026.105560.
[7] European Environment Agency (EEA) Air Quality Download Service using validated measurement data (E1a)
[8] Copernicus Climate Change Service, Climate Data Store, (2025): ERA5 Land hourly time-series data from 1950 to present. Copernicus Climate Change Service (C3S) Climate Data Store (CDS). DOI: 10.24381/ee82e357

PREPARATION AND COMPREHENSIVE CHARACTERIZATION OF TWELVE NOVEL PANTHENOL-BASED NATURAL DEEP EUTECTIC SYSTEMS (NADES) FOR RESVERATROL SOLUBILIZATION

Milica Petković[1,2], Branko Kordić[2], Branislav Jović[2], Boris M. Popović[1]

[1] *University of Novi Sad, Faculty of Agriculture, Trg Dositeja Obradovića 8, Novi Sad, Serbia*
[2] *University of Novi Sad, Faculty of Sciences, Trg Dositeja Obradovića 3, Novi Sad, Serbia*
e-mail: milica.petkovic@polj.edu.rs

Natural Deep Eutectic Solvents (NADES) represent green solvents formed via hydrogen bonding between hydrogen bond donors (HBD) and acceptors (HBA). Previous studies have demonstrated that hydrophilic NADES are successfully applied to enhance the solubility of resveratrol, a bioactive polyphenol whose therapeutic and cosmetic potential is severely constrained by its poor aqueous solubility [1]. D-panthenol, as an alcoholic analogue of vitamin B5 and a precursor to coenzyme A, presents a suitable structural component for NADES formulation, combining tissue-regenerative properties [2] and functional groups capable of establishing a hydrogen-bonding network. To overcome these limitations, this study focuses on the preparation and comprehensive characterization of novel panthenol-based NADES systems as eco-friendly delivery vehicles. Twelve distinct panthenol-based NADES were successfully synthesized via an ultrasound-assisted method by combining panthenol with urea, glycerol, proline, betaine, choline chloride, 1,2-propanediol, sorbitol, citric acid, lactic acid, tartaric acid, malic acid, or mandelic acid. All systems were prepared at a 1:1 molar ratio with the addition of 20% water (wt%). The structural integrity and intermolecular interactions within the systems were confirmed via Fourier-transform infrared spectroscopy (FT-IR), which demonstrating the successful formation of NADES via intermolecular interactions, with no side reactions or new compounds formed. Furthermore, the prepared NADES systems exhibited densities from 1.08g/mL to 1.22g/mL, conductivities from 0.22 to 16.69 mS cm^{-1}, pH values from 1.92 to 9.88, and polarity values spanning from 47.76 to 49.87 kcal mol^{-1}, all measured at 24 ± 1 °C. Resveratrol solubility across all 12 NADES systems, water, and organic solvents (ethanol, methanol and dimethyl sulfoxide DMSO) was evaluated by adding an excess of resveratrol (100 mg/mL) under continuous stirring at 25 °C for 2 hours. Among the tested conventional solvents, DMSO exhibited the highest solubilization capacity (99.94 ± 3.52 mg/mL), followed by ethanol (97.59 ± 0.41 mg/mL) and methanol (76.87 ± 3.82 mg/mL), while the solubility in pure water was extremely low (0.0306 ± 0.0010 mg/mL). Notably, the highest resveratrol solubility among the eutectic media was achieved by panthenol:betaine NADES 89.00 ± 6.94 mg/mL, followed by panthenol:choline chloride NADES 88.25 ± 2.37 mg/mL and panthenol:proline NADES 85.96 ± 5.62 mg/mL. These panthenol-NADES formulations dissolved resveratrol better than methanol and water, reaching efficiency close to ethanol and DMSO. Therefore, they represent a safe, non-toxic, and biocompatible alternative.

Acknowledgements
The authors would like to thank the Ministry of Science, Technological Development and Innovation of the Republic of Serbia for financial support through Contract No. 451-03-34/2026-03/200117 and 451-03-33/2026-03/200117 .

References
[1] Uka, D., Blagojević, B., Alioui, O., Boublia, A., Elboughdiri, N., Benguerba, Y., ... & Popović, B. M. (2023). An innovative and environmentally friendly approach for resveratrol

solubilization and bioaccessibility enhancement by using natural deep eutectic solvents. Journal of Molecular Liquids, 391, 123411.
[2] Zheng, P., Ren, J., Zheng, J., Liu, F., Han, X., & Yu, B. (2025). De novo biosynthesis of D-panthenol in engineered E. coli with rationally designed L-homoserine decarboxylase. Metabolic Engineering.

FROM BERRY TO BIOACTIVE: EXPLORING THE POTENTIAL OF A BERRY EXTRACT AS A MICROBIOME-FRIENDLY COSMETIC INGREDIENT

Anja Petrov Ivanković[1], Marija Ćorović[2], Ana Milivojević[2], Ana Vukoičić[1], Milica Veljković[1], Dejan Bezbradica[2]

[1]Innovation Centre of Faculty of Technology and Metallurgy, Belgrade, Serbia
[2]University of Belgrade, Faculty of Technology and Metallurgy, Belgrade, Serbia
e-mail: apetrov@tmf.bg.ac.rs

Abstract

The skin microbiota plays a crucial role in maintaining cutaneous homeostasis, and selective modulation of microbial communities has emerged as a promising strategy for the development of microbiome-friendly cosmetic ingredients [1]. Plant polyphenols are increasingly recognized as multifunctional bioactive compounds in skin care due to their antioxidant properties and their potential contribution to the maintenance of cutaneous homeostasis [2]. In this study, a phenolic-rich blackcurrant extract obtained by enzyme-assisted extraction was evaluated for its effects on representative skin microorganisms and healthy skin microbiota sample. Biological activity was investigated using a simplified *in vitro* stratum corneum model consisting of agar overlaid with callus, which provides a physiologically relevant nutrient environment for microbial growth. At low concentrations (5–10 µg GAE/mL), the extract significantly enhanced the viability of the commensal bacterium *Staphylococcus epidermidis*, increasing its growth by 50 % compared to the control. In contrast, the opportunistic pathogen *Staphylococcus aureus* was inhibited across the tested concentration range, with the strongest effect observed at 25 µg GAE/mL. The response of *Cutibacterium acnes* was concentration-dependent, with no significant effect observed at lower concentration and reduced growth at higher polyphenol concentration. When applied to a skin microbiota sample, the extract did not significantly affect total aerobic or anaerobic microbial counts. However, a significant increase (~45 %) in coagulase-negative bacteria was observed at 5 µg GAE/mL, indicating a selective stimulation of beneficial commensal populations without disturbing overall microbial balance. The ability of the blackcurrant extract to stimulate commensal bacteria while suppressing opportunistic pathogens highlights its potential to support microbiome equilibrium. Such selective modulation may help restore microbial balance in dysbiosis-associated skin conditions, including atopic dermatitis and acnes, supporting its use as a microbiome-friendly cosmetic ingredient.

Acknowledgements

This work was funded by the Ministry of Science, Technological Development, and Innovation of the Republic of Serbia (contract no. 451-03-33/2026-03/200287 and 451-03-34/2026-03/200135).

References

[1] K. Wojciechowska, K. Dos Santos Szewczyk. Molecules 30 (2025) 4363.
[2] O.V. Zillich, U. Schweiggert-Weisz, P. Eisner, M. Kerscher. *Int J Cosmet Sci* 37 (2015) 5.

TEMPERATURE DEPENDENCE OF THE CRITICAL MICELLE CONCENTRATION OF SELECTED SURFACTANTS IN AQUEOUS ELECTROLYTE AND POLYMER-CONTAINING SOLUTIONS

Ana Pilipović, Zita Farkaš Agatić, Kosta Popović, Vesna Tepavčević, Mihalj Poša

Department of Pharmacy, Faculty of Novi Sad, University of Novi Sad, Hajduk Veljkova 3, 21000 Novi Sad, Serbia
e-mail: ana.pilipovic@mf.uns.ac.rs

Abstract
The temperature dependence of the critical micelle concentration (CMC) of sodium cholate (SC), sodium decyl sulfate (SDS) and Brij S20 (BS20) was investigated in aqueous media and in the presence of NaCl, CsCl and Pluronic F68. CMC values were determined by pyrene fluorescence spectroscopy over the temperature range 278.15–303.15 K. In pure water, SC and SDS exhibited opposite temperature dependences, with increasing and decreasing CMC values, respectively, whereas BS20 showed only minor changes. Both electrolytes substantially decreased the CMC of all surfactants, with CsCl producing lower CMC values than NaCl for SC and SDS. Pluronic F68 further modified the micellization behavior, with effects depending on surfactant type, polymer concentration and electrolyte composition. The combined effects of F68 and electrolytes were non-additive, indicating complex interactions among surfactant, polymer, electrolyte and water. These findings demonstrate that temperature and solution composition can markedly influence surfactant self-assembly in complex aqueous media.

Introduction
Surfactants are amphiphilic compounds that self-assemble into micelles in aqueous media above the critical micelle concentration (CMC), which is an important parameter for characterizing surfactant aggregation. The CMC is affected by several factors, including surfactant structure, temperature, electrolyte composition and the presence of other solutes or polymers [1]. In particular, electrolytes can modify the interactions between charged surfactant head groups and influence the micellization process, while polymeric additives may introduce additional surfactant–polymer interactions. The aim of this study was to investigate the temperature dependence of the CMC of sodium cholate (SC), sodium decyl sulfate (SDS) and Brij S20 (BS20) in aqueous media and to evaluate the individual and combined effects of NaCl, CsCl and Pluronic F68.

Experimental
CMC values were determined in pure water, in aqueous solutions containing 300 mM NaCl or 300 mM CsCl, and in solutions containing 1 wt% or 5 wt% Pluronic F68. Additional measurements were performed in mixed media containing 5 wt% F68 with 300 mM NaCl or 300 mM CsCl. All systems were investigated at six temperatures between 278.15 and 303.15 K (5–30 °C). CMC values were determined by spectrofluorimetric measurements using pyrene as a polarity-sensitive fluorescent probe. The first (I_1) and third (I_3) vibronic bands of pyrene were monitored at 373 and 384 nm, respectively, and the I_1/I_3 ratio was plotted as a function of surfactant concentration. The CMC was determined from the inflection point of the resulting sigmoidal curves by Boltzmann fitting using OriginLab 9 software [2,3] (Figure 1.).

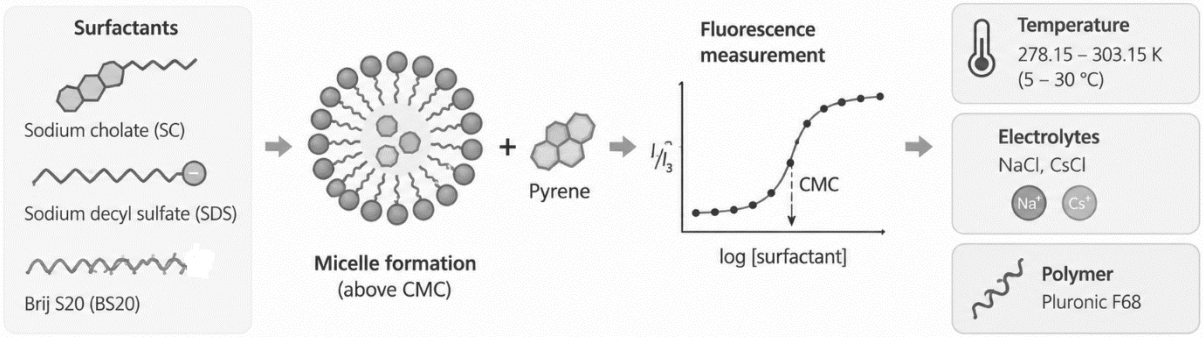


Figure 1. Schematic representation of experimental conditions and methodology for the determination of critical micelle concentration (CMC).

Results and discussion

The obtained results presnted on the Figure 2 revealed pronounced surfactant-specific and medium-dependent temperature effects. In pure water, SC and SDS exhibited opposite temperature dependences of the CMC, with the CMC of SC increasing from approximately 14.8 to 16.3, whereas that of SDS decreased from approximately 32.2 to 29.0 over the investigated temperature range. BS20 showed comparatively small changes in CMC. The addition of 300 mM NaCl or CsCl substantially decreased the CMC values of all three surfactants. Moreover, CsCl produced lower CMC values than NaCl for SC and SDS, indicating that the nature of the electrolyte and, in particular, the identity of the counterion, influences the aggregation behavior. The presence of F68 further modified the micellization behavior, with the magnitude and direction of the effect depending on surfactant type and F68 concentration. Particularly pronounced changes were observed for SDS in F68-containing media, while SC exhibited a distinct temperature dependence in the presence of 5 wt% F68 and CsCl. The combined effects of F68 and electrolytes were not simply additive, demonstrating that the micellization behavior is governed by complex interactions between surfactant, polymer, electrolyte and water.

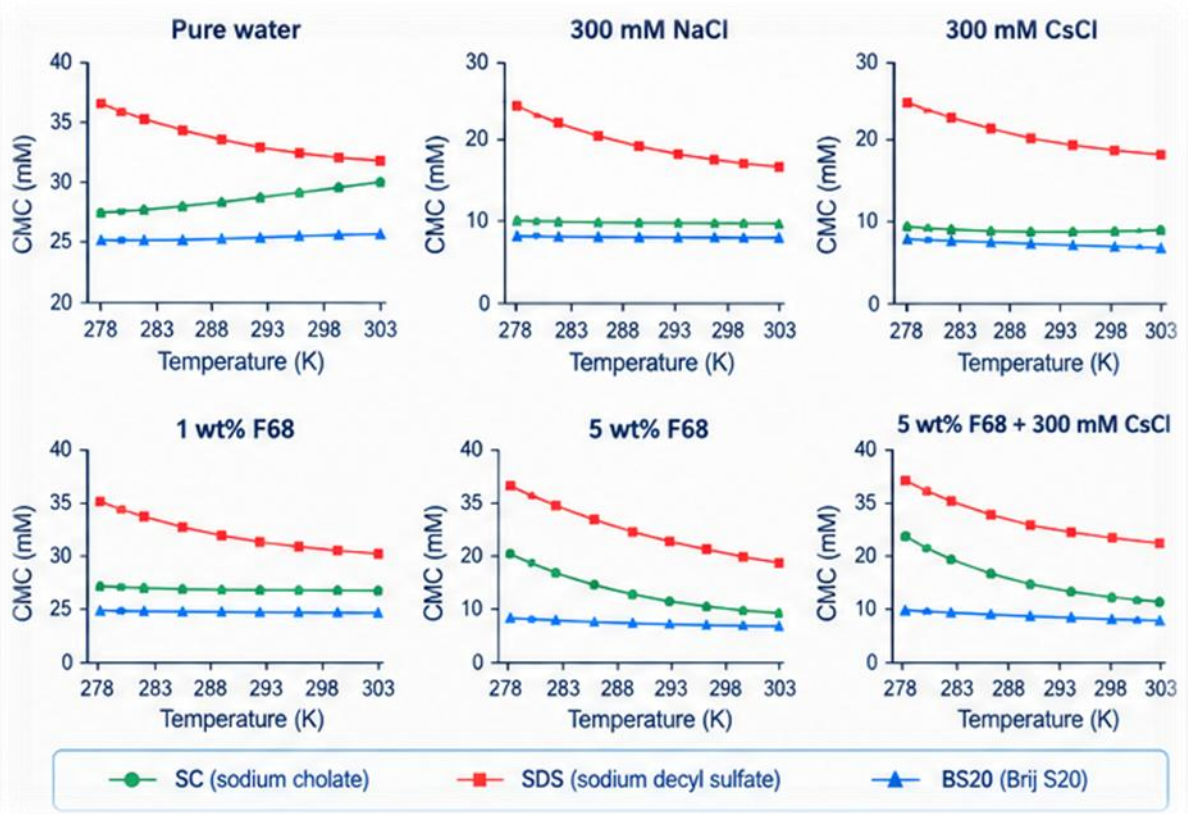


Figure 2. Temperature dependance of CMC

Conclusion

These findings demonstrate that temperature, electrolyte identity and polymer concentration can strongly modulate surfactant micellization and that their combined effects are highly dependent on surfactant structure. The results provide insight into the physicochemical factors governing surfactant self-assembly in complex aqueous media.

Acknowledgements

This research was carried out within the project "Development of Innovative Pharmaceutical-Technological Preparations for the Pediatric Population in the Republic of Serbia" ("Razvoj inovativnih farmaceutsko-tehnoloških preparata za pedijatrijsku populaciju u Republici Srbiji"), funded by the Provincial Secretariat for Higher Education and Scientific Research of the Autonomous Province of Vojvodina, Republic of Serbia, under Project No. 003817825 2025 09418 003 000 000 001.

References

[1] Y. Moroi, Adv. Colloid Interface Sci. 45 (1993) 1.
[2] A. Mohr, P. Talbiersky, H.-G. Korth, R. Sustmann, R. Boese, D. Bläser, H. Rehage, J. Phys. Chem. B 111 (2007) 12985.
[3] K. Popović, Z. Farkaš Agatić, A. Pilipović, M. Poša, Int. J. Mol. Sci. 27 (2026) 6284.

CATALYST EXTRUDATE DEVELOPMENT FOR DIRECT CO_2 HYDROGENATION

Ádám Pitó[1], András Sápi[1], Imre Szenti[1,2] , Ákos Kukovecz[1], Zoltán Kónya[1,2]

[1]University of Szeged, Department of Applied and Environmental Chemistry, H-6720, Rerrich Béla square 1, Szeged, Hungary
[2] HUN-REN–SZTE Reaction Kinetics and Surface Chemistry Research Group, H-6720, Szeged, Hungary
e-mail: pito.adam@chem.u-szeged.hu

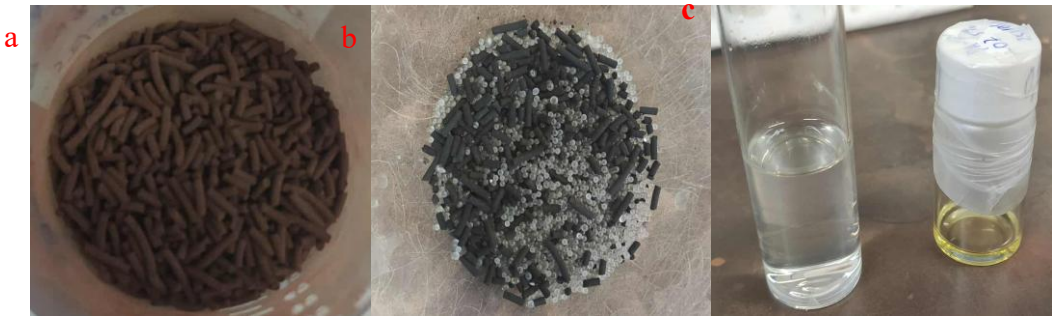
Abstract

Anthropogenic CO_2 emissions represent both a climate protection challenge and a potential source of raw materials. Due to the stability of carbon dioxide, a catalyst is required for its activation and conversion. Modified iron oxide-based catalysts offer a cost-effective option for CO_2 hydrogenation, with high conversion and favorable selectivity. In our research group's previous work, we successfully synthesized the mixed iron oxide catalyst precursor and, from it, the sodium-promoted Na-Fe_3O_4 catalyst. For industrial-scale application, it became necessary to scale up the synthesis, during which we developed the technological steps required for the production of large quantities of the catalyst [1–3]. Upscaled catalyst testing occours in the 'Energy Innovation Test Station' – EIT (1. figure), where industrial scale fuel prodiction happens.



1.figure: EIT test station for industral catalyst testing

This study focuses on the production of extrudates from catalyst powder, their optimization, and their structural and catalytic characterization (2. figures).



2. figure: a) Fresh catalyst extrudate, b) spent catalyst extrudate, c) produced e-fuel

During the extrusion process, I prepared samples containing various amounts of inorganic binder (1–33%) and then examined their mechanical stability and catalytic

performance. Based on the experimental results, it was possible to determine the optimal range (5–10% binder) in which the catalyst extrudate exhibits both stable mechanical properties and acceptable catalytic activity. For further fine-tuning, I used a restricted mixture design, which allowed me to determine the ideal ratios of inorganic and organic binders, as well as the catalyst powder. This second set of extrudets were more focused on finding the optimal mixture ratios, while the same catalytic, mechanichal and characterization steps were taken, paving the way for further extrudate developement.

References

[1] Najari, Sara, et al. "Synergistic enhancement of CO2 hydrogenation to C5+ hydrocarbons using mixed Fe5C2 and Na-Fe3O4 catalysts: effects of oxide/carbide ratio, proximity, and reduction." Chemical Engineering Journal 485 (2024): 149787.
[2] Khoshroo, Ghazaleh, et al. "Pure Ni-based and trimetallic Ni-Co-Fe catalysts for the dry reforming of methane: Effect of K promoter and the calcination temperature." Catalysis Letters 153.9 (2023): 2755-2762.
[3] Boldizsár, Tamás, et al. "Optimalization of ceramic-based noble metal-free catalysts for CO oxidation reactions." Reaction Kinetics, Mechanisms and Catalysis 135.2 (2022): 575-587.

INFLUENCE OF CONVECTIVE DRYING ON THE BIOACTIVE POTENTIAL OF GRAPE POMACE WITHIN A CIRCULAR ECONOMY FRAMEWORK

Mariana-Atena Poiana[1], Diana Moigradean[1*], Andreea Ghitulescu[1], Florina Radu[1], Daniela Stoin[1], Corina Megyesi[1], Ariana Velciov[1], Despina Bordean[1], Sofia Popescu[1], Mihaela Lacatus[1], Antoanela Cozma[2], Laura Radulescu[1], Alexandru Rinovetz[1]

[1]Faculty of Food Engineering, University of Life Sciences "King Mihai I" from Timisoara, Calea Aradului No. 119, 300645 Timisoara, Romania
[2]Faculty of Agriculture, University of Life Sciences "King Mihai I" from Timisoara, Calea Aradului No. 119, 300645 Timisoara, Romania
[*] corresponding author, e-mail: dianamoigradean@usvt.ro

Abstract
This study investigates the influence of convective drying on the bioactive potential of grape pomace (GP) from the *Feteasca Neagra* variety, with emphasis on its sustainable valorization within a circular economy framework. GP, the main by-product of the winemaking process, consists mainly of skins and seeds and represents a valuable source of naturally occurring bioactive compounds. However, its high moisture content limits its stability and further utilization. Therefore, to ensure the chemical, biochemical, and microbiological stability of GP for its subsequent use as an ingredient in various food applications, the effects of different convective drying conditions on the preservation of bioactive properties were evaluated. The results showed that drying at 60°C for 16 h reduced the moisture content to below 5%, providing a material suitable for subsequent storage and valorization. Although convective drying led to losses in antioxidant capacity and bioactive compound content, the dried GP retained considerable bioactive potential. Increasing the drying temperature resulted in more pronounced losses, highlighting the importance of selecting appropriate processing conditions to balance effective moisture removal with the preservation of bioactive properties. The findings demonstrate that controlled convective drying represents a suitable conditioning strategy for transforming GP from a perishable winery by-product into a stable and valuable raw material. Its valorization may contribute to reducing winery waste and promoting development of value-added food ingredients in accordance with circular economy principles.

Introduction
The wine sector is an important component of the food industry, particularly in countries with favorable conditions for viticulture. Romania is one of the major wine-producing countries in Europe and is recognized for its native grape varieties. Among these, Feteasca Neagra is highly valued for its technological characteristics and for producing red wines rich in phenolic compounds, anthocyanins, and aromatic constituents [7]. Winemaking generates substantial amounts of by-products, among which grape pomace represents the main solid fraction, consisting primarily of skins, seeds, stems, and residual pulp after pressing [8]. Grape pomace accounts for approximately 20–30% of the processed grape mass, depending on cultivar, maturity stage, and vinification technology [5, 6, 13]. Traditionally, it has been used for distillate production, animal feed, or organic fertilizers [3, 12]. However, after red grape vinification, significant amounts of phenolic compounds and anthocyanins remain in the skin and seed matrices [14,15], making this by-product a valuable source of bioactive compounds with potential for further valorization [1]. The high moisture content of fresh grape pomace limits its storage stability and promotes biochemical deterioration and microbial spoilage. Dehydration is therefore an important stabilization step, as moisture removal contributes to reducing water activity and extending storage life [10]. However, drying may also affect

thermally sensitive bioactive compounds, making the selection of appropriate processing parameters essential to achieve effective stabilization while minimizing bioactive losses [6]. Assessment of antioxidant capacity, total phenolic content, and anthocyanin content provides relevant information on GP quality and its potential as a value-added food ingredient [6, 7]. Therefore, this study aimed to evaluate the influence of convective drying conditions on the physicochemical characteristics and bioactive potential of *Feteasca Neagra* GP, with emphasis on identifying suitable processing parameters for stabilization while preserving its bioactive constituents.

Experimental

Convective drying of grape pomace

Grape pomace (GP) from the Feteasca Neagra variety, originating from the Recas viticultural area in Western Romania (Timis County), was used in this study. Prior to processing, fresh GP was stored at −18°C. Convective drying was performed in a Froilabo AC60 laboratory oven (France, 1000 W). In the first experimental stage, GP was dried at 60 and 70°C for 4 and 8 h. The effect of these drying conditions on the preservation of bioactive potential was assessed by determining ferric reducing antioxidant power (FRAP), total phenolic content (TPC), and total monomeric anthocyanin content (TMA). Based on the results of this preliminary screening, 60°C was selected for further conditioning, as it provided the highest retention of the investigated bioactive parameters. GP was subsequently dried at 60°C until a residual moisture content below 5% was achieved, requiring a total drying time of 16 h. After drying, GP was ground using a Grindomix Retsch GM 200 laboratory mill. The resulting powder was characterized in terms of proximate composition, FRAP, TPC, and TMA.

Analytical procedures

Fresh and dried GP samples were analyzed for proximate composition, TPC, TMA, and FRAP value. The proximate composition of GP, including moisture, ash, crude protein, and fat contents, was determined according to official AOAC methods [2].

Preparation of hydroalcoholic extracts for phytochemical and antioxidant analyses. Hydroalcoholic extracts were prepared by adding 20 mL of 45% (v/v) ethanol to 2 g of GP. The mixture was continuously stirred for 120 min at 25°C to promote the extraction of bioactive compounds. Subsequently, the suspension was centrifuged at approximately 4000 rpm for 10–15 min, and the resulting supernatant was collected [7]. The remaining solid residue was subjected to a second extraction under the same conditions, followed by centrifugation. The supernatants obtained from the two extraction steps were combined and homogenized and subsequently used for the determination of TPC, TMA, and FRAP.

Determination of total phenolic content. TPC of the GP extracts was determined using the Folin–Ciocalteu method. The hydroalcoholic extracts were diluted 1:10 (v/v), mixed with Folin–Ciocalteu reagent and sodium carbonate, and incubated for 30 min at 50°C. Absorbance was measured at 750 nm, and TPC was quantified using a gallic acid calibration curve [11] and expressed as mg gallic acid equivalents (GAE)/100 g dry weight (d.w.) of sample.

Determination of total monomeric anthocyanin content. TMA of the grape pomace extracts was determined using the pH differential method. The difference in absorbance between the two pH conditions was used for quantification, and TMA was calculated using an adapted Beer–Lambert law equation [9]. Results were expressed as mg cyanidin-3-glucoside (C3G) equivalents per 100 g d.w.

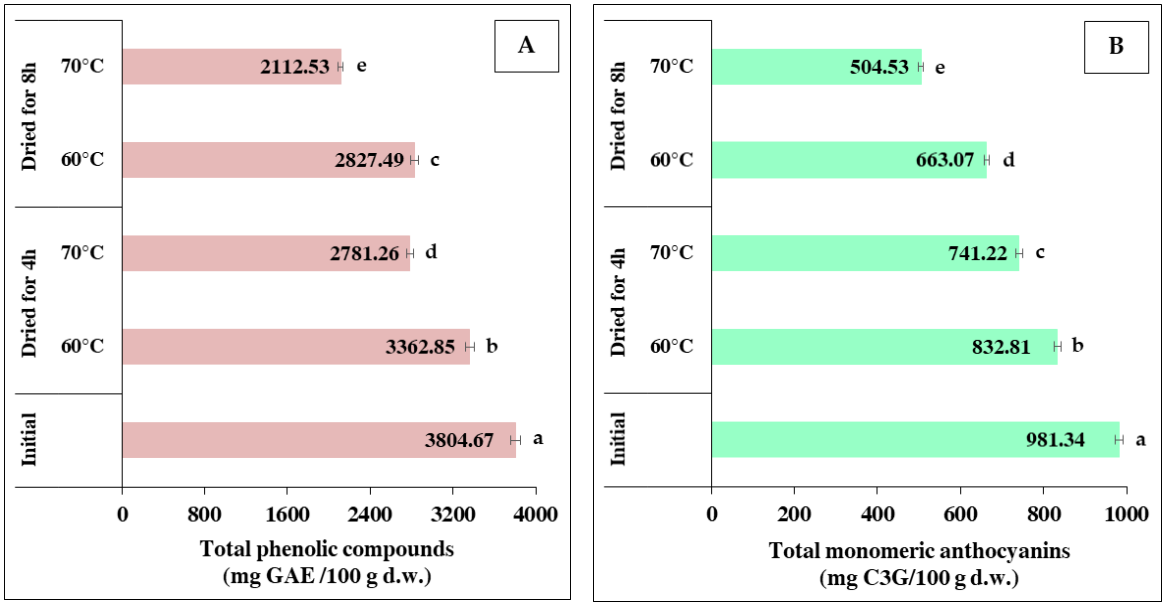
Antioxidant capacity. The antioxidant capacity of the GP extracts was determined by the FRAP assay, measuring the Fe^{2+}–TPTZ complex at 593 nm after 30 min of incubation at 37°C. Results were quantified using a $FeSO_4$ calibration curve [4] and expressed as µmol Fe^{2+}/g d.w.

Statistical analysis

All results were expressed as mean ± standard deviation (SD) of triplicate determinations (n = 3). Differences among samples were evaluated using one-way analysis of variance (ANOVA). Statistical significance was established at $p < 0.05$.

Results and discussion

Figure 1 illustrates the effect of drying temperature and time on the bioactive potential of Feteasca Neagra GP, expressed as total phenolic content (TPC, Figure 1A), total monomeric anthocyanin content (TMA, Figure 1B), and antioxidant capacity (FRAP, Figure 1C).



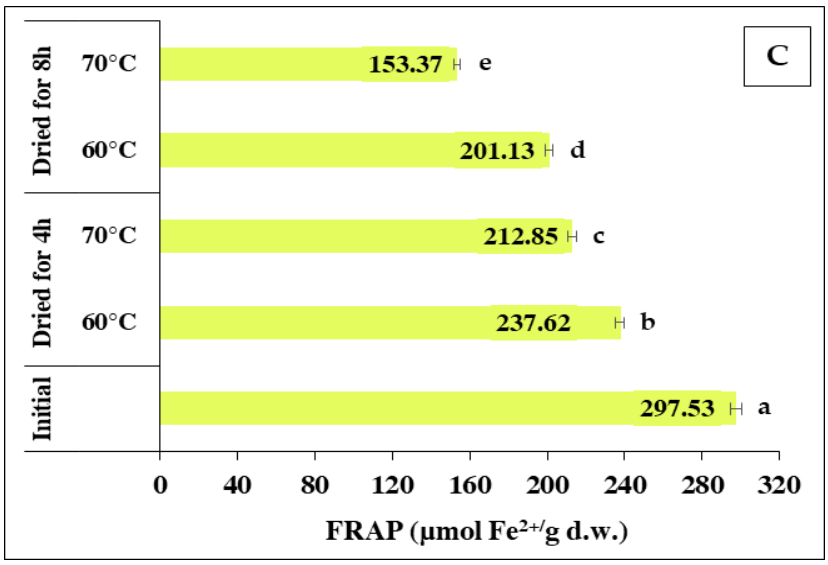


Figure 1. Effect of drying conditions on TPC (A), TMA (B), and FRAP value (C) of Feteasca Neagra GP. Different letters (a–e) indicate significant differences among samples ($p < 0.05$).

In all cases, convective drying resulted in a progressive decrease in the analyzed parameters compared with the fresh GP, and the magnitude of this reduction depended on both temperature and drying time. The fresh GP exhibited an initial TPC of 3804.67 mg GAE/100 g d.w., a TMA content of 981.34 mg C3G/100 g d.w., and a FRAP value of 297.53 µmol Fe^{2+}/g d.w., confirming the substantial bioactive potential characteristic of red grape-derived matrices [6, 7]. After drying at 60°C for 4 and 8 h, TPC decreased by 11.6% and 25.7%, respectively, while TMA declined by 15.1% and 32.4%, and FRAP by 20.1% and 32.4%. At 70°C, the reductions were more pronounced, reaching 26.9% and 44.5% for TPC, 24.5% and 48.6% for TMA, and 28.5% and 48.5% for FRAP after 4 and 8 h, respectively. The marked decrease in TMA at the higher temperature is consistent with the known thermal sensitivity of anthocyanins, whose degradation is intensified by increased temperature and prolonged heat exposure [6, 7].

The results demonstrate that increasing drying temperature and exposure time negatively affected the retention of TPC, TMA and antioxidant capacity in GP. Drying at 60 °C for 4 h provided the best preservation, whereas the greatest losses occurred at 70 °C for 8 h. Therefore, 60 °C was selected for further conditioning of GP to a residual moisture content below 5%.

The proximate composition of GP in the fresh state and after convective drying at 60°C for 16 h is presented in Table 1. The results indicate substantial changes in the proximate composition of GP following convective drying. Fresh GP exhibited a moisture content of 59.39%, which decreased to 4.78% after drying at 60°C for 16 h. This value was below the targeted 5% threshold and supports improved storage stability of the conditioned material [13]. Moisture removal resulted in a relative increase in the proportion of solid constituents. Accordingly, ash content increased from 2.73 to 6.71%, crude protein from 5.22 to 13.69%, fat from 3.31 to 8.54%, and carbohydrates from 29.35 to 66.28%. These increases primarily reflect the concentration effect associated with water removal. Convective drying effectively reduced the moisture content of *Feteasca Neagra* GP and produced a material suitable for subsequent use as a value-added food ingredient.

Table 1. Proximate composition of fresh and conditioned Feteasca Neagra GP

Sample	Moisture (%)	Ash (%)	Crude protein (%)	Fat (%)	CRB (%)
Fresh GP	59.39 ± 0.15	2.73 ± 0.04	5.22 ± 0.09	3.31 ± 0.10	29.35 ± 0.12
Dried GP	4.78 ± 0.07	6.71 ± 0.06	13.69 ± 0.11	8.54 ± 0.08	66.28 ± 0.14

Values are expressed as % of the sample. CRB: carbohydrates calculated by difference.

Table 2 compares the bioactive potential of fresh and dried GP after drying at 60°C for 16 h.

Tabelul 2. Influence of convective drying (60°C, 16 h) on the bioactive potential of GP

Sample	TPC (mg GAE/100 g d.w.)	TMA (mg C3G /100 g d.w.)	FRAP (µmol Fe^{2+}/g d.w.)
Fresh GP	3804.67 ± 3.09	981.34 ± 2.56	297.53 ± 2.43
Dried GP	2315.61 ± 2.63	539.95 ± 2.19	163.93 ± 1.82

Drying resulted in a marked decrease in all investigated parameters. FRAP was reduced from 297.53 to 163.93 µmol Fe^{2+}/g d.w., while TPC declined from 3804.67 to 2315.61 mg GAE/100 g d.w. A similar trend was observed for TMA, which decreased from 981.34 to 539.95 mg C3G/100 g d.w. Despite these reductions, the dried GP retained considerable phenolic content and antioxidant capacity, preserving a substantial proportion of its bioactive potential, in agreement with previous findings [6, 7].

Conclusion

The findings provide evidence that *Feteasca Neagra* grape pomace is a valuable source of bioactive compounds, with high phenolic and monomeric anthocyanin contents and antioxidant capacity. Preliminary drying trials showed that increasing temperature and prolonged exposure time negatively affected these parameters, with 60°C ensuring better retention than 70°C. Consequently, 60°C was selected for conditioning. Drying for 16 h reduced the moisture content from 59.39% to 4.78%, reaching the targeted level below 5% and improving storage suitability. Although drying at 60°C for 16 h decreased TPC, TMA, and FRAP values, the conditioned GP retained substantial bioactive potential. Moisture removal also increased the relative proportion of the major solid constituents. Controlled convective drying at 60°C therefore represents a suitable conditioning strategy for *Feteasca Neagra* GP, providing effective moisture reduction while preserving relevant bioactive properties. The resulting material shows potential for valorization as a value-added food ingredient, supporting the sustainable use of winery by-products within a circular economy framework.

Acknowledgements

The authors express their gratitude for the technical support provided by the University of Life Sciences "King Mihai I" from Timisoara, Faculty of Food Engineering.

References

[1] B. Antonić, S. Jančíková, D. Dordević, B. Tremlová, Foods. 9 (2020) 1627.
[2] AOAC. Determination of Moisture, Ash, Protein and Fat in: Official Method of Analysis of the Association of Analytical Chemists. 18th Edition, AOAC, Washington DC. 2005.
[3] I.S. Arvanitoyannis, A. Kassaveti, S. Stefanatos, Int. J. Food Sci. Technol. 42 (2007) 852-867.
[4] I.F. Benzie, J.J. Strain, Anal Biochem. 239 (1996) 70-76.
[5] C. Beres, G.N. Costa, I. Cabezudo, N.K. da Silva-James, A.S. Teles, A.P. Cruz, S.P. Freitas, Waste Manag. 68 (2017) 581-594.
[6] Y., Carmona-Jiménez, M. V., García-Moreno,., C. García-Barroso. Plant Foods Hum. Nutr., 73 (2018), 74-81.
[7] C. Gaita, E. Alexa, I. Popescu, S. Popescu, M. Negrea, M.A. Poiana, J. Agroaliment. Processes Technol. 23 (2017) 141-147.

[8] L. Laguna, B. Bartolomé, M.V. Moreno-Arribas. Trends Food Sci. Technol. 59 (2017) 49-59.
[9] J. Lee, R.W. Durst, R.E. Wrolstad, J. AOAC Int. 88 (2005) 1269.
[10] T. Maier, A. Schieber, D.R. Kammerer, R. Carle, Food Chem. 112 (2009) 551-559.
[11] V.L. Singleton, R. Orthofer, R.M. Lamuela-Raventós, Methods Enzymol. 299 (1999) 152-178.
[12] G. Spigno, L. Marinoni, G.D. Garrido. State of the art in grape processing by-products in Handbook of Grape Processing By-Products. Academic Press, 2017, pp. 1-27.
[13] G.Toscano, G. Riva, D. Duca, E.F. Pedretti, F. Corinaldesi, G. Rossini, Biomass Bioenergy. 55 (2013) 260-267.
[14] P. Vašeková, M. Juráček, D. Bíro, M. Šimko,.B., Gálik, M., Rolinec, O. Hanušovský, R. Kolláthová, E. Ivanišová, E. Bioactive compounds and fatty acid profile of grape pomace. Acta Fytotechn. Zootechn, 23 (2020) 230-235.
[15] J. Yu,, M. Ahmedna. Int. J. Food Sci. Technol. 48 (2013), 221-237.

STRUCTURE–PROPERTY RELATIONSHIPS IN RARE-EARTH (Er, Tm and Tb) DOPED CaF_2 AND BaF_2 SINGLE CRYSTALS

Maria Poienar[1]*, Gabriel Buse[1], Matthias Gutmann[2], Marius Stef[3], Carla Zeicu[3], Philippe Veber[1,3] and Daniel Vizman[1,3]

[1]*ICAM, West University of Timisoara, Bvd. V.Parvan, No.4, Timisoara (Romania)*
[2]*Rutherford Appleton Laboratory, ISIS Facility, Chilton Didcot, Oxfordshire OX11 0QX (United Kingdom)*
[3]*Physics Faculty, West University of Timisoara, Bvd. V.Parvan, No.4, Timisoara (Romania)*
e-mail: maria.poienar@e-uvt.ro

Abstract

Rare-earth (RE)-doped fluoride crystals represent an important class of functional materials for multiple applications, owing to their low phonon energies, broad UV–VIS–NIR transparency, and chemical stability [1–4]. The incorporation of RE ions into alkaline-earth fluorides such as CaF_2 and BaF_2 offers a means of tailoring their optical response, but the resulting properties are strongly influenced by the local structural environment and the mechanisms involved in charge compensation.

In this work, we investigate the structural and optical properties of Er, Tm, and Tb doped CaF_2 and BaF_2 single crystals. The crystals were synthesized by the vertical Bridgman–Stockbarger method [5] and systematically characterized by single-crystal and powder X-ray diffraction and neutron diffraction. These complementary techniques were used to examine the evolution of the host lattice and to identify local structural distortions associated with the substitution of M^{2+} cations by RE ions. Particular attention was given to the relationship between RE concentration, charge-compensation mechanisms and defect formation. The structural observations were further correlated with the optical response, including absorption features associated with the different valence states and local environments of the RE ions [6]. The combined diffraction and spectroscopic results demonstrate that RE incorporation modifies the local structural environment of the fluorite lattice, with the magnitude and nature of these effects depending on both the host matrix and the RE dopant. These findings contribute to a better understanding of the structure–property relationships governing RE-doped CaF_2 and BaF_2 crystals and provide useful insights for the design of fluoride-based materials with tailored optical and functional properties.

Acknowledgements

This work is supported by a grant PNRR/2022/C9/MCID/I8, project title "Enhanced Single Crystal Applications and Research in the Growth of new Optical rare earth-based compounds for sustainable and efficient Technologies (ESCARGOT), contact number 136/15.11.2022.

References

[1] A. A. Kaminskii. Crystalline Lasers: Physical Processes and Operating Schemes (CRC Press) 1996.
[2] N. Sarukura, T.Nawata, H. Ishibashi, M. Ishii, T. Fukuda. Handbook of Crystal Growth: Bulk Crystal Growth vol 2 2nd edn (Elsevier), 131–68, 2015.
[3] D. Hahn, Opt. Photonik **9**, 45–8, 2014.
[4] D. L. Dexter, J. Chem. Phys. **21**, 836–50, 1953.
[5] D. Nicoara, I. Nicoara, Mater. Sci. Eng. A **102**, L1–L5, 1988.
[6] G. Buse *et al*, J. of Alloys and Compounds, **1010**, (2025) pp.177784.

ADVANCED HPLC METHOD DEVELOPMENT AND COMPREHENSIVE VALIDATION FOR THE SIMULTANEOUS ASSAY AND RELATED SUBSTANCES DETERMINATION OF PYRITINOL DIHYDROCHLORIDE IN ORAL SOLUTION

Andrada Daniela Pop Szmical, Thomas Dippong
Technical University of Cluj-Napoca, Faculty of Science, 76 Victoriei Street, 430122, Baia Mare, Romania;
e-mail: thomas.dippong@cb.utcluj.ro

Abstract
Pyritinol dihydrochloride (Pyr-HCl), a synthetic derivative of vitamin B6 (pyridoxine), is a widely prescribed neurotropic agent employed in the management of cognitive disorders, peripheral neuropathies, and as an adjuvant therapy in post-traumatic syndromes, yet its hygroscopic nature and susceptibility to oxidative and hydrolytic degradation pose significant challenges to pharmaceutical technology, as the presence of impurities such as free pyridoxine or oxidative degradation products may compromise both therapeutic potency and safety profile, necessitating stringent control of related substances throughout the product's shelf-life, and while the existing literature reports several reversed-phase HPLC methods for this compound, these often involve complex phosphate buffers or lengthy gradient elution programs rendering them inadequate for routine, high-throughput quality control, prompting the present study to develop and validate an innovative modified normal-phase HPLC method employing an amino-bonded stationary phase (APS-2 Amino Hypersil, 250 mm × 4.0 mm, 5 µm) that enables both the precise quantification of the active pharmaceutical ingredient and the optimal resolution of potential impurities within a simple, isocratic, and cost-effective chromatographic framework fully compliant with ICH Q2(R1) guidelines and FDA stability testing requirements [1-5]. The method was comprehensively validated according to ICH Q2(R1) guidelines, beginning with specificity assessment through forced degradation studies wherein samples were subjected to acidic (0.1N HCl, 60 °C, 6 hours), alkaline (0.1N NaOH, 60 °C, 4 hours), oxidative (3% H_2O_2, ambient temperature, 24 hours), and photolytic (UV light at 254 nm, 48 hours) stress conditions, demonstrating excellent separation of all degradation peaks from the principal peak with resolution factors Rs > 2.0 for all detectable impurities, confirmed by DAD peak purity assessment yielding a similarity index exceeding 99.5%. Linearity and range were established for the assay between 80% – 120% of the nominal oral solution concentration, with the linear regression equation y = 28765x + 1243.3 yielding a correlation coefficient of R^2 = 0.9976 demonstrating robust linear correlation with minimal data dispersion, while for impurities linearity was verified from the reporting threshold (0.05%) up to the specification limit (0.5%) demonstrating adequate sensitivity for detecting impurities at toxicologically relevant levels. Accuracy assessed via the standard addition method at three concentration levels (80%, 100%, 120%) for the API and three levels for impurities (50%, 100%, 150% of the specification limit) yielded mean recoveries ranging between 99.02% and 101.45%, confirming method accuracy and the absence of matrix interference from excipients such as sorbitol, preservatives, and flavoring agents which are often problematic in oral solutions. Precision studies demonstrated repeatability with six replicate determinations yielding Relative Standard Deviation (RSD) of 0.41% for the assay and 1.20% for impurities, while intermediate precision over two different days performed by two different analysts yielded a cumulative RSD of 0.87% for the assay confirming reproducibility under normal laboratory conditions. The limit of detection (LOD) and limit of quantification (LOQ) based on signal-to-noise ratio (S/N = 3:1 and 10:1, respectively) were established at 0.02 µg/mL and 0.06 µg/mL, values substantially below the regulatory reporting limit (0.1%) providing a considerable analytical safety margin. Robustness evaluated through a One-Factor-at-a-Time approach with deliberate variations to critical

parameters (±2 °C for temperature, ±2% for mobile phase pH, and ±0.1 mL/min for flow rate) demonstrated excellent robustness with only minor variations in retention time (RSD < 1.5%) without affecting the critical resolution between Pyr-HCl and adjacent impurities. The chromatographic system enabled rapid elution with a total run time under 10 minutes per analysis, optimizing solvent consumption and analysis time as a crucial economic factor in routine quality control laboratories, with the principal Pyr-HCl peak exhibiting a symmetry factor (As) of 1.05 indicating minimal interaction with free silanols attributable to the acidified mobile phase and precise thermal control, while the impurity profile revealed through forced degradation indicated the presence of three major degradation products all separated with a resolution Rs > 2.5, a particularly significant finding as some of these impurities (e.g., pyridoxamine analogues) may possess distinct pharmacological activity or exhibit potential toxicity, thus validating that the finished product maintains its purity specifications throughout its proposed shelf-life [1-5]. In conclusion, the HPLC method developed and validated in this study constitutes a superior analytical tool for the quality control of pyritinol dihydrochloride oral solution, as the combination of an amino stationary phase with an isocratic acidified mobile phase provides an optimal balance between resolution, sensitivity, and analytical speed surpassing the limitations of conventional reversed-phase methodologies, with principal advantages including absolute specificity towards excipients and degradation products essential for ICH stability studies, statistically confirmed precision and accuracy meeting the most stringent pharmaceutical acceptance criteria (RSD < 2%), and industrial applicability owing to the low cost of reagents and short run time making it eligible for technological transfer to manufacturing units [1-5]. From a pharmaceutical perspective, this method not only ensures compliance with international regulatory standards but also provides a guarantee of patient safety by enabling rigorous monitoring of chemical purity and, consequently, the safety and efficacy of neurotropic therapy, with future studies extending the method's applicability to the analysis of industrial-scale production batches and the evaluation of real-time degradation kinetics.

Acknowledgements: This work was supported by the **Technical University of Cluj-Napoca** through the doctoral research program within the **IOSUD-UTCN**. The authors gratefully acknowledge the financial support for participating in this conference.

References

[1] Satyanarayana Reddy Y, Himabindu G, Prasad AVSS, Ramadas C, Sharma HK. Development and validation of orthogonal RP-HPLC methods for the determination of organic impurities in penicillamine drug substance. Separation Science Plus, 8(1), (2025), e202400145.
[2] Altwala A, Algohary, A.M., Alhalafi, M.H., Eraqi. M.M., Ibrahim A.M. An ICH Q14-guided AQbD framework for the development of an HPLC method: Analysis of siponimod fumarate and its impurities. Electrophoresis. 46(23), (2025), 1661-1672.
[3] Eberle M, Wasylenko JT, Kostelac D, Kiehna S, Schellinger A, Zhang Z, Ehrick JD. A modern framework for analytical procedure development and lifecycle management based on ICH Q14 principles. Analytical Chemistry. 97(1), (2025) 12-21.
[4] Kumar A, Sharma S, Singh R. Recent advances in stability-indicating HPLC methods for pharmaceutical analysis: A comprehensive review. Journal of Pharmaceutical and Biomedical Analysis. 238, (2024) 115843.
[5] Mendes G, Oliveira R, Santos M. Method validation in pharmaceutical analysis: Current perspectives and future trends under ICH Q2(R2) and Q14. Journal of Pharmaceutical Sciences. 114(2), (2025) 1456-1468.

DEVELOPMENT, CHARACTERIZATION AND HACCP PLAN DESIGN FOR AN INNOVATIVE VEGETABLE-ENRICHED BREAD

Viorica Mirela Popa[1*], Camelia Moldovan[1], Delia Gabriela Dumbravă[1], Diana Nicoleta Raba[2], Mariana Atena Poiană[1], Petru Bogdan Rădoi[1]

[1] Faculty of Food Engineering, University of Life Sciences "King Mihai I" from Timişoara, Calea Aradului 119A, 300645, Romania
[2]Faculty of Management and Rural Tourism, University of Life Sciences "King Mihai I" from Timişoara, Calea Aradului 119A, 300645, Romania
e-mail: mirelapopa@usvt.ro

Abstract
Growing interest in functional foods has spurred the development of innovative bakery products with enhanced nutritional and health-promoting properties. In this context, the present study aimed to develop and evaluate the characteristics of an innovative vegetable-enriched bread, produced by incorporating carrots and leeks into a whole-wheat flour recipe. The proposed recipe was designed to combine the nutritional benefits of whole grains with the valuable bioactive compounds naturally found in vegetables, resulting in a product with enhanced functional potential. Whole-wheat flour was selected due to its higher content of fiber, protein, and micronutrients compared to refined flour, while the chosen vegetables served to improve both the nutritional profile and the sensory properties of the final product. The baking process involved conventional technological stages: dough preparation, fermentation, shaping, proofing, and baking. The resulting product was evaluated based on its physicochemical, nutritional, and sensory characteristics. A HACCP analysis highlighted the importance of controlling raw material quality, dough fermentation conditions, baking temperature, and storage practices to minimize food safety risks. Appropriate monitoring procedures, corrective actions, and verification measures were proposed to ensure consistent product quality and consumer protection. The vegetable-enriched bread offered a healthier alternative to conventional bakery products, featuring enhanced nutritional value and a food safety management system based on HACCP principles.

Keywords: vegetable-enriched bread, whole wheat flour, carrot, leek, HACCP

DESIGN AND EVALUATION OF A FUNCTIONAL MALT-ENRICHED YOGURT SUPPORTED BY HACCP PRINCIPLES

Viorica Mirela Popa[1*], Camelia Moldovan[1], Delia Gabriela Dumbravă[1], Diana Nicoleta Raba[2], Corina Dana Mișcă[1], Aurica Breica Borozan[3]

[1]Faculty of Faculty of Food Engineering, University of Life Sciences "King Mihai I" from Timişoara, Calea Aradului 119A, 300645, Romania
[2] Faculty of Management and Rural Tourism, University of Life Sciences "King Mihai I" from Timişoara, Calea Aradului 119A, 300645, Romania
[3]Faculty of Engineering and Applied Technologies, Calea Aradului 119, Timisoara 300645, Romania
e-mail: mirelapopa@usvt.ro

Abstract
The development of innovative dairy products represents a significant trend in the food industry, driven by the growing demand for foods with superior nutritional value and functional benefits. In this context, the present research aimed to develop and characterize an innovative yogurt variety based on whole goat milk—enriched with malt, honey, and inactive yeast—and to establish the necessary elements for implementing a food safety system based on HACCP principles. The primary raw material used was whole goat milk, valued for its high digestibility and valuable nutrient content, specifically 3.0–3.5% protein, 3.5–4.5% fat, and 4.0–4.6% lactose. The technological process involved standardization, pasteurization, cooling, and inoculation with starter cultures consisting of *Lactobacillus bulgaricus* and *Streptococcus thermophilus*, microorganisms responsible for lactose fermentation and the formation of the yogurt's characteristic texture. Malt, honey, and inactive yeast (*Saccharomyces cerevisiae*) were added to enhance the product's functional value. Malt provided fermentable carbohydrates, amino acids, and bioactive compounds, while honey contributed to improved sensory properties and nutritional value through its content of simple sugars and enzymes. The use of inactive yeast allowed for the enrichment of the nutritional profile without negatively affecting the lactic fermentation process or the product's sensory characteristics.

Keywords: goat milk yogurt, malt, honey, inactive yeast, HACCP

PHOTOCATALYTIC DEGRADATION OF CONGO RED USING A FUNCTIONALIZED STYRENE–6.7% DIVINYLBENZENE COPOLYMER AS ACTIVE MATERIAL

Adriana Popa[1*], Izabela-Denisa Arjocu[2], Aurelia Visa[1], Laura Cocheci[2*]

[1.] *"Coriolan Drăgulescu" Institute of Chemistry, 24 M. Viteazul Blv., 300223 Timisoara, Romania*

[2.] *Politehnica University Timişoara, Faculty of Chemical Engineering, Biotechnology and Environmental Protection, 6 Vasile Parvan Blvd., 300223, Timisoara, Romania*

[*]*coresponding e-mail:* laura.cocheci@upt.ro; apopa_ro@yahoo.com

Abstract

The styrene–6.7% divinylbenzene copolymers functionalized with chloromethyl or amino-acid groups was evaluated as an active material for the photocatalytic reduction and degradation of Congo Red (CR) from aqueous solutions. Its three-dimensional cross-linked structure ensures high stability, while the introduced -CH_2Cl and -NH-C_6H_4-COOH groups create reactive centers that facilitate electron transfer and enhance photocatalytic performance.

Introduction

Congo Red is an anionic azo dye, frequently used in the textile industry, for dyeing cotton fibers, but also as a chemical indicator and biological dye in laboratories [1]. It has a complex aromatic structure, with two azo groups (-N=N-), which gives it high chemical stability and a characteristic deep red color. Due to its stability and resistance to biodegradation, Congo Red is considered a hazardous pollutant of industrial wastewater [2]. Its presence in the aquatic environment reduces light penetration, affects photosynthesis of aquatic organisms and can have toxic or potentially carcinogenic effects. Photocatalytic degradation of Congo Red represents an advanced method for treating contaminated water [3]. The method is considered efficient and environmentally friendly for the treatment of industrial wastewater [4].

The paper presents the evaluation of styrene-6.7% divinylbenzene copolymer functionalized with chloromethyl / amino-acid groups, used as an active material in photocatalytic processes for the reduction and degradation of the azo dye Congo Red from aqueous solutions. The three-dimensional cross-linked structure, obtained by copolymerization, gives the material high mechanical and chemical stability, as well as a suitable surface for functionalization (Figure 1). The introduction of -CH_2Cl/-NH-C_6H_4-COOH groups on the aromatic nuclei generates reactive centers capable of facilitating electron transfer processes and interaction with the species involved in photocatalytic reactions.

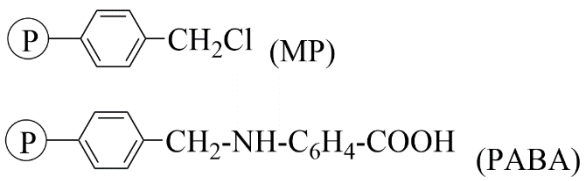


Figure 1. Functionalized styrene–6.7% divinylbenzene copolymer.

Experimental

The photocatalysis tests were performed using a batch photocatalytic reactor, model PhotoLAB B400-700 Basic L, equipped with a medium-pressure mercury lamp, 150 W. The system temperature did not exceed 20°C. The Congo Red dye solution was used in a volume of 700 cm^3 and was magnetically stirred together with a certain amount of sample (MP or PABA), so that the catalyst concentration was 0.5, 1, and 1.5 g/L. At well-established time intervals, 5 mL

aliquots were taken, filtered through a Millipore syringe filter and analyzed spectrophotometrically. The spectra were recorded in the range 200–800 nm, and the maximum absorption values at λ = 498 nm were monitored. The Lambert-Beer law was used to establish the relationship between absorption and CR concentration. The CR removal efficiency was calculated using the equation:

$$\text{Efficiency}(\%) = \frac{c_0 - c}{c_0} \cdot 100$$

where: R – efficiency (%); C_0 – initial concentration (mg/L); C –concentration at time t (mg/L).

Results and discussion

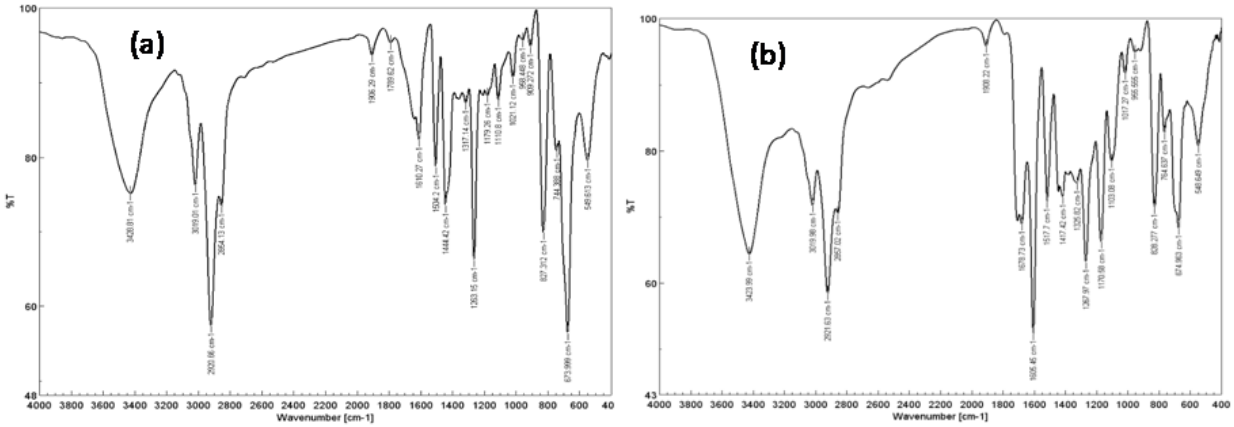


Figure 2. FTIR spectra for MP (a) and PABA (b).

Figure 2 (a, b) highlights the bands corresponding to the MP copolymer, as well as the absorption bands of the PABA sample. It was observed in the spectrum of Fig 2b, a decrease in the intensity of the γCH₂Cl band at 1263 cm^{-1}, and respectively the presence of the carbonyl C=O band at 1625 cm^{-1}.

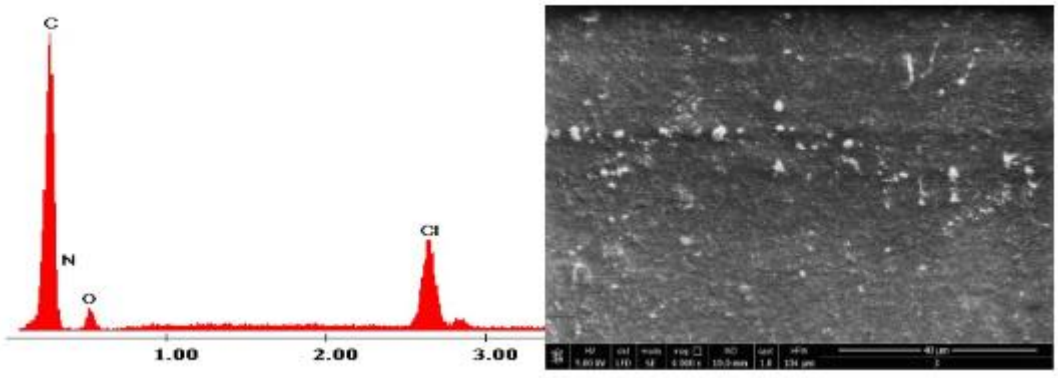
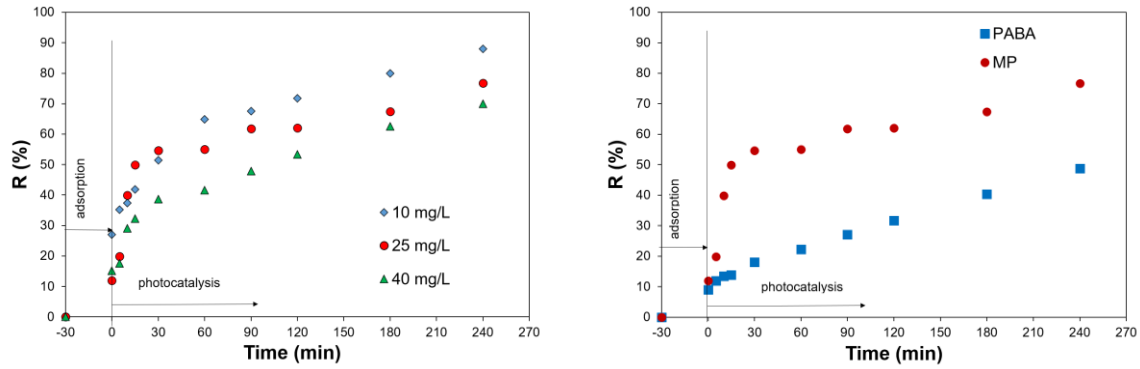


Figure 3. EDX and SEM images for PABA.

The energy dispersive X-ray (EDX) analysis and the scanning electron microscopy (SEM) image of the PABA sample are shown in Figure 3(a,b).

The photocatalytic activity was investigated under UV-Vis irradiation, under controlled conditions of initial dye concentration and exposure time (Figures 4a and 4b). Under the action of radiation, the functionalized polymer system favors the formation of reactive species (hydroxyl radicals •OH and other oxidative species) through electronic excitation and charge transfer processes. Chloromethyl groups contribute to the stabilization of radical intermediates

and to the improvement of the separation of electron-hole pairs, reducing their recombination and increasing the efficiency of the process.



(a) (b)

Figure 4. Influence of initial concentration and time of exposure on the photocatalytic degradation of Congo Red on MP copolymer, where: S:L = 1g/L (a) and PABA, MP copolymers, where: c_i = 25 mg/L, S:L = 1g/L (b).

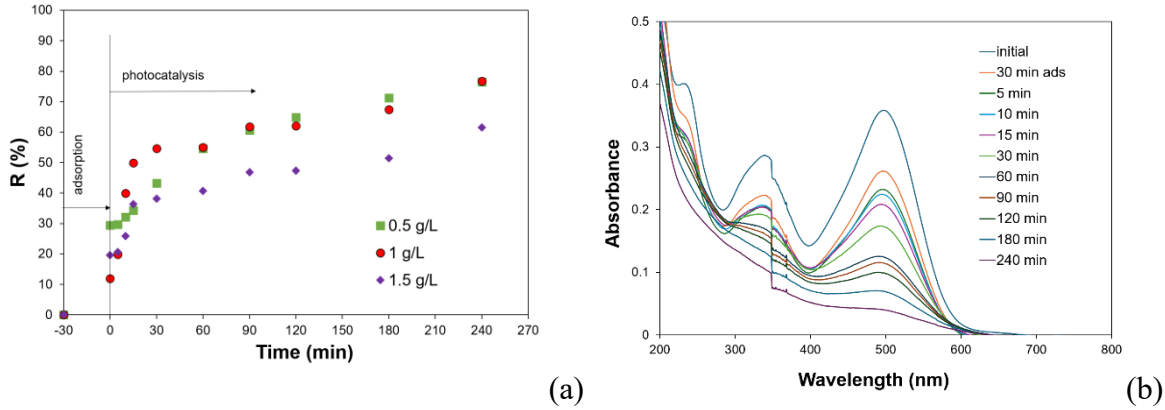
The degradation monitoring was carried out by UV-Vis spectrophotometry, highlighting the decrease in the intensity of the characteristic absorption band in the visible range, associated with the discoloration and progressive degradation of the dye. The obtained results indicate an increase in the degradation yield in the presence of the functionalized copolymer, demonstrating its potential for the treatment of wastewater contaminated with azo dyes, within the framework of advanced oxidation processes.

The MP photocatalyst performed better under the same experimental conditions: R = 76.7 % compared to R = 48.8 % when using the PABA photocatalyst. Therefore, the MP photocatalyst was further used to study the influence of the initial CR dye concentration and the S:L ratio.

The study of the influence of the initial CR solution concentration highlighted the fact that a higher dye concentration can inhibit the degradation process. Three initial CR concentrations were used in this study: 10 mg/L, 25 mg/L and 40 mg/L, keeping the same S:L ratio = 1 g/L. The highest process yield, R = 88.0 %, was obtained at the lowest initial concentration.

The S:L ratio was then varied, using the ratios 0.5 g/L, 1 g/L and 1.5 g/L and keeping the initial concentration of the CR solution ci = 25 mg/L (Figures 5a and 5b). The S:L ratios of 0.5 g/L and 1 g/L had almost equal yields, R = 76.5 % for S:L = 0.5 g/L and R = 76.7 % for S:L = 1 g/L. An S:L ratio greater than 1 g/L decreases the yield of the photocatalysis process.

The UV-VIS spectra of the sample solutions taken during the process show that the studied process is efficient not only in terms of color removal, but also degrades the entire dye molecule.



(a) (b)

Figure 5. Influence of S:L ratio and time of exposure on the photocatalytic degradation of Congo Red on MP copolymer, where: c_i = 25 mg/L (a) and UV-VIS spectra of Congo Red solutions during the experiment, where c_i = 10 mg/L and S:L= 1 g/L (b)

Conclusion

In conclusion, it is shown that the MP photocatalyst is more efficient than PABA in the degradation of the CR dye, achieving the best results at low initial concentrations of the dye, while an S:L ratio higher than 1 g/L negatively affects the efficiency of the process. The analysis of the UV–VIS spectra confirms that the photocatalysis not only removes the color of the solution, but also leads to the complete degradation of the dye molecule.

References

[1] Robinson, T., McMullan, G., Marchant, R., & Nigam, P. (2001). Remediation of dyes in textile effluent: a critical review. *Bioresource Technology*, 77, 247–255.

[2] Forgacs, E., Cserháti, T., & Oros, G. (2004). Removal of synthetic dyes from wastewaters: a review. *Environment International*, 30, 953–971.

[3] Daneshvar, N., Salari, D., & Khataee, A. R. (2004). Photocatalytic degradation of azo dye acid red 14 in water: investigation of the effect of operational parameters. *Journal of Photochemistry and Photobiology A: Chemistry*, 157, 111–116.

[4] Herrmann, J. M. (1999). Heterogeneous photocatalysis: fundamentals and applications to the removal of various types of aqueous pollutants. *Catalysis Today*, 53, 115–129.

DESIGN OF A SINGLE-ROW POTATO PLANTER WITH LOW ENVIRONMENTAL IMPACT

Daniel Popa[1], Anișoara Duma Copcea[2] Attila Blenesi-Dima [1], Sorin Tiberiu Bungescu[1] Casiana Mihut[2], Okros Adalbert[2]

[1]Department of Agricultural Tehnologies, University of Life Sciences `King Mihai I from Timisoara, 119 Calea Aradului, Romania
[2]Department of Soil Sciences, University of Life Sciences `King Mihai I from Timisoara, 119 Calea Aradului, Romania
e-mail: anisoaradumacopcea@usvt.ro

Abstract

This paper presents the design, construction, and experimental testing of a functional prototype of a single-row potato planter intended for use on smallholdings and micro-farms. The aim of this work is to demonstrate the technical, economic, and environmental feasibility of constructing a prototype single-row potato planter. The project seeks to reduce physical exertion, optimize energy consumption by using a low-power engine (a 7 HP motor hoe), and protect the soil structure by reducing the total mass of the machinery unit.

The primary objective was to develop an efficient agricultural implement with low environmental impact and a minimal carbon footprint, manufactured entirely in-house using accessible workshop technologies (mechanical cutting, MMA arc welding). The machine operates coupled with a 7 HP motor hoe and features a distribution mechanism using cups mounted on a motorcycle chain, an angled-disc covering system, and a 50 kg hopper.

Field tests demonstrated high planting uniformity (28–32 cm spacing between tubers at a speed of 3–4 km/h), a mechanical damage rate of less than 1%, and low fuel consumption. From an economic perspective, the total material production cost was 420 RON, representing a cost reduction of at least 60% compared to similar commercial equipment.

Introduction

The potato (*Solanum tuberosum*) is one of the most important food crops globally and nationally. [1]On small-scale farms and in individual households, planting is often carried out manually—entailing considerable physical effort and significant time investment—or by using large, oversized machinery that causes excessive soil compaction and high fossil fuel consumption. [2, 3]

Small-scale mechanization plays a crucial role in the transition toward sustainable agriculture. [4]Designing agricultural equipment tailored to smallholdings—using recyclable materials or those readily available on the local market—significantly reduces the carbon footprint associated with industrial manufacturing and transport processes. [5,6]

Planting is one of the most critical agronomic operations in potato cultivation. [7]Planting depth, uniform spacing between tubers within the row, and ridge geometry directly influence branching, root system development, tuber aeration, and, ultimately, crop yield and quality. [8,9]

Traditional planting methods (manual planting with a hoe or walking backwards along furrows opened by a plow) present major disadvantages: [10]

Low labor productivity: a large volume of strenuous physical work concentrated within short timeframes.

•Lack of uniformity: variable spacing between tubers leads to unbalanced competition for light, water, and nutrients. [11]

•Tuber exposure: the prolonged interval between opening the furrow and covering it causes significant soil moisture loss. [12]

On the other hand, industrial planters (2-, 4-, or 6-row models) are designed for large areas and require medium- to high-horsepower tractors (over 50–80 HP). Using them on small or fragmented plots is uneconomical and damages the soil structure. [13,14]

Experimental

The prototype was designed, built, and assembled entirely in-house at the personal workshop (M.S.).

Materials used and structural design

Standardized metal profiles and adapted components—sourced from metal suppliers and hardware stores—were used to construct the equipment:

Main frame: constructed from square steel tubing (2.5 × 2.5 cm, 2 mm wall thickness), providing optimal mechanical resistance to torsion and bending.

Furrow-opening system: a share made of 2 mm thick steel plate—resistant to abrasive wear—that creates a continuous furrow with a triangular profile.

Distribution mechanism: a system featuring metal cups (6 cm diameter) welded onto a motorcycle chain. Motion is transmitted synchronously from the wheel axle. Tubers are guided into the soil through a 100 mm diameter PVC pipe.

Feed hopper: made of 1 mm thick galvanized sheet metal, with a load capacity of approximately 50 kg.

Running and traction system: two metal wheels (30 cm diameter) made of steel flat bar, equipped with asymmetrically arranged lugs (2 cm and 3 cm high) to prevent slippage on wet soil.

Covering/ridging system: composed of two steel half-discs (40 cm diameter) mounted at an angle.

Attachment system: adjustable adapter for connection to a standard 7 HP motor hoe.

Field testing methodology

Functional testing was carried out using a 7 HP motor hoe on previously prepared land. The parameters monitored during the experiments were:

-uniformity of planting spacing within the row at a travel speed of 3–4 km/h.

-mechanical damage rate of tubers and sprouts.

-quality of the ridge (height and degree of coverage).

Economic efficiency and investment cost (analysis of the material cost estimate).

Results and discussion

Functional analysis and mechanical performance

Field tests demonstrated excellent kinematic synchronization between the unit's forward speed and the rotation of the distribution mechanism.

Planting precision: the use of a motorcycle chain eliminated sprocket slippage, maintining the spacing between tubers within the optimal agrotechnical range of 28–32 cm. The 100 mm guide tube prevented tuber bounce.

Planting material integrity: the 6 cm cups with finished edges ensured a mechanical damage rate for the skin and sprouts of less than 1%.

Ridging quality: the 40 cm half-discs efficiently gathered the displaced soil, creating an aerated, uniform ridge 15–18 cm high—optimal for root system development.

Environmental impact assessment

Soil protection: the machine's low mass and its coupling with a 7 HP power tiller exert low pressure on the soil, preventing excessive compaction (destruction of macropores and formation of a hardpan layer).

Energy efficiency: low fossil fuel consumption per unit area reduces direct CO_2 and pollutant emissions.

Reduced manufacturing footprint: The use of common materials and the potential to recycle certain components (transmission mechanisms, mounts) reduce embodied energy compared to industrial mass production.

Economic analysis and bill of materials

Material and component acquisition costs are detailed in Table 1.

Table 1

Bill of materials for the prototype

Machine component	Specified material	Estimated quantity	Market price (RON)
Frame	Square steel tube (25×25×2 mm	~6 m (1 bar)	50
Feed hopper	1 mm galvanized sheet metal	1 sheet (1000×2000 mm)	90
Covering system	2 discs (40 cm)	Raw material / 2 pcs.	100
Timing mechanism	Motorcycle chain + sprockets + cups Ø=6" cm"	1 set	—
Guide tube	PVC drainage pipe Ø=100 mm	1 m	20
Opening hoe	2 mm steel sheet	Sample piece / scrap	30
Mounting system	Motor hoe mounting adapter	Adapted component	10
Workshop consumables	MMA electrodes, cutting discs, paint	1 package	80
TOTAL MATERIALE			**420 RON**

Labor cost savings: In-house execution (estimated at 16–24 working hours) saved between 800 and 1,200 RON (based on a workshop rate of 50 RON/hour).

Financial efficiency: The total cost of 420 RON represents a reduction of at least 60% compared to the market price of similar industrial equipment (1,500–2,500 RON).

Operational limitations and versatile advantages

Advantages: nicreased labor productivity, reduced physical exertion, versatility (can also be adapted for planting onion sets).

Disadvantages: requires constant monitoring due to hopper capacity (50 kg); tubers with long or tangled sprouts require pre-sorting to prevent hopper blockages.

Conclusion

Techno-economic feasibility: the project demonstrates the feasibility of manufacturing a reliable and precise agricultural implement in-house, with a budget of only 420 RON.

Sustainability and environmental impact: operation in combination with a 7 HP motor hoe ensures a low carbon footprint, reduced fuel consumption, and enhanced soil protection by preventing compaction.

Agrotechnical performance: the chain-and-cup mechanism and ridging half-discs ensure uniform planting (28–32 cm), a minimal damage rate (<1%), and a well-formed ridge (15–18 cm).

Recommendations

Installation of a sprocket-changing system to adjust planting spacing according to the potato variety.
Lining the cups with a polymer or rubber layer to provide extra protection for delicate sprouts.
Integration of a small secondary hopper for the localized application of granular fertilizers.

References

[1]Băneșu, A. & Biriș, S. Ș. (2018) Mecanica agregatelor agricole și optimizarea consumurilor energetice, Editura Printech, București.
[2]Căproiu, Ș., Scripnic, V., & Vlăduț, V. (2008) Mașini agricole de lucrat solul, semănat și plantat, Editura Didactică și Pedagogică, București.
[3]Ghereș, M., & Rusu, T. (2014) Tehnologii și mașini pentru lucrarea solului și înființarea culturilor în agricultura durabilă, Editura Risoprint, Cluj-Napoca.
[4]Lal, R. (2004) – „Soil carbon sequestration impacts on global climate change and food security", Science, 304(5677), 1623-1627.
[5]Maniu, I., & Popescu, S. (2011) Fundamentele proiectării mașinilor agricole, Editura Universității Transilvania, Brașov.
[6]Nagy, Z., & Drocas, I. (2017) – Mecanizarea culturii cartofului: Tehnologii și echipamente moderne, Editura AcademicPres, Cluj-Napoca.
[7]Neculăesa, V., & Cojocaru, I. (2016) – „Cercetări privind optimizarea parametrilor funcționali ai organelor de lucru pentru plantat cartofi", Revista Construcția de Mașini, 68(3), 45-52.
[8]Poienaru, I. & Vlăduț, V. (2015) Echipamente tehnologice pentru reducerea gradului de tasare a solului, Editura INMA, București.
[9]Popa, D., & Bungescu, S. (2019) Impactul mecanic al agregatelor agricole asupra structurii solului, Editura Politehnica, Timișoara.
[10]Raper, R. L. (2005) „Agricultural traffic impacts on soil compaction", Journal of Terramechanics, 42(3-4), 259-280.
[11]Stoorvogel, J. J., & Bouma, J. (2010) „Precision agriculture and the environment: Designing sustainable crop management systems", Soil and Tillage Research, 108(1-2), 12-21.
[12]Tenu, I., Cârlescu, P., & Cojocariu, R. (2015) Modelarea și simularea proceselor mecanice în agricultura de precizie, Editura Ion Ionescu de la Brad, Iași.
[13]Vander Zaag, P., & Demagante, A. L. (1990) „Potato planting geometry and mechanical optimization for reduced soil erosion", Potato Research, 33(4), 485-496.
[14]Voicu, G., Toma, U., & Cardei, P. (2012) Modelarea matematică a proceselor din mașinile agricole, Editura Matrix Rom, București.

EFFECT OF ROSEHIP POWDER ADDITION ON SELECTED PHYSICOCHEMICAL PROPERTIES OF QUINCE JELLIES

Sofia Popescu[1], Manuel Amzoiu [2], Maria Stanciugelu[3], Emilia Amzoiu[2], Florina Radu[1], Corina Megyesi[1], Laura Radulescu[1], Mariana Poiana[1], Patricia Tarkanyi[1], Despina Bordean[1]

[1]Faculti of Food Engineering, University of Life Sciences "King Mihai I" from Timisoara, 300645, 119 Calea Aradului, Romania
[2]Faculty of Pharmacy of the University of Medicine and Pharmacy of Craiova. 2-4 Petru Rares Street Craiova , Romania
[3]Brukenthal National Museum, Natural History Museum, Sibiu, Romania
e-mail: sofiapopescu@yahoo.com, sofiapopescu@usvt.ro

Abstract
This study aimed to evaluate the effect of rosehip (Rosa canina L.) powder addition on the physicochemical characteristics of jellies prepared from aqueous quince (Cydonia oblonga Mill.) extract. Four formulations were developed: a control sample without rosehip powder (QJ-C) and three formulations enriched with 2%, 4%, and 6% rosehip powder (QJ-RP2, QJ-RP4, and QJ-RP6, respectively). The physicochemical characterization included the determination of moisture, dry matter, ash content, and apparent total soluble solids (TSS). Increasing the rosehip powder concentration from 0 to 6% was associated with a progressive decrease in moisture content from 62.60% to 55.62% and a corresponding increase in dry matter from 37.40% to 44.38%. Ash content increased from 0.893% in the control sample to 1.003% in the formulation containing 4% rosehip powder. Estimated apparent TSS values increased from 7.38 to 10.75 °Brix, corresponding to a relative increase of approximately 45.6%. These findings indicate that rosehip powder addition modifies the physicochemical composition of quince jellies and supports its potential use as a plant-based ingredient in the development of diversified fruit-based formulations.

Keywords: *quince jelly; rosehip powder; moisture content; ash content; total soluble solids*

Introduction

Quince (*Cydonia oblonga Mill.*) is a fruit used in the food industry for the production of processed products, including jams, preserves, jellies, and other fruit-based preparations [1, 2]. Its chemical composition, particularly the presence of pectin, carbohydrates, organic acids, and other plant constituents, contributes to its technological suitability for the development of gelled food products [1, 3]. The physicochemical characteristics of the final products are influenced by both raw material composition and processing conditions [2].
Rosehips (*Rosa canina L.)* are plant materials known for their content of vitamin C, phenolic compounds, carotenoids, and mineral constituents [4]. The incorporation of rosehip powder into food formulations introduces additional plant-derived components that may influence the composition and physicochemical characteristics of the final products.
Moisture and dry matter contents are important parameters for characterizing the composition of gelled food products. Ash content provides information on the total inorganic residue remaining after incineration, while refractometric determination of apparent total soluble solids (TSS) enables the assessment of changes associated with constituents influencing the refractive index [2, 5]. Together, these parameters provide information on the compositional changes associated with the incorporation of powdered plant-based ingredients.

The aim of this study was to develop and physicochemically characterize jellies prepared from aqueous quince extract and enriched with rosehip powder at concentrations of 2%, 4%, and 6% (w/w), compared with a control formulation without rosehip powder. Moisture, dry matter, ash content, and apparent TSS were evaluated to investigate changes associated with increasing rosehip powder concentrations.

Experimental

Raw materials and preparation of quince jellies. Ripe quince fruits (Cydonia oblonga Mill.) were selected, washed, and cut into pieces, retaining the peel. The fruits were mixed with water at a ratio of 1:1 (w/v), boiled for approximately 30 min, and filtered to obtain an aqueous quince extract.

The jelly formulation was adapted from Poiana et al. [6]. Invert sugar syrup (25 g, 80 °Brix) and food-grade gelatin (20 g) were added to 800 mL of aqueous quince extract. The mixture was heated to approximately 55 °C under continuous stirring until the gelatin was completely dissolved and a homogeneous mixture was obtained.

Four portions of 200.00 g each were weighed from the base formulation. One portion served as the control (QJ-C), while 4.08, 8.33, and 12.77 g of food-grade rosehip (Rosa canina L.) powder were incorporated into the remaining portions to obtain final concentrations of 2% (QJ-RP2), 4% (QJ-RP4), and 6% (QJ-RP6), respectively. The samples were individually homogenized, transferred into identical containers, and stored at 4 °C for 24 h to allow gelation and stabilization.

Determination of moisture, dry matter, and ash content. The moisture and dry matter contents were determined gravimetrically by drying the samples to constant mass, while the total ash content was determined by incineration at 550 °C to constant mass, according to AOAC (2019) methods. The results were expressed as g/100 g of product (%).

Moisture content was determined gravimetrically by drying the samples to constant mass, while dry matter content was calculated by difference (100 − moisture content). Total ash content was determined by incineration at 550 °C to constant mass, following the applicable AOAC procedures [7]. The results were expressed as percentages (g/100 g of product).

Determination of Apparent Total Soluble Solids (TSS). The apparent total soluble solids (TSS) content was evaluated by refractometry using a procedure adapted for jelly samples with a gelled structure. The principle of refractometric determination is based on the relationship between the refractive index of the sample and the equivalent sucrose concentration, expressed in degrees Brix (°Brix) [5].

For each formulation (QJ-C, QJ-RP2, QJ-RP4, and QJ-RP6), 10.00 g of jelly was weighed and mixed with 50.00 g of distilled water, corresponding to a sample-to-water ratio of 1:5 (w/w). The mixtures were gently heated to 40–45 °C under stirring to disperse the gelled structure while minimizing water loss through evaporation. After cooling to approximately 20 °C, the initial mass of the mixture was restored, if necessary, by adding distilled water. The clarified liquid phase was then used for refractometric determination.

The measured values were multiplied by the nominal dilution factor of 6 and reported as estimated apparent TSS values (°Brix). Three determinations were performed for each sample, and the results were expressed as mean ± standard deviation (SD).

The method employed represents an adaptation of the refractometric principle described in ISO 2173:2003 [5]. The dilution-corrected values should be regarded as estimates, since the effects of gelatin and other matrix constituents on the refractive index are not completely eliminated by this correction.

Statistical analysis. Results were expressed as mean ± standard deviation (SD) based on three determinations (n = 3). Descriptive statistics were used to summarize the variation in the

measured physicochemical parameters. Moisture and dry matter were interpreted jointly because dry matter was calculated as the complement of moisture content.

Results and discussion

The technological process used to prepare quince jellies enriched with rosehip powder is presented in Figure 1. Four experimental formulations were obtained: a control sample without rosehip powder (QJ-C) and three formulations enriched with 2% (QJ-RP2), 4% (QJ-RP4), and 6% (QJ-RP6) rosehip powder. The use of the same base formulation and processing conditions allowed the influence of rosehip powder concentration on the physicochemical characteristics of the developed products to be investigated.

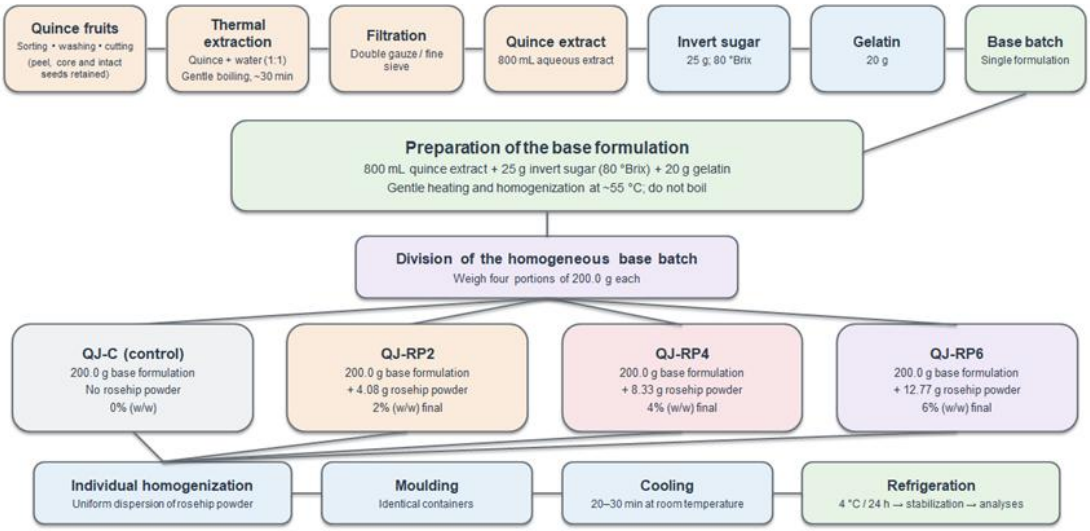


Figure 1. Technological scheme for the preparation of quince jellies enriched with rosehip powder

The physicochemical characteristics of quince jellies containing different concentrations of rosehip powder are presented in Table 1. The results revealed progressive changes in moisture, dry matter, ash content, and apparent total soluble solids (TSS) with increasing rosehip powder concentration.

Table 1. Physicochemical characteristics of quince jellies enriched with rosehip powder

Sample	Moisture (%)	Dry matter (%)	Total ash (%)	TSS (°Brix)
QJ-C	62.60 ± 0.46	37.40 ± 0.46	0.893 ± 0.025	7,38 ± 0,04
QJ-RP2	60.02 ± 0.63	39.98 ± 0.63	0.940 ± 0.046	8,21 ± 0,02
QJ-RP4	58.09 ± 0.50	41.91 ± 0.50	1.003 ± 0.050	9,08 ± 0,03
QJ-RP6	55.62 ± 0.56	44.38 ± 0.56	1.097 ± 0.035	10,75 ± 0,05

Values are expressed as mean ± SD (n = 3). TSS values represent apparent estimates obtained using a nominal dilution correction factor of 6.

Moisture content decreased progressively with increasing rosehip powder concentration, from 62.60 ± 0.46% in the control sample (QJ-C) to 60.02 ± 0.63%, 58.09 ± 0.50%, and 55.62 ± 0.56% in QJ-RP2, QJ-RP4, and QJ-RP6, respectively. Conversely, dry matter content increased from 37.40 ± 0.46% to 44.38 ± 0.56%. These changes may be attributed to the incorporation of additional solids through rosehip powder, which reduced the relative proportion of water in the final formulations. Najman et al. [2] reported moisture contents of 81.40 ± 0.16% in fresh quince and 84.71 ± 0.38% in boiled quince, with corresponding dry matter contents of 18.60 ± 0.16% and 15.29 ± 0.38%, respectively. The higher dry matter content observed in the present jelly formulations may reflect differences in product composition, particularly the incorporation of invert sugar syrup, gelatin, and rosehip powder. However, direct comparison is limited by differences in the investigated matrices and processing procedures.

Ash content also increased progressively with rosehip powder addition, from 0.893 ± 0.025% in QJ-C to 0.940 ± 0.046%, 1.003 ± 0.050%, and 1.097 ± 0.035% in QJ-RP2, QJ-RP4, and QJ-RP6, respectively. The highest ash content was recorded in the formulation containing 6% rosehip powder, representing an increase of approximately 22.8% compared with the control. This trend suggests that rosehip powder contributed additional inorganic constituents to the jelly formulations. Nevertheless, ash content represents the total inorganic residue remaining after incineration and does not provide information on individual mineral elements.

The aqueous quince extract exhibited a mean soluble solids value of 5.30 ± 0.04 °Brix. Following the addition of invert sugar syrup and gelatin, the estimated apparent TSS value increased to 7.38 ± 0.04 °Brix in the control jelly. Further increases were observed with rosehip powder addition, reaching 8.21 ± 0.02, 9.08 ± 0.03, and 10.75 ± 0.05 °Brix in QJ-RP2, QJ-RP4, and QJ-RP6, respectively. Compared with the control, these values corresponded to relative increases of approximately 11.2%, 23.0%, and 45.6%. The increasing trend may be associated with soluble constituents introduced by rosehip powder, including sugars and organic acids, as well as changes in the overall composition of the food matrix [4].

For comparison, Najman et al. [2] reported soluble solids values of 12.50 ± 0.50 °Brix in fresh quince, 12.00 ± 0.50 °Brix in boiled quince, and 15.17 ± 0.29 °Brix in quince juice. Sharma et al. [1] reported substantially higher soluble solids contents in conventional quince jam (70 °Brix) and jelly (66 °Brix). These differences may be explained by variations in raw material concentration, sugar addition, processing conditions, and product formulation. In the present study, the jellies were prepared from a diluted aqueous quince extract with a relatively small amount of invert sugar syrup, resulting in a different product composition. Furthermore, the reported TSS values were estimated using a dilution-corrected refractometric procedure and therefore should not be considered directly equivalent to values obtained through conventional refractometric measurements of other fruit products [5, 6].

Overall, the results indicate that increasing rosehip powder concentration was associated with lower moisture content and higher dry matter, ash content, and estimated apparent TSS values. These findings highlight the influence of rosehip powder incorporation on the physicochemical composition of quince jellies.

Conclusion

The incorporation of rosehip (Rosa canina L.) powder influenced the physicochemical characteristics of quince (Cydonia oblonga Mill.) jellies. Increasing the rosehip powder concentration from 0% to 6% resulted in a decrease in moisture content from 62.60% to 55.62%, accompanied by an increase in dry matter from 37.40% to 44.38%. Ash content increased from 0.893% to 1.097%, suggesting a contribution of inorganic constituents from rosehip powder. Similarly, estimated apparent total soluble solids increased from 7.38 to 10.75 °Brix. These findings demonstrate that rosehip powder can be incorporated into quince jelly formulations to modify their physicochemical composition and support the development of diversified fruit-based products. Further investigations are needed to evaluate their bioactive compounds, antioxidant activity, sensory properties, and storage stability.

Acknowledgements

The authors express their gratitude for the technical support provided by the University of Life Sciences "King Mihai I" from Timisoara, Faculty of Food Engineering, Food Science Research Center, where the analyses were conducted.

References

[1] Sharma, R., Joshi, V. K., & Rana, J. C. (2011). Nutritional composition and processed products of quince (Cydonia oblonga Mill.). Indian Journal of Natural Products and Resources, 2(3), 354–357.
[2] Najman, K., Adrian, S., Sadowska, A., Świąder, K., Hallmann, E., Buczak, K., Waszkiewicz-Robak, B., & Szterk, A. (2023). Changes in physicochemical and bioactive properties of quince (Cydonia oblonga Mill.) and its products. Molecules, 28(7), 3066.
[3] Al-Zughbi, I., & Krayem, M. (2022). Quince fruit Cydonia oblonga Mill nutritional composition, antioxidative properties, health benefits and consumers preferences towards some industrial quince products: A review. Food Chemistry, 393, 133362.
[4] Igual, M., García-Herrera, P., Cámara, R. M., Martínez-Monzó, J., García-Segovia, P., & Cámara, M. (2022). Bioactive compounds in rosehip (Rosa canina) powder with encapsulating agents. Molecules, 27(15), 4737.
[5] International Organization for Standardization (ISO). (2003). ISO 2173:2003. Fruit and vegetable products — Determination of soluble solids — Refractometric method. Geneva: ISO.
[6] AOAC International. Official Method 932.12. Solids (Soluble) in Fruits and Fruit Products — Refractometer Method.
[7] AOAC International (2019), Official Methods of Analysis, 21st edition

BIOACTIVE COMPOUNDS AND ANTIOXIDANT ACTIVITY OF QUINCE JELLY ENRICHED WITH ROSEHIP

Sofia Popescu[1], Emilia Amzoiu[2], Florina Radu[1]*, Corina Megyesi[1], Laura Radulescu[1], Despina Bordean[1], Patricia Tarkanyi[1], Manuel Amzoiu [2], Mihaela-Maria Stanciugelu[3], Mariana Poiana[1], Lia S. Rotariu[4], Alexandru Rinovetz[1]

[1]Faculti of Food Engineering, University of Life Sciences "King Mihai I" from Timisoara, 300645, 119 Calea Aradului, Romania
[2]Faculty of Pharmacy of the University of Medicine and Pharmacy of Craiova. 2-4 Petru Rares Street Craiova , Romania
[3]Brukenthal National Museum, Natural History Museum, Sibiu, Romania
[4]Faculty of Management and Rural Tourism, University of Life Sciences "King Mihai I" from Timisoara, 300645, 119 Calea Aradului, Romania
**corresponding author, e-mail: florinaradu@.usvt.ro*

Abstract

This study aimed to develop quince (Cydonia oblonga Mill.) jellies enriched with rosehip (Rosa canina L.) powder and to evaluate the effect of powder concentration on their bioactive properties. Four formulations were prepared using aqueous quince extract and limited amounts of added sugar: a control sample (QJ-C) and three samples containing 2, 4, and 6% (w/w) rosehip powder. Total phenolic content (TPC), vitamin C content, and antioxidant capacity were determined using the Folin–Ciocalteu method, DCPIP titration, and the FRAP assay, respectively. Increasing rosehip powder concentration enhanced the investigated parameters. TPC increased from 88.10 to 110.97 mg GAE/100 g fresh weight, while vitamin C content increased from 12.51 to 23.62 mg/100 g fresh weight. FRAP antioxidant capacity increased by approximately 48.0% compared with the control. The formulation containing 6% rosehip powder exhibited the highest TPC and FRAP values, whereas the difference in vitamin C content between the 4 and 6% formulations was not statistically significant ($p > 0.05$). These findings indicate that rosehip powder can enhance the bioactive characteristics of quince-based jellies and support its potential use in developing fruit-based gelled products.

Keywords: quince jelly; rosehip powder; total phenolic content; antioxidant activity; vitamin C.

Introduction

Quince (Cydonia oblonga Mill.) is a valuable raw material for the food industry due to its natural pectin content and the presence of bioactive compounds, particularly phenolic acids. Although fresh consumption is limited by its firm texture and astringency, quince is widely processed into jams, jellies, marmalades, and other fruit-based products [1, 2]. Its phenolic compounds contribute to its antioxidant potential, and several phenolic constituents have also been identified in processed quince products [3–5].

Rosehips (Rosa canina L.) are valuable sources of vitamin C, phenolic compounds, and carotenoids, making them suitable ingredients for developing foods with enhanced bioactive properties [6]. Previous research has demonstrated that incorporating rosehip powder into fruit-based jellies can increase bioactive compound content and antioxidant capacity, depending on the addition level [7].

Combining aqueous quince extract with rosehip powder may provide an approach for developing gelled products with improved bioactive characteristics. In formulations containing

limited amounts of added sugar, gelatin can serve as the primary gelling agent, while naturally occurring quince pectin may also contribute to product structure [1, 2].

The aim of this study was to develop and characterize quince jellies formulated with a reduced amount of added sugar and enriched with rosehip powder at concentrations of 2, 4, and 6% (w/w), compared with a control sample. The effects of rosehip powder addition on total phenolic content (TPC), vitamin C content, and antioxidant capacity determined by the FRAP assay were evaluated.

Experimental

Raw materials and preparation of quince jellies

Ripe quince fruits (Cydonia oblonga Mill.) were selected, washed, and cut into pieces, retaining the peel. The fruits were mixed with water at a ratio of 1:1 (w/v), boiled for approximately 30 min, and filtered to obtain the aqueous extract.

The jelly formulation was adapted from Poiana et al. [7]. Invert sugar syrup (25 g, 80 °Brix) and food-grade gelatin (20 g) were added to 800 mL of aqueous quince extract. The mixture was heated to approximately 55 °C under continuous stirring until the gelatin was completely dissolved and a homogeneous mixture was obtained.

Four portions of 200.00 g each were weighed from the base formulation. One portion served as the control (QJ-C), while 4.08, 8.33, and 12.77 g of food-grade rosehip (*Rosa canina L.)* powder were incorporated into the remaining portions to obtain final concentrations of 2% (QJ-RP2), 4% (QJ-RP4), and 6% (QJ-RP6, respectively). The samples were individually homogenized, transferred into identical containers, and stored at 4 °C for 24 h to allow gelation and stabilization.

Preparation of extracts for bioactive compound analysis

Extracts were prepared according to the procedure described by Poiana et al. [7]. Each jelly sample (0.5 g) was mixed with 10 mL of 70% (v/v) ethanol, agitated for 2 h at room temperature, and centrifuged at 5000 rpm for 10 min. The residue was re-extracted for 60 min, and the combined supernatants were adjusted to a final volume of 20 mL with 70% (v/v) ethanol. The extracts were stored at −20 °C in the dark until analysis.

Determination of total phenolic content

Total phenolic content (TPC) was determined using the Folin–Ciocalteu method according to Singleton et al. [8], with adaptations described by Poiana et al. [7]. Following reaction with Folin–Ciocalteu reagent and sodium carbonate, the samples were incubated at 50 °C for 30 min, and absorbance was measured at 750 nm. Gallic acid was used as the calibration standard, and the results were expressed as mg gallic acid equivalents (GAE)/100 g fresh weight (f.w.).

Determination of vitamin C content

Vitamin C content was determined titrimetrically using 2,6-dichlorophenolindophenol (DCPIP), following an adaptation of the method described by Poiana et al. [7]. The results were expressed as mg ascorbic acid/100 g fresh weight (f.w.).

Determination of antioxidant capacity by the FRAP assay

Determination of antioxidant capacity by the FRAP assay

Antioxidant capacity was evaluated using the ferric reducing antioxidant power (FRAP) assay according to Benzie and Strain [9], with adaptations described by Poiana et al. [7]. Following reaction with the FRAP reagent, the samples were incubated at 37 °C for 30 min, and absorbance was measured at 593 nm. Results were reported on a fresh-weight basis.

Statistical analysis

Results were expressed as mean ± standard deviation (SD) of three determinations (n = 3). Differences among formulations were evaluated using one-way analysis of variance (ANOVA), followed by Tukey's honestly significant difference (HSD) test for multiple comparisons. Differences were considered statistically significant at $p < 0.05$. Statistical analysis was performed using JASP software, version 0.19.3.

Results and discussion

The incorporation of rosehip powder influenced the bioactive characteristics of quince jellies (Table 1). Increasing rosehip powder concentration from 0 to 6% (w/w) resulted in higher total phenolic content (TPC), vitamin C content, and FRAP antioxidant capacity.

Table 1. Total phenolic content, vitamin C content, and FRAP antioxidant capacity of quince jellies enriched with rosehip powder

Sample	TPC (mg GAE/100 g f.w.)	Vitamin C (mg/100 g f.w.)	FRAP (µmol Fe^{2+}/g f.w.)
QJ-C	88.10 ± 0.40^{d}	12.51 ± 0.17^{c}	12.06 ± 0.23^{d}
QJ-RP2	96.23 ± 0.73^{c}	16.58 ± 0.76^{b}	13.72 ± 0.76^{c}
QJ-RP4	105.08 ± 0.98^{b}	22.47 ± 0.55^{a}	16.04 ± 0.23^{b}
QJ-RP6	110.97 ± 0.16^{a}	23.62 ± 0.47^{a}	17.85 ± 0.21^{a}

Values are expressed as mean ± standard deviation (SD), n = 3. Means sharing no common superscript letters within the same column differ significantly according to Tukey's HSD test ($p < 0.05$). TPC – total phenolic content; FRAP – ferric reducing antioxidant power; f.w. – fresh weight.

Total phenolic content increased progressively from 88.10 mg GAE/100 g f.w. in the control sample (QJ-C) to 110.97 mg GAE/100 g f.w. in QJ-RP6, corresponding to an increase of approximately 26.0%. Significant differences were observed among all formulations ($p < 0.05$). This increase may be attributed to phenolic compounds introduced through rosehip powder. Similar findings were reported by Poiana et al. [7], who observed enhanced bioactive compound content in orange-based jellies enriched with rosehip powder. Quince also contains phenolic compounds that contribute to its antioxidant properties [4, 5, 10].

Vitamin C content increased from 12.51 mg/100 g f.w. in QJ-C to 23.62 mg/100 g f.w. in QJ-RP6, representing an increase of approximately 88.8%. The formulations containing 4 and 6% rosehip powder exhibited the highest vitamin C values (22.47 and 23.62 mg/100 g f.w., respectively), with no statistically significant difference between them ($p > 0.05$). These results highlight the contribution of rosehip powder to the vitamin C content of the developed jellies, consistent with the composition of rosehips reported in the literature [6, 7].

FRAP antioxidant capacity increased from 12.06 µM Fe^{2+}/g f.w. in QJ-C to 17.85 µM Fe^{2+}/g f.w. in QJ-RP6, corresponding to an increase of approximately 48.0%. All formulations differed significantly ($p < 0.05$). The increase in FRAP values alongside TPC suggests that phenolic compounds may contribute to the reducing capacity of the products. Similar relationships between phenolic composition and antioxidant properties in processed quince products have been discussed by Baroni et al. [11].

Overall, increasing rosehip powder concentration improved the investigated bioactive characteristics of quince jellies. The 6% formulation showed the highest TPC and FRAP values, while vitamin C content did not differ significantly between the 4 and 6% formulations. These findings support the potential use of rosehip powder to enhance the bioactive properties of quince-based gelled products.

Conclusion

The incorporation of rosehip (Rosa canina L.) powder at concentrations of 2, 4, and 6% (w/w) improved the bioactive characteristics of quince (Cydonia oblonga Mill.) jellies. Increasing rosehip powder concentration resulted in significant increases in total phenolic content (TPC) and FRAP antioxidant capacity, reaching approximately 26.0% and 48.0%, respectively, compared with the control. Vitamin C content also increased by approximately 88.8% in the formulation containing 6% rosehip powder, although the difference between the 4 and 6% formulations was not statistically significant. These findings highlight the potential of rosehip powder as an ingredient for enhancing the bioactive properties of quince-based jellies. Further studies on sensory acceptability and storage stability are needed to determine the most suitable formulation for food applications.

Acknowledgements

The authors express their gratitude for the technical support provided by the University of Life Sciences "King Mihai I" from Timisoara, Faculty of Food Engineering, Food Science Research Center, where the analyses were conducted.

References

[1] Al-Zughbi, I., & Krayem, M. (2022). Quince fruit Cydonia oblonga Mill nutritional composition, antioxidative properties, health benefits and consumers preferences towards some industrial quince products: A review. Food Chemistry, 393, 133362. https://doi.org/10.1016/j.foodchem.2022.133362

[2] Sharma, R., Joshi, V. K., & Rana, J. C. (2011). Nutritional composition and processed products of quince (Cydonia oblonga Mill.). Indian Journal of Natural Products and Resources, 2(3), 354–357.

[3] Silva, B. M., Andrade, P. B., Valentão, P., Mendes, G. C., Seabra, R. M., & Ferreira, M. A. (2000). Phenolic profile in the evaluation of commercial quince jellies authenticity. Food Chemistry, 71(2), 281–285. https://doi.org/10.1016/S0308-8146(00)00134-5

[4] Silva, B. M., Andrade, P. B., Ferreres, F., Domingues, A. L., Seabra, R. M., & Ferreira, M. A. (2002). Phenolic profile of quince fruit (Cydonia oblonga Miller) (pulp and peel). Journal of Agricultural and Food Chemistry, 50(16), 4615–4618. https://doi.org/10.1021/jf0203139

[5] Silva, B. M., Andrade, P. B., Valentão, P., Ferreres, F., Seabra, R. M., & Ferreira, M. A. (2004). Quince (Cydonia oblonga Miller) fruit (pulp, peel, and seed) and jam: Antioxidant activity. Journal of Agricultural and Food Chemistry, 52(15), 4705–4712. https://doi.org/10.1021/jf040057v

[6] Igual, M., García-Herrera, P., Cámara, R. M., Martínez-Monzó, J., García-Segovia, P., & Cámara, M. (2022). Bioactive compounds in rosehip (Rosa canina) powder with encapsulating agents. Molecules, 27(15), 4737. https://doi.org/10.3390/molecules27154737

[7] Poiana, M.-A., Moigradean, D., Radu, F., Stoin, D., Lacatus, M., Bordean, D.-M., Velciov, A., Megyesi, C., Popescu, S., & Rinovetz, A. (2025). Formulation of functional orange jellies enriched with rosehip powder. Proceedings of the 31st International Symposium on Analytical and Environmental Problems (ISAEP), Szeged, 190–194.

[8] Singleton, V. L., Orthofer, R., & Lamuela-Raventós, R. M. (1999). Analysis of total phenols and other oxidation substrates and antioxidants by means of Folin–Ciocalteu reagent. Methods in Enzymology, 299, 152–178. https://doi.org/10.1016/S0076-6879(99)99017-1

[9] Benzie, I. F. F., & Strain, J. J. (1996). The ferric reducing ability of plasma (FRAP) as a measure of "antioxidant power": The FRAP assay. Analytical Biochemistry, 239(1), 70–76. https://doi.org/10.1006/abio.1996.0292

[10] Najman, K., Adrian, S., Sadowska, A., Świąder, K., Hallmann, E., Buczak, K., Waszkiewicz-Robak, B., & Szterk, A. (2023). Changes in physicochemical and bioactive properties of quince (Cydonia oblonga Mill.) and its products. Molecules, 28(7), 3066. https://doi.org/10.3390/molecules28073066

[11] Baroni, M. V., Gastaminza, J., Podio, N. S., Lingua, M. S., Wunderlin, D. A., Rovasio, J. L., Dotti, R., Rosso, J. C., Ghione, S., Ribotta, P. D., & Pérez, G. T. (2018). Changes in the antioxidant properties of quince fruit (Cydonia oblonga Miller) during jam production at industrial scale. Journal of Food Quality, 2018, Article 1460758. https://doi.org/10.1155/2018/1460758

NATIVE AND MALTED CEREALS IN WORT PRODUCTION: EXPLORING ALTERNATIVES TO BARLEY MALT

Milana Pribić, Lenka Grubač, Jelena Pejin

Department of Biotechnology, Faculty of Technology Novi Sad, University of Novi Sad, Bulevar cara Lazara 1, 21000 Novi Sad, Serbia
e-mail: milana.pribic@uns.ac.rs

Abstract

The use of unmalted cereals as partial substitutes for barley malt is a common practice in brewing and may contribute to more resource-efficient beer production. Unlike malting, which requires additional water, energy, and processing steps, the direct use of native cereals can reduce the resources associated with malt production. Therefore, the application of unmalted cereals represents a potential approach towards more sustainable wort production, provided that their technological limitations can be overcome.

This study evaluated the potential of barley, oats, and dark wheat, in both native and malted forms, as partial replacements for barley malt. Grists containing 25% and 50% of the cereals were used for wort production, with and without the addition of the commercial enzyme Termamyl® BrewQ to enhance starch degradation. Two mashing regimes, congress and modified (54 °C for 30 min, 64 °C for 45 min, and 80 °C for 10 min), were applied, and the quality of the resulting worts was evaluated.

Increasing the proportion of native cereals generally resulted in lower wort extract, whereas the congress mashing regime produced higher extract contents compared with the modified regime. Among the worts produced from native cereals, the highest extract content was obtained with 25% dark wheat, enzyme addition, and congress mashing (8.435±0.02%). The addition of Termamyl® BrewQ increased wort extract and shortened the saccharification time, demonstrating its contribution to starch degradation. In contrast, increasing the proportion of malted cereals resulted in higher extract contents, with the highest value obtained for wort containing 50% malted dark wheat with enzyme addition under the congress regime (8.524±0.02%), exceeding the control wort. The modified mashing regime resulted in higher soluble nitrogen content and lower wort viscosity compared with the congress regime.

The results indicate that native dark wheat and barley can be incorporated into grists at levels of up to 25% when supported by commercial enzyme addition, while malted barley and dark wheat can be used at levels of up to 50% without negatively affecting wort quality. These findings highlight the potential of native cereals to partially replace malt and reduce the processing requirements associated with malting, while maintaining acceptable wort quality.

Acknowledgements

This work was funded by the Ministry of Science, Technological Development and Innovation of the Republic of Serbia (No. 451-03-34/2026-03/ 200134 and 451-03-33/2026-03/ 200134) and by the Provincial Secretariat for Higher Education and Scientific Research, Republic of Serbia, Autonomous Province of Vojvodina (No. 002365668 2026 09418 002 000 000 001 04 002).

STOMATAL DENSITY AS A SELECTION MARKER FOR IMPROVED RESILIENCE TO DROUGHT

Putnik-Delić M.[1], Trkulja D.[2], Sakić A.[1], Mirosavljević M.[2], Mikić S.[2], Kastori R.[1], Maksimović I.[1]

[1]University of Novi Sad, Faculty of Agriculture, Trg Dositeja Obradovića 8, Novi Sad, Serbia
[2]Institute of Field and Vegetable Crops, Maksima Gorkog 30, Novi Sad, Serbia
e-mail: putnikdelic@polj.uns.ac.rs

Abstract
Drought severely threatens global wheat production, necessitating the breeding of resilient cultivars with improved water-use efficiency. Stomatal traits, particularly stomatal density (SD), play a crucial role in balancing photosynthesis and transpirational water loss. As part of the joint Serbian-Italian PHENO-DROP project, this study evaluated flag leaf SD across 50 bread wheat (*Triticum aestivum* L.) cultivars of various origins to characterize drought-tolerance mechanisms. Samples were collected from adaxial and abaxial leaf surfaces of field-grown plants. Statistical analysis revealed significant variations among genotypes, with SD ranging between 40 and 90 stomata/mm² alongside significant differences in the abaxial/adaxial SD ratio. These findings highlight substantial genetic diversity in stomatal patterning within germplasm, providing valuable wheat with significantly increased resilience to drought.

Introduction
Wheat production is increasingly jeopardized by drought, which can cause yield losses over 50% if present during critical phenological phases, such as anthesis and grain filling (Farooq et al., 2009). Therefore, breeding drought-resilient varieties has become a primary goal. Developing drought-tolerant cultivars relies on natural genetic variation found in landraces, wild relatives (*Triticum dicoccoides*, *Aegilops* spp.), and elite germplasm. Key targets include stomatal traits, such as density, size, and conductance, which regulate the balance between photosynthesis and transpirational water loss.
Mediterranean landraces and wild relatives offer novel alleles for drought tolerance, improved water-use efficiency (WUE), deep roots, and optimized stomatal control (Lopes et al., 2011; Monneveux et al., 2012). Wheat genotypes deploy three main survival strategies: drought escape (early flowering), drought avoidance (root uptake, leaf rolling, stomatal regulation), and drought tolerance (osmotic adjustment, antioxidants) (Ghosh et al., 2021). Among these, stomatal regulation is the frontline defense connecting water preservation to carbon fixation. The joint Serbian-Italian project PHENO-DROP addresses this issue by applying phenomics and genomics to hexaploid wheat panels, aiming to identify traits associated with drought resilience and high water-use efficiency (WUE).

Experimental
To characterize drought tolerance, this study evaluated SD on the flag leaf across 50 bread wheat cultivars from the Institute of Field and Vegetable Crops in Novi Sad. Plants were at mid-grain filling growth stage. Plots were 5 m long and 1 m wide, with 10 rows per plot, with target density of 500 plants per square meter.
Stomatal prints were collected from four plants per genotype from both the adaxial and abaxial leaf surfaces. Each sample was counted across 10 fields of view using an electric microscope at 100× magnification.
Statistical analysis of data was performed by Statistica 14. Significance of obtained differences between means was established by LSD test.

Results and discussion

Stomatal density on the flag leaf varies significantly across wheat cultivars. The number of stomata varied between 40 and 90 stomata per mm^2 of the leaf (Figure 1). According to the literature, depending on the species and variety, that number can vary between 40 and 180 stomata per mm^2, depending on side of the leaf blade (adaxial vs. abaxial), leaf position, ploidy level, and genetic background (Khazaei et al., 2010). The results also showed the statistically significant differences in the ratio of the number of stomata on the adaxial and abaxial leaf surfaces among the varieties (Figure 1 and 2).

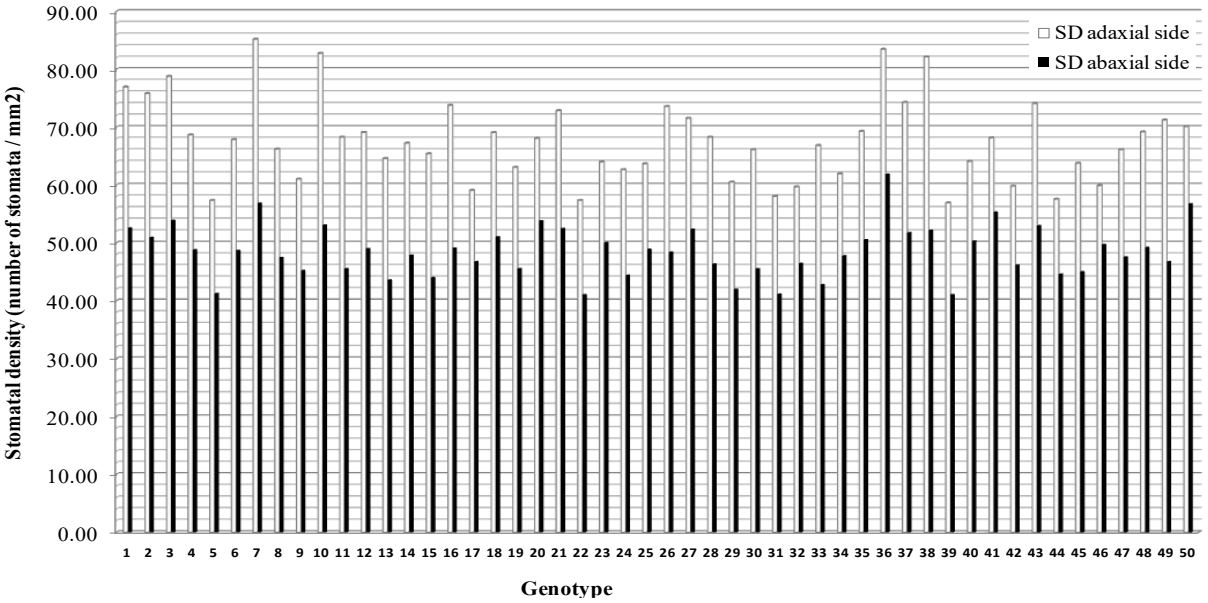


Figure 1. Stomatal density on adaxial and abaxial side of 50 wheat genotypes

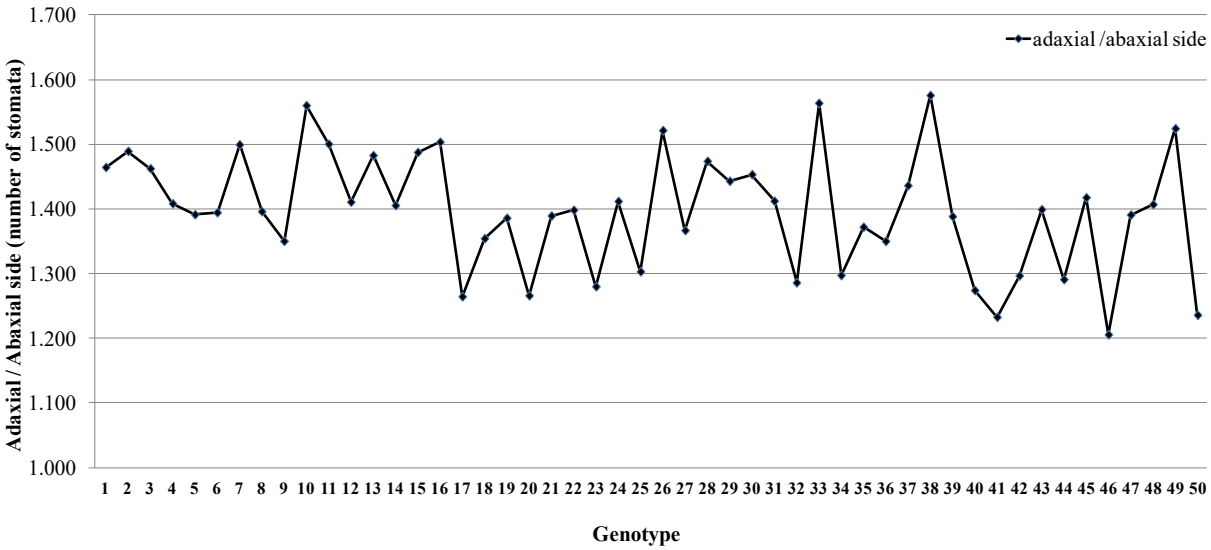


Figure 2. Ratio of stomata on the adaxial and abaxial side of the flag leaf of 50 wheat genotypes

Diploid wild relatives (e.g., *Triticum boeoticum*) generally display higher stomatal densities with smaller stomata, whereas hexaploid bread wheat (*Triticum aestivum*) exhibits lower stomatal density combined with larger guard cells due to genome duplication effects (Miskin

and Rasmusson, 1971). Wheat leaves are amphistomatic, featuring stomata on both the upper (adaxial) and lower (abaxial) surfaces of the leaf blade. Generally, the adaxial surface maintains a higher stomatal density than the abaxial surface. Research demonstrates that genotypes capable of altering the adaxial-to-abaxial density ratio under stress demonstrate finer micro-environmental acclimation (Wang and Clark, 1993).

Selecting wheat genotypes with inherently lower stomatal density is considered as an effective breeding strategy for water-limited environments. Plants with lower stomatal density exhibit reduced baseline transpiration under non-limiting conditions, conserving subsoil water reserve. Higher leaf water potential is necessary to be sustained for longer periods during progressive drought. Also, prevention of premature flag leaf senescence and maintainance of photosynthetic activity during grain filling is necessary. Research by Hepworth et al. (2015) demonstrated that genetic manipulation or phenotypic selection targeting reduced stomatal density in cereals yields drought tolerant plants without compromising yield potential under well-watered conditions. Across diverse wheat germplasm collections, an inverse correlation is frequently observed between stomatal density and stomatal size. Genotypes with smaller stomata can adjust stomatal aperture faster in response to sudden increases in vapor pressure deficiency or soil drying because small guard cells have a higher surface area to volume ratio, facilitating rapid ion fluxes (Hetherington and Woodward, 2003).

Therefore, the ideal drought-resilient ideotype often combines moderate to low stomatal density with smaller, more responsive stomata, allowing high maximum WUE and agile physiological regulation under fluctuating climate conditions.

Conclusion

Developing drought tolerant wheat genotypes is essential for ensuring global food security under escalating climatic volatility. Exploiting the broad genetic diversity present within available breeding material provides the foundation for successful breeding. The observed variation in stomatal density and the adaxial/abaxial stomatal density ratio highlights the potential of stomatal traits as useful characteristics for the selection of drought-resilient wheat genotypes. Stomatal density represents a reliable, highly heritable anatomical marker that directly governs water-use efficiency and drought avoidance. Genotypes characterized by reduced stomatal density, combined with rapid stomatal responsiveness, maintain higher physiological water potentials, exibit higher WUE and yield stability during water deficits. In the near future, combining high throughput digital microscopy with molecular markers for genes involved in stomatal development will provide wheat breeders with tools to select and develop resilient cultivars tailored for arid and semi-arid production environments.

Acknowledgements

Grant for the project "New PHENO-ideotypes for DROught resilience in hexaPloid wheat, PHENO-DROP", is highly acknowledged.

References

[1] M. Farooq, A. Wahid, N. Kobayashi, D. Fujita, S.M.A. Basra, Agron. Sustain. Dev. 29 (2009) 185-212.
[2] U.K. Ghosh, M.N. Islam, M.N. Siddiqui, M.A.R. Khan, Plant Signal. Behav. 16(8) (2021).
[3] C. Hepworth, T.W. Doheny-Adams, L. Hunt, D.D. Cameron, J.E. Gray, New Phytol. 208 (2015) 336-341.
[4] A. Hetherington, F. Woodward, Nature 424 (2003) 901-908.
[5] H. Khazaei, P. Monneveux, S. Hongbo S. Mohammady, Genet. Resour. Crop Evol. 57 (2010) 307-314.
[6] M.S. Lopes, J.L. Araus, P.D. van Heerden, C.H. Foyer, J. Exp. Bot. 62 (2011) 3135-3153.

[7] K.E. Miskin, D.C. Rasmusson, Crop Sci. 10 (1971) 575-578.
[8] P. Monneveux, R. Jing, S.C. Misra Front. Physio. 3 (2012) 429.
[9] H. Wang, J.M. Clarke, Canadian J. Plant Sci. 73 (1993) 671-678.

EVALUATION OF THE NUTRITIONAL COMPOSITION OF CATFISH PÂTÉS AND PASTE SUPPLEMENTED WITH WILD SPICE HERBS

Robert Daniel Neagu[1], Camelia Moldovan[2], Delia Gabriela Dumbravă[2], Viorica Mirela Popa[2], Corina Dana Mișcă[2], Aurica Breica Borozan[3], Diana Nicoleta Raba[4*]

[1] University of Life Sciences "King Michael I" from Timisoara, Doctoral School "Engineering of Vegetable and Animal, Calea Aradului 119, Timisoara 300645, Romania
[2]Faculty of Food Engineering, University of Life Sciences "King Mihai I" from Timișoara, Calea Aradului 119A, 300645, Romania
[3]Faculty of Engineering and Applied Technologies, Calea Aradului 119, Timisoara 300645, Romania
[4]Faculty of Management and Rural Tourism, University of Life Sciences "King Mihai I" from Timișoara, Calea Aradului 119A, 300645, Romania
e-mail: diana.raba@usvt.ro

Abstract
The growing consumer demand for nutritionally enhanced fish products has stimulated the development of innovative formulations incorporating natural plant ingredients. This study aimed to evaluate the nutritional composition of pâtés and spread produced from Danube-caught catfish (*Silurus glanis*) enriched with selected wild herbs originating from spontaneous flora, namely wild garlic (*Allium ursinum*), sorrel (*Rumex acetosa L.*), and patience dock (*Rumex patientia*), used individually or as a mixed herb formulation. The nutritional characteristics of raw herbs and sixteen experimental samples, including control fish pâtés and herb-enriched variants, were determined using standardized analytical methods. he analyzed fish pâtés exhibited moisture contents ranging from 43.90 to 49.85%, crude protein contents between 14.82 and 16.67%, lipid contents between 26.62 and 30.74%, and energy values of 330.09 to 354.88 kcal/100 g. The incorporation of wild herbs increased the carbohydrate fraction and contributed additional minerals, resulting in products with improved nutritional diversity. Among the experimental variants, pâtés containing mixed herbs presented the highest energy value (354.88 kcal/100 g), while liver-based pâtés enriched with herbs showed carbohydrate contents up to 11.55%. The results demonstrate that the incorporation of wild edible herbs into catfish-based pâtés can generate value-added products with desirable nutritional attributes and a balanced fatty acid composition. These formulations represent a promising strategy for enhancing the nutritional value and functional potential of fish-based foods while promoting the utilization of locally available wild plant resources.

Keywords: *Silurus glanis*, fish pâté, wild herbs, *Allium ursinum, Rumex acetosa, Rumex patientia*, nutritional composition.

SOME CRITICAL FACTORS INFLUENCING THE FOLIN-CIOCALTEU ASSAY FOR THE DETERMINATION OF TOTAL PHENOLIC CONTENT IN FOODS

Florina Radu[1], Georgeta-Sofia Popescu[1], Cerasela Petolescu[2], Diana Moigradean[1], Mariana-Atena Poiana[1], Daniela Stoin[1], Antoanela Cozma[3]

[1]Faculty of Food Engineering, University of Life Sciences "King Mihai I" from Timisoara, Romania, Aradului Street No 119, 300645 Timisoara, Romania
[2]Faculty of Engineering and Applied Technology, University of Life Sciences "King Mihai I" from Timisoara, Romania, Aradului Street No 119, 300645 Timisoara, Romania
[3]Faculty of Agriculture, University of Life Sciences "King Mihai I" from Timişoara, Aradului Street No 119, 300645 Timisoara, Romania
e-mail: florinaradu@usvt.ro

Abstract
The Folin–Ciocalteu (F–C) assay remains one of the most widely used colorimetric methods for estimating total phenolic content (TPC) in food, plant extracts, and biological samples. Despite its popularity, the assay is not specific to phenols and is influenced by pH, reaction stoichiometry, reagent stability, and the presence of non-phenolic reducing agents. This review synthesizes the chemical mechanism, structural determinants of reactivity, analytical limitations, and recent methodological improvements, with emphasis on the role of phenol structure, assay pH, and matrix interferences.

1. Introduction

Phenolic compounds constitute one of the most important classes of plant secondary metabolites, including phenolic acids, flavonoids, tannins, stilbenes, lignans, and lignins, and play essential roles in plant defense, oxidative stability, and the sensory properties of foods [1,2]. Their nutritional and functional relevance derives from their high antioxidant capacity, associated with reduced risk of chronic diseases and improved food quality, which makes the evaluation of total phenolic content (TPC) fundamental in food science. Measuring TPC provides a global indicator of antioxidant potential, enables comparison of varieties, processing technologies, and food matrices, supports the assessment of processing effects, and allows estimation of phenolic intake in dietary patterns such as the Mediterranean diet, where polyphenol consumption is high (800–900 mg/day) [3]. The Folin–Ciocalteu (FC) assay was first developed for tyrosine quantification and later adapted to measure polyphenols in red wine [4]. Its popularity stems from its simplicity and reproducibility. Antioxidants reduce the FC reagent to a blue chromophore measurable spectrophotometrically. The FC assay is widely used to estimate total polyphenol content in plant extracts and juices [5,6,7].The Folin–Ciocalteu (F–C) method is the most widely used colorimetric technique for determining TPC, based on the reduction of phosphomolybdic and phosphotungstic heteropoly anions under alkaline conditions, forming a blue complex measured at 760–765 nm [4,8]. Its simplicity, reproducibility, and broad applicability have established F–C as a standard analytical tool; however, the method is non-specific, as the reagent can also be reduced by non-phenolic compounds such as ascorbic acid, dehydroascorbic acid, reducing sugars, aromatic amino acids, organic acids, or lignocellulosic degradation products [1,9]. These interferences lead to overestimation of TPC, prompting the development of correction strategies including solid-phase extraction (SPE), calculation of corrected TPC values, oxidative pretreatments with H_2O_2, or dual-stage absorbance measurements (acidic and alkaline phases) [10]. In this context, a critical evaluation of the experimental factors influencing the accuracy of the F–C assay is

essential for rigorous interpretation and reliable use of this method in the analysis of phenolic compounds in foods.

2. Overview of the Folin–Ciocalteu (F–C) assay

The Folin–Ciocalteu method is a redox assay based on a single-electron transfer (SET) mechanism, widely used for determining the total phenolic content (TPC) in foods, plant extracts, and biological samples. It is considered a reference method due to its simplicity, reproducibility, and sensitivity [4,8,11]. Although its exact composition is not disclosed, the reagent is believed to contain heteropolyacids such as phosphomolybdic and phosphotungstic acids. The color change reflects the stepwise reduction of molybdenum species (Mo(VI) → Mo(V) → Mo(IV)(Equation 1).

$$\text{Mo (VI) (yellow)} + e^- \rightarrow \text{Mo (V) (blue)} + e^- \rightarrow \text{Mo (IV)} \qquad (1)$$

Under alkaline conditions (pH ≈ 10), phenolic compounds act as electron donors, reducing Mo(VI) and W(VI) to their partially reduced forms Mo(V) and W(V), generating an intense blue complex with maximum absorbance at 760–765 nm (Figure 1) [12,13].

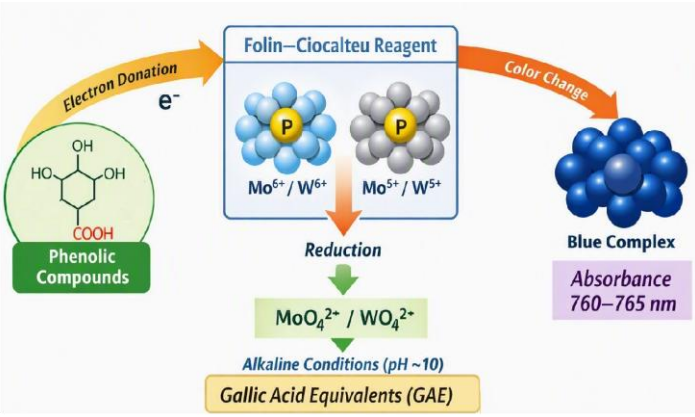


Figure 1. Folin Ciocalteu redox reaction mechanism

The color intensity is proportional to the reducing capacity of the phenolic compounds, and results are usually expressed as gallic acid equivalents (GAE), although other standards such as catechin, chlorogenic acid, or ferulic acid may also be used [1,2]. The reaction involves a sequence of reversible one or two electron transfer processes influenced by the phenolic structure, particularly by the number and position of hydroxyl and methoxy groups and by the stabilization of thephenoxyl radical through intramolecular hydrogen bonding [14-16]. Although robust, the method is not specific for phenolics, since any reducing compound (ascorbate, sulfites, amino acids, reducing sugars) may contribute to the signal, leading to overestimation of TPC [11, 17]. Interferences depend on the food matrix, pH, temperature, incubation time, and solvent; therefore, modified versions of the method have been proposed, including adaptations for lipophilic antioxidants [18]. Overall, the theoretical foundation of the F–C method relies on the reduction of Mo/W heteropolyoxometalates within a Keggin architecture (Eq. 1), the formation of blue reduced species (Figure 1), and the correlation between signal intensity and the electron-transfer capacity of phenolic compounds, explaining the close relationship between phenolic structure and analytical response.

3. Critical factors influencing the F-C assay

3.1. Influence of pH on the Folin–Ciocalteu reaction

The Folin–Ciocalteu (F-C) assay is fundamentally governed by the acid–base environment in which the redox reaction occurs. The pH determines both the **speciation of phenolic substrates** and the **redox potential of the heteropoly-molybdate/tungstate complex**, thereby controlling the kinetics and magnitude of blue chromophore formation (Figure 2).

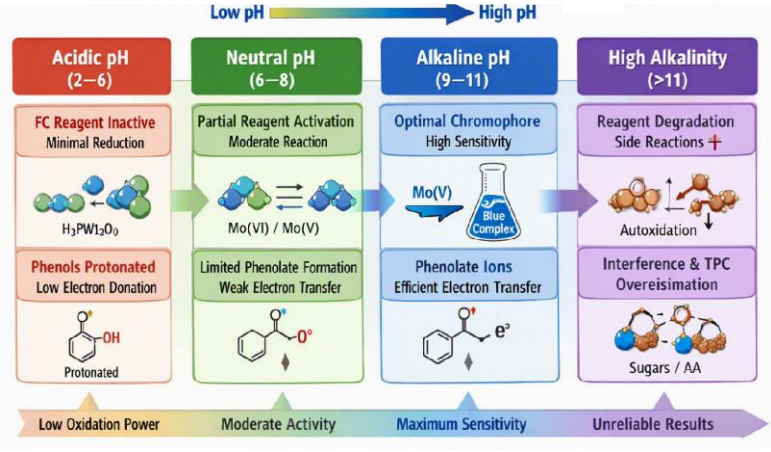


Figure 2. pH-dependent reactivity of phenolics and interfering compounds in the F-C assay

Because the F-C reagent is strongly acidic (pH ≈ 3), and the reaction is subsequently alkalinized to pH ≈ 10 by sodium carbonate, the assay proceeds through two mechanistically distinct phases: an **acidic pre-reaction phase** and an **alkaline electron-transfer phase**. At the initial acidic pH, phenolic compounds remain largely protonated and are **poor electron donors**. However, several non-phenolic reducing agents, such as, ascorbic acid (AA), dehydroascorbic acid (DHA), certain amino acids, and some sugars, are readily oxidized under these conditions. As described by Sánchez-Rangel et al. [1], AA and DHA (both enediols) reduce the phosphotungstate/phosphomolybdate complex **before phenolate formation occurs**, generating an immediate blue coloration. This early absorbance is therefore **not attributable to phenolics**, but to interfering reductants present in the matrix. This phenomenon explains why matrices rich in vitamin C (citrus, kiwifruit, strawberries) systematically overestimate total phenolic content (TPC) unless corrected. Upon addition of sodium carbonate, the reaction mixture reaches pH ≈ 10. Under these alkaline conditions, phenolic hydroxyl groups undergo **deprotonation**, forming phenolate ions with significantly enhanced electron-donating capacity. These phenolates reduce Mo(VI) to Mo(V), generating the characteristic blue chromophore [4, 19]. The alkaline pH therefore serves two essential functions: i) f**ormation of phenolate ions**, the active reducing species; ii) a**djustment of the redox potential** of the heteropoly complex, enabling efficient electron transfer. Excessive alkalinity (>10.5) destabilizes the blue complex and promotes precipitation of molybdate/tungstate salts, particularly in methanol-containing systems. Controlled carbonate concentration (5% w/v) minimizes this effect.

3.2. Structural determinants of phenolic reactivity

The reactivity of phenolic compounds in the Folin–Ciocalteu assay is governed by a set of structural parameters that modulate electron-donating ability, phenoxyl radical stability, and the kinetics of Mo(VI) → Mo(V) reduction. Although the F-C reagent is not selective for phenols, phenolic structures exhibit predictable reactivity patterns that correlate strongly with their antioxidant capacity and redox behavior in alkaline medium [4, 20] (Figure 3).

3.2.1. Number and position of hydroxyl groups. Hydroxylation degree is the primary determinant of phenolic reactivity. Each phenolic –OH group contributes to electron donation through homolytic O–H bond cleavage and formation of resonance-stabilized phenoxyl radicals. Trihydroxylated structures such as gallic acid exhibit the highest reducing capacity, explaining why gallic acid is consistently the most responsive calibration standard in the F-C assay [9, 20]. The catechol motif (3′,4′-dihydroxy) dramatically enhances reactivity due to intramolecular hydrogen bonding and stabilization of the resulting semiquinone radical. This structural feature explains the high reactivity of caffeic acid, catechol, quercetin, and other ortho-dihydroxylated phenolics [13, 20]. In contrast, para-hydroxylation alone (e.g., p-coumaric acid, 4-hydroxybenzoic acid) yields significantly lower reactivity because the phenoxyl radical lacks resonance stabilization across the aromatic ring.

3.2.2. Conjugation and extended π-systems. Phenolics with **extended conjugation** (flavonoids,

stilbenes, hydroxycinnamic acids) demonstrate higher reducing capacity because

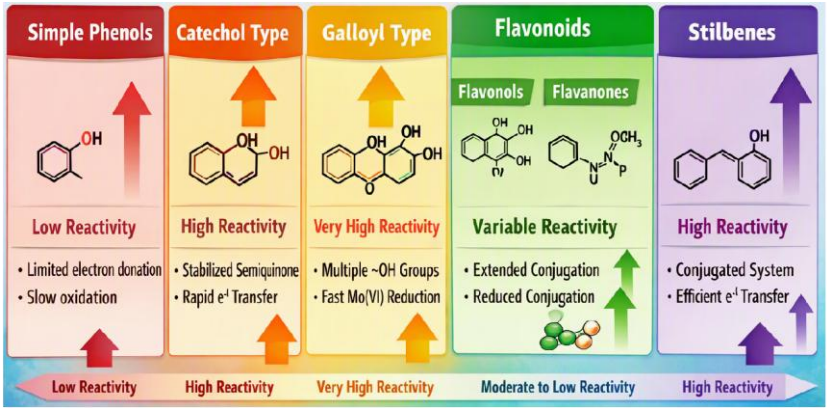


Figure 3. Structural determinants of phenolic reactivity in the F-C assay

delocalization of π-electrons facilitates electron transfer to the FC reagent. Flavonoids containing a **C2=C3 double bond and 4-oxo group** (e.g., quercetin) show particularly high reactivity due to the formation of **stable quinone-type structures** upon oxidation [8, 21]. The **B-ring catechol** in quercetin further enhances reactivity, making it one of the strongest FC-reactive flavonoids. Conversely, flavanones lacking the C2=C3 double bond (e.g., naringenin) exhibit significantly lower FC response.

3.2.3. Influence of substituents: electron-donating vs. electron-withdrawing groups. Electron-donating substituents (–OH, –OCH_3) increase phenolic reactivity by raising electron density on the aromatic ring, thereby facilitating oxidation. Methoxylated phenols (e.g., ferulic acid) show intermediate reactivity: the methoxy group donates electrons but also reduces the number of free hydroxyls available for oxidation. Electron-withdrawing substituents (–COOH, –NO_2) decrease reactivity by stabilizing the phenolic form and increasing oxidation potential. For example, *p*-nitrophenol exhibits minimal FC response despite being a phenolic compound **[15]**.

3.2.4. Steric hindrance and accessibility of phenolic hydroxyls. Bulky substituents near hydroxyl groups reduce FC reactivity by limiting access of the reagent to the phenolic oxygen. This effect is particularly relevant in **polymeric phenolics** (tannins) and **highly glycosylated flavonoids**, where steric shielding reduces oxidation rate. Glycosylation at the 3-or 7-position of flavonoids significantly decreases FC response compared to their aglycones [9].

4. Interfering Compounds and Their Mitigation

Although the Folin–Ciocalteu (FC) assay is widely used for estimating total phenolic content, its analytical signal is not exclusive to phenolic compounds. The reagent responds to any species capable of reducing the phosphomolybdic–phosphotungstic complex under alkaline conditions, leading to systematic overestimation when non-phenolic reductants are present **[4, 19]**. Interfering compounds originate from several chemical classes (ascorbates, reducing sugars, amino acids and proteins, organic acids and carbonyl compounds, Maillard reaction products, and inorganic reductants) each contributing distinct mechanistic pathways. Understanding these pathways and applying appropriate mitigation strategies is essential for improving assay specificity.

4.1. Ascorbic Acid and Dehydroascorbic Acid

Ascorbic acid (AA) is the most aggressive interferent due to its extremely rapid electron-transfer kinetics. AA reduces the FC reagent even under mildly acidic conditions, generating premature chromophore formation before phenolate ions are produced **[1]**. This leads to substantial overestimation of TPC in vitamin C rich matrices such as citrus fruits, berries, and tropical juices. Mitigation requires selective removal or neutralization of AA while preserving phenolic integrity. **Controlled oxidative pretreatment with hydrogen peroxide** is one of the most effective approaches. Raposo et al. [21] demonstrated that low concentration H_2O_2 oxidizes AA to non-reducing species without degrading phenolics, reducing interference by up to 40% [21]. **Ascorbate oxidase** offers high selectivity, particularly in foods where AA concentrations are substantial. Analytically, **dual phase or dual wavelength measurement**

allows subtraction of AA contribution by recording absorbance before and after alkalinization **[1]**. Finally, **solid-phase extraction** using C18 or polymeric sorbents effectively removes AA from aqueous extracts,

4.2. Organic Acids, Carbonyl Compounds, and Maillard Reaction Products

Organic acids (formic, acetic) and carbonyl compounds can reduce the FC reagent at high pH, especially in thermally processed foods. **Maillard reaction products**, particularly melanoidins, are strong reductants and represent major interferents in roasted, baked, or fermented matrices such as coffee, cocoa, cereals, and bread [22]. Mitigation depends on molecular size and solubility. **Dialysis and ultrafiltration** effectively remove high molecular weight melanoidins while retaining phenolics. **Differential solvent extraction** exploits solubility differences: phenolics partition into hydroalcoholic solvents, while melanoidins remain in the aqueous phase. For matrices heavily affected by Maillard products, Raposo et al. [21] recommend the **Fast Blue BB assay** as a complementary or confirmatory method, as it is less susceptible to interference from carbonyl compounds and melanoidins.

Conclusion

The Folin–Ciocalteu assay remains indispensable for estimating total phenolic content, but its lack of specificity requires careful interpretation. Understanding reagent chemistry, pH effects, structural determinants of phenolic reactivity, and the influence of interfering compounds is essential for accurate quantification. Mitigation strategies, ranging from oxidative pretreatment to SPE and matrix matched calibration, significantly improve assay reliability. The integrated perspective presented here provides a robust foundation for developing standardized protocols and enhancing analytical accuracy in complex matrices.

References

[1] J.C.S. Rangel, J. Benavides, J.B. Heredia, L.C. Zevallos, D.A.J. Velázquez, *Food Chem.* 141 (2013) 188–194.
[2] B. Xu, S.K.C. Chang, *J. Agric. Food Chem.* 55 (2007) 7164–7170.
[3] S. Dudonné, X. Vitrac, P. Coutière, M. Woillez, *Agric. Food Chem.* 57 (2009) 1772.
[4] V.L. Singleton, J.A. Rossi Jr., Am. J. Enol. Vitic. 16 (1965) 145.
[5] R. Kaur, P. Kapoor, Ind. Crops Prod. 169 (2021) 113640.
[6] M. Suleria, S. Barrow, F. Dunshea, Food Chem. 405 (2023) 134903.
[7] A. de Souza, L. Costa, M. Silva, J. Food Compos. Anal. 109 (2022) 104540.
[8] V.L. Singleton, R. Orthofer, R.M. Lamuela Raventós, *Methods Enzymol.* 299 (1999) 156.
[9] K. Bastola, S. Guragain, S. Bhadriraju, R. Vadlani, *Food Anal. Methods* 10 (2017) 3505.
[10] S.L. Nixdorf, I. Hermosín Gutiérrez, Anal. Chim. Acta 659 (2010) 208–215.
[11] D. Huang, B. Ou, R.L. Prior, J. Agric. Food Chem. 53 (2005) 1841–1856.
[12] L.M. Magalhães, F. Santos, M.A. Segundo, S. Reis, J. Lima, *Food Chem.*119 (2010) 695.
[13] I.G. Munteanu, C. Apetrei, Int. J. of Molecular Sciences 22 (2021) 3380.
[14] Y.Z. Cai, Q. Luo, M. Sun, H. Corke, Life Sciences 78 (2006) 2157–2184.
[15] H. Ma, P.C.K. Cheung, J. Agric. Food Chem. 55 (2007) 1010–1016.
[16] M. Platzer, A. Kiese, S. Herfellner, V. Weisz, J. Agric. Food Chem. 69 (2021) 12378.
[17] M. Samara, A. Nasser, U. Mingelgrin, Am. J. Anal. Chem. 13 (2022) 480.
[18] K. Berker, F. Olgun, D. Özyurt, B. Demirata, J. Agric. Food Chem. 61 (2013) 4786.
[19] J.D. Everette, Q.M. Bryant, A.M. Green, Y.A. Abbey, G.W. Wangila, R.B. Walker, *J. Agric. Food Chem.* 58 (2010) 813–820.
[20] S. Pérez Jiménez, M. Díaz Ruiz, A. Saura Calixto, Food Chem. 405 (2023) 135079.
[21] A. Raposo, M. Barreiros, M. Carvalho, A. Santos, M. Ferreira, Foods 13 (2024) 811.
[22] N. Cicco, V. Lattanzio, J. Agric. Food Chem. 59 (2011) 10872.

SOL–GEL SYNTHESIS, CATION DISTRIBUTION, AND ACID–BASE TAILORING OF CR-SUBSTITUTED ZINC FERRITE NANOSTRUCTURES

Raul Marius Reiz, Anamaria-Magdalena Savolszki-Madaras, Thomas Dippong

Technical University of Cluj-Napoca, Faculty of Science, 76 Victoriei Street, 430122, Baia Mare, Romania;
e-mail: thomas.dippong@cb.utcluj.ro

Abstract

Zinc ferrite ($ZnFe_2O_4$) is an oxide ceramic material featuring a spinel crystal structure, highly valued for its exceptional chemical and thermal stability, along with remarkable electrical and magnetic properties [1,2]. Its functional characteristics can be precisely tailored by doping it with various metal ions, making its final properties directly dependent on modifications in chemical composition, synthesis routes, and processing conditions [1]. Spinel ferrites have attracted significant attention due to their unique combination of physical traits, including high coercivity, low eddy current losses, low saturation magnetization, and high electrical resistivity [3]. Furthermore, substituting divalent and trivalent cations within spinel ferrite nanoparticles can fundamentally alter their structural, vibrational, morphological, and magnetic properties [3].

Chromium doping enhances the functional performance of zinc ferrite by replacing Fe^{3+} with Cr^{3+} ions [1]. This substitution alters the distribution within the spinel lattice, directly tuning the structural, electrical, optical, and electrochemical properties [1]. Due to the high structural compatibility of Cr^{3+}, these stable materials allow electronic transfer processes to be controlled without disrupting the primary crystalline phase [1]. Furthermore, nanostructured Zn-Cr ferrites exhibit increased specific surface area and enhanced surface-related phenomena, making them highly advantageous for diverse technological applications [1].

Chromium-doped zinc ferrite adopts a cubic spinel structure, which is characteristic of compounds with the general formula AB_2O_4 [1,2]. Within this configuration, Zn^{2+} ions predominantly occupy tetrahedral (A) sites, whereas Fe^{3+} and Cr^{3+} ions are distributed across octahedral (B) sites [1,2]. This cationic arrangement underpins the structural stability of the material, providing an effective pathway for tuning its properties through controlled metal ion substitution [1]. X-ray diffraction (XRD) investigations have demonstrated that chromium incorporation does not trigger the formation of secondary phases; all analysed compositions strictly retain the characteristic spinel framework of zinc ferrite [1]. Nevertheless, replacing Fe^{3+} with Cr^{3+} ions induce variations in the lattice parameters and crystallite size due to the difference in ionic radii between the two species [1].

The incorporation of chromium alters the electronic environment of the crystal lattice and significantly impacts charge transport mechanisms [1]. The electrical properties of chromium-doped zinc ferrite are tightly governed by the structural and electronic changes resulting from the Fe^{3+}/Cr^{3+} replacement. In spinel ferrites, electrical conduction is generally associated with the small polaron hopping mechanism, which involves electron transfer between metal ions occupying octahedral sites [1]. Increasing the Cr^{3+} concentration modifies charge carrier mobility and influences the rate of electron transfer processes, allowing the electrochemical properties of the material to be customized according to specific application requirements [1]. Composition-dependent modifications of the band gap energy and charge-transfer resistance significantly affect the semiconductor behaviour of these doped zinc ferrite materials [1].

While undoped zinc ferrite has high native sensitivity, chromium incorporation allows precise kinetic tuning and optimized functional properties [1]. This enhanced sensing performance stems from the synergistic effect of a porous structure, increased active surface area, and higher

structural defect concentrations, which collectively accelerate gas adsorption and electron exchange at the material–environment interface [4].

In this study, undoped and Cr-doped zinc ferrites were synthesized via the sol–gel method involving precursor hydrolysis/polymerization, gelation, solvent evaporation, and drying. A final calcination step at tailored temperatures was performed to achieve high-purity crystalline phases. A final thermal treatment is typically performed to obtain the target crystalline phase with high purity. Thermal analysis was employed to investigate the formation and decomposition processes of the zinc and chromium succinate precursors. To verify precursor stoichiometry, acid-base properties of samples calcined at 200 °C were evaluated via conductometric and pH-metric titrations. By calculating consumed HCl (for succinate protonation) and NaOH (for Zn^{2+} /Cr^{3+} hydroxide precipitation) across consecutive equivalence points, the precursor nature was determined. A stoichiometric ratio of $H^+/OH^- = 1$ confirms a neutral zinc/chromium succinate precursor, whereas a ratio of $H^+/OH^- = 2$ indicates a basic hydroxysuccinate species. Fourier-transform infrared spectroscopy (FTIR) confirmed the silica matrix formation and characteristic metal–oxygen (M-O) ferrite bonds. Ultimately, these acid-base properties strongly validate thermal and FTIR data, proving that the underlying redox reaction yields coordinated neutral or basic carboxylate complexes that stabilize the target metal ions into highly pure precursor matrices.

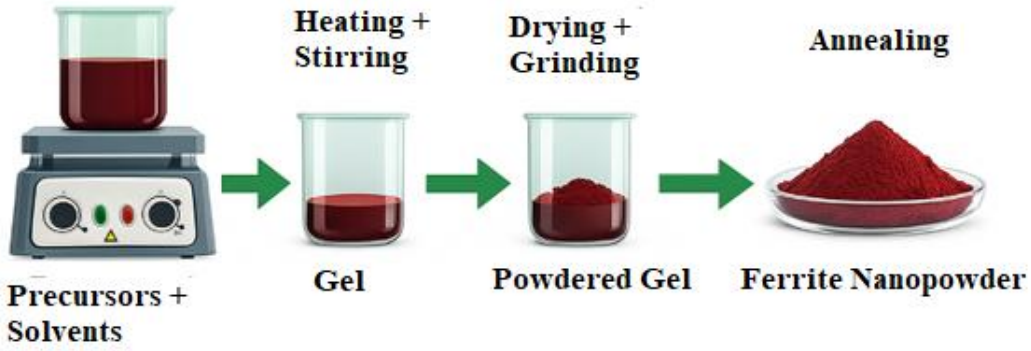


Figure 1. Sol–Gel Synthesis of Chromium-Doped Zinc Ferrite

Acknowledgements: This work was supported by the Technical University of Cluj-Napoca through the doctoral research program within the IOSUD-UTCN. The authors gratefully acknowledge the financial support for participating in this conference.

CARBON-BASED QUANTUM DOTS AND THEIR ROLE IN WASTEWATER TREATMENT

Andrea Rónavári[3], Tamás Bodor[1,2], Zoltán Kónya[3]

[1]Department of Plant Biology, University of Szeged, Szeged, Hungary
[2]Doctoral School of Biology, Faculty of Science and Informatics, University of Szeged, Szeged, Hungary
[3]Department of Applied and Environmental Chemistry, University of Szeged, Szeged, Hungary
e-mail: ronavari@chem.u-szeged.hu

Abstract

Carbon-based nanomaterials are increasingly investigated for applications in environmental, industrial and biomedical technologies, raising growing interest in their potential release into aquatic systems and wastewater treatment processes. Among these materials, graphene quantum dots (GQDs) and carbon quantum dots (CQDs) represent an emerging class of nanoscale carbon materials with unique physicochemical and optical properties. Their small size, high surface area and pronounced interactions with biological interfaces may influence microbial communities and the performance of biological wastewater treatment systems.

In this study, the interactions of graphene quantum dots (GQDs) with aerobic granular sludge (AGS) during biological wastewater treatment were investigated as a model system for assessing the response of microbial aggregates to carbon-based quantum dots. AGS sequencing batch reactors were exposed to GQDs at environmentally relevant concentrations (1, 5 and 10 mg/L) for 10 days, followed by a 14-day recovery period in the absence of the nanomaterial. The study focused on changes in wastewater treatment performance, extracellular polymeric substance (EPS) production, sludge characteristics and the retention and distribution of the fluorescent nanomaterial within the granular sludge system.

GQD exposure caused concentration-dependent changes in AGS performance, EPS production and sludge properties, while the treatment system remained functional. Several responses were reduced during recovery, indicating the adaptability of AGS to nanomaterial exposure.

These findings highlight the relevance of carbon-based quantum dots, including GQDs and CQDs, for understanding nanomaterial behaviour and interactions in biological wastewater treatment systems.

INFLUENCE OF TECHNOLOGICAL ENVIRONMENTS ON CORROSION OF METAL ALLOYS IN MINCED MEAT PROCESSING

Nataliia Rudenko[1], George Daniel Dima[2], Cristian George Vaszilcsin[3], Mircea Laurențiu Dan[2]

[1]University Politehnica Timisoara, Innovation and Technology Transfer Center, University Politehnica Timisoara, 300501 Timisoara, str. Gavriil Musicescu 138, Romania
[2]University Politehnica Timisoara, Faculty of Chemical Engineering, Biotechnologies and Environmental Protection, blvd. Vasile Parvan 6, 300223 Timisoara, Romania
[3]National Institute of Research and Development for Electrochemistry and Condensed Matter, Dr. A. P. Podeanu 144, 300569, Timişoara, Romania
e-mail: mircea.dan@upt.ro

The meat processing industry uses a wide range of metal equipment for receiving and storing raw materials, slicing, chopping, mixing, filling, heat treatment, cooling, washing and sanitizing. During these operations, metal surfaces come into repeated contact with complex environments, characterized by the presence of water, proteins, fats, mineral salts, organic acids, additives, cleaning agents and disinfectants. In the case of minced meat products, the contact between the product and the equipment is particularly important, since the large specific surface area of the food mass, the uneven distribution of moisture and salt, as well as the possibility of retaining organic residues in hard-to-reach areas can favour the initiation and development of localized corrosion.

The issue is of technical, economic and sanitary interest, since the degradation of equipment can affect the durability of the facilities, maintenance costs, the quality of the finished product and food safety.

Iron-based alloys, especially austenitic stainless steels of the AISI 304/304L and AISI 316/316L types, are the predominant materials for food processing equipment due to their corrosion resistance, mechanical properties, cleanability and ability to form a passive film rich in chromium oxides. Under favourable conditions, this film limits the anodic dissolution of the metal and maintains the surface in a passive state. However, passivity is not absolute. It can be affected by the composition of the medium, the process temperature, the pH, the concentration of aggressive ions, aeration, surface roughness, manufacturing defects, the presence of welded joints and sanitation conditions. In minced meat processing, chlorides constitute one of the most important categories of aggressive species. These can come from both sodium chloride added to recipes and from process water, cleaning solutions or chlorine-based disinfectants. Chloride ions can locally destabilize the passive film of stainless steels, leading to pitting and crevice corrosion. These forms of attack are particularly dangerous because they can develop under deposits, in metal-to-gasket contact areas, in pores, at joints and in areas with poor drainage, without being immediately observed during visual inspection. In a recent study on AISI 304L stainless steel in food applications, risks of localized corrosion were reported in environments containing chlorides and chlorinated biocides; the authors emphasize the need to control the chloride concentration and the contact time with sanitizing agents. For AISI 304L steel, the literature indicates the need to limit the chloride concentration in the contact environment, especially under conditions of high temperature or stagnant solutions.



Figure 1. Schematic representation of corrosion-related factors in stainless-steel equipment used for ground meat processing (Created by the authors using an AI-assisted image-generation tool and scientifically reviewed by the authors)

The technological environments in the manufacture of minced meat products are variable. Meat contains water, proteins, lipids, nitrogen compounds, phosphates, salts and metabolites, and formulations may include salt, sodium nitrite, polyphosphates, ascorbate or erythorbate, spices and other ingredients. During processing, food components can form films or deposits on metal surfaces. These deposits can create microzones with different concentrations of oxygen, humidity, pH and ions, favouring the appearance of differential aeration cells. In addition, the accumulation of organic debris in insufficiently cleaned areas can generate corrosion conditions under the deposits and reduce the efficiency of natural passivation of stainless surfaces. Although fats are not usually electrochemically aggressive environments, they can retain impurities, water and saline residues, indirectly contributing to the maintenance of local conditions favourable to corrosion in the crevice.

The correct selection of the alloy must be correlated with the severity of the technological environment and the hygiene requirements. AISI 304L stainless steel is suitable for many applications where the chloride concentration is low, the surface is well finished, and cleaning and rinsing are strictly controlled. In contrast, for components frequently exposed to saline solutions, stagnant humid environments, higher temperatures, or more aggressive cleaning agents, AISI 316L steel can offer superior resistance to localized corrosion due to the addition of molybdenum. However, the use of a higher alloy does not replace the need for proper hygienic design. Areas with crevices, exposed threads, unfinished welds, excessive roughness, dead corners, and insufficient drainage should be avoided, as they allow the accumulation of product and cleaning solutions.

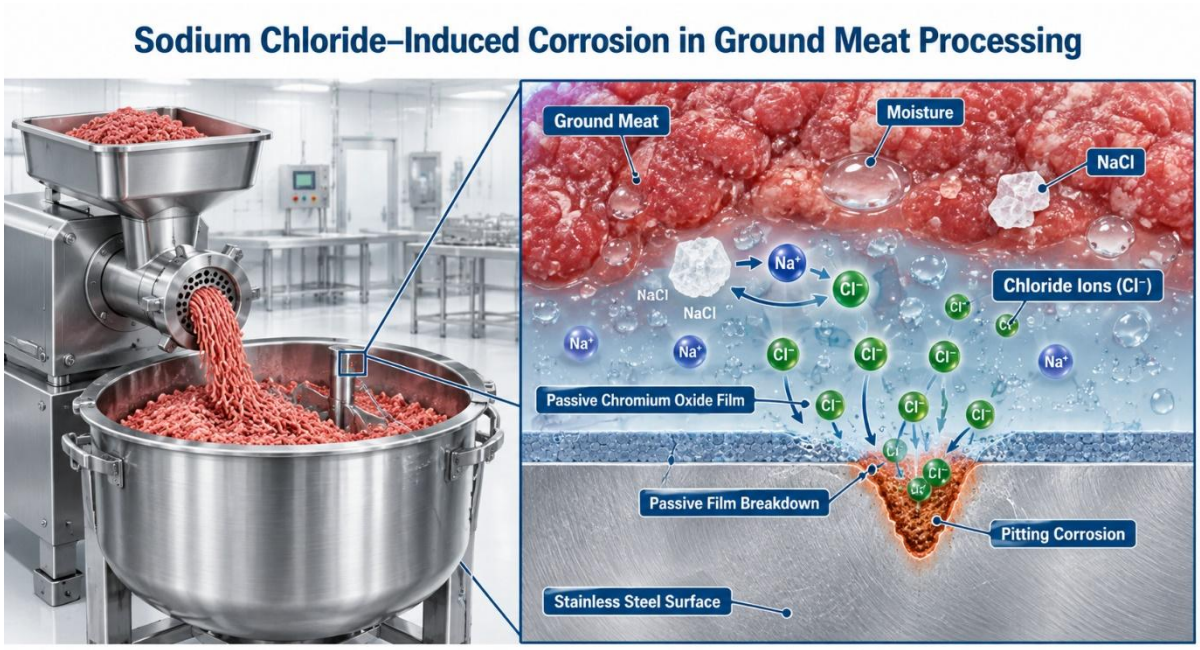


Figure 2. Conceptual illustration of sodium chloride-induced localized corrosion in stainless-steel equipment used for ground meat processing (Created by the authors using an AI-assisted image-generation tool and scientifically reviewed by the authors)

Preventing corrosion in minced meat processing facilities requires a multidisciplinary approach, based on judicious choice of materials, hygienic design, adequate surface finishing, weld inspection, application of validated cleaning and disinfection procedures, water quality monitoring and personnel training. It is recommended to avoid prolonged contact with chlorinated solutions, comply with the concentrations and temperatures prescribed for sanitizing products, perform complete rinsing after disinfection and prevent stagnation of liquids on metal surfaces. Also, periodic inspections of critical areas, electrochemical evaluation of material behaviour and degradation analysis can contribute to the early detection of corrosion mechanisms. In conclusion, corrosion of metal alloys in minced meat processing is determined by the interaction between the composition of the food product, process parameters and the sanitizing regime. Chlorides, oxidizing agents, organic deposits, geometric defects and local differential aeration conditions are the main factors of localized corrosion. By applying integrated measures of material selection, design, operation and maintenance, the service life of the equipment can be increased, and the risk of contamination associated with the degradation of metal surfaces can be reduced.

Acknowledgements

The authors used Perplexity AI image-generation tools to assist in preparing the conceptual illustration presented in Figures 1 and 2. The authors reviewed, edited, and verified the scientific accuracy, terminology, and relevance of the final figure and assume full responsibility for its content.

References

[1] S. Rossi, S.M. Leso, M. Calovi, Materials. 17 (2024) 1617.
[2] R.H. Schmidt, D.J. Erickson, Food Prot. Trends. 32 (2012) 574-584.
[3] A.H. Tuthill, R.A. Covert, FES. 20 (2000) 506-517.
[4] S.H. Mameng, R. Pettersson, J.Y. Jonson, Mater Corros. 68 (2017) 272–283.
[5] A. Azimi Dastgerdi, A. Brenna, M. Ormellese, M.P. Pedeferri, F. Bolzoni, Corros. Sci. 170 (2020) 108–695.

[6] D. Steiner Petrovič, D. Mandrino, Food Control. 73 (2017) 806–815.
[7] M. El-Shenawy, H. Al-Mazeedi, A. Ghoneim, D. Al-Bader, S. Al-Mufti, A. Al-Rasheed, Z. Al-Hajri, F. Al-Hamdan, J. Food Eng. 117 (2013) 34-40.
[8] B. Valdez, M. Schorr, in Corrosion in the Food Industry and Its Control. In Food Industrial Processes – Methods and Equipment, InTech, Rijeka, Croatia, 2012; pp. 367-398.
[9] A.H. Tuthill, R.E. Avery, in Guidelines for the Welded Fabrication of Nickel-Containing Stainless Steels for Corrosion Resistance Services, Nickel Development Institute, Toronto, ON, Canada, 1992.
[10] World Stainless Association. Stainless Steel in the Food and Beverage Industry in Materials and Applications Series, Volume 7, World Stainless Association, Brussels, Belgium, 2006.
[11] A.J. Sedriks, in Corrosion of Stainless Steels, 2nd ed., John Wiley & Sons, New York, NY, USA, 1996.
[12] J.R. Davis, in Ed. Stainless Steels, ASM International, Materials Park, OH, USA, 1994.
[13] R.W. Revie, H.H. Uhlig, in Corrosion and Corrosion Control: An Introduction to Corrosion Science and Engineering, 4th ed., John Wiley & Sons, Hoboken, NJ, USA, 2008.
[14] D.A. Jones, in Principles and Prevention of Corrosion, 2nd ed.; Prentice Hall, Upper Saddle River, NJ, USA, 1996.
[15] R. Scheidegger, R.O. Mueller, Mater. Corros. 31 (1980) 5-12.

MORPHOLOGICAL AND THERMAL BEHAVIOR OF CALCIUM BISMUTHATE ($Ca_2Bi_2O_5$)

[1]Florina Stefania Rus, [1]Alexandra Ioana Bucur, [1]Raul Alin Bucur, [1]Andrei Racu, [1]Cristina Mosoarca, [1]George Dima, [1]Bogdan-Ovidiu Taranu, [1]Radu Banica, [2]Adrian-Ionut Cadis

[1]National Institute of R&D for Electrochemistry and Condensed Matter, 144 Dr. Aurel Păunescu-Podeanu, RO-300569 Timisoara, Romania
[2] "Babes-Bolyai" University, "Raluca Ripan" Institute for Research in Chemistry, Fantanele 30, RO-400294 Cluj-Napoca, Romania;
e-mail: rusflorinastefania@gmail.com

Abstract

Alkaline-earth bismuthates remain an underexplored class of visible-light-responsive semiconductors, with structural and thermal aspects often receiving less attention than their photocatalytic performance. This work focuses on the particle morphology and thermal decomposition behaviour of $Ca_2Bi_2O_5$ powder obtained via a fast precipitation route from calcium and bismuth nitrate solutions, precipitated with ammonium oxalate and calcined at low temperature. Scanning electron microscopy revealed an unusual dumb-bell-shaped particle morphology with an average size of hundreds of nm — a feature that may enhance the material's specific surface area beyond what is typically reported for solid-state-derived bismuthates. Thermogravimetric analysis tracked the decomposition pathway in detail, showing a cumulative mass loss of 15 % across three distinct thermal events, with the material reaching full thermal stability above 660 °C. X-ray diffraction verified the resulting phase as single-phase, triclinic $Ca_2Bi_2O_5$ (space group P–1), confirming that this rapid precipitation route reaches phase purity at a comparatively low calcination temperature. These structural and thermal insights complement existing photocatalytic studies on this compound and offer a morphology-focused perspective that may inform particle-engineering strategies for future Ca–Bi–O photocatalyst design.

Acknowledgements

This work was supported by the Nucleu Program within the National Research Development and Innovation Plan 2022–2027, carried out with the support of MCID, project no PN 23 27 02 01 contract no. 29N/2023.

References

[1] Cadiș, A.I.; Rus, F.Ș.; Gonçalves, J.N.; Ivanovici, M. Preparing a Ca-Bi-O System by the Precipitation Method and Studying Its Intermediate Structural Properties for Applications in Water Treatment. Inorganics 2023, 11(2), 79. https://doi.org/10.3390/inorganics11020079

[2] Ji, X.; Lu, J.-F.; Wang, Q.; Zhang, D. Impurity Doping Approach on Bandgap Narrowing and Improved Photocatalysis of $Ca_2Bi_2O_5$. Powder Technol. 2020, 376, 708–723. https://doi.org/10.1016/j.powtec.2020.08.029

[3] Luo, W.; Tang, J.; Zou, Z.; Ye, J. Preparation and Photophysical Properties of Some Oxides in Ca–Bi–O System. J. Alloys Compd. 2008, 455, 346–352. https://doi.org/10.1016/j.jallcom.2007.01.096

SODIUM BENZOATE AND TRYPTOPHOL: DUAL ACTION INHIBITORS OF BIOFILM FORMATION AND QUORUM SENSING OF FOOD SPOILAGE BACTERIA

Urjinlkham Ryenchindorj[1], Viktória Gulyás[1], Csaba Vágvölgyi[1], Tamás Papp[1,2], Miklós Takó[1], Erika Beáta Kerekes[1]

[1]Department of Biotechnology and Microbiology, Faculty of Science and Informatics, University of Szeged, H-6726 Szeged, Közép fasor 52, Hungary
[2]HUN-REN-SZTE Pathomechanisms of Fungal Infections Research Group, University of Szeged, H-6726 Szeged, Közép fasor 52, Hungary
e-mail: urjeedorj5@gmail.com

Biofilm formation and quorum sensing (QS) allow foodborne microorganisms to persist and adapt to food processing environments where they coordinate virulence, stress tolerance, and resistance that undermine conventional preservation strategies. With broader relevance to microbial ecology and biotechnology, targeting these QS regulated behaviors has emerged as a promising approach for food safety and preservation. Tryptophol, an aromatic alcohol derived from tryptophan, is a QS molecule produced by yeast that can serve as an alternative or supplement to synthetic food preservatives. The aim of this study was to evaluate the minimal inhibitory concentration (MIC), anti-biofilm activity, anti-QS, and the synergistic potential of tryptophol and the synthetic preservative sodium benzoate (SOD) against *Bacillus cereus*, *Bacillus subtilis*, *Staphylococcus aureus*, *Escherichia coli* and *Pseudomonas putida*. Anti-QS activity was assessed using the pigment producing bacteria *Chromobacterium violaceum* and *Serratia marcescens*. The checkerboard method was used for the combined effect of the compounds, and its interaction was calculated using the fractional inhibitory concentration (FIC) index. Tryptophol showed MIC values that ranged from 0.94 mg/mL (*C. violaceum*) to 3.75 mg/mL (*S. aureus*), while SOD MICs ranged from 6.25 mg/mL (*E. coli*) to 50 mg/mL (*S. aureus*). Tryptophol reduced biofilm formation to 17–72% relative to the control at MIC/2 concentration, with the strongest reduction observed against *B. cereus* (17.3% biofilm formation) and the weakest against *P. putida* (72.2% biofilm formation). SOD reduced biofilm formation to 35–85%, with the strongest suppression against *B. subtilis* (35.3% biofilm formation) and the lowest against *P. putida* (84.7% biofilm formation). Pigment production in *C. violaceum* and *S. marcescens* was reduced by both compounds to 16–21%. The combined application of tryptophol and SOD produced an additive effect against *B. cereus*, *B. subtilis*, *P. putida*, and *C. violaceum*. Results indicate that tryptophol and SOD show selective antibacterial activity and can effectively influence QS and biofilm formation. Their combination can be a promising strategy for biofilm inhibition and food preservation.

This research was funded by the National Research, Development and Innovation Office (NKFI grants PD 142122, 2024-1.1.1-KKV_FÓKUSZ-2024-00050 and 2025-1.2.4-TÉT-2025-00033).

CHANGES IN SEED GERMINATION AND INITIAL GROWTH OF SIX DIFFERENT SPECIES IN RESPONSE TO BIOSTIMULANTS

Anastasija Sakić, Milica Miljanić, Marina Putnik-Delić, Ivana Maksimović

University of Novi Sad, Faculty of Agriculture, Trg Dositeja Obradovića 8, Novi Sad, Serbia
e-mail: anastasija.vujovic@polj.edu.rs

Seed germination is a key phase in the life cycle of seed plants since it affects early plant development as well as later productivity. In response to climate change, sustainable agricultural practices, including the use of biostimulants, are attracting more attention for their potential to improve plant growth and tolerance to abiotic stress. The aim of this study was to evaluate the effects of an algae-based (Agro GreenWay) and a *Bacillus*-based (BioticB) biostimulants on germination and initial growth of four vegetable species (cucumber, garden cress, Swiss chard, and cabbage) and two field species (wheat and maize). For each crop and biostimulant, five treatments were applied (in triplicates): the recommended concentration of biostimulant according to the manufacturer's instructions, 10, 50, and 100 times higher, and water as a control. Each Petri dish (R=9cm) contained 20 cucumber seeds or 30 seeds of the other crops placed on filter paper, supplied with 10 mL of the corresponding treatment solution, and covered with a lid. Germination was monitored every 24 hours, while shoot and root fresh mass of seedlings was recorded in cucumber, Swiss chard, cabbage, and wheat. Data were analyzed using one-way ANOVA followed by Fisher's LSD test. Effects of biostimulants varied by crop species and applied concentration. Agro GreenWay initially delayed germination in cucumber, Swiss chard, and wheat, although final germination was comparable to the control. It also increased maize germination, including at concentrations higher than recommended. In cabbage, the 100 times higher concentration significantly increased root fresh mass compared to both the control and the recommended concentration. BioticB reduced Swiss chard germination at all tested concentrations, while maize showed enhanced germination at the concentration 50 times higher than recommended. Germination of garden cress increased at 10 times higher concentration of BioticB, compared to the control. Since these responses were observed under laboratory conditions, they may be different in the field, where interactions between plants, microorganisms, and biostimulants can influence the final outcome.

Keywords: biostimulants; seed germination; cucumber; garden cress; Swiss chard; cabbage; wheat; maize

Acknowledgments: This work was funded by the Ministry of Science, Technological Development and Innovation under Contract No. 451-03-34/2026-03/200117 dated 05 February 2026. In addition, Centre of Outstanding Values for the Adaptation of Agricultural, Urban and Forest Ecosystems to Climate Change (Agro-Ur-For) is also acknowledged.

GRANULOMETRIC RESOLUTION AS A CONTROLLING FACTOR IN THE DETECTION OF RADIONUCLIDE REDISTRIBUTION IN DUST-FORMING MATERIALS

Selena Samardžić Cvijanović[2], Kristina Bikit[1], Tomas Nemeš[2], Robert Lakatoš[2], Jan Hansman[1], Ivana Lončarević[2], Dušan Mrđa[1], Sofija Forkapić[1]

[1]Department of Physics, Faculty of Sciences, University of Novi Sad, Trg Dositeja Obradovića 4, 21000 Novi Sad, Serbia
[2]Faculty of Technical Sciences, University of Novi Sad, Trg Dositeja Obradovića 6, 21000 Novi Sad, Serbia
e-mail: selena@uns.ac.rs

Abstract

Particle-size-resolved gamma spectrometry is increasingly used to assess radionuclide redistribution in comminuted mineral materials. The choice of fraction binning is treated as a practical detail rather than as a factor that conditions the outcome. A set of 27 construction materials and secondary mineral substrates was analysed under a coarse three-class scheme (PSD3: 1000–125, 125–75, <75 μm) and a seven-class scheme (PSD7: >500 to <50 μm) by HPGe gamma spectrometry, with particle-size descriptors obtained by laser diffraction. Under PSD3 the classes separated the samples by size correctly ($\rho = -0.93$ against D[4,3], $p < 0.001$) but detected no redistribution of ^{226}Ra, ^{232}Th or ^{40}K (Friedman $\chi^2(2) = 2.696$, $p = 0.260$). In PSD7 sheme a systematic rise of the activity concentration index toward the fines was found ($\chi^2(6) = 20.368$, $p = 0.002$), and the apparent composition of the index changed with the scheme: under PSD3 the index tracked ^{232}Th ($\rho = 0.893$, $p < 0.01$) with no measurable radium association ($\rho = 0.026$), whereas under PSD7 it tracked ^{40}K ($\rho = 0.685$) and ^{226}Ra ($\rho = 0.532$, both $p < 0.01$) and not ^{232}Th ($\rho = 0.202$). Neither ranking reproduces the bulk baseline, in which all three radionuclides contribute comparably. Coarse binning therefore does not merely attenuate the signal — it can attribute it to the wrong radionuclide.

Keywords: gamma spectrometry; particle size distribution; granulometric resolution; activity concentration index; NORM

Introduction

Indoor environments are the dominant setting for human radiation exposure, and construction materials are a principal source of both external gamma radiation and radionuclide-bearing dust. The activity concentration index Iγ defined in the European Basic Safety Standards is the established screening tool for these materials [2,3]. It is computed from bulk activity concentrations and therefore assumes that radionuclides are distributed uniformly throughout the material. Occupants and workers, however, are exposed to the fine, abradable and respirable fractions released during cutting, milling, sanding, sweeping and demolition, not to the intact bulk product.

That radionuclides are enriched in fine particles is long established, documented since Megumi and Mamuro [5] and reported for soils, sediments, ashes and building materials [6–8]. Its existence is not in question here.

There is a limited number of investigations into the granulometric resolution that examine the core of its influence on radionuclide redistribution. Published work bins particle sizes into classes of widely differing granularity, yet this choice is treated as a methodological detail rather than as a factor that may condition the result. Two consequences follow, and neither has been quantified. Immediately, data grouping at a coarse level average out the activity associated with the transition of material from within the crystal lattice to a surface-bound state. Consequently, the actual redistribution may be so attenuated that it becomes undetectable. This

makes it impossible to distinguish a negative result from one caused by insufficient resolution. Secondly, averaging during this same transition can distort the apparent contribution of individual radionuclides, such that even a positive finding might be erroneously attributed to the wrong radionuclide.The present work quantifies both effects on a single sample set analysed under two binning schemes of different resolution. The radiological consequences of the redistribution for this sample set have been reported previously [1]; the question addressed here is distinct, namely how the choice of fraction binning conditions whether, and to which radionuclide, the redistribution is attributed.

Experimental. Twenty-seven construction materials and secondary mineral substrates (ceramic and granite tiles, stone, brick, roof tile, cement, aerated concrete, gravel, fireclay and biomass-ash pellets) were dry-sieved (Analysette 3 PRO, Fritsch; ISO 3310-1 sieves) into seven size classes (>500, 500–250, 250–125, 125–100, 100–75, 75–50 and <50 µm); where fraction masses fell below that required for representative counting, fractions were pooled into three classes (1000–125, 125–75 and <75 µm). Activity concentrations of ^{226}Ra, ^{232}Th, ^{40}K and ^{137}Cs were measured by low-level HPGe gamma spectrometry (Canberra; 32.4 % and 105.8 % relative efficiency) for approximately 18 h per sample after at least 40 days of secular equilibration, with Genie 2000 and ANGLE 5. Particle-size descriptors were obtained by laser diffraction (Mastersizer 2000, Scirocco 2000 dry dispersion). Statistics (Spearman correlation, Friedman ANOVA by ranks, linear regression) were computed in SPSS v2024 at $\alpha = 0.05$. Full experimental detail is given in [1].

Results and discussion

Composition of the index in bulk samples

Bulk activity concentrations across the 27 samples were 39 ± 23 Bq kg^{-1} for ^{226}Ra, 36 ± 20 Bq kg^{-1} for ^{232}Th and 623 ± 406 Bq kg^{-1} for ^{40}K, giving a mean Iγ of 0.52 with the most active samples approaching the regulatory unity threshold (max Iγ = 0.93) [1]. Spearman correlations between the index and the individual radionuclides show that, at bulk scale, all three contribute comparably: Iγ–^{232}Th $\rho = 0.821$, Iγ–^{226}Ra $\rho = 0.794$ and Iγ–^{40}K $\rho = 0.772$ (all $p < 0.001$). No single radionuclide dominates the index in undivided material. This balanced baseline, obtained where no granulometric separation has taken place, is the reference against which the fraction-resolved results below are read.

Coarse binning: correct size separation without detectable redistribution

The Friedman test within the three-class scheme yielded a result of $\chi^2(2) = 2.696$ ($p = 0.260$) for the Iγ values across the fraction groups. The activity median was slightly elevated in the intermediate group (125–75 µm) and lower in the groups containing the coarsest and finest particles. Furthermore, no monotonic dependence on particle size was observed, and the value distributions across groups overlapped significantly (Figure 1a). Spearman correlations between the PSD3 classification and the measured activities were also not statistically significant for any of the three radionuclides (226Ra $p = 0.482$; 232Th $p = 0.532$; 40K $p = 0.434$). PSD3 correlates strongly and negatively with every particle-size descriptor — d(0.5) $\rho = -0.866$ ($p < 0.001$), D[3,2] $\rho = -0.721$ ($p = 0.001$) and D[4,3] $\rho = -0.931$ ($p < 0.001$) — confirming that the three classes separate the samples by size as intended. The null result therefore cannot be attributed to faulty sieving or to a failure of the binning to track granulometry; the explanation that remains is that three classes average over the size range across which the redistribution occurs.

A caveat is warranted at the outset. The three-class scheme was applied to granite and ceramic tiles—materials with a dense, low-porosity matrix in which radionuclides are largely retained within the crystal lattice. Consequently, resolution and material type are partially interrelated,

and the mineral structure of these materials likely contributes to a weak granulometric signal, regardless of classification.

High-resolution binning: emergence of the gradient

When the same measurement is resolved into seven classes, on the subset of samples with sufficient mass per fraction (schist, biomass-ash pellets, ceramic tiles and fireclay), the Friedman test on Iγ yields $\chi^2(6) = 20.368$, $p = 0.002$, with mean ranks rising monotonically from the coarsest fraction (>500 µm, mean rank ≈ 1.50) toward the finest (75–50 µm, ≈ 6.50; <50 µm, ≈ 5.50) (Figure 1b). Correlations between Iγ and the particle-size descriptors are uniformly negative — d(0.1) $\rho = -0.65$, d(0.5) $\rho = -0.68$, d(0.9) $\rho = -0.71$ and D[3,2] $\rho = -0.68$ ($p < 0.01$) — while the Span correlates positively ($r = 0.563$, $p < 0.001$), indicating that polydisperse materials are more prone to fines-driven enrichment. Regression of Iγ on the cumulative passing fraction at 75 µm is significant ($R = 0.675$, $p < 0.001$) but explains less than half the variance ($R^2 \approx 0.46$), confirming that particle size is a real but not exclusive control. This is the first of the two effects examined here: the same procedure, applied to the same measurements, returns a null result at three classes and a significant monotonic gradient at seven.

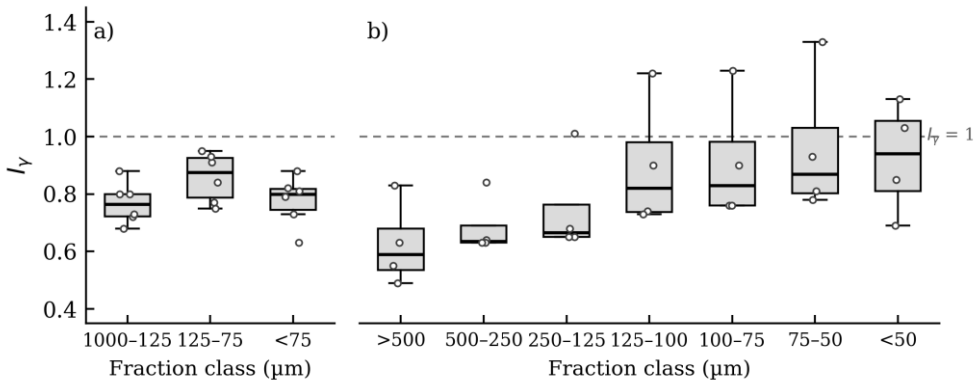


Figure 1. Distribution of Iγ across (a) the three PSD3 fraction classes (n = 6 each) and (b) the seven PSD7 fraction classes (n = 4 each), on a common vertical scale; circles are individual samples, the dashed line the unity screening criterion.

Resolution-dependent attribution

The second effect concerns not whether the gradient is detected but to which radionuclide it is attributed (Table 1).

Table 1. Spearman rank correlations among radionuclides and Iγ under the coarse (PSD3, n = 18) and high-resolution (PSD7, n = 35) schemes (* $p < 0.05$; ** $p < 0.01$).

Variable	^{226}Ra	^{232}Th	^{40}K	Iγ
PSD3 (three classes)				
^{226}Ra	1.000			
^{232}Th	−0.037	1.000		
^{40}K	−0.551	0.533*	1.000	
Iγ	0.026	0.893**	0.697**	1.000
PSD7 (seven classes)				
^{226}Ra	1.000			
^{232}Th	0.567**	1.000		
^{40}K	−0.064	−0.233	1.000	
Iγ	0.532**	0.202	0.685**	1.000

Under the coarse scheme the index appears to be carried by thorium (Iγ–^{232}Th $\rho = 0.893$, $p < 0.01$), with a secondary potassium contribution ($\rho = 0.697$, $p < 0.01$) and no measurable association with radium ($\rho = 0.026$). Under the seven-class scheme the ranking is reversed: the index tracks ^{40}K ($\rho = 0.685$) and ^{226}Ra ($\rho = 0.532$, both $p < 0.01$), while the association with ^{232}Th falls out of significance ($\rho = 0.202$). The ^{232}Th–^{40}K correlation also loses its positive sign, from +0.533 ($p < 0.05$) under PSD3 to −0.233 under PSD7. The matrix is computed on all fractionated series, as in the correlation analysis of [1]; restricting it to the four materials of the preceding section (n = 28) leaves the pattern unchanged (Iγ–^{40}K $\rho = 0.629$, Iγ–^{226}Ra $\rho = 0.476$, Iγ–^{232}Th $\rho = -0.008$), so the effect does not depend on which fractionated series are included.

Thus, a single set of measurements supports two mutually inconsistent descriptions of which radionuclide determines a given index—depending solely on how the fractions are grouped—and neither reproduces the balanced reference value for the total sample. In fact, broad classification averages the activity as it shifts from being associated with the crystal lattice to being associated with the surface. Within the 1000–125 μm size class, the contribution of the finest material (where activity is concentrated on the surface) is diluted by that of the coarser material (where activity is lattice-bound); consequently, the resulting index primarily reflects radionuclides bound to the mineral structure. Dividing the material into seven classes makes it possible to observe this transition and isolate the component determined by surface properties.

In any case, one limitation should be noted. Analyses based on three- and seven-category roughness schemes were conducted on different subsets of the material, meaning that resolution and material type were not fully decoupled; consequently, the result is presented as a resolution-dependent difference in attribution rather than as a proven inversion of the underlying mechanism. Nevertheless, its practical implication is significant: neither the absence of findings nor an attribution based on a crude schema can be taken for granted.

Conclusion

Grouping into classes based on particle size constitutes a methodological variable rather than a technical detail. When analyzing a set of construction materials and materials containing secondary minerals, a three-class scheme correctly classified the samples by particle size but failed to indicate the presence of redistribution ($\chi^2(2) = 2.696$; $p = 0.260$), whereas a seven-class scheme applied to the same data revealed a systematic increase in Iγ values towards the finer fractions ($\chi^2(6) = 20.368$; $p = 0.002$). More importantly, these two models disagree on which

radionuclide carries the index—232Th in the three-class scheme, and 40K and 226Ra in the seven-class scheme—with neither reproducing the overall reference value, to which all three elements contribute comparably. Considering only those radionuclides whose behaviour is governed by surface processes exhibits a granulometric gradient; a coarse classification based on particle size simultaneously weakens the signal and misattributes its origin.

A seven-class scheme is therefore proposed as the minimum resolution for granulometric NORM studies of construction products; three classes verify the sieving, not the redistribution.

Acknowledgements

This research was funded by the Provincial Secretariat for Higher Education and Scientific Research of Vojvodina through the project “Acoustics, Urban environment, Radionuclides from dust, and microclimate Assessment in construction and infrastructure projects in Vojvodina” (grant no. 003864834 2025 09418 003 000 000 001 04 004), by the Ministry of Science, Technological Development and Innovation (Contract No. 451-03-34/2026-03/200156) and by the Faculty of Technical Sciences, University of Novi Sad (No. 01-3609/1).

References

[1] Bikit, K.; Samardžić Cvijanović, S.; Nemeš, T.; Lakatoš, R.; Hansman, J.; Lončarević, I.; Vučinić Vasić, M.; Mrđa, D.; Forkapić, S. Radionuclide accumulation in fine fractions: implications for occupational and environmental exposure. Environments 2026, 13, 436.

[2] European Commission. Radiation Protection 112: Radiological Protection Principles Concerning the Natural Radioactivity of Building Materials; EC: Luxembourg, 1999.

[3] Council Directive 2013/59/Euratom of 5 December 2013. Off. J. Eur. Union 2014, L13, 1–73.

[4] UNSCEAR. Sources, Effects and Risks of Ionizing Radiation, 2008 Report to the General Assembly; United Nations: New York, 2008.

[5] Megumi, K.; Mamuro, T. Concentration of uranium-series radionuclides in soils and rocks. J. Geophys. Res. 1977, 82, 353–356.

[6] Elnobi, S.; Khater, A.E.M.; Abbady, A.G.E. Influence of grain size on radionuclide activity concentrations and radiological hazard of building material samples. Appl. Radiat. Isot. 2017, 130, 43–48.

[7] He, Q.; Walling, D.E. Interpreting particle size effects in the adsorption of ^{137}Cs and unsupported ^{210}Pb by mineral soils and sediments. J. Environ. Radioact. 1996, 30, 117–137.

[8] Knežević Radić, J.; Hansman, J.; Mrđa, D.; Demirhan, K.; Velimirović, D.; Kuzmanović, P.; Forkapić, S. Survey of radiological properties of some commonly used building materials: cement, chamotte and refractory products. J. Radioanal. Nucl. Chem. 2025, 334, 1715–1727.

SERUM GANGLIOSIDE PROFILING BY HIGH-RESOLUTION MASS SPECTROMETRY AND FRAGMENTATION ANALYSIS FOR BIOMARKER DISCOVERY IN FRONTOTEMPORAL DEMENTIA

Mirela Sarbu[1], Raluca Ica[1,2], Livia Deveseleanu-Corici[3], David E. Clemmer[4], and Alina D. Zamfir[1,5]

[1]Department of Condensed Matter, National Institute for Research and Development in Electrochemistry and Condensed Matter, Timişoara, Romania
[2]Department of Mathematics-Informatics, Aurel Vlaicu University of Arad, Arad, Romania
[3]Romanian Academy, "Coriolan Drăgulescu" Institute of Chemistry, Timişoara, Romania
[4]Department of Chemistry, The College of Arts & Science, Indiana University, Bloomington, Indiana, USA
[5]Department of Technical and Natural Sciences, Aurel Vlaicu University of Arad, Arad, Romania
mirela.sarbu86@yahoo.co.uk

Abstract
Serum ganglioside profiles were investigated in cohorts of frontotemporal dementia (FTD) patients and healthy controls using an integrated analytical workflow combining high-performance thin-layer chromatography (HPTLC) and ion mobility mass spectrometry (IMS-MS). FTD sera were characterized by a predominance of GD3 and GD2, together with increased levels of simple gangliosides, whereas control sera were dominated by complex gangliosides that were markedly reduced or absent in FTD. These results provide a solid foundation for the discovery and validation of serum lipid biomarkers with diagnostic and mechanistic relevance in FTD.

Introduction

FTD, is a group of non-Alzheimer neurodegenerative disorders characterized by progressive impairment of behavior, language, and executive functions, with frontal and temporal lobe atrophy. Despite being the third most common neurodegenerative dementia and the leading cause of early-onset dementia, FTD remains substantially underdiagnosed [1].
Increasing evidence implicates dysregulated glycosphingolipid metabolism, particularly gangliosides, in FTD pathogenesis, suggesting their potential as biomarkers [2]. In this context, we investigated serum ganglioside profiles in cohorts of FTD patients and healthy controls using an integrated analytical workflow combining HPTLC and IMS-MS.

Experimental

Patients were selected according to internationally accepted criteria for the behavioral variant (bvFTD) and primary progressive aphasia (PPA), together with age-matched healthy controls. Serum gangliosides were profiled using an integrated analytical workflow combining HPTLC, for high-resolution, reproducible separation and quantification, with ion mobility mass spectrometry, for structural screening and confirmation of ganglioside heterogeneity.

Results and discussion

HPTLC analysis showed high resolution and reproducibility, revealing marked differences between FTD and control sera. FTD samples were characterized by a predominance of GD3 and GD2 (~51% of total gangliosides), along with increased levels of GM3, GM2, and other simple gangliosides.
In contrast, control sera were dominated by complex gangliosides (GM1, GD1a, GD1b, GT1b), which were markedly reduced or absent in FTD. IMS-MS screening further supported the

ganglioside heterogeneity associated with FTD, confirming the structural distinctions observed by HPTLC.

Conclusion

This integrated TLC-IMS-MS approach enables robust correlation of ganglioside alterations with the molecular processes underlying FTD and provides a solid foundation for the discovery and validation of serum lipid biomarkers with potential diagnostic and mechanistic relevance.

Acknowledgements

This work was supported by the Romanian National Authority for Scientific Research, UEFISCDI, through the projects PN-IV-P2-2.1-TE-2023-0175

References

[1] Y.A. Ambaw, P.A. Ljubenkov, S. Singh, A. Hamed, S. Boland, A.L. Boxer, T.C. Walther, R.V. Farese Jr., Alzheimers Dement. 21 (2025) e70631.
[2] M. Sarbu, R. Ica, M.R. Biricioiu, L. Dehelean, A.D. Zamfir, Biomedicines 13 (2025) 2854.

AN IN SILICO FRAMEWORK FOR ENHANCING THE ORAL BIOAVAILABILITY OF AHAS INHIBITORS

Radu Daniel Săvulescu, Ana Borota, Sorin Alin Marinescu

"Coriolan Dragulescu" Institute of Chemistry, 24 M. Viteazu Ave, 300223 Timisoara, Romania, rsavulescu@acad-icht.tm.edu.ro

Abstract

The alarming increase in fungal infections resistant to conventional treatments demands the urgent development of innovative drug discovery strategies, with an effective approach being the repurposing of herbicides[1] that inhibit the acetohydroxyacid synthase (AHAS) enzyme. Because the AHAS-mediated biosynthetic pathway is essential for the survival of pathogens such as *Candida albicans* and is completely absent in mammals, these chemical structures offer excellent selectivity and minimal risk of systemic toxicity to the host. However, the transition of these compounds from the agricultural environment to clinical practice is hindered by poor oral bioavailability, as they were initially optimized to penetrate rigid plant barriers.

To overcome these pharmacokinetic barriers, the present work proposes an integrated methodology combining pharmacophore-based screening, advanced structural optimization techniques such as scaffold hopping, and fragment-based design. All structural modifications were designed to ensure strict compliance with Lipinski's Rule of Five, significantly improving drug-likeness properties. In parallel, a rigorous ADME filter targeting toxicological alerts associated with liver injury were applied, successfully transforming the original agrotoxins into safe, viable pharmaceutical candidates for future antifungal clinical applications.

References

[1] Garcia MD, Chua SMH, Low YS, Lee YT, Agnew-Francis K, Wang JG, Nouwens A, Lonhienne T, Williams CM, Fraser JA, Guddat LW. Commercial AHAS-inhibiting herbicides are promising drug leads for the treatment of human fungal pathogenic infections. Proc Natl Acad Sci U S A. 2018 Oct 9;115(41):E9649-E9658. doi: 10.1073/pnas.1809422115. Epub 2018 Sep 24. PMID: 30249642; PMCID: PMC6187177.

Acknowledgments

This work was partially supported by Program no 1, from the "Coriolan Dragulescu" Institute of Chemistry Timisoara, Romania.

DETERMINATION OF BIOMETRIC AND CHEMICAL PARAMETERS OF FRUITS FROM CERTAIN PLUM CULTIVARS

Scedei Daniela Nicoleta[1], Mihuț Casiana[2], Anisoara Copcea Duma[2], Molnar Levente[3], Moatar Maria Mihaela[4], Stefan Carolina[4], Petru Ioan Dragomir[4], Mihaela Malaescu[1], Petre Alexandru Panici[4], Liana Maria Alda[5]

[1]Department of Horticulture, University of Life Sciences "King Michael I" from Timisoara, 300645, Timisoara, Romania; e-mail: daniela.scedei@usvt.ro
[2]Department of Soil, University of Life Sciences "King Michael I" from Timisoara, 300645, Timisoara, casiana_mihut@usvt.ro
[3]Department of Plant Protection, University of Life Sciences "King Michael I" from Timisoara, 300645, Timisoara, leventemolnar@usvt.ro
[4]Department of Forestry, University of Life Sciences "King Michael I" from Timisoara, 300645, Timisoara, mihaela.moatar@usvt.ro
[5]Department of Chemistry, *University of Life Sciences "King Michael I" from Timisoara, 300645, Timisoara, lianaalda@usvt.ro*

Abstract

The plum tree (*Prunus domestica* L.) is the most widely grown fruit tree in Romania, cultivated for its tasty, nutrient-rich fruit. It occupies the largest area among fruit species in the country and adapts easily to diverse soil types and climatic conditions. The fruit is consumed fresh, dried, or processed into plum butter (*magiun*), jam, compote, and *țuică* (plum brandy); in terms of health benefits, plums aid digestion, provide fiber and vitamins, and support heart health. Frequent consumption supports memory function, helps prevent heart disease, regulates blood sugar levels, relieves constipation, and—being low in calories—is suitable for those aiming to maintain a balanced physique.

For this study, 20 fruits from each of three plum cultivars (*Tuleu gras*, *Anna Späth*, and *Stanley*) were analyzed. The samples were harvested from a family orchard in Beregsău Mare, Timiș County, during the 2025 experimental year. The fruit underwent biometric and qualitative analysis, focusing on the following parameters: major diameter (mm), minor diameter (mm), height (mm), weight (g), soluble solids content (°Brix), sugar content (%), and fruit firmness. Based on the results obtained for the physico-chemical (biometric) parameters, the following observations can be made: for the 'Tuleu Gras' plum variety, the mean value for the major diameter is 36.73 mm, while the highest value was recorded by the 'Anna Späth' variety (38.29 mm), with an overall experimental mean of 37.23 mm. Regarding soluble solids (°Brix) and sugar content, the 'Anna Späth' variety recorded the highest values for these parameters, specifically 22.47 °Brix and 21.37 °Brix, respectively.

Introduction

The plum tree (*Prunus domestica* L.) is a fruit-bearing tree belonging to the Rosaceae family. Its fleshy, dark blue or yellowish fruits have multiple uses in the food industry—such as in preserves or jams—and are also consumed fresh. However, its most well-known use is in the production of plum brandy (*brandy *), with the spirit sometimes even aged in barrels made from the tree's own wood. The unripe fruit is occasionally used in pickling.

The tree grows successfully across all geographical regions of Romania, as it is not demanding regarding climatic conditions. It is a tree of moderate vigor, featuring oval leaves with serrated edges and white blossoms. Plums can be utilized in various ways: fresh, dried, as preserves, or in the alcohol industry. They contain carbohydrates, organic acids, albumin, cellulose, vitamins (A, B, C), iron, calcium, magnesium, phosphorus, sodium, and more.

The plum tree has moderate temperature requirements. The best results are achieved in areas with an average annual temperature between 8°C and 11°C. It can withstand winter temperatures as low as -31°C. Flower buds tolerate temperatures down to -4°C, whereas blossoms are damaged by temperatures below -0.5°C. Temperatures exceeding 35°C cause scorching on young leaves. The tree thrives in areas with annual precipitation of 600–700 mm. It does not have high light requirements. Provided that all growing conditions are optimal, the plum tree will thrive in any soil type. It can even be planted on sandy soils, provided irrigation is available.

Currently, cultivated varieties also exhibit great diversity regarding environmental preferences, as certain varieties have adapted to various climatic conditions in temperate zones suitable for fruit growing. Plum trees are cultivated across all five continents, with total production exceeding 11 million tonnes [9]. The plum is a fruit species widely distributed around the globe—particularly in the temperate zones of the Northern Hemisphere—ranking fourth after the apple, peach, and pear [8, 4, 5];

Of the 23.8 million hectares comprising Romania's territory, 61.7% constitutes the country's agricultural land, with 1.5% of this area occupied by orchards and fruit tree nurseries [6,7].

In Romania, as in all neighboring countries, plum trees are highly popular due to their adaptability to local climate and soil conditions, their resilience, their nutritional value, and local tradition. Orchards account for approximately 1.4% of Romania's agricultural land; in 2018, 46.90% (over 65,900 hectares) of this area was planted with plum trees, placing Romania fourth among the world's leading plum producers. The local germplasm pool includes numerous foreign varieties (developed in the USA, other Eastern European countries, etc.)—six of which are particularly widespread—as well as a diverse range of locally developed varieties. Over the past six decades, research centers such as those in Bistrița, Pitești, Strejești, Vâlcea, and Voinești have developed more than 40 Romanian varieties and produced approximately 1,000 hybrids [1,2,3].

Experimental

Regarding biometric parameters, fruit samples (20 fruits per cultivar) were analyzed for major diameter, minor diameter, and height.

External fruit characteristics of the studied cultivars were measured using calipers, while soluble solids content was determined using a digital refractometer. Fruit weight was determined by weighing on a digital analytical balance.



Figure 1. Analytical balance



Figure 2. Digital refractometer (original photo)

Soluble sugar content (°Brix) was measured using a digital refractometer (Fig. 2). The plums were grated, and the juice was squeezed onto the lens, ensuring no pulp fell onto it. The plastic cover was carefully lowered over the juice, and readings were taken. Testing the refractometer with plain water should yield a reading of zero.

The sugar percentage in the juice obtained from the sampled fruit was determined using the formula:

% = (N × 4.25) / 4 – 2.5, where: N = the refractometer reading; 4.25 = juice (must) density; 4 = established coefficient; 2.5 = percentage of non-sugar dry matter.

Results and discussion

The results indicate that the 'Anna Späth' plum variety recorded the highest values for both major and minor diameters, with averages of 38.29 mm and 36.96 mm, respectively. Regarding fruit height and weight, the 'Tuleu Gras' variety showed the highest values: 50.48 mm and 42.87 g (Table 1, Figure 3).

Table 1. Results obtained for the plum varieties under study

No. crt.	Variety	Large diameter (mm)	Small diameter (mm)	Height (mm)	Weight (g)
1	Tuleu gras	36.73	35.67	50.48	42.87
2	Anna Späth	38.29	36.96	41.93	39.08
3	Stanley	36.68	34.55	48.99	42.63
	Average experience	37.23	41.62	47.13	41.52

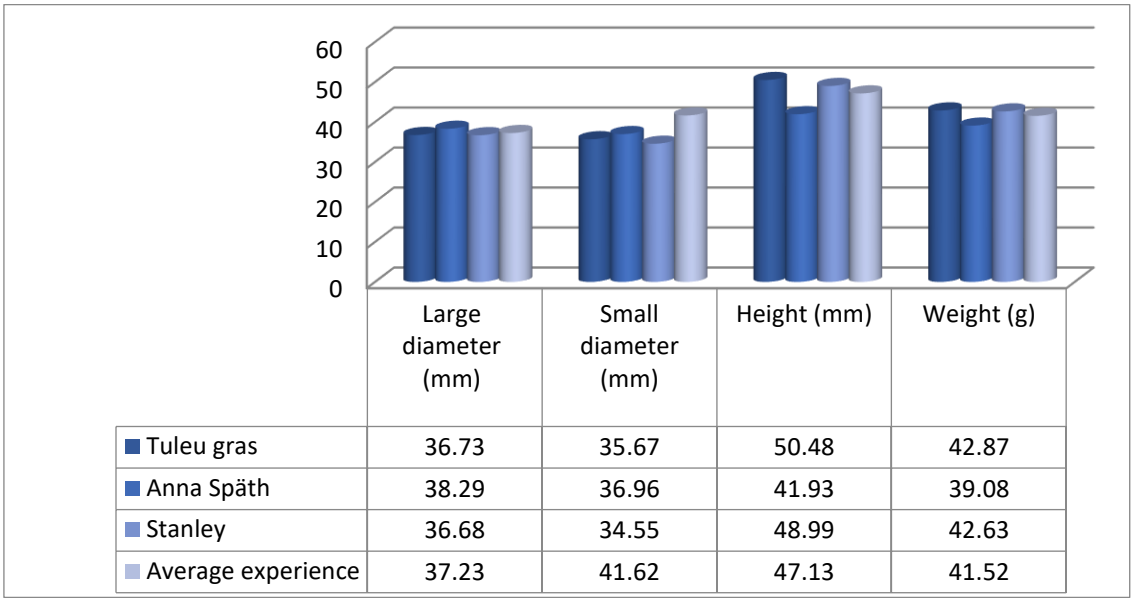
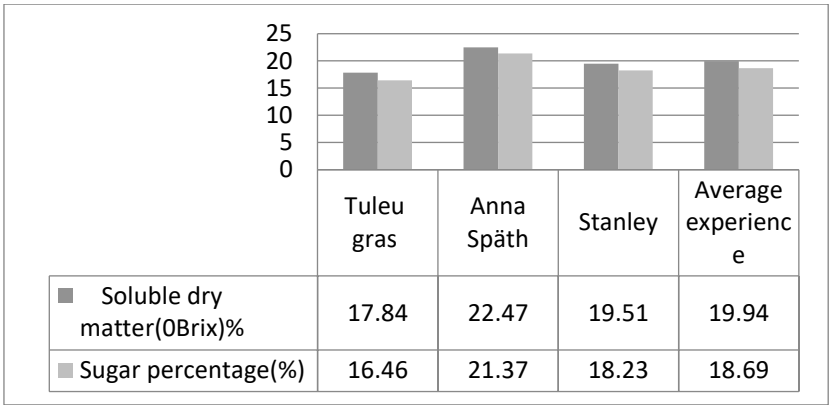


Figure 3. Graphical representation of the data obtained from biometric parameters

Regarding the carbohydrate content of the analyzed plum cultivars under 2025 conditions, the results show that the Anna Späth cultivar recorded the highest sugar percentage (21.37%), followed by the Stanley cultivar (18.23%) (Table 2, Figure 4).

Table 2. Results obtained on the fruits of the plum varieties studied

No. crt.	Variety	Soluble dry matter (^{0}Brix)%	Sugar percentage (%)
1	Tuleu gras	17.84	16.46
2	Anna Späth	22.47	21.37
3	Stanley	19.51	18.23
	Average experience	19.94	18.69



	Tuleu gras	Anna Späth	Stanley	Average experience
Soluble dry matter(0Brix)%	17.84	22.47	19.51	19.94
Sugar percentage(%)	16.46	21.37	18.23	18.69

Figure 4. Graphical representation of data obtained for carbohydrates

Conclusion

Based on the results obtained for the plum varieties under study, the following can be observed:
•regarding the major diameter: the mean value is 36.73 mm for 'Tuleu Gras' plums, 38.29 mm for the 'Anna Späth' variety, and 36.68 mm for 'Stanley' plums;
•regarding the minor diameter: the mean value is 35.67 mm for 'Tuleu Gras' plums, 36.96 mm for the 'Anna Späth' variety, and 34.55 mm for 'Stanley' plums;
•regarding fruit height: the mean value is 50.48 mm for 'Tuleu Gras' plums, 41.93 mm for the 'Anna Späth' variety, and 48.99 mm for 'Stanley' plums;
•regarding fruit weight: the mean value is 42.87 g for 'Tuleu Gras' plums, 39.08 g for the 'Anna Späth' variety, and 42.63 g for 'Stanley' plums;
•regarding sugar content: the mean value is 16.46% for 'Tuleu Gras' plums, 21.37% for the 'Anna Späth' variety, and 18.23% for 'Stanley' plums;

References

[1]. Butac, M., Botu, M., Militaru, M., Mazilu, C., Dutu, I., Nicolae S., **2019**. Plum germplasm resources and breeding in Romania. Proc. Latv. Acad. Sci. B Nat. Exact Appl. Sci. 2019, 73, 214–219.
[2]. Cătuneanu, I., Iordăchescu, M., Petre, A., Frîncu, M., Iliescu, L., Udroște, A., Bădulescu, L., **2022**. Physico-chemical characterization for several Romanian plum cultivars at the time of harvest. J. Hortic. For. Biotechnol. 2022, 26, 8–16.
[3]. Micu S.M., Popoviciu D.R., Grosu M.I., Radu M.D., **2024**. Biochemical Characterization of Some Plum Cultivars Available on the Romanian Market. *Appl. Sci.* 2024, *14*, 11311. https://doi.org/10.3390/app142311311
[4]. Iordănescu O.A., Olaru D.N., **2014**. Pomologie. Ed. Agroprint. Timişoara.
[5]. Chiţu V., Butac M., Chiţu E., **2007**. Studiul calităţi fructelor unor hibrizi de prun pretabili pentru deshidratare. https://ibn.idsi.md/sites/default/files/imag_file/83-86_27.pdf
[6]. Dragunescu A. A., Scedei D. N., Dobrei A. G., Malaescu I. M., **2021**.Tehnologii horticole. Editura Agroprint.
[7]. Selka S., Mkedder I., Ilias F., Gaouar S.B.S., **2024**. Morpho-Pomological Study of Plum Trees (Prunus domestica L.) in Western Algeria. *Biol. Life Sci. Forum* 2024, *36*, 12. https://doi.org/10.3390/blsf2024036012
[8]. Vișanu F., Botu M., Ștefănescu F., Vicol I., Cernătescu A., **2012**. Structure of the plum cultivar assortment for the region of Oltenia, Romania. Acta Horticulturae (ISHS, nr. 968, p. 115-120).

[9]. Milošević J., Žeželj I., Gorton M., Barjolle D., 2012. Understanding the motives for food choice in Western Balkan Countries. Elsevier, Vol. 58, Issue 1, 205-214.
[10]. *Sharma R., Joshi V.K., Rana J.C.,* ***2011****.Nutritional composition and processed products of Quince (Cydonia oblonga Mill.) Indian J. Nat. Prod. Resour.;2:354–357.*

DETERMINATION OF BIOMETRIC AND CHEMICAL PARAMETERS OF FRUITS FROM CERTAIN QUINCE CULTIVARS (Cydonia Oblonga Miller)

Scedei Daniela Nicoleta[1], Casiana Mihuț [2], Cozma Antoanela[2], Alina Georgeta Dobrei[1], Anisoara Copcea - Duma[2], Moatar Maria Mihaela[3], Stefan Carolina[3], Adalbert Ocrosi[2], Petru Ioan Dragomir[3], Alexandru Panici[3]

[1]Department of Horticulture, University of Life Sciences "King Michael I" from Timisoara, 300645, Timisoara, Romania; e-mail: daniela.scedei@usvt.ro
[2]Department of Soil, University of Life Sciences "King Michael I" from Timisoara, 300645, Timisoara, casiana_mihut@usvt.ro
[3] Department of Forestry, University of Life Sciences "King Michael I" from Timisoara, 300645, Timisoara, mihaela.moatar@usvt.ro

Abstract

The quince (*Cydonia oblonga* Miller) is a plant commonly cultivated worldwide, known for centuries for its valuable nutritional and medicinal properties. Although quince fruits are highly aromatic, their extreme hardness and sour, astringent, and bitter taste make them unsuitable for direct consumption in their raw state.

For this study, 20 fruits from each of five quince cultivars (Bereczki_RO, Champion_HU, De Portugalia_TR, Constantinopol_RO, and Aromate_RO), purchased from a supermarket during the 2025 experimental year - were analyzed for qualitative and biometric characteristics. The parameters examined included major diameter (mm), minor diameter (mm), height (mm), weight (g), soluble solids (°Brix), sugar content (%), and fruit firmness. An analysis of the physicochemical (biometric) data revealed the following: regarding the Bereczki_RO cultivar, the mean major diameter was 80.43 mm, while the highest values were recorded for the Constantinopol_RO and Aromate_RO cultivars (88.66 mm and 87.12 mm, respectively), against an overall experimental mean of 83.41 mm. Regarding soluble solids (°Brix) and sugar content, the Bereczki_RO cultivar exhibited the highest values for these parameters, recording 14.02 °Brix and 12.40%, respectively.

Introduction

The common quince (*Cydonia oblonga* Miller) is the sole representative of the *Cydonia* genus and belongs to the Rosaceae family, which also includes apple and pear trees [1]. Its region of origin is considered to be Western Asia, although it has since spread to other continents; it is found growing wild, planted in home gardens and parks as an ornamental plant, and cultivated for its edible fruit [2]. Turkey is the largest global producer and distributor (supplying 25% of global output), followed by China, Iran, Argentina, and Morocco (supplying 10% of global output) [3,4]. Turkey's quince fruit production increased by approximately 66% between 2006 and 2020 [5].

Quince fruit is increasingly attracting the interest of scientists and consumers alike due to its wide-ranging health benefits, which include hypoglycemic, anti-inflammatory, anticancer, antibacterial, antiallergic, and anti-ulcer properties [7,10,11,12,13,14].

Global quince production in 2022 totaled 700,479.34 tonnes, a 0.1% decrease from 2021, when the total output was 701,204.4 tonnes. Turkey was the leading global producer, accounting for over a quarter (28.2%) of total worldwide production [1].

In 2023, global production stood at 687,036 tonnes, down 1.92% from the previous year. Turkey remained the world's largest producer, accounting for 27.98% of total global production[1].

In 2017 (the most recent year for which data was reported to the FAO), the area covered by quince orchards in Romania was 883 hectares, ranking 13th globally and 3rd in the European Union, behind Spain and Belgium. Production volume ranked 2nd in the European Union—behind Spain—and 12th globally. Productivity in Romania stood at 7,407.9 kg/ha, ranking 5th in the European Union (behind Greece, Italy, Hungary, and Portugal) and 26th globally, a figure lower than the global average of 8,583.5 kg/ha[1]. The data is sourced from the FAOSTAT database of the Food and Agriculture Organization of the United Nations (FAO)[1].

Experimental

Regarding biometric parameters, fruit samples (20 fruits per cultivar) were analyzed for major diameter, minor diameter, and height.

External fruit characteristics of the studied cultivars were measured using calipers, while soluble solids content was determined using a digital refractometer. Fruit weight was determined by weighing on a digital analytical balance.



Figure 1. Analytical balance (original photo)



Figure 2. The digital refractometer (original photo)

Soluble sugar content (°Brix) was measured using a digital refractometer (Fig. 2). The quinces were grated, and the juice was squeezed onto the lens, ensuring no pulp fell onto it. The plastic cover was carefully lowered over the juice, and readings were taken. Testing the refractometer with plain water should yield a reading of zero.

The sugar percentage in the juice obtained from the sampled fruit was determined using the formula:

% = (N × 4.25) / 4 − 2.5, where: N = the refractometer reading; 4.25 = juice (must) density; 4 = established coefficient; 2.5 = percentage of non-sugar dry matter. Firmness was determined using the PCE-PTR 200N penetrometer; unlike analog models, this digital penetrometer offers higher measurement precision and resolution.

Results and discussion

Based on the obtained data, regarding the large diameter (mm), the highest value was recorded by the Constantinopol_RO cultivar (88.66 mm), followed by the Aromate_RO cultivar (mean of 87.12 mm), while the Champion_HU cultivar showed the lowest value (78.36 mm) (Table 1); regarding the small diameter parameter, the Constantinopol_RO cultivar again recorded the highest value (83.35 mm), with an experimental mean of 83.36 mm; finally, concerning fruit height and weight, the Constantinopol_RO cultivar once more recorded the highest values, specifically 90.59 mm and 303.92 g.

Table 1. Results obtained for the fruits of the quince cultivars under study

No. crt.	Variety	Large diameter (mm)	Small diameter (mm)	Height (mm)	Weight (g)
1	Bereczki_RO	80.43	74.69	87.55	247.22
2	Champion_HU	78.36	68.88	88.32	211.64
3	De Portugalia_TR	82.44	77.81	89.14	258.95
4	Constantinopol_RO	88.66	83.36	90.59	303.92
5	Aromate_RO	87.12	81.44	88.11	248.10
	Media experientei	83.41	77.24	88.74	253.97

Based on the data obtained regarding soluble solids (°Brix) and sugar content, it can be observed that the Bereczki_RO cultivar recorded the highest values for these parameters, 14.02°Brix and 12.40%, respectively (Table 2). Regarding firmness, the data show that the Bereczki_RO cultivar exhibited the highest value at 10.88 lb, followed by the Aromate_RO cultivar with a firmness of 9.08 lb (table 2).

Table 2. Results obtained for the fruits of the quince cultivars under study

No. crt.	Variety	Soluble dry matter (^{0}Brix)%	Sugar percentage (%)	Firmness lb (livre)
1	Bereczki_RO	14.02	12.40	10.88
2	Champion_HU	13.19	11.51	8.07
3	De Portugalia_TR	13.14	11.46	7.98
4	Constantinopol_RO	12.54	10.82	8.30
5	Aromate_RO	12.61	10.90	9.08
	Media experientei	13.10	11.42	8.86

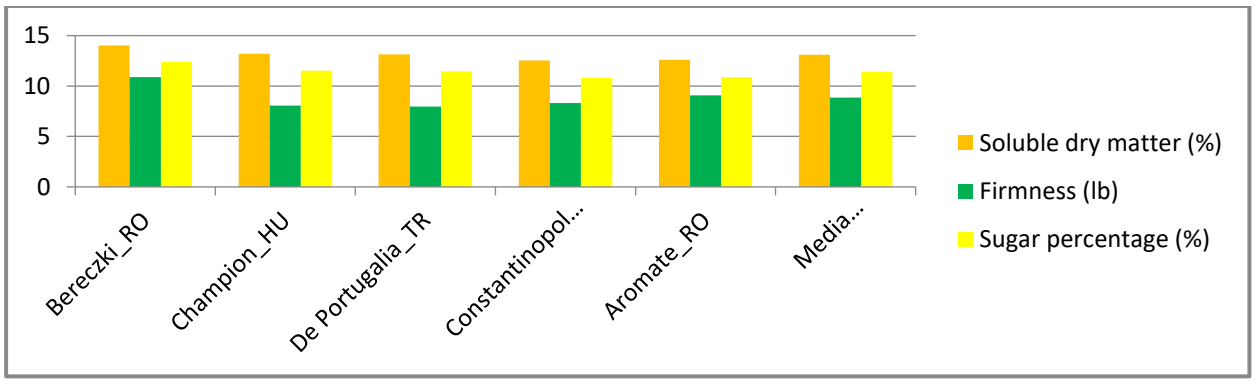


Figure 3. Graphical representation of data obtained for carbohydrates and firmness

Conclusions

Based on the results obtained for the quince fruits of the varieties under study, the following can be observed:

•regarding the major diameter: the mean value is 80.43 mm for Bereczki_RO, 78.36 mm for Champion_HU, 82.44 mm for De Portugalia_TR, 87.12 mm for Aromate_RO, and 88.66 mm for Constantinopol_RO; the overall experimental mean is 83.41 mm.

•regarding the minor diameter: the mean value is 74.69 mm for Bereczki_RO, 68.88 mm for Champion_HU, 77.81 mm for De Portugalia_TR, 81.44 mm for Aromate_RO, and 83.36 mm for Constantinopol_RO; the overall experimental mean is 77.24 mm.

•regarding fruit height: the mean value is 87.55 mm for Bereczki_RO, 88.32 mm for Champion_HU, 89.14 mm for De Portugalia_TR, and 90.59 mm for Constantinopol_RO; the overall experimental mean is 88.74 mm. • Basic fruit weight indicators: for Bereczki_RO quinces, the mean weight is 247.22 g; for Champion_HU quinces, 211.64 g; for De Portugalia_TR quinces, 258.95 g; and for Constantinopol_RO quinces, 303.93 g; with an overall experimental mean of 253.97 g.

•basic sugar content indicators: for Bereczki_RO quince varieties, the mean sugar content is 12.40%; for Champion_HU quinces, 11.51%; for De Portugalia_TR quinces, 11.46%; for Aromate_RO quinces, 10.90%; and for Constantinopol_RO quinces, 10.82%; with an overall experimental mean of 11.42%.

References

[1]. Butac, M., Botu, M., Militaru, M., Mazilu, C., Dutu, I., Nicolae S., **2019**. Plum germplasm resources and breeding in Romania. Proc. Latv. Acad. Sci. B Nat. Exact Appl. Sci. 2019, 73, 214–219.

[2]. Cătuneanu, I., Iordăchescu, M., Petre, A., Frîncu, M., Iliescu, L., Udroşte, A., Bădulescu, L., **2022**. Physico-chemical characterization for several Romanian plum cultivars at the time of harvest. J. Hortic. For. Biotechnol. 2022, 26, 8–16.

[3]. Micu S.M., Popoviciu D.R., Grosu M.I., Radu M.D., **2024**. Biochemical Characterization of Some Plum Cultivars Available on the Romanian Market. *Appl. Sci.* 2024, *14*, 11311. https://doi.org/10.3390/app142311311

[4]. Iordănescu O.A., Olaru D.N., **2014**. Pomologie. Ed. Agroprint. Timişoara.

[5]. Chiţu V., Butac M., Chiţu E., **2007**. Studiul calităţi fructelor unor hibrizi de prun pretabili pentru deshidratare. https://ibn.idsi.md/sites/default/files/imag_file/83-86_27.pdf

[6]. Dragunescu A. A., Scedei D. N., Dobrei A. G., Malaescu I. M., **2021**.Tehnologii horticole. Editura Agroprint.

[7]. Selka S., Mkedder I., Ilias F., Gaouar S.B.S., **2024**. Morpho-Pomological Study of Plum Trees (Prunus domestica L.) in Western Algeria. *Biol. Life Sci. Forum* 2024, *36*, 12. https://doi.org/10.3390/blsf2024036012

[8]. Vişanu F., Botu M., Ştefănescu F., Vicol I., Cernătescu A., **2012**. Structure of the plum cultivar assortment for the region of Oltenia, Romania. Acta Horticulturae (ISHS, nr. 968, p. 115-120).

[9]. Milošević J., Žeželj I., Gorton M., Barjolle D., 2012. Understanding the motives for food choice in Western Balkan Countries. Elsevier, Vol. 58, Issue 1, 205-214.

[10]. *Sharma R., Joshi V.K., Rana J.C., **2011**. Nutritional composition and processed products of Quince (Cydonia oblonga Mill.) Indian J. Nat. Prod. Resour;2:354–357.*

[11]. Silva B.M., Andrade P.B., Martins R.C., Valentão P., Ferreres F., Seabra R.M., Ferreira M.A., **2005**. Quince (Cydonia oblonga Miller) fruit characterization using principal component analysis. J. Agric. Food Chem.; 53:111–122. doi: 10.1021/jf040321k.

[12]. *Rop O., Balík J., Řezníček V., Juríková T., Škardová P., Salaš P., Kramářová D.,* ***2011****. Chemical characteristics of fruits of some selected quince (Cydonia oblonga Mill.) cultivars. Czech J. Food Sci.;29:65–73. doi: 10.17221/212/2009-CJFS.*
[13]. *Najman K., Adrian S., Hallmann E., Sadowska A., Buczak K., Waszkiewicz-Robak B., Szterk A.,* ***2023****. Effect of various drying methods on physicochemical and bioactive properties of quince fruit (Cydonia oblonga Mill.) Agriculture;13:446. doi: 10.3390/agriculture13020446.*
[14]. *Al-Zughbi I., Krayem M.,* ***2022****. Quince fruit Cydonia oblonga Mill nutritional composition, antioxidative properties, health benefits and consumers preferences towards some industrial quince products: A review. Food Chem.;393:133362.*
[15]. http://pomiifructiferi.blogspot.ro/2012/02/marul_29.html
[16]. https://pepiniera-luca.ro/product/gutui-bereczki/
[17]. https://pepinierele-roman.ro/produs/de-portugalia/
[18]. https://bulbshop.ro/acasa/2469-gutui-pom-fructifer-constantinopol.html
[19].https://www.google.com/search?q=balanta+analitica&rlz=1C1GCEA_enRO945RO945&oq=balanta+&aqs=chrome.3.69i57j0i512j46i512j0i512l5j0i131i433i512i650j0i512.6775j0j15&sourceid=chrome&ie=UTF-8

PRELIMINARYTREATMENT OF COMPOST LEACHATE

Marjana Simonič

Faculty of Chemistry and Chemical Engineering, University of Maribor, 2000 Maribor, Smetanova 17, Slovenia
e-mail: marjana.simonic@um.si

Abstract
In the present study, the compost leachate was sampled at a real composting plant and treated in laboratory scale using a combination of various methods. Based on treatment efficiency and cost effectiveness, the following methods were chosen: settling, crushed recycled glass filtration, and lime treatment as pretreatment methods, followed by aerobic degradation of organic compounds in a sequencing batch reactor (SBR). Chemical analyses were carried out. Chemical oxygen demand (COD) was measured as the most important organic parameter, while the focus was on heavy metals removal among inorganic pollutants during pre-tretment stage. The results showed that the pretreatment methods contribute to efficient COD removal.

Key words: Compost leachate, SBR, filtration, lime, crushed recycled glass

Introduction
Composting is the controlled decomposition of organic material by microorganisms into stable soil. A major problem associated with composting is leachate [1]. Compost can consist of material with a high water content, water from irrigation, and water produced during biodegradation processes. This water seeps through the compost and eventually leaves it as leachate. The amount of leachate produced during composting is influenced by various factors, including the composition of the raw material, the composting techniques used, and local weather conditions [2]. Leachate can contain a high proportion of organic, biological and inorganic material. Due to the content of dissolved and particulate organic material in the compost, the chemical oxygen demand (COD) and turbidity are very high. High COD indicates high organic matter availability for microbes, but not necessarily high nutrient availability for plants. Excessive COD in compost leachate create conditions that can suppress plant growth.Compost eachate treatment generally requires various combined processes, such as pretreatment combined with SBR [3]. Pre-treatment is therefore necessary. Based on literature research and cost effectiveness, the following methods have been chosen: aerobic degradation in a sequencing batch reactor (SBR) after settling and glass filtration or lime treatment [4]. Lime could remove up to 40 % of COD [5]. With age, the concentration of nitrogen, mostly as ammonia, in leachates increases. However, it can be reamoved by microbial community treatment, such as applied in SBR. The SBR is easy to maintain, the stirring period duration as well as aeration can be controled and periodically changed. Consequently the microorganisms growth is promoted and efficiency could be increased. Nitrogen removal occurred through biosynthesis, nitrification, and denitrification. The concentration of dissolved oxygen should be maintained in range from 2 mg/L to 4 mg/L [6].

Experimental
Leachate sampling was carried out in accordance with the SIST ISO 5667-10:1996 standard in Kogal composting plant, Slovenia (Figure 1). The sample was first left to settle in a funnel for 2 hours. Filtration through recycled crushed glass, 0.4–0.8 mm (Maribor company, Slovenia), as pretreatment in comparison with settling was performed prior to the SBR. Alternatively, lime was applied (Zagorje near Sava, Slovenia). In the last step, the samples were poured into the SBR reactor with an effective volume of 2 L. Aerobic bacteria were added (Kogal company,

Slovenia). Aeration of the leachate was provided by a tank pump to maintain the disolved oxygen concentration just above 2 mg/L at room temperature.



Figure 1: Sampling location at Kogal composting plant, Slovenia

Figure 2 shows the crushed recycled glass filter. UV-Visible Spectrophotometer Cary 50 Bio, Agilent, USA, Multi 3410 WTW pH meter and COND 3110 WTW conductometer were used.The metals were determined based on Flame atomic absorption spectrometric methods, ISO 8288 (2002).Chromium(VI) was determined by Atomic absorption spectrometric method, ISO 9174 (1998).The metal ions were determined in cooperation with IOS company (Maribor, Slovenia).Chemical oxygen demand was determined following SIST ISO 6060 (1989). High dilution was required for measurement of the parameters due to high organic content in accordance with another study [3].



Figure 1. The crushed recycled glass filter

Results and discussion

Table 1 shows the results of chemical analysis before and after settling.The changes in pH were negigible as expected. Several samples were taken and COD range was wide. The results were presented on one average leachate sample. After the settling only a slight decrease in COD was observed at 10 %. After settling a small percentage of condutivity decrease was observed and pH remains the same. Most physical parameters and measured metal ion concentrations did not decrease much afetr settling. The observed decrease of Zn^{2+} concentration after simple settling can be attributed to its association with suspended organic matter and colloidal particles present in compost leachate. Zinc is known to form complexes with humic substances and particulate organic matter, which subsequently settle under quiescent conditions [7]. Since the pH remained acidic, no hydroxide precipitates were likely formed. Other metals' concentrations except Ni^{2+} remained practically unchanged.

Table 1. Chemical analysis of leachate

Parameter	**Standard**	**Raw leachate**	**Leachate after settling**
General			
pH	SIST ISO 10523:1996	5.45	5.45
Conductivity [mS/cm]	SIST EN 27888:1998	15.6 (20.4˚C)	12.4 (22.4˚C)
SAK [m^{-1}] at 254 nm	Mod. (ISO 7887:1985)	5910	5310
Organic			
COD [mg/L O_2]	SIST ISO 6060:1989	53420	47900
Inorganic			
Cu [mg/L]	ISO 8288(2002)	0.22	0.21
Zn [mg/L]	ISO 8288(2002)	4.54	1.19
Cd[mg/L]	ISO 8288(2002)	0.03	0.03
Cr [mg/L]	ISO 9174(1998)	0.40	0.40
Ni [mg/L]	ISO 8288(2002)	0.86	0.73
Pb [mg/L]	ISO 8288(2002)	0.06	0.06

The sample was then treated with lime and afterwards in SBR. The results are seen from Table 2 and the same standard methods were used (please see Table 1). The SAK removal remains the same after lime treatment compared with removal after settling. A lime treatment removed additional 22 % of COD. Regarding the metals Zn^{2+} was further removed at 33 % and Cu^{2+} at 10 %. pH increased to 8.26. At this value Zn and Cu precipitate as $Zn(OH)_2$ and $Cu(OH)_2$, which is the main reason for removal [8]. The results showed that the SBR was very efficient organic compounds removal process. The compost leachate was treated in the SBR for 7 days. COD removal reached 81 %, after combination of settling, lime and SBR treatment.
The sample was then treated with a combination of following methods: settling, recycled glass filtration and SBR. The results are seen from Table 3 and the same standard methods were used (please see Table 1). A recycled glass filtration was superior in comparison with the lime treatment, achieving COD removal of 31 %, which is about 10 % more compared to lime removal of COD. The overall COD removal increased to 85 %. Among the metals removal Zn^{2+} and Cu^{2+} ions were removed at 29 % and 15 %, while other metals removal efficiency was negligible. In neutral range glass surfaces are covered by silanol groups $\equiv Si - OH$.

Table 2. Chemical analysis of leachate after SBR treatment

Parameter	**Leachate after settling and lime**	**Leachate after settling, lime and SBR**
General		
pH	5.45	8.26
Conductivity [mS/cm]	12.4 (20.4˚C)	12.4 (22.4˚C)
SAK [m^{-1}] at 254 nm	5310	5300

Organic		
COD [mg/L O_2]	42700	9050
Inorganic		
Cu [mg/L]	0.19	0.18
Zn [mg/L]	0.80	0.80
Cd[mg/L]	0.03	0.03
Cr [mg/L]	0.40	0.36
Ni [mg/L]	0.71	0.67
Pb [mg/L]	0.06	0.06

Table 3. Chemical analysis of leachate after recycled glass filtration

Parameter	**Leachate after settling and recycled glass filter**	**Leachate after settling, glass filter and SBR**
General		
pH	5.49	7.49
Conductivity [mS/cm]	12.4 (22.4°C)	12.4 (22.4°C)
SAK [m^{-1}] at 254nm	5249	4628
Organic		
COD [mg/L O_2]	37065	7960
Inorganic		
Cu [mg/L]	0.18	0.17
Zn [mg/L]	0.85	0.85
Cd[mg/L]	0.03	0.03
Cr [mg/L]	0.40	0.28
Ni [mg/L]	0.67	0.65
Pb [mg/L]	0.06	0.06

Above the point of zero charge, these groups deprotonate (eq.1):

$$\equiv Si - OH \rightleftharpoons \equiv SiO^- + H^+ \quad (1)$$

The negatively charged sites can bind metal ions in Eqs (2) and (3) [8]:

$$\equiv SiO^- + Cu^{2+} \rightarrow \equiv SiOCu^+ \quad (2)$$

$$\equiv SiO^- + Zn^{2+} \rightarrow \equiv SiOZn^+ \quad (3)$$

The results were in accordance with another study, in which the COD removal percentage was reported as 84.25 % [3]. The results confirm the hypothesis that the nature of the leachate and the presence of various impurities have a significant influence on COD removal. It is also

important that the ratio of SAK to DOC, decreases in the SBR, with the leachate becoming more hydrophilic and mobility is increased due to hydrophilic fractions in compost leachate [9].

Conclusion

Pretreatment processes such as lime addition and filtration through a recycled glass filter were carried out to improve SBR compost leachate treatment. According to the results, SBR performance in removing organic matter is satisfactory, and overall COD removal efficiency reached 85 % when filtration with crushed recycled glass was used, and 80 % in the case of lime application as preatreatment. Higher SAK decrease with crushed recycled glass at 22 % was measured compared with lime at 10 %.

Acknowledgements

The author would like to thank the Slovenian Research and Innovation Agency Programme P2-0414.

References

[1] K. Brown, A. J. Ghoshdastidar, J. Hanmore, J. Frazee, and A. Z. Tong, Waste Manag., 33 (2013) 2188. https://doi.org/10.1016/j.wasman.2013.04.006
[2] M. J. Tahsini, M.Nikaeen, A. H. Nafez, Environmental Technology & Innovation, 36 (2024) 103859. https://doi.org/10.1016/j.eti.2024.103859
[3] H. Hashemi, T. Jasemi Zad, Z. Derakhshan, A. A. Ebrahimi, Health Scope. 6(3) (2017) e13356. doi: https://doi.org/10.5812/jhealthscope.13356
[4] M. Gałwa-Widera, Desalin Water Treat 231 (2025) 101025. https://doi.org/10.1016/j.dwt.2025.101025
[5] L. Kinidi, S.F. Salleh, Int J Chem Eng 2020 (2020) 3687165. https://doi.org/10.1155/2020/3687165
[6] R. Soret, J.R. Loup, P.E. Fontaine, J Water Process Eng 77 (2025) 108312. https://doi.org/10.1016/j.jwpe.2025.108312
[7] M. Simonič, L. F. Zemljič, International Conference Ružička days, Today Science-Tomorrow industry, Proceedings, Vukovar, Croatia, 21-23.September, 2016, pp.311-317.
[8] M.C.Benalia, L.Youcef, M.G.Buaziz, S. Achour, H. Menasra, Arab J Sci Eng 47 (2022) 5587–5599. https://doi.org/10.1007/s13369-021-05525-7
[9] Y.Wang, Y. Ge, Y. Deng, X. Xu, Y. Zhang, L. Li, and Z. Xu, Front. Microbiol., 14 (2023) 1320302. doi: 10.3389/fmicb.2023.1320302

EFFECT OF *ASCOPHYLLUM NODOSUM* EXTRACT ON THE GROWTH PARAMETERS AND YIELD OF MINT

Aleksandra Stanojković-Sebić[1], Aleksandar Stanojković[2]

[1]Institute of Soil Science, Teodora Drajzera 7, 11000 Belgrade, Republic of Serbia
[2]Institute for Animal Husbandry, Autoput 16, 11080 Belgrade- Zemun, Serbia
e-mail: astanojkovic@yahoo.com

Abstract

The present study aimed to evaluate the significance of variations in the yield, morphological traits (stem length, leaf length, average number of leaves, and root length), and physiological parameters (nitrogen balance index, chlorophyll, flavonoids, and anthocyanins) of mint plants treated with different concentrations of *Ascophyllum nodosum* extract (ANE) diluted in distilled water (0, 2, 4, and 6 mL/L). The experiment was conducted in a greenhouse using pots from the second week of April to the fourth week of July 2026. Each pot contained 1.4 kg of homogenized Eutric Cambisol soil, characterized by a very clayey texture and an acidic reaction. Physiological parameters were measured using a Dualex leaf clip sensor. The results demonstrated a pronounced effect of all ANE application rates on the evaluated plant parameters compared with the untreated control. Among the tested treatments, ANE applied at 4 mL/L produced the most substantial improvements in yield, morphological characteristics, and physiological parameters. Further research under larger-scale soil cultivation conditions is recommended to explore additional possibilities for the application of ANE in mint production and other vegetable crops from an ecological and sustainable perspective.

Introduction

Mint (*Mentha piperita* L.) is a perennial herb with a branched green stem with underground and above-ground shoots. The leaves are opposite and covered with short hairs on the reverse side, and the root is veiny and poorly developed. In modern pharmacy, the leaf (Menthae piperitae folium), aerial parts (Menthae piperitae herba) and essential oil (Menthae piperitae aetheroleum) are used as a stomachic, carminative, disinfectant, stimulant. Mint essential oil (pure menthol) has a strong bactericidal effect. It is also widespread as a spice plant, so it is used to improve the taste of drinks and sweets. In terms of environmental conditions, mint thrives best in humid coastal areas, but it also suits a moderate climate. All species of the genus Mentha, and especially *M. piperita*, have high moisture and nutrient requirements, and no high heat requirements. It prefers humus, structural and fertile soils, neutral to slightly acidic reactions, and does not tolerate highly compacted and heavy soils [1].

Although mint is mostly grown in the open field, greenhouse cultivation is more prevalent, since with controlled climate growth and constant soil moisture, it allows production of stable harvest up to four times per season [2], especially within organic farming systems. Due to the exclusion of synthetic pesticides and inorganic fertilizers, organically grown mint has become highly popular among health-conscious consumers. Organic agriculture relies on natural processes, such as crop rotation, cover crops, intercropping, and minimal tillage, alongside natural substances like organic fertilizers, biostimulants, and symbiotic associations. By restricting or fully eliminating synthetic chemicals, this approach preserves ecosystems through the integration of biological cycles and biodiversity [3].

To enhance the sustainability and economic viability of organic farming, biostimulants derived from seaweed extracts have emerged as a highly promising solution. Utilizing natural seaweed as a fertilizer allows for the progressive replacement of conventional inorganic fertilizers. These marine extracts are inherently biodegradable, non-toxic, non-polluting, and completely safe for

humans, wildlife, and birds. Their extensive positive impact on plant development stems from a rich composition of growth regulators (auxins, cytokinins, gibberellins, betaines), macronutrients (Ca, K, P), and essential micronutrients (Fe, Cu, Zn, B, Mn, Co and Mo) [4]. Numerous studies have demonstrated that the application of *ANE*, either through foliar spraying or soil application, can enhance the growth and development of various field, fruit, and vegetable crops [5, 6]. Extracts from the brown seaweed ANE are widely commercialized in organic farming as a viable alternative to chemical inputs, demonstrating a strong potential to boost both the quality and quantity of crop yields [7]. The application of ANE on mint herbs enhanced the morphological and the physiological performance of the plants [8]. Soil and foliar application of ANE, particularly in the organic sector, has been shown to maximize chlorophyll levels, grain yield, and essential oil content in parsley [9], as well as increase carvacrol concentration in savory essential oil [10]. Furthermore, these extracts function as potent biostimulants that enhance crop vigor, improve seed germination, promote lateral root development, optimize water and nutrient use efficiency, raise flavonoids content, mitigate both biotic and abiotic stresses in various crops, and stimulate beneficial soil microorganisms [11, 12].

This study aimed to investigate how varying doses of *A. nodosum* extract (ANE) influence the yield, as well as the morphological and physiological characteristics, of mint grown on Eutric Cambisol soil under semi-controlled greenhouse conditions.

Experimental

The experiment was conducted from the second week of April to the fourth week of July 2026, in a semi-controlled greenhouse at the Institute of Soil Science, utilizing plastic pots. Each pot contained 1.4 kg of homogenized Eutric Cambisol soil [13]. The soil was collected from a field in Mladenovac town, located about 55 km from Belgrade, Serbia (grid reference: 44°24' N, 20°40' E). Based on the soil surface characterization from our previous research [14], Eutric Cambisol is characterized by acid reaction, high available potassium, medium to high available phosphorus, and medium total nitrogen and organic carbon supply. According to granulometric composition, Eutric Cambisol is a clay loam. In every plastic pot, six mint seeds were sown on April 16. Once the seedlings emerged and reached a height of approximately 3 cm above the soil surface, they were thinned to maintain a uniform density of three plants per pot. Cultivation followed standard agricultural practices, including systematic irrigation and manual weed removal, without the application of any chemical plant protection products. The experimental design comprised four distinct treatments arranged in three replications: Control (ANE 0 mL/L distilled water) - T1, ANE at concentrations of 0.2% (2 mL/L distilled water) - T2, 0.4% (4 mL/L distilled water) - T3, and 0.6% (6 mL/L distilled water) - T4. According to the manufacturer's specification, the *A. nodosum* extract is classified as a liquid nitrogenous organic fertilizer of plant (algal) origin. The initial application of the designated ANE doses was performed via soil spraying immediately after sowing. Following seedling emergence (at approximately 3 cm plant height) and thinning, subsequent treatments were performed every 7 days through combined soil and foliar spraying. The pots were regularly irrigated to ensure optimal and continuous soil moisture throughout the cultivation period. Seven days prior to the final harvest, morphological traits, specifically stem length (SL), leaf length (LL), and number of leaves (NL), along with physiological parameters of the aerial biomass were evaluated. These

physiological indicators, which included the nitrogen balance index (NBI), chlorophyll (CHL), flavonoids (FLV), and anthocyanins (ANT), were recorded using a portable Dualex optical leafclip sensor (FORCE-A, Orsay, France). On July 30, 7 days after the measurements, the mint plants were completely harvested from the pots, ensuring minimal damage during the separation of roots from the soil matrix. The root system was subsequently washed thoroughly with distilled water to remove remaining soil particles, and the root length (RL) was measured for each treatment. To determine the yield, the fresh weight of the aerial biomass per treatment was recorded immediately, after which the plant material was dried to determine the dry weight, with both yield parameters expressed in g/pot.

All collected data relevant to the treatment effects on tested plant parameters were subjected to a one-way analysis of variance (ANOVA) using SPSS 22.0 software. Statistically significant differences among the treatment means were determined using Duncan's multiple range test (DMRT) at a significance level of $p < 0.05$.

Results and discussion

The values of the yield, morphological and physiological traits of mint showed distinct responses under influence of treatment with different doses of ANE.

Statistical analysis of the differences between the treatments for individual comparison of plant morphological traits is presented in Table 1. The obtained data indicated a statistically significant effect ($p < 0.05$) of all applied doses of ANE on plant morphological traits in relation to soil not treated with ANE. The most pronounced significant effect ($p < 0.05$) on all plant morphological traits compared to other tested treatments was determined in the treatment where ANE at 4 mL/L was applied, followed by treatments sprayed with ANE at 6 and 2 mL/L.

Table 1. Effect of treatments on morphological traits of mint

Treatments	Morphological traits (per pot)[1]			
	SL (cm)	LL (cm)	NL	RL (cm)
T1 - ANE (0 ml/l)	13.44 ± 0.94 c	1.55 ± 0.08 c	18.86 ± 0.56 c	2.89 ± 0.35 c
T2 - ANE (2 ml/l)	16.69 ± 0.77 b	2.59 ± 0.60 b	23.03 ± 0.77 b	4.07 ± 0.22 b
T3 - ANE (4 ml/l)	20.64 ± 1.51 a	3.74 ± 0.52 a	26.98 ± 1.51 a	6.26 ± 0.25 a
T4 - ANE (6 ml/l)	17.55 ± 0.91 b	2.66 ± 0.27 b	23.89 ± 0.91 b	4.66 ± 0.58 b

[1]Means ± STDEV (n = 3); stem length (SL), leaf length (LL), number of leaves (NL), root length (RL); Duncan's test at $p \leq 0.05$ - values followed by the same letter in a column are not significantly different.

Previous research [15] reported that the application of ANE at a concentration of 10 mL/L enhanced the root length of *Mentha spicata* L. compared with the control treatment. Similarly, the application of *ANE* through drench and foliar treatments increased leaf number and plant height in mint plants. Among the tested treatments, drench application of ANE at 7 mL/L produced the highest values for both leaves per plant and plant height compared with applications at 0 and 5 mL/L [8].

Statistical analysis of the differences between the treatments for individual comparison of plant physiological parameters is presented in Figure 1. The obtained results mainly indicated a statistically significant effect ($p < 0.05$) of all applied doses of ANE on all plant physiological parameters in relation to soil not treated with ANE. The most pronounced significant effect ($p < 0.05$) on all plant physiological parameters compared to T1, T2 and T4 treatments was determined in the treatments where ANE at 4 mL/L was applied, followed by ANE at 2 mL/L.

Consistent with the present findings, moderate ANE application doses, particularly 2 mL/L, obtained in previous work [5], have been shown to improve chlorophyll, carotenoid, and

flavonoid concentrations, as well as antioxidant capacity, in basil cultivated under fully controlled plant factory conditions. Similarly, foliar application of ANE at a concentration of 0.3% enhanced chlorophyll content and increased the activity of anthocyanins in okra plants under drought stress [6]. *ANE* has also been reported to stimulate flavonoid biosynthesis and increase total flavonoid content in spinach [11].

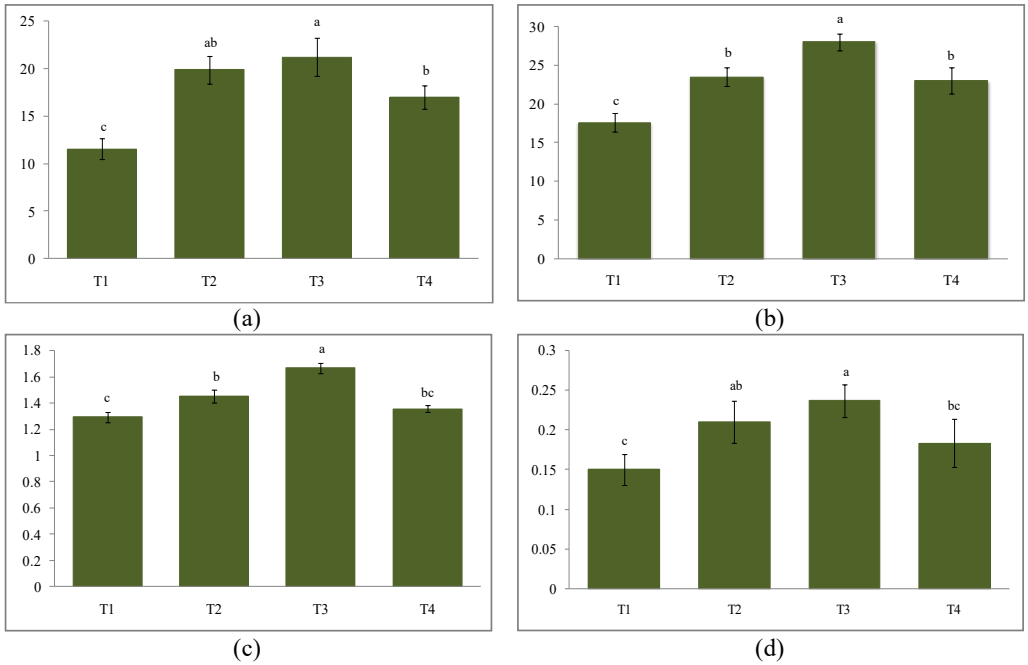


Figure 1. Effect of treatments on mint physiological parameters: a) nitrogen balance index (NBI); b) chlorophyll (CHL, µg/cm^2); c) flavonoids (FLV, µg/cm^2); d) anthocyanins (ANT, µg/cm^2); Duncan's test at $p \leq 0.05$ - different lowercase letters represent significance in differences between treatment means (± STDEV, n = 3).

Differences in the values of fresh and air-dried biomass yield between the treatments indicated a statistically significant effect ($p < 0.05$) of all applied doses of ANE on mint yield in relation to soil not treated with ANE. The treatments where ANE was applied at 4 mL/L, followed by those sprayed with ANE at 6 mL/L, showed the most pronounced significant effect ($p < 0.05$) on plant yield.

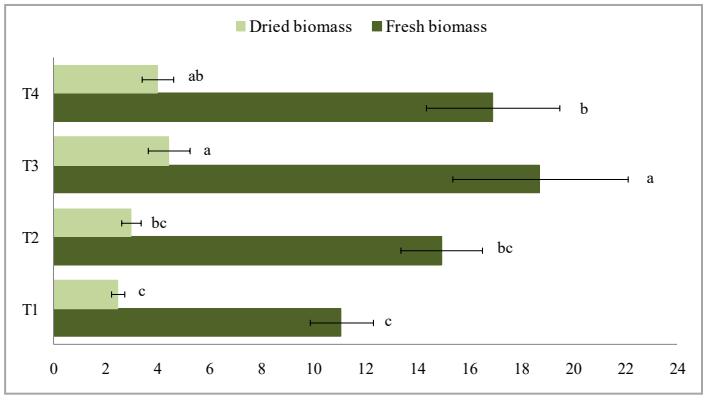


Figure 2. Effect of treatments on mint yield (g/pot); Duncan's test at $p \leq 0.05$ - different lowercase letters represent significance in differences between treatment means (± STDEV, n = 3).

Similar to these findings regarding better results with higher ANE doses, drench application of ANE at 7 mL/L resulted in the highest stem dry weight compared with applications at 0 and 5 mL/L in mint [8]. Research investigating the effects of *ANE* on the growth and yield of savory demonstrated that both soil and foliar applications of the seaweed extract significantly increased plant dry weight [10]. According to the findings of Pappachan et al. [18], the application of ANE at a lower concentration (0.5 mL/L) significantly increased mulberry leaf production compared with the application of 1 mL/L.

Conclusion

The results of the present study demonstrated that ANE application at concentrations of 2, 4, and 6 mL/L significantly affected all evaluated parameters of mint compared with the untreated control. Among the tested treatments, the application of ANE at 4 mL/L produced the most pronounced effects on yield, morphological characteristics, and physiological parameters, and may be recommended for mint cultivation under greenhouse pot conditions. Nevertheless, further research under larger-scale soil cultivation conditions is needed to validate these findings and assess the applicability of this treatment in practical production systems.

Acknowledgements

The study was supported by the Ministry of Science, Technological Development and Innovation of the Republic of Serbia, Project 451-03-33/2026-03/200011, and Project 451-03-33/2026-03/200022.

References

[1] J. Kišgeci, Lekovito bilje - Gajenje, sakupljanje, upotreba, Partenon, Belgrade, Serbia, 2002, pp. 212-213 (in Serbian).
[2] S.R. Sommano, N. Kanthawang, C. Janpen, P. ai Norkum, M. Wongkaew, C. Inkham, H. Van Doan, R. Cheewangkoon, Front. Sustain. Food Syst. 5 (2022) 808327.
[3] D.D. Treadwell, G.J. Hochmuth, R.C. Hochmuth, E.H. Simonne, S.A. Sargent, L.L. Davis, W.L. Laughlin, A. Berry, Hort. Technology *21* (2011) 162-169.
[4] M. Begum, B.C. Bordoloi, D.D. Singha, N.J. Ojha, Agric. Rev. 39 (2018) 321-326.
[5] V.P. Lam, G. Bok, D.N. Loi, M.C. Do, J. Park, Plants 14 (2025) 3271.
[6] J. Ali, I. Jan, H. Ullah, N. Ahmed, M. Alam, R. Ullah, M. El-Sharnouby, H. Kesba, M. Shukry, S. Sayed, T. Nawaz, Plants 11 (2022) 790.
[7] T. Frioni, J. Vanderweide, A. Palliotti, S. Tombesi, S. Poni, P. Sabbatini, *Sci. Hortic.* 277 (2021) e109807.
[8] H.O. Elansary, K. Yessoufou, S. Shokralla, E.A. Mahmoud, K. Skalicka-Woźniak, Ind. Crops Prod. 92 (2016) 50-56.
[9] M.K.A. Aly, E.T. Ahmed, M.A.H. Mohamed, E.Z.N. Youssef, *Sci. J. Flowers Ornam.* Plants 8 (2021) 235-249.
[10] Y. Nasiri, H. Kochakkhani, M. Asadi, Pesq. Agropec. Trop. 55 (2025), e81375.
[11] S. Kumari, K.D. Sehrawat, D. Phogat, A.R. Sehrawat, R. Chaudhary, S.N. Sushkova, M.S.Voloshina, V.D. Rajput, A.N. Shmaraeva, R. Marc, S. Shende, Agriculture 13 (2023) 1179.
[12] N. Çöl Keskin, M. Tanur Erkoyuncu, TURJAF 13 (2025) 1169-1181.
[13] IUSS Working Group WRB, In: International Soil Classification System for Naming Soils and Creating Legends for Soil Maps, 4th ed, Vienna, Austria: International Union of Soil Sciences, 2022.
[14] D. Latković, J. Maksimović, Z. Dinić, R. Pivić, A. Stanojković, A. Stanojković-Sebić, Biology 9 (2020), 452.

[15] P.F. Luna-Rodríguez, H.M. Munguia-Falcon, I.E. Mogollón-Ortega, E.E. Saavedra-Flores, C.P. Romero-Ayala, M.F. Siancas-Carrasco, M.A. Márquez-Bautista, C.E. Figueroa-Serrudo, I.M. Montes-Yarasca, H.B. Cántaro-Segura, Agron. Costarricense 48 (2024) 151-158.
[16] A. Pappachan, L. Bariampan, K. Trivedy, Biosci. Discov. 8 (2017) 235-240.

GLUTEN-FREE BISCUITS ENRICHED WITH ACORN FLOUR: NUTRITIONAL, PHYSICAL, PHYTOCHEMICAL, AND SENSORY CHARACTERIZATION

Daniela Stoin [1*], Calin Jianu[1], Ersilia Alexa[1], Mariana-Atena Poiana[1], Ariana-Bianca Velciov[1], Florina Radu[1], Diana Moigradean[1], Liana Alda[1], Corina Megyesi[1], Laura Rădulescu[1], Alexandru Rinovetz[1], Antoanela Cozma[2]

[1]Faculty of Food Engineering, University of Life Sciences „King Michael I" from Timisoara, Romania, Aradului Street No 119, 300645 Timisoara, Romania
[2] Faculty of Agriculture, Banat's University of Life Sciences „King Michael I" from Timisoara, Romania, Aradului Street No 119, 300645 Timisoara, Romania
[*]author's email address: alexandrurinovetz@usvt.ro

Abstract

In response to growing consumer interest in foods with enhanced nutritional and functional properties, acorn flour (AF) represents a promising ingredient for the development of value-added products. This study aimed to develop and characterize gluten-free biscuits enriched with AF through partial substitution of rice flour (RF). Four formulations were prepared with 0, 5, 15, and 25% AF substitution, corresponding to BC, B5AF, B15AF, and B25AF, respectively. Proximate composition, physical properties, total phenolic content (TPC), DPPH radical-scavenging activity, and sensory attributes were evaluated. AF incorporation increased fat, ash, and total dietary fiber contents, while available carbohydrates decreased from 40.02 to 35.55 g/100 g. Increasing AF levels reduced biscuit thickness and increased diameter, weight, and spread ratio, which rose from 5.28 in BC to 5.64 in B25AF. TPC increased from 38.43 to 63.82 mg GAE/100 g DM, while DPPH radical-scavenging activity increased from 31.49% to 64.37%. All formulations showed good sensory acceptability, with moderate AF substitution providing a favorable balance between sensory quality and functional properties. Overall, AF incorporation represents a promising strategy for developing functional gluten-free biscuits with improved nutritional and antioxidant characteristics while maintaining favorable physical and sensory properties.

Keywords: *acorn flour, gluten-free biscuits, sensory evaluation, functional ingredient*

Introduction

The increasing prevalence of celiac disease and gluten sensitivity has driven the diversification of gluten-free products. However, many of these products are formulated primarily with starches and refined flours and contain lower amounts of dietary fiber, vitamins, minerals, and bioactive compounds than conventional wheat-based products [1]. Consequently, research has increasingly focused on alternative raw materials that are naturally gluten-free and possess a superior nutritional profile. Among these, acorns, the fruits of species belonging to the genus *Quercus*, represent an underutilized resource that is widely available in Romania.

Acorn flour (AF) has a valuable nutritional and functional profile, although its composition is influenced by species, pedoclimatic conditions, and processing technology. In general, it contains approximately 75–84% carbohydrates, 5% protein, 8.5–13% lipids, 9.5–15% dietary fiber, and around 2% minerals [2]. It is also an important source of unsaturated fatty acids and bioactive compounds, including polyphenols such as gallic acid, ellagic acid, catechin, and rutin, as well as vitamin E and minerals, which contribute to its antioxidant potential [3,4]. Previous studies have highlighted the beneficial effects of incorporating acorn flour into bakery products. Beltrão Martins et al. (2020) [3] reported increases in phenolic compound content and antioxidant activity in gluten-free bread, while Levent and Aktaş (2024) [5] observed improvements in protein, phenolic compound, and mineral contents. Nevertheless, high

substitution levels may adversely affect technological properties by reducing dough extensibility and final product volume, effects mainly associated with the high fiber content and increased water absorption capacity of acorn flour [6,7]. Depending on the product, acorn flour may be incorporated at levels ranging from approximately 10 to 60%, with gluten-free applications considered particularly promising from a nutritional perspective [8]. Despite this potential, studies specifically addressing the incorporation of acorn flour into gluten-free biscuits remain limited, particularly regarding its combined effects on nutritional, functional, physical, and sensory properties. Therefore, the present study evaluated different acorn flour substitution levels to determine their influence on the proximate composition, physical characteristics, total phenolic content, antioxidant activity, and sensory acceptability of gluten-free biscuits.

Experimental

Technological process for the production of gluten-free biscuits

RF, AF and the other ingredients used in this study were purchased from local market in Timisoara town, Romania.

The gluten-free biscuits were prepared according to the procedure described by Stoin et al. (2025) [9], with modifications adapted to the present formulation. Briefly, the dry ingredients, including rice flour, acorn flour, Jerusalem artichoke flour, carob powder, and stevia, were thoroughly mixed to ensure uniform distribution. Coconut butter and coconut milk were then added, and the mixture was kneaded until a homogeneous dough was obtained. The dough was refrigerated at 4 °C for 60 min, rolled to a thickness of 4 mm, and cut into circular pieces using a 6 cm diameter cutter. The biscuits were baked at 175 °C for 20 min and subsequently cooled to room temperature before further analyses. Three independent batches were prepared for each formulation (n = 3).

Analytical procedures

The proximate composition of the gluten-free biscuits was determined using standard AOAC methods [11,12]. Moisture, lipid, protein, and total dietary fiber contents were determined according to AOAC Official Methods 925.10, 922.06, 920.87, and 991.43, respectively. Available carbohydrate content was calculated by difference. The physical properties of the biscuits, including weight, diameter, thickness, and spread ratio, were evaluated according to previously described procedures [9,10], with the spread ratio calculated as the ratio of biscuit diameter to thickness (D/T). TPC was determined using the Folin–Ciocalteu method and expressed as mg gallic acid equivalents (GAE)/100 g dry matter (DM) [9]. Antioxidant activity was assessed using the DPPH (2,2-diphenyl-1-picrylhydrazyl) radical-scavenging assay, and the results were expressed as percentage inhibition [9,10]. All determinations were performed in triplicate, and the results were expressed as mean ± standard deviation (SD).

Sensory evaluation

Sensory evaluation was conducted using a consumer acceptance test with 25 untrained panelists (n = 25). A nine-point hedonic scale ranging from 1 (“dislike extremely”) to 9 (“like extremely”) was used to evaluate five sensory attributes: color, appearance, odor, flavor, and overall acceptability. The biscuit samples were coded with random three-digit numbers and presented to the panelists in randomized order. Water was provided for palate cleansing between samples [13].

Results and discussion

Proximate composition of biscuit samples

As shown in Table 1, the incorporation of AF progressively modified the proximate composition of the gluten-free biscuits.

Table 1. Proximate composition and energy value of AF-enriched gluten-free biscuit formulations

Chemical Parameters	**Gluten-free biscuits**			
	BC	B5AF	B15AF	B25AF
Moisture (%)	5.12 ± 0.06	5.38 ± 0.22	5.61 ± 0.38	5.84 ± 0.21
Fat (%)	28.14 ± 0.22	29.03 ± 0.35	29.87 ± 0.14	30.44 ± 0.12
Protein (%)	6.48 ± 0.19	6.43 ± 0.28	6.34 ± 0.22	6.25 ± 0.19
Ash (%)	1.52 ± 0.18	1.57 ± 0.18	1.63 ± 0.22	1.71 ± 0.29
Total Dietary Fiber (%)	18.72 ± 0.14	19.05 ± 0.23	19.63 ± 0.25	20.21 ± 0.34
Available CRB (%)	40.02 ± 0.18	38.54 ± 0.42	36.92 ± 0.25	35.55 ± 0.33
Energy Value (kcal/100 g)	476.70 ± 0.27	479.25 ± 0.14	481.13 ± 0.31	481.58 ± 0.26

All determinations were done in triplicate and the results were reported as average value ± standard deviation (SD). ***BC*** *– control Biscuits prepared with 100% rice flour (RF);* ***B5AF*** *– Biscuits prepared with 95% RF and 5% AF;* ***B15AF*** *– Biscuits prepared with 85% RF and 15% AF;* ***B25AF*** *– Biscuits prepared with 75% RF and 25% AF.*

Moisture content increased slightly from 5.12% in BC to 5.84% in B25AF, which may be related to the higher water-binding capacity associated with the fiber-rich fraction of AF. Fat content increased from 28.14 to 30.44%, whereas protein content showed a slight decrease from 6.48 to 6.25%. This trend is consistent with the composition of AF reported by Beltrão Martins et al. (2022) [4], who found that AF contained considerably more fat but less protein than RF. Ash and total dietary fiber contents increased progressively, reaching 1.71 and 20.21%, respectively, in B25AF. Similar increases in dietary fiber following AF incorporation into gluten-free biscuits have been reported by Korus et al. (2017) [14], supporting the potential of AF to improve the nutritional value of gluten-free bakery products. In parallel, available carbohydrate content decreased from 40.02 to 35.55%, reflecting the replacement of carbohydrate-rich rice flour with acorn flour containing higher amounts of lipids and fiber. The energy value increased only slightly, from 476.70 to 481.58 kcal/100 g, mainly due to the higher lipid content. Overall, these results are consistent with previous studies describing acorn flour as a relatively high-fat, fiber-rich ingredient with moderate protein content [4,15].

Table 2. Physical characteristics of AF-enriched gluten-free biscuit formulations

Physical characteristics	**Gluten-free biscuits**			
	BC	B5AF	B15AF	B25AF
Thickness (mm)	7.82 ± 0.22	7.71 ± 0.28	7.58 ± 0.31	7.43 ± 0.39
Diameter (mm)	41.25 ± 0.19	41.43 ± 0.61	41.68 ± 0.48	41.90 ± 0.55
Weight (g)	7.54 ± 0.26	7.61 ± 0.18	7.67 ± 0.24	7.72 ± 0.20
Spread Ratio	5.28 ± 0.11	5.38 ± 0.15	5.50 ± 0.11	5.64 ± 0.17

As shown in Table 2, increasing AF substitution progressively affected the physical characteristics of the gluten-free biscuits. Biscuit thickness decreased from 7.82 mm in BC to 7.43 mm in B25AF, whereas diameter and weight slightly increased from 41.25 to 41.90 mm and from 7.54 to 7.72 g, respectively. Consequently, the spread ratio increased from 5.28 to 5.64, indicating greater lateral spreading at higher AF levels. A comparable decrease in thickness accompanied by increases in diameter and spread ratio has been reported for biscuits containing alternative flour sources [10]. These changes may be associated with modifications in dough consistency and water-binding behavior resulting from the higher fiber content and specific functional properties of the incorporated flour [6,7]. Overall, AF incorporation

produced moderate changes in biscuit geometry while maintaining the physical integrity of the final products.

Table 3. Total phenolic content (TPC) and DPPH radical scavenging activity of AF-enriched gluten-free biscuit formulations

Samples	**Phytochemical parameters**	
	TPC (mg GAE/100g DM)	**DPPH Inhibition (%)**
BC	38.43 ±0.22	31.49 ± 0.35
B5AF	42.17 ± 0.32	38.62 ± 0.43
B15AF	51.35± 0.25	51.74 ± 0.39
B25AF	63.82± 0.34	64.37± 0.28

As shown in Table 3, increasing AF substitution resulted in a progressive enhancement of the phytochemical and antioxidant properties of the gluten-free biscuits. TPC increased from 38.43 mg GAE/100 g DM in BC to 63.82 mg GAE/100 g DM in B25AF, corresponding to an increase of approximately 66%. Similarly, DPPH radical-scavenging activity increased from 31.49% to 64.37%, more than doubling at the highest substitution level. This trend can be attributed to the naturally high content of phenolic compounds in AF, including gallic acid, ellagic acid, catechin, and rutin, which contribute substantially to its antioxidant potential [3,4]. Similar improvements in phenolic content and antioxidant activity following AF incorporation have been reported by Beltrão Martins et al. (2022) [3] in gluten-free bakery products. The parallel increase in TPC and DPPH inhibition observed in the present study suggests that the enrichment of biscuits with AF enhanced their antioxidant potential, with B25AF showing the highest functional value.

Table 4. Sensory evaluation of AF-enriched gluten-free biscuit formulations

Sensory evaluation	**Gluten-free biscuits**			
	BC	B5AF	B15AF	B25AF
Color	7.82 ± 0.25	7.75 ± 1.22	7.53 ± 0.11	7.21 ± 0.28
Appearance	7.65 ± 0.14	7.70 ± 0.12	7.78 ± 0.14	7.54 ± 0.14
Odor	7.44 ± 0.17	7.52 ± 0.36	7.61 ± 0.11	7.48 ± 0.33
Flavor	7.23 ± 0.27	7.38 ± 0.13	7.51 ± 0.25	7.33 ± 0.18
Overall acceptability	7.53 ± 0.33	7.61 ± 0.14	7.72 ± 0.26	7.38 ± 0.41

All biscuit formulations showed good sensory acceptability, with mean scores above 7 for all evaluated attributes (Table 4). B15AF achieved the highest scores for appearance, odor, flavor, and overall acceptability, whereas color scores decreased with increasing AF incorporation. The slight decline observed at 25% substitution suggests that moderate AF levels may provide a better balance between functional enhancement and sensory quality, in agreement with previous findings for flour-enriched bakery products [10,13].

Conclusions

The incorporation of acorn flour improved the nutritional and functional profile of gluten-free biscuits, particularly by increasing total dietary fiber, phenolic content, and antioxidant activity, while reducing available carbohydrate content. Increasing AF substitution also induced moderate changes in the physical properties of the biscuits, including a higher spread ratio and lower thickness. All formulations maintained good sensory acceptability, with the 15% AF formulation showing the most favorable overall sensory profile. These findings support the use

of AF as a promising functional ingredient for the development of gluten-free biscuits with enhanced nutritional and antioxidant properties while maintaining acceptable technological and sensory characteristics.

References

[1] G. Vici, L. Belli, M. Biondi, M., V. Polzonetti,. Gluten free diet and nutrient deficiencies: A review. Clinical Nutrition, 35(6), (2016), 1236–1241.
[2] S. Silva, E.M. Costa, A. Borges, A.P. Carvalho, M.J. Monteiro, M.M.E. Pintado, M. M. E., Nutritional characterization of acorn flour (a traditional component of the Mediterranean gastronomical folklore). Journal of Food Measurement and Characterization, 10(3), (2016).
[3] R. Beltrão Martins, I. Gouvinhas, M.C. Nunes, J. Alcides Peres, A. Raymundo, A.I. Barros, Acorn flour as a source of bioactive compounds in gluten-free bread. Molecules, *25*(16), (2020), 3568.
[4] R. Beltrão Martins, I. Gouvinhas, M.C. Nunes, L.M. Ferreira, J.A. Peres, A. Raymundo, A.I. Barros,. Acorn flour from holm oak (*Quercus rotundifolia*): Assessment of nutritional, phenolic, and technological profile. Current Research in Food Science, 5, (2022), 2211-2218.
[5] A. Levent, K. Aktaş, K., Nutritional composition and staling properties of gluten-free bread-added fermented acorn flour. Food Science & Nutrition, 12(3), (2023), 1955-1964.
[6] M.E.H. Kaykha, A., Forouhar, H. Saberian, H., Functional cakes: The effect of acorn flour and hydrocolloids and emulsifier on texture, nutritional and sensory properties. Food Science & Nutrition, 13(8), (2025), e70703.
[7] E. Szabłowska, M. Tańska, Effects of acorn flour addition on baking characteristics of wheat flour. Foods, 14(2), (2025), 190.
[8] E. Szabłowska, M. Tańska, Acorn flour properties depending on the production method and laboratory baking test results: A review. Comprehensive Reviews in Food Science and Food Safety, 20(1), (2021), 980–1008.
[9] D. Stoin, M.A. Poiana, E. Alexa, I. Cocan, M. Negrea, C. Jianu, & C. Ianasi, C., Current trends in gluten-free biscuit formulation using rice flour enriched with chestnut flour and fruit powders. *Foods*, *14*(23), (2025), 4074.
[10] S. Dossa, C. Neagu, D. Lalescu, M. Negrea, D. Stoin, C. Jianu, & E. Alexa, E. Evaluation of the Nutritional, Rheological, Functional, and Sensory Properties of Cookies Enriched with Taro (*Colocasia esculenta*) Flour as a Partial Substitute for Wheat Flour. Foods, 14(20), (2025), 3526.
[11] A.O.A.C., "Official Methods of Analysis" Association Official Analytical Chemists of the 16" Ed. International, Washington, D.C., U.S.A. (1995).
[12] AOAC (Association of Official Analytical Chemists) Official Methods of Analysis International. 17th, Ed. Washington, DC: AOAC (2000).
[13] S. Frauenhoffer, E. Ola, S. Jervis, S.E. Gauch, S.H. Seo, Comparison Analyses of Consumer Acceptance, Evoked Emotions, and Purchase Intent Between Gluten-Containing Versus Gluten-Free Chocolate Chip Cookie Products. Journal of Food Science, 90(5), (2025) e70276.
[14] A. Korus, D. Gumul, M. Krystyjan, L. Juszczak, L., & J. Korus, Evaluation of the quality, nutritional value and antioxidant activity of gluten-free biscuits made from corn-acorn flour or corn-hemp flour composites. European Food Research and Technology, 243(8), (2017)1429-1438.
[15] A. Pasqualone, F.Z. Makhlouf, M. Barkat, G. Difonzo, C. Summo, G. Squeo, & F. Caponio, Effect of acorn flour on the physico-chemical and sensory properties of biscuits. *Heliyon*, *5*(8). (2019).

SOUS-VIDE PROCESSING AS A SUSTAINABLE THERMAL PROCESS FOR THE FOOD INDUSTRY

Alexandru Rinovetz[1], Diana Radu[3], Daniela Stoin[3]*, Corina-Iuliana Megyesi[1], Laura Rădulescu[1], Ariana-Bianca Velciov[1], Bogdan Rădoi[3], Mariana-Atena Poiană[3], Florina Radu[3], Corina Mișcă[2]

[1]University of Life Sciences "King Mihai I" Timisoara, Faculty of Food Engineering, Food Science Department, Calea Aradului, 300645, Timisoara, Romania;
[2]University of Life Sciences "King Mihai I" Timisoara, Faculty of Food Engineering, Food Control and Expertise Department, Calea Aradului, 300645, Timisoara, Romania;
[3]University of Life Sciences "King Mihai I" Timisoara, Faculty of Food Engineering, Food Technologies Department, Calea Aradului, 300645, Timisoara, Romania.
**corresponding author: danielastoin@usvt.ro*

Abstract
Sous-vide processing (French for 'under vacuum') is a controlled thermal-processing technique widely used in gastronomy and increasingly applied in the food industry to preserve the sensory and nutritional quality of foods. The process involves vacuum packaging followed by mild heat treatment at a constant, accurately controlled temperature, generally within 50–90°C in a thermostatically controlled water bath. Treatment time is selected according to the food matrix (red or white meat, fish, vegetables, fruit, or eggs), physicochemical properties, characteristic thickness, and the required level of microbiological safety. Accurate control of these variables promotes uniform heating while limiting water loss, oxidation, loss of volatile compounds, and excessive structural damage. Reduced oxygen exposure and processing below the boiling point can decrease lipid oxidation and the degradation of heat-sensitive vitamins, while controlled protein denaturation can improve texture, tenderness, and juiciness. When the vacuum, time–temperature profile, rapid cooling, and refrigerated storage are validated and monitored, sous-vide processing can contribute to the control of foodborne pathogens, including *Listeria monocytogenes* and *Salmonella* spp. The principal technological advantages are uniform processing, improved process yield, extended refrigerated shelf life, recipe standardization, and high reproducibility through digital control of the operating parameters.
Keywords: sous-vide, controlled thermal processing, nutrient retention, heat transfer, food safety, sustainability.

Introduction
Thermal processing is essential for microbiological stabilization and for establishing the sensory properties of foods; however, high temperatures and direct contact with water or air can intensify mass loss, oxidation, and the migration of soluble constituents. Sous-vide processing mitigates these effects by hermetically packaging the food, removing air, and heating it in a controlled, thermostatically regulated medium at a temperature close to the target value at the product core. This approach contributes to pathogen inactivation, texture improvement, flavor development, enhanced digestibility, and the attainment of sensory properties accepted by consumers. Thermal treatment may nevertheless cause losses of nutritional and bioactive constituents, including water-soluble vitamins, sensitive pigments, phenolic compounds, amino acids susceptible to browning reactions, and volatile aroma compounds. The literature identifies two major disadvantages of conventional thermal processing: high energy consumption and degradation of heat-sensitive nutrients. Over the past decade, these limitations have stimulated the development and integration of alternative technologies with lower environmental impact and/or improved quality attributes. The defining

operation in sous-vide processing is the packaging of food in heat-resistant food-contact materials, followed by partial or near-complete air removal and thermal treatment at controlled, relatively mild temperatures compared with boiling, baking, or frying. Its principal characteristics are therefore temperature stability, uniform heat transfer, limited oxygen exposure, and reduced losses through evaporation or dissolution in the processing medium [1–5]. This topic is relevant to the food industry because sous-vide products can be integrated into centralized production systems, catering, refrigerated retail, HoReCa operations, and supply chains for high-quality semi-prepared foods. The technique supports portion standardization and reproducible sensory quality, improves yield, and allows thermal treatment, cooling, storage, and finishing to be separated operationally, thereby offering a viable approach to reducing food waste [2].

Sustainability is no longer defined solely by equipment energy consumption, it also encompasses processing yield, mass losses, water consumption, shelf life, refrigeration requirements, packaging impact, and product acceptability. Sous-vide may be regarded as a sustainable thermal process when phase-specific operating conditions are optimized, including the loading of the thermostatically controlled bath, equipment insulation, packaging selected according to product characteristics, and implementation of a validated HACCP plan. Consequently, the process cannot be defined solely by the immersion-bath temperature; it must also account for the thermal history at the slowest-heating point, portion thickness, pH, water activity, composition, initial contamination, and storage duration [1,6–9].

Experimental

2.1. Materials

A systematic technological review of the literature supports the selection of three representative food matrices: meat, fish, and vegetables. The principal factors considered were the thermal regime, sample geometry, conventional reference method, quality indicators, and resource-consumption indicators (Table 1).

Table 1. Proposed experimental treatments [2,3]

Code	Food matrix	Sous-vide regime (°C/min)	Assessment criterion
V1	Chicken breast	63/90	Safety and juiciness
V2	Pork loin	60/180	Tenderness and yield
V3	Salmon fillet	50/40	Texture and reduced losses
V4	Broccoli	85/25	Color, vitamin C, and phenolics
V5	Carrot	85/60	Carotenoids and texture
V6	Potato	90/80	Starch gelatinization
M1	Same raw materials	Boiling (100 °C)	Reference for leaching
M2	Same raw materials	Oven/steam cooking	Quality reference

The processing line comprises a chamber vacuum-packaging machine, heat-resistant oxygen-barrier packaging, a thermostatically controlled immersion bath, a temperature probe, a temperature-data logging system, and a blast chiller or an ice-water bath. The packaging material must provide mechanical stability and chemical inertness over the applied temperature range. Close contact between the package and the product promotes uniform heat transfer and heat flux [1,2].

2.2. Methods

The recommended analytical methods are summarized in Table 2.

Table 2. Recommended analytical methods [2,3,10–14].

Parameter	Recommended method	Unit	Relevance
Moisture	Oven drying/moisture analyzer	%	Water loss and juiciness
Protein	Kjeldahl/Dumas	%	Nutritional value and protein matrix
Lipids	Soxhlet extraction	%	Energy value, oxidation, and juiciness
Ash	Incineration	%	Total mineral content
Vitamin C	HPLC/titration	mg/100 g	Heat-labile marker
Amino acids	Capillary electrophoresis/HPLC	%	Protein denaturation

Minerals	ICP-OES/AAS	mg/100 g	Mineral retention
Total phenolics	Folin–Ciocalteu assay	mg GAE/100 g	Bioactive compounds
Carotenoids	HPLC/spectrophotometry	mg/100 g	Colored vegetables
Antioxidant capacity	DPPH, ABTS, FRAP	% / μmol TE	Antioxidant capacity
Color	CIE L*a*b* colorimetry	L*, a*, b* units	Appearance and acceptability
Texture	Warner–Bratzler/texture analyzer	N	Tenderness and firmness
Microbiology	Specific ISO/GOST methods	CFU/g	Safety and hygiene

Results and discussion

Published studies confirm that heating time varies nonlinearly with product geometry. For a characteristic thickness d = 20 mm, the time required for the product center to approach the immersion-bath temperature is approximately 50 min for a slab, 30 min for a cylinder, and 20 min for a sphere. At d = 60 mm, the corresponding values increase to 285, 150, and 120 min, respectively. These differences arise from the diffusion distance and the heat- and mass-transfer area available relative to product volume (Figure 1).

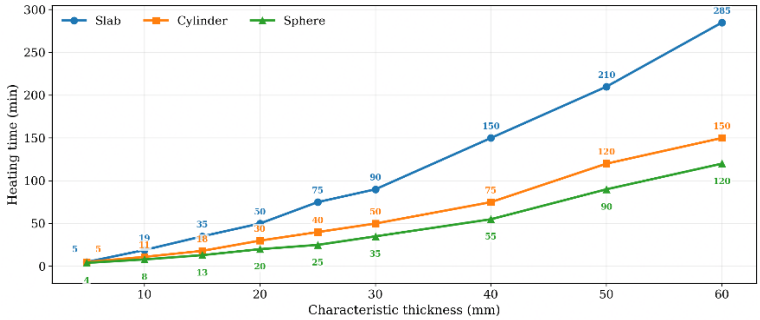


Figure 1. Effects of product thickness and geometry on heating time [adapted from 1].

Total product mass cannot substitute for thickness as a process-design variable. Samples should be portioned uniformly, and packages should be arranged so that water circulation is not restricted. Any change in sample dimensions, geometry, or equipment load requires revalidation of the temperature profile at the geometric center. Sous-vide processing limits oxygen exposure and prevents contact with external process water, into which soluble bioconstituents would otherwise migrate. This effect is particularly relevant to vitamin C, thiamine, folates, potassium, and magnesium; however, percentage retention remains dependent on temperature, treatment time, pH, structure, and the subsequent use of the exudate. Sous-vide processing does not prevent thermal degradation; its principal advantage is the reduction of oxidation and leaching of soluble biocomponents. In cauliflower, vitamin C loss was 19.9% after sous-vide processing and 47.0% after boiling, corresponding to a 27.1% reduction. In carrot, the a* color parameter decreased by 12% under sous-vide conditions and by 30% after boiling, indicating better preservation of red-orange hues. This response is not universal: browning has been reported in asparagus, and prolonged exposure may eliminate the benefit associated with reduced oxygen availability in some vegetables (Table 3) [3,10–14].

Table 3. Factors relevant to the quality of sous-vide products.

Component	Mechanism	Potential beneficial effect	Critical condition
Muscle proteins	Denaturation and contraction	Uniform texture and tenderization	Avoid excessive time above 65°C
Collagen	Gradual solubilization	Tenderization of tough cuts	Extended treatment at 60–75°C
Vitamin C	Oxidation and degradation	Reduced leaching	Minimum time compatible with safety
Minerals	Migration into liquid	Retention within the package	Reintegration of exudate
Carotenoids	Release from the matrix	Increased bioaccessibility	Appropriate temperature and lipid content
Chlorophylls	Conversion to pheophytins	Color retention under mild processing	Control of pH, time, and temperature

For meat, the 55–65°C range represents an effective compromise among myofibrillar protein denaturation, partial collagen solubilization, and water loss. Above 65°C, longitudinal

myofibrillar contraction and the exudation of biocomponents become more pronounced [15–17].

Sustainability should be evaluated per unit of finished product rather than solely as a function of processing temperature. The compiled data indicate a specific energy consumption of 0.65 kWh/kg and processing losses of 6% for an optimized sous-vide system. The corresponding reference values are 1.10 kWh/kg and 18% for oven cooking, 0.95 kWh/kg and 15% for boiling, and 1.25 kWh/kg and 20% for grilling. Under this scenario, optimized sous-vide processing reduces specific energy consumption by 32–48% and mass losses by 60–70% relative to conventional methods (Figure 2).

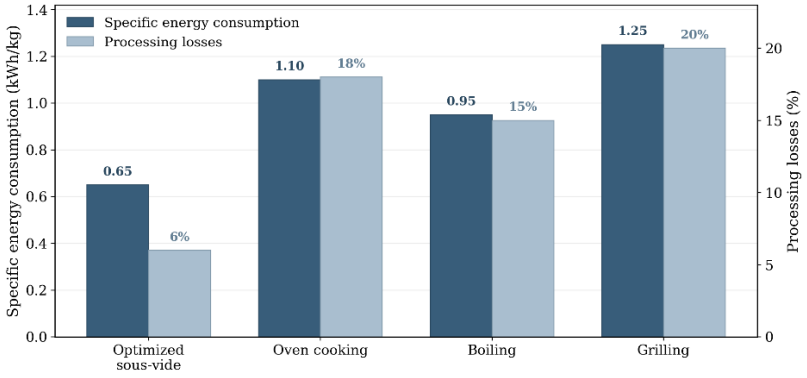


Figure 2. Specific energy consumption and processing losses for the compared methods [adapted from 18].

The yield advantage can offset part of the energy demand associated with long processing times because resources invested in raw-material production are not lost through evaporation or drip loss. When equipment is operated at a low load, fixed energy consumption is distributed over a smaller product mass and specific energy consumption, E_s, increases. Batch planning, thermal insulation, and prompt equipment shutdown are therefore prerequisites for environmental performance. Sous-vide products require a process-specific HACCP plan because vacuum conditions, moderate temperatures, and refrigerated storage may create favorable conditions for anaerobic and psychotropic microorganisms. Relevant hazards include *Salmonella spp*., *Listeria monocytogenes*, *Clostridium perfringens*, and non-proteolytic strains of *Clostridium botulinum*. Selection of the target microorganism must be based on the food matrix, pH, water activity, processing temperature, storage temperature, and intended shelf life [6–9,19].

Process validation should include dynamic monitoring of the thermal profile under worst-case operating conditions: the product with the greatest characteristic dimension, the maximum equipment load, the lowest initial product temperature, and the location exhibiting the lowest heat-transfer rate.

Conclusions

Sous-vide processing enables the process parameters—moderate temperature, thermal-treatment duration, and vacuum-packaging conditions—to be matched to the compositional, structural, and thermophysical characteristics of the food matrix. Method performance depends on precise operational control and reproducibility. Industrial implementation should therefore be supported by sensory and physicochemical assessments, quantification of the retention of nutritional and bioactive compounds, monitoring of specific resource and energy consumption, and application of a validated HACCP plan. Robust sustainability comparisons additionally require life-cycle assessment that integrates the production and end-of-life impact of packaging, the energy demand of thermal processing and refrigeration, resource consumption, processing yield, and the contribution of the process to reducing food losses and waste.

Acknowledgements
The authors acknowledge the University of Life Sciences 'King Mihai I' from Timișoara, Faculty of Food Engineering, for financial and technical support.

References

[1] Baldwin, D. E.,**2012**, Sous vide cooking: A review. International Journal of Gastronomy and Food Science, 1(1), pp. 15–30. https://doi.org/10.1016/j.ijgfs.2011.11.002
[2] Berdigaliuly, S., Baybolova, L., Davydenko, N., et al., **2022**, Perspectives for the application of sous-vide cooking in products for public catering. Potravinarstvo Slovak Journal of Food Sciences, 16, pp. 137–148.
[3] Zavadlav, S., Blažić, M., Van de Velde, F., et al., **2020**, Sous-Vide as a technique for healthy and high-quality vegetable and seafood products. Foods, 9(11), pp. 1537.
[4] Gazda, P., & Glibowski, P., **2024**, Advanced technologies in food processing—Development perspective. Applied Sciences, 14(9), pp. 3617.
[5] Rondanelli, M., Daglia, M., Meneghini, S., et al., **2017**, Nutritional advantages of sous-vide cooking compared to boiling on cereals and legumes. Food Science & Nutrition, 5(4), pp. 827–833.
[6] Hyytiä-Trees, E., Skyttä, E., Mokkila, M., et al., **2000**, Safety evaluation of sous vide-processed products with respect to nonproteolytic Clostridium botulinum. Applied and Environmental Microbiology, 66(1), pp. 223–229.
[7] Food Safety Authority of Ireland, **2014**, Sous Vide and Food Safety. Catering Factsheet Series.
[8] Codex Alimentarius Commission, **2022**, General Principles of Food Hygiene, CXC 1-1969.
[9] Regulation (EC) No 852/2004 of the European Parliament and of the Council on the hygiene of foodstuffs.
[10] Kosewski, G., Kowalówka, M., Drzymała-Czyż, S., & Przysławski, J., **2023**, Impact of culinary processing, including sous-vide, on polyphenols, vitamin C and antioxidant status. Foods, 12(11), pp. 2121.
[11] Florkiewicz, A., Socha, R., Filipiak-Florkiewicz, A., & Topolska, K., **2019**, Sous-vide and antioxidant properties of Brassica vegetables. Journal of the Science of Food and Agriculture, 99(1), pp. 173–182.
[12] Florkiewicz, A., & Berski, W., **2017**, Sous-vide method to maximize mineral retention. Journal of Food Processing and Preservation, 42(2), pp. 13491.
[13] Chiavaro, E., Mazzeo, T., Visconti, A., et al., **2012**, Nutritional quality of sous vide cooked carrots and Brussels sprouts. Journal of Agricultural and Food Chemistry, 60(23), pp. 6019–6025.
[14] Patras, A., Brunton, N. P., & Butler, F., **2010**, Effect of immersion and sous-vide on antioxidants, carotenoids and colour of carrot disks. Journal of Food Processing and Preservation, 34, pp. 1009–1023.
[15] Dominguez-Hernandez, E., Salaseviciene, A., & Ertbjerg, P., **2018**, Low-temperature long-time cooking of meat. Meat Science, 143, pp. 104–113.
[16] Roldán, M., Antequera, T., Martín, A., et al., **2013**, Effects of temperature–time combinations on sous-vide cooked lamb loins. Meat Science, 93(3), pp. 572–578.
[17] Tornberg, E., **2005**, Effects of heat on meat proteins. Meat Science, 70(3), pp. 493–508.
[18] Głuchowski, A., Czarniecka-Skubina, E., Buła, M., **2020**, Sous-vide poultry: nutrition protection versus energy consumption. Sustainability, 12(18), pp. 7606.
[19] ISO 22000:2018. Food safety management systems—Requirements for any organization in the food chain.

ORGANIC CARBON FRACTIONS AS INDICATORS OF SOIL ORGANIC MATTER STABILITY UNDER DIFFERENT LAND USES

Mirna Štrbac[1], Maja Manojlović[1], Vladimir Ćirić[1], Ranko Čabilovski[1], Klara Petković[1], Dragan Kovačević[1], Mirjana Vijuk[1]

[1]Department of Field and Vegetable Crops, Faculty of Agriculture, University of Novi Sad, Trg Dositeja Obradovića 8, 21000 Novi Sad, Serbia
e-mail: mirna.strbac@polj.uns.ac.rs

Abstract

Soil organic matter is a key component of soil quality, while its content and stability are strongly influenced by land use and agricultural management practices. Total soil organic carbon (SOC) provides important information on soil organic matter status; however, SOC fractions differing in their susceptibility to oxidation may provide additional insight into management-induced changes. The aim of this study was to evaluate the distribution of SOC fractions under different agricultural management practices and land uses, as well as to assess their potential as indicators of soil quality. Three soil types were investigated: Chernozem, Gleysol and Planosol, under organic and conventional farming, with pasture used as a reference land-use system. In Chernozem, two durations of organic farming (5–10 and >10 years) were additionally considered. Soil organic matter resistance to decomposition was assessed by determining four SOC fractions (F1–F4) with different degrees of oxidizability using the modified Walkley–Black method according to Chan et al. (2001). The response of individual SOC fractions to management differed among soil types. In Chernozem, F1, representing the most labile fraction, did not differ significantly among the investigated systems, whereas F2, a transitional fraction between rapidly mineralizable and more stable organic matter, showed greater sensitivity to management, with a higher proportion under long-term organic farming than under organic farming for 5–10 years. No significant differences were observed for F3, while F4, representing the most stable fraction, showed the most pronounced differences among land-use systems, with the highest proportion recorded under pasture compared with cultivated soils. In Gleysol, F1–F3 showed relatively limited sensitivity to management, whereas the most pronounced differences were observed for the F4 fraction, with the highest proportion under pasture. In contrast, Planosol showed a different response pattern, with the F1 fraction being more sensitive to management, showing differences between organic and conventional farming, while no significant differences among the investigated systems were observed for F2–F4. The results indicate that the sensitivity of SOC fractions to land management is soil-type dependent, with labile and stable fractions showing different response patterns among the investigated soils. These findings highlight the importance of considering soil type when using SOC fractions to assess changes in soil organic matter stability under different land uses. Assessment of SOC fractions with different degrees of oxidizability may therefore complement total SOC determination and provide additional information on soil quality.

Keywords: soil quality, organic farming, agricultural management, pasture, soil type

THE INFLUENCE OF PEDOGENETIC AND CLIMATIC FACTORS ON THE PHYSICAL AND CHEMICAL PROPERTIES OF SOILS IN THE SOCODOR AREA OF ARAD COUNTY

Marius Stroia[1], Marcel Ciprian Stroia[2], Casiana Mihuț[1], Anișoara Duma-Copcea[1], Adalbert Okros[1]

[1]Department of Soil Sciences, Faculty of Agriculture, "King Mihai I" University of Life Sciences in Timișoara, Calea Aradului no. 119, 300645 Timișoara, Timiș country, Romania
[2] Department of biology and plant protection, Faculty of Agriculture, "King Mihai I" University of Life Sciences in Timișoara, Calea Aradului no. 119, 300645 Timișoara, Timiș country, Romania
E-mail: casianamihut@usvt.ro

Abstract
This study aims to characterize the physical and chemical properties of representative soils in the Socodor area, Arad county, western Romania, and to evaluate the influence of pedogenetic factors on soil formation. The investigated area, part of the Western Plain, is characterized by loess and clay deposits, low altitudes (90–120 m), and a temperate-continental climate with moderate precipitation (580–600 mm/year). Three soil types were analyzed: eutric fluvisol, vertic chernozems, and gleyic solonchaks. Laboratory analyses (pH, humus content, cation exchange capacity, base saturation, and carbonate content) revealed significant differences among soils. The study confirms that climate, parent material, topography, groundwater, vegetation, biological activity, and anthropic interventions collectively shape soil properties. The results underline the need for site-specific management practices, including pH correction, organic and mineral fertilization, controlled drainage, and irrigation, to ensure sustainable utilization of the pedological resources in Socodor.

Introduction

Soil is an essential component of terrestrial ecosystems, playing a crucial role in supporting agriculture, regulating the water and nutrient cycles, and maintaining ecological balance [1]. In the context of agricultural intensification and climate change, assessing soil properties and the factors influencing them has become imperative for the sustainable management of agricultural lands [2,3]. The main pedogenetic factors-climate, parent rock, relief, vegetation, organisms, water, and human activity-interact in a complex manner, leading to the formation of soils with distinct characteristics [4,5,6].

At the European level, studies in the Pannonian Plain have highlighted the diversity of soils and their vulnerability to processes such as gleying, erosion, and salinization [7,8]. In Romania, pedological research in the Western Plain has shown that loess and clay soils exhibit high fertility, yet they are sensitive to compaction, excess moisture, and loss of organic matter [9,10]. Several studies have emphasized that agricultural management profoundly affects soil structure and chemical properties, thereby modifying pedogenetic processes over time [11,12].

The Socodor area, Arad County, located in western Romania, is characterized by predominantly flat relief, low altitudes (90–120 m), and a loess-clay substrate. The temperate-continental climate, with annual precipitation of 580–600 mm and mean temperatures of 10.8°C, favors humification processes but also promotes vertisolization during dry years [13,14,15]. The dominant soils include eutric fluvisol, vertic chernozems, and gleyic solonchaks, each differently influenced by the groundwater level, parent material, and human activity [16,17]. The aim of this study is the comparative characterization of the three soil types in Socodor through morphological description and chemical analysis, and the interpretation of

the results in relation to pedogenetic factors. The main objectives include identifying the morphological and physicochemical properties of the soils, analyzing their differences, and evaluating the implications for soil fertility and the sustainable management of agricultural lands.

Experimental

The study was conducted within the administrative territory of the commune of Socodor, located in western Romania, Arad County, approximately 25 km west of the city of Arad, on the right bank of the Mureș River (46°08′N, 21°04′E). Geographically, the area belongs to the Mureș Plain, part of the Western Plain, characterized by low altitudes (90–120 m), flat or gently fragmented relief, and loess or clay deposits that constitute the parent material of the soils. The climate is moderately temperate-continental, with oceanic and subMediterranean influences. The multi-annual mean temperature is 10.8°C, and the average annual precipitation is 580–600 mm, unevenly distributed, with the highest amounts recorded in spring and at the end of summer. The natural vegetation belongs to the foreststeppe zone; however, most of the area is currently used for agriculture, predominantly for field crops such as wheat, maize, and sunflower. For soil characterization, three representative profiles were excavated and described: eutric fluvisol, vertic chernozems, and gleyic solonchaks. Morphological description was carried out following standard methodologies [1,3,4], analyzing horizon depth and thickness, color (Munsell), texture, structure, consistency, porosity, presence of concretions and coatings, signs of gleying, and carbonatation. The obtained data were compiled and compared among the analyzed soils to identify pedogenetic differences and their implications for fertility and agricultural use.

Results and Discussion

1. Distribution and Characteristics of Soils

The administrative area of the Socodor commune covers 14,717 ha, of which 10,197 ha are agricultural land. Among the agricultural lands, the predominant soils are: chernozems (3,417 ha), solonchaks (2,661 ha), and alluviosols (540 ha).

In this study, three of the identified soil types are described: eutric fluvisol, vertic chernozems, and gleyic solonchaks. The three studied soils develop on loess and clay deposits and exhibit significant differences in morphological and chemical properties.

2. Analysis of Pedogenetic Factors

Moderate precipitation and a mean temperature of 10.8°C favor the humification of organic matter, while drought induces large cracks in chernozems and vertisolization.

Slightly higher interfluves allow better drainage and promote the development of chernozems, whereas micro-depressions favor water stagnation and gleying.

Loess and heavy clays influence texture, water retention, and cation exchange capacity.

Humus content is higher in chernozems due to the original forest-steppe vegetation and intense biological activity. The analyzed soils are mature, having formed during the Holocene; however, pedogenetic processes are still active. Vertisolization, gleying, and carbonatation demonstrate continuous pedogenetic activity influenced by climate changes and human activity.

Mechanical soil work and intensive agriculture modify horizon structure, reduce porosity, and promote compaction. Intensive plowing and mechanical interventions have altered the structure of the Ap horizons, decreasing porosity and increasing compaction.

The analyzed soils are mature, having formed during the Holocene; however, pedogenetic processes are still active. Vertisolization, gleying, and carbonatation demonstrate continuous pedogenetic activity influenced by climate changes and human activity.

Mechanical soil work and intensive agriculture modify horizon structure, reduce porosity, and promote compaction. Intensive plowing and mechanical interventions have altered the structure of the Ap horizons, decreasing porosity and increasing compaction.

Table 1. The physical and chemical proprirty of Eutric Fluvisol

Horizons	**Ao**	**C**
Depths (cm)	0-27	27-75
Coarse sand (2.0-0.2 mm)%	31,8	25,8
Fine sand (0.02-0.0.02 mm)%	36,0	39,2
Dust (0.0-0.02 mm)%	11,9	16,3
Clay 2 (under 0.002 mm)%	20,3	18,7
TEXTREA	**LN**	**LN**
pH (în H_2 O)	4,65	5,05
Humus (%)	3,28	1,19
P mobil (ppm)	3,9	2,8
K mobil (ppm)	44	26
Hydrogen changeable (SH me.e./100 g soil)	9,03	2,57
Spare bases (SB m.e./100 g soil)	12,29	8,55
Cationic exchange capacity (T me/100 g soil)	21,32	11,12
Degree of saturation at bases (V%)	57,64	76,88

The natural fertility of these soils is relatively good. The assortment of crops that can be grown includes almost the entire range of plants specific to the conditions in our country: corn, sugar beet, sunflower, potato, rice, wheat, fodder plants, vegetables, vines, etc.

Table 2. The physical and chemical proprirty of Vertic Chernozems

Horizons	**Ap**	**Am**	**ABy**	**Bvy**	**Ccay**	**Ccaygsc-ac**	**Ccayg**	**CcayGo**
Depths (cm)	0-16	16-32	32-45	45-63	63-85	85-125	125-150	150-230
Coarse sand (2.0-0.2 mm)%	0,5	0,4	0,2	0,3	0,3	0,3	0,7	0,4
Fine sand (0.02-0.0.02 mm)%	34,1	32,6	30,8	32,8	31,5	36,3	32,1	34,9
Dust (0.0-0.02 mm)%	26,4	26,8	28,1	26,3	28,5	26,3	23,8	22,4
Clay 2 (under 0.002 mm)%	39,0	40,2	40,9	40,6	39,7	37,1	43,4	42,3
Physical clay (below 0.01 mm) %	49,3	51,8	52,8	52,5	51,1	47,4	52,9	52,8
TEXTREA	TT	TT	TT	TT	TT	TT	TT	TT
Specific Density (D g/cm^3)	2,69	2,73	2,68	2,75				
Apparent Density (DA g/cm^3)	1,50	1,39	1,35	1,34				
Total porosity (PT %)	44,23	49,08	49,62	51,27				
Aircraft porosity (PA %)	11,09	15,26	15,71	17,43				
Degree of settlement (GT %)	13,86	4,78	3,94	0,66				
pH (în H_2 O)	6,16	6,46	6,47	7,18	8,10	8,42	8,42	8,44
Carbonates ($CaCO_3$%)					13,1	16,7	15,7	14,7
Humus (%)	2,68	2,31	2,18	1,73				
Spare bases (SB m.e./100 g soil)	25,19	26,66	23,90					
Hydrogen changeable (SH	15,1	14,3	15,8					
Cationic exchange capacity (T	30,0	31,43	28,07			17,40		
Degree of saturation at bases	83,96	84,82	85,14					

Vertic Chernozems have good fertility and are grown with grains, technical plants, vegetables, vineyards and trees. The application of irrigation complementing water scarcity during dry periods, administering organic fertilizers and minerals contributes to obtaining large productions.

Table 3. The physical and chemical proprirty of Gleyic solonchaks

Horizons	At	Aonasck	Aonasck	Btnasck	Btnasck	BtnascG	CnascGo
Depths (cm)	0-2	2-12	12-35	35-80	80-100	100-135	135-160
Coarse sand (2.0-0.2 mm)%	0,1	0,1	0,1	0,1	0,2	0,1	0,1
Fine sand (0.02-0.0.02 mm)%	48,5	44,8	43,2	39,2	35,2	38,4	43,9
Dust (0.0-0.02 mm)%	27,2	28,9	30,1	27,8	29,2	28,5	26,4
Clay 2 (under 0.002 mm)%	24,2	26,2	26,6	32,9	35,0	33,0	29,6
Physical clay (below 0.01 mm) %	34,5	38,2	39,0	45,3	48,4	44,9	41,2
TEXTREA	**LL**	**LL**	**LL**	**TT**	**TT**	**TT**	**LL**
Specific Density (D g/ cm^3)	2,40	2,70	2,70	2,70	2,70		
Apparent Density (DA g/cm^3)	1,0	1,55	1,55	1,58	1,57		
Total porosity (PT %)	58,83	42,59	42,59	41,48	41,85		
pH (în H_2 O)	9,76	9,85	10,02	10,16	9,87	9,70	9,60
Carbonates ($CaCO_3$%)	6,71	7,04	8,45	19,3	24,3	22,4	19,2
Humus (%)	2,19	2,11	2,07	0,42			
Na changeable (me/ 100 g soil)	7,55	10,55	12,87	18,12	9,88	5,42	2,70
Na changeable (%from T)	28,45	52,75	67,21	75,72	46,34	25,42	16,77
Soluble salts (1:5)(mg/100 g soil)	165,17	177,87	181,69	241,40	155,0	133,11	118,16
Na^+ (m.e./100 g soil)	2,46	2,75	2,79	4,24	2,31	1,98	1,65

Poor physical and chemical properties (high degree of compaction, low aeration porosity, extremely low waterproofing, strong alkaline reaction) and the presence of low-depth soluble salts that have caused salinization phenomena, sharply limit the fertility of the soil and assortment of plants that can be grown on this soil.

Conclusions

The soils of the Socodor area show marked differences in physical and chemical properties as a result of the combined influence of parent material, relief, climate, groundwater regime, and anthropogenic activity. The three investigated soil types—Eutric Fluvisol, Vertic Chernozem, and Gleyic Solonchak—therefore have different fertility levels and agricultural limitations.

Vertic Chernozem has the highest agricultural potential among the investigated soils, with relatively favorable chemical properties and good natural fertility. In contrast, the Eutric Fluvisol is characterized by an acidic reaction and lower nutrient availability, requiring management adapted to its specific properties.

Gleyic Solonchak presents the most severe limitations for agricultural use, due to its strongly alkaline reaction, high exchangeable sodium and soluble salt contents, compaction, and poor aeration. These properties considerably restrict soil fertility and the range of suitable crops.

Sustainable agricultural use in the Socodor area requires soil-specific management rather than uniform practices. Maintaining soil structure, limiting compaction, applying fertilization and amendments according to soil analyses, and adequately managing irrigation and drainage are essential for conserving fertility and reducing soil degradation.

Bibliography

[1] Brady, N.C.; Weil, R.R. The Nature and Properties of Soils, 15th ed.; Pearson: New York, NY, USA, 2017.

[2] Lal, R. Soil Conservation and Management for Sustainable Agriculture. Springer: Berlin/Heidelberg, Germany, 2020.

[3] FAO. World Reference Base for Soil Resources 2015: International Soil Classification System for Naming Soils and Creating Legends for Soil Maps; FAO: Rome, Italy, 2015.

[4] Buol, S.W.; Southard, R.J.; Graham, R.C.; McDaniel, P.A. Soil Genesis and Classification, 7th ed.; Wiley: Hoboken, NJ, USA, 2011.

[5] Jenny, H. Factors of Soil Formation: A System of Quantitative Pedology; Dover Publications: New York, NY, USA, 1994.
[6] Mihuț, C., Niță L., 2018, Atmospheric Factors used to characterize soil resources https://www.rjas.ro/issue_detail/44, Timișoara, pag. 114-120.
[7] Jones, R.J.A.; Montanarella, L.; Jones, R.; Hiederer, R.; Panagos, P. Soil Vulnerability and Erosion in Europe. Geoderma 2012, 189–190, 40–53.
[8] Tóth, G.; Hermann, T.; Da Silva, M.R.; Montanarella, L. Soil Resources of Europe: Status, Challenges and Policy Support. European Commission, 2018.
[9] Florea, N.; Munteanu, N. Pedologie: Fundamentele Solurilor și Gestionarea Resurselor Pedologice; Risoprint: Cluj-Napoca, Romania, 2012.
[10] Pătruț, V. Caracterizarea solurilor loessoase din Câmpia de Vest a României. Lucrări Științifice USAMV Cluj-Napoca 2014, 57, 45–56.
[11] Tóth, Z.; Szabó, J.; Hermann, T. Influence of Land Use on Soil Properties in Hungary. Catena 2010, 82, 63–71.
[12] Florea, N.; Stoica, M.; Munteanu, N. Pedogenetic Processes and Soil Fertility in Western Romania. J. Soil Sci. Agric. Eng. 2015, 6, 12–23.
[13] Okros, A., Pirsan, P., Borcean, A., Mihut, C., Nita, S., Mircov, V.D., Shahzod, H., Abdumanon, G., 2019, Intensive Agriculture Management In The North-West Area Of The Banat Region Under The Influence Of Different Bio-Pedo-Climatic Conditions. Proceedings of the InternationaL Conference on Life Sciences. Proceedings Edition July, 2020, pp. 176-178.
[14] Ciobanu, D.; Panin, A.; Popescu, C. Climate Influence on Soil Formation in the Romanian Plain. Romanian Agric. Res. 2013, 30, 23–32.
[15] Szabó, R.; Tóth, G. Soil Classification and Mapping in Câmpia Panonică. Geoderma Regional 2017, 10, 90–101.
[16] Munteanu, N.; Florea, N. Morphological and Chemical Characterization of Loess-Derived Soils. Soil Sci. Annu. 2016, 67, 7–18.
[17] Pătruț, V.; Stoica, M. Pedological Zonation and Fertility Assessment of Western Romanian Plains. AgroLife Sci. J. 2018, 7, 45–57.

STABILITY AND ECOTOXIC EFFECTS OF LEAD-FREE PEROVSKITES ON ISOPODS

Lilla Szalma[1], Adrienn Dorisz-Dávid[2], Kincső Kozma[2], Tamás Bukor[1], Máté Fekete[1], Tamás Gyulavári[1], Zsolt Pap[1,2,3]

[1]Department of Applied and Environmental Chemistry, University of Szeged, H-6720 Szeged, Rerrich Béla tér 1, Hungary
[2]Faculty of Biology and Geology, Hungarian Department of Biology and Ecology, Babeş-Bolyai University, RO-400015 Cluj-Napoca, Republicii str. 42, Romania
[1]STAR-UBB Institute, Babeş-Bolyai University, RO-400015 Cluj-Napoca, Mihail Kogălniceanu str. 1, Romania
e-mail: szalma.lilla.klara@szte.hu

Abstract
Our aim was to investigate the environmental impact of Cs_2SnI_6 and Cs_3MnI_5 synthesized as lead-free alternative semiconductors to $CsPbI_3$. Furthermore, our investigations were extended to include the characterization of perovskite materials to identify correlations between structural changes, stability, and ecotoxic effects.

Introduction
$CsPbX_3$ semiconductor perovskites are considered promising materials for various optoelectronic applications. However, their lead-related toxicity raises several concerns, including oxidative stress, carcinogenicity, and developmental toxicity. One possibility to reduce their toxicity is to replace lead with tin or manganese.

Experimental
Lead-free perovskites were synthesized using a solvothermal method at different temperatures (120 °C, 150 °C, and 180 °C). The structural, morphological, and optical properties of the samples were characterized using X-ray diffraction (XRD), scanning electron microscopy (SEM), and diffuse reflectance spectroscopy (DRS).
In the toxicological experiment, the effect of the selected semiconductors was investigated on the population isopods (*Porcellio laevis*), while considering the stability issues in the environment. The protocol was to follow the life cycle of 15 individuals over a one-month period. The experimental soil contained 0, 0.1 and 0.5 wt.% of perovskites and four replicates were prepared for each experiment in order to assure statistical validity.

Results and discussion
Stability testing revealed that all perovskites remained stable in air but degraded rapidly upon contact with water, losing their crystalline structure. However, recrystallization occurred after drying, indicating partial reversibility. The relative stability decreased in the sequence: $CsPbI_3$ > Cs_2SnI_6 > Cs_3MnI_5.
A significant decline in population size was observed as the perovskite concentration increased. Lower perovskite stability led to higher mortality rates within a short period of time. This was attributed not only to the presence of Pb, Sn, and Mn, but also to the highly acidic pH resulting from HI release under the influence of moisture, which became increasingly pronounced as stability decreased.

Conclusion

The synthesized lead-free perovskite alternatives (Cs_2SnI_6 and Cs_3MnI_5) show lower overall environmental stability compared to $CsPbI_3$, with water contact leading to rapid decomposition. Furthermore, ecotoxicity testing reveals a direct link between lower material stability and increased mortality in *Porcellio laevis* populations at higher concentrations.

Acknowledgements

The authors are grateful for the financial support of the 2021-1.2.6-TÉT-IPARI-MA-2022-00009 project. Zsolt Pap acknowledges the funding provided by the Bolyai János Research Scholarship of the Hungarian Academy of Sciences. Kincső Kozma acknowledges the funding provided by the Márton Áron Talent Development Scholarship of the Balassi Bálint Scholarship Program. Adrienn-Dorisz Dávid is grateful for the financial support provided by the Collegium Talentum program. Lilla Szalma and Máté Fekete are grateful for the financial support provided by the Pannónia Scholarship Programme.

MACHINE LEARNING-BASED DECOMPOSITION OF OVERLAPPING GAS ABSORPTION SPECTRA

László Ábel Szűcs[1], Csilla Gombi[1], Zoltán Bozóki[1,2], Anna Szabó[1,2]

[1]Department of Optics and Quantum Electronics, University of Szeged, H-6720 Szeged, Dóm tér 9, Hungary
[2]HUN-REN-SZTE Research Group for Photoacoustic Monitoring of Environmental Processes, University of Szeged, 6720 Szeged, Hungary
e-mail:szucs.laszlo.abel@szte.hu

Abstract

The decomposition of overlapping gas absorption spectra is a challenging inverse problem, particularly when multiple gases exhibit similar spectral features. Machine learning approaches provide a promising framework for the simultaneous estimation of gas concentrations from overlapping absorption spectra [1]. In this study, synthetic spectra of eight gas species were generated using reference spectra from the HITRAN database [2]. The number of active gases was varied between 2 and 8, while the concentrations of inactive gases were set to zero, requiring the models to identify both present and absent gas components. The effects of spectral coverage and measurement noise on prediction accuracy were also systematically investigated. Partial Least Squares (PLS) regression and a feed-forward neural network (NN) were compared. For the NN, two optimization approaches were evaluated: conventional Mean Squared Error (MSE) loss based on concentration errors and a custom spectral residual loss based on the reconstruction of the absorption spectrum from the predicted concentrations. Model performance was assessed using the Root Mean Squared Error (RMSE) of the predicted concentrations.

The results show that spectral coverage has the strongest influence on prediction accuracy, while increasing the number of active gases also reduces performance. The NN trained with MSE substantially outperformed PLS across the investigated conditions. Within the relative error range of ±5%, 60.64% of the NN predictions were within this interval, compared with 11.81% for PLS. These results demonstrate the potential of NN for the decomposition of strongly overlapping gas absorption spectra and highlight the importance of sufficient spectral coverage for reliable multi-gas concentration estimation.

References

[1] M.A.Z. Chowdhury, M.A. Oehlschlaeger, Sensors 24 (2024) 1873.
[2] I.E. Gordon, L.S. Rothman, R.J. Hargreaves, et al., J. Quant. Spectrosc. Radiat. Transf. 277 (2022) 107949

ANALYSIS OF GERMINATED AND NON-GERMINATED SORGHUM EXTRACTS FERMENTED WITH MARE'S MILK *LACTOBACILLUS* ISOLATES

Nermin Tahboub[1], Tamás Kovács[2], Panna Herczeg[1], Levente Szilágyi[1], Judit Krisch[2], Csaba Vágvölgyi[1], Tamás Papp[1,3], Miklós Takó[1]

[1]Department of Biotechnology and Microbiology, Faculty of Science and Informatics, University of Szeged, Közép fasor 52, H-6726 Szeged, Hungary
[2]Department of Food Engineering, Faculty of Engineering, University of Szeged, Mars tér 7, H-6724 Szeged, Hungary
[3]HUN-REN-SZTE Pathomechanisms of Fungal Infections Research Group, University of Szeged, Közép fasor 52, H-6726 Szeged, Hungary
e-mail: nermin.tahboub@gmail.com

Sorghum grain is a gluten-free cereal with a rich phenolic profile, including flavonoids and tannins. Fermentation with lactic acid bacteria (LAB) is a traditional method to adjust the nutritional and functional properties of grains. Our aim was the characterization of extracts obtained after LAB fermentation of sorghum samples. In this study, *lactobacilli obtained from mare's milk (Airag) were used to ferment* ground sorghum under aerobic conditions at 37 °C. Germinated and non-germinated sorghum were inoculated with *L. paracasei, L. paracasei subsp. tolerans, and L. helveticus* separately. Bacterial viability and pH were monitored, and the total phenolic and flavonoid content, antioxidant activity, hydrolase activities, reducing sugars and proteins were analyzed from the cell-free supernatant obtained after 24-h cultivation. *L. paracasei subsp. tolerans* recorded the highest growth in the non-germinated sorghum samples. No significant increase in phenolic or flavonoid content was observed post-fermentation. Fermented non-germinated sorghum showed elevated cellulase and lipase activities over germinated samples. Germination of sorghum led to a marked reduction in all tested enzymes, although it showed a significant increase in reducing sugar content. These findings highlight the complex biochemical interactions during LAB fermentation. The probiotic-enriched sorghum ferments can be used as a bioactive additive in functional food developments. This research was supported by the projects 2024-1.1.1-KKV_FÓKUSZ-2024-00050 and 2025-1.2.4-TÉT-2025-00033.

PHYTOTOXIC EFFECT OF IVERMECTIN IN DICOTYLEDON AND MONOCOTYYLEDON INDICATOR SPECIES

Eszter Takács, Miléna Tünde Tóth, Szandra Klátyik, Borbála Gémes, András Székács

Agro-Environmental Research Center, Institute of Environmental Sciences, Hungarian University of Agriculture and Life Sciences, Tessedik S. st. 4, Gödöllő, H-2100, Hungary
e-mail: takacs.eszter84@uni-mate.hu

Abstract

Ivermectin is a widely used antiparasitic drug in veterinary and human medicine that has raised substantial ecological concerns due to its persistence and bioactivity [1]. Following administration to livestock, about 90% of ivermectin and its metabolites are excreted via feces and about 1% eliminated through urine [2]. This continuous excretion creates a heavy environmental load, making ivermectin a ubiquitous contaminant in livestock-rearing terrestrial ecosystems [1]. Because ivermectin possesses high lipophilicity and strong binding affinity for organic matter, it tends to persist in soil and dung for extended periods rather than rapidly degrading [1,3]. While its lethal effects on non-target coprophagous organisms like dung beetles and flies are well established [2], recent research emphasizes its overlooked impacts on flora. Plants growing in contaminated soils absorb ivermectin through their root systems, distributing the compound into stems, leaves, and reproductive structures. The resulting phytotoxic effects can disrupt fundamental physiological processes, including seed germination and seedling emergence. At the cellular level, exposure to ivermectin alters plant antioxidant enzyme activities, indicating severe oxidative stress. Higher concentrations can shorten root length, suppress biomass production, and impair photosynthetic pigment composition in macrophyte species [4].

In this study, the inhibitory effect of ivermectin was investigated on the dicotyledon white mustard (*Sinapis alba*) and on the monocotyledon wheat (*Triticum aestivum*) indicator species. Seedling emergence and early growth experiments were performed based on the OECD 208 guideline. Sixteen seeds per replicates of each species were exposed to ivermectin at 23°C under dark conditions and evaluated for effects on the 3rd and 7th day for mustard and wheat, respectively. Endpoints measured were the percentage of the germinated seedlings, as well as the shoot and root lengths. No significant differences were detected between the untreated control and solvent control group regarding the parameters determined. Ivermectin had a slight, but significant effect on emergence and seedling growth in both species investigated.

Acknowledgements

This research was supported by the Research Excellence Programme and the Flagship Research Groups Program of the Hungarian University of Agriculture and Life Sciences.

References

[1] D. Efrain Merma Chacca, I. Maldonado, F. Z. Vilca, Front. Environ. Sci. 10 (2022).
[2] S. Belete, H. Adunga, T. Yirsa, PLoS One. 20(4) (2025) e0320867.
[3] B. Förster, A. Boxall, A. Coors, J. Jensen, M. Liebig, L. Pope, T. Moser, J. Römbke, Ecotoxicology. 20(1) (2010), 234–245.
[4] M. Navrátilová, L. Raisová Stuchlíková, K. Moťková, B. Szotáková, L. Skálová, L. Langhansová, R. Podlipná, Molecules, 25(16) (2020), 3655.

PHENOLIC CONTENT AND ANTIOXIDANT ACTIVITY OF CAPIA PEPPER RESIDUES BEFORE AND AFTER FERMENTATION WITH THE PROBIOTIC YEAST *SACCHAROMYCES BOULARDII*

Miklós Takó[1], Nermin Tahboub[1], Erika Beáta Kerekes[1], Csilla Veres[1], Marija Petrović[2], Marina Jovanović[2], Tamás Kovács[3], Csaba Vágvölgyi[1], Tamás Papp[1,4]

[1]Department of Biotechnology and Microbiology, Faculty of Science and Informatics, University of Szeged, Közép fasor 52, H-6726 Szeged, Hungary
[2]Institute of General and Physical Chemistry, Studentski trg 12, 11070 Belgrade, Serbia
[3]Institute of Food Engineering, Faculty of Engineering, University of Szeged, Mars tér 7, H-6724 Szeged, Hungary
[4]HUN-REN-SZTE Pathomechanisms of Fungal Infections Research Group, University of Szeged, Közép fasor 52, H-6726 Szeged, Hungary
e-mail: tako78@bio.u-szeged.hu

Pepper processing residues are rich in various bioactive compounds, including phenolic glycosides and phenolic esters. These compounds may serve as sources of phenolic substances with antioxidant activity, and their availability can potentially be enhanced by microbiological and enzymatic treatments. Valorization of these residues may therefore provide an opportunity to develop phenol-enriched products for use as natural ingredients in food and feed. Fermentation with probiotic microorganisms is a promising technique for obtaining bioactive extracts enriched with probiotic cells from plant residues; however, this approach has been less extensively studied using pepper-derived substrates. In this study, residues of capia-type red pepper (*Capsicum annuum* L.) were subjected to fermentation with the probiotic yeast *Saccharomyces boulardii*. After 24 and 72 h of cultivation, cell counts, total phenolic content (TPC), total flavonoid content (TFC), and antioxidant activity were determined in the crude fermentation extracts. The results showed a significant 1.15-fold increase in cell count after 24 h of incubation. While the TPC remained unchanged during fermentation, the TFC increased after both 24 and 72 h compared with the non-inoculated control. Furthermore, ferric reducing antioxidant power and cupric ion reducing antioxidant capacity values increased after 72 h of fermentation, indicating enhanced antioxidant activity. Overall, fermentation of capia pepper residues with *S. boulardii* resulted in a probiotic cell-enriched extract with increased flavonoid content and antioxidant activity, highlighting its potential for further investigation as a bioactive ingredient for food and feed applications. This research was supported by the projects PD 142122, 2024-1.1.1-KKV_FÓKUSZ-2024-00050 and 2025-1.2.4-TÉT-2025-00033.

EFFECT OF PORPHYRIN ADDITIVES ON SOLID POLYMER ELECTROLYTE MEMBRANES FOR LITHIUM-ION BATTERIES

Milica Țară-Lungă-Mihali*, Anca Lascu, Ionela Frîngu, Nicoleta Pleșu, Aurelia Vișa

[1]*„Coriolan Dragulescu" Institute of Chemistry, 24 Mihai Viteazu Ave, 300223 Timisoara, Romania*
**milicamihali22@gmail.com*

Organophosphorus-based polymers have attracted increasing attention as solid polymer electrolyte (SPE) materials because they offer a combination of ionic conductivity, mechanical stability, chemical and intrinsic flame-retardant properties. The incorporation of fillers into SPE is aimed at enhancing ionic conductivity, particularly at low temperatures. The presence of inorganic or organic additives within the polymer matrix can also modify the structural and thermal properties of the electrolyte by suppressing polymer recrystallization and can reduce the glass transition temperature. These effects increase the mobility of the polymer chains and facilitate ion transport, contributing to improved ionic conductivity [1,2].

We prepared solid polymer electrolyte (SPE) membranes based on polyphosphonate and PEG (molar mass 2000), containing 10 wt% lithium perchlorate ($LiClO_4$) [3]. The aim of this study was to improve the ionic conductivity of the SPE by incorporating different amounts of 5,10,15,20-tetrakis-(4-allyloxyphenyl)-porphyrin (TAPP) [4] into the membrane formulation at room temperature. The evolution of the membrane conductivity as a function of porphyrin content and temperature was investigated by impedance spectroscopy (EIS). The conductivity of the membranes increases with increasing porphyrin content, which can be attributed to the higher number of charge carriers resulting from improved salt dispersion within the membrane. With increasing temperature the ionic conductivity of all membranes increases, which can be attributed to the enhanced mobility of the charge carriers and the polymer chains. As the temperature rises, increased segmental motion of the polymer chains facilitates ion transport through the polymer matrix. Consequently, this enhanced mobility promotes the formation of continuous pathways for charge transport and increases the number of accessible coordination sites for the charge carriers, resulting in higher ionic conductivity.

References

1. Yang X., Liu J., Pei N., Chen Z., Li R., Fu L., Zhang P., Zhao J., Nano-Micro Lett., 2023, 15, 74.
2. Fu J., Li Z., Zhou X., Guo X., Mater. Adv., 2022, 3, 3809–3819.
3. Iliescu S., Zubizarreta L., Plesu N.; Macarie L., Popa A., Ilia G.,Chem. Cent. J., 2012, 6, 132.
4. Dudás Z., Enache C., Fagadar-Cosma G., Armeanu I., Fagadar-Cosma E., Mater. Res. Bull., 2010,45,1150–1156.

TEM ANALYSIS OF AN ASYMMETRICALLY SUBSTITUTED Zn(II)-METALATED PORPHYRIN APPLIED ON TEM GRIDS FROM DIFFERENT ORGANIC SOLVENTS

Bogdan-Ovidiu Taranu, Alexandra Ioana Bucur, Raul Alin Bucur, Florina Stefania Rus, Radu Banica, Cristina Mosoarca, Andrei Racu, George Dima

National Institute of Research and Development for Electrochemistry and Condensed Matter, Dr. Aurel Paunescu Podeanu Street, No. 144, 300569, Timisoara, Romania
e-mail: b.taranu84@gmail.com

Abstract

Zn(II) 5-(4-carboxyphenyl)-10,15,20-tris(4-phenoxyphenyl)-porphyrin (ZnCOOHPP) is an asymmetrically substituted metalloporphyrin in which the porphyrin macrocycle chelates the Zn^{2+} cation [1]. This study focuses on the self-assembling behavior of ZnCOOHPP molecules, as revealed by transmission electron microscopy (TEM) analysis. Zn(II)-porphyrin solutions were prepared using organic solvents of different polarities (dichloromethane, tetrahydrofuran, benzonitrile, N,N-dimethylformamide, and dimethylsulfoxide) [2,3]. Subsequently, a small volume (a few microliters) was taken from each solution and applied onto TEM grids made of Cu mesh covered with a thin, amorphous, and uninterrupted carbon film. The specimens were analyzed after solvent evaporation using a transmission electron microscope, namely a dedicated Titan G2 80–200 microscope from FEI Company (Hillsboro, OR, USA), as well as software such as Digital Micrograph v. 2.12.1579.0 and TEM Imaging & Analysis v. 4.7. The images were recorded at 200 KV acceleration voltage using two modes of operation: Bright Field TEM and STEM. The images of the sample obtained by applying the metalloporphyrin from dichloromethane reveal a discontinuous film resulting from the self-assembly of ZnCOOHPP molecules. When Zn(II)-porphyrin molecules were applied from tetrahydrofuran, they again organized into a discontinuous layer. However, this layer was dotted with circular islands. The metalloporphyrin's tendency to form interrupted layers was also observed when the solvents used to obtain the studied samples were benzonitrile and N,N-dimethylformamide, respectively. However, when dimethylsulfoxide - the most polar solvent in the investigated series - was used, the Zn(II)-porphyrin molecules self-assembled into more complex aggregates, resembling filaments and islands. At lower magnification, the submicrometric islands appear circular, while irregular shapes are observed at higher magnification. The two types of formations can interact to form beads-on-string-type higher-order architectures. The TEM analysis of the asymmetrically substituted ZnCOOHPP metalloporphyrin, drop-cast onto TEM grids from solutions prepared in different organic solvents, advances current knowledge of the spontaneous association of metalloporphyrin molecules.

References

[1] A.-M. Belean, Cromofori de tip porfirine și complecșii lor cu metale tranziționale. Elaborarea de noi senzori cu aplicabilitate în medicină, chimie și chimia mediului, Ph.D. thesis, Institute of Chemistry Timisoara of the Romanian Academy, Timisoara, Romania, 2017, pp. 58.
[2] L.R. Snyder, J.J. Kirkland, J.L. Glajch, Practical HPLC Method Development, 2nd ed., JohnWiley & Sons, Inc., Hoboken, USA, 1997, pp. 721.
[3] Z. Szabadai, L.Sbarcea, L. Udrescu, Analiza fizica si chimica a medicamentului, Victor Babes Publishing House, Timisoara, Romania, 2016, pp. 243.

NUTRITIONAL CHARACTERISTICS OF *URTICA DIOICA* AND *LAMIUMPURPUREUM*-COMPARATIVE STUDY

Patricia-Cristina Tarkanyi[1], Mihaela Lăcătuș[1], Ersilia Alexa[1,2], Adrian Riviș[1,2], Diana Nicoleta Raba[1,3], Georgeta-Sofia Popescu[2], Ioan Ladislau Caba[4], Aurica Breica Borozan[5], Despina-Maria Bordean[1,2*]

[1]Doctoral School of Plant and Animal Resources Engineering, Food Engineering, University of Life Sciences "King Mihai I" from Timisoara, Calea Aradului 119, Timisoara, Romania;
[2]Faculty of Food Engineering, University of Life Sciences "King Mihai I" from Timisoara, Calea Aradului 119, Timisoara, Romania;
[3]Faculty Of Management and Rural Tourism, University of Life Sciences "King Mihai I" from Timisoara, Calea Aradului 119, Timisoara, Romania;
[4]National Institute of Research-Development for Machines and Installations Designed to Agriculture and Food Industry-INMA, 013813 Bucharest, Romania;
[5]Faculty of Engineering and Applied Technologies, University of Life Sciences "King Mihai I" from Timisoara, 300645 Timisoara, Romania
**Corresponding authors: sofiapintilie1@usvt.ro*

Abstract
Structural characteristics still play a major role in the identification of plants, classification, and ecological interpretation, besides molecular techniques, which have been increasingly incorporated in systematics nowadays. The aim of this study was to compare the nutritional characteristics of *Urtica dioica* L. and *Lamium purpureum* L. The study was based on a review of scientific literature. The literature review showed that both species are valuable sources of nutrients and bioactive compounds, although *Urtica dioica* generally contains higher levels of minerals, vitamin C, proteins, and total phenolic compounds than *Lamium purpureum*. These findings highlight the nutritional potential of both plants and indicate the need for further studies on *L. purpureum* to better understand its nutritional value and possible applications.

Keywords: stinging nettle, dead nettle, comparative analysis, phenolic compounds, wild edible plants

Introduction

Both species are widely distributed in temperate regions and often coexist in similar environments, including grasslands, disturbed soils, field margins, and ruderal habitats. *U. dioica* prefers nutrient-rich, moist soils and often forms dense populations, whereas *L. purpureum* is more associated with disturbed agricultural areas and exhibits rapid colonization through seed production [3, 5].

Urtica dioica L., commonly known as stinging nettle, is a herbaceous perennial species belonging to the family Urticaceae. It is widely distributed across temperate regions of Europe, Asia, North Africa, and North America [3]. The species is characterized by erect stems (up to 1–3 m), opposite serrated leaves, and the presence of specialized stinging trichomes containing irritant compounds such as histamine and acetylcholine [12].

Lamium purpureum L., often called purple deadnettle, is a fast growing, annual herb of the Lamiaceae family. The plant is originally from Eurasia, but it has spread so much that it has almost become a wild plant in various other parts of the world. It is very often found in places that have been recently disturbed, e.g. cultivated land, gardens, roadsides [7].

Besides their morphological significance, both *Urtica dioica* and *Lamium purpureum* are celebrated for their nutritional and phytochemical potentials. *U. dioica* has been recognized as

a mineral-rich plant (iron, calcium, and magnesium) with a good amount of vitamins (A, C, and K) and phenolics possessing antioxidant properties [3]. *L. purpureum* is known for its flavonoids, phenolic acids, and micronutrients, which are the basis of its use as a healthy food and medicinal herb [8].
The aim of this review was to compare the nutritional characteristics of *Urtica dioica* and *Lamium purpureum* based on the available literature and to identify similarities and differences that may contribute to understanding their nutritional potential value as wild edible plants.

Experimental
The present study is based on a review of scientific literature concerning the nutritional characteristics of *Urtica dioica* L. and *Lamium purpureum* L. Publications relevant to the topic were collected from Google Scholar, PubMed, Scopus, and Web of Science and were used for the comparative evaluation of the two species.

Results and discussion
Urtica dioica is a perennial herbaceous species widely distributed in temperate regions and associated with nutrient-rich habitats [13]. *Lamium purpureum* is an annual herbaceous species occurring in temperate ecosystems [7].
Urtica dioica is consumed as a wild vegetable, while *Lamium purpureum* has also been reported among wild plants used for food [9, 10].
Urtica dioica L. has attracted increasing interest as a wild edible plant due to its remarkable nutritional and phytochemical composition [11]. The leaves are an important source of essential minerals, including calcium, iron, magnesium, and potassium, as well as vitamins such as vitamin C, provitamin A (β-carotene), and vitamin K [3, 6]. *Urtica dioica* contains protein, which adds to its nutritional value [12]. The plant is also characterized by a rich profile of phenolic compounds and flavonoids, which are associated with significant antioxidant activity and potential health-promoting effects [3, 6].
Lamium purpureum is much less researched but inspires the appetite by showing several nutritional virtues. Phenolic compounds and flavonoids, as well as quite appreciable amounts of minerals such as calcium and potassium, are found in the aerial parts of the plant [5]. These are the compounds that carry antioxidant and anti-inflammatory properties. Even though its nutrient profile is generally less abundant in comparison to that of *U. dioica*, *L. purpureum* enhances food variety and can be a phytochemical source complementing a traditional diet.
Table 1 presents a comparison of the nutritional composition of *Urtica dioica* and *Lamium purpureum* based on literature data. In general, *U. dioica* contains higher levels of minerals, vitamin C, proteins, and total phenolic content than *L. purpureum* [1, 2]. *Lamium purpureum* also contains valuable amounts of nutrients and phenolic compounds [4, 8].

Table 1. Comparative nutritional composition of *Urtica dioica* and *Lamium purpureum*

Component	***Urtica dioica***	***Lamium purpureum***
Minerals	Ca: 480-1700 mg/100 g DW; Fe: 10-40 mg/100 g DW; Mg: 150-400 mg/100 g DW [1, 2]	Ca: 300-800 mg/100 g DW [4]
Vitamins	Vitamin C: 100-300 mg/100 g FW [1, 2]	Vitamin C: 20-80 mg/100 g FW [4]
Proteins	20-30% DW [1, 2]	10-18% DW [4]
Total phenolic content	150-400 mg GAE/g extract (Devkota et al., 2022) [2]	90-130 mg GAE/g extract [4, 8]

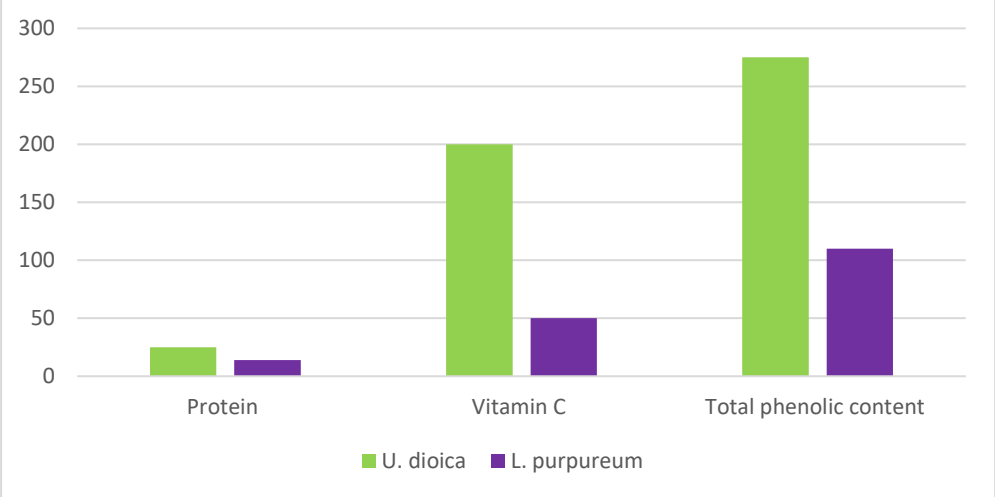


Figure 1. Protein (% DW), vitamin C (mg/100 g FW), and total phenolic content (mg GAE/g extract) in *Urtica dioica* and *Lamium purpureum*

Figure 1 shows a visual comparison of protein, vitamin C, and total phenolic content in the two species. *Urtica dioica* presents higher values for all three parameters than *Lamium purpureum*. Both species represent valuable sources of nutrients, although *Urtica dioica* generally contains higher levels of minerals and vitamins. The observed differences in composition may be associated with species-specific characteristics and environmental adaptations. Together with their morphological traits, these nutritional properties highlight the potential use of these plants in nutrition, functional foods, and phytotherapy.

Conclusion

Both *Urtica dioica* and *Lamium purpureum* are valuable sources of nutrients and bioactive compounds. Based on the reviewed literature, *Urtica dioica* shows higher levels of minerals, vitamin C, proteins, and total phenolic compounds. The nutritional properties of both species support their potential use in human nutrition, functional foods, and phytotherapy. Compared with *U. dioica*, information on the nutritional composition of *L. purpureum* remains limited, highlighting the need for further studies to better characterize its nutritional value and potential applications.

Acknowledgements

This study was funded by the University of Life Sciences "King Mihai I" from Timisoara" and the results will be included in the PhD Thesis of Tarkanyi Patricia Cristina, under the supervision of Prof.Habil.Dr.Eng. Despina-Maria Bordean.

The authors would like to thank to the Doctoral School "Engineering of Vegetable and Animal Resources", University of Life Sciences "*King Mihai I*" from Timişoara (Calea Aradului 119, 300645 Timişoara, Romania), for the academic support and resources provided throughout the development of this research.

References

[1] Bhusal, K. K., Magar, S. K., Thapa, R., Lamsal, A., Bhandari, S., Maharjan, R., Shrestha, S., & Shrestha, J. (2022). *Nutritional and pharmacological importance of stinging nettle (Urtica dioica L.): A review*. *Heliyon, 8*(6), e09717. https://doi.org/10.1016/j.heliyon.2022.e09717

[2] Devkota, H. P., Paudel, K. R., Khanal, S., Baral, A., Panth, N., Adhikari-Devkota, A., Jha, N. K., Das, N., Singh, S. K., Chellappan, D. K., Dua, K., & Hansbro, P. M. (2022). *Stinging nettle (Urtica dioica L.): Nutritional composition, bioactive compounds, and food functional properties*. *Molecules, 27*(16), 5219. https://doi.org/10.3390/molecules27165219

[3] Grauso, L., de Falco, B., Lanzotti, V., & Motti, R. (2020). *Stinging nettle, Urtica dioica L.: Botanical, phytochemical and pharmacological overview*. Phytochemistry Reviews, 19(6), 1341–1377.https://doi.org/10.1007/s11101-020-09680-x

[4] Grujić, S. M., Džamić, A. M., Mitić, V. D., Stankov-Jovanović, V., Marin, P. D., & Stojanović, G. S. (2017). *Effects of solvent extraction system on antioxidant activity of Lamium purpureum L. Hemijska Industrija, 71*(5), 361-370. https://doi.org/10.2298/HEMIND160518047G

[5] Ionescu, N., Popescu, D., & Badea, O. (2022). Variability of morphological characteristics of *Lamium purpureum*. *Annals of the University of Craiova*.

[6] Paulauskienė, A., Tarasevičienė, Ž., & Laukagalis, V. (2021). Influence of harvesting time on the chemical composition of wild stinging nettle (*Urtica dioica* L.). *Plants, 10*(4), 686. https://doi.org/10.3390/plants10040686

[7] Plants of the World Online. (2026). *Lamium purpureum* L. Royal Botanic Gardens, Kew.

[8] Ranjbar, A., Moghadam, A. L., Kutani, S. H., Naderkhani, R., & Maham, M. (2026). *A comprehensive phytochemical analysis, antioxidant, and antibacterial properties of Lamium purpureum L. Chemistry & Biodiversity, 23*(7), e02866. https://doi.org/10.1002/cbdv.202502866

[9] Redžić, S. (2010). Use of wild and semi-wild edible plants in nutrition and survival of people in 1430 days of siege of Sarajevo during the war in Bosnia and Herzegovina (1992–1995). *Collegium antropologicum*, *34*(2), 551-570.

[10] Rutto, Laban K., Xu, Yixiang, Ramirez, Elizabeth, Brandt, Michael, Mineral Properties and Dietary Value of Raw and Processed Stinging Nettle (*Urtica dioica* L.), *International Journal of Food Science*, 2013, 857120, 9 pages, 2013. https://doi.org/10.1155/2013/857120

[11] Sahal, A., Hussain, A., Kumar, S., Dobhal, A., Ahmad, W., Chand, K., ... & Lohani, U. C. (2025). Nettle (Urtica dioica) leaves as a novel food: Nutritional, phytochemical profiles, and bioactivities. *Food Chemistry: X*, *28*, 102607.https://doi.org/10.1016/j.fochx.2025.102607

[12] Singh, M., & Sengar, B. (2021). *Urtica dioica* L. (Stinging nettle): Morphological, phytochemical, cultivation practices and biological potential: A review. *International Journal of Pharmacognosy and Phytochemical Research, 13*(2), 1-7.

[13] Taylor, K. (2009), Biological Flora of the British Isles: *Urtica dioica* L. Journal of Ecology, 97: 1436-1458. https://doi.org/10.1111/j.1365-2745.2009.01575.x

RADIATION-INDUCED SURFACE FUNCTIONALIZATION OF GROUND TIRE RUBBER FOR ENHANCED COPPER ION ADSORPTION

Lorant Kiss[1], Renata Homlok[2], Petra Toth[1], Anna Tegze[2], Laszlo Meszaros[1,3]

[1]Department of Polymer Engineering, Faculty of Mechanical Engineering, Budapest University of Technology and Economics, Muegyetem rkp. 3, Budapest H-1111, Hungary
[2]Radiation Chemistry Group, Surface Chemistry and Catalysis Department, Institute for Energy Security and Environmental Safety, HUN-REN Centre for Energy Research, Konkoly-Thege M. Street 29-33, Budapest H-1121, Hungary
[3]HUN-REN-BME Research Group for Composite Science and Technology, Budapest University of Technology and Economics, Muegyetem rkp. 3, Budapest H-1111, Hungary
e-mail: kiss.lorant@gpk.bme.hu, homlok.renata@ek.hun-ren.hu

Abstract

The increasing amount of end-of-life tires represents an important environmental challenge, while the utilization of waste tire rubber as a secondary raw material offers opportunities for developing new functional materials. Ground tire rubber (GTR), obtained from waste tires, has potential for environmental applications, although its relatively hydrophobic surface limits its interaction with dissolved contaminants.

In this study, radiation-modified GTR was investigated as a potential material for copper-ion removal from aqueous solution. GTR samples were irradiated using a TESLA LINAC LPR-4 electron accelerator operated at 4 MeV and subsequently grafted with methyl methacrylate (MMA) or maleic anhydride (MAH). The resulting materials were characterized by Fourier-transform infrared spectroscopy (FTIR) and scanning electron microscopy (SEM). Copper-ion adsorption was investigated in batch experiments by examining the effects of initial copper concentration, contact time, and absorbed radiation dose.

The applied treatment resulted in changes in the chemical structure and surface morphology of GTR. Differences in copper-ion adsorption were observed between untreated and modified materials. The results indicate that radiation-modified and grafted GTR can be considered as potential low-cost materials for copper-ion removal from aqueous solutions.

This work demonstrates a possible approach for combining waste tire valorization and water treatment, using radiation-modified polymeric materials for environmental applications.

Introduction

The large amount of end-of-life tires generated worldwide presents an environmental challenge and increases the need for their efficient utilization. Ground tire rubber (GTR), produced from waste tires, is an abundant secondary material that can be incorporated into new applications [1]. Due to its relatively low cost and availability, GTR is of interest for the development of materials for environmental purposes.

Copper ions can occur in industrial wastewater and their removal from contaminated water is an important environmental issue. Adsorption is a widely used method for metal-ion removal, and waste-derived materials have attracted attention as potential low-cost adsorbents [2].

The surface properties of GTR can be modified by different physical and chemical treatments. Ionizing radiation is capable of generating reactive sites in polymeric materials, which can subsequently be used for grafting reactions. In the present work, radiation-modified GTR was investigated for its potential application in copper-ion removal from aqueous solution [3].

Experimental

Ground tire rubber samples were irradiated using a TESLA LINAC LPR-4 electron accelerator operated at 4 MeV. Irradiation was performed under different conditions, including treatment in air and in an aqueous medium.

Following irradiation, grafting was carried out using methyl methacrylate (MMA) and maleic anhydride (MAH). MMA was used without dilution, while MAH was applied at 10 wt% in acetone. The grafting reactions were performed at 50 °C.

The untreated and modified GTR samples were characterized by FTIR and SEM. Copper-ion adsorption experiments were performed in batch systems. The effects of initial copper concentration, contact time, and absorbed radiation dose were investigated.

Results and discussion

Electron beam irradiation followed by grafting resulted in changes in the chemical structure and surface morphology of GTR. FTIR analysis indicated changes associated with the grafting treatment, while SEM observations revealed modifications of the surface structure.

The modified GTR samples exhibited different copper-ion adsorption behaviour compared with untreated GTR. The adsorption depended on the investigated experimental conditions, including the initial copper concentration, contact time, and absorbed radiation dose.

The observed changes indicate that radiation treatment and subsequent grafting can influence the surface properties of GTR and consequently its interaction with copper ions in aqueous solution. The use of waste tire rubber as the starting material also provides an opportunity to combine material modification with waste valorisation.

Conclusion

Radiation-modified and grafted ground tire rubber was investigated for copper-ion removal from aqueous solution. Electron beam treatment followed by grafting with MMA or MAH resulted in changes in the chemical and morphological characteristics of GTR.

Differences in copper-ion adsorption were observed between untreated and modified materials. The results demonstrate the potential of radiation-modified GTR as a waste-derived material for water treatment applications

Acknowledgements

This work was supported by the EKÖP-25-4-I-BME-277 University Research Scholarship Programme of the Ministry for Culture and Innovation, financed from the National Research, Development and Innovation Fund.

The authors also acknowledge the International Atomic Energy Agency (IAEA) for financial support under the Coordinated Research Project F23036.

References

1] F. Calisir, F.R. Roman, L. Alamo, O. Perales, M.A. Arocha, S. Akman, Desalination 249 (2009) 515.

[2] Y. Liu, L. Luo, G. Chen, M. Xie, Z. Yu, Iranian Polymer Journal 19 (2010) 207.

[3] L. Kiss, R. Homlok, A. Tegze, L. Mészáros, Macromolecular Materials and Engineering 311 (2026) e70328.

METAL-DEPENDENT OZONE ACTIVATION OVER GREEN TEA-SYNTHESIZED Fe, Ag AND Au–ZnO NANOCATALYSTS FOR PHENOL DEGRADATION

Razvan State[1], Anna Tegze[2], Florica Papa*[1], Ioan Balint[1], Liubovi Cretu[1], Anca Vasile[1], Krisztina Kovacs[2], Renata Homlok[2], Monica Pavel[1]

[1]"Ilie Murgulescu" Institute of Physical Chemistry of the Romanian Academy, 202 Spl. Independentei,060021 Bucharest, Romania
[2]Radiation Chemistry Group, Surface Chemistry and Catalysis Department, Institute for Energy Security and Environmental Safety, HUN-REN Centre for Energy Research, Konkoly-Thege Miklós út 29-33, H-1121 Budapest, Hungary
e-mail: frusu@icf.ro

The development of efficient ozone-activation catalysts through sustainable synthesis routes remains a key challenge in advanced oxidation processes. Herein, we demonstrate a green-tea-assisted strategy for engineering metal–ZnO interfaces in which Fe, Au, and Ag nanoparticles are synthesized and stabilized by tea-derived polyphenols and subsequently employed as a catalytic system for phenol ozonation. The principal novelty lies in correlating the nature of the deposited metal with the mechanism of ozone activation and the resulting oxidation performance. Structural and spectroscopic characterization revealed distinct metal–ZnO interactions, with Fe incorporation associated with highly dispersed iron species and modified defect structures, while Au and Ag exhibited characteristic metallic nanoparticle phases. The catalysts displayed markedly different ozonation activities, with Fe_ZnO achieving 97% phenol conversion after 180 min and an apparent rate constant of 0.0181 min^{-1}, compared with 90%, 75%, and 46% conversion for Au_ZnO, Ag_ZnO, and pristine ZnO, respectively. Mechanistically, the results indicate that the superior activity of Fe_ZnO originates from a redox-mediated ozone activation pathway involving the Fe^{2+}/Fe^{3+} couple, in contrast to the predominantly interfacial electronic activation proposed for the noble-metal Au_ZnO and Ag_ZnO catalysts. HPLC analysis further revealed a sequential oxidation pathway from hydroquinone, benzoquinone, and dihydroxybenzene to low-molecular-weight carboxylic acids, evidencing aromatic-ring cleavage and progressive oxidation. These findings establish metal character and interfacial redox chemistry as decisive factors governing ozone activation and demonstrate the potential of green-synthesized Fe_ZnO as an effective catalyst for phenolic wastewater treatment.

SYNTHESIS OF BIOACTIVE-LOADED MICROBEADS FROM MARINE ALGAE EXTRACTS

Vesna Teofilovic[1], Halis Can Mörel[2], Davut Laçin[3], Tamara Erceg[1], Jelena Pavlicevic[1], Bojana Ikonic[1], Emine Okudan[4], Ayşe Zehra Aroğuz[2]

[1]University of Novi Sad, Faculty of Technology, Bul. Cara Lazara 1, 21000 Novi Sad, Serbia
[2] Faculty of Pharmacy, Biruni University, Merkezefendi, 75. Sokak No: 1-13 (M.G), 34015 Zeytinburnu/Istanbul, TÜRKİYE
[3] Department of Geology Engineering, Istanbul University-Cerrahpaşa, Avcılar Yerleşkesi, Mühendislik Fakültesi, J Blok, 34320 Avcılar/ Istanbul, TÜRKİYE
[4]Akdeniz University, Faculty of Fisheries, Department of Basic Aquatic Science, Section of Marine Biology, Dumlupınar Bulvarı, 07058 Konyaaltı/Antalya, TÜRKİYE
**Corresponding author's e-mail address: vesnateofilovic@uns.ac.rs*

Renewable sources of bioactive compounds, such as marine algae, offer numerous potential applications across various fields, particularly in medicine, agriculture, and biotechnology. Incorporating these extracts into polymeric microbeads allows for their effective handling and delivery in easy-to-use formulations. This study explores the preparation of bioactive-loaded microbeads using the brown algae *Sargassum vulgare*, collected from the Marmara Sea, as a polymer source. Extract-loaded microbeads were prepared alongside extract-free control beads, both utilizing sodium alginate as the polymer backbone, to evaluate the influence of extract incorporation on bead formation and material characteristics. The primary formulation employed an O1/W/O2 phase system, where the algal extract was incorporated into the O1 phase and encapsulated with the assistance of surfactants and sodium alginate in the aqueous W phase. Subsequently, slow internal gelation was triggered within the O1/W system, which was then introduced into the continuous O2 phase to yield solid microbeads. Initial observations confirmed successful microbead formation. Fourier-transform infrared (FTIR) spectroscopy confirmed the successful incorporation of the algal bioactive components and indicated key functional group interactions within the polymeric network. Overall, this work provides a foundation for developing marine algae-derived microbeads intended for agricultural applications, with ongoing studies focusing on their functional performance and biological efficacy.

Keywords: Marine algae, bioactive substances, microbeads, biopolymers, drug delivery.

Acknowledgement: This research was funded by the Bilateral Scientific cooperation between The Ministry of Science, Technological Development and Innovation of the Republic of Serbia (NITRA) (Nr. 026 02 11) and Scientific and Technological Research Council of Türkiye (TUBITAK) (Nr. 123N938), as well as by programs of Ministry of Science, Technological Development, and Innovation, Republic of Serbia No. 451-03-33/2026-03/200134 and 451-03-34/2026-03/200134

DEVELOPMENT AND PHYSICOCHEMICAL CHARACTERIZATION OF LAMOTRIGINE-LOADED LIPOSOMES STABILIZED WITH TWEEN 80 AND POLOXAMER 188

Vesna Tepavčević[1], Mijat Brenjo[1], Ana Pilipović[1], Mihalj Poša[1], Kosta Popović[1], Mladena Lalić-Popović[1], Nemanja Todorović[1], Zita Farkaš Agatić[1]

[1]Department of Pharmacy, Faculty of Medicine, University of Novi Sad, Hajduk Veljkova 3, 21000 Novi Sad, Serbia
e-mail: vesna.tepavcevic@mf.uns.ac.rs

Abstract

Lamotrigine is an antiepileptic drug with limited aqueous solubility, and liposomal carriers represent a potential approach for modifying its release and permeation characteristics [1]. The aim of this study was to develop and physicochemically characterize lamotrigine-loaded liposomes stabilized with the non-ionic surfactants Tween 80 and Poloxamer 188. Nine formulations were prepared using the thin-film hydration method. The amounts of lecithin and Tween 80 were kept constant, while the concentration of Poloxamer 188 (0.03–0.06% w/v) and the lecithin-to-cholesterol ratio (6:1, 4:1 and 3:1) were varied. Particle-size distribution was determined by dynamic light scattering, encapsulation efficiency by UV–Vis spectrophotometry following ultracentrifugation, and lamotrigine release and permeation using Franz diffusion cells. Release kinetics were evaluated using the Higuchi and Weibull models [2–4]. Most formulations showed median particle diameters in the submicrometer range. Formulation 9 showed a median particle diameter d(0.5) of 0.304 µm and a mean diameter D(4,3) of 0.439 µm, together with the highest encapsulation efficiency of 84.36%. Higuchi coefficients for the liposomal formulations ranged from 21.42 to 40.98 $\mu g \cdot cm^{-2} \cdot min^{-1/2}$, compared with 245.78 $\mu g \cdot cm^{-2} \cdot min^{-1/2}$ for free lamotrigine. Similarly, permeation flux decreased from 11.65 $\mu g \cdot cm^{-2} \cdot min^{-1}$ for free lamotrigine to 0.36–2.08 $\mu g \cdot cm^{-2} \cdot min^{-1}$ for the liposomal formulations. Weibull analysis indicated that lamotrigine release involved both diffusion and structural characteristics of the liposomal system. Overall, Formulation 9, containing 0.06% Poloxamer 188 and a lecithin-to-cholesterol ratio of 3:1, provided the most favorable combination of particle size, homogeneity, encapsulation efficiency and permeation characteristics.

Acknowledgements

This work was supported by the projects *"Development of Innovative Pharmaceutical-Technological Preparations for the Pediatric Population in the Republic of Serbia"*, *"Integration of Digitalization and 3D Printing Supported by Artificial Intelligence in the Development of Solid and Liquid Pharmaceutical Dosage Forms"*, and *"Genetic Characterization of Rapidly Mutating Y-STR Markers in the Population of Vojvodina"*, funded by the Provincial Secretariat for Higher Education and Scientific Research of Vojvodina.

References

[1] Praveen A, et al. *Colloids Surf B Biointerfaces.* 2019;174:553–562.
[2] Jain A, Jain SK. *Chem Phys Lipids.* 2016;201:28–40.
[3] Siepmann J, Peppas NA. *Int J Pharm.* 2011;418(1):6–12.
[4] Papadopoulou V, et al. *Int J Pharm.* 2006;309(1–2):44–50.

ANALYTICAL POTENTIAL OF CARBON NANOTUBE BASED NANOMATERIALS WITH 1D RANDOM OR 1D ORDERED STRUCTURES

Ildikó Y. Tóth

Department of Applied and Environmental Chemistry, University of Szeged, H-6720, Szeged, Rerrich Béla tér 1, Hungary
e-mail: ildiko.toth@chem.u-szeged.hu, ilditoth84@gmail.com

Abstract
The evaporation of liquids from porous films is a very complex phenomenon, which can be followed by simultaneous weight monitoring, electric resistance measurement, infrared imaging and contact angel measurement. The appropriate evaluation of these measurement results can carry both quantitative and qualitative analytical information. The aim of our work is to demonstrate this opportunity through the example of the wetting and evaporation of simple solvents from (1D nano) carbon nanotube (CNT) based materials with 1D random or 1D ordered structures.

Introduction
Recent developments in nanotechnology have highlighted the importance of the classical topics of wetting, droplet spreading and evaporation due to their pronounced effect in different nanotechnological applications. The multiple phenomena (wetting, spreading, capillary filling, gravity induced convective flow, adsorption, evaporation from the surface, evaporation from the pores, etc.) take place simultaneously when a fluid sessile droplet contacts a porous surface can be studied by different techniques: TEM, SEM, contact angle measurement, high speed camera recordings, thermography, etc.
The wetting and evaporation of a sessile droplet can be followed by an equipment assembled at the Department of Applied and Environmental Chemistry, University of Szeged: this equipment can guide simultaneous weight monitoring, electric resistance measurement and thermography at a controlled temperature. There are several experimental results characteristics for the wetting and evaporation process, the most important ones being the total evaporation time, time of evaporation only from the surface, full width at half maximum of the time-dependent mass and resistance curves, evaporation rate, initial area of the droplet, and the wetted area at the moment of total evaporation from the surface, etc. [1-6].
The main goal of this work was to demonstrate the analytical possibilities of the mass and resistivity measurements and thermography through the example of sessile droplet evaporation from carbon nanotube (CNT) based composites with 1D random or 1D ordered structures.

Experimental
Pure materials. The multiwall carbon nanotubes were synthesized by catalytic chemical vapor deposition. These nanotubes were called non-functionalized carbon nanotubes (nf-CNTs). Carbon nanotube functionalization was performed by oxidation using 8-hour nitric acid reflux, the product is the so-called functionalized carbon nanotubes (f-CNTs). (Outer diameter: 14.1±7.5 nm, inner diameter: 5.8±1.7 nm, length: 23.9±3.6 μm). [1,2,5,6]. The hydrophilic goethite nanowires (GNWs) were prepared by oxidation-precipitation. (Length: 378 ± 163 nm, diameter: 38.3 ± 19.5 nm.) [5,6] The hydrophilic imogolite nanotubes (INTs) were produced by purification from a natural mineral collected in Japan. (Outer diameter: ~2 nm, inner diameter: ~1 nm, length: 23.9±3.6 μm.) [6] The hydrophilic ZnMgAl-LDO (layered double oxide) particles (diameter: ~25 μm) were prepared by precipitation, ageing, drying and calcination processes and the hydrophobic fluoropolymer (FP) (poli (1H, 1H, 2H, 2H-perfluor-

decil-akrilát) was synthetized by UV-polymerization and dissolved in toluene. The studied LDO/fluoropolymer layer was prepared by spray-coating from the mixed suspension with 80/20 w/w % LDO/p(PFDAk) ratio [4].

1D random structured materials – buckypaper (BP) preparation. The nf-CNTs or f-CNTs were converted into pure buckypaper (BP) by filtering 100 cm^3 of their 0.1 g/dm^3 suspensions through a 0.45 μm nominal pore diameter Whatmann nylon membrane filter. The nf-CNTs / f-CNTs were suspended by ultrasonication in N,N dimethylformamide (DMF) / water. The self-supporting BP was ready after drying process [1,2,5,6]. Mixed structured BP was prepared by dead-end filtration from the physical mixture of the studied material's suspensions (e.g., actual ratio of nf-CNT in DMF and f-CNT in water or nf-CNT in DMF and GNW in water (90/10 w/w%) [5]. Layered structured BP was prepared by doping of the already prepared pure nf-CNT BP, e.g. filtration of aqueous suspensions of INT or GNW onto nf-CNT BP [5,6] or spray-coating of LDO/fluoropolymer dispersion onto nf-CNT BP [4]. After drying, layered structured samples were obtained.

1D ordered structured nanomaterials - CNT forests preparation. Vertically aligned carbon nanotubes, so-called CNT forests were prepared by catalytic chemical vapor deposition (CCVD) method. By varying the reaction time and the water content, a series of samples with different heights (CNT lengths ~700 μm, ~1000 μm, ~1400 μm, ~2000 μm) and a series of samples with different macroscopic surface roughness were prepared.

The wetting and evaporation of liquid droplets (acetone, methanol, ethanol,2-proanol, water, ethanol-water mixtures, etc.) was studied from the CNT based nanomaterials. The temperature, the electric resistance and weight variations could be simultaneously monitored by the equipment assembled at the Department of Applied and Environmental Chemistry, University of Szeged [1-6]. The solid nanomaterial was placed onto a purpose-built sample holder. The setup included a type K thermocouple in contact with the non-wetted part, which data was fed back to the temperature controller that maintained a base solid temperature (typically 50.0 ± 0.5 °C) by continuously adjusting the heater power using fuzzy logic control. The sample holder was placed on a Sartorius Cubis microbalance with 0.01 mg readability and the weigh variation during droplet evaporation was recorded. For thermography a FLIR A655sc infrared (IR) camera (with thermal sensitivity of 30 mK and accuracy of ±2 °C for temperatures up to 650 °C at 640x480 resolution) was used. Its uncooled microbolometer detector has a spectral range of 7.5-14.0 μm. The IR camera is equipped with a 2.9x (50 μm) IR close-up lens, with 32x24 mm field of view and 50 μm spatial resolution. The recorded images are transferred to a PC with FLIR ResearchIR Max software. Each CNT based nanomaterial's emissivity (ε_S) was determined by calibration at the initial film temperature (25 °C) with a black electrical tape (ε = 0.95). The sample holder plastic plate with the 0.7 cm radius gap in the center was equipped with two copper electrical connections at the opposite edges of the gap on the bottom of the sheet. The BP was fixed to the bottom of the plastic section with magnetic clips. The copper electrodes were contacted to the source meter by 0.3 mm diameter copper wires. The computer recorded the electrical resistance (R) of the buckypaper as measured by a Keithley 2612A Source Meter. The R was not measured in case of CNT forests. The ambient air temperature and the relative humidity of the ambient atmosphere were kept constant (at 25 °C and 55 RH%, respectively). Before the measurements, the solid was mounted in the assembly and heating at initial temperature was applied until the electrical resistance and the sample weight both stabilized. Then all three recordings (resistivity, IR imaging and sample weight) were started a few seconds before dropping. The selected solvent droplets (5 μL or 10 μL, 25 °C) were instilled with an Eppendorf Xplorer electronic pipette on the surface of the porous solids, and the IR video, the weight and the R variation were recorded until they returned to their original values.

Results and discussion

In general, at the moment, we drop the liquid on the buckypaper film (t_0), the liquid starts to diffuse immediately into the pores of the solid, but a part of it remains spread on the surface of the sample. The evaporation of this liquid from the surface takes place together with the diffusion. Once all liquid evaporates from the surface, namely the primary surface evaporation is complete (t_s), liquid is left only in the pores. The solvent gradually evaporates from the pores as well. The complete evaporation of the solvent (t_t) was confirmed by the fact that the weight and the resistivity of the solid returned to the baseline.

In case of a typical weight variation, the m increased as soon as the solvent was dropped to the solid (t_0) and this is followed by a quasi-linear weight decrease. Once the primary surface evaporation is complete (t_s), the weight of the sample decreases as linear (within experimental error) functions of time due to the continuous evaporation of the solvent. The total evaporation time (t_t) was at the moment when the weight of the solid returned to the baseline. At the linear weight decreasing ranges, the rate of evaporation (-dm/dt) is constant. The change of -dm/dt value suggests the change of the dominant evaporation process, e.g., evaporation of the droplet sitting on the surface of the solid sample, evaporation of the condensed water from the porous system or the evaporation of the adsorbed water from the microscopical surface of the porous system. From this measurement, the typical experimentally determined data are the shape of the curve: m_{max}, area, FWHM, t_s and t_t, evaporation rate -dm/dt and its change, and the t_i and m_i values at these points. These parameters are characteristic for the measured system and can be used to identify them.

In case of the thermography analysis, the IR videos were evaluated at selected representative moments. During liquid surface evaporation the temperature was determined by taking into account the emissivity of the liquid ($\varepsilon_L = 0.95$); after surface evaporation, the emissivity of the wetted solids was calculated as the average between ε_L and ε_S. Based on the exported pictures at the representative moments, it is possible to determine the spot area and average temperature of the drop (S_d, T_d) and of the wetted region (S_w, T_w) as a function of time. The S_d and S_w values at t_0 and t_s are very characteristic.

In case of a typical electric resistance variation as a function of time, the R increased as soon as the solvent was dropped to the solid (t_0) and reached the maximum (R_{max}) usually at t_s, then this is followed by a monotone R decrease. The total evaporation time (t_t) was at the moment when the R of the solid returned to the baseline. These curves are characteristic for the fluid-solid pair, can be called as evaporation profiles and described by their shape: R_{max}, t_s, t_t, FWHM, area, etc. However, in some cases other special characteristics can also be observed in the evaporation profiles, for example the appearance of a negative peak next to the typical maximum peak (e.g. water - nf-CNT BP), which can further increase the analytical possibilities of the measurement method.

Qualitative and quantitative analytical possibilities based on the application of Origin, SPSS, different statistical methods (PCC correlation matrix, principal component analysis) modeling, etc. The following 3 main areas can be distinguished.

A) Characterization/determination of solid, porous samples (Fig.1.) [5]

B) Determination of solvents (water, acetone, methanol, ethanol, 2-propanol, 1,4-dioxane, etc.) (Fig.2.) [5,6]

C) Determination of the composition of ethanol-water solvent mixture (Fig.3.) [4]

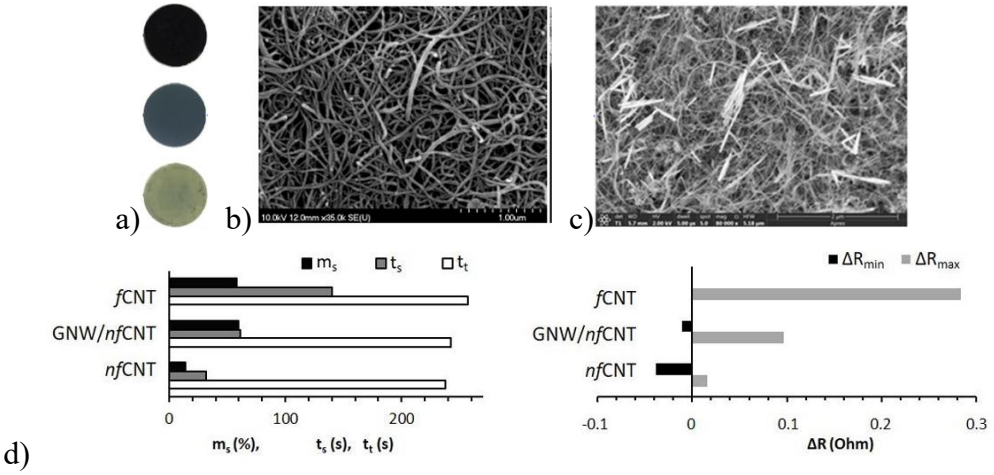
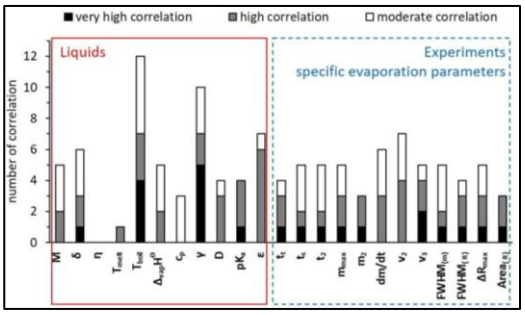


Figure 1. Photo (a), SEM (b,c) and characteristic experimental parameters of water wetting and evaporation {5 µL, 50°C} (d) from the surface of pure nf-CNT BP (a1,b,d), pure f-CNT BP (d), GNW/nf-CNT BP with mixed structured (a2,c,d) and GNW/nf-CNT BP with layered structured (a3) [1,2,5].

	t_t	t_s	t_2	m_{max}	m_2	dm/dt	v_2	v_3	$FWHM_{(m)}$	$FWHM_{(R)}$	ΔR_{max}	$Area_{(R)}$
M	-0.466	-0.570	-0.538	0.186	-0.064	0.419	-0.722	0.375	-0.617	-0.470	0.807	0.254
ρ	-0.449	-0.239	0.617	-0.611	-0.856	0.878	-0.679	0.971	-0.397	-0.432	-0.270	-0.497
η	0.120	-0.051	-0.190	0.476	-0.208	-0.376	0.252	0.061	0.057	0.109	0.294	0.289
T_{melt}	0.272	0.226	0.094	0.254	0.071	-0.401	0.260	0.073	0.235	0.291	0.193	0.338
T_{boil}	0.772	0.608	0.636	0.985	-0.958	-0.781	0.563	0.957	0.651	0.760	0.541	0.929
$\Delta_{vap}H^0$	0.582	0.433	0.492	0.557	-0.392	-0.847	0.824	-0.019	0.584	0.564	-0.048	0.363
c_p	-0.453	-0.543	-0.493	0.132	-0.093	0.416	-0.618	0.246	-0.569	-0.457	0.605	0.116
γ	0.971	0.992	0.985	0.639	-0.808	-0.673	0.742	0.613	0.965	0.976	-0.089	0.625
D	-0.246	-0.008	0.266	-0.766	0.262	0.566	-0.164	-0.650	-0.084	-0.233	-0.840	-0.770
pKa	-0.233	-0.059	0.042	-0.762	0.433	0.308	0.098	0.791	-0.044	-0.228	0.962	-0.855
ε	0.772	0.860	0.847	0.164	-0.369	-0.572	0.831	0.043	0.877	0.775	-0.617	0.101



	$t_{t(m)}$	$t_{t(R)}$	$t_{s(R)}$	m_{max}	dm/dt	dm/dt_2	$FWHM_{(m)}$	$FWHM_{(R)}$	ΔR_{max}	$Area_{(R)}$
M	-0.86	-0.85	-0.81	-0.84	0.50	-0.80	-0.83	-0.84	-0.78	-0.84
δ	0.97	0.97	1.00	0.92	-0.92	0.74	0.98	0.83	1.00	0.97
η	0.04	0.06	-0.05	0.18	-0.09	0.33	0.07	0.21	-0.03	0.08
T_{melt}	0.38	0.40	0.34	0.36	0.08	0.41	0.31	0.57	0.28	0.39
T_{boil}	0.84	0.84	0.77	0.90	-0.77	0.89	0.86	0.82	0.79	0.85
$\Delta_{vap}H^0$	0.56	0.56	0.42	0.70	-0.38	0.84	0.57	0.68	0.43	0.57
c_p	-0.66	-0.65	-0.63	-0.63	0.28	-0.58	-0.62	-0.64	-0.59	-0.63
γ	0.97	0.97	1.00	0.91	-0.91	0.73	0.98	0.83	1.00	0.97
D	-0.34	-0.34	-0.15	-0.50	-0.06	-0.75	-0.31	-0.59	-0.13	-0.34
pK_a	-0.82	-0.81	-0.69	-0.90	0.43	-0.99	-0.79	-0.92	-0.67	-0.81
ε	0.98	0.96	0.97	0.93	-0.82	0.79	0.97	0.85	0.96	0.96

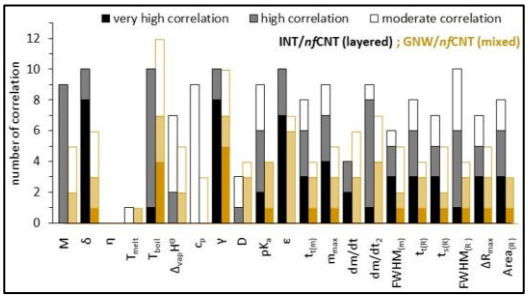


Figure 2. Relevant PCC matrix (left) and its analysis (right) in case of the different fluid's wetting and evaporation experiments {5 µL, 50°C} from the surface of the mixed structured GNW/nf-CNT BP (up) [5] and from the surface of the layered structured INT/nf-CNT BP (down) [6].

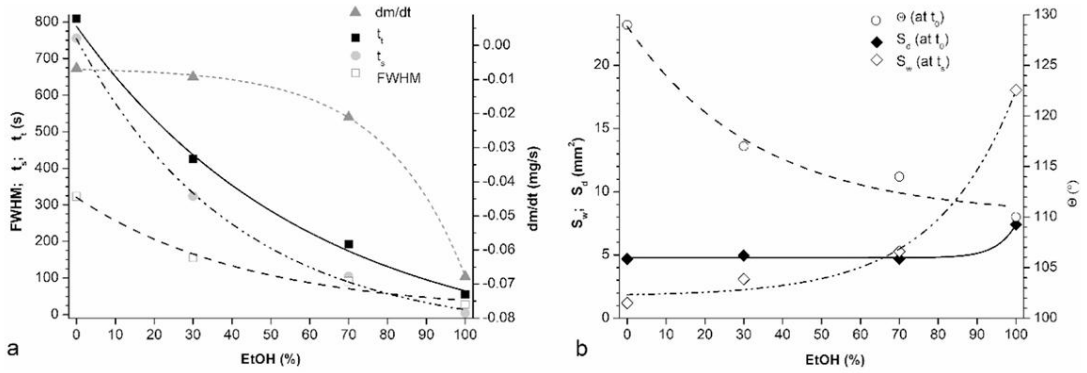


Figure 3. Results of wetting and evaporation of EtOH-water mixtures {5 µL, 50°C} from the

surface of glass coated by LDO/fluoropolymer layer. This superhydrophobic layer can be doped onto nf-CNT BP [4]. (Initial contact angle of water: LDO/FP_glass: 129°, LDO/FP_nf-CNT BP: 125°, nf-CNT BP:73°.)

Conclusion

The weight monitoring of the evaporation of liquids from porous materials can provide information about the mechanism of wetting and vaporization which is a significant area of the basic researches. Furthermore, it can be proved by using appropriate statistical methods (e.g., matrix of Pearson correlation coefficients, hierarchical cluster analysis, functional analysis, etc.), that the experimentally determined characteristic values are specific for the physical properties of the solvents, and they are also dependent on the quality of the solid materials, therefore, they can be used for qualitative chemical analysis via the estimation of physical properties. The results allow us to presume the possibility of this experimental setup and theoretical approach for a potential future application in the field of analytics.

Acknowledgements

I.Y. Toth acknowledge the support by the János Bolyai Research Scholarship of the Hungarian Academy of Sciences.

References

[1] Schuszter et al., Liquid droplet evaporation from buckypaper: on the fundamental properties of the evaporation profile. Microporous Mesoporous Mater. 209 (2015) 105.
[2] Bogya et al., Surface pinning explains the low heat transfer coefficient between water and a carbon nanotube film. Carbon 100 (2016) 27.
[3] Nagy et al., Wetting and evaporation on a carbon cloth type gas diffusion layer for passive direct alcohol fuel cells. J. Mol. Liq. 304 (2020) 112698.
[4] Tóth et al., Characterization of the solvent specific evaporation from a fluoropolymer surface roughened by layered double oxide (LDO) particles. J. Mol. Liq. 305 (2020) 112826.
[5] Tóth et al., Characterization of the solvent specific evaporation from a carbon nanotube buckypaper doped by goethite nanowires. J. Mol. Liq. 389 (2023) 122816.
[6] Tóth and Kukovecz, Solvent specific evaporation properties from the surface of carbon nanotube buckypapers doped by hydrophilic 1D nanomaterials. J. Mol. Liq. 435 (2025) 128089.

GREENHOUSE GAS AND AMMONIA EMISSIONS IN *ARABIDOPSIS THALIANA* USING A RHIZOBOX INTEGRATION AND CRDS ANALYSIS

Saeid Toghiani Khorasgani [1], Anna Szabó [2], Csilla Gombi [2], Miklós Hóvári [3], Milan Szabó [3], Melinda Tar [4]

[1] Doctoral School of Environmental Sciences, University of Szeged, Szeged, Hungary
[2]Department of Optics and Quantum Electronics, University of Szeged, Szeged, Hungary
[3] Institute of Plant Biology, HUN-REN Biological Research Centre, Szeged, Hungary
[4] Faculty of Agriculture, University of Szeged, Hódmezővásárhely, Hungary
e-mail: Toghiani.Khorasgani.Saeid@stud.u-szeged.hu

Abstract

It is crucial to measure trace gases such as CO_2 and NH_3 to understand the dynamics of carbon and nitrogen in agricultural and environmental systems. Accurately separating the emissions of these gases from plant biological activities and from intrinsic soil emissions is a major challenge. To achieve this physical separation, we utilized a rhizobox. The rhizobox was square-shaped and created by sealing a 50-µm nylon mesh using an electrothermal sealer. It isolated the root zone and prevented mixing with the soil mass. We planted *Arabidopsis thaliana* (Col-0) in a fully controlled, clay-free peat substrate. For gas analysis, we utilized a Cavity Ring-Down Spectroscopy (CRDS)-based highly sensitive gas concentration analyzer (Picarro G2509). Measurements were recorded continuously in three separate steps: total combined gas concentration, isolated plant gas exchange, and isolated soil emission. Through this approach, we captured the normalized CO_2 concentration dynamics of plant-mediated gas exchange using a background normalization method applied to the extracted curves, distinctly separating it from the background soil gas concentration. This normalization visibly decoupled the plant-mediated NH_3 concentration gradient from the soil bulk gas concentration. These preliminary observations demonstrate the technical feasibility of separating plant and soil gas fluxes and indicate that plant-specific NH_3 concentrations may be relevant compared to intrinsic soil gas concentrations. Finally, the integration of the rhizobox structure together with the CRDS measurement protocol provides a promising methodological framework for investigating trace gas dynamics associated with different biological and agricultural processes, such as fertilizer application, and for distinguishing between biological and microbial gas sources.

Keywords: Trace gas emissions, Cavity Ring-Down Spectroscopy (CRDS), Rhizobox, *Arabidopsis thaliana*, Ammonia volatilization, Soil gas emissions.

DEVELOPMENT AND CHARACTERIZATION OF NOVEL IONIC LIQUID-FUNCTIONALIZED ADSORBENT MATERIALS FOR PALLADIUM RECOVERY FROM AQUEOUS SOLUTIONS

Dan Cristian Roşu[1], Nick Samuel Ţolea[1], Adina Căta[1], Paula Sfîrloagă[1], Ioana M.C. Ienaşcu[1,2], Lavinia Lupa[3], Radu Lazau[3], Laura Cocheci[3]

[1]National Institute of Research and Development for Electrochemistry and Condensed Matter, Dr. A. P. Podeanu 144, 300569, Timişoara, Romania
[2]"Vasile Goldiş" Western University of Arad, Faculty of Pharmacy, Liviu Rebreanu 86, 310045, Arad, Romania
[3] Politehnica University of Timişoara, Faculty of Industrial Chemistry and Environmental Engineering, 6 Vasile Parvan Blvd, 300223, Timisoara, Romania
e-mail: samy_nick2008@yahoo.com

Abstract

Palladium (Pd) is a platinum group metal (PGM) with unique chemical and physical properties, including high chemical stability and excellent electrical conductivity, which have contributed to its extensive use in a wide range of technological applications. Its increasing demand, together with its strategic importance for various industrial sectors, has led to its recognition by the European Commission as a critical raw material of economic importance. As a result of its widespread use, significant amounts of palladium can accumulate in secondary resources, increasing the interest in its recovery from these sources. In particular, the recovery of Pd from aqueous solutions has become an important research topic [1]. Among the available recovery methods, adsorption represents an attractive approach due to its operational simplicity, efficiency, and potential for developing selective solid-phase adsorbents [2,3].

In this context, the present study focuses on the synthesis of Mg_3Al- and Zn_3Al-LDHs and their functionalization with Cyphos IL-101 (trihexyl tetradecylphosphonium chloride) for the recovery of palladium metal ions from aqueous solutions. The ionic liquid was incorporated using two approaches, ultrasonication-assisted functionalization and co-synthesis. The obtained materials were characterized by X-ray diffraction (XRD), scanning electron microscopy (SEM), Fourier-transform infrared spectroscopy (FTIR), BET surface area analysis, and thermogravimetric analysis (TGA). Palladium adsorption was investigated in batch systems by evaluating the effects of pH, contact time, and initial metal ion concentration.
A pH of 3.5 was selected for the adsorption experiments, as lower pH values may compromise LDH stability, whereas increasing the pH can promote palladium precipitation and interfere with the adsorption measurements. For all materials, adsorption equilibrium was reached within approximately 60 min, while the adsorption capacity increased with increasing equilibrium palladium concentration. The kinetic data were best described by the pseudo-second-order model, whereas the equilibrium data were well represented by the Langmuir isotherm. Functionalization with Cyphos IL-101 approximately doubled the maximum palladium adsorption capacity compared with the corresponding pristine LDHs. Moreover, Mg_3Al-based materials exhibited higher maximum adsorption capacities than the Zn_3Al-based materials.
The results demonstrate that Cyphos IL-101 functionalization enhances the performance of LDH-based adsorbents and highlights their potential for the recovery of palladium metal ions from aqueous solutions.

References

[1] C. Vancea, M. Mihailescu, A. Negrea, G. Mosoarca, M. Ciopec N. Duteanu, P. Negrea, V.Minzatu, Batch and Fixed-Bed Column Studies on Palladium Recovery from Acidic Solution by Modified $MgSiO_3$, Int. J. Environ. Res. Public Health, 17(24), 9500, (2020).

[2] J. Kameliya, A.Verma, P. Dutta, C. Arora, S. Vyas, R.S. Varma, Layered Double Hydroxide Materials: A Review on Their Preparation, Characterization, and Applications, Inorganics, 11(3), 121, (2023).

[3] A.S.K. Kumar, S. Sharma, R.S. Reddy, M. Barathi, N. Rajesh, Comprehending the interaction between chitosan and ionic liquid for the adsorption of palladium, Int. J. Biol. Macromol., 72, 633–639, (2015).

HYDRODYNAMIC INTENSIFICATION OF SWEET WHEY ULTRAFILTRATION AND DIAFILTRATION USING A 3D-PRINTED FLOW PROMOTER

Tímea Lilla Urr[1], Zoltán Péter Jákói[2], Balázs P. Szabó[1], Szabolcs Kertész[2], Réka Dobozi[1]

[1]Department of Food Engineering, Faculty of Engineering, University of Szeged, H-6725 Moszkvai krt. 5-7., Hungary
[2]Department of Biosystems Engineering, Faculty of Engineering, University of Szeged, H6725 Moszkvai krt. 9., Hungary
e-mail: urr.lilla07@gmail.com

Abstract

The recovery of whey proteins from dairy side streams requires an efficient separation strategy combining protein retention with the removal of lactose and other low-molecular-weight constituents. Although ultrafiltration is well suited for this purpose, its performance may decline due to concentration polarization and deposit formation at the membrane surface. In this study, a multistage ultrafiltration–diafiltration *(UF-DF)* process was investigated together with a 3D-printed flow-modifying insert designed to improve membrane-side hydrodynamics. Polyethersulfone *(PES)* membranes with nominal molecular weight cut-offs of 10, 30, and 50 kDa were tested in a stirred filtration cell at a transmembrane pressure of 2.5 bar and a stirring rate of 500 rpm. Ultrafiltration was followed by three consecutive batch diafiltration stages. For each membrane, experiments were conducted both without an insert and with a backward-oriented spiral-vane element.

Process performance was evaluated based on permeate production, hydraulic resistance, and changes in retentate composition. Successive diafiltration increased the protein fraction of the retained solids while progressively reducing lactose content. After the third diafiltration cycle, protein content on a dry-matter basis reached approximately 76.1%, 77.1%, and 74.9% for the 10, 30, and 50 kDa membranes, respectively, with the flow-modifying insert. In the final retentates obtained with the 30 kDa membrane, lactose concentration decreased below the analytical detection limit of 100 mg L^{-1}.

The spiral-vane insert also improved hydraulic performance throughout the *UF-DF* sequence. Compared with the insert-free system, mean total filtration resistance decreased by 10.6-29.6% across the investigated membrane–stage combinations, reaching 5.602, 4.312 and 4.372 × 10^{13} m^{-1} at *DF3* for the 10, 30 and 50 kDa membranes, respectively. This improvement was mainly associated with lower reversible resistance, indicating reduced accumulation of hydraulically removable deposits near the membrane surface.

These findings indicate that repeated diafiltration and local hydrodynamic modification are complementary approaches for sweet whey fractionation. Diafiltration enhanced protein enrichment and lactose removal, while the 3D-printed insert improved hydraulic performance without compromising product composition. The combined approach may support the further development of intensified membrane processes for protein-enriched whey fractions.

Acknowledgements

The Authors are grateful for the support provided by the Ministry of Culture and Innovation's University Research Scholarship Program, financed by the National Research, Development and Innovation Fund (EKÖP-26-1-SZTE-238 and EKÖP-26-3-SZTE-244). Furthermore, this study was supported by the 142414 FK and 2022-1.2.6-TÉT-IPARI TR2022-00011 projects from the National Research, Development, and Innovation Office (NKFI), Hungary.

VALORIZATION OF BLACKBERRY PRUNING RESIDUES FOR THE REMEDIATION OF Cr(VI) CONTAMINATED WATER

Vesna Vasić[1], Dragana Lukić[1], Teodora Subić[1], Jelena Prodanović[1]

[1]University of Novi Sad, Faculty of Technology Novi Sad, Bul. cara Lazara 1, 21000 Novi Sad, Serbia
e-mail: vesna.vasic@uns.ac.rs

Abstract

Heavy metal contamination of aquatic environments remains an important environmental concern due to the persistence, toxicity and potential accumulation of these pollutants in living organisms. Industrial activities represent one of the major sources of metals in water, and insufficiently treated industrial effluents may contribute to their release into surface waters and groundwater [1]. Among inorganic contaminants, hexavalent chromium (Cr(VI)) is of particular concern because of its high toxicity and mobility in aquatic systems. Cr(VI) containing effluents may originate from several industrial activities, including metal processing, textile and leather production, dye manufacturing and wood preservation. A variety of physicochemical approaches, including chemical precipitation, ion exchange, membrane processes, electrochemical treatment and adsorption, have been applied for the removal of metal ions from contaminated waters. However, their practical application may be constrained by high operational costs, consumption of chemicals and energy, or the generation of secondary waste [1,2]. Consequently, increasing attention has been directed towards the development of cost-effective and environmentally sustainable materials for water remediation. Agricultural and lignocellulosic residues are particularly attractive in this context because they are renewable, widely available and contain surface functional groups capable of interacting with dissolved metal species [3,4]. Their conversion into functional materials for water treatment additionally supports the principles of circular economy by transforming low-value residual biomass into a resource for environmental remediation. Pruning residues represent an abundant but insufficiently utilized fraction of agricultural biomass and could therefore provide a suitable feedstock for the development of low-cost remediation materials. The aim of this study was to evaluate blackberry stems generated during pruning as a lignocellulosic biosorbent for the removal of Cr(VI) from water and to assess their potential for the sustainable remediation of chromium-contaminated aqueous systems.

Blackberry pruning residues were ground and sieved, and the particle-size fraction of 224-400 μm was used throughout the experiments. In order to improve their sorption properties, the prepared material was chemically treated using either 0.5%H_2SO_4 or 1%NaOH. Acid treatment was performed at a solid-to-liquid ratio of 1:15 for 2 h at room temperature, followed by washing and drying at 30 °C. Preliminary experiments showed better Cr(VI) removal with the acid-treated material, which was therefore selected for further experiments. Batch experiments were conducted at room temperature using model Cr(VI) solutions prepared from $K_2Cr_2O_7$. The biosorbent dosage was 1 g/L, while the initial pH of the model solution was adjusted to 2. The influence of contact time was investigated in the range of 5-180 min, and the remaining Cr(VI) concentration was determined titrimetrically using sodium thiosulfate with starch as an indicator. Cr(VI) removal was relatively rapid. The major part of the uptake occurred during the first 30 min of contact, after which only minor changes were observed. Accordingly, 30 min was selected as the equilibrium contact time for subsequent batch experiments. The initial rapid removal can be associated with the large number of readily accessible sites on the external surface of the lignocellulosic material, followed by a slower stage involving progressively less

accessible sites and diffusion into the internal structure of the biosorbent. The experimental kinetic data were evaluated using pseudo-first-order, pseudo-second-order and intraparticle diffusion models. The pseudo-first-order model showed poor agreement with the experimental data (R^2=0.3933). In contrast, the pseudo-second-order model provided an excellent fit, with R^2=0.9998 and a calculated equilibrium uptake capacity of 10.31 mg/g. Analysis using the intraparticle diffusion model resulted in two distinct linear regions (R^2=1.000 and 0.9688 for the first and second regions, respectively). Since the fitted lines did not indicate a single diffusion-controlled region, the results suggest that intraparticle diffusion was not the sole rate-controlling process and that Cr(VI) removal involved more than one mass-transfer step. Equilibrium data were evaluated using Langmuir and Freundlich adsorption models. The Langmuir model provided a substantially better description of the experimental data (R^2=0.9997) than the Freundlich model (R^2=0.8299). The maximum Cr(VI) uptake capacity estimated from the Langmuir model was 10.24 mg/g, while the Langmuir affinity constant was 0.5377 L/mg. These findings demonstrate a measurable affinity of the chemically treated blackberry pruning residues towards Cr(VI) and confirm their potential as a low-cost material for chromium removal from aqueous systems.

In addition to Cr(VI) removal efficiency, possible secondary contamination originating from the lignocellulosic biosorbent was considered. This aspect is particularly important for minimally processed plant-derived materials because soluble organic constituents may be released into the treated water. Chemical oxygen demand (COD) was therefore determined for water exposed to both untreated and chemically treated blackberry residues. A pronounced difference was observed: COD was 794 mg/L for the untreated material and only 59.6 mg/L for the treated biomass. Thus, chemical pretreatment reduced the contribution of the biosorbent to the organic load of the aqueous phase by approximately 92.5%, representing an important additional advantage of the treated material. Chemical treatment also affected the surface properties of the biomass. The point of zero charge (pHpzc) was approximately 5 for untreated blackberry residues and approximately 4 following treatment. Since the Cr(VI) removal experiments were conducted at pH 2, i.e. below the pH_{pzc} of the treated material, its surface was expected to be predominantly positively charged under the applied experimental conditions, favouring interactions with negatively charged Cr(VI) species present in acidic aqueous solution.

Overall, the results demonstrate that blackberry stems generated as pruning residues can be converted into a functional material for Cr(VI) removal from water. Acid treatment provided a material combining effective chromium uptake, rapid removal kinetics and substantially reduced release of organic matter into the treated water. The use of this readily available residual biomass therefore represents a promising waste-to-resource strategy, simultaneously addressing agricultural residue valorization and remediation of metal-contaminated water. Further studies using real wastewater matrices, regeneration experiments and continuous-flow systems would be required to evaluate its applicability under environmentally relevant and operational conditions.

Acknowledgements
This work is a result of the programs 451-03-34/2026-03/200134 and 451-03-33/2026-03/200134 supported by the Ministry of Education, Science and Technological Development of the Republic of Serbia.

References
[1] F. Fu, Q.Wang, J. Environ. Manage. 92 (2011) 407-418.

[2] T.A. Kurniawan, G.Y.S. Chan, W.H. Lo, S. Babel, Chem. Eng. J. 118 (2006) 83-98.
[3] A. Demirbas, J. Hazard. Mater. 157 (2008) 220–229.
[4] T.A.H. Nguyen, H.H. Ngo, W.S. Guo, S. Liang, Q.Y. Yue, Q. Li, T.V. Nguyen, Bioresour. Technol. 148 (2013) 574-585.

MINERAL PROFILE OF *PRUNUS SPINOSA* L. DRIED FRUITS AND THEIR POTENTIAL CONTRIBUTION TO ESSENTIAL MINERAL INTAKE

Ariana-Bianca Velciov[1], Diana Utu[2], Antoanela Cozma[1], Daniela Stoin[1], Corina Megyesi[1], Mariana-Atena Poiană[1], Laura Rădulescu[1], Diana Moigrădean[1], Marioara Drugă[1], Alda Liana – Maria[1], Alexandru Rinovetz[1], Maria Rada[2*]

[1]University of Life Sciences "King Michael I" Timisoara, Calea Aradului, 300645, Timisoara, Romania
[2]Victor Babeș University of Medicine and Pharmacy, Faculty of Pharmacy, 2 Eftimie Murgu Square, Timișoara 300041, Romania
corresponding author, e-mail: radamariam@gmail.com

Abstract
This study evaluated the mineral composition and potential contribution to essential mineral intake of dried wild blackthorn fruits (*Prunus spinosa* L.) obtained from local agri-food markets. Potassium was the predominant mineral (1754–1862 mg/100 g dry matter), followed by calcium (142–157 mg/100 g), magnesium (88.7–94.6 mg/100 g), and sodium (54.8–63.2 mg/100 g). The essential trace elements Fe, Mn, Zn, and Cu ranged from 2.63–3.84, 0.49–0.61, 0.89–1.12, and 0.34–0.44 mg/100 g, respectively. Lead and cadmium concentrations were below the quantification limits (<0.10 and <0.02 mg/100 g, respectively). A 25 g serving of dried fruits provided a notable contribution to the reference intake of K (12.90–17.90%), Mg (5.28–7.63%), Fe (3.65–12.00%), Mn (5.33–8.47%), and Cu (9.44–12.22%). Overall, the mineral profile and estimated mineral contribution indicate the potential of dried *P. spinosa* fruits as a natural mineral-rich ingredient for the development of nutritionally enhanced food products.

Keywords: *Prunus spinosa* L.; wild blackthorn, essential minerals; mineral intake.

Introduction

Prunus spinosa L., commonly known as blackthorn or sloe, is a wild species belonging to the Rosaceae family and widely distributed throughout Europe, northwestern Africa, and western Asia [1]. Its small blue-black drupes have a characteristic tart and astringent taste and typically ripen in autumn [2]. Traditionally consumed as food and used in the preparation of jams, compotes, liqueurs, and fermented beverages, blackthorn fruits have attracted increasing scientific interest due to their nutritional and functional potential [3,4]. They contain carbohydrates, dietary fiber, organic acids, vitamins, minerals, and a broad spectrum of bioactive compounds [2,5–7]. Phytochemical studies have particularly highlighted the presence of phenolic acids, flavonoids, and anthocyanins, with caffeoylquinic acids among the predominant phenolic constituents [3,4,8,9].

Previous studies have shown that wild blackthorn fruits (*Prunus spinosa* L.) possess a diverse mineral profile, characterized by the predominance of the macroelements K, Ca, Mg, and P, together with several essential trace elements [5,7–13]. In fruits from Turkey, concentrations reported on a dry weight basis were 18,706.98 mg/kg for K, 1,524.22 mg/kg for Ca, 968.15 mg/kg for Mg, and 1,514.10 mg/kg for P, whereas Na, B, Al, and Fe were detected at lower concentrations [7]. For fresh *P. spinosa* fruits collected in Romania, Cosmulescu et al. (2017) reported 32.20 mg/100 g Ca, 11.83 mg/100 g Mg, 0.48 mg/100 g Na, and 1.11 mg/100 g Fe, together with Mn, Cu, Cr, and Zn at trace levels [8].

Studies of fruits collected from wild populations have consistently identified K as the predominant mineral, accompanied by substantial amounts of Ca, Mg, and P. Babalau-Fuss et

al. (2018, 2020) reported K concentrations of 17,291–17,925 mg/kg, followed by P (1,498–1,675 mg/kg), Ca (1,425–1,476 mg/kg), Mg (896–954 mg/kg), and Na (490–591 mg/kg), together with several trace and potentially toxic elements. In wild *P. spinosa* populations from Bosnia and Herzegovina, Dedić et al. (2021) reported lower mineral concentrations and considerable variability among sampling sites, indicating differences in elemental composition according to geographical origin. Similarly, Ozzengin et al. (2023) identified K as the predominant element in Turkish wild populations (2,014.23 ± 1,087.10 mg/kg), followed by Ca and Mg, together with Fe, Zn, Cu, and Mn. For wild populations from Romania, Vlaicu et al. (2026) reported concentrations of 44.87 mg/kg Fe, 8.54 mg/kg Zn, 7.02 mg/kg Mn, and 3.47 mg/kg Cu, providing additional data on the distribution of essential trace elements in Romanian *P. spinosa* fruits.

A comprehensive elemental profile of wild blackthorn fruits collected from western and central Romania, including areas subject to different levels of anthropogenic impact, was reported by Vlad et al. (2026). Among the macroelements, K showed the highest concentrations (16,868–19,028 mg/kg), followed by S (4,925.51–5,026.77 mg/kg), P (1,411–1,629 mg/kg), Ca (1,365–1,562 mg/kg), and Mg (871–982 mg/kg). The essential trace elements included Fe (17.9–38.9 mg/kg), Zn (5.9–14.8 mg/kg), Mn (3.5–9.8 mg/kg), and Cu (2.0–4.8 mg/kg). Other elements detected included Al (11.76–36.58 mg/kg), Si (43.68–88.73 mg/kg), Sr (2.96–8.36 mg/kg), and Rb (2.18–6.07 mg/kg). Potentially toxic elements, including Ni (1.71–4.47 mg/kg) and Cr (2.96–7.88 mg/kg), were also detected, whereas Pb (0.019–0.052 mg/kg), Cd (0.016–0.036 mg/kg), As (0.171–0.421 mg/kg), and Hg (0.018–0.039 mg/kg) occurred at considerably lower concentrations. The variation in elemental concentrations across sampling areas suggests that differences in environmental conditions and anthropogenic influence may contribute to the variability observed in the elemental composition of wild *P. spinosa* fruits.

Overall, the available literature indicates that *P. spinosa* fruits possess a diverse mineral profile, with K consistently reported as the predominant element, followed by Ca, P, and Mg, although the relative concentrations vary according to geographical origin, growing conditions, and analytical methodology. Fe, Mn, Zn, and Cu represent important components of the essential trace-element fraction. The variation reported among populations and geographical regions may be associated with differences in pedoclimatic characteristics, soil composition, habitat conditions, and environmental factors.

In this context, characterizing the mineral profile of dried *P. spinosa* fruits is of particular interest because drying reduces water content, thereby increasing the concentration of minerals per unit of product and facilitating their use as a powder or food ingredient. The assessment of essential macro- and trace elements, together with potentially toxic elements such as Pb and Cd, provides complementary information on the nutritional characteristics and elemental quality of the dried fruit. Furthermore, relating the measured mineral concentrations to reference intakes allows the potential contribution of a defined serving of dried *P. spinosa* fruits to daily mineral intake to be estimated.

Experimental

A 200 g sample of fruits was collected from each of three local farmers' markets (LFM), where wild blackthorn fruits were offered for sale by local foragers. The fruits were harvested at optimal ripeness and coded as LFM-1, LFM-2, and LFM-3, according to their market origin. Fresh fruits (Figure 1a) were thoroughly washed, drained, and dried at 60 °C (Figure 1b). The dried fruits were subsequently ground using a grinder, passed through a sieve (Figure 1c), and stored under refrigerated conditions (approximately 5 °C) until analysis.

The concentrations of essential mineral elements (Na, K, Ca, Mg, Fe, Mn, Zn, and Cu) and potentially toxic elements (Pb and Cd) were determined by flame atomic absorption spectrometry (FAAS) using an air–acetylene flame. Prior to analysis, the samples were

subjected to dry ashing, followed by dissolution of the resulting ash in nitric acid. The obtained solutions were analyzed using a Varian AA-240 FS atomic absorption spectrometer [13]. All samples were analyzed in triplicate.



a b c

Figure 1. Fresh (a), dried (b), and powdered (c) fruits of wild blackthorn (*Prunus spinosa* L.)

Results and discussion

The concentrations of mineral elements determined in the analyzed wild blackthorn (*Prunus spinosa* L.) fruit samples are presented in Table 1.

Table 1. Mean concentrations of essential and toxic mineral elements in wild blackthorn fruits (*Prunus spinosa*)

Sample code	Mineral element, mean value (mg/100g DM)									
	Na	K	Ca	Mg	Fe	Mn	Zn	Cu	Pb	Cd
LFM-1	54.8± 0.90	1754± 48	142± 2.44	88.7± 1.10	2.63± 0.18	0.49± 0.04	0.89± 0.09	0.34± 0,04	< 0.10	< 0.02
LFM-2	63.2± 0.86	1862± 7.79	157± 3.27	94,6± 2.48	3,84± 0.14	0.61± 0.09	1.12± 0.11	0.44± 0.05	< 0.10	< 0.02
LFM-3	56.2± 0.90	1811± 7.25	152± 2.94	93.1± 2.57	3.68± 0.20	0.53± 0.09	1.08± 0.09	0.41± 0.06	< 0.10	< 0.02

LFM-1- local farmers' market 1, LFM-2 (local farmers' market 2 and LFM-3 (local farmers' market 3. DM-dried matter.

The results (Table 1) showed a clear predominance of potassium (K) in the mineral profile of *Prunus spinosa* fruits, with concentrations ranging from 1754 to 1862 mg/100 g dry matter, the highest values among the analyzed elements. Calcium (Ca) and magnesium (Mg) were present at intermediate concentrations, ranging from 142 to 157 and 88.7 to 94.6 mg/100 g, respectively, whereas sodium (Na) concentrations ranged from 54.8 to 63.2 mg/100 g.

Among the essential trace elements, iron (Fe) showed the highest concentrations (2.63–3.84 mg/100 g), followed by zinc (Zn) (0.89–1.12 mg/100 g), manganese (Mn) (0.49–0.61 mg/100 g), and copper (Cu) (0.34–0.44 mg/100 g). Although the absolute differences among samples were relatively small, Mn exhibited the greatest relative variation. Overall, LFM-2 showed the highest concentrations of most essential elements analyzed, indicating that mineral composition in P. spinosa fruits varies by market origin.

The potentially toxic elements Pb and Cd were below the respective quantification limits in all samples (<0.10 and <0.02 mg/100 g dry matter, respectively), indicating very low levels in the investigated fruits. Overall, the wild *P. spinosa* fruits exhibited a mineral profile dominated by K, Ca, and Mg, together with appreciable concentrations of Fe, Zn, Mn, and Cu. The differences observed among the three LFM samples may be associated with variations in microhabitat, soil characteristics, environmental conditions, and geographical origin.

Overall, the elemental profile determined in the present study was broadly consistent with that reported for wild *P. spinosa* populations, with K as the predominant element, followed by Ca, Mg, and Na. The concentrations of the macroelements and essential trace elements were generally comparable to those reported by Babalau-Fuss et al. (2018, 2020), Ozzengin et al. (2023), and Vlad et al. (2026), particularly for K, Ca, Mg, Fe, Mn, Zn, and Cu. Pb and Cd concentrations were below the analytical method's quantification limits (<0.10 and <0.02

mg/100 g dry matter, respectively), indicating very low levels in the investigated samples and consistent with the low concentrations reported for wild *P. spinosa* populations.
Based on the experimental mineral composition and the methodology described by Rada et al. (2024), the contribution of a 25 g serving of dried wild blackthorn fruits to the reference intake of selected minerals was estimated, as presented in Table 2 [15].

Table 5. Contribution of a 25-g serving of dried wild blackthorn fruits (Prunus spinosa L.) to the recommended daily mineral intake

Element	Persons	Mineral intake,%			Element	Persons	Mineral intake, %		
		LFM-1	LFM-2	LFM-3			LFM-1	LFM-2	LFM-3
Na	Men	0.91	1.05	0.94	Fe	Men	8.22	12.00	11.50
	Women	0.91	1.05	0.94		Women	3.65	5.33	5.11
K	Men	12.90	13.69	13.32	Mn	Men	5.33	6.63	5.76
	Women	16.87	17.90	17.41		Women	6.81	8.47	7.36
Ca	Men	3.55	3.92	3.80	Zn	Men	2.02	2.55	2.45
	Women	3.55	3.92	3.80		Women	2.78	3.50	3.38
Mg	Men	5.28	5.63	5.54	Cu	Men	9.44	12.22	11.39
	Women	7.15	7.63	7.51		Women	9.44	12.22	11.39

Note: Values are expressed as percentages (%) of the recommended daily intake contributed by a 25-g serving of dried fruits. Men and women aged 19–50 years were considered.
LFM-1, LFM-2, and LFM-3 denote dried P. spinosa fruit samples obtained from local farmers' markets 1, 2, and 3, respectively

A 25 g serving of dried *P. spinosa* fruits provided measurable contributions to the reference intake of essential minerals, with the highest contribution observed for K (438.5–465.5 mg; 12.90–17.90%), followed by Cu (9.44–12.22%), Mn (5.33–8.47%), Mg (5.28–7.63%), Fe (3.65–12.00%), and Zn (2.02–3.50%). Calcium contributed approximately 3.55–3.92% of the reference intake, whereas sodium contributed only 0.91–1.05%. LFM-2 showed the highest contribution for most minerals, consistent with the higher concentrations observed for this sample in Table 1. Overall, a 25 g serving of dried *P. spinosa* fruits provided a notable contribution to K intake and smaller contributions to the intake of several other essential minerals.

Conclusion

Dried *Prunus spinosa* L. fruits exhibited a mineral profile dominated by K, followed by Ca and Mg, together with appreciable levels of Fe, Mn, Zn, and Cu. The mineral composition was broadly consistent with previous reports for wild *P. spinosa* populations, particularly those from Romania. A 25 g serving provided a notable contribution to K intake and smaller contributions to the intake of Mg, Fe, Mn, and Cu. The differences observed among fruit sources may be associated with geographical and environmental conditions. Pb and Cd concentrations were below the quantification limits in all samples. Overall, the mineral composition of dried *P. spinosa* fruits indicates their potential as a source of essential minerals and as a functional ingredient for the development of nutritionally enhanced food products.

References

[1] Popescu, I. & Caudullo, G., Prunus spinosa in Europe: distribution, habitat, usage and threats. In: San-Miguel-Ayanz, J., de Rigo, D., Caudullo, G., Houston Durrant, T., Mauri, A. (Eds.), European Atlas of Forest Tree Species. Publ. Off. EU, Luxembourg, 2016, pp e018f4e+.
[2] Bei M.F., Apahidean A.I., Budău R., Rosan C.A., Popovici R., Memete A.R., Domocos D., Vicas S.I., An Overview of the Phytochemical Composition of Different Organs of *Prunus spinosa* L., Their Health Benefits and Application in Food Industry. Horticulturae vol 10/issue29. 2024.

[3] Tamayo-Vives C., Úbeda M. Morales P., García-Herrera P., Sánchez-Mata M.C., Crataegus monogyna Jacq., Sorbus aria (L.) Crantz and Prunus spinosa L.: From Edible Fruits to Functional Ingredients: A Review, Foods vol.14, 2299, 2025,
[4] Marčetić M., Samardžić S., Ilić T., Božić D.D., Vidović B., Phenolic Composition, Antioxidant, Anti-Enzymatic, Antimicrobial and Prebiotic Properties of *Prunus spinosa* L. Fruits, Foods, 2023, vol. 11/issue 20, 3289.
[5] Vlaicu P. A., Varzaru I., Turcu R. P., Oancea A. G., Untea A. E., Comparative evaluation of wild plum (*Prunus spinosa* L.) stone fruits and leaves: Insights into nutritional composition, antioxidant properties, and polyphenol profile. Foods, vo. 15/issue 1, 142, 2026.
[6] Babalau-Fuss V., Becze A., Moldovan A., Grebla O. B., Pop A. I., Talos I., Tofană M., Evaluation of nutritional value of blackthorn and rose fruits, Hop and Medicinal Plants, Year XXVIII, no. 1-2, 2020.
[7] Marakoglu T., Arslan D., Özcan M., Hacıseferogulları H., Proximate composition and technological properties of fresh blackthorn (Prunus spinosa L. subsp dasyphylla (Schur.)) fruits, Journal of Food Engineering, vol. 68/issue 2, pp 137-142, 2005
[8] Ozzengin B., Zannou O., Koca I.. Quality attributes and antioxidant activity of three wild plums from *Prunus spinosa* and *Prunus domestica* species. Measurement: food, vol. 10, 100079, 2023.
[9] Cosmulescu S., Trandafir I., Nour V., Phenolic acids and flavonoids profiles of extracts from edible wild fruits and their antioxidant properties, International Journal Of Food Properties, vol. 20/issue 12, pp 3124–3134, 2017
[10] Babalau-Fuss V., Grebla O.B., Cadar O., Hoaghia M.-A., Kovacs M.-E., Moldovan A., Maria Tofana M., Determination of chemical composition and fatty acids of blackthorn fruits (*Prunus spinosa*) grown near Cluj-Napoca, NW Romania, Agricultura vol. 1–2/105-106, pp 90-95, 2018.
[11] Dedić A., Dţudţević-Čančar H., Alispahić A., Tahirović I., Muratović, E., In-vitro antioxidant and antimicrobial activity of aerial parts of *Prunus spinosa* L. growing wild in Bosnia and Herzegovina, Int. J. Pharm. Sci. Res, vol.12/issue 7, pp 3643-3653, 2021.
[12] Vlad A. I., Bartha S., Timiș-Gânsac V., Burescu L. I. N., Adrian T., Bei M. F., Rebrean F.A., Calugar A., Motiu P. T., Bora, F. D., Multi-Element Composition of Wild Prunus spinosa Fruits Across Contrasting Environments: Implications for Food Safety and Quality. Foods, vol.15/issue 10, 1726, 2026.
[13] Velciov A. B., Popescu G. S., Cozma A., Brei L., Stoin D., Lalescu V. D., Rădulescu L., Megyesi C. I., Rada, M. M., Preliminary research on garlic peel powder as a source of essential mineral elements. Journal of Agroalimentary Processes and technologies, vol.30/issue 4, 463-470, 2024
[14] European Commission. Commission Regulation (EU) 2023/915 of 25 April 2023 on maximum levels for certain contaminants in food and repealing Regulation (EC) No 1881/2006. Official Journal of the European Union, L 119, pp 103–157, 2023
[15] Rada M., Alda, S. Velciov A., Scedei D., Anghel I. M., Dobrei A., Nistor E., Danci M., Evaluation of some essential elements in walnut kernel, Scientific Papers, Series B. Horticulture, vol. 68/issue 1, pp 129, 2024

MATHEMATICAL MODELING AND ARTIFICIAL INTELLIGENCE FOR MULTI-CRITERIA ASSESSMENT OF ENVIRONMENTAL PRESSURES FROM ENERGY SYSTEMS: EVIDENCE FROM THE REPUBLIC OF SERBIA

Bojana Velečković Gajinović[1], Nebojša Ralević[1], Vladimir Đaković[1], Andrija Blesić[1], Dejan Ćebić[2]

[1]University of Novi Sad, Faculty of Technical Sciences, Trg Dositeja Obradovića 6, 21000 Novi Sad, Serbia
[2]University of Belgrade, Faculty of Mining and Geology, Đušina 7, 11000 Belgrade, Serbia
e-mail: veleckovic.gajinovic.dt1.2024@uns.rs

Abstract
Large energy systems are important sources of environmental pressure due to atmospheric emissions. This study proposes an integrated mathematical-artificial intelligence framework for multi-criteria assessment of major Serbian thermal-energy systems. Plant-level European Environment Agency data for 2018-2023 were analysed using sulphur oxides (SOx), nitrogen oxides (NOx) and particulate matter (PM10). A composite Environmental Pressure Index (EPI) was constructed by min-max normalization and Shannon entropy weighting. Panel-wide weights were 0.2940 for SOx, 0.3487 for NOx and 0.3573 for PM10. TENT A ranked first and TENT B second in every analysed year, although their EPI values decreased by approximately 18.0% and 17.5% between 2018 and 2023. K-means clustering of standardized plant-year observations achieved the highest silhouette score for K=3 (0.591). Principal component analysis showed that the first two components explained 97.4% of total variance. The combined approach provides complementary information through interpretable ranking and unsupervised identification of characteristic emission profiles.
Keywords: environmental pressure; entropy weighting; K-means; PCA; energy systems; Artificial Intelligence

Introduction
Large combustion and thermal-energy systems are relevant sources of atmospheric pollutants, making their environmental assessment inherently multi-dimensional. An energy system may perform differently across pollutants, limiting the usefulness of single-indicator rankings. Multi-criteria assessment is therefore appropriate when several non-equivalent environmental indicators must be interpreted jointly [1–4]. In this study, Shannon entropy is used for objective weighting, assigning greater information-based weight to criteria with higher dispersion across observations. This improves reproducibility, although the resulting weights reflect statistical discrimination rather than environmental toxicity.
Environmental pressure is also relevant to operational and strategic risk assessment, as changing emission profiles may affect regulatory compliance, resource allocation and long-term planning. The proposed framework is therefore intended as a decision-support layer for environmental risk monitoring, rather than a substitute for toxicological, health-risk or regulatory assessment.
Unsupervised machine-learning methods provide a complementary perspective by identifying groups with similar emission profiles without predefined environmental classes. K-means partitions standardized observations by minimizing within-cluster squared distances, while silhouette analysis supports the selection of the cluster number [5,6]. Principal component analysis (PCA) provides a low-dimensional representation of multivariate structure [7]. The methodological contribution lies in combining a transparent composite index with unsupervised

pattern recognition: the former provides an interpretable longitudinal assessment, while the latter identifies characteristic emission profiles independently of the EPI.

The study also builds on the authors' previous research in artificial intelligence, quantitative modelling and optimization. Earlier work examined AI applications and responsible use of AI-supported methods [8], while quantitative optimization approaches were investigated in investment analysis and portfolio management [9]. These studies provide a methodological basis for integrating mathematical modelling, data-driven weighting and unsupervised machine learning in the assessment of environmental pressures in energy systems.

The analysis uses plant-level records from the European Environment Agency industrial reporting dataset [10]. The broader EEA industrial reporting system contains administrative information and pollutant releases for major industrial sites and includes detailed reporting for large combustion plants. For the present case study, seven Serbian thermal-energy systems with comparable SOx, NOx and PM10 records over 2018-2023 were selected: RB Kolubara - Prerada, TE Kolubara, TE Morava, TENT A, TENT B, TE Kostolac A and TE Kostolac B. The resulting panel contains 42 potential plant-year observations; one observation is incomplete because PM10 for RB Kolubara - Prerada in 2020 is missing. No imputation was performed, leaving 41 complete three-pollutant observations for multivariate analysis.

The three indicators were normalized over the complete 2018-2023 panel using min-max normalization, as shown in Eq. (1):

$$z_{ij} = \frac{x_{ij} - {x_j}^{min}}{{x_j}^{max} - {x_j}^{min}} \quad (1)$$

Using a common normalization range for the entire panel, rather than recalculating the scale separately for each year, preserves the longitudinal meaning of changes in EPI.

Objective criterion weights were then obtained by Shannon entropy. The normalized proportion of each observation was calculated using Eq. (2):

$$p_{ij} = \frac{z_{ij}}{\sum_{i=1}^{n} z_{ij}} \quad (2)$$

and the corresponding entropy of criterion j using Eq. (3):

$$e_j = -\frac{1}{ln\, n} \sum_{i=1}^{n} p_{ij}\, ln\, p_{ij} \quad (3)$$

For $p_{ij} = 0$, the standard convention $p_{ij} ln\left(p_{ij}\right) = 0$ was used.

The degree of diversification of each criterion is given by Eq. (4):

$$d_j = 1 - e_j \quad (4)$$

and the final, normalized entropy weight by Eq. (5):

$$w_j = \frac{d_j}{\sum_{j=1}^{m} d_j} \quad (5)$$

The composite Environmental Pressure Index (EPI) was then calculated for each observation using Eq. (6):

$$EPI_i = \sum_{j=1}^{m} w_j z_{ij} \quad (6)$$

The resulting panel-wide entropy weights were wSOx=0.2940, wNOx=0.3487 and wPM10=0.3573.

Complete plant-year observations were standardized according to Eq. (7) before K-means clustering, because Euclidean-distance methods are scale-sensitive:

$${x_{ij}}^* = \frac{x_{ij} - \mu_j}{\sigma_j} \quad (7)$$

Candidate solutions K=2,...,6 were compared using the silhouette coefficient defined in Eq. (8):

$$s(i) = \frac{b(i) - a(i)}{max\{a(i), b(i)\}} \quad (8)$$

and PCA was applied to the same standardized matrix. A fixed random initialization was used for reproducibility. The EPI is a relative emission-pressure index and should not be interpreted as a toxicological or health-risk measure.

The complete analysis pipeline was implemented as a reproducible workflow. Normalization limits, entropy weights, cluster centroids and PCA loadings were estimated consistently on the 2018–2023 panel. A fixed random initialization was used for K-means. The pollutant series were checked for outliers and unit consistency, with no additional filtering beyond exclusion of the single incomplete PM10 observation.

Results and discussion

Entropy weighting produced wSOx=0.2940, wNOx=0.3487 and wPM10=0.3573. The weights are relatively balanced, with PM10 providing the largest data-driven discrimination. They represent statistical information content in the analysed sample and should not be interpreted as relative toxicity.

Table 1. Environmental Pressure Index (EPI) by energy system, 2018-2023.

Energy system	**2018**	**2019**	**2020**	**2021**	**2022**	**2023**
TENT A	0.905	0.883	0.951	0.852	0.842	0.742
TENT B	0.702	0.594	0.629	0.446	0.483	0.579
TE Kostolac B	0.606	0.349	0.469	0.212	0.230	0.280
TE Kostolac A	0.267	0.214	0.243	0.323	0.262	0.274
TE Kolubara	0.369	0.396	0.424	0.373	0.174	0.160
TE Morava	0.054	0.050	0.060	0.037	0.125	0.067
RB Kolubara - Prerada	0.008	0.007	N/A*	0.004	0.023	0.026

** N/A - PM10 value for RB Kolubara - Prerada in 2020 was not reported; the incomplete observation was excluded from analyses requiring all three pollutants.*

Source: Authors' calculations based on European Environment Agency (EEA) data [10].

TENT A and TENT B occupied the first two EPI positions throughout 2018-2023, while their EPI values declined by approximately 18.0% and 17.5%, respectively. Larger reductions occurred for TE Kolubara (56.6%) and TE Kostolac B (53.9%). The panel mean declined from its 2020 local maximum of 0.463 to 0.304 in 2023, showing that lower average pressure can coexist with persistent differences among individual energy systems.

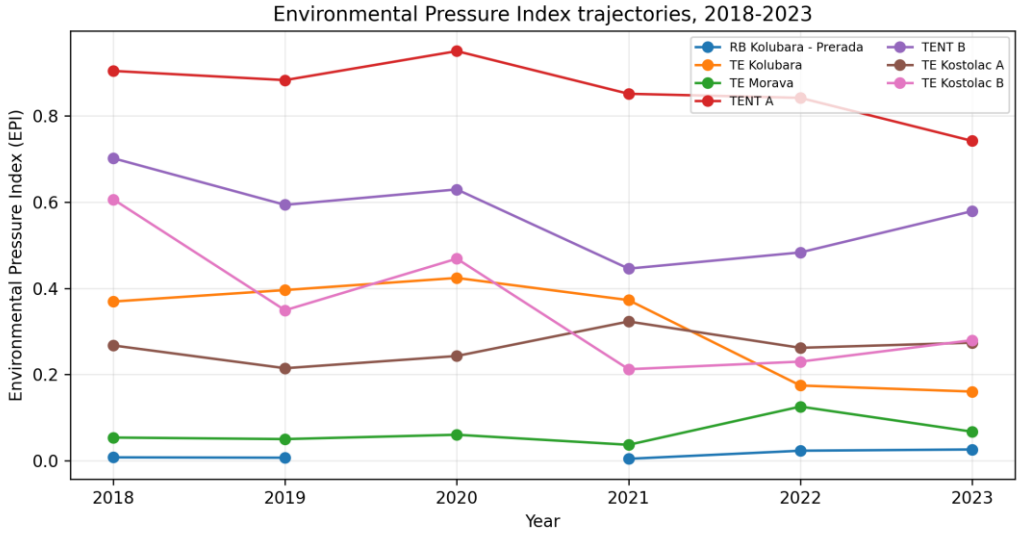


Figure 1. EPI trajectories of the analysed Serbian energy systems, 2018-2023.

Source: Authors' calculations and visualization based on European Environment Agency (EEA) data [10].

For the 41 complete plant-year observations, K=3 achieved the highest silhouette score (0.591), while K=6 was nearly equivalent (0.590). The three-cluster solution was therefore retained as

the more parsimonious and interpretable representation of the dominant emission-profile structure.

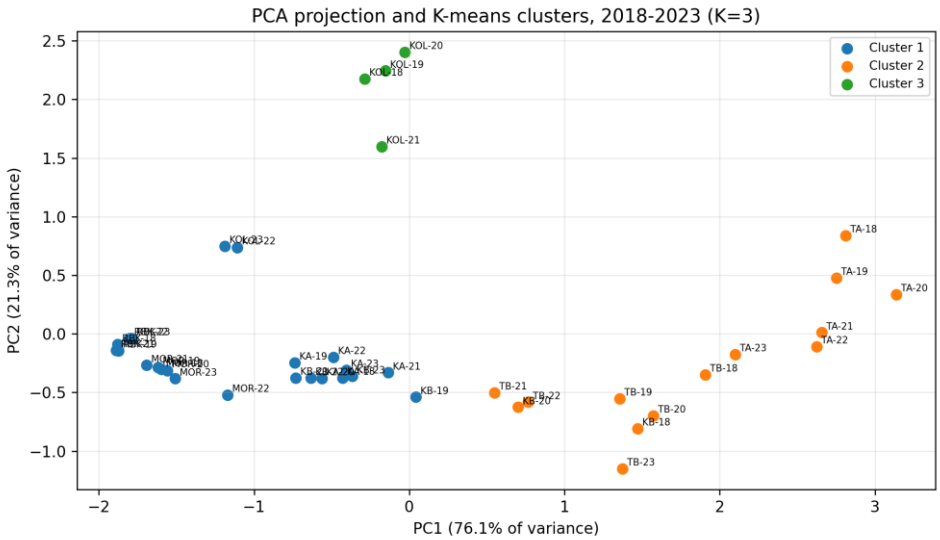


Figure 2. PCA projection of standardized SOx, NOx and PM10 observations with K-means clusters (K=3).

Source: Authors' calculations and visualization based on European Environment Agency (EEA) data [10].

PC1 explained 76.1% and PC2 21.3% of total variance (97.4% combined). TENT A and TENT B observations lie toward the high-PC1 region, while several TE Kolubara observations show a distinct high-PC2 pattern. Thus, EPI provides an interpretable weighted ranking, whereas clustering and PCA preserve differences in pollutant composition; their agreement is complementary rather than an independent validation because all methods use the same pollutant variables.

The EPI measures relative absolute emission pressure rather than operational emission efficiency because plant-level energy input was unavailable. It is sample- and period-dependent, entropy weights reflect dispersion rather than toxicity or health impact, and K-means results are exploratory given the modest sample and Euclidean geometry assumption. The missing 2020 PM10 observation was excluded rather than imputed.

Conclusion

The proposed framework combines transparent multi-criteria aggregation with unsupervised pattern recognition to assess environmental pressure from Serbian thermal-energy systems. EPI summarizes relative combined pressure, while clustering and PCA reveal differences in emission-profile structure. The results indicate persistent differences among energy systems despite overall reductions in pressure and demonstrate the complementary value of interpretable indexing and multivariate analysis.

For energy-systems management, the framework can support environmental-risk monitoring by identifying persistent high-pressure patterns and changes in multivariate emission profiles. Future research should integrate plant-level energy-input data, additional pollutants and operational variables, test alternative weighting and clustering methods, and connect environmental-pressure indicators with quantitative risk-management and energy-system planning models.

Acknowledgements
This research was partly supported by the Science Fund of the Republic of Serbia, GRANT No. 7632, Project "Mathematical Methods in Image Processing under Uncertainty"-MaMIPU. This research was supported by the Ministry of Science, Technological Development and Innovation and the Faculty of Technical Sciences, University of Novi Sad, through the project "Improvement of Teaching Quality in the Study Programmes of the Department through the Implementation of Scientific Research Results in the Field of Industrial Engineering and Management". The authors were also financially supported by the project of the Department of Fundamental Disciplines in Engineering, "Artificial Intelligence and the Possibilities of its Application for the Improvement of the Teaching Process in General Disciplines". Additionally, this research was supported by the Ministry of Science, Technological Development and Innovation (Contract No. 451-03-34/2026-03/200156) and the Faculty of Technical Sciences, University of Novi Sad, through the project "Scientific-Research and Artistic-Research Work of Researchers in Teaching and Associate Positions at the Faculty of Technical Sciences, University of Novi Sad 2026" (No. 01-3609/1).

References
[1] Filar, J.A., Ross, N.P., Wu, M.-L. Environmental Assessment Based on Multiple Indicators. Calcutta Statistical Association Bulletin, 2003, 54(1-2), 93-104.
[2] Shannon, C.E. A Mathematical Theory of Communication. Bell System Technical Journal, 1948, 27, 379-423, 623-656.
[3] Saraswat, S.K., Digalwar, A.K. Evaluation of energy alternatives for sustainable development of energy sector in India: An integrated Shannon entropy fuzzy multi-criteria decision approach. Renewable Energy, 2021, 171, 58-74.
[4] Gan, X., Fernandez, I.C., Guo, J., Wilson, M., Zhao, Y., Zhou, B., Wu, J. When to use what: Methods for weighting and aggregating sustainability indicators. Ecological Indicators, 2017, 81, 491-502. https://doi.org/10.1016/j.ecolind.2017.05.068.
[5] Lloyd, S. Least squares quantization in PCM. IEEE Transactions on Information Theory, 1982, 28(2), 129-137.
[6] Rousseeuw, P.J. Silhouettes: A graphical aid to the interpretation and validation of cluster analysis. Journal of Computational and Applied Mathematics, 1987, 20, 53-65.
[7] Jolliffe, I.T., Cadima, J. Principal component analysis: a review and recent developments. Philosophical Transactions of the Royal Society A, 2016, 374, 20150202.
[8] Velečković Gajinović, B., Ralević, N., Đaković, V. Mogućnosti i rizici primene veštačke inteligencije u obrazovnom sistemu Republike Srbije [Opportunities and Risks of the Application of Artificial Intelligence in the Education System of the Republic of Serbia]. XXXI Skup TRENDOVI RAZVOJA – TREND 2025, Vrnjačka Banja, Serbia, 3-5 December 2025, pp. 178-180.
[9] Velečković Gajinović, B.G., Ralevic, N.M., Djakovic, V.Dj. Quantitative Investment Analysis and Portfolio Management: An Optimization Perspective. Proceedings of the International Symposium on Analytical and Environmental Problems, 2025, Vol. 31, pp. 308-311. University of Szeged, Szeged. ISBN 978-963-688-078-1.
[10] European Environment Agency. Industrial Reporting under the Industrial Emissions Directive 2010/75/EU and European Pollutant Release and Transfer Register Regulation (EC) No 166/2006. European Industrial Emissions Portal, dataset used for the present analysis: 2007-2023 release.

MACROPOROUS RESIN MODIFICATION FOR COVALENT FRUCTOSYLTRANSFERASE IMMOBILIZATION AND APPLICATION OF THE RESULTING BIOCATALYST IN FRUCTO-OLIGOSACCHARIDE PRODUCTION

Milica Veljković[1], Milica Simović[2], Katarina Banjanac[1], Anja Petrov Ivanković[1], Ana Vukoičić[1], Dejan Bezbradica[2]

[1]Innovation Center of Faculty of Technology and Metallurgy, Belgrade, Serbia
[2]Faculty of Technology and Metallurgy, University of Belgrade, Belgrade, Serbia
e-mail: mveljkovic@tmf.bg.ac.rs

Abstract

Fructosyltransferases (FT) are biocatalysts that catalyze the transfructosylation of sucrose, enabling the production of fructo-oligosaccharides (FOS), established prebiotics with numerous well-documented health benefits [1]. However, their sensitivity to process conditions may affect their performance in industrial processes, making enzyme immobilization a widely used approach for enhancing stability, allowing reuse, and enabling continuous production processes [2]. In this study, FT from the commercial enzyme preparation Pectinex® Ultra SP-L was immobilized onto the macroporous ion-exchange resin Purolite® A109, whose surface was modified with glutaraldehyde (GA) and epichlorohydrin (EP) to introduce aldehyde and epoxy functional groups, respectively, and enable covalent bonding with functional groups of the enzyme. The immobilization process was optimized in terms of pH, buffer ionic strength, immobilization time, and enzyme concentration. Under the determined optimal conditions, the catalytic activities of the immobilized preparations ranged from 243 to 371 IU/g of support. Although the lowest activity was achieved using the epoxy-functionalized support, this preparation exhibited the highest selectivity towards FT relative to pectinases, indicating the possibility of simultaneously immobilizing the target enzyme, FT, while partially purifying it from pectinases and other hydrolytic enzymes present in the commercial preparation. The obtained immobilized preparations were further evaluated in the synthesis of FOS using sucrose for 24 h at 50 °C. The proportion of FOS in total carbohydrates increased throughout the reaction for all tested preparations, with the epoxy-functionalized support showing the most favorable performance, reaching a maximum FOS proportion of 53% after 9 h. In comparison, approximately 50% FOS was achieved after 21 h using the GA-activated supports. These results demonstrate the suitability of the epoxy-functionalized Purolite® A109 resin as a support for the development of a stable and selective immobilized FT biocatalyst that could be further evaluated in various reactor systems for FOS production.

Acknowledgements

This work was funded by the Ministry of Science, Technological Development, and Innovation of the Republic of Serbia (contract no. 451-03-33/2026-03/200287 and 451-03-34/2026-03/200135).

References

[1] G.S. Dias, A.C. Vieira, G. Baioni e Silva, N.F. Simões, T.S. Milessi, L.S. Saraiva, M.C.A. Xavier, A.A. Longati, M.F.A. Rodrigues, S. Fernandes, et al., Processes 13 (2025) 1252.
[2] A.A. Homaei, R. Sariri, F. Vianello, R. Stevanato, J. Chem. Biol. 6 (2013) pp.185–205.

DYEING AND FUNCTIONALIZATION OF SILK FABRICS VIA *IN SITU* ENZYMATIC POLYMERIZATION OF ESCULIN

Ana Vukoičić[1], Aleksandra Ivanovska[1], Anja Petrov Ivanković[1], Marija Ćorović[2], Ana Milivojević[2], Dejan Bezbradica[2]

[1]Innovation Centre of Faculty of Technology and Metallurgy, Belgrade, Serbia
[2]University of Belgrade, Faculty of Technology and Metallurgy, Belgrade, Serbia
e-mail: avukoicic@tmf.bg.ac.rs

Abstract

Green dyeing technologies are gaining more and more attention due to the negative effects of conventional chemical-based processes. Natural dyes have received much attention and there is a growing need for finding environmentally friendly and sustainable dyeing methods. For this purpose, the combination of green enzymes such as laccases and naturally occurring compounds like flavonoids is being explored [1]. This reaction can yield novel colored, bioactive oligomeric/polymeric products [2, 3]. In this work, enzymatic oligomerization of esculin has been applied for *in situ* dyeing and functionalization of silk fabric (SILK) and chitosan-modified silk fabric (SILK-CH). As a catalyst, laccase from *Trametes versicolor* has been used. Functionalized SILK and SILK-CH fabrics showed excellent antioxidant activity of 80.53% and 96.01% respectively, which remained in the same range after washing cycle. Both fabrics showed yellow coloration after the reaction, but SILK-CH showed better ability to bond synthesized oligomers, indicated by higher color strength values for this fabric. These results indicate that the presented dyeing method can be successfully applied for simultaneous dyeing and functionalization of silk fabric.

Acknowledgements

This work was funded by the Ministry of Science, Technological Development, and Innovation of the Republic of Serbia (contract no. 451-03-33/2026-03/200287 and 451-03-34/2026-03/200135).

References

[1] J. Polak, J., A. Jarosz-Wilkolazka, Process Biochem. 47 (2012) 9
[2] S. Borah, R.M. Kalita, S. Hazarika, P. Gogoi, Acid. Ind. Eng. Chem. Res. 63 (2024) 35
[3] A. Vukoičić, A, A. Ivanovska, M. Ćorović, A. Petrov Ivanković, A. Milivojević, D. Bezbradica, Textiles 6 (2026) 18

GREEN EXTRACTION OF POLYPHENOLS FROM PEPPER SEED BY-PRODUCTS USING NATURAL DEEP EUTECTIC SOLVENTS (NADES)

Jelena Vukosavljević[1], Sara Hourani[1], Boris M. Popović[2], Branimir Pavlić[1]

[1] Faculty of Technology Novi Sad, University of Novi Sad, Blvd. cara Lazara 1, 21000 Novi Sad, Serbia
[2] Faculty of Agriculture, University of Novi Sad, Trg Dositeja Obradovića 8, 21000 Novi Sad, Serbia
e-mail: jelena.vukosavljevic@uns.ac.rs

Abstract

The valorization of agro-industrial waste has gained increasing attention as a sustainable approach for recovering valuable bioactive compounds while reducing waste generation [1]. Pepper seed by-products, generated during pepper processing, represent an underutilized source of phenolic compounds with potential antioxidant properties. In this study, natural deep eutectic solvents (NADES) were investigated as environmentally friendly extraction media for the recovery of bioactive compounds from pepper seed by-products. Fifteen different NADES systems were prepared and tested using dried and ground pepper seed by-products. A one-factor-at-a-time (OFAT) approach was applied, with the type of NADES serving as the test variable, while extraction temperature, time, and solid-liquid ratio were kept constant. The extraction performance was evaluated based on the total phenolic content (TPC) and DPPH radical scavenging activity. The TPC values obtained ranged from 3.79 to 8.55 mg GAE/g DW, with the highest value obtained using N5, composed of choline chloride, lactic acid and fructose (2:1:1). The DPPH radical scavenging activity ranged from 0.64 to 3.26 mg TE/g DW, with the highest value observed for N11, composed of proline and glycerol (1:2). The differences among the tested systems demonstrated that the composition of NADES plays an important role in the extraction of phenolic and antioxidant compounds from pepper seed by-products. Based on the screening results, the most promising NADES system will be selected for further optimization of the extraction process. In the next stage, extraction temperature, time, and solid-to-liquid ratio will be systematically investigated with the aim of maximizing polyphenol recovery. Overall, the present findings demonstrate the potential of NADES as environmentally friendly extraction media for the valorization of pepper seed by-products and provide a basis for further process optimization.

Acknowledgements

The authors would like to thank the Ministry of Science, Technological Development and Innovation of the Republic of Serbia for financial support through Contract No 451-03-33/2026-03/200007.

References

[1] Yadav, S., Malik, K., Moore, J. M., Kamboj, B. R., Malik, S., Malik, V. K., ... & Bishnoi, D. K. (2024). Valorisation of agri-food waste for bioactive compounds: recent trends and future sustainable challenges. *Molecules*, *29*(9), 2055.

CYCLIC ION MOBILITY MASS SPECTROMETRY REVEALS NEW HUMAN BRAIN-ASSOCIATED GLYCOLIPID BIOMARKERS

Mirela Sarbu[1], Raluca Ica[1,2], Livia Deveseleanu-Corici[3], David E. Clemmer[4], Alina D. Zamfir[1,5]

[1]National Institute for Research and Development in Electrochemistry and Condensed Matter, Timişoara, Romania
[2]Faculty of Exact Sciences, Aurel Vlaicu University of Arad, Arad, Romania
[3]Romanian Academy, "Coriolan Drăgulescu" Institute of Chemistry, Timişoara, Romania
[4]Department of Chemistry, The College of Arts & Science, Indiana University, Bloomington, Indiana, USA
[5]Department of Technical and Natural Sciences, Faculty of Food Engineering, Tourism and Environmental Protection, Aurel Vlaicu University of Arad, Romania
e-mail: alina.zamfir@uav.ro

Abstract
Cyclic ion mobility mass spectrometry (cIMS) was applied to human brain gangliosides, extending previous work in ion mobility mass spectrometry (IMS-MS) and tandem MS (MS/MS)of this structurally complex glycolipid class. The enhanced power of cIMS, **achieved through its extended path length** resolved isomeric and low-abundance ganglioside species that might unseparated by traveling-wave IMS, leading to the discovery of new human brain-associated glycolipid structures, several of which showed disease-associated alterations. These results establish cIMS as a promising tool for glycolipid biomarker discovery in neurological disorders and cancer.

Introduction
IMS-MS extends MS by separating ions according to their size, shape, and charge, adding a further dimension of resolution beyond *m/z*. This is particularly valuable for gangliosides, a structurally diverse class of brain glycolipids in which isomeric species sharing the same nominal mass are difficult to distinguish by mass alone. The recent introduction of cIMS, with its extended-path, high-resolution mobility separation, has substantially advanced this capability, enabling the resolution of closely related ganglioside isomers directly from human brain tissue and opening new possibilities for glycolipid biomarker discovery [1].
Previous work has established workflows for the separation and characterization of isomeric complex gangliosides directly from brain extracts, differentiating species sharing the same nominal mass but differing in glycan branching, sialylation pattern, or ceramide composition, and defining structural fingerprints based on collision cross section measurements combined with high-resolution MS/MS [2]. Building on this foundation, the present study explores the added value of cIMS for resolving ganglioside isomers and discovering new glycolipid biomarkers in human brain tissue.

Experimental
Ganglioside extracts from human brain-derived tissue were analyzed by cIMS MS operated with an extended, tunable separation path, allowing tunable, high-resolution separation of isomeric and closely related species. Structural assignment of the mobility-resolved ions was performed by collision-induced dissociation tandem mass spectrometry (CID MS/MS) in negative ion mode.

Results and discussion

Applying cIMS to human brain ganglioside extracts, we resolved isomeric and low-abundance species that remained unseparated by traveling-wave IMS, revealing differences in glycan branching, sialylation pattern, and ceramide composition that were previously inaccessible. This increased resolution led to the identification of several new human brain-associated glycolipid structures, including species not previously reported in the literature.

Comparison with pathological profiles further indicated that a subset of these newly resolved species show altered expression, glycan and ceramide composition, or unsaturation in disease-associated brain samples, pointing to their potential as candidate biomarkers. By reducing spectral overlap in complex mixtures, cIMS further strengthened the confidence of biomarker identification, complementing previous IMS-MS approaches.

Conclusion

Cyclic IMS represents a significant advance over IMS-MS for the analysis of brain gangliosides, providing the resolving power needed to distinguish closely related isomers directly from human brain tissue. Applied to this challenging lipid class, cIMS enabled the discovery of new human brain-associated glycolipid biomarkers, extending our previous findings in neuro-glycolipidomics and highlighting cyclic IMS as a promising tool for future biomarker research in neurological disorders and cancer.

Acknowledgements

This work was supported by the Romanian National Authority for Scientific Research, UEFISCDI, through the projects PN-III-P4-ID-PCE-2020-0209 and PN-IV-P2-2.1-TE-2023-0175.

References

[1] K. Giles, J. Ujma, J. Wildgoose, S. Pringle, K. Richardson, D. Langridge, M. Green, Anal. Chem. 91 (2019) 8564.

[2] M. Sarbu, R. Ica, Ž. Vukelić, D.E. Clemmer, A.D. Zamfir, Int. J. Mol. Sci. 26 (2025) 12029.

BIOLOGICAL POTENTIAL OF SUNFLOWER AND MAIZE IN RAINWATER QUALITY MONITORING

Brankica Kartalović[1],Antonije Žunić[2], Vojislava Bursić[2], Vladimira Žunić[2], Dušan Marinković[2]

[1]BioSense Institute, Dr Zorana Đinđića 1, 21000, University of Novi Sad, Serbia
[2]Faculty of Agriculture, Trg Dositelja Obradovića 8, 21000, University of Novi Sad, Serbia
e-mail: antonije.zunic@polj.edu.rs

Abstract

Under the pressures of climate change and frequent droughts, rainwater becomes an important supplementary source for irrigation. Hence, the quality evaluation of rainwater for irrigation plays a decisive role in preserving the crops productivity in the Autonomous Province of Vojvodina, Serbia. During 2025/26, samples were taken from three representative sites: Kikinda, Sremska Mitrovica and Sombor. Sunflower (*Helianthus annuus*) and maize (*Zea mays)* serve as practical plants for laboratory biotests in evaluating rainwater irrigation suitability. Chemical characterization of the collected samples indicated that pH values were at the boundary between slightly acidic and neutral reaction (6.2-7.4), while electrical conductivity ranged from 120 to 350 µS/cm, suggesting low to moderate mineralization. Distilled water was used as the control treatment. Germination percentages and morphological traits were recorded from 100 seeds per replicate, with four replicates per treatment. Statistical evaluation was performed in R using ANOVA and Fisher's LSD at the 95% confidence level. Both species responded positively to rainwater exposure, maize germination was enhanced by 5%, shoot lenght (0.3 cm, +27.7%), roots (0.6 cm, +44%), and greater biomass (5 g, +33%), in comparison to the control variant. Sunflower exhibited slightly different stimulation: germination was increased by 7%, shoot elongation (0.2 cm, +14%), root extension (0.7 cm, +35%), and biomass (1.5 g, +23%). Overall, rainwater promoted growth compared to the control, confirming its potential as an irrigation resource. These findings confirm that rainwater can effectively support early crop development and represents a valuable resource for sustainable agriculture under climate change and drought conditions.

Keywords: biotest, water, irrigation, crops, corn, sunflower.

Acknowledgements
This research was funded by the Provincial Secretariat for Higher Education and Scientific Research of the Autonomous Province of Vojvodina (Contract No. 003795622-2025-09418).

ANALYTICAL AND REGULATORY ASSESSMENT OF PESTICIDE RESIDUES IN DRIED PARSLEY UNDER TRACTOR SPRAYER AND DRONE APPLICATIONS

Antonije Žunić[1], Marko Bojin[1], Brankica Kartalović[2], Vojislava Bursić[1], Dušan Marinković[1]

[1]*Faculty of Agriculture, Trg Dositelja Obradovića 8, 21000, University of Novi Sad, Serbia*
[2]*BioSense Institute, Dr Zorana Đinđića 1, 21000, University of Novi Sad, Serbia*
e-mail: antonije.zunic@polj.edu.rs

Abstract

Parsley (*Petroselinum crispum*) represents an economically important aromatic and medicinal plant widely cultivated in diverse agro-ecological systems. Ensuring effective crop protection and sustainable management practices is essential for maintaining both yield and quality. Conventional application of plant protection products using tractor-mounted sprayers has long been the standard approach in parsley cultivation. However, recent advances in precision agriculture have introduced unmanned aerial vehicles i.e. drones as innovative tools for pesticide application, offering potential benefits in terms of efficiency, reduced environmental impact, and improved coverage uniformity. This study aims to compare parsley crop treatments applied via tractor-mounted sprayers and drone-based systems, using spectrophotometry, GC–MS/MS, and LC–MS/MS analyses, as well as evaluating compliance with maximum residue levels (MRLs) prescribed by current European regulations. Samples of dried parsley leaves (Italian Gigant variety) were collected in Serbia (AP Vojvodina, Orom locality). A representative 1 kg composite sample was taken from all plots (15 ha) at the end of June, following routine control procedures. Samples were properly packaged and transported to an accredited laboratory in accordance with established protocols. Pesticide residue analysis was conducted using a validated multiresidue method compliant with SRPS EN 15662, employing gas chromatography with tandem mass spectrometry (GC–MS/MS) and liquid chromatography with tandem mass spectrometry (LC–MS/MS). Quality control and method validation followed the guidelines of Analytical quality control and method validation procedures for pesticide residues analysis in food and feed (SANTE/11312/2021, version 2026). Given the widespread use of parsley and its proven antioxidant and potential anticancer properties, the study examined a broad spectrum of active substances and relevant pesticide metabolites, including insecticides, fungicides, and herbicides. Results revealed residues above the limit of quantification (LOQ), including aclonifen, boscalid, difenoconazole, pendimethalin, pyraclostrobin, terbuthylazine, and metolachlor (including isomeric forms). However, most detected compounds were present at low concentrations, while many pesticides tested were below the LOQ. By integrating physiological and residue-level evaluations, this research provides evidence-based recommendations for optimizing crop protection strategies in parsley cultivation, contributing to the broader goals of sustainable agriculture and precision crop management. The findings highlight the importance of comprehensive multiresidue monitoring in dried culinary herbs, considering their frequent dietary use and the potential for increased residue concentrations during the drying process.

Keywords: parsley; pesticide; residues; drone; sprayer; food safety.

Acknowledgements

The research funds were provided by the Ministry of Science, Technological Development and Innovation under Contract No. 451-03-34/2026-03/200117.

TARGETED ISOLATION AND CHARACTERIZATION OF HYDROCARBON-DEGRADING BACTERIA FOR REMEDIATION APPLICATIONS

Ingrid Zsilinszky[1], Alexandra Nóra Piti[1], Eszter Csákvári[1], Balázs Fehér[1]

[1]Department of Applied Microbiology, Division for Biotechnology, Bay Zoltán Nonprofit Ltd. for Applied Research, H-6726 Szeged, Derkovits fasor 2., Hungary
e-mail: ingrid.zsilinszky@bayzoltan.hu

Abstract
The efficiency of biological remediation of hydrocarbon-contaminated sites can be enhanced by the application of target-specific microorganisms with high degradation activity. The aim of our study was to isolate and characterize bacteria active under aerobic and anoxic/denitrifying conditions from environmental samples contaminated with TPH and BTEX. Among the aerobic TPH degraders, isolate ZR05 resulted in a 96.03% decrease in EPH concentration within 14 days, while its 16S rDNA gene sequence showed 100% identity with *Rhodococcus qingshengii* CCM 4446. Under denitrifying conditions, isolate BA1 reduced the concentrations of xylenes and alkylbenzenes by 49–84% within seven days, and based on its 16S sequence, it was assigned to the genus *Pseudomonas*. Based on the results, both isolates may be promising candidates for bioaugmentation of hydrocarbon-contaminated sites.

Introduction
Increasing the efficiency of bioremediation may require the application of microorganisms capable of degrading target compounds with high activity under the prevailing environmental conditions. For field applications, the selection and molecular characterization of pollutant-degrading microorganisms can support the development of targeted bioaugmentation strategies [1]. The aim of our study was to isolate and select bacterial strains with high TPH- and BTEX-degrading activity.

Experimental
Selective enrichment cultures were established from TPH- and BTEX-contaminated soil samples. Diesel fuel, BTEX compounds, xylenes and other alkylbenzenes were used as carbon sources. The enrichment cultures were incubated under aerobic and anoxic/denitrifying conditions, and pure isolates were subsequently obtained from cultures showing microbial growth.
Among the aerobic TPH degraders, the activity of eight individual isolates and two microbial consortia was investigated in diesel-containing microcosm systems. Changes in contaminant concentrations were determined by EPH analysis after 14 days of incubation. The activity of isolate BA1 was investigated for seven days under anoxic conditions in denitrifying microcosms containing xylenes and alkylbenzenes, using nitrate as an alternative electron acceptor. The selected isolates were identified by 16S rDNA gene sequencing.

Results and discussion
All tested isolates and consortia showed significant TPH-degrading activity in the aerobic microcosms. During the 14-day incubation period, the decrease in EPH concentration ranged between 92 and 97%. Among the individual isolates, ZR05 showed the highest activity, with a 96.03% reduction, while a 97.06% reduction was measured in the BGB consortium.
The 16S rRNA gene sequence of isolate ZR05 showed 100% identity with *Rhodococcus qingshengii* CCM 4446. Members of the genus *Rhodococcus* are known for their metabolic versatility and their ability to degrade a broad range of petroleum-derived hydrocarbons.

Rhodococcus qingshengii has been reported to utilize crude oil and individual hydrocarbons, while other *Rhodococcus* strains have also demonstrated the ability to degrade all major BTEX components [2,3].
The anoxic BA1 isolate reduced the concentrations of the investigated xylene and alkylbenzene components by 49–84% within seven days, whereas only a 1–10% change was observed in the abiotic control. The strain was also able to utilize benzene, toluene and ethylbenzene. Its 16S rRNA gene sequence showed 99% similarity to *Pseudomonas fluorescens*, *P. migulae* and *P. putida*. The ability of *Pseudomonas* species to degrade aromatic hydrocarbons is well documented, with *P. putida* and *P. fluorescens* strains showing activity toward several BTEX components [4,5].

Conclusion

Using a targeted isolation procedure, we successfully selected an aerobic *Rhodococcus* isolate with high TPH-degrading activity and an anoxic/denitrifying *Pseudomonas* strain with broad substrate specificity. Based on the results, the selected isolates may be promising candidates for bioaugmentation of hydrocarbon-contaminated sites. Further studies will include de novo genome sequencing of the strains and the development of strain-specific qPCR methods.

Acknowledgements

The studies were carried out within the framework of project 2020-1.1.2-PIACI-KFI-2020-00119, entitled “Development of a Bioexplosion Technology for the In Situ Remediation of Soils Contaminated with Petroleum-Derived Hydrocarbons.”

References

[1] Dueholm M.S., Marques I.G., Karst S.M., D'Imperio S., Tale V.P., Lewis D., Nielsen P.H., Nielsen J.L. *Survival and activity of individual bioaugmentation strains.* Bioresource Technology, 2015, 186, 192–199. DOI: 10.1016/j.biortech.2015.02.111.
[2] L. Iminova, Y. Delegan, E. Frantsuzova, A. Bogun, A. Zvonarev, N. Suzina, S. Anbumani, I. Solyanikova, *Physiological and biochemical characterization and genome analysis of Rhodococcus qingshengii strain 7B capable of crude oil degradation and plant stimulation*, Biotechnology Reports 35 (2022) e00741. DOI: 10.1016/j.btre.2022.e00741.
[3] J. You, M. Du, H. Chen, X. Zhang, S. Zhang, J. Chen, Z. Cheng, D. Chen, J. Ye, *BTEX degradation by a newly isolated bacterium: Performance, kinetics, and mechanism*, International Biodeterioration & Biodegradation 129 (2018) 202–208. DOI: 10.1016/j.ibiod.2018.02.012.
[4] You Y., Shim J., Cho C.-H., Ryu M.-H., Shea P.J., Kamala-Kannan S., Chae J.-C., Oh B.-T. *Biodegradation of BTEX mixture by Pseudomonas putida YNS1 isolated from oil-contaminated soil.* Journal of Basic Microbiology, 2013, 53, 469–475. DOI: 10.1002/jobm.201200067.
[5] Shim H., Yang S.-T. *Biodegradation of benzene, toluene, ethylbenzene, and o-xylene by a coculture of Pseudomonas putida and Pseudomonas fluorescens immobilized in a fibrous-bed bioreactor.* Journal of Biotechnology, 1999, 67, 99–112. DOI: 10.1016/S0168-1656(98)00166-7.

OCCUPATIONAL RISK ASSESSMENT OF PARTICULATE MATTER AND NOISE DURING INDOOR APARTMENT RECONSTRUCTION IN NOVI SAD

Miljan Šunjević[1], Maja Brborić[1], Aleksandra Čavić[2], Branka Nakomčić-Smaragdakis[1] and Sonja Dmitrašinović[1]

[1]Department of Environmental Engineering and Occupational Safety and Health, Faculty of Technical Sciences, University of Novi Sad, Trg Dositeja Obradovića 6, Novi Sad, Serbia
[2] Faculty of Economy and Engineering Management in Novi Sad, University Business Academy in Novi Sad, Cvecarska 2, 21000 Novi Sad, Serbia
e-mail: msunjevic@uns.ac.rs

Abstract

Indoor apartment reconstruction combines dust generating and acoustically intensive activities within a confined environment, creating highly variable worker exposure. The research paper presents a time-weighted occupational risk screening method applied to a monitoring dataset of 47 m^2 apartment reconstruction. The scenario contains 108 five-minute observations from 08:35 to 17:30 (8 h 55 min) for PM2.5, PM10 and noise. Timestamp-integrated TWA concentrations were 96.2 $\mu g/m^3$ for PM2.5 and 144.1 $\mu g/m^3$ for PM10. When the total monitored concentration-time exposure was normalized to an 8h reference period, the values were 107.3 and 160.6 $\mu g/m^3$, respectively. For occupational screening only, these values were compared with the OSHA particulate limits of 5 mg/m^3 for respirable dust and 15 mg/m^3 for total dust, giving screening quotients of 0.021 and 0.011. The energy-equivalent noise level was 79.9 dB and the normalized daily exposure indicator was LEX,8h = 80.4 dB, slightly above the EU lower action value of 80 dB(A). Despite low generic dust screening quotients, PM peaks were more than three times the daily TWA and noise reached 94.0 dB. The results demonstrate why average exposure, peak structure and metric compatibility must be interpreted together in reconstruction risk assessment.

Introduction

Indoor reconstruction activities such as demolition, drilling, wall chasing, sanding, cutting and debris handling can generate substantial short-term particulate emissions. Unlike open construction sites, apartment work takes place in small enclosed rooms where source to worker distances is short and pollutant dilution depends strongly on ventilation. Reviews of construction particulate monitoring have emphasized large temporal variability and the importance of linking exposure metrics to work activities and health protection objectives [1]. Personal sampling during indoor demolition and renovation has likewise shown that dust and respirable crystalline silica exposure can vary greatly by task, with mechanical demolition and removal of demolished material among the higher exposure activities [2].

Noise is a second major exposure domain. Construction workers frequently experience daily levels at or above commonly used occupational action values, particularly during power tools operation [3]. A combined time-resolved approach is therefore useful because particulate and acoustic peaks can occur together but do not represent the same hazard and cannot be combined into a single physical exposure limit.

The objective of the research is to asses and develop a compact occupational screening assessment for one representative apartment reconstruction day using: timestamp-weighted particulate TWA, 8h normalized concentration-time exposure, comparison with broad occupational dust limits through a screening quotient, and energy equivalent noise assessment against EU daily action and limit values.

Experimental

The analyzed dataset contains 108 records at 5 minute resolution between 08:35 and 17:30 on 07.07.2026., corresponding to a monitored duration of 8.92 h. The PM2.5, PM10 and noise series were detected using a Bettair Static Node (MK2 Series). According to the manufacturer, the platform uses electrochemical sensors for gaseous pollutants and an optical particle counter for PM1, PM2.5, and PM10, and also records ambient noise profile.

Time-weighted particulate exposure and OEL screening

For each particulate fraction, exposure was integrated over the actual time sequence. The monitored period time-weighted average was calculated as TWA corresponding interval duration. Because the monitored work period was longer than the nominal 8h reference period, an 8h normalized concentration was additionally calculated. This expresses the complete monitored concentration time burden on an 8h basis.

No occupational exposure limit is defined specifically for optical environmental PM2.5 or PM10 fractions. To provide a transparent numerical screen, the OSHA permissible exposure limits for particulates not otherwise regulated (PNOR) were used as non-equivalent benchmarks: 5 mg/m^3 for the respirable fraction and 15 mg/m^3 for total dust [4]. A screening quotient was defined as SQ = C_8h/OEL. SQ < 1 means that the measured optical mass concentration is numerically below the selected broad dust limit; it does not demonstrate compliance because PM2.5 is not identical to occupational respirable dust and PM10 is not identical to total or inhalable dust.

Noise exposure assessment

Noise was evaluated logarithmically. The energy equivalent level for the monitoring period was calculated from the 5 minute observations, and the daily normalized level was obtained as $L_{EX,8h} = L_{eq,T} + 10 \log_{10}(T/8)$, where T is the monitored duration in hours. The resulting indicator was compared with Directive 2003/10/EC, which specifies a lower daily exposure action value of 80 dB(A), an upper action value of 85 dB(A), and an exposure limit value of 87 dB(A) [5].

Descriptive and temporal analysis

Median, standard deviation, 95th percentile (P95), 99th percentile and maximum were calculated for PM and noise. P95 and maximum to TWA ratios were used to describe episodic amplification. Spearman correlation was used to characterize temporal covariation among PM2.5, PM10 and noise. The accumulated duration of observations at or above 80, 85, 87 and 90 dB was also calculated as a descriptive indicator of high noise periods.

Results

The representative workday showed a strongly episodic particulate profile (Figure 1. and Table 1.). PM2.5 TWA was 96.2 µg/m^3 and PM10 TWA was 144.1 µg/m^3. The P95 values increased to 248.2 and 340.3 µg/m^3, while maxima reached 322.3 and 436.2 µg/m^3. The peak to TWA ratios were therefore 3.35 for PM2.5 and 3.03 for PM10. PM2.5 and PM10 were very strongly correlated (Spearman $\rho = 0.976$, $p < 0.001$), as expected for nested particle size fractions.

Table 1. Modeled monitoring data

Metric	**PM**2.5	**PM**10
TWA, monitored period (µg/m^3)	96.2	144.1
8h normalized concentration (µg/m^3)	107.3	160.6
Median (µg/m^3)	76.5	117.8
P95 (µg/m^3)	248.2	340.3
P99 (µg/m^3)	308.6	428.9
Maximum (µg/m^3)	322.3	436.2

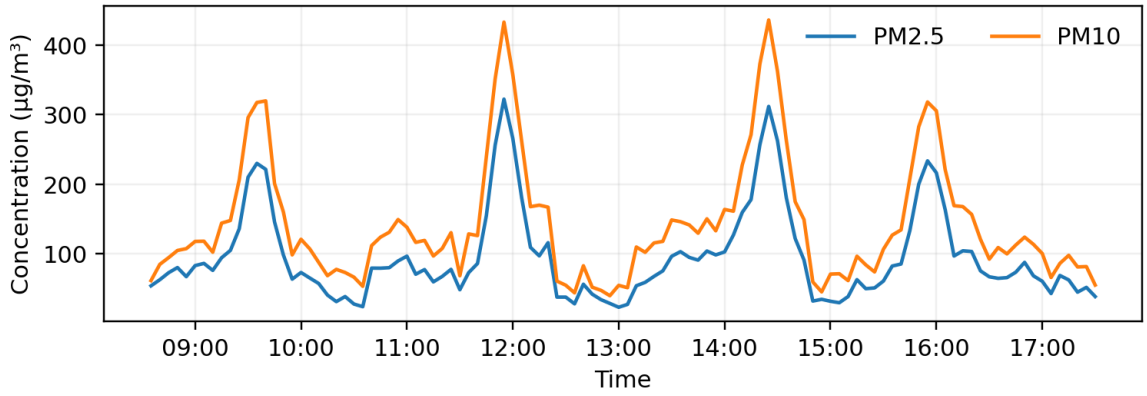


Figure 1. Time series of PM2.5 and PM10 concentrations during the representative 8 h 55 min reconstruction scenario.

TWA/OEL occupational screening

Normalization of the complete 8.92 h exposure to an 8h reference period produced C_8h values of 0.107 mg/m^3 for PM2.5 and 0.161 mg/m^3 for PM10. Relative to the selected OSHA PNOR benchmarks, the screening quotients were 0.021 and 0.011, equivalent to 2.15% and 1.07% of the respective benchmark concentrations. Numerically, the daily mass concentrations were therefore well below these broad nuisance dust limits. However, the low quotients should not be interpreted as evidence that renovation dust was intrinsically low risk because the sensor fractions and the regulated occupational fractions are not equivalent, and the chemical/mineral composition of the aerosol is unknown.

Indicator	**8h value**	**Benchmark**	**SQ / margin**	**Screening result**	**Interpretation**
PM2.5	0.107 mg/m^3	5 mg/m^3 respirable PNOR	0.021	Below benchmark	Non-equivalent proxy
PM10	0.161 mg/m^3	15 mg/m^3 total PNOR	0.011	Below benchmark	Non-equivalent proxy
Noise	80.4 dB	80 dB(A) lower action	+0.4 dB	Action level reached	Screening only
Noise	80.4 dB	85 / 87 dB(A)	−4.6 / −6.6 dB	Below upper/limit	Screening only

Table 2. TWA/OEL and noise action value screening.

Noise exposure profile

The arithmetic mean of the noise observations was 71.6 dB, but the energy equivalent value was substantially higher because decibels are logarithmic. Leq,T for the 8.92h period was 79.9 dB and the normalized daily exposure indicator was LEX,8h = 80.4 dB. The maximum recorded level was 94.0 dB and P95 was 86.1 dB. Approximately 65 min of observations occurred at or

above 80 dB, 40 min at or above 85 dB, 20 min at or above 87 dB, and 10 min at or above 90 dB. PM2.5-noise and PM10-noise correlations were positive ($\rho = 0.762$ and 0.801; $p < 0.001$), indicating that high noise periods often coincided with dust generating activity in the synthetic scenario.

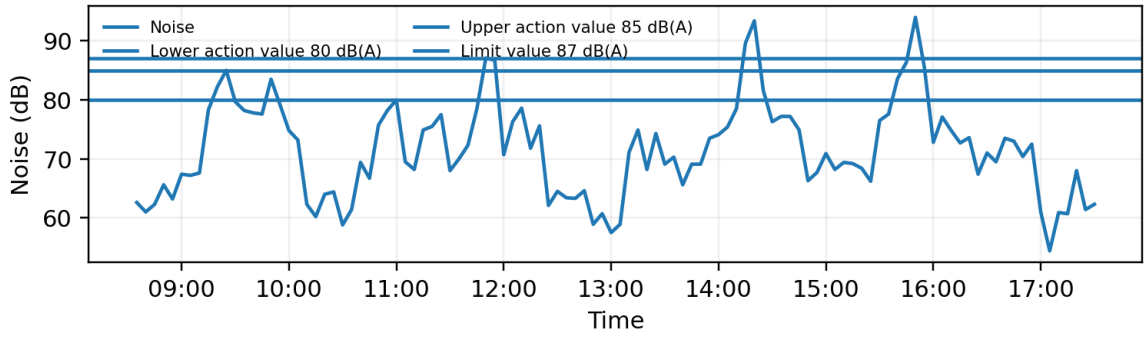


Figure 2. Noise time series with the EU lower action, upper action and exposure limit reference levels.

Discussion

The primary methodological finding is that a very low generic dust screening quotient can coexist with a strongly episodic exposure pattern. The PM2.5 and PM10 8h values represented only 2.15% and 1.07% of the broad PNOR benchmarks, yet P95 concentrations were more than twice the monitored period TWA and maxima exceeded TWA by approximately threefold. Occupational interpretation based only on SQ would therefore under describe the short periods that dominate exposure variability. Similar task dependent variability has been reported during refurbishment, drilling and demolition [2,6].

The most important limitation of the OEL comparison is metric compatibility. Optical PM2.5 and PM10 are useful for detecting temporal changes and identifying high emission periods, but they are not interchangeable with the respirable, thoracic or inhalable conventions used in occupational hygiene. The difference is particularly important in renovation because mineral containing materials may generate respirable crystalline silica, for which health-based limits are much lower than generic nuisance dust limits.

The normalized noise result reached the EU lower action value by approximately 0.4 dB while remaining below the upper action and exposure limit values. This indicates a different risk profile from the generic particulate comparison: the daily acoustic burden was close to a level at which preventive action becomes relevant, and short periods exceeded 85 and 87 dB. The positive PM-noise correlations suggest that some high energy tasks may drive both hazards simultaneously, but the relationship is not sufficiently specific for noise to serve as a surrogate for particulate exposure.

Conclusion

The representative monitoring data produced a PM2.5 TWA of 96.2 µg/m^3 and a PM10 TWA of 144.1 µg/m^3 over 8h 55min. Normalization to 8h yielded 0.107 and 0.161 mg/m^3, corresponding to generic PNOR screening quotients of 0.021 and 0.011. These low numerical ratios do not establish occupational compliance because optical PM2.5/PM10 are not equivalent to regulated occupational dust fractions. Particulate peaks exceeded the daily TWA by approximately threefold. The energy equivalent noise assessment produced LEX,8h = 80.4 dB, marginally above the EU lower action value, with several shorter periods above 85 and 87 dB. The combined findings support a risk assessment approach that uses TWA/OEL screening

together with peak event analysis and metric specific personal measurements rather than relying on a single daily average.

Acknowledgements
This research has been supported by the Ministry of Science, Technological Development and innovation (No. 451-03-33/2026-03/200156), and by the Autonomous Province of Vojvodina (No. 003870771 2025 09418 003 000 000 001; 003858394 2025 09418 003 000 000 001 04 002 and 002497912 2026 09418 002 000 000 001 04 006).

References

[1] Fang X, Chang R, Zhang Y, Zuo J, Zou Y, Han Y. Monitoring airborne particulate matter from building construction: A systematic review. Journal of Building Engineering. 2024;86:108708. doi:10.1016/j.jobe.2024.108708.
[2] Halvorsen JØ, Graff P, Gjengedal ELF, Ervik TK. Measurements of dust and respirable crystalline silica during indoor demolition and renovation. Annals of Work Exposures and Health. 2025;69(1):48-58. doi:10.1093/annweh/wxae082.
[3] Lewkowski K, Li IW, Fritschi L, Williams W, Heyworth JS. A systematic review of full-shift noise exposure levels among construction workers: Are we improving? Annals of Work Exposures and Health. 2018;62(7):771-782. doi:10.1093/annweh/wxy051.
[4] Occupational Safety and Health Administration. 29 CFR 1910.1000 Table Z-1: Limits for Air Contaminants - Particulates Not Otherwise Regulated. OSHA, Washington, DC.
[5] European Parliament and Council. Directive 2003/10/EC on minimum health and safety requirements regarding the exposure of workers to risks arising from physical agents (noise). Official Journal of the European Union. 2003;L42:38-44.
[6] Azarmi F, Kumar P, Mulheron M, Colaux JL, Jeynes C, Adhami S, Watts JF. Physicochemical characteristics and occupational exposure to coarse, fine and ultrafine particles during building refurbishment activities. Journal of Nanoparticle Research. 2015;17:343. doi:10.1007/s11051-015-3141-z.
[7] Nazaroff WW. Indoor particle dynamics. Indoor Air. 2004;14(Suppl 7):175-183. doi:10.1111/j.1600-0668.2004.00286.x.
[8] Yang X, Yu Q, Zhang Y, Ma W. Occupational health risk assessment of construction workers caused by particulate matter exposure on construction sites. Heliyon. 2023;9(10):e20433. doi:10.1016/j.heliyon.2023.e20433.

ASSESSMENT OF THE EFFECT OF PHYSICOCHEMICAL PARAMETERS ON THE UPTAKE OF PESTICIDE ACTIVE INGREDIENTS

Jomana Alrwashdeh[1], Mária Mörtl[2], László Balázs[3], András Szekács[2]

[1]Doctoral School of Natural Sciences, Institute of Environmental Sciences, Hungarian University of Agriculture and Life Sciences (MATE),2100 Gödöllő, Tessedik Sámuel u. 2, Hungary
[2]Agro-Environmental Research Centre, Institute of Environmental Sciences, Hungarian University of Agriculture and Life Sciences (MATE),2100 Gödöllő, Tessedik Sámuel u. 2, Hungary
[3]Institute of Agronomy, Department of Agronomy, Hungarian University of Agriculture and Life Sciences,2100 Gödöllő, Páter Károly u. 1, Hungary
e-mail: Alrwashdeh.Jomana.AbedAlkareem.Mahmoud.1@phd.uni-mate.hu

Abstract:
Neonicotinoids have been widely used in agriculture as plant protection products since the nineties as market-leading insecticides. However, these systemic compounds, acting on the nicotinic acetylcholine receptors in insects, raised significant environmental concerns about their effects on pollinators and other beneficial non-target species. Consuming guttation liquid produced by plants, which may serve as a water source for various insects, provides an exposure route particularly for bees. As a result, neonicotinoid insecticides were restricted and eventually banned in Europe. Anthranilic diamide insecticides, targeting insect ryanodine receptors as their mode of action, were introduced a decade later as an alternative; however, research into their toxicity to non-target species, such as bees, remains limited.
Plant uptake depends on numerous physicochemical parameters, and levels of systemic active ingredients in the plant guttation liquid also vary. The goal of this study is to evaluate plant uptake levels of four neonicotinoid insecticide active ingredients, thiamethoxam (TMX), clothianidin (CLO), imidacloprid (IMI) and thiacloprid (TCL), as well as an anthranilic diamide chlorantraniliprole (CHL), under two different light intensities at four different wavelength ratios. The light effect on corn plant development, which might affect the amount of excreted guttation droplets, has been investigated by measuring their insecticide content using instrumental analysis. Results showed significantly greater plant development, as measured by biomass, in the group illuminated with higher light intensity than in the group illuminated with lower light intensity. For active ingredient concentrations, TMX concentrations were highest under both conditions. Regarding the effect of four different wavelength ratios on plant biomass, lower ratios resulted in longer root and shoot lengths; however, for mass, there appeared to be no significant differences. Finally, among the wavelength ratios, medium and low ratios had the highest concentrations of active ingredients for both illumination conditions.

Acknowledgements
This study was funded by the Tempus Public Foundation under the Stipendium Hungaricum scholarship.

EXPLORING THE PHENOLIC CONTENT AND ANTIOXIDATIVE PROPERTIES OF THE INVASIVE PLANT SPECIES *AMORPHA FRUTICOSA*

Mijat Brenjo, Milica Vidić, Nevena Grujić-Letić, Branislava Teofilović, Emilia Gligorić

Department of Pharmacy, Faculty of Medicine, University of Novi Sad, Hajduk Veljkova 3, 21000 Novi Sad, Serbia
e-mail: emilia.gligoric@mf.uns.ac.rs

Abstract
Amorpha fruticosa L. is among the most invasive plant species in Northern Serbia, in the Vojvodina region. Its detrimental impact on the autochthonous species has been known for years. The aim of this study was to evaluate the efficiency of different NADES systems in extracting phenolic and flavonoid compounds from the leaves of *A. fruticosa* and to assess the antioxidant capacity of the resulting extracts in comparison with those obtained using conventional solvents.

Introduction
Invasive plants aggressively spread outside of their natural range, take up soil, nutrients, sunlight and in doing so crowd out native plants, thereby negatively changing the composition of existing ecosystems drastically. The heightened fecundity of these species degrades biodiversity, leading to the extinction of endemic species, changes in the food chain, negative impacts on human health, such as allergies, as well as increasing economic costs for the removal of these invasive species [1]. *Amorpha fruticosa* L. is widely distributed in the Vojvodina region, with anthropogenic habitats being most susceptible to its invasion [2]. Sustainable strategies to valorize *A. fruticosa* can turn an environmental challenge into an attractive source of bioactive compounds. In line with one of the 12 principles of green chemistry, which advocates for the use of environmentally friendly solvents and substances, natural deep eutectic solvents (NADES) have emerged as a promising alternative to conventional organic solvents for extracting bioactive compounds [3]. Therefore, this study aimed to evaluate the efficiency of various NADES systems for the extraction of phenolic and flavonoid compounds from the leaves of *A. fruticosa* and to determine the antioxidant potential of the obtained extracts in comparison to conventional solvents.

Experimental
Air-dried leaves of *A. fruticosa* were ground and sieved. NADES were synthesized by heating and stirring using choline chloride (ChCl), glycerol (Gly), lactic acid (LA), glucose (Glu), and urea (U). Four types of NADES were obtained by mixing these compounds in different molar ratios: NADES1 (ChCl:Gly=1:2), NADES2 (ChCl:LA=1:2), NADES3 (Glu:LA=1:5), NADES4 (U:LA=1:4). Microwave-assisted extraction (MAE) was carried out at 180W for a total of 24 s, divided into three cycles, using NADES, water (H_2O) and 70% ethanol (EtOH) as extraction solvents. After MAE, the extracts were filtered and diluted for further analysis. The total phenolic content (TPC) and total flavonoid content (TFC) of extracts were determined spectrophotometrically. The antioxidant potential of extracts was evaluated by the 2,2-diphenyl-1-picrylhydrazyl (DPPH) radical scavenging test and the cupric reducing antioxidant capacity (CUPRAC) assay [4].

Results and discussion

The total phenolic content (TPC) and total flavonoid content (TFC) of extracts obtained using the four NADES along with water and ethanol as reference solvents, are presented in Figure 1.

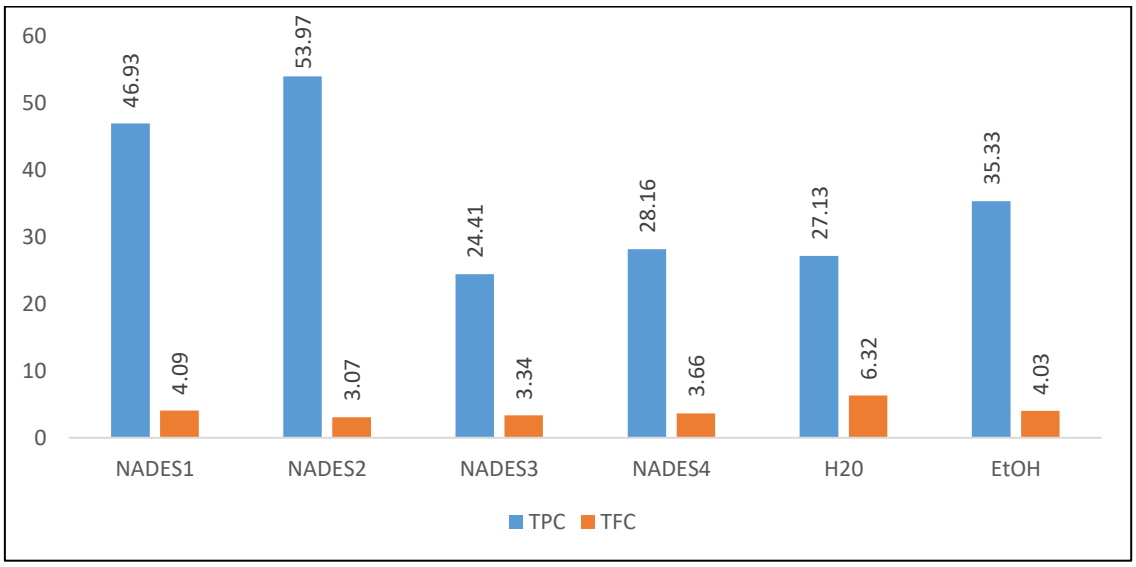


Figure 1. Total phenolic content (mg GAE/g dw) and total flavonoid content (mg eq QE/g dw) of various *A. fruticosa* leaf extracts.

TPC values ranged from 24.41 to 53.97 mg gallic acid equivalent (GAE)/g dry weight (dw), with NADES2 yielding the highest phenolic recovery, outperforming the other NADES as well as conventional solvents. TFC values ranged from 3.07 to 6.32 mg quercetin equivalents (QE)/g dw. The highest TFC was obtained using water as the extraction agent, followed by NADES1, whereas NADES2 yielded the lowest flavonoid recovery. The contrasting TPC and TFC values obtained with NADES2 suggest a distinct extraction profile, possibly related to its polarity and hydrogen-bonding capacity. These properties can influence solvent–solute interactions and selective solubilization of phenolic subclasses. Matching NADES polarity to that of target phenolic compounds was shown to modulate both extraction efficiency and compound-class selectivity [5].

The values of the DPPH test, expressed as mg of Trolox equivalents (TE)/g dw are shown in Figure 2.

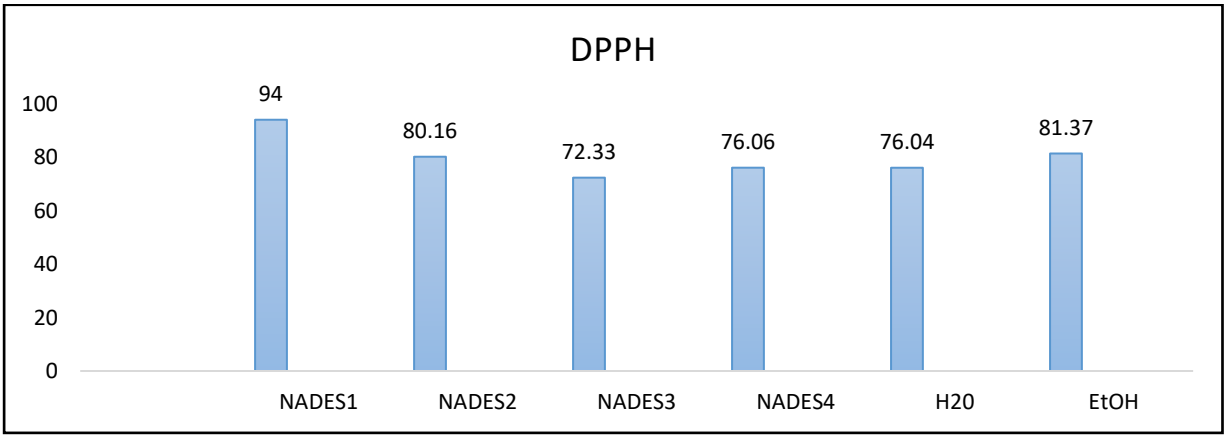


Figure 2. DPPH radical-scavenging activity of *A. fruticosa* leaf extracts (mg TE/g dw).

The extract obtained with NADES1 exhibited the highest DPPH radical-scavenging activity, followed by those obtained with ethanol and NADES2, whereas the NADES3 extract showed the lowest activity.

The values of the CUPRAC assay, expressed as mg TE/g dw are shown in Figure 3. Extracts obtained with NADES1 and NADES2 demonstrated the highest reducing capacity, consistent with their TPC results.

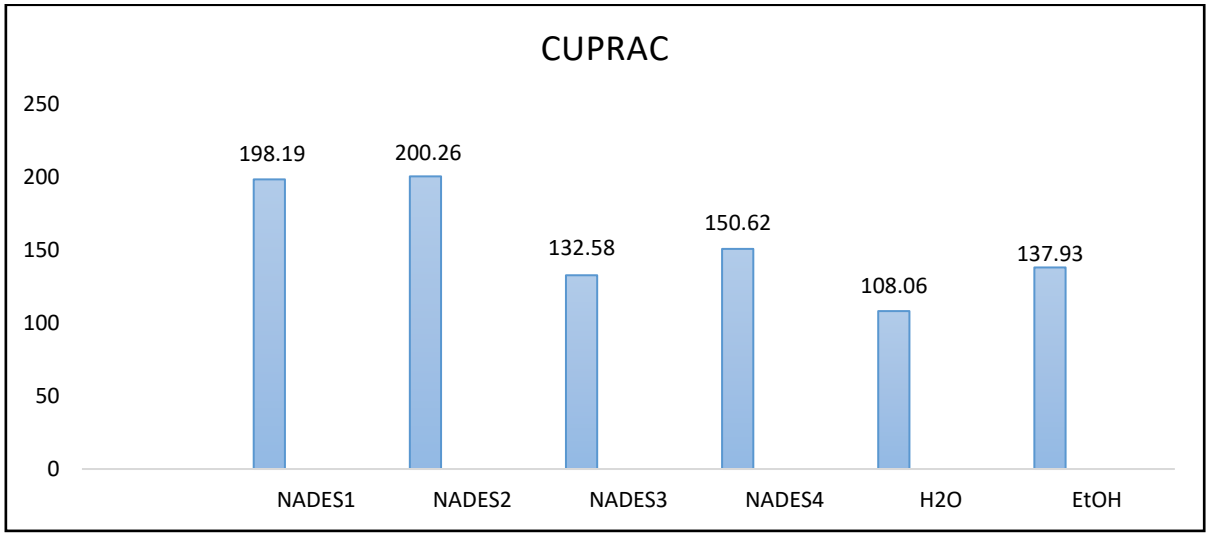


Figure 3. Antioxidant activity of *A. fruticosa* extracts assessed by the CUPRAC assay (mg TE/g dw).

A certain discrepancy was observed between Figures 2 and 3, with the CUPRAC assay yielding higher Trolox equivalent (TE) values per gram of dry weight than the DPPH assay. This difference may be attributed to the distinct reaction mechanisms and experimental conditions of the two assays. CUPRAC is performed at a near-neutral buffered pH, which may favour the deprotonation and electron-transfer reactions of certain antioxidant compounds. In contrast, the unbuffered, slightly acidic conditions used in the DPPH assay may limit the ionisation of certain antioxidant compounds, thereby affecting their reactivity and, consequently, the measured antioxidant activity of the investigated extracts. Another possible explanation for the observed variation in antioxidant activity between the two assays involves steric effects, as copper ions are more accessible to antioxidant molecules, whereas interactions with the relatively bulky DPPH radical may be affected by steric hindrance [6].

The results obtained in this study indicate that NADES can provide an effective alternative to conventional extraction solvents for obtaining extracts with antioxidant activity. In particular, three of the four investigated NADES extracts exhibited higher antioxidant capacity than the water and ethanol extracts in the CUPRAC assay (Figure 3). These findings highlight the potential of NADES-based extraction for improving the recovery of antioxidant compounds from the investigated plant material.

NADES1 and NADES2, both containing choline chloride as the hydrogen-bond acceptor, generally exhibited higher values across the investigated antioxidant and phenolic assays, as reflected by their TPC, DPPH, and CUPRAC results (Figures 1–3). This may indicate that the physicochemical properties of these NADES systems, including their ability to establish hydrogen-bonding and other solvent–solute interactions, were favourable for the extraction of compounds contributing to the measured phenolic content and antioxidant activity.

Conclusion

Based on the findings of the present study and previous reports, NADES show considerable potential as extraction media for obtaining phenolic compounds and extracts with antioxidant activity. However, further optimisation of NADES composition and extraction conditions is needed to identify systems that are best suited to the targeted compounds and plant matrices. The results of this study also indicate that the leaves of the highly invasive plant species *Amorpha fruticosa* L. contain appreciable levels of phenolic compounds and exhibit antioxidant activity, highlighting their potential as a source of bioactive compounds. Further studies should investigate a broader range of NADES systems and other plant parts, as well as assess the toxicological and pharmacological properties of the resulting extracts and their major bioactive constituents.

Acknowledgements

This work was supported by the Provincial Secretariat for Higher Education and Scientific Research, Province of Vojvodina (Grant No. 003874431 2025 09418 003 000 000 001).

References

[1] Prabakaran K, Li J, Anandkumar A, Leng Z, Zou CB, Du D. Managing environmental contamination through phytoremediation by invasive plants: A review. Ecol Eng. 2019;138:28-37.

[2] Anačkov G, Rat M, Radak B, Igić R, Vukov D, Rućando M, et al. Alien invasive neophytes of the Southeastern part of the Pannonian Plain. Cent Eur J Biol. 2013 Oct;8(10):1032-43.

[3] Wypych G. Handbook of Solvents, Volume 2: Use, Health, and Environment. 3rd ed. Amsterdam: Elsevier; 2019.

[4] Teofilović B, Gligorić E, Ninić M, Vukmirović S, Gagić Ž, Mandić-Kovačević N, et al. Green Extraction Combined with Chemometric Approach: Profiling Phytochemicals and Antioxidant Properties of Ten Species of the Lamiaceae Family. Separations. 2025; 12(6):155.

[5] Esnal-Yeregi L, Labidi J, Jauregi P. Modulation of phenolic extraction from grape seeds by varying the composition of natural deep eutectic solvents. Biofuels, Bioproducts and Biorefining. 2025;19(5):1364-77.

[6] Apak R, Güçlü K, Demirata B, Özyürek M, Çelik SE, Bektaşoğlu B, et al. Comparative evaluation of various total antioxidant capacity assays applied to phenolic compounds with the CUPRAC assay. Molecules. 2007;12(7):1496-547.

ULTRASOUND-ASSISTED EXTRACTION OF PHENOLIC COMPOUNDS AND ASCORBIC ACID FROM CITRUS RETICULATA BLANCO PEEL USING CHOLINE CHLORIDE-BASED NATURAL DEEP EUTECTIC SOLVENT

Nevena Grujić-Letić, Milica Vidić, Branislava Teofilović, Emilia Gligorić

Department of Pharmacy, Faculty of Medicine, University of Novi Sad, Hajduk Veljkova 3, Novi Sad, Serbia
e-mail: nevena.grujic-letic@mf.uns.ac.rs

Abstract

Citrus Reticulata Blanco peel represents an important source of bioactive compounds and its valorization can contribute to the development of sustainable approaches for the utilization of agro-industrial waste. In this study, a choline chloride based natural deep eutectic solvent (NADES) was investigated for the ultrasound-assisted extraction of phenolic compounds and ascorbic acid from *Citrus reticulata* Blanco (mandarin) peel. The NADES was prepared by mixing choline chloride and lactic acid at a molar ratio of 1:2. Ultrasound-assisted extraction was applied to enhance the recovery of bioactive compounds from the citrus peel matrix. The obtained extract was characterized by high-performance liquid chromatography with diode-array detection (HPLC-DAD). The detected phenolic compounds comprised gallic, chlorogenic, caffeic, sinapic and ferulic acids, as well as the flavonoids rutin, epicatechin, quercetin and naringenin. Ascorbic acid was also quantified in the obtained extract. The results demonstrated that ChCl-based NADES combined with ultrasound enabled the recovery of several phenolic compounds and ascorbic acid from *C. reticulata* Blanco peel. The obtained phytochemical profile confirms the potential of this extraction approach for the valorization of citrus peel as a renewable source of bioactive compounds. The study provides a basis for the further development of NADES-based extraction strategies for the sustainable utilization of citrus processing residues.

Introduction

The processing of citrus fruits generates considerable amounts of peel residues, which are often treated as waste despite their high content of valuable bioactive compounds. Citrus peels contain phenolic acids, flavonoids, ascorbic acid and other phytochemicals with potential nutritional and functional value. Their recovery therefore represents an attractive strategy for converting an abundant agro-industrial residue into a source of value-added compounds. The extraction of plant bioactives is strongly influenced by the properties of the extraction solvent. Conventional organic solvents are widely used for this purpose, but their use can be associated with environmental, health and safety concerns. NADES are typically formed by combining two or more naturally occurring metabolites, including organic acids, sugars, amino acids, and choline chloride, which interact primarily through hydrogen bonding to produce a eutectic mixture with a reduced melting point. Their tunable physicochemical properties and broad solubilization capacity have made NADES promising alternative media for the efficient extraction of diverse phytochemicals from natural sources. Choline chloride-based NADES have been extensively investigated for the extraction of bioactive compounds from plant materials. In particular, the combination of choline chloride and lactic acid can provide an extraction medium capable of interacting with and solubilizing polar plant metabolites. The use of ultrasound-assisted extraction can further facilitate the release of intracellular compounds through acoustic cavitation, improved solvent penetration and enhanced mass transfer. The aim of this study was to investigate the potential of a choline chloride:lactic acid NADES (molar ratio 1:2) combined with ultrasound-assisted extraction for the recovery of phenolic compounds

and ascorbic acid from *Citrus reticulata* Blanco peel. The obtained extract was characterized using HPLC-DAD to determine its individual phenolic and total ascorbic acid content.

Experimental

Citrus reticulata Blanco was collected from a local supplier and originated from Turkey. The peels were separated from the pulp and ground using a food grinder. Subsequently, the peels were dried in an oven at 100 ± 0.2 °C until a constant weight was achieved to ensure complete moisture removal. NADES was prepared using choline chloride and lactic acid at a molar ratio of 1:2. The ideal water content has been demonstrated to be 20% (v/v). NADES extraction involved measuring 0.2 g of mandarin peel, adding 2 mL of NADES and 5 mL of distilled water, heating and mixing at 45º C. This was followed by a centrifugation for 15 minutes at 3000 revolutions. The resulting mandarin peel, NADES, and water mixture was put in an ultrasonic bath for NADES-UAE extraction. The extraction process took 20 minutes (180 W). Following the previously described centrifugation, 2 mL of the supernatant was filtered through a membrane filter in a vial. Total ascorbic acid was determined after the reduction of dehydroascorbic acid. The analysis of *C. reticulata* Blanco peel was conducted using Agilent HP 1100 HPLC-diode array detection (HPLC-DAD) system with an autosampler injector. A modified HPLC method was applied for the analysis of phenolic acids and flavonoids, using a Zorbax CB-C18 column (4.6 mm × 150 mm, i.d., 5 µm particle size) and gradient mode flow rate of 1 mL/min was used to provide a mobile phase consisting of 0.1% aqueous acetic acid (A) and 0.1% acetic acid in acetonitrile (B). The injection volume was 10 µL, and the UV detector was set at 280 nm. Ascorbic acid in mandarin peel extracts was determined by HPLC using a Zorbax C18 analytical column (4.6 × 150 mm, 5 µm particle size). Isocratic elution was performed with a methanol buffer (70:30, v/v; pH 6.8) mobile phase at a flow rate of 1 mL/min. Detection was carried out at 254 nm, while the column temperature was maintained at 25 °C.

Results and discussion

The HPLC-DAD analysis demonstrated that ultrasound-assisted extraction using ChCl:lactic acid (1:2) NADES enabled the recovery of several phenolic compounds from *C. reticulata* Blanco peel. The obtained extract contained both phenolic acids and flavonoids, confirming the suitability of the applied extraction system for the recovery of compounds belonging to different phytochemical classes. Among the investigated phenolic acids, gallic acid, chlorogenic acid and ferulic acid were particularly represented. Gallic acid was detected at a concentration of 207.12 µg/g DW, while chlorogenic and ferulic acids were determined at concentrations of 102.82 and 442.46 µg/g DW, respectively. Caffeic and sinapic acids were also detected at concentrations of 125.52 and 35.00 µg/g DW, respectively. Among the analyzed flavonoids, rutin was detected at a concentration of 280.58 µg/g DW. Epicatechin, quercetin and naringenin were also present in the extract at concentrations of 22.27, 183.65 and 267.18 µg/g DW, respectively. The obtained concentrations are comparable with those reported in recent studies employing deep eutectic solvents for the extraction of phytochemicals from *C. reticulata* peel. For example, Wang et al. investigated the recovery of polyphenols from *C. reticulata* Blanco peels using a choline chloride:glycol (1:4) deep eutectic solvent within an integrated extraction–resin adsorption process. Their approach focused on total polyphenol recovery, process optimization and subsequent compositional and bioactivity assessment. In contrast, the present study employed a single ChCl-based natural deep eutectic solvent in combination with ultrasonic assistance and provided the individual determination of five phenolic acids and four flavonoids. This represents a simpler extraction approach while providing detailed information on the individual phytochemical composition of the obtained extract. The achieved results demonstrate that the ChCl:lactic acid (1:2) NADES was capable of extracting a broad range of phenolic compounds from the citrus peel matrix. The extraction efficiency can be attributed to

the physicochemical characteristics of the NADES, including its hydrogen-bonding capacity and interactions with compounds present in the plant matrix. The application of ultrasound may additionally promote the disruption of plant tissues and facilitate the transfer of phytochemicals into the extraction medium. Ascorbic acid was also successfully detected in the obtained extract, with a concentration of 421.82 μg/g DW. While recent studies have primarily focused on polyphenol recovery or other fractions of citrus biomass, the present approach provides a broader analytical characterization by including both phenolic compounds and ascorbic acid in the same extraction study. The simultaneous recovery of phenolic compounds and ascorbic acid is particularly relevant because it demonstrates the potential of the applied extraction system to obtain extracts containing different classes of nutritionally relevant bioactive compounds. The phytochemical profile obtained in this study highlights the potential of *C. reticulata* Blanco peel as a valuable source of naturally occurring compounds. The use of ChCl-based NADES in combination with ultrasound provides an alternative extraction approach that may contribute to reducing the reliance on conventional organic solvents and improving the utilization of citrus processing residues.

Conclusion

The present study demonstrated the potential of choline chloride acid:lactic acid (1:2) natural deep eutectic solvent combined with ultrasound-assisted extraction for the recovery of phenolic compounds and ascorbic acid from *Citrus reticulata* Blanco peel. HPLC-DAD analysis confirmed the presence of several phenolic acids and flavonoids, including gallic, chlorogenic, caffeic, sinapic and ferulic acids, as well as rutin, epicatechin, quercetin and naringenin. Ascorbic acid was also successfully detected in the obtained extract. The results indicate that the ChCl:lactic acid (1:2) NADES can serve as a suitable extraction medium for the recovery of different classes of bioactive compounds from mandarin peel. The combination of NADES and ultrasound-assisted extraction represents a promising approach for the sustainable valorization of citrus peel waste and the generation of phytochemical-rich extracts with potential applications in food, nutraceutical and other bio-based fields.

Acknowledgements

The authors are grateful for the financial support of Provincial Secretariat for Higher Education and Scientific Research, grant number: 003874431 2025 09418 003 000 000 001.

References

[1] G. Domínguez-Rodríguez, V.M. Amador-Luna, M. Castro-Puyana, E. Ibáñez, M.L. Marina, Food Res. Int. 202 (2025) 115713.
[2] M. Plaza, M.L. Marina, Microchem. J. 212 (2025) 113366.
[3] U. Miljić, V. Puškaš, J. Cvejić Hogervorst, L. Torović, Int. J. Food Prop. 20 (2017) 2022–2033.
[4] S. Wang, Y. Feng, X. Yu, Z. Yang, P. Jiao, Q. Niu, Sep. Purif. Technol. 355 (2025) 129560.

MEMBRANE-BASED VALORIZATION OF SLUDGE DIGESTATES: LINKING PRETREATMENT EFFECTS TO SEPARATION PERFORMANCE

Anar Imamverdiyev[1], Zoltán Péter Jákói[2], Cecilia Hodúr[2], Sándor Beszédes[2]

[1]Doctoral School of Environmental Sciences, University of Szeged, H-6720 Szeged, Hungary
[2]Department of Biosystems Engineering, Faculty of Engineering, University of Szeged, H-6725 Szeged, Hungary
e-mail: a.imamverdiyev@outlook.com

Abstract

Anaerobic digestion residues are increasingly treated as secondary resources for water, nutrient and energy recovery rather than as wastes for disposal, a shift reinforced in the European Union by the recast Urban Wastewater Treatment Directive. Membrane processes are leading candidates for fractionating the liquid fraction of digestate, but their stability depends on feed properties that upstream pretreatment strongly modifies. This contribution summarizes a recently published review [1] that treats pretreatment and membrane separation as one conditioning-to-separation pathway. Evidence on thermal hydrolysis, microwave, alkaline, ozone and enzymatic conditioning is linked to the behavior of pressure-driven membranes (MF, UF, NF, RO), electrodialysis and bipolar membrane electrodialysis (ED, BMED) and membrane distillation (MD). Pretreatments that raise solubilization and improve bulk rheology can also increase the load of soluble biopolymers and fine colloids: microwave treatment of activated sludge at 80 °C, for example, lowered the median particle size from 228 to 45 µm while the sludge filter resistance increased about twentyfold. The reported indicators show that ammonium is the most consistently recoverable or removable target, that a staged UF–selective ED–RO train raised clean-water recovery from about 38% to 88% at pilot scale, and that digestate-specific energy data exist mainly for electro-driven processes. Condition-explicit reporting and long-term operation on real digestate are identified as the main prerequisites for scale-up.

Introduction

Municipal wastewater treatment plants are being reframed as water resource recovery facilities, in which sludge and digestate are regarded as sources of energy, nutrients, organic carbon and water rather than as residues to be stabilized and disposed of. In the European Union, the recast Urban Wastewater Treatment Directive (Directive (EU) 2024/3019), in effect since 1 January 2025, strengthens nutrient-removal and resource-recovery requirements, introduces quaternary treatment for micropollutants and pushes the sector toward energy and climate neutrality [2]. Within such schemes, membranes can split the liquid fraction of digestate (LFD) into a clarified permeate and a concentrate, reduce transport volumes, and prepare process-ready streams for struvite crystallization, ammonia stripping and absorption, or electrochemical recovery [3].

Digestate is, however, a challenging membrane feed. It behaves as a non-Newtonian suspension, and its soluble extracellular polymeric substances (EPS) and soluble microbial products (SMP) – proteins, polysaccharides, humic-like substances and other cell- or hydrolysis-derived compounds – can adsorb on membrane surfaces, constrict or block pores and promote gel-layer formation [4–6]. Because hydrolysis usually limits the rate of anaerobic digestion, sludge is often pretreated before digestion [7], and this pretreatment changes the rheology, particle-size distribution and soluble-organic content of the digestate that later reaches the membranes. Existing reviews usually treat digestate management, pretreatment, membrane nutrient recovery and fouling separately, and few follow how upstream choices carry through to flux, fouling, scaling and energy demand.

This contribution presents the main findings of our recent review [1], which addresses that gap by (i) relating pretreatment-induced changes in digestate properties to membrane behavior, (ii) compiling reported performance indicators for membrane options applied to real digestate-type streams, and (iii) identifying the fouling, scaling, energy and reporting constraints that currently limit scale-up.

Review methodology

The work was prepared as a structured narrative review. Web of Science, Scopus and ScienceDirect were searched, with Google Scholar and the reference lists of key papers used as supplementary sources, covering 2000 to June 2026 with emphasis on studies published from 2010 onward. Search strings combined feedstock terms (e.g., sludge digestate, liquid fraction of digestate, digested sludge centrate) with membrane terms (MF, UF, NF, RO, ED, BMED, MD) and outcome terms (nutrient, ammonium, phosphorus and potassium recovery, volatile fatty acids, fouling, scaling) using Boolean operators. Studies reporting quantitative indicators – permeate flux, recovery, fouling resistance, solubilization, particle-size change or specific energy consumption – were prioritized, and pilot- and full-scale data were preferred where available. Non-peer-reviewed sources were used only for regulatory and market context. Because feeds, operating conditions and performance metrics differ widely between studies, results were not pooled statistically; reported trends, mechanisms and performance ranges were compared instead, and quantitative values were tabulated with their metric type and scale.

Results and discussion

Pretreatment effects on digestate properties

Pretreatment disrupts flocs and EPS networks, often lowering the yield stress and consistency index of the Herschel–Bulkley model and thereby improving pumping and mixing. Improved bulk rheology does not, however, guarantee improved separability, because membrane performance is often limited by colloidal and soluble-biopolymer loading rather than by viscosity [1,6]. Thermal hydrolysis (commonly around 150–170 °C under pressure, followed by rapid decompression) is frequently associated with some of the largest viscosity reductions and generally improves dewaterability [8], but it also moves organic matter into the liquid phase: in thermally pretreated secondary sludge, about 30% of the particulate organic matter and 34% of the volatile solids fed were shifted to the liquid fraction [9]. At high severity, colored and more refractory melanoidin-like compounds can form [10], adding to the organic load on NF/RO polishing.

Microwave conditioning shows the clearest particle-size trade-off. In waste activated sludge treated at 80 °C for 5 min, soluble COD increased from 88.5 to 2380 mg/L, d_{50} decreased from 228 to 44.6 µm, d_{90} from 368 to 72.8 µm, and sludge filter resistance rose from 1.02×10^{13} to 2.15×10^{14} m/kg [11]. Although measured before digestion, these data show how severe disintegration can move the dominant resistance from largely reversible cake filtration toward more persistent pore-scale deposition by fines; MW pretreatment should therefore be paired with an upstream MF/UF barrier or equivalent solids management before tighter membranes. Alkaline treatment (pH ≈ 10–12) raises ionic strength and the precipitation potential of carbonate and phosphate minerals, whereas controlled under-stoichiometric ozonation increased UF flux of digestate by about 50–80% [12]; overdosing, however, can fragment organics and damage polymeric membranes. Combined pretreatments can intensify these effects: ultrasonic–alkaline treatment increased the fraction of organics above 300 kDa from 7.8% to 42.3% [13], a macromolecular fraction closely related to gel-layer formation, adsorption and pore blocking. Most of these pretreatment data, however, come from raw or thickened sludge rather than digestate liquors.

Membrane processes and reported performance

The behavior of pressure-driven membranes on digestate can be interpreted with the resistance-in-series model and the concentration-polarization (CP) relation [6,14]:

$$J = \Delta P / [\mu\,(R_m + R_c + R_f + R_{cp})], \qquad C_w = C_b \exp(J/k) \tag{1}$$

where R_m, R_c, R_f and R_{cp} are the membrane, cake, pore-blocking/adsorption and polarization resistances, and k is the mass-transfer coefficient. Lower viscosity helps hydraulics, but more soluble biopolymers and fines increase R_f and CP-driven gel formation, which is why conservative flux targets relative to a system-specific critical flux are typically decisive for stable operation [14]. In practical applications (Figure 1), MF/UF serve as front-end clarification, NF acts as an intermediate concentrator, and RO provides final refining for reusable water. Selective ED and BMED are placed after clarification to recover ionic nutrients or generate acid and base, and MD can use low-grade heat (50–90 °C) available from combined heat and power units for ammonia recovery [1,3].

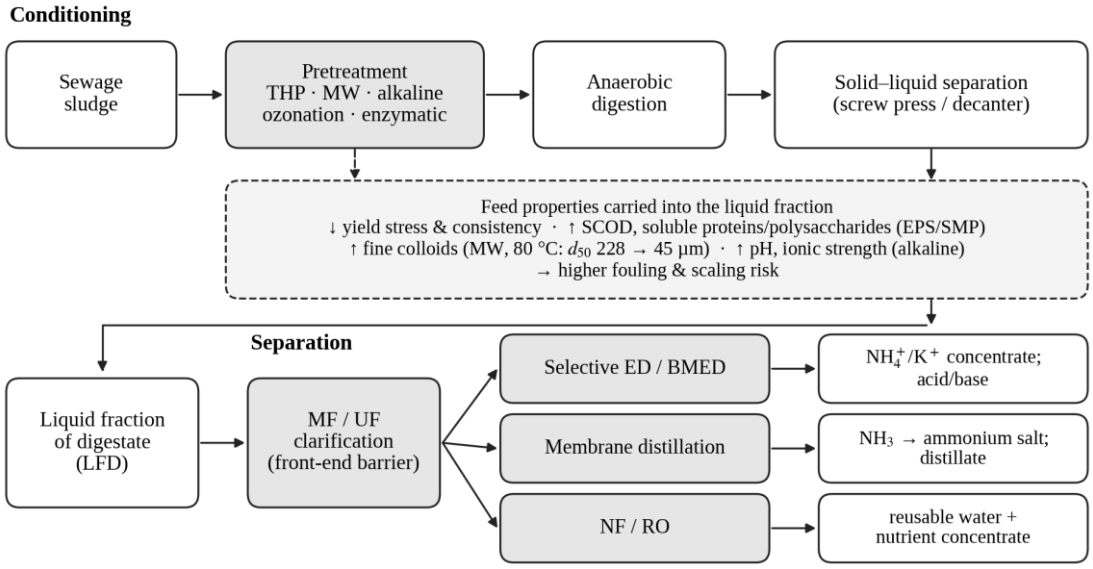


Figure 1. Conditioning-to-separation pathway for membrane-based digestate valorization; downstream stages may be used alone or in series, e.g., UF–selective ED–RO (schematic summary based on [1])

Representative indicators are compiled in Table 1. Among the pressure-driven examples, UF showed the highest real-feed flux, while NF and RO/ULPRO (ultra low-pressure RO) gave lower initial fluxes, in line with higher selectivity and greater susceptibility to CP, organic fouling and scaling. MD flux is thermally driven and ED performance is expressed through removal, recovery and energy, so these values are not ranked against hydraulic flux. Ammonium is the most consistently recoverable or removable target, particularly through selective ED, BMED and MD-based ammonia recovery. Phosphate behavior is route-dependent: selective ED mobilizes only part of the phosphate into a liquid product [15], whereas full-scale pressure-driven cascades remove most phosphorus upstream of RO into solid or concentrate fractions [16,17], so phosphate removal should not be equated with recovery.

Fouling, scaling and energy constraints

Fouling remains the main technical limitation. EPS proteins and polysaccharides form cohesive deposits and gel-like layers, dissolved and colloidal SMP intensify pore constriction, higher fractions of fine flocs are associated with denser cake layers, and elevated pH and CP at the membrane surface favor precipitation of struvite and calcium carbonate, particularly in NF and RO [1,6]. Mitigation is best framed as a combination of staged clarification, feed conditioning

(oxidation or pH control where appropriate), conservative flux relative to the critical flux and hydrodynamic enhancement, e.g., vibratory shear-enhanced processing. Digestate-specific energy data are concentrated in electro-driven processes: about 0.44 kWh/m^3 at ~93% total ion removal and 0.24–15.2 kWh/kg N depending on the removal target in laboratory ED [18], and 4.9 ± 1.5 kWh/kg N in pilot ED on digester centrate [19]. Specific thermal energy for MD on real post-digestion digestate and comparable kWh/m^3 values for pressure-driven digestate treatment are not consistently reported, so these are reporting gaps rather than evidence of favorable or unfavorable energetics. Because electrical, thermal and pressure-driven energy metrics are physically distinct, they should be reported by driving force rather than ranked together.

Table 1. Representative indicators reported for membrane treatment of real digestate-type streams (metric types differ and are not directly comparable across rows; *scale given where reported in [1])

Process	Feed; scale*	Reported indicator	Ref.
UF (PES, 5–50 kDa)	Swine-manure digestate	Flux ≈60 L m^{-2} h^{-1} (3 bar, 25 °C)	[20]
NF (NF90) / ULPRO (XLE)	Liquid digestate	Initial flux ≈27 / ≈20 L m^{-2} h^{-1} (5 bar)	[21]
MD	Anaerobic digestate; lab	Vapor flux ≈5.5 L m^{-2} h^{-1} (70 °C); 40% water recovery	[22]
UF–selective ED–RO	Digested sludge liquid fraction; pilot	Clean-water recovery 38% → 88%; permeate TDS 869.0 → 10.3 mg/L	[23]
Selective ED	Digested sludge liquor; pilot	>95% NH_4^+ and K^+ recovery; ≈55% PO_4^{3-}	[15]
ED	Swine digestate; lab	~93% total ion removal at 0.44 kWh/m^3	[18]
Vacuum MD	Liquid digestate; lab	Ammonia removal fraction >0.85	[24]
UF–RO cascade	Co-digestion digestate; full scale	>99% of P removed before RO; RO permeate 48% of feed	[17]

Conclusion

Membrane-based valorization of sludge digestate is technically promising, but its outcome depends strongly on upstream conditioning: pretreatment that improves digestion and rheology can simultaneously raise the soluble-biopolymer, fine-colloid and scaling-ion load that governs membrane fouling. Hybrid trains in which MF/UF protect selective ED/BMED, MD or NF/RO stages, operated at conservative flux relative to the critical flux, are currently the most defensible configuration. Progress toward full-scale application will depend on standardized, condition-explicit reporting of flux, recovery, rejection and energy; on long-term pilot operation with real digestate; and on measuring pretreatment severity and membrane fouling on the same feed rather than inferring the link across separate studies.

References

[1] A. Imamverdiyev, Z.P. Jákói, C. Hodúr, S. Beszédes, Water 18 (2026) 1505. https://doi.org/10.3390/w18121505
[2] European Parliament and Council of the European Union, Directive (EU) 2024/3019 of 27 November 2024 concerning urban wastewater treatment (recast), https://eur-lex.europa.eu/eli/dir/2024/3019/oj/eng (accessed 16 April 2026).
[3] M. Zielińska, K. Bułkowska, Membranes 15 (2025) 45.
[4] G.-P. Sheng, H.-Q. Yu, X.-Y. Li, Biotechnol. Adv. 28 (2010) 882.
[5] H. Lin, M. Zhang, F. Wang, F. Meng, B.-Q. Liao, H. Hong, J. Chen, W. Gao, J. Membr. Sci. 460 (2014) 110.
[6] P. Le-Clech, V. Chen, T.A.G. Fane, J. Membr. Sci. 284 (2006) 17.

[7] H. Carrère, C. Dumas, A. Battimelli, D.J. Batstone, J.P. Delgenès, J.P. Steyer, I. Ferrer, J. Hazard. Mater. 183 (2010) 1.
[8] W.P.F. Barber, Water Res. 104 (2016) 53.
[9] S.I. Pérez-Elvira, I. Sapkaite, F. Fdz-Polanco, Braz. J. Chem. Eng. 33 (2016) 699.
[10] J. Dwyer, D. Starrenburg, S. Tait, K. Barr, D.J. Batstone, P. Lant, Water Res. 42 (2008) 4699.
[11] A. Alhraishawi, S. Aslan, Eur. J. Sustain. Dev. Res. 8 (2024) em0255.
[12] T. Gienau, A. Ehrmanntraut, M. Kraume, S. Rosenberger, Membranes 10 (2020) 64.
[13] X. Tian, C. Wang, A.P. Trzcinski, L. Lin, W.J. Ng, J. Environ. Sci. 29 (2015) 97.
[14] P. Bacchin, P. Aimar, R.W. Field, J. Membr. Sci. 281 (2006) 42.
[15] V. Proskynitopoulou, I. Garagounis, A. Vourros, P. Dimopoulos Toursidis, S. Lorentzou, A. Zouboulis, K. Panopoulos, J. Environ. Manage. 353 (2024) 120166.
[16] J.L. Van Puffelen, C. Brienza, I.C. Regelink, I. Sigurnjak, F. Adani, E. Meers, O.F. Schoumans, Sep. Purif. Technol. 297 (2022) 121501.
[17] A. Chiumenti, F. da Borso, F. Teri, R. Chiumenti, B.B. Piaia, Appl. Eng. Agric. 29 (2013) 985.
[18] C.-Y. Wei, S.-Y. Pan, Y.-I. Lin, T.N.-D. Cao, Water Res. 224 (2022) 119066.
[19] A.J. Ward, K. Arola, E. Thompson Brewster, C.M. Mehta, D.J. Batstone, Water Res. 135 (2018) 57.
[20] C. Yue, H. Dong, Y. Chen, B. Shang, Y. Wang, S. Wang, Z. Zhu, Membranes 11 (2021) 179.
[21] C. Tsaridou, A. Karanasiou, K.V. Plakas, A.J. Karabelas, Membranes 13 (2023) 297.
[22] M. Aquino, S. Santoro, G. Di Profio, M.F. La Russa, C. Limonti, S. Straface, G. D'Andrea, E. Curcio, A. Siciliano, Sep. Purif. Technol. 315 (2023) 123687.
[23] V. Proskynitopoulou, A. Vourros, I. Garagounis, P. Dimopoulos Toursidis, S. Lorentzou, A. Zouboulis, K. Panopoulos, J. Environ. Chem. Eng. 12 (2024) 112675.
[24] A. Karanasiou, K. Angistali, K.V. Plakas, M. Kostoglou, A.J. Karabelas, Sep. Purif. Technol. 314 (2023) 123602.

CHALLENGES IN SAMPLE PREPARATION OF BUILDING MATERIALS FOR GAMMA SPECTROMETRY

Robert Lakatoš[1], Tomas Nemeš[1], Selena Samardžić Cvijanović[1], Sofija Forkapić[2], Ivana Lončarević[1], Milica Vučinić Vasić[1], Jan Hansman[2]

[1]Faculty of Technical Sciences, University of Novi Sad, Serbia
[2]Faculty of Sciences, Department of Physics, University of Novi Sad, Serbia
e-mail: laki@uns.ac.rs

Abstract

The reliability with which natural radionuclides in building materials are determined by gamma-ray spectrometry depends on how faithfully the counted sample represents the material as a whole, and this is a question of sample preparation. The present work examines the practical limits of particle-size-resolved sample preparation on a set of 27 samples of granite, ceramic tiles, natural stone and related products. After comminution and sieving into narrow size classes, the mass was distributed very unevenly: individual fractions failed to reach the mass required for satisfactory counting statistics and for reproducible filling of the counting container. Adjacent classes were therefore pooled into composite samples exceeding 100 g, which reduced seven size classes to three. The comminution method governs this behaviour: mechanical milling yields an excess of fine material and depletes the coarse classes, whereas manual crushing preserves the coarse classes but is slow and poorly reproducible. Comparing sieving with laser diffraction revealed a further limitation, this time of the classification itself: below about 125 µm fine particles stick together into aggregates that the sieve passes as coarse grains, so the nominal class ceases to describe the actual particle size — and the size at which this happens depends on the material. The results define a trade-off between granulometric resolution, attainable sample mass and practical feasibility, and argue for preparation protocols matched to the material.

Introduction

Building materials of mineral origin contain the primordial radionuclides ^{226}Ra, ^{232}Th and ^{40}K and contribute to the indoor radiation exposure of occupants [1]. This contribution is subject to regulatory control [2,3], and surveys of building-material radioactivity by gamma-ray spectrometry with high-purity germanium (HPGe) detectors are therefore carried out routinely [4,5]. Every such survey rests on the assumption that the portion of sample placed in the counting container faithfully represents the material as a whole — and for building materials that assumption is not trivial.

Many of these materials are heterogeneous at the grain scale, and the radionuclides of interest are not distributed uniformly among the mineral phases: potassium resides mainly in feldspars and micas, whereas uranium and thorium are concentrated in accessory minerals such as zircon, monazite and apatite. These phases differ from the bulk matrix in hardness and cleavage, so comminution does not distribute them evenly across the size classes. The measured specific activity may consequently depend systematically on grain size [6,7], which means that any procedure altering the particle-size distribution can also alter the reported result.

Resolving that dependence experimentally requires the comminuted sample to be divided into narrow size classes and each of them counted separately. At this point a constraint appears that is imposed not by the material but by the measurement: gamma-ray spectrometry of low-activity samples requires a minimum sample mass, both to reach acceptable counting statistics within a realistic counting time and to fill the counting container reproducibly. The two

requirements act against each other, because the narrower the classes, the less material remains in each of them. This work examines where the preparation procedure fails, why it fails for particular material types, and what this implies for the design of future protocols.

Experimental

Samples and comminution

Twenty-seven samples of building materials in common use were investigated: granite, ceramic tiles, natural stone and slate, fireclay and ash pellets, selected to span a range of mineralogical composition and mechanical hardness. Two comminution routes were compared: mechanical milling, and manual crushing with a hammer followed by grinding in a mortar. The comminuted material passed in its entirety through a 1 mm aperture.

Particle-size characterisation

Size fractionation was carried out by dry sieving on an electromagnetic vibratory sieve shaker (Analysette 3 PRO, Fritsch GmbH, Germany) with a set of analytical sieves conforming to ISO 3310-1 [8]. Charges of about 150 g were sieved in repeated 10 min cycles at a vertical amplitude of 1.5 mm. Sieving was not continued to constant mass; instead it was repeated until enough material had accumulated in the classes of interest for gamma counting, and the excess from abundant classes was discarded. Fractionation was performed on ten samples — four according to the PSD7 scheme and six according to the PSD3 scheme — while the remaining samples were counted as bulk material. Six sieves were used, of 500, 250, 125, 100, 75 and 50 µm aperture, giving seven size classes: >500, 500–250, 250–125, 125–100, 100–75, 75–50 and <50 µm (denoted PSD7). Classes that did not reach the mass required for counting were merged with the neighbouring ones into a three-class scheme: >125, 125–75 and <75 µm (denoted PSD3). The PSD3 scheme is a true pooling of PSD7 — its first class covers the first three PSD7 classes, its second the next two and its third the last two — so the two schemes are mutually consistent and can be compared.

Each separated fraction was additionally characterised by laser diffraction (Mastersizer 2000 with a Scirocco dry-dispersion unit, Malvern Instruments, UK) over the range 0.02–2000 µm in accordance with ISO 13320 [9]. Refractive index, absorption and density were specified individually for each material, and the dry-dispersion parameters were adjusted to suppress the sticking together of particles, which was apparent during trial measurements. The distributions were summarised by the mean diameters D[3,2] and D[4,3], the percentiles d(0.1), d(0.5) and d(0.9), and the cumulative fractions below given diameters. Since these diameters correspond to the apertures of the sieves used, the proportion of each fraction that actually lies below the lower limit of the class into which sieving placed it can be calculated.

Gamma-ray spectrometry

Activity concentrations were determined on two liquid-nitrogen-cooled coaxial HPGe detectors of 32.4% and 105.8% relative efficiency. Fractions were sealed in cylindrical polypropylene containers 70 mm in diameter and 62 mm high and stored for at least 40 days before counting, to establish secular equilibrium between ^{226}Ra and the short-lived radon progeny; this period corresponds to more than ten half-lives of ^{222}Rn. The counting time was approximately 18 h per sample, at masses in the range 100–250 g. Efficiency transfer between the different filling heights and densities was performed in ANGLE [10]. A fraction mass of at least about 100 g was taken as the working requirement that the preparation procedure has to satisfy.

Results and discussion

Distribution of mass across the size classes

The dominant practical problem was not the sieving itself but the distribution of mass that it revealed. For most of the harder and more heterogeneous materials the mass was spread very unevenly across the seven target classes, and at least one class — most often an intermediate or a fine one — remained well below the required mass. Prolonged sieving helped only to a limited extent, because the shortfall does not arise from incomplete sieving: the amount of material in a given class is set by how the material fractures, not by the choice of sieve apertures. The class boundaries are chosen by the operator, but how much material ends up in each of them is determined by the sample.

Insufficient mass degrades the measurement in two ways. First, it reduces the number of counts recorded, so that for a fixed counting time the statistical uncertainty grows — and for low-activity samples this is the dominant contribution in any case. Second, it changes the counting geometry: a smaller mass means a lower filling height and a different bulk density from those for which the detector was calibrated. This second effect can be corrected by efficiency transfer, but the accuracy of the correction depends on how well the filling height and density are known — and these are least well defined precisely at small masses, when the layer of material in the container becomes thin and uneven.

Pooling of fractions as a working compromise

Merging adjacent classes proved effective: composite samples above 100 g could be assembled consistently once seven classes had been reduced to three. The full PSD7 scheme was retained only for materials that yielded sufficient mass per class. The price of that compromise is a loss of granulometric resolution, and it falls on the harder and more heterogeneous materials — those for which a dependence of specific activity on grain size would be most likely [6,7]. The pooling scheme applied should therefore be reported as an integral part of the result rather than as an incidental detail of sample handling.

Influence of the comminution method

How severe the mass problem became depended on the choice between milling and manual crushing. Mechanical milling produced a disproportionate quantity of fine material: the fine classes were amply supplied, the coarse ones systematically depleted, and prolonging milling in order to process more material only shifted the distribution further towards the fines. Manual preparation with hammer and mortar gave a more balanced distribution and preserved the coarse classes, but at a considerable cost in time and consistency; its outcome depended on the operator and on the material, so the results were less reproducible and the achievable throughput too low for a larger sample set. The two routes therefore fail in complementary ways — milling is reproducible but biased towards the fines, manual crushing is unbiased in that respect but poorly reproducible — so neither can be recommended as universal. The comminution route should be chosen with the target size classes in mind.

Nominal sieve class and actual particle size

The limits of the preparation lie not only in the available mass. Every separated fraction was also measured by laser diffraction, which made it possible to establish how much of it is in fact finer than the nominal sieve class claims. Figure 1 shows that proportion. Were the sieve classifying correctly, it would be close to zero.

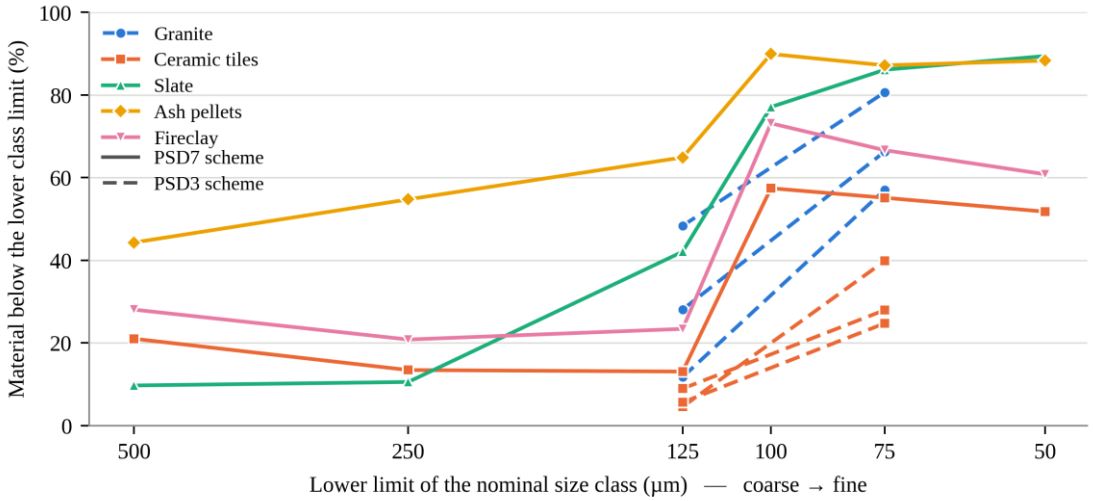


Figure 1. Proportion of material that, according to laser diffraction, is finer than the lower limit of the size class into which sieving placed it. Solid lines — samples sieved according to the PSD7 scheme; dashed lines — according to the PSD3 scheme.

The deviations are large and grow towards the finer classes. For slate the coarse classes are well classified: in the >500 µm class only 9.7% of the material is finer than 500 µm. Yet in the 125–100 µm class 77% lies below the lower limit, and in the 75–50 µm class as much as 89%. The same pattern recurs in the other materials with differing severity — for ceramic tiles the proportion rises from 13% in the 250–125 µm class to 57% in the 125–100 µm class, while for ash pellets it is high in every class, from 44% upwards. The difference between materials is clearest in the PSD3 scheme: the nominally coarse class (>125 µm) contains between 12% and 48% of material finer than 125 µm for granite, but only 4.6–8.9% for ceramic tiles.

Two conclusions follow. First, there is a break at about 125 µm: above it the sieve classifies satisfactorily, below it the nominal class ceases to describe the actual particle size. Second, that break is not the same for all materials, so the same nominal class cannot be taken to mean the same thing for two different materials.

The main cause is the sticking together of fine particles. A cluster of fine grains behaves on the sieve as a single coarse grain, does not pass through the aperture and is assigned to a coarser class; during the laser measurement the stream of compressed air breaks these clusters apart, so the instrument sees the individual particles. That such sticking does occur was confirmed during the measurements themselves, in which the dispersion parameters had to be adjusted specifically in order to suppress it. Since the sieve classifies aggregates while laser diffraction classifies individual particles, the two methods must diverge once sticking becomes pronounced — and it does so precisely in the finer classes, which matches the shape of the curves in Figure 1. Two further mechanisms probably contribute to the same deviation. Sieving was not continued to constant mass, so some fine material may have remained unclassified. In addition, the two methods differ in what they measure: the sieve classifies particles by their intermediate dimension, whereas laser diffraction returns an equivalent-sphere diameter, which for non-spherical particles cannot coincide even in the ideal case. The proportion shown is a property of the fraction itself and does not depend on how much material from it was retained for counting.

Implications for future protocols

Taken together, these observations argue against a single sieving protocol for all building materials. The comminution route and the choice of sieve set should be matched to the expected fracture behaviour of the material; laser diffraction on small sub-samples can be used in advance

to estimate both the distribution of mass and the reliability of the classification, so that the pooling scheme can be fixed before samples enter the counting procedure; and where a fraction cannot be enlarged by further pooling without losing the resolution that motivated the experiment, it is the measurement that should be adapted — by a smaller calibrated geometry or a longer counting time.

Conclusion

Particle-size-resolved sample preparation for gamma-ray spectrometry is governed by a trade-off between granulometric resolution, attainable sample mass and practical feasibility. Narrow size classes could not be maintained across the whole sample set: fractions had to be pooled into three classes in order to reach the mass required for reliable counting, and the seven-class scheme survived only for materials that comminuted favourably. The comminution route governed this outcome — milling shifts the distribution towards the fines, while manual crushing sacrifices reproducibility in order to preserve the coarse classes. Comparison with laser diffraction showed in addition that below about 125 µm the nominal sieve class ceases to describe the actual particle size reliably, and that the size at which this occurs depends on the material. Preparation protocols matched to the material, shaped jointly by granulometric measurement and by the mass requirement of the counting geometry, are a practical route towards more reliable gamma-spectrometric assessment of heterogeneous building materials.

Acknowledgements

This research was funded by the Provincial Secretariat for Higher Education and Scientific Research of Vojvodina through the project No. 003864834 2025 09418 003 000 000 001 04 004, and supported by the Ministry of Science, Technological Development and Innovation and the Faculty of Technical Sciences, University of Novi Sad, Contracts: No. 451-03-34/2026-03/200156 and No. 01-3609/1.

References

[1] UNSCEAR, Sources, Effects and Risks of Ionizing Radiation, UNSCEAR 2024 Report Vol. II, United Nations, New York, 2024.

[2] IAEA, Regulatory Control of Exposure due to Radionuclides in Building Materials and Construction Materials, Safety Reports Series No. 117, IAEA, Vienna, 2023.

[3] Council Directive 2013/59/Euratom, Off. J. Eur. Union L13 (2014) 1.

[4] N. Todorović, I. Bikit, M. Krmar, D. Mrđa, J. Hansman, et al., Int. J. Environ. Sci. Technol. 12 (2015) 705.

[5] L. Laghi, A. Zappi, D. Mostacci, L. Tositti, Environ. Sci. Pollut. Res. 32 (2025) 7651.

[6] S. Elnobi, S. Harb, N.K. Ahmed, Appl. Radiat. Isot. 130 (2017) 43.

[7] M.I. Savva, D.J. Karangelos, M.J. Anagnostakis, S.E. Simopoulos, Appl. Radiat. Isot. 109 (2016) 563.

[8] ISO 3310-1:2016, Test Sieves — Technical Requirements and Testing — Part 1: Test Sieves of Metal Wire Cloth, International Organization for Standardization, Geneva, 2016.

[9] ISO 13320:2020, Particle Size Analysis — Laser Diffraction Methods, International Organization for Standardization, Geneva, 2020.

[10] S. Jovanović, A. Dlabač, N. Mihaljević, Nucl. Instrum. Methods Phys. Res. A 622 (2010) 385.

PHYSICOCHEMICAL AND SENSORY EVALUATION OF COOKIES WITH TURMERIC AND ROSEMARY

Laura Rădulescu[1], Ariana-Bianca Velciov[1], Corina-Iuliana Megyesi[1], Mariana Poiană[1], Liana Maria Alda[1], Carmen Daniela Petcu[3], Sofia Popescu[1], Patricia Tarkanyi[1], Simion Alda[2], Mihaela Lacatuș[1], Diana Moigradean[1], Antoanela Cozma[5], Ioan Ladislau Caba[4], Alexandru Panici[2] , Despina-Maria Bordean[1]

[1]Faculty of Food Engineering, University of Life Sciences "King Michael I" from Timisoara, 300645, Timisoara, Romania
[2]Faculty of Engineering and Applied Technologies, University of Life Sciences "King Michael I" from Timisoara, 300645, Timisoara, Romania
[3]Faculty of Veterinary Medicine, University of Agronomic Sciences and Veterinary Medicine of Bucharest, 105 Independentei Spl., District 5, 050097, Bucharest, Romania
[4]National Institute of Research – Development for Machines and Installations Designed for Agriculture and Food Industry – INMA, 013813, Bucharest, Romania
[5]Faculty of Agriculture,, University of Life Sciences "King Michael I" from Timisoara, 300645, Timisoara, Romania
e-mail: corina.megyesi@usvt.ro

Abstract
The aim of this study was to evaluate the physicochemical and sensory characteristics of butter cookies enriched with turmeric (*Curcuma longa* L.) powder and dried rosemary (*Rosmarinus officinalis* L.). Three variants were prepared from the same basic recipe: a control without spices, a sample with 2 g turmeric and 2 g rosemary, and a sample with 5 g turmeric and 5 g rosemary per batch (approximately 1120 g of dough). Sensory evaluation was carried out by five assessors on a 5-point hedonic scale for external appearance, odour, texture, taste and overall appearance. Dry matter, moisture, fat, total ash and pH were determined, and the nutritional and energy values were calculated from the recipe. Both enriched samples obtained higher scores than the control for all attributes, and the sample with 5 g turmeric and 5 g rosemary obtained the highest mean score (4.9, compared with 4.1 and 3.0), with the largest gains for external appearance and taste. Dry matter ranged from 79.1 to 79.7%, moisture from 20.3 to 20.9% and fat from 19.0 to 19.5%, whereas total ash increased from 0.95 to 1.18% and pH decreased slightly from 6.52 to 6.31 as the level of addition increased. The calculated energy value was 84 kcal per 20 g cookie. The incorporation of turmeric and rosemary improved the sensory profile of the cookies while maintaining a similar basic composition, highlighting the potential of these spices for the development of innovative bakery products.
Keywords: turmeric, rosemary, cookies, sensory evaluation, physicochemical characteristics, bakery products

Introduction
Innovation plays a fundamental role in the pastry industry, contributing to product diversification, quality improvement and meeting the needs of modern consumers. It may concern the ingredients used, production technologies, product design and presentation, as well as health and sustainability aspects, and it is essential for developing new value-added products. In recent years, the fortification of bakery products, including biscuits and cookies, with functional ingredients has become a successful strategy for meeting consumer demand and supporting industry growth [1]. Turmeric and rosemary offer both sensory and nutritional benefits and can give cookies a distinctive, slightly exotic flavour, different from that of

conventional products, which may attract consumers looking for functional foods and new taste experiences.

Curcumin, the main polyphenol of turmeric, has been associated with antioxidant and anti-inflammatory effects and with the management of metabolic conditions [2]. Besides its bioactive properties, turmeric is widely used as a spice and natural colourant [3], and it can give cookies a golden-yellow hue without the need for artificial colourants. Turmeric powder has already been tested in bakery products: in cakes, replacing up to 6% of the wheat flour gave acceptable sensory scores [4], while in bread its effects on quality and antioxidant properties have been evaluated [5].

Rosemary is rich in phenolic diterpenes (carnosic acid and carnosol), rosmarinic acid and essential oil [6]. Owing to its antioxidant and antimicrobial activity, it is considered an effective natural preservative, and it has also been linked to gastrointestinal health in *in vivo* studies [7]. In cookies, spice extracts including rosemary improved the oxidative stability of the fat fraction, and cookies with 0.02% rosemary extract were sensorially acceptable [8]. From a sensory point of view, rosemary adds a fresh, Mediterranean note that complements the aroma of turmeric.

The aim of this study was to evaluate the physicochemical characteristics (dry matter, moisture, fat, ash and pH) and the sensory acceptability of butter cookies enriched with two levels of turmeric powder and dried rosemary (2 g + 2 g and 5 g + 5 g per batch), compared with a control without additions.

Experimental

Materials and samples. The cookies were prepared from wheat flour (500 g), butter (250 g), sugar (200 g), eggs (three eggs, approximately 150 g), grated lemon zest and baking powder, giving approximately 1120 g of dough per batch (56 cookies of 20 g each). Three variants were prepared: Sample 1 (control), without turmeric or rosemary; Sample 2, with 2 g turmeric powder and 2 g dried rosemary; and Sample 3, with 5 g turmeric powder and 5 g dried rosemary (approximately 0.45% of each in the dough). All samples were prepared under controlled laboratory conditions, using the same basic recipe and processing method.

Cookie preparation. The raw materials were weighed according to the recipes. The butter was creamed with the sugar, the eggs and lemon zest were added, and the dry ingredients (flour, baking powder, turmeric powder and dried rosemary) were gradually incorporated until a homogeneous dough was obtained. The dough was kept at 4 °C for approximately 30 min, rolled out to a thickness of 5–7 mm, cut with cookie cutters and placed on trays lined with baking paper. The cookies were baked in a preheated oven at 160–170 °C for 15–20 min and then left to cool at room temperature.

Sensory analysis. The three variants were evaluated comparatively by a panel of five assessors, using a 5-point scale (1 = dislike extremely, 2 = dislike, 3 = neither like nor dislike, 4 = like, 5 = like very much) for external appearance, odour, texture, taste and overall appearance. The results are expressed as mean ± standard deviation (n = 5).

Physicochemical analyses. Dry matter was determined gravimetrically by drying approximately 5 g of homogenised sample at 103 ± 2 °C to constant mass; moisture was calculated as 100 − dry matter. Total fat was determined by Soxhlet extraction (petroleum ether, approximately 6 h) on approximately 5 g of ground sample. Total ash was determined by dry ashing of 3–5 g of sample in a muffle furnace at 550 ± 25 °C to constant mass. The pH was measured potentiometrically on a 1:10 (w/v) suspension (10 g of sample in 90 mL of distilled water, homogenised for 5 min), using a pH meter calibrated with pH 4.00 and 7.00 buffers. The nutritional and energy values were calculated from the recipe composition, using the nutritional values per 100 g of each ingredient.

Results and discussion

A. Sensory evaluation

The mean sensory scores are presented in Table 1 and Figure 1. The addition of turmeric and rosemary increased the scores for all attributes: the control (Sample 1) obtained the lowest overall mean score (3.0), followed by Sample 2 (4.1) and Sample 3 (4.9). The largest differences were recorded for external appearance (1.8 for the control vs. 4.4 and 4.8), consistent with the golden-yellow colour conferred by turmeric, and for taste (2.6 vs. 3.8 and 5.0). Odour was also rated higher in the enriched samples (4.4 and 4.8 vs. 3.8), reflecting the aromatic contribution of rosemary and turmeric. Texture scores were similar for the control and Sample 2 (3.8 and 4.0) and higher for Sample 3 (4.8); the control also showed the widest dispersion of texture scores (SD 1.3). All five assessors gave Sample 3 the maximum score for taste and overall appearance, which indicates that, at the highest level tested (approximately 0.45% of each spice in the dough), no off-flavours such as the bitterness that may occur at excessive levels of these spices affected acceptability. Since only two addition levels were tested and the panel consisted of five assessors, the results are indicative, and the optimum level may lie above the range studied.

Table 1. Mean sensory scores of the cookie samples (mean ± SD, n = 5 assessors)

Attribute	Sample 1 (control)	Sample 2 (2 g + 2 g)	Sample 3 (5 g + 5 g)
External appearance	1.8 ± 0.8	4.4 ± 0.9	4.8 ± 0.4
Odour	3.8 ± 0.4	4.4 ± 0.5	4.8 ± 0.4
Texture	3.8 ± 1.3	4.0 ± 0.7	4.8 ± 0.4
Taste	2.6 ± 0.9	3.8 ± 0.4	5.0 ± 0.0
Overall appearance	3.2 ± 0.8	4.0 ± 0.0	5.0 ± 0.0
Mean of all attributes	**3.0**	**4.1**	**4.9**

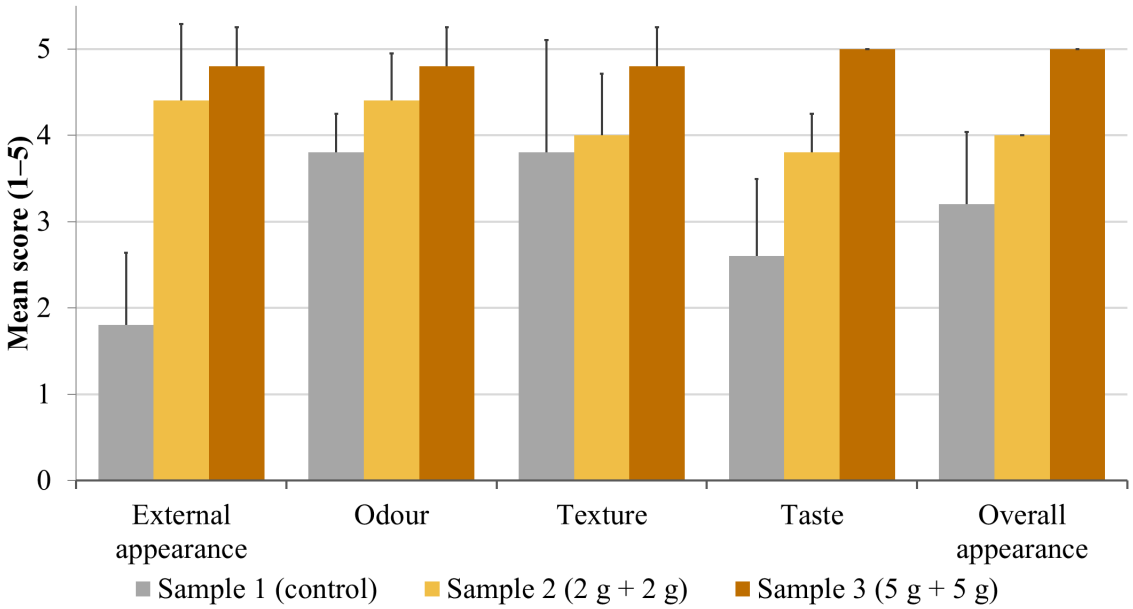


Figure 1. Mean sensory scores of the cookie samples (error bars: SD, n = 5; Sample 1: control; Sample 2: 2 g turmeric + 2 g rosemary; Sample 3: 5 g turmeric + 5 g rosemary)

B. Physicochemical characterisation

The results are given in Table 2. Dry matter ranged from 79.1 to 79.7% and moisture from 20.9 to 20.3%; the differences between samples were below 0.6 percentage points, and the slight decrease in moisture may be related to the dry plant material added. Fat content varied only marginally (19.0–19.5%), since butter and eggs, the main lipid sources, were identical in all variants; the small increase in the enriched samples may reflect the solvent-extractable essential oils and lipophilic compounds of turmeric and rosemary. In contrast, total ash increased with the level of addition, from 0.95 g/100 g in the control to 1.05 g/100 g (+11%) and 1.18 g/100 g (+24%) in Samples 2 and 3, consistent with the mineral contribution of the added spices. The pH values were slightly acidic, as expected for flour–butter–sugar products, and decreased slightly from 6.52 (control) to 6.31 (Sample 3), probably due to the phenolic compounds and organic acids of turmeric and rosemary; this change does not alter the general character of the product.

Table 2. Physicochemical characteristics of the cookie samples

Sample	Dry matter (%)	Moisture (%)	Fat (%)	Total ash (%)	pH
1 (control)	79.1	20.9	19.0	0.95	6.52
2 (2 g + 2 g)	79.3	20.7	19.2	1.05	6.44
3 (5 g + 5 g)	79.7	20.3	19.4–19.5	1.18	6.31

C. Nutritional value

For the Sample 3 formulation, the calculated values per batch (approximately 1120 g of dough, 56 cookies) were 4679 kcal, 71 g protein, 227.8 g fat and 595.5 g carbohydrates, corresponding to 84 kcal, 1.3 g protein, 4.1 g fat and 10.6 g carbohydrates per 20 g cookie. Turmeric and rosemary contribute approximately 35 kcal per batch (<1% of the total energy), so their effect is mainly sensory rather than energetic.

Conclusion

The addition of turmeric powder and dried rosemary markedly improved the sensory acceptability of butter cookies without major changes in their basic composition. The cookies with 5 g turmeric and 5 g rosemary per batch obtained the highest mean sensory score (4.9, compared with 4.1 for the 2 g + 2 g variant and 3.0 for the control), with the largest gains for external appearance and taste. Dry matter (79.1–79.7%), moisture (20.3–20.9%) and fat (19.0–19.5%) varied only slightly, total ash increased progressively (from 0.95 to 1.18%) and pH decreased slightly (from 6.52 to 6.31). The calculated energy value was 84 kcal per 20 g cookie. These results, obtained with a panel of five assessors, indicate that turmeric and rosemary are promising ingredients for innovative bakery products. Further work should include larger consumer panels, additional addition levels and the determination of antioxidant capacity, oxidative stability and shelf life.

Acknowledgements

The authors wish to express their gratitude to all who contributed to the completion of this study.

References

[1] N. Chakraborty, R. Chakraborty, Curr. Nutr. Food Sci. 19 (2023) 615–641. https://doi.org/10.2174/1573401319666221104100217

[2] S.J. Hewlings, D.S. Kalman, Foods 6 (2017) 92. https://doi.org/10.3390/foods6100092

[3] S. Prasad, B.B. Aggarwal, in: I.F.F. Benzie, S. Wachtel-Galor (Eds.), Herbal Medicine: Biomolecular and Clinical Aspects, 2nd ed., CRC Press/Taylor & Francis, Boca Raton, 2011, pp. 263–288.
[4] S.H. Park, H.S. Lim, S.Y. Hwang, Food Sci. Technol. Int. 18 (2012) 435–443. https://doi.org/10.1177/1082013211428220
[5] H.S. Lim, S.H. Park, K. Ghafoor, S.Y. Hwang, J. Park, Food Chem. 124 (2011) 1577–1582.
[6] J.M. Andrade, C. Faustino, C. Garcia, D. Ladeiras, C.P. Reis, P. Rijo, Future Sci. OA 4 (2018) FSO283. https://doi.org/10.4155/fsoa-2017-0124
[7] J.P. Veenstra, J.J. Johnson, Int. J. Nutr. 6 (2021) 1–10.
[8] M. Kozłowska, A. Żbikowska, E. Gruczyńska, K. Żontała, A. Półtorak, J. Therm. Anal. Calorim. 118 (2014) 1697–1705. https://doi.org/10.1007/s10973-014-4058-y

ANTINUTRITIONAL FACTORS AND PROCESSING NEEDS - MITIGATION STRATEGIES

Mihaela Lacatus[1], Patricia Cristina Tarkanyi[1], Alexandru-Erne Rinovetz[2*], Laura Radulescu[2], Liana Maria Alda[2], Luminita Pirvulescu[4], Ioan Ladislau Caba[3], Mariana-Atena Poiana[1,2], Despina Maria Bordean[1,2]

[1]Doctoral School "Engineering of Vegetable and Animal Resources", University of Life Sciences "King Mihai I" from Timisoara, Calea Aradului 119, Timisoara, Romania;
[2]Faculty of Food Engineering, University of Life Sciences "King Mihai I" from Timisoara, 300645, Timisoara, Romania;
[3]National Institute of Research Development for Machines and Installations designed to Agriculture and Food Industry INMA,
Bucharest 013813, Romania.
[4]Faculty of Management and Rural Tourism, University of Life Sciences "King Mihai I" from Timisoara, Calea Aradului 119, 300645-Timisoara, Romania
e-mail: alexandrurinovetz@usvt.ro

Abstract
This study aims to review the antinutritional compounds in *Amaranthus* species, and the approaches reported for their reduction content. Literature data was used to summarize nitrates, oxalates, saponins, phytates, tannins and protease inhibitors. Analytical methods were also described. The reported information was compiled in a comparative table, while a schematic figure was prepared for *Amaranthus retroflexus* L. to highpoint the main factors: antinutrient levels, their potential nutritional implications and possible reduction strategies. Processing treatments (soaking, germination, fermentation and thermal treatments) have been reported to reduce or modify antinutritional compounds. Although their efficiency varies depending on the compound and treatment conditions. Understanding these aspects may support the nutritional valorization of *Amaranthus* and its safer use in food and plant-based functional products.

Keywords: ***Amaranthus retroflexus* L., *analytical methods, food safety, nutrients.***

Introduction

Although *Amaranthus* is well known as a appreciated source of nutrients and bioactive compounds, its nutritional utilization may be limited because the presence of antinutritional factors. Among these: nitrates, oxalates, phytate, tannins and saponins have a particular interest. Their presence and concentration can influence nutrient availability and the suitability of plant material for the human and animal consumption [1].
Phytic acid is distributed throughout the grain, and its removal via simple abrasion or washing with water is relatively ineffective. Consequently, various processing methods have been investigated to reduce antinutritional compounds in amaranth [1]. Olawoye (2009) reported that defatting, blanching, germination, fermentation, and autoclaving improved protein digestibility and reduced specific antinutritional compounds in *Amaranthus viridis* seeds [2]. Germination at 30°C for 72 hours yielded the greatest improvement in protein digestibility, reaching approximately 82%, while fermentation resulted in an increase of about 76%. Blanching and autoclaving proved effective in reducing tannins and oxalates. Similarly, Bordean et al. (2025) found that boiling improved protein digestibility and reduced the content of tannins, oxalates, and phytates [2]. In another study, Kanensi (2011) reported that soaking for 5 hours and germination for 24 hours led to a significant reduction in antinutritional compounds [3].

Tannins are phenolic compounds associated with the bitter taste of plant materials. They are typically found in seed coats, fruits, and vegetables, including *amaranthus* [4]. Although considered antinutritional compounds, their effects depend on chemical structure and concentration [5]. Oxalates represent another significant antinutritional factor, particularly in amaranth leaves. They can bind to calcium to form insoluble calcium oxalate, thereby reducing calcium availability [6]. *Amaranth* can also accumulate considerable amounts of nitrates, with levels influenced by environmental and agronomic conditions, including drought, low temperatures, herbicide exposure, and excessive nitrogen fertilization.

The commonly used methods for the determination of the antinutritional factors were identified and are based on an extensive review from the scientific literature. For each method, a brief description is provided below:

1. *Determination of phytate content.*

The quantitative determination of phytate can be carried out using the colorimetric procedure described by Wheeler and Ferrel (1971) [7]. In this method, phytate is first extracted from the plant material using hydrochloric acid. Following extraction, phytate is precipitated in the form of ferric phytate, and the iron associated with the precipitate is subsequently determined spectrophotometrically. The measured iron content is then converted into phytate concentration using an appropriate conversion factor[7].

2. *Determination of saponins.*

The method proposed by Obadoni and Ochuko (2001) is based on the extraction and gravimetric determination of saponins from plant material [8]. Finely ground samples are extracted with 20% aqueous ethanol under controlled heating and continuous stirring. After filtration, the remaining plant material is subjected to a second extraction, and the resulting extracts are combined and concentrated. Concentrated extract is subsequently purified by partitioning with diethyl ether to remove non-polar compounds. The aqueous fraction containing the saponins is then extracted with n-butanol; butanolic fractions are washed with sodium chloride solution and evaporated to obtain the dry saponin residue; after drying to constant weight, the saponin content is calculated gravimetrically by relating the mass of the dried residue to the initial mass of the plant sample [8].

3. *Determination of tannins.*

The determination of tannins may be performed according to the colorimetric method described by Van-Burden and Robinson (1981) [9]. Tannins are extracted from the plant material using distilled water; the resulting extract is then reacted with ferric chloride in an acidic medium, together with potassium ferrocyanide. The result is a colored complex that can be quantified spectrophotometrically [9].

4. *Determination of oxalates.*

Oxalate content can be determined using the procedure described by Locke et. al., (1987). It involves acid extraction followed by titrimetric quantification. Initially, the plant material is treated with dilute hydrochloric acid to release the oxalates into the extraction medium. After filtration, the resulting solution is titrated against a standardized potassium permanganate solution. The reaction is final when is indicated by the appearance of a faint pink coloration that remains stable for a short period. The oxalate concentration is then calculated from the volume of potassium permanganate consumed during the titration [10].

5. *Determination of nitratest.*

Nitrates are an important source of inorganic nitrogen in plants. Excessive accumulation may have nutritional implications due to their conversion into nitrites and N-nitroso compounds. The colorimetric method of Cataldo et al. (1975) is based on the reaction of nitrates with salicylic acid in sulfuric acid, followed by the development of a yellow color under alkaline conditions [11].

The aim of this study was to provide an overview of antinutritional factors in *Amaranthus retroflexus* plant parts with the focus on: phytates, saponins, tannins, oxalates, protease

inhibitors and nitrates. With the overall objective of supporting nutritional quality and safer consumption of amaranth-based products, we review the analytical methods reported in the scientific literature for their determination and the processing strategies proposed for their decreasing content.

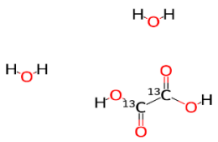
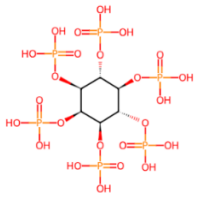
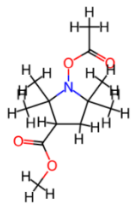
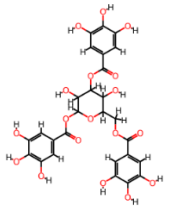
Experimental

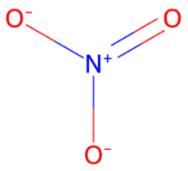
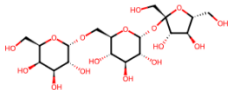
For the experimental part of this study, the aproach was based on data collected from scientific literature. The reported compounds and their determination methods were reviewed and compiled in table and figure. The schematic representation was developed with the help of ChatGPT (OpenAI, 2026) [12].

Results and discussion

Antinutritional factors refer to naturally occurring substances in foods that can negatively affect nutritional value by reducing nutrient availability, interfering with digestion, or limiting nutrient utilization [1]. These compounds may be of biological or chemical origin and can interfere with metabolic processes, thereby affecting the utilization of nutrients in both humans and animals [1], [13], [14]. The main antinutritional factors reported in *Amaranthus retroflexus* are summarized in Table 1.

Table 1. Antinutrients in *Amaranthus retroflexus* [1], [15].

Common name	IUPAC NAME	Molecular formula	Chemical structure
Oxalic acid	(~13~C_2_)Ethanedioic acid dihydrate	13C2H6O6	
Phytic acid	(1R,2S,3r,4R,5S,6s)-1,2,3,4,5,6-Cyclohexanehexayl hexakis[dihydrogen (phosphate)]	C6H18O24P6	
Saponin	Methyl 1-acetoxy-2,2,5,5-tetramethyl-3-pyrrolidinecarboxylate	C12H21NO4	
Tanin	1,3,6-Tris-O-(3,4,5-trihydroxybenzoyl)hexopyranose	C27H24O18	

Nitrate	Nitrate	NO3	
Lectin	β-D-Fructofuranosyl α-D-galactopyranosyl-(1->6)-α-D-glucopyranoside	C18H32O16	

The data synthesized in Figure 1 highlights the multifactorial nature of antinutritional compounds in *Amaranthus retroflexus*. Their presence is not constant, but may vary with plant organ, genotype, environmental conditions and post-harvest handling. As a result, the nutritional implications of these compounds and the capability of their reduction should be considered in relation to both the plant material and the processing conditions applied.

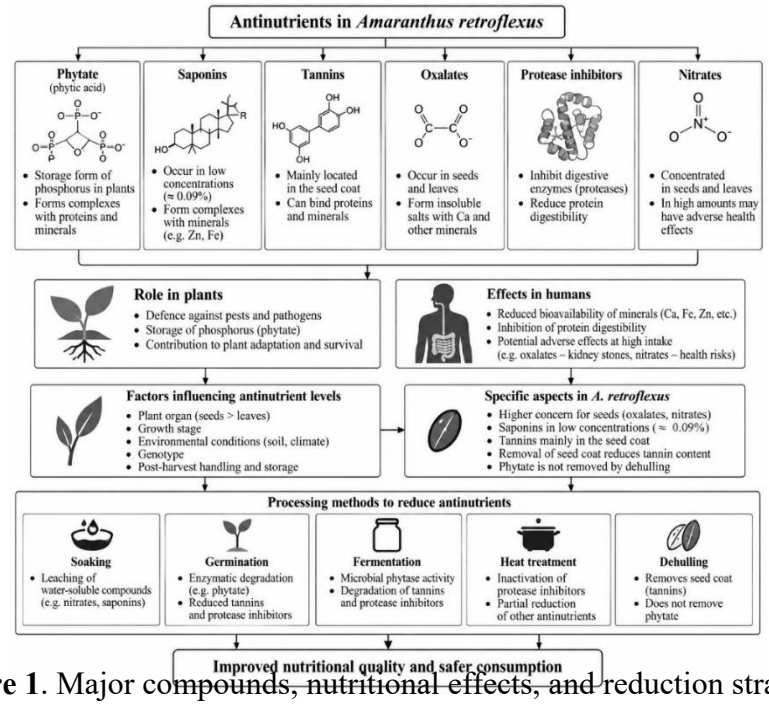


Figure 1. Major compounds, nutritional effects, and reduction strategies.
Adapted from Dobos (1992) and Cuadrado et al. (2019). Created by the authors with the assistance of ChatGPT (OpenAI, 2026) [12], [11], [16].

Conclusion

The *Amaranthus retroflexus* represent a valuable plant resources, but its potential is influenced by the presence of antinutritional factors. From the reviewed scientific literature results that these compounds vary with the plant organ, environmental conditions and cultivation practices. With the combined assessment of antinutritional factors and correct processing methods, for this plant, the nutritional quality and safety can be improved.
Overall, these approaches can support the nutritional valorization for the use in functional foods and plant-based ingrendients.

Acknowledgements
This study was funded by the University of Life Sciences "King Mihai I" from Timisoara" and the results will be included in the PhD Thesis of Mihaela Lăcătuș under the supervision of Prof. Habil.Dr.Eng. Despina-Maria Bordean. The authors would like to thank to the Doctoral School "Engineering of Vegetable and Animal Resources", University of Life Sciences "King Mihai I" from Timişoara, Calea Aradului 119, 300645, Timişoara, Romania), for the academic support and resources provided throughout the development of this research.

References
[1]. Bordean, D.-M., Caba, I. L., Mișcă, C. D., Poiană, M.-A., Borozan, A.-B., Tarkanyi, P., Lăcătuș, M., & Poiană, T.-A. (2025). Bioresources and sustainability: From alternative food to ecosystem regeneration. Eurobit. ISBN 978-630-326-183-6;
[2]. Olawoye, B. T., & Gbadamosi, S. O. (2017). Effect of different treatments on in vitro protein digestibility, antinutrients, antioxidant properties and mineral composition of Amaranthus viridis seed. Cogent Food & Agriculture, 3(1), 1296402. https://doi.org/10.1080/23311932.2017.1296402;
[3]. Kanensi, O. J., Ochola, S., Gikonyo, N. K., & Makokha, A. (2011). Optimization of the period of steeping and germination for amaranth grain. Journal of Agriculture and Food Technology, 1(6), 101-105.https://www.researchgate.net/publication/264788165_Optimization_of_the_Period_of_Steeping_and_Germination_for_Amaranth_Grain ;
[4]. Makkar, H. P. (2003). Effects and fate of tannins in ruminant animals, adaptation to tannins, and strategies to overcome detrimental effects of feeding tannin-rich feeds. *Small ruminant research, 49(3)*, 241-256. https://doi.org/10.1016/S0921-4488(03)00142-1 ;
[5]. Hassanpour, S., MaheriSis, N., & Eshratkhah, B. (2011). Plants and secondary metabolites (Tannins): A Review. https://www.researchgate.net/publication/216069956_Plants_and_secondary_metabolites_Tannins_A_Review ;
[6]. Agbaire, P. O. (2012). Levels of anti-nutritional factors in some common leafy edible vegetables of southern Nigeria. *African Journal of Food Science and Technology*, 3(4), 99-101;
[7]. Wheeler, E. L., & Ferrel, R. E. (1971). A method for phytic acid determination in wheat and wheat fractions. https://www.cabidigitallibrary.org/doi/full/10.5555/19721492732 ;
[8]. Obadoni, B. O., & Ochuko, P. O. (2002). Phytochemical studies and comparative efficacy of the crude extracts of some haemostatic plants in Edo and Delta States of Nigeria. *Global Journal of pure and applied sciences*, *8*(2), 203-208. DOI: 10.4314/gjpas.v8i2.16033 ;
[9]. Van Buren, J. P., & Robinson, W. B. (1969). Formation of complexes between protein and tannic acid. *Journal of Agricultural and Food Chemistry*, *17*(4), 772-777. https://doi.org/10.1021/jf60164a003;
[10]. Locke, D. C., & Grossman, W. E. (1987). The curriculum in quantitative analysis: results of a survey. *Analytical Chemistry*, *59*(13), 829A-835A. https://doi.org/10.1021/ac00140a001 ;
[11]. Cuadrado, C., Takacs, K., Szabó, E. E., & Pedrosa, M. M. (2019). Non-nutritional factors: Lectins, phytic acid, protease inhibitors, allergens. In M. Á. Martín-Cabrejas (Ed.), *Legumes: Nutritional quality, processing and potential health benefits* (pp. 152–176). Royal Society of Chemistry. https://doi.org/10.1039/9781788015721-00152 ;
[12]. ChatGPT (version GPT-5.6, developed by OpenAI, San Francisco, CA, USA). Available online: https://chat.openai.com/ (accessed on 23 September 2026);
[13]. Venskutonis, P. R., & Kraujalis, P. (2013). Nutritional components of amaranth seeds and vegetables: a review on composition, properties, and uses. *Comprehensive reviews in food science and food safety*, *12*(4), 381-412. https://doi.org/10.1111/1541-4337.12021 ;

[14]. Soetan, K. O., & Oyewole, O. E. (2009). The need for adequate processing to reduce the anti-nutritional factors in plants used as human foods and animal feeds: A review. *African Journal of food science*, *3*(9), 223-232. https://academicjournals.org/journal/AJFS/article-full-text-pdf/8CA575F20441.pdf ;
[15]. ChemSpider. Royal Society of Chemistry. https://www.chemspider.com / (accessed in 01 August 2025);
[16]. Dobos, G. (1992). Körneramaranth als neue *Kulturpflanze in Österreich: Introduktion und züchterische Aspekte*. Doctoral dissertation, University of Agricultural Sciences Vienna;

COMPARATIVE GREEN EXTRACTION OF PHENOLICS FROM *SATUREJA MONTANA* BY MICROWAVE- AND ULTRASOUND-ASSISTED TECHNIQUES USING CHOLINE CHLORIDE-GLYCEROL NADES

Milica Vidić, Nevena Grujić-Letić, Branislava Teofilović, Emilia Gligorić

Department of Pharmacy, Faculty of Medicine, University of Novi Sad, Hajduk Veljkova 3, 21000 Novi Sad, Serbia
e-mail: milica.vidic@mf.uns.ac.rs

Abstract

This study aimed to chemically characterize *Satureja montana* L. (Lamiaceae) extracts obtained by microwave-assisted extraction (MAE) and ultrasound-assisted extraction (UAE) using choline chloride: glycerol natural deep eutectic solvent (NADES $_{ChCl:Gly}$). This system was evaluated as a greener alternative to conventional solvents, and the efficiency of MAE and UAE was additionally compared. NADES$_{ChCl: Gly}$ was synthesized by heating and stirring. The plant material-to-solvent ratio was 1:10, with NADES$_{ChCl: Gly}$, 70% ethanol, and water used as solvents. MAE was carried out at a power of 180 W, with three irradiation cycles of 5 s each, while UAE was performed for 30 min at 40 °C, with an ultrasonic frequency of 40 kHz and a power of 360 W. Rosmarinic acid, trans-cinnamic acid, rutin, quercetin, and naringenin were identified and quantified by high-performance liquid chromatography with diode-array detection (HPLC-DAD). The application of NADES$_{ChCl: Gly}$ resulted in comparable or higher phenolic contents than those obtained using conventional solvents. Both green techniques provided high efficiency in the extraction of phenolics. However, MAE enabled efficient phenolic extraction performed at half the power of UAE with a total irradiation time of only 15 s, demonstrating its efficiency in terms of extraction time and energy consumption. This study represents an initial step towards the application of *S. montana* extracts obtained using green extraction approaches.

Introduction

Satureja montana L. (Lamiaceae) is a shrub distributed throughout the Mediterranean region, which has traditionally been used for its antiseptic, digestive, and antispasmodic properties [1]. Moreover, the extracts of this species are rich in phenolic compounds, which contribute to its antioxidant activity [2].

Ultrasound-assisted extraction (UAE) is a green extraction technique that employs ultrasonic waves (>20 kHz) to facilitate the extraction of active principles from a sample in the presence of a suitable solvent [3]. Microwave-assisted extraction (MAE) is another widely applied green extraction technique that involves exposing plant material in a suitable solvent to electromagnetic radiation with frequencies ranging from 0.3 to 300 GHz [4]. Compared with conventional extraction methods, these approaches provide higher extraction efficiency and greater recovery of phytochemicals, while requiring less time, energy, and solvent [5].
Natural deep eutectic solvents (NADES) have emerged as environmentally friendly and cost-effective alternatives to conventional solvents, with high potential for the extraction of phenolic compounds [6].

An innovative approach to extraction involves combining novel extraction techniques, including MAE and UAE, with green solvents such as NADES. Therefore, this study aimed to chemically characterize extracts of *S. montana* obtained by MAE and UAE in combination with choline chloride: glycerol NADES (NADES$_{ChCl: Gly}$). Furthermore, the NADES$_{ChCl: Gly}$ was investigated as a greener alternative to conventional solvents, along with a comparison of MAE and UAE efficiency.

Experimental

Dried aerial parts of *S. montana*, obtained from the Institute for Medicinal Plant Research "Dr. Josif Pančić", were ground (Bosch, Gerlingen, Germany) and sieved through a 0.35 mm sieve (Retsch GmbH & Co. KG, Haan, Germany). $NADES_{ChCl:\ Gly}$ at a molar ratio of 1:2 was synthesized by heating and stirring, with 20 % water added [7]. For the extraction, the plant material-to-solvent ratio was 1:10, with $NADES_{ChCl:\ Gly}$, 70% ethanol, and water used as solvents. MAE was carried out in a microwave oven (Bosch BFL523MS0/06, Munich, Germany) at a power of 180 W, with three irradiation cycles of 5 s each (total time 15 s). UAE was performed in an ultrasonic bath (Vabsonic, Niš, Serbia) for 30 min at 40 °C, with an ultrasonic frequency of 40 kHz and a power of 360 W [8]. Following extraction, all samples were centrifuged at 3500 rpm for 25 min in a centrifuge (SIGMA Laborzentrifugen GmbH, Osterode am Harz, Germany), after which the supernatants were collected and filtered. The chemical characterization of *S. montana* extracts was performed using a modified HPLC method on an Agilent HP 1100 high-performance liquid chromatography system with diode-array detection (HPLC-DAD) and an autosampler injector (Santa Clara, CA, USA) [9]. Statistical analysis was conducted using IBM SPSS Statistics, version 22. Differences among the means of the measured parameters were assessed by one-way ANOVA followed by Duncan's post hoc test, with statistical significance set at $p < 0.05$.

Results and discussion

In this study, the phenolic compound efficiency of $NADES_{ChCl:\ Gly}$ was investigated and compared with conventional solvents. Additionally, the efficiency of two green extraction techniques, UAE and MAE, was evaluated. **Table 1** presents the results of the chemical characterization of *S. montana* herb.

Table 1. Chemical characterization of *S. montana* herb extracts (mg/g DM)

Active principle	Type of extraction	Solvent		
		$NADES_{ChCl:\ Gly}$	70% EtOH	H2O
Rosmarinic acid	MAE	4.7 ± 0.34 ^{a}	4.39 ± 0.25 $^{a, b}$	0.85 ± 0.06 ^{c}
	UAE	4.09 ± 0.02 ^{b}	4.7 ± 0.34 ^{a}	0.61 ± 0.04 ^{c}
Trans-cinnamic acid	MAE	0.04 ± 0.01 ^{a}	0.03 ± 0.01 $^{a, b}$	0.02 ± 0.01 $^{a, b}$
	UAE	0.04 ± 0.01 ^{a}	0.03 ± 0.01 $^{a, b}$	n.d.
Rutin	MAE	2.26 ± 0.06	1.7 ± 0.02	0.94 ± 0.06
	UAE	2.05 ± 0.02	1.92 ± 0.03	0.81 ± 0.03
Quercetin	MAE	0.76 ± 0.14 ^{a}	0.79 ± 0.09 ^{a}	0.71 ± 0.12 ^{a}
	UAE	0.76 ± 0.14 ^{a}	0.8 ± 0.1 ^{a}	n.d.
Naringenin	MAE	1.61 ± 0.06 ^{a}	1.55 ± 0.05 ^{a}	1.53 ± 0.05 ^{a}
	UAE	1.62 ± 0.06 ^{a}	1.56 ± 0.01 ^{a}	1.54 ± 0.05 ^{a}

DM, dried matter; MAE, microwave-assisted extraction; UAE, ultrasound-assisted extraction, n.d., not detected.
Different superscript letters within the same active principle or their absence (rutin) indicate significant differences between means at the 0.05 level (Duncan test).

HPLC analysis revealed the presence of five bioactive compounds in *S. montana* extracts, including the phenolic acids - rosmarinic and trans-cinnamic acid, as well as the flavonoids - rutin, quercetin, and naringenin.

Rosmarinic acid was the most abundant active principle in all extracts, as also reported as the main phenolic compound in a decoction of *S. montana* [10]. The rosmarinic acid content ranged from 0.85 to 4.70 mg/g DM in extracts obtained by MAE and from 0.61 to 4.70 mg/g DM in extracts obtained by UAE. The highest contents were found in the MAE-$NADES_{ChCl: Gly}$ and UAE-70% EtOH extracts, which did not differ significantly. The extract obtained by MAE with 70% EtOH also showed no significant difference from both of these extracts. Additionally, no statistically significant differences were observed between the MAE-70% EtOH and UAE-$NADES_{ChCl: Gly}$ extracts, or between the MAE-water and UAE-water extracts. In combination with MAE and UAE, $NADES_{ChCl: Gly}$ yielded 5.5- and 6.7-fold higher amounts of this phenolic acid than water, respectively.

Trans-cinnamic acid was the least abundant phenolic, ranging from 0.02 to 0.04 mg/g DM for MAE and from 0.03 to 0.04 mg/g DM for UAE. The highest content was obtained with $NADES_{ChCl: Gly}$ under both extraction methods, whereas this compound was not detected in the UAE-water extract. No statistically significant differences were observed among the $NADES_{ChCl: Gly}$-MAE, $NADES_{ChCl: Gly}$-UAE, 70% EtOH-MAE, 70% EtOH-UAE, and water-MAE extracts, nor among the water-MAE, 70% EtOH-MAE, and 70% EtOH-UAE extracts.

Rutin was the second most abundant compound, with amounts ranging from 0.94 to 2.26 mg/g DM for MAE and from 0.81 to 2.05 mg/g DM for UAE. $NADES_{ChCl: Gly}$ yielded the highest content under both extraction methods, 2.4- and 2.5-fold higher than water for MAE and UAE, respectively.

Quercetin was present at concentrations ranging from 0.71 to 0.79 mg/g DM in extracts obtained by MAE and from 0.76 to 0.80 mg/g DM in those obtained by UAE. 70% EtOH showed higher extraction efficiency for this compound with both green extraction methods compared with the other solvents. Quercetin was not detected in the UAE-water extract. The other five extracts did not differ significantly.

The content of naringenin ranged from 1.53 to 1.61 mg/g DM in extracts obtained by MAE and from 1.54 to 1.62 mg/g DM in those obtained by UAE. The highest content was obtained with $NADES_{ChCl: Gly}$ under both extraction methods. However, no statistically significant differences were observed among the six extracts.

The extraction efficiency of rosmarinic acid, trans-cinnamic acid, and rutin depended on the applied solvent. $NADES_{ChCl: Gly}$ enabled the extraction of comparable (rosmarinic acid, and quercetin) or higher (trans-cinnamic acid, rutin, and naringenin) amounts of active compounds than the applied conventional solvents. Moreover, water was the least effective solvent for phenolic compound extraction. The high solubility of bioactive compounds in NADES can be attributed to hydrogen bonding and dipole–dipole interactions between the solvent components and the target compounds [11]. These results highlight NADES as a green alternative to conventional solvents for the extraction of phenolics from *S. montana* herb.

Additionally, the contents of rosmarinic acid and rutin varied with the applied extraction method. Performed at half the power of UAE and for only 15 s, MAE enabled comparable or higher phenolic compound contents. During MAE, the solvent absorbs microwave radiation and converts it into heat, promoting disruption of the plant matrix and the release of bioactive compounds. Due to their compatibility with NADES, high extraction efficiency can be achieved [12].

Conclusion

The chemical composition of *S. montana* herb extracts obtained by MAE and UAE using $NADES_{ChCl: Gly}$, 70% ethanol, and water as extraction solvents was determined. The extraction efficiency of $NADES_{ChCl: Gly}$ and conventional solvents was compared, along with the efficiency of MAE and UAE.

NADES comply with the principles of green chemistry and provide efficient extraction, making them suitable for use with both novel extraction techniques for the isolation of phenolic compounds from *S. montana*. The application of $NADES_{ChCl:\ Gly}$ resulted in comparable or higher phenolic contents than those obtained using conventional solvents.
When comparing the two green extraction methods, MAE provided efficient extraction within 15 s at 180 W, highlighting its potential for energy-efficient extraction of phenolics.
This study represents an initial step towards the application of these green extracts. The next stage of the research should involve determining their total phenolic and flavonoid contents, followed by evaluation of antioxidant activity to further characterize their bioactive potential.

Acknowledgements
This work was supported by the Provincial Secretariat for Higher Education and Scientific Research, Province of Vojvodina (Grant No. 003874431 2025 09418 003 000 000 001).

References
[1] F. Coban, Y. Lan, G. Yetisgin, H. Yuca, B. Aydın, H. Angın, B. Demirci, S. Karakaya, Phytochemical Composition and Bioactivities of *Satureja montana* L. and *Satureja hortensis* L.: Culinary Herbs with Antidiabetic, Anticholinesterase, and Antioxidant Potential, PLoS One 20 (2025) e0332178.
[2] N. Hudz, E. Makowicz, M. Shanaida, M. Białoń, I. Jasicka-Misiak, O. Yezerska, L. Svydenko, P.P. Wieczorek, Phytochemical Evaluation of Tinctures and Essential Oil Obtained from *Satureja montana* Herb, Molecules 25 (2020) 4763.
[3] M. Mosić, A. Dramićanin, P. Ristivojević, D. Milojković-Opsenica, Extraction as a Critical Step in Phytochemical Analysis, J. AOAC Int. 103 (2020) 365-372.
[4] N. Wang, H. Zhu, M. Wang, S. Zhao, G. Sun, Z. Li, Recent Advancements in Microwave-Assisted Extraction of Flavonoids: A Review, Food Bioproc. Tech. 18 (2025) 2083-2100.
[5] H. Valisakkagari, C. Chaturvedi, H.P.V. Rupasinghe, Green Extraction of Phytochemicals from Fresh Vegetable Waste and Their Potential Application as Cosmeceuticals for Skin Health, Processes 12 (2024) 742.
[6] G. Puma-Isuiza, J.M. García-Chacón, C. Osorio, I. Betalleluz-Pallardel, J. Chue, M. Inga, Extraction of Phenolic Compounds from Lucuma (*Pouteria lucuma*) Seeds with Natural Deep Eutectic Solvents: Modelling Using Response Surface Methodology and Artificial Neural Networks, Front. Sustain. Food Syst. 8 (2024) 1401825.
[7] M. Vidić, N. Grujić-Letić, B. Teofilović, E. Gligorić, Towards a Green and Sustainable Valorization of *Salix amplexicaulis*: Integrating Natural Deep Eutectic Solvents and Microwave-Assisted Extraction for Enhanced Recovery of Phenolic Compounds, Sustainability 17 (2025) 6347.
[8] B.M. Popovic, N. Micic, A. Potkonjak, B. Blagojevic, K. Pavlovic, D. Milanov, T. Juric, Novel Extraction of Polyphenols from Sour Cherry Pomace Using Natural Deep Eutectic Solvents – Ultrafast Microwave-Assisted NADES Preparation and Extraction, Food Chem. 366 (2022) 130562.
[9] U. Miljić, V. Puškaš, J. Cvejić Hogervorst, L. Torović, Phenolic Compounds, Chromatic Characteristics and Antiradical Activity of Plum Wines, Int. J. Food Prop. 20 (2017) 2022–2033.
[10] F. Gomes, M.I. Dias, Â. Lima, L. Barros, M.E. Rodrigues, I.C.F.R. Ferreira, M. Henriques, *Satureja montana* L. and *Origanum majorana* L. Decoctions: Antimicrobial Activity, Mode of Action and Phenolic Characterization, Antibiotics 9 (2020) 294.
[11] N.P.E. Hikmawanti, D. Ramadon, I. Jantan, A. Mun'im, Natural Deep Eutectic Solvents (NADES): Phytochemical Extraction Performance Enhancer for Pharmaceutical and Nutraceutical Product Development, Plants 10 (2021) 2091.

[12] M. Ivanović, M. Islamčević Razboršek, M. Kolar, Innovative Extraction Techniques Using Deep Eutectic Solvents and Analytical Methods for the Isolation and Characterization of Natural Bioactive Compounds from Plant Material, Plants 9 (2020) 1428.

SUSTAINABLE MICROWAVE-ASSISTED EXTRACTION OF BIOACTIVE COMPOUNDS FROM *SATUREJA MONTANA* USING CHOLINE CHLORIDE-BASED NATURAL DEEP EUTECTIC SOLVENTS

Milica Vidić, Nevena Grujić-Letić, Branislava Teofilović, Emilia Gligorić

[1]*Department of Pharmacy, Faculty of Medicine, University of Novi Sad, Hajduk Veljkova 3, 21000 Novi Sad, Serbia*
e-mail: milica.vidic@mf.uns.ac.rs

Abstract

Natural deep eutectic solvents (NADES) have emerged as promising alternatives to conventional solvents. They represent liquid systems at room temperature, formed through the combination of hydrogen bond acceptors (HBA) and hydrogen bond donors (HBD). Choline chloride, a quaternary ammonium salt, is one of the most widely used HBA reported in the literature, owing to its low cost and favorable safety profile. High extraction efficiency has been reported when NADES are combined with green extraction techniques for the isolation of phytochemicals from medicinal plants. Therefore, this study evaluated the preliminary chemical composition and antioxidant potential of four *Satureja montana* L. (Lamiaceae) herb extracts obtained by microwave-assisted extraction (MAE) employing two NADES composed of choline chloride as the HBA and lactic and malic acids as the HBD, as well as 70% ethanol and water. The choline chloride: lactic acid (1:2) and choline chloride: malic acid (1:1) NADES were synthesized by heating and stirring, with the addition of 20% water. MAE was performed in three cycles of 5 s each, at a microwave power of 180 W. The total phenolic content (TPC) was determined using the Folin–Ciocalteu colorimetric method, while the total flavonoid content (TFC) was assessed using the aluminum chloride colorimetric assay. Antioxidant activity was evaluated spectrophotometrically employing the 2,2-diphenyl-1-picrylhydrazyl (DPPH) radical scavenging assay and the cupric reducing antioxidant capacity (CUPRAC) assay. The highest TPC and the strongest antioxidant activity according to the CUPRAC assay were observed in the extract obtained using choline chloride: lactic acid NADES. MAE with 70% ethanol resulted in the highest TFC and the strongest antioxidant activity according to the DPPH assay. The lower viscosity of choline chloride: lactic acid NADES compared with choline chloride: malic acid NADES may have contributed to the higher TPC and TFC, as well as the strongest antioxidant activity observed in the choline chloride: lactic acid NADES extract. These findings support the use of sustainable extraction approaches and highlight the medicinal potential of *S. montana* extracts.

Acknowledgements

This work was supported by the Provincial Secretariat for Higher Education and Scientific Research, Province of Vojvodina (Grant No. 003874431 2025 09418 003 000 000 001).

TRANSITION FROM LINEAR TO CIRCULAR ECONOMY: CASE STUDY NOVI SAD WASTE MANAGEMENT REGION

Višnja Mihajlović

Technical Faculty Mihajlo Pupin, University of Novi Sad, Zrenjanin, Djure Djakovica 1A, Serbia
e-mail: visnjamihajlovic@uns.ac.rs

Abstract
The European Union's Circular Economy Package sets ambitious targets for 2030. Aligning its waste management system with these requirements while expanding the use of waste as secondary raw materials remains a major challenge for Serbia, an EU candidate country. The Novi Sad Waste Management Region is one of the 26 regions that will need to transform from linear to circular waste management. This paper aims to analyze current situation in the region regarding circular economy and identify the priority streams with the greatest potential to yield secondary raw materials and support the region's transition. The analysis identified four priority streams—biodegradable waste, paper/cardboard, plastics, metals,—that have the greatest potential. In 2030, the total amount of generated municipal solid waste in the region will be 292,342 tons, whereas priority streams will include 193,393 tons of secondary raw materials.

Introduction
For organisations that aim to be profitable and to create value, the circular economy (CE) is increasingly seen as a strategic priority. Firms that hold Environmental Management System (EMS) certification, are committed to improving their environmental performance, and have adopted sustainable business models tend to implement CE practices more extensively [1]. By promoting sustainable development, CE helps lower risks while avoiding environmental damage and the depletion of natural resources [2]. The circular economy can provide business models that combine economic growth with sustainability. Companies across a range of industries that adopt these models show better environmental performance and gain a number of benefits, including more rational use of resources, lower costs, economies of scale, and greater flexibility in production. The European Union (EU) introduced the circular economy concept in 2014 with a long-term strategy focused on minimizing, recycling, or repurposing waste and recognizing waste as a secondary raw material [3]. In 2020, the EU adopted the new circular economy action plan 2020, with one of the aims to reduce waste and focus on the sectors that use the most resources and where the potential for circularity is high, for example, packaging waste plastics, setting 70% 55% targets by 2030. At the EU level in 2021, the average EU recycling rate was 64%, while the highest recycling rate among EU members was Belgium at 80%, the Netherlands at 78%, Slovakia at 74 %, and Luxembourg and Italy at 73% for monitoring compliance with policy targets, by type of packaging. In contrast, Europe's circular material use rate slightly increases to 11,5% [4]. Less than 12% of all materials used in the EU are recycled. Following EU waste management practices, in 2020, Serbia adopted a Circular Economy Roadmap aimed at transitioning from a linear to circular economy within the country. The roadmap, through the adoption of circular business models, promotes the creation of new job opportunities in the industry and supports business innovation by identifying sustainable solutions in the market [5]. Transition and developing economies often enter the circular economy through waste management, the so-called "end-of-pipe" approach, because eco-design, green public procurement, and industrial symbiosis remain underdeveloped. Improving collection, sorting, recycling, and landfill diversion is therefore the most feasible starting point. This "waste-first" pathway lets public authorities show visible environmental results while

gradually building the institutional, technical, and market capacity that more advanced circular strategies require. The paper identifies the municipal waste flows and volumes with potential to serve as secondary raw materials, thereby contributing to sustainable development in the Novi Sad Waste Management Region (NSWMR) and the transition to a circular model.

Experimental

NSWMC represents one of 27 waste management centers defined by the National Waste Management Strategy. It comprises about 3000 km2 and hosts a population of 500,000 inhabitants generating 190,000 t of municipal solid waste (MSW). As in the majority of waste management regions, landfilling is the dominant method of waste treatment. In addition, there is separate collection of plastic bottles, glass, paper, and cardboard in some parts of the region, mostly in the core of Novi Sad City. Biodegradable waste is not separated at the source; it is landfilled without any pretreatment [6].

Regarding the waste quantities generated in NSWMR, the projected waste generation growth rate of 2% was used, considering the influence of GDP on waste generation growth rate and GDP fluctuations in Serbia. Therefore, in 2030, the total amount of MSW generated in NSWMR will be 292.342 tons, since in 2008 was 189.089 tons [6]. The morphological composition of MSW in NSWMC is given in Table 1.

Table 1. Morphological composition of MSW in NSWMC

Garden waste	14,0%
Biodegradable waste	33,0%
Paper	7,0%
Glass	6,0%
Cardboard	7,0%
Waxed cardboard	0,7%
Al.-coated cardboard	0,9%
Metal pack. and other	1,0%
Metal – Al cans	0,3%
Plastic pack. waste	4,0%
Plastic bags	6,0%
Hard plastic	4,0%
Textiles	4,0%
Leather	0,5%
Nappies	3,6%
Fine waste particles	8,0%
Total	100%

Results and discussion

For the year 2030 the total waste generation is calculated to be 292.342 Table 2. Regarding the potential secondary raw material of landfilled waste, 47% is biodegradable waste, 14% paper and cardboard, 4% PET packaging, and 4% other plastic waste. In contrast, other potential secondary raw materials include glass, metal, metal-aluminum cans, other plastic waste, plastic bags, and textiles and leather, accounting for 23% of landfilled waste. Fine elements and other materials account for 12% of landfilled waste. Therefore, excluding fine elements and other potential secondary raw materials, which are landfilled, is 88%.

Table 2. Projected MSWquantites in 2030. in NSWMR

MSW morphological composition	2030 (t/year)
Garden waste	40.928
Biodegradable waste	96.473
Paper	20.464
Glass	17.540
Cardboard	20.464
Waxed cardboard	2.046
Al.-coated cardboard	2.631
Metal pack. and other	2.923
Metal – Al cans	731
Plastic pack. waste	11.694
Plastic bags	17.540
Hard plastic	11.694
Textiles	11.694
Leather	1.462
Nappies	10.524
Fine waste particles	23.387
Total	292.342

The largest share of landfilled waste is biodegradable waste (137.401 tons), of which only 1.32% was recycled in Serbia (SEPA, 2023a). The rise in landfilled waste shows that CE is not at a satisfactory level, and landfilled waste is a lost SRM that can be used instead of virgin materials, which cost more and increase costs in the production chain. NSWMR has limited domestic supplies of primary raw materials, and the price of waste fluctuates over the course of the year. In addition, virgin materials remain cheaper and more attractive than recycled ones, which cost more. Because of this price gap, large quantities of plastic waste still end up in landfills instead of being recycled. Even metal and plastic are attractive SRM, metal prices are higher and more stable, which keeps metals attractive, while plastic and paper prices fluctuate sharply in the country. Although the NSWMR promotes the separate collection of paper, cardboard, PET, and glass, the volumes collected remain too low to realise economies of scale. Based on waste quantities and their ease of reuse, recycle and substituon of virgin materials several waste stream can be identified as priority streams for circular-economy action:
biodegradable waste which is suitable for composting and anaerobic digestion to produce biogas and compost; Paper and cardboard - can be efficiently recycled within existing industrial capacities; Metals - offering high recycling value and direct substitution for virgin materials; Plastics - particularly packaging fractions, which are price-sensitive.
Focusing on these four material streams first would enchance progress toward higher recycling rates and less landfilling, giving a practical base for its transition to a circular economy in NSWMR.

Conclusion

A circular economy business model strengthens economic resilience by reducing waste and improving resource efficiency. The transition from the linear model requires investment, yet its early stage can be relatively low-cost and market-driven, which makes it less sensitive to fluctuations in waste quantity and quality and more sustainable in the long term. Public

awareness of the circular economy must grow alongside it. In the long run, the circular economy creates jobs, reduces unemployment, promotes sustainable resource use, limits waste, advances clean technologies, encourages innovation, and supports a sustainable society.

References

[1] Fonseca, L.M. et al. (2018) "Assessment of Circular Economy within Portuguese Organizations," Sustainability, 10(7), p. 2521. Available at: https://doi.org/10.3390/su10072521.

[2] Ghisellini, P., Cialani, C. and Ulgiati, S. (2016) "A review on circular economy: the expected transition to a balanced interplay of environmental and economic systems," Journal of Cleaner Production, 114, pp. 11–32. Available at: https://doi.org/10.1016/j.jclepro.2015.09.007.

[3] European Commission (2018) Circular Economy. Closing the Loop. Available at: http://ec.europa. eu/environment/ circular-economy/index_en.html

[4] Eurostat (2024) Recycling rates of packaging waste for monitoring compliance with policy targets, by type of packaging, Waste statistics. Available at: https://ec.europa.eu/eurostat/databrowser/view/env_waspacr/default/table?lang=en&category=env.env_was.env_wasst

[5] Ministry of Environmental Protection (2020) "Roadmap for circular economy in Serbia." Serbian Ministry of Environmental Protection.

[6] Mihajlović, V. et al. (2016) "Financial implications of compliance with EU waste management goals: Feasibility and consequences in a transition country," Waste Management & Research: The Journal for a Sustainable Circular Economy, 34(9), pp. 923–932. Available at: https://doi.org/10.1177/0734242X16652962.